Industria y Comercio
SUPERINTENDENCIA

Espacio reservado para el adhesivo de radicación

DIRECCIÓN DE NUEVAS CREACIONES
Procedimiento acelerado de exámenes de patente (PPH)

1	**NÚMERO DE SOLICITUD ANTE LA SIC NC2017/0013432**		
2	**GLOBAL - PPH** ☐ PAÍS	**3**	**PCT – PPH** ☐ PAÍS
4	**PROSUR** ☐ PAÍS	**5**	**Alianza del Pacifico (AdP)** ☐ PAÍS
6	**OFICINA DE PRIMERA PRESENTACIÓN (OPP)** ☒	**7**	**OFICINA DE EXAMEN ANTERIOR (OEA)** ☐
8	**NÚMERO DE SOLICITUD O PUBLICACIÓN DE LA SOLICITUD (OPP)** ☒ **NÚMERO DE SOLICITUD EN OFICINA DE EXAMEN ANTERIOR (OEA):** ☐ **NÚMERO DE SOLICITUD PCT:** ☐	1. 15/167,373	
9	☐ **REPRESENTANTE LEGAL** ☒ **APODERADO**		

APELLIDOS	NOMBRES	IDENTIFICACIÓN
DAZA MONTALVO	CAROLINA MERCEDES	C.C. 66783790 T.P. 141563 CSJ

DIRECCIÓN	Carrera 11 No. 86-53 Piso 3	No. TELÉFONO	6181088
CIUDAD	Bogotá	CORREO ELECTRÓNICO	notificaciones@clarkemodet.com.co
PAÍS	Colombia	No. RADICACIÓN O PROTOCOLO DE PODER GENERAL	

10 CONDICIONES PARA ACCEDER A ESTE PROCESO:

10.1. DATOS DE PRIORIDAD ☒ SI ☐ NO

(33) PAÍS DE ORIGEN	CÓDIGO PAÍS	(31) NÚMERO	(32) FECHA (AAAA/MM/DD)
1. ESTADOS UNIDOS DE AMÉRICA	US	62/168,581	2015/05/29
2. ESTADOS UNIDOS DE AMÉRICA	US	62/168,529	2015/05/29
3. ESTADOS UNIDOS DE AMÉRICA	US	62/269,745	2015/05/29

10.2. DATOS SOLICITUD INTERNACIONAL PCT ☒ SI ☐ NO

Solicitud Internacional No.	PCT/US2016/034782	**Fecha**	2016/05/27
Publicación Internacional No.	WO/2016/196346	**Fecha**	2016/12/08

*El solicitante presenta una copia de la(s) reivindicación(es) patentable(s) u otorgable(s) de la solicitud de la Oficina de Primera Presentación que profirió el examen de patentabilidad, junto con una traducción al castellano. ☒ SI ☐ NO

*El solicitante presenta los resultados de búsqueda de la Oficina de Examen Anterior, junto con una traducción al castellano ☒ SI ☐ NO

REQUISITOS PARA EL RECONOCIMIENTO DE LOS RESULTADOS DE EXÁMENES DE PATENTABILIDAD EFECTUADOS A SOLICITUDES EXTRANJERAS

Para que la Superintendencia de Industria y Comercio pueda reconocer los resultados de exámenes de patentabilidad producidos por otras Oficinas de Propiedad Industrial se debe cumplir con las siguientes condiciones:

(a) Al momento de solicitar el examen de patentabilidad, si el solicitante pide que se reconozcan exámenes de patentabilidad de otras oficinas extranjeras, deberá aportar junto con el pago de la tasa correspondiente, los siguientes anexos:

(i) Copia de las resoluciones, fallos o decisiones que han sido relevantes para la determinación de la patentabilidad de la(s) solicitud(es) en la Oficina que haya proferido el examen de patentabilidad que contienen reivindicaciones patentables u otorgables que son la base de la petición, y si es del caso, su traducción al castellano. ☒ SI ☐ NO

(ii) Copia de todas las reivindicaciones determinadas como patentables u otorgables en la Oficina que profirió el examen de patentabilidad y, si es del caso, su traducción al castellano. ☒ SI ☐ NO

(iii) Copia de los antecedentes, información o documentos citados por el examinador de la Oficina de Primera Presentación del examen de patentabilidad, en las resoluciones, fallos o decisiones correspondientes, incluyendo la literatura no patente. Los documentos de patente deberán presentarse siempre y cuando no estén disponibles para la Superintendencia de Industria y Comercio mediante el simple acceso a bases de datos gratuitas. ☒ SI ☐ NO

(iv) Una tabla de correspondencias de las reivindicaciones que han sido determinadas como patentables u otorgables en la solicitud de la Oficina que haya proferido el examen de patentabilidad. . ☒ SI ☐ NO

11 FIRMA DEL SOLICITANTE, DEL APODERADO O DEL REPRESENTANTE LEGAL
Junto a cada firma, indicar el nombre del firmante y su calidad (si tal calidad no es obvia al leer el petitorio)



UNITED STATES PATENT AND TRADEMARK OFFICE

UNITED STATES DEPARTMENT OF COMMERCE
United States Patent and Trademark Office
Address: COMMISSIONER FOR PATENTS
P.O. Box 1450
Alexandria, Virginia 22313-1450
www.uspto.gov

NOTICE OF ALLOWANCE AND FEE(S) DUE

21839 7590 06/21/2017

BUCHANAN, INGERSOLL & ROONEY PC
POST OFFICE BOX 1404
ALEXANDRIA, VA 22313-1404

EXAMINER
SOROUSH, LAYLA

ART UNIT	PAPER NUMBER
1627	

DATE MAILED: 06/21/2017

APPLICATION NO.	FILING DATE	FIRST NAMED INVENTOR	ATTORNEY DOCKET NO.	CONFIRMATION NO.
15/167,373	05/27/2016	Mark BOCK	0080171-000253-T1	2421

TITLE OF INVENTION: TETRASUBSTITUTED ALKENE COMPOUNDS AND THEIR USE

APPLN. TYPE	ENTITY STATUS	ISSUE FEE DUE	PUBLICATION FEE DUE	PREV. PAID ISSUE FEE	TOTAL FEE(S) DUE	DATE DUE
nonprovisional	UNDISCOUNTED	$960	$0	$0	$960	09/21/2017

THE APPLICATION IDENTIFIED ABOVE HAS BEEN EXAMINED AND IS ALLOWED FOR ISSUANCE AS A PATENT. PROSECUTION ON THE MERITS IS CLOSED. THIS NOTICE OF ALLOWANCE IS NOT A GRANT OF PATENT RIGHTS. THIS APPLICATION IS SUBJECT TO WITHDRAWAL FROM ISSUE AT THE INITIATIVE OF THE OFFICE OR UPON PETITION BY THE APPLICANT. SEE 37 CFR 1.313 AND MPEP 1308.

THE ISSUE FEE AND PUBLICATION FEE (IF REQUIRED) MUST BE PAID WITHIN THREE MONTHS FROM THE MAILING DATE OF THIS NOTICE OR THIS APPLICATION SHALL BE REGARDED AS ABANDONED. THIS STATUTORY PERIOD CANNOT BE EXTENDED. SEE 35 U.S.C. 151. THE ISSUE FEE DUE INDICATED ABOVE DOES NOT REFLECT A CREDIT FOR ANY PREVIOUSLY PAID ISSUE FEE IN THIS APPLICATION. IF AN ISSUE FEE HAS PREVIOUSLY BEEN PAID IN THIS APPLICATION (AS SHOWN ABOVE), THE RETURN OF PART B OF THIS FORM WILL BE CONSIDERED A REQUEST TO REAPPLY THE PREVIOUSLY PAID ISSUE FEE TOWARD THE ISSUE FEE NOW DUE.

HOW TO REPLY TO THIS NOTICE:

I. Review the ENTITY STATUS shown above. If the ENTITY STATUS is shown as SMALL or MICRO, verify whether entitlement to that entity status still applies.

If the ENTITY STATUS is the same as shown above, pay the TOTAL FEE(S) DUE shown above.

If the ENTITY STATUS is changed from that shown above, on PART B - FEE(S) TRANSMITTAL, complete section number 5 titled "Change in Entity Status (from status indicated above)".

For purposes of this notice, small entity fees are 1/2 the amount of undiscounted fees, and micro entity fees are 1/2 the amount of small entity fees.

II. PART B - FEE(S) TRANSMITTAL, or its equivalent, must be completed and returned to the United States Patent and Trademark Office (USPTO) with your ISSUE FEE and PUBLICATION FEE (if required). If you are charging the fee(s) to your deposit account, section "4b" of Part B - Fee(s) Transmittal should be completed and an extra copy of the form should be submitted. If an equivalent of Part B is filed, a request to reapply a previously paid issue fee must be clearly made, and delays in processing may occur due to the difficulty in recognizing the paper as an equivalent of Part B.

III. All communications regarding this application must give the application number. Please direct all communications prior to issuance to Mail Stop ISSUE FEE unless advised to the contrary.

IMPORTANT REMINDER: Utility patents issuing on applications filed on or after Dec. 12, 1980 may require payment of maintenance fees. It is patentee's responsibility to ensure timely payment of maintenance fees when due.

PART B - FEE(S) TRANSMITTAL

Complete and send this form, together with applicable fee(s), to: Mail **Mail Stop ISSUE FEE**
Commissioner for Patents
P.O. Box 1450
Alexandria, Virginia 22313-1450
or Fax (571)-273-2885

INSTRUCTIONS: This form should be used for transmitting the ISSUE FEE and PUBLICATION FEE (if required). Blocks 1 through 5 should be completed where appropriate. All further correspondence including the Patent, advance orders and notification of maintenance fees will be mailed to the current correspondence address as indicated unless corrected below or directed otherwise in Block 1, by (a) specifying a new correspondence address; and/or (b) indicating a separate "FEE ADDRESS" for maintenance fee notifications.

CURRENT CORRESPONDENCE ADDRESS (Note: Use Block 1 for any change of address)

21839 7590 06/21/2017
BUCHANAN, INGERSOLL & ROONEY PC
POST OFFICE BOX 1404
ALEXANDRIA, VA 22313-1404

Note: A certificate of mailing can only be used for domestic mailings of the Fee(s) Transmittal. This certificate cannot be used for any other accompanying papers. Each additional paper, such as an assignment or formal drawing, must have its own certificate of mailing or transmission.

Certificate of Mailing or Transmission
I hereby certify that this Fee(s) Transmittal is being deposited with the United States Postal Service with sufficient postage for first class mail in an envelope addressed to the Mail Stop ISSUE FEE address above, or being facsimile transmitted to the USPTO (571) 273-2885, on the date indicated below.

(Depositor's name)
(Signature)
(Date)

APPLICATION NO.	FILING DATE	FIRST NAMED INVENTOR	ATTORNEY DOCKET NO.	CONFIRMATION NO.
15/167,373	05/27/2016	Mark BOCK	0080171-000253-T1	2421

TITLE OF INVENTION: TETRASUBSTITUTED ALKENE COMPOUNDS AND THEIR USE

APPLN. TYPE	ENTITY STATUS	ISSUE FEE DUE	PUBLICATION FEE DUE	PREV. PAID ISSUE FEE	TOTAL FEE(S) DUE	DATE DUE
nonprovisional	UNDISCOUNTED	$960	$0	$0	$960	09/21/2017

EXAMINER	ART UNIT	CLASS-SUBCLASS
SOROUSH, LAYLA	1627	514-333000

1. Change of correspondence address or indication of "Fee Address" (37 CFR 1.363).
- ❑ Change of correspondence address (or Change of Correspondence Address form PTO/SB/122) attached.
- ❑ "Fee Address" indication (or "Fee Address" Indication form PTO/SB/47; Rev 03-02 or more recent) attached. **Use of a Customer Number is required.**

2. For printing on the patent front page, list
(1) The names of up to 3 registered patent attorneys or agents OR, alternatively,
(2) The name of a single firm (having as a member a registered attorney or agent) and the names of up to 2 registered patent attorneys or agents. If no name is listed, no name will be printed.
1 _____
2 _____
3 _____

3. ASSIGNEE NAME AND RESIDENCE DATA TO BE PRINTED ON THE PATENT (print or type)

PLEASE NOTE: Unless an assignee is identified below, no assignee data will appear on the patent. If an assignee is identified below, the document has been filed for recordation as set forth in 37 CFR 3.11. Completion of this form is NOT a substitute for filing an assignment.

(A) NAME OF ASSIGNEE (B) RESIDENCE: (CITY and STATE OR COUNTRY)

Please check the appropriate assignee category or categories (will not be printed on the patent) : ❑ Individual ❑ Corporation or other private group entity ❑ Government

4a. The following fee(s) are submitted:
- ❑ Issue Fee
- ❑ Publication Fee (No small entity discount permitted)
- ❑ Advance Order - # of Copies _____

4b. Payment of Fee(s): **(Please first reapply any previously paid issue fee shown above)**
- ❑ A check is enclosed.
- ❑ Payment by credit card. Form PTO-2038 is attached.
- ❑ The director is hereby authorized to charge the required fee(s), any deficiency, or credits any overpayment, to Deposit Account Number _____ (enclose an extra copy of this form).

5. **Change in Entity Status** (from status indicated above)
- ❑ Applicant certifying micro entity status. See 37 CFR 1.29 — NOTE: Absent a valid certification of Micro Entity Status (see forms PTO/SB/15A and 15B), issue fee payment in the micro entity amount will not be accepted at the risk of application abandonment.
- ❑ Applicant asserting small entity status. See 37 CFR 1.27 — NOTE: If the application was previously under micro entity status, checking this box will be taken to be a notification of loss of entitlement to micro entity status.
- ❑ Applicant changing to regular undiscounted fee status. — NOTE: Checking this box will be taken to be a notification of loss of entitlement to small or micro entity status, as applicable.

NOTE: This form must be signed in accordance with 37 CFR 1.31 and 1.33. See 37 CFR 1.4 for signature requirements and certifications.

Authorized Signature _____ Date _____

Typed or printed name _____ Registration No. _____

PTOL-85 Part B (10-13) Approved for use through 10/31/2013. OMB 0651-0033 U.S. Patent and Trademark Office; U.S. DEPARTMENT OF COMMERCE

UNITED STATES PATENT AND TRADEMARK OFFICE

UNITED STATES DEPARTMENT OF COMMERCE
United States Patent and Trademark Office
Address: COMMISSIONER FOR PATENTS
P.O. Box 1450
Alexandria, Virginia 22313-1450
www.uspto.gov

APPLICATION NO.	FILING DATE	FIRST NAMED INVENTOR	ATTORNEY DOCKET NO.	CONFIRMATION NO.
15/167,373	05/27/2016	Mark BOCK	0080171-000253-T1	2421

21839 7590 06/21/2017

BUCHANAN, INGERSOLL & ROONEY PC
POST OFFICE BOX 1404
ALEXANDRIA, VA 22313-1404

EXAMINER	
SOROUSH, LAYLA	

ART UNIT	PAPER NUMBER
1627	

DATE MAILED: 06/21/2017

Determination of Patent Term Adjustment under 35 U.S.C. 154 (b)
(Applications filed on or after May 29, 2000)

The Office has discontinued providing a Patent Term Adjustment (PTA) calculation with the Notice of Allowance.

Section 1(h)(2) of the AIA Technical Corrections Act amended 35 U.S.C. 154(b)(3)(B)(i) to eliminate the requirement that the Office provide a patent term adjustment determination with the notice of allowance. See Revisions to Patent Term Adjustment, 78 Fed. Reg. 19416, 19417 (Apr. 1, 2013). Therefore, the Office is no longer providing an initial patent term adjustment determination with the notice of allowance. The Office will continue to provide a patent term adjustment determination with the Issue Notification Letter that is mailed to applicant approximately three weeks prior to the issue date of the patent, and will include the patent term adjustment on the patent. Any request for reconsideration of the patent term adjustment determination (or reinstatement of patent term adjustment) should follow the process outlined in 37 CFR 1.705.

Any questions regarding the Patent Term Extension or Adjustment determination should be directed to the Office of Patent Legal Administration at (571)-272-7702. Questions relating to issue and publication fee payments should be directed to the Customer Service Center of the Office of Patent Publication at 1-(888)-786-0101 or (571)-272-4200.

OMB Clearance and PRA Burden Statement for PTOL-85 Part B

The Paperwork Reduction Act (PRA) of 1995 requires Federal agencies to obtain Office of Management and Budget approval before requesting most types of information from the public. When OMB approves an agency request to collect information from the public, OMB (i) provides a valid OMB Control Number and expiration date for the agency to display on the instrument that will be used to collect the information and (ii) requires the agency to inform the public about the OMB Control Number's legal significance in accordance with 5 CFR 1320.5(b).

The information collected by PTOL-85 Part B is required by 37 CFR 1.311. The information is required to obtain or retain a benefit by the public which is to file (and by the USPTO to process) an application. Confidentiality is governed by 35 U.S.C. 122 and 37 CFR 1.14. This collection is estimated to take 12 minutes to complete, including gathering, preparing, and submitting the completed application form to the USPTO. Time will vary depending upon the individual case. Any comments on the amount of time you require to complete this form and/or suggestions for reducing this burden, should be sent to the Chief Information Officer, U.S. Patent and Trademark Office, U.S. Department of Commerce, P.O. Box 1450, Alexandria, Virginia 22313-1450. DO NOT SEND FEES OR COMPLETED FORMS TO THIS ADDRESS. SEND TO: Commissioner for Patents, P.O. Box 1450, Alexandria, Virginia 22313-1450. Under the Paperwork Reduction Act of 1995, no persons are required to respond to a collection of information unless it displays a valid OMB control number.

Privacy Act Statement

The Privacy Act of 1974 (P.L. 93-579) requires that you be given certain information in connection with your submission of the attached form related to a patent application or patent. Accordingly, pursuant to the requirements of the Act, please be advised that: (1) the general authority for the collection of this information is 35 U.S.C. 2(b)(2); (2) furnishing of the information solicited is voluntary; and (3) the principal purpose for which the information is used by the U.S. Patent and Trademark Office is to process and/or examine your submission related to a patent application or patent. If you do not furnish the requested information, the U.S. Patent and Trademark Office may not be able to process and/or examine your submission, which may result in termination of proceedings or abandonment of the application or expiration of the patent.

The information provided by you in this form will be subject to the following routine uses:

1. The information on this form will be treated confidentially to the extent allowed under the Freedom of Information Act (5 U.S.C. 552) and the Privacy Act (5 U.S.C 552a). Records from this system of records may be disclosed to the Department of Justice to determine whether disclosure of these records is required by the Freedom of Information Act.
2. A record from this system of records may be disclosed, as a routine use, in the course of presenting evidence to a court, magistrate, or administrative tribunal, including disclosures to opposing counsel in the course of settlement negotiations.
3. A record in this system of records may be disclosed, as a routine use, to a Member of Congress submitting a request involving an individual, to whom the record pertains, when the individual has requested assistance from the Member with respect to the subject matter of the record.
4. A record in this system of records may be disclosed, as a routine use, to a contractor of the Agency having need for the information in order to perform a contract. Recipients of information shall be required to comply with the requirements of the Privacy Act of 1974, as amended, pursuant to 5 U.S.C. 552a(m).
5. A record related to an International Application filed under the Patent Cooperation Treaty in this system of records may be disclosed, as a routine use, to the International Bureau of the World Intellectual Property Organization, pursuant to the Patent Cooperation Treaty.
6. A record in this system of records may be disclosed, as a routine use, to another federal agency for purposes of National Security review (35 U.S.C. 181) and for review pursuant to the Atomic Energy Act (42 U.S.C. 218(c)).
7. A record from this system of records may be disclosed, as a routine use, to the Administrator, General Services, or his/her designee, during an inspection of records conducted by GSA as part of that agency's responsibility to recommend improvements in records management practices and programs, under authority of 44 U.S.C. 2904 and 2906. Such disclosure shall be made in accordance with the GSA regulations governing inspection of records for this purpose, and any other relevant (i.e., GSA or Commerce) directive. Such disclosure shall not be used to make determinations about individuals.
8. A record from this system of records may be disclosed, as a routine use, to the public after either publication of the application pursuant to 35 U.S.C. 122(b) or issuance of a patent pursuant to 35 U.S.C. 151. Further, a record may be disclosed, subject to the limitations of 37 CFR 1.14, as a routine use, to the public if the record was filed in an application which became abandoned or in which the proceedings were terminated and which application is referenced by either a published application, an application open to public inspection or an issued patent.
9. A record from this system of records may be disclosed, as a routine use, to a Federal, State, or local law enforcement agency, if the USPTO becomes aware of a violation or potential violation of law or regulation.

Examiner-Initiated Interview Summary	Application No.	Applicant(s)	
	15/167,373	BOCK ET AL.	
	Examiner	Art Unit	
	LAYLA SOROUSH	1627	

All participants (applicant, applicant's representative, PTO personnel):

(1) *LAYLA SOROUSH*. (3)_____.

(2) *Duane A. Stewart*. (4)_____.

Date of Interview: *23 May 2017*.

Type: ☒ Telephonic ☐ Video Conference
☐ Personal [copy given to: ☐ applicant ☐ applicant's representative]

Exhibit shown or demonstration conducted: ☐ Yes ☐ No.
If Yes, brief description: _____.

Issues Discussed ☐101 ☐112 ☐102 ☐103 ☐Others
(For each of the checked box(es) above, please describe below the issue and detailed description of the discussion)

Claim(s) discussed: _____.

Identification of prior art discussed: _____.

Substance of Interview
(For each issue discussed, provide a detailed description and indicate if agreement was reached. Some topics may include: identification or clarification of a reference or a portion thereof, claim interpretation, proposed amendments, arguments of any applied references etc...)

In the interest of compact prosecution, a proposal was made to the Applicant to overcome the remaining issues and proceed to allowance. Applicant agreed and gave the Examiner authorization to make the appropriate claim amendments in an Examiner's Amendment .

Applicant recordation instructions: It is not necessary for applicant to provide a separate record of the substance of interview.

Examiner recordation instructions: Examiners must summarize the substance of any interview of record. A complete and proper recordation of the substance of an interview should include the items listed in MPEP 713.04 for complete and proper recordation including the identification of the general thrust of each argument or issue discussed, a general indication of any other pertinent matters discussed regarding patentability and the general results or outcome of the interview, to include an indication as to whether or not agreement was reached on the issues raised.

☐ Attachment

Notice of Allowability	Application No. 15/167,373	Applicant(s) BOCK ET AL.	
	Examiner LAYLA SOROUSH	Art Unit 1627	AIA (First Inventor to File) Status Yes

-- The MAILING DATE of this communication appears on the cover sheet with the correspondence address--

All claims being allowable, PROSECUTION ON THE MERITS IS (OR REMAINS) CLOSED in this application. If not included herewith (or previously mailed), a Notice of Allowance (PTOL-85) or other appropriate communication will be mailed in due course. **THIS NOTICE OF ALLOWABILITY IS NOT A GRANT OF PATENT RIGHTS.** This application is subject to withdrawal from issue at the initiative of the Office or upon petition by the applicant. See 37 CFR 1.313 and MPEP 1308.

1. ☒ This communication is responsive to *the arguments filed on 3/22/17*.
   ☐ A declaration(s)/affidavit(s) under **37 CFR 1.130(b)** was/were filed on_____.
2. ☐ An election was made by the applicant in response to a restriction requirement set forth during the interview on _____; the restriction requirement and election have been incorporated into this action.
3. ☒ The allowed claim(s) is/are *1-3, 5-7, 11, 17-27, 29, 33, 38-43, and 47-52* . As a result of the allowed claim(s), you may be eligible to benefit from the **Patent Prosecution Highway** program at a participating intellectual property office for the corresponding application. For more information, please see http://www.uspto.gov/patents/init_events/pph/index.jsp or send an inquiry to PPHfeedback@uspto.gov .
4. ☐ Acknowledgment is made of a claim for foreign priority under 35 U.S.C. § 119(a)-(d) or (f).

   Certified copies:

   a) ☐ All b) ☐ Some *c) ☐ None of the:
   1. ☐ Certified copies of the priority documents have been received.
   2. ☐ Certified copies of the priority documents have been received in Application No. _____ .
   3. ☐ Copies of the certified copies of the priority documents have been received in this national stage application from the International Bureau (PCT Rule 17.2(a)).

   * Certified copies not received: _____.

Applicant has THREE MONTHS FROM THE "MAILING DATE" of this communication to file a reply complying with the requirements noted below. Failure to timely comply will result in ABANDONMENT of this application.
THIS THREE-MONTH PERIOD IS NOT EXTENDABLE.

5. ☐ CORRECTED DRAWINGS (as "replacement sheets") must be submitted.
   ☐ including changes required by the attached Examiner's Amendment / Comment or in the Office action of Paper No./Mail Date _____.

   Identifying indicia such as the application number (see 37 CFR 1.84(c)) should be written on the drawings in the front (not the back) of each sheet. Replacement sheet(s) should be labeled as such in the header according to 37 CFR 1.121(d).
6. ☐ DEPOSIT OF and/or INFORMATION about the deposit of BIOLOGICAL MATERIAL must be submitted. Note the attached Examiner's comment regarding REQUIREMENT FOR THE DEPOSIT OF BIOLOGICAL MATERIAL.

Attachment(s)

1. ☐ Notice of References Cited (PTO-892)
2. ☐ Information Disclosure Statements (PTO/SB/08), Paper No./Mail Date _____
3. ☐ Examiner's Comment Regarding Requirement for Deposit of Biological Material
4. ☒ Interview Summary (PTO-413), Paper No./Mail Date *23 May 2017* .
5. ☒ Examiner's Amendment/Comment
6. ☒ Examiner's Statement of Reasons for Allowance
7. ☐ Other _____.

DETAILED ACTION

Applicant's response filed on March 22, 2017 is acknowledged in response to the office action mailed on 12/23/2016.

The present application, filed on or after March 16, 2013, is being examined under the first inventor to file provisions of the AIA.

Claim Status

Claims 1-3, 5-7, 11, 17-27, 29, 33, 38-43, and 47-52 are pending.

Claims 1-3, 5-7, 11, 17-27, 29, 33, 38-43, and 47-52 are allowed.

Withdrawn Rejections

The objection over the specification is withdrawn.

The rejection of claims 18, 20, 22, 29, 33, and 48 rejected under 35 U.S.C. 103 as being unpatentable over Krushner et al. (US 8063249 B1) is withdrawn.

Reasons for Allowance

The following is an examiner's statement of reasons for allowance:

The prior art does not teach or suggest a compound given by formula II of claim 1, formula I of claim 2, and formula III of claim 20.

Accordingly, the claims are found to patentable over the prior art.

Any comments considered necessary by applicant must be submitted no later than the payment of the issue fee and, to avoid processing delays, should preferably accompany the issue fee. Such submissions should be clearly labeled "Comments on Statement of Reasons for Allowance."

Any inquiry concerning this communication or earlier communications from the examiner should be directed to LAYLA SOROUSH whose telephone number is (571)272-5008. The examiner can normally be reached on 8:30a.m.-5:00p.m..

If attempts to reach the examiner by telephone are unsuccessful, the examiner's supervisor, Sreenivasan Padmanabhan can be reached on (571)272-0629. The fax phone number for the organization where this application or proceeding is assigned is 571-273-8300.

Information regarding the status of an application may be obtained from the Patent Application Information Retrieval (PAIR) system. Status information for published applications may be obtained from either Private PAIR or Public PAIR. Status information for unpublished applications is available through Private PAIR only. For more information about the PAIR system, see http://pair-direct.uspto.gov. Should you have questions on access to the Private PAIR system, contact the Electronic Business Center (EBC) at 866-217-9197 (toll-free). If you would like assistance from a USPTO Customer Service Representative or access to the automated information system, call 800-786-9199 (IN USA OR CANADA) or 571-272-1000.

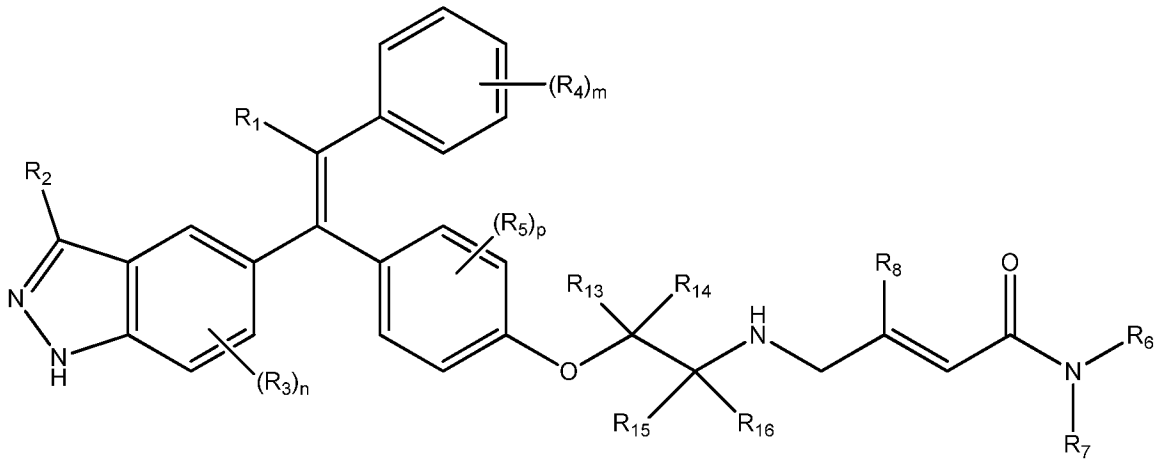
/LAYLA SOROUSH/

Art Unit 1627

Listing of Claims

This Listing of Claims replaces all previous listings of claims in this application.

1. (Withdrawn) A compound given by formula II:



II

wherein:

R_1 is selected from the group consisting of methyl, ethyl, cyclobutyl, cyclopropyl, propyl, isopropyl, $-CH_2CF_3$, $-CH_2CH_2F$, and $-CH_2CH_2Cl$;

R_2 is selected from the group consisting of H and F;

n is 0-1;

R_3 is F when n=1;

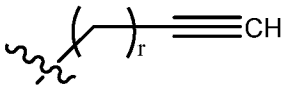
m is 0-2;

R_4 are the same or different and are independently selected from the group consisting of F, CF_3, Cl, isopropyl, $-OCH_3$, $-OCHF_2$, $-OCF_3$, ethyl and methyl;

p is 0-1;

R_5 is F when p=1;

R_6 and R_7 are the same or different and are independently selected from the group consisting of methyl, ethyl, propyl, $-CH_2CH_2OH$ and



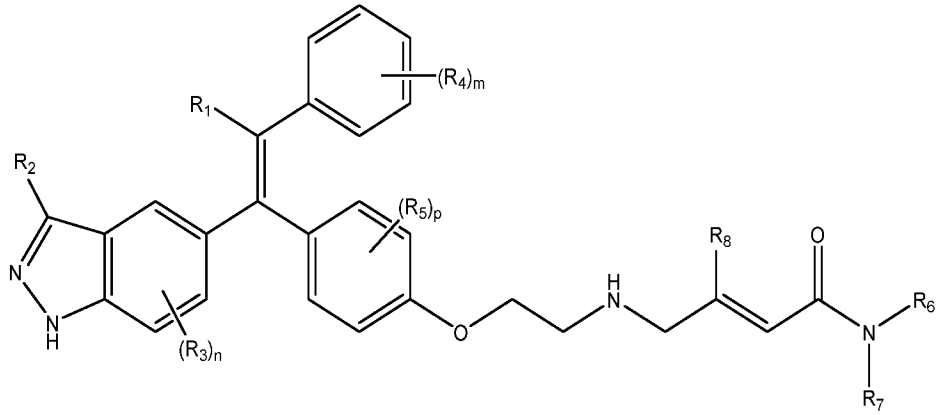
, wherein r is 1 or 2; or, wherein R_6 and R_7 form a 4-6 membered heterocyclic ring with the N to which they are attached, wherein said heterocyclic ring optionally includes an oxygen atom, and wherein said heterocyclic ring is optionally substituted with F, or $-CH_2F$;

R_8 is selected from the group consisting of H and $-CH_3$;

and R_{13}, R_{14}, R_{15}, and R_{16} are independently selected from the group consisting of –H or $-CH_3$;

or a pharmaceutically acceptable salt thereof.

2. (Withdrawn) The compound or pharmaceutically acceptable salt of claim 1, given by formula I:



I

wherein:

R_1 is selected from the group consisting of methyl, ethyl, cyclobutyl, cyclopropyl and $-CH_2CH_2Cl$;

R_2 is selected from the group consisting of H and F;

n is 0-1;

R_3 is F when n=1;

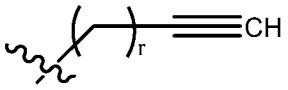
m is 0-2;

R_4 are the same or different and are independently selected from the group consisting of F, CF_3, Cl, isopropyl, $-OCH_3$, $-OCHF_2$, $-OCF_3$, ethyl and methyl;

p is 0-1;

R_5 is F when p=1;

R_6 and R_7 are the same or different and are independently selected from the group consisting of methyl, ethyl, propyl, $-CH_2CH_2OH$ and



, wherein r is 1 or 2;

or, wherein R_6 and R_7 form a 4-6 membered heterocyclic ring with the N to which they are attached, wherein said heterocyclic ring optionally includes an oxygen atom, and wherein said heterocyclic ring is optionally substituted with F, or $-CH_2F$;

R_8 is selected from the group consisting of H and CH_3;

or a pharmaceutically acceptable salt thereof.

3. (Withdrawn) The compound or pharmaceutically acceptable salt according to claim 2, wherein R_1 is ethyl.

4. (Cancelled)

5. (Withdrawn) The compound or pharmaceutically acceptable salt according to claim 2, wherein R_6 and R_7 are both methyl.

6. (Withdrawn) The compound or pharmaceutically acceptable salt according to claim 2, wherein R_2 and R_8 are H.

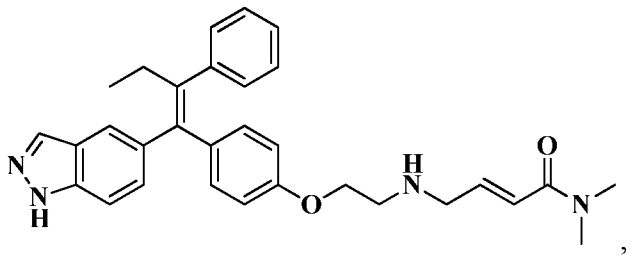
7. (Withdrawn) The compound or pharmaceutically acceptable salt according to claim 2, wherein R_2 is F.

8-10. (Cancelled)

11. (Withdrawn) The compound or pharmaceutically acceptable salt according to claim 2, wherein m, n, and p are 0.

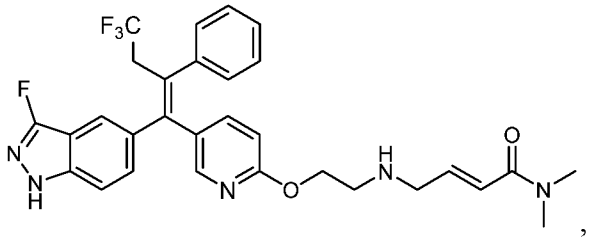
12-16. (Cancelled)

17. (Withdrawn) The compound of claim 2, having the following formula:



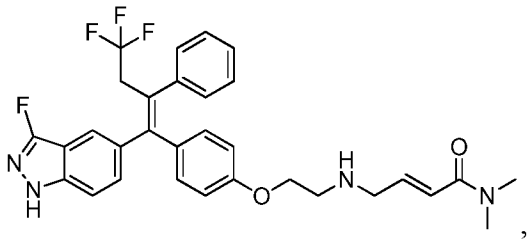
or a pharmaceutically acceptable salt thereof.

18. (Original) A compound having the following formula:



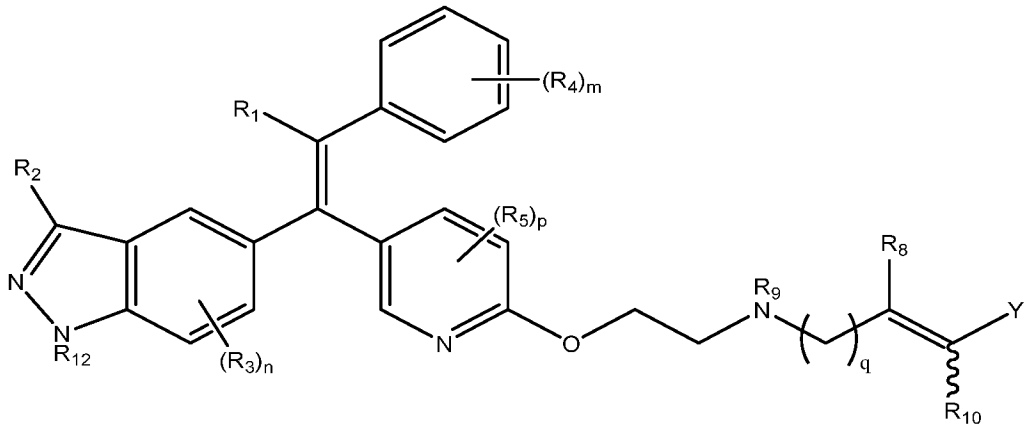
or a pharmaceutically acceptable salt thereof.

19. (Withdrawn) The compound of claim 1 having the following formula:



or a pharmaceutically acceptable salt thereof.

20. (Original) A compound given by formula III:



III

wherein:

R_1 is selected from the group consisting of C_1-C_6 alkyl, C_3-C_6 cycloalkyl, $-CH_2CF_3$, and a 4-6 membered heterocyclic ring;

R_2 is selected from the group consisting of H, halogen, hydroxy, C_1-C_3 alkyl, C_3-C_4 cycloalkyl and C_4 heterocyclic ring;

when n is not 0, R_3 are the same or different, and are independently selected from the group consisting of H, halogen, C_1-C_6 alkyl and C_1-C_3 alkoxy optionally substituted with at least one halogen;

n is 0-3;

when m is not zero, R_4 are the same or different and are independently selected from the group consisting of H, halogen, C_1-C_6 alkyl, and OR_{11}, wherein R_{11} is selected from the group consisting of C_3-C_6 cycloalkyl, C_1-C_6 alkyl, aryl, heteroaryl and a 4-6 membered heterocyclic ring;

m is 0-5;

when p is not 0, R_5 are the same or different and are independently selected from the group consisting of H, halogen, C_1-C_4 alkyl, C_1-C_4 alkoxy, C_3-C_4 cycloalkyl, C_3-C_6 cycloalkoxy and C_4 heterocycle;

p is 0-3;

q is 1-2;

R_8 and R_{10} are the same or different and are independently selected from the group consisting of halogen, H and C_1-C_3 alkyl;

R_9 is selected from the group consisting of H, C_1-C_6 alkyl and C_3-C_6 cycloalkyl;

Y is selected from the group consisting of $-S(O)_2R_6$, $-S(O)_2NR_6R_7$, $-C(O)NR_6R_7$,

-C(O)R_6, -C(O)OR_6, -CN; or wherein Y and R_{10} both represent $-CF_3$;

R_6 and R_7 are the same or different and are independently selected from the group consisting of H, C_1-C_6 alkyl, C_3-C_6 cycloalkyl, aryl, heteroaryl and a 4-6 membered heterocyclic ring wherein said alkyl is saturated or unsaturated or wherein R_6 and R_7 form a 4-6 membered heterocyclic ring with the N to which they are attached, optionally also containing an O atom;

R_{12} is selected from the group consisting of H, C_3-C_4 cycloalkyl and C_1-C_6 alkyl; and

wherein any carbon containing moiety of R_1-R_{12} may be optionally substituted with one or more halogen atoms, fluoromethane, difluoromethane or trifluoromethane, or –OH;

or pharmaceutically acceptable salts thereof.

21. (Withdrawn) The compound or pharmaceutically acceptable salt according to claim 20, wherein R_1 is selected from the group consisting of C_1-C_6 alkyl, C_3-C_6 cycloalkyl, and a 4-6 membered heterocyclic ring.

22. (Currently Amended) The compound or pharmaceutically ~~accepatable~~ acceptable salt according to claim 20, wherein:

R_2 is selected from the group consisting of H, halogen, methyl and ethyl;

R_3 are the same or different, and are independently selected from the group consisting of H, halogen, methyl and ethyl;

R_4 are the same or different and are independently selected from the group consisting of H, halogen, C_1-C_6 alkyl and C_1-C_6 alkoxy;

R_5 are the same or different and are independently selected from the group consisting of H, halogen, methyl and ethyl;

R_8 and R_{10} are the same or different and are independently selected from the group consisting of H and methyl;

R_9 is selected from the group consisting of H, methyl and ethyl; and

R_6 and R_7 are the same or different and are independently selected from the group consisting of H and C_1-C_6 alkyl or wherein R_6 and R_7 form a 4-6 atom heterocyclic ring with the N to which they are attached, optionally also containing an O atom.

23. (Previously Presented) The compound or pharmeutically acceptable salt of claim 20, wherein Y is $-C(O)NR_6R_7$.

24. (Previously Presented) The compound or pharmaceutically acceptable salt of claim 20, wherein R_6 and R_7 are methyl.

25. (Withdrawn) The compound or pharmaceutically acceptable salt of claim 23, wherein R_2, R_8 , R_9, and R_{10} are each H.

26. (Withdrawn) The compound or pharmaceutically acceptable salt of claim 23, wherein R_1 is ethyl.

27. (Withdrawn) The compound or pharmaceutically acceptable salt of claim 23, wherein R_1 is cyclobutyl.

28. (Cancelled)

29. (Previously Presented) The compound or pharmaceutically acceptable salt of claim 23, wherein R_2 is F.

30-32. (Cancelled)

33. (Previously Presented) The compound or pharmaceutically acceptable salt of claim 23, wherein m, n, and p are 0.

34-37. (Cancelled)

38. (Withdrawn) A method of treating breast cancer comprising administering to a subject a compound or pharmaceutically acceptable salt of claim 20.

39. (Withdrawn) The method of claim 38, wherein said breast cancer is an ER-positive breast cancer.

40. (Withdrawn) The method of claim 39, where said subject expresses a mutant ER-α protein.

41. (Withdrawn) A method of treating breast cancer comprising administering to a subject a compound or pharmaceutically acceptable salt of claim 18.

42. (Withdrawn) The method of claim 41, wherein said breast cancer is an ER-positive breast cancer.

43. (Withdrawn) The method of claim 42, where said subject expresses a mutant ER-α protein.

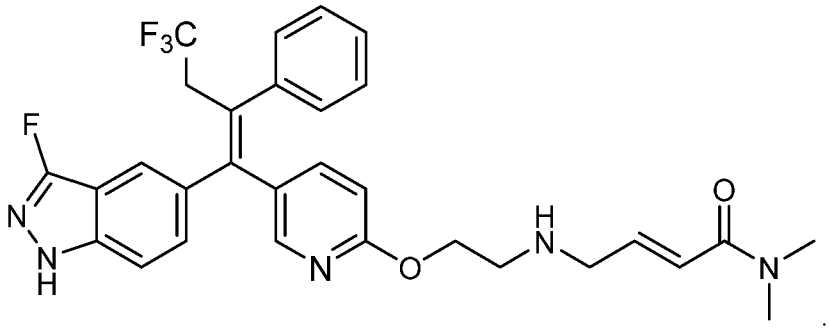
44-46. (Cancelled)

47. (Withdrawn) A pharmaceutical composition comprising the compound of claim 17 or a pharmaceutically acceptable salt thereof, and further comprising a pharmaceutically acceptable excipient.

48. (Previously Presented) A pharmaceutical composition comprising the compound of claim 18 or a pharmaceutically acceptable salt thereof, and further comprising a pharmaceutically acceptable excipient.

49. (Withdrawn) A pharmaceutical composition comprising the compound of claim 19 or a pharmaceutically acceptable salt thereof, and further comprising a pharmaceutically acceptable excipient.

50. (New) The compound of claim 18, having the following formula:



51. (New) A pharmaceutical composition comprising the compound of claim 50, and further comprising a pharmaceutically acceptable excipient.

52. (New) A pharmaceutical composition comprising the compound of claim 20 or a pharmaceutically acceptable salt thereof, and further comprising a pharmaceutically acceptable excipient.

Notificación de Concesión	**Solicitud No.** 15/167,373	**Solicitante(s)** BOCK ET AL.	
	Examinador LAYLA SOROUSH	**Unidad de Arte** 1627	**Estado AIA (Primer Inventor en Presentar)** Sí

-- La FECHA DE ENVIO de esta comunicación aparece en la hoja de cubierta con la dirección de correspondencia--

Todas las reivindicaciones son concedidas, TRÁMITE SOBRE EL FONDO ESTÁ (O PERMANECE) CERRADO en esta solicitud. Si no se incluye acá (o enviada previamente), una Notificación de Concesión (PTOL-85) u otra comunicación adecuada será enviada en su debido momento. **ESTA NOTIFICACION DE CONCESION NO ES UNA CONCESION DE DERECHOS DE PATENTE**. Esta solicitud está sujeta a retiro de emisión a la iniciativa de la Oficina o a petición del solicitante. Ver 37 CFR 1.313 y MPEP 1308.

1. Esta comunicación responde a los argumentos presentados el 3/22/17.

Una declaración bajo **37 CFR 1.130(b)** se presentó el_____.

2. Se hizo una elección por el solicitante en respuesta a un requerimiento de restricción definido durante la entrevista el ____; el requerimiento de restricción y la elección se han incorporado en esta acción.

3. Las reivindicaciones concedidas son *1-3, 5-7, 11, 17-27, 29, 33, 38-43, y 47-52*. Como resultado de las reivindicaciones aceptadas, usted puede ser elegible del beneficio del programa de **Trámite de Patente Acelerado** en una oficina de propiedad intelectual participante para la correspondiente solicitud. Para más información, por favor ver http://www.uspto.gov/patents/init_events/pph/index.jsp o enviar una pregunta a PPHfeedback@uspto.gov.

4. Se reconoce una reivindicación de prioridad extranjera bajo 35 USC sección 119(a)-(d) o (f).

Copias certificadas:

a) Todas b) Algunas c) Ninguna de las:

1. Copias certificadas de los documentos de prioridad se han recibido.

2. Copias certificadas de los documentos de prioridad se han recibido en la Solicitud No. ____.

3. Copias de las copias certificadas de los documentos de prioridad se han recibido en esta solicitud de fase nacional de la Oficina Internacional (Regla PCT 17.2 (a)).

* Copias certificadas no recibidas: _____.

El Solicitante tiene TRES MESES A PARTIR DE LA “FECHA DE ENVIO” de esta comunicación para presentar una respuesta que cumpla con los requerimientos indicados anteriormente. Falla en cumplir a tiempo resultará en el ABANDONO de esta solicitud.

ESTE PERIODO DE TRES MESES NO ES EXTENSIBLE

5. Se deben presentar FIGURAS CORREGIDAS (como “hojas de reemplazo”).

Incluyendo cambios requeridos por la Enmienda/Comentario del Examinador adjunto o en la Acción Oficial de Papel No./Fecha de Envío ____.

Los indicios de identificación tal como el número de solicitud (ver 37 CFR 1.84(c)) se deben escribir en las figuras en el frente (no atrás) de cada hoja. Las hojas de reemplazo deben estar etiquetadas como tal en el encabezado de acuerdo con 37 CFR 1.121(d).

6. Se debe presentar DEPOSITO DE y/o INFORMACIÓN acerca del depósito de MATERIAL BIOLOGICO. Note el comentario del Examinador adjunto con relación al REQUERIMIENTO PARA EL DEPOSITO DE MATERIAL BIOLOGICO.

Adjunto(s)

1. Notificación de Referencias Citadas (PTO-892)
2. Declaraciones de Divulgación de Información (PTO/SB/08), Papel No./Fecha Envío ____
3. Comentario del Examinador con Relación a Requerimiento para Depósito de Material Biológico
4. Resumen de Entrevista (PTO-413), Papel [X] No./Fecha Envío __23/05/2017__.
5. Enmienda/Comentario del Examinador [X]
6. Declaración del Examinador de Razones para Concesión. [X]
7. Otro ____.

ACCION DETALLADA

Se reconoce la respuesta del Solicitante presentada el 22 de marzo de 2017 en respuesta a la acción oficial enviada el 23/12/2016.

La presente solicitud, presentada en o después del 16 de marzo de 2013, es examinada bajo las disposiciones de primer inventor en presentar del AIA.

Estado de la Reivindicación

Las reivindicaciones 1-3, 5-7, 11, 17-27, 29, 33, 38-43, y 47-52 están pendientes.

Las reivindicaciones 1-3, 5-7, 11, 17-27, 29, 33, 38-43, y 47-52 son aceptadas.

Objeciones Retiradas

La objeción sobre la descripción es retirada.

La objeción de las reivindicaciones 18, 20, 22, 29, 33, y 48 rechazadas bajo 35 U.S.C. 103 por ser no patentables sobre Krushner y otros (US 8063249 B1) es retirada.

Razones para Concesión

La siguiente es una declaración del examinador de las razones para la concesión:

El arte previo no enseña ni sugiere un compuesto dado por la fórmula II de la reivindicación 1, fórmula 1 de la reivindicación 2, y fórmula III de la reivindicación 20.

En consecuencia, se encontró que las reivindicaciones son patentables sobre el arte previo.

Cualquier comentario considerado como necesario por el solicitante debe ser presentado no después del pago de la tasa de emisión y, para evitar demoras de procesamiento, debe preferiblemente acompañar la tasa de emisión. Dichas presentaciones deben ser etiquetadas claramente como “Comentarios sobre

Declaración de Razones para Concesión”.

Cualquier duda relacionada con esta comunicación o comunicaciones anteriores del examinador se deben dirigir a LAYLA SOROUSH cuyo número telefónico es (571)272-5008. El examinador se puede encontrar normalmente de 8:30 am-5:00 pm.

Si los intentos para comunicarse con el examinador no son exitosos, el supervisor del examinador, Sreenivasan Padmanabhan se puede encontrar en (571)272-0629. El número de fax para la organización donde esta solicitud o procedimiento es asignada es 571-273-8300.

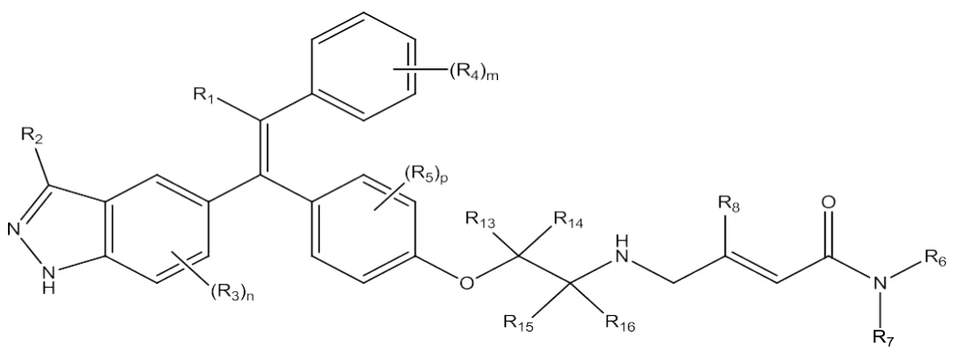
La información relacionada con el estado de una solicitud se puede obtener del sistema de Recuperación de Información de Solicitud de Patente (PAIR). La información del estado para solicitudes publicadas se puede obtener el PAIR Privado o el PAIR Público. La información del estado para solicitudes no publicadas está disponible únicamente a través del PAIR Privado. Si tiene alguna pregunta sobre el acceso al sistema PAIR Privado, contacte el Centro de Negocios Electrónicos (EBC) al 866-217-9197 (línea gratuita). Si desea asistencia de un Representante de Servicio al Cliente de la USPTO o acceso al sistema de información automatizada, llame al 800-786-9199 (EN USA O CANADA) o 571-272-1000.

/LAYLA SOROUSH/

Unidad del Arte 1627

REIVINDICACIONES

1. (Retirada) Un compuesto dado por la Fórmula II:



II

en donde:

R_1 se selecciona del grupo que consiste de metilo, etilo, ciclobutilo, ciclopropilo, propilo, isopropilo, $-CH_2CF_3$, $-CH_2CH_2F$, y $-CH_2CH_2Cl$;

R_2 se selecciona del grupo que consiste de H y F; n es 0-1;

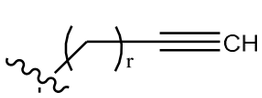
R_3 es F cuando n=1;

m es 0-2;

R_4 son los mismos o diferentes y se seleccionan independientemente del grupo que consiste de F, CF_3, Cl, isopropilo, $-OCH_3$, $-OCHF_2$, $-OCF_3$, etilo y metilo;

p es 0-1;

R_5 es F cuando p=1;

R_6 y R_7 son los mismos o diferentes y se seleccionan independientemente del grupo que consiste de metilo, etilo, propilo, $-CH_2CH_2OH$ y 

en donde r es 1 o 2; o, en donde R_6 y R_7 forman un anillo heterocíclico de 4-6 miembros con la N a la cual se enlazan, en donde dicho anillo heterocíclico opcionalmente incluye cero un átomo de oxígeno, y en donde dicho anillo heterocíclico es opcionalmente sustituido con F, o $–CH_2F$;

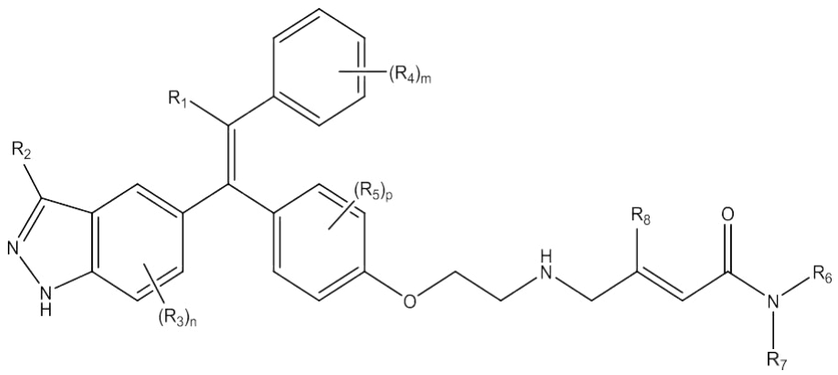
R_8 se selecciona del grupo que consiste de H y $-CH_3$;

y R_{13}, R_{14}, R_{15}, y R_{16} se seleccionan independientemente del grupo que

consiste de –H o $–CH_3$;

o una sal farmacéuticamente aceptable de los mismos.

2. (Retirada) El compuesto o sal farmacéuticamente aceptable de la reivindicación 1, dado por la Fórmula I:



I

en donde:

R_1 se selecciona del grupo que consiste de metilo, etilo, ciclobutilo, ciclopropilo y $-CH_2CH_2Cl$;

R_2 se selecciona del grupo que consiste de H y F;

n es 0-1;

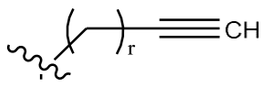
R_3 es F cuando n=1;

m es 0-2;

R_4 son los mismos o diferentes y se seleccionan independientemente del grupo que consiste de F, CF_3, Cl, isopropilo, $-OCH_3$, $-OCHF_2$, $-OCF_3$, etilo y metilo;

p es 0-1;

R_5 es F cuando p=1;

R_6 y R_7 son los mismos o diferentes y se seleccionan independientemente del grupo que consiste de metilo, etilo, propilo, $-CH_2CH_2OH$ y 

en donde r es 1 o 2;

o, en donde R_6 y R_7 forman un anillo heterocíclico de 4-6 miembros con la N a la cual se enlazan, en donde dicho anillo heterocíclico opcionalmente incluye un

átomo de oxígeno, y en donde dicho anillo heterocíclico es opcionalmente sustituido con F, o $–CH_2F$;

R_8 se selecciona del grupo que consiste de H y CH_3;

o una sal farmacéuticamente aceptable de los mismos.

3. (Retirada) El compuesto o sal farmacéuticamente aceptable de acuerdo con la reivindicación 2, en donde R_1 es etilo.

4. (Cancelada)

5. (Retirada) El compuesto o sal farmacéuticamente aceptable de acuerdo con la reivindicación 2, en donde R_6 y R_7 ambos son metilo.

6. (Retirada) El compuesto o sal farmacéuticamente aceptable de acuerdo con la reivindicación 2, en donde R_2 y R_8 son H.

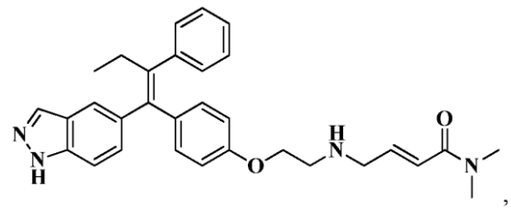
7. (Retirada) El compuesto o sal farmacéuticamente aceptable de acuerdo con la reivindicación 2, en donde R_2 es F.

8-10. (Canceladas)

11. (Retirada) El compuesto o sal farmacéuticamente aceptable de acuerdo con la reivindicación 2, en donde m, n, y p son 0.

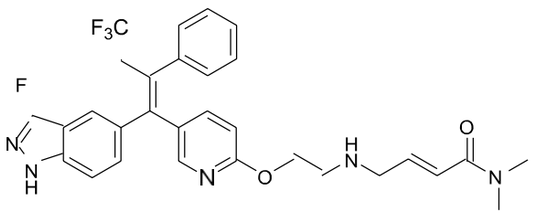
12-16. (Canceladas)

17. (Retirada) El compuesto de la reivindicación 2, que tiene la siguiente fórmula:



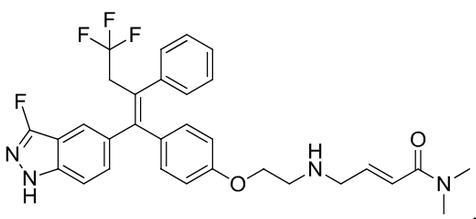
o una sal farmacéuticamente aceptable del mismo.

18. (Original) Un compuesto que tiene la siguiente fórmula:



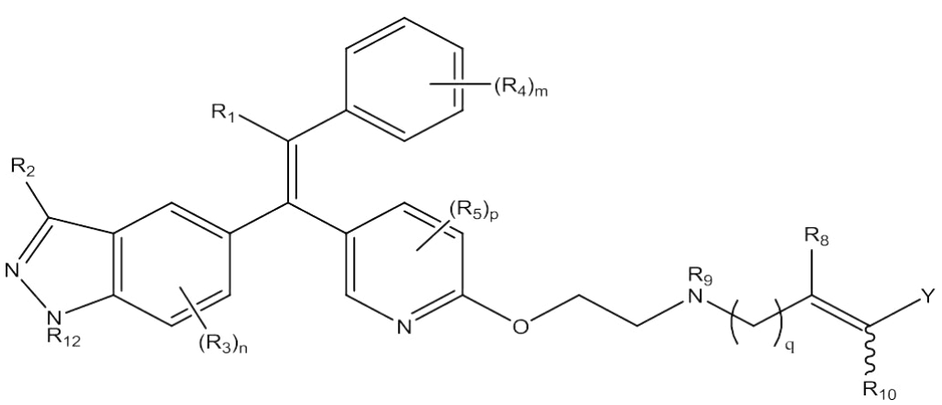
o una sal farmacéuticamente aceptable del mismo.

19. (Retirada) El compuesto de la reivindicación 1, que tiene la siguiente fórmula:



o una sal farmacéuticamente aceptable del mismo.

20. (Original) Un compuesto dado por la Fórmula III:



III

en donde:

R_1 se selecciona del grupo que consiste de alquilo C_1-C_6, cicloalquilo C_3-C_6, - CH_2CF_3, y un anillo heterocíclico de 4-6 miembros;

R_2 se selecciona del grupo que consiste de H, halógeno, hidroxi, alquilo C_1-C_3, cicloalquilo C_3-C_4 y anillo heterocíclico C_4;

cuando n no es 0, R_3 son los mismos o diferentes, y se seleccionan independientemente del grupo que consiste de H, halógeno, alquilo C_1-C_6 y alcoxi C_1-C_3 opcionalmente sustituido con al menos un halógeno;

n es 0-3;

cuando m no es cero, R_4 son los mismos o diferentes y se seleccionan independientemente del grupo que consiste de H, halógeno, alquilo C_1-C_6, y OR_{11}, en donde R_{11} se selecciona del grupo que consiste de cicloalquilo C_3-C_6, alquilo C_1-C_6, arilo, heteroarilo y un anillo heterocíclico de 4-6 miembros;

m es 0-5;

cuando p no es 0, R_5 son los mismos o diferentes y se seleccionan independientemente del grupo que consiste de H, halógeno, alquilo C_1-C_4, alcoxi C_1-C_4, cicloalquilo C_3-C_4, cicloalcoxi C_3-C_6 y heterociclo C_4;

p es 0-3;

q es 1-2;

R_8 y R_{10} son los mismos o diferentes y se seleccionan independientemente del grupo que consiste de halógeno, H y alquilo C_1-C_3;

R_9 se selecciona del grupo que consiste de H, alquilo C_1-C_6 y cicloalquilo C_3-C_6;

Y se selecciona del grupo que consiste de $-S(O)_2R_6$, $-S(O)_2NR_6R_7$, $-C(O)NR_6R_7$, $-C(O)R_6$, $-C(O)OR_6$, -CN; o en donde Y, y R_{10} ambos representan $–CF_3$;

R_6 y R_7 son los mismos o diferentes y se seleccionan independientemente del grupo que consiste de H, alquilo C_1-C_6, cicloalquilo C_3-C_6, arilo, heteroarilo y un anillo heterocíclico de 4-6 miembros en donde dicho alquilo es saturado o insaturado o en donde R_6 y R_7 forman un anillo heterocíclico de 4-6 miembros con la N a la cual

se enlazan, opcionalmente también incluye átomo O;

R_{12} se selecciona del grupo que consiste de H, cicloalquilo C_3-C_4 y alquilo C_1-C_6; y

en donde cualquier carbono que contiene porción de R_1-R_{12} se puede sustituir opcionalmente con uno o más átomos de halógeno, fluorometano, difluorometano o trifluorometano, o -OH;

o sales farmacéuticamente aceptables de los mismos.

21. (Retirada) El compuesto o sal farmacéuticamente aceptable de acuerdo con la reivindicación 20, en donde R_1 se selecciona del grupo que consiste de alquilo C_1-C_6, cicloalquilo C_3-C_6, y un anillo heterocíclico de 4-6 miembros.

22. (Actualmente Modificada) El compuesto o sal farmacéuticamente aceptable de acuerdo con la reivindicación 20, en donde:

R_2 se selecciona del grupo que consiste de H, halógeno, metilo y etilo;

R_3 son los mismos o diferentes, y se seleccionan independientemente del grupo que consiste de H, halógeno, metilo y etilo;

R_4 son los mismos o diferentes y se seleccionan independientemente del grupo que consiste de H, halógeno, alquilo C_1-C_6 y alcoxi C_1-C_6;

R_5 son los mismos o diferentes y se seleccionan independientemente del grupo que consiste de H, halógeno, metilo y etilo;

R_8 y R_{10} son los mismos o diferentes y se seleccionan independientemente del grupo que consiste de H y metilo;

R_9 se selecciona del grupo que consiste de H, metilo y etilo; y

R_6 y R_7 son los mismos o diferentes y se seleccionan independientemente del grupo que consiste de H y alquilo C_1-C_6 o en donde R_6 y R_7 forman un anillo heterocíclico de 4-6 átomos con la N a la cual se enlazan, opcionalmente también contienen un átomo O.

23. (Presentada Anteriormente) El compuesto o sal farmacéuticamente aceptable de la reivindicación 20, en donde Y es -C(O)NR_6R_7.

24. (Presentada Anteriormente) El compuesto o sal farmacéuticamente aceptable de la reivindicación 20, en donde R_6 y R_7 son metilo.

25. (Retirada) El compuesto o sal farmacéuticamente aceptable de la reivindicación 23, en dondeo porque R_2, R_8, R_9 y R_{10} son cada uno H.

26. (Retirada) El compuesto o sal farmacéuticamente aceptable de la reivindicación 23, en donde R_1 es etilo.

27. (Retirada) El compuesto o sal farmacéuticamente aceptable de la reivindicación 23, en donde R_1 es ciclobutilo.

28. (Cancelada)

29. (Presentada Anteriormente) El compuesto o sal farmacéuticamente aceptable de la reivindicación 23, en donde R_2 es F.

20-32. (Cancelado)

33. (Presentada Anteriormente) El compuesto o sal farmacéuticamente aceptable de la reivindicación 23, en donde m, n, y p son 0.

34-37 (Cancelada)

38. (Retirada) Un método para tratar cáncer de seno que comprende administrar a un sujeto un compuesto o sal farmacéuticamente aceptable de la reivindicación 20.

39. (Retirada) El método de la reivindicación 38, en donde dicho cáncer de seno es un cáncer de seno positivo ER.

40. (Retirada) El método de la reivindicación 39, en donde dicho sujeto expresa una proteína ER-α mutante.

41. (Retirada) Un método para tratar cáncer de seno que comprende administrar a un sujeto un compuesto o sal farmacéuticamente aceptable de la reivindicación 18.

42. (Retirada) El método de la reivindicación 41, en donde dicho cáncer de seno es un cáncer de seno positivo ER.

43. (Retirada) El método de la reivindicación 42, en donde dicho sujeto expresa una proteína ER-α mutante.

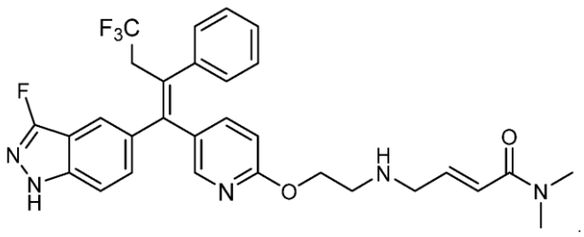
44-46. (Cancelada)

47. (Retirada) Una composición farmacéutica que comprende el compuesto de la reivindicación 17 o una sal farmacéuticamente aceptable del mismo, y además comprende un excipiente farmacéuticamente aceptable.

48. (Presentada Anteriormente) Una composición farmacéutica que comprende el compuesto de la reivindicación 18 o una sal farmacéuticamente aceptable del mismo, y que además comprende un excipiente farmacéuticamente aceptable.

49. (Retirada) Una composición farmacéutica que comprende el compuesto de la reivindicación 19 o una sal farmacéuticamente aceptable del mismo, y que además comprende un excipiente farmacéuticamente aceptable.

50. (Nueva) El compuesto de la reivindicación 18, que tiene la siguiente fórmula:

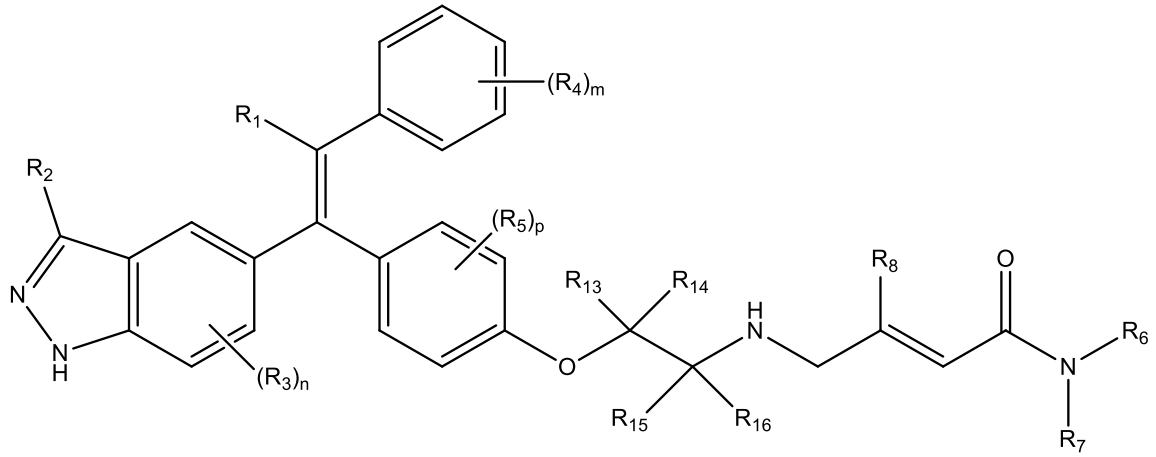


51. (Nueva) Una composición farmacéutica que comprende el compuesto de la reivindicación 50, y que además comprende un excipiente farmacéuticamente aceptable.

52. (Nueva) Una composición farmacéutica que comprende el compuesto de la reivindicación 20 o una sal farmacéuticamente aceptable del mismo, y que además comprende un excipiente farmacéuticamente aceptable.

GRANTED CLAIMS IN US 9,796,683 B2

1. A compound given by formula II:



II

wherein:

R_1 is selected from the group consisting of methyl, ethyl, cyclobutyl, cyclopropyl, propyl, isopropyl, $-CH_2CF_3$, $-CH_2CH_2F$, and $-CH_2CH_2Cl$;

R_2 is selected from the group consisting of H and F;

n is 0-1;

R_3 is F when n=1;

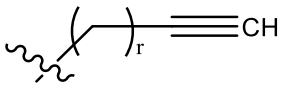
m is 0-2;

R_4 are the same or different and are independently selected from the group consisting of F, CF_3, Cl, isopropyl, $-OCH_3$, $-OCHF_2$, $-OCF_3$, ethyl and methyl;

p is 0-1;

R_5 is F when p=1;

R_6 and R_7 are the same or different and are independently selected from the group consisting of methyl, ethyl, propyl, $-CH_2CH_2OH$ and



, wherein r is 1 or 2; or, wherein R_6 and R_7 form a 4-6 membered heterocyclic ring with the N to which they are attached, wherein said heterocyclic

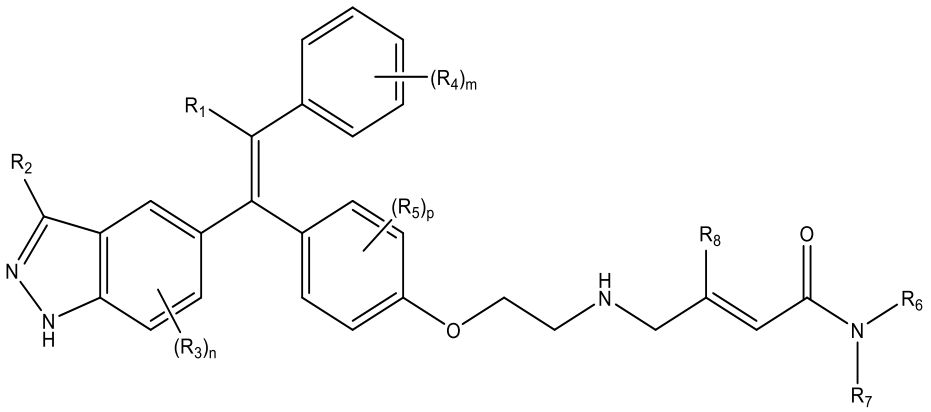
ring further includes an oxygen atom, and wherein said heterocyclic ring is optionally unsubstituted with F, or $–CH_2F$;

R_8 is selected from the group consisting of H and $-CH_3$;

and R_{13}, R_{14}, R_{15}, and R_{16} are independently selected from the group consisting of –H or $–CH_3$;

or a pharmaceutically acceptable salt thereof.

2. The compound or pharmaceutically acceptable salt of claim 1, given by formula I:



I

wherein:

R_1 is selected from the group consisting of methyl, ethyl, cyclobutyl, cyclopropyl and $-CH_2CH_2Cl$;

R_2 is selected from the group consisting of H and F;

n is 0-1;

R_3 is F when n=1;

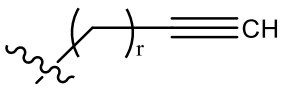
m is 0-2;

R_4 are the same or different and are independently selected from the group consisting of F, CF_3, Cl, isopropyl, $-OCH_3$, $-OCHF_2$, $-OCF_3$, ethyl and methyl;

p is 0-1;

R_5 is F when p=1;

R_6 and R_7 are the same or different and are independently selected from the group consisting of methyl, ethyl, propyl, $-CH_2CH_2OH$ and



, wherein r is 1 or 2;

or, wherein R_6 and R_7 form a 4-6 membered heterocyclic ring with the N to which they are attached, wherein said heterocyclic ring optionally includes an oxygen atom, and wherein said heterocyclic ring is optionally substituted with F, or $–CH_2F$;

R_8 is selected from the group consisting of H and CH_3;

or a pharmaceutically acceptable salt thereof.

3. The compound or pharmaceutically acceptable salt according to claim 2, wherein R_1 is ethyl.

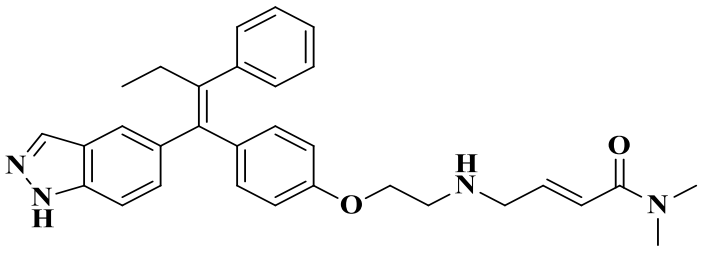
4. The compound or pharmaceutically acceptable salt according to claim 2, wherein R_6 and R_7 are both methyl.

5. The compound or pharmaceutically acceptable salt according to claim 2, wherein R_2 and R_8 are H.

6. The compound or pharmaceutically acceptable salt according to claim 2, wherein R_2 is F.

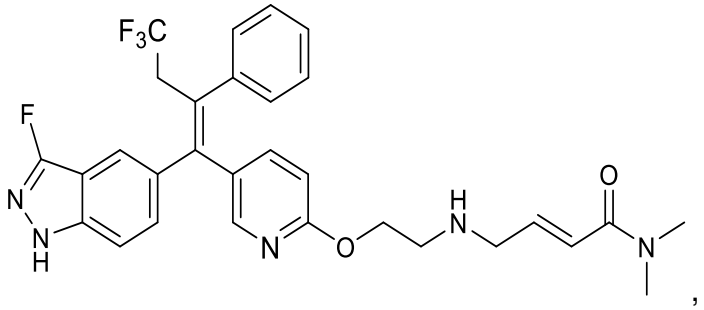
7. The compound or pharmaceutically acceptable salt according to claim 2, wherein m, n, and p are 0.

8. The compound of claim 2, having the following formula:



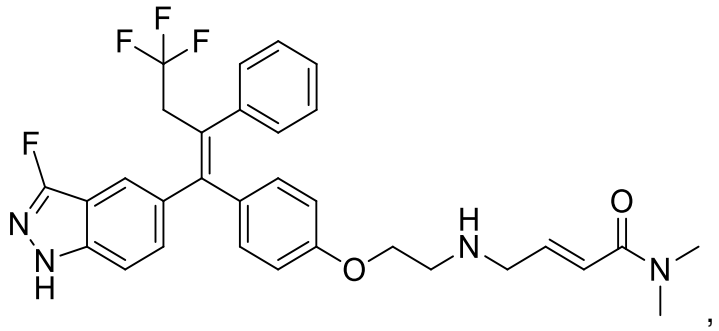
or a pharmaceutically acceptable salt thereof.

9. A compound having the following formula:



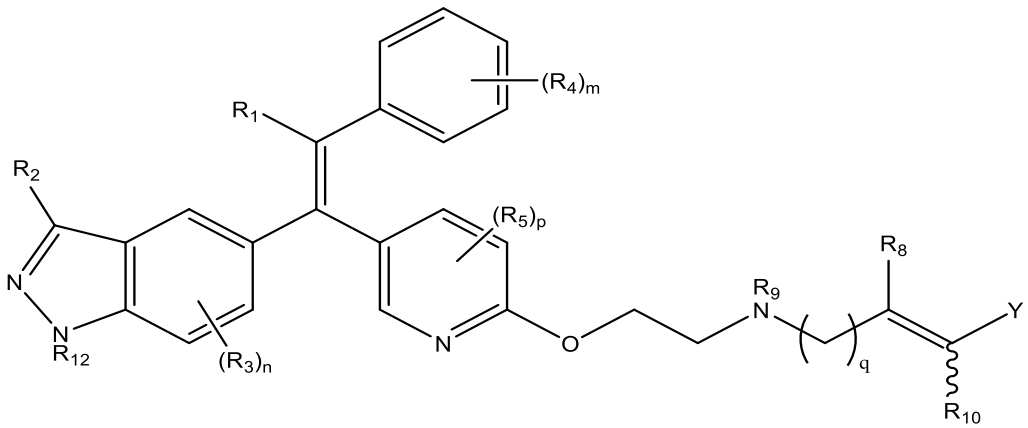
or a pharmaceutically acceptable salt thereof.

10. The compound of claim 1, having the following formula:



or a pharmaceutically acceptable salt thereof.

11. A compound given by formula III:



III

wherein:

R_1 is selected from the group consisting of C_1-C_6 alkyl, C_3-C_6 cycloalkyl, -CH_2CF_3, and a 4-6 membered heterocyclic ring;

R_2 is selected from the group consisting of H, halogen, hydroxy, C_1-C_3 alkyl, C_3-C_4 cycloalkyl and C_4 heterocyclic ring;

when n is not 0, R_3 are the same or different, and are independently selected from the group consisting of H, halogen, C_1-C_6 alkyl and C_1-C_3 alkoxy optionally substituted with at least one halogen;

n is 0-3;

when m is not zero, R_4 are the same or different and are independently selected from the group consisting of H, halogen, C_1-C_6 alkyl, and OR_{11}, wherein R_{11} is selected from the group consisting of C_3-C_6 cycloalkyl, C_1-C_6 alkyl, aryl, heteroaryl and a 4-6 membered heterocyclic ring;

m is 0-5;

when p is not 0, R_5 are the same or different and are independently selected from the group consisting of H, halogen, C_1-C_4 alkyl, C_1-C_4 alkoxy, C_3-C_4 cycloalkyl, C_3-C_6 cycloalkoxy and C_4 heterocycle;

p is 0-3;

q is 1-2;

R_8 and R_{10} are the same or different and are independently selected from the group consisting of halogen, H and C_1-C_3 alkyl;

R_9 is selected from the group consisting of H, C_1-C_6 alkyl and C_3-C_6 cycloalkyl;

Y is selected from the group consisting of $-S(O)_2R_6$, $-S(O)_2NR_6R_7$, $-C(O)NR_6R_7$, $-C(O)R_6$, $-C(O)OR_6$, -CN; or wherein Y and R_{10} both represent $–CF_3$;

R_6 and R_7 are the same or different and are independently selected from the group consisting of H, C_1-C_6 alkyl, C_3-C_6 cycloalkyl, aryl, heteroaryl and a 4-6 membered heterocyclic ring wherein said alkyl is saturated or unsaturated or wherein R_6 and R_7 form a 4-6 membered heterocyclic ring with the N to which they are attached, optionally also containing an O atom;

R_{12} is selected from the group consisting of H, C_3-C_4 cycloalkyl and C_1-C_6 alkyl; and

wherein any carbon containing moiety of R_1-R_{12} may be optionally substituted with one or more halogen atoms, fluoromethane, difluoromethane or trifluoromethane, or –OH;

or pharmaceutically acceptable salts thereof.

12. The compound or pharmaceutically acceptable salt according to claim 11, wherein R_1 is selected from the group consisting of C_1-C_6 alkyl, C_3-C_6 cycloalkyl, and a 4-6 membered heterocyclic ring.

13. The compound or pharmaceutically acceptable salt according to claim 11, wherein:

R_2 is selected from the group consisting of H, halogen, methyl and ethyl;

R_3 are the same or different, and are independently selected from the group consisting of H, halogen, methyl and ethyl;

R_4 are the same or different and are independently selected from the group consisting of H, halogen, C_1-C_6 alkyl and C_1-C_6 alkoxy;

R_5 are the same or different and are independently selected from the group consisting of H, halogen, methyl and ethyl;

R_8 and R_{10} are the same or different and are independently selected from the group consisting of H and methyl;

R_9 is selected from the group consisting of H, methyl and ethyl; and

R_6 and R_7 are the same or different and are independently selected from the group consisting of H and C_1-C_6 alkyl or wherein R_6 and R_7 form a 4-6 atom heterocyclic ring with the N to which they are attached, optionally also containing an O atom.

14. The compound or pharmaceutically acceptable salt of claim 11, wherein Y is -$C(O)NR_6R_7$.

15. The compound or pharmaceutically acceptable salt of claim 11, wherein R_6 and R_7 are methyl.

16. The compound or pharmaceutically acceptable salt of claim 14, wherein R_2, R_8, R_9, and R_{10} are each H.

17. The compound or pharmaceutically acceptable salt of claim 14, wherein R_1 is ethyl.

18. The compound or pharmaceutically acceptable salt of claim 14, wherein R_1 is cyclobutyl.

19. The compound or pharmaceutically acceptable salt of claim 14, wherein R_2 is F.

20. The compound or pharmaceutically acceptable salt of claim 14, wherein m, n, and p are 0.

21. A method of treating breast cancer comprising administering to a subject a compound or pharmaceutically acceptable salt of claim 11.

22. The method of claim 21, wherein said breast cancer is an ER-positive breast cancer.

23. The method of claim 22, where said subject expresses a mutant ER-α protein.

24. A method of treating breast cancer comprising administering to a subject a compound or pharmaceutically acceptable salt of claim 9.

25. The method of claim 24, wherein said breast cancer is an ER-positive breast cancer.

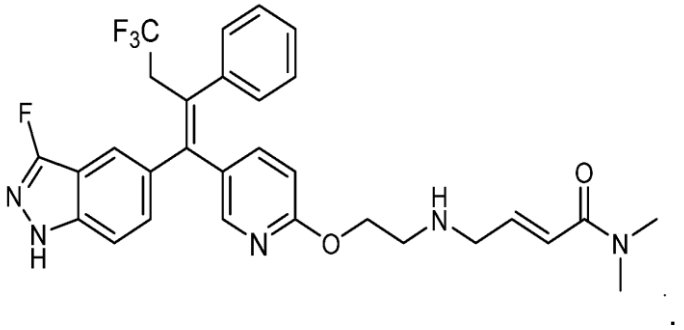
26. The method of claim 25, where said subject expresses a mutant ER-α protein.

27. A pharmaceutical composition comprising the compound of claim 8 or a pharmaceutically acceptable salt thereof, and further comprising a pharmaceutically acceptable excipient.

28. A pharmaceutical composition comprising the compound of claim 9 or a pharmaceutically acceptable salt thereof, and further comprising a pharmaceutically acceptable excipient.

29. A pharmaceutical composition comprising the compound of claim 10 or a pharmaceutically acceptable salt thereof, and further comprising a pharmaceutically acceptable excipient.

30. The compound of claim 9, having the following formula:

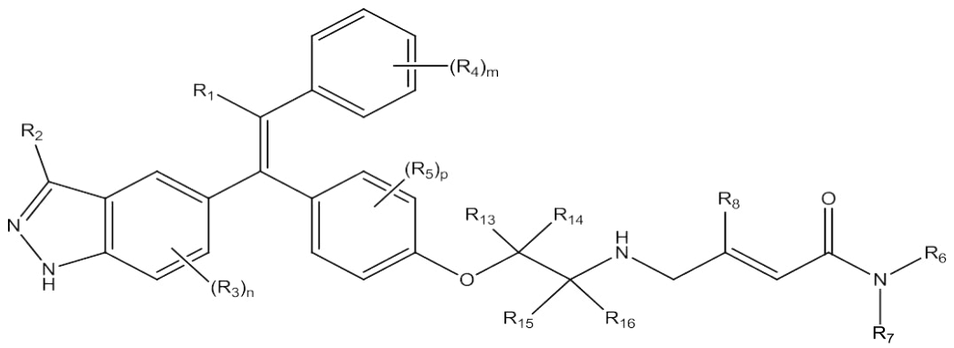


31. A pharmaceutical composition comprising the compound of claim 30, and further comprising a pharmaceutically acceptable excipient.

32. A pharmaceutical composition comprising the compound of claim 11 or a pharmaceutically acceptable salt thereof, and further comprising a pharmaceutically acceptable excipient.

REIVINDICACIONES CONCEDIDAS USPTO
US 9,796,683 B2

1. Un compuesto dado por la Fórmula II:



II

en donde:

R_1 se selecciona del grupo que consiste de metilo, etilo, ciclobutilo, ciclopropilo, propilo, isopropilo, $-CH_2CF_3$, $-CH_2CH_2F$, y $-CH_2CH_2Cl$;

R_2 se selecciona del grupo que consiste de H y F;

n es 0-1;

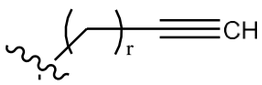
R_3 es F cuando n=1;

m es 0-2;

R_4 son los mismos o diferentes y se seleccionan independientemente del grupo que consiste de F, CF_3, Cl, isopropilo, $-OCH_3$, $-OCHF_2$, $-OCF_3$, etilo y metilo;

p es 0-1;

R_5 es F cuando p=1;

R_6 y R_7 son los mismos o diferentes y se seleccionan independientemente del grupo que consiste de metilo, etilo, propilo, $-CH_2CH_2OH$ y 

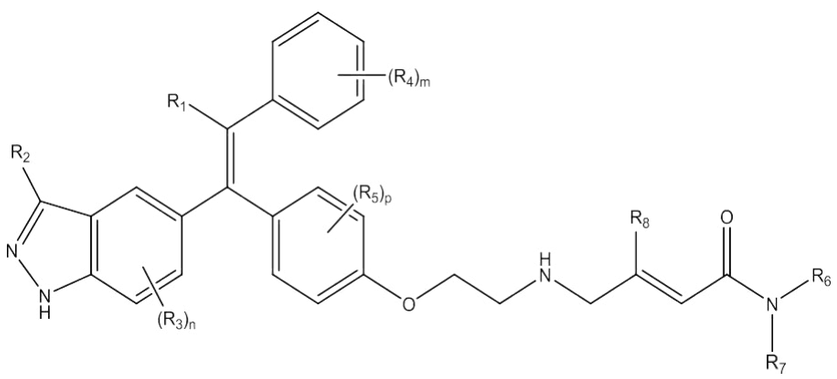
en donde r es 1 o 2; o, en donde R_6 y R_7 forman un anillo heterocíclico de 4-6 miembros con la N a la cual se enlazan, en donde dicho anillo heterocíclico opcionalmente incluye un átomo de oxígeno, y en donde dicho anillo heterocíclico es opcionalmente sustituido con F, o $–CH_2F$;

R_8 se selecciona del grupo que consiste de H y $-CH_3$;

y R_{13}, R_{14}, R_{15}, y R_{16} se seleccionan independientemente del grupo que consiste de –H o $–CH_3$;

o una sal farmacéuticamente aceptable de los mismos.

2. El compuesto o sal farmacéuticamente aceptable de la reivindicación 1, dado por la Fórmula I:



I

en donde:

R_1 se selecciona del grupo que consiste de metilo, etilo, ciclobutilo, ciclopropilo y $-CH_2CH_2Cl$;

R_2 se selecciona del grupo que consiste de H y F;

n es 0-1;

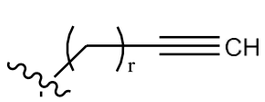
R_3 es F cuando n=1;

m es 0-2;

R_4 son los mismos o diferentes y se seleccionan independientemente del grupo que consiste de F, CF_3, Cl, isopropilo, $-OCH_3$, $-OCHF_2$, $-OCF_3$, etilo y metilo;

p es 0-1;

R_5 es F cuando p=1;

R_6 y R_7 son los mismos o diferentes y se seleccionan independientemente del grupo que consiste de metilo, etilo, propilo, $-CH_2CH_2OH$ y 

en donde r es 1 o 2;

o, en donde R_6 y R_7 forman un anillo heterocíclico de 4-6 miembros con la N

a la cual se enlazan, en donde dicho anillo heterocíclico opcionalmente incluye un átomo de oxígeno, y en donde dicho anillo heterocíclico es opcionalmente sustituido con F, o $–CH_2F$;

R_8 se selecciona del grupo que consiste de H y CH_3;

o una sal farmacéuticamente aceptable de los mismos.

3. El compuesto o sal farmacéuticamente aceptable de acuerdo con la reivindicación 2, en donde R_1 es etilo.

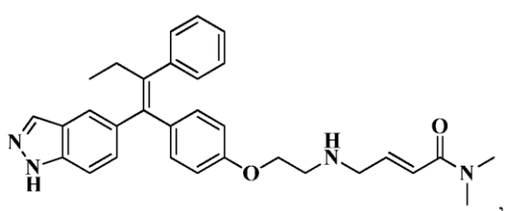
4. El compuesto o sal farmacéuticamente aceptable de acuerdo con la reivindicación 2, en donde R_6 y R_7 ambos son metilo.

5. El compuesto o sal farmacéuticamente aceptable de acuerdo con la reivindicación 2, en donde R_2 y R_8 son H.

6. El compuesto o sal farmacéuticamente aceptable de acuerdo con la reivindicación 2, en donde R_2 es F.

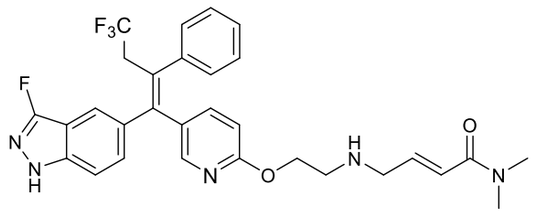
7. El compuesto o sal farmacéuticamente aceptable de acuerdo con la reivindicación 2, en donde m, n, y p son 0.

8. El compuesto de la reivindicación 2, que tiene la siguiente fórmula:



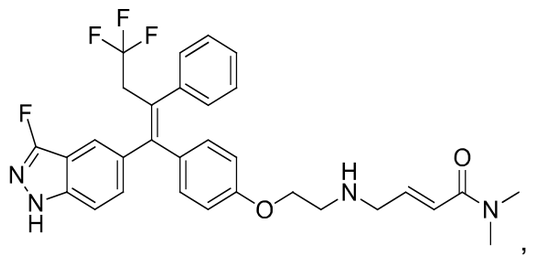
o una sal farmacéuticamente aceptable del mismo.

9. Un compuesto que tiene la siguiente fórmula:



o una sal farmacéuticamente aceptable del mismo.

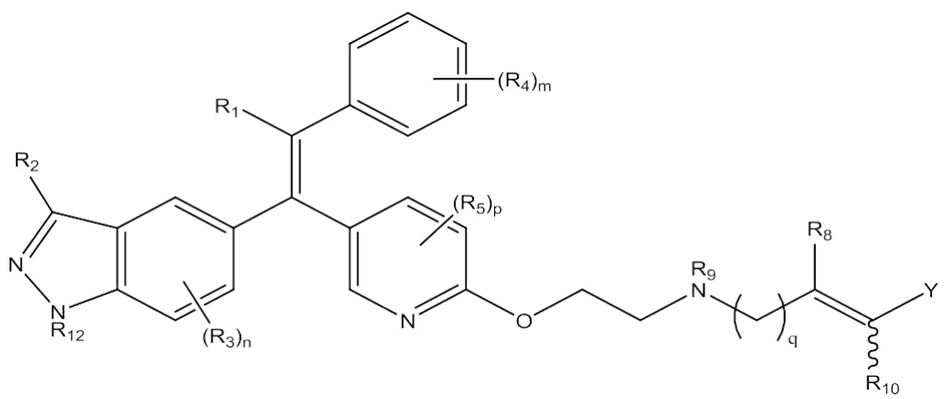
10. El compuesto de la reivindicación 1, que tiene la siguiente fórmula:



,

o una sal farmacéuticamente aceptable del mismo.

11. Un compuesto dado por la Fórmula III:



III

en donde:

R_1 se selecciona del grupo que consiste de alquilo C_1-C_6, cicloalquilo C_3-C_6, - CH_2CF_3, y un anillo heterocíclico de 4-6 miembros;

R_2 se selecciona del grupo que consiste de H, halógeno, hidroxi, alquilo C_1-C_3, cicloalquilo C_3-C_4 y anillo heterocíclico C_4;

cuando n no es 0, R_3 son los mismos o diferentes, y se seleccionan

independientemente del grupo que consiste de H, halógeno, alquilo C_1-C_6 y alcoxi C_1-C_3 opcionalmente sustituido con al menos un halógeno;

n es 0-3;

cuando m no es cero, R_4 son los mismos o diferentes y se seleccionan independientemente del grupo que consiste de H, halógeno, alquilo C_1-C_6, y OR_{11}, en donde R_{11} se selecciona del grupo que consiste de cicloalquilo C_3-C_6, alquilo C_1-C_6, arilo, heteroarilo y un anillo heterocíclico de 4-6 miembros;

m es 0-5;

cuando p no es 0, R_5 son los mismos o diferentes y se seleccionan independientemente del grupo que consiste de H, halógeno, alquilo C_1-C_4, alcoxi C_1-C_4, cicloalquilo C_3-C_4, cicloalcoxi C_3-C_6 y heterociclo C_4;

p es 0-3;

q es 1-2;

R_8 y R_{10} son los mismos o diferentes y se seleccionan independientemente del grupo que consiste de halógeno, H y alquilo C_1-C_3;

R_9 se selecciona del grupo que consiste de H, alquilo C_1-C_6 y cicloalquilo C_3-C_6;

Y se selecciona del grupo que consiste de $-S(O)_2R_6$, $-S(O)_2NR_6R_7$, $-C(O)NR_6R_7$, $-C(O)R_6$, $-C(O)OR_6$, -CN; o en donde Y, y R_{10} ambos representan $–CF_3$;

R_6 y R_7 son los mismos o diferentes y se seleccionan independientemente del grupo que consiste de H, alquilo C_1-C_6, cicloalquilo C_3-C_6, arilo, heteroarilo y un anillo heterocíclico de 4-6 miembros en donde dicho alquilo es saturado o insaturado o en donde R_6 y R_7 forman un anillo heterocíclico de 4-6 miembros con la N a la cual se enlazan, opcionalmente también incluye un átomo O;

R_{12} se selecciona del grupo que consiste de H, cicloalquilo C_3-C_4 y alquilo C_1-C_6; y

en donde cualquier carbono que contiene porción de R_1-R_{12} se puede sustituir opcionalmente con uno o más átomos de halógeno, fluorometano,

difluorometano o trifluorometano, o -OH;

o sales farmacéuticamente aceptables de los mismos.

12. El compuesto o sal farmacéuticamente aceptable de acuerdo con la reivindicación 11, en donde R_1 se selecciona del grupo que consiste de alquilo C_1-C_6, cicloalquilo C_3-C_6, y un anillo heterocíclico de 4-6 miembros.

13. El compuesto o sal farmacéuticamente aceptable de acuerdo con la reivindicación 11, en donde:

R_2 se selecciona del grupo que consiste de H, halógeno, metilo y etilo;

R_3 son los mismos o diferentes, y se seleccionan independientemente del grupo que consiste de H, halógeno, metilo y etilo;

R_4 son los mismos o diferentes y se seleccionan independientemente del grupo que consiste de H, halógeno, alquilo C_1-C_6 y alcoxi C_1-C_6;

R_5 son los mismos o diferentes y se seleccionan independientemente del grupo que consiste de H, halógeno, metilo y etilo;

R_8 y R_{10} son los mismos o diferentes y se seleccionan independientemente del grupo que consiste de H y metilo;

R_9 se selecciona del grupo que consiste de H, metilo y etilo; y

R_6 y R_7 son los mismos o diferentes y se seleccionan independientemente del grupo que consiste de H y alquilo C_1-C_6 o en donde R_6 y R_7 forman un anillo heterocíclico de 4-6 átomos con la N a la cual se enlazan, opcionalmente también contienen un átomo O.

14. El compuesto o sal farmacéuticamente aceptable de la reivindicación 11, en donde Y es $-C(O)NR_6R_7$.

15. El compuesto o sal farmacéuticamente aceptable de la reivindicación 11, en donde R_6 y R_7 son metilo.

16. El compuesto o sal farmacéuticamente aceptable de la reivindicación 14, en donde R_2, R_8, R_9 y R_{10} son cada uno H.

17. El compuesto o sal farmacéuticamente aceptable de la reivindicación 14, en donde R_1 es etilo.

18. El compuesto o sal farmacéuticamente aceptable de la reivindicación 14, en donde R_1 es ciclobutilo.

19. El compuesto o sal farmacéuticamente aceptable de la reivindicación 14, en donde R_2 es F.

20. El compuesto o sal farmacéuticamente aceptable de la reivindicación 14, en donde m, n, y p son 0.

21. Un método para tratar cáncer de seno que comprende administrar a un sujeto un compuesto o sal farmacéuticamente aceptable de la reivindicación 11.

22. El método de la reivindicación 21, en donde dicho cáncer de seno es un cáncer de seno positivo ER.

23. El método de la reivindicación 22, en donde dicho sujeto expresa una proteína ER-α mutante.

24. Un método para tratar cáncer de seno que comprende administrar a un sujeto un compuesto o sal farmacéuticamente aceptable de la reivindicación 9.

25. El método de la reivindicación 24, en donde dicho cáncer de seno es un cáncer de seno positivo ER.

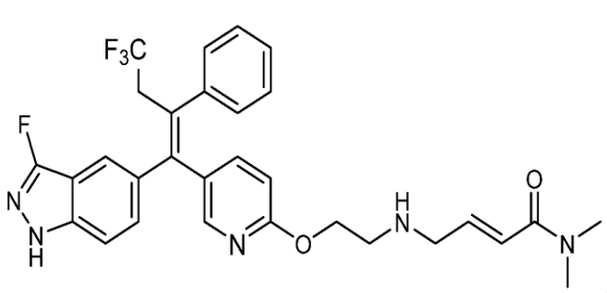
26. El método de la reivindicación 25, en donde dicho sujeto expresa una proteína ER-α mutante.

27. Una composición farmacéutica que comprende el compuesto de la reivindicación 8 o una sal farmacéuticamente aceptable del mismo, y además comprende un excipiente farmacéuticamente aceptable.

28. Una composición farmacéutica que comprende el compuesto de la reivindicación 9 o una sal farmacéuticamente aceptable del mismo, y además comprende un excipiente farmacéuticamente aceptable.

29. Una composición farmacéutica que comprende el compuesto de la reivindicación 10 o una sal farmacéuticamente aceptable del mismo, y que además comprende un excipiente farmacéuticamente aceptable.

30. El compuesto de la reivindicación 9, que tiene la siguiente fórmula:



31. Una composición farmacéutica que comprende el compuesto de la reivindicación 30, y además comprende un excipiente farmacéuticamente aceptable.

32. Una composición farmacéutica que comprende el compuesto de la reivindicación 11 o una sal farmacéuticamente aceptable del mismo, y además comprende un excipiente farmacéuticamente aceptable.

PTO/SB/08a (03-15)
Approved for use through 07/31/2016. OMB 0651-0031
U.S. Patent and Trademark Office; U.S. DEPARTMENT OF COMMERCE
Under the Paperwork Reduction Act of 1995, no persons are required to respond to a collection of information unless it contains a valid OMB control number.

INFORMATION DISCLOSURE STATEMENT BY APPLICANT

(Not for submission under 37 CFR 1.99)

Application Number	15167373
Filing Date	2016-05-27
First Named Inventor	Mark Bock
Art Unit	1627
Examiner Name	Layla Soroush
Attorney Docket Number	0080171-000253-T1

U.S.PATENTS Remove

Examiner Initial*	Cite No	Patent Number	Kind Code[1]	Issue Date	Name of Patentee or Applicant of cited Document	Pages,Columns,Lines where Relevant Passages or Relevant Figures Appear
	1	8063249	B1	2011-11-22	Kushner et al.	
	2	9399646	B2	2016-07-26	Smith et al.	
	3	8299112	B2	2012-10-30	Smith et al.	
	4	8455534	B2	2013-06-04	Smith et al.	

If you wish to add additional U.S. Patent citation information please click the Add button. Add

U.S.PATENT APPLICATION PUBLICATIONS Remove

Examiner Initial*	Cite No	Publication Number	Kind Code[1]	Publication Date	Name of Patentee or Applicant of cited Document	Pages,Columns,Lines where Relevant Passages or Relevant Figures Appear
	1	20130231333	A1	2013-09-05	Smith et al.	
	2	20020103229	A1	2002-08-01	Bhagwat et al.	

INFORMATION DISCLOSURE STATEMENT BY APPLICANT (Not for submission under 37 CFR 1.99)		
	Application Number	15167373
	Filing Date	2016-05-27
	First Named Inventor	Mark Bock
	Art Unit	1627
	Examiner Name	Layla Soroush
	Attorney Docket Number	0080171-000253-T1

	3	20150105403	A1	2015-04-16	Smith et al.	

If you wish to add additional U.S. Published Application citation information please click the Add button. Add

FOREIGN PATENT DOCUMENTS Remove

Examiner Initial*	Cite No	Foreign Document Number[3]	Country Code[2]	Kind Code[4]	Publication Date	Name of Patentee or Applicant of cited Document	Pages,Columns,Lines where Relevant Passages or Relevant Figures Appear	T[5]
	1	2009120999	WO	A2	2009-10-01	Olema Pharmaceuticals Inc.		
	2	2011129837	WO	A1	2011-10-20	Olema Pharmaceuticals Inc.		
	3	2007058626	WO	A1	2007-05-24	S BIO PTE Ltd.		
	4	2012037411	WO	A2	2012-03-22	Aragon Pharmaceuticals Inc.		
	5	2013142266	WO	A1	2013-09-26	Seragon Pharmaceuticals Inc.		

If you wish to add additional Foreign Patent Document citation information please click the Add button Add

NON-PATENT LITERATURE DOCUMENTS Remove

Examiner Initials*	Cite No	Include name of the author (in CAPITAL LETTERS), title of the article (when appropriate), title of the item (book, magazine, journal, serial, symposium, catalog, etc), date, pages(s), volume-issue number(s), publisher, city and/or country where published.	T[5]
	1	International Search Report and Written Opinion for PCT/US16/34764, dated August 30, 2016	

INFORMATION DISCLOSURE STATEMENT BY APPLICANT (Not for submission under 37 CFR 1.99)		
	Application Number	15167373
	Filing Date	2016-05-27
	First Named Inventor	Mark Bock
	Art Unit	1627
	Examiner Name	Layla Soroush
	Attorney Docket Number	0080171-000253-T1

	2	Search History accompanying International Search Report for PCT/US2016/34764 dated August 1, 2016
	3	PubChem, Compound Summary for CID 69281185, dated December 1, 2012.
	4	PubChem, Compound Summary for CID 89780731, dated February 13, 2015.
	5	International Search Report and Written Opinion for PCT/US2016/34774, dated September 7, 2016.
	6	Search History accompanying International Search Report for PCT/US16/34774 dated July 26, 2016.
	7	International Search Report and Written Opinion for PCT/US2016/034782, dated August 23, 2016.
	8	Search History accompanying International Search Report for PCT/US2016/034782 dated July 25, 2016.

If you wish to add additional non-patent literature document citation information please click the Add button Add

EXAMINER SIGNATURE

Examiner Signature		Date Considered	

*EXAMINER: Initial if reference considered, whether or not citation is in conformance with MPEP 609. Draw line through a citation if not in conformance and not considered. Include copy of this form with next communication to applicant.

[1] See Kind Codes of USPTO Patent Documents at www.USPTO.GOV or MPEP 901.04. [2] Enter office that issued the document, by the two-letter code (WIPO Standard ST.3). [3] For Japanese patent documents, the indication of the year of the reign of the Emperor must precede the serial number of the patent document. [4] Kind of document by the appropriate symbols as indicated on the document under WIPO Standard ST.16 if possible. [5] Applicant is to place a check mark here if English language translation is attached.

INFORMATION DISCLOSURE STATEMENT BY APPLICANT

(Not for submission under 37 CFR 1.99)

Application Number	15167373
Filing Date	2016-05-27
First Named Inventor	Mark Bock
Art Unit	1627
Examiner Name	Layla Soroush
Attorney Docket Number	0080171-000253-T1

CERTIFICATION STATEMENT

Please see 37 CFR 1.97 and 1.98 to make the appropriate selection(s):

That each item of information contained in the information disclosure statement was first cited in any communication from a foreign patent office in a counterpart foreign application not more than three months prior to the filing of the information disclosure statement. See 37 CFR 1.97(e)(1).

OR

☐ That no item of information contained in the information disclosure statement was cited in a communication from a foreign patent office in a counterpart foreign application, and, to the knowledge of the person signing the certification after making reasonable inquiry, no item of information contained in the information disclosure statement was known to any individual designated in 37 CFR 1.56(c) more than three months prior to the filing of the information disclosure statement. See 37 CFR 1.97(e)(2).

See attached certification statement.

The fee set forth in 37 CFR 1.17 (p) has been submitted herewith.

☒ A certification statement is not submitted herewith.

SIGNATURE

A signature of the applicant or representative is required in accordance with CFR 1.33, 10.18. Please see CFR 1.4(d) for the form of the signature.

Signature	/Duane A. Stewart III/	Date (YYYY-MM-DD)	2016-11-15
Name/Print	Duane A. Stewart III	Registration Number	54468

This collection of information is required by 37 CFR 1.97 and 1.98. The information is required to obtain or retain a benefit by the public which is to file (and by the USPTO to process) an application. Confidentiality is governed by 35 U.S.C. 122 and 37 CFR 1.14. This collection is estimated to take 1 hour to complete, including gathering, preparing and submitting the completed application form to the USPTO. Time will vary depending upon the individual case. Any comments on the amount of time you require to complete this form and/or suggestions for reducing this burden, should be sent to the Chief Information Officer, U.S. Patent and Trademark Office, U.S. Department of Commerce, P.O. Box 1450, Alexandria, VA 22313-1450. DO NOT SEND FEES OR COMPLETED FORMS TO THIS ADDRESS. **SEND TO: Commissioner for Patents, P.O. Box 1450, Alexandria, VA 22313-1450.**

Privacy Act Statement

The Privacy Act of 1974 (P.L. 93-579) requires that you be given certain information in connection with your submission of the attached form related to a patent application or patent. Accordingly, pursuant to the requirements of the Act, please be advised that: (1) the general authority for the collection of this information is 35 U.S.C. 2(b)(2); (2) furnishing of the information solicited is voluntary; and (3) the principal purpose for which the information is used by the U.S. Patent and Trademark Office is to process and/or examine your submission related to a patent application or patent. If you do not furnish the requested information, the U.S. Patent and Trademark Office may not be able to process and/or examine your submission, which may result in termination of proceedings or abandonment of the application or expiration of the patent.

The information provided by you in this form will be subject to the following routine uses:

1. The information on this form will be treated confidentially to the extent allowed under the Freedom of Information Act (5 U.S.C. 552) and the Privacy Act (5 U.S.C. 552a). Records from this system of records may be disclosed to the Department of Justice to determine whether the Freedom of Information Act requires disclosure of these record s.

2. A record from this system of records may be disclosed, as a routine use, in the course of presenting evidence to a court, magistrate, or administrative tribunal, including disclosures to opposing counsel in the course of settlement negotiations.

3. A record in this system of records may be disclosed, as a routine use, to a Member of Congress submitting a request involving an individual, to whom the record pertains, when the individual has requested assistance from the Member with respect to the subject matter of the record.

4. A record in this system of records may be disclosed, as a routine use, to a contractor of the Agency having need for the information in order to perform a contract. Recipients of information shall be required to comply with the requirements of the Privacy Act of 1974, as amended, pursuant to 5 U.S.C. 552a(m).

5. A record related to an International Application filed under the Patent Cooperation Treaty in this system of records may be disclosed, as a routine use, to the International Bureau of the World Intellectual Property Organization, pursuant to the Patent Cooperation Treaty.

6. A record in this system of records may be disclosed, as a routine use, to another federal agency for purposes of National Security review (35 U.S.C. 181) and for review pursuant to the Atomic Energy Act (42 U.S.C. 218(c)).

7. A record from this system of records may be disclosed, as a routine use, to the Administrator, General Services, or his/her designee, during an inspection of records conducted by GSA as part of that agency's responsibility to recommend improvements in records management practices and programs, under authority of 44 U.S.C. 2904 and 2906. Such disclosure shall be made in accordance with the GSA regulations governing inspection of records for this purpose, and any other relevant (i.e., GSA or Commerce) directive. Such disclosure shall not be used to make determinations about individuals.

8. A record from this system of records may be disclosed, as a routine use, to the public after either publication of the application pursuant to 35 U.S.C. 122(b) or issuance of a patent pursuant to 35 U.S.C. 151. Further, a record may be disclosed, subject to the limitations of 37 CFR 1.14, as a routine use, to the public if the record was filed in an application which became abandoned or in which the proceedings were terminated and which application is referenced by either a published application, an application open to public inspections or an issued patent.

9. A record from this system of records may be disclosed, as a routine use, to a Federal, State, or local law enforcement agency, if the USPTO becomes aware of a violation or potential violation of law or regulation.

Substitute for PTO/SB/08a&b (07-09)
Approved for use through 07/31/2012. OMB 0651-0031
U.S. Patent and Trademark Office; U.S. DEPARTMENT OF COMMERCE
Under the Paperwork Reduction Act of 1995, no persons are required to respond to a collection of information unless it contains a valid OMB control number.

Substitute for form 1449/PTO **INFORMATION DISCLOSURE STATEMENT BY APPLICANT** ***(Use as many sheets as necessary)***				***Complete if Known***	
				Application Number	15/167,373
				Filing Date	May 27, 2016
				First Named Inventor	Mark BOCK
				Art Unit	1629
				Examiner Name	Unassigned
Sheet	1	of	2	*Attorney Docket Number*	0080171-000253-T1

U.S. PATENT DOCUMENTS

Examiner Initials'	Cite No.[1]	Document Number **Number-Kind Code**[2] *(if known)*	Publication Date MM-DD-YYYY	Name of Patentee or Applicant of Cited Document	Pages, Columns, Lines, Where Relevant Passages or Relevant Figures Appear
		US-2013/0336962 A1	12-19-2013	ANDERSEN et al.	
		US-2014/0199236 A1	07-17-2014	CHEN et al.	
		US-8,785,501 B2	07-22-2014	WITT-ENDERBY et al.	
		US-			
		US-			
		US-			
		US-			
		US-			

FOREIGN PATENT DOCUMENTS

Examiner Initials'	Cite No.[1]	Foreign Patent Document Country Code[3] Number[4] Kind Code [5] *(if known)*	Publication Date MM-DD-YYYY	Name of Patentee or Applicant of Cited Document	Pages, Columns, Lines, Where Relevant Passages or Relevant Figures Appear	T[6]
		WO 2014/205136 A1	12-24-2014	SERAGON PHARMACEUTICALS, INC.		
		WO 2014/205138 A1	12-24-2014	SERAGON PHARMACEUTICALS, INC.		
		WO 2013/056178 A2	04-18-2013	FOUNDATION MEDICINE, INC.		
		WO 2012/037410 A2	03-22-2012	ARAGON PHARMACEUTICALS, INC.		
		WO 2012/037411 A2	03-22-2012	ARAGON PHARMACEUTICALS, INC.		
		WO 2015/000868 A1	01-08-2015	GLAXOSMITHKLINE INTELLECTUAL PROPERTY DEVELOPMENT		
		WO 2015/136016 A2	09-17-2015	HOFFMANN LA ROCHE et al.		
		WO 90/10638 A1	09-20-1990	EISENBRAND, Gerhard		

NON PATENT LITERATURE DOCUMENTS

Examiner Initials*	Cite No.[1]	Include name of the author (in CAPITAL LETTERS), title of the article (when appropriate), title of the item (book, magazine, journal, serial, symposium, catalog, etc.), date, page(s), volume-issue number(s), publisher, city and/or country where published.	T[2]
		MATTRAS et al., "Identification by MALDI-TOF Mass Spectrometry of 17α-Bromoacetamidopropylestradiol Covalent Attachment Sites on Estrogen Receptor α", Biochemistry, 2002, pp. 15713-15727, vol 41, no. 52.	
		REESE et al., "Mutagenesis of Cysteines in the Hormone Binding Domain of the Human Estrogen Receptor", The Journal of Biological Chemistry, June 1991, pp. 10880-10887, vol. 266, no. 17.	
		FISHER et al., "Endometrial Cancer in Tamoxifen-Treated Breast Cancer Patients: Findings From the National Surgical Adjuvant Breast and Bowel Project (NSABP) B-14", Journal of the National Cancer Institute, April 1994, pp. 527-537, vol. 86, no. 7.	

Examiner Signature		Date Considered	

*EXAMINER: Initial if reference considered, whether or not citation is in conformance with MPEP 609. Draw line through citation if not in conformance and not considered. Include copy of this form with next communication to applicant. [1] Applicant's unique citation designation number (optional). [2] See Kinds Codes of USPTO Patent Documents at www.uspto.gov or MPEP 901.04. [3] Enter Office that issued the document, by the two-letter code (WIPO Standard ST.3). [4] For Japanese patent documents, the indication of the year of the reign of the Emperor must precede the serial number of the patent document. [5] Kind of document by the appropriate symbols as indicated on the document under WIPO Standard ST.16 if possible. [6] Applicant is to place a check mark here if English language Translation is attached.

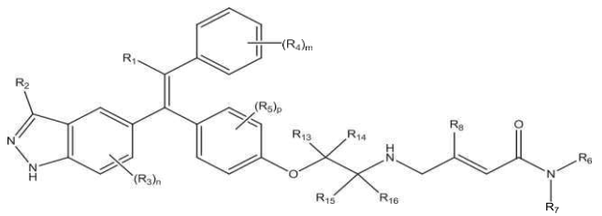
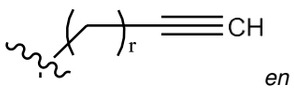
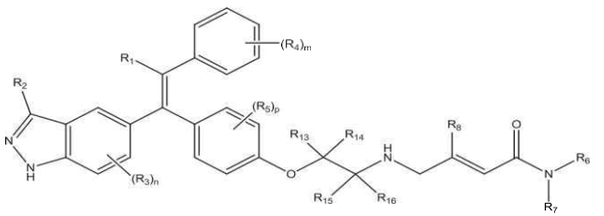
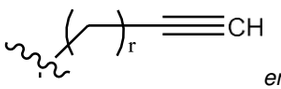
Substitute for PTO/SB/08a&b (07-09)
Approved for use through 07/31/2012. OMB 0651-0031
U.S. Patent and Trademark Office; U.S. DEPARTMENT OF COMMERCE
Under the Paperwork Reduction Act of 1995, no persons are required to respond to a collection of information unless it contains a valid OMB control number.

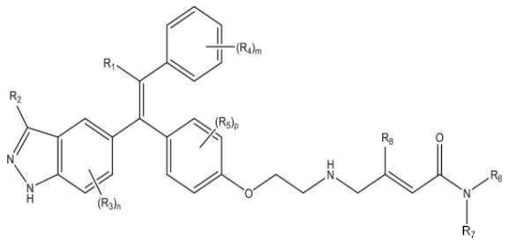
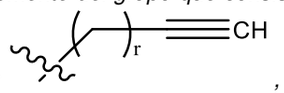
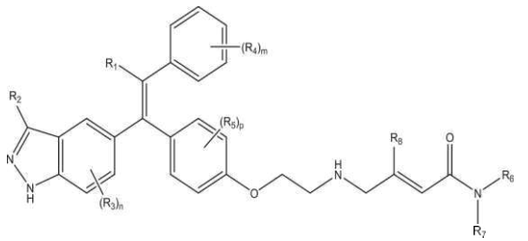
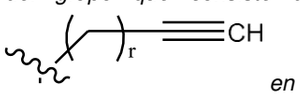
Substitute for form 1449/PTO **INFORMATION DISCLOSURE STATEMENT BY APPLICANT** ***(Use as many sheets as necessary)***				***Complete if Known***	
				Application Number	15/167,373
				Filing Date	May 27, 2016
				First Named Inventor	Mark BOCK
				Art Unit	1629
				Examiner Name	Unassigned
Sheet	2	of	2	*Attorney Docket Number*	0080171-000253-T1

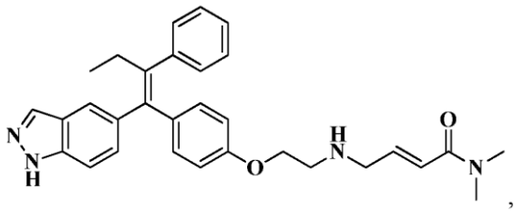
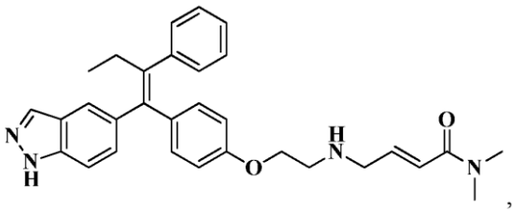
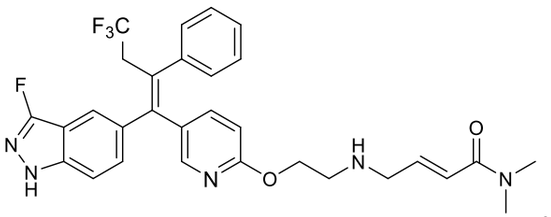
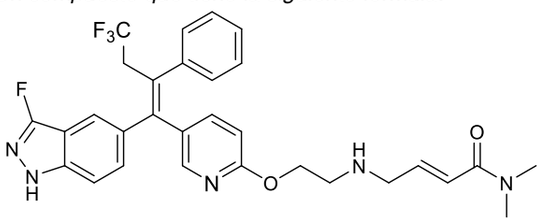
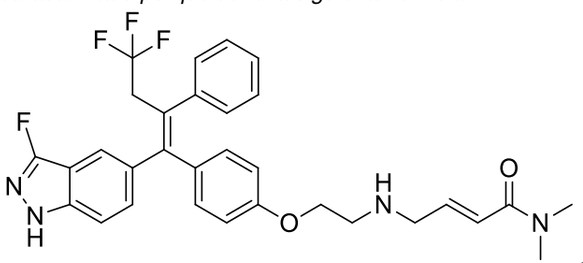
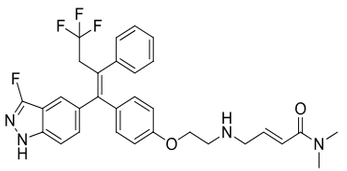
NON PATENT LITERATURE DOCUMENTS			
Examiner Initials*	Cite No.[1]	Include name of the author (in CAPITAL LETTERS), title of the article (when appropriate), title of the item (book, magazine, journal, serial, symposium, catalog, etc.), date, page(s), volume-issue number(s), publisher, city and/or country where published.	T[2]
		LI et al., "Endocrine-Therapy-Resistant ESR1 Variants Revealed by Genomic Characterization of Breast-Cancer-Derived Xenografts", Cell Reports, September 2013, pp. 1116-1130, vol. 4.	
		JESELSOHN et al., "Emergence of Constitutively Active Estrogen Receptor-α Mutations in Pretreated Advanced Estrogen Receptor–Positive Breast Cancer", Clin Cancer Res, April 2014, pp. 1757-1767, vol. 20, no. 7.	
		MERENBAKH-LAMIN et al., "D538G Mutation in Estrogen Receptor-α: A Novel Mechanism for Acquired Endocrine Resistance in Breast Cancer", Cancer Res, December 2013, pp. 6856-6864, vol. 72, no. 23.	
		OSBORNE et al., "Role of the Estrogen Receptor Coactivator AIB1 (SRC-3) and HER-2/neu in Tamoxifen Resistance in Breast Cancer", Journal of the National Cancer Institute, March 2003, pp. 353-361, vol. 95, no. 5.	
		OSBORNE et al., "Mechanisms of Endocrine Resistance in Breast Cancer", Annu. Rev. Med., 2011, pp. 233-247, vol. 62.	
		SEGAL et al., "Estrogen Receptor Mutations in Breast Cancer—New Focus on an Old Target", Clin Cancer Res, April 2014, pp. 1724-1726, vol. 20, no. 7.	
		SHOU et al., "Mechanisms of Tamoxifen Resistance: Increased Estrogen Receptor-HER2/neu Cross-Talk in ER/HER2–Positive Breast Cancer", Journal of the National Cancer Institute, June 2004, pp. 926-935, vol. 96, no. 12.	
		TOY et al., "ESR1 ligand-binding domain mutations in hormone-resistant breast cancer", Nature Genetics, December 2013, pp. 1439-1445, vol. 45, no. 12.	
		VAN LEEUWEN et al., "Risk of endometrial cancer after tamoxifen treatment of breast cancer", The Lancet, February 1994, pp. 448-452, vol. 343.	
		YU et al., "Ex vivo culture of circulating breast tumor cells for individualized testing of drug susceptibility", Science Mag, July 2014, pp. 216-220, vol. 345, issue 6193.	
		ROBINSON et al., "Activating ESR1 mutations in hormone-resistant metastatic breast cancer", Nature Genetics, December 2013, pp. 1446-1451, vol. 45, no. 12.	
		LAI et al., "Identification of GDC-0810 (ARN-810), an Orally Bioavailable Selective Estrogen Receptor Degrader (SERD) that Demonstrates Robust Activity in Tamoxifen-Resistant Breast Cancer Xenografts", Journal of Medicinal Chemistry, 2015, pp. 4888-4904, vol. 58.	
		KEELY et al., "Design, Synthesis and Biochemical Evaluation of Estrogen Receptor Ligand Conjugates as Tumour Targeting Agents", Letters in Drug Design & Discovery, 2012, pp. 295-304, vol. 9, no. 3.	
		MCDONNELL, "The Molecular Pharmacology of SERMs", TEM, 1999, pp. 301-311, vol. 10, no. 8.	
		WANG et al., "A second binding site for hydroxytamoxifen within the coactivator-binding groove of estrogen receptor β", PNAS, pp. 9908-9911, June 2006, vol. 103, no. 26.	
		Coser et al., "Global analysis of ligand sensitivity of estrogen inducible and suppressible genes in MCF7BUS breast cancer cells by DNA microarray", PNAS, November 2003, pp. 13994-13999, vol. 100, no. 24.	
		The Cancer Genome Atlas Research Network, "Integrated genomic characterization of endometrial carcinoma", Nature, 2013, pp. 1-5, vol. 000.	

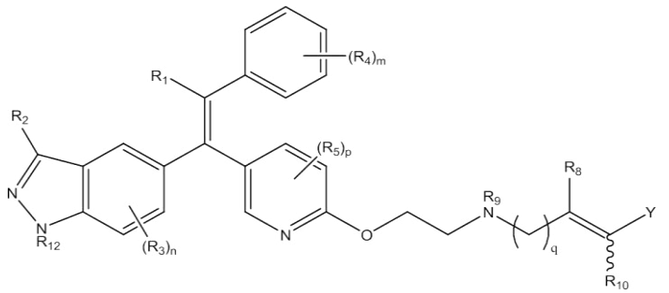
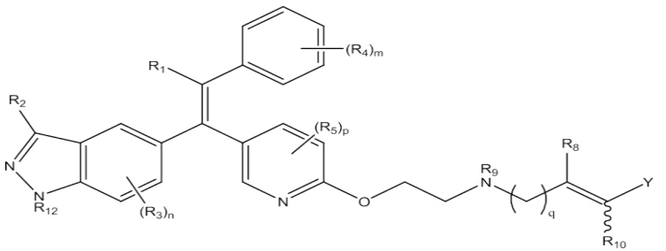
Examiner Signature		Date Considered	

*EXAMINER: Initial if reference considered, whether or not citation is in conformance with MPEP 609. Draw line through citation if not in conformance and not considered. Include copy of this form with next communication to applicant. [1] Applicant's unique citation designation number (optional). [2] See Kinds Codes of USPTO Patent Documents at www.uspto.gov or MPEP 901.04. [3] Enter Office that issued the document, by the two-letter code (WIPO Standard ST.3). [4] For Japanese patent documents, the indication of the year of the reign of the Emperor must precede the serial number of the patent document. [5]Kind of document by the appropriate symbols as indicated on the document under WIPO Standard ST.16 if possible. [6] Applicant is to place a check mark here if English language Translation is attached.

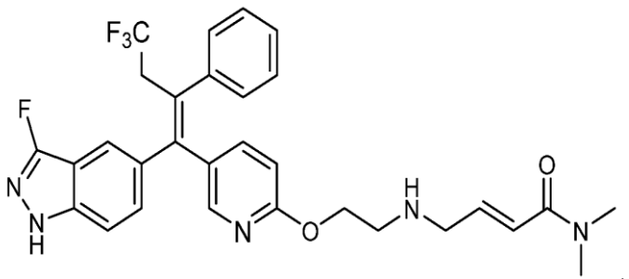
10 (iv)	**TABLA DE CORRESPONDENCIA DE REIVINDICACIONES**	
Reivindicaciones en la solicitud en Colombia **(NOTA. LAS REIVINDICACIONES ACÁ INDICADAS CORRESPONDEN A AQUELLAS MODIFICADAS EN MODIFICACIÓN VOLUNTARIA EL 9 DE NOVIEMBRE DE 2018)**	Reivindicaciones otorgables en la solicitud internacional	Explicación sobre la suficiente correspondencia ó Comentarios que explican la correspondencia
1. Un compuesto que tiene la fórmula II:  II *en donde:* *R_1 se selecciona del grupo que consiste de metilo, etilo, ciclobutilo, ciclopropilo, propilo, isopropilo, $-CH_2CF_3$, $-CH_2CH_2F$, y $-CH_2CH_2Cl$;* *R_2 se selecciona del grupo que consiste de H y F;* *n es 0-1;* *R_3 es F cuando n=1;* *m es 0-2;* *R_4 son los mismos o diferentes y se seleccionan independientemente del grupo que consiste de F, CF_3, Cl, isopropilo, $-OCH_3$, $-OCHF_2$, $-OCF_3$, etilo y metilo;* *p es 0-1;* *R_5 es F cuando p=1;* *R_6 y R_7 son los mismos o diferentes y se seleccionan independientemente del grupo que consiste de metilo, etilo, propilo,*  *CH_2CH_2OH y* *en donde r es 1 o 2; o, en donde R_6 y R_7 forman un anillo heterocíclico de 4-6 miembros con la N a la cual se enlazan, en donde dicho anillo heterocíclico opcionalmente incluye un átomo de oxígeno, y en donde dicho anillo heterocíclico es opcionalmente sustituido con F, o $-CH_2F$;* *R_8 se selecciona del grupo que consiste de H y $-CH_3$;* *y R_{13}, R_{14}, R_{15}, y R_{16} se seleccionan independientemente del grupo que consiste de –H o $-CH_3$;* *o una sal farmacéuticamente aceptable de los mismos.*	*1. Un compuesto que tiene la fórmula II:*  II *en donde:* *R_1 se selecciona del grupo que consiste de metilo, etilo, ciclobutilo, ciclopropilo, propilo, isopropilo, $-CH_2CF_3$, $-CH_2CH_2F$, y $-CH_2CH_2Cl$;* *R_2 se selecciona del grupo que consiste de H y F;* *n es 0-1;* *R_3 es F cuando n=1;* *m es 0-2;* *R_4 son los mismos o diferentes y se seleccionan independientemente del grupo que consiste de F, CF_3, Cl, isopropilo, $-OCH_3$, $-OCHF_2$, $-OCF_3$, etilo y metilo;* *p es 0-1;* *R_5 es F cuando p=1;* *R_6 y R_7 son los mismos o diferentes y se seleccionan independientemente del grupo que consiste de metilo, etilo, propilo, $-CH_2CH_2OH$ y*  *en donde r es 1 o 2; o, en donde R_6 y R_7 forman un anillo heterocíclico de 4-6 miembros con la N a la cual se enlazan, en donde dicho anillo heterocíclico opcionalmente incluye un átomo de oxígeno, y en donde dicho anillo heterocíclico es opcionalmente sustituido con F, o $-CH_2F$;* *R_8 se selecciona del grupo que consiste de H y $-CH_3$;* *y R_{13}, R_{14}, R_{15}, y R_{16} se seleccionan independientemente del grupo que consiste de –H o $-CH_3$;* *o una sal farmacéuticamente aceptable de los mismos.*	*Corresponde a la reivindicación 1 de la solicitud colombiana*

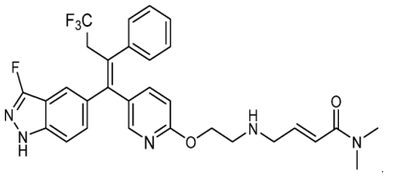
2. Un compuesto que tiene la fórmula I:  I *caracterizado porque:* *R_1 se selecciona del grupo que consiste de metilo, etilo, ciclobutilo, ciclopropilo y -CH_2CH_2Cl;* *R_2 se selecciona del grupo que consiste de H y F;* *n es 0-1;* *R_3 es F cuando n=1;* *m es 0-2;* *R_4 son los mismos o diferentes y se seleccionan independientemente del grupo que consiste de F, CF_3, Cl, isopropilo, -OCH_3, -$OCHF_2$, -OCF_3, etilo y metilo;* *p es 0-1;* *R_5 es F cuando p=1;* *R_6 y R_7 son los mismos o diferentes y se seleccionan independientemente del grupo que consiste de metilo, etilo, propilo, -CH_2CH_2OH y*  *, en donde r es 1 o 2;* *o, en donde R_6 y R_7 forman un anillo heterocíclico de 4-6 miembros con la N a la cual se enlazan, en donde dicho anillo heterocíclico incluye un átomo de oxígeno, y en donde dicho anillo heterocíclico está sustituido o no sustituido con F, o –CH_2F;* *R_8 se selecciona del grupo que consiste de H y CH_3;* *o una sal farmacéuticamente aceptable de los mismos.*	*2. Un compuesto que tiene la fórmula I:*  I *en donde:* *R_1 se selecciona del grupo que consiste de metilo, etilo, ciclobutilo, ciclopropilo y -CH_2CH_2Cl;* *R_2 se selecciona del grupo que consiste de H y F;* *n es 0-1;* *R_3 es F cuando n=1;* *m es 0-2;* *R_4 son los mismos o diferentes y se seleccionan independientemente del grupo que consiste de F, CF_3, Cl, isopropilo, -OCH_3, -$OCHF_2$, -OCF_3, etilo y metilo;* *p es 0-1;* *R_5 es F cuando p=1;* *R_6 y R_7 son los mismos o diferentes y se seleccionan independientemente del grupo que consiste de metilo, etilo, propilo, -CH_2CH_2OH y*  *en donde r es 1 o 2;* *o, en donde R_6 y R_7 forman un anillo heterocíclico de 4-6 miembros con la N a la cual se enlazan, en donde dicho anillo heterocíclico opcionalmente incluye un átomo de oxígeno, y en donde dicho anillo heterocíclico es opcionalmente sustituido con F, o –CH_2F;* *R_8 se selecciona del grupo que consiste de H y CH_3;* *o una sal farmacéuticamente aceptable de los mismos.*	*Corresponde a la reivindicación 2 de la solicitud colombiana*
3. El compuesto o sal farmacéuticamente aceptable de conformidad con la reivindicación 2, caracterizado porque R_1 es etilo.	*3. El compuesto o sal farmacéuticamente aceptable de acuerdo con la reivindicación 2, en donde R_1 es etilo.*	*Corresponde a la reivindicación 3 de la solicitud colombiana*
4. El compuesto o sal farmacéuticamente aceptable de conformidad con la reivindicación 2, caracterizado porque R_6 y R_7 ambos son metilo.	*4. El compuesto o sal farmacéuticamente aceptable de acuerdo con la reivindicación 2, en donde R_6 y R_7 ambos son metilo.*	*Corresponde a la reivindicación 4 de la solicitud colombiana*

5. El compuesto o sal farmacéuticamente aceptable de conformidad la reivindicación 2, caracterizado porque R_2 y R_8 son H.	*5. El compuesto o sal farmacéuticamente aceptable de acuerdo con la reivindicación 2, en donde R_2 y R_8 son H.*	*Corresponde a la reivindicación 5 de la solicitud colombiana*
6. El compuesto o sal farmacéuticamente aceptable de conformidad con la reivindicación 2, caracterizado porque R_2 es F.	*6. El compuesto o sal farmacéuticamente aceptable de acuerdo con la reivindicación 2, en donde R_2 es F.*	*Corresponde a la reivindicación 6 de la solicitud colombiana*
7. El compuesto o sal farmacéuticamente aceptable de conformidad con la reivindicación 2, caracterizado porque m, n y p son 0.	*7. El compuesto o sal farmacéuticamente aceptable de acuerdo con la reivindicación 2, en donde m, n, y p son 0.*	*Corresponde a la reivindicación 7 de la solicitud colombiana*
8. El compuesto de conformidad con la reivindicación 2, que tiene la siguiente fórmula:  *o una sal farmacéuticamente aceptable del mismo.*	*8. El compuesto de la reivindicación 2, que tiene la siguiente fórmula:*  *o una sal farmacéuticamente aceptable del mismo.*	*Corresponde a la reivindicación 8 de la solicitud colombiana*
9. Un compuesto, caracterizado porque tiene la siguiente fórmula:  *o una sal farmacéuticamente aceptable del mismo.*	*9. Un compuesto que tiene la siguiente fórmula:*  *o una sal farmacéuticamente aceptable del mismo.*	*Corresponde a la reivindicación 9 de la solicitud colombiana*
10. El compuesto de conformidad con la reivindicación 1, caracterizado porque tiene la siguiente fórmula:  *o una sal farmacéuticamente aceptable del mismo.*	*10. El compuesto de la reivindicación 1, que tiene la siguiente fórmula:*  *o una sal farmacéuticamente aceptable del mismo.*	*Corresponde a la reivindicación 10 de la solicitud colombiana*

11. Un compuesto dado por la Fórmula III:  *III* *caracterizado porque:* *R_1 se selecciona del grupo que consiste de alquilo C_1-C_6, cicloalquilo C_3-C_6, -CH_2CF_3, y un anillo heterocíclico de 4-6 miembros;* *R_2 se selecciona del grupo que consiste de H, halógeno hidroxi, alquilo C_1-C_3, cicloalquilo C_3-C_4 y anillo heterocíclico C_4;* *cuando n no es 0, R_3 son los mismos o diferentes, y se seleccionan independientemente del grupo que consiste de H, halógeno, alquilo C_1-C_6 y alcoxi C_1-C_3 sustituido o no sustituido con al menos un halógeno;* *n es 0-3;* *cuando m no es cero, R_4 son los mismos o diferentes y se seleccionan independientemente del grupo que consiste de H, halógeno, alquilo C_1-C_6, y OR_{11}, en donde R_{11} se selecciona del grupo que consiste de cicloalquilo C_3-C_6, alquilo C_1-C_6, arilo, heteroarilo y un anillo heterocíclico de 4-6 miembros;* *m es 0-5;* *cuando p no es 0, R_5 son los mismos o diferentes y se seleccionan independientemente del grupo que consiste de H, halógeno, alquilo C_1-C_4, alcoxi C_1-C_4, cicloalquilo C_3-C_4, cicloalcoxi C_3-C_6 y heterociclo C_4;* *p es 0-3;* *q es 1-2;* *R_8 y R_{10} son los mismos o diferentes y se seleccionan independientemente del grupo que consiste de halógeno, H y alquilo C_1-C_3;* *R_9 se selecciona del grupo que consiste de H, alquilo C_1-C_6 y cicloalquilo C_3-C_6;* *Y se selecciona del grupo que consiste de -$S(O)_2R_6$, -$S(O)_2NR_6R_7$, -$C(O)NR_6R_7$, -$C(O)R_6$, -$C(O)OR_6$, -CN; o en donde Y, y R_{10} ambos representan –CF_3;* *R_6 y R_7 son los mismos o diferentes y se seleccionan independientemente del grupo que consiste de H, alquilo C_1-C_6,*	*11. Un compuesto dado por la Fórmula III:*  *III* *en donde:* *R_1 se selecciona del grupo que consiste de alquilo C_1-C_6, cicloalquilo C_3-C_6, - CH_2CF_3, y un anillo heterocíclico de 4-6 miembros;* *R_2 se selecciona del grupo que consiste de H, halógeno, hidroxi, alquilo C_1-C_3, cicloalquilo C_3-C_4 y anillo heterocíclico C_4;* *cuando n no es 0, R_3 son los mismos o diferentes, y se seleccionan independientemente del grupo que consiste de H, halógeno, alquilo C_1-C_6 y alcoxi C_1-C_3 opcionalmente sustituido con al menos un halógeno;* *n es 0-3;* *cuando m no es cero, R_4 son los mismos o diferentes y se seleccionan independientemente del grupo que consiste de H, halógeno, alquilo C_1-C_6, y OR_{11}, en donde R_{11} se selecciona del grupo que consiste de cicloalquilo C_3-C_6, alquilo C_1-C_6, arilo, heteroarilo y un anillo heterocíclico de 4-6 miembros;* *m es 0-5;* *cuando p no es 0, R_5 son los mismos o diferentes y se seleccionan independientemente del grupo que consiste de H, halógeno, alquilo C_1-C_4, alcoxi C_1-C_4, cicloalquilo C_3-C_4, cicloalcoxi C_3-C_6 y heterociclo C_4;* *p es 0-3;* *q es 1-2;* *R_8 y R_{10} son los mismos o diferentes y se seleccionan independientemente del grupo que consiste de halógeno, H y alquilo C_1-C_3;* *R_9 se selecciona del grupo que consiste de H, alquilo C_1-C_6 y cicloalquilo C_3-C_6;* *Y se selecciona del grupo que consiste de -$S(O)_2R_6$, -$S(O)_2NR_6R_7$, -$C(O)NR_6R_7$, -$C(O)R_6$, -$C(O)OR_6$, -CN; o en donde Y, y R_{10} ambos representan –CF_3;* *R_6 y R_7 son los mismos o diferentes y se seleccionan independientemente del grupo que consiste de H, alquilo C_1-C_6, cicloalquilo C_3-C_6, arilo, heteroarilo y un*	*Corresponde a la reivindicación 11 de la solicitud colombiana*

cicloalquilo C_3-C_6, arilo, heteroarilo y un anillo heterocíclico de 4-6 miembros en donde dicho alquilo es saturado o no saturado o en donde R_6 y R_7 forman un anillo heterocíclico de 4-6 miembros con la N a la cual se enlazan, también incluye un átomo O; *R_{12} se selecciona del grupo que consiste de H, cicloalquilo C_3-C_4 y alquilo C_1-C_6; y* *en donde cualquier carbono que contiene porción de R_1-R_{12} está sustituido o no sustituido con uno o más átomos de halógeno, fluorometano, difluorometano o trifluorometano, o -OH;* *o sales farmacéuticamente aceptables de los mismos.*	*anillo heterocíclico de 4-6 miembros en donde dicho alquilo es saturado o insaturado o en donde R_6 y R_7 forman un anillo heterocíclico de 4-6 miembros con la N a la cual se enlazan, opcionalmente también incluye un átomo O;* *R_{12} se selecciona del grupo que consiste de H, cicloalquilo C_3-C_4 y alquilo C_1-C_6; y* *en donde cualquier carbono que contiene porción de R_1-R_{12} se puede sustituir opcionalmente con uno o más átomos de halógeno, fluorometano, difluorometano o trifluorometano, o -OH;* *o sales farmacéuticamente aceptables de los mismos.*	
12. El compuesto o sal farmacéuticamente aceptable de conformidad con la reivindicación 11, caracterizado porque R_1 se selecciona del grupo que consiste de alquilo C_1-C_6, cicloalquilo C_3-C_6, y un anillo heterocíclico de 4-6 miembros.	*12. El compuesto o sal farmacéuticamente aceptable de acuerdo con la reivindicación 11, en donde R_1 se selecciona del grupo que consiste de alquilo C_1-C_6, cicloalquilo C_3-C_6, y un anillo heterocíclico de 4-6 miembros.*	*Corresponde a la reivindicación 12 de la solicitud colombiana*
13. El compuesto o sal farmacéuticamente aceptable de conformidad con la reivindicación 11, caracterizado porque: *R_2 se selecciona del grupo que consiste de H, halógeno, metilo y etilo;* *R_3 son los mismos o diferentes, y se seleccionan independientemente del grupo que consiste de H, halógeno, metilo y etilo;* *R_4 son los mismos o diferentes y se seleccionan independientemente del grupo que consiste de H, halógeno, alquilo C_1-C_6 y alcoxi C_1-C_6;* *R_5 son los mismos o diferentes y se seleccionan independientemente del grupo que consiste de H, halógeno, metilo y etilo;* *R_8 y R_{10} son los mismos o diferentes y se seleccionan independientemente del grupo que consiste de H y metilo;* *R_9 se selecciona del grupo que consiste de H, metilo y etilo; y* *R_6 y R_7 son los mismos o diferentes y se seleccionan independientemente del grupo que consiste de H y alquilo C_1-C_6 o en donde R_6 y R_7 forman un anillo heterocíclico de 4-6 átomos con la N a la cual se enlazan, también contienen un átomo O.*	*13. El compuesto o sal farmacéuticamente aceptable de acuerdo con la reivindicación 11, en donde:* *R_2 se selecciona del grupo que consiste de H, halógeno, metilo y etilo;* *R_3 son los mismos o diferentes, y se seleccionan independientemente del grupo que consiste de H, halógeno, metilo y etilo;* *R_4 son los mismos o diferentes y se seleccionan independientemente del grupo que consiste de H, halógeno, alquilo C_1-C_6 y alcoxi C_1-C_6;* *R_5 son los mismos o diferentes y se seleccionan independientemente del grupo que consiste de H, halógeno, metilo y etilo;* *R_8 y R_{10} son los mismos o diferentes y se seleccionan independientemente del grupo que consiste de H y metilo;* *R_9 se selecciona del grupo que consiste de H, metilo y etilo; y* *R_6 y R_7 son los mismos o diferentes y se seleccionan independientemente del grupo que consiste de H y alquilo C_1-C_6 o en donde R_6 y R_7 forman un anillo heterocíclico de 4-6 átomos con la N a la cual se enlazan, opcionalmente también contienen un átomo O.*	*Corresponde a la reivindicación 13 de la solicitud colombiana*
14. El compuesto o sal farmacéuticamente aceptable de conformidad con la reivindicación 11, caracterizado porque Y es -C(O)NR_6R_7.	*14. El compuesto o sal farmacéuticamente aceptable de la reivindicación 11, en donde Y es -C(O)NR_6R_7.*	*Corresponde a la reivindicación 14 de la solicitud colombiana*
15. El compuesto o sal farmacéuticamente aceptable de conformidad con la reivindicación 11, caracterizado porque R_6 y R_7 son metilo.	*15. El compuesto o sal farmacéuticamente aceptable de la reivindicación 11, en donde R_6 y R_7 son metilo.*	*Corresponde a la reivindicación 15 de la solicitud colombiana*
16. El compuesto o sal farmacéuticamente aceptable de conformidad con la reivindicación 14, caracterizado porque R_2, R_8, R_9 y R_{10} son cada uno H.	*16. El compuesto o sal farmacéuticamente aceptable de la reivindicación 14, en donde R_2, R_8, R_9 y R_{10} son cada uno H.*	*Corresponde a la reivindicación 16 de la solicitud colombiana*
17. El compuesto o sal farmacéuticamente aceptable de conformidad con la reivindicación 14, caracterizado porque R_1 es etilo.	*17. El compuesto o sal farmacéuticamente aceptable de la reivindicación 14, en donde R_1 es etilo.*	*Corresponde a la reivindicación 17 de la solicitud colombiana*

18. El compuesto o sal farmacéuticamente aceptable de conformidad con la reivindicación 14, caracterizado porque R_1 es ciclobutilo.	*18. El compuesto o sal farmacéuticamente aceptable de la reivindicación 14, en donde R_1 es ciclobutilo.*	*Corresponde a la reivindicación 18 de la solicitud colombiana*
19. El compuesto o sal farmacéuticamente aceptable de conformidad con la reivindicación 14, caracterizado porque R_2 es F.	*19. El compuesto o sal farmacéuticamente aceptable de la reivindicación 14, en donde R_2 es F.*	*Corresponde a la reivindicación 19 de la solicitud colombiana*
20. El compuesto o sal farmacéuticamente aceptable de conformidad con la reivindicación 14, caracterizado porque m, n y p son 0.	*20. El compuesto o sal farmacéuticamente aceptable de la reivindicación 14, en donde m, n, y p son 0.*	*Corresponde a la reivindicación 20 de la solicitud colombiana*
21. Una composición farmacéutica que comprende el compuesto de la reivindicación 8 o una sal farmacéuticamente aceptable del mismo, y además comprende un excipiente farmacéuticamente aceptable.	*21. Un método para tratar cáncer de seno que comprende administrar a un sujeto un compuesto o sal farmacéuticamente aceptable de la reivindicación 11.*	*Eliminada en la respuesta de Forma*
22. Una composición farmacéutica que comprende el compuesto de la reivindicación 9 o una sal farmacéuticamente aceptable del mismo, y además comprende un excipiente farmacéuticamente aceptable.	*22. El método de la reivindicación 21, en donde dicho cáncer de seno es un cáncer de seno positivo ER.*	*Eliminada en la respuesta de Forma*
23. Una composición farmacéutica que comprende el compuesto de la reivindicación 10 o una sal farmacéuticamente aceptable del mismo, y que además comprende un excipiente farmacéuticamente aceptable.	*23. El método de la reivindicación 22, en donde dicho sujeto expresa una proteína ER-α mutante.*	*Eliminada en la respuesta de Forma*
24. El compuesto de la reivindicación 9, que tiene la siguiente fórmula: 	*24. Un método para tratar cáncer de seno que comprende administrar a un sujeto un compuesto o sal farmacéuticamente aceptable de la reivindicación 9.*	*Eliminada en la respuesta de Forma*
25. Una composición farmacéutica que comprende el compuesto de la reivindicación 24, y además comprende un excipiente farmacéuticamente aceptable.	*25. El método de la reivindicación 24, en donde dicho cáncer de seno es un cáncer de seno positivo ER.*	*Eliminada en la respuesta de Forma*
26. Una composición farmacéutica que comprende el compuesto de la reivindicación 11 o una sal farmacéuticamente aceptable del mismo, y además comprende un excipiente farmacéuticamente aceptable.	*26. El método de la reivindicación 25, en donde dicho sujeto expresa una proteína ER-α mutante.*	*Eliminada en la respuesta de Forma*
	27. Una composición farmacéutica que comprende el compuesto de la reivindicación 8 o una sal farmacéuticamente aceptable del mismo, y además comprende un excipiente farmacéuticamente aceptable.	*Corresponde a la reivindicación 21 de la solicitud colombiana*
	28. Una composición farmacéutica que comprende el compuesto de la reivindicación 9 o una sal farmacéuticamente aceptable del mismo, y además comprende un excipiente farmacéuticamente aceptable.	*Corresponde a la reivindicación 22 de la solicitud colombiana*
	29. Una composición farmacéutica que comprende el compuesto de la reivindicación 10 o una sal farmacéuticamente aceptable del mismo, y que además comprende un excipiente farmacéuticamente aceptable.	*Corresponde a la reivindicación 23 de la solicitud colombiana*

	30. El compuesto de la reivindicación 9, que tiene la siguiente fórmula: 	*Corresponde a la reivindicación 24 de la solicitud colombiana*
	31. Una composición farmacéutica que comprende el compuesto de la reivindicación 30, y además comprende un excipiente farmacéuticamente aceptable.	*Corresponde a la reivindicación 25 de la solicitud colombiana*
	32. Una composición farmacéutica que comprende el compuesto de la reivindicación 11 o una sal farmacéuticamente aceptable del mismo, y además comprende un excipiente farmacéuticamente aceptable.	*Corresponde a la reivindicación 26 de la solicitud colombiana*

US009796683B2

(12) **United States Patent**
Bock et al.

(10) **Patent No.: US 9,796,683 B2**
(45) **Date of Patent: Oct. 24, 2017**

(54) **TETRASUBSTITUTED ALKENE COMPOUNDS AND THEIR USE**

(71) Applicant: **Eisai R&D Management Co., Ltd.**, Tokyo (JP)

(72) Inventors: **Mark Bock**, Boston, MA (US); **Ming-Hong Hao**, Quincy, MA (US); **Manav Korpal**, Winchester, MA (US); **Vijay Kumar Nyavanandi**, Andhra Pradesh (IN); **Xiaoling Puyang**, Cambridge, MA (US); **Susanta Samajdar**, Kamataka (IN); **Peter Gerard Smith**, Arlington, MA (US); **John Wang**, Andover, MA (US); **Guo Zhu Zheng**, Lexington, MA (US); **Ping Zhu**, Boxborough, MA (US)

(73) Assignee: **Eisai R&D Management Co., Ltd.**, Tokyo (JP)

(*) Notice: Subject to any disclaimer, the term of this patent is extended or adjusted under 35 U.S.C. 154(b) by 0 days.

(21) Appl. No.: **15/167,373**

(22) Filed: **May 27, 2016**

(65) **Prior Publication Data**

US 2016/0347717 A1 Dec. 1, 2016

Related U.S. Application Data

(60) Provisional application No. 62/168,581, filed on May 29, 2015, provisional application No. 62/168,529, filed on May 29, 2015, provisional application No. 62/269,745, filed on Dec. 18, 2015.

(51) **Int. Cl.**

A01N 43/40	(2006.01)
A61K 31/44	(2006.01)
C07D 231/56	(2006.01)
C07D 403/12	(2006.01)
C07D 471/14	(2006.01)
C07D 403/06	(2006.01)
C07D 401/06	(2006.01)
C07D 401/14	(2006.01)

(52) **U.S. Cl.**

CPC ***C07D 231/56*** (2013.01); ***C07D 401/06*** (2013.01); ***C07D 401/14*** (2013.01); ***C07D 403/06*** (2013.01); ***C07D 403/12*** (2013.01); ***C07D 471/14*** (2013.01)

(58) **Field of Classification Search**

USPC 514/333

See application file for complete search history.

(56) **References Cited**

U.S. PATENT DOCUMENTS

8,063,249	B1	11/2011	Kushner et al.
8,299,112	B2	10/2012	Smith et al.
8,455,534	B2	6/2013	Smith et al.
8,785,501	B2	7/2014	Witt-Enderby et al.
9,399,646	B2	7/2016	Smith et al.
2002/0103229	A1	8/2002	Bhagwat et al.
2013/0231333	A1	9/2013	Smith et al.
2013/0336962	A1	12/2013	Andersen et al.
2014/0199236	A1	7/2014	Chen et al.
2015/0105403	A1	4/2015	Smith et al.

FOREIGN PATENT DOCUMENTS

WO	WO 90/10638	A1	9/1990
WO	2007058626	A1	5/2007
WO	2009120999	A2	10/2009
WO	2011129837	A1	10/2011
WO	2012037411	A2	3/2012
WO	WO 2012/037410	A2	3/2012
WO	WO 2012/037411	A2	3/2012
WO	WO 2013/056178	A2	4/2013
WO	2013142266	A1	9/2013
WO	WO 2014/205136	A1	12/2014
WO	WO 2014/205138	A1	12/2014
WO	WO 2015/000868	A1	1/2015
WO	WO 2015/136016	A2	9/2015

OTHER PUBLICATIONS

International Search Report and Written Opinion for PCT/US16/34764, dated Aug. 30, 2016.

Search History accompanying International Search Report for PCT/US2016/34764 dated Aug. 1, 2016.

PubChem, Compound Summary for CID 69281185, dated Dec. 1, 2012.

PubChem, Compound Summary for CID 89780731, dated Feb. 13, 2015.

International Search Report and Written Opinion for PCT/US2016/34774, dated Sep. 7, 2016.

Search History accompanying International Search Report for PCT/US16/34774 dated Jul. 26, 2016.

International Search Report and Written Opinion for PCT/US2016/034782, dated Aug. 23, 2016.

Search History accompanying International Search Report for PCT/US2016/034782 dated Jul. 25, 2016.

Mattras et al., "Identification by MALDI-TOF Mass Spectrometry of 17α-Bromoacetamidopropylestradiol Covalent Attachment Sites on Estrogen Receptor α", Biochemistry, 2002, pp. 15713-15727, vol. 41, No. 52.

Reese et al., "Mutagenesis of Cysteines in the Hormone Binding Domain of the Human Estrogen Receptor", The Journal of Biological Chemistry, Jun. 1991, pp. 10880-10887, vol. 266, No. 17.

Fisher et al., "Endometrial Cancer in Tamoxifen-Treated Breast Cancer Patients: Findings From the National Surgical Adjuvant Breast and Bowel Project (NSABP) B-14", Journal of the National Cancer Institute, Apr. 1994, pp. 527-537, vol. 86, No. 7.

(Continued)

Primary Examiner — Layla Soroush

(74) *Attorney, Agent, or Firm* — Buchanan Ingersoll & Rooney PC

(57) **ABSTRACT**

Disclosed herein are compounds, or pharmaceutically acceptable salts thereof, and methods of using the compounds for treating breast cancer by administration to a subject in need thereof a therapeutically effective amount of the compounds or pharmaceutically acceptable salts thereof. The breast cancer may be an ER-positive breast cancer and/or the subject in need of treatment may express a mutant ER-α protein.

32 Claims, 5 Drawing Sheets

(56) **References Cited**

OTHER PUBLICATIONS

Li et al., "Endocrine-Therapy-Resistant ESR1 Variants Revealed by Genomic Characterization of Breast-Cancer-Derived Xenografts", Cell Reports, Sep. 2013, pp. 1116-1130, vol. 4.

Jeselsohn et al., "Emergence of Constitutively Active Estrogen Receptor-α Mutations in Pretreated Advanced Estrogen Receptor-Positive Breast Cancer", Clin Cancer Res, Apr. 2014, pp. 1757-1767, vol. 20, No. 7.

Merenbakh-Lamin et al., "D538G Mutation in Estrogen Receptor-α: A Novel Mechanism for Acquired Endocrine Resistance in Breast Cancer", Cancer Res, Dec. 2013, pp. 6856-6864, vol. 72, No. 23.

Osborne et al., "Role of the Estrogen Receptor Coactivator AlB1 (SRC-3) and HER-2/neu in Tamoxifen Resistance in Breast Cancer", Journal of the National Cancer Institute, Mar. 2003, pp. 353-361, vol. 95, No. 5.

Osborne et al., "Mechanisms of Endocrine Resistance in Breast Cancer", Annu. Rev. Med., 2011, pp. 233-247, vol. 62.

Segal et al., "Estrogen Receptor Mutations in Breast Cancer—New Focus on an Old Target", Clin Cancer Res, Apr. 2014, pp. 1724-1726, vol. 20, No. 7.

Shou et al., "Mechanisms of Tamoxifen Resistance: Increased Estrogen Receptor-HER2/neu Cross-Talk in ER/HER2-Positive Breast Cancer", Journal of the National Cancer Institute, Jun. 2004, pp. 926-935, vol. 96, No. 12.

Toy et al., "ESR1 ligand-binding domain mutations in hormone-resistant breast cancer", Nature Genetics, Dec. 2013, pp. 1439-1445, vol. 45, No. 12.

Van Leeuwen et al., "Risk of endometrial cancer after tamoxifen treatment of breast cancer", The Lancet, Feb. 1994, pp. 448-452, vol. 343.

Yu et al., "Ex vivo culture of circulating breast tumor cells for individualized testing of drug susceptibility", Science Mag, Jul. 2014, pp. 216-220, vol. 345, issue 6193.

Robinson et al., "Activating ESR1 mutations in hormone-resistant metastatic breast cancer", Nature Genetics, Dec. 2013, pp. 1446-1451, vol. 45, No. 12.

Lai et al., "Identification of GDC-0810 (ARN-810), an Orally Bioavailable Selective Estrogen Receptor Degrader (SERD) that Demonstrates Robust Activity in Tamoxifen-Resistant Breast Cancer Xenografts", Journal of Medicinal Chemistry, 2015, pp. 4888-4904, vol. 58.

Keely et al., "Design, Synthesis and Biochemical Evaluation of Estrogen Receptor Ligand Conjugates as Tumour Targeting Agents", Letters in Drug Design & Discovery, 2012, pp. 295-304, vol. 9, No. 3.

McDonnell, "The Molecular Pharmacology of SERMs", TEM, 1999, pp. 301-311, vol. 10, No. 8.

Wang et al., "A second binding site for hydroxytamoxifen within the coactivator-binding groove of estrogen receptor β", PNAS, pp. 9908-9911, Jun. 2006, vol. 103, No. 26.

Coser et al., "Global analysis of ligand sensitivity of estrogen inducible and suppressible genes in MCF7BUS breast cancer cells by DNA microarray", PNAS, Nov. 2003, pp. 13994-13999, vol. 100, No. 24.

The Cancer Genome Atlas Research Network, "Integrated genomic characterization of endometrial carcinoma", Nature, 2013, pp. 1-5, vol. 000.

FIG. 1

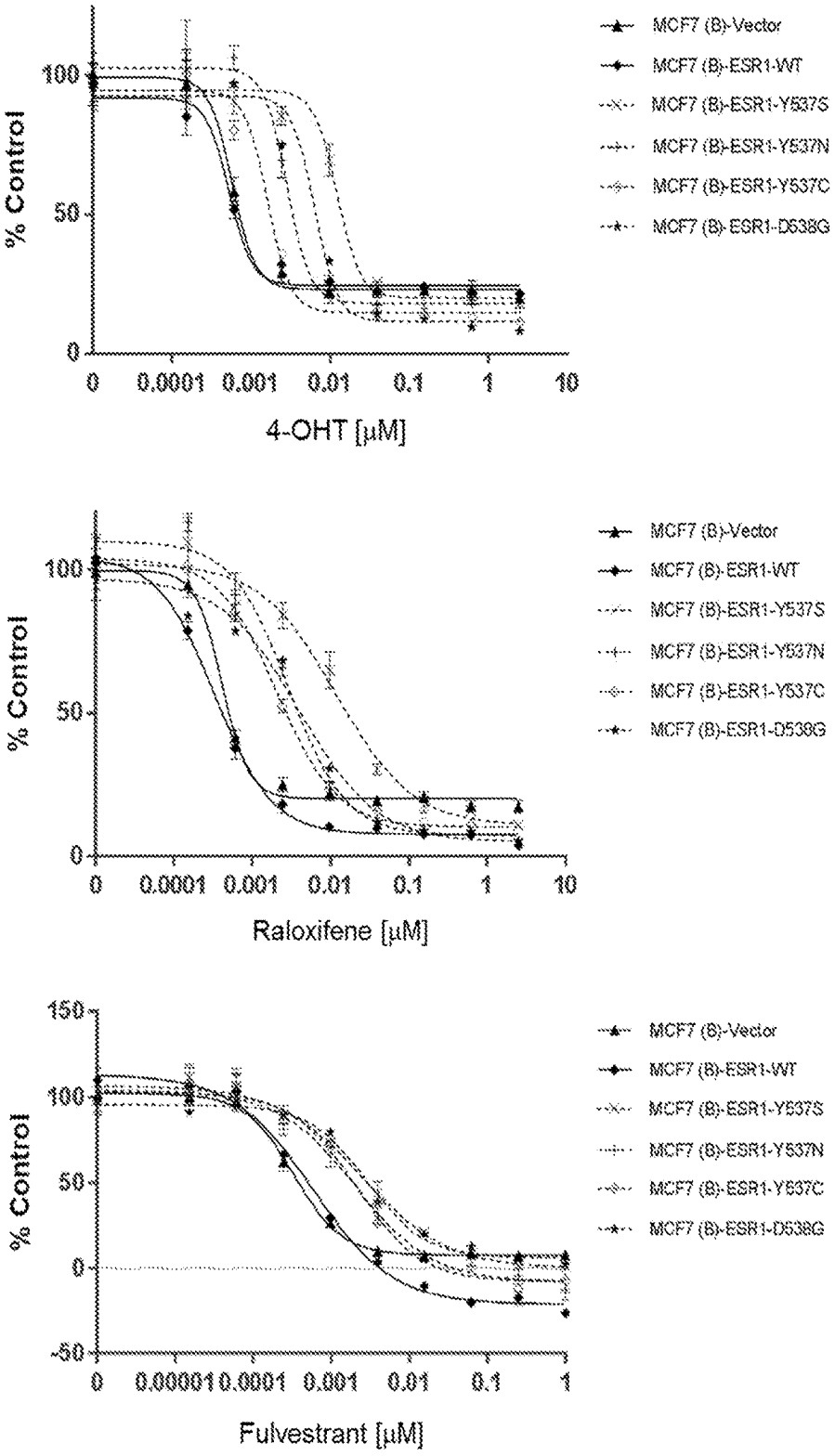

% Control
100
50
0
0 0.0001 0.001 0.01 0.1 1 10
4-OHT [μM]
MCF7 (B)-Vector
MCF7 (B)-ESR1-WT
MCF7 (B)-ESR1-Y537S
MCF7 (B)-ESR1-Y537N
MCF7 (B)-ESR1-Y537C
MCF7 (B)-ESR1-D538G
% Control
100
50
0
0 0.0001 0.001 0.01 0.1 1 10
Raloxifene [μM]
MCF7 (B)-Vector
MCF7 (B)-ESR1-WT
MCF7 (B)-ESR1-Y537S
MCF7 (B)-ESR1-Y537N
MCF7 (B)-ESR1-Y537C
MCF7 (B)-ESR1-D538G
% Control
150
100
50
0
-50
0 0.00001 0.0001 0.001 0.01 0.1 1
Fulvestrant [μM]
MCF7 (B)-Vector
MCF7 (B)-ESR1-WT
MCF7 (B)-ESR1-Y537S
MCF7 (B)-ESR1-Y537N
MCF7 (B)-ESR1-Y537C
MCF7 (B)-ESR1-D538G

FIG. 2

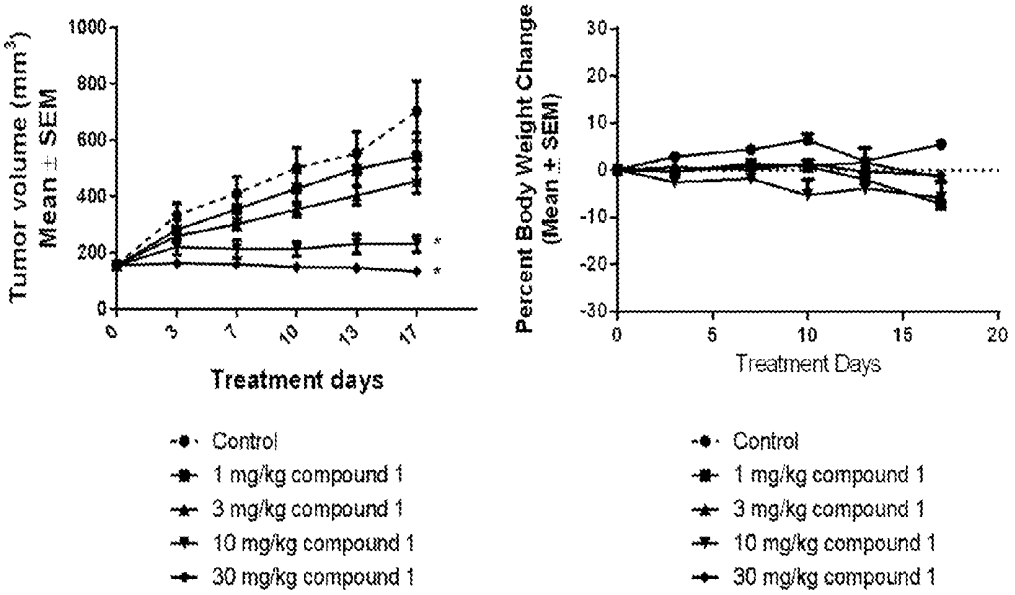

Tumor volume (mm³)
Mean ± SEM
1000
800
600
400
200
0
0
3
7
10
13
17
Treatment days
Control
1 mg/kg compound 1
3 mg/kg compound 1
10 mg/kg compound 1
30 mg/kg compound 1
Percent Body Weight Change
(Mean + SEM)
30
20
10
0
-10
-20
-30
0
5
10
15
20
Treatment Days
Control
1 mg/kg compound 1
3 mg/kg compound 1
10 mg/kg compound 1
30 mg/kg compound 1

FIG. 3

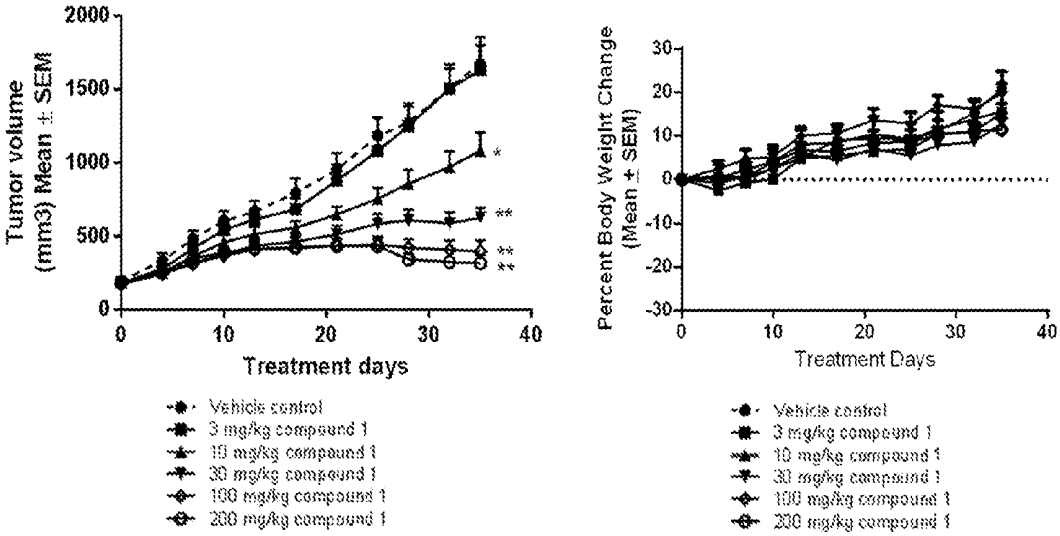

Tumor volume
(mm3) Mean ± SEM
2000
1500
1000
500
0
0
10
20
30
40
Treatment days
Vehicle control
3 mg/kg compound 1
10 mg/kg compound 1
30 mg/kg compound 1
100 mg/kg compound 1
200 mg/kg compound 1
Percent Body Weight Change
(Mean + SEM)
30
20
10
0
-10
-20
-30
0
10
20
30
40
Treatment Days
Vehicle control
3 mg/kg compound 1
10 mg/kg compound 1
30 mg/kg compound 1
100 mg/kg compound 1
200 mg/kg compound 1

FIG. 4

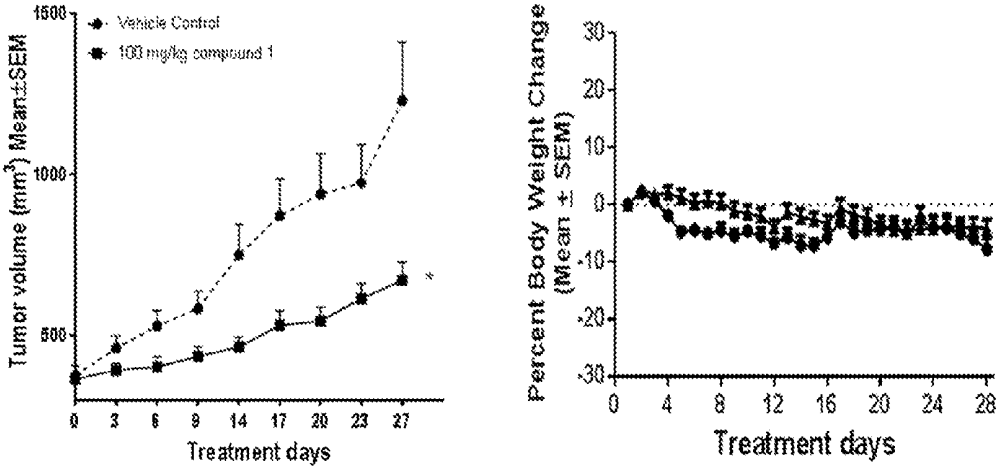

Vehicle Control
100 mg/kg compound 1
Tumor volume (mm3) Mean±SEM
1500
1000
500
0 3 6 9 14 17 20 23 27
Treatment days
Percent Body Weight Change (Mean ± SEM)
30
20
10
0
-10
-20
-30
0 4 8 12 16 20 24 28
Treatment days

FIG. 5

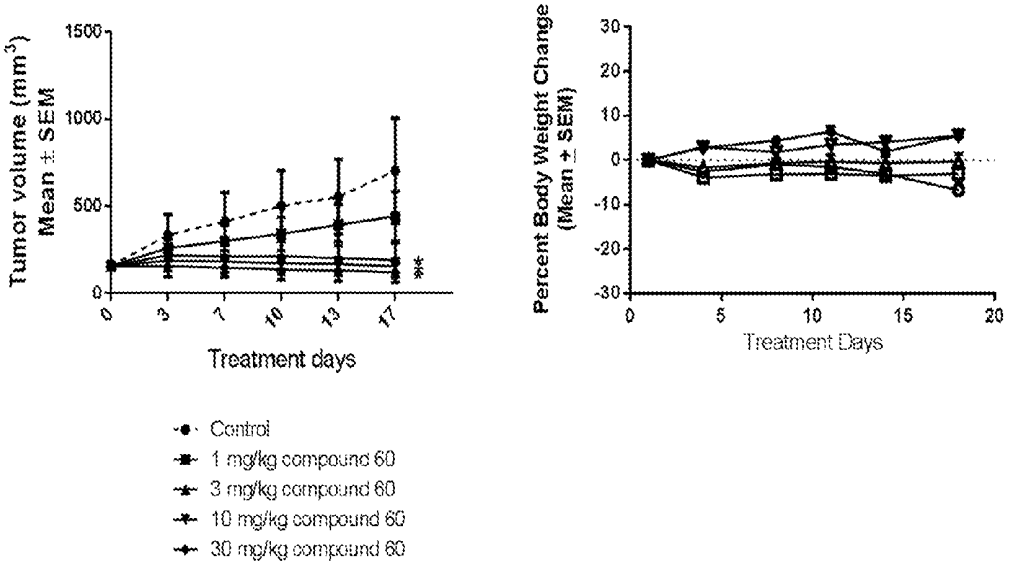

Tumor volume (mm3) Mean ± SEM
1500
1000
500
0
0 3 7 10 13 17
Treatment days
**
Percent Body Weight Change (Mean ± SEM)
30
20
10
0
-10
-20
-30
0 5 10 15 20
Treatment Days
Control
1 mg/kg compound 60
3 mg/kg compound 60
10 mg/kg compound 60
30 mg/kg compound 60

FIG. 6

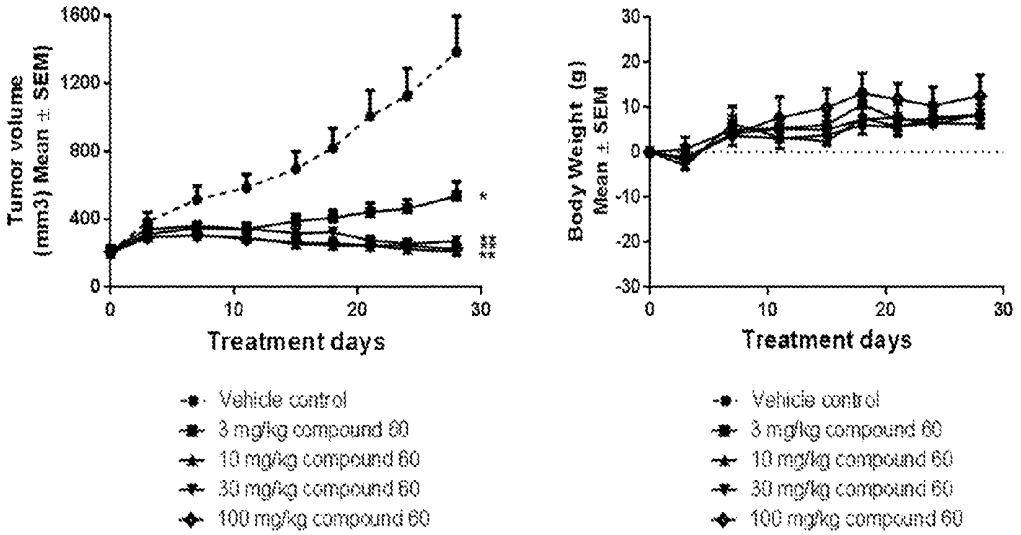

Tumor volume (mm3) Mean ± SEM
1600
1200
800
400
0
0
10
20
30
Treatment days
*
**
***
Vehicle control
3 mg/kg compound 60
10 mg/kg compound 60
30 mg/kg compound 60
100 mg/kg compound 60
Body Weight (g) Mean ± SEM
30
20
10
0
-10
-20
-30
0
10
20
30
Treatment days
Vehicle control
3 mg/kg compound 60
10 mg/kg compound 60
30 mg/kg compound 60
100 mg/kg compound 60

FIG. 7

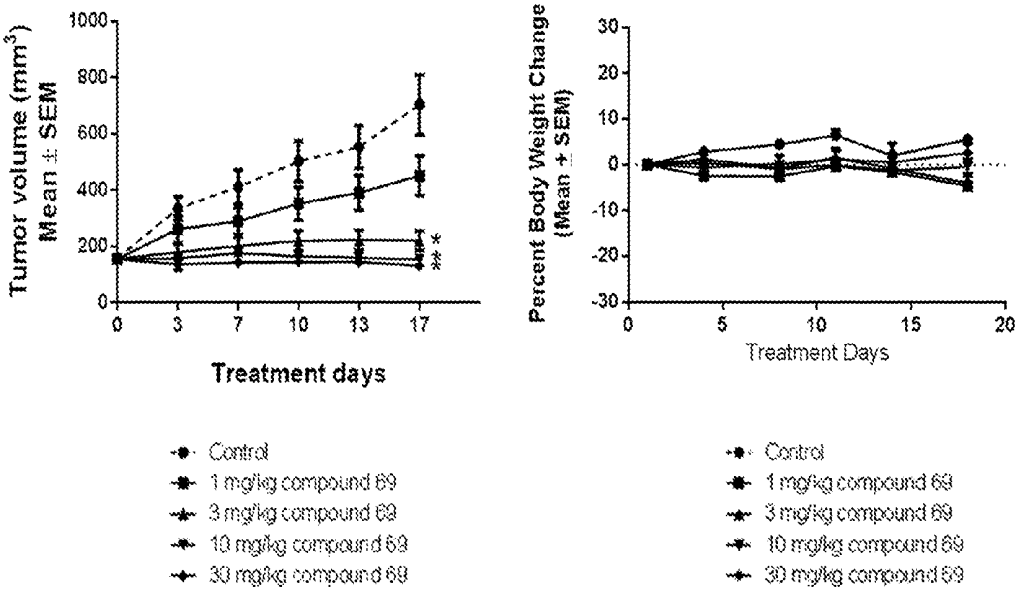

Tumor volume (mm3) Mean ± SEM
1000
800
600
400
200
0
0
3
7
10
13
17
Treatment days
**
*
Control
1 mg/kg compound 69
3 mg/kg compound 69
10 mg/kg compound 69
30 mg/kg compound 69
Percent Body Weight Change (Mean ± SEM)
30
20
10
0
-10
-20
-30
0
5
10
15
20
Treatment Days
Control
1 mg/kg compound 69
3 mg/kg compound 69
10 mg/kg compound 69
30 mg/kg compound 69

FIG. 8

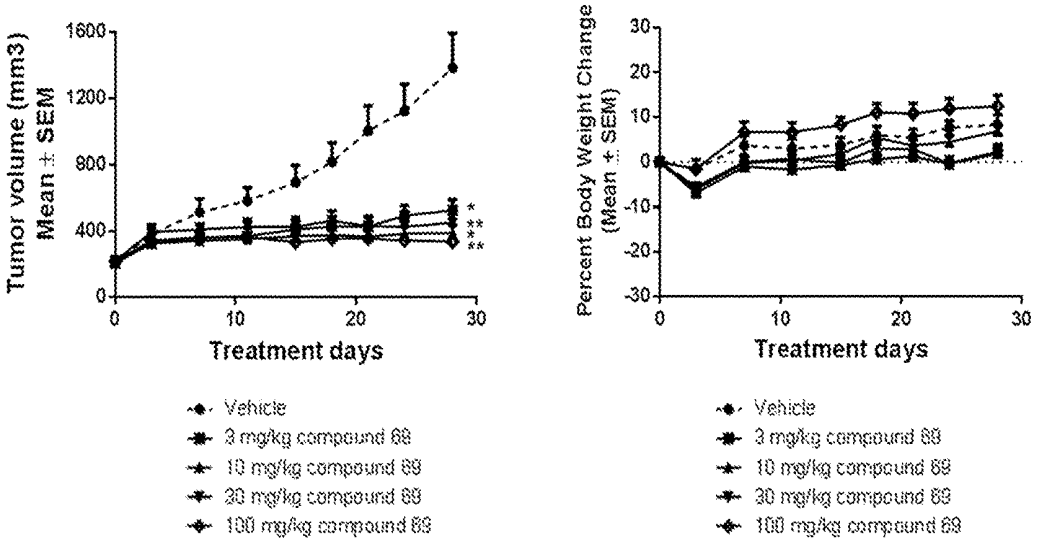
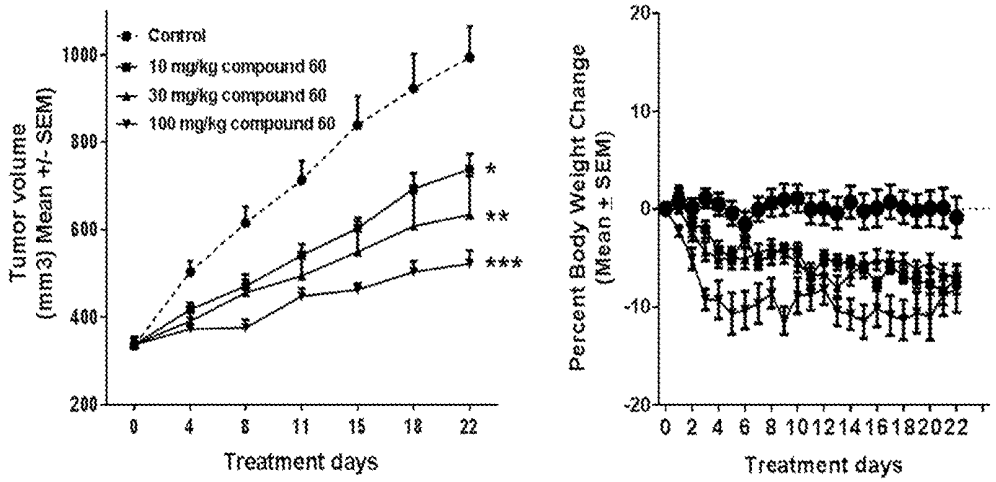

Tumor volume (mm3)
Mean ± SEM
1600
1200
800
400
0
0
10
20
30
Treatment days
*
***
**
Vehicle
3 mg/kg compound 69
10 mg/kg compound 69
20 mg/kg compound 69
100 mg/kg compound 69
Percent Body Weight Change
(Mean ± SEM)
30
20
10
0
-10
-20
-30
0
10
20
30
Treatment days
Vehicle
3 mg/kg compound 69
10 mg/kg compound 69
30 mg/kg compound 69
100 mg/kg compound 69

FIG. 9


Control
10 mg/kg compound 60
30 mg/kg compound 60
100 mg/kg compound 60
Tumor volume
(mm3) Mean +/- SEM)
1000
800
600
400
200
0
4
8
11
15
18
22
Treatment days
*
**
***
Percent Body Weight Change
(Mean ± SEM)
20
10
0
-10
-20
0 2 4 6 8 10 12 14 16 18 20 22
Treatment days

TETRASUBSTITUTED ALKENE COMPOUNDS AND THEIR USE

CROSS-REFERENCE TO RELATED APPLICATIONS

This application claims priority to U.S. Provisional Application No. 62/168,581, filed on May 29, 2015, to U.S. Provisional Patent Application No. 62/168,529, filed on May 29, 2015, and to U.S. Provisional Application No. 62/269,745, filed on Dec. 18, 2015, all of which are incorporated by reference herein.

BACKGROUND

Breast cancer is the most commonly diagnosed malignancy among women today with nearly 200,000/1.7 million new cases diagnosed in the US/worldwide each year respectively. Since about 70% of breast tumors are positive for the estrogen receptor alpha (ERα)—a key oncogenic driver in this subset of tumors—several classes of therapies have been developed to antagonize ERα function, including 1) selective estrogen receptor downregulators (SERDs) of which fulvestrant is an example, 2) selective estrogen receptor modulators (SERMs) of which tamoxifen is an example and 3) aromatase inhibitors that reduce systemic levels of estrogen.

These therapies have been largely effective in the clinic reducing occurrence and progression of ERα+ breast tumors. However there are on-target liabilities associated with these different classes of compounds. For example, tamoxifen has been shown to activate signaling activity in the endometrium leading to an increase in risk of endometrial cancers in the clinic (Fisher et al., (1994) *J Natl Cancer Inst*. April 6; 86(7):527-37; van Leeuwen et al., (1994) *Lancet* February 19; 343(8895):448-52). In contrast, since fulvestrant is a pure antagonist, it can lead to loss of bone density in post-menopausal women as ERα activity is critical for bone building. In addition to on-target side effects, clinical resistance is also beginning to emerge to these classes of ERα antagonists highlighting the need to develop next-generation compounds.

Several mechanisms of resistance have been identified using in vitro and in vivo models of resistance to various endocrine therapies. These include increased ERα/HER2 "crosstalk" (Shou et al., (2004) *J Natl Cancer Inst*. June 16; 96(12):926-35), aberrant expression of ERα coactivators/corepressors (Osborne et al., (2003) *J Natl Cancer Inst*. March 5; 95(5):353-61) or loss of ERα altogether to allow ER-independent growth (Osborne C K, Schiff R (2011) *Annu Rev Med* 62: 233-47).

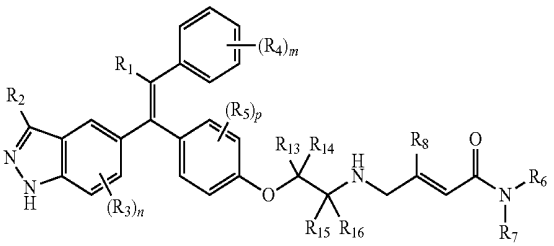
In the hopes of identifying clinically relevant mechanisms of resistance, great effort has also recently gone into deeply characterizing the genetics of endocrine-therapy resistant metastases isolated from patients. Several independent labs have recently published the multitude of genetic lesions observed in the resistant vs the primary tumors (Li et al., (2013) *Cell Rep*. September 26; 4(6): 116-30; Robinson et al., (2013) *Nat Genet*. December; 45(12):1446-51; Toy et al., (2013) *Nat Genet*. 2013 December; 45(12):1439-45). Among these are the highly recurrent mutations in the ligand-binding domain of ESR1 (gene which encodes ERα protein) found to be significantly enriched in about 20% of resistant tumors relative to endocrine therapy naïve tumors (Jeselsohn et al., (2014) *Clin Cancer Res*. April 1; 20(7): 1757-67; Toy et al., (2013) *Nat Genet*. 2013 December; 45(12):1439-45; Robinson et al., (2013) *Nat Genet*. December; 45(12):1446-51; Merenbakh-Lamin et al., (2013) *Cancer Res*. December 1; 73(23):6856-64; Yu et al., (2014) *Science* July 11; 345(6193):216-20; Segal and Dowsett (2014), *Clin Cancer Res* April 1; 20(7):1724-6), suggesting the potential for these mutations to functionally drive clinical resistance. In contrast to the enrichment in ESR1 mutations observed in therapy-resistant tumors, mutations in other cancer-related genes failed to show such a robust enrichment strongly implying the importance of ERα mutations in promoting resistance (Jeselsohn et al., (2014) *Clin Cancer Res*. April 1; 20(7):1757-67).

ER+ breast cancer patients on average are treated with seven independent therapies including chemotherapies and various anti-estrogen therapies such as tamoxifen, fulvestrant and aromatase inhibitors. Recent genomic profiling has revealed that the ERα pathway remains a critical driver of tumor growth in the resistant setting as activating mutations in ERα have emerged. Thus, it is critical that more potent ER-directed therapies be developed that can overcome resistance in the clinical setting. Hence, there is a need for novel compounds that can potently suppress the growth of both wild-type (WT) and ER α-mutant positive tumors.

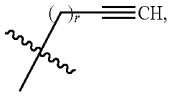
SUMMARY

Described herein are novel compounds useful for treating cancer. In embodiments, such novel compounds are described by Formula II:

II

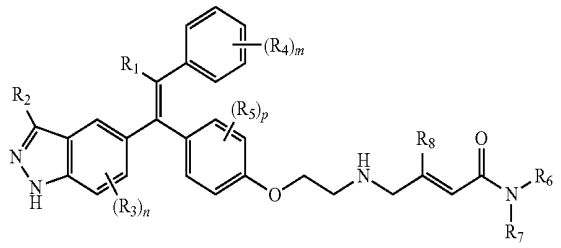


wherein: R_1 is selected from the group consisting of methyl, ethyl, cyclobutyl, cyclopropyl and —CH_2CH_2Cl, propyl, isopropyl, —CH_2CF_3, and —CH_2CH_2F; R_2 is selected from the group consisting of H and F; n is 0-1; R_3 is F; m is 0-2; R_4 are the same or different and are independently selected from the group consisting of F, CF_3, Cl, isopropyl, —OCH_3, —$OCHF_2$, —OCF_3, ethyl and methyl; p is 0-1; R_5 is F; R_6 and R_7 are the same or different and are independently selected from the group consisting of methyl, ethyl, propyl, —CH_2CH_2OH and

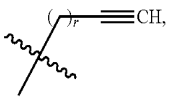


wherein r is 1 or 2; or, wherein R_6 and R_7 form a 4-6 membered heterocyclic ring with the N to which they are attached, wherein said heterocyclic ring optionally includes an oxygen atom, and wherein said heterocyclic ring is optionally substituted with F, or —CH_2F; R_8 is selected from the group consisting of H and —CH_3; and R_{13}, R_{14}, R_{15}, and R_{16} are independently selected from the group consisting of —H or —CH_3; or pharmaceutically acceptable salts thereof.

In further embodiments, such novel compounds are described by Formula I:



wherein: R_1 is selected from the group consisting of methyl, ethyl, cyclobutyl, cyclopropyl and —CH_2CH_2Cl; R_2 is selected from the group consisting of H and F; n is 0-1; R_3 is F; m is 0-2; R_4 are the same or different and are independently selected from the group consisting of F, CF_3, Cl, isopropyl, —OCH_3, —$OCHF_2$, —OCF_3, ethyl and methyl; p is 0-1; R_5 is F; R_6 and R_7 are the same or different and are independently selected from the group consisting of methyl, ethyl, propyl, —CH_2CH_2OH and



wherein r is 1 or 2; or, wherein R_6 and R_7 form a 4-6 membered heterocyclic ring with the N to which they are attached, wherein said heterocyclic ring optionally includes an oxygen atom, and wherein said heterocyclic ring is optionally substituted with F, or —CH_2F; R_8 is selected from the group consisting of H and —CH_3; or pharmaceutically acceptable salts thereof.

In embodiments, the compounds of Formula I may have the following preferred permutations or preferred combination of permutations: R_1 is ethyl or cyclobutyl; R_6 and R_7 are both methyl; R_8 is H; R_2 is H or F; m is 2 and one of R_4 is F and the other R_4 is Cl; m is 2 and both of R_4 are F; m is 0; R_3 is F; n is 0; p is 1 and R_5 is F; and p is 0.

In embodiments, the compounds of Formula I have the following permutation: R_1 is ethyl; R_2 is H; n is 0; m is 0; p is 0; R_6 and R_7 are the same and are methyl; R_8 is H; or pharmaceutically acceptable salts thereof.

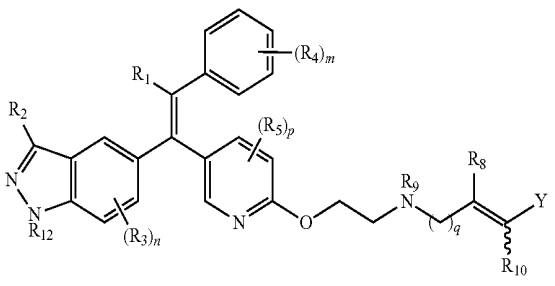
In embodiments, the compounds of Formula I have the following permutation: R_1 is ethyl; R_2 is F; n is 0; m is 2 and one R_4 is F and one R_4 is Cl; p is 0; R_6 and R_7 are the same and are methyl; R_8 is H; or pharmaceutically acceptable salts thereof.

In embodiments, the compounds of Formula I are selected from the group consisting of (E)-4-((2-(4-((E)-1-(1H-indazol-5-yl)-2-phenylbut-1-en-1-yl)phenoxy) ethyl) amino)-N,N-dimethylbut-2-enamide; (E)-4-((2-(4-((E)-1-(3-fluoro-1H-indazol-5-yl)-2-phenyl but-1-en-1-yl) phenoxy)ethyl) amino)-N,N-dimethylbut-2-enamide; (E)-4-((2-(4-((E)-1-(3-fluoro-1H-indazol-5-yl)-2-(3-fluoro-5-(trifluoromethyl) phenyl)but-1-en-1-yl)phenoxy)ethyl)amino)-N,N-dimethylbut-2-enamide; (E)-4-((2-(4-((E)-1-(4-fluoro-1H-indazol-5-yl)-2-phenyl but-1-en-1-yl) phenoxy) ethyl)amino)-N,N-dimethylbut-2-enamide; (E)-4-((2-(4-((E)-2-(3,5-difluorophenyl)-1-(1H-indazol-5-yl)but-1-en-1-yl) phenoxy)ethyl)amino)-N,N-dimethylbut-2-enamide; (E)-4-((2-(4-((E)-2-(3,4-difluorophenyl)-1-(1H-indazol-5-yl)but-1-en-1-yl) phenoxy)ethyl)amino)-N,N-dimethylbut-2-enamide; (E)-4-((2-(4-((E)-2-(3-chloro-5-fluorophenyl)-1-(1H-indazol-5-yl)but-1-en-1-yl) phenoxy)ethyl)amino)-N,N-dimethylbut-2-enamide; (E)-4-((2-(4-((E)-1-(1H-indazol-5-yl)-2-phenylbut-1-en-1-yl)phenoxy) ethyl) amino)-N-methyl-N-(prop-2-yn-1-yl)but-2-enamide; (E)-4-((2-(4-((E)-1-(1H-indazol-5-yl)-2-phenylbut-1-en-1-yl)phenoxy) ethyl) amino)-N-(but-3-yn-1-yl)-N-methylbut-2-enamide; (E)-4-((2-(4-((E)-1-(1H-indazol-5-yl)-2-phenylbut-1-en-1-yl)phenoxy)ethyl) amino)-1-(azetidin-1-yl)but-2-en-1-one; (E)-4-((2-(4-((E)-1-(1H-indazol-5-yl)-2-phenylbut-1-en-1-yl)phenoxy)ethyl) amino)-1-(pyrrolidin-1-yl)but-2-en-1-one; (E)-4-((2-(4-((E)-1-(1H-indazol-5-yl)-2-phenylbut-1-en-1-yl)phenoxy)ethyl) amino)-1-(piperidin-1-yl)but-2-en-1-one; (E)-4-((2-(4-((E)-2-cyclobutyl-1-(1H-indazol-5-yl)-2-phenylvinyl)phenoxy) ethyl)amino)-N,N-dimethylbut-2-enamide; (E)-4-((2-(4-((E)-2-cyclobutyl-1-(3-fluoro-1H-indazol-5-yl)-2-phenylvinyl) phenoxy)ethyl)amino)-N,N-dimethylbut-2-enamide 2,2,2-trifluoro acetate; (E)-4-((2-(4-((E)-1-(1H-indazol-5-yl)-2-phenylbut-1-en-1-yl)phenoxy) ethyl) amino)-1-morpholinobut-2-en-1-one; (E)-4-((2-(4-((E)-1-(1H-indazol-5-yl)-2-phenylbut-1-en-1-yl)phenoxy) ethyl) amino)-N-ethyl-N-methylbut-2-enamide; (E)-4-((2-(4-((E)-1-(1H-indazol-5-yl)-2-phenylbut-1-en-1-yl) phenoxy)ethyl) amino)-N-methyl-N-propylbut-2-enamide; (E)-4-((2-(4-((E)-1-(1H-indazol-5-yl)-2-phenylbut-1-en-1-yl)phenoxy)ethyl)amino)-N-(2-hydroxyethyl)-N-methyl-but-2-enamide; (E)-4-((2-(4-((E)-2-(2-chloro-4-fluorophenyl)-1-(3-fluoro-1H-indazol-5-yl)but-1-en-1-yl)phenoxy) ethyl)amino)-N,N-dimethylbut-2-enamide; (E)-4-((2-(4-((E)-1-(1H-indazol-5-yl)-2-phenylbut-1-en-1-yl)phenoxy) ethyl) amino)-N,N,3-trimethylbut-2-enamide; (Z)-4-((2-(4-((E)-1-(1H-indazol-5-yl)-2-phenylbut-1-en-1-yl)phenoxy) ethyl) amino)-N,N-dimethylbut-2-enamide; (E)-4-((2-(4-((E)-2-cyclobutyl-1-(1H-indazol-5-yl)-2-phenylvinyl) phenoxy) ethyl)amino)-1-morpholinobut-2-en-1-one; (E)-4-((2-(4-((E)-2-cyclobutyl-1-(4-fluoro-1H-indazol-5-yl)-2-phenylvinyl) phenoxy)ethyl)amino)-N,N-dimethylbut-2-enamide; (E)-4-((2-((5-((Z)-1-(1H-indazol-5-yl)-2-phenylbut-1-en-1-yl)pyridin-2-yl) oxy)ethyl)amino)-N,N-dimethylbut-2-enamide; (E)-4-((2-(4-((E)-1-(1H-indazol-5-yl)-2-(o-tolyl)but-1-en-1-yl)phenoxy) ethyl)amino)-N-(2-hydroxyethyl)-N-methylbut-2-enamide; (E)-4-((2-(4-((E)-2-(2-chloro-4-fluorophenyl)-1-(3-fluoro-1H-indazol-5-yl) but-1-en-1-yl)phenoxy)ethyl)amino)-N-(2-hydroxyethyl)-N-methylbut-2-enamide; (E)-4-((2-(4-((E)-1-(1H-indazol-5-yl)-2-(4-isopropyl phenyl)but-1-en-1-yl) phenoxy)ethyl) amino)-N,N-dimethylbut-2-enamide; (E)-4-((2-(4-((E)-4-chloro-1-(1H-indazol-5-yl)-2-phenyl but-1-en-1-yl) phenoxy) ethyl)amino)-N,N-dimethylbut-2-enamide; (E)-4-((2-(4-((E)-1-(1H-indazol-5-yl)-2-(4-isopropyl phenyl)but-1-en-1-yl) phenoxy)ethyl)amino)-N,N-dimethylbut-2-enamide; (E)-4-((2-(4-((E)-2-(2-(difluoromethoxy)phenyl)-1-(1H-indazol-5-yl)but-1-en-1-yl)phenoxy)ethyl)amino)-N,N-dimethylbut-2-enamide; (E)-4-((2-(4-((E)-1-(1H-indazol-5-yl)-2-(2-(trifluoro-methoxy)phenyl)but-1-en-1-yl) phenoxy)ethyl)amino)-N,N-dimethylbut-2-enamide; (E)-4-((2-(4-((E)-1-(1H-indazol-5-yl)-2-(2-isopropyl phenyl)but-1-en-1-yl) phenoxy)ethyl)amino)-N,N-dimethylbut-2-enamide; (E)-4-((2-(4-((E)-2-(2-ethylphenyl)-1-(1H-indazol-5-yl)but-1-en-1-yl)phenoxy) ethyl)amino)-N,N-dimethylbut-2-enamide; (E)-4-((2-(4-((E)-1-(1H-indazol-5-yl)-2-(o-tolyl)but-1-en-1-yl)phenoxy)ethyl) amino)-N,N-dimethylbut-2-enamide; (E)-4-((2-((5-((Z)-1-(1H-indazol-5-yl)-2-phenylbut-1-en-1-yl)pyrimidin-2-yl) oxy)ethyl) amino)-N,N-dimethylbut-2-enamide; (E)-1-(azetidin-1-yl)-

4-((2-(4-((E)-2-cyclobutyl-1-(1H-indazol-5-yl)-2-phenylvinyl) phenoxy)ethyl)amino)but-2-en-1-one; (E)-1-(azetidin-1-yl)-4-((2-(4-((E)-2-cyclobutyl-1-(3-fluoro-1H-indazol-5-yl)-2-phenylvinyl)phenoxy)ethyl)amino)but-2-en-1-one; (E)-4-((2-(4-((E)-2-cyclobutyl-1-(1H-indazol-5-yl)-2-phenylvinyl) phenoxy) ethyl)amino)-N-(2-hydroxyethyl)-N-methylbut-2-enamide; (E)-1-(azetidin-1-yl)-4-((2-(4-((E)-2-cyclobutyl-1-(1H-indazol-5-yl)-2-(o-tolyl) vinyl)phenoxy) ethyl)amino)but-2-en-1-one; (E)-4-((2-(4-((E)-1-(3-fluoro-1H-indazol-5-yl)-2-(2-fluoro phenyl)but-1-en-1-yl) phenoxy)ethyl)amino)-N,N-dimethylbut-2-enamide; (E)-4-((2-(4-((E)-1-(3-fluoro-1H-indazol-5-yl)-2-(3-fluoro phenyl)but-1-en-1-yl) phenoxy)ethyl)amino)-N,N-dimethylbut-2-enamide; (E)-4-((2-(4-((E)-1-(3-fluoro-1H-indazol-5-yl)-2-(3-fluorophenyl)but-1-en-1-yl) phenoxy)ethyl) amino)-N,N-dimethylbut-2-enamide; (E)-4-((2-(4-((E)-2-(2-chloro-4-fluorophenyl)-2-cyclobutyl-1-(3-fluoro-1H-indazol-5-yl)vinyl)phenoxy)ethyl)amino)-N,N-dimethylbut-2-enamide; (E)-4-((2-(2-fluoro-4-((Z)-1-(3-fluoro-1H-indazol-5-yl)-2-phenylbut-1-en-1-yl)phenoxy) ethyl)amino)-N,N-dimethylbut-2-enamide; (E)-4-((2-(4-((E)-2-(2,6-difluorophenyl)-1-(3-fluoro-1H-indazol-5-yl) but-1-en-1-yl)phenoxy)ethyl)amino)-N,N-dimethylbut-2-enamide; (E)-4-((2-(4-((E)-1-(3-fluoro-1H-indazol-5-yl)-2-(pyridin-3-yl)but-1-en-1-yl)phenoxy)ethyl)amino)-N,N-dimethylbut-2-enamide; (E)-4-((2-(4-((E)-1-(3-fluoro-1H-indazol-5-yl)-2-(pyridin-4-yl)but-1-en-1-yl)phenoxy)ethyl) amino)-N,N-dimethylbut-2-enamide; (E)-4-((2-(4-((E)-1-(1H-indazol-5-yl)-2-phenylprop-1-en-1-yl)phenoxy)ethyl) amino)-N,N-dimethylbut-2-enamide; (E)-4-((2-(4-((E)-2-cyclopropyl-1-(1H-indazol-5-yl)-2-phenylvinyl)phenoxy) ethyl)amino)-N,N-dimethylbut-2-enamide; (E)-4-((2-(4-((E)-2-(2-chloro-4-fluorophenyl)-1-(4-fluoro-1H-indazol-5-yl)but-1-en-1-yl)phenoxy)ethyl)amino)-N,N-dimethylbut-2-enamide; (E)-4-((2-((5-((Z)-2-(2-chloro-4-fluorophenyl)-1-(3-fluoro-1H-indazol-5-yl)but-1-en-1-yl)pyridin-2-yl) oxy)ethyl)amino)-N,N-dimethylbut-2-enamide; (E)-4-((2-((5-((Z)-2-(2-chloro-4-fluorophenyl)-4,4,4-trifluoro-1-(3-fluoro-1H-indazol-5-yl)but-1-en-1-yl)pyridin-2-yl)oxy) ethyl)amino)-N,N-dimethylbut-2-enamide; (E)-N,N-dimethyl-4-((2-((5-((Z)-4,4,4-trifluoro-1-(3-fluoro-1H-indazol-5-yl)-2-phenylbut-1-en-1-yl)pyridin-2-yl)oxy) ethyl)amino)but-2-enamide; (E)-N,N-dimethyl-4-((2-(4-((E)-4,4,4-trifluoro-1-(3-fluoro-1H-indazol-5-yl)-2-(3-fluoropyridin-4-yl)but-1-en-1-yl)phenoxy)ethyl)amino)but-2-enamide; (E)-N,N-dimethyl-4-((2-((5-((Z)-4,4,4-trifluoro-1-(3-fluoro-1H-indazol-5-yl)-2-(3-fluoropyridin-4-yl)but-1-en-1-yl)pyridin-2-yl)oxy)ethyl)amino)but-2-enamide; (E)-N,N-dimethyl-4-((2-(4-((E)-2-phenyl-1-(1H-pyrazolo[4,3-b]pyridin-5-yl)but-1-en-1-yl)phenoxy)ethyl)amino)but-2-enamide; (E)-4-((2-(3-fluoro-4-((Z)-1-(3-fluoro-1H-indazol-5-yl)-2-phenylbut-1-en-1-yl)phenoxy)ethyl) amino)-N,N-dimethylbut-2-enamide; (E)-4-((2-(4-((E)-2-(2,4-difluorophenyl)-1-(3-fluoro-1H-indazol-5-yl)but-1-en-1-yl)phenoxy)ethyl)amino)-N,N-dimethylbut-2-enamide; (E)-4-((2-(4-((E)-1-(3,6-difluoro-1H-indazol-5-yl)-2-phenylbut-1-en-1-yl)phenoxy)ethyl)amino)-N,N-dimethylbut-2-enamide; (E)-4-((2-(4-((E)-1-(3-fluoro-1H-indazol-5-yl)-2-(pyridin-2-yl)but-1-en-1-yl)phenoxy)ethyl)amino)-N,N-dimethylbut-2-enamide; (E)-4-((2-((5-((Z)-1-(3-fluoro-1H-indazol-5-yl)-2-phenylbut-1-en-1-yl)pyridin-2-yl)oxy) ethyl)amino)-N,N-dimethylbut-2-enamide; (E)-N,N-dimethyl-4-((2-(4-((E)-4,4,4-trifluoro-1-(3-fluoro-1H-indazol-5-yl)-2-phenylbut-1-en-1-yl)phenoxy)ethyl)amino) but-2-enamide; (E)-4-((2-((5-((Z)-2-cyclobutyl-1-(3-fluoro-1H-indazol-5-yl)-2-phenylvinyl)pyridin-2-yl)oxy)ethyl) amino)-N,N-dimethylbut-2-enamide; (E)-4-((2-(4-((E)-2-(2-chlorophenyl)-1-(3-fluoro-1H-indazol-5-yl)but-1-en-1-yl)phenoxy)ethyl)amino)-N,N-dimethylbut-2-enamide; (E)-4-((2-(4-((E)-2-(2-chloro-4-fluorophenyl)-1-(1H-indazol-5-yl)but-1-en-1-yl)phenoxy)ethyl)amino)-N,N-dimethylbut-2-enamide; (E)-4-((2-(4-((E)-1-(3-fluoro-1H-indazol-5-yl)-2-(pyridin-4-yl)but-1-en-1-yl)phenoxy)ethyl)amino)-N-(2-hydroxyethyl)-N-methylbut-2-enamide; (E)-4-((2-(4-((E)-1-(7-fluoro-1H-indazol-5-yl)-2-phenylbut-1-en-1-yl) phenoxy)ethyl)amino)-N,N-dimethylbut-2-enamide; (E)-4-((2-(4-((E)-1-(3-fluoro-1H-indazol-5-yl)-2-phenylpent-1-en-1-yl)phenoxy)ethyl)amino)-N,N-dimethylbut-2-enamide; (E)-4-((2-(4-((E)-1-(3,7-difluoro-1H-indazol-5-yl)-2-phenylbut-1-en-1-yl)phenoxy)ethyl)amino)-N,N-dimethylbut-2-enamide; (E)-4-((2-(4-((E)-2-(2,5-difluorophenyl)-1-(3-fluoro-1H-indazol-5-yl)but-1-en-1-yl) phenoxy)ethyl)amino)-N,N-dimethylbut-2-enamide; (E)-4-((2-(4-((E)-1-(3-fluoro-1H-indazol-5-yl)-2-(3-fluoropyridin-4-yl)but-1-en-1-yl)phenoxy)ethyl)amino)-N,N-dimethylbut-2-enamide; (E)-4-((2-(4-((E)-1-(3-fluoro-1H-indazol-5-yl)-3-methyl-2-phenylbut-1-en-1-yl) phenoxy)ethyl)amino)-N,N-dimethylbut-2-enamide; (E)-5-((2-(4-((E)-4-fluoro-1-(3-fluoro-1H-indazol-5-yl)-2-phenylbut-1-en-1-yl)phenoxy)ethyl)amino)-N,N-dimethylpent-2-enamide; (E)-5-((2-(4-((E)-2-(2-chloro-4-fluorophenyl)-1-(3-fluoro-1H-indazol-5-yl)but-1-en-1-yl) phenoxy)ethyl)amino)-N,N-dimethylpent-2-enamide; (E)-4-((2-(4-((E)-2-(2-chloro-4-fluorophenyl)-1-(3-fluoro-1H-indazol-5-yl)but-1-en-1-yl)phenoxy)ethyl)amino)-N,N,2-trimethylbut-2-enamide; (E)-4-((2-(4-((E)-2-(2-chloro-4-fluorophenyl)-4,4,4-trifluoro-1-(3-fluoro-1H-indazol-5-yl) but-1-en-1-yl)phenoxy)ethyl)amino)-N,N-dimethylbut-2-enamide; (E)-4-((2-(4-((E)-1-(1H-indazol-5-yl)-2-(phenyl-d5)but-1-en-1-yl)phenoxy)ethyl)amino)-N,N-dimethylbut-2-enamide; (E)-4-((2-(4-((E)-1-(1H-indazol-5-yl)-2-phenylbut-1-en-1-yl)phenoxy)ethyl)amino)-N,N-dimethylpent-2-enamide; (E)-4-((2-(4-((E)-1-(1H-indazol-5-yl)-2-phenylbut-1-en-1-yl)phenoxy)propyl)amino)-N,N-dimethylbut-2-enamide; (E)-4-((1-(4-((E)-1-(1H-indazol-5-yl)-2-phenylbut-1-en-1-yl)phenoxy)propan-2-yl)amino)-N,N-dimethylbut-2-enamide; (E)-4-((2-((6-((Z)-1-(3-fluoro-1H-indazol-5-yl)-2-phenylbut-1-en-1-yl)pyridin-3-yl)oxy) ethyl)amino)-N,N-dimethylbut-2-enamide; (E)-4-((3-(4-((E)-1-(1H-indazol-5-yl)-2-phenylbut-1-en-1-yl)phenoxy) propyl)amino)-N,N-dimethylbut-2-enamide; (E)-4-((3-(4-((E)-1-(1H-indazol-5-yl)-2-phenylbut-1-en-1-yl)phenoxy) butan-2-yl)amino)-N,N-dimethylbut-2-enamide; (E)-4-((1-(4-((E)-1-(1H-indazol-5-yl)-2-phenylbut-1-en-1-yl) phenoxy)-2-methylpropan-2-yl)amino)-N,N-dimethylbut-2-enamide; (E)-4-((2-(4-((E)-1-(1H-indazol-5-yl)-2-phenylbut-1-en-1-yl)phenoxy)-2-methylpropyl)amino)-N,N-dimethylbut-2-enamide; and (E)-4-((2-(4-((E)-2-cyclobutyl-1-(3-fluoro-1H-indazol-5-yl)-2-phenylvinyl) phenoxy)ethyl)amino)-N-(2-hydroxyethyl)-N-methylbut-2-enamide, and pharmaceutically acceptable salts thereof.

In some embodiments, such novel compounds are described by Formula III:

III



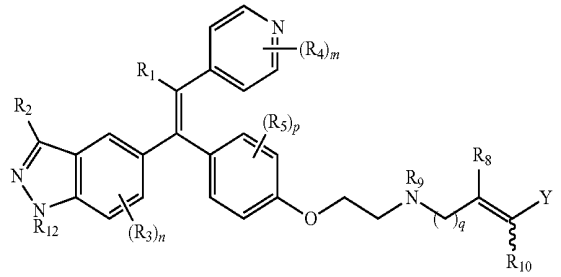
wherein: R_1 is selected from the group consisting of C_1-C_6 alkyl, —CH_2CF_3, C_3-C_6 cycloalkyl and a 4-6 membered heterocyclic ring; R_2 is selected from the group consisting of H, halogen, hydroxy, C_1-C_3 alkyl, C_3-C_4 cycloalkyl and C_4

heterocyclic ring; R_3 are the same or different, and are independently selected from the group consisting of H, halogen, C_1-C_6 alkyl and C_1-C_3 alkoxy optionally substituted with at least one halogen; n is 0-3; R_4 are the same or different and are independently selected from the group consisting of H, halogen, C_1-C_6 alkyl, and OR_{11}, wherein R_{11} is selected from the group consisting of C_3-C_6 cycloalkyl, C_1-C_6 alkyl, aryl, heteroaryl and a 4-6 membered heterocyclic ring; m is 0-5; R_5 are the same or different and are independently selected from the group consisting of H, halogen, C_1-C_4 alkyl, C_1-C_4 alkoxy, C_3-C_4 cycloalkyl, C_3-C_6 cycloalkoxy and C_4 heterocycle; p is 0-3; q is 1-2; R_8 and R_{10} are the same or different and are independently selected from the group consisting of halogen, H and C_1-C_3 alkyl; R_9 is selected from the group consisting of H, C_1-C_6 alkyl and C_3-C_6 cycloalkyl; Y is selected from the group consisting of $—S(O)_2R_6$, $—S(O)_2NR_6R_7$, $—C(O)NR_6R_7$, $—C(O)R_6$, $—C(O)OR_6$, —CN; or wherein Y and R_{10} both represent $—CF_3$; R_6 and R_7 are the same or different and are independently selected from the group consisting of H, C_1-C_6 alkyl, C_3-C_6 cycloalkyl, aryl, heteroaryl and a 4-6 membered heterocyclic ring wherein said alkyl is saturated or unsaturated or wherein R_6 and R_7 form a 4-6 membered heterocyclic ring with the N to which they are attached, optionally also containing an O atom; R_{12} is selected from the group consisting of H, C_3-C_4 cycloalkyl and C_1-C_6 alkyl; and wherein any carbon containing moiety of R_1-R_{12} may be optionally substituted with one or more halogen atoms, fluoromethane, difluoromethane or trifluoromethane, or —OH; or pharmaceutically acceptable salts thereof.

In a further embodiment, R_1 is selected from the group consisting of C_1-C_6 alkyl, C_3-C_6 cycloalkyl and a 4-6 membered heterocyclic ring. In a further embodiment, R1 is $—CH_2CF_3$. In more specific embodiments, such novel compounds are described by Formula III, wherein: R_2 is selected from the group consisting of H, halogen, methyl and ethyl; R_3 are the same or different, and are independently selected from the group consisting of H, halogen, methyl and ethyl; R_4 are the same or different and are independently selected from the group consisting of H, halogen, C_1-C_6 alkyl and C_1-C_6 alkoxy; R_5 are the same or different and are independently selected from the group consisting of H, halogen, methyl and ethyl; R_8 and R_{10} are the same or different and are independently selected from the group consisting of H and methyl; R_9 is selected from the group consisting of H, methyl and ethyl; and R_6 and R_7 are the same or different and are independently selected from the group consisting of H and C_1-C_6 alkyl or wherein R_6 and R_7 form a 4-6 atom heterocyclic ring with the N to which they are attached, optionally also containing an O atom. In further embodiments, R_1 is cyclobutyl, ethyl, or $—CH_2CF_3$; R_2 is —H or —F; n is 0; m is 0 or 2, and when m is 2, then one R_4 is —Cl and the other R_4 is —F; p is 0; Y is $—CON(CH_3)_2$, and R_8, R_9, R_{10}, and R_{12} are all —H.

In some embodiments, such novel compounds are described by Formula IV:

IV

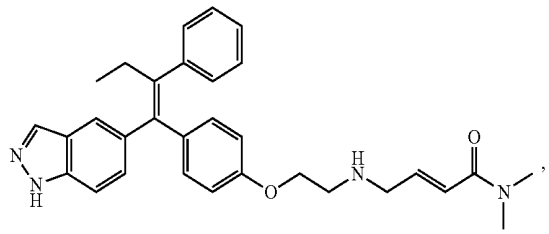


wherein: R_1 is selected from the group consisting of C_1-C_6 alkyl, C_3-C_6 cycloalkyl and a 4-6 membered heterocyclic ring; R_2 is selected from the group consisting of H, halogen, hydroxy, C_1-C_3 alkyl, C_3-C_4 cycloalkyl and C_4 heterocyclic ring; R_3 are the same or different, and are independently selected from the group consisting of H, halogen, C_1-C_6 alkyl and C_1-C_3 alkoxy optionally substituted with at least one halogen; n is 0-3; R_4 are the same or different and are independently selected from the group consisting of H, halogen, C_1-C_6 alkyl, and OR_{11}, wherein R_{11} is selected from the group consisting of C_3-C_6 cycloalkyl, C_1-C_6 alkyl, aryl, heteroaryl and a 4-6 membered heterocyclic ring; m is 0-4; R_5 are the same or different and are independently selected from the group consisting of H, halogen, C_1-C_4 alkyl, C_1-C_4 alkoxy, C_3-C_4 cycloalkyl, C_3-C_6 cycloalkoxy and C_4 heterocycle; p is 0-4; q is 1-2; R_8 and R_{10} are the same or different and are independently selected from the group consisting of halogen, H and C_1-C_3 alkyl; R_9 is selected from the group consisting of H, C_1-C_6 alkyl and C_3-C_6 cycloalkyl; Y is selected from the group consisting of $—S(O)_2R_6$, $—S(O)_2NR_6R_7$, $—C(O)NR_6R_7$, $—C(O)R_6$, $—C(O)OR_6$, —CN; or wherein Y and R_{10} both represent $—CF_3$; R_6 and R_7 are the same or different and are independently selected from the group consisting of H, C_1-C_6 alkyl, C_3-C_6 cycloalkyl, aryl, heteroaryl and a 4-6 membered heterocyclic ring wherein said alkyl is saturated or unsaturated or wherein R_6 and R_7 form a 4-6 membered heterocyclic ring with the N to which they are attached, optionally also containing an O atom; R_{12} is selected from the group consisting of H, C_3-C_4 cycloalkyl and C_1-C_6 alkyl; and wherein any carbon containing moiety of R_1-R_{12} may be optionally substituted with one or more halogen atoms, fluoromethane, difluoromethane or trifluoromethane, or —OH; or pharmaceutically acceptable salts thereof.

In more specific embodiments, such novel compounds are described by Formula IV, wherein: R_2 is selected from the group consisting of H, halogen, methyl and ethyl; R_3 are the same or different, and are independently selected from the group consisting of H, halogen, methyl and ethyl; R_4 are the same or different and are independently selected from the group consisting of H, halogen, C_1-C_6 alkyl and C_1-C_6 alkoxy; R_8 are the same or different and are independently selected from the group consisting of H, halogen, methyl and ethyl; R_8 and R_{10} are the same or different and are independently selected from the group consisting of H and methyl; R_9 is selected from the group consisting of H, methyl and ethyl; and R_6 and R_7 are the same or different and are independently selected from the group consisting of H and C_1-C_6 alkyl or wherein R_6 and R_7 form a 4-6 atom heterocyclic ring with the N to which they are attached, optionally also containing an O atom.

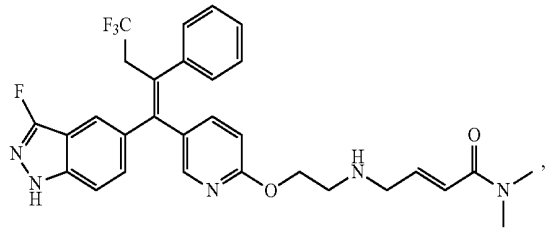
In some embodiments, the compounds of Formula III or Formula IV have the following permutations or combinations of permutations: Y is $—C(O)NR_6R_7$; R_6 and R_7 are methyl; R_8 and R_{10} are both H; R_1 is ethyl or cyclobutyl; R_9 is H; R_2 is F or H; m is 2 and one of R_4 is F and the other R_4 is Cl; m is 2 and both of R_4 are F; m is 0; n is 1 and R_3 is F; n is 0; p is 1 and R_5 is F; or p is 0.

An embodiment may provide a compound having the following formula:



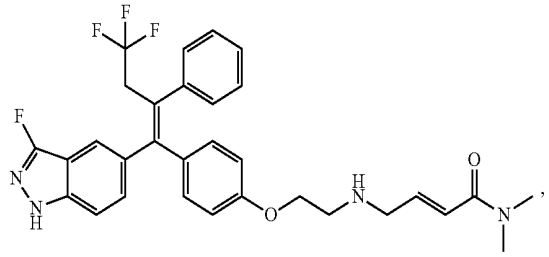
or a pharmaceutically acceptable salt thereof.

An embodiment may provide a compound having the following formula:



or a pharmaceutically acceptable salt thereof.

An embodiment may provide a compound having the following formula:



or a pharmaceutically acceptable salt thereof.

A further embodiment may provide a method of treating breast cancer comprising administering to a subject a compound according to any one of the preceding paragraphs. The breast cancer may be an ER-positive breast cancer. The subject may express a mutant ER-α protein. An embodiment may provide use of a compound as in the paragraphs above for treating breast cancer. In some embodiments the breast cancer is an ER-positive breast cancer. In some embodiments said subject expresses a mutant ER-α protein. In some embodiments a compound as presented above is used in the preparation of a medicament for treatment of breast cancer.

In embodiments, the compounds disclosed herein are useful for inhibiting the cell culture growth of MCF7 ER-alpha (wildtype) and MCF7 ER-alpha (Y537S mutant) cells. Other compounds (e.g., tamoxifen, raloxifene and fulvestrant) known to inhibit the cell culture growth of MCF7 ER-alpha (wildtype) cells are currently used to treat breast cancer in human patients. Hence, the compounds disclosed herein are useful for treating ER-alpha expressing breast cancer in human patients, and are useful for treating Y537S mutant ER-alpha expressing breast cancer in human patients.

In embodiments, the compounds disclosed herein are useful for treating breast cancer. In embodiments, the breast cancer is ER-α+. In embodiments, the breast cancer expresses an ER-α mutation, which is L536Q (Robinson et al. *Nat Genet.* 2013 December; 45(12)), L536R (Toy et al. *Nat Genet.* 2013 December; 45(12):1439-45), Y537S (Toy et al. *Nat Genet.* 2013 December; 45(12):1439-45; Robinson et al. *Nat Genet.* 2013 December; 45(12); Jeselsohn et al. *Clin Cancer Res.* 2014 Apr. 1; 20(7):1757-67), Y537N (Toy et al. *Nat Genet.* 2013 December; 45(12):1439-45; Jeselsohn et al. *Clin Cancer Res.* 2014 Apr. 1; 20(7): 1757-67), Y537C (Toy et al. *Nat Genet.* 2013 December; 45(12): 1439-45; Jeselsohn et al. *Clin Cancer Res.* 2014 Apr. 1; 20(7):1757-67) and D538G (Toy et al. *Nat Genet.* 2013 December; 45(12):1439-45; Robinson et al. *Nat Genet.* 2013 December; 45(12); Jeselsohn et al. *Clin Cancer Res.* 2014 Apr. 1; 20(7):1757-67; Merenbakh-Lamin et al. *Cancer Res.* 2013 Dec. 1; 73(23):6856-64); and Yu et al., (2014) *Science* July 11; 345(6193):216-20, all of which are incorporated by reference in their entireties for their teachings of ER-α mutations.

BRIEF DESCRIPTION OF THE DRAWINGS

FIG. **1** shows in vitro proliferation effects of wild-type and mutant ER-bearing MCF7 lines to clinical therapies 4-hydroxytamoxifen (4-OHT), raloxifene and fulvestrant, where phenotypic resistance observed in mutant-bearing lines relative to control lines to existing clinical compounds, whereby MCF7 cells engineered to overexpress various $ER\alpha^{MUT}$ showed partial resistance to various endocrine therapies.

FIG. **2** shows antitumor and body weight effects of oral Compound 1 in MCF7 xenograft bearing female balb/c nude mice.

FIG. **3** shows antitumor and body weight effects of oral Compound 1 in PDX-Y537S xenograft bearing athymic nude (Crl:NU(NCr)-Foxnlnu) female mice.

FIG. **4** shows antitumor and body weight effects of oral Compound 1 in WHUM20 xenograft bearing SCID-bg female mice.

FIG. **5** shows antitumor and body weight effects of oral Compound 60 in MCF7 xenograft bearing female Balb/c nude mice.

FIG. **6** shows antitumor and body weight effects of oral Compound 60 in PDX-Y537S xenograft bearing athymic nude (Crl:NU(NCr)-Foxnlnu) female mice.

FIG. **7** shows antitumor and body weight effects of oral Compound 69 in MCF7 xenograft bearing female Balb/c nude mice.

FIG. **8** shows antitumor and body weight effects of oral Compound 69 in PDX-Y537S xenograft bearing athymic nude (Crl:NU(NCr)-Foxnlnu) female mice.

FIG. **9** shows the anti-tumor and body weight effects of Compound 60 in the ER+ WHIM20 PDX model bearing a homozygous Y537S mutation.

DETAILED DESCRIPTION

All publications and patent documents cited herein are incorporated herein by reference as if each such publication or document was specifically and individually indicated to be incorporated herein by reference. Where the text of this disclosure and the text of one or more documents incorporated by reference conflicts, this disclosure controls. Citation of publications and patent documents is not intended as an admission that any is pertinent prior art, nor does it constitute any admission as to the contents or date of the same. The embodiments described herein having now been described by way of written description, those of skill in the art will

recognize that the embodiments described herein may be practiced in a variety of embodiments and that the description and examples provided herein are for purposes of illustration and not limitation of the claims.

As used herein, "alkyl", "C_1, C_2, C_3, C_4, C_5 or C_6 alkyl" or "C_1-C_6 alkyl" is intended to include C_1, C_2, C_3, C_4, C_5 or C_6 straight chain (linear) saturated aliphatic hydrocarbon groups and C_3, C_4, C_5 or C_6 branched saturated aliphatic hydrocarbon groups. For example, C_1-C_6 alkyl is intended to include C_1, C_2, C_3, C_4, C_5 and C_6 alkyl groups. Examples of alkyl include moieties having from one to six carbon atoms, such as, but not limited to, methyl, ethyl, n-propyl, i-propyl, n-butyl, s-butyl, t-butyl, n-pentyl, s-pentyl or n-hexyl.

In certain embodiments, a straight chain or branched alkyl has six or fewer carbon atoms (e.g., C_1-C_6 for straight chain, C_3-C_6 for branched chain), and in another embodiment, a straight chain or branched alkyl has four or fewer carbon atoms.

As used herein, the term "cycloalkyl" refers to a saturated or unsaturated nonaromatic hydrocarbon ring having 3 to 7 carbon atoms (e.g., C_3-C_7). Examples of cycloalkyl include, but are not limited to, cyclopropyl, cyclobutyl, cyclopentyl, cyclohexyl, cycloheptyl, cyclopentenyl, cyclohexenyl, and cycloheptenyl.

The term "heterocycloalkyl" refers to a saturated or unsaturated nonaromatic 3-8 membered monocyclic groups, 7-10 membered fused bicyclic groups having one or more heteroatoms (such as O, N, or S), unless specified otherwise. Examples of heterocycloalkyl groups include, but are not limited to, piperidinyl, piperazinyl, pyrrolidinyl, dioxanyl, tetrahydrofuranyl, isoindolinyl, indolinyl, imidazolidinyl, pyrazolidinyl, oxazolidinyl, isoxazolidinyl, triazolidinyl, oxiranyl, azetidinyl, oxetanyl, thietanyl, 1,2,3,6-tetrahydropyridinyl, tetrahydropyranyl, tetrahydrothiophene, dihydropyranyl, pyranyl, morpholinyl, 1,4-diazepanyl, 1,4-oxazepanyl, and the like.

Additional examples of heterocycloalkyl groups include, but are not limited to, acridinyl, azocinyl, benzimidazolyl, benzofuranyl, benzothiofuranyl, benzothiophenyl, benzoxazolyl, benzoxazolinyl, benzthiazolyl, benztriazolyl, benztetrazolyl, benzisoxazolyl, benzisothiazolyl, benzimidazolinyl, carbazolyl, 4aH-carbazolyl, carbolinyl, chromanyl, chromenyl, cinnolinyl, decahydroquinolinyl, 2H,6H-1,5,2-dithiazinyl, dihydrofuro[2,3-b]tetrahydrofuran, furanyl, furazanyl, imidazolidinyl, imidazolinyl, imidazolyl, 1H-indazolyl, indolenyl, indolinyl, indolizinyl, indolyl, 3H-indolyl, isatinoyl, isobenzofuranyl, isochromanyl, isoindazolyl, isoindolinyl, isoindolyl, isoquinolinyl, isothiazolyl, isoxazolyl, methylenedioxyphenyl, morpholinyl, naphthyridinyl, octahydroisoquinolinyl, oxadiazolyl, 1,2,3-oxadiazolyl, 1,2,4-oxadiazolyl, 1,2,5-oxadiazolyl, 1,3,4-oxadiazolyl, 1,2,4-oxadiazol5(4H)-one, oxazolidinyl, oxazolyl, oxindolyl, pyrimidinyl, phenanthridinyl, phenanthrolinyl, phenazinyl, phenothiazinyl, phenoxathinyl, phenoxazinyl, phthalazinyl, piperazinyl, piperidinyl, piperidonyl, 4-piperidonyl, peperonyl, pteridinyl, purinyl, pyranyl, pyrazinyl, pyrazolidinyl, pyrazolinyl, pyrazolyl, pyridazinyl, pyridooxazole, pyridoimidazole, pyridothiazole, pyridinyl, pyridyl, pyrimidinyl, pyrrolidinyl, pyrrolinyl, 2H-pyrrolyl, pyrrolyl, quinazolinyl, quinolinyl, 4H-quinolizinyl, quinoxalinyl, quinuclidinyl, tetrahydrofuranyl, tetrahydroisoquinolinyl, tetrahydroquinolinyl, tetrazolyl, 6H-1,2,5-thiadiazinyl, 1,2,3-thiadiazolyl, 1,2,4-thiadiazolyl, 1,2,5-thiadiazolyl, 1,3,4-thiadiazolyl, thianthrenyl, thiazolyl, thienyl, thienothiazolyl, thienooxazolyl, thienoimidazolyl, thiophenyl, triazinyl, 1,2,3-triazolyl, 1,2,4-triazolyl, 1,2,5-triazolyl, 1,3,4-triazolyl and xanthenyl.

The term "optionally substituted alkyl" refers to unsubstituted alkyl or alkyl having designated substituents replacing one or more hydrogen atoms on one or more carbons of the hydrocarbon backbone. Such substituents may include, for example, alkyl, alkenyl, alkynyl, halogen, hydroxyl, alkylcarbonyloxy, arylcarbonyloxy, alkoxycarbonyloxy, aryloxycarbonyloxy, carboxylate, alkylcarbonyl, arylcarbonyl, alkoxycarbonyl, aminocarbonyl, alkylaminocarbonyl, dialkylaminocarbonyl, alkylthiocarbonyl, alkoxyl, phosphate, phosphonato, phosphinato, amino (including alkylamino, dialkylamino, arylamino, diarylamino and alkylarylamino), acylamino (including alkylcarbonylamino, arylcarbonylamino, carbamoyl and ureido), amidino, imino, sulfhydryl, alkylthio, arylthio, thiocarboxylate, sulfates, alkylsulfinyl, sulfonato, sulfamoyl, sulfonamido, nitro, trifluoromethyl, cyano, azido, heterocyclyl, alkylaryl, or an aromatic or heteroaromatic moiety.

An "arylalkyl" or an "aralkyl" moiety is an alkyl substituted with an aryl (e.g., phenylmethyl(benzyl)). An "alkylaryl" moiety is an aryl substituted with an alkyl (e.g., methylphenyl).

"Alkenyl" includes unsaturated aliphatic groups analogous in length and possible substitution to the alkyls described above, but that contain at least one double bond. For example, the term "alkenyl" includes straight chain alkenyl groups (e.g., ethenyl, propenyl, butenyl, pentenyl, hexenyl), and branched alkenyl groups. In certain embodiments, a straight chain or branched alkenyl group has six or fewer carbon atoms in its backbone (e.g., C_2-C_6 for straight chain, C_3-C_6 for branched chain). The term "C_2-C_6" includes alkenyl groups containing two to six carbon atoms. The term "C_3-C_6" includes alkenyl groups containing three to six carbon atoms.

The term "optionally substituted alkenyl" refers to unsubstituted alkenyl or alkenyl having designated substituents replacing one or more hydrogen atoms on one or more hydrocarbon backbone carbon atoms. Such substituents may include, for example, alkyl, alkenyl, alkynyl, halogen, hydroxyl, alkylcarbonyloxy, arylcarbonyloxy, alkoxycarbonyloxy, aryloxycarbonyloxy, carboxylate, alkylcarbonyl, arylcarbonyl, alkoxycarbonyl, aminocarbonyl, alkylaminocarbonyl, dialkylaminocarbonyl, alkylthiocarbonyl, alkoxyl, phosphate, phosphonato, phosphinato, amino (including alkylamino, dialkylamino, arylamino, diarylamino and alkylarylamino), acylamino (including alkylcarbonylamino, arylcarbonylamino, carbamoyl and ureido), amidino, imino, sulfhydryl, alkylthio, arylthio, thiocarboxylate, sulfates, alkylsulfinyl, sulfonato, sulfamoyl, sulfonamido, nitro, trifluoromethyl, cyano, heterocyclyl, alkylaryl, or an aromatic or heteroaromatic moiety.

"Alkynyl" includes unsaturated aliphatic groups analogous in length and possible substitution to the alkyls described above, but which contain at least one triple bond. For example, "alkynyl" includes straight chain alkynyl groups (e.g., ethynyl, propynyl, butynyl, pentynyl, hexynyl), and branched alkynyl groups. In certain embodiments, a straight chain or branched alkynyl group has six or fewer carbon atoms in its backbone (e.g., C_2-C_6 for straight chain, C_3-C_6 for branched chain). The term "C_2-C_6" includes alkynyl groups containing two to six carbon atoms. The term "C_3-C_6" includes alkynyl groups containing three to six carbon atoms.

The term "optionally substituted alkynyl" refers to unsubstituted alkynyl or alkynyl having designated substituents replacing one or more hydrogen atoms on one or more hydrocarbon backbone carbon atoms. Such substituents may include, for example, alkyl, alkenyl, alkynyl, halogen,

hydroxyl, alkylcarbonyloxy, arylcarbonyloxy, alkoxycarbonyloxy, aryloxycarbonyloxy, carboxylate, alkylcarbonyl, arylcarbonyl, alkoxycarbonyl, aminocarbonyl, alkylaminocarbonyl, dialkylaminocarbonyl, alkylthiocarbonyl, alkoxyl, phosphate, phosphonato, phosphinato, amino (including alkylamino, dialkylamino, arylamino, diarylamino and alkylarylamino), acylamino (including alkylcarbonylamino, arylcarbonylamino, carbamoyl and ureido), amidino, imino, sulfhydryl, alkylthio, arylthio, thiocarboxylate, sulfates, alkylsulfinyl, sulfonato, sulfamoyl, sulfonamido, nitro, trifluoromethyl, cyano, azido, heterocyclyl, alkylaryl, or an aromatic or heteroaromatic moiety.

Other optionally substituted moieties (such as optionally substituted cycloalkyl, heterocycloalkyl, aryl, or heteroaryl) include both the unsubstituted moieties and the moieties having one or more of the designated substituents. For example, substituted heterocycloalkyl includes those substituted with one or more alkyl groups, such as 2,2,6,6-tetramethyl-piperidinyl and 2,2,6,6-tetramethyl-1,2,3,6-tetrahydropyridinyl.

"Aryl" includes groups with aromaticity, including "conjugated," or multicyclic systems with at least one aromatic ring and do not contain any heteroatom in the ring structure. Examples include phenyl, benzyl, 1,2,3,4-tetrahydronaphthalenyl, etc.

"Heteroaryl" groups are aryl groups, as defined above, except having from one to four heteroatoms in the ring structure, and may also be referred to as "aryl heterocycles" or "heteroaromatics." As used herein, the term "heteroaryl" is intended to include a stable 5-, 6-, or 7-membered monocyclic or 7-, 8-, 9-, 10-, 11- or 12-membered bicyclic aromatic heterocyclic ring which consists of carbon atoms and one or more heteroatoms, e.g., 1 or 1-2 or 1-3 or 1-4 or 1-5 or 1-6 heteroatoms, or e.g., 1, 2, 3, 4, 5, or 6 heteroatoms, independently selected from the group consisting of nitrogen, oxygen and sulfur. The nitrogen atom may be substituted or unsubstituted (i.e., N or NR' wherein R' is H or other substituents, as defined). The nitrogen and sulfur heteroatoms may optionally be oxidized (i.e., N—O and $S(O)_p$, where p=1 or 2). It is to be noted that total number of S and O atoms in the aromatic heterocycle is not more than 1.

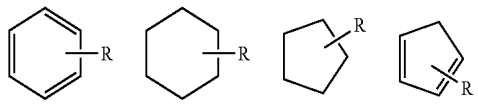
Examples of heteroaryl groups include pyrrole, furan, thiophene, thiazole, isothiazole, imidazole, triazole, tetrazole, pyrazole, oxazole, isoxazole, pyridine, pyrazine, pyridazine, pyrimidine, and the like.

Furthermore, the terms "aryl" and "heteroaryl" include multicyclic aryl and heteroaryl groups, e.g., bicyclic. Nonlimiting example of such aryl groups include, e.g., naphthalene, benzoxazole, benzodioxazole, benzothiazole, benzoimidazole, benzothiophene, methylenedioxyphenyl, quinoline, isoquinoline, naphthrydine, indole, benzofuran, purine, benzofuran, deazapurine, indolizine.

In the case of multicyclic aromatic rings, only one of the rings needs to be aromatic (e.g., 2,3-dihydroindole), although all of the rings may be aromatic (e.g., quinoline).

The cycloalkyl, heterocycloalkyl, aryl, or heteroaryl ring may be substituted at one or more ring positions (e.g., the ring-forming carbon or heteroatom such as N) with such substituents as described above, for example, alkyl, alkenyl, alkynyl, halogen, hydroxyl, alkoxy, alkylcarbonyloxy, arylcarbonyloxy, alkoxycarbonyloxy, aryloxycarbonyloxy, carboxylate, alkylcarbonyl, alkylaminocarbonyl, aralkylaminocarbonyl, alkenylaminocarbonyl, alkylcarbonyl, arylcarbonyl, aralkylcarbonyl, alkenylcarbonyl, alkoxycarbonyl, aminocarbonyl, alkylthiocarbonyl, phosphate, phosphonato, phosphinato, amino (including alkylamino, dialkylamino, arylamino, diarylamino and alkylarylamino), acylamino (including alkylcarbonylamino, arylcarbonylamino, carbamoyl and ureido), amidino, imino, sulfhydryl, alkylthio, arylthio, thiocarboxylate, sulfates, alkylsulfinyl, sulfonato, sulfamoyl, sulfonamido, nitro, trifluoromethyl, cyano, azido, heterocyclyl, alkylaryl, or an aromatic or heteroaromatic moiety. Aryl and heteroaryl groups may also be fused with alicyclic or heterocyclic rings, which are not aromatic so as to form a multicyclic system (e.g., tetralin, methylenedioxyphenyl).

When a bond to a substituent is shown to cross a bond connecting two atoms in a ring (as shown by the examples below with substituent R), then such substituent may be bonded to any atom in the ring.



When any variable (e.g., R1) occurs more than one time in any constituent or formula for a compound, its definition at each occurrence is independent of its definition at every other occurrence. Thus, for example, if a group is shown to be substituted with 0-2 R_1 moieties, then the group may optionally be substituted with up to two R_1 moieties and R_1 at each occurrence is selected independently from the definition of R_1.

The term "hydroxy" or "hydroxyl" includes groups with an —OH or —O^-.

As used herein, "halo" or "halogen" refers to fluoro, chloro, bromo and iodo. The term "perhalogenated" generally refers to a moiety wherein all hydrogen atoms are replaced by halogen atoms. The term "haloalkyl" or "haloalkoxyl" refers to an alkyl or alkoxyl substituted with one or more halogen atoms.

"Alkoxyalkyl," "alkylaminoalkyl," and "thioalkoxyalkyl" include alkyl groups, as described above, wherein oxygen, nitrogen, or sulfur atoms replace one or more hydrocarbon backbone carbon atoms.

The term "alkoxy" or "alkoxyl" includes substituted and unsubstituted alkyl, alkenyl and alkynyl groups covalently linked to an oxygen atom. Examples of alkoxy groups or alkoxyl radicals include, but are not limited to, methoxy, ethoxy, isopropyloxy, propoxy, butoxy and pentoxy groups. Examples of substituted alkoxy groups include halogenated alkoxy groups. The alkoxy groups may be substituted with groups such as alkenyl, alkynyl, halogen, hydroxyl, alkylcarbonyloxy, arylcarbonyloxy, alkoxycarbonyloxy, aryloxycarbonyloxy, carboxylate, alkylcarbonyl, arylcarbonyl, alkoxycarbonyl, aminocarbonyl, alkylaminocarbonyl, dialkylaminocarbonyl, alkylthiocarbonyl, alkoxyl, phosphate, phosphonato, phosphinato, amino (including alkylamino, dialkylamino, arylamino, diarylamino, and alkylarylamino), acylamino (including alkylcarbonylamino, arylcarbonylamino, carbamoyl and ureido), amidino, imino, sulfhydryl, alkylthio, arylthio, thiocarboxylate, sulfates, alkylsulfinyl, sulfonato, sulfamoyl, sulfonamido, nitro, trifluoromethyl, cyano, azido, heterocyclyl, alkylaryl, or an aromatic or heteroaromatic moieties. Examples of halogen substituted alkoxy groups include, but are not limited to, fluoromethoxy, difluoromethoxy, trifluoromethoxy, chloromethoxy, dichloromethoxy and trichloromethoxy.

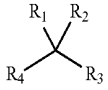
"Isomerism" means compounds that have identical molecular formulae but differ in the sequence of bonding of their atoms or in the arrangement of their atoms in space. Isomers that differ in the arrangement of their atoms in space

are termed "stereoisomers." Stereoisomers that are not mirror images of one another are termed "diastereoisomers," and stereoisomers that are non-superimposable mirror images of each other are termed "enantiomers" or sometimes optical isomers. A mixture containing equal amounts of individual enantiomeric forms of opposite chirality is termed a "racemic mixture."

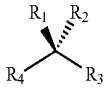
A carbon atom bonded to four nonidentical substituents is termed a "chiral center."

"Chiral isomer" means a compound with at least one chiral center. Compounds with more than one chiral center may exist either as an individual diastereomer or as a mixture of diastereomers, termed "diastereomeric mixture." When one chiral center is present, a stereoisomer may be characterized by the absolute configuration (R or S) of that chiral center. Absolute configuration refers to the arrangement in space of the substituents attached to the chiral center. The substituents attached to the chiral center under consideration are ranked in accordance with the Sequence Rule of Cahn, Ingold and Prelog. (Calm et al., Angew. Chem. Inter. Edit. 1966, 5, 385; errata 511; Cahn et al., Angew. Chem. 1966, 78, 413; Cahn and Ingold, J. Chem. Soc. 1951 (London), 612; Calm et al., Experientia 1956, 12, 81; Cahn, J. Chem. Educ. 1964, 41, 116).

In the present specification, each incidence of a chiral center within a structural formula, such as the non-limiting example shown here:



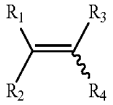
is meant to depict all possible stereoisomers. In contrast, a chiral center drawn with hatches and wedges, such as the non-limiting example shown here:



is meant to depict the stereoisomer as indicated (here in this sp^3 hybridized carbon chiral center, R_3 and R_4 are in the plane of the paper, R_1 is above the plane of paper, and R_2 is behind the plane of paper).

"Geometric isomer" means the diastereomers that owe their existence to hindered rotation about double bonds or a cycloalkyl linker (e.g., 1,3-cyclobutyl). These configurations are differentiated in their names by the prefixes cis and trans, or Z and E, which indicate that the groups are on the same or opposite side of the double bond in the molecule according to the Cahn-Ingold-Prelog rules.

In the present specification, each incidence within a structural formula including a wavy line adjacent to a double bond as shown:



is meant to depict both geometric isomers. In contrast, such structures drawn without a wavy line is meant to depict a compound having the geometric configuration as drawn.

"Tautomer" is one of two or more structural isomers that exist in equilibrium and is readily converted from one isomeric form to another. This conversion results in the formal migration of a hydrogen atom accompanied by a switch of adjacent conjugated double bonds. Tautomers exist as a mixture of a tautomeric set in solution. In solutions where tautomerization is possible, a chemical equilibrium of the tautomers will be reached. The exact ratio of the tautomers depends on several factors, including temperature, solvent and pH. The concept of tautomers that are interconvertible by tautomerizations is called tautomerism.

Where the present specification depicts a compound prone to tautomerization, but only depicts one of the tautomers, it is understood that all tautomers are included as part of the meaning of the chemical depicted. It is to be understood that the compounds disclosed herein may be depicted as different tautomers. It should also be understood that when compounds have tautomeric forms, all tautomeric forms are intended to be included, and the naming of the compounds does not exclude any tautomer form.

Of the various types of tautomerism that are possible, two are commonly observed. In keto-enol tautomerism a simultaneous shift of electrons and a hydrogen atom occurs. Ring-chain tautomerism arises as a result of the aldehyde group (—CHO) in a sugar chain molecule reacting with one of the hydroxy groups (—OH) in the same molecule to give it a cyclic (ring-shaped) form as exhibited by glucose.

Common tautomeric pairs are: ketone-enol, amide-nitrile, lactam-lactim, amide-imidic acid tautomerism in heterocyclic rings (e.g., in nucleobases such as guanine, thymine and cytosine), imine-enamine and enamine-enamine.

Furthermore, the structures and other compounds disclosed herein include all atropic isomers thereof, it being understood that not all atropic isomers may have the same level of activity. "Atropic isomers" are a type of stereoisomer in which the atoms of two isomers are arranged differently in space. Atropic isomers owe their existence to a restricted rotation caused by hindrance of rotation of large groups about a central bond. Such atropic isomers typically exist as a mixture, however as a result of recent advances in chromatography techniques, it has been possible to separate mixtures of two atropic isomers in select cases.

The term "crystal polymorphs", "polymorphs" or "crystal forms" means crystal structures in which a compound (or a salt or solvate thereof) may crystallize in different crystal packing arrangements, all of which have the same elemental composition. Different crystal forms usually have different X-ray diffraction patterns, infrared spectral, melting points, density hardness, crystal shape, optical and electrical properties, stability and solubility. Recrystallization solvent, rate of crystallization, storage temperature, and other factors may cause one crystal form to dominate. Crystal polymorphs of the compounds may be prepared by crystallization under different conditions. It is understood that the compounds disclosed herein may exist in crystalline form, crystal form mixture, or anhydride or hydrate thereof.

The compounds disclosed herein include the compounds themselves, as well as their salts and solvates, if applicable. A salt, for example, may be formed between an anion and a positively charged group (e.g., amino) on an aryl- or heteroaryl-substituted benzene compound. Suitable anions include chloride, bromide, iodide, sulfate, bisulfate, sulfamate, nitrate, phosphate, citrate, methanesulfonate, trifluoroacetate, glutamate, glucuronate, glutarate, malate, maleate, succinate, fumarate, tartrate, tosylate, salicylate, lactate, naphthalenesulfonate, and acetate (e.g., trifluoroacetate). The term "pharmaceutically acceptable anion" refers

to an anion suitable for forming a pharmaceutically acceptable salt. Likewise, a salt may also be formed between a cation and a negatively charged group (e.g., carboxylate) on an aryl- or heteroaryl-substituted benzene compound. Suitable cations include sodium ion, potassium ion, magnesium ion, calcium ion, and an ammonium cation such as tetramethylammonium ion. The aryl- or heteroaryl-substituted benzene compounds also include those salts containing quaternary nitrogen atoms.

Additionally, the compounds disclosed herein, for example, the salts of the compounds, may exist in either hydrated or unhydrated (the anhydrous) form or as solvates with other solvent molecules. Nonlimiting examples of hydrates include monohydrates, dihydrates, etc. Nonlimiting examples of solvates include ethanol solvates, acetone solvates, etc.

As used herein, "pharmaceutically acceptable salts" refer to derivatives of the compounds disclosed herein wherein the parent compound is modified by making acid or base salts thereof. Examples of pharmaceutically acceptable salts include, but are not limited to, mineral or organic acid salts of basic residues such as amines, alkali or organic salts of acidic residues such as carboxylic acids, and the like. The pharmaceutically acceptable salts include the conventional non-toxic salts or the quaternary ammonium salts of the parent compound formed, for example, from non-toxic inorganic or organic acids. For example, such conventional non-toxic salts include, but are not limited to, those derived from inorganic and organic acids selected from 2-acetoxybenzoic, 2-hydroxyethane sulfonic, acetic, ascorbic, benzene sulfonic, benzoic, bicarbonic, carbonic, citric, edetic, ethane disulfonic, 1,2-ethane sulfonic, fumaric, glucoheptonic, gluconic, glutamic, glycolic, glycollyarsanilic, hexylresorcinic, hydrabamic, hydrobromic, hydrochloric, hydroiodic, hydroxymaleic, hydroxynaphthoic, isethionic, lactic, lactobionic, lauryl sulfonic, maleic, malic, mandelic, methane sulfonic, napsylic, nitric, oxalic, pamoic, pantothenic, phenylacetic, phosphoric, polygalacturonic, propionic, salicyclic, stearic, subacetic, succinic, sulfamic, sulfanilic, sulfuric, tannic, tartaric, toluene sulfonic, and the commonly occurring amine acids, e.g., glycine, alanine, phenylalanine, arginine, etc.

Other examples of pharmaceutically acceptable salts include hexanoic acid, cyclopentane propionic acid, pyruvic acid, malonic acid, 3-(4-hydroxybenzoyl)benzoic acid, cinnamic acid, 4-chlorobenzenesulfonic acid, 2-naphthalenesulfonic acid, 4-toluenesulfonic acid, camphorsulfonic acid, 4-methylbicyclo-[2.2.2]-oct-2-ene-1-carboxylic acid, 3-phenylpropionic acid, trimethylacetic acid, tertiary butylacetic acid, muconic acid, and the like. The present disclosure also encompasses salts formed when an acidic proton present in the parent compound either is replaced by a metal ion, e.g., an alkali metal ion, an alkaline earth ion, or an aluminum ion; or coordinates with an organic base such as ethanolamine, diethanolamine, triethanolamine, tromethamine, N-methylglucamine, and the like. In the salt form, it is understood that the ratio of the compound to the cation or anion of the salt may be 1:1, or any ratio other than 1:1, e.g., 3:1, 2:1, 1:2, or 1:3.

It should be understood that all references to pharmaceutically acceptable salts include solvent addition forms (solvates) or crystal forms (polymorphs) as defined herein, of the same salt.

"Solvate" means solvent addition forms that contain either stoichiometric or non stoichiometric amounts of solvent. Some compounds have a tendency to trap a fixed molar ratio of solvent molecules in the crystalline solid state, thus forming a solvate. If the solvent is water the solvate formed is a hydrate; and if the solvent is alcohol, the solvate formed is an alcoholate. Hydrates are formed by the combination of one or more molecules of water with one molecule of the substance in which the water retains its molecular state as H_2O.

Chemicals as named or depicted are intended to include all naturally occurring isotopes of atoms occurring in the present compounds. Isotopes include those atoms having the same atomic number but different mass numbers. By way of general example and without limitation, isotopes of ^{1}H hydrogen include tritium and deuterium, and isotopes of ^{12}C carbon include ^{13}C and ^{14}C.

It will be understood that some compounds, and isomers, salts, esters and solvates thereof, of the compounds disclosed herein may exhibit greater in vivo or in vitro activity than others. It will also be appreciated that some cancers may be treated more effectively than others, and may be treated more effectively in certain species of subjects that others, using the compounds, and isomers, salts, esters and solvates thereof, of the compounds disclosed herein.

As used herein, "treating" means administering to a subject a pharmaceutical composition to ameliorate, reduce or lessen the symptoms of a disease. As used herein, "treating" or "treat" describes the management and care of a subject for the purpose of combating a disease, condition, or disorder and includes the administration of a compound disclosed herein, or a pharmaceutically acceptable salt, polymorph or solvate thereof, to alleviate the symptoms or complications of a disease, condition or disorder, or to eliminate the disease, condition or disorder. The term "treat" may also include treatment of a cell in vitro or an animal model.

Treating cancer may result in a reduction in size of a tumor. A reduction in size of a tumor may also be referred to as "tumor regression." Preferably, after treatment, tumor size is reduced by 5% or greater relative to its size prior to treatment; more preferably, tumor size is reduced by 10% or greater; more preferably, reduced by 20% or greater; more preferably, reduced by 30% or greater; more preferably, reduced by 40% or greater; even more preferably, reduced by 50% or greater; and most preferably, reduced by greater than 75% or greater. Size of a tumor may be measured by any reproducible means of measurement. The size of a tumor may be measured as a diameter of the tumor.

Treating cancer may result in a reduction in tumor volume. Preferably, after treatment, tumor volume is reduced by 5% or greater relative to its size prior to treatment; more preferably, tumor volume is reduced by 10% or greater; more preferably, reduced by 20% or greater; more preferably, reduced by 30% or greater; more preferably, reduced by 40% or greater; even more preferably, reduced by 50% or greater; and most preferably, reduced by greater than 75% or greater. Tumor volume may be measured by any reproducible means of measurement.

Treating cancer may result in a decrease in number of tumors. Preferably, after treatment, tumor number is reduced by 5% or greater relative to number prior to treatment; more preferably, tumor number is reduced by 10% or greater; more preferably, reduced by 20% or greater; more preferably, reduced by 30% or greater; more preferably, reduced by 40% or greater; even more preferably, reduced by 50% or greater; and most preferably, reduced by greater than 75%. Number of tumors may be measured by any reproducible means of measurement. The number of tumors may be measured by counting tumors visible to the naked eye or at

a specified magnification. Preferably, the specified magnification is 2×, 3×, 4×, 5×, 10×, or 50×.

Treating cancer may result in a decrease in number of metastatic lesions in other tissues or organs distant from the primary tumor site. Preferably, after treatment, the number of metastatic lesions is reduced by 5% or greater relative to number prior to treatment; more preferably, the number of metastatic lesions is reduced by 10% or greater; more preferably, reduced by 20% or greater; more preferably, reduced by 30% or greater; more preferably, reduced by 40% or greater; even more preferably, reduced by 50% or greater; and most preferably, reduced by greater than 75%. The number of metastatic lesions may be measured by any reproducible means of measurement. The number of metastatic lesions may be measured by counting metastatic lesions visible to the naked eye or at a specified magnification. Preferably, the specified magnification is 2×, 3×, 4×, 5×, 10×, or 50×.

As used herein, "subject" or "subjects" refers to any animal, such as mammals including rodents (e.g., mice or rats), dogs, primates, lemurs or humans.

Treating cancer may result in an increase in average survival time of a population of treated subjects in comparison to a population receiving carrier alone. Preferably, the average survival time is increased by more than 30 days; more preferably, by more than 60 days; more preferably, by more than 90 days; and most preferably, by more than 120 days. An increase in average survival time of a population may be measured by any reproducible means. An increase in average survival time of a population may be measured, for example, by calculating for a population the average length of survival following initiation of treatment with an active compound. An increase in average survival time of a population may also be measured, for example, by calculating for a population the average length of survival following completion of a first round of treatment with an active compound.

Treating cancer may result in an increase in average survival time of a population of treated subjects in comparison to a population of untreated subjects. Preferably, the average survival time is increased by more than 30 days; more preferably, by more than 60 days; more preferably, by more than 90 days; and most preferably, by more than 120 days. An increase in average survival time of a population may be measured by any reproducible means. An increase in average survival time of a population may be measured, for example, by calculating for a population the average length of survival following initiation of treatment with an active compound. An increase in average survival time of a population may also be measured, for example, by calculating for a population the average length of survival following completion of a first round of treatment with an active compound.

Treating cancer may result in increase in average survival time of a population of treated subjects in comparison to a population receiving monotherapy with a drug that is not a compound disclosed herein, or a pharmaceutically acceptable salt thereof. Preferably, the average survival time is increased by more than 30 days; more preferably, by more than 60 days; more preferably, by more than 90 days; and most preferably, by more than 120 days. An increase in average survival time of a population may be measured by any reproducible means. An increase in average survival time of a population may be measured, for example, by calculating for a population the average length of survival following initiation of treatment with an active compound. An increase in average survival time of a population may also be measured, for example, by calculating for a population the average length of survival following completion of a first round of treatment with an active compound.

Treating cancer may result in a decrease in the mortality rate of a population of treated subjects in comparison to a population receiving carrier alone. Treating cancer may result in a decrease in the mortality rate of a population of treated subjects in comparison to an untreated population. Treating cancer may result in a decrease in the mortality rate of a population of treated subjects in comparison to a population receiving monotherapy with a drug that is not a compound disclosed herein, or a pharmaceutically acceptable salt, prodrug, metabolite, analog or derivative thereof. Preferably, the mortality rate is decreased by more than 2%; more preferably, by more than 5%; more preferably, by more than 10%; and most preferably, by more than 25%. A decrease in the mortality rate of a population of treated subjects may be measured by any reproducible means. A decrease in the mortality rate of a population may be measured, for example, by calculating for a population the average number of disease-related deaths per unit time following initiation of treatment with an active compound. A decrease in the mortality rate of a population may also be measured, for example, by calculating for a population the average number of disease-related deaths per unit time following completion of a first round of treatment with an active compound.

Treating cancer may result in a decrease in tumor growth rate. Preferably, after treatment, tumor growth rate is reduced by at least 5% relative to number prior to treatment; more preferably, tumor growth rate is reduced by at least 10%; more preferably, reduced by at least 20%; more preferably, reduced by at least 30%; more preferably, reduced by at least 40%; more preferably, reduced by at least 50%; even more preferably, reduced by at least 50%; and most preferably, reduced by at least 75%. Tumor growth rate may be measured by any reproducible means of measurement. Tumor growth rate may be measured according to a change in tumor diameter per unit time.

Treating cancer may result in a decrease in tumor regrowth, for example, following attempts to remove it surgically. Preferably, after treatment, tumor regrowth is less than 5%; more preferably, tumor regrowth is less than 10%; more preferably, less than 20%; more preferably, less than 30%; more preferably, less than 40%; more preferably, less than 50%; even more preferably, less than 50%; and most preferably, less than 75%. Tumor regrowth may be measured by any reproducible means of measurement. Tumor regrowth is measured, for example, by measuring an increase in the diameter of a tumor after a prior tumor shrinkage that followed treatment. A decrease in tumor regrowth is indicated by failure of tumors to reoccur after treatment has stopped.

Treating or preventing a cell proliferative disorder may result in a reduction in the rate of cellular proliferation. Preferably, after treatment, the rate of cellular proliferation is reduced by at least 5%; more preferably, by at least 10%; more preferably, by at least 20%; more preferably, by at least 30%; more preferably, by at least 40%; more preferably, by at least 50%; even more preferably, by at least 50%; and most preferably, by at least 75%. The rate of cellular proliferation may be measured by any reproducible means of measurement. The rate of cellular proliferation is measured, for example, by measuring the number of dividing cells in a tissue sample per unit time.

Treating or preventing a cell proliferative disorder may result in a reduction in the proportion of proliferating cells.

Preferably, after treatment, the proportion of proliferating cells is reduced by at least 5%; more preferably, by at least 10%; more preferably, by at least 20%; more preferably, by at least 30%; more preferably, by at least 40%; more preferably, by at least 50%; even more preferably, by at least 50%; and most preferably, by at least 75%. The proportion of proliferating cells may be measured by any reproducible means of measurement. Preferably, the proportion of proliferating cells is measured, for example, by quantifying the number of dividing cells relative to the number of nondividing cells in a tissue sample. The proportion of proliferating cells may be equivalent to the mitotic index.

Treating or preventing a cell proliferative disorder may result in a decrease in size of an area or zone of cellular proliferation. Preferably, after treatment, size of an area or zone of cellular proliferation is reduced by at least 5% relative to its size prior to treatment; more preferably, reduced by at least 10%; more preferably, reduced by at least 20%; more preferably, reduced by at least 30%; more preferably, reduced by at least 40%; more preferably, reduced by at least 50%; even more preferably, reduced by at least 50%; and most preferably, reduced by at least 75%. Size of an area or zone of cellular proliferation may be measured by any reproducible means of measurement. The size of an area or zone of cellular proliferation may be measured as a diameter or width of an area or zone of cellular proliferation.

Treating or preventing a cell proliferative disorder may result in a decrease in the number or proportion of cells having an abnormal appearance or morphology. Preferably, after treatment, the number of cells having an abnormal morphology is reduced by at least 5% relative to its size prior to treatment; more preferably, reduced by at least 10%; more preferably, reduced by at least 20%; more preferably, reduced by at least 30%; more preferably, reduced by at least 40%; more preferably, reduced by at least 50%; even more preferably, reduced by at least 50%; and most preferably, reduced by at least 75%. An abnormal cellular appearance or morphology may be measured by any reproducible means of measurement. An abnormal cellular morphology may be measured by microscopy, e.g., using an inverted tissue culture microscope. An abnormal cellular morphology may take the form of nuclear pleiomorphism.

As used herein, the term "alleviate" is meant to describe a process by which the severity of a sign or symptom of a disorder is decreased. Importantly, a sign or symptom may be alleviated without being eliminated. In a preferred embodiment, the administration of pharmaceutical compositions disclosed herein leads to the elimination of a sign or symptom, however, elimination is not required. Effective dosages are expected to decrease the severity of a sign or symptom. For instance, a sign or symptom of a disorder such as cancer, which may occur in multiple locations, is alleviated if the severity of the cancer is decreased within at least one of multiple locations.

As used herein, the term "severity" is meant to describe the potential of cancer to transform from a precancerous, or benign, state into a malignant state. Alternatively, or in addition, severity is meant to describe a cancer stage, for example, according to the TNM system (accepted by the International Union Against Cancer (UICC) and the Amerimay Joint Committee on Cancer (AJCC)) or by other art-recognized methods. Cancer stage refers to the extent or severity of the cancer, based on factors such as the location of the primary tumor, tumor size, number of tumors, and lymph node involvement (spread of cancer into lymph nodes). Alternatively, or in addition, severity is meant to describe the tumor grade by art-recognized methods (see, National Cancer Institute, www.cancer.gov). Tumor grade is a system used to classify cancer cells in terms of how abnormal they look under a microscope and how quickly the tumor is likely to grow and spread. Many factors are considered when determining tumor grade, including the structure and growth pattern of the cells. The specific factors used to determine tumor grade vary with each type of cancer. Severity also describes a histologic grade, also called differentiation, which refers to how much the tumor cells resemble normal cells of the same tissue type (see, National Cancer Institute, www.cancer.gov). Furthermore, severity describes a nuclear grade, which refers to the size and shape of the nucleus in tumor cells and the percentage of tumor cells that are dividing (see, National Cancer Institute, www.cancer.gov).

In another aspect of embodiments described herein, severity describes the degree to which a tumor has secreted growth factors, degraded the extracellular matrix, become vascularized, lost adhesion to juxtaposed tissues, or metastasized. Moreover, severity describes the number of locations to which a primary tumor has metastasized. Finally, severity includes the difficulty of treating tumors of varying types and locations. For example, inoperable tumors, those cancers which have greater access to multiple body systems (hematological and immunological tumors), and those which are the most resistant to traditional treatments are considered most severe. In these situations, prolonging the life expectancy of the subject and/or reducing pain, decreasing the proportion of cancerous cells or restricting cells to one system, and improving cancer stage/tumor grade/histological grade/nuclear grade are considered alleviating a sign or symptom of the cancer.

As used herein the term "symptom" is defined as an indication of disease, illness, injury, or that something is not right in the body. Symptoms are felt or noticed by the individual experiencing the symptom, but may not easily be noticed by non-health-care professionals.

A "pharmaceutical composition" is a formulation containing a compound disclosed herein in a form suitable for administration to a subject. In one embodiment, the pharmaceutical composition is in bulk or in unit dosage form. The unit dosage form is any of a variety of forms, including, for example, a capsule, an IV bag, a tablet, a single pump on an aerosol inhaler or a vial. The quantity of active ingredient (e.g., a formulation of the disclosed compound or salt, hydrate, solvate or isomer thereof) in a unit dose of composition is an effective amount and is varied according to the particular treatment involved. One skilled in the art will appreciate that it is sometimes necessary to make routine variations to the dosage depending on the age and condition of the patient. The dosage will also depend on the route of administration. A variety of routes are contemplated, including oral, pulmonary, rectal, parenteral, transdermal, subcutaneous, intravenous, intramuscular, intraperitoneal, inhalational, buccal, sublingual, intrapleural, intrathecal, intranasal, and the like. Dosage forms for the topical or transdermal administration of a compound disclosed herein include powders, sprays, ointments, pastes, creams, lotions, gels, solutions, patches and inhalants. In one embodiment, the active compound is mixed under sterile conditions with a pharmaceutically acceptable carrier, and with any preservatives, buffers, or propellants that are required.

As used herein, the phrase "pharmaceutically acceptable" refers to those compounds, anions, cations, materials, compositions, carriers, and/or dosage forms which are, within the scope of sound medical judgment, suitable for use in

contact with the tissues of human beings and animals without excessive toxicity, irritation, allergic response, or other problem or complication, commensurate with a reasonable benefit/risk ratio.

"Pharmaceutically acceptable excipient" means an excipient that is useful in preparing a pharmaceutical composition that is generally safe, non-toxic and neither biologically nor otherwise undesirable, and includes excipient that is acceptable for veterinary use as well as human pharmaceutical use. A "pharmaceutically acceptable excipient" as used in the specification and claims includes both one and more than one such excipient.

The present disclosure also provides pharmaceutical compositions comprising any compound disclosed herein in combination with at least one pharmaceutically acceptable excipient or carrier.

A pharmaceutical composition disclosed herein is formulated to be compatible with its intended route of administration. Examples of routes of administration include parenteral, e.g., intravenous, intradermal, subcutaneous, oral (e.g., inhalation), transdermal (topical), and transmucosal administration. Solutions or suspensions used for parenteral, intradermal, or subcutaneous application may include the following components: a sterile diluent such as water for injection, saline solution, fixed oils, polyethylene glycols, glycerine, propylene glycol or other synthetic solvents; antibacterial agents such as benzyl alcohol or methyl parabens; antioxidants such as ascorbic acid or sodium bisulfite; chelating agents such as ethylenediaminetetraacetic acid; buffers such as acetates, citrates or phosphates, and agents for the adjustment of tonicity such as sodium chloride or dextrose. The pH may be adjusted with acids or bases, such as hydrochloric acid or sodium hydroxide. The parenteral preparation may be enclosed in ampoules, disposable syringes or multiple dose vials made of glass or plastic.

A compound or pharmaceutical composition disclosed herein may be administered to a subject in many of the well-known methods currently used for chemotherapeutic treatment. For example, for treatment of cancers, a compound disclosed herein may be injected directly into tumors, injected into the blood stream or body cavities or taken orally or applied through the skin with patches. The dose chosen should be sufficient to constitute effective treatment but not so high as to cause unacceptable side effects. The state of the disease condition (e.g., cancer, precancer, and the like) and the health of the patient should preferably be closely monitored during and for a reasonable period after treatment.

The term "therapeutically effective amount", as used herein, refers to an amount of a pharmaceutical agent to treat, ameliorate, or prevent an identified disease or condition, or to exhibit a detectable therapeutic or inhibitory effect. The effect may be detected by any assay method known in the art. The precise effective amount for a subject will depend upon the subject's body weight, size, and health; the nature and extent of the condition; and the therapeutic or combination of therapeutics selected for administration. Therapeutically effective amounts for a given situation may be determined by routine experimentation that is within the skill and judgment of the clinician. In a preferred aspect, the disease or condition to be treated is cancer. In another aspect, the disease or condition to be treated is a cell proliferative disorder.

For any compound, the therapeutically effective amount may be estimated initially either in cell culture assays, e.g., of neoplastic cells, or in animal models, usually rats, mice, rabbits, dogs, or pigs. The animal model may also be used to determine the appropriate concentration range and route of administration. Such information may then be used to determine useful doses and routes for administration in humans. Therapeutic/prophylactic efficacy and toxicity may be determined by standard pharmaceutical procedures in cell cultures or experimental animals, e.g., ED_{50} (the dose therapeutically effective in 50% of the population) and LD_{50} (the dose lethal to 50% of the population). The dose ratio between toxic and therapeutic effects is the therapeutic index, and it may be expressed as the ratio, LD_{50}/ED_{50}. Pharmaceutical compositions that exhibit large therapeutic indices are preferred. The dosage may vary within this range depending upon the dosage form employed, sensitivity of the patient, and the route of administration.

Dosage and administration are adjusted to provide sufficient levels of the active agent(s) or to maintain the desired effect. Factors which may be taken into account include the severity of the disease state, general health of the subject, age, weight, and gender of the subject, diet, time and frequency of administration, drug combination(s), reaction sensitivities, and tolerance/response to therapy. Long-acting pharmaceutical compositions may be administered every 3 to 4 days, every week, or once every two weeks depending on half-life and clearance rate of the particular formulation.

The pharmaceutical compositions containing active compounds disclosed herein may be manufactured in a manner that is generally known, e.g., by means of conventional mixing, dissolving, granulating, dragee-making, levigating, emulsifying, encapsulating, entrapping, or lyophilizing processes. Pharmaceutical compositions may be formulated in a conventional manner using one or more pharmaceutically acceptable carriers comprising excipients and/or auxiliaries that facilitate processing of the active compounds into preparations that may be used pharmaceutically. Of course, the appropriate formulation is dependent upon the route of administration chosen.

Pharmaceutical compositions suitable for injectable use include sterile aqueous solutions (where water soluble) or dispersions and sterile powders for the extemporaneous preparation of sterile injectable solutions or dispersion. For intravenous administration, suitable carriers include physiological saline, bacteriostatic water, Cremophor EL™ (BASF, Parsippany, N.J.) or phosphate buffered saline (PBS). In all cases, the composition must be sterile and should be fluid to the extent that easy syringeability exists. It must be stable under the conditions of manufacture and storage and must be preserved against the contaminating action of microorganisms such as bacteria and fungi. The carrier may be a solvent or dispersion medium containing, for example, water, ethanol, polyol (for example, glycerol, propylene glycol, and liquid polyethylene glycol, and the like), and suitable mixtures thereof. The proper fluidity may be maintained, for example, by the use of a coating such as lecithin, by the maintenance of the required particle size in the case of dispersion and by the use of surfactants. Prevention of the action of microorganisms may be achieved by various antibacterial and antifungal agents, for example, parabens, chlorobutanol, phenol, ascorbic acid, thimerosal, and the like. In many cases, it will be preferable to include isotonic agents, for example, sugars, polyalcohols such as mannitol and sorbitol, and sodium chloride in the composition. Prolonged absorption of the injectable compositions may be brought about by including in the composition an agent which delays absorption, for example, aluminum monostearate and gelatin.

Sterile injectable solutions may be prepared by incorporating the active compound in the required amount in an

appropriate solvent with one or a combination of ingredients enumerated above, as required, followed by filtered sterilization. Generally, dispersions are prepared by incorporating the active compound into a sterile vehicle that contains a basic dispersion medium and the required other ingredients from those enumerated above. In the case of sterile powders for the preparation of sterile injectable solutions, methods of preparation are vacuum drying and freeze-drying that yields a powder of the active ingredient plus any additional desired ingredient from a previously sterile-filtered solution thereof.

Oral compositions generally include an inert diluent or an edible pharmaceutically acceptable carrier. They may be enclosed in gelatin capsules or compressed into tablets. For the purpose of oral therapeutic administration, the active compound may be incorporated with excipients and used in the form of tablets, troches, or capsules. Oral compositions may also be prepared using a fluid carrier for use as a mouthwash, wherein the compound in the fluid carrier is applied orally and swished and expectorated or swallowed. Pharmaceutically compatible binding agents, and/or adjuvant materials may be included as part of the composition. The tablets, pills, capsules, troches and the like may contain any of the following ingredients, or compounds of a similar nature: a binder such as microcrystalline cellulose, gum tragacanth or gelatin; an excipient such as starch or lactose, a disintegrating agent such as alginic acid, Primogel, or corn starch; a lubricant such as magnesium stearate or Sterotes; a glidant such as colloidal silicon dioxide; a sweetening agent such as sucrose or saccharin; or a flavoring agent such as peppermint, methyl salicylate, or orange flavoring.

The active compounds may be prepared with pharmaceutically acceptable carriers that will protect the compound against rapid elimination from the body, such as a controlled release formulation, including implants and microencapsulated delivery systems. Biodegradable, biocompatible polymers may be used, such as ethylene vinyl acetate, polyanhydrides, polyglycolic acid, collagen, polyorthoesters, and polylactic acid. Methods for preparation of such formulations will be apparent to those skilled in the art.

It is especially advantageous to formulate oral or parenteral compositions in dosage unit form for ease of administration and uniformity of dosage. Dosage unit form as used herein refers to physically discrete units suited as unitary dosages for the subject to be treated; each unit containing a predetermined quantity of active compound calculated to produce the desired therapeutic effect in association with the required pharmaceutical carrier. The specification for the dosage unit forms of the compounds disclosed herein are dictated by and directly dependent on the unique characteristics of the active compound and the particular therapeutic effect to be achieved.

In therapeutic applications, the dosages of the pharmaceutical compositions used in accordance with embodiments described herein vary depending on the agent, the age, weight, and clinical condition of the recipient patient, and the experience and judgment of the clinician or practitioner administering the therapy, among other factors affecting the selected dosage. Generally, the dose should be sufficient to result in slowing, and preferably regressing, the growth of the tumors and also preferably causing complete regression of the cancer. Dosages may range from about 0.01 mg/kg per day to about 5000 mg/kg per day. In preferred aspects, dosages may range from about 1 mg/kg per day to about 1000 mg/kg per day. In an aspect, the dose will be in the range of about 0.1 mg/day to about 50 g/day; about 0.1 mg/day to about 25 g/day; about 0.1 mg/day to about 10 g/day; about 0.1 mg to about 3 g/day; or about 0.1 mg to about 1 g/day, in single, divided, or continuous doses (which dose may be adjusted for the patient's weight in kg, body surface area in m^2, and age in years). An effective amount of a pharmaceutical agent is that which provides an objectively identifiable improvement as noted by the clinician or other qualified observer. For example, regression of a tumor in a patient may be measured with reference to the diameter of a tumor. Decrease in the diameter of a tumor indicates regression. Regression is also indicated by failure of tumors to reoccur after treatment has stopped. As used herein, the term "dosage effective manner" refers to amount of an active compound to produce the desired biological effect in a subject or cell.

The pharmaceutical compositions may be included in a container, pack, or dispenser together with instructions for administration.

Techniques for formulation and administration of the compounds disclosed herein may be found in Remington: the Science and Practice of Pharmacy, 19th edition, Mack Publishing Co., Easton, Pa. (1995). In an embodiment, the compounds described herein, and the pharmaceutically acceptable salts thereof, may be used in pharmaceutical preparations in combination with a pharmaceutically acceptable carrier or diluent. Suitable pharmaceutically acceptable carriers include inert solid fillers or diluents and sterile aqueous or organic solutions. The compounds will be present in such pharmaceutical compositions in amounts sufficient to provide the desired dosage amount in the range described herein.

Exemplary cancers that may be treated using one or more compounds disclosed herein include, but are not limited to, breast cancer, uterine endometrial, ovarian carcinoma, sarcoma, thyroid carcinoma, prostate, lung adenocarcinoma, and hepatocellular carcinoma.

In embodiments, the compounds disclosed herein may be useful for treating breast cancer. In embodiments, the breast cancer is ER-α+. In embodiments, the breast cancer expresses an ER-α mutation, which may be L536Q (Robinson et al. *Nat Genet.* 2013 December; 45(12)), L536R (Toy et al. *Nat Genet.* 2013 December; 45(12):1439-45), Y537S (Toy et al. *Nat Genet.* 2013 December; 45(12):1439-45; Robinson et al. *Nat Genet.* 2013 December; 45(12); Jeselsohn et al. *Clin Cancer Res.* 2014 Apr. 1; 20(7):1757-67), Y537N (Toy et al. *Nat Genet.* 2013 December; 45(12): 1439-45; Jeselsohn et al. *Clin Cancer Res.* 2014 Apr. 1; 20(7):1757-67), Y537C (Toy et al. *Nat Genet.* 2013 December; 45(12):1439-45; Jeselsohn et al. *Clin Cancer Res.* 2014 Apr. 1; 20(7):1757-67) and D538G (Toy et al. *Nat Genet.* 2013 December; 45(12):1439-45; Robinson et al. *Nat Genet.* 2013 December; 45(12); Jeselsohn et al. *Clin Cancer Res.* 2014 Apr. 1; 20(7):1757-67; Merenbakh-Lamin et al. *Cancer Res.* 2013 Dec. 1; 73(23):6856-64), all of which are incorporated by reference in their entireties for their teachings of ER-α mutations.

Thus, the compounds disclosed herein may be also useful for additional indications and genotypes. ESR1 mutations (Y537C/N) were recently discovered in 4 of 373 cases of endometrial cancers (Kandoth et al. *Nature* 2013 May 2; 497(7447):67-73; Robinson et al. *Nat Genet.* 2013 December; 45(12)). Since it has been shown that ESR1 mutations Y537C/N significantly drive resistance to currently marketed SOC therapies, the compounds disclosed herein may be useful for treating $ER\alpha^{MUT}$ endometrial cancers.

Exemplary cell proliferative disorders that may be treated using one or more compounds disclosed herein include, but are not limited to breast cancer, a precancer or precancerous condition of the breast, benign growths or lesions of the breast, and malignant growths or lesions of the breast, and metastatic lesions in tissue and organs in the body other than the breast. Cell proliferative disorders of the breast may include hyperplasia, metaplasia, and dysplasia of the breast.

A breast cancer that is to be treated may arise in a male or female subject. A breast cancer that is to be treated may arise in a premenopausal female subject or a postmenopausal female subject. A breast cancer that is to be treated

may arise in a subject 30 years old or older, or a subject younger than 30 years old. A breast cancer that is to be treated has arisen in a subject 50 years old or older, or a subject younger than 50 years old. A breast cancer that is to be treated may arise in a subject 70 years old or older, or a subject younger than 70 years old.

A compound disclosed herein, or a pharmaceutically acceptable salt thereof, may be used to treat or prevent a cell proliferative disorder of the breast, or to treat or prevent breast cancer, in a subject having an increased risk of developing breast cancer relative to the population at large, or used to identify suitable candidates for such purposes. A subject with an increased risk of developing breast cancer relative to the population at large is a female subject with a family history or personal history of breast cancer. A subject with an increased risk of developing breast cancer relative to the population at large is a female who is greater than 30 years old, greater than 40 years old, greater than 50 years old, greater than 60 years old, greater than 70 years old, greater than 80 years old, or greater than 90 years old.

A cancer that is to be treated may include a tumor that has been determined to be less than or equal to about 2 centimeters in diameter. A cancer that is to be treated may include a tumor that has been determined to be from about 2 to about 5 centimeters in diameter. A cancer that is to be treated may include a tumor that has been determined to be greater than or equal to about 3 centimeters in diameter. A cancer that is to be treated may include a tumor that has been determined to be greater than 5 centimeters in diameter. A cancer that is to be treated may be classified by microscopic appearance as well differentiated, moderately differentiated, poorly differentiated, or undifferentiated. A cancer that is to be treated may be classified by microscopic appearance with respect to mitosis count (e.g., amount of cell division) or nuclear pleiomorphism (e.g., change in cells). A cancer that is to be treated may be classified by microscopic appearance as being associated with areas of necrosis (e.g., areas of dying or degenerating cells). A cancer that is to be treated may be classified as having an abnormal karyotype, having an abnormal number of chromosomes, or having one or more chromosomes that are abnormal in appearance. A cancer that is to be treated may be classified as being aneuploid, triploid, tetraploid, or as having an altered ploidy. A cancer that is to be treated may be classified as having a chromosomal translocation, or a deletion or duplication of an entire chromosome, or a region of deletion, duplication or amplification of a portion of a chromosome.

The compounds, or pharmaceutically acceptable salts thereof may be administered orally, nasally, transdermally, pulmonary, inhalationally, buccally, sublingually, intraperintoneally, subcutaneously, intramuscularly, intravenously, rectally, intrapleurally, intrathecally and parenterally. In one embodiment, the compound is administered orally. One skilled in the art will recognize the advantages of certain routes of administration.

The dosage regimen utilizing the compounds may be selected in accordance with a variety of factors including type, species, age, weight, sex and medical condition of the patient; the severity of the condition to be treated; the route of administration; the renal and hepatic function of the patient; and the particular compound or salt thereof employed. An ordinarily skilled physician or veterinarian may readily determine and prescribe the effective amount of the drug required to prevent, counter, or arrest the progress of the condition.

EXAMPLES

Hereby are provided non-limiting examples of embodiments of compounds disclosed herein. If there is any discrepancy between a compound's depicted chemical structure and its chemical name, the depicted chemical structure will control.

TABLE 1

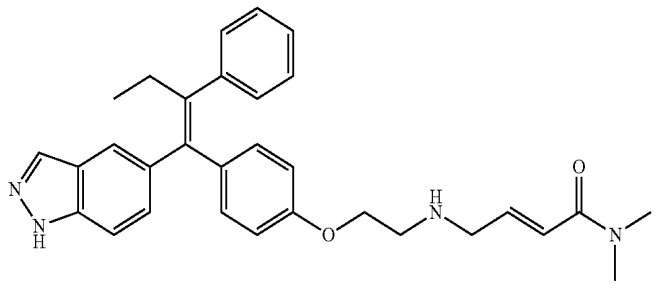
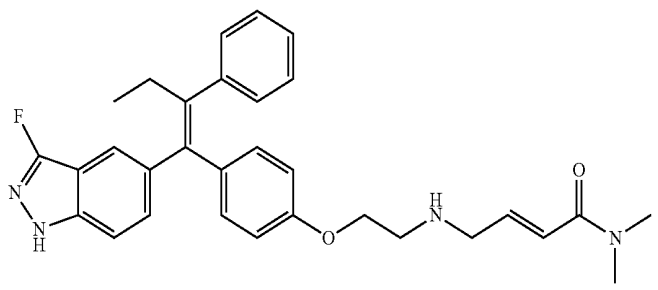
Compound #	Structure	GI50 WT (nM)	GI50 MUT (Y537S) (nM)
1		1.69 ± 0.54 (2)	20.59 ± 7.01 (2)
2		5.56 ± 2.84 (2)	64.85 ± 37.24 (2)

TABLE 1-continued

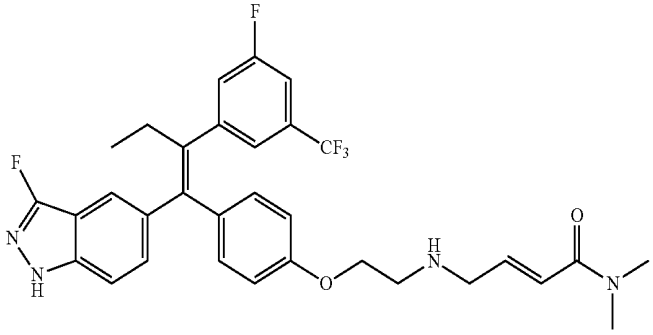
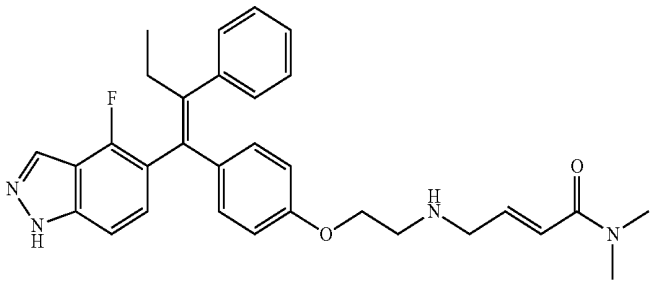
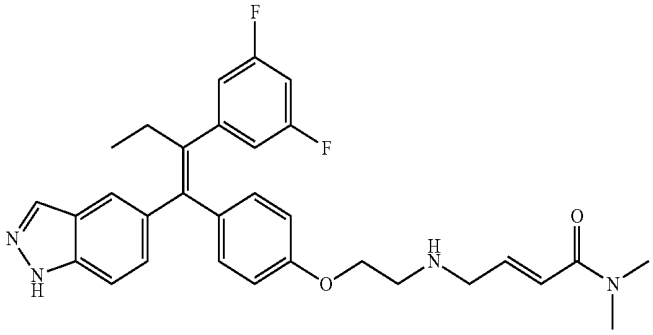
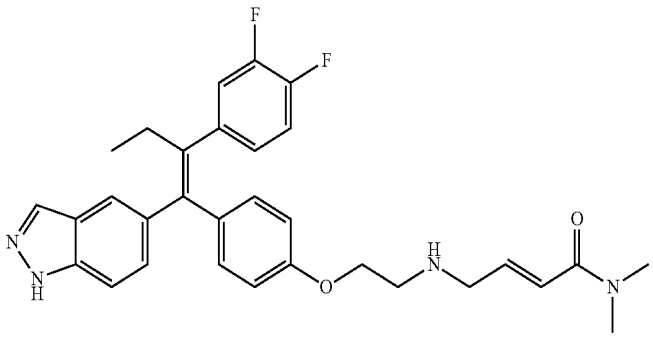
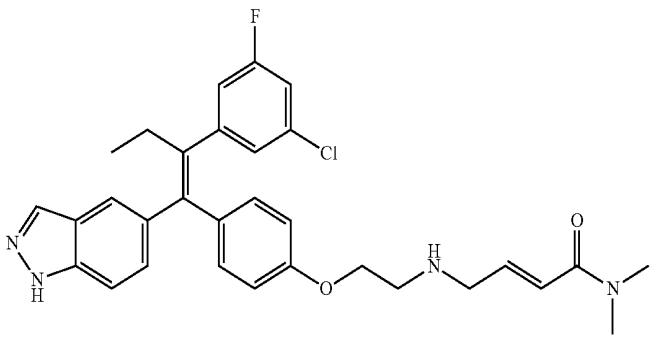
Compound #	Structure	GI50 WT (nM)	GI50 MUT (Y537S) (nM)
3		6.95 ± 2.47 (2)	159.04 ± 91.80 (2)
4		4.55 ± 3.34 (2)	36.29 ± 15.99 (2)
5		8.44 ± 3.87 (2)	81.42 ± 45.75 (2)
6		2.93 ± 2.83 (2)	111.21 ± 124.43 (2)
7		1.92	74.09 ± 55.2 (2)

TABLE 1-continued

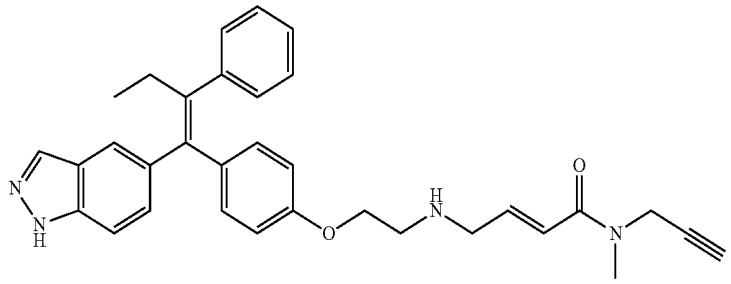
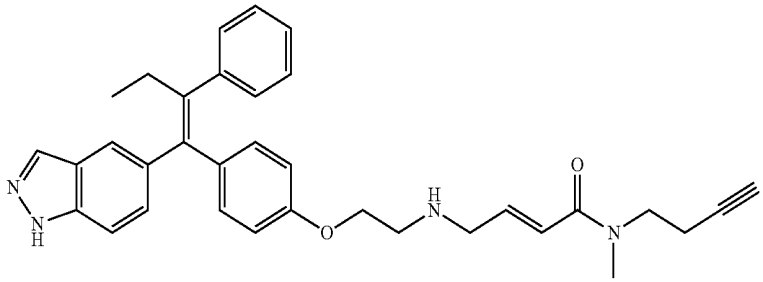
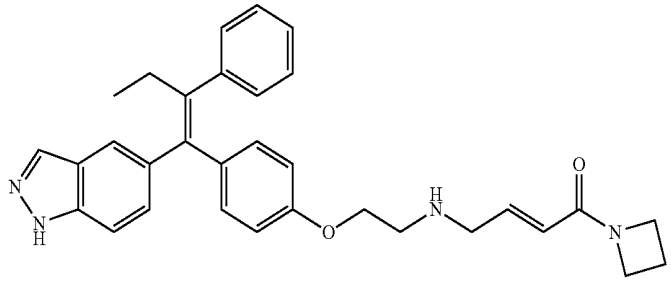
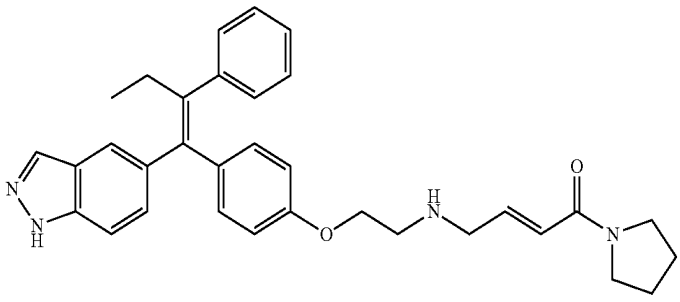
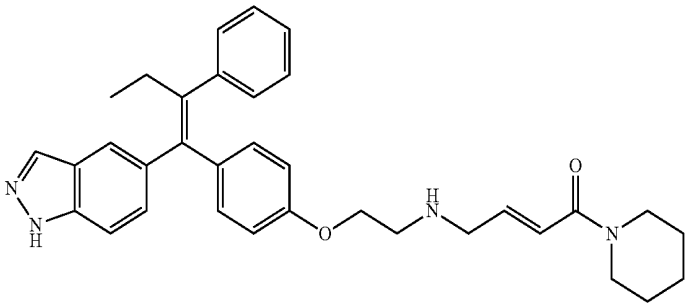
Compound #	Structure	GI50 WT (nM)	GI50 MUT (Y537S) (nM)
8		1.59	22.31
9		5.57	117.8
10		2.22 ± 2.34 (3)	21.22 ± 17.22 (3)
11		0.76	13.97
12		1.69	36.68

TABLE 1-continued

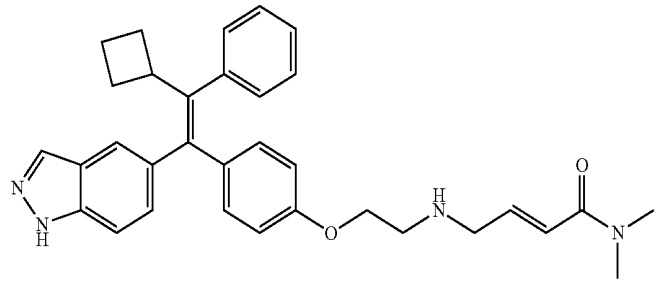
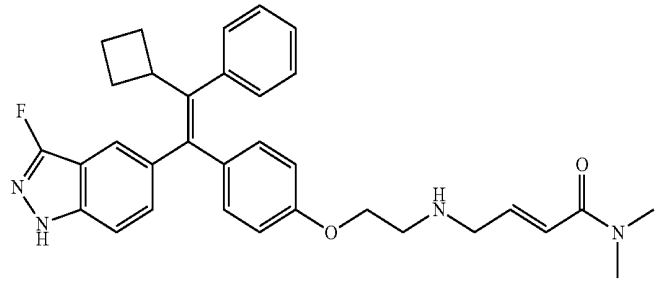
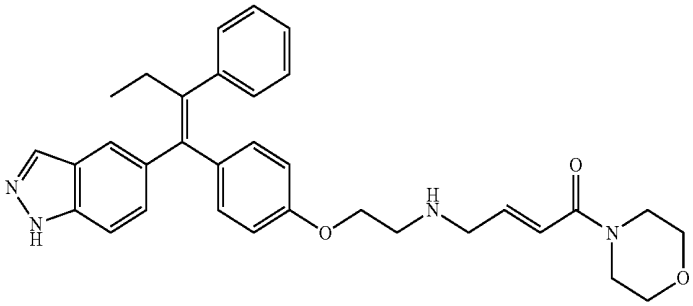
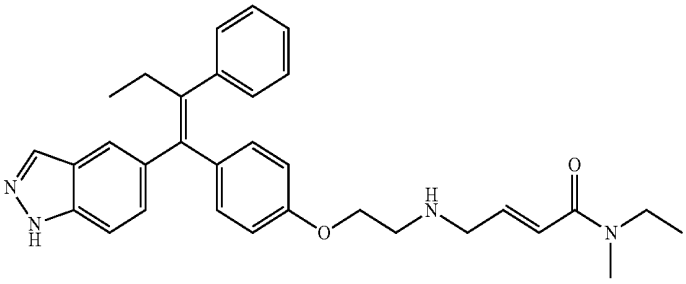
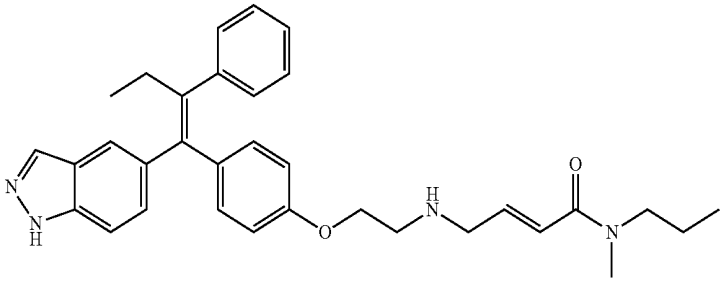
Compound #	Structure	GI50 WT (nM)	GI50 MUT (Y537S) (nM)
13		2.08 ± 1.57 (3)	20.02 ± 13.71 (3)
14		2.46 ± 1.43 (2)	30.67 ± 4.02 (2)
15		1.84 ± 1.09 (3)	25.53 ± 13.78 (3)
16		1.66	21.89
17		2.18	25.18

TABLE 1-continued

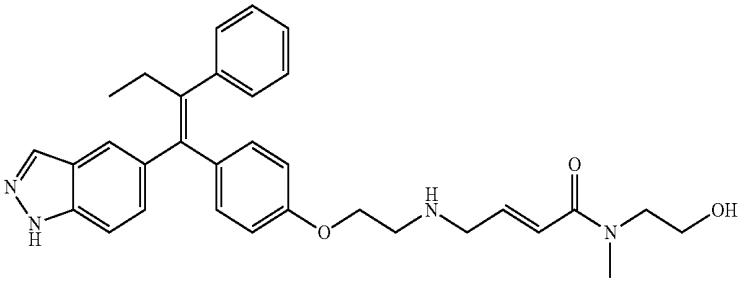
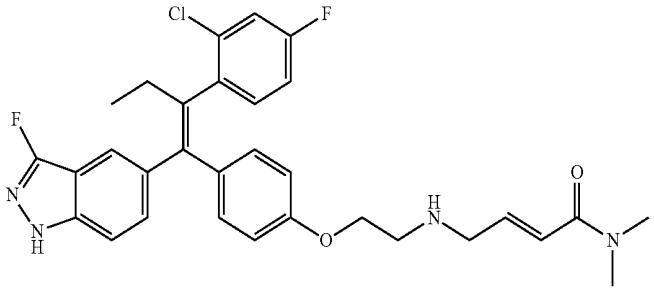
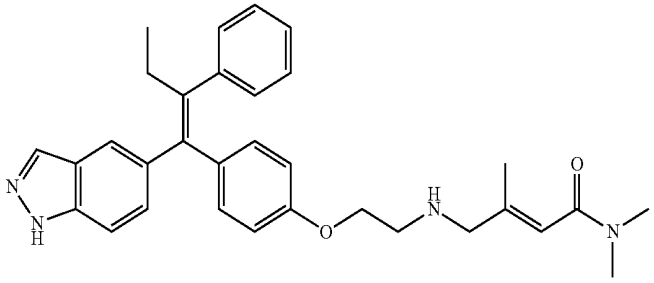
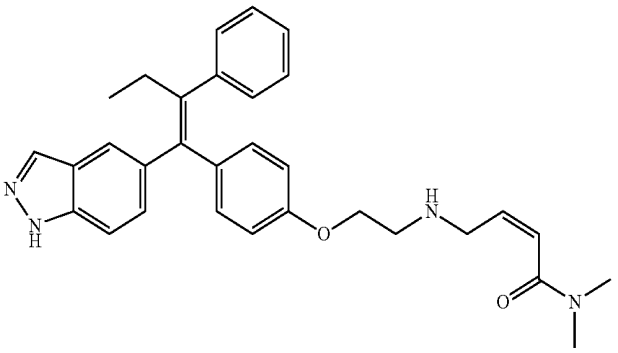
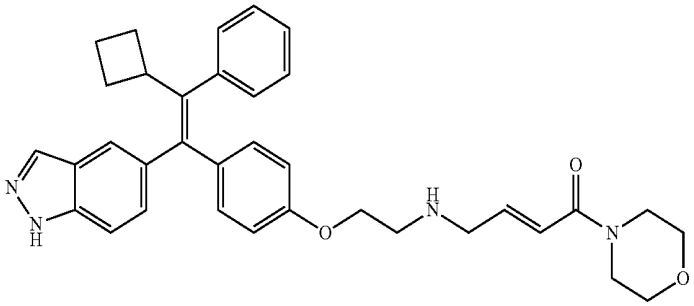
Compound #	Structure	GI50 WT (nM)	GI50 MUT (Y537S) (nM)
18		1.63 ± 1.41 (3)	21.35 ± 15.03 (3)
19		1.58	18.57
21		26.57 ± 21.84 (2)	153.62 ± 51.68 (2)
22		2.42 ± 1.95 (2)	21.64 ± 0.26 (2)
23		1.52 ± 1.05 (2)	24.23 ± 6.57 (2)

TABLE 1-continued

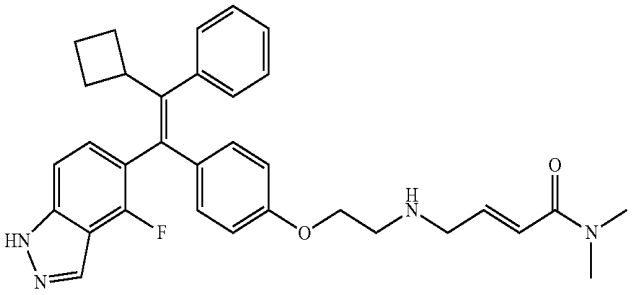
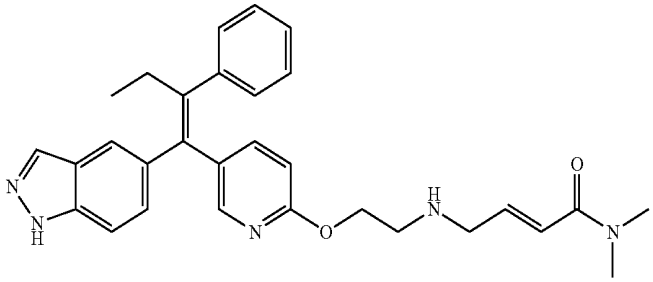
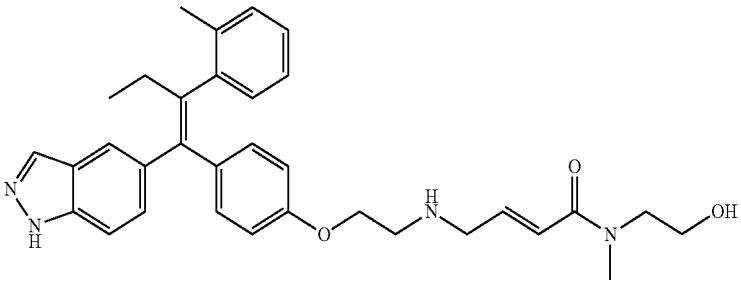
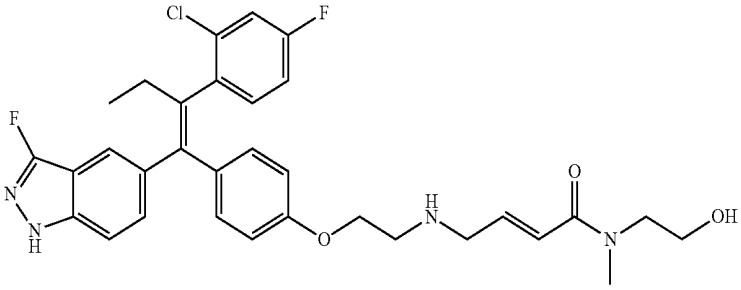
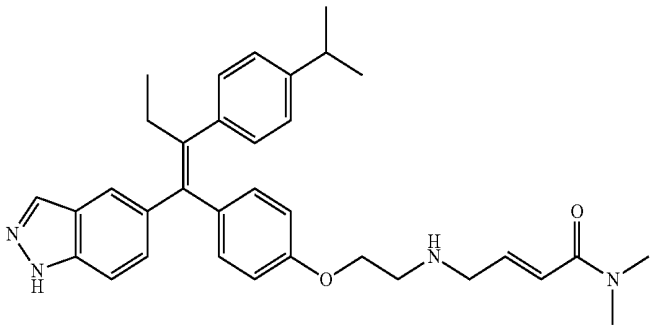
Compound #	Structure	GI50 WT (nM)	GI50 MUT (Y537S) (nM)
24		1.05 ± 0.30 (2)	19.86 ± 3.58 (2)
25		1.15 ± 0.30 (2)	19.64 ± 4.26 (2)
26		2.18 ± 0.87 (2)	32.48 ± 16.72 (2)
28		3.16	69.7
29		3.37	58.66

TABLE 1-continued

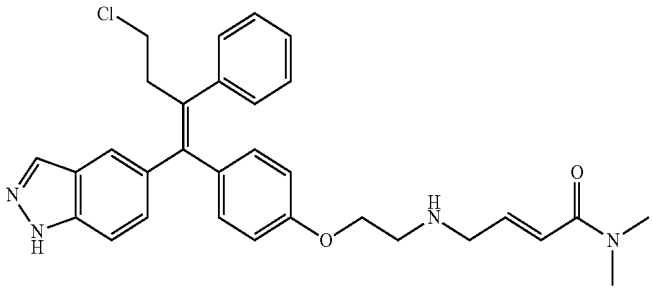
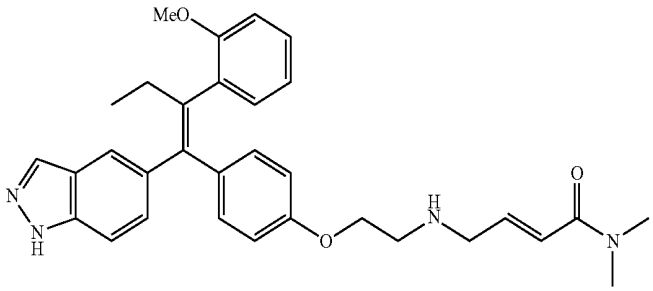
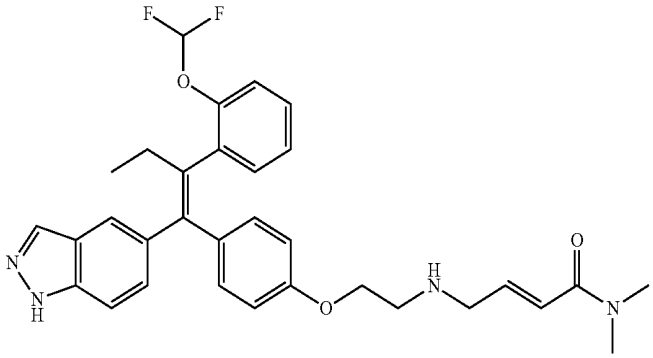
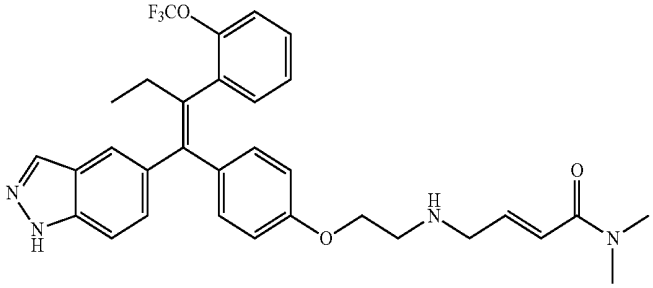
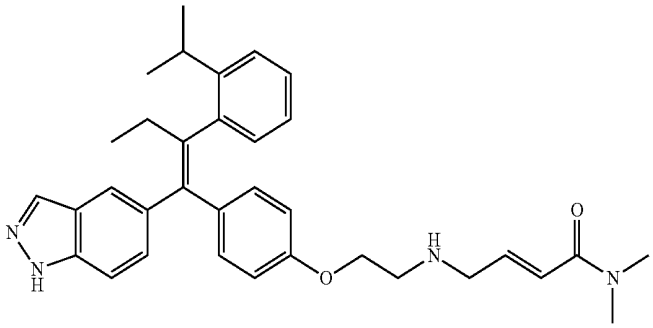
Compound #	Structure	GI50 WT (nM)	GI50 MUT (Y537S) (nM)
30		2.74 ± 1.06 (2)	61.26 ± 9.98 (2)
31		0.83	13.09
32		1.28	22.89
33		2.5	29.3
34		10.52	93.62

TABLE 1-continued

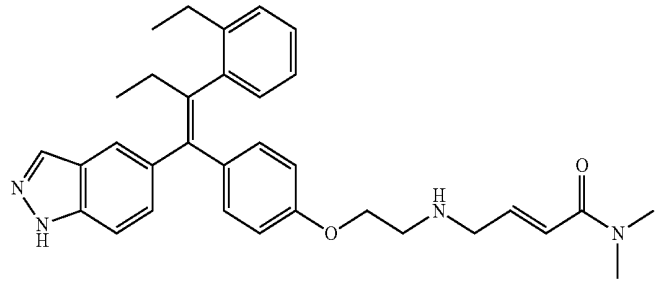
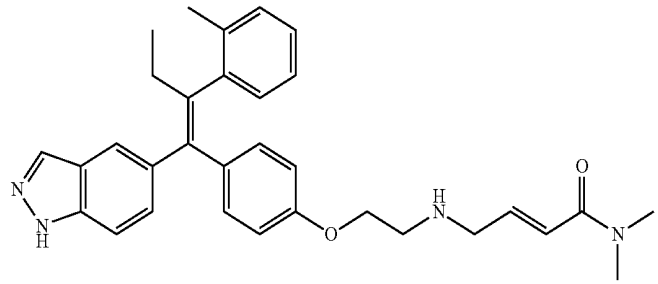
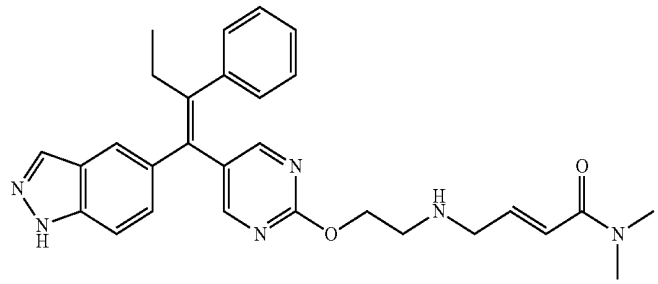
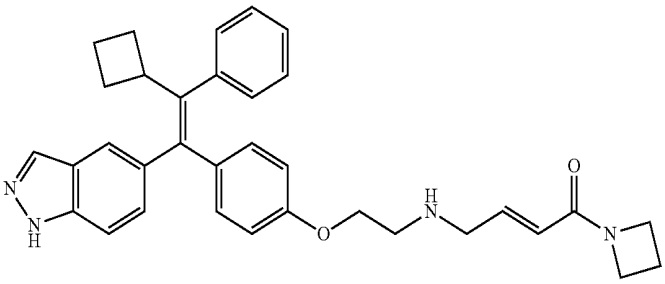
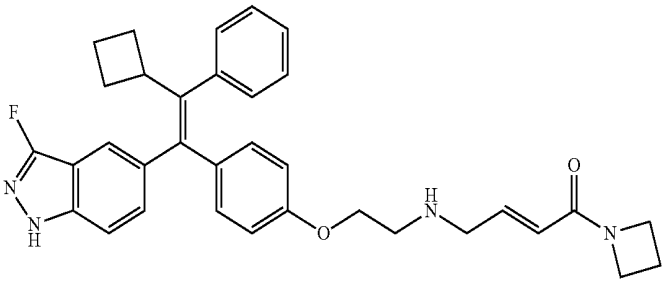
Compound #	Structure	GI50 WT (nM)	GI50 MUT (Y537S) (nM)
35		6.22 ± 0.58 (2)	47.82 ± 15.58 (2)
36		4.96 ± 3.10 (3)	25.04 ± 21.87 (3)
38		8.23 ± 5.32 (3)	158.56 ± 127.8 (3)
39		1.79 ± 0.47 (2)	31.82 ± 4.85 (2)
40		7.52 ± 4.52 (3)	94.55 ± 20.82 (3)

TABLE 1-continued

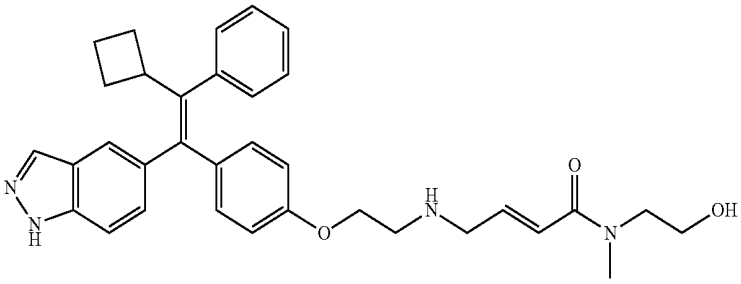
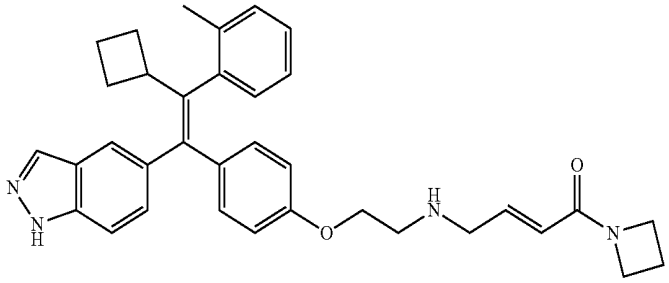
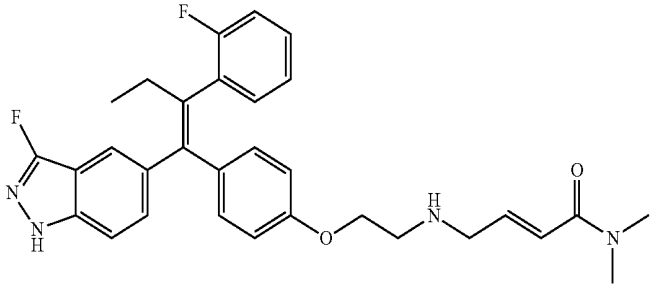
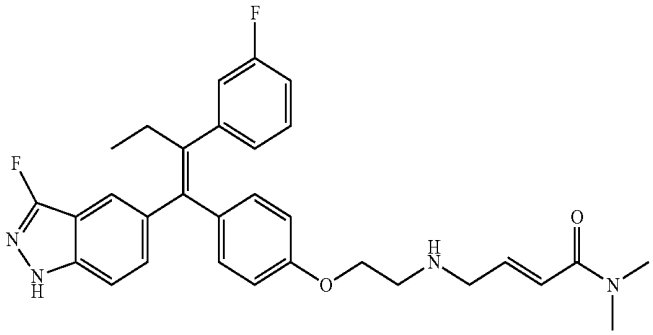
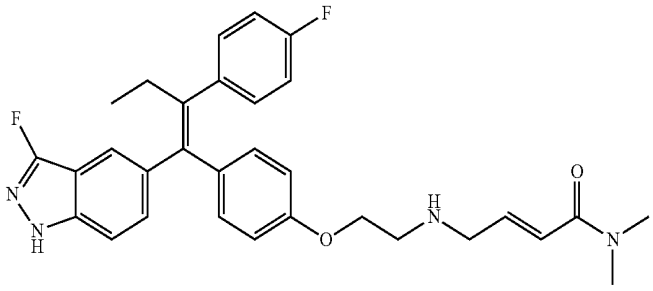
Compound #	Structure	GI50 WT (nM)	GI50 MUT (Y537S) (nM)
41		3.84	66.31
42		2.68 ± 1.66 (2)	69.43 ± 29.08 (2)
43		1.94	47.31
44		4.91	179.86
45		4.14	103.76

TABLE 1-continued

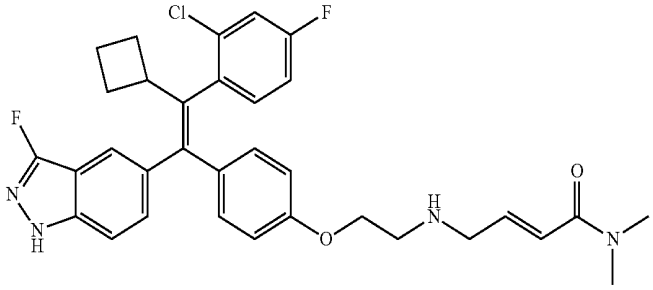
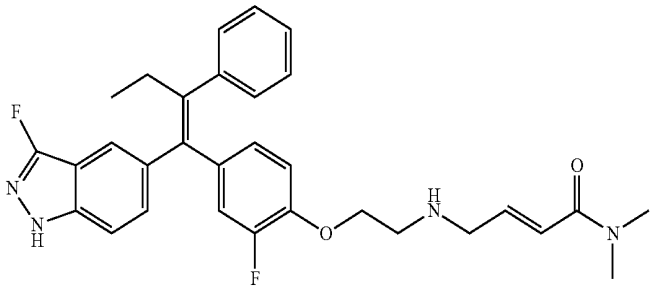
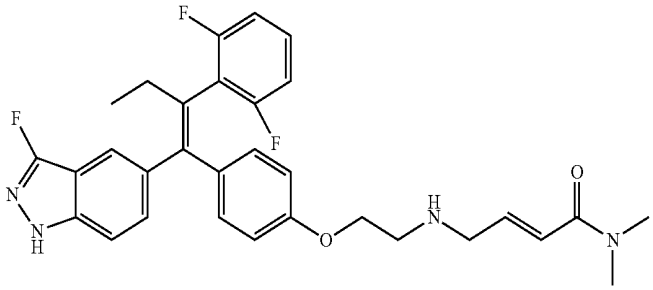
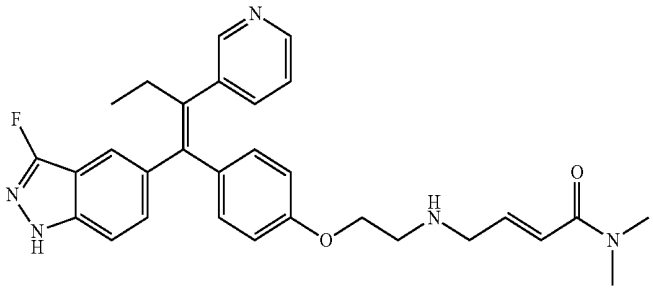
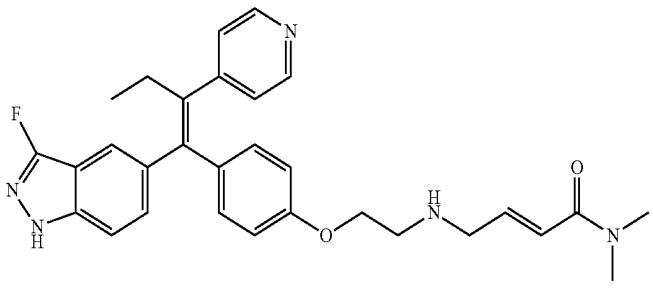
Compound #	Structure	GI50 WT (nM)	GI50 MUT (Y537S) (nM)
46		0.95	12.36
49		5.4	288.09
50		2.46	67.53
51		20.89	347
52		2.9	85.75

TABLE 1-continued

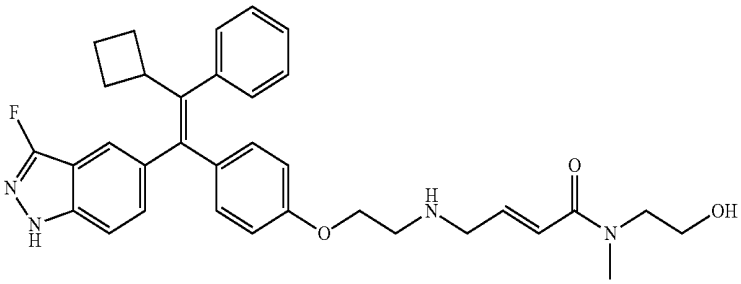
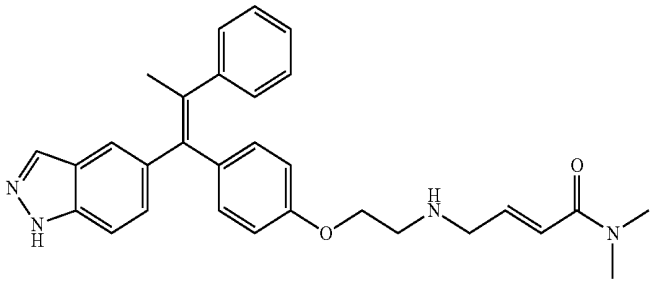
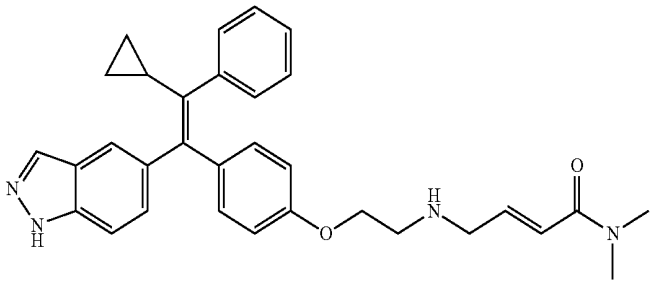
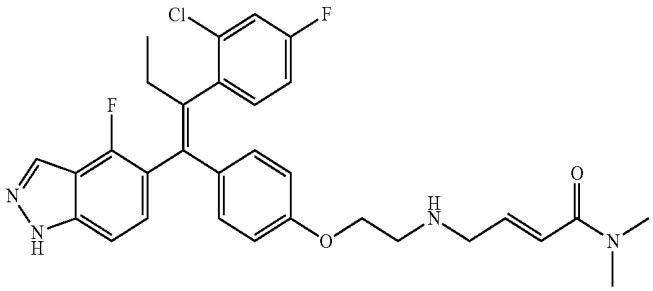
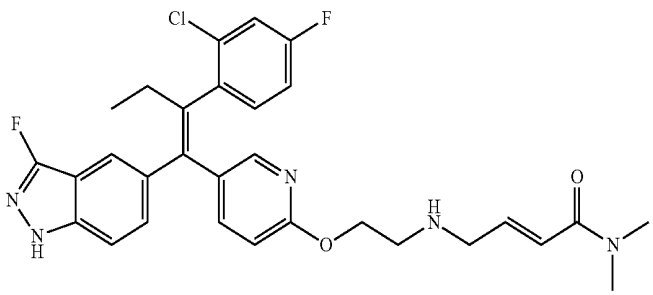
Compound #	Structure	GI50 WT (nM)	GI50 MUT (Y537S) (nM)
53		3.59	76.55
54		7.97 ± 1.65 (2)	160.02 ± 39.63 (2)
56		3.78 ± 1.75 (2)	63.59 ± 18.38 (2)
57		1.9	36.2
58		1.3 ± 0.4 (n = 2)	17.9 ± 4.5 (n = 2)

TABLE 1-continued

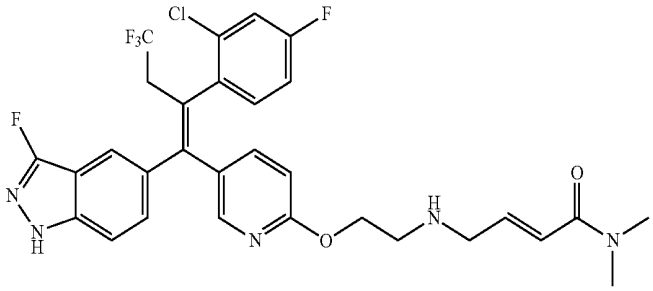
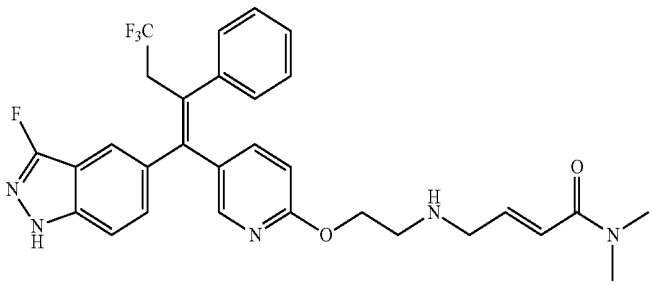
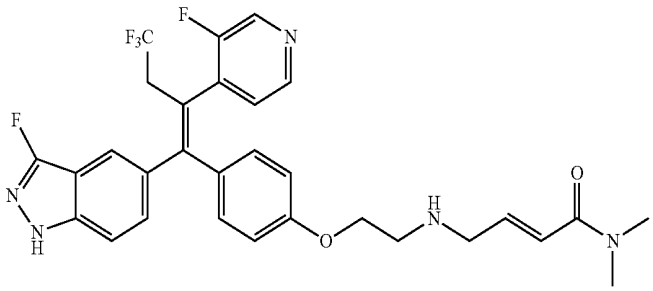
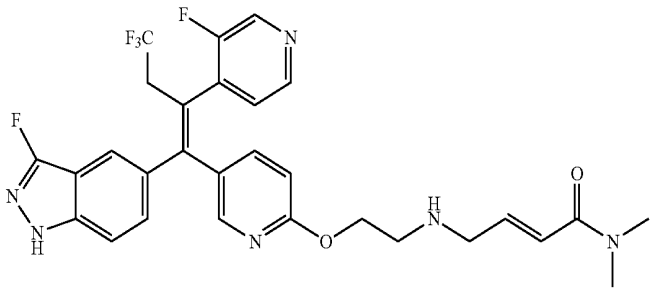
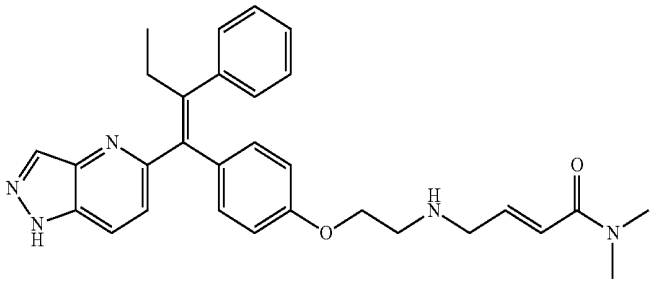
Compound #	Structure	GI50 WT (nM)	GI50 MUT (Y537S) (nM)
59		0.33 ± 0.18 (n = 2)	15.24 ± 3.7 (n = 2)
60		0.34	4.26
61		0.30 ± 0.1 (n = 2)	4.0 ± 1.5 (n = 2)
62		0.3	1.3
63		2.8	65.7

TABLE 1-continued

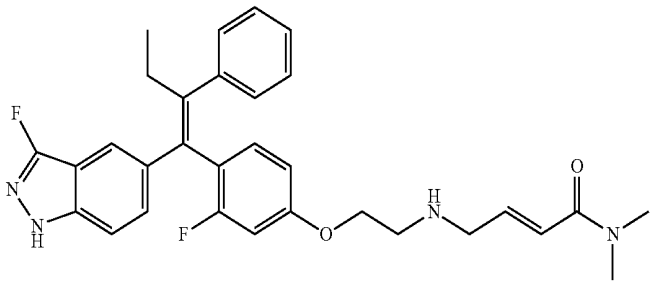
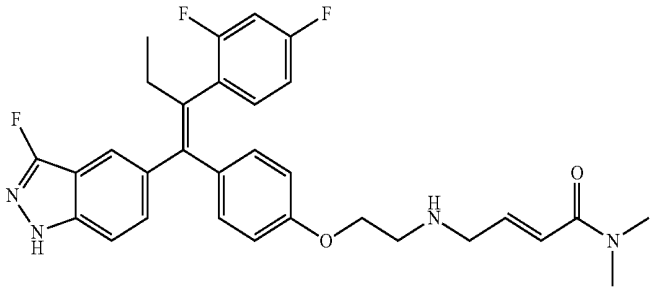
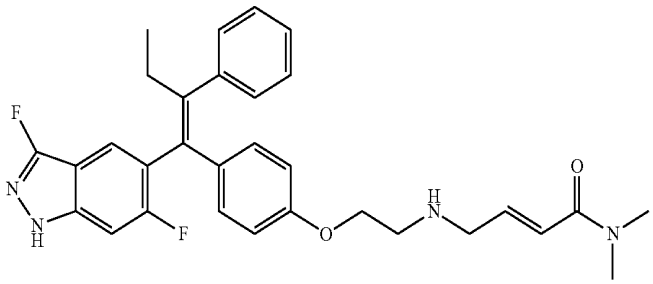
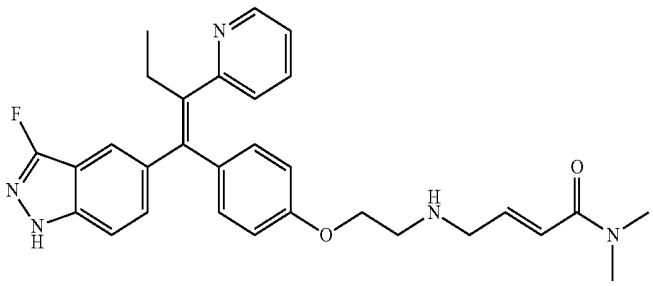
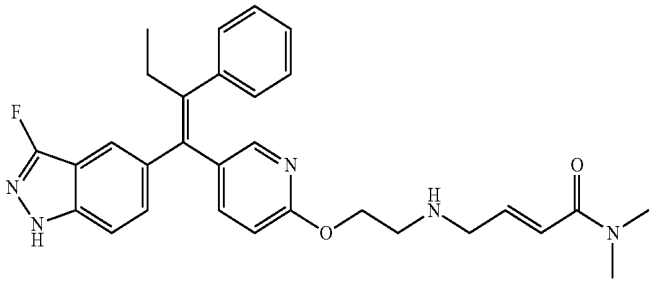
Compound #	Structure	GI50 WT (nM)	GI50 MUT (Y537S) (nM)
64		3.1	58.3
65		4.0	66.0
66		32.1	826.8
67		10.5	192.9
68		2.8	30.3

TABLE 1-continued

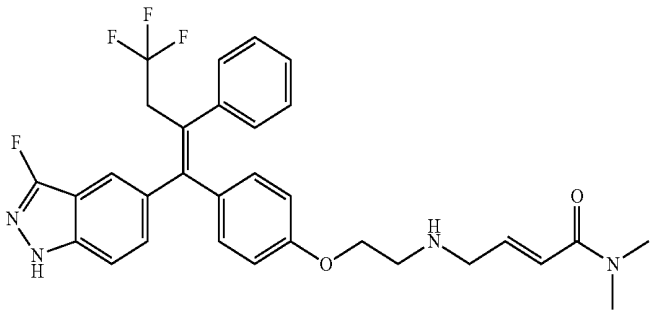
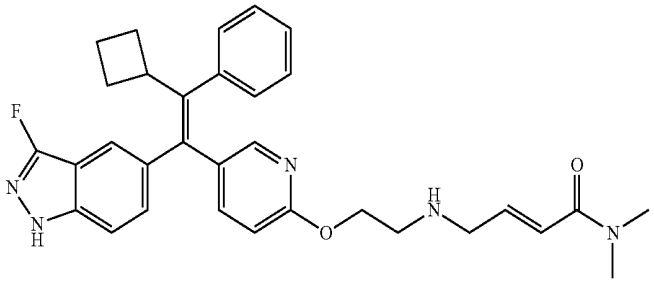
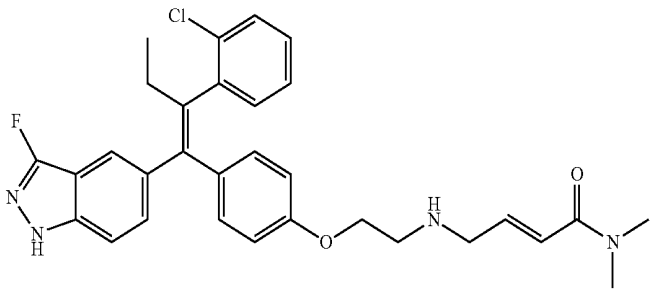
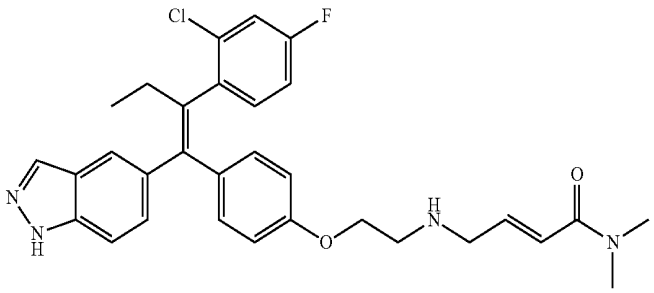
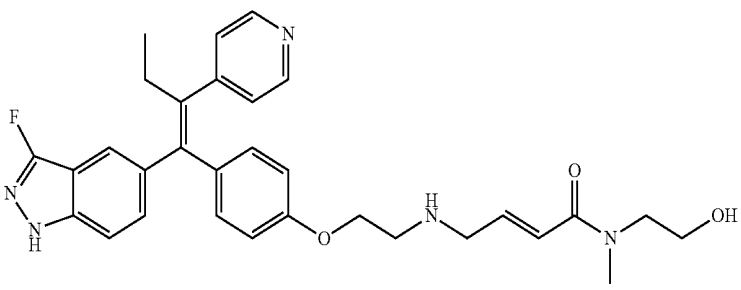
Compound #	Structure	GI50 WT (nM)	GI50 MUT (Y537S) (nM)
69		1.0	16.2
72		2.0	32.7
73		1.7	40.5
74		1.8 ± 0.5 (n = 2)	28.8 ± 14.0 (n = 2)
75		3.2	72.2

TABLE 1-continued

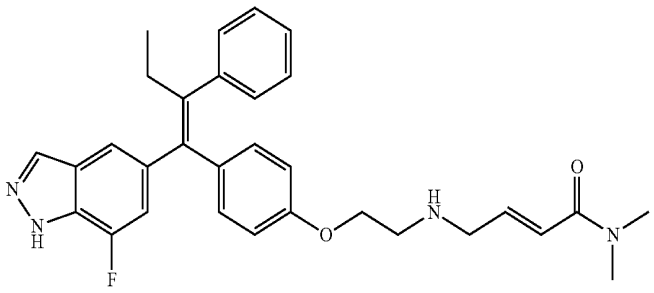
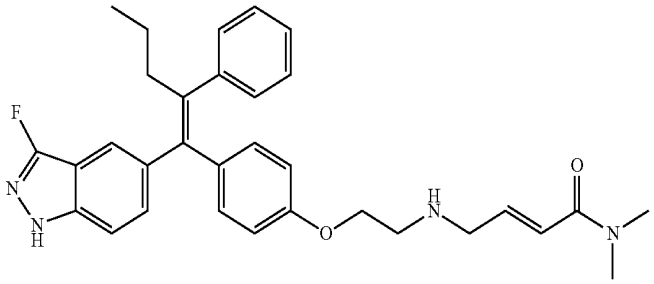
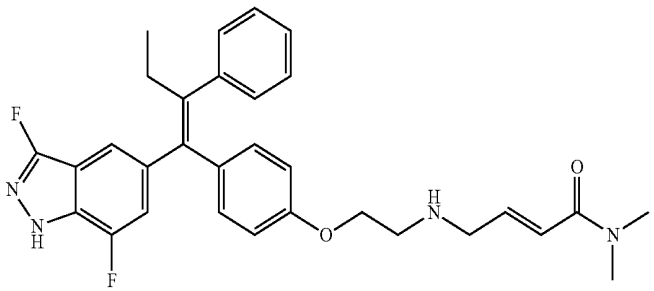
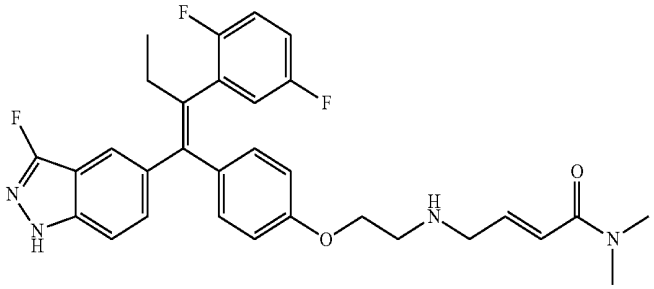
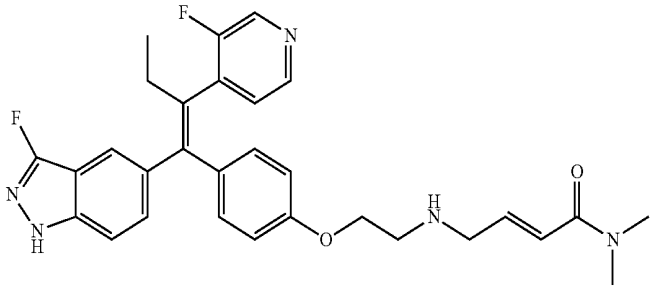
Compound #	Structure	GI50 WT (nM)	GI50 MUT (Y537S) (nM)
76		1.2	32.2
77		2.4	35.0
79		6.9	92.5
80		2	33.6
81		0.3	13.0

TABLE 1-continued

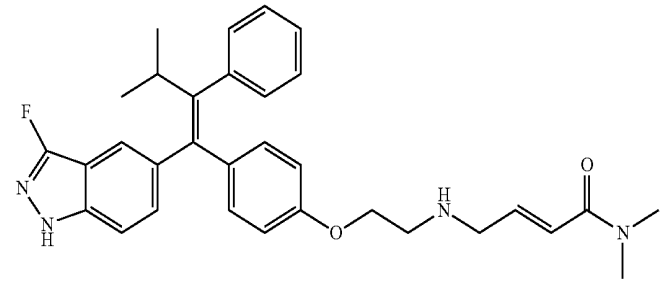
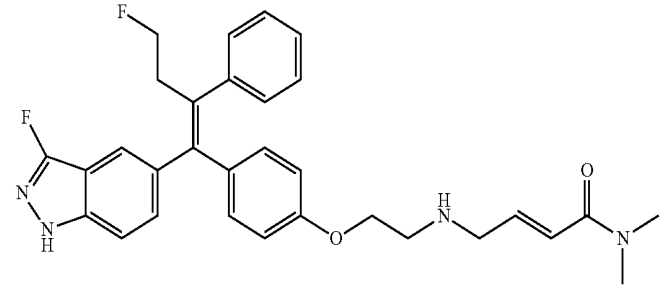
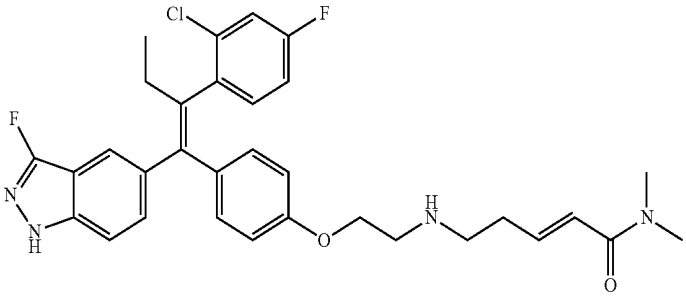
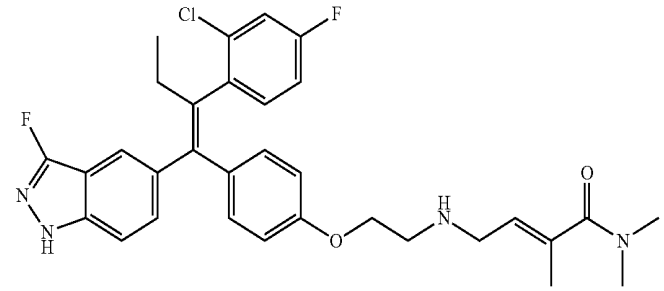
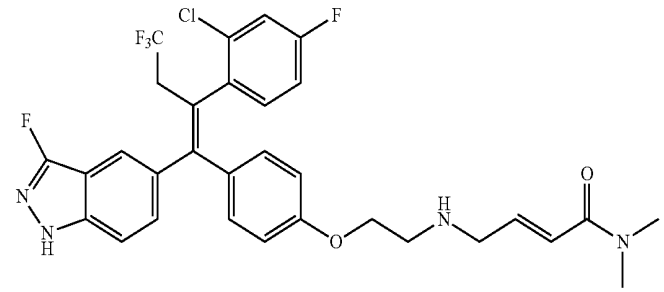
Compound #	Structure	GI50 WT (nM)	GI50 MUT (Y537S) (nM)
82		4.65 ± 2.9 (n = 2)	93.66 ± 6.3 (n = 2)
84		2.15 ± 0.15 (n = 2)	34.93 ± 1.5 (n = 2)
85		1.56 ± 0.56 (n = 2)	28.40 ± 2.9 (n = 2)
86		1.73 ± 1.0 (n = 2)	29.43 ± 4.7 (n = 2)
87		0.25	21.91

TABLE 1-continued

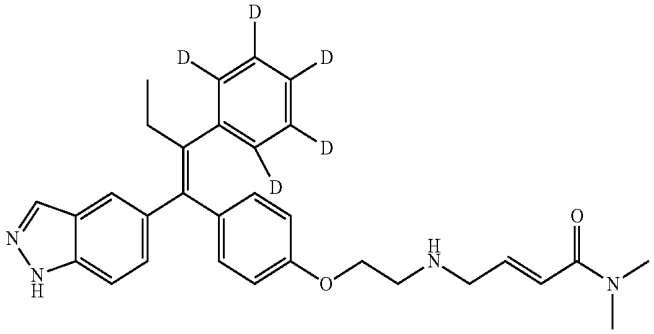
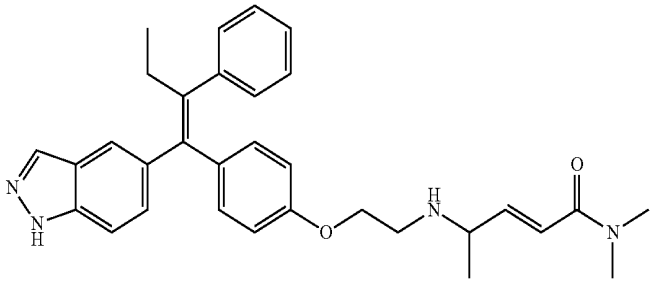
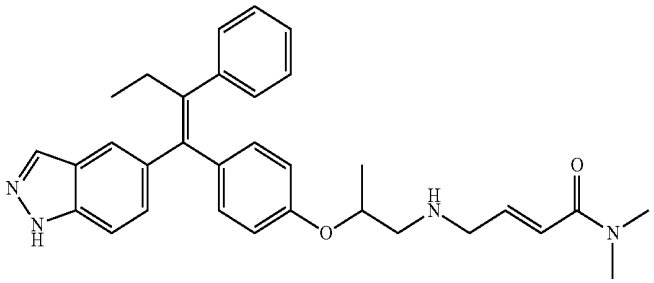
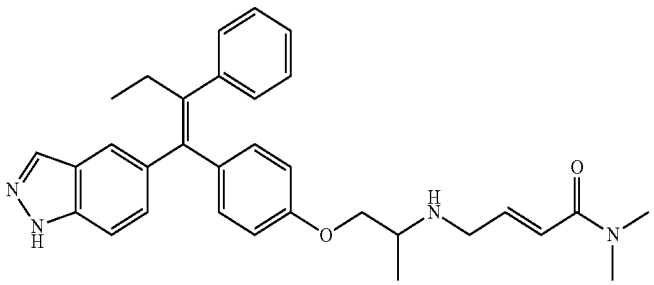
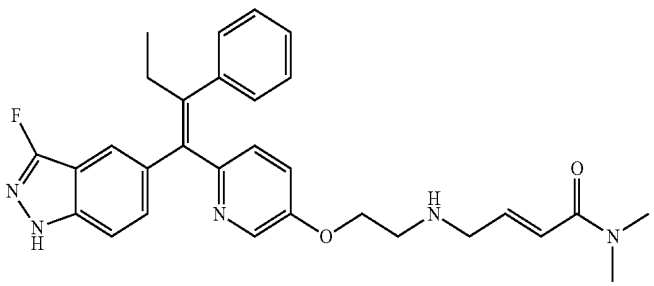
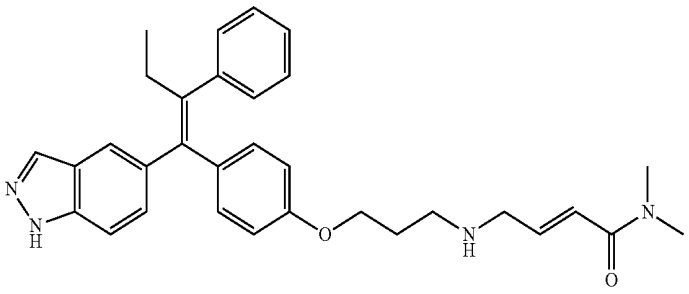
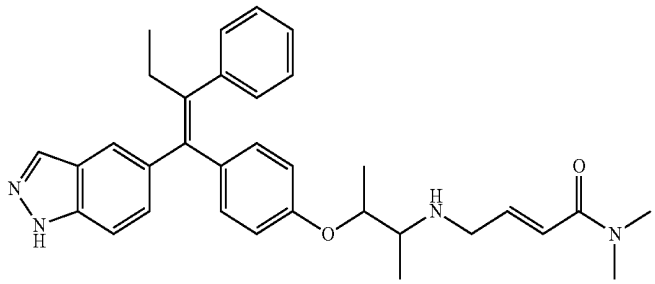
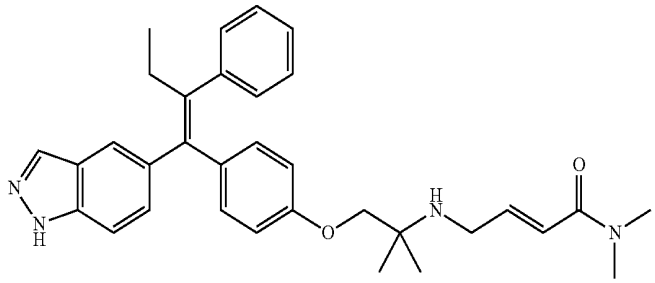
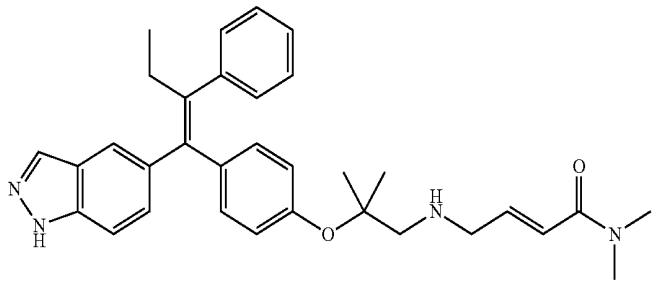
Compound #	Structure	GI50 WT (nM)	GI50 MUT (Y537S) (nM)
88		0.7	12.5
89		2.8	35
90		2.5	22.7
92		2.3	26.9
93		12.4	368.9

TABLE 1-continued

Compound #	Structure	GI50 WT (nM)	GI50 MUT (Y537S) (nM)
95		1.8	32.4
96		2	27.2
98		0.4	13.4
99		2.7	81.4

General Procedures

The following abbreviations may be used herein:

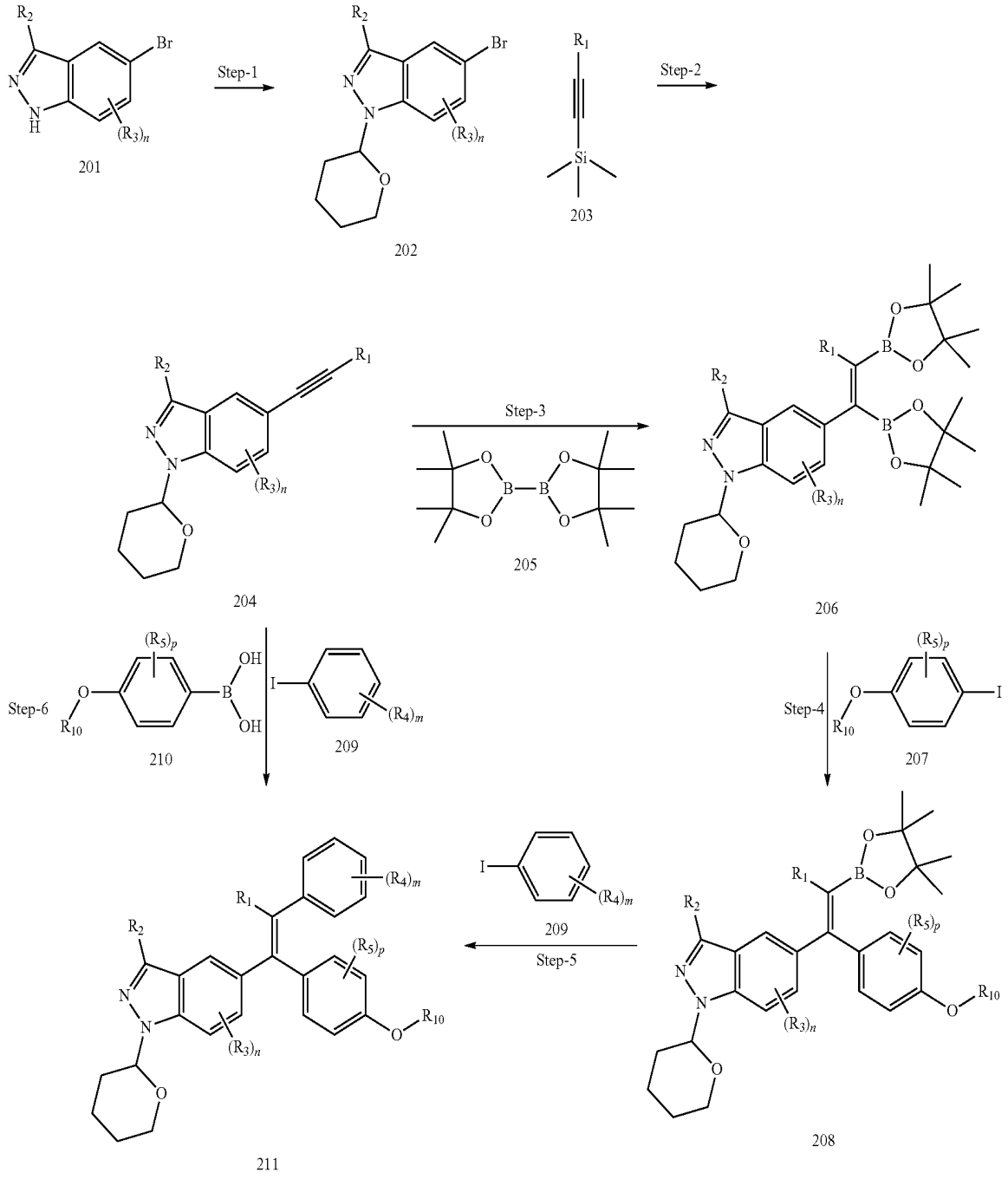
ACN: Acetonitrile
BOC: tert-butyloxycarbonyl
CAN: ceric ammonium nitrate
Conc.: concentrated
Cs_2CO_3: Cesium carbonate
DABCO: 1,4-Diazabicyclo[2.2.2]octane
DCM: Dichloromethane
DHP: Dihydropyran
DIPEA: N,N-diisopropylethylamine, Hunig's base
DMA: Dimethylacetamide
DMF: Dimethylformamide
DMSO: dimethylsulfoxide
DPEphos: (Oxydi-2,1-phenylene)bis(diphenylphosphine)
EDCI.HCl: N-(3-Dimethylaminopropyl)-N-ethylcarbodiimide hydrochloride
EtOH: Ethanol
EtOAc: Ethyl acetate
Et_3N: Triethylamine
Ex.: Example
h: Hours
HATU: 1-[Bis(dimethylamino)methylene]-1H-1,2,3-triazolo[4,5-b]pyridinium 3-oxid hexafluorophosphate
HCl: Hydrochloric acid
HMPA: Hexamethylphosphoramide
HPLC: High-performance liquid chromatography
H_2SO_4: Sulfuric acid
IPA: Isopropyl alcohol
K2CO3: Potassium carbonate
KOH: Potassium hydroxide
LCMS: Liquid chromatography—mass spectrometry
MeOH: Methanol

Na_2CO_3: Sodium carbonate
NBS: n-bromosuccinimide
nBuLi: n-Butyllithium
NH_4Cl: Ammonium chloride
NH4OH: Ammonium hydroxide
NMR: nuclear magnetic resonance
on or o.n.: overnight
Pd/C: Palladium (0) on carbon

TFA: Trifluoroacetic acid
THF: Tetrahydrofuran
TLC: Thin-layer chromatography
Pt/C: Platinum (0) on carbon

Unless indicated otherwise, ^1H NMR spectra were taken on a Varian Mercury Plus 400 MHz NMR.

Scheme 1:



$Pd_2(dba)_3$: Tris(dibenzylideneacetone)dipalladium(0)
PPTS: pyridinium p-toluenesulfonate
PTSA: p-toluenesulfonic acid
RT or r.t.: room temperature
TBAF: Tetrabutylammonium fluoride
TEA: Triethylamine

Step-1:

To a stirred solution of 5-bromo-1H-indazole (201, 23.5 mmol) in dry dichloromethane (50 mL) at 23° C. was added dihydro pyran (9.9 g, 118 mmol) followed by addition of pyridinium p-toluene sulfonate (0.6 g, 2.4 mmol). The resulting mixture was stirred at room 23° C. temperature for

16 h. Upon completion by TLC, the reaction mixture was quenched with water (50 mL) and extracted with dichloromethane (2×100 mL). The combined organic extracts were washed with water, brine, dried over sodium sulphate and concentrated. The crude material was purified by column chromatography over 230-400 mesh silica using 4-5% ethyl acetate in hexane to afford 5-bromo-1-(tetrahydro-2H-pyran-2-yl)-1H-indazole (202, 20 mmol, 86%) as a pale yellow oil.

Step-2a:

To a stirred solution of 5-bromo-1-(tetrahydro-2H-pyran-2-yl)-1H-indazole (202, 3.6 mmol) in 10 mL of MeOH:DMA:H_2O (1:1:1), in a sealed tube, were added copper iodide (0.068 g, 0.3 mmol) and cesium carbonate (1.62 g, 4.9 mmol) at 23° C. This mixture was degassed with three vacuum/N_2 cycles, and then but-1-yn-1-yltrimethylsilane (203, 0.899 g, 7.1 mmol) followed by $Pd(PPh_3)_2Cl_2$ (0.125 g, 0.1 mmol) were added. The pressure tube was sealed and heated at 80° C. for 1-12 h. Upon completion by TLC, the reaction mixture was quenched with water (10 mL) and extracted with ethyl acetate (2×50 mL). The combined organic extracts were washed with water, brine, dried over sodium sulphate and concentrated. The crude product was purified over 230-400 mesh silica column chromatography using 4-5% ethyl acetate in hexane to afford 204 (1.4 mmol, 55%) as a pale yellow oil.

Step-2b:

To a stirred solution of 5-bromo-3-fluoro-1-(tetrahydro-2H-pyran-2-yl)-1H-indazole (202, 2.5 g, 8.3 mmol) in 30 mL of DMA, in a sealed tube, were added copper iodide (79 mg, 0.41 mmol) and cesium carbonate (4 g, 12.4 mmol) at room temperature. reaction mixture was degassed with three vacuum/N_2 cycles, (cyclobutylethynyl)trimethylsilane (203, 1.78 g, 11.74 mmol) followed by $Pd(OAc)_2$ (92 mg, 0.41 mmol) and dppf (228 mg, 0.041 mmol) were added. The pressure tube was sealed and heated at 90° C. for 2 h. Upon completion by TLC, the reaction mixture was cooled to room temperature and diluted with water (25 mL), extracted with ethyl acetate (100 mL). The combined organic extracts were washed with water followed by brine. The organic layer was dried over anhydrous sodium sulphate and concentrated under reduced pressure. The crude product was purified over 230-400 mesh silica column chromatography using 10% ethyl acetate in n-hexane as an eluent to afford 5-(cyclobutylethynyl)-3-fluoro-1-(tetrahydro-2H-pyran-2-yl)-1H-indazole (204, 2.15 g, 86%).

Step-3:

To a stirred solution of 204 (39.37 mmol) in 2-methyl THF (80 mL), was added bis(pinacolato) diboron (10.09 g, 39.76 mmol), tetrakis(triphenylphosphine)platinum(0) (372 mg, 0.299 mmol) under nitrogen atmosphere, reaction mixture was refluxed for 6 h. After completion of reaction, reaction mixture was diluted with water and extracted with EtOAc. The Organic layer was dried over anhydrous sodium sulphate and concentrated under reduced pressure. The crude material was used in next step without further purification (206, 39 mmol, quantitative) as brown color oil.

Step-4:

To a stirred solution of 207 (2.34 g, 10.61 mmol), bis(triphenylphosphine) palladium(II) dichloride (372 mg, 0.530 mmol), cesium carbonate (6.9 g, 21.23 mmol) and 2-methyl THF (60 mL) were added. This mixture was degassed with nitrogen and water (5 mL) was added. This mixture was stirred at room temperature for 12 h. After completion of reaction, reaction mixture was diluted with water and extracted with EtOAc. The Organic layer was dried over anhydrous sodium sulphate and concentrated under reduced pressure. The crude material was purified by column chromatography over 230-400 mesh silica gel using MeOH in dichloromethane (1.6:98.4) to afford 208 (5.5 mmol, 43%).

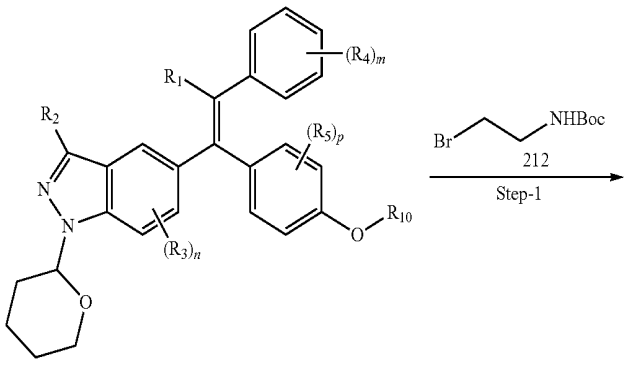
Step-5:

To a stirred solution of 208 (1.8 mmol) in 2-methyl THF (30 mL), iodobenzene (209, 1.8 mmol), 4M aqueous KOH (5 mL) and $Pd(PPh_3)_2Cl_2$ (63 mg, 0.09 mmol) were added and the mixture was degassed with nitrogen for 15 min and heated at 80-90° C. for 8-12 h. Upon completion, the reaction mixture was diluted with EtOAc. Organic layer was washed with water followed by brine, dried over anhydrous sodium sulphate, filtered and concentrated. The crude product was purified by silica gel chromatography (2:8 EtOAc in n-hexane) to give a desired product (211, 0.74 mmol, 41%).

Step-6:

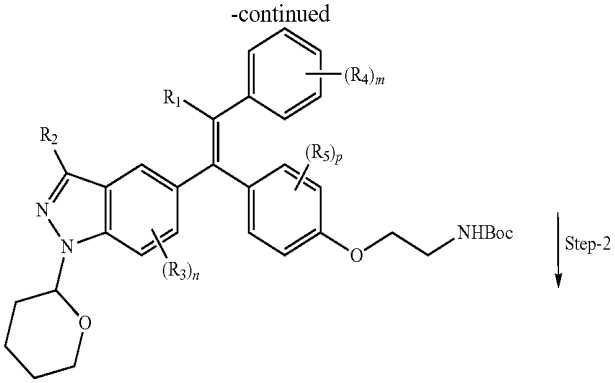
To a solution of 5-(but-1-yn-1-yl)-1-(tetrahydro-2H-pyran-2-yl)-1H-indazole (204, 27.5 mmol), iodobenzene (209, 17 g, 82.7 mmol), 4-hydroxy phenyl boronic acid (210, 11.4 g, 82.7 mmol), in N,N-dimethyl formamide/water (2:1, 50 mL) was added K_2CO_3 (11.4 g, 82.7 mmol). The contents were degassed with three vacuum/N_2 cycles, and then heated at 45° C. for 1 h until the solution was homogeneous. A solution of $Pd(PhCN)_2Cl_2$ (0.528 g, 1.4 mmol) in N,N-dimethyl formamide (1 mL) was added and the resulting mixture was stirred at 45° C. for 16 h. Upon completion by TLC, the reaction mixture was quenched with water (500 mL) and extracted with ethyl acetate (2×500 mL). The combined organic extracts were washed with water, brine, dried over sodium sulphate and concentrated. The crude material was purified over 230-400 mesh silica column chromatography using 20% ethyl acetate in hexane to afford the desired compound (211, 11.8 mmol, 43%) as a pale yellow oil.

Scheme 2:

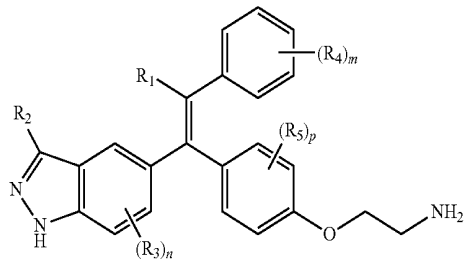


211a

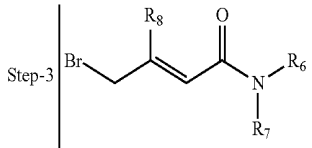
-continued



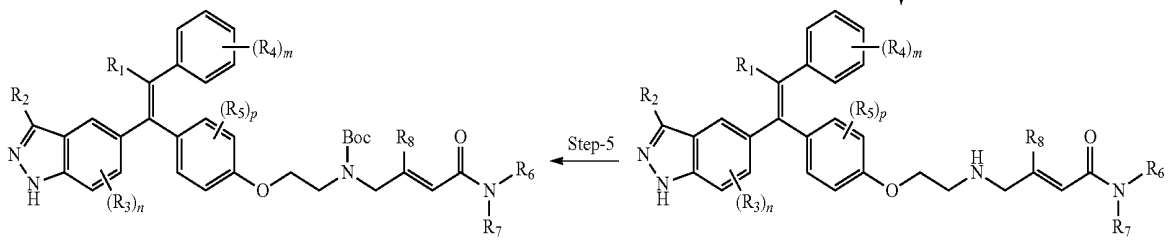
211b



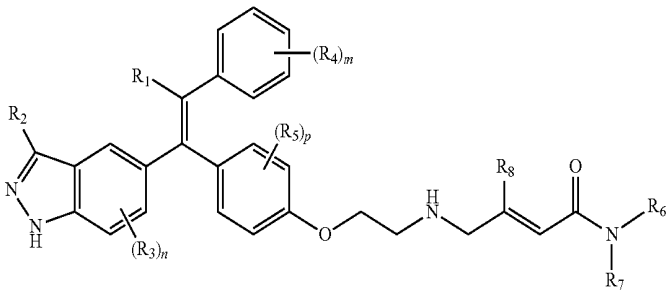
213



214



211c 215



216

Step-1:

To a solution of 211a (3.4 mmol) in DMF (30 mL), at 0° C., were added sequentially potassium carbonate (1.4 g, 10.1 mmol) and tert-butyl (2-bromoethyl)-carbamate (212, 8.5 mmol). The reaction mixture was stirred at 80° C. for 16 h, was diluted with ethyl acetate, washed with water, brine, dried over sodium sulphate and concentrated under reduced pressure. The crude material was purified by column chromatography over 230-400 mesh silica gel using 15% ethyl acetate in n-hexane to afford the desired product (211b, 1.8 mmol, 53%) as a light brown colour gummy mass.

Step-2a:

To a stirred solution of 211b (2.5 mmol) in ethanol (10 mL) was added at 0° C., 2M HCl in ether (10 mL). The

reaction mixture was stirred for 16-24 h at 23° C. After completion of reaction, reaction mixture was basified with saturated $NaHCO_3$, extracted with 10% MeOH in dichloromethane. Organic layer was concentrated under reduced pressure and the crude material was purified by column chromatography over 230-400 mesh silica gel using (4-5%) MeOH in DCM to afford the desire product (13, 1.25 mmol, 50%) as a brown coloured semi solid.

Step-2b:

To a stirred solution of 211 (1.5 g, 2.3 mmol) in ethanol (3 mL) was added at 0° C., 2M HCl in ditheyl ether (15 mL). The reaction mixture was stirred for 24 h at room temperature. After completion of reaction, reaction mixture was basified with saturated $NaHCO_3$, extracted with ethyl acetate. Organic layer was concentrated under reduced pressure to afford crude desired product (213, 1.1 g crude).

Step-3a:

To a stirred solution of 213 (1.24 mmol) in DMF (5 mL) was added at 0° C., (E)-4-bromo-N,N-dimethylbut-2-enamide (214, 1.24 mmol) and DIPEA (0.321 g, 2.49 mmol). The reaction mixture was stirred for 12-48 h at 23° C., was diluted with cold water (50 mL) and extracted with dichloromethane. The organic layer was washed with water followed by brine, dried over anhydrous sodium sulphate and concentrated under reduced pressure to give a crude mixture of 215.

Step-3b:

To a stirred solution of 213 (1.1 g, 2 mmol) in DMF (22 mL) was added DIPEA (0.62 g, 4 mmol) at room temperature, stirred for 15 min at same temperature. A solution of (E)-4-bromo-N,N-dimethylbut-2-enamide and (E)-4-chloro-N,N-dimethylbut-2-enamide mixture (214, 0.41 g, 2 mmol) in DMF (5 mL) was added drop wise, reaction mixture was stirred for 16 h at room temperature, after completion of reaction (monitored by TLC), reaction mixture was diluted with cold water (50 mL) and extracted with dichloromethane. The organic layer was washed with water followed by saturated NaCl solution, dried over anhydrous sodium sulphate and concentrated under reduced pressure to deliver crude product 215 (1.8 g).

Step-4:

The crude material obtained from previous step was purified by preparative HPLC to afford pure isomer 216 (0.06 mmol, 5%) as a white solid. The ^1H NMR, HPLC and MS data were collected.

Step-5:

To a stirred solution of 215 (1.25 mmol) in DCM (10 mL) was added di-tert-butyl dicarbonate (0.546 g, 2.5 mmol). The reaction mixture was stirred for 1 h at 23° C., after completion of reaction, reaction mixture was diluted with cold water (50 mL) and extracted with dichloromethane (100 mL). The organic layer was washed with water followed by brine, dried over anhydrous sodium sulphate and concentrated under reduced pressure. Crude compound was purified by column chromatography using 2% MeOH in DCM to afford 211c (0.63 mmol, 50%) as a light brown semi-solid.

Step-6a:

To a stirred solution of 211c (0.622 mmol) in MeOH (5 mL) was added at 0° C., 2M HCl in ether (10 mL). The reaction mixture was stirred for 16 h at 23° C. After completion of reaction, reaction mixture was basified with saturated $NaHCO_3$, extracted with 10% MeOH in DCM. Organic layer was concentrated under reduced pressure to obtain crude compound (215, 0.07 mmol) as an off-white solid. Crude compound was purified by preparative HPLC to afford desired pure isomer (216, 0.03 mmol, 4.1%) as an white solid. The ^1H NMR, HPLC and MS data were collected.

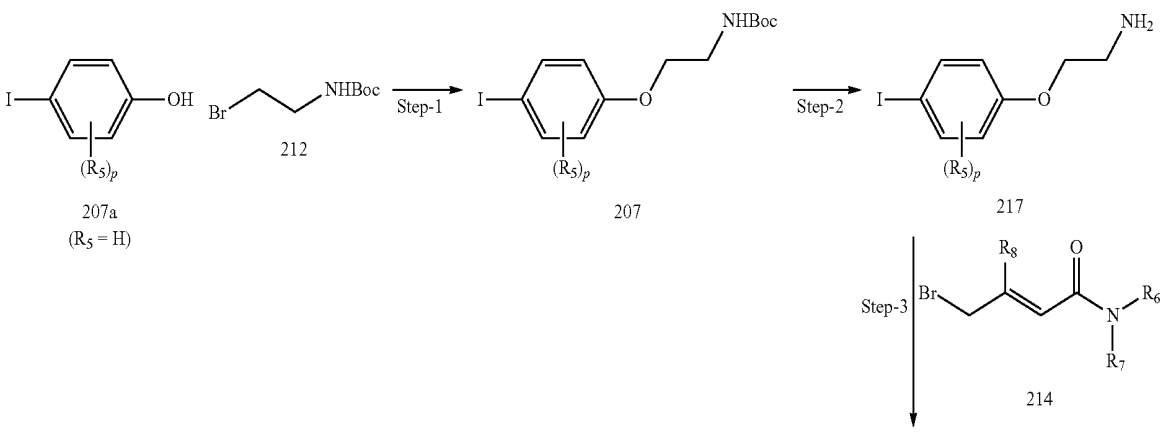
Step-6b:

To a stirred solution of 211c (0.081 mmol) in dichloromethane (1.2 mL) at 0° C., was added TFA (0.3 mL). The reaction mixture was stirred at 23° C. for 30 min to 2 h. After completion of reaction, the solution was basified with saturated $NaHCO_3$ solution and extracted with dichloromethane. Combined organic layer was dried over anhydrous sodium sulfate and concentrated under reduced pressure. The crude material was purified by preparative HPLC to afford desired pure isomer (216, 0.12 mmol, 33.3%) as an white solid. The ^1H NMR, HPLC and MS data were collected.

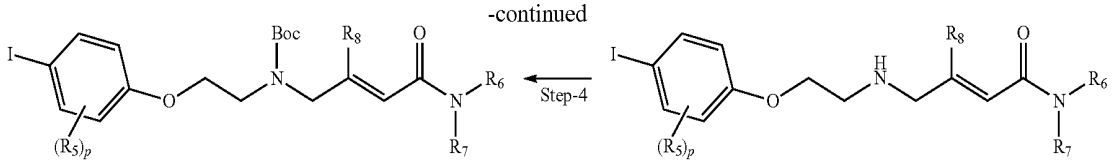
Step-6c:

To a stirred solution of 211c (0.504 mmol) in EtOH (3 mL) was added at 0° C., 2M HCl in diethyl ether (5 mL). The reaction mixture was stirred for 12 h at room temperature. After completion of reaction (monitored by TLC), reaction mixture was basified with saturated $NaHCO_3$ solution at 0° C. extracted with 10% MeOH in dichloromethane. The organic layer was washed with water, saturated NaCl solution and concentrated under reduced pressure to obtain crude compound, crude compound was purified by preparative TLC to afford desired compound 216 (74 mg, 27%).

Scheme 3:



-continued



207c 218

Step-1:

To a stirred solution of 4-iodophenol (207a, 227 mmol) in DMF (750 mL) was added potassium carbonate (188 g, 1.363 mol) and stirred for 30 min at 23° C., to the above mixture tert-butyl (2-bromoethyl)carbamate (212, 71.27 g, 318 mmol) was added. The contents were stirred at 70° C. for 12 h. After completion of reaction, reaction mixture was poured onto ice cold water, solid separated was filtered and dried under reduced pressure to obtain desired compound tert-butyl (2-(4-iodophenoxy)-ethyl)carbamate as an off-white solid (207b, 220 mmol, 97%).

Step-2:

To a stirred solution of tert-butyl (2-(4-iodophenoxy) ethyl)carbamate (207b, 68.6 mmol) in ethanol (50 mL) was added at 0° C., 2M HCl in ether (250 mL). The reaction mixture was stirred for 12 h at 23° C. After completion of reaction, reaction mixture was basified with saturated $NaHCO_3$, extracted with 10% MeOH in DCM. Organic layer was concentrated under reduced pressure and the crude material was used in next step without further purification (217, 60 mmol, 88%).

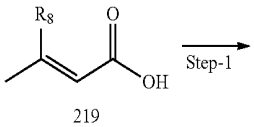
Step-3:

To a stirred solution of 2-(4-iodophenoxy)ethan-1-amine (217, 60.6 mmol) in DMF (65 mL) was added at 0° C., 4-bromo-N,N-dimethylbut-2-enamide (214, 42.4 mmol) and DIPEA (11.72 g, 90.9 mmol). The reaction mixture was stirred for 5 h at room temperature, was diluted with cold water (250 mL) and extracted with dichloromethane. The organic layer was washed with water followed by brine, dried over anhydrous sodium sulphate and concentrated under reduced pressure. The crude material was used in next step without further purification (218, 50 mmol, 83%, crude).

Step-4:

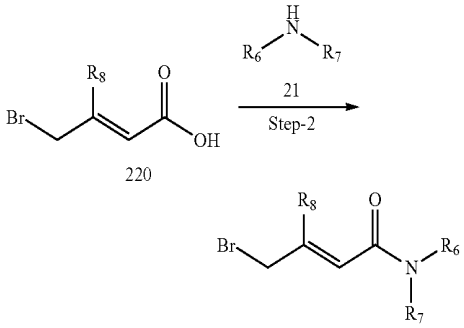
To a stirred solution of 218 (50.26 mmol) in dry dichloromethane (150 mL) was added DIPEA (6.4 g, 50.2 mmol) at 0° C., stirred for 15 min at 0° C. To the above reaction mixture, was added di-tert-butyl dicarbonate (13.1 g, 60.3 mmol), resulting mixture was stirred at 23° C. for 12 h. Upon completion by TLC, the reaction mixture was cooled to 0° C., quenched with ice cold water (500 mL) and extracted with dichloromethane (500 mL). The combined organic extracts were washed with water, followed by brine, dried over anhydrous sodium sulphate and concentrated under reduced pressure. The crude material was purified by column chromatography over 230-400 mesh silica using 3% MeOH in dichloromethane as an eluent to afford 207c (19 mmol, 37.8%).

Scheme 4:



219

-continued



220 214

Step-1:

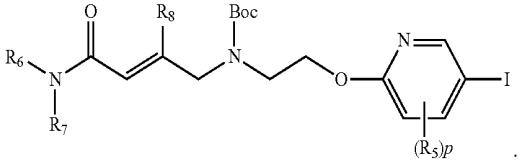
To a stirred solution of but-2-enoic acid (219, 116.0 mmol) in benzene (150 mL) was added N-Bromo succinamide (31.4 g, 120.0 mmol) followed by Benzoyl peroxide (0.200 g, 1.4 mmol) at 23° C. The reaction mixture was heated to reflux for 4 h, which resulted in precipitation of succinamide crystals. The crystals were filtered off and the filtrate was concentrated. The crude was recrystallized with minimum amount of hexane and washed with hexane to afford 4-bromobut-2-enoic acid (220, 42.5 mmol, 37%) as a white solid.

Step-2:

bromobut-2-enoic acid (220, 9 mmol) was taken in dichloromethane (30 mL) and cooled to 0° C. To this solution oxalyl chloride (1.6 mL, 18 mmol), DMF (0.1 mL) were added and stirred for 0.5 h at 23° C. The reaction mixture was concentrated under nitrogen atmosphere, residue was diluted with THF (30 mL), cooled to 0° C. and was basified with DIPEA (3.1 mL, 18 mmol). To this mixture, an amine (221, 9 mmol) was added slowly as a solution in dichloromethane and the contents were stirred at 23° C. for 1 h. The volatiles were removed by concentration under reduced pressure and the residue was partitioned between water and ethyl acetate. The organic layer was washed with water, brine, dried over sodium sulphate and concentrated. The crude material was purified by column chromatography over 230-400 mesh silica gel using 3-7% ethyl acetate in hexane to afford the desired amide (214, 0.85 mmol, 9.4%) as a brown colour liquid.

Scheme 5:

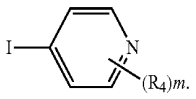
Compounds of formula III may be prepared by substituting the following compound for Compound 207 in Step-4 of Scheme 1:



The compound shown here in Scheme 5 may be prepared by using the process as outlined in Scheme 3 by substituting the appropriate pyridyl for compound 207a.

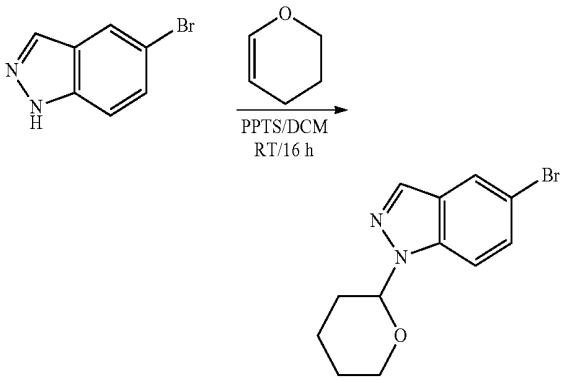
Scheme 6:

Compounds of formula IV may be prepared by substituting the following compound for Compound 209 in Step-5 or Step-6 of Scheme 1:



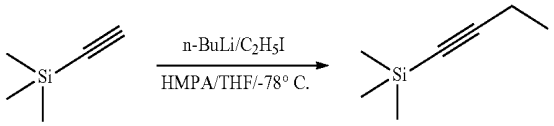
Example 1: Synthesis of (E)-4-((2-(4-((E)-1-(1H-indazol-5-yl)-2-phenylbut-1-en-1-yl)phenoxy) ethyl) amino)-N,N-dimethylbut-2-enamide (Compound 1)

Step-1: Synthesis of 5-bromo-1-(tetrahydro-2H-pyran-2-yl)-1H-indazole



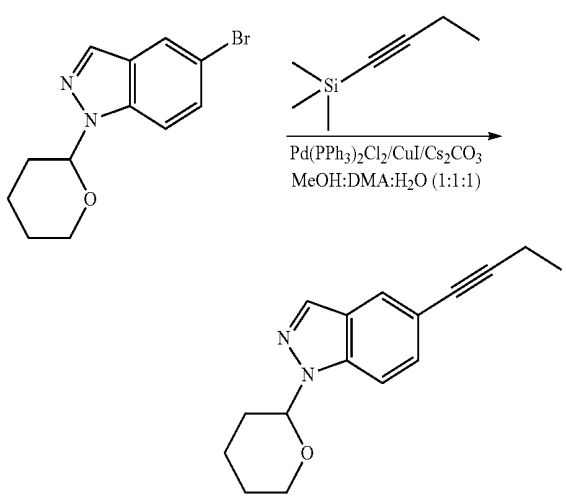
The reaction was carried out according to Scheme 1, Step-1, substituting 5-bromo-1H-indazole (5 g, 23.5 mmol) for Compound 201. The crude material was purified by column chromatography over 230-400 mesh silica using 4-5% ethyl acetate in hexane to afford the title compound of Ex. 1 Step-1 (12.6 g, 86%) as a pale yellow oil.

Step-2: Synthesis of but-1-yn-1-yltrimethylsilane



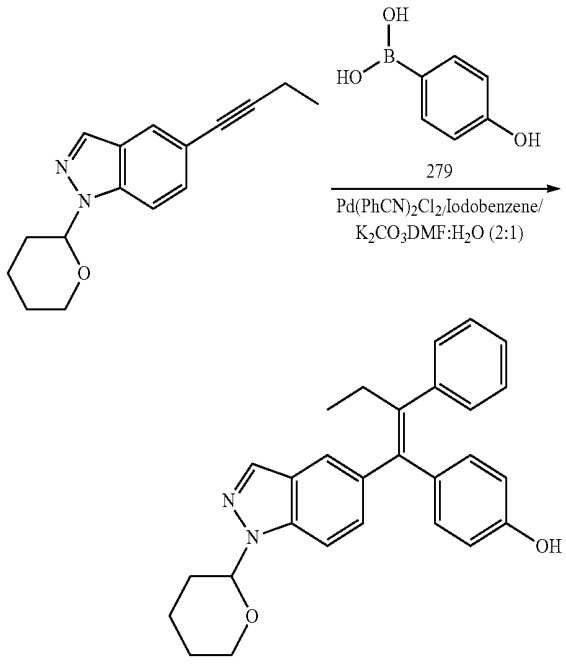
To a stirred solution of (trimethylsilyl)acetylene (116 g, 1.19 mol) in dry THF (400 mL) was added n-BuLi (2.5M in THF, 500 mL) at −78° C. over 2 h. The resulting mixture was warmed to 0° C. for 10 min. The reaction mixture was again cooled to −78° C., HMPA (234 g, 1.13 mol) was added to the above mixture and stirred at −78° C. for 30 min. To the above reaction mixture iodoethane (200 g, 1.28 mol) was added and the resulting mixture was stirred at room temperature for 16 h. After completion of reaction, the reaction mixture was quenched with water, extracted with ethyl acetate (1000 mL). The organic layer was washed with brine, dried over anhydrous sodium sulphate and concentrated under reduced pressure. The product but-1-yn-1-yltrimethylsilane was distilled between 125-135° C. to afford the the title compound of Ex. 1 Step-2 (91 g, 61%) as a colourless liquid.

Step-3: Synthesis of 5-(but-1-yn-1-yl)-1-(tetrahydro-2H-pyran-2-yl)-1H-indazole



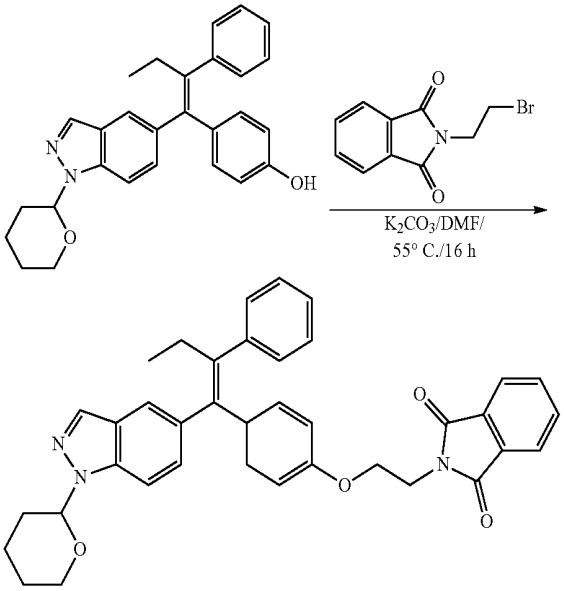
The reaction was carried out according to Scheme 1, Step-2a, using 5-bromo-1-(tetrahydro-2H-pyran-2-yl)-1H-indazole (1 g, 3.6 mmol) for compound 202. The crude product was purified over 230-400 mesh silica column chromatography using 4-5% ethyl acetate in hexane to afford the title compound of Ex. 1 Step-3 (0.5 g, 55%) as a pale yellow oil.

Step-4: Synthesis of (E)-4-(2-phenyl-1-(1-(tetrahydro-2H-pyran-2-yl)-1H-indazol-5-yl)but-1-en-1-yl)phenol



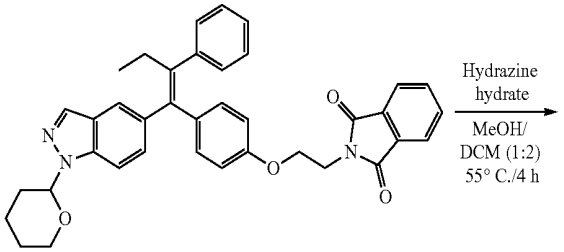
The reaction was carried out according to Scheme 1, Step-6 using 5-(but-1-yn-1-yl)-1-(tetrahydro-2H-pyran-2-yl)-1H-indazole (7 g, 27.5 mmol) for compound 204, iodobenzene (17 g, 82.7 mmol), and 4-hydroxy phenyl boronic acid (11.4 g, 82.7 mmol) for compound 210. The crude material was purified over 230-400 mesh silica column chromatography using 20% ethyl acetate in hexane to the title compound of Ex. 1 Step-4 (5 g, 43%) as a pale yellow oil.

Step-5: Synthesis of (E)-2-(2-(4-(2-phenyl-1-(1-(tetrahydro-2H-pyran-2-yl)-1H-indazol-5-yl) but-1-en-1-yl) phenoxy) ethyl) isoindoline-1,3-dione

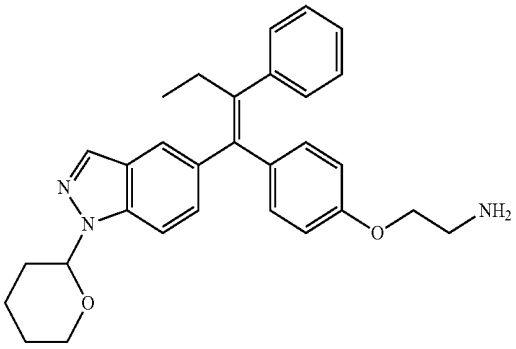


The reaction was carried out according to Scheme 2, Step-1 substituting (E)-4-(2-phenyl-1-(1-(tetrahydro-2H-pyran-2-yl)-1H-indazol-5-yl)but-1-en-1-yl) phenol (1 g, 2.3 mmol) for compound 211a and 2-(2-bromoethyl) isoindoline-1,3-dione (6 g, 23.5 mmol) for compound 212. The reaction mixture was stirred at 55° C. for 16 h, was diluted with ethyl acetate, washed with water, brine, dried over sodium sulphate and concentrated under reduced pressure. The crude material was purified by silica gel chromatography using 30-35% ethyl acetate in n-hexane to afford the title compound of Ex. 1 Step-5 (0.5 g, 36%) as a light brown colour gummy mass.

Step-6: Synthesis of (E)-2-(4-(2-phenyl-1-(1-(tetrahydro-2H-pyran-2-yl)-1H-indazol-5-yl)but-1-en-1-yl) phenoxy) ethan-1-amine

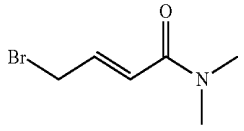


-continued

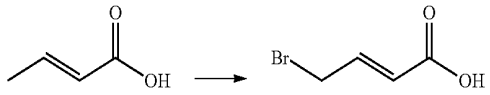


To a solution of (E)-2-(2-(4-(2-phenyl-1-(1-(tetrahydro-2H-pyran-2-yl)-1H-indazol-5-yl)but-1-en-1-yl)phenoxy) ethyl)isoindoline-1,3-dione (1 g, 1.6 mmol) in MeOH/DCM (1:2, 20 mL) was added hydrazine hydrate (14 mL) at room temperature. The reaction mixture was stirred at 55° C. for 4 h, quenched with NH_4OH and extracted with dichloromethane. The organic layer was washed with water, brine, dried over sodium sulphate and concentrated under reduced pressure. The crude material was purified by column chromatography over 100-200 mesh silica gel using 3% methanol in DCM to afford the title compound of Ex. 1 Step-6 (0.500 g, 64%) as a gummy compound.

Step-7: Synthesis of (E)-4-bromo-N,N-dimethylbut-2-enamide

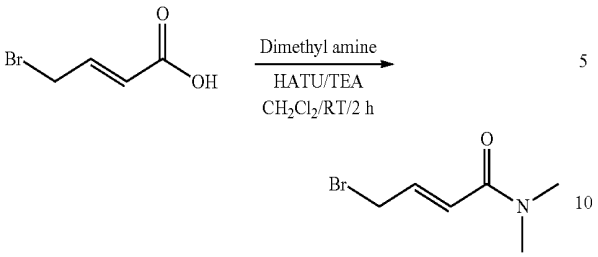


Step-7.1: Synthesis of (E)-4-bromobut-2-enoic acid



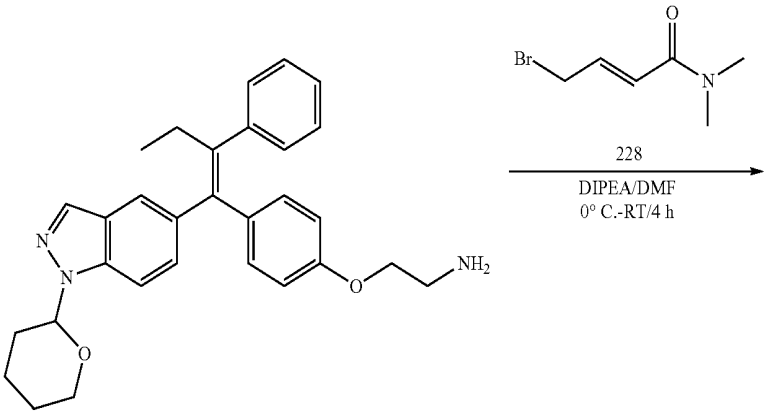
To a stirred solution of (E)-but-2-enoic acid (10.0 g, 116.0 mmol) in benzene (150 mL) was added N-Bromosuccinamide (31.4 g, 120.0 mmol) followed by Benzoyl peroxide (0.200 g, 1.4 mmol) at 23° C. The reaction mixture was heated to reflux for 4 h, which resulted in precipitation of succinamide crystals. The crystals were filtered off and the filtrate was concentrated. The crude was recrystallized with minimum amount of hexane and washed with hexane to afford (E)-4-bromobut-2-enoic acid (6.97 g, 37%) as a white solid.

Step-7.2: Synthesis of (E)-4-bromo-N,N-dimethylbut-2-enamide

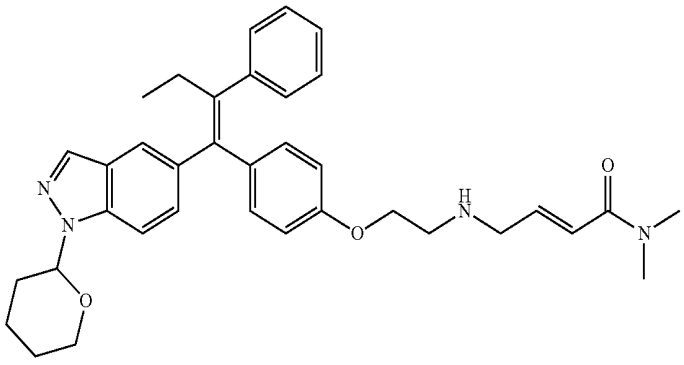


(E)-4-bromobut-2-enoic acid (2 g, 12.2 mmol) was taken in dichloromethane (20 mL) and at 0° C. were added HATU (5.5 g, 14 mmol), triethyl amine (2.56 mL, 18.4 mmol) and stirred for 10 min at RT. To this mixture N,N-dimethyl amine (9.2 mL, 18 mmol) was added slowly and the contents were stirred at room temperature for 2 h. The volatiles were removed under reduced pressure and the residue was partitioned between water and ethyl acetate. The organic layer was washed with water, brine, dried over sodium sulphate and concentrated. The crude material was purified by column chromatography over 100-200 silica gel using 20% ethyl acetate in n-hexane to afford (E)-4-bromo-N,N-dimethylbut-2-enamide (0.4 g, 17%) as a pale green colour liquid.

Step-8: Synthesis of (E)-N,N-dimethyl-4-((2-(4-((E)-2-phenyl-1-(1-(tetrahydro-2H-pyran-2-yl)-1H-indazol-5-yl)but-1-en-1-yl) phenoxy) ethyl) amino) but-2-enamide

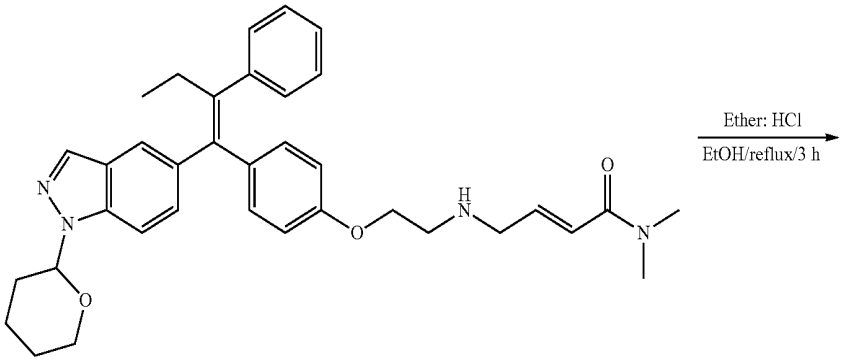


229



The reaction was carried out according to Scheme 2, Step-3a using 2-(4-(2-phenyl-1-(1-(tetrahydro-2H-pyran-2-yl)-1H-indazol-5-yl)but-1-en-1-yl)phenoxy)ethan-1-amine (0.450 g, 0.96 mmol) for compound 213. The reaction mixture was stirred for 4 h at room temperature, was diluted with cold water (50 mL) and extracted with dichloromethane. The organic layer was washed with water followed by brine, dried over anhydrous sodium sulphate and concentrated under reduced pressure. The crude material was purified by column chromatography over 230-400 mesh silica gel using 1% methanol in dichloromethane to afford the title compound of Ex. 1 Step-8 (0.200 g, 36%) as a gummy solid.

Step-9: Synthesis of (E)-4-((2-(4-((E)-1-(1H-indazol-5-yl)-2-phenylbut-1-en-1-yl)phenoxy)ethyl)amino)-N, N-dimethylbut-2-enamide (Compound 1)



1

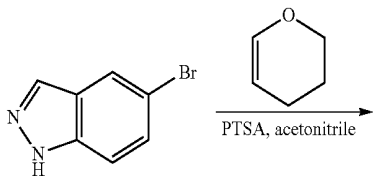
To a stirred solution of (E)-N,N-dimethyl-4-((2-(4-((E)-2-phenyl-1-(1-(tetrahydro-2H-pyran-2-yl)-1H-indazol-5-yl)but-1-en-1-yl)phenoxy)ethyl)amino)but-2-enamide (0.180 g, 0.31 mmol) in ethanol (10 mL), at 0° C. was added 2M HCl in ether (10 mL). The reaction mixture was stirred for 3 h at reflux temperature, was diluted with cold water (50 mL) and extracted with ethyl acetate. The organic layer was washed with water followed by brine, dried over anhydrous sodium sulphate and concentrated under reduced pressure. The crude material was purified by column chromatography over 230-400 mesh silica gel using 3-4% methanol in DCM to afford Compound 1 (0.035 g, 23%) as a colourless solid.

Compound 1:

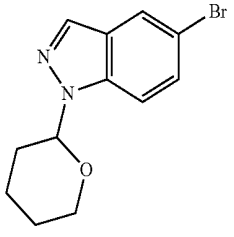
^{1}H NMR (400 MHz, $CDCl_3$) δ 10.16 (bs, 1H), 8.07 (s, 1H), 7.66 (s, 1H), 7.5 (d, J=8.8 Hz, 1H), 7.26-7.11 (m, 6H), 6.93-6.87 (m, 1H), 6.78 (d, J=8.8 Hz, 2H), 6.56 (d, J=8.8, 2H), 6.42 (d, J=15.2 Hz, 1H), 3.948 (t, J=4.9 Hz 2H), 3.45 (m, 2H), 3.06 (s, 3H), 2.99 (s, 3H), 2.50-2.45 (m, 2H), 0.95 (t, J=7.2 Hz, 3H). LCMS: 526.3 $[M+H]^+$.

Example 1A—Synthesis of Hydrochloride Salt of Compound 1

Step-1A: Synthesis of 5-bromo-1-(tetrahydro-2H-pyran-2-yl)-1H-indazole)



-continued



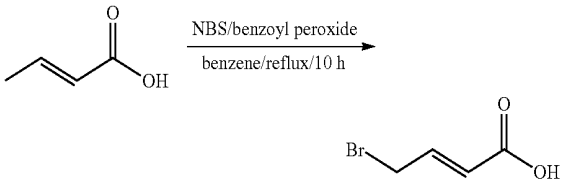
300

In to clean, dry, nitrogen flushed 2001 Glass reactor, charged 5-bromo indazole (11.0 Kg, 0.055 mol) actonitrile (110 Lit) and PTSA (1.0 Kg g, 0.055 mol), the reaction mixture were stirred at 28-30° C. for 30 min. To the above solution, dihydropyran (7.03 Kg, 2.55 mol) was added drop wise over a period of 20 min. The resulting mixture was stirred at room temperature for 16 h. Upon completion by TLC, the reaction mixture was quenched with water (500 mL) and acetonitrile was concentrated under reduced pres-

sure. Obtained product was extracted with ethyl acetate (25 l*3), combined organic extracts were washed with water followed by brine, dried over anhydrous sodium sulphate and concentrated under reduced pressure to get desired compound which was taken as it is for next stage without further purification (14 Kg, 89% Yield, 93.93% HPLC purity)

^{1}H NMR (300 MHz, CDCl3): δ 7.95 (s, 1H), 7.85 (s, 1H), 7.45-7.55 (d, 2H), 5.62-5.82 (d, 1H), 3.95-4.05 (d, 1H), 3.75-3.85 (d, 1H), 2.55-2.65 (t, 1H), 2.1-2.2 (m, 2H), 1.65-1.85 (m, 4H), HPLC: 93.93% at 210 nm.

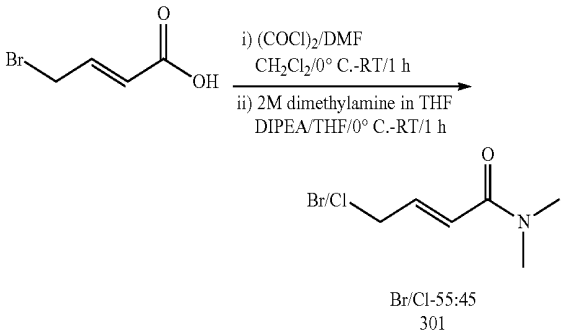
Step-2A: Synthesis of (E)-4-bromobut-2-enoic acid



To a stirred solution of (E)-but-2-enoic acid (5.0 Kg, 59.52 mol) in benzene (50.0 Lit) was added N-Bromo succinamide (10.58 Kg, 59.52 mol) followed by benzoyl peroxide (144 g, 0.595 mol) at room temperature. The reaction mixture was heated to reflux for 10 h, which resulted in precipitation of succinamide crystals. The crystals were filtered off and the filtrate was concentrated. The crude was purified by crystallisation using hexane to afford (E)-4-bromobut-2-enoic acid (2.5 Kg, 26.5% Yield) as a white solid.

^{1}H NMR (300 MHz, $CDCl_3$): δ 7.07-7.17 (m, 1H), 6.05-6.8 (d, 1H), 4.05-4.1 (d, 2H) HPLC; 84.1% at 210 nm

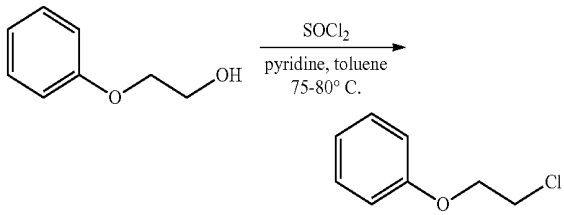
Step-3A: Synthesis of
(E)-4-bromo-N,N-dimethylbut-2-enamide



(E)-4-bromobut-2-enoic acid (5.0 Kg g, 0.030 mol) was taken in dichloromethane (600 mL) and cooled to 0° C. To this solution oxalyl chloride (5.1 Kg, 0.039 mol), catalytic amount DMF (500 mL) were added at the same temperature and stirred for 2 h at room temperature. It was cooled to 0° C. and was basified with sodium carbonate (5.79 Kg, 0.054 mol). To this mixture 2M dimethylamine in THF (15 L, 2M solution) was added slowly (6-8 h) and the contents were stirred at room temperature for 1-2 h. The volatiles were removed by concentration under reduced pressure and the residue was partitioned between water and ethyl acetate. The organic layer was washed with water, brine, dried over sodium sulphate and concentrated. The crude material was purified by column chromatography over 230-400 mesh silica gel using 3-7% ethyl acetate in hexane to afford (E)-4-bromo (chloro)-N,N-dimethylbut-2-enamide (301, 55:45/Br:Cl, 2.5 Kg, 73%) as a brown colour liquid.

^{1}H NMR (300 MHz, $CDCl_3$): δ 6.84-6.94 (m, 1H), 6.4-6.5 (m, 1H), 4.15-4.2 (d, 1H), 3.95-4.0 (d, 1H), 2.9-2.95 (s, 3H), 2.95-3.0 (s, 3H), HPLC: 68.23 and 25.7% at 210 nm.

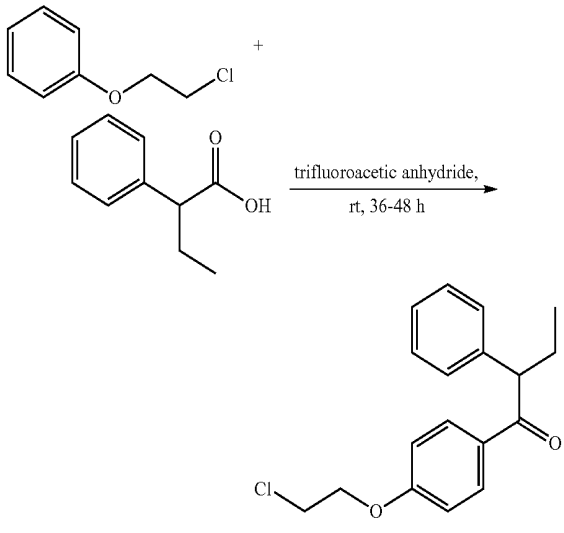
Step-4A: Synthesis of 2-Phenoxyethyl Chloride



In to clean, dry, nitrogen flushed 750 l GLR, charged toluene (150 L), 2-phenoxyethanol (15 kg, 0.108 mol) and pyridine (1.2 kg, 0.162 mol, 0.15 equiv). reaction mass was cooled to 10-15° C., added thionyl chloride (19.3 kg, 0.162 mol, 1.5 equiv) over 90 min. The reaction mixture was then heated to reflux and maintained for 10-12 h. After the reaction completion, it was cooled to 10-15° C. and quenched with water (500 L). The aqueous phase was separated and discarded. The washing procedure was repeated one more time before the vessel was set for vacuum distillation and heated at less than 60° C. until toluene (500 L) had been removed. The residue was then cooled to 30-35° C. before being transferred to a smaller vessel (16 kg, 94%, 95.89% HPLC purity).

^{1}H NMR (400 MHz, DMSO-d6): δ 7.27-7.31 (t, 2H), 6.94-6.96 (t, 3H), 4.22-4.25 (t, 2H), 3.95-4.0 (t, 2H); HPLC: 95.89% at 210 nm.

Step-5A. Synthesis of
1-[4-(2-Chloroethoxy)phenyl]-2-phenyl-1-butanone

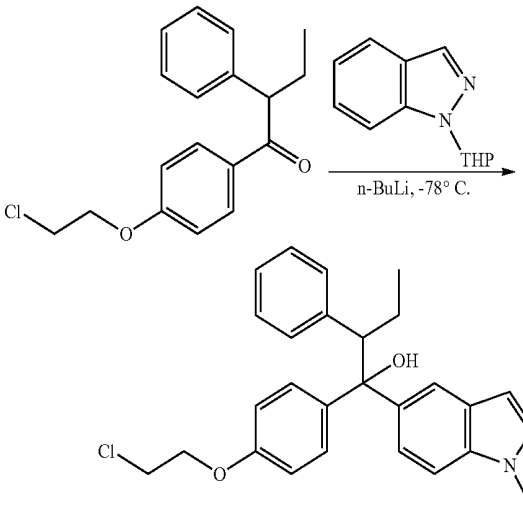


In to clean, dry, nitrogen flushed 2001 Glass reactor, charged 2-Phenoxyethyl chloride (17.0 kg, 69.94 kg at

100%, 1035 mol) and trifluoroacetic anhydride (13 Lt kg) it was stirred for 30 min at 20-25° C. Added 2-Phenylbutyric acid (17.8 kg at 98.7%, 17.9 kg at 100%, 1038 mol). The reaction mixture was maintained at 25-30° C. for 3 days, after completion of the reaction it was quenched with water and basified with potassium carbonate. Obtained product was extracted with DCM (25 l*3), it was washed with water (25 l*2) followed by brine (25 l). Organic layer was dried with sodium sulphate and concentrated under reduced pressure. The solution was cooled to 20° C., and hexane (25 l) was added. The suspension was cooled to 5° C. and stirred at 0-5° C. for 1 h. The product was isolated by filtration and washed with cold hexane (5 l). The wet product was air dried to give ketone (24 kg, 78% Yield, 98.82% HPLC purity).

^{1}H NMR (400 MHz, $CDCl_3$): δ 7.95-7.97 (d, 2H), 7.286-7.28 (m, 4H), 7.18-7.22 (m, 1H), 6.86-6.88 (d, 2H), 4.38-4.40 (t, 1H), 4.22-4.25 (t, 2H), 3.78-3.85 (t, 2H), 2.18-2.22 (m, 1H), 1.85-1.90 (m, 1H), 0.95-0.98 (t, 3H), HPLC; 98.83% at 210 nm, LCMS: 303[M+H]$^+$.

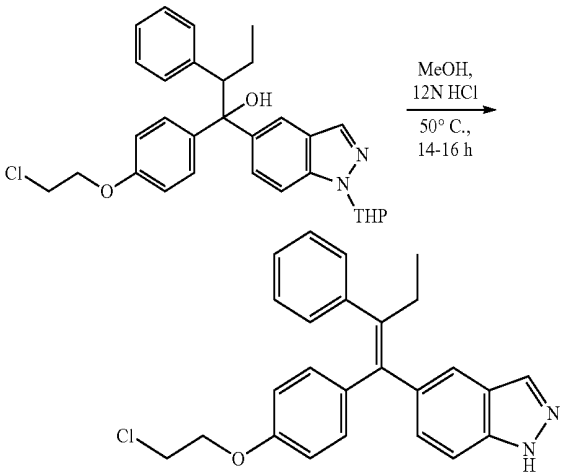
Step-6A: Synthesis of 1-(4-(2-chloroethoxy)phenyl)-2-phenyl-1-(1-(tetrahydro-2H-pyran-2-yl)-1H-indazol-5-yl)butan-1-ol



In to clean, dry, nitrogen flushed 2001 Glass reactor, charged 1-[4-(2-Chloroethoxy) phenyl]-2-phenyl-1-butanone (compound 3)(11 kg, 0.0364 mol, 1 equiv) Compound 300 (10.2 kg, 0.0364 mol, 1.0 equiv THF (110 L) cooled to −78° C. Added n-BuLi (19 L 2.5 molar 13. equiv) in 6-7 h. reaction mass maintained at −78° C. for 2 hr, after completion of the reaction it was quenched with saturated ammonium chloride (4-51) at the same time in 2-3 h and the reaction mass was allowed to warm for the room temperature gradually (8-10 h). Added 25 l of water and the product was extracted with 25 l of ethyl acetate, organic layer was separated and concentrated under reduced vacuum. Obtained crude product was purified through 60-120 silica gel using 0-20ethyl acetate in hexane to get pure compound 4 (6.7 kg, 36.5% Yield, 97.83% HPLC purity)

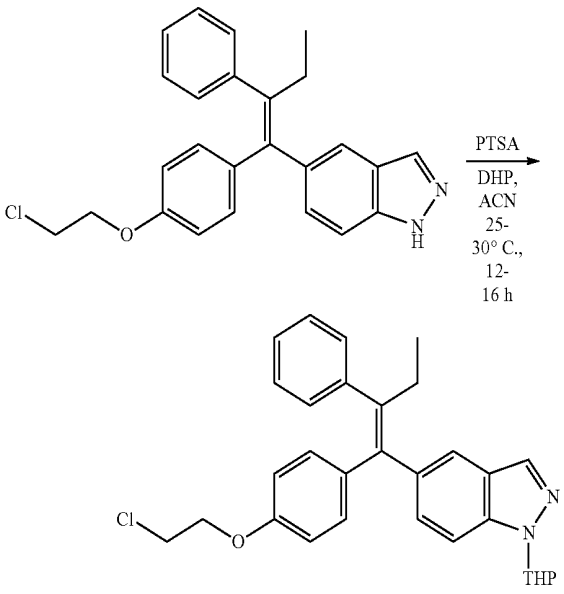
^{1}H NMR (400 MHz, DMSO-d6): δ 8.10 (s, 1H), 7.69-7.72 (d, 1H), 7.65-7.70 (s, 1H), 7.10-7.23 (m, 6H), 6.72-6.74 (d, 2H), 6.55-6.59 (d, 2H), 5.82-5.86 (d, 1H), 3.85-3.90 (s, 1H), 3.75-3.8 (t, 3H), 2.75-2.80 (t, 2H), 1.35-1.40 (m, 3H), 1.95-2.0 (t, 2H), 1.2-2.0 (m, 7H), 0.85-0.90 (t, 3H). HPLC; 97.83% at 210 nm

Step-7A: Synthesis of (E)-5-(1-(4-(2-chloroethoxy) phenyl)-2-phenylbut-1-en-1-yl)-1H-indazole



In to clean, 2001 Glass reactor, charged compound 4 (6.4 Kg, 12.67 mol), methanol (64 L, 10 Vol), and 11N HCl (13 L, 2.5 Vol), the reaction mixture were maintained at 50° C. for 14-16 h. After the reaction completion, methanol was concentrated under reduced pressure and the obtained product was extracted with ethyl acetate (25 l*3), organic layer was washed with water (25 l), dried over anhydrous sodium sulphate and concentrated under reduced pressure. Obtained product was slurry washed with hexane (10 l) to get pure compound 5 as off white solid (4.4 kg, 86.37% Yield, 52.92:46.5 isomer ratio)

Step-8A: Synthesis of (E)-5-(1-(4-(2-chloroethoxy) phenyl)-2-phenylbut-1-en-1-yl)-1-(tetrahydro-2H-pyran-2-yl)-1H-indazole

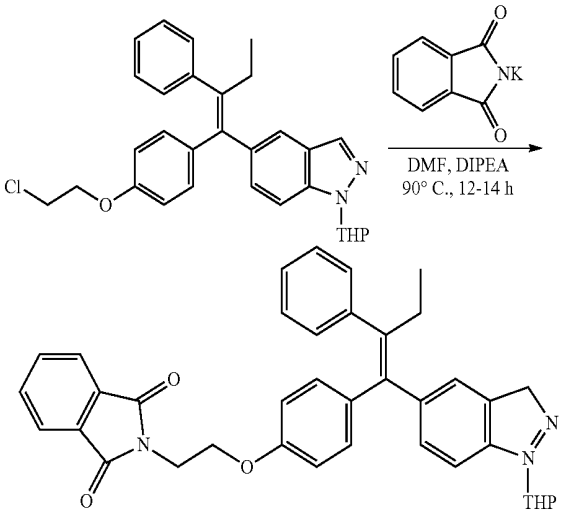


In to clean, dry, nitrogen flushed 2001 Glass reactor, charged compound 5 (5.1 Kg, 12.686 mol) actonitrile (5 Lit) and PTSA (241 g, 1.268 mol), the reaction mixture were

stirred at 28-30° C. for 30 min. To the above solution, dihydropyran 1.6 Kg, 19.03 mol) was added drop wise over a period of 20 min. The resulting mixture was stirred at room temperature for 16 h. Upon completion by TLC, the reaction mixture was quenched with water (500 mL) and acetonitrile was concentrated under reduced pressure. Obtained product was extracted with ethyl acetate (25 l*3), combined organic extracts were washed with water followed by brine, dried over anhydrous sodium sulphate and concentrated under reduced pressure to get the compound 6 (6.Kg, 97% Yield,) as a pale yellow gummy material.

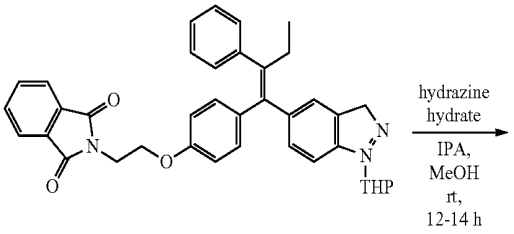
^{1}H NMR (400 MHz, DMSO-d6): compound is having both geometrical isomers in the ratio 39.2:50.4.

Step-9A: Synthesis of (E)-2-(2-(4-(2-phenyl-1-(1-(tetrahydro-2H-pyran-2-yl)-1H-indazol-5-yl)but-1-en-1-yl)phenoxy)ethyl)isoindoline-1,3-dione

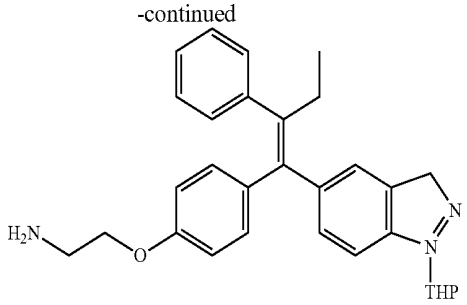


In to clean, dry, nitrogen flushed 200 L Glass reactor, charged compound 6 (5.8 Kg, 11.9 mol, 1.1 equiv), DMF (6 L), potassium phthalamide (2.42 Kg, 13.11 mol), DIPEA (4.6 Kg, 35.7 mol, 3.0 equiv), reaction mass were heated to 90° C. and maintained for 12-14 h. After the reaction completion, it was cooled to 30° C., quenched with 50 L of water and the obtained product was extracted with ethyl acetate, washed with 20 L of water, organic layer was dried over anhydrous sodium sulphate and concentrated under reduced pressure. Obtained solid was stirred with 25 L of 1:1 ethyl acetate and hexane for 5-6 h, filtered the undissolved Z isomer and concentrated the filtrate and the process was repeated till the isomeric purity becomes >80% by HPLC (4.0 kg, 50% Desired isomer).

Step-10A: Synthesis of (E)-2-(4-(2-phenyl-1-(1-(tetrahydro-2H-pyran-2-yl)-1H-indazol-5-yl)but-1-en-1-yl)phenoxy)ethan-1-amine

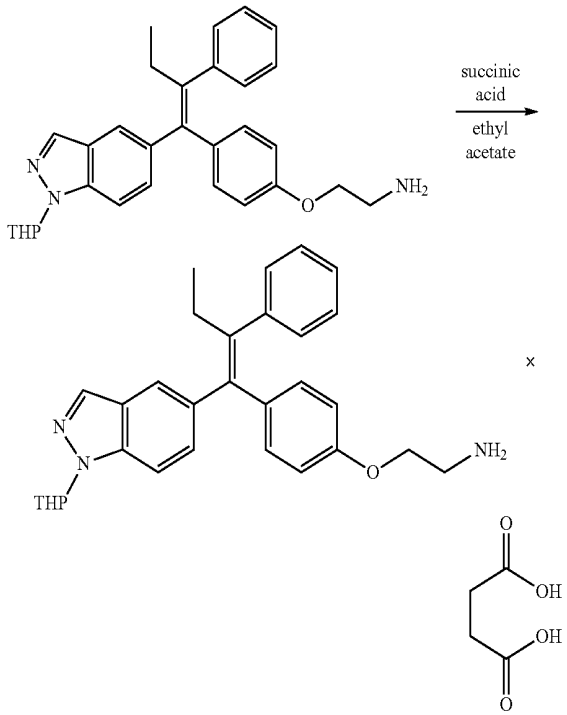


-continued



In to clean, dry, nitrogen flushed 2001 Glass reactor, charged compound 7(6.0 Kg, 10.04 mol), methanol (6 L), IPA (60 L) was cooled to 5-10° C. and added Hydrazine hydrate (10 L, 1.5 vol), After the reaction mass were stirred at 30° C. for 14-16 h. After completion of the reaction, it was filtered to remove succinamide, filtrate was quenched with 10 L of water and the alcohols were concentrated under reduced pressure. Obtained product was extracted with ethyl acetate (25 l*2), organic layer was separated washed with water 25 l, dried over anhydrous sodium sulphate, concentrated to get compound 8 of (4.5 Kg 59.45% Desired isomer purity. 15% Other isomer).

Step-11A: Synthesis of (E)-2-(4-(2-phenyl-1-(1-(tetrahydro-2H-pyran-2-yl)-1H-indazol-5-yl)but-1-en-1-yl)phenoxy)ethan-1-amine succinate salt

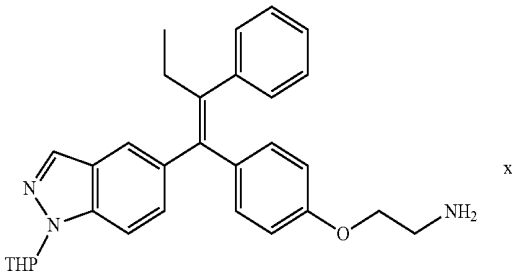


In to clean, dry, nitrogen flushed 2001 Glass reactor, added succinic acid (1.2 Kg, 10.3 mol), ethyl acetate (15 L, 3 vol) and heated to reflux, added compound 8 (4.8 Kg, 10.3 mol) dissolved in (20 L, 4 vol) of ethyl acetate in 20-30 min and continued the reflux for another 30 min. the reaction mass was cooled to 30-40° C. and filtered the solids and washed with (25 L) of ethyl acetate, dried to get 2.1 Kg of desired compound with 93.6% of HPLC purity (2% of undesired geometrical isomer).

^{1}H NMR (300 MHz, DMSO-d6): δ 8.10 (s, 1H), 7.65-7.72 (m, 2H), 7.13-7.21 (m, 6H), 6.75-6.78 (d, 2H), 6.62-6.64 (d, 2H), 3.87-4.01 (m, 4H), 3.69-3.73 (m, 4H), 3.04-

3.05 (t, 3H), 2.27-2.38 (m, 5H), 1.98-2.0 (d, 1H), 1.6 (s, 1H), 0.85-0.90 (t, 2H). HPLC; 93.6% at 210 nm

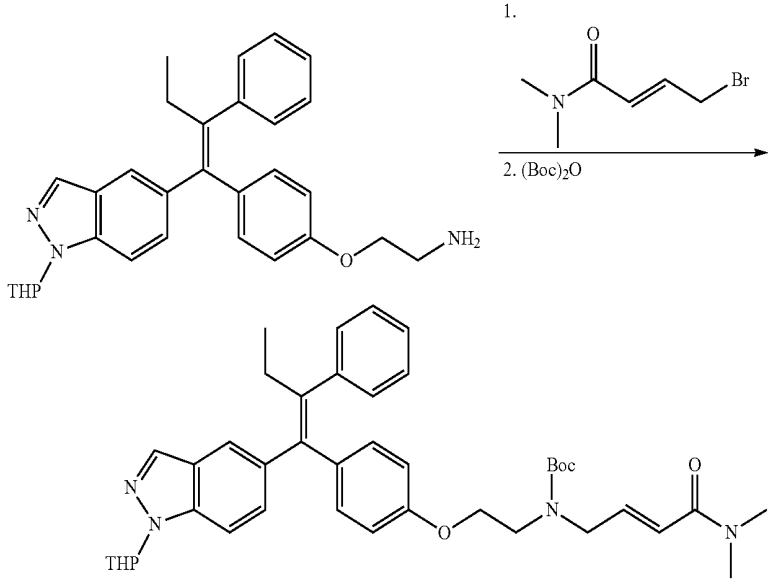
Step-12A: Synthesis of (E)-2-(4-(2-phenyl-1-(1-(tetrahydro-2H-pyran-2-yl)-1H-indazol-5-yl)but-1-en-1-yl)phenoxy)ethan-1-amine



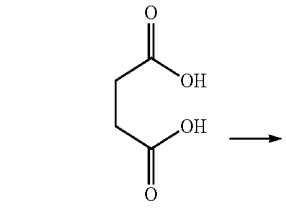
x

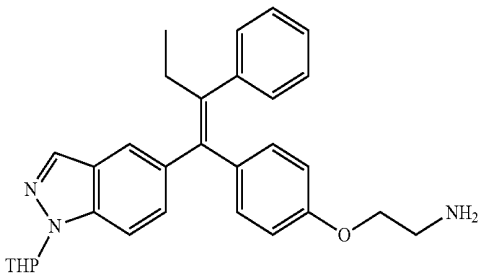
In to a clean 201 four necked RBF, equipped with mechanical stirrer added water 1, compound 9 (2.1 kg, 3.58 mol) and cooled to 10-15° C., added potassium carbonate solution till the pH becomes 9-10, obtained base was extracted with 5 l*3 of DCM. Combined organic layer was washed with water, dried over anhydrous sodium sulphate, concentrated under reduced pressure to get desired compound (1.5 kg, 89% Yield, 90% HPLC, 2.5% other isomer)

Step-13A: Synthesis of (E)-N,N-dimethyl-4-((2-(4-((E)-2-phenyl-1-(1-(tetrahydro-2H-pyran-2-yl)-1H-indazol-5-yl)but-1-en-1-yl) phenoxy) ethyl) amino) but-2-enamide



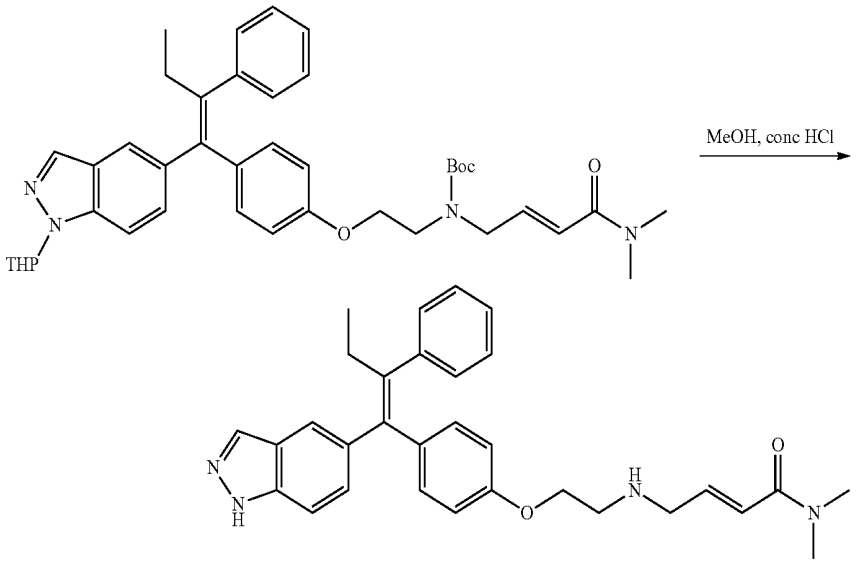
-continued





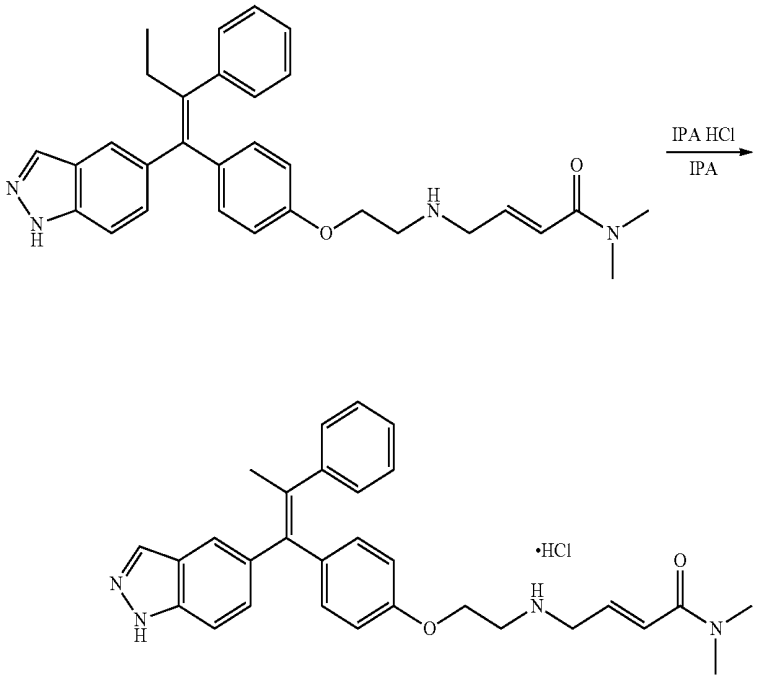
In to a clean, dry, nitrogen flushed 101 four necked RBF, equipped with mechanical stirrer added compound 10 (1.5 Kg, 3.211 mol) DCM (9 L), DIPEA (1.24 Kg, 9.63 mol, 3.0 equiv) and reaction mixture were cooled to 0-5° C. Added (E)-4-bromo (chloro)-N,N-dimethylbut-2-enamide (0.616 Kg, 3.2 mol) dissolved in DCM (2 L) using dropping funnel in 30-40 min (E)-4-bromo (chloro)-N,N-dimethylbut-2-enamide as prepared in Steps and reaction mass was slowly warmed to rt and kept for 24 hr under stirring. It was cooled to 0-5° C., added Boc anhydride (1.05 Kg, 4.81 mol, 1.5 equiv) in DCM (2 L), and stirred for 4-5 hr. After completion of the reaction, it was quenched with water, DCM layer was separated, washed with brine and dried over anhydrous sodium sulphate and concentrated under reduced pressure to desired crude compound which was purified by 60-120 mesh silica gel using 0-20 ethyl acetate in hexane to get (1.23 Kg, 55.3% Yield, 94.3% HPLC of desired product and 2.1% Other isomer.

Step-14A: Synthesis of tert-butyl ((E)-4-(dimethylamino)-4-oxobut-2-en-1-yl)(2-(4-((E)-2-phenyl-1-(1-(tetrahydro-2H-pyran-2-yl)-1H-indazol-5-yl)but-1-en-1-yl)phenoxy)ethyl)carbamate



In to a clean, dry, nitrogen flushed 101 four necked RBF, equipped with mechanical stirrer and reflux condenser, added methanol (12 L) and compound 11 (1.2 Kg, 1.76 mol) reaction mixture were cooled to 0-5° C., added concentrated HCl (2.4 L, 2 vol) using dropping funnel in 30 min and the reaction mixture slowly warmed to room temperature followed by 50° C. It was maintained at the same temperature for 4-6 h, after completion of the reaction, methanol was concentrated under reduced pressure. The reaction mixture was basified with sodium carbonate solution at 10-15° C. and the obtained product was extracted with 2 l*3 of ethyl acetate, washed with water and dried over anhydrous sodium sulphate and concentrated under reduced to get the desired product (1.0 Kg, 80% Yield, 98.22% HPLC purity)

Step-15A: Synthesis of (E)-4-((2-(4-((E)-1-(1H-indazol-5-yl)-2-phenylbut-1-en-1-yl)phenoxy)ethyl)amino)-N,N-dimethylbut-2-enamide hydrochloride



In to a clean, dry, nitrogen flushed 51 four necked RBF, equipped with mechanical stirrer, added compound 11 (600 gm, 1.21 mol) dissolved in 9 L of IPA. It was cooled to 5-10° C., added IPA.HCl till the pH becomes 2.5-3 and stirred at the same temperature for 30 min and filtered the solid formed and washed with 3 L of cold IPA and dried well to 550 (85% Yield) of desired compound (98.07% HPLC).

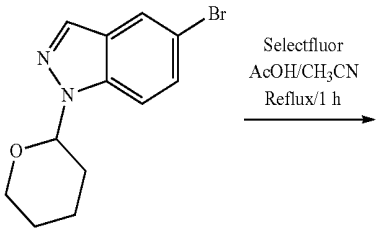
HPLC: 98.07%(210 nm), LCMS (ESI, m/z), 494.5 $[M+H]^+$. Melting point: 220-221° C.

Compound 1 (Hydrochloride Salt):

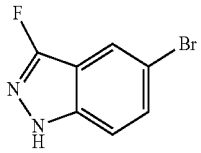
^1H NMR (300 MHz, DMSO-d6): δ 13.05 (s, 1H), 9.28 (s, 2H), 8.07 (s, 1H), 7.60 (s, 1H), 7.5-7.52 (d, J=8.8 Hz, 1H), 7.1-7.22 (m, 6H), 6.78-6.84 (m, 3H), 6.52-6.66 (m, 3H), 4.11-4.13 (t, J=4.4 Hz, 2H), 3.76-3.80 (m, 2H), 3.26-3.3 (m, 2H), 3.03 (s, 3H), 2.86 (s, 3H), 2.40-2.41 (m, 2H), 0.86-0.89 (t, J=7.4 Hz, 3H). HPLC; 98.07% at 210 nm.

Example 2: Synthesis of (E)-4-((2-(4-((E)-1-(3-fluoro-1H-indazol-5-yl)-2-phenyl but-1-en-1-yl) phenoxy) ethyl)amino)-N,N-dimethylbut-2-enamide (Compound 2)

Step-1: Synthesis of 5-bromo-3-fluoro-1H-indazole

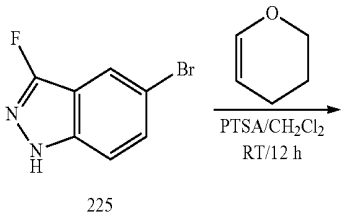


270



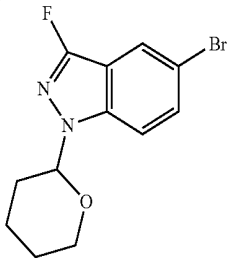
To a stirred solution of 5-bromo-1-(tetrahydro-2H-pyran-2-yl)-1H-indazole (10 g, 35.7 mmol, as prepared in Example 1, Step-1) in 100 mL of acetonitrile, were added acetic acid (4 mL) and selectfluor (25.2 g, 71.4 mmol) at room temperature. Reaction mixture was refluxed for 1 h. Upon completion by TLC, the reaction mixture was diluted with water (100 mL) and extracted with ethyl acetate (200 mL). The combined organic extracts were washed with water, brine, dried over anhydrous sodium sulphate and concentrated under reduced pressure. The crude product was purified over 230-400 mesh silica column chromatography using 1% ethyl acetate in n-hexane to afford 5-bromo-3-fluoro-1H-indazole (6 g, 78%) as a brown oil.

Step-2: Synthesis of 5-bromo-3-fluoro-1-(tetrahydro-2H-pyran-2-yl)-1H-indazole



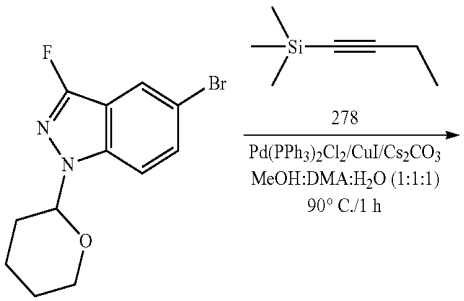
225

-continued

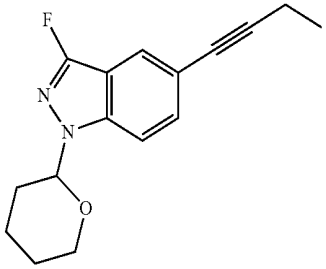


The reaction was carried out according to Scheme 1, Step-1 to give a crude product, which was purified over 230-400 mesh silica column chromatography using 1% ethyl acetate in n-hexane to afford the title compound of Ex. 2 Step-2 (5 g, 60%) as a brown oil.

Step-3: Synthesis of 5-(but-1-yn-1-yl)-3-fluoro-1-(tetrahydro-2H-pyran-2-yl)-1H-indazole

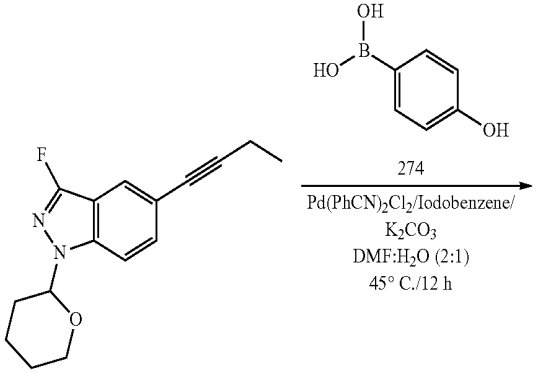


273

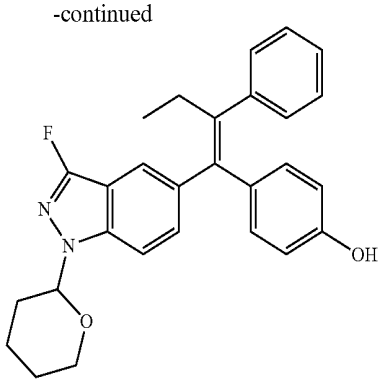


The reaction was carried out according to Scheme 1, Step-2a to afford the title compound of Ex. 2 Step-3 (4.2 g, 99%) as a brown oil.

Step-4: Synthesis of (E)-4-(1-(3-fluoro-1-(tetrahydro-2H-pyran-2-yl)-1H-indazol-5-yl)-2-phenyl-but-1-en-1-yl)phenol

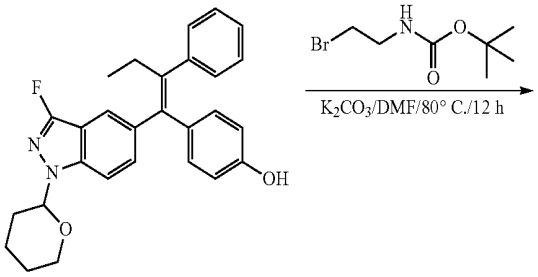


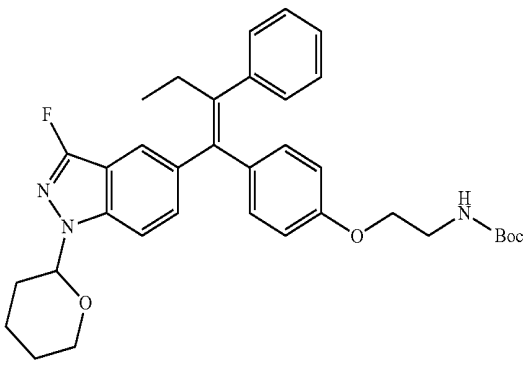
-continued



The reaction was carried out according to Scheme 1, Step-6 to afford the title compound of Ex. 2 Step-4 (1 g, 22%).

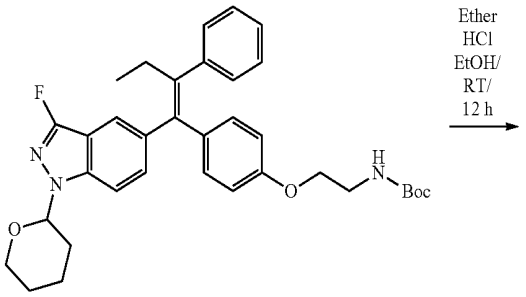
Step-5: Synthesis of tert-butyl (E)-(2-(4-(1-(3-fluoro-1-(tetrahydro-2H-pyran-2-yl)-1H-indazol-5-yl)-2-phenylbut-1-en-1-yl)phenoxy)ethyl)carbamate

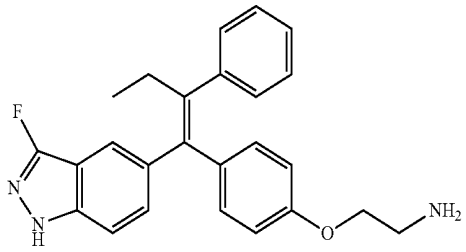




The reaction was carried out according to Scheme 2, Step-1 to give a crude product which was purified by column chromatography over 230-400 mesh silica gel using 10% ethyl acetate in n-hexane to afford the title compound of Ex. 2 Step-5 (1 g, 75%) as a light brown colour gummy mass.

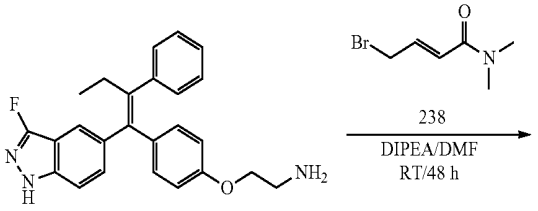
Step-6: Synthesis of (E)-2-(4-(1-(3-fluoro-1H-indazol-5-yl)-2-phenylbut-1-en-1-yl)phenoxy)ethanamine



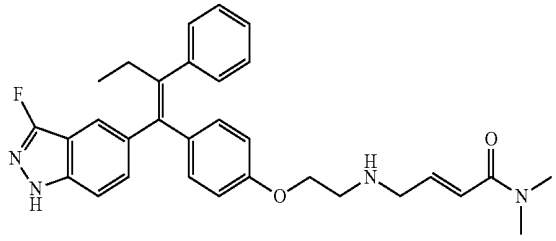


The reaction was carried out according to Scheme 2, Step-2a using (E)-(2-(4-(1-(3-fluoro-1-(tetrahydro-2H-pyran-2-yl)-1H-indazol-5-yl)-2-phenylbut-1-en-1-yl)phenoxy)ethyl)carbamate (0.8 g, 1.61 mmol) for compound 211b. The crude material was purified by silica gel chromatography using (2:98) MeOH in DCM to afford the title compound of Ex. 2 Step-6 (0.23 g) as a white solid.

Step-7: Synthesis of (E)-4-((2-(4-((E)-1-(3-fluoro-1H-indazol-5-yl)-2-phenylbut-1-en-1-yl)phenoxy)ethyl)amino)-N,N-dimethylbut-2-enamide (Compound 2)



237



2

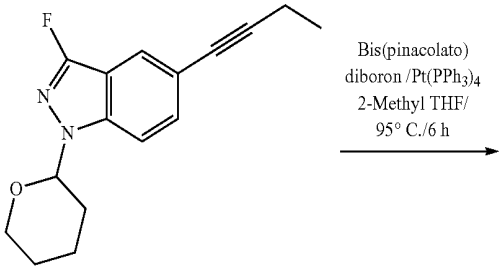
The reaction was carried out according to Scheme 2, Step-3a to afford the title compound of Ex. 2 Step-7 (0.13 g, crude), which was purified by HPLC to give a pure isomer (0.07 g, 37%) as an off-white solid.

Compound 2:

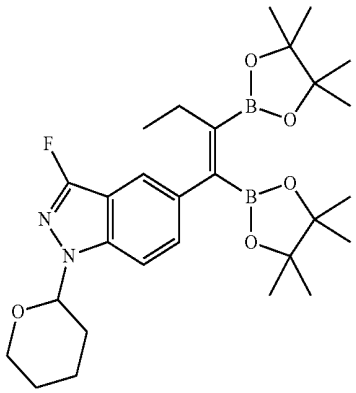
^{1}H NMR (400 MHz, DMSO-d_6) δ 12.57 (s, 1H), 7.50 (s, 1H), 7.47 (dd, J1=8.8 Hz, J2=2.0 Hz, 1H), 7.22-7.19 (m, 6H), 6.77 (s, 1H), 6.74 (s, 1H), 6.74-6.58 (m, 3H), 6.51-6.48 (m, 1H), 3.87 (t, J=5.6 Hz, 2H), 2.98 (s, 3H), 2.79 (s, 3H), 2.73 (t, J=5.6 Hz, 2H), 2.49-2.38 (m, 2H), 0.87 (t, J=7.2 Hz, 3H). ES (MS) 513.2 $[M+H]^+$.

Example 3: Synthesis of (E)-4-((2-(4-((E)-1-(3-fluoro-1H-indazol-5-yl)-2-(3-fluoro-5-(trifluoromethyl) phenyl)but-1-en-1-yl)phenoxy)ethyl)amino)-N,N-dimethylbut-2-enamide (Compound 3)

Step-1: Synthesis of (Z)-5-(1, 2-bis(4,4,5,5-tetramethyl-1,3,2-dioxaborolan-2-yl)but-1-en-1-yl)-3-fluoro-1-(tetrahydro-2H-pyran-2-yl)-1H-indazole

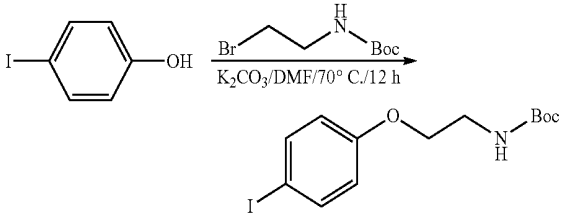


252



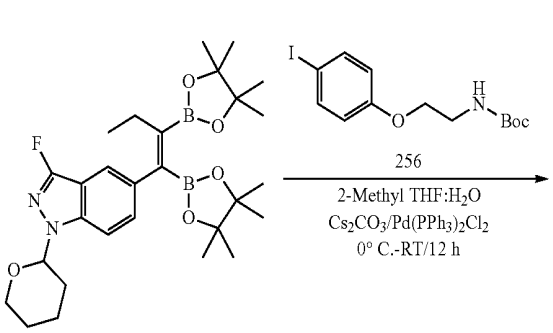
The reaction was carried out according to Scheme 1, Step-3 using 5-(but-1-yn-1-yl)-3-fluoro-1-(tetrahydro-2H-pyran-2-yl)-1H-indazole (2.0 g, 7.29 mmol, as prepared in Example 2, Step-3) for compound 204. The crude material was purified by column chromatography over 230-400 mesh silica gel using 2% EtOAc in n-hexane to afford the title compound of Ex. 3, Step-1 (2.5 g, 65%).

Step-2: Synthesis of tert-butyl (2-(4-iodophenoxy)ethyl)carbamate

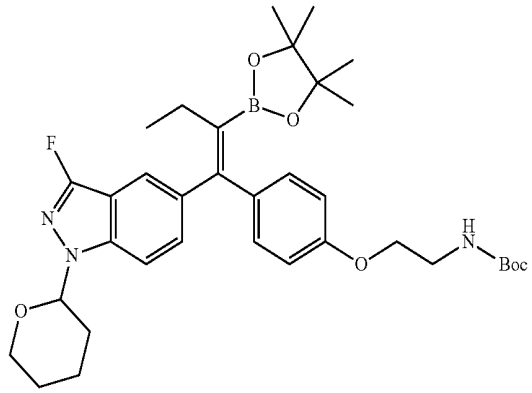


The reaction was carried out according to Scheme 3, Step-1 to obtain the title compound of Ex. 3 Step-2 as an off-white solid (80 g, 97%).

Step-3: Synthesis of tert-butyl (Z)-(2-(4-(1-(3-fluoro-1-(tetrahydro-2H-pyran-2-yl)-1H-indazol-5-yl)-2-(4,4,5,5-tetramethyl-1,3,2-dioxaborolan-2-yl) but-1-en-1-yl)phenoxy)ethyl)carbamate

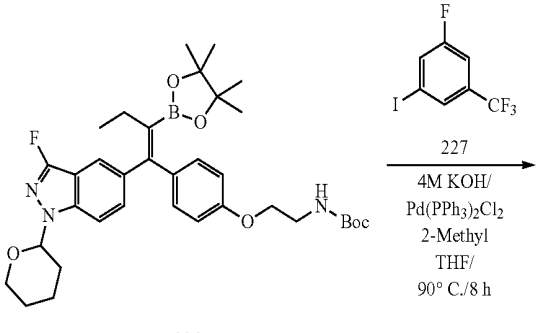


255



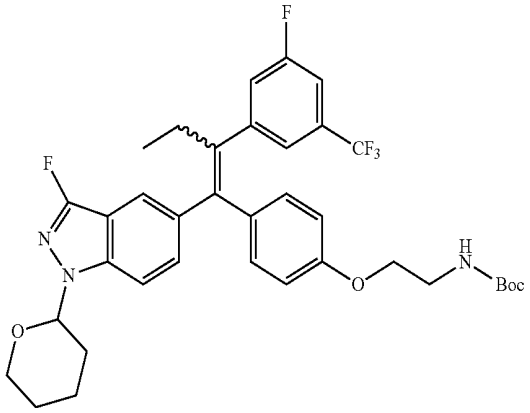
The reaction was carried out according to Scheme 1, Step-4 using (Z)-5-(1,2-bis(4,4,5,5-tetramethyl-1,3,2-dioxaborolan-2-yl)but-1-en-1-yl)-3-fluoro-1-(tetrahydro-2H-pyran-2-yl)-1H-indazole (1.5 g, 2.85 mmol) for compound 206 and tert-butyl (2-(4-iodophenoxy)ethyl)carbamate (1.03 g, 2.85 mmol) for compound 207. The crude product containing the title compound of Ex. 3, Step-3 was used in next step without further purification (2 g).

Step-4: Synthesis of tert-butyl (E)-(2-(4-(1-(3-fluoro-1-(tetrahydro-2H-pyran-2-yl)-1H-indazol-5-yl)-2-(3-fluoro-5-(trifluoromethyl)phenyl)but-1-en-1-yl)phenoxy)ethyl)carbamate



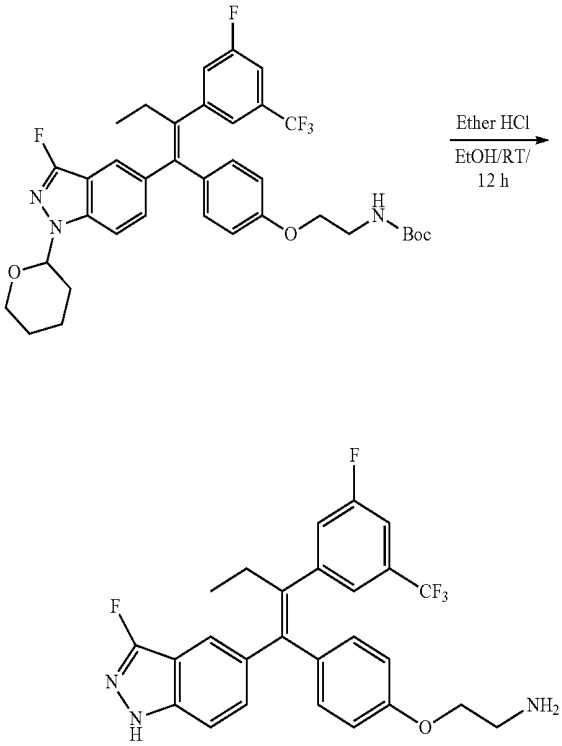
226

-continued



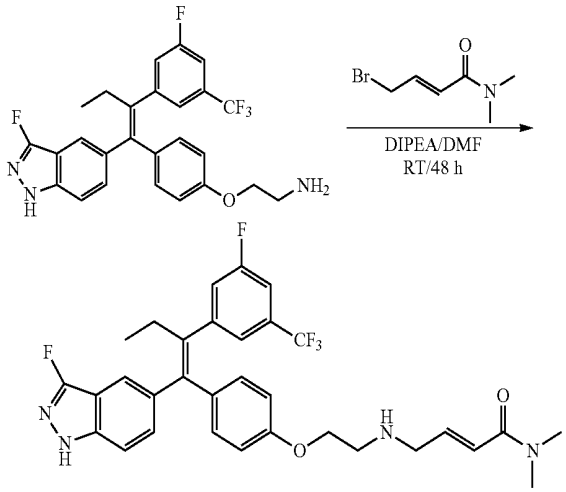
The reaction was carried out according to Scheme 1, Step-5, using tert-butyl (Z)-(2-(4-(1-(3-fluoro-1-(tetrahydro-2H-pyran-2-yl)-1H-indazol-5-yl)-2-(4,4,5,5-tetramethyl-1,3,2-dioxaborolan-2-yl)but-1-en-1-yl)-phenoxy)ethyl)carbamate (950 mg, 1.8 mmol) for compound 208 and 1-fluoro-3-iodo-5-(trifluoromethyl)benzene (523 mg, 1.8 mmol) for compound 209. The crude product was purified by silica gel chromatography (2:8 EtOAc in n-hexane) to give the title compound of Ex. 3, Step-4 (0.5 g, 41%).

Step-5: Synthesis of (E)-2-(4-(1-(3-fluoro-1H-indazol-5-yl)-2-(3-fluoro-5-(trifluoro-methyl)phenyl)but-1-en-1-yl)phenoxy)ethan-1-amine



The reaction was carried out according to Scheme 2, Step-2a to afford the title compound of Ex. 3, Step-5 (0.24 g, 66%) as a brown coloured semi solid.

Step-6: Synthesis of (E)-4-((2-(4-((E)-1-(3-fluoro-1H-indazol-5-yl)-2-(3-fluoro-5-(trifluoromethyl) phenyl)but-1-en-1-yl)phenoxy)ethyl)amino)-N,N-dimethylbut-2-enamide (Compound 3)



3

The reaction was carried out according to Scheme 2, Step-3a to afford the title compound of Ex. 3, Step-6 (0.1 g, 29%) as a white solid.

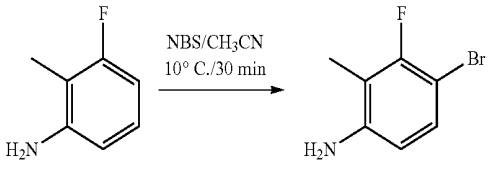
Compound 3:

^{1}H NMR (400 MHz, DMSO-d_6): δ 12.60 (s, 1H), 7.57 (s, 1H), 7.48 (dd, J1=8.8 Hz, J2=6.8 Hz, 1H), 7.41 (t, J=8.8 Hz, 2H), 7.27 (s, 1H), 7.23 (dd, J1=8.4 Hz, J2=0.8 Hz, 1H), 6.80 (d, J=8.8 Hz, 2H), 6.68-6.47 (m, 4H), 3.89 (t, J=5.2 Hz, 2H), 2.99 (s, 3H), 2.84 (s, 3H), 2.77 (t, J=5.6 Hz, 2H), 2.49-2.42 (m, 2H), 0.89 (t, J=7.2 Hz, 3H). ES (MS): 599.3 $[M+H]^+$.

Example 4: Synthesis of (E)-4-((2-(4-((E)-1-(4-fluoro-1H-indazol-5-yl)-2-phenyl but-1-en-1-yl) phenoxy) ethyl)amino)-N,N-dimethylbut-2-enamide. (Compound 4)

The compound was synthesized following the approach as outlined in Example 2 by substituting into Step-2 5-bromo-4-fluoro-1H-indazole (preparation shown below in Ex. 4 Steps 1-2) for compound 225 to afford Compound 4 (0.03 g, 5%) as a white solid.

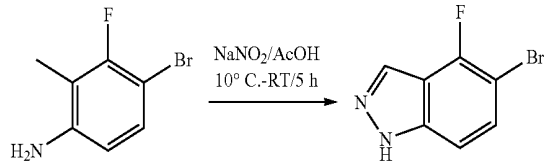
Step-1: Synthesis of 4-bromo-3-fluoro-2-methylaniline



To a stirred solution of 3-fluoro-2-methylaniline (15 g, 0.1199 mol) in acetonitrile (300 mL) was added N-bromo succinamide (23.5 g, 0.131 mol) at 0° C. The reaction mixture was stirred for 30 min at 10° C., after completion of reaction (monitored by TLC), the reaction mixture was

diluted with EtOAc. Organic layer was washed with water followed by brine, dried over anhydrous sodium sulphate, filtered and concentrated under reduced pressure. The crude product was used in next step without further purification to afford 4-bromo-3-fluoro-2-methylaniline (25 g, crude) as a white solid.

Step-2: Synthesis of 5-bromo-4-fluoro-1H-indazole



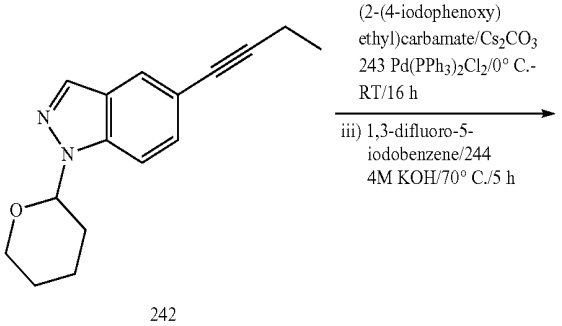
To a stirred solution of 4-bromo-3-fluoro-2-methylaniline (20 g, 98 mmol) in acetic acid was added sodium nitrite (8.1 g, 117 mmol) at 10° C., and the contents were stirred at room temperature for 5 h. After completion of reaction (monitored by TLC), the reaction mixture was cooled to 0° C., 50% NaOH solution was added drop wise till the pH of the solution becomes 9. Reaction mixture was diluted with ethyl acetate and the organic layer was washed with water followed by brine. The organic layer was dried over anhydrous Na_2SO_4 and concentrated under reduced pressure. The crude compound was purified by column chromatography over 230-400 mesh silica gel using (10-15%) ethyl acetate in n-hexane as an eluent to obtain title compound of Ex. 4 Step-2 (6.1 g, 29%) as a yellow solid.

Compound 4:

^{1}H NMR (400 MHz, DMSO-d_6): δ 13.39 (s, 1H), 8.17 (s, 1H), 7.39 (d, J=8.4 Hz, 1H), 7.24-7.2 (m, 2H), 7.18-7.15 (m, 4H), 6.77 (d, J=8.4 Hz, 2H), 6.62-6.57 (m, 3H), 6.51-6.47 (m, 1H), 3.86 (t, J=5.6 Hz, 2H), 3.31 (m, 2H), 2.98 (s, 3H), 2.83 (s, 3H), 2.77 (t, J=5.4 Hz, 2H), 2.33-2.30 (m, 2H), 0.89 (t, J=7.4 Hz, 3H). ES (MS): 513.3 $[M+H]^+$.

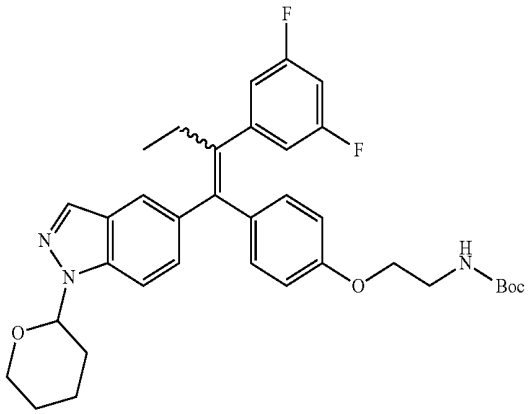
Example 5: Synthesis of (E)-4-((2-(4-((E)-2-(3,5-difluorophenyl)-1-(1H-indazol-5-yl)but-1-en-1-yl) phenoxy)ethyl)amino)-N,N-dimethylbut-2-enamide (Compound 5)

Step-1: Synthesis of tert-butyl (E)-(2-(4-(2-(3, 5-difluorophenyl)-1-(1-(tetrahydro-2H-pyran-2-yl)-1H-indazol-5-yl)but-1-en-1-yl)phenoxy)ethyl)carbamate



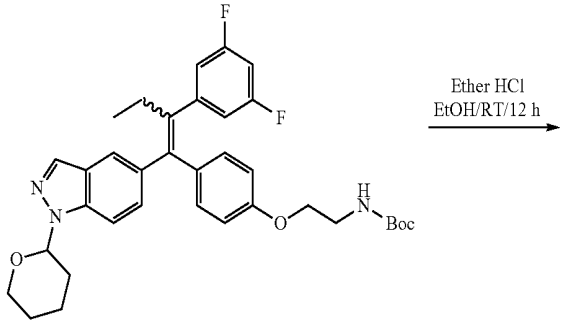
242

-continued

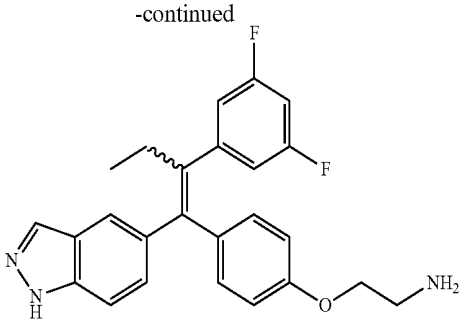


To a stirred solution of 5-(but-1-yn-1-yl)-1-(tetrahydro-2H-pyran-2-yl)-1H-indazole (0.4 g, 1.574 mmol, Example 1, Step-3) in 2-methyl THF (5 mL), was added bis(pinacolato)diboron (0.44 g, 1.732 mmol), tetrakis(triphenylphosphine)platinum(0) (14.6 mg, 0.0118 mmol) under nitrogen atmosphere, reaction mixture was heated at 90° C. for 5 h. After completion of reaction (monitored by TLC), reaction mixture was allowed to cool to 4° C. and tert-butyl (2-(4-iodophenoxy)ethyl)carbamate (571 mg, 1.574 mmol, Example 3, Step-2), bis(triphenylphosphine)palladium(II) dichloride (55 mg, 0.078 mmol), cesium carbonate (1.023 g, 3.140 mmol) and 2-methyl THF (5 mL) were added. This mixture was degassed with nitrogen and water (1.2 mL) was added. Reaction mixture was stirred at room temperature for 16 h. After completion of reaction (monitored by TLC), 1,3-difluoro-5-iodobenzene (528 mg, 2.20 mmol) and 4M aqueous KOH (3 mL) were added and the mixture was degassed with nitrogen and heated at 70° C. for 5 h. Upon completion, the reaction mixture was filtered through a celite/silicagel pad and washed with EtOAc. The filtrate was washed with water, brine, dried over anhydrous sodium sulphate, filtered and concentrated under reduced pressure. The crude product was purified by silica gel chromatography (2:8 EtOAc in n-hexane) to give title compound of Ex. 5 Step-1 (500 mg, 54%).

Step-2: Synthesis of (E)-2-(4-(2-(3, 5-difluorophenyl)-1-(1H-indazol-5-yl)but-1-en-1-yl)phenoxy) ethan-1-amine

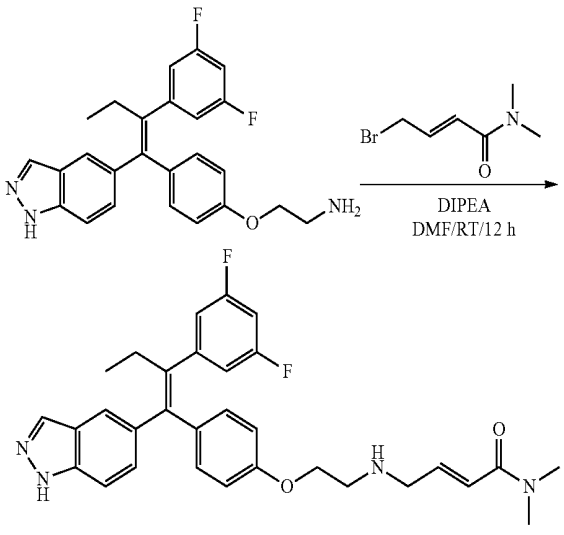


-continued



The reaction was carried out according to Scheme 2, Step-2a by substituting in tert-butyl (E)-(2-(4-(2-(3,5-difluorophenyl)-1-(1-(tetrahydro-2H-pyran-2-yl)-1H-indazol-5-yl)but-1-en-1-yl)phenoxy)ethyl)carbamate for compound 211b to afford title compound of Ex. 5 Step-2 (0.340 g, 97%) as a white solid.

Step-3: Synthesis of (E)-4-((2-(4-((E)-2-(3,5-difluorophenyl)-1-(1H-indazol-5-yl)but-1-en-1-yl)phenoxy) ethyl)amino)-N,N-dimethylbut-2-enamide (Compound 5)



The compound was made according to Scheme 2, Step-3a by substituting in (E)-2-(4-(2-(3,5-difluorophenyl)-1-(1H-indazol-5-yl)but-1-en-1-yl)phenoxy)ethan-1-amine for compound 213 to afford Compound 5 (60 mg, 14%) as a white solid.

Compound 5:

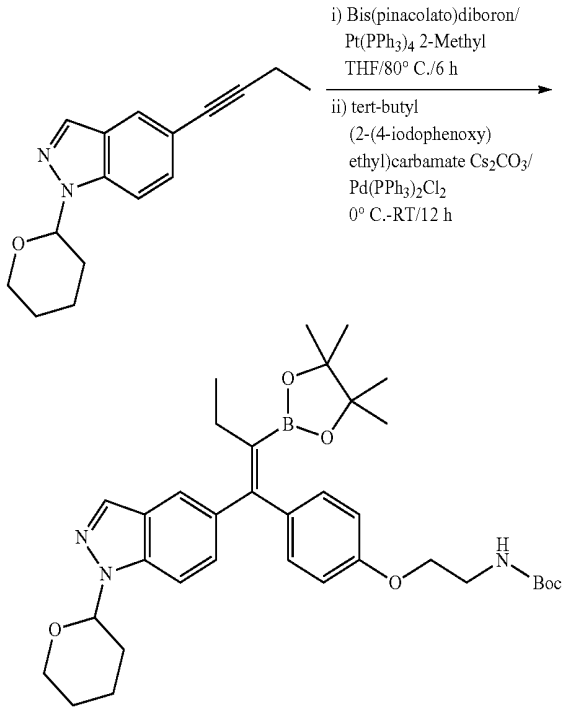
^{1}H NMR (400 MHz, DMSO-d_6): δ 13.08 (s, 1H), 8.07 (s, 1H), 7.61 (s, 1H), 7.52 (d, J=8.8 Hz, 1H), 7.12 (d, J=8.4 Hz, 1H), 6.99 (m, 1H), 6.868 (m, 1H), 6.795 (d, J=8.8 Hz, 2H), 6.67 (d, J=8.8 Hz, 2H), 6.63-6.58 (m, 1H), 3.9 (t, J=5.6 Hz, 2H), 3.31 (m, 2H), 2.99 (s, 3H), 2.84 (s, 3H), 2.79 (t, J=5.6 Hz, 2H), 2.39 (q, J=7.2 Hz, 2H), 0.89 (t, J=7.4 Hz, 3H).

LCMS: 531.3 $[M+H]^+$.

Example 6: Synthesis of (E)-4-((2-(4-((E)-2-(3,4-difluorophenyl)-1-(1H-indazol-5-yl)but-1-en-1-yl) phenoxy)ethyl)amino)-N,N-dimethylbut-2-enamide (Compound 6)

The compound was synthesized following the approach as outlined in Example 3 substituting into Step-4 tert-butyl (E)-(2-(4-(2-(3,4-difluorophenyl)-1-(1-(tetrahydro-2H-pyran-2-yl)-1H-indazol-5-yl)but-1-en-1-yl)phenoxy)ethyl) carbamate for compound 226 (preparation shown below in Example 6, Step-1) and 1,2-difluoro-5-iodobenzene for compound 227 to afford Compound 6 (50 mg, 8%) as a white solid.

Step-1: Synthesis of tert-butyl (E)-(2-(4-(2-(3,4-difluorophenyl)-1-(1-(tetrahydro-2H-pyran-2-yl)-1H-indazol-5-yl)but-1-en-1-yl)phenoxy)ethyl)carbamate



To a stirred solution of 5-(but-1-yn-1-yl)-1-(tetrahydro-2H-pyran-2-yl)-1H-indazole (2.5 g, 9.84 mmol, as prepared in Example 1, Step-3) in 2-methyl THF (20 mL), was added bis(pinacolato)diboron (2.52 g, 9.94 mmol), tetrakis(triphenylphosphine)platinum(0) (93 mg, 0.0748 mmol) under nitrogen atmosphere, reaction mixture was heated at 80° C. for 6 h. The solution was allowed to cool to 4° C., and tert-butyl (2-(4-iodophenoxy)ethyl)carbamate (3.57 g, 9.84 mmol, as prepared in Example 3, Step-2), bis(triphenylphosphine)palladium(II) dichloride (345 mg, 0.492 mmol), cesium carbonate (6.4 g, 19.68 mmol) and 2-methyl THF (10 mL) were added. This mixture was degassed with nitrogen and water (6 mL) was added. This mixture was stirred at room temperature for 12 h. After completion of reaction, reaction mixture was diluted with water and extracted with EtOAc. The Organic layer was dried over anhydrous sodium sulphate and concentrated under reduced pressure. The crude material was purified by column chromatography over 230-400 mesh silica gel using EtOAc in n-hexane (3:7) to afford the title compound of Ex. 6 Step-1 (3.85 g, 64%) as a gummy solid.

Compound 6:

^{1}H NMR (400 MHz, DMSO-d_6): δ 13.09 (s, 1H), 8.07 (s, 1H), 7.60 (s, 1H), 7.51 (d, J=8.0 Hz, 1H), 7.29-7.20 (m, 2H), 7.11 (d, J=8.8 Hz, 1H), 6.94 (bs, 1H), 6.77 (d, J=8.80 Hz, 2H), 6.65 (d, J=8.8 Hz, 2H), 6.63-6.48 (m, 2H), 3.71 (t,

J=5.6 Hz, 2H), 2.99 (s, 3H), 2.84 (s, 3H), 2.78 (t, J=5.2 Hz, 2H), 2.43-2.32 (m, 2H), 0.89 (t, J=7.2 Hz, 3H). LCMS: 531.3 $[M+H]^+$.

Example 7: Synthesis of (E)-4-((2-(4-((E)-2-(3-chloro-5-fluorophenyl)-1-(1H-indazol-5-yl)but-1-en-1-yl) phenoxy)ethyl)amino)-N,N-dimethylbut-2-enamide

The compound was synthesized following the approach as outlined in Example 3 by substituting into Step-4 tert-butyl (Z)-(2-(4-(1-(1-(tetrahydro-2H-pyran-2-yl)-1H-indazol-5-yl)-2-(4,4,5,5-tetramethyl-1,3,2-dioxaborolan-2-yl)but-1-en-1-yl)phenoxy)-ethyl)carbamate (1.5 g, 2.43 mmol, as prepared in Example 6, Step-1) for compound 226 and 1-chloro-3-fluoro-5-iodobenzene for compound 227 in step-4 to afford the title compound (50 mg, 9%) as a white solid.

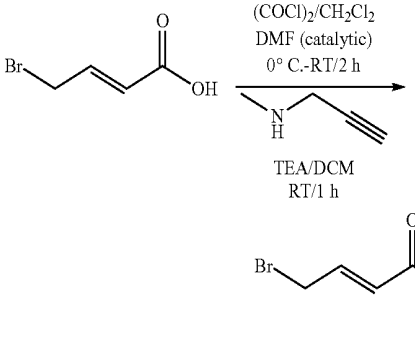
Compound 7:

^{1}H NMR (400 MHz, DMSO-d_6): δ 13.10 (s, 1H), 8.08 (s, 1H), 7.61 (s, 1H), 7.52 (d, J=8.8 Hz, 1H), 7.19 (d, J=8.8 Hz, 1H), 7.12 (d, J=8.6 Hz, 1H), 7.05 (s, 2H), 7.00 (d, J=8.8 Hz, 2H), 6.68 (d, J=8.8 Hz, 2H), 6.63-6.58 (m, 1H), 6.52-6.48 (m, 1H), 3.9 (t, J=5.6 Hz, 2H), 3.33-3.31 (m, 2H), 2.99 (s, 3H), 2.84 (s, 3H), 2.79 (t, J=5.6 Hz, 2H), 2.44-2.32 (m, 2H), 0.89 (t, J=7.4 Hz, 3H). ESMS: 547.3 $[M+H]^+$.

Example 8: Synthesis of (E)-4-((2-(4-((E)-1-(1H-indazol-S-yl)-2-phenylbut-1-en-1-yl)phenoxy) ethyl) amino)-N-methyl-N-(prop-2-yn-1-yl)but-2-enamide (Compound 8)

The compound was synthesized following the approach as outlined in Example 1 by substituting into Step-8 (E)-4-bromo-N-methyl-N-(prop-2-yn-1-yl)but-2-enamide (preparation shown below in Ex. 8 Step-1) for compound 228 and 2-(4-(1-(1H-indazol-5-yl)-2-phenylbut-1-en-1-yl)phenoxy) ethan-1-amine (preparation shown below in Ex. 9, Step 4-5) for compound 229 to afford Compound 8 (4 mg, yield: 5%) as a light green solid.

Step-1: Synthesis of (E)-4-bromo-N-methyl-N-(prop-2-yn-1-yl)but-2-enamide



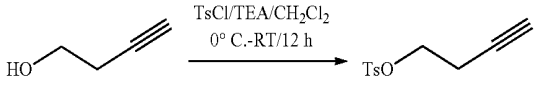
The reaction was carried out according to Scheme 4, Step-2, using N-methylprop-2-yn-1-amine for compound 221 to afford a mixture of (E)-4-bromo-N-methyl-N-(prop-2-yn-1-yl)but-2-enamide (0.5 g, 19%) as a brown colour liquid.

Compound 8:

^{1}H NMR (400 MHz, DMSO-d_6): δ 13.06 (s, 1H), 8.06 (s, 1H), 7.61 (s, 1H), 7.51 (d, J=7.2 Hz, 1H), 7.22-7.10 (m, 6H), 6.74 (d, J=8.8 Hz, 2H), 6.60-6.52 (m, 4H), 4.22-4.16 (m, 2H), 3.87 (t, J=5.2 Hz, 2H), 3.02 (s, 2H), 2.87 (bs, 1H), 2.78 (t, J=5.6 Hz, 2H), 2.43-2.37 (m, 2H), 0.87 (t, J=7.6 Hz, 3H). ESMS: 519.2 $[M+H]^+$.

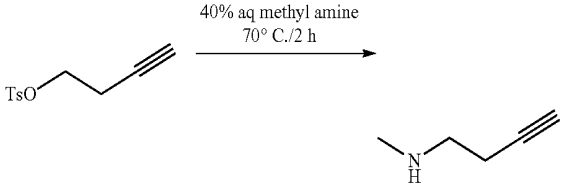
Example 9: Synthesis of (E)-4-((2-(4-((E)-1-(1H-indazol-5-yl)-2-phenylbut-1-en-1-yl)phenoxy)ethyl) amino)-N-(but-3-yn-1-yl)-N-methylbut-2-enamide (Compound 9)

Step-1: Synthesis of but-3-yn-1-yl 4-methylbenzenesulfonate



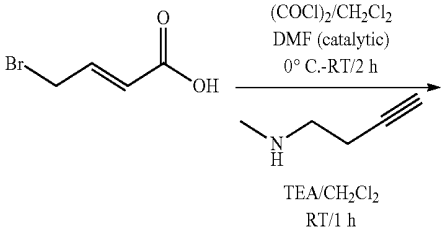
To a stirred solution of but-3-yn-1-ol (5 g, 0.0714 mmol) in dichloromethane (50 mL) at 0° C. was added triethylamine (10.82 g, 0.107 mmol) and tosyl chloride (13.61 g, 0.0714 mmol). The reaction mixture was stirred at room temperature for 12 h, after completion of reaction (monitored by TLC), reaction mixture was diluted with dichloromethane. The organic layer was washed with water, brine and dried over anhydrous Na_2SO_4 and concentrated under reduced pressure to afford but-3-yn-1-yl 4-methylbenzenesulfonate (13 g, 81%).

Step-2: Synthesis of N-methylbut-3-yn-1-amine

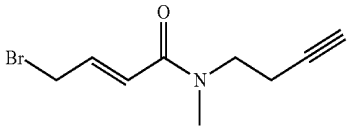


But-3-yn-1-yl 4-methylbenzenesulfonate (10 g, 44.6 mmol) was added to 40% aqueous methylamine (30 mL). The contents were heated at 70° C. under nitrogen for 2 h. After completion of reaction, reaction mixture was cooled to room temperature, the volatiles removed under vacuum and extracted with dichloromethane (250 mL). The organic layer was washed with water, brine and dried over anhydrous sodium sulphate. Organic layer was dried under reduced pressure to give N-methylbut-3-yn-1-amine (3.7 g, crude).

Step-3: Synthesis of (E)-4-bromo-N-(but-3-yn-1-yl)-N-methylbut-2-enamide

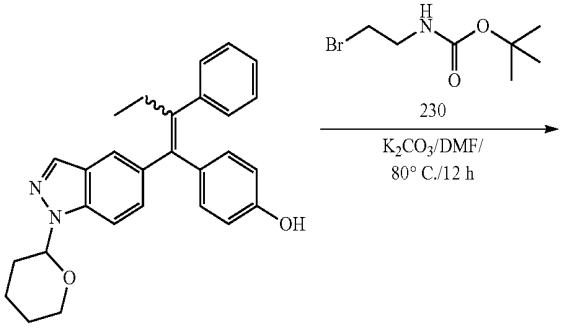


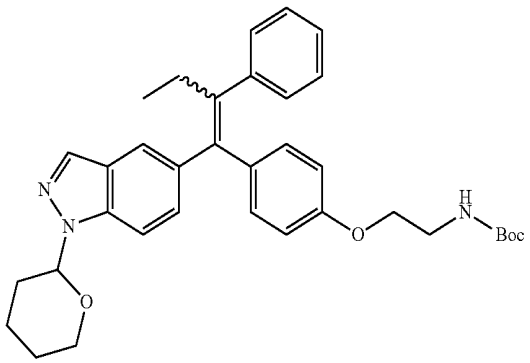
-continued



The reaction was carried out according to Scheme 4, Step-2, using N-methylbut-3-yn-1-amine for compound 221, to afford a mixture of (E)-4-bromo-N-(but-3-yn-1-yl)-N-methylbut-2-enamide (1.8 g, crude) as a brown colour liquid.

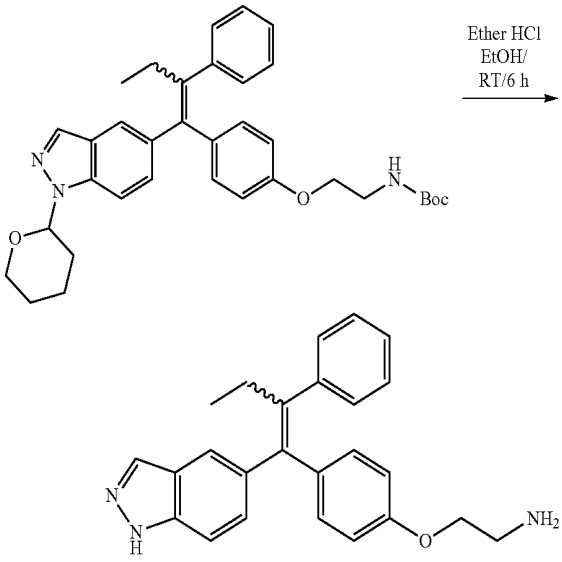
Step-4: Synthesis of tert-butyl (2-(4-(2-phenyl-1-(1-(tetrahydro-2H-pyran-2-yl)-1H-indazol-5-yl)but-1-en-1-yl)phenoxy)ethyl)carbamate





To a solution of (E)-4-(2-phenyl-1-(1-(tetrahydro-2H-pyran-2-yl)-1H-indazol-5-yl)but-1-en-1-yl)phenol (3 g, 7.0 mmol, as prepared in Example 1, Step-4) in DMF (30 mL), were added sequentially potassium carbonate (4.8 g, 35.3 mmol) and tert-butyl (2-bromoethyl)carbamate (3.16 g, 14.1 mmol). The reaction mixture was stirred at 80° C. for 12 h, after completion of reaction, reaction mixture was poured on ice cold water. The solid separated was filtered and dried under reduced pressure to afford the title compound of Ex.9 Step-4 (2.5 g, 64%) as an off-white solid.

Step-5: Synthesis of 2-(4-(1-(1H-indazol-5-yl)-2-phenylbut-1-en-1-yl)phenoxy)ethan-1-amine



The reaction was carried out according to Scheme 2, Step-2a using tert-butyl (2-(4-(2-phenyl-1-(1-(tetrahydro-2H-pyran-2-yl)-1H-indazol-5-yl)but-1-en-1-yl)phenoxy) ethyl)carbamate (2.5 g, 4.4 mmol) for compound 211b to afford the title compound of Ex 9. Step-5 (0.8 g, 47%) as an off-white solid.

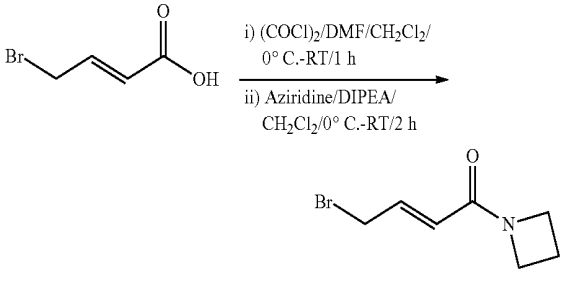
Compound 9:

^{1}H NMR (400 MHz, DMSO-d_6): δ 13.07 (s, 1H), 8.06 (s, 1H), 7.61 (s, 1H), 7.51 (d, J=8.8 Hz, 1H), 7.20-7.11 (m, 6H), 6.74 (d, J=8.8 Hz, 2H), 6.60-6.57 (m, 4H), 3.86 (t, J=4.8 Hz, 2H), 3.49-3.38 (m, 3H), 3.03 (s, 2H), 2.86-2.84 (m, 3H), 2.77 (t, J=6.40 Hz, 2H), 2.43-2.32 (m, 4H), 0.87 (t, J=7.2 Hz, 3H). LCMS: 533.4 $[M+H]^+$.

Example 10: Synthesis of (E)-4-((2-(4-((E)-1-(1H-indazol-5-yl)-2-phenylbut-1-en-1-yl)phenoxy)ethyl) amino)-1-(azetidin-1-yl)but-2-en-1-one (Compound 10)

The compound was synthesized following the approach as outlined in Example 9 by substituting into Step-4 (E)-1-(azetidin-1-yl)-4-bromobut-2-en-1-one (preparation shown below in Ex. 10 Step-1) for compound 230 to afford compound 10 (22 mg, 4.1%) as a white solid.

Step-1: Synthesis of (E)-1-(azetidin-1-yl)-4-bromobut-2-en-1-one



The reaction was carried out according to Scheme 4, Step-2, using aziridine for compound 221, to afford (E)-1-(azetidin-1-yl)-4-bromobut-2-en-1-one (1 g, 27%) as a brown colour liquid.

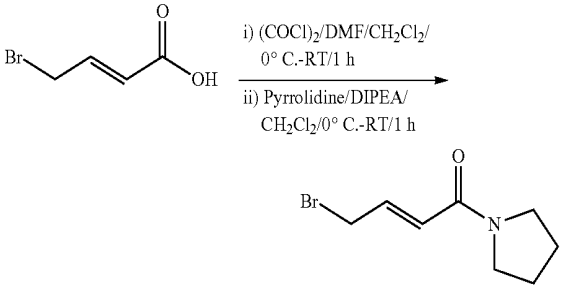
Compound 10:

^{1}H NMR (400 MHz, DMSO-d_6): δ 13.08 (s, 1H), 8.07 (s, 1H), 7.6 (s, 1H), 7.51 (d, J=8.4 Hz, 1H), 7.2 (d, J=7.6 Hz, 2H), 7.15-7.11 (m, 4H), 6.75 (d, J=8.8 Hz, 2H), 6.61-6.57 (m, 3H), 6.04 (d, J=16 Hz, 1H), 4.12 (t, J=7.6 Hz, 2H), 3.88-3.84 (m, 4H), 3.32-3.3 (m, 2H), 2.77 (t, J=5.6 Hz, 2H), 2.42-2.4 (m, 2H), 2.19-2.15 (m, 2H), 0.88 (t, J=7.6 Hz, 3H). LCMS: 507.1 $[M+H]^+$.

Example 11: Synthesis of (E)-4-((2-(4-((E)-1-(1H-indazol-5-yl)-2-phenylbut-1-en-1-yl)phenoxy)ethyl) amino)-1-(pyrrolidin-1-yl)but-2-en-1-one (Compound 11)

The compound was synthesized following the approach as outlined in Example 9 by substituting into Step-4 (E)-4-bromo-1-(pyrrolidin-1-yl)but-2-en-1-one (preparation shown below in Ex. 9 Step-1) for compound 230 to afford title compound 11 (7.5 mg, 6.6%) as a white solid.

Step-1: Synthesis of (E)-4-bromo-1-(pyrrolidin-1-yl)but-2-en-1-one



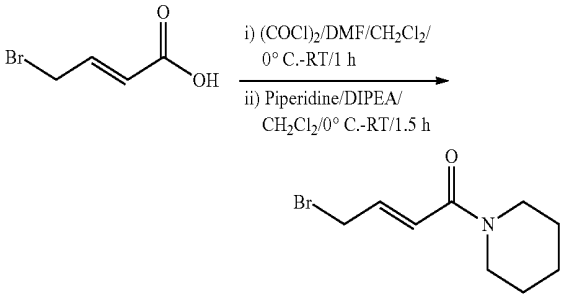
The reaction was carried out according to Scheme 4, Step-2, using pyrrolidine to afford (E)-4-bromo-1-(pyrrolidin-1-yl)but-2-en-1-one (0.31 g, 6%) as a brown colour liquid.

Compound 11:

^{1}H NMR (400 MHz, DMSO-d_6): δ 13.06 (s, 1H), 8.07 (s, 1H), 7.61 (s, 1H), 7.51 (d, J=8.8 Hz, 1H), 7.22-7.11 (m, 6H), 6.75 (d, J=8.8 Hz, 2H), 6.65-6.58 (m, 3H), 6.31 (d, J=15.2 Hz, 1H), 3.86 (t, J=5.6 Hz, 2H), 3.45 (t, J=6.8 Hz, 2H), 2.77 (t, J=5.6 Hz, 2H), 2.43-2.38 (m, 2H), 1.9-1.73 (m, 6H), 0.88 (t, J=7.2 Hz, 5H). LCMS: 521.3 $[M+H]^+$.

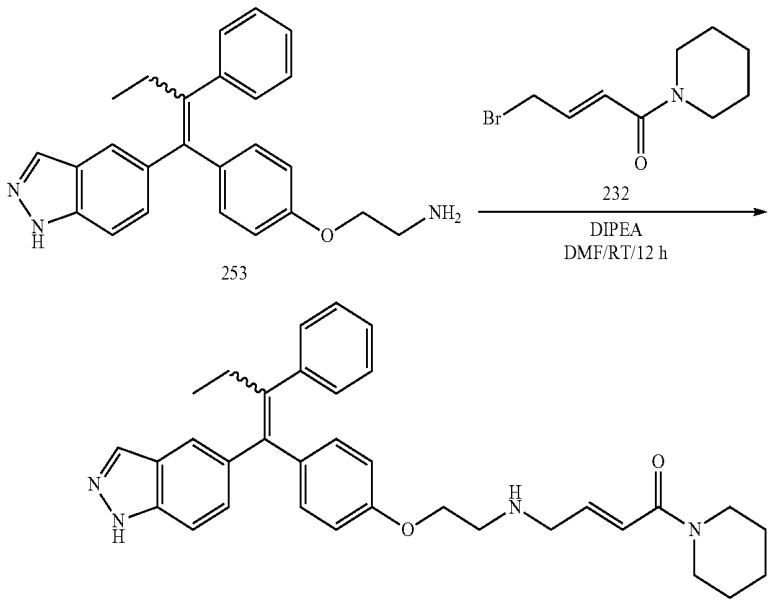
Example 12: Synthesis of (E)-4-((2-(4-((E)-1-(1H-indazol-5-yl)-2-phenylbut-1-en-1-yl)phenoxy)ethyl) amino)-1-(piperidin-1-yl)but-2-en-1-one (Compound 12)

Step-1: Synthesis of (E)-4-bromo-1-(piperidin-1-yl) but-2-en-1-one



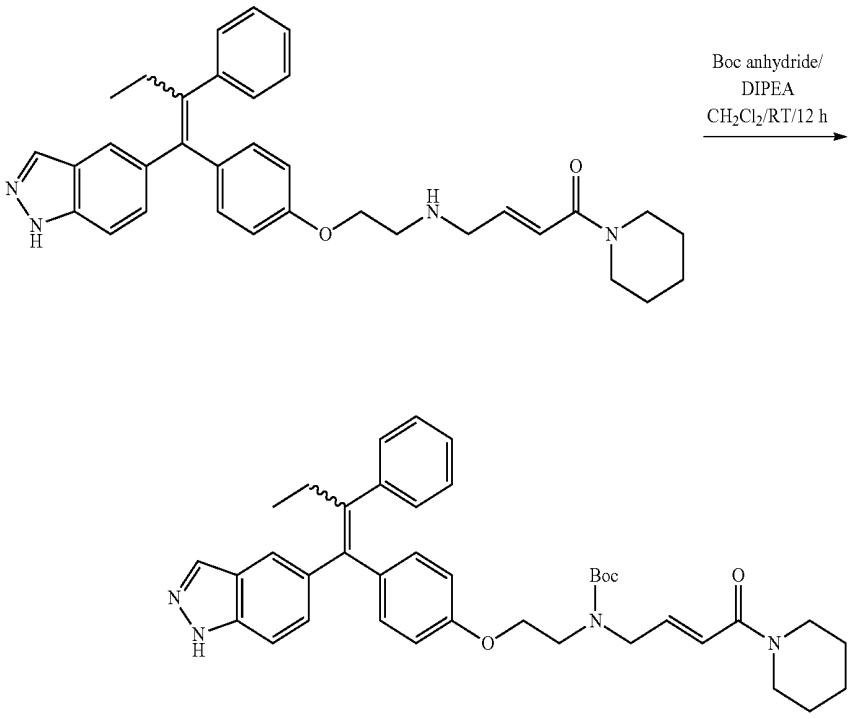
The reaction was carried out according to Scheme 4, Step-2, using piperidine, for compound 221 to afford (E)-4-bromo-1-(piperidin-1-yl)but-2-en-1-one (3.9 g, 55%) as a brown colour liquid.

Step-2: Synthesis of (2E)-4-((2-(4-(1-(1H-indazol-5-yl)-2-phenylbut-1-en-1-yl)phenoxy)ethyl)amino)-1-(piperidin-1-yl)but-2-en-1-one



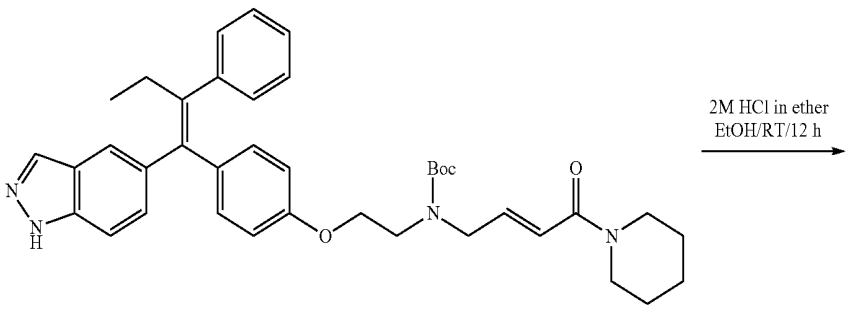
The reaction was carried out according to Scheme 2, Step-3a, using 2-(4-(1-(1H-indazol-5-yl)-2-phenylbut-1-en-1-yl)phenoxy)-ethan-1-amine (as prepared in Example 9, Step 4-5) for compound 213 to give a crude material which was used in next step without further purification (716 mg, crude).

Step-3: Synthesis of tert-butyl (2-(4-(1-(1H-indazol-5-yl)-2-phenylbut-1-en-1-yl)phenoxy)ethyl) ((E)-4-oxo-4-(piperidin-1-yl)but-2-en-1-yl)carbamate

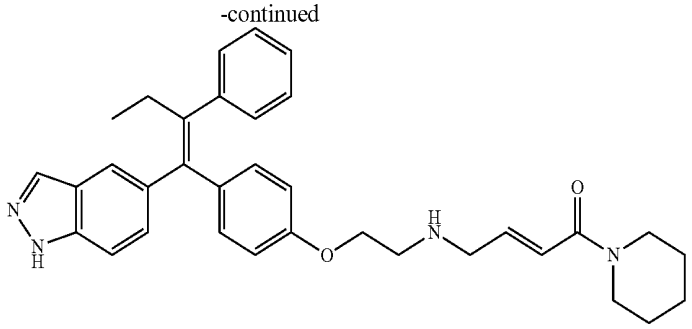


The reaction was carried out according to Scheme 2, Step-5, using (2E)-4-((2-(4-(1-(1H-indazol-5-yl)-2-phenylbut-1-en-1-yl)phenoxy)ethyl)amino)-1-(piperidin-1-yl)but-2-en-1-one (0.716 g, 1.34 mmol) for compound 215. The crude compound was purified by column chromatography using 4% MeOH in dichloromethane to afford the title compound of Ex. 12 Step-3 (0.32 g, 37%).

Step-4: Synthesis of (E)-4-((2-(4-((E)-1-(1H-indazol-5-yl)-2-phenylbut-1-en-1-yl)phenoxy)ethyl) amino)-1-(piperidin-1-yl)but-2-en-1-one (Compound 12)



-continued



12

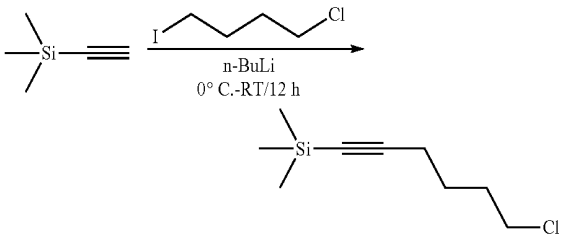
The reaction was carried out according to Scheme 2, Step-6c, using tert-butyl (2-(4-(1-(1H-indazol-5-yl)-2-phenylbut-1-en-1-yl)phenoxy)ethyl)((E)-4-oxo-4-(piperidin-1-yl)but-2-en-1-yl)carbamate (0.32 g, 0.504 mmol) for compound 211c to deliver crude compound, which was purified by preparative TLC to afford compound 12 (74 mg, 27%).

Compound 12:

^{1}H NMR (400 MHz, DMSO-d_6): δ 13.06 (s, 1H), 8.06 (s, 1H), 7.61 (s, 1H), 7.51 (d, J=8.8 Hz, 1H), 7.2 (d, J=7.6 Hz, 2H), 7.15-7.1 (m, 4H), 6.75 (d, J=8.4 Hz, 2H), 6.6-6.5 (m, 4H), 3.86 (t, J=6 Hz, 2H), 3.42 (t, J=5.6 Hz, 4H), 2.77 (t, J=5.6 Hz, 2H), 2.5 (m, 3H), 2.43-2.38 (m, 2H), 1.58-1.53 (m, 2H), 1.42 (d, J=3.6 Hz, 4H), 0.87 (t, J=7.2 Hz, 3H). LCMS: 535.3 $[M+H]^+$.

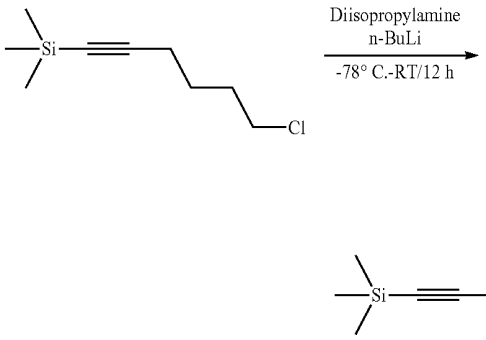
Example 13: Synthesis of (E)-4-((2-(4-((E)-2-cyclobutyl-1-(1H-indazol-5-yl)-2-phenylvinyl)phenoxy) ethyl)amino)-N,N-dimethylbut-2-enamide (Compound 13)

Step-1: Synthesis of (6-chlorohex-1-yn-1-yl)trimethylsilane



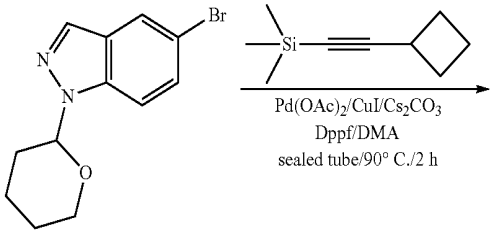
A solution of trimethylsilylacetylene (10 g, 101 mmol) in dry tetrahydrofuran (90 mL) was stirred at 0° C. under nitrogen atmosphere; n-BuLi (44.5 mL of 2.6M solution in hexane, 111.2 mmol) was added drop wise. The solution was stirred for 30 minutes, a solution of 1-chloro-4-iodobutane (13.6 mL, 111.2 mmol) in dry tetrahydrofuran (30 mL) was added. The reaction mixture was allowed to warm to 20° C. and stirred for 12 h. The reaction mixture was poured into water, the aqueous mixture was extracted with diethyl ether. The ethereal extracts were washed with water and dried over anhydrous sodium sulphate. The solvent was removed under reduced pressure to obtain 6-chloro-1-trimethylsilylhex-1-yne (18 g) as a yellow liquid and was used in next step without further purification.

Step-2: Synthesis of (cyclobutylethynyl)trimethylsilane

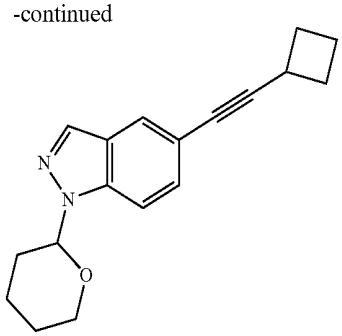


To a solution of diisopropylamine (17 mL, 95.7 mmol) in anhydrous THF (50 mL) at 0° C., n-BuLi (2.6M in hexane, 36.8 mL, 95.7 mmol) was added dropwise. The mixture was stirred for 20 minutes at 0° C. and then cooled to −78° C. To this mixture, a solution of (6-chlorohex-1-yn-1-yl)trimethylsilane (9 g, 47 mmol) in anhydrous THF (50 mL) was added drop wise. The resulting mixture was allowed to warm to room temperature and stirred for 12 h. The reaction mixture was carefully quenched at room temperature with saturated aqueous NH_4Cl (100 mL), extracted with pentane (200 mL). The combined organic layers were washed with brine and dried over anhydrous Na_2SO_4. The solvent was evaporated under reduced pressure. The residue was distilled at 160-162° C./760 Torr to afford the title compound as a colourless liquid (4 g, 55%).

Step-3: Synthesis of 5-(cyclobutylethynyl)-1-(tetrahydro-2H-pyran-2-yl)-1H-indazole

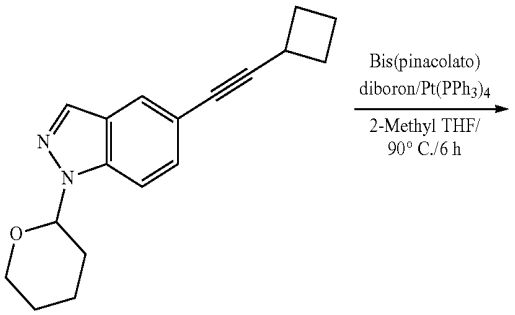


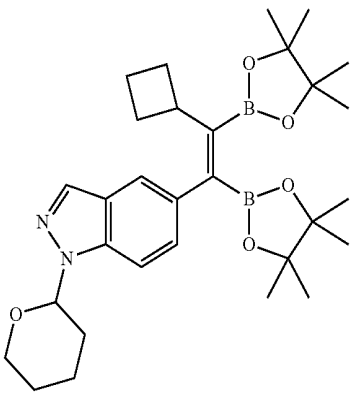
-continued



The reaction was carried out according to Scheme 1, Step-2, using cyclobutylethynyl)trimethylsilane for compound 203, to afford the title compound of Ex. 13 Step-3 (450 mg, 84%) as a brown oil.

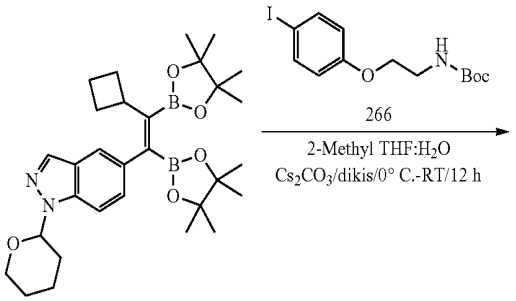
Step-4: Synthesis of (Z)-5-(2-cyclobutyl-1, 2-bis(4, 4,5,5-tetramethyl-1,3,2-dioxaborolan-2-yl)vinyl)-1-(tetrahydro-2H-pyran-2-yl)-1H-indazole



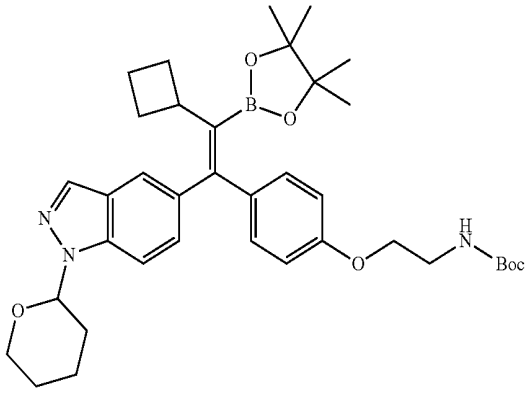


The reaction was carried out according to Scheme 1, Step-3 to afford the title compound of Ex. 13 Step-4 (0.5 g, 66%).

Step-5: Synthesis of tert-butyl (Z)-(2-(4-(2-cyclobutyl-1-(1-(tetrahydro-2H-pyran-2-yl)-1H-indazol-5-yl)-2-(4,4,5,5-tetramethyl-1,3,2-dioxaborolan-2-yl) vinyl)phenoxy)-ethyl)carbamate

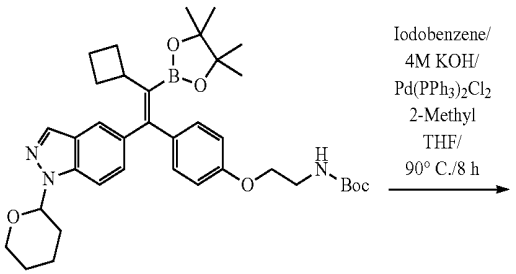


254

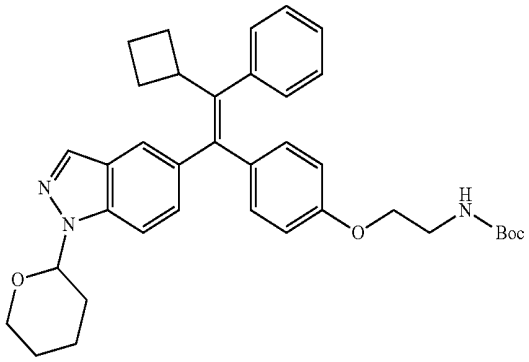


The reaction was carried out according to Scheme 1, Step-4, using tert-butyl (2-(4-iodophenoxy)ethyl)carbamate (as prepared in Example 3, Step-2) for compound 207 to afford the title compound of Ex. 13 Step-5 (0.36 g, 50%).

Step-6: Synthesis of tert-butyl (E)-(2-(4-(2-cyclobutyl-2-phenyl-1-(1-(tetrahydro-2H-pyran-2-yl)-1H-indazol-5-yl)vinyl)phenoxy)ethyl)carbamate

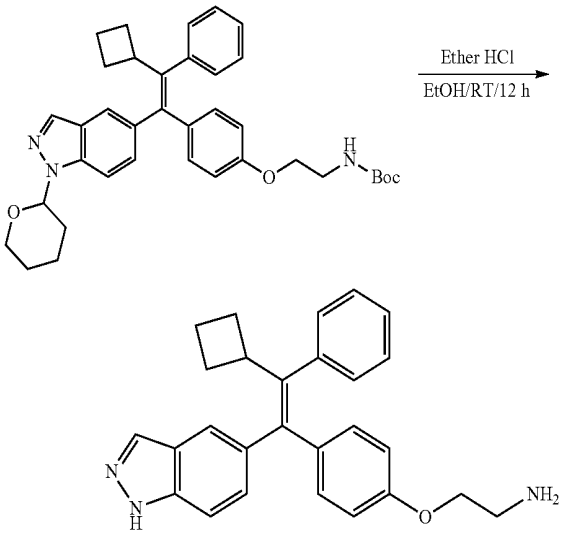


-continued



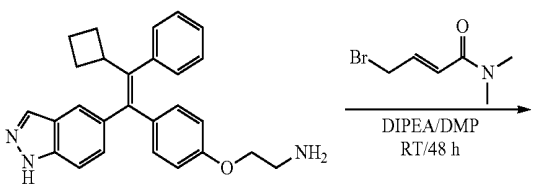
The reaction was carried out according to Scheme 1, Step-5, using iodobenzene for compound 209 to give the title compound of Ex. 13 Step-6 (0.17 g, 51%).

Step-7: Synthesis of (E)-2-(4-(2-cyclobutyl-1-(1H-indazol-5-yl)-2-phenylvinyl) phenoxy)ethan-1-amine

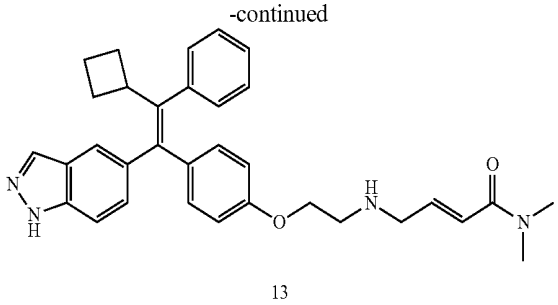


The reaction was carried out according to Scheme 2, Step-2a to afford the title compound of Ex. 13 Step-7 (0.04 g, 34%) as a brown coloured semi solid.

Step-8: Synthesis of (E)-4-((2-(4-((E)-2-cyclobutyl-1-(H-indazol-5-yl)-2-phenylvinyl)phenoxy) ethyl) amino)-N,N-dimethylbut-2-enamide (Compound 13)



-continued



13

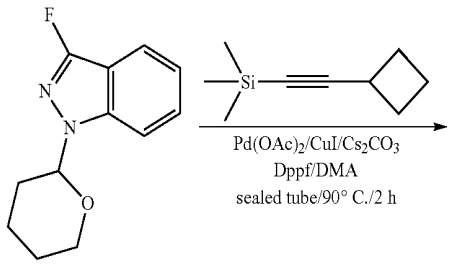
The reaction was carried out according to Scheme 2, Step-3a, using (E)-4-bromo-N,N-dimethylbut-2-enamide (as prepared in Example 1, Step-7) for compound 214 to afford compound 13 (0.2 g, 40%) as a white solid.

Compound 13:

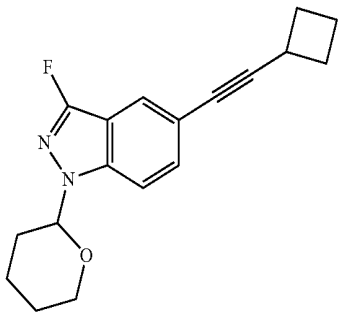
^{1}H NMR (400 MHz, DMSO-d_6): δ 13.06 (s, 1H), 8.07 (s, 1H), 7.58 (s, 1H), 7.51 (d, J=6.8 Hz, 1H), 7.24 (d, J=5.2 Hz, 2H), 7.17-7.09 (m, 4H), 6.78 (d, J=6.8 Hz, 2H), 6.60-6.46 (m, 4H), 3.83 (t, J=4.4 Hz, 2H), 3.50-3.39 (m, 2H), 2.97 (s, 3H), 2.83 (s, 3H), 2.75 (t, J=4.4 Hz, 2H), 1.8-1.77 (m, 4H), 1.57-1.55 (m, 1H), 1.36-1.24 (m, 2H). LC (MS) 521.3 $[M+H]^+$.

Example 14: Synthesis of (E)-4-((2-(4-((E)-2-cyclobutyl-1-(3-fluoro-1H-indazol-5-yl)-2-phenylvinyl) phenoxy)ethyl)amino)-N,N-dimethylbut-2-enamide 2,2,2-trifluoro acetate (Compound 14)

Step-1: Synthesis of 5-(cyclobutylethynyl)-3-fluoro-1-(tetrahydro-2H-pyran-2-yl)-1H-indazole

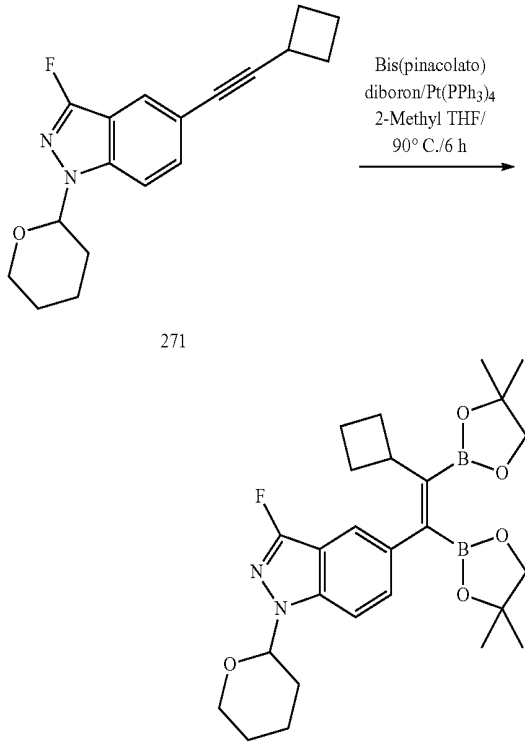


240



The reaction was carried out according to Scheme 1, Step-2b, using 5-bromo-3-fluoro-1-(tetrahydro-2H-pyran-2-yl)-1H-indazole (as prepared in Example 2, Step-2) for compound 202 and cyclobutylethynyl)trimethylsilane (as prepared in Example 13, Step-3) for compound 203 to afford the title compound in Ex. 14 Step-1 (2.15 g, 86%).

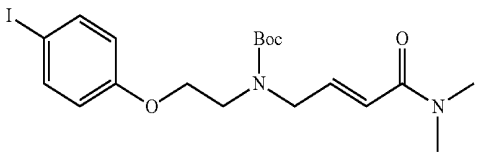
Step-2: Synthesis of (Z)-5-(2-cyclobutyl-1, 2-bis(4, 4,5,5-tetramethyl-1,3,2-dioxaborolan-2-yl)vinyl)-3-fluoro-1-(tetrahydro-2H-pyran-2-yl)-1H-indazole



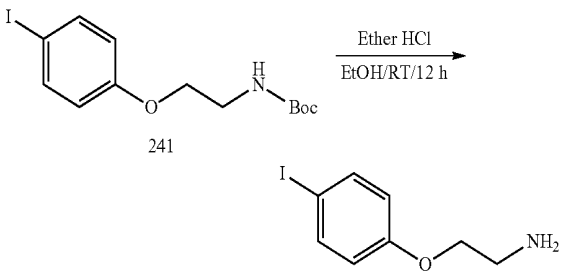
271

The reaction was carried out according to Scheme 1, Step-3 to afford the title compound of Ex. 14 Step-2 (4.3 g, 51.8%).

Step-3: Synthesis of tert-butyl (E)-(4-(dimethyl-amino)-4-oxobut-2-en-1-yl)(2-(4-iodophenoxy) ethyl) carbamate



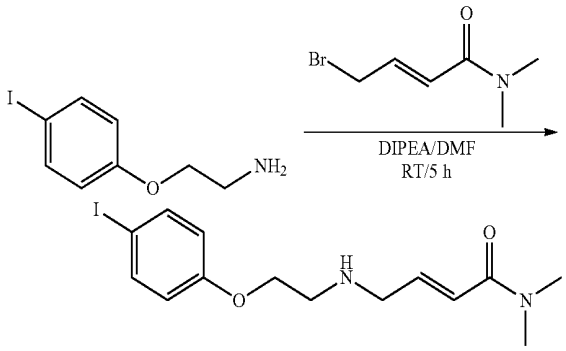
Step-3.1: Synthesis of 2-(4-iodophenoxy)ethan-1-amine



241

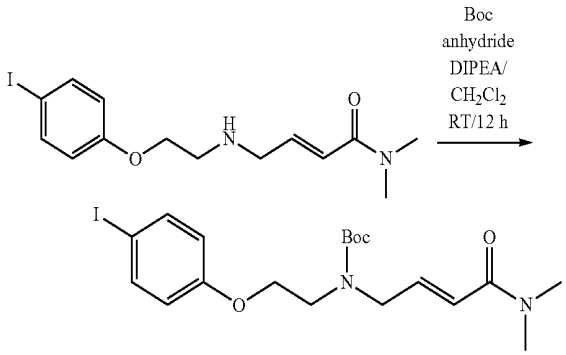
To a stirred solution of tert-butyl (2-(4-iodophenoxy) ethyl)carbamate (25 g, 68.6 mmol, Example 3, Step-2) in ethanol (50 mL) was added at 0° C., 2M HCl in ether (250 mL). The reaction mixture was stirred for 12 h at room temperature. After completion of reaction, reaction mixture was basified with saturated $NaHCO_3$, extracted with 10% MeOH in DCM. Organic layer was concentrated under reduced pressure and the crude material was used in next step without further purification (16 g, 88%).

Step-3.2: Synthesis of (E)-4-((2-(4-iodophenoxy) ethyl)amino)-N,N-dimethylbut-2-enamide



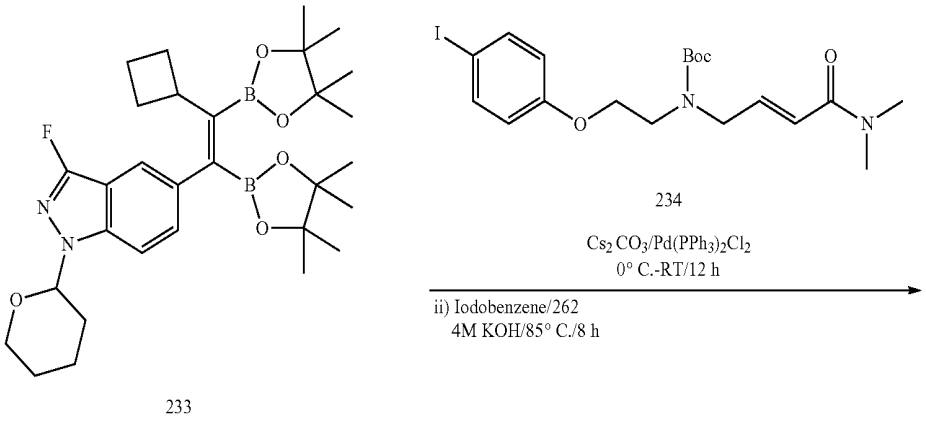
The reaction was carried out according to Scheme 2, Step-3a, using (E)-4-bromo-N,N-dimethylbut-2-enamide (Example 1, Step-7) for compound 214 to give a crude product which was used in next step without further purification (18.8 g, crude).

Step-3.3: Synthesis of tert-butyl (E)-(4-(dimethyl-amino)-4-oxobut-2-en-1-yl)(2-(4-iodophenoxy) ethyl)carbamate

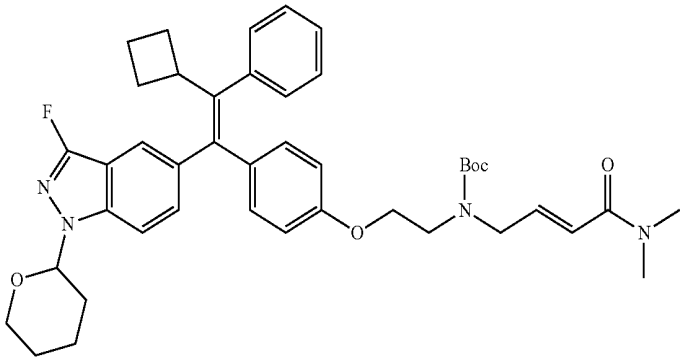


To a stirred solution of (E)-4-((2-(4-iodophenoxy)ethyl) amino)-N,N-dimethylbut-2-enamide (18.8 g, 50.26 mmol) in dry dichloromethane (150 mL) was added DIPEA (6.4 g, 50.2 mmol) at 0° C., stirred for 15 min at 0° C. To the above reaction mixture, was added boc anhydride (13.1 g, 60.3 mmol), resulting mixture was stirred at room temperature for 12 h. Upon completion by TLC, the reaction mixture was cooled to 0° C., quenched with ice cold water (500 mL) and extracted with dichloromethane (500 mL). The combined organic extracts were washed with water, followed by brine, dried over anhydrous sodium sulphate and concentrated under reduced pressure. The crude material was purified by column chromatography over 230-400 mesh silica using 3% MeOH in dichloromethane as an eluent to afford tert-butyl (E)-(4-(dimethylamino)-4-oxobut-2-en-1-yl)(2-(4-iodophenoxy)ethyl)carbamate (9 g, 37.8%).

Step-4: Synthesis of tert-butyl (2-(4-((E)-2-cyclobutyl-1-(3-fluoro-1-(tetrahydro-2H-pyran-2-yl)-1H-indazol-5-yl)-2-phenylvinyl)phenoxy)ethyl) ((E)-4-(dimethylamino)-4-oxobut-2-en-1-yl)carbamate

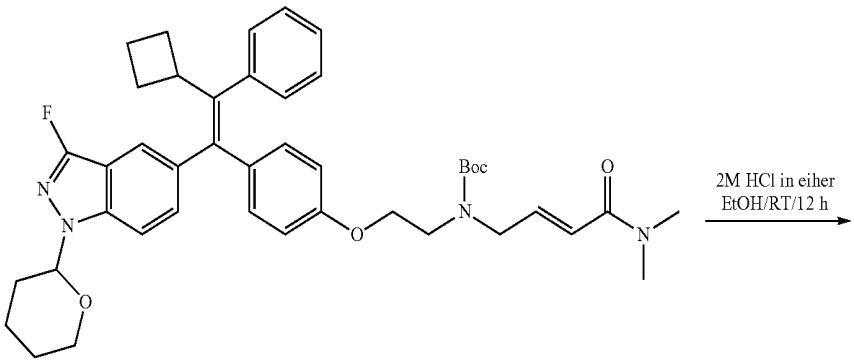


233

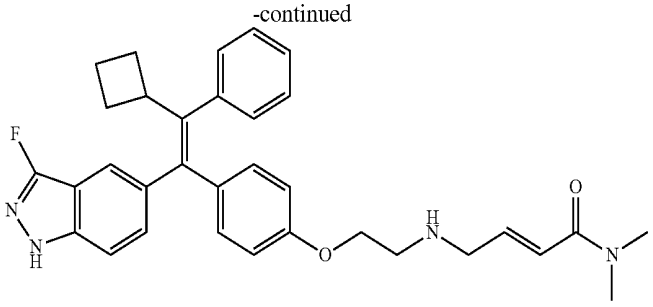


The reaction was carried out according to Scheme 1, Step-4 and Step-5 to give a crude product. The crude product containing the title compound of Ex. 14 Step-4, which was used in next step without further purification (340 mg, crude).

Step-5: Synthesis of (E)-4-((2-(4-((E)-2-cyclobutyl-1-(3-fluoro-1H-indazol-5-yl)-2-phenylvinyl)phenoxy) ethyl)amino)-N,N-dimethylbut-2-enamide 2,2,2-trifluoroace-tate (Compound 14)



-continued



14

The reaction was carried out according to Scheme 2, Step-6c to provide a crude compound, which was purified by preparative HPLC to afford compound 14 (15 mg, 7%) as an off-white solid.

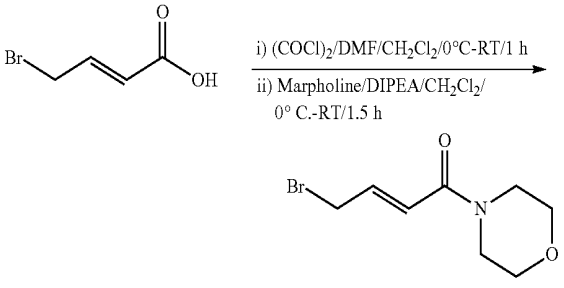
Compound 14:

^{1}H NMR (400 MHz, DMSO-d_6): δ 12.59 (s, 1H), 8.08 (s, 1H), 7.49-7.27 (m, 2H), 7.26-7.21 (m, 3H), 7.2-7.16 (m, 1H), 7.1 (d, J=6.8 Hz, 2H), 6.78 (d, J=14.8 Hz, 1H), 6.63 (d, J=8.8 Hz, 2H), 6.57-6.52 (m, 2H), 4.05 (t, J=4.8 Hz, 2H), 3.78 (d, J=6.0 Hz, 2H), 3.38-3.36 (m, 1H), 3.24 (s, 2H), 3.02 (s, 3H), 2.87 (s, 3H), 1.8-1.76 (m, 4H), 1.6-1.5 (m, 1H), 1.35 (m, 1H). LCMS: 539.3 $[M+H]^+$.

Example 15: Synthesis of (E)-4-((2-(4-((E)-1-(1H-indazol-5-yl)-2-phenylbut-1-en-1-yl)phenoxy)ethyl) amino)-1-morpholinobut-2-en-1-one (Compound 15)

The compound was synthesized following the approach as outlined in Example 9 by substituting into Step-4 (E)-4-bromo-1-morpholinobut-2-en-1-one (preparation shown below in Ex. 15 Step-1) for compound 230 to afford compound 15 (15 mg, 3.2%) as a white solid.

Step-1: Synthesis of (E)-4-bromo-1-morpholinobut-2-en-1-one



The reaction was carried out according to Scheme 4, Step-2, using morphorline for compound 221, to afford (E)-4-bromo-1-(piperidin-1-yl)but-2-en-1-one (2.1 g, 29.6%) as a brown colour liquid.

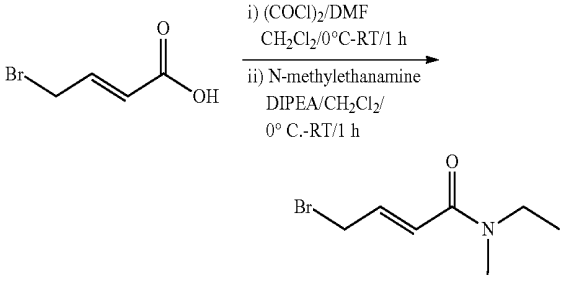
Compound 15:

^{1}H NMR (400 MHz, DMSO-d_6) δ 13.08 (s, 1H), 8.07 (s, 1H), 7.61 (s, 1H), 7.51 (d, J=6.8 Hz, 1H), 7.21-7.11 (m, 6H), 6.74 (d, J=8.8 Hz, 2H), 6.7-6.62 (m, 1H), 6.59 (d, J=8.4 Hz, 2H), 6.51 (d, J=15.2 Hz, 1H), 3.86 (t, J=5.2 Hz, 2H), 3.58-3.4 (m, 10H), 2.77 (t, J=5.2 Hz, 2H), 2.41-2.39 (m, 2H), 0.88 (t, J=7.2 Hz, 3H). LCMS: 537.1 $[M+H]^+$.

Example 16: Synthesis of (E)-4-((2-(4-((E)-1-(1H-indazol-5-yl)-2-phenylbut-1-en-1-yl)phenoxy)ethyl) amino)-N-ethyl-N-methylbut-2-enamide (Compound 16)

The compound was synthesized following the approach as outlined in Example 12 by substituting into Step-2 (E)-4-bromo-N-ethyl-N-methylbut-2-enamide (preparation shown below in Ex. 16 Step-1) for compound 232 to afford compound 16 (0.147 g, 96%).

Step-1: Synthesis of (E)-4-bromo-N-ethyl-N-methylbut-2-enamide



The reaction was carried out according to Scheme 4, Step-2, using (E)-4-bromobut-2-enoic acid (Example 1, Step-7) and N-methylethylamine, to give a crude material, which was purified by column chromatography over 230-400 mesh silica gel using 15% ethyl acetate in n-hexane to afford (E)-4-bromo-N-ethyl-N-methylbut-2-enamide (2.8 g, 44%).

Compound 16:

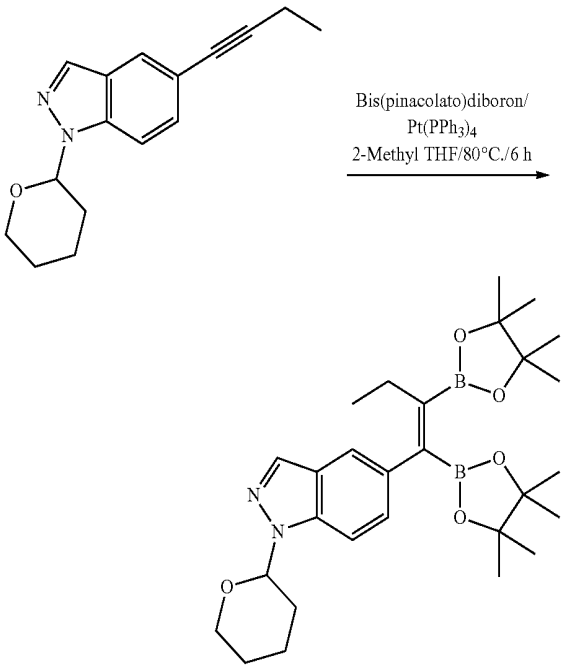
^{1}H NMR (400 MHz, DMSO-d_6): δ 13.06 (s, 1H), 8.06 (s, 1H), 7.61 (s, 1H), 7.51 (d, J=8.8 Hz, 1H), 7.22-7.1 (m, 6H), 6.74 (d, J=8.8 Hz, 2H), 6.6-6.65 (m, 3H), 6.46 (d, J=15.2 Hz, 1H), 3.87 (t, J=5.6 Hz, 2H), 3.36-3.35 (m, 3H), 2.96 (s, 2H), 2.82 (s, 2H), 2.79-2.76 (t, J=5.6 Hz, 2H), 2.43-2.38 (m, 2H), 1.06-0.97 (m, 3H), 0.88 (t, J=7.2 Hz, 3H). LCMS: 509.4 $[M+H]^+$.

Example 17: Synthesis of (E)-4-((2-(4-((E)-1-(1H-indazol-5-yl)-2-phenylbut-1-en-1-yl)phenoxy)ethyl) amino)-N-methyl-N-propylbut-2-enamide (Compound 17)

The compound was synthesized following the approach as outlined in Example 9 by substituting into Step-4 (E)-4-bromo-N-methyl-N-propylbut-2-enamide (preparation

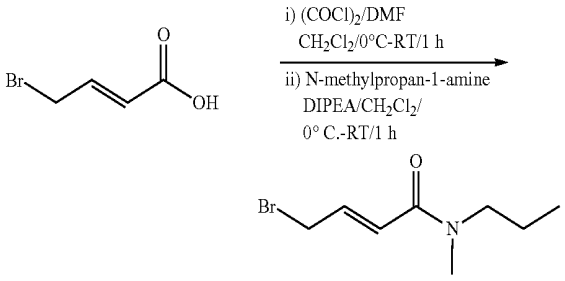
shown below in Ex. 17 Step-2) for compound 230 to afford compound 17 (0.015 g, 3.1%).

Step-1: Synthesis of (Z)-5-(1,2-bis(4,4,5,5-tetramethyl-1,3,2-dioxaborolan-2-yl)but-1-en-1-yl)-1-(tetrahydro-2H-pyran-2-yl)-1H-indazole



The reaction was carried out according to Scheme 1, Step-3 using 5-(but-1-yn-1-yl)-1-(tetrahydro-2H-pyran-2-yl)-1H-indazole (as prepared in Ex. 1, Step-3) for compound 204. The crude material containing the title compound of Ex. 17 Step-1 was used in next step without further purification (20 g) as brown color oil.

Step-2: Synthesis of (E)-4-bromo-N-methyl-N-propylbut-2-enamide



The reaction was carried out according to Scheme 4, Step-2, using (E)-4-bromobut-2-enoic acid (as prepared in Example 1, Step-7.1) for compound 204 and N-methylpropylamine, to give a crude material, which was purified by column chromatography over 230-400 mesh silica gel using 15% ethyl acetate in n-hexane to afford (E)-4-bromo-N-methyl-N-propylbut-2-enamide (0.536 g, 23%).

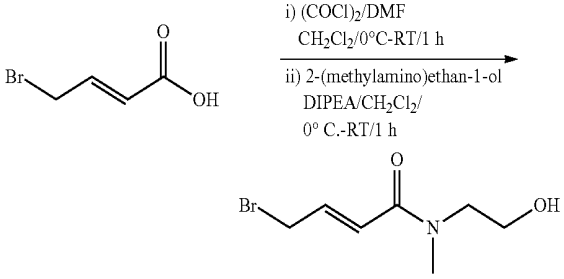
Compound 17:

^{1}H NMR (400 MHz, DMSO-d_6): δ 13.08 (s, 1H), 8.07 (s, 1H), 7.61 (s, 1H), 7.51 (d, J=8.4 Hz, 1H), 7.22-7.19 (m, 2H), 7.18-7.11 (m, 4H), 6.75 (d, J=8.8 Hz, 2H), 6.59 (d, J=8.8 Hz, 3H), 7.5-7.44 (d, J=15.2 Hz, 1H), 3.86 (t, J=5.6 Hz, 2H), 3.32-3.30 (m, 4H), 2.96 (s, 1H), 2.83 (s, 2H), 2.67 (d, J=2.0 Hz, 2H), 2.44-2.38 (m, 2H), 1.49-1.45 (m, 2H), 0.88 (t, J=7.2 Hz, 3H), 0.80 (t, 7.2 Hz, 3H). LCMS: 523.2 [M+H]$^+$.

Example 18: Synthesis of (E)-4-((2-(4-((E)-1-(1H-indazol-5-yl)-2-phenylbut-1-en-1-yl)phenoxy)ethyl)amino)-N-(2-hydroxyethyl)-N-methylbut-2-enamide (Compound 18)

The compound was synthesized following the approach as outlined in Example 9 by substituting into Step-4 (E)-4-bromo-N-(2-hydroxyethyl)-N-methylbut-2-enamide (preparation shown below in Ex. 18 Step-1) for compound 230 to afford compound 18 (0.017 g, 3.1%).

Step-1: Synthesis of (E)-4-bromo-N-(2-hydroxyethyl)-N-methylbut-2-enamide



The reaction was carried out according to Scheme 4, Step-2, using (E)-4-bromobut-2-enoic acid (Example 1, Step-7) for compound 220 and 2-(methylamino)ethan-1-ol for compound 221, to give a crude material, which was purified by column chromatography over 230-400 mesh silica gel using 30% ethyl acetate in n-hexane to afford (E)-4-bromo-N-(2-hydroxyethyl)-N-methylbut-2-enamide (1 g, 25%).

Compound 18:

^{1}H NMR (400 MHz, DMSO-d_6): δ 13.08 (s, 1H), 8.06 (s, 1H), 7.61 (s, 1H), 7.51 (d, J=8.3 Hz, 1H), 7.21 (d, J=7.3 Hz, 2H), 7.19-7.11 (m, 4H), 6.74 (d, J=8.8 Hz, 2H), 6.59 (d, J=8.8 Hz, 3H), 6.53-6.51 (m, 1H), 4.79-4.66 (m, 1H), 3.86 (t, J=5.1 Hz, 2H), 3.49 (d, J=8.8 Hz, 2H), 3.39-3.35 (m, 2H), 3.03 (s, 1H), 2.86 (s, 2H), 2.77 (s, 2H), 2.40 (d, J=7.4 Hz, 2H), 0.87 (t, J=7.3 Hz, 3H). LCMS: 525.2 [M+H]$^+$.

Example 19: Synthesis of (E)-4-((2-(4-((E)-2-(2-chloro-4-fluorophenyl)-1-(3-fluoro-1H-indazol-5-yl)but-1-en-1-yl)phenoxy)ethyl)amino)-N,N-dimethylbut-2-enamide (Example 19)

The compound was synthesized following the approach as outlined in Example 14 by substituting into Step-4 (Z)-5-(1,2-bis(4,4,5,5-tetramethyl-1,3,2-dioxaborolan-2-yl)but-1-en-1-yl)-3-fluoro-1-(tetrahydro-2H-pyran-2-yl)-1H-indazole (as prepared in Example 3, Step-1) for compound 233 and 2-chloro-4-fluoro-1-iodobenzene to afford compound 19 (0.11 g, 12%) as an off-white solid.

Compound 19:

^{1}H NMR (400 MHz, DMSO-d_6): δ 12.6 (s, 1H), 7.6 (s, 1H), 7.5 (d, J=6.0 Hz, 1H), 7.35-7.31 (m, 2H), 7.25 (d, J=1.2 Hz, 1H), 7.14-7.10 (m, 1H), 6.83 (d, J=6.8 Hz, 2H), 6.63 (d,

J=7.4 Hz, 2H), 6.59 (t, J=4 Hz, 1H), 6.5 (d, J=8.8 Hz, 1H), 3.87 (t, J=4.4 Hz, 2H), 2.99 (s, 3H), 2.84 (s, 3H), 2.77 (t, J=4.4 Hz, 2H), 3.3 (m, 2H), 2.4 (q, J=6 Hz, 2H), 0.88 (t, J=6.0 Hz, 3H). LCMS: 565.3 $[M+H]^+$.

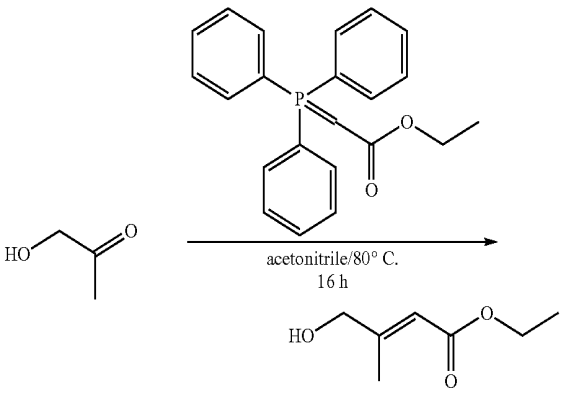
Example 20

There is no Example 20.

Example 21: Synthesis of (E)-4-((2-(4-((E)-1-(1H-indazol-5-yl)-2-phenylbut-1-en-1-yl)phenoxy)ethyl) amino)-N,N,3-trimethylbut-2-enamide (Compound 21)

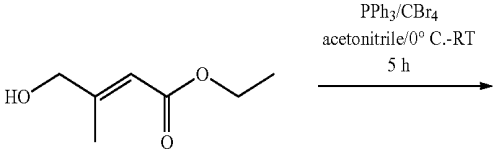
The compound was synthesized following the approach as outlined in Example 14 by substituting into Step-4 (Z)-5-(1,2-bis(4,4,5,5-tetramethyl-1,3,2-dioxaborolan-2-yl)but-1-en-1-yl)-1-(tetrahydro-2H-pyran-2-yl)-1H-indazole (as prepared in Example 17, Step-1) for compound 233 and tert-butyl (E)-(4-(dimethylamino)-2-methyl-4-oxobut-2-en-1-yl)(2-(4-iodophenoxy) ethyl)carbamate (preparation shown below in Steps 1-6) for compound 234 to afford compound 21 (35 mg, 10%).

Step-1: Synthesis of ethyl (E)-4-hydroxy-3-methylbut-2-enoate

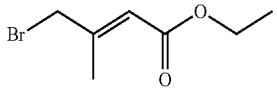


To a stirred solution of 1-hydroxypropan-2-one (10 g, 134 mmol) in acetonitrile (300 mL), was added ethyl 2-(triphenylphosphoranylidene)acetate (56 g, 161 mmol) and the reaction was heated to 80° C. for 16 h. Reaction mixture was evaporated under reduced pressure, diluted with diethyl ether (200 mL) then filtered by using buckner funnel, solid was washed with diethyl ether (2×100 mL), filtrate was evaporated to get the crude product which was purified through column chromatography over silica gel and the column eluting with 15% EtoAc in n-hexane as an eluent to afford the title compound of Ex. 21 Step-1 as a colourless waxy liquid (13.8 g, 71%).

Step-2: Synthesis of ethyl (E)-4-bromo-3-methylbut-2-enoate

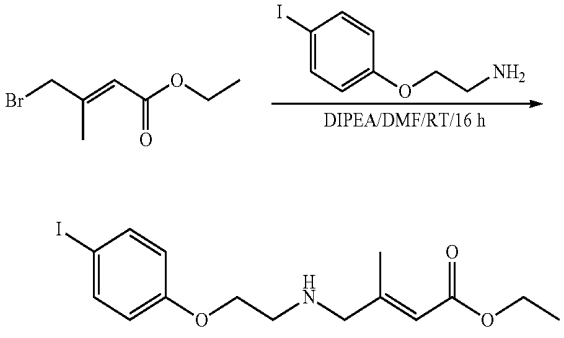


-continued



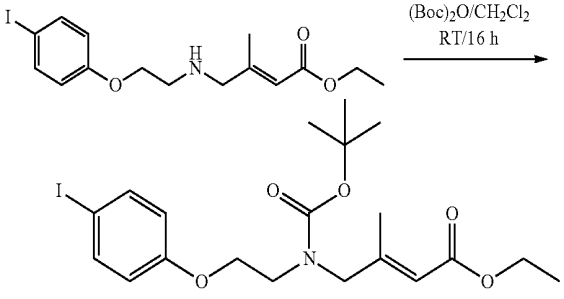
To an ice cooled solution of ethyl (E)-4-hydroxy-3-methylbut-2-enoate (10 g, 6.9 mmol) in acetonitrile (20 mL), were added triphenyl phosphine (18.2 g, 6.9 mmol) and carbon tetra bromide (23 g, 6.9 mmol) and the reaction was allowed to room temperature for 5 h. Reaction mixture was concentrated to get the crude product, which was purified through column chromatography over silica gel and the column eluting with 10% EtoAc in n-hexane as a eluent to afford the title compound of Ex. 21 Step-2 as a colourless oil (8.5 g, 59%).

Step-3: Synthesis of ethyl (E)-4-((2-(4-iodophenoxy)ethyl)amino)-3-methylbut-2-enoate



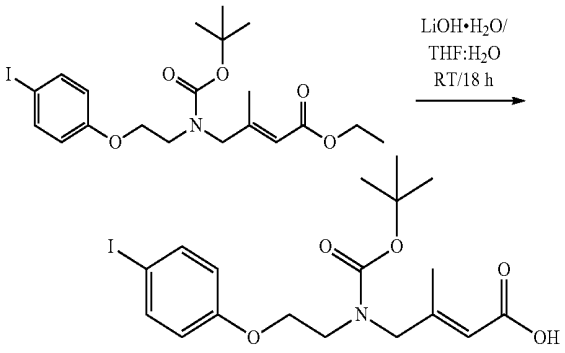
The reaction was carried out according to Scheme 3, Step-3 to give a crude product, which was purified through column chromatography over silica gel, and the column was eluting with 30% EtoAc in n-hexane as a eluent to get the title compound of Ex. 21 Step-3 (3.1 g, 42%).

Step-4: Synthesis of ethyl (E)-4-((tert-butoxycarbonyl)(2-(4-iodophenoxy)-ethyl)amino)but-2-enoate



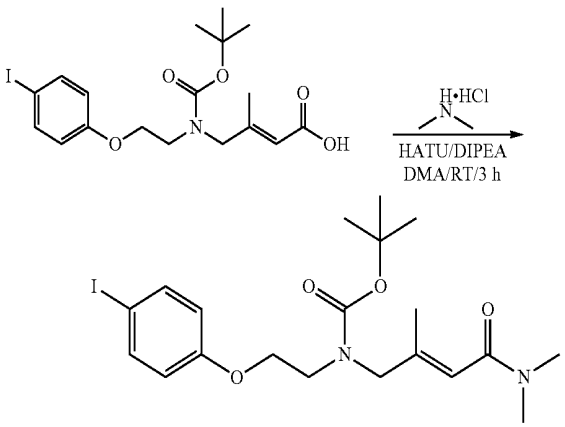
The reaction was carried out according to Scheme 3, Step-4 to give a crude product which was purified through column chromatography over silica gel and the column eluting with 20% EtoAc in n-hexane as an eluent to get the title compound of Ex. 21 Step-4 as colourless oil (3.8 g, 97%).

Step-5: Synthesis of (E)-4-((tert-butoxycarbonyl)(2-(4-iodophenoxy)ethyl)amino)-3-methylbut-2-enoic acid



To a stirred solution ethyl (E)-4-((tert-butoxycarbonyl)(2-(4-iodophenoxy) ethyl)amino)but-2-enoate (3.8 g, 7.7 mmol) in THF:H_2O (40:10 mL), was added lithium hydroxide monohydrate (0.65 g, 15.5 mmol) and the reaction was stirred for 18 h at room temperature. Water was added to the reaction mixture, washed with diethyl ether (100 mL) aqueous layer was adjusted to pH 2-3 by using 10% citric acid then extracted with dichloromethane (2×100 mL), organic layer was dried over anhydrous sodium sulphate, concentrated to get the title compound of Ex. 21 Step-5 (1.7 g, 48%).

Step-6: Synthesis of tert-butyl (E)-(4-(dimethylamino)-2-methyl-4-oxobut-2-en-1-yl)(2-(4-iodophenoxy) ethyl)carbamate



The reaction was carried out as described in Example 1 by substituting into Step-7.2 (E)-4-((tert-butoxycarbonyl)(2-(4-iodophenoxy)ethyl)amino)-3-methylbut-2-enoic acid for compound 235 and substituting DMA for CH_2Cl_2 as the solvent to afford the title compound of Ex. 21 Step-6 (2.5 g, crude).

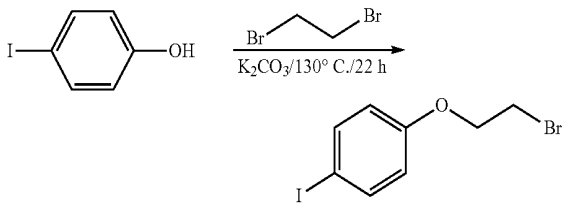
Compound 21:

^{1}H NMR (400 MHz, DMSO-d_6): δ 13.08 (s, 1H), 8.07 (s, 1H), 7.61 (s, 1H), 7.51 (d, J=8.8 Hz, 1H), 7.22-7.21 (m, 2H), 7.19-7.11 (m, 4H), 6.74 (d, J=8.4 Hz, 2H), 6.59 (d, J=8.8 Hz, 2H), 6.04 (s, 1H), 3.87 (t, J=5.2 Hz, 2H), 3.14 (s, 2H), 2.9 (s, 3H), 2.8 (s, 3H), 2.74 (t, J=5.2 Hz, 2H), 2.43-2.38 (m, 2H), 1.75 (s, 3H), 0.88 (t, J=6.8 Hz, 3H). LCMS: 509.3[M+H]$^+$.

Example 22: Synthesis of (Z)-4-((2-(4-((E)-1-(1H-indazol-5-yl)-2-phenylbut-1-en-1-yl)phenoxy)ethyl) amino)-N,N-dimethylbut-2-enamide (Compound 22)

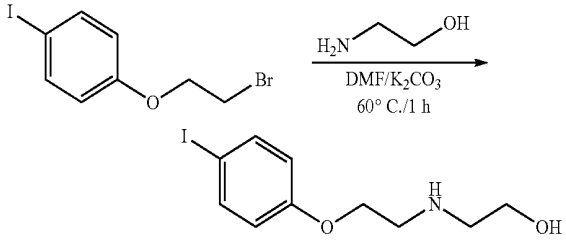
The compound was synthesized following the approach as outlined in Example 14 by substituting into Step-4 (Z)-5-(1,2-bis(4,4,5,5-tetramethyl-1,3,2-dioxaborolan-2-yl)but-1-en-1-yl)-1-(tetrahydro-2H-pyran-2-yl)-1H-indazole (as prepared in Example 17, Step-1) for compound 233 and tert-butyl (Z)-(4-(dimethylamino)-4-oxobut-2-en-1-yl)(2-(4-iodophenoxy) ethyl) carbamate (preparation shown below in Ex. 22 Steps 1-7) for compound 234 to afford compound 22 (0.27 g, 38%).

Step-1: Synthesis of 1-(2-bromoethoxy)-4-iodobenzene



To a stirred solution of 4-iodophenol (20 g, 90 mmol) was added potassium carbonate (9.4 g, 136 mmol) and stirred for 10 min at 0° C., to the above mixture 1,2-dibromoethane (145 g, 772 mmol) was added. The contents were stirred at 130° C. for 22 h. After completion of reaction, reaction mixture was poured onto ice cold water, and extracted with ethyl acetate. The combined organic layers were washed with water followed by saturated NaCl solution, dried over anhydrous Na_2SO_4 and concentrated under reduced pressure. The crude material was purified by column chromatography over 230-400 mesh silica using 3% EtOAc in n-hexane as an eluent to obtain desired compound 1-(2-bromoethoxy)-4-iodobenzene (20.1 g, 67.6%).

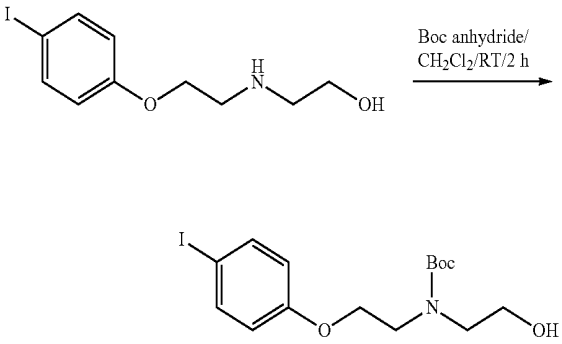
Step-2: Synthesis of 2-((2-(4-iodophenoxy)ethyl) amino)ethan-1-ol



To a stirred solution of 1-(2-bromoethoxy)-4-iodobenzene (20 g, 61 mmol) in DMF (100 mL) was 2-aminoethan-1-ol (37.36 g, 610 mmol). The reaction mixture was stirred for 1 h at 60° C., after completion of reaction (monitored by TLC), reaction mixture was diluted with cold water (50 mL)

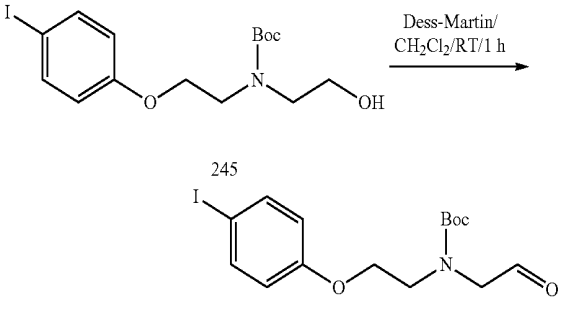
and extracted with ethyl acetate. The combined organic layers were washed with water followed by saturated NaCl solution, dried over anhydrous Na_2SO_4 and concentrated under reduced pressure. The crude material was purified by column chromatography over 230-400 mesh silica using 20% MeOH in dichloromethane as an eluent to obtain desired compound 2-((2-(4-iodophenoxy)ethyl)amino) ethan-1-ol (13.2 g, 70.58%).

Step-3: Synthesis of tert-butyl (2-hydroxyethyl)(2-(4-iodophenoxy)ethyl)carbamate



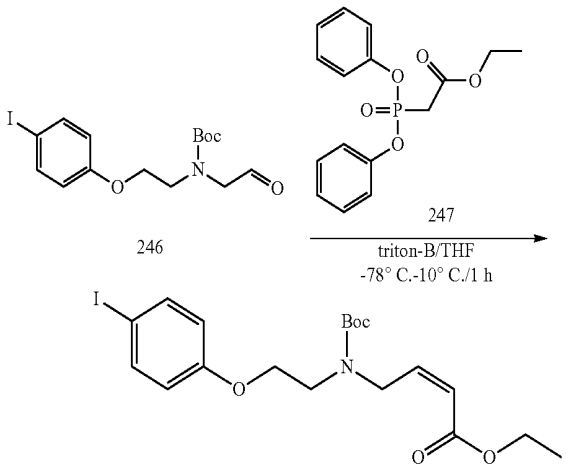
The reaction was carried out according to Scheme 4, Step-4 to give a crude material, which was purified by column chromatography over 230-400 mesh silica using 7% MeOH in dichloromethane as an eluent to obtain desired compound tert-butyl (2-hydroxyethyl)(2-(4-iodophenoxy) ethyl)carbamate (16.7 g, 95.9%).

Step-4: Synthesis of tert-butyl (2-(4-iodophenoxy) ethyl)(2-oxoethyl)carbamate



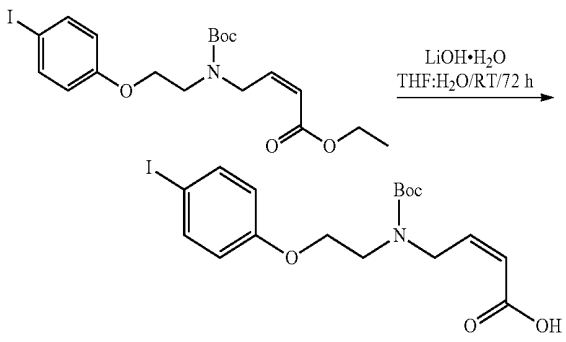
To a stirred solution of tert-butyl (2-hydroxyethyl)(2-(4-iodophenoxy)ethyl)carbamate (6.7 g, 16.4 mmol) in dichloromethane (150 mL) was added Dess-Martin periodinane (10.46 g, 24.6 mmol). The reaction mixture was stirred for 1 h at room temperature, after completion of reaction (monitored by TLC), reaction mixture was diluted with 1:1 mixture of hypo and $NaHCO_3$ solution and extracted with dichloromethane (100 mL). The organic layer was washed with water followed by saturated NaCl solution, dried over anhydrous Na_2SO_4 and concentrated under reduced pressure. The crude product was used in next step without further purification (5.9 g, 89.9%).

Step-5: Synthesis of ethyl ethyl (Z)-4-((tert-butoxycarbonyl)(2-(4-iodophenoxy)ethyl)amino)but-2-enoate



To a stirred solution of ethyl 2-(diphenoxyphosphoryl) acetate (4.71 g, 14.7 mmol) and triton-B (9.39 mL, 17.7 mmol) in THF (70 mL) at −78° C., tert-butyl (2-(4-iodophenoxy)ethyl)(2-oxoethyl)carbamate (5.97 g, 14.7 mmol) in THF (30 mL) was added was added dropwise. The reaction mixture was stirred for 1 h at 10° C., after completion of reaction (monitored by TLC), reaction mixture was diluted with ammonium chloride solution and extracted with EtOAc (100 mL). The organic layer was washed with water followed by saturated NaCl solution, dried over anhydrous Na_2SO_4 and concentrated under reduced pressure. The crude product was purified by column chromatography over 230-400 mesh silica-gel by eluting with 9% EtOAc in n-hexane to afford title compound of Ex. 22 Step-5 (0.82 g, 11.7%).

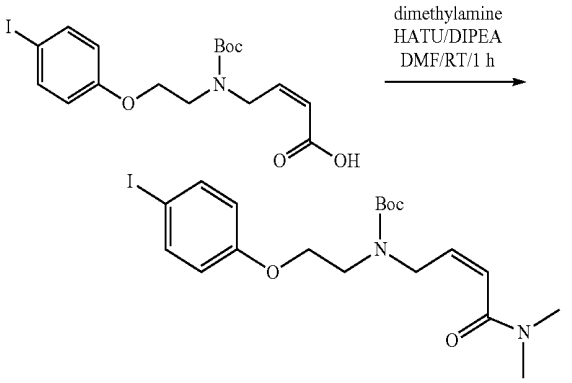
Step-6: Synthesis of (Z)-4-((tert-butoxycarbonyl)(2-(4-iodophenoxy)ethyl)amino)but-2-enoic acid



To a stirred solution of ethyl (Z)-4-((tert-butoxycarbonyl) (2-(4-iodophenoxy)ethyl) amino)but-2-enoate (0.8 g, 1.6 mmol) in THF (10 mL) was added $LiOH.H_2O$ (0.353 g, 8.4 mmol) and water (5 mL). The reaction mixture was stirred for 72 h at room temperature, after completion of reaction (monitored by TLC), reaction mixture was diluted with water and extracted with dichloromethane (100 mL). The organic layer was washed with water followed by saturated NaCl solution, dried over anhydrous Na_2SO_4 and concen-

trated under reduced pressure. The crude product was used in next step without further purification (0.705 g, 93.7%).

Step-7: Synthesis of tert-butyl (Z)-(4-(dimethylamino)-4-oxobut-2-en-1-yl)(2-(4-iodophenoxy) ethyl) carbamate



The reaction was carried out as described in Example 1, Step-7.2 by substituting (Z)-4-((tert-butoxycarbonyl)(2-(4-iodophenoxy)ethyl)amino)but-2-enoic acid for compound 235 and substituting DMF for CH_2C_2 as the solvent to give a crude product, which was purified by column chromatography over 230-400 mesh silica-gel by eluting with 40-70% EtOAc in n-hexane to afford title compound of Ex. 22 Step-7 (0.97 g, 70.8%).

Compound 22:

^{1}H NMR (400 MHz, DMSO-d_6): δ 13.06 (s, 1H), 8.06 (s, 1H), 7.61 (s, 1H), 7.51 (d, J=8.8 Hz, 2H), 7.12-7.10 (m, 4H), 674 (d, J=8.8 Hz, 2H), 6.58 (d, J=8.8 Hz, 2H), 6.15 (d, J=11.6 Hz, 2H), 5.93-5.86 (m, 1H), 3.84 (t, J=5.4 Hz, 2H), 3.40 (dd, J_1=6.4 Hz, J_2=1.6 Hz, 2H), 2.93 (s, 3H), 2.80 (s, 3H), 2.77 (t, J=5.6 Hz, 2H), 2.40 (q, J=7.3 Hz, 2H), 0.88 (t, J=7.2 Hz, 3H). LCMS: 495.3 $[M+H]^+$.

Example 23: Synthesis of (E)-4-((2-(4-((E)-2-cyclobutyl-1-(1H-indazol-5-yl)-2-phenylvinyl)phenoxy) ethyl)amino)-1-morpholinobut-2-en-1-one (Compound 23)

The reaction was carried out following the approach as outlined by Example 2, Step-7, by substituting into Ex. 2, Step-7 (E)-2-(4-(2-cyclobutyl-1-(1H-indazol-5-yl)-2-phenylvinyl)phenoxy)ethanamine (as prepared in Example 13, Step-7) for compound 237 and (E)-4-bromo-1-morpholinobut-2-en-1-one (as prepared in Example 15, Step-1) for compound 238 to afford Compound 23 (0.045 g, 5%).

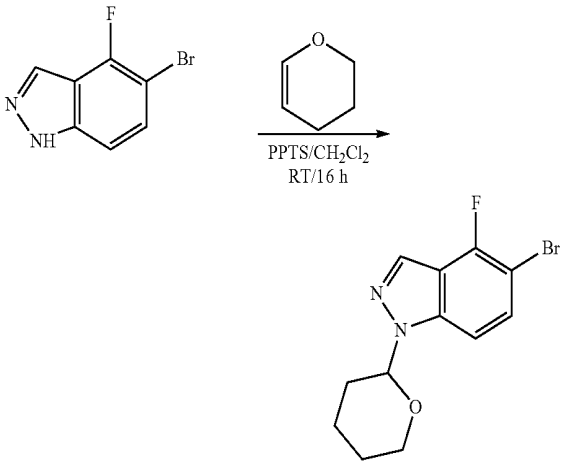
Compound 23:

^{1}H NMR (400 MHz, DMSO-d_6): δ 13.06 (s, 1H), 8.07 (s, 1H), 7.58 (s, 1H), 7.51 (d, J=8.8 Hz, 1H), 7.27-7.23 (m, 2H), 7.17-7.13 (m, 2H), 7.11-7.08 (m, 2H), 6.77 (d, J=8.8 Hz, 2H), 6.66-6.61 (m, 1H), 6.53 (d, J=8.8 Hz, 3H), 3.82 (t, J=5.6 Hz, 2H), 3.51-3.49 (m, 8H), 3.40 (t, J=8.5 Hz, 1H), 3.29 (s, 2H), 2.74 (t, J=5.7 Hz, 2H), 1.82-1.76 (m, 4H), 1.57-1.54 (m, 1H), 1.23 (m, 1H). LCMS: 563.3 $[M+H]^+$.

Example 24: Synthesis of (E)-4-((2-(4-((E)-2-cyclobutyl-1-(4-fluoro-1H-indazol-5-yl)-2-phenylvinyl) phenoxy)ethyl)amino)-N,N-dimethylbut-2-enamide (Compound 24)

The compound was synthesized following the approach as outlined in Example 14 by substituting into Step-1 5-bromo-4-fluoro-1-(tetrahydro-2H-pyran-2-yl)-1H-indazole (preparation shown below in Ex.24 Step-1) for compound 240 to afford Compound 24 (0.03 g, 5%).

Step-1: Synthesis of 5-bromo-4-fluoro-1-(tetrahydro-2H-pyran-2-yl)-1H-indazole



The reaction was carried out according to Scheme 1, Step-1 to give a crude material which was purified by column chromatography over 230-400 mesh silica using 3-4% ethyl acetate in n-hexane to afford 5-bromo-4-fluoro-1-(tetrahydro-2H-pyran-2-yl)-1H-indazole (5 g, 72%) as a brown oil.

Compound 24:

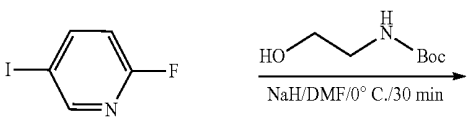
^{1}H NMR (400 MHz, DMSO-d_6): δ 13.4 (s, 1H), 8.2 (s, 1H), 7.39 (d, J=8.8 Hz, 1H), 7.29-2.26 (m 2H), 7.2-7.16 (m, 2H), 7.11 (d, J=7.2 Hz, 2H), 6.8 (d, J=8.8 Hz, 2H), 6.6-6.54 (m, 3H), 6.52 (d, J=16.0 Hz, 1H), 3.84 (t, J=5.6 Hz, 2H), 3.3-3.26 (m, 3H), 2.97 (s, 3H), 2.83 (s, 3H), 2.76 (t, J=5.6 Hz, 2H), 1.8-1.7 (m, 4H), 1.56-1.5 (m, 1H), 1.34-1.3 (m, 1H).

LCMS: 539.3 $[M+H]^+$.

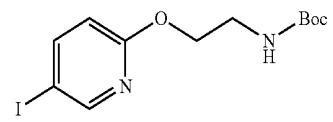
Example 25: Synthesis of (E)-4-((2-((5-((Z)-1-(1H-indazol-5-yl)-2-phenylbut-1-en-1-yl)pyridin-2-yl) oxy)ethyl)amino)-N,N-dimethylbut-2-enamide

The compound was synthesized following the approach as outlined in Example 14 by substituting into Step-4 (Z)-5-(1,2-bis(4,4,5,5-tetramethyl-1,3,2-dioxaborolan-2-yl)but-1-en-1-yl)-1-(tetrahydro-2H-pyran-2-yl)-1H-indazole (as prepared in Example 17, Step-1) for compound 233 and tert-butyl (E)-(4-(dimethylamino)-4-oxobut-2-en-1-yl)(2-((5-iodopyridin-2-yl)oxy) ethyl)carbamate (preparation shown below in Ex. 25 Steps 1-2) for compound 234 to afford Compound 25 (80 mg, 18%) as an off-white solid.

Step-1: Synthesis of tert-butyl (2-((5-iodopyridin-2-yl)oxy)ethyl)carbamate

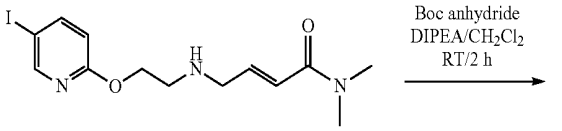


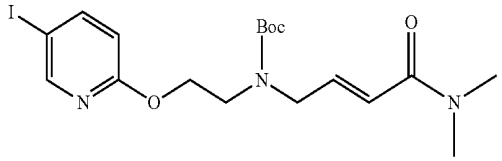
-continued



To a stirred solution of 2-fluoro-5-iodopyridine (5 g, 22.4 mmol) in DMF (25 mL) was added sodium hydride (0.7 g, 33.5 mmol) and stirred for 10 min at 0° C., to the above mixture tert-butyl (2-hydroxyethyl)carbamate (1.8 g, 11.2 mmol) was added. The contents were stirred at 0° C. for 30 min. After completion of reaction, reaction mixture was poured onto ice cold water, and extracted with ethyl acetate. The combined organic layers were washed with water followed by saturated NaCl solution, dried over anhydrous Na_2SO_4 and concentrated under reduced pressure. The crude material was purified by column chromatography over 230-400 mesh silica using 15% EtOAc in n-hexane as an eluent to obtain desired compound tert-butyl (2-((5-iodopyridin-2-yl)oxy)ethyl)carbamate as an off-white solid (3.5 g, 43%).

Step-2: Synthesis of tert-butyl (E)-(4-(dimethylamino)-4-oxobut-2-en-1-yl)(2-((5-iodopyridin-2-yl)oxy)ethyl)carbamate





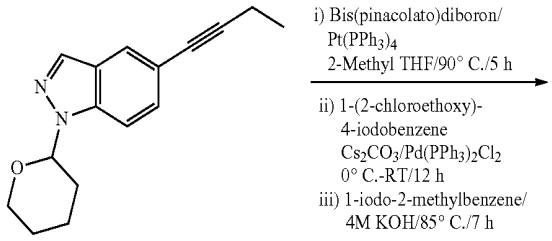
The reaction was carried out following the approach as outlined by Example 14, Step-3.1, by substituting into Ex. 14, Step-3.1 tert-butyl (2-((5-iodopyridin-2-yl)oxy)ethyl) carbamate for compound 241 to deliver the title compound of Ex. 25 Step-2 (3.6 g, 47%).

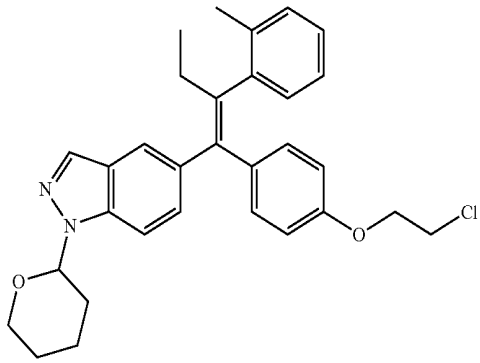
Compound 25:

^{1}H NMR (400 MHz, DMSO-d_6): δ 13.1 (s, 1H), 8.1 (s, 1H), 7.65 (s, 1H), 7.58 (d, J=2.0 Hz, 1H), 7.54 (d, J=8.0 Hz, 1H), 7.23 (d, J=6.8 Hz, 2H), 7.17-7.12 (m, 5H), 6.6-6.5 (m, 1H), 6.5-6.47 (m, 2H), 4.1 (t, J=5.6 Hz, 2H), 3.3 (m, 2H), 2.98 (s, 3H), 2.84 (s, 3H), 2.75 (t, J=5.6 Hz, 2H), 2.46-2.40 (m, 2H), 0.89 (t, J=7.2 Hz, 3H). LCMS: 496.3 $[M+H]^+$.

Example 26: Synthesis of (E)-4-((2-(4-((E)-1-(1H-indazol-5-yl)-2-(o-tolyl)but-1-en-1-yl)phenoxy)ethyl)amino)-N-(2-hydroxyethyl)-N-methylbut-2-enamide (Compound 26)

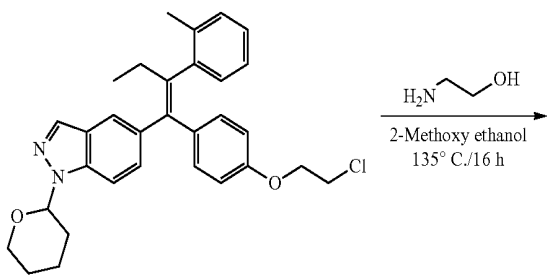
Step-1: Synthesis of (E)-5-(1-(4-(2-chloroethoxy)phenyl)-2-(o-tolyl)but-1-en-1-yl)-1-(tetrahydro-2H-pyran-2-yl)-1H-indazole



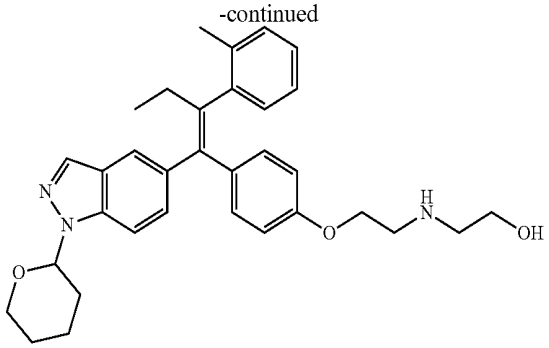


The same procedures as described in Example 5 by substituting into Step-1 (i) 5-(but-1-yn-1-yl)-1-(tetrahydro-2H-pyran-2-yl)-1H-indazole (as prepared in Example 1, Step-3) for compound 242, (ii) 1-(2-chloro-ethoxy)-4-iodobenzene for compound 243, and (iii) 1-iodo-2-methylbenzene for compound 244, to give crude material, which was purified by column chromatography over 230-400 mesh silica gel using 5% EtOAc in n-hexane to afford the title compound of Ex. 26 Step-1 (2.9 g, 29.8%) as an off-white solid.

Step-2: Synthesis of (E)-2-((2-(4-(1-(1-(tetrahydro-2H-pyran-2-yl)-1H-indazol-5-yl)-2-(o-tolyl)but-1-en-1-yl)phenoxy)ethyl)amino)ethan-1-ol

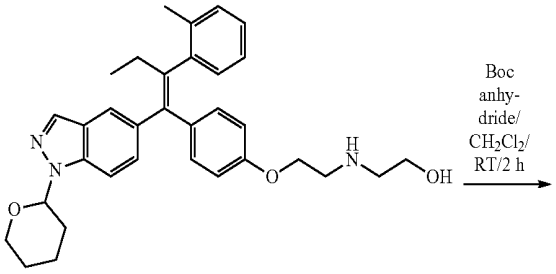


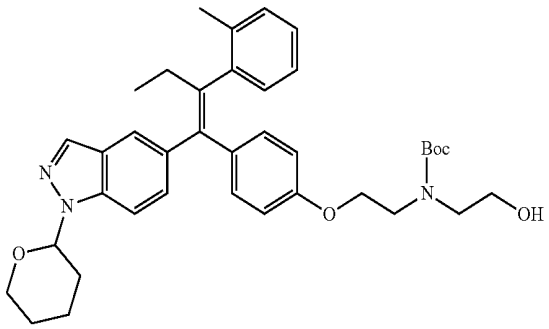
-continued



To a stirred solution of (E)-5-(1-(4-(2-chloroethoxy)phenyl)-2-(o-tolyl)but-1-en-1-yl)-1-(tetrahydro-2H-pyran-2-yl)-1H-indazole (2.8 g, 5.6 mmol) in 2-methoxy ethanol (28 mL) was 2-aminoethan-1-ol (3.3 mL, 56 mmol). The reaction mixture was stirred for 16 h at 135° C., after completion of reaction (monitored by TLC), reaction mixture was diluted with cold water (50 mL) and extracted with ethyl acetate. The combined organic layers were washed with water followed by saturated NaCl solution, dried over anhydrous Na_2SO_4 and concentrated under reduced pressure. The crude product was used in next step without further purification (3.2 g, crude).

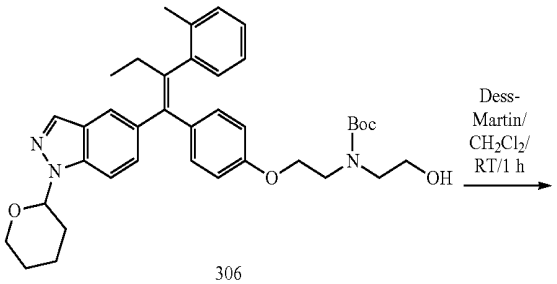
Step-3: Synthesis of tert-butyl (E)-(2-hydroxyethyl)(2-(4-(1-(1-(tetrahydro-2H-pyran-2-yl)-1H-indazol-5-yl)-2-(o-tolyl)but-1-en-1-yl)phenoxy)ethyl)carbamate



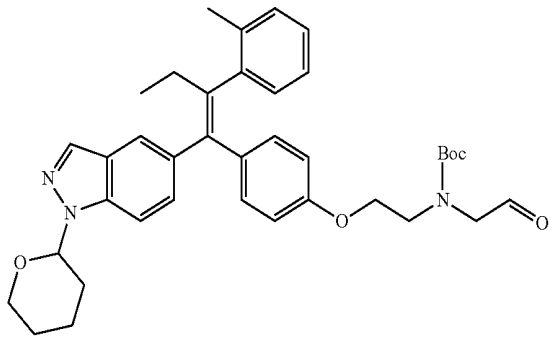


The reaction was carried out according to Scheme 3, Step-4 to give a crude product which was used in next step without further purification (3.8 g, crude).

Step-4: Synthesis of tert-butyl (E)-(2-oxoethyl)(2-(4-(1-(1-(tetrahydro-2H-pyran-2-yl)-1H-indazol-5-yl)-2-(o-tolyl)but-1-en-1-yl)phenoxy)ethyl)carbamate



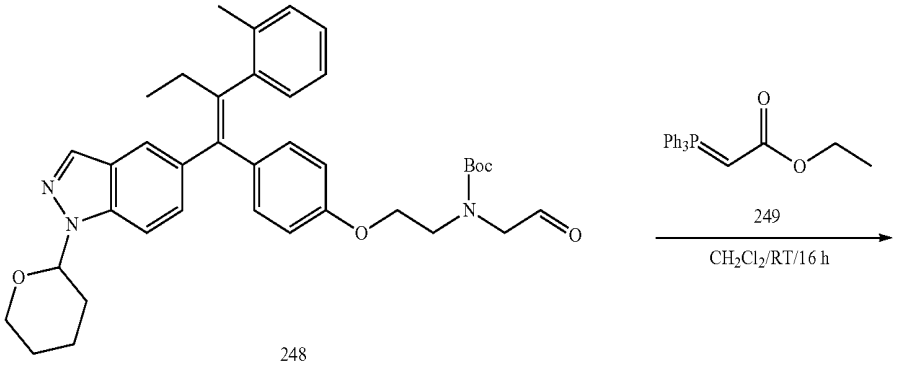
306



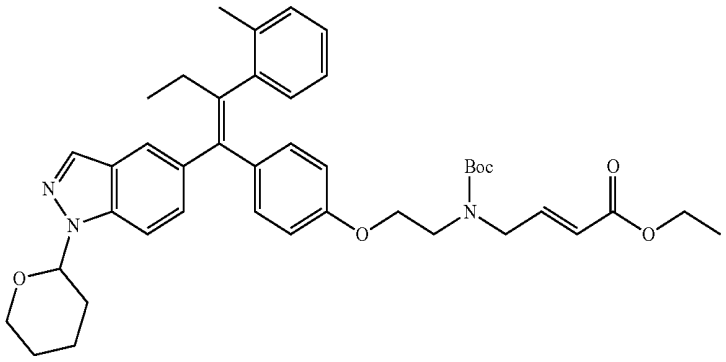
307

The reaction was carried out as described in Example 22, Step-4, substituting compound 306 for compound 245 to give a crude product which was purified by column chromatography over 100-200 mesh silica-gel by eluting with 30% EtOAc in n-hexane to afford the title compound of Ex. 26 Step-4 (1.5 g, 40%).

Step-5: Synthesis of ethyl (E)-4-((tert-butoxycarbonyl)(2-(4-((E)-1-(1-(tetrahydro-2H-pyran-2-yl)-1H-indazol-5-yl)-2-(o-tolyl)but-1-en-1-yl)phenoxy)ethyl)amino)but-2-enoate

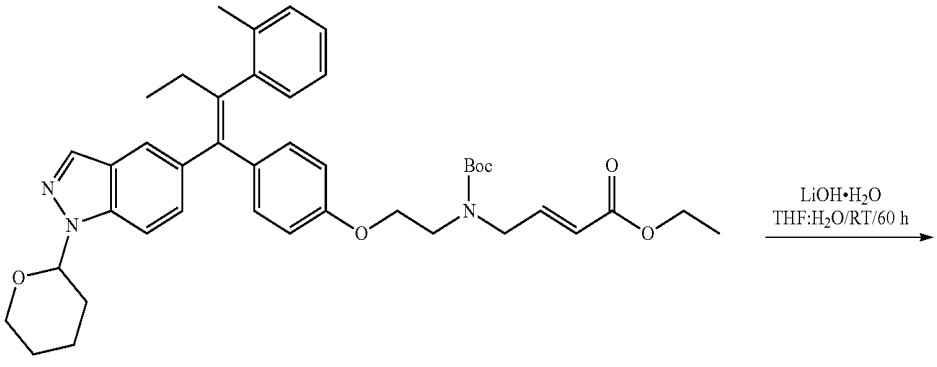


248

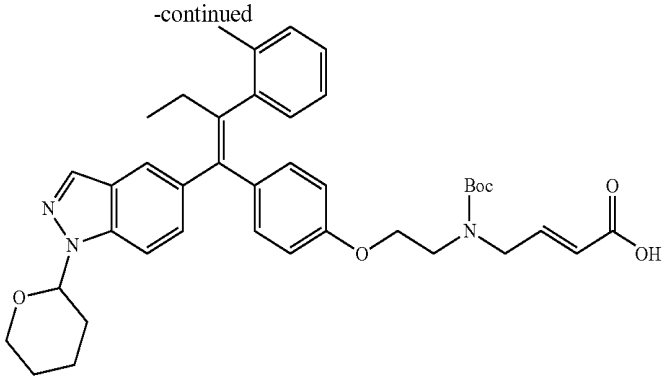


The reaction was carried out as described in Example 22, Step-5, substituting compound 248 for compound 246 and substituting compound 249 for compound 247 to give a crude product which was purified by column chromatography over 230-400 mesh silica-gel by eluting with 20% EtOAc in n-hexane to afford title compound of Ex. 26 Step-5 (1.37 g, 82%).

Step-6: Synthesis of (E)-4-((tert-butoxycarbonyl)(2-(4-((E)-1-(1-(tetrahydro-2H-pyran-2-yl)-1H-indazol-5-yl)-2-(o-tolyl)but-1-en-1-yl)phenoxy)ethyl)amino)but-2-enoic acid



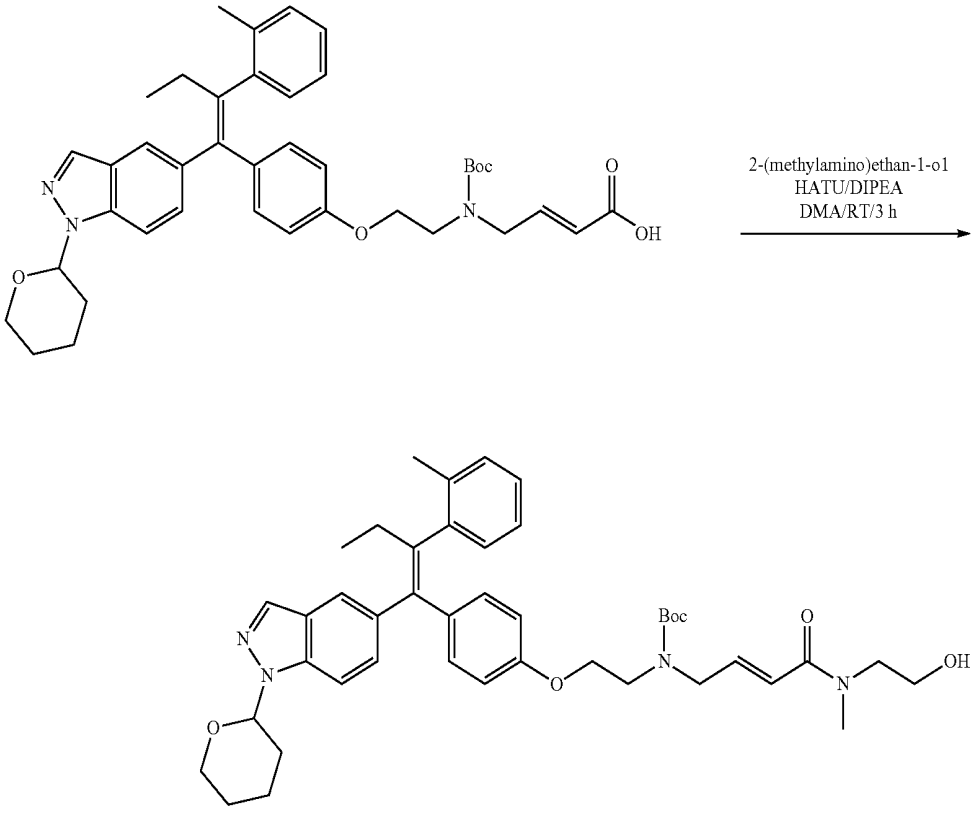
-continued



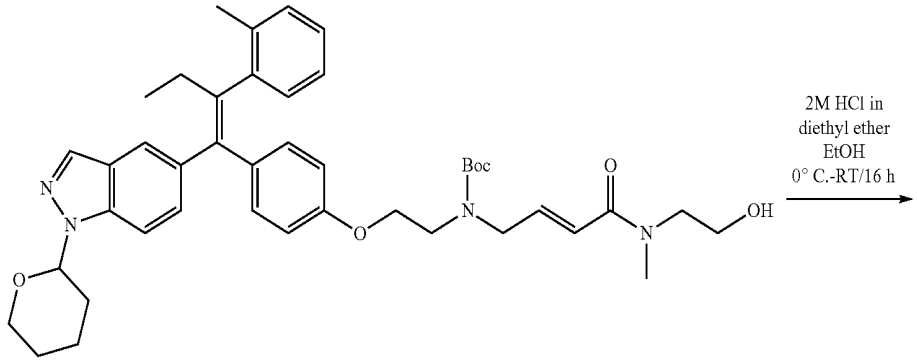
To a stirred solution of ethyl (E)-4-((tert-butoxycarbonyl)(2-(4-((E)-1-(1-(tetrahydro-2H-pyran-2-yl)-1H-indazol-5-yl)-2-(o-tolyl)but-1-en-1-yl)phenoxy)ethyl)amino)but-2-enoate (0.38 g, 0.54 mmol) in THF (16 mL) was added $LiOH.H_2O$ (0.15 g, 3.78 mmol) and water (4 mL). The reaction mixture was stirred for 60 h at room temperature, after completion of reaction (monitored by TLC), reaction mixture was diluted with water and extracted with dichloromethane (100 mL). The organic layer was washed with water followed by saturated NaCl solution, dried over anhydrous Na_2SO_4 and concentrated under reduced pressure. The crude product was purified by combi-flash to afford title compound of Ex. 26 Step-7 (0.33 g, 91%).

Step-8: Synthesis of tert-butyl ((E)-4-((2-hydroxyethyl)(methyl)amino)-4-oxobut-2-en-1-yl)(2-(4-((E)-1-(1-(tetrahydro-2H-pyran-2-yl)-1H-indazol-5-yl)-2-(o-tolyl)but-1-en-1-yl)phenoxy)ethyl)carbamate

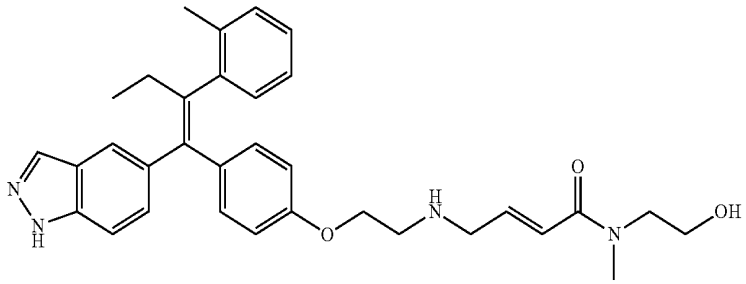
To a stirred solution of (E)-4-((tert-butoxycarbonyl)(2-(4-((E)-1-(1-(tetrahydro-2H-pyran-2-yl)-1H-indazol-5-yl)-2-(o-tolyl)but-1-en-1-yl)phenoxy)ethyl)amino)but-2-enoic acid (0.33 g, 0.49 mmol) in DMA (14 mL) was added DIPEA (0.25 mL, 1.47 mmol), HATU (0.18 g, 0.49 mmol) and 2-(methylamino)ethan-1-ol (0.036 g, 0.49 mmol). The reaction mixture was stirred for 3 h at room temperature, after completion of reaction (monitored by TLC), reaction mixture was diluted with water and extracted with dichloromethane (100 mL). The organic layer was washed with water followed by saturated NaCl solution, dried over anhydrous Na_2SO_4 and concentrated under reduced pressure. The crude product was purified by column chromatography over 230-400 mesh silica-gel by eluting with 3% MeOH in dichloromethane to afford title compound of Ex. 26 Step-8 (0.4 g, crude).



Step-9: Synthesis of (E)-4-((2-(4-((E)-1-(1H-indazol-5-yl)-2-(o-tolyl)but-1-en-1-yl)phenoxy)ethyl)amino)-N-(2-hydroxyethyl)-N-methylbut-2-enamide (Compound 26)



250



26

The reaction was carried out according to Scheme 2, Step-6c, substituting compound 250 for compound 211c to give a crude product which was purified by preparative HPLC to afford the Compound 26 (20 mg).

Compound 26:

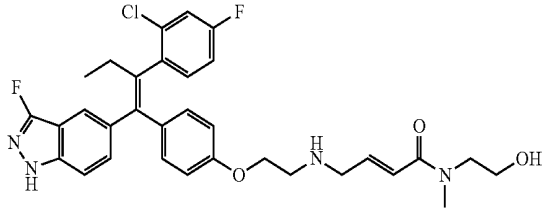
^{1}H NMR (400 MHz, DMSO-d_6): δ 13.07 (s, 1H), 8.08 (s, 1H), 7.65 (s, 1H), 7.53 (d, J=8.4 Hz, 1H), 7.23 (d, J=8.8 Hz, 1H), 7.16-7.12 (m, 2H), 7.09-7.03 (m, 3H), 6.74 (d, J=8.8 Hz, 2H), 6.63-6.46 (m, 4H), 4.76-4.64 (m, 1H), 3.84 (t, J=5.2 Hz, 2H), 3.50-3.47 (m, 2H), 3.39-3.36 (m, 2H), 3.02 (s, 4H), 2.86 (s, 1H), 2.75-2.67 (m, 1H), 2.33-2.30 (m, 2H), 2.10 (s, 3H), 2.0 (bs, 1H), 0.86 (t, J=7.4 Hz, 3H). LCMS: 539.4 $[M+H]^+$.

Example 27

There is no Example 27.

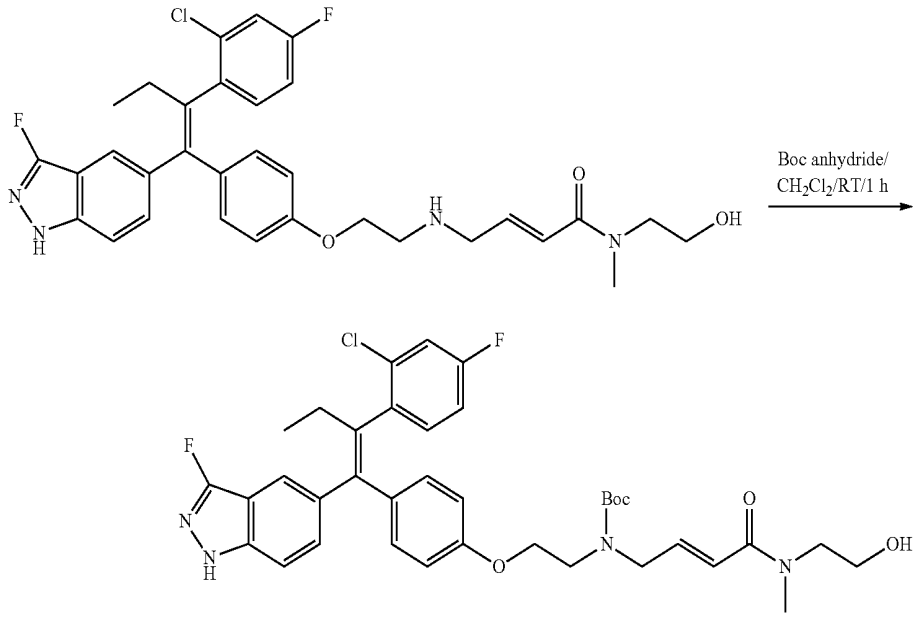
Example 28: Synthesis of (E)-4-((2-(4-((E)-2-(2-chloro-4-fluoro-(3-fluoro-1H-indazol-5-yl)but-1-en-1-yl)phenoxy)ethyl)amino)-N-(2-hydroxyethyl)-N-methylbut-2-enamide (Compound 28)

Step-1: Synthesis of (E)-4-((2-(4-((E)-2-(2-chloro-4-fluorophenyl)-1-(3-fluoro-1H-indazol-5-yl)but-1-en-1-yl)phenoxy)ethyl)amino)-N-(2-hydroxyethyl)-N-methylbut-2-enamide



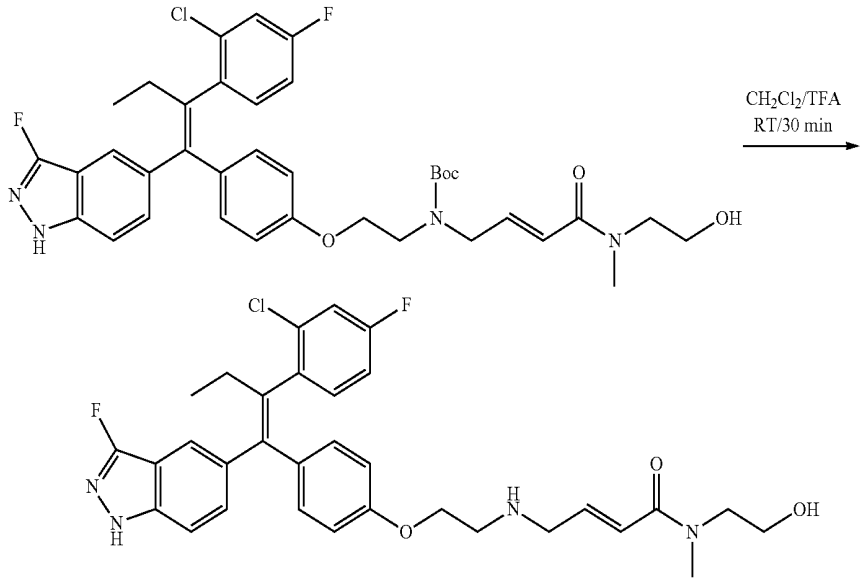
The compound was synthesized by following the approach as outlined in Example 3 by (i) substituting into Step-4 2-chloro-4-fluoro-1-iodobenzene for compound 227 and (ii) substituting into Step-6 of Ex. 3 (E)-4-bromo-N-(2-hydroxyethyl)-N-methylbut-2-enamide (as prepared in Example 18, Step-1) for compound 251 to afford the title compound as a crude (0.5 g) and used without further purification.

Step-2: Synthesis of tert-butyl (2-(4-((E)-2-(2-chloro-4-fluorophenyl)-1-(3-fluoro-1H-indazol-5-yl) but-1-en-1-yl)phenoxy)ethyl)((E)-4-((2-hydroxy-ethyl)(methyl)-amino)-4-oxobut-2-en-1-yl) carbamate



The reaction was carried out according to Scheme 2, Step-5 to give a crude product which was purified by preparative HPLC to obtain pure title compound of Step-2 Ex. 28 (0.28 g, 48%).

Step-3: Synthesis of (E)-4-((2-(4-((E)-2-(2-chloro-4-fluorophenyl)-1-(3-fluoro-1H-indazol-5-yl)but-1-en-1-yl)phenoxy)ethyl)amino)-N-(2-hydroxyethyl)-N-methylbut-2-enamide (Compound 28)

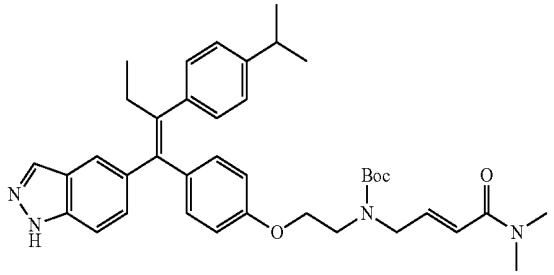


The reaction was carried out according to Scheme 2, Step-6b to give a crude product, which was purified by preparative HPLC to obtain compound 28 (0.025 g, 11%). Compound 28:

^{1}H NMR (400 MHz, DMSO-d_6): δ 12.59 (s, 1H), 7.54 (s, 1H), 7.49 (d, J=8.8 Hz, 1H), 7.34-7.31 (m, 2H), 7.24 (d, J=8.8 Hz, 1H), 7.14-7.11 (m, 1H), 6.83 (d, J=8.4 Hz, 2H), 6.63 (d, J=8.3 Hz, 2H), 6.59-6.52 (m, 2H), 4.76-4.64 (m, 1H), 3.87 (t, J=4.7 Hz, 2H), 3.50-3.46 (m, 2H), 3.40-3.38 (m, 4H), 3.03 (s, 1H), 2.86-2.81 (m, 4H), 2.36-2.33 (m, 2H), 0.88 (t, J=7.3 Hz, 3H). LCMS: 595.2 $[M+H]^+$.

Example 29: Synthesis of (E)-4-((2-(4-((E)-1-(1H-indazol-5-yl)-2-(4-isopropyl phenyl)but-1-en-1-yl) phenoxy)ethyl)amino)-N,N-dimethylbut-2-enamide (Compound 29)

Step-1: Synthesis of tert-butyl (2-(4-((E)-1-(1H-indazol-5-yl)-2-(4-isopropylphenyl)but-1-en-1-yl) phenoxy)ethyl)((E)-4-(dimethylamino)-4-oxobut-2-en-1-yl)carbamate



The compound was synthesized following the approach as outlined in Example 3 by substituting (i) into Step-1 5-(but-1-yn-1-yl)-1-(tetrahydro-2H-pyran-2-yl)-1H-indazole (prepared in Example 1, Step-3) for compound 252 and (ii) into Step-4 4-isopropyliodobenzene for compound 227. The resulting intermediate was subjected to the reaction conditions described in Scheme 2, Step-5 to give a crude product which was purified through column chromatography over 230-400 mesh silica-gel, column was eluted with 2% MeOH in dichloromethane as an eluent to afford the title compound of Ex. 29 Step-1 (0.096 g, 29%).

Step-2: Synthesis of (E)-4-((2-(4-((E)-1-(1H-indazol-5-yl)-2-(4-isopropylphenyl)but-1-en-1-yl)phenoxy)ethyl)amino)-N,N-dimethylbut-2-enamide (Compound 29)

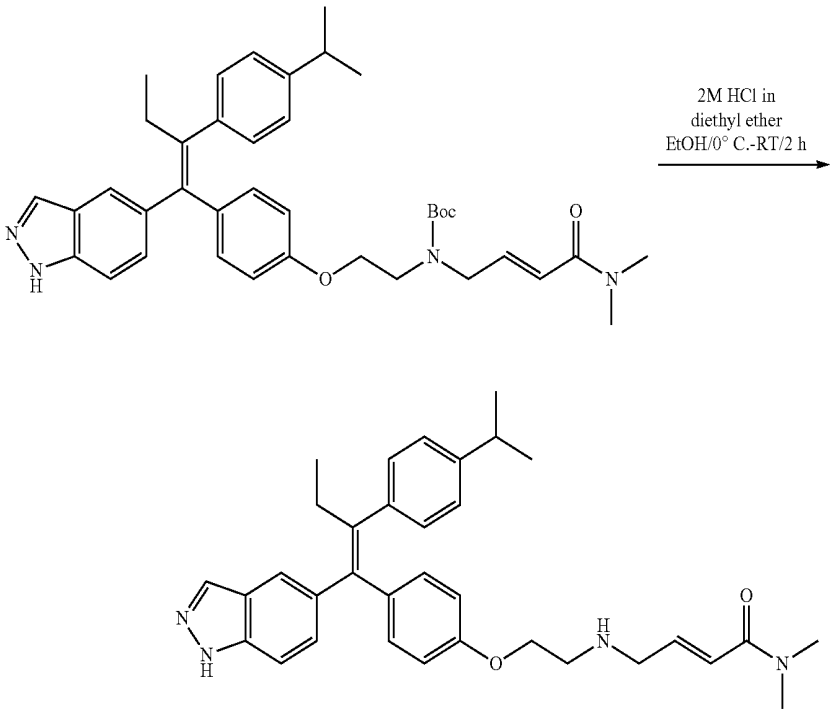
The reaction was carried out according to Scheme 2, Step-6c to give a crude compound was purified by preparative HPLC to afford Compound 29 (0.010 g, 12%).

Compound 29:

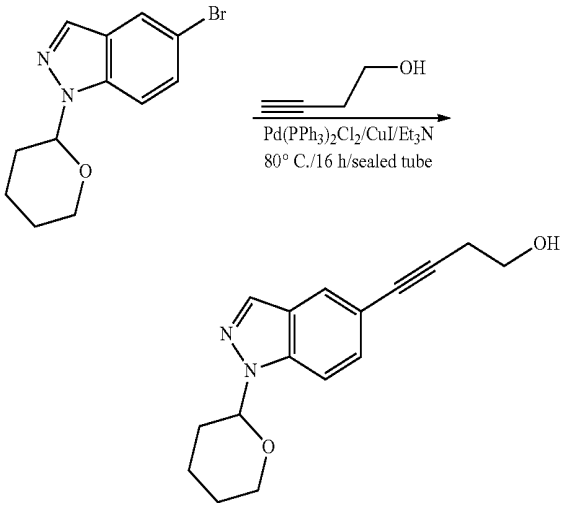
^{1}H NMR (400 MHz, DMSO-d_6): δ 13.05 (s, 1H), 8.06 (s, 1H), 7.6 (s, 1H), 7.5 (d, J=8.8 Hz, 1H), 7.1-7.05 (m, 5H), 6.74 (d, J=8.8 Hz, 2H), 6.63-6.58 (m, 3H), 6.5 (d, J=15.2 Hz, 1H), 3.66 (t, J=5.6 Hz, 2H), 3.31 (m, 2H), 2.98 (s, 3H), 2.84 (s, 3H), 2.82-2.76 (m, 3H), 2.4-2.35 (m, 2H), 1.16 (d, J=6.8 Hz, 6H), 0.88 (t, J=7.3 Hz, 3H). LCMS: 537.4 $[M+H]^+$.

Example 30: Synthesis of (E)-4-((2-(4-((E)-4-chloro-1-(1H-indazol-5-yl)-2-phenyl but-1-en-1-yl) phenoxy) ethyl)amino)-N,N-dimethylbut-2-enamide (Compound 30)

The compound was synthesized following the approach as outlined in Example 5 by substituting into Step-1 5-(4-chlorobut-1-yn-1-yl)-1-(tetrahydro-2H-pyran-2-yl)-1H-indazole (preparation shown below in Ex. 30 Steps 1-2) for compound 242, tert-butyl (E)-(4-(dimethylamino)-4-oxobut-2-en-1-yl)(2-(4-iodophenoxy)ethyl)carbamate (as prepared in Example 14, Step-3) for compound 243, and iodobenzene for compound 244 and continuing with Ex. 5 Step-2 to afford Compound 30 (0.04 g, 6%).

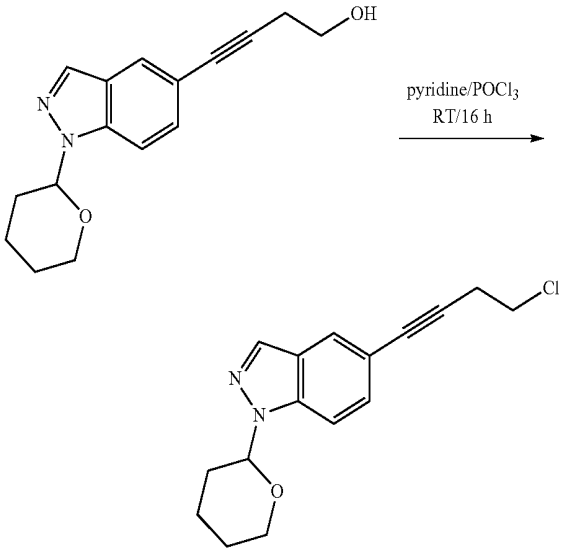


Step-1: Synthesis of 4-(1-(tetrahydro-2H-pyran-2-yl)-1H-indazol-5-yl)but-3-yn-1-ol



The reaction was carried out according to Scheme 1, Step-2, using 5-bromo-1-(tetrahydro-2H-pyran-2-yl)-1H-indazole (Example 1, Step-3) for compound 202 and but-3-yn-1-ol for compound 203, to give a crude product which was purified over silica-gel column chromatography using 15% ethyl acetate in n-hexane to afford the title compound of Ex. 30 Step-1 (1.3 g, 54%).

Step-2: Synthesis of 5-(4-chlorobut-1-yn-1-yl)-1-(tetrahydro-2H-pyran-2-yl)-1H-indazole



To an ice cold solution of 4-(1-(tetrahydro-2H-pyran-2-yl)-1H-indazol-5-yl)but-3-yn-1-ol (2.6 g, 9.6 mmol) in pyridine (36 mL), was added $POCl_3$. Reaction mixture was allowed to room temperature for 16 h. Upon completion of reaction, excess of $POCl_3$ was removed under vacuum, basified with sodium bicarbonate solution, extracted with ethyl acetate (2×100 mL), combined organic layers were washed with brine solution and dried over anhydrous sodium sulphate. Organic layer was concentrated to dryness to afford the crude product, which was purified by column chromatography over silica-gel, column was eluting with 10% EtOAc in n-hexane to obtain the title compound of Ex. 30 Step-2 (1.5 g, 54%).

Compound 30:

^{1}H NMR (400 MHz, DMSO-d_6): δ 13.1 (s, 1H), 8.08 (s, 1H), 7.7 (s, 1H), 7.53 (d, J=8.8 Hz, 1H), 7.26-7.16 (m, 6H), 6.77 (d, J=8.8 Hz, 2H), 6.6 (d, J=8.0 Hz, 3H), 6.5 (t, J=5.2 Hz, 1H), 3.87 (d, J=5.6 Hz, 2H), 3.46 (t, J=6.8 Hz, 2H), 3.3 (m, 2H), 2.98 (s, 3H), 2.89 (t, J=7.2 Hz, 2H), 2.84 (s, 3H), 2.77 (t, J=5.2 Hz, 2H). LCMS: 529.3 $[M+H]^+$.

Example 31: Synthesis of (E)-4-((2-(4-((E)-1-(1H-indazol-5-yl)-2-(4-isopropyl phenyl)but-1-en-1-yl) phenoxy)ethyl)amino)-N,N-dimethylbut-2-enamide (Compound 31)

The compound was synthesized following the approach as outlined in Example 3 by substituting into Step-4 (Z)-tert-butyl (2-(4-(1-(1-(tetrahydro-2H-pyran-2-yl)-1H-indazol-5-yl)-2-(4,4,5,5-tetramethyl-1,3,2-dioxaborolan-2-yl)but-1-en-1-yl)phenoxy)ethyl)carbamate (as prepared in Example 6, Step-1) for compound 226 and 2-iodo-1-methoxybenzene for compound 227 to afford Compound 31 (0.014 g, 3%).

Compound 31:

^{1}H NMR (400 MHz, DMSO-d_6): δ 13.05 (s, 1H), 8.07 (s, 1H), 7.6 (s, 1H), 7.5 (d, J=8.4 Hz, 1H), 7.15-7.11 (m, 2H), 6.94 (d, J=8.4 Hz, 1H), 6.87 (d, J=7.2 Hz, 1H), 6.78-6.72 (m, 3H), 6.58-6.54 (m, 3H), 6.5 (d, J=15.2 Hz, 1H), 3.85 (t, J=5.6 Hz, 2H), 3.77 (s, 3H), 3.31 (m, 2H), 2.98 (s, 3H), 2.84 (s, 3H), 2.76 (t, J=5.6 Hz, 2H), 2.33 (s, 2H), 0.88 (t, J=7.2 Hz, 3H). LCMS: 525.3 $[M+H]^+$.

Example 32: Synthesis of (E)-4-((2-(4-((E)-2-(2-(difluoromethoxy)phenyl)-1-(1H-indazol-5-yl)but-1-en-1-yl)phenoxy)ethyl)amino)-N,N-dimethylbut-2-enamide (Compound 32)

The compound was synthesized following the approach as outlined in Example 3 by substituting into Step-4 (Z)-tert-butyl (2-(4-(1-(1-(tetrahydro-2H-pyran-2-yl)-1H-indazol-5-yl)-2-(4,4,5,5-tetramethyl-1,3,2-dioxaborolan-2-yl)but-1-en-1-yl)phenoxy)ethyl)carbamate (as prepared in Example 6, Step-1) for compound 226 and 2-iodo-1-difluromethoxy-benzene for compound 227 to afford Compound 32 (0.022 g, 4%).

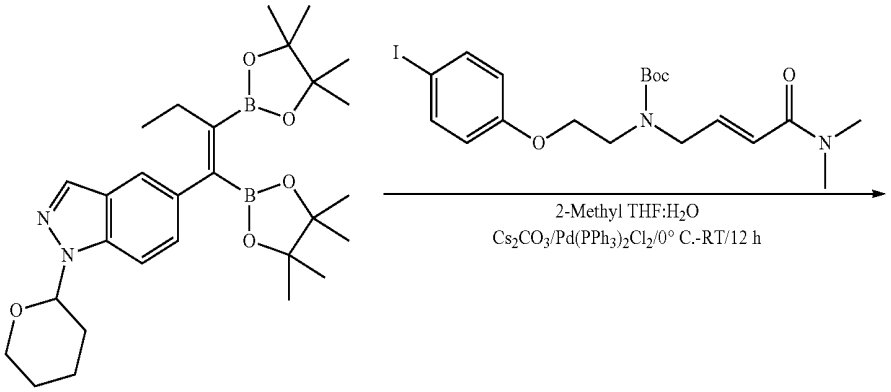
Compound 32:

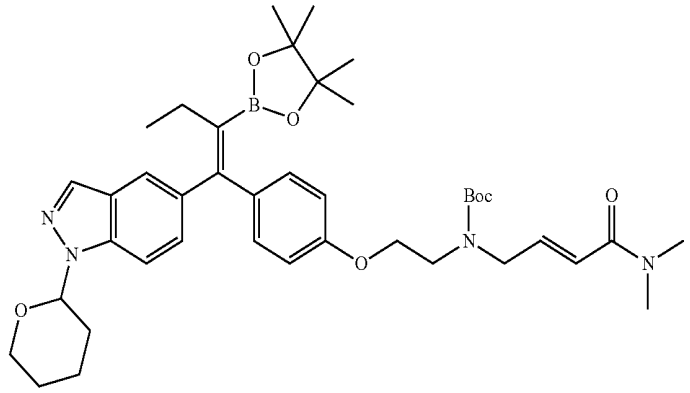
^{1}H-NMR (400 MHz, DMSO-d_6): δ 13.08 (s, 1H), 8.09 (s, 1H), 7.62 (s, 1H), 7.53 (d, J=8.8 Hz, 1H), 7.25-7.23 (m, 1H), 7.22-7.08 (m, 5H), 6.78 (d, J=8.8 Hz, 2H), 6.62-6.57 (m, 3H), 6.5 (d, J=15.2 Hz, 1H), 3.85 (t, J=5.2 Hz, 2H), 3.32-3.3 (m, 2H), 2.98 (s, 3H), 2.84 (s, 3H), 2.77 (t, J=5.2 Hz, 2H), 2.33 (m, 2H), 0.87 (t, J=7.2 Hz, 3H), LC-MS: 561.3 $[M+H]^+$.

Example 33: Synthesis of (E)-4-((2-(4-((E)-1-(1H-indazol-5-yl)-2-(2-(trifluoro-methoxy)phenyl)but-1-en-1-yl)phenoxy)ethyl)amino)-N,N-dimethylbut-2-enamide (Compound 33)

The compound was synthesized following the approach as outlined in Example 3 by substituting into Step-4 tert-butyl ((E)-4-(dimethylamino)-4-oxobut-2-en-1-yl)(2-(4-((Z)-1-(1-(tetrahydro-2H-pyran-2-yl)-1H-indazol-5-yl)-2-(4,4,5,5-tetramethyl-1,3,2-dioxaborolan-2-yl)but-1-en-1-yl)phenoxy)ethyl)carbamate (preparation shown below in Ex. 33 Step-1) for compound 226 and 2-iodo-1-trifluromethoxy-benzene for compound 227 and continuing with Ex. 3 Step-5 to afford Compound 33 (0.030 g, 26%).

Step-1: Synthesis of tert-butyl ((E)-4-(dimethylamino)-4-oxobut-2-en-1-yl)(2-(4-((Z)-1-(1-(tetrahydro-2H-pyran-2-yl)-1H-indazol-5-yl)-2-(4,4,5,5-tetramethyl-1,3,2-dioxaborolan-2-yl)but-1-en-1-yl)phenoxy)ethyl)carbamate





The reaction was carried out according to Scheme 1, Step-4, using (Z)-5-(1,2-bis(4,4,5,5-tetramethyl-1,3,2-dioxaborolan-2-yl)but-1-en-1-yl)-1-(tetrahydro-2H-pyran-2-yl)-1H-indazole (as prepared in Example 17, Step-1) for compound 206 and tert-butyl (E)-(4-(dimethylamino)-4-oxobut-2-en-1-yl)(2-(4-iodophenoxy)ethyl)carbamate (as prepared in Example 14, Step-3) for compound 207, to give a crude material which was purified by column chromatography over 230-400 mesh silica gel using MeOH in dichloromethane (1.6:98.4) to afford the title compound of Ex. 33 Step-1 (4.04 g, 43%).

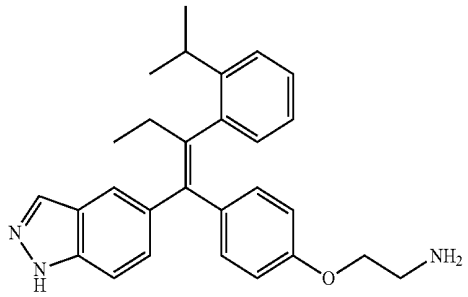
Compound 33:

^{1}H-NMR (400 MHz, DMSO-d_6): δ 13.10 (s, 1H), 8.1 (s, 1H), 7.6 (s, 1H), 7.5 (d, J=8.8 Hz, 1H), 7.42-7.39 (m, 1H), 7.38-7.26 (m, 2H), 7.22-7.18 (m, 1H), 7.13-7.11 (m, 1H), 6.74 (d, J=8.80 Hz, 2H), 6.62-6.58 (m, 3H), 6.51-6.48 (d, J=15.2 Hz, 1H), 3.86 (t, J=5.6 Hz, 2H), 3.31-3.3 (m, 2H), 2.98 (s, 3H), 2.84 (s, 3H), 2.76 (t, J=5.6 Hz, 2H), 2.43-2.42 (m, 2H), 0.86 (t, J=7.60 Hz, 3H). LCMS: 579.0 $[M+H]^+$.

Example 34: Synthesis of (E)-4-((2-(4-((E)-1-(1H-indazol-5-yl)-2-(2-isopropyl phenyl)but-1-en-1-yl)phenoxy)ethyl)amino)-N,N-dimethylbut-2-enamide (Compound 34)

The compound was synthesized following the approach as outlined in Example 12 by substituting into Step-2 (E)-2-(4-(1-(1H-indazol-5-yl)-2-(2-isopropylphenyl)but-1-en-1-yl)phenoxy)ethan-1-amine (preparation shown below in Ex. 34 Step-1) for compound 253 and (E)-4-bromo-N,N-dimethylbut-2-enamide (as prepared in Example 1, Step-7) for compound 232 to afford Compound 34 (0.010 g, 6%).

Step-1: Synthesis of tert-butyl (E)-(2-(4-(2-(2-isopropylphenyl)-1-(1-(tetrahydro-2H-pyran-2-yl)-1H-indazol-5-yl)but-1-en-1-yl)phenoxy)ethyl)carbamate



The compound was synthesized following the approach as outlined in Example 7 by substituting 2-iodo-1-iospropyl-benzene in Step-1, continuing with Step-2, and proceeding directly to Step 4 to obtain the title compound (0.5 g, 98%).

Compound 34:

^{1}H-NMR (400 MHz, DMSO-d_6): δ 13.07 (s, 1H), 8.10 (s, 1H), 7.64 (s, 1H), 7.53 (d, J=8.8 Hz, 1H), 7.24 (d, J=6.8 Hz, 1H), 7.19-7.14 (m, 4H), 6.72 (d, J=8.8 Hz, 2H), 6.6-6.46 (m, 4H), 3.84 (t, J=5.6 Hz, 2H), 3.30 (m, 2H), 3.17 (t, J=6.80 Hz, 1H), 2.98 (s, 3H), 2.84 (s, 3H), 2.75 (t, J=5.6 Hz, 1H), 2.67 (t, J=6.0 Hz, 1H), 2.36-2.30 (m, 2H), 1.13 (d, J=6.8 Hz, 3H), 0.86 (t, J=7.60 Hz, 3H), 0.61 (d, J=6.80 Hz, 3H), LC-MS: 537.3 $[M+H]^+$.

Example 35: Synthesis of (E)-4-((2-(4-((E)-2-(2-ethylphenyl)-1-(1H-indazol-5-yl)but-1-en-1-yl)phenoxy) ethyl)amino)-N,N-dimethylbut-2-enamide (Compound 35)

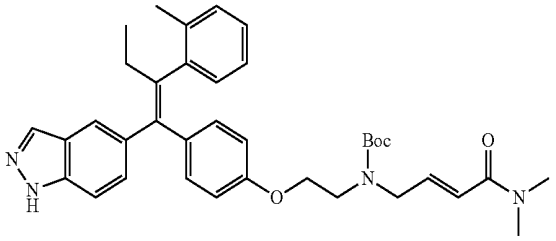
The compound was synthesized following the approach as outlined in Example 5 by substituting into Step-1 tert-butyl (E)-(4-(dimethylamino)-4-oxobut-2-en-1-yl)(2-(4-iodophenoxy) ethyl) carbamate (as prepared in Example 14, Step-3) for compound 243 and 2-iodo-1-methylbenzene for compound 244 and continuing with Step-2 to deliver Compound 35 (0.079 g, 10%).

Compound 35:

^{1}H NMR (400 MHz, DMSO-d_6): δ 13.06 (s, 1H), 8.08 (s, 1H), 7.64 (s, 1H), 7.53 (d, J=8.4 Hz, 1H), 7.2-7.13 (m, 5H), 6.73 (d, J=8.8 Hz, 2H), 6.6-6.47 (m, 4H), 3.84 (t, J=5.6 Hz, 2H), 3.3-3.29 (m, 2H), 2.98 (s, 3H), 2.84 (s, 3H), 2.75 (t, J=5.6 Hz, 2H), 2.67-2.63 (m, 1H), 2.41-2.26 (m, 3H), 1.02 (t, J=7.6 Hz, 3H), 0.86 (t, J=7.6 Hz, 3H) LCMS: 523.3 $[M+H]^+$.

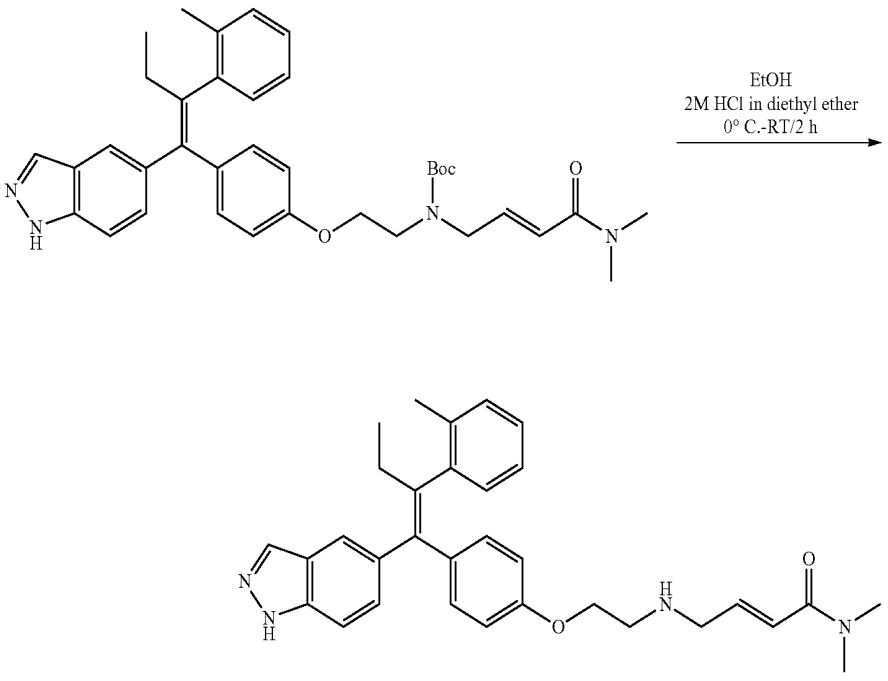
Example 36: Synthesis of (E)-4-((2-(4-((E)-1-(1H-indazol-5-yl)-2-(o-tolyl)but-1-en-1-yl)phenoxy) ethyl) amino)-N,N-dimethylbut-2-enamide (Compound 36)

Step-1: Synthesis of tert-butyl (2-(4-((E)-1-(1H-indazol-5-yl)-2-(o-tolyl)but-1-en-1-yl)phenoxy) ethyl)((E)-4-(dimethylamino)-4-oxobut-2-en-1-yl) carbamate



The compound was synthesized following the approach as outlined in Example 3 by substituting into Step-4 (Z)-tert-butyl (2-(4-(1-(1-(tetrahydro-2H-pyran-2-yl)-1H-indazol-5-yl)-2-(4,4,5,5-tetramethyl-1,3,2-dioxaborolan-2-yl)but-1-en-1-yl)phenoxy)ethyl)carbamate (as prepared in Example 6, Step-1) for compound 226 and 2-iodo-1-methylbenzene for compound 227. The resulting intermediate was subjected to the reaction conditions described in Scheme 2, Step-5 to give a crude product, which was purified through silica gel chromatography with with 2% MeOH in dichloromethane as an eluent to afford the title compound of Ex. 36 Step-1 (0.12 g, 27%).

Step-2: Synthesis of (E)-4-((2-(4-((E)-1-(1H-indazol-5-yl)-2-(o-tolyl)but-1-en-1-yl)phenoxy)ethyl) amino)-N,N-dimethylbut-2-enamide (Compound 36)



The reaction was carried out according to Scheme 2, Step-6c, to afford the crude product, which was purified by preparative TLC to afford the title compound of Ex. 36 Step-2(0.015 g, 15%).

Compound 36:

^{1}H NMR (400 MHz, DMSO-d_6): δ 13.08 (s, 1H), 8.08 (s, 1H), 7.65 (s, 1H), 7.53 (d, J=8.8 Hz, 1H), 7.4 (d, J=7.2 Hz, 1H), 7.16-7.13 (m, 2H), 7.1-7.03 (m, 2H), 6.74 (d, J=8.8 Hz, 2H), 6.6-6.47 (m, 4H), 3.84 (t, J=5.6 Hz, 2H), 3.29-3.1 (m, 2H), 2.98 (s, 3H), 2.84 (s, 3H), 2.76 (t, J=5.6 Hz, 2H), 2.33-2.31 (m, 2H), 2.1 (s, 3H), 0.86 (t, J=7.6 Hz, 3H). LCMS: 509.3 $[M+H]^+$.

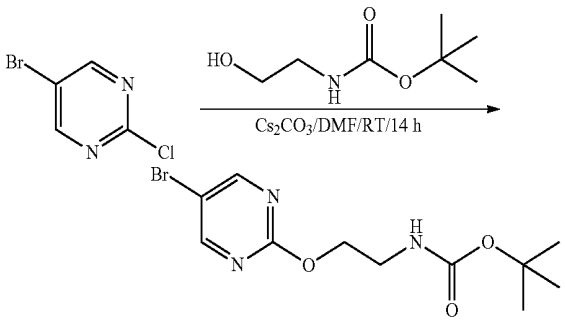
Example 37

There is no Example 37.

Example 38: Synthesis of (E)-4-((2-((5-((Z)-1-(1H-indazol-5-yl)-2-phenylbut-1-en-1-yl)pyrimidin-2-yl)oxy)ethyl)amino)-N,N-dimethylbut-2-enamide (Compound 38)

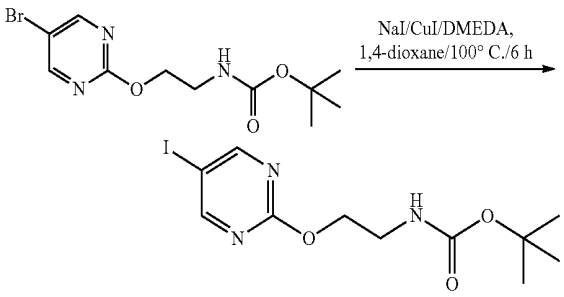
The compound was synthesized following the approach as outlined in Example 12 by substituting into Step-2 (E)-4-((2-((5-((Z)-1-(1H-indazol-5-yl)-2-phenylbut-1-en-1-yl)pyrimidin-2-yl)oxy) ethyl)amino)-N,N-dimethylbut-2-enamide (preparation shown below in Ex. 38 Steps 1-4) for compound 253 and (E)-4-bromo-N,N-dimethylbut-2-enamide (as prepared in Example 1, Step-7) for compound 232 to afford Compound 38 (0.11 g, 13%).

Step-1: Synthesis of tert-butyl (2-((5-bromopyrimidin-2-yl)oxy)ethyl)carbamate



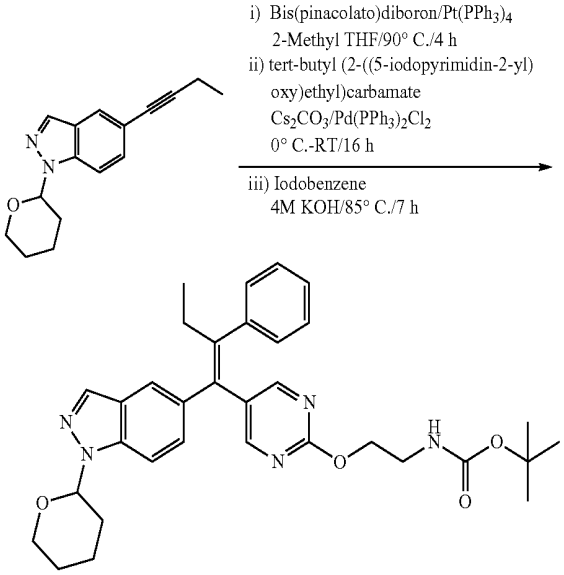
To a stirred solution of tert-butyl (2-hydroxyethyl)carbamate (3.25 g, 20.2 mmol) in DMF (90 mL), was added cesium carbonate (7.57 g, 23.3 mmol). Reaction mixture was stirred for about 15 min at room temperature, 5-Bromo-2-chloropyrimidine (3.0 g, 15.5 mmol) was added to the reaction mixture and stirred for 14 h. Upon completion, reaction mixture was diluted with water, extracted with ethyl acetate, the combined organic layers were washed with water followed by brine. The organic layer was dried over anhydrous sodium sulphate, concentrated to dryness under reduced pressure. The crude product was purified through column chromatography over silica gel, eluting with 15-20% EtoAc in n-hexane to afford the title compound (4.5 g, 55%).

Step-2: Synthesis of tert-butyl (2-((5-iodopyrimidin-2-yl)oxy)ethyl)carbamate



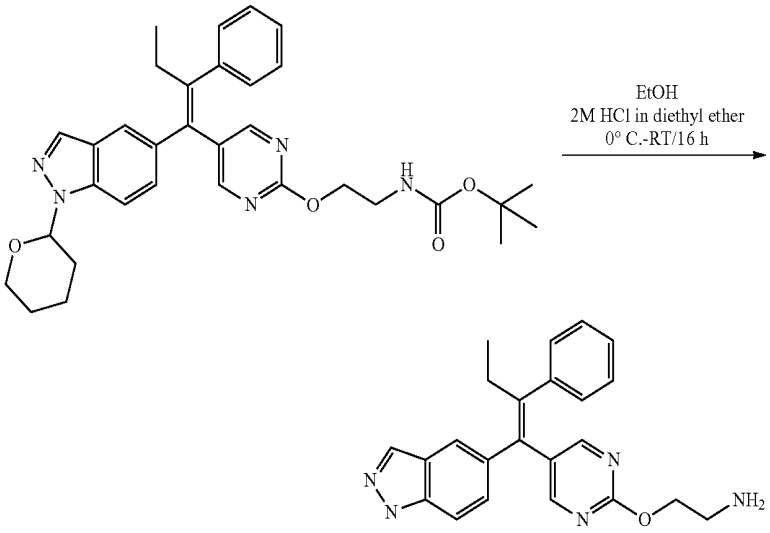
To a stirred solution of tert-butyl (2-((5-bromopyrimidin-2-yl)oxy)ethyl)carbamate (4.0 g, 12.6 mmol) in 1,4-dioxane (80 mL), were added NaI (3.78 g, 25.2 mmol), CuI (2.4 g, 12.6 mmol) and N,N'-dimethylethylenediamine (2.2 g, 25.2 mmol). The reaction mixture was heated to 100° C. for 6 h. Upon completion, reaction mixture was cooled to room temperature, filtered through celite pad and the celite pad was washed with ethyl acetate (200 mL). The obtained filtrate was washed with water, brine and dried over anhydrous sodium sulphate and concentrated to dryness. The crude product was purified through column chromatography over silica gel, eluting with 15% EtOAc in n-hexane to afford the title compound of Ex. 38 Step-1 (3.2 g, 69%).

Step-3: Synthesis of tert-butyl (Z)-(2-((5-(2-phenyl-1-(1-(tetrahydro-2H-pyran-2-yl)-1H-indazol-5-yl)but-1-en-1-yl)pyrimidin-2-yl)oxy)ethyl)carbamate



The reactions were carried out as described in Example 5, Step-1, using 5-(but-1-yn-1-yl)-1-(tetrahydro-2H-pyran-2-yl)-1H-indazole (Example 1, Step-3) and substituting Iodobenzene for compound 244 to give a crude product which was purified by silica gel chromatography, eluting with 25-30% EtOAc in n-hexane to obtain the title compound of Ex. 38 Step-3 (2.9 g, crude).

Step-4: Synthesis of (Z)-2-((5-(1-(1H-indazol-5-yl)-2-phenylbut-1-en-1-yl)pyrimidin-2-yl)oxy)ethan-1-amine



The reaction was carried out according to Scheme 2, Step-2b to afford the title compound of Ex. 38 Step-4 (1.6 g, 85%).

Compound 38:

^{1}H NMR (400 MHz, DMSO-d_6): δ 13.12 (s, 1H), 8.09 (s, 1H), 7.99 (s, 2H), 7.69 (s, 1H), 7.56 (d, J=8.4 Hz, 1H), 7.3-7.17 (m, 6H), 6.62-6.47 (m, 2H), 4.18 (t, J=6 Hz, 2H), 3.30-3.28 (m, 2H), 2.98 (s, 3H), 2.83 (s, 3H), 2.68 (t, J=6 Hz, 2H), 2.46-2.42 (m, 2H), 0.90 (t, J=7.2 Hz, 3H). LCMS: 497.3 $[M+H]^+$.

Example 39: Synthesis of (E)-1-(azetidin-1-yl)-4-((2-(4-((E)-2-cyclobutyl-1-(1H-indazol-5-yl)-2-phenylvinyl) phenoxy)ethyl)amino)but-2-en-1-one (Compound 39)

The compound was synthesized following the approach as outlined in Example 12 by substituting into Step-2 (E)-2-(4-(2-cyclobutyl-1-(1H-indazol-5-yl)-2-phenylvinyl) phenoxy)ethan-1-amine (as prepared in Example 13, Step-7) for compound 253 and (E)-1-(azetidin-1-yl)-4-bromobut-2-en-1-one (as prepared in Example 10, Step-1) for compound 232 to afford Compound 39 (0.030 g, 4%).

Compound 39:

^{1}H NMR (400 MHz, DMSO-d_6): δ 13.06 (s, 1H), 8.07 (s, 1H), 7.58 (s, 1H), 7.51 (d, J=8.8 Hz, 1H), 7.27-7.23 (m, 2H), 7.17-7.08 (m, 5H), 6.79-6.76 (m, 2H), 6.59 (t, J=5.2 Hz, 1H), 6.57-6.53 (m, 2H), 6.04-5.75 (m, 1H), 4.11 (t, J=7.6 Hz, 2H), 3.87-3.80 (m, 4H), 3.41 (t, J=8.8 Hz, 1H), 3.29-3.27 (m, 2H), 2.74 (t, J=5.6 Hz, 2H), 2.17 (t, J=7.6 Hz, 2H), 1.82-1.76 (m, 4H), 1.59-1.55 (m, 1H), 1.36-1.32 (m, 1H). LCMS: 533.3 $[M+H]^+$.

Example 40: Synthesis of (E)-1-(azetidin-1-yl)-4-((2-(4-((E)-2-cyclobutyl-1-(3-fluoro-1H-indazol-5-yl)-2-phenylvinyl)phenoxy)ethyl)amino)but-2-en-1-one (Compound 40)

The compound was synthesized following the approach as outlined in Example 3 by (i) substituting into Step-4 (Z)-5-(1,2-bis(4,4,5,5-tetramethyl-1,3,2-dioxaborolan-2-yl)but-1-en-1-yl)-3-fluoro-1-(tetrahydro-2H-pyran-2-yl)-1H-indazole (as prepared in Example 3, Step-1) for compound 226 and iodobenzene for compound 227 and (ii) substituting into Step-6 (E)-1-(azetidin-1-yl)-4-bromobut-2-en-1-one (as prepared in Example 10, Step-1) for compound 251 to deliver the title compound (0.007 g, 3%).

Compound 40:

^{1}H NMR (400 MHz, DMSO-d_6): δ 12.57 (s, 1H), 7.49 (s, 1H), 7.46 (d, J=8.0 Hz, 1H), 7.27-7.1 (m, 6H), 6.8 (d, J=8.8 Hz, 2H), 6.6 (t, J=5.2 Hz, 1H), 6.55 (d, J=8.8 Hz, 2H), 6.02 (d, J=15.6 Hz, 1H), 4.12 (t, J=7.4 Hz, 2H), 3.87-3.83 (m, 4H), 3.4-3.37 (m, 1H), 3.29-3.27 (m, 2H), 2.74 (t, J=5.6 Hz, 2H), 2.2-2.1 (m, 2H), 1.83-1.75 (m, 4H), 1.6-1.56 (m, 1H), 1.34-1.24 (m, 1H). LCMS: 551.3 $[M+H]^+$.

Example 41: Synthesis of (E)-4-((2-(4-((E)-2-cyclobutyl-1-(1H-indazol-5-yl)-2-phenylvinyl) phenoxy) ethyl)amino)-N-(2-hydroxyethyl)-N-methylbut-2-enamide (Compound 41)

The compound was synthesized following the approach as outlined in Example 12 by substituting into Step-2 (E)-2-(4-(2-cyclobutyl-1-(1H-indazol-5-yl)-2-phenylvinyl) phenoxy)ethan-1-amine (as prepared in Example 13, Step-7) for compound 253 and (E)-4-bromo-N-(2-hydroxyethyl)-N-methylbut-2-enamide (as prepared in Example 18, Step-1) for compound 232 to afford Compound 41 (0.012 g, 9%).

Compound 41:

^{1}H NMR (400 MHz, DMSO-d_6): δ 13.06 (s, 1H), 8.08 (s, 1H), 7.58 (s, 1H), 7.51 (d, J=8.0 Hz, 1H), 7.27-7.24 (m, 2H), 7.17-7.09 (m, 4H), 7.78 (d, J=7.6 Hz, 2H), 6.58-6.52 (m, 4H), 4.77-4.64 (m, 1H), 3.85 (t, J=5.2 Hz, 2H), 3.51-3.41 (m, 2H), 3.39-3.34 (m, 5H), 3.03 (s, 1H), 2.86 (s, 2H), 2.80-2.79 (m, 2H), 1.82-1.76 (m, 4H), 1.57-1.55 (m, 1H), 1.35-1.32 (m, 1H), LCMS: 551.3 $[M+H]^+$.

Example 42: Synthesis of (E)-1-(azetidin-1-yl)-4-((2-(4-((E)-2-cyclobutyl-1-(1H-indazol-5-yl)-2-(o-tolyl) vinyl)phenoxy)ethyl)amino)but-2-en-1-one (Compound 42)

The compound was synthesized following the approach as outlined in Example 3 by (i) substituting into Step-4 (Z)-tert-butyl (2-(4-(2-cyclobutyl-1-(1-(tetrahydro-2H-pyran-2-yl)-1H-indazol-5-yl)-2-(4,4,5,5-tetramethyl-1,3,2-dioxaborolan-2-yl)vinyl)phenoxy)ethyl)carbamate (as prepared in Example 13, Step-5) for compound 226 and 1-iodo-2-methylbenzene for compound 227 and (ii) substituting into Step-6 (E)-1-(azetidin-1-yl)-4-bromobut-2-en-1-one (as prepared in Example 10, Step-1) for compound 251 to afford Compound 42 (0.05 g, 4.5%).

Compound 42:

^{1}H NMR (400 MHz, DMSO-d_6): δ 13.07 (s, 1H), 8.09 (s, 1H), 7.60 (s, 1H), 7.53 (d, J=2.0 Hz, 1H), 7.16-7.08 (m, 5H), 6.77 (d, J=8.8 Hz, 2H), 6.61-6.57 (m, 1H), 6.54 (d, J=8.8 Hz, 2H), 6.03 (d, J=15.6 Hz, 1H), 4.11 (t, J=7.6 Hz, 2H), 3.87-3.82 (m, 4H), 3.43-3.39 (m, 1H), 3.31 (s, 2H), 2.77 (t, J=5.6 Hz, 2H), 2.19-2.15 (m, 2H), 2.12 (s, 3H), 1.89-1.73 (m, 3H), 1.61-1.53 (m, 2H), 1.36-1.32 (m, 1H). LCMS: 547.3 [M+H]$^+$.

Example 43: Synthesis of (E)-4-((2-(4-((E)-1-(3-fluoro-1H-indazol-5-yl)-2-(2-fluoro phenyl)but-1-en-1-yl)phenoxy)ethyl)amino)-N,N-dimethylbut-2-enamide (Compound 43)

The compound was synthesized following the approach as outlined in Example 3 by substituting into Step-4 1-iodo-2-fluorobenzene for compound 227 to afford Compound 43 (0.025 g, 10%).

Compound 43:

^{1}H NMR (400 MHz, DMSO-d_6): δ 12.59 (s, 1H), 7.52 (s, 1H), 7.48 (dd, J_1=8.8 Hz, J_2=2.0 Hz, 1H), 7.24-7.18 (m, 3H), 7.08-7.03 (m, 2H), 6.80 (d, J=8.4 Hz, 2H), 6.63-6.57 (m, 3H), 6.49 (d, J=5.2 Hz, 1H), 3.86 (t, J=5.6 Hz, 2H), 3.33-3.31 (m, 2H), 2.98 (s, 3H), 2.84 (s, 3H), 2.77 (t, J=5.6 Hz, 2H), 2.37-2.32 (m, 2H), 0.88 (t, J=7.2 Hz, 3H). LCMS: 531.3 [M+H]$^+$.

Example 44: Synthesis of (E)-4-((2-(4-((E)-1-(3-fluoro-1H-indazol-5-yl)-2-(3-fluoro phenyl)but-1-en-1-yl) phenoxy)ethyl)amino)-N,N-dimethylbut-2-enamide (Compound 44)

The compound was synthesized following the approach as outlined in Example 3 by substituting into Step-4 1-iodo-3-fluorobenzene for compound 227 to afford Compound 44 (0.010 g, 4%).

Compound 44:

^{1}H NMR (400 MHz, DMSO-d_6): δ 12.60 (s, 1H), 7.52 (s, 1H), 7.47 (d, J=8.8 Hz, 1H), 7.25-7.19 (m, 2H), 6.99-6.94 (m, 3H), 6.78 (d, J=8.8 Hz, 2H), 6.64 (d, J=8.8 Hz, 2H), 6.59 (t, J=5.2 Hz, 1H), 6.50 (d, J=15.2 Hz, 1H), 3.88 (d, J=5.6 Hz, 2H), 3.33-3.31 (m, 2H), 2.99 (s, 3H), 2.84 (s, 3H), 2.78 (t, J=5.2 Hz, 2H), 2.42-2.38 (m, 2H), 0.88 (t, J=7.6 Hz, 3H). LCMS: 531.3 [M+H$^+$].

Example 45: Synthesis of (E)-4-((2-(4-((E)-1-(3-fluoro-1H-indazol-5-yl)-2-(3-fluorophenyl)but-1-en-1-yl) phenoxy)ethyl)amino)-N,N-dimethylbut-2-enamide (Compound 45)

The compound was synthesized following the approach as outlined in Example 3 by substituting into Step-4 1-iodo-4-fluorobenzene for compound 227 to afford Compound 45 (0.008 g, 3.8%).

Compound 45:

^{1}H NMR (400 MHz, DMSO-d_6): δ 12.60 (s, 1H), 7.51 (s, 1H), 7.47 (dd, J_1=8.8 Hz, J_2=1.6 Hz, 1H), 7.21-7.19 (m, 3H), 7.18-7.02 (m, 2H), 6.75 (d, J=8.8 Hz, 2H), 6.64-6.58 (m, 3H), 6.51 (d, J=15.2 Hz, 1H), 3.88 (t, J=5.6 Hz, 2H), 3.31 (d, J=4.4 Hz, 2H), 2.99 (s, 3H), 2.84 (s, 3H), 2.78 (t, J=5.2 Hz, 2H), 2.39-2.37 (m, 2H), 0.87 (t, J=7.2 Hz, 3H). LCMS: 531.3 [M+H]$^+$.

Example 46: Synthesis of (E)-4-((2-(4-((E)-2-(2-chloro-4-fluorophenyl)-2-cyclobutyl-1-(3-fluoro-1H-indazol-5-yl)vinyl)phenoxy)ethyl)amino)-N,N-dimethylbut-2-enamide (Compound 46)

The compound was synthesized following the approach as outlined in Example 3 by (i) substituting into Step-3 (Z)-5-(2-cyclobutyl-1,2-bis(4,4,5,5-tetramethyl-1,3,2-dioxaborolan-2-yl)vinyl)-3-fluoro-1-(tetrahydro-2H-pyran-2-yl)-1H-indazole (as prepared in Example 14, Step-2) for compound 255 and (E)-tert-butyl (4-(dimethylamino)-4-oxobut-2-en-1-yl)(2-(4-iodophenoxy)ethyl)-carbamate (as prepared in Example 14, Step-3) for compound 256 and (ii) substituting into Step-4 2-chloro-4-fluoro-1-iodobenzene for compound 227 and (iii) continuing with Step-5 to afford Compound 46 (0.02 g, 10%).

Compound 46:

^{1}H NMR (400 MHz, DMSO-d_6): δ 12.6 (s, 1H), 7.49 (d, J=5.2 Hz 2H), 7.37-7.31 (m, 2H), 7.23 (d, J=8.8 Hz, 1H), 7.18-7.15 (m, 1H), 6.87 (d, J=8.8 Hz, 2H), 6.63-6.57 (m, 3H), 6.5 (d, J=15.2 Hz, 1H), 3.87 (t, J=5.6 Hz, 2H), 3.51 (s, 1H), 3.39-3.33 (m, 2H), 2.98 (s, 3H), 2.84 (s, 3H), 2.79 (t, J=5.4 Hz, 2H), 1.87-1.78 (m, 3H), 1.68-1.58 (m, 2H), 1.38-1.36 (m, 1H). LCMS: 591.2 [M+H]$^+$.

Example 47

There is no Example 47.

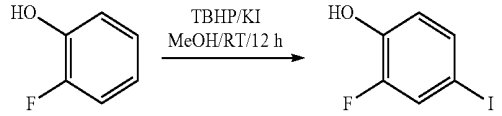
Example 48

There is no Example 48.

Example 49: Synthesis of (E)-4-((2-(2-fluoro-4-((Z)-1-(3-fluoro-1H-indazol-5-yl)-2-phenylbut-1-en-1-yl)phenoxy)ethyl)amino)-N,N-dimethylbut-2-enamide (Compound 49)

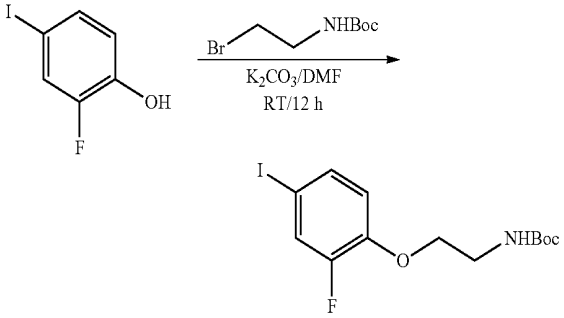
The compound was synthesized following the approach as outlined in Example 12 by substituting into Step-2 (Z)-2-(2-fluoro-4-(1-(3-fluoro-1H-indazol-5-yl)-2-phenylbut-1-en-1-yl)phenoxy)ethan-1-amine (preparation shown below in Ex. 49 Steps 1-3) for compound 253 and (E)-4-bromo-N,N-dimethylbut-2-enamide and (E)-4-chloro-N,N-dimethylbut-2-enamide mixture (preparation shown below in Ex. 49 Step 4) for compound 232 to afford Compound 49 (0.03 g, 7%).

Step-1: Synthesis of 2-fluoro-4-iodophenol



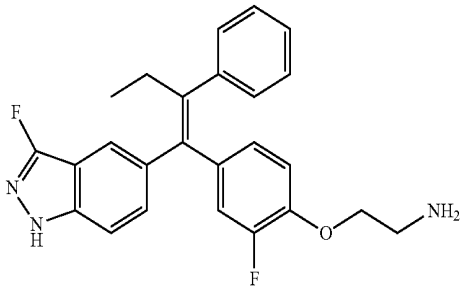
A mixture of 2-fluorophenol (5 g, 44 mmol) and potassium iodide (8.14 g, 49 mmol) in methanol (150 mL) was added tert-butyl hydroperoxide (6.43 mL, 66.9 mmol) and stirred at room temperature for 12 h. After completion of reaction, reaction mixture was quenched with sodium thiosulphate and extracted with EtOAc. Organic layer was washed water followed by brine, concentrated under reduced pressure to obtain the crude compound. Crude material was purified by column chromatography over 230-400 mesh silica gel using 15% EtOAc in n-hexane to give the title compound (5.7 g).

Step-2: Synthesis of tert-butyl (2-(2-fluoro-4-iodophenoxy)ethyl)carbamate



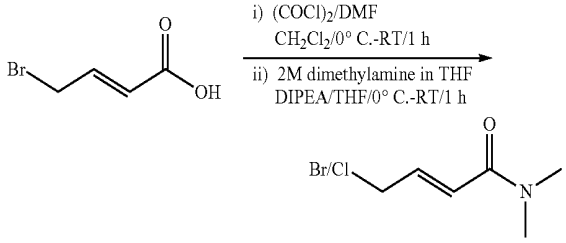
To a solution of 2-fluoro-4-iodophenol (4.6 g, 21 mmol) in DMF (40 mL) was added potassium carbonate (16 g, 116 mmol) and tert-butyl (2-bromoethyl)carbamate (8.62 g, 38.6 mmol). The reaction mixture was stirred at room temperature for 12 h. The reaction mixture was quenched with water and extracted with ethyl acetate (250 mL×2). The combined organic layers were washed with water, brine, dried over anhydrous sodium sulphate and concentrated under reduced pressure. The crude material was purified by column chromatography over 230-400 mesh silica gel using 30% ethyl acetate in n-hexane to afford tert-butyl (2-(2-fluoro-4-iodophenoxy)ethyl)carbamate (4.53 g, 61%).

Step-3: Synthesis of (Z)-2-(2-fluoro-4-(1-(3-fluoro-1H-indazol-5-yl)-2-phenylbut-1-en-1-yl)phenoxy) ethan-1-amine



The compound was synthesized following the approach as outlined in Example 3 by substituting tert-butyl (2-(2-fluoro-4-iodophenoxy)ethyl)carbamate for compound 256 in Step-3, and substituting iodobenzene for compound 227 in Step-4. The crude material was used in next step without further purification (2.1 g).

Step-4: Synthesis of (E)-4-bromo-N,N-dimethylbut-2-enamide and (E)-4-chloro-N,N-dimethylbut-2-enamide mixture



(~60:40/Br:Cl)

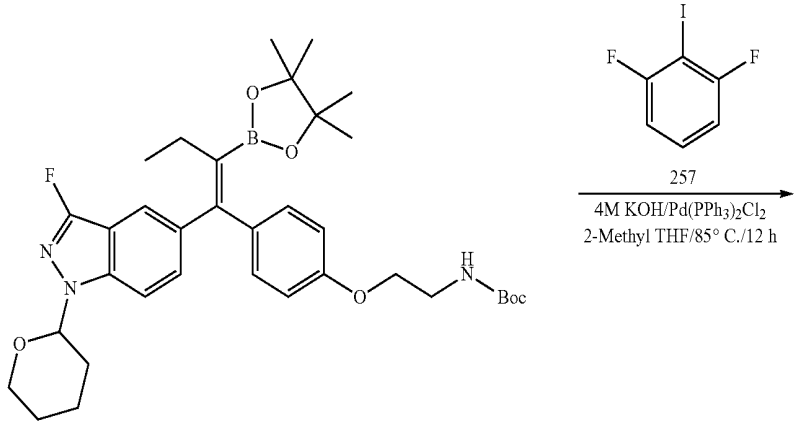
The reaction was carried out according to Scheme 4, Step-2 using (E)-4-bromobut-2-enoic acid (Example 1, Step-7.1) and dimethylamine to give crude material, which was purified by silica column chromatography to afford (E)-4-bromo-N,N-dimethylbut-2-enamide and (E)-4-chloro-N,N-dimethylbut-2-enamide mixture (~60:40/Br:Cl, 18 g, 51%) as a brown colour liquid. ^{1}H NMR (400 MHz, DMSO-d_6): δ 6.95-6.86 (m, 1H), 6.57-6.46 (m, 1H), 4.19-4.18 (m, 1H), 4.05-4.03 (m, 1H), 3.09-3.05 (m, 3H), 3.0-2.98 (m, 3H). LCMS: 194.0 and 148.1 $[M+H]^+$

Compound 49:

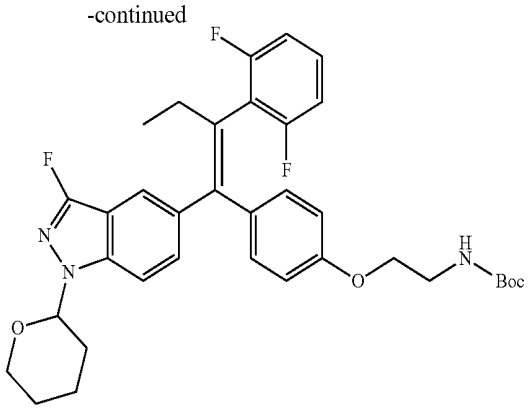
^{1}H NMR (400 MHz, DMSO-d_6): 12.59 (s, 1H), 7.54 (s, 1H), 7.48 (d, J=7.2 Hz, 1H), 7.25-7.22 (m, 3H), 7.17-7.15 (m, 3H), 6.84 (t, J=8.6 Hz, 1H), 6.64-6.47 (m, 4H), 3.94 (t, J=5.4 Hz, 2H), 3.31-3.20 (m, 2H), 2.98 (s, 3H), 2.84 (s, 3H), 2.79 (t, J=5.8 Hz, 2H), 2.41 (q, J=6.8 Hz, 2H), 0.86 (t, J=7.6 Hz, 3H). LCMS: 531.3 $[M+H]^+$

Example 50: Synthesis of (E)-4-((2-(4-((E)-2-(2,6-difluorophenyl)-1-(3-fluoro-1H-indazol-5-yl)but-1-en-1-yl)phenoxy)ethyl)amino)-N,N-dimethylbut-2-enamide (Compound 50)

Step-1: Synthesis of tert-butyl (E)-(2-(4-(2-(2,6-difluorophenyl)-1-(3-fluoro-1-(tetrahydro-2H-pyran-2-yl)-1H-indazol-5-yl)but-1-en-1-yl)phenoxy)ethyl) carbamate

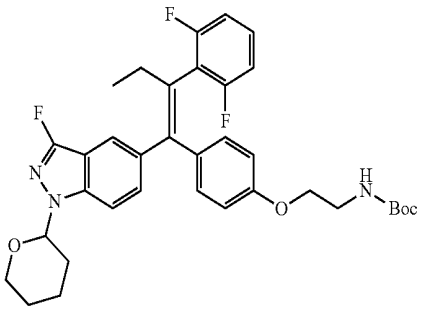


-continued



The reaction was carried out according to Scheme 1, Step-5, using tert-butyl (Z)-(2-(4-(1-(3-fluoro-1-(tetrahydro-2H-pyran-2-yl)-1H-indazol-5-yl)-2-(4,4,5,5-tetramethyl-1,3,2-dioxaborolan-2-yl)but-1-en-1-yl)phenoxy)ethyl)carbamate (2.79 g, 4.39 mmol, as prepared in Example 3, Step-3) for compound 208. The crude product was purified by silica gel chromatography using 5-15% EtOAc in n-hexane to give title compound of Ex. 50 Step-1 (2.1 g, 77.2%).

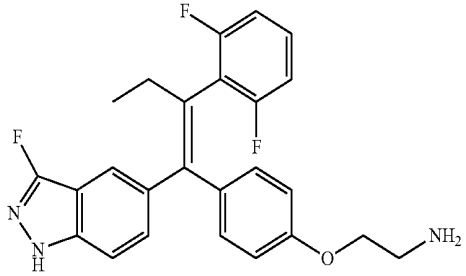
Step-2: Synthesis of (E)-2-(4-(2-(2,6-difluorophenyl)-1-(3-fluoro-1H-indazol-5-yl)but-1-en-1-yl)phenoxy)ethan-1-amine



261

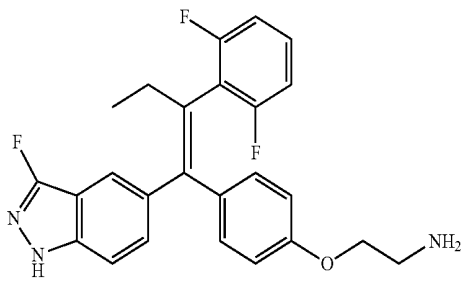
EtOH
2M HCl
diethyl ether
RT/12 h

-continued

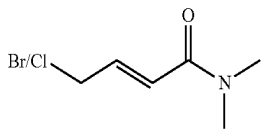


The reaction was carried out according to Scheme 2, Step-2b, using tert-butyl (E)-(2-(4-(2-(2,6-difluorophenyl)-1-(3-fluoro-1-(tetrahydro-2H-pyran-2-yl)-1H-indazol-5-yl)but-1-en-1-yl)phenoxy)ethyl)carbamate (2.1 g, 3.38 mmol, as prepared in Example 50, Step 1). The crude material was used in next step without further purification (1.2 g, crude).

Step-3: Synthesis of (E)-4-((2-(4-((E)-2-(2,6-difluorophenyl)-1-(3-fluoro-1H-indazol-5-yl)but-1-en-1-yl)phenoxy)ethyl)amino)-N,N-dimethylbut-2-enamide



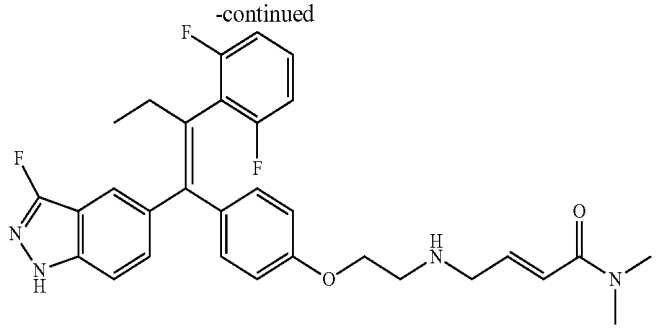
258



259

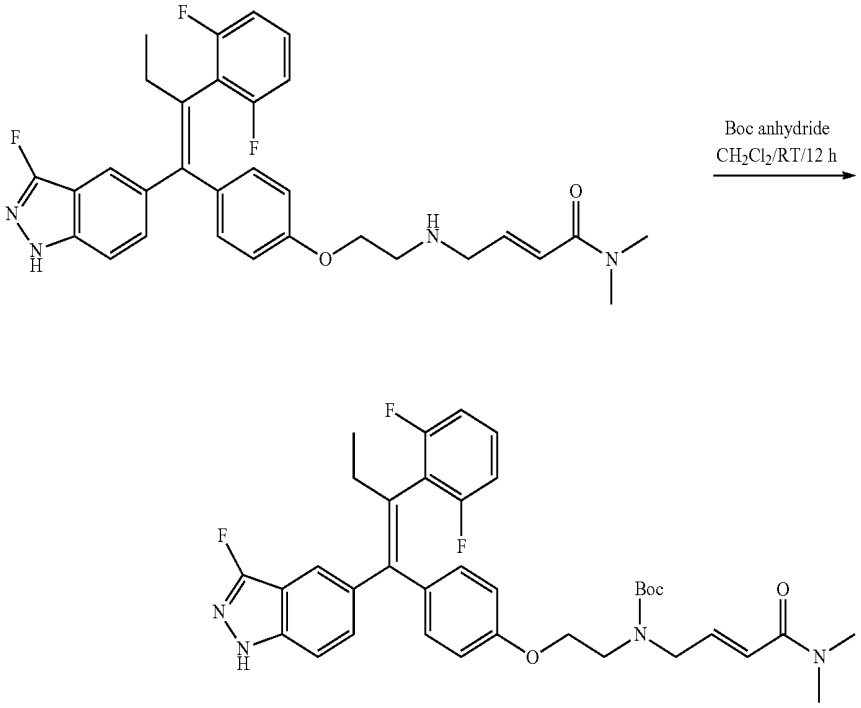
(~60:40)
DIPEA/IRA/RT/12 h

-continued



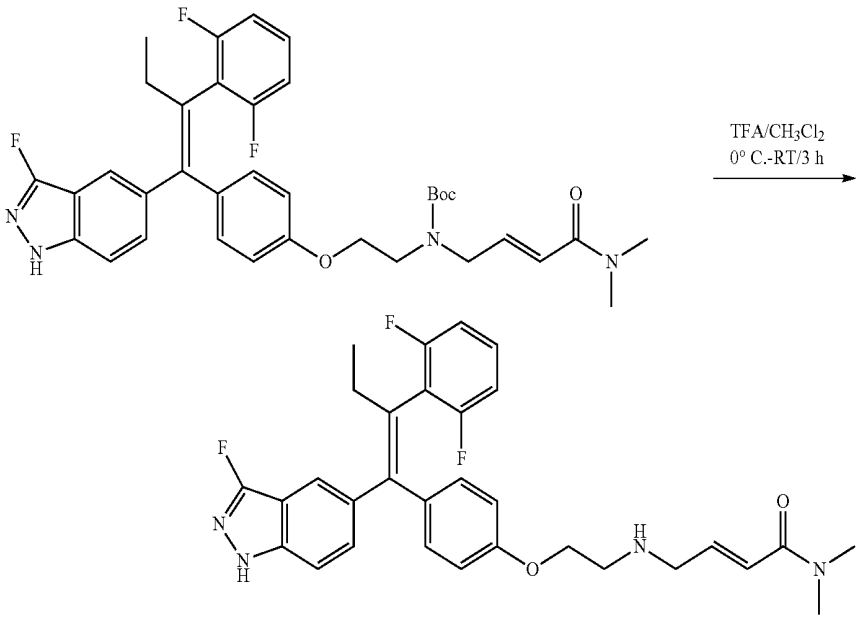
The reaction was carried out according to Scheme 2, Step-3b using (E)-2-(4-(2-(2,6-difluorophenyl)-1-(3-fluoro-1H-indazol-5-yl)but-1-en-1-yl)phenoxy)ethan-1-amine (1.2 g, 2.7 mmol) and (E)-4-bromo-N,N-dimethylbut-2-enamide for compound 213 and (E)-4-chloro-N,N-dimethylbut-2-enamide mixture (as prepared in Example 49, Step-4) for compound 214 to obtain crude product, which was used in next step without further purification (1.15 g, crude).

Step-4: Synthesis of tert-butyl (2-(4-((E)-2-(2,6-difluorophenyl)-1-(3-fluoro-1H-indazol-5-yl)but-1-en-1-yl)phenoxy)ethyl)((E)-4-(dimethylamino)-4-oxobut-2-en-1-yl)carbamate



The reaction was carried out according to Scheme 2, Step-5 using (E)-4-((2-(4-((E)-2-(2,6-difluorophenyl)-1-(3-fluoro-1H-indazol-5-yl)but-1-en-1-yl)phenoxy)ethyl) amino)-N,N-dimethylbut-2-enamide (1.15 g, 2.13 mmol) for compound 215. Crude material was purified by column chromatography over 230-400 mesh silica gel using (2.5%) MeOH in dichloromethane to obtain the title compound of Ex. 50 Step-4 (0.3 g, 22.2%).-

Step-5: Synthesis of (E)-4-((2-(4-((E)-2-(2,6-difluorophenyl)-1-(3-fluoro-1H-indazol-5-yl)but-1-en-1-yl)phenoxy)ethyl)amino)-N,N-dimethylbut-2-enamide



The reaction was carried out according to Scheme 2, Step-6b, using tert-butyl (2-(4-((E)-2-(2,6-difluorophenyl)-1-(3-fluoro-1H-indazol-5-yl)but-1-en-1-yl)phenoxy)ethyl) ((E)-4-(dimethylamino)-4-oxobut-2-en-1-yl)carbamate (0.3 g, 0.462 mmol) for compound 211c. Crude compound was purified by preparative HPLC to afford Compound 50 (0.065 g, 25.6%).

Compound 50:

^{1}H NMR (400 MHz, DMSO-d_6): δ 12.60 (s, 1H), 7.52 (s, 1H), 7.49 (dd, J_1=8.8 Hz, J_2=1.2 Hz, 1H), 7.23-7.12 (m, 1H), 7.11-7.02 (m, 3H), 6.83 (d, J=8.4 Hz, 2H), 6.65 (d, J=8.4 Hz, 2H), 6.62-6.48 (m, 2H), 3.88 (t, J=5.6 Hz, 2H), 3.32-3.31 (m, 2H), 2.99 (s, 3H), 2.84 (s, 3H), 2.79 (t, J=5.4 Hz, 2H), 2.35 (q, J=7.0 Hz, 2H), 0.91 (t, J=7.4 Hz, 3H). LCMS: 549.3 $[M+H]^+$

Example 51: Synthesis of (E)-4-((2-(4-((E)-1-(3-fluoro-1H-indazol-5-yl)-2-(pyridin-3-yl)but-1-en-1-yl)phenoxy)ethyl)amino)-N,N-dimethylbut-2-enamide (Compound 51)

The compound was synthesized following the approach as outlined in Example 50 by substituting into Step-1 3-iodopyridine for compound 257 to afford Compound 51 (0.02 g, 10%).

Compound 51:

^{1}H NMR (400 MHz, DMSO-d_6): δ 12.59 (s, 1H), 8.31-8.30 (m, 1H), 8.26 (d, J=2 Hz, 1H), 7.62 (dd, J_1=6.0 Hz, J_2=2.0 Hz, 1H), 7.54 (s, 1H), 7.48 (dd, J_1=8.0 Hz, J_2=2.0 Hz, 1H), 7.28-7.24 (m, 1H), 7.22 (dd, J=8.8 Hz, J_2=1.2 Hz, 1H), 6.79-6.77 (m, 2H), 6.65-6.60 (m, 3H), 6.58-6.48 (m, 1H), 3.89 (t, J=5.4 Hz, 2H), 3.32-3.31 (m, 2H), 2.99 (s, 3H), 2.84 (s, 3H), 2.79 (t, J=5.4 Hz, 2H), 2.42 (q, J=7.4 Hz, 2H), 0.88 (t, J=7.4 Hz, 3H). LCMS: 514.3 $[M+H]^+$

Example 52: Synthesis of (E)-4-((2-(4-((E)-1-(3-fluoro-1H-indazol-5-yl)-2-(pyridin-4-yl)but-1-en-1-yl)phenoxy)ethyl)amino)-N,N-dimethylbut-2-enamide (Compound 52)

The compound was synthesized following the approach as outlined in Example 50 by substituting into Step-1 4-iodopyridine for compound 257 to afford the title Compound 52 (0.05 g, 19.9%).

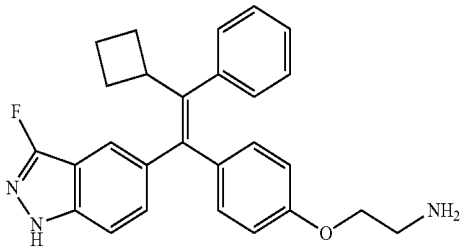
Compound 52:

^{1}H NMR (400 MHz, DMS-d_6): δ 12.60 (s, 1H), 8.39-8.37 (m, 2H), 7.53 (s, 1H), 7.50-7.47 (m, 1H), 7.21 (dd, J_1=8.6 Hz, J_2=1.4 Hz, 1H), 7.14-7.13 (m, 2H), 6.80-6.78 (m, 2H), 6.66-6.60 (m, 2H), 6.59-6.48 (m, 2H), 3.89 (t, J=5.4 Hz, 2H), 3.33-3.31 (m, 2H), 2.99 (s, 3H), 2.84 (s, 3H), 2.79 (t, J=5.8 Hz, 2H), 2.42 (q, J=7.4 Hz, 2H), 0.87 (t, J=7.2 Hz, 3H). LCMS: 514.3 $[M+H]^+$

Example 53: Synthesis of (E)-4-((2-(4-((E)-2-cyclobutyl-1-(3-fluoro-1H-indazol-5-yl)-2-phenylvinyl)phenoxy)ethyl)amino)-N-(2-hydroxyethyl)-N-methylbut-2-enamide (Compound 53)

The compound was synthesized following the approach as outlined in Example 50 by substituting into Step-3 (E)-2-(4-(2-cyclobutyl-1-(3-fluoro-1H-indazol-5-yl)-2-phenylvinyl)phenoxy)ethan-1-amine (preparation shown below in Ex. 53 Step-1) for compound 258 and (E)-4-bromo-N-(2-hydroxyethyl)-N-methylbut-2-enamide (as prepared in Example 18, Step-1) for compound 259 to afford Compound 53 (0.011 g, 5%).

Step-1: Synthesis of (E)-2-(4-(2-cyclobutyl-1-(3-fluoro-1H-indazol-5-yl)-2-phenylvinyl)phenoxy) ethan-1-amine



The compound was synthesized following the approach as outlined in Example 3 substituting tert-butyl (Z)-(2-(4-(2-cyclobutyl-1-(1-(tetrahydro-2H-pyran-2-yl)-1H-indazol-5-yl)-2-(4,4,5,5-tetramethyl-1,3,2-dioxaborolan-2-yl)vinyl) phenoxy)-ethyl)carbamate (as prepared in Example 13, Step-5) for compound 226 and iodobenzene for compound 227 in Step-4 and following Step-5 to deliver the title compound (0.85, crude).

Compound 53:

^{1}H NMR (400 MHz, DMSO-d_6): δ 12.56 (s, 1H), 7.48 (s, 2H), 7.46-7.23 (m, 4H), 7.21 (dd, J1=8.8 Hz, J_2=1.6 Hz, 2H), 6.80-6.78 (m, 2H), 6.60-6.47 (m, 4H), 4.77-4.64 (m, 1H), 3.85 (t, J=5.2 Hz, 2H), 3.51-3.41 (m, 2H), 3.39-3.34 (m, 4H), 3.03 (s, 1H), 2.86 (s, 2H), 2.80-2.79 (m, 2H), 1.82-1.76 (m, 4H), 1.57-1.55 (m, 1H), 1.35-1.32 (m, 1H). LCMS: 569.3 $[M+H]^+$

Example 54: Synthesis of (E)-4-((2-(4-((E)-1-(1H-indazol-5-yl)-2-phenylprop-1-en-1-yl)phenoxy) ethyl)amino)-N,N-dimethylbut-2-enamide (Compound 54)

The title compound was synthesized following the approach as outlined in Example 1. Without wishing to be bound by theory, it is believed that Compound 54 resulted due to inclusion of methyl iodide in the ethyl iodide used in Step-2 of Example 1.

Compound 54:

^{1}H NMR (400 MHz, DMSO-d_6): δ 13.05 (s, 1H), 8.05 (s, 1H), 7.6 (s, 1H), 7.50 (d, J=8.4 Hz, 1H), 7.21-7.09 (m, 6H), 6.75 (d, J=8.8 Hz, 2H), 6.62-6.48 (m, 4H), 3.88 (t, J=5.2 Hz, 2H), 3.31 (d, J=4.8 Hz, 2H), 2.99 (s, 3H), 2.84 (s, 3H), 2.79-2.77 (m, 2H), 2.07 (s, 3H). LCMS: 481.3 $[M+H]^+$

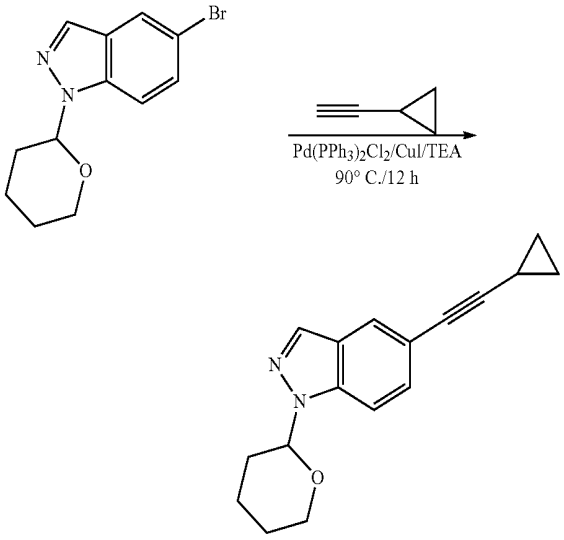
Example 55

There is no Example 55.

Example 56: Synthesis of (E)-4-((2-(4-((E)-2-cyclopropyl-1-(1H-indazol-5-yl)-2-phenylvinyl)phenoxy) ethyl)amino)-N,N-dimethylbut-2-enamide (Compound 56)

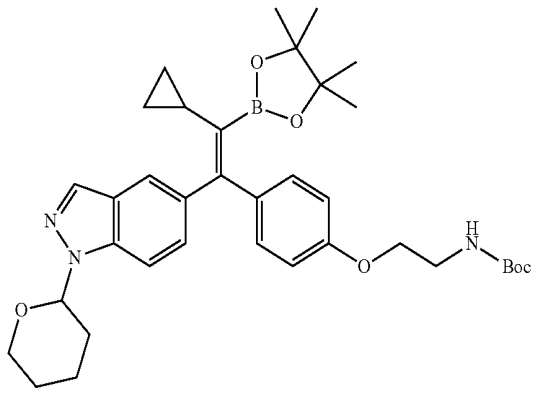
The compound was synthesized following the approach as outlined in Example 50 by substituting into Step-1 tert-butyl (Z)-(2-(4-(2-cyclopropyl-1-(1-(tetrahydro-2H-pyran-2-yl)-1H-indazol-5-yl)-2-(4,4,5,5-tetramethyl-1,3,2-dioxaborolan-2-yl)vinyl)phenoxy)ethyl)carbamate (preparation shown below in Step 1-2) for compound 260 and iodobenzene for compound 257 to afford Compound 56 (0.12 g).

Step-1: Synthesis of 5-(cyclopropylethynyl)-1-(tetrahydro-2H-pyran-2-yl)-1H-indazole



The reaction was carried out according to Scheme 1, Step-2 substituting 5-bromo-1-(tetrahydro-2H-pyran-2-yl)-1H-indazole (5.5 g, 19.57 mmol) in 88 mL of triethyl amine and ethynylcyclopropane (2.5 g, 39.14 mmol) and heated at 90° C. for 12 h. Upon completion by TLC, the reaction mixture was quenched with water (10 mL) and extracted with ethyl acetate (2×50 mL). The combined organic extracts were washed with water, brine, dried over sodium sulphate and concentrated. The crude product was purified over 230-400 mesh silica column chromatography using 5% ethyl acetate in n-hexane to afford 5-(cyclopropylethynyl)-1-(tetrahydro-2H-pyran-2-yl)-1H-indazole (4.5 g, 86%).

Step-2: Synthesis of tert-butyl (Z)-(2-(4-(2-cyclopropyl-1-(1-(tetrahydro-2H-pyran-2-yl)-1H-indazol-5-yl)-2-(4,4,5,5-tetramethyl-1,3,2-dioxaborolan-2-yl) vinyl)phenoxy)ethyl)carbamate



The compound was synthesized following the approach as outlined in Example 3 by substituting into Step-1 5-(cyclopropylethynyl)-1-(tetrahydro-2H-pyran-2-yl)-1H-indazole for compound 252, and continuing with Steps 2-3 to afford the crude material containing the title compound of Ex. 56 Step-2, which was used in next step without further purification (6 g, crude).

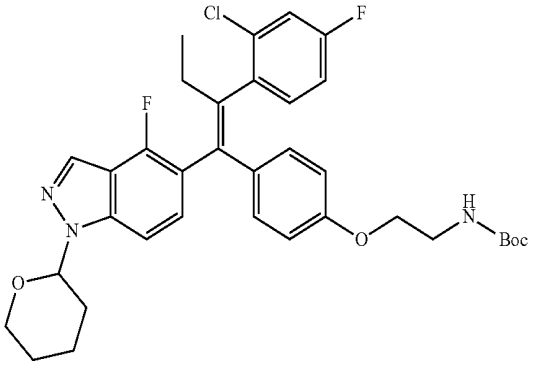
Compound 56:

^{1}H NMR (400 MHz, DMSO-d_6): δ 13.04 (s, 1H), 8.06 (s, 1H), 7.73 (s, 1H), 7.51 (d, J=8.8 Hz, 1H), 7.27 (d, J=8.4 Hz, 1H), 7.21-7.04 (m, 5H), 6.72 (d, J=8.4 Hz, 2H), 6.61-6.46 (m, 4H), 3.83 (t, J=5.6 Hz, 2H), 3.31-3.29 (m, 2H), 2.98 (s, 3H), 2.83 (s, 3H), 2.75 (t, J=5.2 Hz, 2H), 2.0-2.30 (m, 1H), 1.74-1.71 (m, 1H), 0.58-0.56 (m, 2H), 0.21-0.20 (m, 2H). LCMS: 507.4 $[M+H]^+$

Example 57: Synthesis of (E)-4-((2-(4-((E)-2-(2-chloro-4-fluorophenyl)-1-(4-fluoro-1H-indazol-5-yl) but-1-en-1-yl)phenoxy)ethyl)amino)-N,N-dimethyl-but-2-enamide (Compound 57)

The compound was synthesized following the approach as outlined in Example 50 by substituting into Step-2 tert-butyl (E)-(2-(4-(2-(2-chloro-4-fluorophenyl)-1-(4-fluoro-1-(tetrahydro-2H-pyran-2-yl)-1H-indazol-5-yl)but-1-en-1-yl)phenoxy)ethyl)carbamate (preparation shown below in Step-1) for compound 261 to afford Compound 57 (0.04 g, 15.7%).

Step-1: Synthesis of tert-butyl (E)-(2-(4-(2-(2-chloro-4-fluorophenyl)-1-(4-fluoro-1-(tetrahydro-2H-pyran-2-yl)-1H-indazol-5-yl)but-1-en-1-yl)phenoxy)ethyl)carbamate



The compound was synthesized following the approach as outlined in Example 3 by substituting 5-(but-1-yn-1-yl)-4-fluoro-1-(tetrahydro-2H-pyran-2-yl)-1H-indazole (Example 4, Step-4) for compound 252 in Step-1, proceeding directly to Step-3, and substituting 2-chloro-4-fluoro-1-iodobenzene for compound 227 in Step-4 to afford the title compound of this step. The crude product was purified by silica gel column chromatography, eluting with 2% MeOH in dichloromethane to afford the title compound (1.3 g, 16%).

Compound 57:

^{1}H NMR (400 MHz, DMSO-d_6): δ 13.42 (s, 1H), 8.18 (s, 1H), 7.42 (d, J=6.4 Hz, 1H), 7.36 (dd, J_1=7.2 Hz, J_2=2.0 Hz, 1H), 7.31 (dd, J_1=6.8 Hz, J_2=5.2 Hz, 1H), 7.25-7.22 (m, 1H), 7.14 (dt, J_1=6.8 Hz, J_2=5.2 Hz, 1H), 6.84 (d, J=7.2 Hz, 2H), 6.63 (d, J=7.2 Hz, 2H), 6.61-6.57 (m, 1H), 6.49 (d, J=12.4 Hz, 1H), 3.87 (t, J=4.4 Hz, 2H), 3.33-3.31 (m, 2H), 2.97 (s, 3H), 2.84 (s, 3H), 2.78 (t, J=4.4 Hz, 2H), 2.30-2.25 (m, 2H), 0.82 (t, J=6.2 Hz, 3H). LCMS: 565.3 $[M+H]^+$

Example 58: Synthesis of (E)-4-((2-((5-((Z)-2-(2-chloro-4-fluorophenyl)-1-(3-fluoro-1H-indazol-5-yl) but-1-en-1-yl)pyridin-2-yl)oxy)ethyl)amino)-N,N-dimethylbut-2-enamide (Compound 58)

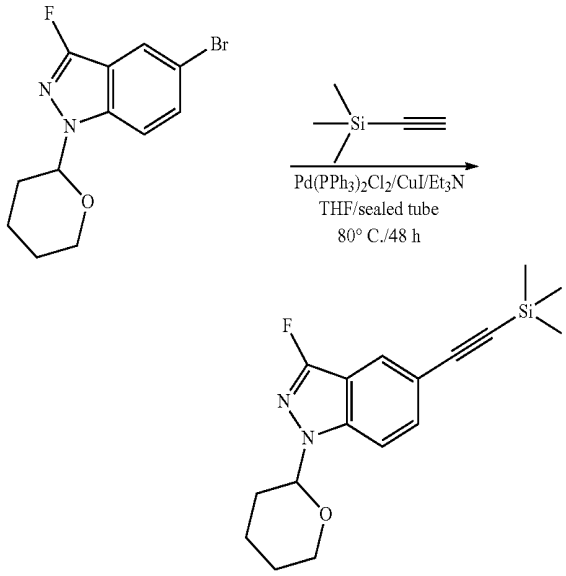
The compound was synthesized following the approach as outlined in Example 14 by substituting into Step-4 (i) (Z)-5-(1,2-bis(4,4,5,5-tetramethyl-1,3,2-dioxaborolan-2-yl) but-1-en-1-yl)-3-fluoro-1-(tetrahydro-2H-pyran-2-yl)-1H-indazole (as prepared in Example 3, Step-1) for compound 233, (ii) tert-butyl (E)-(4-(dimethylamino)-4-oxobut-2-en-1-yl)(2-((5-iodopyridin-2-yl)oxy)ethyl)carbamate (as prepared in Example 25, Step-2) for compound 234, and (iii) 2-chloro-4-fluoro-1-iodobenzene for compound 262 to deliver Compound 58 (0.115 g, 10%).

Compound 58:

^{1}H NMR (400 MHz, DMSO-d_6): δ 12.63 (s, 1H), 7.69 (d, J=2.0 Hz, 1H), 7.59 (s, 1H), 7.51 (dd, J_1=8.6 Hz, J_2=1.8 Hz, 1H), 7.43-7.35 (m, 2H), 7.29 (d, J=1.4 Hz, 1H), 7.27-7.15 (m, 2H), 6.62-6.47 (m, 3H), 4.14 (t, J=5.9 Hz, 2H), 2.93 (s, 3H), 2.84 (s, 3H), 2.78 (t, J=5.8 Hz, 2H), 2.37 (q, J=7.3 Hz, 2H), 0.89 (t, J=7.3 Hz, 3H). LCMS: 566.3 $[M+H]^+$.

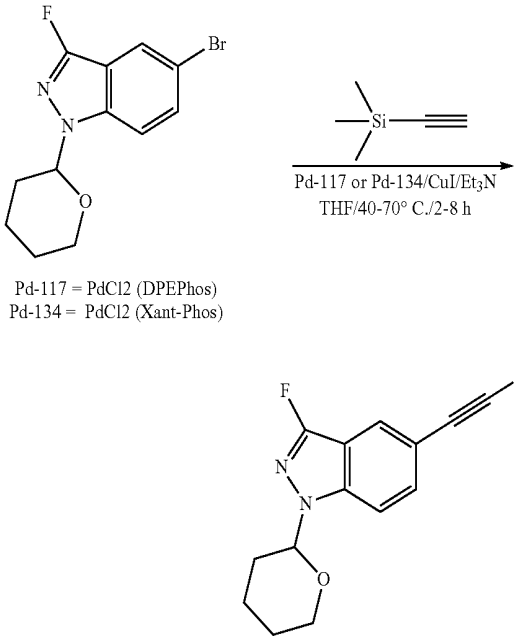
Example 59: Synthesis of (E)-4-((2-((5-((Z)-2-(2-chloro-4-fluorophenyl)-4,4,4-trifluoro-1-(3-fluoro-1H-indazol-5-yl)but-1-en-1-yl)pyridin-2-yl)oxy) ethyl)amino)-N,N-dimethylbut-2-enamide (Compound 59)

Step-1: Synthesis of 3-fluoro-1-(tetrahydro-2H-pyran-2-yl)-5-((trimethylsilyl)ethynyl)-1H-indazole



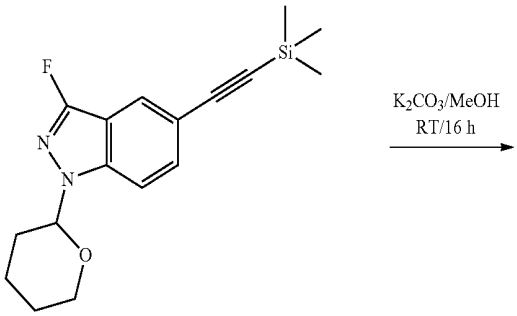
To a stirred solution of 5-bromo-3-fluoro-1-(tetrahydro-2H-pyran-2-yl)-1H-indazole (4.5 g, 15 mmol, as prepared in Example 2, Step-2) in 35 mL of THF:Et_3N (5:1) in a sealed tube, were added copper iodide (0.288 g, 1.5 mmol) at room temperature. This mixture was degassed with three vacuum/N_2 cycles, and were added ethynyltrimethylsilane (2.22 g, 22 mmol) followed by $Pd(PPh_3)_2Cl_2$ (0.5 g, 0.7 mmol). The pressure tube was sealed and heated at 80° C. for 48 h. Upon completion by TLC, the reaction mixture was diluted with water (250 mL) and extracted with EtOAc (2×100 mL). The combined organic extracts were washed with water, brine, dried over anhydrous sodium sulphate and concentrated under reduced pressure. The crude product was purified by combo-flash using 5% EtOAc in n-hexane to afford 3-fluoro-1-(tetrahydro-2H-pyran-2-yl)-5-((trimethylsilyl) ethynyl)-1H-indazole (3.2 g, 72%).

Step-1A: Alternative Synthesis of 3-fluoro-1-(tetrahydro-2H-pyran-2-yl)-5-((trimethylsilyl)ethynyl)-1H-indazole

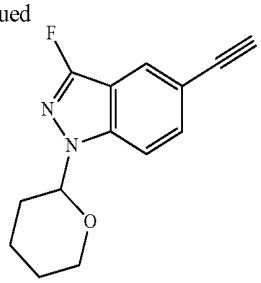


Step-1A presents a proposed alternative to Step-1 of Example 59, for the possible preparation of 3-fluoro-1-(tetrahydro-2H-pyran-2-yl)-5-((trimethylsilyl)ethynyl)-1H-indazole, which may be used as intermediate for further synthetic routes that include that compound. To a stirred solution of 5-bromo-3-fluoro-1-(tetrahydro-2H-pyran-2-yl)-1H-indazole (5 g, 16.71 mmol) in 30 mL of 2-Methyl THF(6V) in a 100 ml RBF, were added triethylamine (5.07 g, 50 mmol), copper iodide (0.16 g, 0.84 mmol) at room temperature. This mixture was degassed with three vacuum/N_2 cycles, and were added ethynyltrimethylsilane (4.10 g, 41.74 mmol) followed by Pd-134 (0.31 g, 0.41 mmol) or Pd-117. The reaction mixture heated at 40° C.-75° C. for 3-8 h. Upon completion by TLC, the reaction mixture was filtered through celite bed and washed with 30 ml 2-Methyl THF. Filtrate washed with brine and concentrated under reduced pressure to afford 3-fluoro-1-(tetrahydro-2H-pyran-2-yl)-5-((trimethylsilyl)ethynyl)-1H-indazole crude (6.1 g) and used for next stage as considering 100% yield.

Step-2: Synthesis of 5-ethynyl-3-fluoro-1-(tetrahydro-2H-pyran-2-yl)-1H-indazole

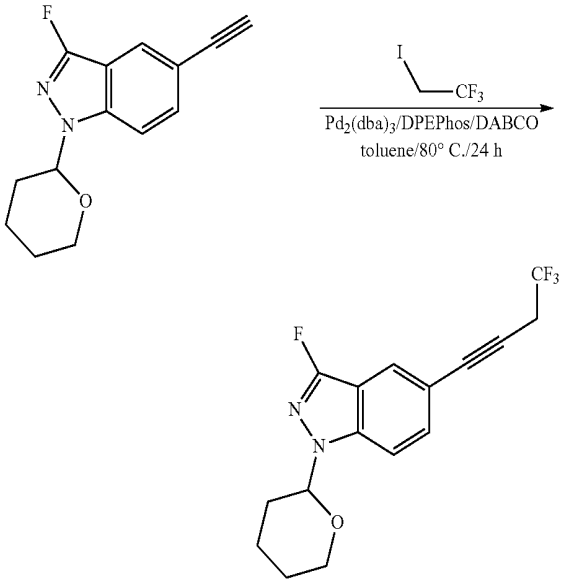


-continued



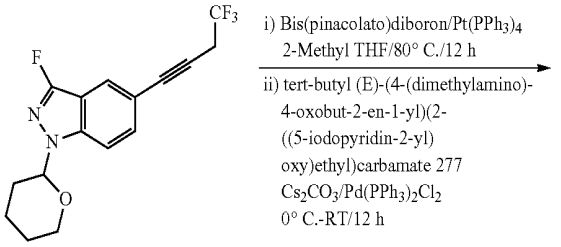
To a stirred solution of 3-fluoro-1-(tetrahydro-2H-pyran-2-yl)-5-((trimethylsilyl)ethynyl)-1H-indazole (3.2 g, 10 mmol) in methanol 32 mL was added potassium carbonate (0.151 g, mmol), reaction mixture was stirred for 16 h at room temperature. After completion of reaction, reaction mixture was diluted with ethyl acetate and the organic layer was washed with water followed by brine. The organic layer was dried over anhydrous Na_2SO_4 and concentrated under reduced pressure to obtain title compound of Ex. 59 Step-2 (2.8 g, crude).

Step-3: Synthesis of 3-fluoro-1-(tetrahydro-2H-pyran-2-yl)-5-(4,4,4-trifluorobut-1-yn-1-yl)-1H-indazole

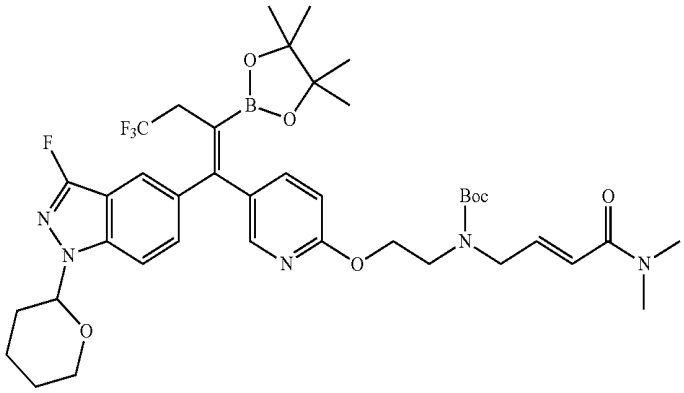


To a stirred solution of 5-ethynyl-3-fluoro-1-(tetrahydro-2H-pyran-2-yl)-1H-indazole (2.6 g, 10.6 mmol) in 20 mL of toluene, were added 1,1,1-trifluoro-2-iodoethane (4.47 g, 21.3 mmol) at room temperature. This mixture was degassed with three vacuum/N_2 cycles, and were added $Pd_2(dba)_3$ (0.487 g, 0.5 mmol) followed by DPEphos (1.14 g, 2.1 mmol) and DABCO (2.39 g, 21.3 mmol). Reaction mixture was heated at 80° C. for 24 h. Upon completion by TLC, the reaction mixture was diluted with water (250 mL) and extracted with EtOAc (2×100 mL). The combined organic extracts were washed with water, brine, dried over anhydrous sodium sulphate and concentrated under reduced pressure. The crude product was purified by column chromatography using 5% EtOAc in n-hexane to afford 3-fluoro-1-(tetrahydro-2H-pyran-2-yl)-5-(4,4,4-trifluorobut-1-yn-1-yl)-1H-indazole (1.6 g, 46%).

Step-4: Synthesis of tert-butyl ((E)-4-(dimethylamino)-4-oxobut-2-en-1-yl)(2-((5-((E)-4,4,4-trifluoro-1-(3-fluoro-1-(tetrahydro-2H-pyran-2-yl)-1H-indazol-5-yl)-2-(4,4,5,5-tetramethyl-1,3,2-dioxaborolan-2-yl)but-1-en-1-yl)pyridin-2-yl)oxy)ethyl)carbamate

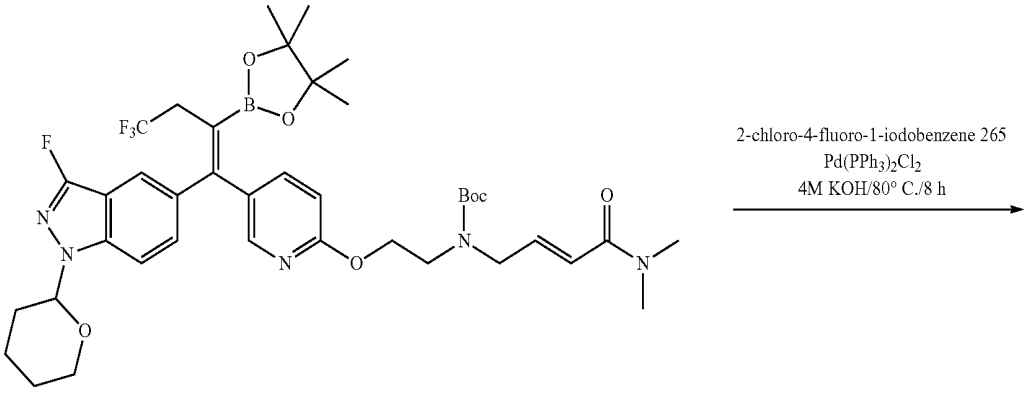


276



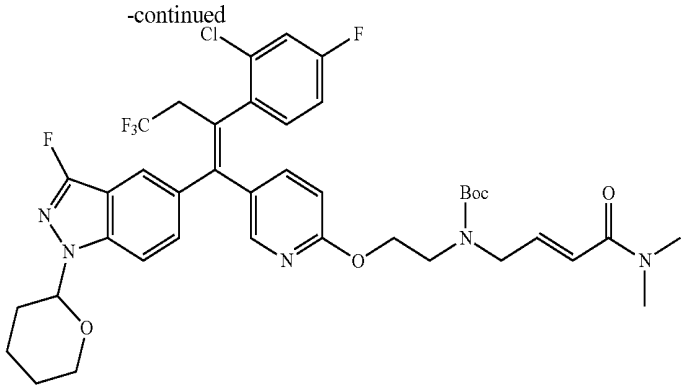
To a stirred solution of 3-fluoro-1-(tetrahydro-2H-pyran-2-yl)-5-(4,4,4-trifluorobut-1-yn-1-yl)-1H-indazole (1 g, 3.06 mmol) in 2-methyl THF (20 mL), was added bis(pinacolato) diboron (0.934 g, 3.68 mmol), tetrakis(triphenylphosphine) platinum (0) (0.026 g, 0.02 mmol) under nitrogen atmosphere, reaction mixture was stirred at 80° C. for 12 h. The solution was allowed to cool to room temperature and tert-butyl (E)-(4-(dimethylamino)-4-oxobut-2-en-1-yl)(2-((5-iodopyridin-2-yl)oxy)ethyl)carbamate (1.12 g, 2.37 mmol), bis(triphenylphosphine)palladium (II) dichloride (0.092 g, 0.13 mmol), cesium carbonate (1.7 g, 5.26 mmol) and 2-methyl THF (20 mL) were added. This mixture was degassed with nitrogen and water (0.3 mL) was added. This mixture was stirred at room temperature for 12 h. After completion of reaction, reaction mixture was diluted with water followed by extracted with ethyl acetate, organic layer was dried over anhydrous sodium sulphate and concentrated under reduced pressure to afford the crude compound. Crude compound was purified by combi-flash using 3% MeOH in dichloromethane to afford the title compound of Ex. 59 Step-4 (1.2 g).

Step-5: Synthesis of tert-butyl (2-((5-((Z)-2-(2-chloro-4-fluorophenyl)-4,4,4-trifluoro-1-(3-fluoro-1-(tetrahydro-2H-pyran-2-yl)-1H-indazol-5-yl)but-1-en-1-yl)pyridin-2-yl)oxy)ethyl)((E)-4-(dimethylamino)-4-oxobut-2-en-1-yl)carbamate



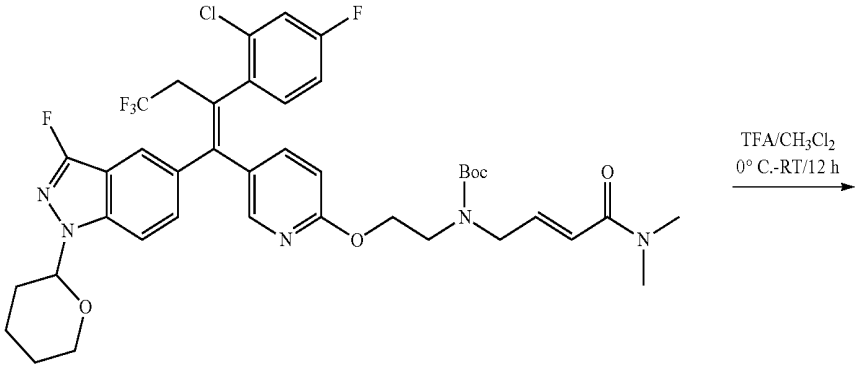
278

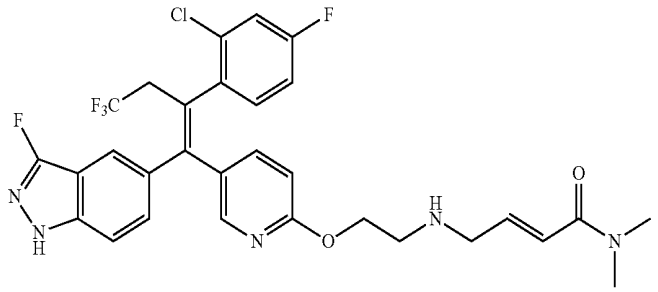
-continued



The reaction was carried out according to Scheme 1, Step-5 using tert-butyl ((E)-4-(dimethylamino)-4-oxobut-2-en-1-yl)(2-((5-((E)-4,4,4-trifluoro-1-(3-fluoro-1-(tetrahydro-2H-pyran-2-yl)-1H-indazol-5-yl)-2-(4,4,5,5-tetramethyl-1,3,2-dioxaborolan-2-yl)but-1-en-1-yl)pyridin-2-yl)oxy)ethyl)carbamate (1.2 g, 1.49 mmol) for compound 208 in 2-m and 2-chloro-4-fluoro-1-iodobenzene (0.383 g, 1.49 mmol) for compound 209. Reaction mixture was stirred at 80° C. for 8 h. The crude material was purified by combiflash using 3% MeOH in dichloromethane to afford the title compound of Ex. 59 Step-5 (0.92 g, 76%).

Step-6: Synthesis of (E)-4-((2-((5-((Z)-2-(2-chloro-4-fluorophenyl)-4,4,4-trifluoro-1-(3-fluoro-1H-indazol-5-yl)but-1-en-1-yl)pyridin-2-yl)oxy)ethyl)amino)-N,N-dimethylbut-2-enamide





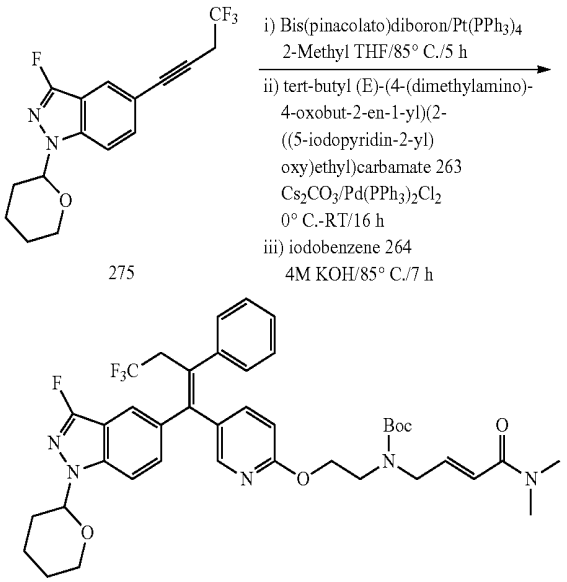
The reaction was carried out according to Scheme 2, Step-6b using tert-butyl (2-((5-((Z)-2-(2-chloro-4-fluorophenyl)-4,4,4-trifluoro-1-(3-fluoro-1-(tetrahydro-2H-pyran-2-yl)-1H-indazol-5-yl)but-1-en-1-yl)pyridin-2-yl)oxy)ethyl)((E)-4-(dimethylamino)-4-oxobut-2-en-1-yl)carbamate (0.92 g, 1.14 mmol) for compound 211c to afford crude compound, which was purified by preparative HPLC to afford Compound 59 (0.27 g, 38%) as a free base.

Compound 59:

^{1}H NMR (400 MHz, DMSO-d_6): δ 12.71 (s, 1H), 7.71 (d, J=2 Hz, 2H), 7.65 (m, 2H), 7.57-7.52 (m, 2H), 7.37 (dd, J_1=8.8 Hz, J_2=2.4 Hz, 1H), 7.28-7.19 (m, 3H), 6.62-6.46 (m, 3H), 4.15 (t, J=4.1 Hz, 2H), 3.54-3.40 (m, 2H), 3.37-3.28 (m, 2H), 2.98 (s, 3H), 2.84 (s, 3H), 2.76 (t, J=4.1 Hz, 2H). LCMS: 620.2 $[M+H]^+$.

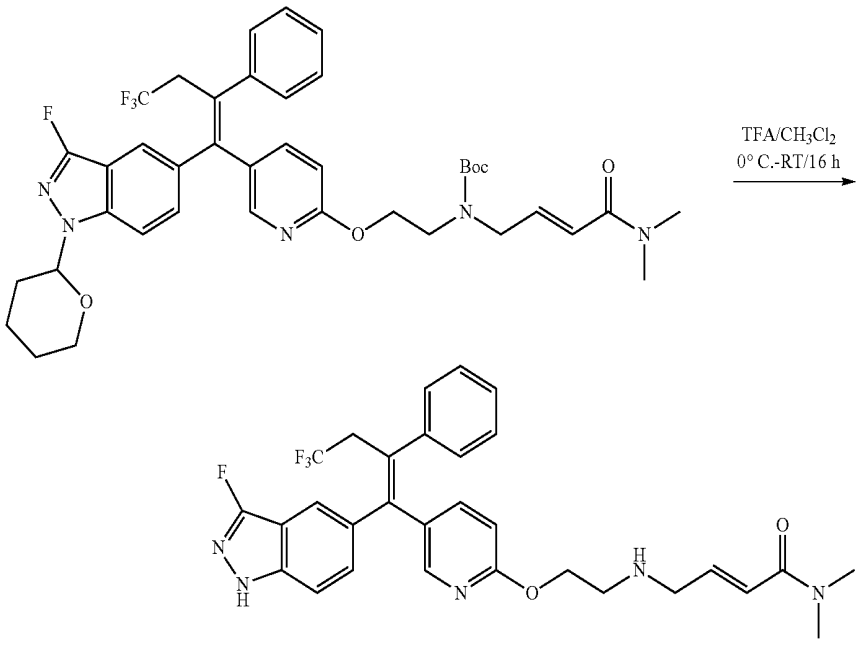
Example 60: Synthesis of (E)-N,N-dimethyl-4-((2-((5-((Z)-4,4,4-trifluoro-1-(3-fluoro-1H-indazol-5-yl)-2-phenylbut-1-en-1-yl)pyridin-2-yl)oxy)ethyl)amino)but-2-enamide (Compound 60)

Step-1: Synthesis of tert-butyl ((E)-4-(dimethylamino)-4-oxobut-2-en-1-yl)(2-((5-((Z)-4,4,4-trifluoro-1-(3-fluoro-1-(tetrahydro-2H-pyran-2-yl)-1H-indazol-5-yl)-2-phenylbut-1-en-1-yl)pyridin-2-yl)oxy)ethyl)carbamate



2.02 mmol, prepared as outlined in Example 59, Step-1 through Step-3) in 2-methyl THF (10 mL), was added bis(pinacolato)diboron (0.566 g, 2.22 mmol), tetrakis(triphenylphosphine)platinum (0) (0.025 g, 0.02 mmol) under nitrogen atmosphere, reaction mixture was stirred at 85° C. for 5 h. The solution was allowed to cool to room temperature and tert-butyl (E)-(4-(dimethylamino)-4-oxobut-2-en-1-yl)(2-((5-iodopyridin-2-yl)oxy)ethyl)carbamate (0.72 g, 1.51 mmol, as prepared in Example 25, Step-2), bis(triphenylphosphine)palladium (II) dichloride (0.071 g, 0.1 mmol), cesium carbonate (1.3 g, 4.04 mmol) and 2-methyl THF (10 mL) were added. This mixture was degassed with nitrogen and water (0.12 mL) was added. This mixture was stirred at room temperature for 16 h. After completion of reaction, to the above reaction mixture 4M KOH (2.78 mL, 11.13 mmol) and iodobenzene (0.33 g, 1.61 mmol) were added. Reaction mixture was stirred at 85° C. for 7 h. After completion of reaction, reaction mixture was cooled to room temperature, diluted with water and extracted with EtOAc. The organic layer was dried over anhydrous sodium sulphate and concentrated under reduced pressure. The crude material was purified by combi-flash using 100% ethyl acetate as an eluent to afford tert-butyl ((E)-4-(dimethylamino)-4-oxobut-2-en-1-yl)(2-((5-((Z)-4,4,4-trifluoro-1-(3-fluoro-1-(tetrahydro-2H-pyran-2-yl)-1H-indazol-5-yl)-2-phenylbut-1-en-1-yl)pyridin-2-yl)oxy)ethyl)carbamate (0.35 g, 23%).

Step-2: Synthesis of (E)-N,N-dimethyl-4-((2-((5-((Z)-4,4,4-trifluoro-1-(3-fluoro-1H-indazol-5-yl)-2-phenylbut-1-en-1-yl)pyridin-2-yl)oxy)ethyl)amino)but-2-enamide



To a stirred solution of 3-fluoro-1-(tetrahydro-2H-pyran-2-yl)-5-(4,4,4-trifluorobut-1-yn-1-yl)-1H-indazole (0.66 g,

To a stirred solution of tert-butyl ((E)-4-(dimethylamino)-4-oxobut-2-en-1-yl)(2-((5-((Z)-4,4,4-trifluoro-1-(3-fluoro-

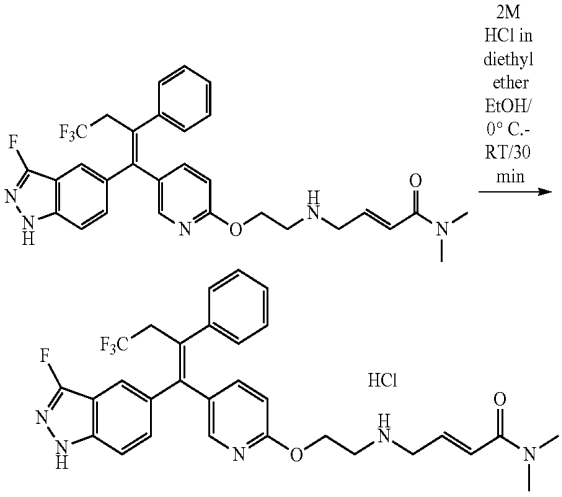
1-(tetrahydro-2H-pyran-2-yl)-1H-indazol-5-yl)-2-phenylbut-1-en-1-yl)pyridin-2-yl)oxy)ethyl)carbamate (0.35 g, 0.46 mmol) in dichloromethane (10 mL) was added at 0° C., TFA (1 mL). The reaction mixture was stirred for 16 h at room temperature. After completion of reaction, reaction mixture was basified with saturated $NaHCO_3$, extracted with ethyl acetate. Organic layer was concentrated under reduced pressure to afford crude compound, which was purified by preparative HPLC to afford desired compound (E)-N,N-dimethyl-4-((2-((5-((Z)-4,4,4-trifluoro-1-(3-fluoro-1H-indazol-5-yl)-2-phenylbut-1-en-1-yl)pyridin-2-yl)oxy)ethyl)amino)but-2-enamide (0.03 g, 11%).

Compound 60:

^{1}H NMR (400 MHz, DMSO-d_6): δ 12.71 (s, 1H), 7.63 (s, 2H), 7.54 (m, 1H), 7.26-7.18 (m, 7H), 6.62-6.46 (m, 3H), 4.13 (t, J=5.8 Hz, 2H), 3.51-3.43 (m, 2H), 3.34-3.28 (m, 2H), 2.98 (s, 3H), 2.83 (s, 3H), 2.75 (t, J=5.8 Hz, 2H). LCMS: 568.2 $[M+H]^+$.

Example 60A: Synthesis of Hydrochloride Salt of Compound 60

Step-1: Synthesis of (E)-N,N-dimethyl-4-((2-((5-((Z)-4,4,4-trifluoro-1-(3-fluoro-1H-indazol-5-yl)-2-phenylbut-1-en-1-yl)pyridin-2-yl)oxy)ethyl)amino)but-2-enamide hydrochloride



To a stirred solution of (E)-N,N-dimethyl-4-((2-((5-((Z)-4,4,4-trifluoro-1-(3-fluoro-1H-indazol-5-yl)-2-phenylbut-1-en-1-yl)pyridin-2-yl)oxy)ethyl)amino)but-2-enamide (4.1 g, 7.23 mmol) in ethanol (24 mL) was added 2M HCl in diethyl ether (7.5 mL) at 0° C. A white solid was observed in the reaction mixture after stirring for 30 min at room temperature. Reaction mixture was concentrated under vacuum at 35° C. and the solid obtained was co-distilled with dichloromethane under vacuum at 45° C. The solid obtained was washed with n-pentane and dried under vacuum at 50° C. for 4 h to obtain the title compound (E)-N,N-dimethyl-4-((2-((5-((Z)-4,4,4-trifluoro-1-(3-fluoro-1H-indazol-5-yl)-2-phenylbut-1-en-1-yl)pyridin-2-yl)oxy)ethyl)amino)but-2-enamide hydrochloride (4.3 g, 98%). ^{1}H NMR (400 MHz, DMSO-d_6): δ 12.74 (s, 1H), 9.26 (bs, 2H), 7.69-7.34 (m, 3H), 7.28-7.17 (m, 7H), 6.81 (d, J=15.2 Hz, 1H), 6.62-6.53 (m, 2H), 4.37 (t, J=4.4 Hz, 2H), 3.77-3.76 (m, 2H), 3.51-3.43 (m, 2H), 3.23 (bs, 2H), 3.03 (s, 3H), 2.86 (s, 3H). LCMS: 568.3 $[M+H]^+$

Example 60B: Synthesis of Hydrochloride Salt of Compound 60

To a stirred solution of (E)-N,N-dimethyl-4-((2-((5-((Z)-4,4,4-trifluoro-1-(3-fluoro-1H-indazol-5-yl)-2-phenylbut-1-en-1-yl)pyridin-2-yl)oxy)ethyl)amino)but-2-enamide (0.200 g, 0.35 mmol) in ethanol (0.6 mL) was added 2M HCl in diethyl ether (0.88 mL) at 0° C. A white solid was observed in the reaction mixture after stirring for 30 min at room temperature. Reaction mixture was concentrated under vacuum at 35° C. and the solid obtained was co-distilled with dichloromethane under vacuum at 45° C. The solid obtained was washed with n-pentane and dried under vacuum at 50° C. for 4 h to obtain the title compound (E)-N,N-dimethyl-4-((2-((5-((Z)-4,4,4-trifluoro-1-(3-fluoro-1H-indazol-5-yl)-2-phenylbut-1-en-1-yl)pyridin-2-yl)oxy)ethyl)amino)but-2-enamide hydrochloride (0.150 g, 67%).

^{1}H NMR (400 MHz, DMSO-d_6): δ 12.71 (s, 1H), 9.07 (bs, 2H), 7.69-7.54 (m, 3H), 7.26-7.18 (m, 7H), 6.80 (d, J=15.2 Hz, 1H), 6.62-6.46 (m, 2H), 4.35 (m, 2H), 3.75 (m, 2H), 3.51-3.43 (m, 2H), 3.34-3.28 (m, 2H), 2.98 (s, 3H), 2.83 (s, 3H). LCMS: 568.2 $[M+H]^+$.

Example 61: Synthesis of (E)-N,N-dimethyl-4-((2-(4-((E)-4,4,4-trifluoro-1-(3-fluoro-1H-indazol-5-yl)-2-(3-fluoropyridin-4-yl)but-1-en-1-yl)phenoxy)ethyl)amino)but-2-enamide (Compound 61)

The compound was synthesized following the approach as outlined in Example 60 by substituting into Step-1 tert-butyl (E)-(4-(dimethylamino)-4-oxobut-2-en-1-yl)(2-(4-iodophenoxy)ethyl)carbamate (as prepared in Example 14, Step-3) for compound 263 and 3-fluoro-4-iodopyridine for compound 264 to afford Compound 61 (0.02 g, 5.8%).

Compound 61:

^{1}H NMR (400 MHz, DMSO-d_6): δ 12.71 (s, 1H), 8.39 (s, 1H), 8.34 (d, J=2 Hz, 1H), 7.59 (s, 1H), 7.56-7.49 (m, 2H), 7.20 (d, J=2.4 Hz, 1H), 6.85 (d, J=8.9 Hz, 2H), 6.85 (d, 1H), 6.68 (d, J=8.9 Hz, 2H), 6.63-6.47 (m, 1H), 4.15 (m, 2H), 3.79 (t, J=5.7 Hz, 2H), 3.45 (q, J=10.8 Hz, 2H), 3.25 (m, 2H), 2.98 (s, 3H), 2.84 (s, 3H). LCMS: 586.2 $[M+H]^+$.

Example 62: Synthesis of (E)-N,N-dimethyl-4-((2-((5-((Z)-4,4,4-trifluoro-1-(3-fluoro-1H-indazol-5-yl)-2-(3-fluoropyridin-4-yl)but-1-en-1-yl)pyridin-2-yl)oxy)ethyl)amino)but-2-enamide (Compound 62)

The compound was synthesized following the approach as outlined in Example 59 by substituting into Step-5 3-fluoro-4-iodopyridine for compound 265 to afford Compound 62 (0.07 g, 12%).

Compound 62:

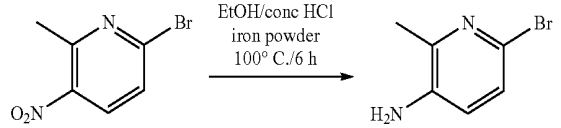
^{1}H NMR (400 MHz, DMSO-d_6): δ 12.76 (s, 1H), 8.43-8.39 (m, 2H), 7.72-7.56 (m, 4H), 7.28-7.24 (m, 2H), 6.62-6.48 (m, 3H), 4.15 (t, J=5.8 Hz, 2H), 4.15 (m, 2H), 3.51-3.46 (m, 2H), 3.38-3.31 (m, 2H), 2.98 (s, 3H), 2.84 (s, 3H). LCMS: 587.2 $[M+H]^+$

Example 63: Synthesis of (E)-N,N-dimethyl-4-((2-(4-((E)-2-phenyl-1-(1H-pyrazolo[4,3-b]pyridin-5-yl)but-1-en-1-yl)phenoxy)ethyl)amino)but-2-enamide (Compound 63)

The compound was synthesized following the approach as outlined in Example 50 by substituting into Step-2 tert-butyl (E)-(2-(4-(2-phenyl-1-(1-(tetrahydro-2H-pyran-2-yl)-1H-

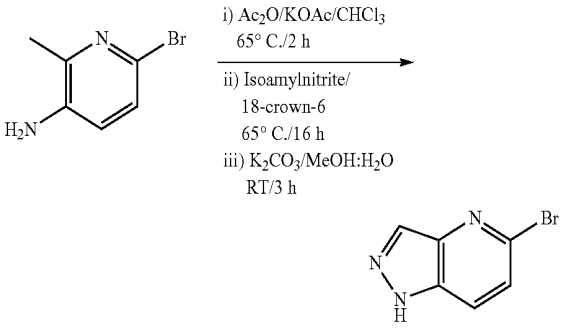
pyrazolo[4,3-b]pyridin-5-yl)but-1-en-1-yl)phenoxy)ethyl) carbamate (preparation shown below in Ex. 63 Step 1-6) for compound 261 to afford Compound 63 (0.013 g, 5.2%).

Step-1: Synthesis of 6-bromo-2-methylpyridin-3-amine



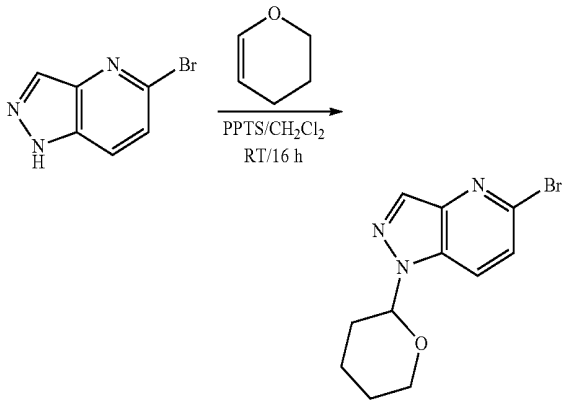
To a stirred solution of 6-bromo-2-methyl-3-nitropyridine (15 g, 69.12 mmol) in ethanol (280 mL) was added iron powder (57.9 g, 1036 mmol) followed by conc HCl (30 mL). The reaction mixture was stirred for 6 h at 100° C., after completion of reaction (monitored by TLC), reaction mixture was cooled to room temperature, filtered through celite. Filterate was basified with saturated $NaHCO_3$ solution, extracted with EtOAc. Organic layer was washed with water followed by brine, dried over anhydrous sodium sulphate, filtered and concentrated under reduced pressure. The crude product was used in next step without further purification to afford desired compound (5.6 g, 65%) as an off-white solid.

Step-2: Synthesis of 5-bromo-1H-pyrazolo[4,3-b]pyridine



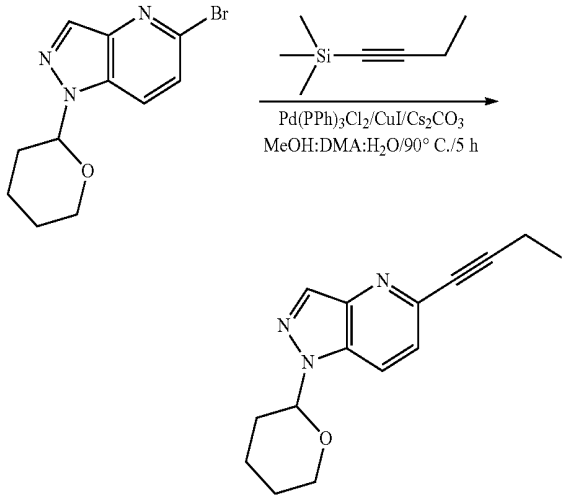
To a stirred solution of 6-bromo-2-methyl-3-nitropyridine (5 g, 26.73 mmol) in chloroform was added potassium acetate (3.14 g, 32.08 mmol) and acetic anhydride (10.9 g, 106 mmol) at 10° C., the contents were stirred at 65° C. temperature for 2 h. After completion of reaction (monitored by TLC), the reaction mixture was cooled to room temperature, isoamylnitrite (3.75 g, 32.06 mmol) was added drop wise over a period of 15 min, followed by 18-crown-6 (0.7 g, 2.67 mmol) was added, reaction mixture was stirred at 65° C. for 16 h. After completion of reaction (monitored by TLC), the reaction mixture was cooled to room temperature, methanol and water mixture 120 mL (1:1) was added to the reaction mixture followed by potassium carbonate (34.48 g, 24.99 mmol) and KOH (4.2 g, 74.97 mmol), reaction mixture was stirred for 3 h at room temperature. After completion of reaction, reaction mixture was added diluted with ethyl acetate and the organic layer was washed with water followed by brine. The organic layer was dried over anhydrous Na_2SO_4 and concentrated under reduced pressure to obtain this title compound (5 g) as an off-white solid.

Step-3: Synthesis of S-bromo-1-(tetrahydro-2H-pyran-2-yl)-1H-pyrazolo[4,3-b]pyridine



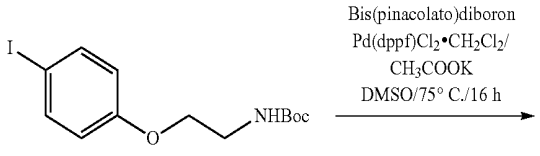
The reaction was carried out according to Scheme 1, Step-1 to give crude material, which was purified by column chromatography over 230-400 mesh silica using 10-15% ethyl acetate in n-hexane to afford 5-bromo-1-(tetrahydro-2H-pyran-2-yl)-1H-pyrazolo[4,3-b]pyridine (5 g, 78%).

Step-4: Synthesis of 5-(but-1-yn-1-yl)-1-(tetrahydro-2H-pyran-2-yl)-1H-pyrazolo[4,3-b]pyridine

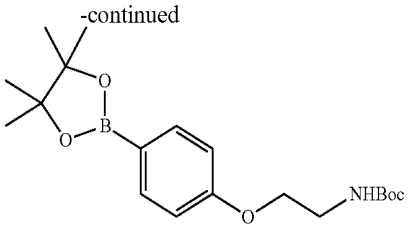


The reaction was carried out according to Scheme 1, Step-2 to give crude material, which was purified over 230-400 mesh silica column chromatography using 10-15% ethyl acetate in n-hexane to afford the title compound of Ex. 63 Step-4 (3.5 g, 77.7%) as a brown oil.

Step-5: Synthesis of tert-butyl (2-(4-(4,4,5,5-tetramethyl-1,3,2-dioxaborolan-2-yl)phenoxy)ethyl)carbamate

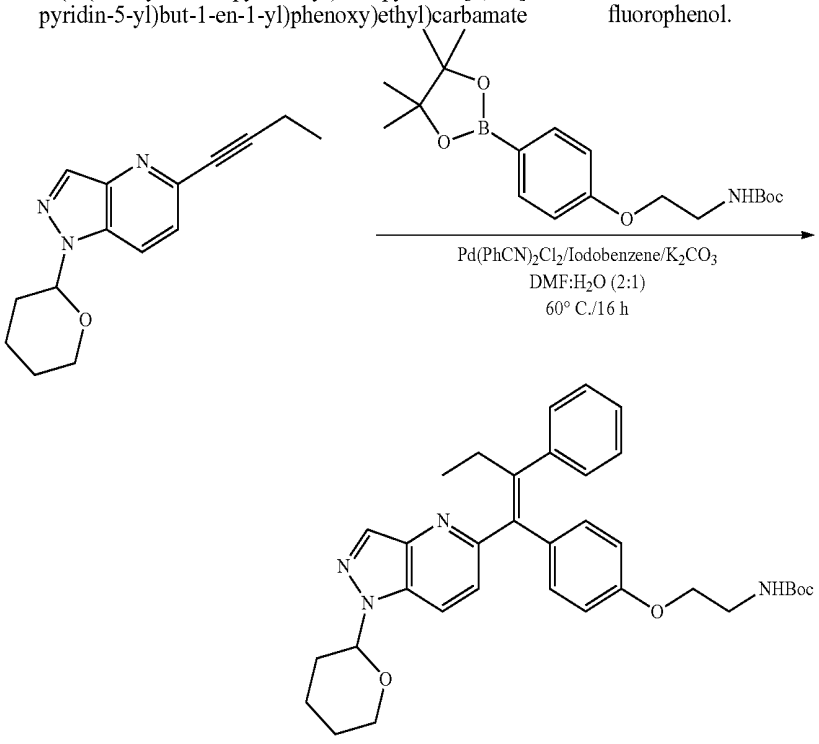


-continued



To a solution of tert-butyl (2-(4-iodophenoxy)ethyl)carbamate (25 g, 68.87 mmol) in DMSO (200 mL) was added potassium acetate (20.24 g, 206.6 mmol) and bis(pinacolato) diboron (34.98 g, 137.74 mmol). The contents were degassed with three vacuum/N_2 cycles, $Pd(dppf)Cl_2.CH_2Cl_2$ (2.8 g, 3.44 mmol) was added and the resulting mixture was stirred at 75° C. for 16 h. Upon completion by TLC, the reaction mixture was quenched with water (500 mL) and extracted with ethyl acetate (2×250 mL). The combined organic extracts were washed with water, brine, dried over anhydrous sodium sulphate and concentrated under reduced pressure. The crude material was purified by column chromatography, eluted with 10-15% ethyl acetate in n-hexane to afford the title compound of Ex. 63 Step-5 (50 g, mixture with bis(pinacolato)diboron).

Step-6: Synthesis of tert-butyl (E)-(2-(4-(2-phenyl-1-(1-(tetrahydro-2H-pyran-2-yl)-1H-pyrazolo[4,3-b]pyridin-5-yl)but-1-en-1-yl)phenoxy)ethyl)carbamate



The reaction was carried according to Scheme 1, Step-6 using 5-(but-1-yn-1-yl)-1-(tetrahydro-2H-pyran-2-yl)-1H-pyrazolo[4,3-b]pyridine for compound 204, iodobenzene for compound 209, tert-butyl (2-(4-(4,4,5,5-tetramethyl-1,3,2-dioxaborolan-2-yl)phenoxy)ethyl)carbamate for compound 210 to obtain crude material, which was purified by silica column chromatography to afford the title compound of Ex. 63 Step-6 (4 g, crude).

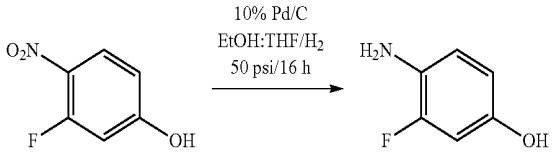
Compound 63:

^1H NMR (400 MHz, DMSO-d_6): δ 13.29 (s, 1H), 8.26 (s, 1H), 7.97 (s, J=8.8 Hz, 1H), 7.24-7.13 (m, 6H), 6.75 (d, J=8.8 Hz, 2H), 6.62-6.57 (m, 3H), 6.50 (d, J=15.2 Hz, 1H), 3.87 (t, J=5.6 Hz, 2H), 3.3-3.29 (m, 2H), 2.98 (s, 3H), 2.84 (s, 3H), 2.78 (t, J=5.4 Hz, 2H), 2.37-2.30 (m, 2H), 0.86 (t, J=7.6 Hz, 3H). LCMS: 496.4 $[M+H]^+$.

Example 64: Synthesis of (E)-4-((2-(3-fluoro-4-((Z)-1-(3-fluoro-1H-indazol-5-yl)-2-phenylbut-1-en-1-yl)phenoxy)ethyl)amino)-N,N-dimethylbut-2-enamide (Compound 64)

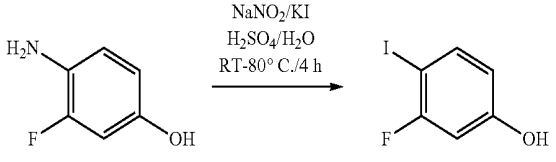
The compound was synthesized following the approach as outlined in Example 50 by substituting into Step-2 tert-butyl (Z)-(2-(3-fluoro-4-(1-(3-fluoro-1-(tetrahydro-2H-pyran-2-yl)-1H-indazol-5-yl)-2-phenylbut-1-en-1-yl)phenoxy)ethyl) carbamate (preparation shown below in Step 1-4) for compound 261 to afford Compound 64 (0.16 g, 17.4%).

Step-1: Synthesis of 4-amino-3-fluorophenol



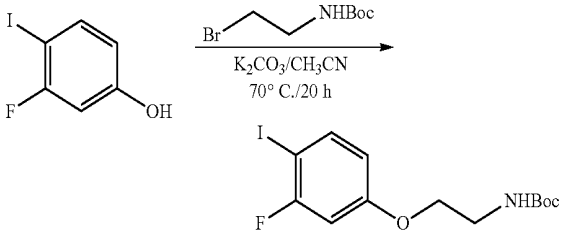
A mixture of 3-fluoro-4-nitrophenol (6 g, 38.4 mmol) and 10% Pd/C (1.8 g) in EtOH (60 mL) and THF (36 mL) was stirred under H_2 (1 atm) for 16 h. After filtration, the filtrate was concentrated to yield 4.68 g (96.5%) of 4-amino-3-fluorophenol.

Step-2: Synthesis of 3-fluoro-4-iodophenol



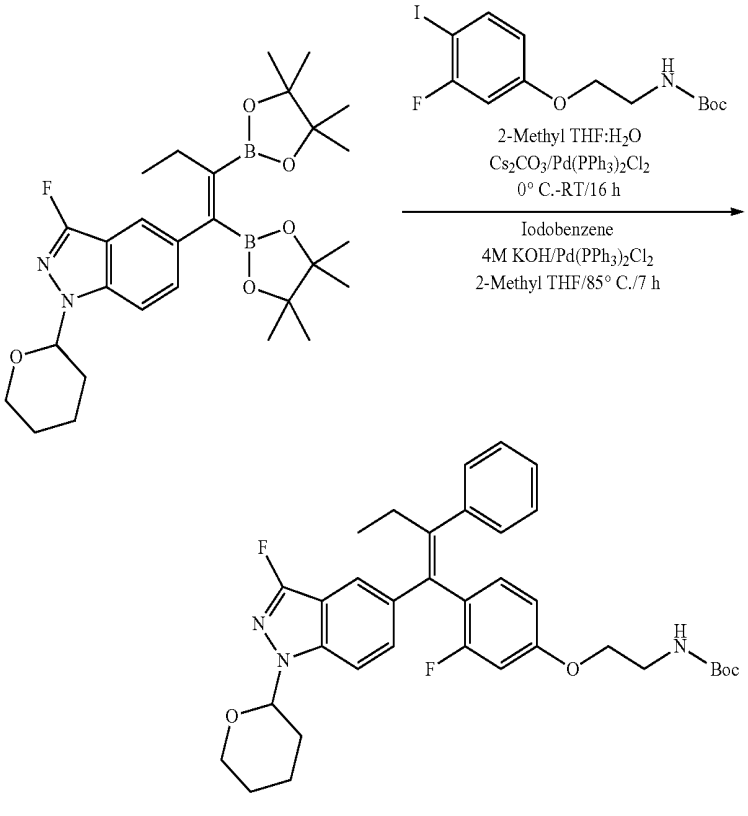
4-Amino-3-fluorophenol (5 g, 39.4 mmol) was suspended in 15 mL water and H_2SO_4 (4.62 g), mixture was cooled in an ice-salt bath to −5° C. To this mixture was added, dropwise, a solution of sodium nitrite (2.71 g, 39.4 mmol) in 15 mL water. The internal temperature was kept below +2° C. The resulting brown solution was stirred for a further 15 min at −5° C., then a solution of potassium iodide (7.87 g, 47.2 mmol) in 30 mL water was slowly added dropwise. After complete addition, the reaction was stirred at room temperature for 4 h. Upon completion, the reaction mixture was diluted with EtOAc. Organic layer was washed with water followed by brine, dried over anhydrous sodium sulphate, filtered and concentrated to give the title compound of Ex. 64 Step-2 (5 g, 53.3%).

Step-3: Synthesis of tert-butyl (2-(3-fluoro-4-iodophenoxy)ethyl)carbamate



The reaction was carried out according to Scheme 3, Step-1 using 3-fluoro-4-iodophenol and tert-butyl (2-bromoethyl)carbamate to obtain crude material, which was purified by silica gel column chromatography to afford tert-butyl (2-(3-fluoro-4-iodophenoxy)ethyl)carbamate (5 g).

Step-4: Synthesis of tert-butyl (Z)-(2-(3-fluoro-4-(1-(3-fluoro-1-(tetrahydro-2H-pyran-2-yl)-1H-indazol-5-yl)-2-phenylbut-1-en-1-yl)phenoxy)ethyl)carbamate



The reaction was carried out following the approach as outlined by Example 50, Step-1, by substituting (Z)-5-(1,2-bis(4,4,5,5-tetramethyl-1,3,2-dioxaborolan-2-yl)but-1-en-1-yl)-3-fluoro-1-(tetrahydro-2H-pyran-2-yl)-1H-indazole (8 g, 15.19 mmol) for compound 260 and tert-butyl (2-(3-fluoro-4-iodophenoxy)ethyl)carbamate (5.4 g, 14.43 mmol) for compound 257 to afford crude material. It was purified by silica gel chromatography using 15% EtOAc in n-hexane to give the title compound of Ex. 64 Step-4 (3.5 g, 38%).

Compound 64:

^{1}H NMR (400 MHz, DMSO-d_6): δ 12.57 (s, 1H), 7.49 (s, 1H), 7.46 (d, J=2.0 Hz, 1H), 7.27 (dd, J_1=8.5 Hz, J_2=1.2 Hz, 1H), 7.21-7.09 (m, 3H), 6.92 (t, J=8.6 Hz, 1H), 6.62-6.47 (m, 4H), 3.88 (t, J=5.6 Hz, 2H), 3.30 (s, 2H), 2.98 (s, 3H), 2.83 (s, 3H), 2.76 (t, J=5.6 Hz, 2H), 2.44 (q, J=7.8 Hz, 2H), 2.10 (bs, 1H), 0.89 (t, J=7.3 Hz, 3H). LCMS: 531.3 $[M+H]^+$.

Example 65: Synthesis of (E)-4-((2-(4-((E)-2-(2,4-difluorophenyl)-1-(3-fluoro-1H-indazol-5-yl)but-1-en-1-yl)phenoxy)ethyl)amino)-N,N-dimethylbut-2-enamide (Compound 65)

The compound was synthesized following the approach as outlined in Example 50 by substituting into Step-1 2,4-difluoro-1-iodobenzene to afford Compound 65 (0.06 g, 23.7%).

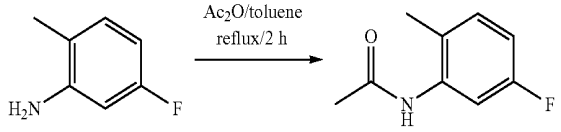
Compound 65:

^{1}H NMR (400 MHz, DMSO-d_6): δ 12.59 (s, 1H), 7.52 (s, 1H), 7.49 (dd, J_1=8.8 Hz, J_2=1.2 Hz, 1H), 7.28-7.21 (m, 2H), 7.09 (dd, J_1=10 Hz, J_2=2.4 Hz, 1H), 6.97 (dd, J_1=8.4 Hz, J_2=2.4 Hz, 1H), 6.80 (d, J=8.4 Hz, 2H), 6.64 (d, J=8.8 Hz, 2H), 6.63-6.58 (m, 1H), 6.50 (d, J=15.2 Hz, 1H), 3.88 (t, J=5.6 Hz, 2H), 3.32-3.31 (m, 2H), 2.98 (s, 3H), 2.84 (s, 3H), 2.78 (t, J=5.4 Hz, 2H) 2.34 (q, J=7.6 Hz, 2H), 0.89 (t, J=7.6 Hz, 3H). LCMS: 549.3 $[M+H]^+$

Example 66: Synthesis of (E)-4-((2-(4-((E)-1-(3,6-difluoro-1H-indazol-5-yl)-2-phenylbut-1-en-1-yl) phenoxy)ethyl)amino)-N,N-dimethylbut-2-enamide (Compound 66)

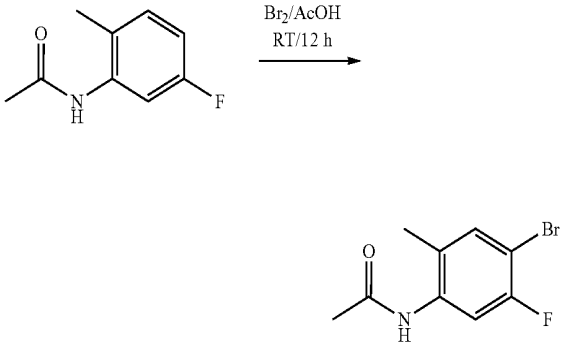
The compound was synthesized following the approach as outlined in Example 50 by (i) substituting into Step-1 tert-butyl (Z)-(2-(4-(1-(3,6-difluoro-1-(tetrahydro-2H-pyran-2-yl)-1H-indazol-5-yl)-2-(4,4,5,5-tetramethyl-1,3,2-dioxaborolan-2-yl)but-1-en-1-yl)phenoxy)ethyl)carbamate (preparation shown below in Ex. 66 Steps 1-7) for compound 260 and iodobenzene for compound 251, and (ii) conducting Step-5 of Ex. 50 by following the reaction conditions described in Scheme 2, Step-6b to deliver Compound 66 (0.012 g).

Step-1: Synthesis of N-(5-fluoro-2-methylphenyl)acetamide



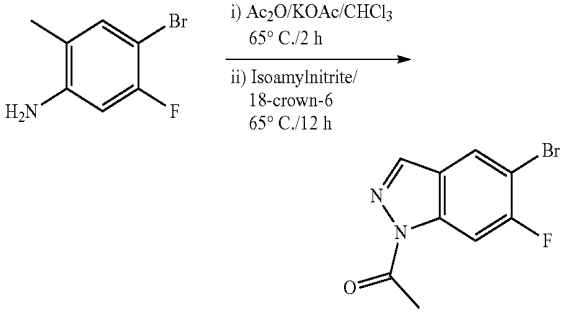
To a stirred solution of 5-fluoro-2-methylaniline (25 g, 200 mmol) in toluene was added acetic anhydride (25 mL) at 10° C., the contents were stirred at reflux temperature for 2 h. After completion of reaction (monitored by TLC), the reaction mixture was cooled to room temperature, solid obtained was filtered and washed with diethyl ether and hexane to obtain desired compound (28 g, 84%).

Step-2: Synthesis of N-(4-bromo-5-fluoro-2-methylphenyl)acetamide



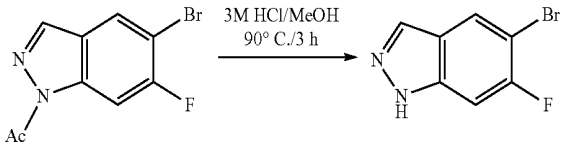
To a stirred solution of N-(5-fluoro-2-methylphenyl)acetamide (28 g, 167 mmol) in acetic acid (150 mL) was added bromine (9.6 mL, 186 mmol) at 10° C. The reaction mixture was stirred for 12 h at room temperature, after completion of reaction (monitored by TLC), solid separated was filtered and dried under reduced pressure. The crude product was used in next step without further purification to afford N-(4-bromo-5-fluoro-2-methylphenyl)acetamide (40 g, 97%).

Step-3: Synthesis of 1-(5-bromo-6-fluoro-1H-indazol-1-yl)ethan-1-one



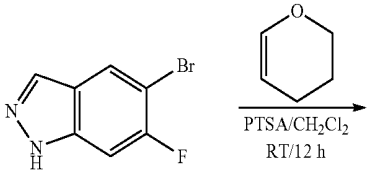
To a stirred solution of 4-bromo-5-fluoro-2-methylaniline (40 g, 163 mmol) in chloroform (400 mL) was added potassium acetate (32 g, 326 mmol) and acetic anhydride (45 mL) at 10° C., the contents were stirred at 65° C. temperature for 2 h. After completion of reaction (monitored by TLC), the reaction mixture was cooled to room temperature, isoamylnitrite (50 mL, 371 mmol) was added drop wise over a period of 15 min, followed by 18-crown-6 (2.16 g, 8.18 mmol) was added, reaction mixture was stirred at 65° C. for 12 h. After completion of reaction (monitored by TLC), the reaction mixture was cooled to room temperature, diluted with ethyl acetate. Organic layer was washed with water followed by brine. The organic layer was dried over anhydrous Na_2SO_4 and concentrated under reduced pressure to obtain title compound of Ex. 66 Step-3 (38.3 g, 44%).

Step-4: Synthesis of 5-bromo-6-fluoro-1H-indazole

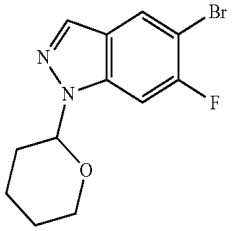


To a stirred solution of 1-(5-bromo-6-fluoro-1H-indazol-1-yl)ethan-1-one (20 g, 78.43 mmol) in 3M HCl (400 mL) was added methanol (80 mL), reaction mixture was stirred at 90° C. for 3 h. After completion of reaction (monitored by TLC), the reaction mixture was cooled to room temperature and basified with 1M NaOH, solid separated was filtered and dried under reduced pressure to obtain title compound of Ex. 66 Step-4 (7.6 g, 45%).

Step-5: Synthesis of 5-bromo-6-fluoro-1-(tetrahydro-2H-pyran-2-yl)-1H-indazole

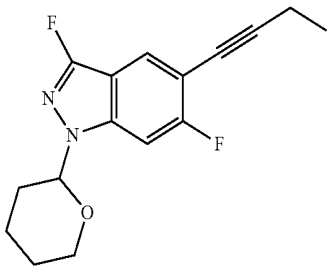


-continued



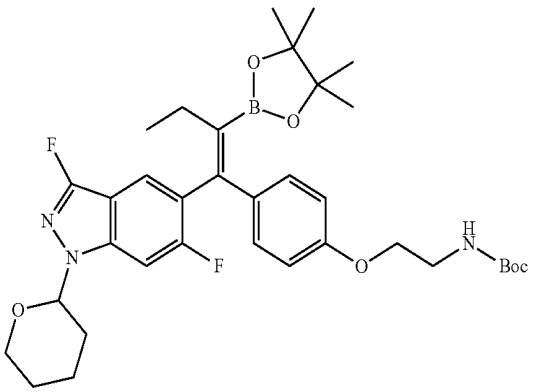
The reaction was run according to Scheme 1, Step-1 using 5-bromo-6-fluoro-1H-indazole (7.6 g, 35.34 mmol) for compound 201. The crude material from the reaction was purified by silica gel chromatography using 4% ethyl acetate in n-hexane to afford 5-bromo-6-fluoro-1-(tetrahydro-2H-pyran-2-yl)-1H-indazole (8.83 g, 84%).

Step-6: Synthesis of 5-(but-1-yn-1-yl)-3,6-difluoro-1-(tetrahydro-2H-pyran-2-yl)-1H-indazole



The compound was synthesized following the approach as outlined in Example 2 by (i) substituting into Step-1 5-bromo-6-fluoro-1-(tetrahydro-2H-pyran-2-yl)-1H-indazole for compound 270 and (ii) following the reaction conditions of Steps 2 and 3 of Ex. 2. to afford the title compound of Ex. 66 Step-6 (12.19 g, 87%).

Step-7: Synthesis of tert-butyl (Z)-(2-(4-(1-(3,6-difluoro-1-(tetrahydro-2H-pyran-2-yl)-1H-indazol-5-yl)-2-(4,4,5,5-tetramethyl-1,3,2-dioxaborolan-2-yl) but-1-en-1-yl)phenoxy)ethyl)carbamate



The compound was synthesized following the approach as outlined in Example 14 by (i) substituting into Step-2 5-(but-1-yn-1-yl)-3,6-difluoro-1-(tetrahydro-2H-pyran-2-yl)-1H-indazole for compound 271 and (ii) substituting into Step-4 tert-butyl (2-(4-iodophenoxy)ethyl)carbamate (as prepared in Example 3, Step-2) for compound 234 to deliver the title compound in Ex. 66 Step-7.

Compound 66:

^{1}H NMR (400 MHz, DMSO-d_6): δ 12.65 (s, 1H), 7.69 (d, J=6.8 Hz, 1H), 7.34 (dd, J_1=6.0 Hz, J_2=2.0 Hz, 1H), 7.25-7.21 (m, 2H), 7.17-7.14 (m, 3H), 6.79 (d, J=8.8 Hz, 2H), 6.64-6.57 (m, 3H), 6.49 (d, J=15.2 Hz, 1H), 3.87 (t, J=5.6 Hz, 2H), 2.98 (s, 3H), 2.84 (s, 3H), 2.77 (t, J=5.6 Hz, 2H), 2.33-2.31 (m, 2H), 0.81 (t, J=7.6 Hz, 3H). LCMS: 531.3 $[M+H]^+$.

Example 67: Synthesis of (E)-4-((2-(4-((E)-1-(3-fluoro-1H-indazol-5-yl)-2-(pyridin-2-yl)but-1-en-1-yl)phenoxy)ethyl)amino)-N,N-dimethylbut-2-enamide (Compound 67)

The compound was synthesized following the approach as outlined in Example 14 by substituting into Step-4 (Z)-5-(1,2-bis(4,4,5,5-tetramethyl-1,3,2-dioxaborolan-2-yl)but-1-en-1-yl)-3-fluoro-1-(tetrahydro-2H-pyran-2-yl)-1H-indazole (as prepared in Example 3, Step-1) for compound 233 and 2-iodopyridine for compound 262 to deliver Compound 67 (0.010 g) as an off-white solid.

Compound 67:

^{1}H NMR (400 MHz, DMSO-d_6): δ 12.6 (s, 1H), 8.56 (d, J=4.4 Hz, 1H), 7.53 (s, 1H), 7.50-7.45 (m, 2H), 7.21 (dd, J_1=8.8 Hz, J_2=1.4 Hz, 1H), 7.13 (dd, J_1=4.9 Hz, J_2=6.9 Hz, 1H), 6.87 (d, J=7.8 Hz, 1H), 6.72 (d, J=8.8 Hz, 2H), 6.64-6.57 (m, 3H), 6.50 (d, J=15.1 Hz, 1H), 3.88 (t, J=5.7 Hz, 2H), 3.32-3.21 (m, 2H), 299 (s, 3H), 2.84 (s, 3H), 2.78 (t, J=5.6 Hz, 2H), 2.54-2.52 (m, 2H), 0.86 (t, J=7.3 Hz, 3H). LCMS: 514.3 $[M+H]^+$.

Example 68: Synthesis of (E)-4-((2-((5-((Z)-1-(3-fluoro-1H-indazol-5-yl)-2-phenylbut-1-en-1-yl)pyridin-2-yl)oxy)ethyl)amino)-N,N-dimethylbut-2-enamide (Compound 68)

The compound was synthesized following the approach as outlined in Example 14 by substituting into Step-4 (Z)-5-(1,2-bis(4,4,5,5-tetramethyl-1,3,2-dioxaborolan-2-yl)but-1-en-1-yl)-3-fluoro-1-(tetrahydro-2H-pyran-2-yl)-1H-indazole (as prepared in Example 3, Step-1) for compound 233 and tert-butyl (E)-(4-(dimethylamino)-4-oxobut-2-en-1-yl) (2-((5-iodopyridin-2-yl)oxy)ethyl)carbamate (as prepared in Example 25, Step-2) for compound 234 to deliver Compound 68 (0.165 g, 11%).

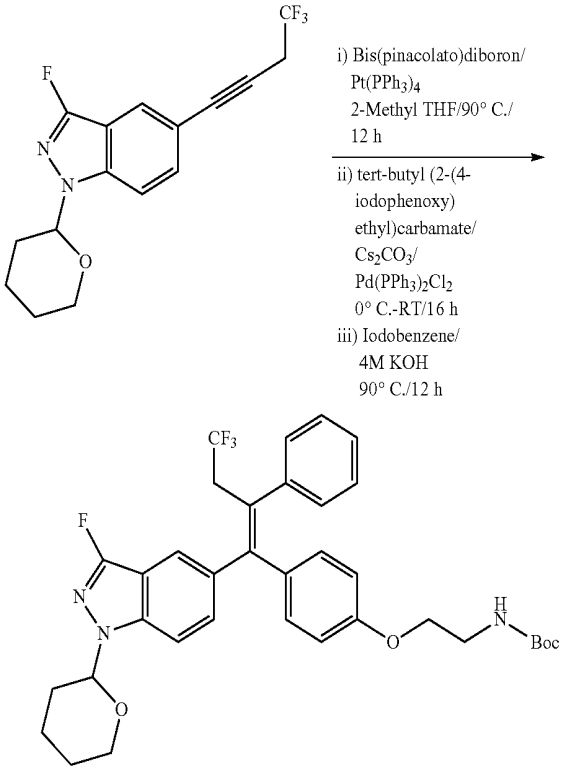
Compound 68:

^{1}H NMR (400 MHz, DMSO-d_6): δ 12.6 (s, 1H), 7.59 (d, J=2.0 Hz, 1H), 7.56 (s, 1H), 7.50 (dd, J_1=8.8 Hz, J_2=2.0 Hz, 1H), 7.26-7.22 (m, 3H), 7.18-7.14 (m, 4H), 6.61-6.56 (m, 1H), 6.51-6.46 (m, 2H), 4.13 (t, J=5:6 Hz, 2H), 3.30-3.29 (m, 2H), 3.29 (s, 3H), 2.84 (s, 3H), 2.76 (t, J=5.9 Hz, 2H), 2.42 (q, J=7.4 Hz, 2H), 2.1-2.0 (bs, 1H), 0.88 (t, J=7.3 Hz, 3H).

LCMS: 514.3 $[M+H]^+$.

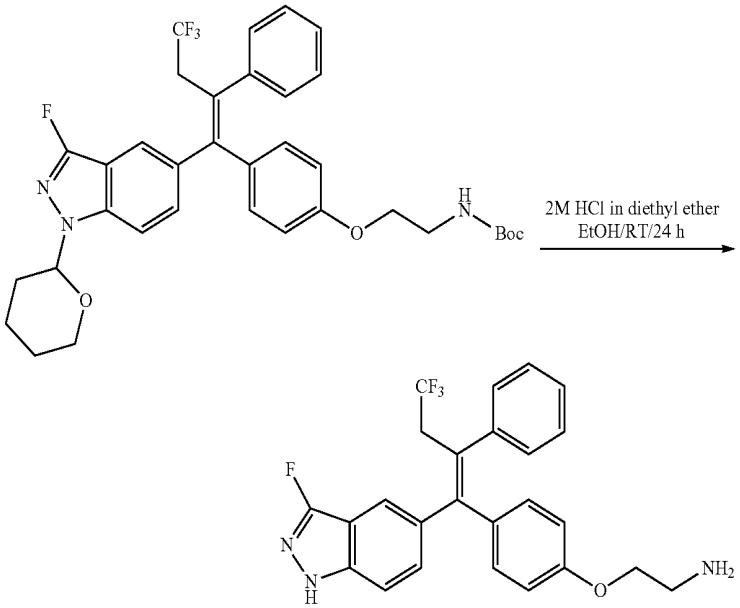
Example 69: Synthesis of (E)-N,N-dimethyl-4-((2-(4-((E)-4,4,4-trifluoro-1-(3-fluoro-1H-indazol-S-yl)-2-phenylbut-1-en-1-yl)phenoxy)ethyl)amino)but-2-enamide (Compound 69)

Step-1: Synthesis of tert-butyl (E)-(2-(4-(4,4,4-trifluoro-1-(3-fluoro-1-(tetrahydro-2H-pyran-2-yl)-1H-indazol-5-yl)-2-phenylbut-1-en-1-yl)phenoxy)ethyl) carbamate



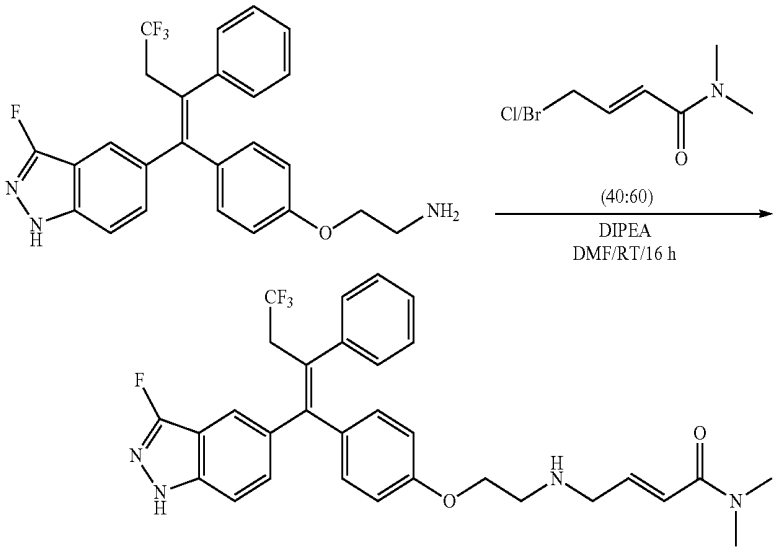
To a stirred solution of 3-fluoro-1-(tetrahydro-2H-pyran-2-yl)-5-(4,4,4-trifluorobut-1-yn-1-yl)-1H-indazole (1.6 g, 4 mmol, Example 59, Step-3) in 2-methyl THF (30 mL), was added bis(pinacolato)diboron (1.24 g, 4 mmol), tetrakis (triphenylphosphine)platinum (0) (0.06 g, 0.04 mmol) under nitrogen atmosphere, reaction mixture was stirred at 90° C. for 12 h. The solution was allowed to cool to room temperature and tert-butyl (2-(4-iodophenoxy)ethyl)carbamate (1.78 g, 4 mmol, Example 3, Step-2), bis(triphenylphosphine)palladium (II) dichloride (0.172 g, 0.2 mmol), cesium carbonate (3.19 g, 9 mmol) and 2-methyl THF (30 mL) were added. This mixture was degassed with nitrogen and water (0.3 mL) was added. This mixture was stirred at room temperature for 16 h. After completion of reaction, to the above reaction mixture 4M KOH (1.47 g, 26 mmol) and iodobenzene (1.95 g, 9 mmol) were added. Reaction mixture was stirred at 90° C. for 12 h. After completion of reaction, reaction mixture was cooled to room temperature, diluted with water and extracted with EtOAc. The organic layer was dried over anhydrous sodium sulphate and concentrated under reduced pressure. The crude material was purified by column chromatography over 230-400 mesh silica gel using 15% EtOAc in n-hexane to afford tert-butyl (E)-(2-(4-(4,4,4-trifluoro-1-(3-fluoro-1-(tetrahydro-2H-pyran-2-yl)-1H-indazol-5-yl)-2-phenylbut-1-en-1-yl)phenoxy)ethyl)carbamate (1.5 g, 50%).

Step-2: Synthesis of (E)-2-(4-(4,4,4-trifluoro-1-(3-fluoro-1H-indazol-5-yl)-2-phenylbut-1-en-1-yl)phenoxy)ethan-1-amine



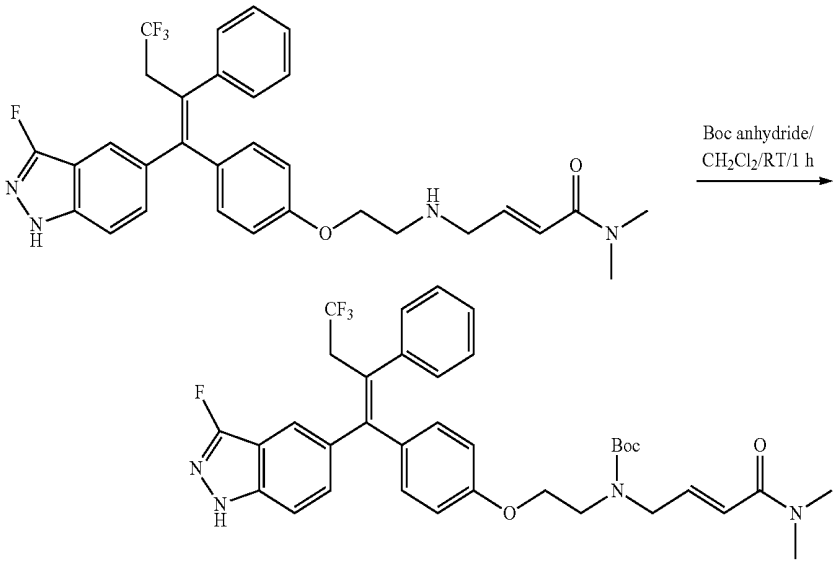
The reaction was carried out according to Scheme 2, Step-2 using tert-butyl (E)-(2-(4-(4,4,4-trifluoro-1-(3-fluoro-1-(tetrahydro-2H-pyran-2-yl)-1H-indazol-5-yl)-2-phenylbut-1-en-1-yl)phenoxy)ethyl)carbamate (1.5 g, 2.3 mmol) to afford crude title compound (1.1 g crude).

Step-3: Synthesis of (E)-N,N-dimethyl-4-((2-(4-((E)-4,4,4-trifluoro-1-(3-fluoro-1H-indazol-5-yl)-2-phenylbut-1-en-1-yl)phenoxy)ethyl)amino)but-2-enamide



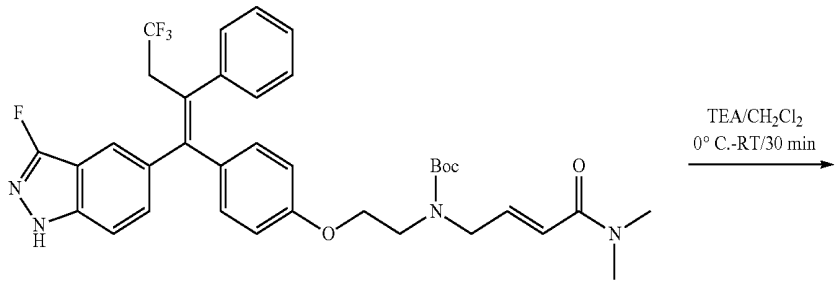
The reaction was carried out according to Scheme 2, Step-3 using (E)-2-(4-(4,4,4-trifluoro-1-(3-fluoro-1H-indazol-5-yl)-2-phenylbut-1-en-1-yl)phenoxy)ethan-1-amine (1.1 g, 2 mmol) and (E)-4-bromo-N,N-dimethylbut-2-enamide and (E)-4-chloro-N,N-dimethylbut-2-enamide mixture (0.41 g, 2 mmol, Example 63, Step-8). The crude material was used in next step without further purification (1.8 g, crude).

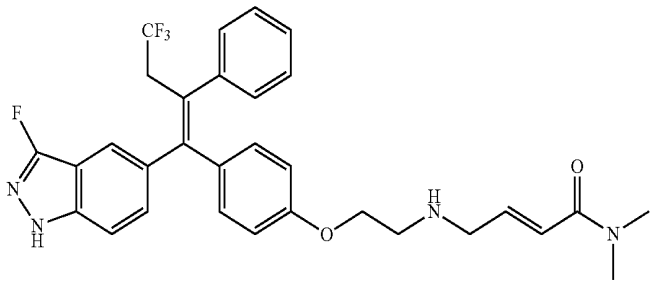
Step-4: Synthesis of tert-butyl ((E)-4-(dimethylamino)-4-oxobut-2-en-1-yl)(2-(4-((E)-4,4,4-trifluoro-1-(3-fluoro-1H-indazol-5-yl)-2-phenylbut-1-en-1-yl)phenoxy)ethyl)carbamate



The procedure described in Scheme 2, Step-5 was used with (E)-N,N-dimethyl-4-((2-(4-((E)-4,4,4-trifluoro-1-(3-fluoro-1H-indazol-5-yl)-2-phenylbut-1-en-1-yl)phenoxy)ethyl)amino)but-2-enamide (1.8 g, 3.18 mmol) to provide crude material, which was purified by silica gel chromatography using (2%) MeOH in dichloromethane to afford tert-butyl ((E)-4-(dimethylamino)-4-oxobut-2-en-1-yl)(2-(4-((E)-4,4,4-trifluoro-1-(3-fluoro-1H-indazol-5-yl)-2-phenylbut-1-en-1-yl)phenoxy)ethyl)carbamate (0.2 g).

Step-5: Synthesis of (E)-N,N-dimethyl-4-((2-(4-((E)-4,4,4-trifluoro-1-(3-fluoro-1H-indazol-5-yl)-2-phenylbut-1-en-1-yl)phenoxy)ethyl)amino)but-2-enamide





69

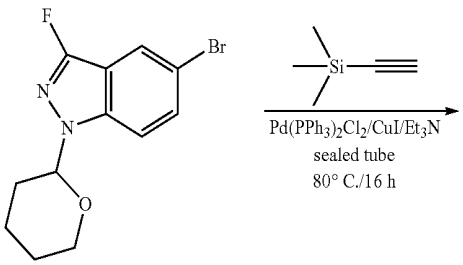
The reaction was carried out according to Scheme 2, Step-6b using tert-butyl ((E)-4-(dimethylamino)-4-oxobut-2-en-1-yl)(2-(4-((E)-4,4,4-trifluoro-1-(3-fluoro-1H-indazol-5-yl)-2-phenylbut-1-en-1-yl)phenoxy)ethyl)carbamate (0.2 g, 0.3 mmol) to afford crude compound, which was purified by preparative TLC to afford desired compound (E)-N,N-dimethyl-4-((2-(4-((E)-4,4,4-trifluoro-1-(3-fluoro-1H-indazol-5-yl)-2-phenylbut-1-en-1-yl)phenoxy)ethyl)amino)but-2-enamide (0.05 g, 29%).

Compound 69:

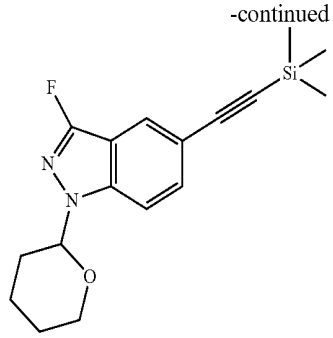
^{1}H NMR (400 MHz, $CDCl_3$): δ 9.40 (s, 1H), 7.66 (s, 1H), 7.39-7.15 (m, 7H), 6.91-6.86 (m, 1H), 6.79 (d, J=8.8 Hz, 2H), 6.56 (d, J=8.8 Hz, 2H), 6.44 (d, J=15.1 Hz, 1H), 3.95 (t, J=5.7 Hz, 2H), 3.46 (q, J=10.8 Hz, 2H), 3.32-3.29 (m, 2H), 3.06 (s, 3H), 3.00 (s, 3H), 2.95 (t, J=5.4 Hz, 2H). LCMS: 567.3 $[M+H]^+$.

Example 69A: Synthesis of (E)-N,N-dimethyl-4-((2-(4-((E)-4,4,4-trifluoro-1-(3-fluoro-1H-indazol-5-yl)-2-phenylbut-1-en-1-yl)phenoxy)ethyl)amino)but-2-enamide hydrochloride

Step-1A: Synthesis of 3-fluoro-1-(tetrahydro-2H-pyran-2-yl)-5-((trimethylsilyl)ethynyl)-1H-indazole

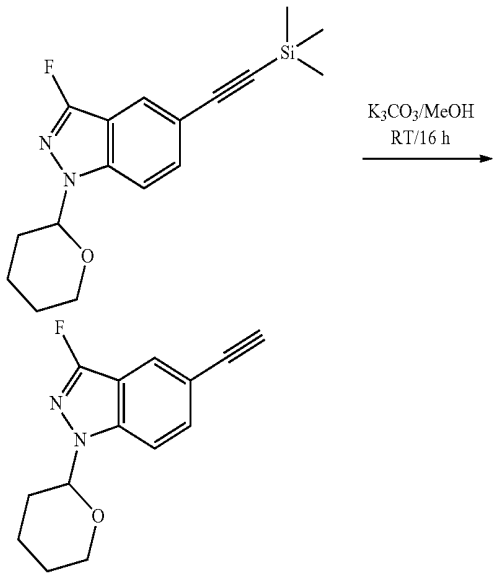


-continued



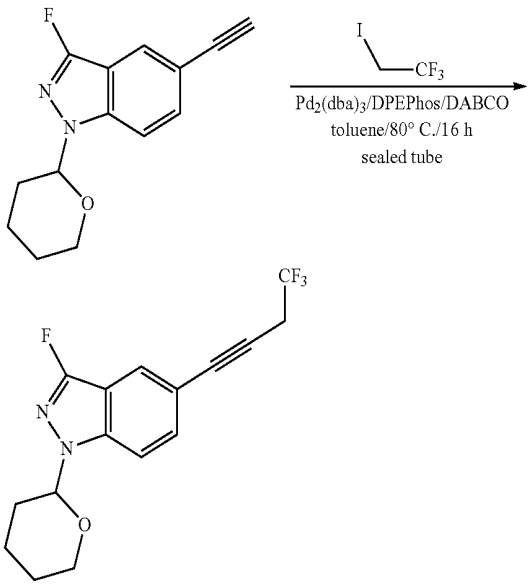
To a stirred solution of 5-bromo-3-fluoro-1-(tetrahydro-2H-pyran-2-yl)-1H-indazole (1.5 Kg, 5.014 mol) in Et_3N (10 L) in a sealed tube, was added copper iodide (95.5 g, 0.501 mol) at room temperature. This mixture was degassed with three vacuum/N_2 cycles, were added ethynyltrimethylsilane (0.73 Kg, 7.52 mol) followed by $Pd(PPh_3)_2Cl_2$ (175 g, 0.25 mol). The pressure tube was sealed and heated at 80° C. for 16 h. Upon completion by TLC, the reaction mixture was diluted with EtOAc (10 L), washed with water. The combined organic extracts were washed with brine, dried over anhydrous sodium sulphate and concentrated under reduced pressure to afford the crude product 3-fluoro-(tetrahydro-2H-pyran-2-yl)-5-((trimethylsilyl)ethynyl)-1H-indazole as dark brown oil (1.71 Kg, crude) 65.7% purity by HPLC.

Step-2A: Synthesis of 5-ethynyl-3-fluoro-1-(tetrahydro-2H-pyran-2-yl)-1H-indazole



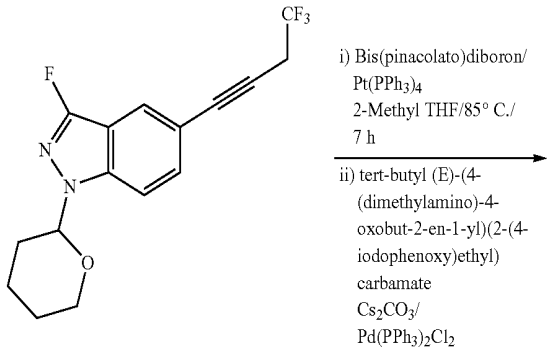
To a stirred solution of 3-fluoro-1-(tetrahydro-2H-pyran-2-yl)-5-((trimethylsilyl)ethynyl)-1H-indazole (1.7 Kg, 5.37 mol) in Methanol 12 L was added potassium carbonate (74.6 g, 0.53 mol), reaction mixture was stirred for 16 h at room temperature. After completion of reaction, methanol was evaporated, residue was diluted with ethyl acetate (6 L) and organic layer was washed with water followed by brine. The combined organic layer was dried over anhydrous Na_2SO_4 and concentrated under reduced pressure to obtain title compound (1.5 Kg crude) 72.3% purity by HPLC.

Step-3A: Synthesis of 3-fluoro-1-(tetrahydro-2H-pyran-2-yl)-5-(4,4,4-trifluorobut-1-yn-1-yl)-1H-indazole

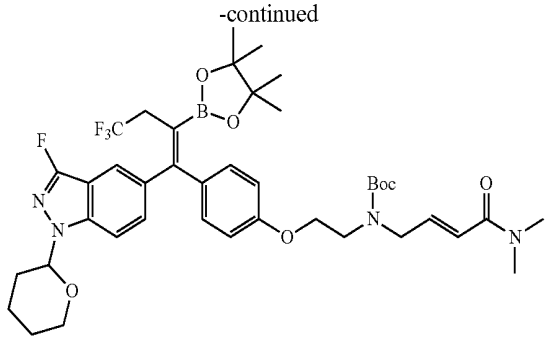


A mixture of $Pd_2(dba)_3$ (0.187 Kg, 0.204 mol), DPEphos (0.44 Kg, 0.818 mol) and DABCO (0.91 Kg, 0.818 mol) under nitrogen atmosphere in toluene (5 L) was added a solution of 5-ethynyl-3-fluoro-1-(tetrahydro-2H-pyran-2-yl)-1H-indazole (1 Kg, 4.093 mol) in toluene (5 L). Reaction mixture was degassed with nitrogen for 10 min, to the above mixture 1,1,1-trifluoro-2-iodoethane (1.71 Kg, 8.187 mol) was added. This mixture was again degassed with three vacuum/N_2 cycles, heated at 80° C. for 16 h. Upon completion by TLC, reaction mixture was cooled to room temperature, filtered through celite. Filtrate was diluted with water and extracted with EtOAc (2×3 L). The organic layer was dried over anhydrous sodium sulphate and concentrated under reduced pressure. The crude material was purified by column chromatography over 60-120 mesh silica-gel using 6% ethyl acetate in n-hexane as an eluent to afford 3-fluoro-1-(tetrahydro-2H-pyran-2-yl)-5-(4,4,4-trifluorobut-1-yn-1-yl)-1H-indazole (1.1 Kg, 82% yield, 78% purity by HPLC).

Step-4A: Synthesis of tert-butyl ((E)-4-(dimethylamino)-4-oxobut-2-en-1-yl)(2-(4-((Z)-4,4,4-trifluoro-1-(3-fluoro-1-(tetrahydro-2H-pyran-2-yl)-1H-indazol-5-yl)-2-(4,4,5,5-tetramethyl-1,3,2-dioxaborolan-2-yl)but-1-en-1-yl)phenoxy)ethyl) carbamate

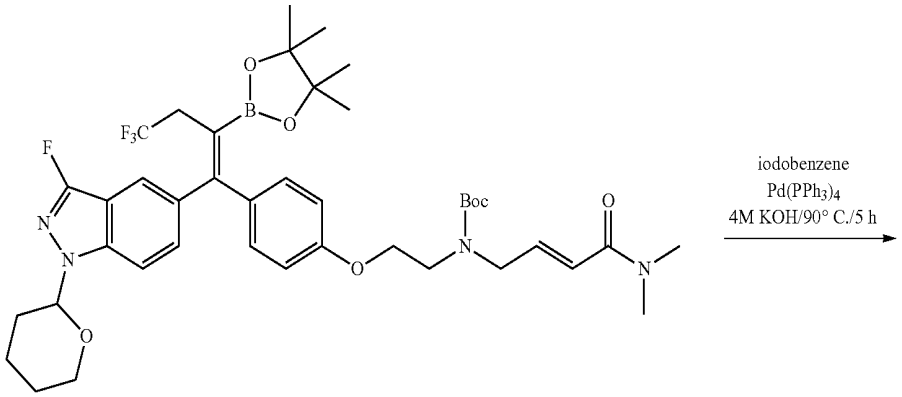


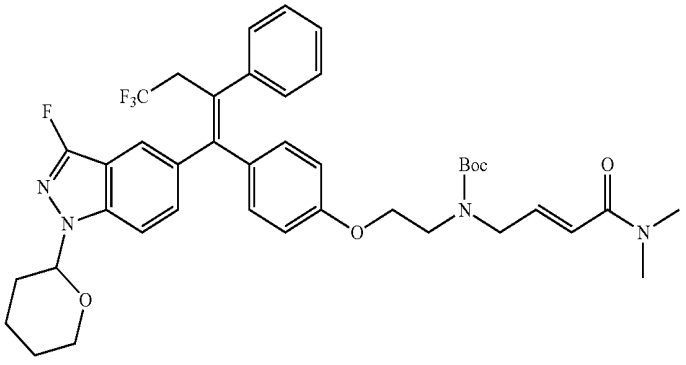
-continued



To a stirred solution of 3-fluoro-1-(tetrahydro-2H-pyran-2-yl)-5-(4,4,4-trifluorobut-1-yn-1-yl)-1H-indazole (500 g, 1.532 mol) in 2-methyl THF (2.5 L), was added bis(pinacolato)diboron (0.39 Kg, 1.532 mol), tetrakis(triphenylphosphine)platinum (0) (19 g, 0.0153 mol) under nitrogen atmosphere, reaction mixture was stirred at 85° C. for 7 h. The reaction mixture was allowed to cool to room temperature, tert-butyl (E)-(4-(dimethylamino)-4-oxobut-2-en-1-yl)(2-(4-iodophenoxy)ethyl)carbamate (0.62 Kg, 1.072 mol), bis (triphenylphosphine)palladium (II) dichloride (53.7 g, 0.076 mol), cesium carbonate (0.6 Kg, 3.064 mol), 2-methyl THF (5 L) and water (250 mL) were added. This mixture was degassed with nitrogen for 15 min, stirred at room temperature for 36 h. After completion of reaction, reaction mixture was cooled to room temperature, filtered through celite. Filtrate was diluted with water and extracted with EtOAc (2×3 L). The organic layer was dried over anhydrous sodium sulphate and concentrated under reduced pressure. The crude material was purified by column chromatography over 60-120 mesh silica-gel using 5% MeOH in dichloromethane as an eluent to afford tert-butyl ((E)-4-(dimethylamino)-4-oxobut-2-en-1-yl)(2-(4-((Z)-4,4,4-trifluoro-1-(3-fluoro-1-(tetrahydro-2H-pyran-2-yl)-1H-indazol-5-yl)-2-(4,4,5,5-tetramethyl-1,3,2-dioxaborolan-2-yl)but-1-en-1-yl)phenoxy)ethyl)carbamate (600 g, 49%), purity by HPLC 58%.

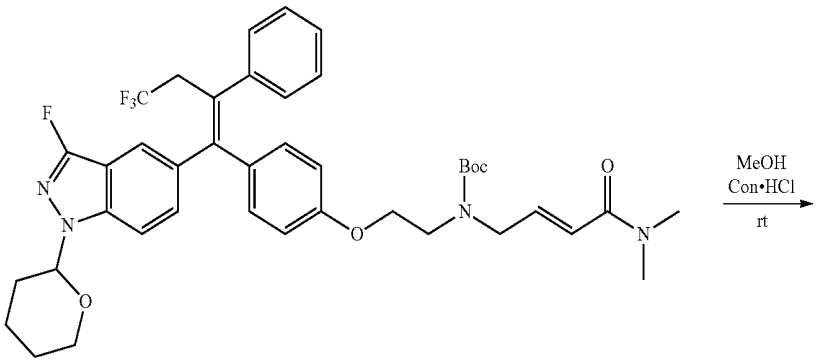
Step-5A: Synthesis of tert-butyl ((E)-4-(dimethylamino)-4-oxobut-2-en-1-yl)(2-(4-((E)-4,4,4-trifluoro-1-(3-fluoro-1-(tetrahydro-2H-pyran-2-yl)-1H-indazol-5-yl)-2-phenylbut-1-en-1-yl)phenoxy)ethyl) carbamate

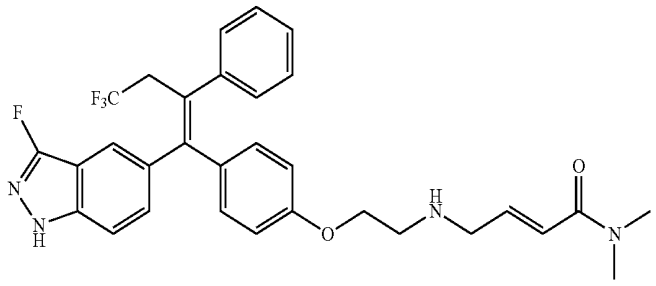




To a stirred solution of tert-butyl ((E)-4-(dimethylamino)-4-oxobut-2-en-1-yl)(2-(4-((Z)-4,4,4-trifluoro-1-(3-fluoro-1-(tetrahydro-2H-pyran-2-yl)-1H-indazol-5-yl)-2-(4,4,5,5-tetramethyl-1,3,2-dioxaborolan-2-yl)but-1-en-1-yl)phenoxy) ethyl)carbamate (600 g, 0.74 mol) in 2-methyl THF (6 L), was added to the above reaction mixture 4M KOH (1.2 L, 2 vol), tetrakis(triphenylphosphine)palladium(0) (43 g, 0.037 mol) and iodobenzene (128 g, 0.62 mol) were added. Reaction mixture was stirred at 90° C. for 5 h. After completion of reaction, reaction mixture was cooled to room temperature followed by filtered through celite. Filtrate was diluted with water and extracted with EtOAc (2×2 L). The organic layer was dried over anhydrous sodium sulphate and concentrated under reduced pressure to afford title compound tert-butyl ((E)-4-(dimethylamino)-4-oxobut-2-en-1-yl)(2-(4-((E)-4,4,4-trifluoro-1-(3-fluoro-1-(tetrahydro-2H-pyran-2-yl)-1H-indazol-5-yl)-2-phenylbut-1-en-1-yl)phenoxy) ethyl)carbamate (700 g, crude) 48% purity by HPLC.

Step-6A. Synthesis of (E)-N,N-dimethyl-4-((2-(4-((E)-4,4,4-trifluoro-1-(3-fluoro-1H-indazol-5-yl)-2-phenylbut-1-en-1-yl)phenoxy)ethyl)amino)but-2-enamide

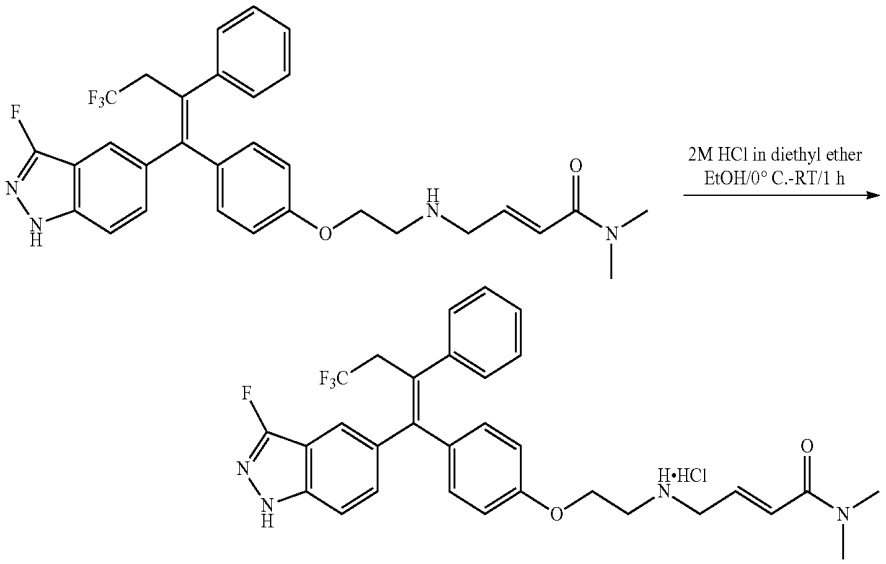




To a stirred solution of tert-butyl ((E)-4-(dimethylamino)-4-oxobut-2-en-1-yl)(2-(4-((E)-4,4,4-trifluoro-1-(3-fluoro-1-(tetrahydro-2H-pyran-2-yl)-1H-indazol-5-yl)-2-phenylbut-1-en-1-yl)phenoxy)ethyl)carbamate (700 g, 0.93 mol) in methanol (3.5 L) was added at 0° C., conc.HCl (2.1 L, 3 vol). The reaction mixture was stirred for 16 h at room temperature. After completion of reaction, reaction mixture was concentrated under reduced pressure. Gummy reaction mass was basified with saturated Na_2CO_3, extracted with dichloromethane (3×2 L). Combined organic layers were dried over anhydrous sodium sulphate and concentrated under reduced pressure to afford crude compound, which was purified by column chromatography over 60-120 mesh silica-gel using 5-7% MeOH in dichloromethane to afford desired compound (E)-N,N-dimethyl-4-((2-(4-((E)-4,4,4-trifluoro-1-(3-fluoro-1H-indazol-5-yl)-2-phenylbut-1-en-1-yl)phenoxy)ethyl)amino)but-2-enamide (260 g,) 65.3% pure by HPLC.

Obtained compound was further purified by combi flash column chromatography to afford the tittle compound with >92% HPLC.

Step-7A: Synthesis of (E)-N,N-dimethyl-4-((2-(4-((E)-4,4,4-trifluoro-1-(3-fluoro-1H-indazol-5-yl)-2-phenylbut-1-en-1-yl)phenoxy)ethyl)amino)but-2-enamide hydrochloride

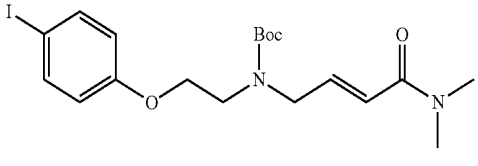


To a stirred solution of (E)-N,N-dimethyl-4-((2-(4-((E)-4,4,4-trifluoro-1-(3-fluoro-1H-indazol-5-yl)-2-phenylbut-1-en-1-yl)phenoxy)ethyl)amino)but-2-enamide (5.6 g, 9.88 mmol) in ethanol (6.6 mL) was added 2M HCl in diethyl ether (56 mL) at 0° C. A white solid was observed after stirring for 1 h at room temperature. Reaction mixture was concentrated under vacuum at 30° C. to remove the excess of ether HCl and ethanol. The solid obtained was dried at 50° C. for 1 h, the residue was triturated with diethyl ether and ether layer was decanted (500 mL×3). Solid obtained was co-distilled with ethyl acetate (300 mL×4), followed by triturated with ethyl acetate (500 mL), filtered and dried under reduced pressure to obtain the title compound (E)-N,N-dimethyl-4-((2-(4-((E)-4,4,4-trifluoro-1-(3-fluoro-1H-indazol-5-yl)-2-phenylbut-1-en-1-yl)phenoxy)ethyl)amino)but-2-enamide hydrochloride (5.4 g, 90%).

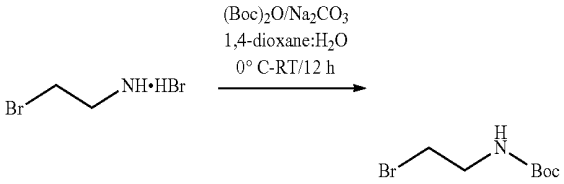
Compound 69 (Hydrochloride Salt):

^{1}H NMR (400 MHz, DMSO-d_6): δ 12.70 (s, 1H), 9.15 (s, 2H), 7.57 (s, 1H), 7.54 (m, 2H), 7.25-7.14 (m, 6H), 6.86-6.79 (m, 3H), 6.69 (d, J=5.8 Hz, 2H), 6.61-6.54 (m, 1H), 4.13 (t, J=4.4 Hz, 2H), 3.79 (m, 2H), 3.48-3.37 (m, 2H), 3.26 (m, 2H) 3.03 (s, 3H), 2.87 (s, 3H). LCMS: 567.2 $[M+H]^+$.

Steps 8A-12A report synthesis of the intermediate tert-butyl (E)-(4-(dimethylamino)-4-oxobut-2-en-1-yl)(2-(4-iodophenoxy)ethyl)carbamate Step 8A: Synthesis of tert-butyl (E)-(4-(dimethylamino)-4-oxobut-2-en-1-yl)(2-(4-iodophenoxy)ethyl)carbamate

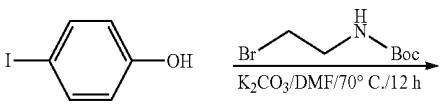


Step-9A: Synthesis of tert-butyl (2-bromoethyl)carbamate

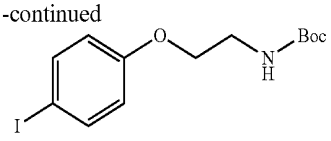


Bromoethylamine hydrobromide (1 Kg, 4.88 mol) was added to a stirred solution of sodium carbonate (1.55 Kg, 14.6 mol), di-t-butyl dicarbonate (1.6 Kg, 7.32 mol) in 1,4-dioxane-water mixture (2:1, 3 L) at 0° C. and the mixture was stirred at room temperature for 12 h. After completion of reaction, excess of 1,4-dioxane was removed under reduced pressure. Reaction mixture was extracted with ethylacetate (2×4 L), organic layer was washed with water followed by brine, dried over anhydrous sodium sulphate, filtered and concentrated under reduced pressure. The crude product was used in next step without further purification (1.1 Kg, %). ^{1}H NMR (400 MHz, DMSO-d_6): δ 7.07 (bs, 1H), 3.42 (t, 2H), 3.31 (t, 2H), 1.38 (s, 9H).

Step-10A. Synthesis of tert-butyl (2-(4-iodophenoxy)ethyl)carbamate

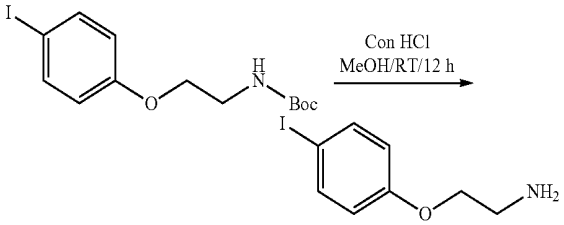


-continued



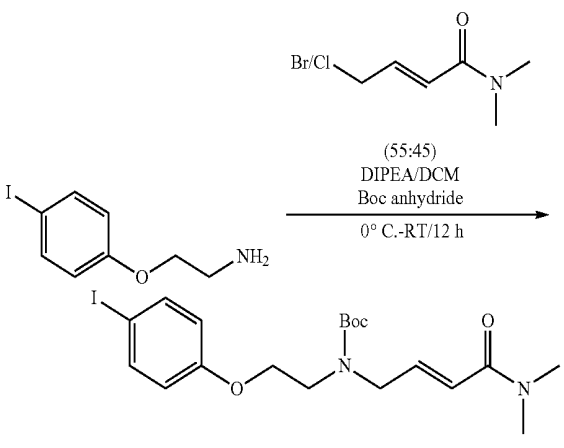
To a stirred solution of 4-iodophenol (1 Kg, 4.54 mol) in DMF (15 L) was added potassium carbonate (1.8 Kg, 13.6 mol) and stirred for 30 min at room temperature, to the above mixture tert-butyl (2-bromoethyl)carbamate (1.48 Kg, 6.36 mol) was added. The contents were stirred at 70° C. for 12 h. After completion of reaction, reaction mixture was poured onto ice cold water, solid separated was filtered and dried under reduced pressure to obtain desired compound tert-butyl (2-(4-iodophenoxy)ethyl)carbamate as an off-white solid (1.4 Kg, 84%). ^{1}H NMR (400 MHz, DMSO-d_6): δ 7.58 (d, J=8.8 Hz, 2H), 7.01 (t, J=5.2 Hz, 1H), 7.78 (d, J=8.8 Hz, 2H), 3.92 (t, J=5.6 Hz, 2H), 1.37 (s, 9H).

Step-11A: Synthesis of 2-(4-iodophenoxy)ethan-1-amine



To a stirred solution of tert-butyl (2-(4-iodophenoxy) ethyl)carbamate (1.4 Kg, 3.85 mol) in methanol (10 L) was added at 0° C., Con.HCl (2.8 L). The reaction mixture was stirred for 12 h at room temperature. After completion of reaction, methanol was evaporated, residue was basified with saturated Na_2CO_3, extracted with 10% MeOH in DCM. Organic layer was concentrated under reduced pressure and the crude material was used in next step without further purification (700 g, 70% yield, 98% pure by HPLC). ^{1}H NMR (400 MHz, DMSO-d_6): δ 7.59-7.55 (m, 2H), 6.80-6.76 (m, 2H), 3.88 (t, J=5.8 Hz, 2H), 3.85 (t, J=6.0 Hz, 2H), 1.61 (bs, 2H).

Step-12A: Synthesis of (E)-4-((2-(4-iodophenoxy) ethyl)amino)-N,N-dimethylbut-2-enamide



To a stirred solution of 2-(4-iodophenoxy)ethan-1-amine (700 g, 2.66 mol) in DCM (4 L) was added DIPEA (1 L, 7.98 mol) and cooled to 0° C. Then, (E)-4-bromo-(chloro)-N,N-dimethylbut-2-enamide (505 g, 2.66 mol) in DCM (2 L) was added dropwise at 0° C. The reaction mixture was stirred for 12 h at room temperature. After that, reaction mixture was cooled to 0° C. and Boc anhydride (870 g, 3.9 mol) in DCM (2 L) was added dropwise and stirred at room temperature for 12 h. Upon completion by TLC, the reaction mixture was cooled to 0° C., quenched with ice cold water (5 L) and extracted with dichloromethane (2 L). The combined organic extracts were washed with water, followed by brine, dried over anhydrous sodium sulphate and concentrated under reduced pressure. The crude material was purified by column chromatography over 60-120 mesh silica using 20% EtOAc in Hexane as an eluent to afford tert-butyl (E)-(4-(dimethylamino)-4-oxobut-2-en-1-yl)(2-(4-iodophenoxy) ethyl)carbamate (480 g, 37% yield). 69% pure by HPLC. ^{1}H NMR (400 MHz, DMSO-d_6): δ 7.58 (d, J=8.8 Hz, 2H), 6.79 (d, J=6.8 Hz, 2H), 6.51-6.39 (m, 2H), 4.0-3.99 (m, 2H), 3.95 (t, J=5.6 Hz, 2H), 3.38 (d, J=5.6 Hz, 2H), 2.96 (s, 3H), 2.84 (s, 3H), 1.37 (s, 9H). LCMS: 595.4 $[M+H]^+$.

Example 70

There is no Example 70.

Example 71

There is no Example 71.

Example 72: Synthesis of (E)-4-((2-((5-((Z)-2-cyclobutyl-1-(3-fluoro-1H-indazol-5-yl)-2-phenylvinyl)pyridin-2-yl)oxy)amino)-N,N-dimethylbut-2-enamide (Compound 72)

The compound was synthesized following the approach as outlined in Example 14 by substituting into Step-4 tert-butyl (E)-(4-(dimethylamino)-4-oxobut-2-en-1-yl)(2-((5-iodopyridin-2-yl)oxy)ethyl)carbamate (as prepared in Example 25, Step-2) for compound 234 and substituting Step-5 with the reaction conditions described in Scheme 2, Step-6b to deliver Compound 72 (0.09 g, 11%).

Compound 72:

^{1}H NMR (400 MHz, DMSO-d_6): δ 12.59 (s, 1H), 7.67 (d, J=2.0 Hz, 1H), 7.54 (s, 1H), 7.49 (dd, J_1=8.8 Hz, J_2=1.6 Hz, 1H), 7.28-7.12 (m, 7H), 6.61-6.44 (m, 3H), 4.09 (t, J=6.0 Hz, 2H), 3.42-3.38 (m, 1H), 3.28-3.27 (m, 2H), 2.97 (s, 3H), 2.83 (s, 3H), 2.73 (t, J=5.8 Hz, 2H), 1.83-1.76 (m, 4H), 1.63-1.58 (m, 1H), 1.35-1.33 (m, 1H). LCMS: 540.3 $[M+H]^+$.

Example 73: Synthesis of (E)-4-((2-(4-((E)-2-(2-chlorophenyl)-1-(3-fluoro-1H-indazol-5-yl)but-1-en-1-yl)phenoxy)ethyl)amino)-N,N-dimethylbut-2-enamide (Compound 73)

The compound was synthesized following the approach as outlined in Example 60 by substituting into Step-1 (i) 5-(but-1-yn-1-yl)-3-fluoro-1-(tetrahydro-2H-pyran-2-yl)-1H-indazole (as prepared in Example 2, Step-3) for compound 275, (ii) tert-butyl (E)-(4-(dimethylamino)-4-oxobut-2-en-1-yl)(2-(4-iodophenoxy)ethyl)carbamate (as prepared in Example 14, Step-3) for compound 263, and (iii) 1-chloro-2-iodobenzene for compound 264 to deliver Compound 73 (0.23 g, 5.6%) as an off-white solid.

Compound 73:

^{1}H NMR (400 MHz, DMSO-d_6): δ 12.59 (s, 1H), 7.54 (s, 1H), 7.49 (dd, J_1=8.8 Hz, J_2=2.0 Hz, 1H), 7.35 (dd, J_1=7.4 Hz, J_2=1.4 Hz, 1H), 7.27-7.16 (m, 4H), 6.83 (d, J=8.8 Hz, 2H), 6.60 (d, J=8.8 Hz, 2H), 6.57-6.47 (m, 2H), 3.86 (t, J=5.6 Hz, 2H), 2.98 (s, 3H), 2.84 (s, 3H), 2.77 (t, J=5.4 Hz, 2H), 2.43-2.32 (m, 4H), 0.88 (t, J=7.4 Hz, 3H). LCMS: 547.2 $[M+H]^+$

Example 74: Synthesis of (E)-4-((2-(4-((E)-2-(2-chloro-4-fluorophenyl)-1-(1H-indazol-5-yl)but-1-en-1-yl)phenoxy)ethyl)amino)-N,N-dimethylbut-2-enamide (Compound 74)

The compound was synthesized following the approach as outlined in Example 60 by substituting into Step-1 (i) 5-(but-1-yn-1-yl)-1-(tetrahydro-2H-pyran-2-yl)-1H-indazole (as prepared in Example 1, Step-3) for compound 275, (ii) tert-butyl (E)-(4-(dimethylamino)-4-oxobut-2-en-1-yl)(2-(4-iodophenoxy)ethyl)carbamate (as prepared in Example 14, Step-3) for compound 263 and (iii) 2-chloro-4-fluoro-1-iodobenzene for compound 264 to isolate Compound 74 (0.26 g, 31%).

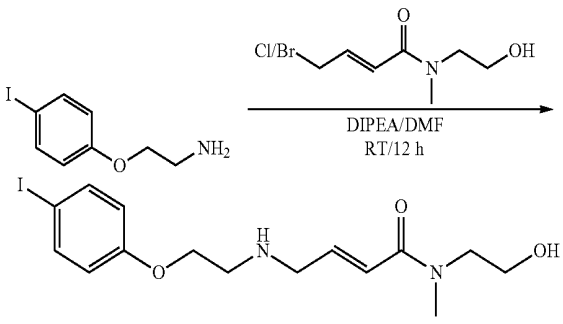
Compound 74:

^{1}H NMR (400 MHz, DMSO-d_6): δ 13.08 (s, 1H), 8.08 (s, 1H), 7.65 (s, 1H), 7.53 (d, J=8.8 Hz, 1H), 7.34-7.17 (m, 2H), 7.16-7.10 (m, 2H), 6.81 (d, J=8.8 Hz, 2H), 6.62-6.47 (m, 4H), 3.86 (t, J=5.6 Hz, 2H), 2.98 (s, 3H), 2.83 (s, 3H), 2.76 (t, J=5.4 Hz, 2H), 2.38-2.33 (m, 3H), 0.88 (t, J=7.4 Hz, 3H). LCMS: 547.3 $[M+H]^+$.

Example 75: Synthesis of (E)-4-((2-(4-((E)-1-(3-fluoro-1H-indazol-5-yl)-2-(pyridin-4-yl)but-1-en-1-yl)phenoxy)ethyl)amino)-N-(2-hydroxyethyl)-N-methylbut-2-enamide (Compound 75)

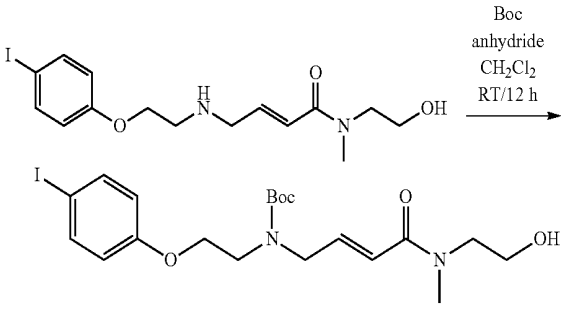
The compound was synthesized following the approach as outlined in Example 14 by (a) substituting into Step-4 (i) (Z)-5-(1,2-bis(4,4,5,5-tetramethyl-1,3,2-dioxaborolan-2-yl)but-1-en-1-yl)-3-fluoro-1-(tetrahydro-2H-pyran-2-yl)-1H-indazole (as prepared in Example 3, Step-1) for compound 233, (ii) tert-butyl (E)-(4-((2-hydroxyethyl)(methyl)amino)-4-oxobut-2-en-1-yl)(2-(4-iodophenoxy)ethyl)carbamate (preparation shown below in Ex. 75 Step 1-2) for compound 234, (iii) 4-iodopyridine for compound 262, and (b) substituting the reaction conditions described in Scheme 2, Step-6b in Ex.14 Step-5 to afford Compound 75 (0.1 g, 20.6%).

Step-1: Synthesis of (E)-N-(2-hydroxyethyl)-4-((2-(4-iodophenoxy)ethyl)amino)-N-methylbut-2-enamide



The reaction was carried out according to Scheme 3, Step-3 using 2-(4-iodophenoxy)ethan-1-amine (7.3 g, 27 mmol, Example 14, Step-3) for compound 217 and (E)-4-bromo-N-(2-hydroxyethyl)-N-methylbut-2-enamide for compound 214 and (E)-4-chloro-N-(2-hydroxyethyl)-N-methylbut-2-enamide (5 g, 27 mmol, Example 50, Step-1) for compound 214. The crude material was used in next step without further purification (9.5 g, crude).

Step-2: Synthesis of tert-butyl (E)-(4-((2-hydroxyethyl)(methyl)amino)-4-oxobut-2-en-1-yl)(2-(4-iodophenoxy)ethyl)carbamate



The reaction was carried out according to Scheme 3, Step-4 using (E)-N-(2-hydroxyethyl)-4-((2-(4-iodophenoxy)ethyl)amino)-N-methylbut-2-enamide (9.5 g, 23.5 mmol) for compound 218. The crude material was purified by column chromatography over 230-400 mesh silica using 3% MeOH in dichloromethane as an eluent to afford the title compound of Ex. 75 Step-2 (2.5 g, 21%).

Compound 75:

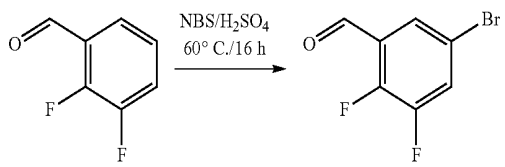
^{1}H NMR (400 MHz, DMSO-d_6): δ 12.60 (s, 1H), 8.38 (dd, J_1=4.4 Hz, J_2=1.7 Hz, 1H), 7.53 (s, 1H), 7.49 (d, J=1.6 Hz, 1H), 7.47 (d, J=2.0 Hz, 1H), 7.22 (d, J=1.6 Hz, 1H), 7.20 (d, J=1.6 Hz, 1H), 7.13 (dd, J_1=4.2 Hz, J_2=1.4 Hz, 2H), 6.79 (d, J=8.8 Hz, 2H), 6.65 (d, J=8.8 Hz, 2H), 6.60-6.51 (m, 2H), 3.88 (t, J=5.4 Hz, 2H), 3.50-3.48 (m, 2H), 3.47-3.34 (m, 2H), 3.03-2.85 (m, 4H), 2.86-2.78 (m, 2H), 2.42 (q, J=7.4 Hz, 2H), 0.87 (t, J=7.2 Hz, 3H).

LCMS: 544.3 $[M+H]^+$.

Example 76: Synthesis of (E)-4-((2-(4-((E)-1-(7-fluoro-1H-indazol-5-yl)-2-phenylbut-1-en-1-yl)phenoxy)ethyl)amino)-N,N-dimethylbut-2-enamide (Compound 76)

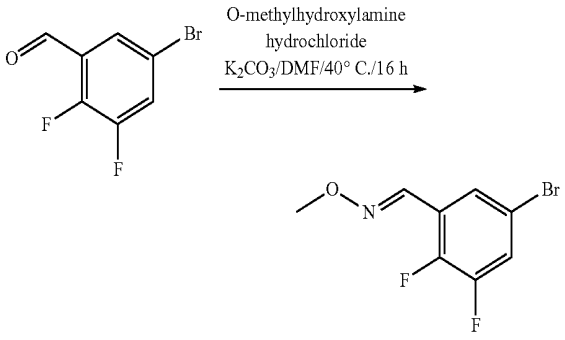
The compound was synthesized following the approach as outlined in Example 14 by substituting into Step-2 5-(but-1-yn-1-yl)-7-fluoro-1-(tetrahydro-2H-pyran-2-yl)-1H-indazole (preparation shown below in Ex. 76 Step 1-5) for compound 271 and substituting Step-5 with reaction conditions outlined in Scheme 2, Step-6c to deliver Compound 76 (0.195 g, 17.7%) as an off-white solid.

Step-1: Synthesis of 5-bromo-2,3-difluorobenzaldehyde



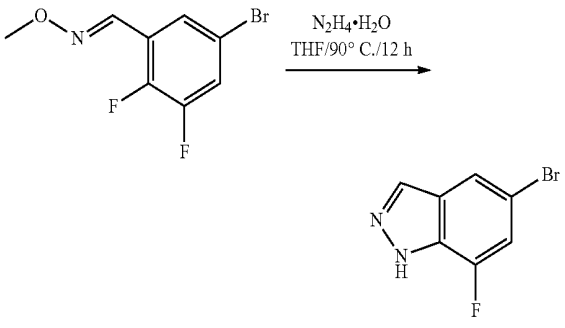
To a stirred solution of 2,3-difluorobenzaldehyde (30 g, 211 mmol) in H_2SO_4 (120 mL) was added N-bromo succinamide (45 g, 253 mmol) at 0° C. The reaction mixture was stirred for 16 h at 60° C., after completion of reaction (monitored by TLC), the reaction mixture was diluted with EtOAc. Organic layer was washed with water followed by brine, dried over anhydrous sodium sulphate, filtered and concentrated under reduced pressure. The crude product was purified by column chromatography by using 0.8% EtOAc in n-hexane to afford 5-bromo-2,3-difluorobenzaldehyde (11.7 g, 23.5%) as a white solid.

Step-2: Synthesis of (E)-5-bromo-2,3-difluorobenzaldehyde O-methyl oxime



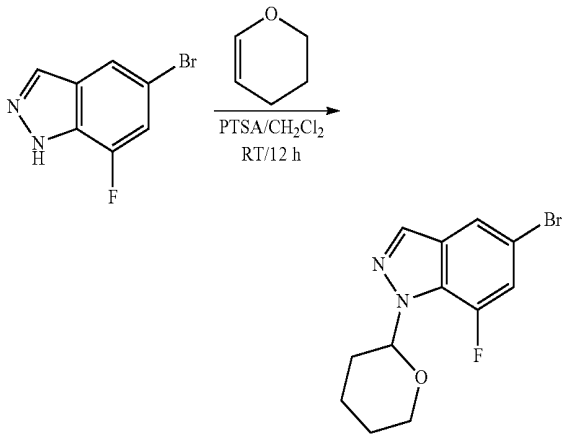
To a stirred solution of 5-bromo-2,3-difluorobenzaldehyde (2 g, 9 mmol) in DMF (20 mL) was added O-methylhydroxylamine hydrochloride (1.51 g, 18 mmol) and K_2CO_3 (2.75 g, 19.9 mmol), contents were stirred at 40° C. for 16 h. After completion of reaction (monitored by TLC), the reaction mixture was cooled to 0° C., diluted with ethyl acetate and the organic layer was washed with water followed by brine. The organic layer was dried over anhydrous Na_2SO_4 and concentrated under reduced pressure. The crude compound was purified by combi-flash using 2% ethyl acetate in n-hexane as an eluent to obtain title compound of Ex. 76 Step-2 (1 g, 44%).

Step-3: Synthesis of 5-bromo-7-fluoro-1H-indazole



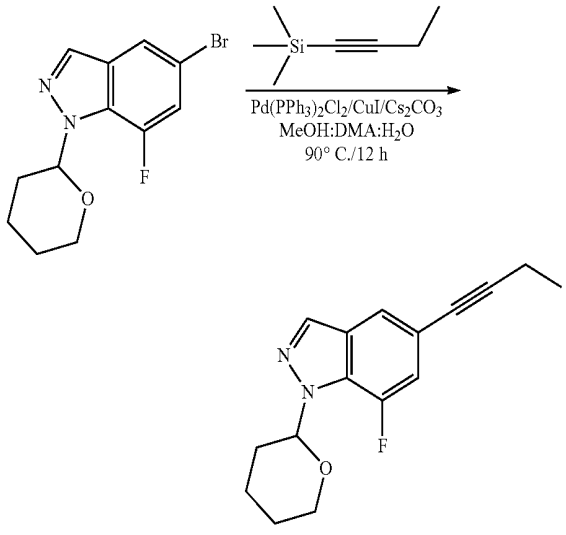
To a stirred solution of (E)-5-bromo-2,3-difluorobenzaldehyde O-methyl oxime (1 g, 4 mmol) in THF (10 mL) was added hydrazine hydrate (4 mL), contents were stirred at 90° C. for 12 h. After completion of reaction (monitored by TLC), the reaction mixture was cooled to 0° C., diluted with ethyl acetate and the organic layer was washed with water followed by brine. The organic layer was dried over anhydrous Na_2SO_4 and concentrated under reduced pressure. The crude compound was purified by combi-flash using 10% ethyl acetate in n-hexane as an eluent to obtain title compound of Ex. 76 Step-3 (0.2 g, 21%).

Step-4: Synthesis of 5-bromo-7-fluoro-1-(tetrahydro-2H-pyran-2-yl)-1H-indazole



The reaction was carried out according to Scheme 1, Step-1 using 5-bromo-7-fluoro-1H-indazole (1.82 g, 8.46 mmol). The crude compound was purified by combi-flash using 5% ethyl acetate in n-hexane as an eluent to obtain the title compound of Ex. 76 Step-4 (2.39 g, 94%).

Step-5: Synthesis of 5-(but-1-yn-1-yl)-7-fluoro-1-(tetrahydro-2H-pyran-2-yl)-1H-indazole



The reaction was carried out according to Scheme 1, Step-2 using 5-bromo-7-fluoro-1-(tetrahydro-2H-pyran-2-yl)-1H-indazole (4.49 g, 15 mmol) and but-1-yn-1-yltrimethylsilane (3.8 g, 30 mmol, Example 1, Step-2). The crude product was purified over 230-400 mesh silica column chromatography using 20% ethyl acetate in n-hexane to afford the title compound of Ex. 76 Step-5 (3.2 g).

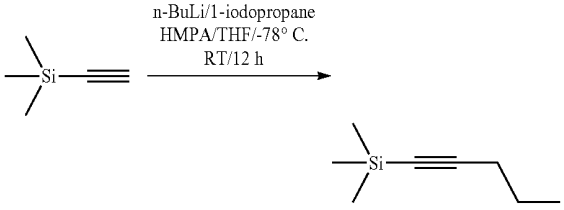
Compound 76:

^{1}H NMR (400 MHz, DMSO-d_6): δ 13.66 (s, 1H), 8.19 (d, J=2.4 Hz, 1H), 7.48 (s, 1H), 7.22-7.21 (m, 2H), 7.19-7.11 (m, 3H), 6.90 (d, J=12.0 Hz, 1H), 6.76 (d, J=8.4 Hz, 2H), 6.63-6.59 (m, 3H), 6.57-6.47 (m, 1H), 3.87 (t, J=5.4 Hz, 2H), 3.37-3.30 (m, 2H), 2.98 (s, 3H), 2.84 (s, 3H), 2.77 (t, J=5.6 Hz, 2H), 2.41 (q, J=7.2 Hz, 2H), 2.32-2.10 (m, 1H), 0.87 (t, J=7.2 Hz, 3H). LCMS: 513.3 $[M+H]^+$.

Example 77: Synthesis of (E)-4-((2-(4-((E)-1-(3-fluoro-1H-indazol-5-yl)-2-phenylpent-1-en-1-yl) phenoxy)ethyl)amino)-N,N-dimethylbut-2-enamide (Compound 77)

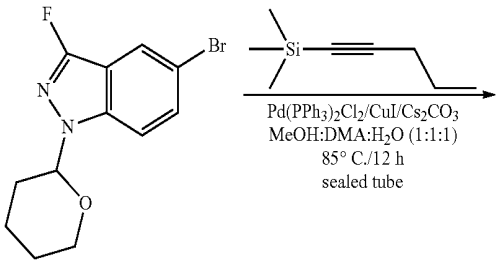
The compound was synthesized following the approach as outlined in Example 59 by (i) substituting into Step-4 3-fluoro-5-(pent-1-yn-1-yl)-1-(tetrahydro-2H-pyran-2-yl)-1H-indazole (preparation shown below in Ex. 77 Step 1-2) for compound 276 and tert-butyl (E)-(4-(dimethylamino)-4-oxobut-2-en-1-yl)(2-(4-iodophenoxy)ethyl)carbamate (as prepared in Example 14, Step-3) for compound 277 and (ii) substituting into Step-5 iodobenzene for compound 265 to afford Compound 77 (0.06 g, 19.3%) as an off-white solid.

Step-1: Synthesis of trimethyl(pent-1-yn-1-yl)silane

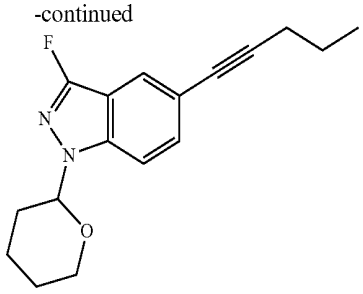


To a stirred solution of (trimethylsilyl)acetylene (29 g, 295 mmol) in dry THF (100 mL) was added n-BuLi (2.5M in THF, 125 mL) at −78° C. over 2 h. The resulting mixture was warmed to 0° C. and stirred for 10 min. The reaction mixture was again cooled to −78° C., HMPA (58 g, 324 mmol) was added to the above mixture and stirred at −78° C. for 30 min. To the above reaction mixture 1-iodopropane (53 g, 315 mmol) was added and the resulting mixture was stirred at room temperature for 12 h. After completion of reaction, the reaction mixture was quenched with water, extracted with ethyl acetate (500 mL). The organic layer was washed with brine, dried over anhydrous sodium sulphate and concentrated under reduced pressure. The product but-1-yn-1-yltrimethylsilane was distilled between 110-160° C. to afford the desired product (38 g).

Step-2: Synthesis of 3-fluoro-5-(pent-1-yn-1-yl)-1-(tetrahydro-2H-pyran-2-yl)-1H-indazole



-continued



The reaction was carried out according to Scheme 1, Step-2 using 5-bromo-3-fluoro-1-(tetrahydro-2H-pyran-2-yl)-1H-indazole (4 g, 13.4 mmol, Example 2, Step-2) for compound 202 and trimethyl(pent-1-yn-1-yl)silane (2.8 g, 20.1 mmol) for compound 203. The crude product was purified over 230-silica gel chromatography using 5% ethyl acetate in n-hexane to afford 3-fluoro-5-(pent-1-yn-1-yl)-1-(tetrahydro-2H-pyran-2-yl)-1H-indazole (1.18 g, 30.8%).

Compound 77:

^{1}H NMR (400 MHz, DMSO-d_6): δ 12.56 (s, 1H), 7.49 (s, 1H), 7.47 (d, J=6.8 Hz, 1H), 7.46-7.11 (m, 6H), 6.77 (d, J=8.8 Hz, 2H), 6.62-6.48 (m, 4H), 3.87 (t, J=5.6 Hz, 2H), 3.33-3.31 (m, 2H), 2.98 (s, 3H), 2.84 (s, 3H), 2.78 (t, J=5.6 Hz, 2H), 2.36-2.32 (m, 2H), 1.29-1.23 (m, 2H), 0.74 (t, J=7.4 Hz, 3H). LCMS: 527.3 $[M+H]^+$.

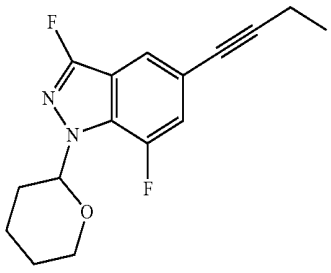
Example 78

There is no Example 78.

Example 79: Synthesis of (E)-4-((2-(4-((E)-1-(3, 7-difluoro-1H-indazol-5-yl)-2-phenylbut-1-en-1-yl) phenoxy)ethyl)amino)-N,N-dimethylbut-2-enamide (Compound 79)

The compound was synthesized following the approach as outlined in Example 14 by substituting into Step-2 5-(but-1-yn-1-yl)-3,7-difluoro-1-(tetrahydro-2H-pyran-2-yl)-1H-indazole (preparation shown below in Ex. 79 Step-1) for compound 271 and substituting Step-5 of Ex. 14 with reaction conditions described in Scheme 2, Step-6b to isolate Compound 79 (0.046 g) as an off-white solid.

Step-1: Synthesis of 5-(but-1-yn-1-yl)-3, 7-difluoro-1-(tetrahydro-2H-pyran-2-yl)-1H-indazole



The compound was synthesized following the approach as outlined in Example 2 by substituting into Step-1 5-bromo-7-fluoro-1-(tetrahydro-2H-pyran-2-yl)-1H-indazole for compound 270 and continuing with Steps 2-3 of Ex. 2 to deliver the title compound of Ex. 79 Step-1 (0.78 g, 76%).

Compound 79:

^{1}H NMR (400 MHz, DMSO-d_6): δ 13.20 (s, 1H), 7.40 (s, 1H), 7.22-7.21 (m, 2H), 7.19-7.11 (m, 3H), 6.90 (d, J=12.0 Hz, 1H), 6.8 (d, J=8.4 Hz, 2H), 6.63-6.59 (m, 3H), 6.57-6.47 (m, 1H), 3.87 (t, J=5.4 Hz, 2H), 3.37-3.30 (m, 2H), 2.98 (s, 3H), 2.84 (s, 3H), 2.77 (t, J=5.6 Hz, 2H), 2.41 (q, J=7.2 Hz, 2H), 0.87 (t, J=7.2 Hz, 3H) LCMS: 531.3 $[M+H]^+$.

Example 80: Synthesis of (E)-4-((2-(4-((E)-2-(2,5-difluorophenyl)-1-(3-fluoro-1H-indazol-5-yl)but-1-en-1-yl)phenoxy)ethyl)amino)-N,N-dimethylbut-2-enamide (Compound 80)

The compound was synthesized following the approach as outlined in Example 14 by substituting into Step-4 (i) (Z)-5-(1,2-bis(4,4,5,5-tetramethyl-1,3,2-dioxaborolan-2-yl) but-1-en-1-yl)-3-fluoro-1-(tetrahydro-2H-pyran-2-yl)-1H-indazole (as prepared in Example 3, Step-1) for compound 233, (ii) tert-butyl (E)-(4-(dimethylamino)-4-oxobut-2-en-1-yl)(2-(4-iodophenoxy)ethyl)carbamate (as prepared in Example 14, Step-3) for compound 234, (iii) 1,4-difluoro-2-iodobenzene for compound 262 and (iv) substituting Ex. 14 Step-5 with reaction conditions described in Scheme 2, Step-6b to isolate Compound 80 (0.16 g, 23.7%) as an off-white solid.

Compound 80:

^{1}H NMR (400 MHz, DMSO-d_6): δ 12.60 (s, 1H), 7.52 (s, 1H), 7.49 (dd, J_1=8.8 Hz, J_2=1.2 Hz, 1H), 7.23-7.12 (m, 1H), 7.11-7.02 (m, 3H), 6.83 (d, J=8.4 Hz, 2H), 6.65 (d, J=8.4 Hz, 2H), 6.62-6.48 (m, 2H), 3.88 (t, J=5.6 Hz, 2H), 3.32-3.31 (m, 2H), 2.99 (s, 3H), 2.84 (s, 3H), 2.79 (t, J=5.4 Hz, 2H), 2.35 (q, J=7.0 Hz, 2H), 0.91 (t, J=7.4 Hz, 3H). LCMS: 549.3 $[M+H]^+$.

Example 81: Synthesis of (E)-4-((2-(4-((E)-1-(3-fluoro-1H-indazol-5-yl)-2-(3-fluoropyridin-4-yl)but-1-en-1-yl)phenoxy)ethyl)amino)-N,N-dimethylbut-2-enamide (Compound 81)

The compound was synthesized following the approach as outlined in Example 14 by substituting into Step-4 (i) (Z)-5-(1,2-bis(4,4,5,5-tetramethyl-1,3,2-dioxaborolan-2-yl) but-1-en-1-yl)-3-fluoro-1-(tetrahydro-2H-pyran-2-yl)-1H-indazole (as prepared in Example 3, Step-1) for compound 233, (ii) tert-butyl (E)-(4-(dimethylamino)-4-oxobut-2-en-1-yl)(2-(4-iodophenoxy)ethyl)carbamate (Example 14, Step-3) for compound 234, and (iii) 3-fluoro-4-iodopyridine for compound 262, and (iv) substituting Ex. 14 Step-5 with reaction conditions described in Scheme 2, Step-6b to isolate Compound 81 (0.24 g, 34%) as an off-white solid.

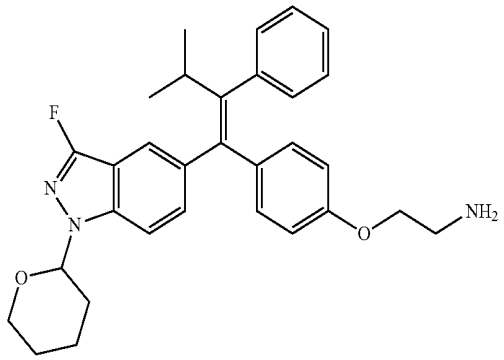
Compound 81:

^{1}H NMR (400 MHz, DMSO-d_6): δ 12.60 (s, 1H), 8.4 (s, 1H), 8.30 (s, 1H), 7.6 (m, 2H), 7.49 (d, J=1.6 Hz, 1H), 7.22 (d, J=1.6 Hz, 1H), 6.8 (d, J=8.8 Hz, 2H), 6.65 (d, J=8.8 Hz, 3H), 6.40 (m, 1H), 3.88 (t, J=5.4 Hz, 2H), 3.03 (s, 3H), 2.80 (s, 3H), 2.78 (t, J=5.4 Hz, 2H), 2.42 (q, J=7.4 Hz, 2H), 0.87 (t, J=7.2 Hz, 3H). LCMS: 532.3 $[M+H]^+$.

Example 82: Synthesis of (E)-4-((2-(4-((E)-1-(3-fluoro-1H-indazol-5-yl)-3-methyl-2-phenylbut-1-en-1-yl)phenoxy)ethyl)amino)-N,N-dimethylbut-2-enamide (Compound 82)

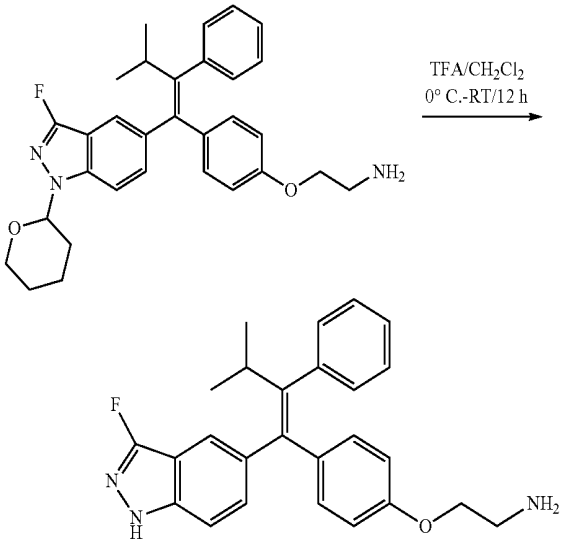
The compound was synthesized following the approach as outlined in Example 50 by (i) substituting into Step-3 (E)-2-(4-(1-(3-fluoro-1-(tetrahydro-2H-pyran-2-yl)-1H-indazol-5-yl)-3-methyl-2-phenylbut-1-en-1-yl)phenoxy) ethan-1-amine (preparation shown below in Ex. 82 Step 1-3) for compound 258 and (ii) substituting Ex. 50 Step-5 with reaction conditions described in Scheme 2, Step-6c to isolate Compound 82 (0.07 g).

Step-1: Synthesis of (E)-2-(4-(1-(3-fluoro-1-(tetrahydro-2H-pyran-2-yl)-1H-indazol-5-yl)-3-methyl-2-phenylbut-1-en-1-yl)phenoxy)ethan-1-amine



The compound was synthesized following the approach as outlined in Example 2 by (i) substituting into Step-3 3-methylbut-1-yne for compound 278, (ii) substituting into Step-4 tert-butyl (2-(4-(4,4,5,5-tetramethyl-1,3,2-dioxaborolan-2-yl)phenoxy)ethyl)carbamate (as prepared in Example 63, Step-5) for compound 274, and (iii) continuing with Ex. 2 Step 6 to isolate the title compound of Ex. 82 Step-1.

Step-2: Synthesis of (E)-2-(4-(1-(3-fluoro-1-(tetrahydro-2H-pyran-2-yl)-1H-indazol-5-yl)-3-methyl-2-phenylbut-1-en-1-yl)phenoxy)ethan-1-amine



To a stirred solution of (E)-2-(4-(1-(3-fluoro-1-(tetrahydro-2H-pyran-2-yl)-1H-indazol-5-yl)-3-methyl-2-phenylbut-1-en-1-yl)phenoxy)ethan-1-amine (1.5 g, 3 mmol) in dichloromethane (20 mL) was added at 0° C., TFA (3.4 mL, 45 mmol). The reaction mixture was stirred for 12 h at room temperature. After completion of reaction, reaction mixture was basified with saturated $NaHCO_3$, extracted with 10%

MeOH in dichloromethane. Organic layer was concentrated under reduced pressure and the crude material was purified by combi-flash using 10% MeOH in dichloromethane to afford the title compound of Ex. 82 Step-2 (1.1 g).

Compound 82:

^{1}H NMR (400 MHz, DMSO-d_6): δ 12.55 (s, 1H), 7.56 (s, 1H), 7.48 (d, J=8.8 Hz, 1H), 7.30 (d, J=8.8 Hz, 1H), 7.23-7.19 (m, 2H), 7.14-7.10 (m, 3H), 6.84 (d, J=8.8 Hz, 2H), 6.61-6.46 (m, 4H), 3.83 (t, J=5.6 Hz, 2H), 3.31 (bs, 2H), 2.97 (s, 3H), 2.83 (m, 4H), 2.75 (t, J=5.4 Hz, 2H), 0.88 (m, 6H). LCMS: 527.3 $[M+H]^+$.

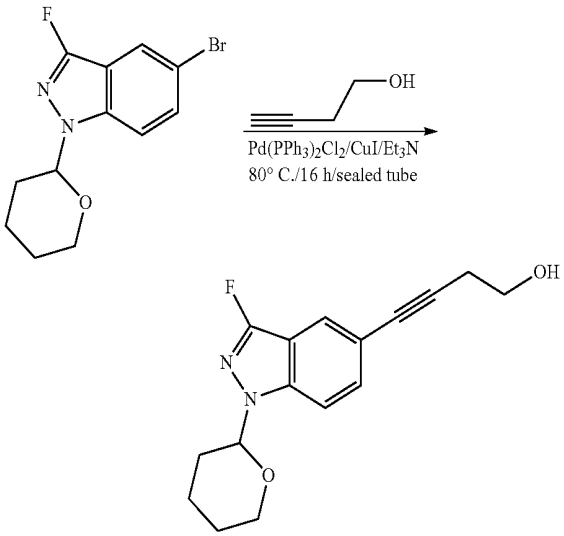
Example 83

There is no Example 83.

Example 84: Synthesis of (E)-S-((2-(4-((E)-4-fluoro-1-(3-fluoro-1H-indazol-S-yl)-2-phenylbut-1-en-1-yl)phenoxy)ethyl)amino)-N,N-dimethylpent-2-enamide (Compound 84)

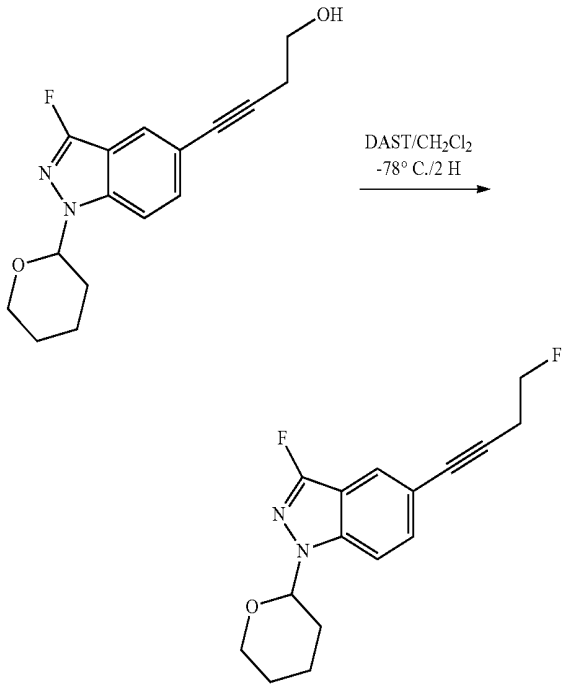
The compound was synthesized following the approach as outlined in Example 60 by substituting into Step-1 3-fluoro-5-(4-fluorobut-1-yn-1-yl)-1-(tetrahydro-2H-pyran-2-yl)-1H-indazole (preparation shown below in Ex. 84 Step 1-2) for compound 275 and tert-butyl (E)-(4-(dimethylamino)-4-oxobut-2-en-1-yl)(2-(4-iodophenoxy)ethyl)carbamate (as prepared in Example 14, Step-3) for compound 263 to isolate Compound 84 (0.075 g, 10%).

Step-1: Synthesis of 4-(3-fluoro-1-(tetrahydro-2H-pyran-2-yl)-1H-indazol-5-yl)but-3-yn-1-ol



The reaction was carried out according to Scheme 1, Step-2 using 5-bromo-3-fluoro-1-(tetrahydro-2H-pyran-2-yl)-1H-indazole (10 g, 33 mmol, as prepared in Example 2, Step-2) and but-3-yn-1-ol (3.52 g, 50 mmol) for compound 202. The crude product was purified over silica-gel column chromatography using 30% ethyl acetate in n-hexane to afford the title compound of Ex. 84 Step-1 (5.7 g, 59%).

Step-2: Synthesis of 3-fluoro-S-(4-fluorobut-1-yn-1-yl)-1-(tetrahydro-2H-pyran-2-yl)-1H-indazole



To a stirred solution of 4-(3-fluoro-1-(tetrahydro-2H-pyran-2-yl)-1H-indazol-5-yl)but-3-yn-1-ol (4 g, 13 mmol) in 40 mL of dichloromethane, was added DAST (3.35 g) at −78° C., reaction mixture was stirred for 2 h. Upon completion by TLC, the reaction mixture was diluted with water (100 mL) and extracted with ethyl acetate (250 mL). The combined organic extracts were washed with water, brine, dried over anhydrous sodium sulphate and concentrated under reduced pressure. The crude product was purified over 230-400 mesh silica column chromatography using 6% ethyl acetate in n-hexane to afford the title compound of Ex. 84 Step-2 (1.2 g, 30%).

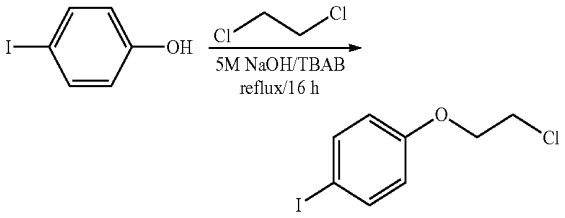
Compound 84:

^{1}H NMR (400 MHz, DMSO-d_6): δ 12.61 (s, 1H), 7.60 (s, 1H), 7.47 (dd, J_1=8.6 Hz, J_2=1.8 Hz, 1H), 7.25-7.13 (m, 6H), 6.9-6.75 (m, 2H), 6.64-6.57 (m, 2H), 6.52-6.48 (m, 2H), 4.36 (t, J=6 Hz, 1H), 4.25 (t, J=6.2 Hz, 1H), 3.87 (t, J=5.6 Hz, 2H), 3.37-3.31 (m, 2H), 2.99 (s, 3H), 2.84 (s, 3H), 2.82-2.70 (m, 4H). LCMS: 531.3 $[M+H]^+$.

Example 85: Synthesis of (E)-5-((2-(4-((E)-2-(2-chloro-4-fluorophenyl)-1-(3-fluoro-1H-indazol-5-yl) but-1-en-1-yl)phenoxy)ethyl)amino)-N,N-dimethyl-pent-2-enamide (Compound 85)

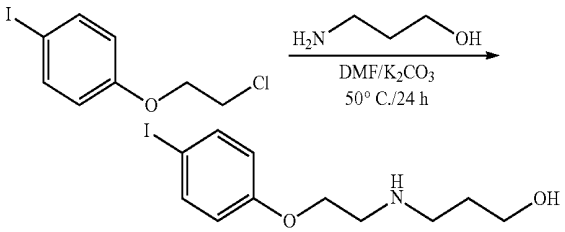
The compound was synthesized following the approach as outlined in Example 60 by substituting into Step-1 (i) tert-butyl (E)-(5-(dimethylamino)-5-oxopent-3-en-1-yl)(2-(4-iodophenoxy)ethyl)carbamate (preparation shown below in Ex. 85 Step 1-7) for compound 263, 5-(but-1-yn-1-yl)-3-fluoro-1-(tetrahydro-2H-pyran-2-yl)-1H-indazole (as prepared in Example 2, Step-3) for compound 275, and 2-chloro-4-fluoro-1-iodobenzene for compound 264 to isolate Compound 85 (0.046 g).

Step-1: Synthesis of 1-(2-chloroethoxy)-4-iodobenzene



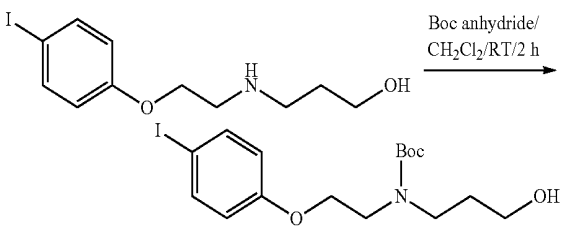
To a stirred solution of 4-iodophenol (15 g, 68 mmol) was added 5M NaOH (90 mL) and stirred for 10 min at 0° C., to the above mixture 1,2-dichloroethane (225 mL) followed by TBAB (0.43 g, 1.36 mmol) were added. The contents were stirred at reflux for 16 h. After completion of reaction, reaction mixture was poured onto ice cold water, and extracted with ethyl acetate. The combined organic layers were washed with water followed by saturated NaCl solution, dried over anhydrous Na_2SO_4 and concentrated under reduced pressure to obtain desired compound 1-(2-chloroethoxy)-4-iodobenzene (20 g, crude).

Step-2: Synthesis of 3-((2-(4-iodophenoxy)ethyl) amino)propan-1-ol



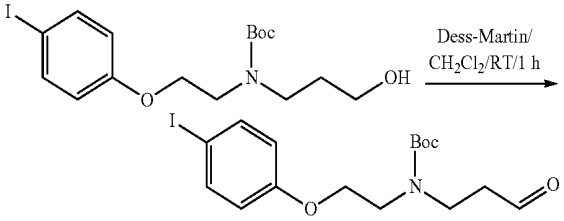
To a stirred solution of 1-(2-chloroethoxy)-4-iodobenzene (10 g, 35 mmol) in DMF (25 mL) was added potassium carbonate (19.5 g, 141 mmol) and 3-aminopropan-1-ol (26.6 g, 350 mmol). The reaction mixture was stirred for 24 h at 50° C., after completion of reaction (monitored by TLC), reaction mixture was diluted with cold water (50 mL) solid separated was filtered and dried under reduced pressure. The crude product was used in next step without further purification (8.6 g, crude).

Step-3: Synthesis of tert-butyl (3-hydroxypropyl)(2-(4-iodophenoxy)ethyl)carbamate



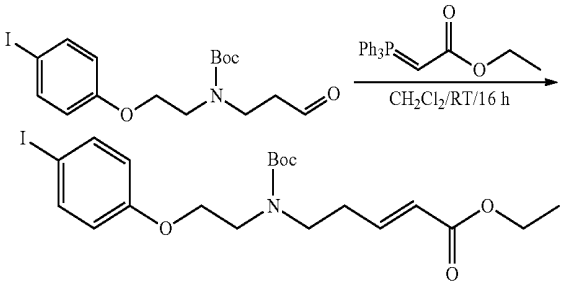
To a stirred solution of 3-((2-(4-iodophenoxy)ethyl) amino)propan-1-ol (8.6 g, 26 mmol) in dichloromethane (86 mL) was added boc anhydride (6.4 g, 29 mmol). The reaction mixture was stirred for 2 h at room temperature, after completion of reaction (monitored by TLC), reaction mixture was diluted with cold water (100 mL) and extracted with dichloromethane (250 mL). The organic layer was washed with water followed by saturated NaCl solution, dried over anhydrous Na_2SO_4 and concentrated under reduced pressure. The crude product purified by combi-flash using 40% EtOAc in n-hexane to get the title compound of Ex. 85 Step-3 (9.5 g).

Step-4: Synthesis of tert-butyl (2-(4-iodophenoxy) ethyl)(3-oxopropyl)carbamate



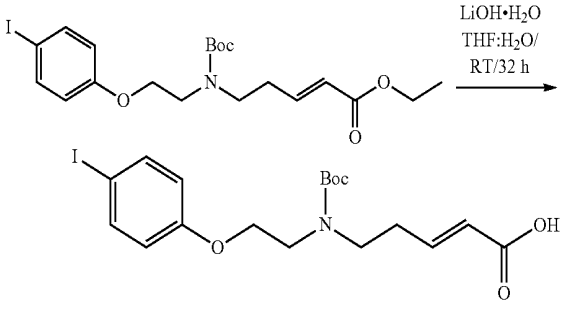
To a stirred solution of tert-butyl (3-hydroxypropyl)(2-(4-iodophenoxy)ethyl)carbamate (9 g, 21 mmol) in dichloromethane (90 mL) was added Dess-Martin periodinane (11.78 g, 27 mmol). The reaction mixture was stirred for 1 h at room temperature, after completion of reaction (monitored by TLC), reaction mixture was diluted with 1:1 mixture of hypo and $NaHCO_3$ solution and extracted with dichloromethane (250 mL). The organic layer was washed with water followed by saturated NaCl solution, dried over anhydrous Na_2SO_4 and concentrated under reduced pressure to afford the title compound of Ex. 85 Step-4 (9 g).

Step-5: Synthesis of ethyl (E)-5-((tert-butoxycarbonyl)(2-(4-iodophenoxy)ethyl)amino)pent-2-enoate



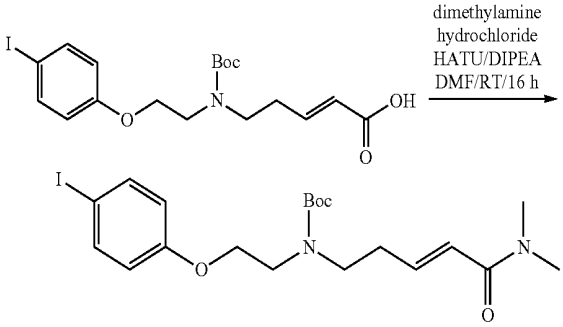
To a stirred solution of tert-butyl (2-(4-iodophenoxy) ethyl)(3-oxopropyl)carbamate (9 g, 28 mmol) in dichloromethane (90 mL) was added ethyl 2-(triphenyl-15-phosphanylidene)acetate (9.8 g, 28 mmol). The reaction mixture was stirred for 16 h at room temperature, after completion of reaction (monitored by TLC), reaction mixture was diluted with water and extracted with dichloromethane (250 mL). The organic layer was washed with water followed by saturated NaCl solution, dried over anhydrous Na_2SO_4 and concentrated under reduced pressure. The crude product was purified by combi-flash eluting with 9% EtOAc in n-hexane to afford the title compound of Ex. 85 Step-5 (6.7 g).

Step-6: Synthesis of (E)-5-((tert-butoxycarbonyl)(2-(4-iodophenoxy)ethyl)amino)pent-2-enoic acid



To a stirred solution of ethyl (E)-5-((tert-butoxycarbonyl)(2-(4-iodophenoxy)ethyl)amino)pent-2-enoate (6.7 g, 13 mmol) in THF (100 mL) was added LiOH.H_2O (2.87 g, 68 mmol) and water (33 mL). The reaction mixture was stirred for 32 h at room temperature, after completion of reaction (monitored by TLC), reaction mixture was diluted with water and neutralized with citric acid, extracted with EtOAc (250 mL). The organic layer was washed with water followed by saturated NaCl solution, dried over anhydrous Na_2SO_4 and concentrated under reduced pressure. The crude product was used in next step without further purification (5.4 g).

Step-7: Synthesis of tert-butyl (E)-(5-(dimethylamino)-5-oxopent-3-en-1-yl)(2-(4-iodophenoxy) ethyl)carbamate



To a stirred solution of (E)-5-((tert-butoxycarbonyl)(2-(4-iodophenoxy)ethyl)amino)pent-2-enoic acid (2.5 g, 5.3 mmol) in DMF (25 mL) was added DIPEA (2.32 mL, 13 mmol), HATU (2.45 g, 6.4 mmol) and dimethylamine hydrochloride (0.526 g, 6.4 mmol). The reaction mixture was stirred for 16 h at room temperature, after completion of reaction (monitored by TLC), reaction mixture was diluted with water and extracted with EtOAc (100 mL). The organic layer was washed with water followed by saturated NaCl solution, dried over anhydrous Na_2SO_4 and concentrated under reduced pressure to afford title compound of Ex. 85 Step-7 (2 g, 71%).

Compound 85:

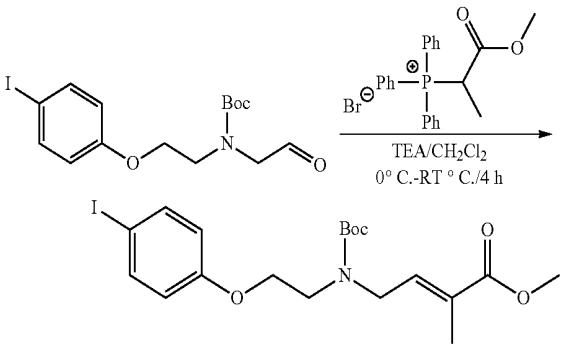
^{1}H NMR (400 MHz, DMSO-d_6): δ 12.62 (s, 1H), 7.54 (s, 1H), 7.49 (dd, J_1=8.8 Hz, J2=1.2 Hz, 1H), 7.36-7.35 (m, 2H), 7.34-7.31 (m, 1H), 7.15-7.11 (m, 1H), 6.82 (d, J=8.8 Hz, 2H), 6.65-6.58 (m, 3H), 6.43-6.39 (m, 1H), 3.85 (t, J=5.7 Hz, 2H), 2.98 (s, 3H), 2.83 (s, 3H), 2.79-2.78 (m, 2H), 2.62 (t, J=6.8 Hz, 2H), 2.33-2.27 (m, 4H), 0.88 (t, J=7.4 Hz, 3H).

LCMS: 579.3 $[M+H]^+$.

Example 86: Synthesis of (E)-4-((2-(4-((E)-2-(2-chloro-4-fluorophenyl)-1-(3-fluoro-1H-indazol-5-yl) but-1-en-yl)phenoxy)ethyl)amino)-N,N,2-trimethyl-but-2-enamide (Compound 86)

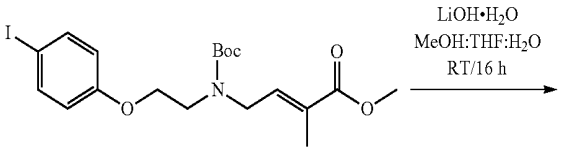
The compound was synthesized following the approach as outlined in Example 59 by substituting into Step-4 5-(but-1-yn-1-yl)-3-fluoro-1-(tetrahydro-2H-pyran-2-yl)-1H-indazole (as prepared in Example 2, Step-3) for compound 276 and tert-butyl (E)-(4-(dimethylamino)-3-methyl-4-oxobut-2-en-1-yl)(2-(4-iodophenoxy)ethyl)carbamate (preparation shown below in Ex. 86 Step 1-3) for compound 277 to isolate Compound 86 (0.11 g, 7.6%).

Step-1: Synthesis of methyl (E)-4-((tert-butoxycarbonyl)(2-(4-iodophenoxy)ethyl)amino)-2-methylbut-2-enoate

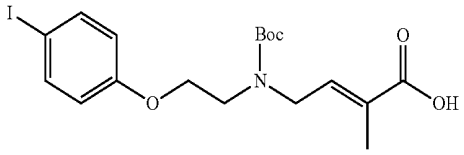


To a stirred solution of (1-methoxy-1-oxopropan-2-yl) triphenylphosphonium bromide (10.8 g, 25 mmol) in dichloromethane (50 mL) was added triethyl amine (6.35 g, 62 mmol) at 0° C., stirred for 30 min. To the above solution, tert-butyl (2-(4-iodophenoxy)ethyl)(2-oxoethyl)carbamate (8.5 g, 20 mmol, Example 22, Step-4) in dichloromethane (35 mL) was added dropwise. The reaction mixture was stirred for 3.5 h at room temperature, after completion of reaction (monitored by TLC), reaction mixture was diluted with ammonium chloride solution and extracted with EtOAc (100 mL). The organic layer was washed with water followed by saturated NaCl solution, dried over anhydrous Na_2SO_4 and concentrated under reduced pressure. The crude product was purified by column chromatography over 230-400 mesh silica-gel by eluting with 5% EtOAc in n-hexane to afford the title compound of Ex. 86 Step-1 (7.1 g, 71.7%).

Step-2: Synthesis of (E)-4-((tert-butoxycarbonyl)(2-(4-iodophenoxy)ethyl)amino)-2-methylbut-2-enoic acid

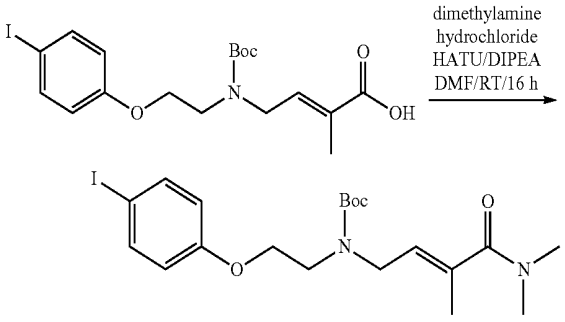


-continued



To a stirred solution of methyl (E)-4-((tert-butoxycarbonyl)(2-(4-iodophenoxy)ethyl)amino)-2-methylbut-2-enoate (7.1 g, 14.9 mmol) in MeOH:THF:H_2O (1:1:1) mixture (70 mL) was added LiOH.H_2O (3.13 g, 74 mmol). The reaction mixture was stirred for 16 h at room temperature, after completion of reaction (monitored by TLC), reaction mixture was diluted with water followed by acidified with 0.5M HCl and extracted with EtOAc (250 mL). The organic layer was washed with water followed by saturated NaCl solution, dried over anhydrous Na_2SO_4 and concentrated under reduced pressure. The crude product was used in next step without further purification (6.5 g, 94%).

Step-3: Synthesis of tert-butyl (E)-(4-(dimethylamino)-3-methyl-4-oxobut-2-en-1-yl)(2-(4-iodophenoxy)ethyl)carbamate



To a stirred solution of (E)-4-((tert-butoxycarbonyl)(2-(4-iodophenoxy)ethyl)amino)-2-methylbut-2-enoic acid (3 g, 6.5 mmol) in DMF (30 mL) was added DIPEA (3.1 g, 16.25 mmol), HATU (2.96 g, 7.8 mmol) and dimethylamine hydrochloride (0.63 g, 7.8 mmol). The reaction mixture was stirred for 16 h at room temperature, after completion of reaction (monitored by TLC), reaction mixture was diluted with water and extracted with dichloromethane (100 mL). The organic layer was washed with water followed by saturated NaCl solution, dried over anhydrous Na_2SO_4 and concentrated under reduced pressure. The crude product was purified by column chromatography over 230-400 mesh silica-gel by eluting with 70% EtOAc in n-hexane to afford the title compound of Ex. 86 Step-3 (2.6 g, 82%).

Compound 86:

^{1}H NMR (400 MHz, DMSO-d_6): δ 12.63 (s, 1H), 7.54 (s, 1H), 7.49 (dd, J_1=8.6 Hz, J_2=1.8 Hz, 1H), 7.36-7.31 (m, 2H), 7.24 (dd, J_1=8.8 Hz, J_2=1.2 Hz, 1H), 7.14 (dd, J_1=8.0 Hz, J_2=2.4 Hz, 1H), 6.82 (d, J=8.8 Hz, 2H), 6.62 (d, J=8.8 Hz, 2H), 5.43-5.40 (m, 1H), 3.86 (t, J=5.6 Hz, 2H), 3.21 (d, J=6.4 Hz, 2H), 2.87-2.75 (m, 8H), 2.33 (q, J=7.2 Hz, 2H), 2.08-1.85 (m, 1H), 1.70 (s, 3H), 0.88 (t, J=7.6 Hz, 3H). LCMS: 579.3 $[M+H]^+$.

Example 87: Synthesis of (E)-4-((2-(4-((E)-2-(2-chloro-4-fluorophenyl)-4,4,4-trifluoro-1-(3-fluoro-1H-indazol-5-yl)but-1-en-1-yl)phenoxy)ethyl)amino)-N,N-dimethylbut-2-enamide (Compound 87)

The compound was synthesized following the approach as outlined in Example 59 by substituting into Step-4 tert-butyl (E)-(4-(dimethylamino)-4-oxobut-2-en-1-yl)(2-(4-iodophenoxy)ethyl)carbamate (as prepared in Example 14, Step-3) for compound 277 to isolate Compound 87 (0.17 g, 24%).

Compound 87:

^{1}H NMR (400 MHz, DMSO-d_6): δ 12.69 (s, 1H), 7.59 (s, 1H), 7.55 (dd, J_1=8.6 Hz, J_2=1.8 Hz, 1H), 7.53 (dd, J_1=8.6 Hz, J_2=1.8 Hz, 1H), 7.43 (dd, J_1=8.6 Hz, J_2=1.8 Hz, 1H), 7.36-7.21 (m, 2H), 6.85 (d, J=8.9 Hz, 2H), 6.67-6.57 (m, 3H), 6.51-6.47 (m, 1H), 3.88 (t, J=5.7 Hz, 2H), 3.45 (q, J=10.8 Hz, 2H), 2.98 (s, 3H), 2.84 (s, 3H), 2.78 (t, J=5.6 Hz, 2H).

LCMS: 619.3 $[M+H]^+$.

Example 88: Synthesis of (E)-4-((2-(4-((E)-1-(1H-indazol-5-yl)-2-(phenyl-d5)but-1-en-1-yl)phenoxy)ethyl)amino)-N,N-dimethylbut-2-enamide (Compound 88)

The compound was synthesized following the approach as outlined in Example 59 by substituting into Step-5 tert-butyl ((E)-4-(dimethylamino)-4-oxobut-2-en-1-yl)(2-(4-((Z)-1-(1-(tetrahydro-2H-pyran-2-yl)-1H-indazol-5-yl)-2-(4,4,5,5-tetramethyl-1,3,2-dioxaborolan-2-yl)but-1-en-1-yl)phenoxy)ethyl)carbamate (as prepared in Example 33, Step-1) for compound 278 and iodobenzene-d_5 for compound 265 to isolate Compound 88 (0.023 mg) as an off-white solid.

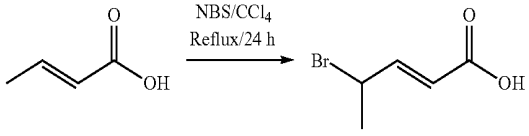
Compound 88:

^{1}H NMR (400 MHz, DMSO-d_6) δ 13.05 (s, 1H), 8.06 (s, 1H), 7.60 (s, 1H), 7.50 (d, J=8.8 Hz, 1H), 7.11 (d, J=8.4 Hz, 1H), 6.73 (d, J=8.8, 2H), 6.59-6.51 (m, 3H), 6.47 (d, J=8.8 Hz, 1H), 3.86 (t, J=5.2 Hz, 2H), 3.31 (d, J=4.8 Hz, 2H), 2.98 (s, 3H), 2.83 (s, 3H), 2.78-2.75 (m, 2H), 2.40 (q, J=7.6 Hz, 2H), 0.89 (t, J=7.6 Hz, 3H). LCMS: 500.4 $[M+H]^+$.

Example 89: Synthesis of (E)-4-((2-(4-((E)-1-(1H-indazol-5-yl)-2-phenylbut-1-en-1-yl)phenoxy)ethyl)amino)-N,N-dimethylpent-2-enamide (Compound 89)

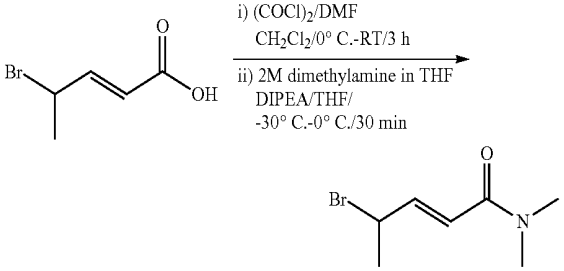
The compound was synthesized following the approach as outlined in Example 59 by substituting into Step-4 5-(but-1-yn-1-yl)-1-(tetrahydro-2H-pyran-2-yl)-1H-indazole (Example 1, Step-3) for compound 276 and tert-butyl (E)-(5-(dimethylamino)-5-oxopent-3-en-2-yl)(2-(4-iodophenoxy)ethyl)carbamate (preparation shown below in Ex. 89 Step 1-4) for compound 277 and substituting into Step-5 iodobenzene for compound 265 to isolate Compound 89 (0.08 g, 5.5%).

Step-1: Synthesis of (E)-4-bromopent-2-enoic acid



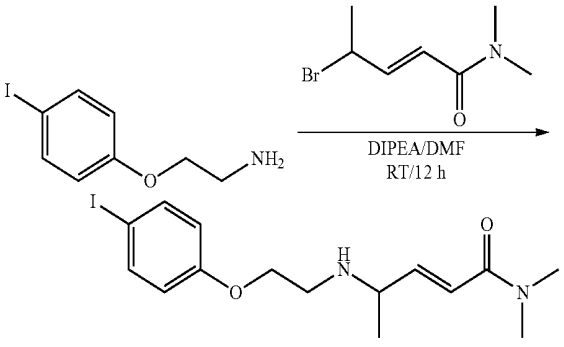
To a stirred solution of (E)-but-2-enoic acid (5 g, 50 mmol) in carbontetrachloride (50 mL) was added N-Bromo succinamide (8.6 g, 65 mmol). The reaction mixture was heated to reflux for 24 h, which resulted in precipitation of succinamide crystals. The crystals were filtered off and the filtrate was concentrated. The crude was recrystallized with minimum amount of hexane and washed with hexane to afford (E)-4-bromopent-2-enoic acid (4 g, 45%) as a white solid.

Step-2: Synthesis of (E)-4-bromo-N,N-dimethylpent-2-enamide



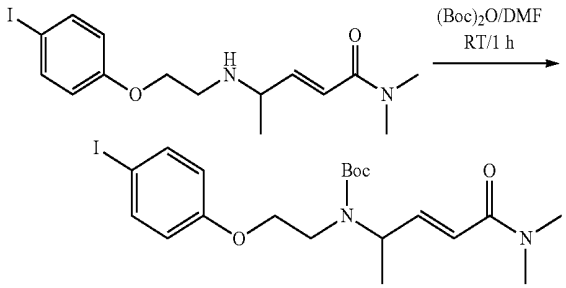
(E)-4-bromopent-2-enoic acid (4 g, 24.2 mmol) was taken in dichloromethane (40 mL) and cooled to 0° C. To this solution oxalyl chloride (3.6 g, 29 mmol), DMF (0.5 mL) were added and stirred for 3 h at room temperature. The reaction mixture was concentrated under nitrogen atmosphere, residue was diluted with dichloromethane (40 mL), cooled to −30° C. and was basified with DIPEA (7.7 mL, 43 mmol). To this mixture 2M dimethylamine in THF (14.3 mL, 28.6 mmol) was added slowly and the contents were stirred at 0° C. for 30 min. The volatiles were removed by concentration under reduced pressure and the residue was partitioned between water and ethyl acetate. The organic layer was washed with water, brine, dried over sodium sulphate and concentrated. The crude material was purified by combi-flash to afford (E)-4-bromo-N,N-dimethylpent-2-enamide (2.3 g, 50%).

Step-3: Synthesis of (E)-4-((2-(4-iodophenoxy) ethyl)amino)-N,N-dimethylpent-2-enamide



The reaction was carried out according to Scheme 3, Step-3 using 2-(4-iodophenoxy)ethan-1-amine (1.5 g, 5.86 mmol, Example 14, Step-3.1) for compound 217 and (E)-4-bromo-N,N-dimethylpent-2-enamide (1.8 g, 5.86 mmol) for compound 214. The crude material was used in next step (3 g, crude).

Step-4: Synthesis of tert-butyl (E)-(5-(dimethylamino)-5-oxopent-3-en-2-yl)(2-(4-iodophenoxy) ethyl)carbamate



The reaction was carried out according to Scheme 3, Step-4 using (E)-4-((2-(4-iodophenoxy)ethyl)amino)-N,N-dimethylpent-2-enamide (4.5 g, 12 mmol) for compound 218 to afford the crude product was purified by combi-flash eluting with 70% ethyl aceate in n-heane to afford the title compound in Ex. 90 Step-4 (2.8 g, 50%).

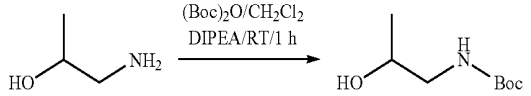
Compound 89:

^{1}H NMR (400 MHz, DMSO-d_6): δ 13.05 (s, 1H), 8.06 (s, 1H), 7.60 (s, 1H), 7.51 (d, J=8.8 Hz, 1H), 7.22-7.10 (m, 6H), 6.74 (d, J=8.8 Hz, 2H), 6.57 (d, J=8.8 Hz, 2H), 6.47-6.41 (m, 2H), 3.84 (t, J=5.6 Hz, 2H), 3.30 (bs, 2H), 2.98 (s, 3H), 2.83 (s, 3H), 2.75-2.66 (m, 2H), 2.43-2.32 (m, 2H), 1.07 (d, J=6.8 Hz, 3H), 0.87 (t, J=7.2 Hz, 3H). LCMS: 509.3 $[M+H]^+$.

Example 90: Synthesis of (E)-4-((2-(4-((E)-1-(1H-indazol-S-yl)-2-phenylbut-1-en-1-yl)phenoxy)propyl)amino)-N,N-dimethylbut-2-enamide (Compound 90)

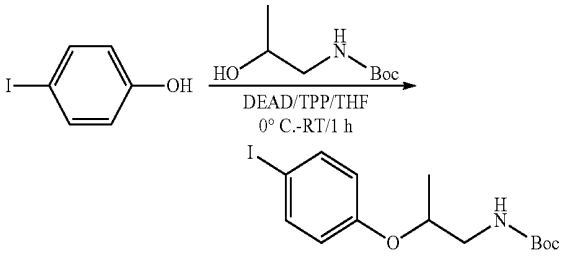
The compound was synthesized following the approach as outlined in Example 59 by substituting into Step-4 5-(but-1-yn-1-yl)-1-(tetrahydro-2H-pyran-2-yl)-1H-indazole (Example 1, Step-3) for compound 276 and tert-butyl (E)-(4-(dimethylamino)-4-oxobut-2-en-1-yl)(2-(4-iodophenoxy) propyl)carbamate (preparation shown below Ex. 90 Step 1-5) for compound 277 and substituting into Step-5 iodobenzene for compound 265 to afford Compound 90 (0.06 g, 10%).

Step-1: Synthesis of tert-butyl (2-hydroxypropyl)carbamate



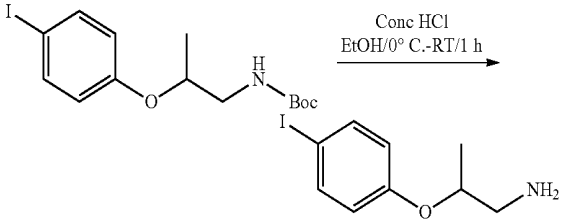
To a stirred solution of 1-aminopropan-2-ol (5 g, 66.6 mmol) in dichloromethane (50 mL), was added boc anhydride (17 mL, 79.92 mmol) and DIPEA (18 mL, 99.9 mmol), the reaction mixture was stirred at room temperature for about 1 h. After completion of reaction, reaction mixture was concentrated under reduced pressure and the crude product was purified by combi-flash eluting with 50% ethyl aceate in n-heane to afford the title compound in Ex. 90 Step-1 (10 g, 86%).

Step-2: Synthesis of tert-butyl (2-(4-iodophenoxy)propyl)carbamate



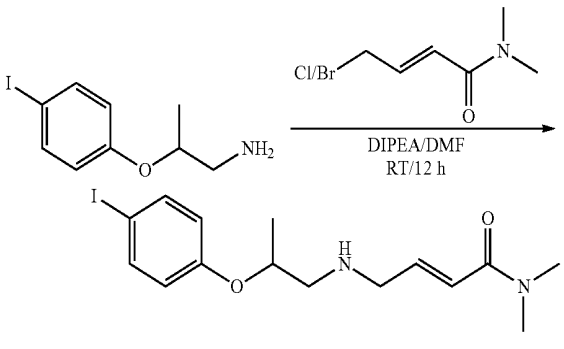
To a mixture of 4-iodophenol (4 g, 18.1 mmol), tert-butyl (2-hydroxypropyl)carbamate (2.6 g, 21.8 mmol), triphenyl phosphine (5.7 g, 21.8 mmol) in THF (40 mL) was added DEAD (3.8 g, 21.8 mmol) dropwise then the reaction mixture was stirred at room temperature for 1 h. After completion of reaction, reaction mixture was quenched with water extracted with ethyl acetate (2×100 mL), combined organic layer was washed with brine solution and dried over anhydrous sodium sulphate. Organic layer was concentrated to afford the crude product which was purified through column chromatography over 100-200 mesh silica gel, eluting with 10% EtoAc in n-hexane to afford the title compound in Ex. 90 Step-2 (2.1 g, 32%).

Step-3: Synthesis of 2-(4-iodophenoxy)propan-1-amine



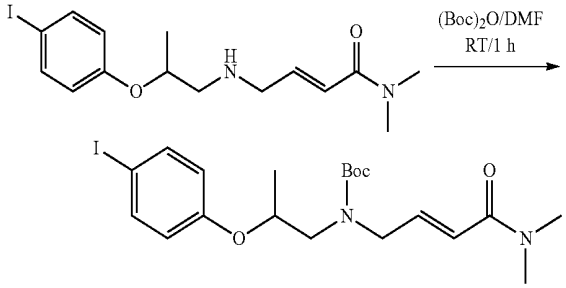
The reaction was carried out according to Scheme 3, Step-2 using tert-butyl (2-(4-iodophenoxy)propyl)carbamate (4.8 g, 12.76 mmol) for compound 207b to afford the crude material, which was used in next step without further purification (2.8 g).

Step-4: Synthesis of (E)-4-((2-(4-iodophenoxy)propyl)amino)-N,N-dimethylbut-2-enamide



The reaction was carried out according to Scheme 3, Step-3 using 2-(4-iodophenoxy)propan-1-amine (1 g, 3.6 mmol) for compound 217 in DMF (10 mL) and (E)-4-chloro-N,N-dimethylbut-2-enamide for compound 214 and (E)-4-bromo-N,N-dimethylbut-2-enamide mixture (0.7 g, 3.6 mmol, Example 63, Step-7) for compound 214. The crude material was used in next step (0.5 g, crude).

Step-5: Synthesis of tert-butyl (E)-(4-(dimethylamino)-4-oxobut-2-en-1-yl)(2-(4-iodophenoxy)propyl)carbamate



The reaction was carried out according to Scheme 3, Step-4 using (E)-4-((2-(4-iodophenoxy)propyl)amino)-N,N-dimethylbut-2-enamide (2 g, 5.3 mmol) for compound 218 to afford the crude product, which was purified by combiflash eluting with 70% ethyl aceate in n-heane to afford the title compound in Ex. 90 Step-5 (0.5 g, 20%).

Compound 90:

^{1}H NMR (400 MHz, DMSO-d_6): δ 13.07 (s, 1H), 8.07 (s, 1H), 7.61 (s, 1H), 7.52 (d, J=11.2 Hz, 1H), 7.22-7.11 (m, 6H), 6.78 (d, J=8.8 Hz, 2H), 6.71-6.52 (m, 4H), 4.52-4.31 (m, 1H), 3.61 (d, J=4.4 Hz, 2H), 3.96-3.04 (m, 5H), 2.86 (s, 3H), 2.42-2.32 (m, 2H), 1.14 (d, J=6.0 Hz, 3H), 0.87 (t, J=7.6 Hz, 3H). LCMS: 509.3 $[M+H]^+$.

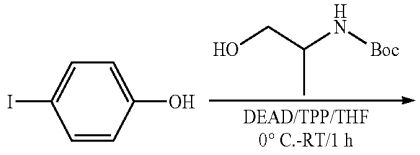
Example 91

There is no Example 91.

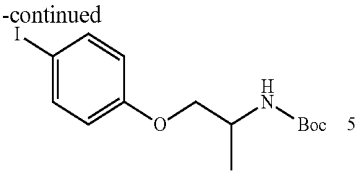
Example 92: Synthesis of (E)-4-((1-(4-((E)-1-(1H-indazol-5-yl)-2-phenylbut-1-en-1-yl)phenoxy)propan-2-yl)amino)-N,N-dimethylbut-2-enamide (Compound 92)

The compound was synthesized following the approach as outlined in Example 59 by (i) substituting into Step-4 5-(but-1-yn-1-yl)-1-(tetrahydro-2H-pyran-2-yl)-1H-indazole (as prepared in Example 1, Step-3) for compound 276 and tert-butyl (E)-(4-(dimethylamino)-4-oxobut-2-en-1-yl)(1-(4-iodophenoxy)propan-2-yl)carbamate (preparation shown below in Ex. 92 Step 1-4) for compound 277 and (ii) substituting into Step-5 iodobenzene for compound 265 to isolate Compound 92 (0.015 g).

Step-1: Synthesis of 2-(3-(4-iodophenyl)propyl)isoindoline-1,3-dione

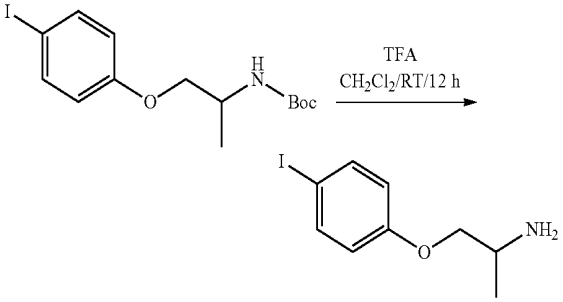


-continued



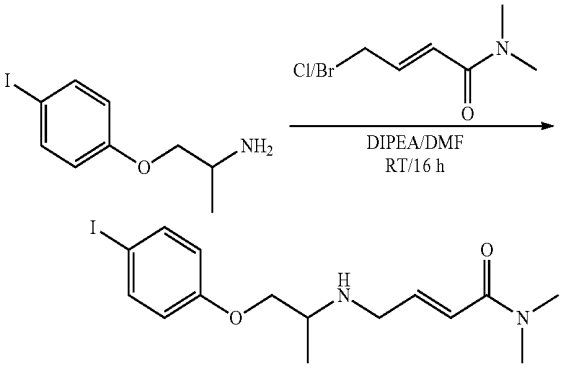
To a mixture of 4-iodophenol (5 g, 22 mmol), tert-butyl (1-hydroxypropan-2-yl)carbamate (4.66 g, 26 mmol), triphenyl phosphine (7.12 g, 26 mmol) in THF (100 mL) was added DEAD (4.66 g, 26 mmol) dropwise then the reaction mixture was stirred at room temperature for 1 h. After completion of reaction, reaction mixture was quenched with water extracted with ethyl acetate (2×100 mL), combined organic layer was washed with brine solution and dried over anhydrous sodium sulphate. Organic layer was concentrated to afford the crude product which was purified through column chromatography over 100-200 mesh silica gel, eluting with 10% EtoAc in n-hexane to afford the title compound in Ex. 92 Step-1 (2 g).

Step-2: Synthesis of 1-(4-iodophenoxy)propan-2-amine



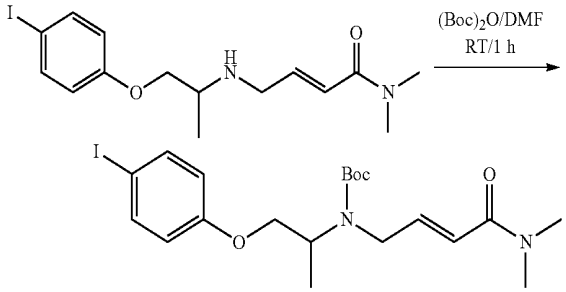
The reaction was carried out according to Scheme 3, Step-2 using tert-butyl (1-(4-iodophenoxy)propan-2-yl)carbamate (4 g, 10.6 mmol) for compound 207b to afford the crude material, which was used in next step without further purification (2 g).

Step-3: Synthesis of (E)-4-((2-(4-iodophenoxy) ethyl)amino)-N,N-dimethylpent-2-enamide



The reaction was carried out according to Scheme 3, Step-3 using 1-(4-iodophenoxy)propan-2-amine (4 g, 14 mmol) in DMF (35 mL) for compound 217 and (E)-4-chloro-N,N-dimethylbut-2-enamide and (E)-4-bromo-N,N-dimethylbut-2-enamide mixture (2.75 g, 14 mmol, Example 63, Step-7) for compound 214. The crude material was used in next step (5.6 g, crude).

Step-4: Synthesis of tert-butyl (E)-(4-(dimethylamino)-4-oxobut-2-en-1-yl)(1-(4-iodophenoxy)propan-2-yl)carbamate



The reaction was carried out according to (E)-4-((1-(4-iodophenoxy)propan-2-yl)amino)-N,N-dimethylbut-2-enamide (5.6 g, 14 mmol) to afford the crude, which was purified by silica gel chromatography with 40% ethyl aceate in n-heane to afford the title compound in Ex. 92 Step-4 (2.5 g).

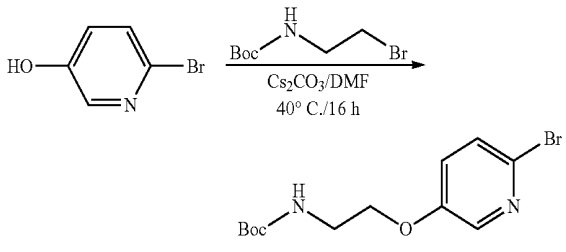
Compound 92:

^{1}H NMR (400 MHz, DMSO-d_6): δ 13.05 (s, 1H), 8.06 (s, 1H), 7.60 (s, 1H), 7.51 (d, J=8.0 Hz, 1H), 7.22-7.11 (m, 6H), 6.75 (d, J=8.4 Hz, 2H), 6.6-6.47 (m, 4H), 3.74-3.71 (m, 1H), 3.65-3.61 (m, 1H), 3.39-3.32 (m, 2H), 2.97 (s, 3H), 2.91-2.83 (m, 4H), 2.43-2.23 (m, 2H), 1.07 (d, J=6.4 Hz, 3H), 0.87 (t, J=7.2 Hz, 3H). LCMS: 509.3 $[M+H]^+$.

Example 93: Synthesis of (E)-4-((2-((6-((Z)-1-(3-fluoro-1H-indazol-5-yl)-2-phenylbut-1-en-1-yl)pyridin-3-yl)oxy)ethyl)amino)-N,N-dimethylbut-2-enamide (Compound 93)

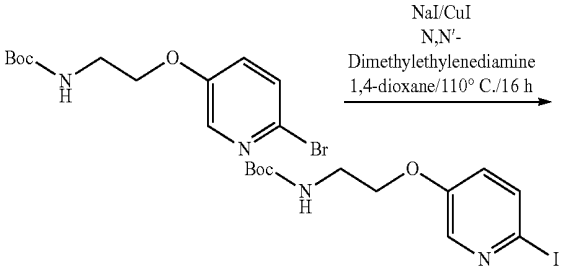
The compound was synthesized following the approach as outlined in Example 3 by (i) substituting into Step-3 of Ex.3 tert-butyl (E)-(4-(dimethylamino)-4-oxobut-2-en-1-yl)(2-((6-iodopyridin-3-yl)oxy)ethyl)carbamate (preparation shown below in Ex. 93 Step 1-5) for compound 256, (ii) substituting into Step-4 of Ex. 3 iodobenzene for compound 227, and (iii) substituting Step-5 of Ex. 3 with reaction conditions described in Scheme 2, Step-6b to afford Compound 93 (0.12 g).

Step-1: Synthesis of tert-butyl (2-((6-bromopyridin-3-yl)oxy)ethyl)carbamate



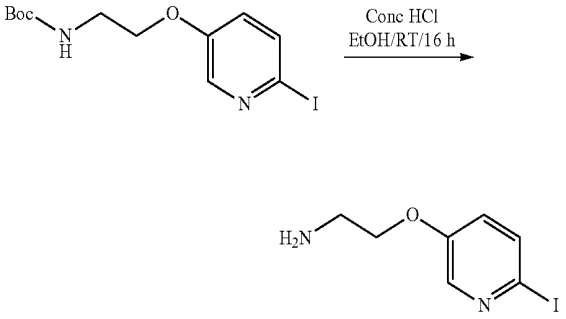
To a stirred solution of 6-bromopyridin-3-ol (5 g, 28.9 mmol) in 50 ml of DMF, cesium carbonate (28.2 g, 86 mmol) and tert-butyl (2-bromoethyl)carbamate (12.89 g, 57.8 mmol) were added. The mixture was then stirred for 16 h at 40° C. After completion of reaction, reaction mixture was added to ice cold water. Solid separated was filtered and dried to obtain tert-butyl (2-((6-bromopyridin-3-yl)oxy) ethyl)carbamate (8.2 g).

Step-2: Synthesis of tert-butyl (2-((6-iodopyridin-3-yl)oxy)ethyl)carbamate



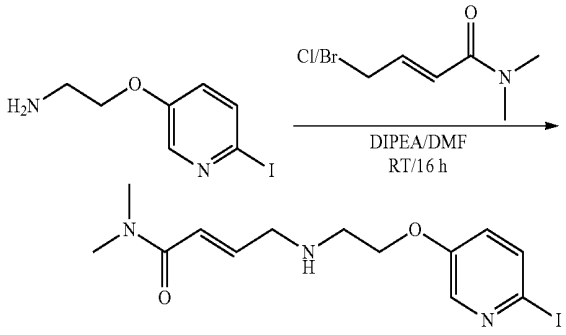
To a stirred solution of tert-butyl (2-((6-bromopyridin-3-yl)oxy)ethyl)carbamate (8.1 g, 25 mmol) in 1,4-dioxane (80 mL) were added sodium iodide (19.2 g, 128 mmol), copper iodide (0.244 g, 1.28 mmol) and N,N'-Dimethylethylenediamine (0.28 mL, 2.5 mmol) stirred for 16 h at 110° C. After completion of reaction, reaction mixture was diluted with ethyl acetate, organic layer was washed with a saturated aqueous solution of sodium chloride, dried over anhydrous sodium sulfate, and then concentrated under reduced pressure. The obtained crude product was used in next step without further purification (8.7 g, crude).

Step-3: Synthesis of 2-((6-iodopyridin-3-yl)oxy) ethan-1-amine



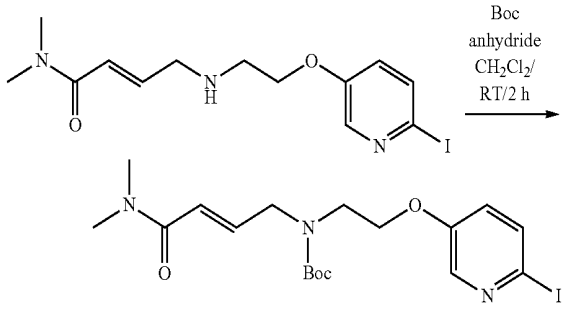
To a stirred solution of tert-butyl (2-((6-iodopyridin-3-yl) oxy)ethyl)carbamate (8 g, 21.97 mmol) in ethanol (2 mL) was added at 0° C., conc HCl (20 mL). The reaction mixture was stirred for 16 h at room temperature. After completion of reaction, reaction mixture was basified with saturated $NaHCO_3$, extracted with ethyl acetate. Organic layer was concentrated under reduced pressure and the crude material was used in next step without further purification (5 g, crude).

Step-4: Synthesis of (E)-4-((2-((6-iodopyridin-3-yl) oxy)ethyl)amino)-N,N-dimethylbut-2-enamide



The reaction was carried out according to Scheme 3, Step-3 using 2-((6-iodopyridin-3-yl)oxy)ethan-1-amine (5 g, 18.9 mmol) in DMF (50 mL) for compound 217 and (E)-4-bromo-N,N-dimethylbut-2-enamide and (E)-4-chloro-N,N-dimethylbut-2-enamide mixture (2.63 g, 15 mmol, Example 63, Step-7) for compound 214. The crude material was used in next step without further purification (7.08 g, crude).

Step-5: Synthesis of tert-butyl (E)-(4-(dimethyl-amino)-4-oxobut-2-en-1-yl)(2-((6-iodopyridin-3-yl) oxy)ethyl)carbamate



The reaction was carried out according to Scheme 3, Step-4 using (E)-4-((2-((6-iodopyridin-3-yl)oxy)ethyl) amino)-N,N-dimethylbut-2-enamide (7.08 g, 18.9 mmol) for compound 218. The crude material was purified by combi-flash eluting with 1.5% MeOH in dichloromethane as an eluent to afford the title compound of Ex. 93 Step-5 (2.7 g, 30%).

Compound 93:

^{1}H NMR (400 MHz, DMSO-d_6): δ 12.5 (s, 1H), 8.03 (s, 1H), 7.48-7.44 (m, 2H), 7.25 (dd, J_1=8.8 Hz, J_2=1.6 Hz, 2H), 7.21-7.10 (m, 4H), 7.02-6.99 (m, 1H), 6.78 (d, J=8.0 Hz, 1H), 6.62-6.47 (m, 2H), 3.94 (t, J=5.6 Hz, 2H), 2.98 (s, 3H), 2.84-2.78 (m, 5H), 2.47-2.42 (m, 2H), 0.87 (t, J=7.2 Hz, 3H). LCMS: 514.3 $[M+H]^+$.

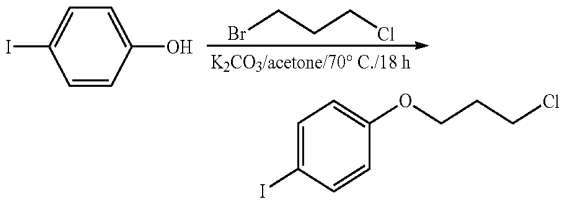
Example 94

There is no Example 94.

Example 95: Synthesis of (E)-4-((3-(4-((E)-1-(1H-indazol-5-yl)-2-phenylbut-1-en-1-yl)phenoxy)propyl)amino)-N,N-dimethylbut-2-enamide (Compound 95)

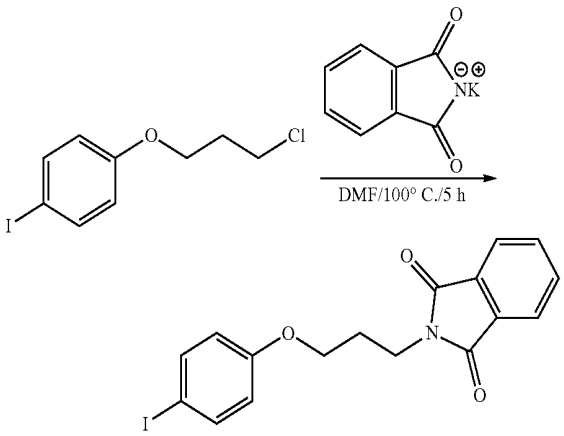
The compound was synthesized following the approach as outlined in Example 59 by (i) substituting into Step-4 of Ex. 59 5-(but-1-yn-1-yl)-1-(tetrahydro-2H-pyran-2-yl)-1H-indazole (as prepared in Example 1, Step-3) for compound 276 and tert-butyl (E)-(4-(dimethylamino)-4-oxobut-2-en-1-yl)(3-(4-iodophenoxy)propyl)carbamate (preparation shown below in Ex. 95 Step 1-5) for compound 277 and (ii) substituting into Step-5 of Ex. 59 iodobenzene for compound 265 to isolate Compound 95 (0.035 g).

Step-1: Synthesis of 1-(3-chloropropoxy)-4-iodobenzene



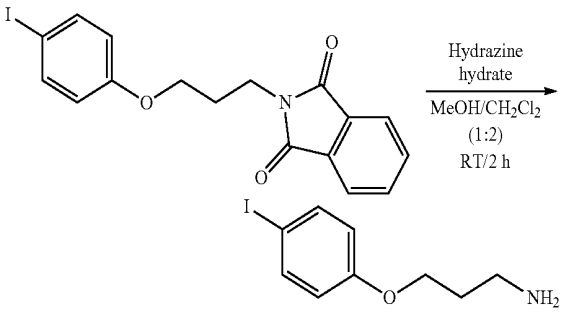
To a stirred solution of 4-iodophenol (10 g, 45.5 mmol) in acetone (150 mL) was added potassium carbonate (12.6 g, 91 mmol) and stirred for 30 min at room temperature, to the above mixture 1-bromo-3-chloropropane (10.75 g, 68.2 mmol) was added. The contents were stirred at 70° C. for 18 h. After completion of reaction, reaction mixture filtered through celite bed, filterate was concentrated under reduced pressure to obtain desired compound 1-(3-chloropropoxy)-4-iodobenzene as a glassy solid (13.2 g, 98%).

Step-2: Synthesis of 2-(3-(4-iodophenoxy)propyl)isoindoline-1,3-dione



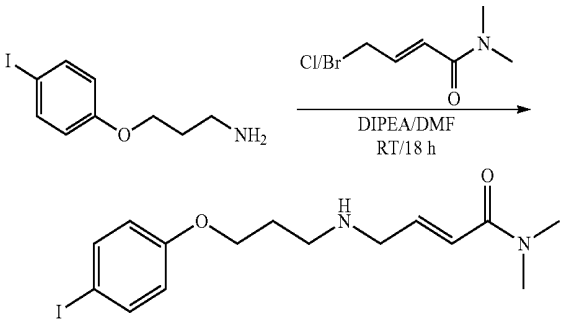
To a stirred solution of 1-(3-chloropropoxy)-4-iodobenzene (12 g, 40.5 mmol) in DMF (100 mL) was added potassium phthalimide (9 g, 48.6 mmol) in one portion at room temperature and the reaction mixture was stirred at 100° C. for 5 h. The reaction mixture cooled to room temperature, diluted with water, solid separated was filtered and dried under reduced pressure to afford the title compound of Ex. 95 Step-2 (15.2 g, 92%).

Step-3: Synthesis of 3-(4-iodophenoxy)propan-1-amine



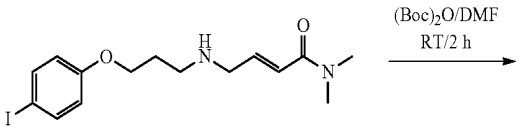
To a solution of 2-(3-(4-iodophenoxy)propyl)isoindoline-1,3-dione (16 g, 39 mmol) in $MeOH/CH_2Cl_2$ (160 mL/1:2) was added hydrazine hydrate (28 mL) at room temperature. The reaction mixture was stirred for 2 h and was quenched with water and extracted with dichloromethane. The organic layer was washed with water, saturated NaCl solution, dried over anhydrous Na_2SO_4 and concentrated under reduced pressure to afford 3-(4-iodophenoxy)propan-1-amine (10.6 g, 97%) as a light brown liquid.

Step-4: Synthesis of (E)-4-((3-(4-iodophenoxy)propyl)amino)-N,N-dimethylbut-2-enamide

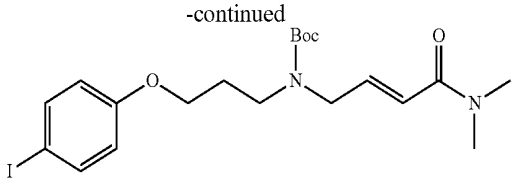


The reaction was carried out according to Scheme 3, Step-3 using 3-(4-iodophenoxy)propan-1-amine (10.6 g, 38 mmol) for compound 217 and (E)-4-chloro-N,N-dimethylbut-2-enamide and (E)-4-bromo-N,N-dimethylbut-2-enamide mixture (5.2 g, 30.6 mmol, Example 63, Step-7) for compound 214. The crude material was used in next step (14.7 g, crude).

Step-5: Synthesis of tert-butyl (E)-(4-(dimethylamino)-4-oxobut-2-en-1-yl)(3-(4-iodophenoxy)propyl)carbamate



-continued



The reaction was carried out according to Scheme 3, Step-4 using (E)-4-((3-(4-iodophenoxy)propyl)amino)-N,N-dimethylbut-2-enamide (14.7 g, 37.8 mmol) for compound 218 to afford crude product, which was purified by column chromatography over 60-120 mesh silica-gel, eluting with 60-80% ethyl aceate in n-heane to afford the title compound of Ex. 95 Step-5 (7.1 g, 39%).

Compound 95:

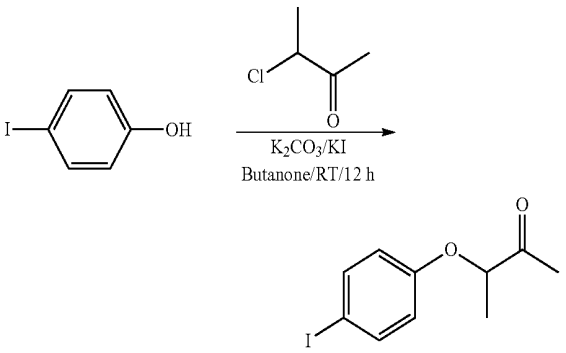
^{1}H NMR (400 MHz, DMSO-d_6): δ 13.05 (s, 1H), 8.06 (s, 1H), 7.60 (s, 1H), 7.52 (d, J=8.4 Hz, 1H), 7.20 (d, J=7.6 Hz, 2H), 7.15-7.11 (m, 4H), 6.74 (d, J=8.4 Hz, 2H), 6.58-6.48 (m, 4H), 3.86 (t, J=6.0 Hz, 2H), 3.25 (d, J=4.8 Hz, 2H), 2.96 (s, 3H), 2.83 (s, 3H), 2.56 (t, J=6.8 Hz, 2H), 2.41 (m, 2H), 1.90 (bs, 1H), 1.76 (t, J=6.0 Hz, 2H), 0.89 (t, J=7.6 Hz, 3H).

LCMS: 509.4 $[M+H]^+$.

Example 96: Synthesis of (E)-4-((3-(4-((E)-1-(1H-indazol-5-yl)-2-phenylbut-1-en-1-yl)phenoxy)butan-2-yl)amino)-N,N-dimethylbut-2-enamide (Compound 96)

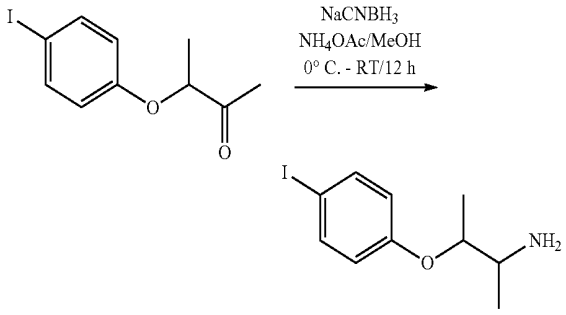
The compound was synthesized following the approach as outlined in Example 59 by substituting into Step-4 of Ex. 59 5-(but-1-yn-1-yl)-1-(tetrahydro-2H-pyran-2-yl)-1H-indazole (as prepared in Example 1, Step-3) for compound 276 and tert-butyl (E)-(4-(dimethylamino)-4-oxobut-2-en-1-yl)(3-(4-iodophenoxy)butan-2-yl)carbamate (preparation shown below in Ex. 96 Step 1-4) for compound 277 and substituting into Step-5 of Ex. 59 iodobenzene for compound 265 to isolate Compound 96 (0.165 g).

Step-1: Synthesis of 3-(4-iodophenoxy)butan-2-one



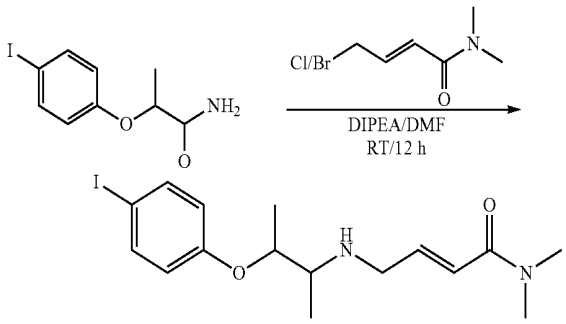
To a stirred solution of 4-iodophenol (5 g, 22.7 mmol) in butanone (100 mL) were added potassium carbonate (4.7 g, 34 mmol) and potassium iodide (0.376 g, 2.27 mmol). Reaction mixture was stirred for 30 min at room temperature, to the above mixture 3-chlorobutan-2-one (2.4 g, 22.7 mmol) was added. The contents were stirred at room temperature for 12 h. After completion of reaction, reaction mixture was poured onto ice cold water and extracted with ethyl acetate (2×250 mL). The combined organic extracts were washed with water, brine, dried over anhydrous sodium sulphate and concentrated under reduced pressure to obtain desired compound 3-(4-iodophenoxy)butan-2-one (6 g, 86%).

Step-2: Synthesis of 3-(4-iodophenoxy)butan-2-amine



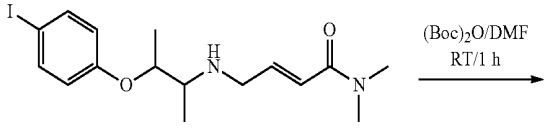
To a stirred solution of 3-(4-iodophenoxy)butan-2-one (3 g, 10.3 mmol) in methanol (50 mL) were added at 0° C., sodium cyanoborohydride (0.98 g, 15.5 mmol) and ammonium acetate (11.8 g, 154.5 mmol). The reaction mixture was stirred for 12 h at room temperature. After completion of reaction, reaction mixture was diluted with conc HCl and water, extracted with diethyl ether. Aqueous layer was basified with 5% NaOH solution, extracted with ethyl acetate. Organic layer was concentrated under reduced pressure and the crude material was used in next step without further purification (2.2 g, 70%).

Step-3: Synthesis of (E)-4-((3-(4-iodophenoxy)butan-2-yl)amino)-N,N-dimethylbut-2-enamide

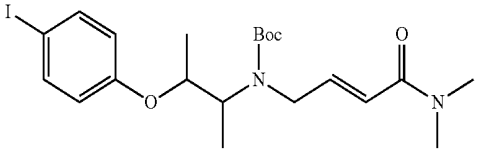


The reaction was carried out according to Scheme 3, Step-3 using 3-(4-iodophenoxy)butan-2-amine (2.9 g, 10.03 mmol) and (E)-4-chloro-N,N-dimethylbut-2-enamide and (E)-4-bromo-N,N-dimethylbut-2-enamide mixture (1.73 g, 9.03 mmol, Example 63, Step-7). The crude material was used in next step (4 g, crude).

Step-4: Synthesis of tert-butyl (E)-(4-(dimethylamino)-4-oxobut-2-en-1-yl)(3-(4-iodophenoxy)butan-2-yl)carbamate



-continued



The reaction was carried out according to Scheme 3, Step-4 using (E)-4-((3-(4-iodophenoxy)butan-2-yl)amino)-N,N-dimethylbut-2-enamide (4 g, 9.9 mmol) for compound 218. The crude product was purified by combi-flash eluting with 70% ethyl aceate in n-heane to afford the title compound of Ex. 96 Step-4 (2.9 g, 60%).

Compound 96:

^{1}H NMR (400 MHz, DMSO-d_6): δ 13.05 (s, 1H), 8.06 (s, 1H), 7.61 (s, 1H), 7.51 (d, J=11.2 Hz, 1H), 7.22-7.10 (m, 6H), 6.74-6.71 (m, 2H), 6.61-6.43 (m, 4H), 4.23-4.20 (m, 1H), 3.35-3.28 (m, 2H), 2.94-2.81 (m, 6H), 2.71-2.67 (m, 1H), 2.42-2.32 (m, 2H), 1.09-0.84 (m, 9H). LCMS: 523.3 $[M+H]^+$.

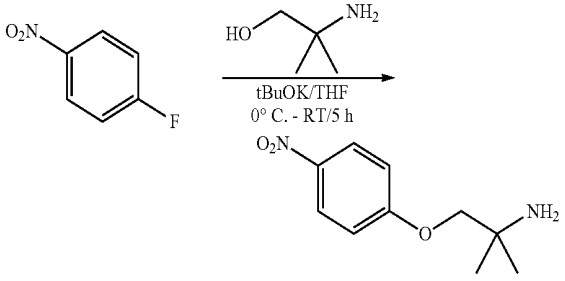
Example 97

There is no Example 97.

Example 98: Synthesis of (E)-4-((1-(4-((E)-1-(1H-indazol-5-yl)-2-phenylbut-1-en-1-yl)phenoxy)-2-methylpropan-2-yl)amino)-N,N-dimethylbut-2-enamide (Compound 98)

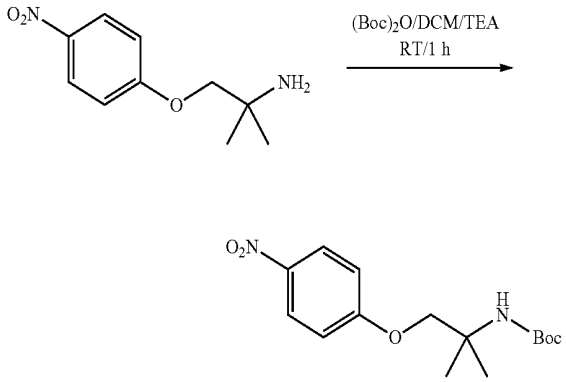
The compound was synthesized following the approach as outlined in Example 3 by (i) substituting into Step-1 of Ex. 3 5-(but-1-yn-1-yl)-1-(tetrahydro-2H-pyran-2-yl)-1H-indazole (as prepared in Example 1, Step-3) for compound 252, (ii) proceeding directly from Step-1 to Step-3 and substituting into Step-3 of Ex. 3 tert-butyl (1-(4-iodophenoxy)-2-methylpropan-2-yl)carbamate (preparation shown below in Ex. 98 Step 1-4) for compound 256, (iii) substituting into Step-4 of Ex. 3 Iodobenzene for compound 227, (iv) substituting Step-5 of Ex. 3 with reaction conditions described in Scheme 2, Step-6b, and (v) substituting into Step-6 of Ex. 3 (E)-4-chloro-N,N-dimethylbut-2-enamide and (E)-4-bromo-N,N-dimethylbut-2-enamide mixture (as prepared in Example 49, Step-4) for compound 251 to afford Compound 98 (0.035 g).

Step-1: Synthesis of 2-methyl-1-(4-nitrophenoxy)propan-2-amine



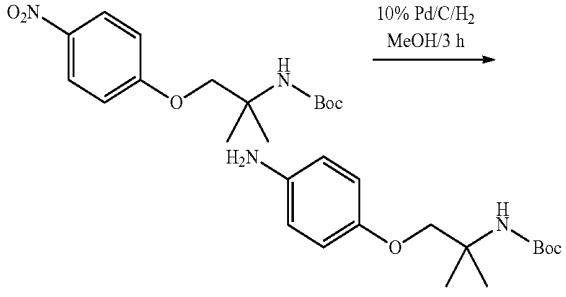
To a stirred solution of 2-amino-2-methylpropan-1-ol (4.5 g) in THF (25 mL) was added a solution of potassium tert-butoxide (5.7 g, 51 mmol) in THF (25 mL) at 0° C., stirred for 1 h at the same temperature. 1-Fluoro-4-nitrobenzene (5 g, 35.4 mmol) was added to the above reaction mixture and the reaction mixture was stirred at room temperature for 4 h. After completion of reaction, reaction mixture was diluted with ice cold water, extracted with EtOAc. The organic layer was dried over anhydrous sodium sulphate and concentrated under reduced pressure to afford the title compound in Ex. 98 Step-1 (6 g, 80%).

Step-2: Synthesis of tert-butyl (2-methyl-1-(4-nitrophenoxy)propan-2-yl)carbamate



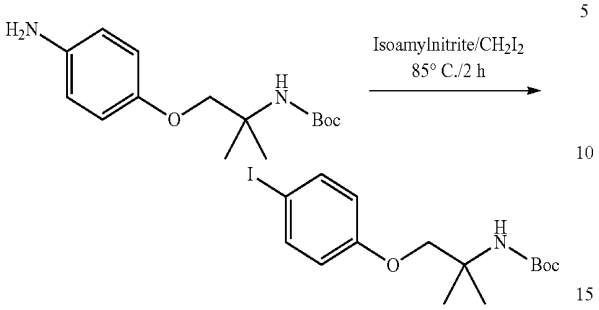
To a stirred solution of 2-methyl-1-(4-nitrophenoxy)propan-2-amine (5 g, 23.5 mmol) in DCM (50 mL) was added TEA (6.3 mL, 35.3 mmol) at room temperature, stirred for 15 min. Boc anhydride (6.1 mL, 28.2 mmol) was added and the reaction mixture was stirred at room temperature for 1 h. After completion of reaction, reaction mixture was diluted with ice cold water, extracted with EtOAc. The organic layer was dried over anhydrous sodium sulphate and concentrated under reduced pressure to afford the title compound in Ex. 98 Step-2 (7.3 g).

Step-3: Synthesis of tert-butyl (1-(4-aminophenoxy)-2-methylpropan-2-yl)carbamate



To a solution of tert-butyl (2-methyl-1-(4-nitrophenoxy)propan-2-yl)carbamate (6 g, 19.35 mmol) in methanol (70 mL) was added 10% Pd/C (1.5 g). Reaction mixture was stirred at room temperature under hydrogen atmosphere for 3 h. After completion of reaction, reaction mixture was filtered through celite, filterate was concentrated under reduced pressure to afford the crude product, crude compound was used in next step without further purification (6 g, crude).

Step-4: Synthesis of tert-butyl (1-(4-iodophenoxy)-2-methylpropan-2-yl)carbamate



A mixture of tert-butyl (1-(4-aminophenoxy)-2-methylpropan-2-yl)carbamate (4 g, 14.2 mmol), isoamylnitrite (19 mL, 142 mmol) and diiodomethane (11.4 mL, 142 mmol) stirred at 85° C. for 2 h. After completion of reaction, reaction mixture was diluted with ice cold water, extracted with EtOAc. The organic layer was dried over anhydrous sodium sulphate and concentrated under reduced pressure to afford the crude product, crude compound was purified by combi-flash eluting with 5% ethyl acetate in n-hexane to afford title compound in Ex. 98 Step-4 (0.9 g, 37%).

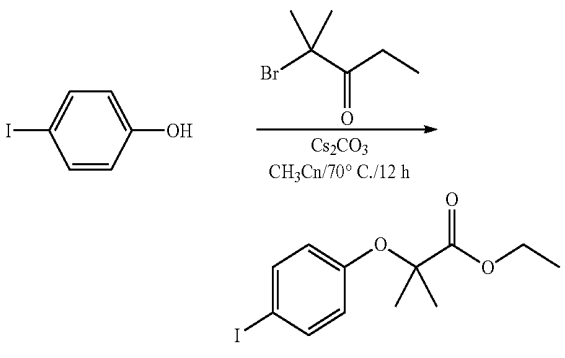
Compound 98:

^{1}H NMR (400 MHz, DMSO-d_6): δ 13.05 (s, 1H), 8.06 (s, 1H), 7.60 (s, 1H), 7.51 (d, J=8.8 Hz, 1H), 7.20 (d, J=7.2 Hz, 1H), 7.15-7.10 (m, 5H), 6.74 (d, J=8 Hz, 2H), 6.65-6.58 (m, 3H), 6.49 (d, J=15.2 Hz, 1H), 3.60 (s, 2H), 3.28-3.06 (m, 2H), 2.98 (s, 3H), 2.89 (s, 3H), 2.40 (d, J=8 Hz, 2H), 1.04 (s, 6H), 0.87 (t, J=7.2 Hz, 3H). LCMS: 523.4 $[M+H]^+$.

Example 99: Synthesis of (E)-4-((2-(4-((E)-1-(1H-indazol-5-yl)-2-phenylbut-1-en-1-yl)phenoxy)-2-methylpropyl)amino)-N,N-dimethylbut-2-enamide (Compound 99)

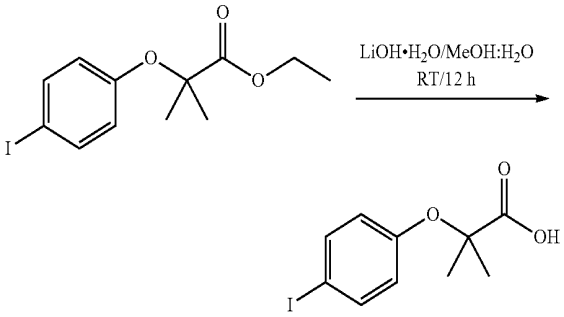
The compound was synthesized following the approach as outlined in Example 59 by (i) substituting into Step-4 of Ex. 59 5-(but-1-yn-1-yl)-1-(tetrahydro-2H-pyran-2-yl)-1H-indazole (sa prepared in Example 1, Step-3) for compound 276 and tert-butyl (E)-(4-(dimethylamino)-4-oxobut-2-en-1-yl)(2-(4-iodophenoxy)-2-methylpropyl)carbamate (preparation shown below Ex. 99 Step 1-5) for compound 277, and (ii) substituting into Step-5 of Ex. 59 iodobenzene for compound 265 to afford Compound 99 (0.19 g).

Step-1: Synthesis of ethyl 2-(4-iodophenoxy)-2-methylpropanoate



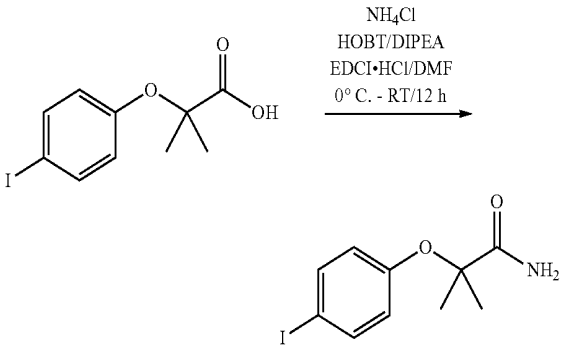
To a stirred solution of 4-iodophenol (10 g, 45.45 mmol) in acetonitrile (100 mL) were added cesium carbonate (29.5 g, 90 mmol) and 2-bromo-2-methylpentan-3-one (8.86 g, 45.45 mmol). The contents were stirred at 70° C. for 12 h. After completion of reaction, reaction mixture was poured onto ice cold water and extracted with ethyl acetate (2×250 mL). The combined organic extracts were washed with water, brine, dried over anhydrous sodium sulphate and concentrated under reduced pressure to obtain desired compound ethyl 2-(4-iodophenoxy)-2-methylpropanoate (15 g).

Step-2: Synthesis of 2-(4-iodophenoxy)-2-methylpropanoic acid



To a stirred solution of ethyl 2-(4-iodophenoxy)-2-methylpropanoate (15 g, 44.91 mmol) in MeOH:H_2O (60 mL, 3:1) was added LiOH.H_2O (3.77 g, 89.82 mmol). The reaction mixture was stirred for 12 h at room temperature, after completion of reaction (monitored by TLC), reaction mixture was diluted with water and acidified with 2M HCl, extracted with EtOAc (300 mL). The organic layer was washed with water followed by saturated NaCl solution, dried over anhydrous Na_2SO_4 and concentrated under reduced pressure. The crude product was used in next step without further purification (12 g).

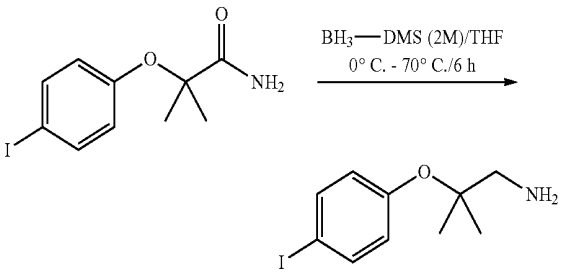
Step-3: Synthesis of 2-(4-iodophenoxy)-2-methylpropanamide



To a stirred solution of 2-(4-iodophenoxy)-2-methylpropanoic acid (13 g, 42.48 mmol) in DMF (25 mL) was added DIPEA (14.6 mL, 84.96 mmol), EDCI.HCl (12.21 g, 63.72 mmol), HOBT (8.6 g, 63.72 mmol) and ammonium chloride (4.58 g, 84.96 mmol). The reaction mixture was stirred for 12 h at room temperature, after completion of reaction (monitored by TLC), reaction mixture was diluted with

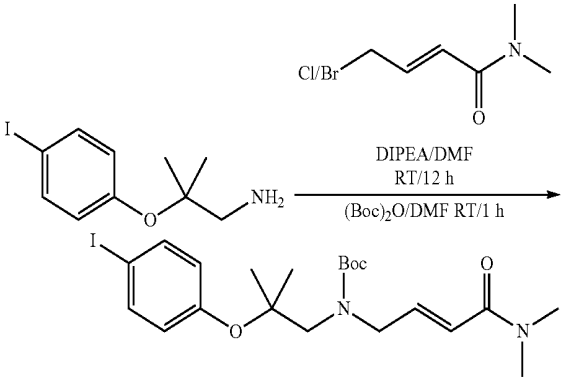
water and extracted with EtOAc (500 mL). The organic layer was washed with water followed by saturated NaCl solution, dried over anhydrous Na_2SO_4 and concentrated under reduced pressure to afford crude compound, crude compound was purified by combi-flash using 2% MeOH in dichloromethane to afford the title compound of Ex. 99 Step-3 (12 g, 97%).

Step-4: Synthesis of 2-(4-iodophenoxy)-2-methylpropan-1-amine



A solution of 2-(4-iodophenoxy)-2-methylpropanamide (11.2 g, 36.72 mmol), in THF (110 mL) was added to a solution of borane-methyl sulphide complex (36.7 mL, 73.44 mmol) was added drop wise and the contents were stirred for 6 h at 70° C. The reaction mixture was quenched with methanol, water was added to the reaction mixture, extracted twice with ethyl acetate. The combined organic layers were washed with water followed by brine solution and dried over anhydrous sodium sulphate. The solvent was removed under reduced pressure to obtain the title compound in Ex. 99 Step-4 (8.5 g, 80%).

Step-5: Synthesis of tert-butyl (E)-(4-(dimethylamino)-4-oxobut-2-en-1-yl)(2-(4-iodophenoxy)-2-methylpropyl)carbamate



The reaction was carried out according to Scheme 3, Step-3 using 2-(4-iodophenoxy)-2-methylpropan-1-amine (5 g, 17.18 mmol) in DMF (50 mL) and (E)-4-chloro-N,N-dimethylbut-2-enamide and (E)-4-bromo-N,N-dimethylbut-2-enamide mixture (2.39 g, 13.74 mmol, Example 63, Step-7). The crude product was purified by combi-flash eluting with 2% MeOH in dichloromethane to afford the title product of Ex. 99 Step 5 (5 g, 58%).

Compound 99:

^{1}H NMR (400 MHz, DMSO-d_6): δ 13.06 (s, 1H), 8.07 (s, 1H), 7.63 (s, 1H), 7.52 (d, J=8.8 Hz, 1H), 7.11-7.10 (m, 5H), 7.09 (d, J=2 Hz, 1H), 6.75 (d, J=8.4 Hz, 2H), 6.63-6.60 (m, 2H), 6.51 (t, J=5.4 Hz, 1H), 6.50 (s, 1H), 2.98 (s, 3H), 2.84 (s, 3H), 2.41 (q, J=7.2 Hz, 2H), 1.12 (s, 6H), 0.87 (t, J=7.2 Hz, 3H). LCMS: 523.3 $[M+H]^+$.

Example 100

There is no Example 100.

EXAMPLES

Example 101—Compounds that Inhibit ER$\alpha^{WT/MUT}$ Activity In Vitro

Cell Culture

MCF7 BUS cells (Coser, et al., (2003) PNAS 100(24): 13994-13999) were maintained in Dulbecco's Modified Eagle Medium supplemented with 10% FBS, 4 mM L-glutamine and 1× non-essential amino acids. Lenti-X 293T cells (Clontech, Cat #632180) were routinely cultured in Dulbecco's Modified Eagle Medium supplemented with 10% FBS.

Site-Direct Mutagenesis and Cell Line Engineering

The QuikChange II XL Site-Directed Mutagenesis Kit (Agilent Technologies, Cat #200523) was used to generate Y537S, Y537C, Y537N and D538G mutations within the ERα exon 8. Wild-type ESR1 cDNA (GeneCopoeia Inc., Cat# GC-A0322, accession no. NM 000125) was used as a template with the following mutagenesis primers (where the underlined nucleotides represent site mutations); Y537S: F-AAG AAC GTG GTG CCC CTC TCT GAC CTG CTG CTG GAG ATG (SEQ ID NO: 1), R-CAT CTC CAG CAG CAG GTC AGA GAG GGG CAC CAC GTT CTT (SEQ ID NO: 2); Y537N: F-AAG AAC GTG GTG CCC CTC AAT GAC CTG CTG CTG GAG ATG (SEQ ID NO: 3), R-CAT CTC CAG CAG CAG GTC ATT GAG GGG CAC CAC GTT CTT (SEQ ID NO: 4); Y537C: F-AAG AAC GTG GTG CCC CTC TGT GAC CTG CTG CTG GAG ATG (SEQ ID NO: 5), R-CAT CTC CAG CAG CAG GTC ACA GAG GGG CAC CAC GTT CTT (SEQ ID NO: 6); D538G: F-AAC GTG GTG CCC CTC TAT GGC CTG CTG CTG GAG ATG CTG (SEQ ID NO: 7), R-CAG CAT CTC CAG CAG CAG GCC ATA GAG GGG CAC CAC GTT (SEQ ID NO: 8). WT and mutant ESR1 cDNAs were cloned into the designation lentiviral vector pLenti6.3/V5-Dest (Invitrogen, Cat #V533-06). To make lentivirus, DNAs (WT and mutant ESR1) were co-transfected with packaging plasmids into Lenti-X 293T cells using TransIT (Mirus, Cat #MIR 2700). 48 h post-transfection, virus containing media was filtered and added to MCF7 cells in the presence of 8 μg/ml polybrene overnight. Two days following infection, cells were placed under selection with 10 μg/ml blasticidin for 2 weeks for stable expression.

In Vitro Proliferation Assays

MCF7-WT and -Y537S cells were seeded at 1500 cells/well in black-walled 96-well plates (assay plates, Costar, Cat #3904). In parallel, cells were also seeded in a separate 96-well plate (8 wells/cell line, control plate) for which a CTG (CellTiter-Glo® Luminescent Viability Assay, Promega, Cat #G7572) was measured the following day (day 0 reading). The day 0 reading was used for the GI_{50} calculation at the termination of the experiment. The day following seeding, compounds were added to assay plates. Briefly, a 1:4 serial dilution was prepared in DMSO at 200× final concentration for a total of 10 concentrations (9 dilutions containing compound and one is DMSO only). Serially

diluted compounds were pipetted into medium to prepare a compound-medium mix at 10× final concentration. 10 μl of compound-medium mix was added to MCF7-WT and -Y537S cells at 3 wells/concentration (triplicate for each concentration). On day 3, media/compound was removed and replaced with fresh media/compound as described above. On day 6, CTG was measured and compared to day 0 readings from control plate to assess GI_{50}.

Results

FIG. **1** shows that ectopic expression of $ER\alpha^{Y537S/N/C, D538G}$ in MCF7 cells conferred phenotypic resistance to currently marketed therapies tamoxifen (SERM), raloxifene (SERM) and fulvestrant (SERD). Similar observations were also recently published by several independent labs (Jeselsohn et al., (2014) *Clin Cancer Res.* April 1; 20(7):1757-67; Toy et al., (2013) *Nat Genet.* 2013 December; 45(12):1439-45; Robinson et al., (2013) *Nat Genet.* December; 45(12): 1446-51; Merenbakh-Lamin et al., (2013) *Cancer Res.* December 1; 73(23):6856-64; Yu et al., (2014) *Science* July 11; 345(6193):216-20). Having confirmed that $ER\alpha^{MUT}$ drive resistance to current endocrine therapies, identification of novel compounds that would reduce proliferation of the $ER\alpha^{MUT}$-bearing MCF7 cells more efficaciously than the corresponding clinical compound 4-hydroxytamoxifen was sought. Using the WT and mutant viability assay as a screening tool, compounds were identified that were more potent towards the Y537S-bearing MCF7 line relative to 4-hydroxytamoxifen. The results of the viability assay screen are shown in Table 1 above.

In Vivo Xenograft Methods

Methods and Materials

In the following examples (Examples 102-109) and in the figures that are referred to in those examples, references to compound 1, compound 60, and compound 69 refer to a hydrochloride salt of the respectively numbered compounds. These hydrochloride salts were prepared as outlined above in Examples 1A, 60A, and 69A.

MCF7 Xenograft Study

The ESR1 wild-type human ER+ breast cancer cell line MCF7 (ATCC) was cultured in DMEM media supplemented with 10% FBS at 37° C. in a 5% CO2 atmosphere and kept in the exponential growth phase. The cells were collected in trypsin and re-suspended in a 1:1 mixture of matrigel and HBSS at a final concentration of 5×10^7 cells/mL. A 0.2 mL aliquot of cells was injected subcutaneously into the 3rd mammary fat pad of 6-8 week old female Balb/c nude mice, giving 1×10^7 cells/mouse. When the average tumor volume reached approximately 155 mm^3, 92 animals were randomized prior to treatment.

Anti-tumor activity in the MCF7 xenograft model was examined using compound 1, compound 60, and compound 69. All of the compounds were dosed orally every day at doses ranging from 1 to 30 mg/kg. Each treatment was started on Day 0 and the administration schedule was continued for 17 days. The administration volume was calculated from the individual mouse body weights prior to dose administration. The body weights were measured daily while the tumor volumes were measured twice a week. Tumor volumes (TV) were calculated based on the formula:

$$TV=length\times width^2\times 0.5$$

length: largest diameter of tumor (mm)

width: diameter perpendicular to length (mm)

The Tumor Growth Inhibition % (TGI) was calculated according to the following formula:

$$\text{Tumor Growth Inhibition \% } (TGI) = \frac{\text{Average Control } TV \text{ Day } X - \text{Treatment } TV \text{ Day } X}{\text{Average Control } TV \text{ Day } X} \times 100$$

Where Day X is the endpoint measurement.

Y537S Positive PDx Xenograft Study

A Patient-Derived Xenograft (PDX) tumor model representing an ESR1-Y537S mutated human ER+ breast cancer, designated as PDX-Y537S, was propagated subcutaneously in immunocompromised mice. The tumors were excised within 60 days of implantation and processed to mixed tumor fragments. Solid tumor tissues were depleted of necrotic components, cut into 70 mg fragments, mixed with matrigel and subcutaneously implanted into the right flank of 6-12 week old female athymic Nude (Crl:NU(NCr)-Foxnlnu) mice. The precise number of fragments and volume of matrigel was determined on a case by case basis. When the average tumor volume reached approximately 200 mm^3, animals were randomized prior to treatment. All of the primary human tumors utilized in this study had undergone approximately 7 passages in vivo.

Anti-tumor activity in the PDX-Y537S model was examined using compound 1, compound 60, and compound 69. Estrogen was not supplemented in the studies. All compounds were dosed orally every day at doses ranging from 3 to 200 mg/kg. Each treatment was started on Day 0 and the administration schedule was continued for up to 35 days. The administration volume was calculated from the individual mouse body weights prior to dose administration. The body weights were measured daily while the tumor volumes were measured twice a week. Tumor volumes were calculated based on the previously described formula.

WHIM20 Xenograft Study

The Patient-Derived Xenograft (PDX) tumor model, WHIM20, representing an ESR1-Y537S mutated human ER+ breast cancer was propagated in mice. The tumors were excised and processed to mixed tumor fragments and the fragments were re-implanted subcutaneously into new recipient mice. For the current work, solid tumor tissues were depleted of necrotic components, cut into fragments, mixed with matrigel and subcutaneously implanted into the right flank of 6-8 week old female SCID-bg mice. The precise number of fragments and volume of matrigel was determined on a case by case basis. When the average tumor volume reached approximately 370 mm^3, animals were randomized prior to treatment. All of the primary human tumors utilized in this study had undergone approximately 4 passages in vivo.

Anti-tumor activity in the WHIM20 patient derived xenograft model was examined using compound 1 and compound 60 in separate studies. Estrogen was not supplemented in WHIM20 studies. Compounds 1 and 60 were dosed orally every day at the indicated doses. Each treatment was started on Day 0 and the administration schedule was continued for the indicated days. The administration volume was calculated from the individual mouse body weights prior to dose administration. The body weights were measured daily while the tumor volumes were measured twice a week. Tumor volumes were calculated based on the previously described formula.

Statistical Analysis

Data are expressed as the mean±SEM for tumor volume and the mean±SEM for body weight. The differences in tumor volume during the study period between the vehicle

treated and compound treated groups were analyzed by two-way analysis of variance (ANOVA) followed by the Dunnett multiple comparison post hoc test. Statistical analyses were performed using the GraphPad Prism® version 5.04 (GraphPad Software, La Jolla, Calif.).

Example 102

FIG. **2** shows the anti-tumor and body weight effects of compound 1 in the MCF7 xenograft model carrying the wild-type ER grown in immunocompromised mice. Compound 1 inhibited xenograft growth in a dose dependent manner with 10 mg/kg QD and 30 mg/kg QD significantly inhibiting growth on day 17 compared to the control (TGI of 68% and 83% and $p<0.0001$ for both doses, respectively). Compound 1 treatment of 1 mg/kg QD and 3 mg/kg QD was not statistically different from the control treated group (TGI of 19% and 41%, respectively). All doses and regimens were well tolerated with no significant body weight loss.

Compound 1 was given orally once daily for the duration of the study. Data in FIG. **2** represent the mean±SEM (Tumor Volume), or the mean±SEM (Body Weight) (N=6 for treatment groups, N=8 for Vehicle control). * $p<0.0001$ versus vehicle control on Day 17 (Two-Way ANOVA followed by the Dunnett multiple comparison test).

Example 103

FIG. **3** shows the anti-tumor and body weight effects of compound 1 in the PDX-Y537S model bearing a heterozygous Y537S mutation. Compound 1 dosed daily inhibited xenograft growth in a dose dependent manner with 10 mg/kg, 30 mg/kg, 100 mg/kg and 200 mg/kg treatments significantly inhibiting growth on day 35 (TGI of 35%, 63%, 76% and 81% and $p<0.01$, $p<0.0001$, $p<0.0001$ and $p<0.0001$, respectively). Compound 1 treated daily at 3 mg/kg was not statistically different from the Vehicle treated group (TGI of 3%). All doses and regimens were well tolerated with no significant body weight loss.

Compound 1 was given orally once daily for the duration of the study. Data represent the mean±SEM (Tumor Volume) or mean±SEM (Body Weight) (N=8 for all groups). *$p<0.01$, **$p<0.0001$ versus vehicle control on Day 35 (Two-Way ANOVA followed by the Dunnett multiple comparison post hoc test).

Example 104

FIG. **4** shows the anti-tumor and body weight effects of compound 1 in the ER+ WHIM20 PDX model bearing a homozygous Y537S mutation. Daily treatment with compound 1 at 100 mg/kg significantly reduced tumor growth relative to the vehicle control (TGI of 45%; $p<0.05$). This dose of compound 1 was tolerated in accordance with internal animal care and use committee guidelines.

Compound 1 was given orally once daily for the duration of the study. Data represent the mean±SEM (Tumor Volume) or mean±SEM (Body Weight) (N=9 for all groups). *$p<0.05$ versus vehicle control on Day 27 (Two-Way ANOVA followed by the Dunnett multiple comparison post hoc test).

Example 105

FIG. **5** shows the antitumor and body weight effects of compound 60 in the MCF7 subcutaneous xenograft model carrying wild-type ER grown in immunocompromised mice. Compound 60 inhibited xenograft growth in a dose dependent manner with 3 mg/kg QD, 10 mg/kg QD and 30 mg/kg QD treatments inhibiting growth on day 17 (TGI of 75%, 80% and 85% and $p<0.0001$ for all doses, respectively). Compound 60 treatment of 1 mg/kg QD×18 did not show a statistically meaningful difference from the control treated group (TGI of 36%, $p>0.05$). All doses and regimens were well tolerated with no significant body weight loss or clinical signs.

Compound 60 was given orally once daily for the duration of the study. Data represent the mean±SEM (Tumor Volume) or mean±SEM (Body Weight) (N=6 for treatment groups, N=8 for Vehicle control). * $p<0.0001$ versus vehicle control on Day 17 (Two-Way ANOVA followed by the Dunnett multiple comparison test).

Example 106

FIG. **6** shows the antitumor and body weight effects of compound 60 in a repeat study in the ER+ PDX-Y537S model bearing a heterozygous Y537S mutation. Compound 60 inhibited xenograft growth in a dose dependent manner with 3 mg/kg QD, 10 mg/kg QD, 30 mg/kg QD and 100 mg/kg QD treatments significantly inhibiting growth on day 28 (TGI of 61%, 85%, 81% and 84% and $p<0.001$, $p<0.0001$, $p<0.0001$ and $p<0.0001$, respectively). All doses were well tolerated with no significant body weight loss or clinical signs.

Compound 60 was given orally once daily for the duration of the study. Data represent the mean±SEM (Tumor Volume) or mean±SEM (Body Weight) (N=6 for compound 60 and N=8 for vehicle). * $p<0.001$, ** $p<0.0001$ versus vehicle control on Day 28 (Two-Way ANOVA followed by the Dunnett multiple comparison test).

Example 107

FIG. **7** shows the antitumor and body weight effects of compound 69 in the MCF7 subcutaneous xenograft model carrying wild-type ER grown in immunocompromised mice. Compound 69 inhibited xenograft growth in a dose dependent manner with 3 mg/kg QD, 10 mg/kg QD and 30 mg/kg QD treatments inhibiting growth on day 17 (TGI of 72%, 80% and 83% and $p<0.0001$ for all doses, respectively). Compound 69 treatment of 1 mg/kg QD did not show statistically meaningful difference from the control treated group (TGI of 42%). All doses were well tolerated with no significant body weight loss or clinical signs.

Compound 69 was given orally once daily for the duration of the study. Data represent the mean±SEM (Tumor Volume) or mean±SEM (Body Weight) (N=6 for treatment groups, N=8 for Vehicle control). * $p<0.0001$ versus vehicle control on Day 17 (Two-Way ANOVA followed by the Dunnett multiple comparison test).

Example 108

FIG. **8** shows the antitumor and body weight effects of compound 69 in the ER+ PDX-Y537S model bearing a heterozygous Y537S mutation. Compound 69 showed significant efficacy with 3 mg/kg QD, 10 mg/kg QD, 30 mg/kg QD and 100 mg/kg QD treatments inhibiting growth on day 28 relative to vehicle treatment group (TGI of 62%, 72%, 67% and 76% and $p<0.001$, $p<0.0001$, $p<0.001$ and $p<0.0001$, respectively). All doses were well tolerated with no significant body weight loss or clinical signs.

Compound 69 was given orally once daily for the duration of the study. Data represent the mean±SEM (Tumor Volume)

or mean±SEM (Body Weight) (N=8). * p<0.001, ** p<0.0001 versus vehicle control on Day 28 (Two-Way ANOVA followed by the Dunnett multiple comparison test).

Example 109

FIG. **9** shows the anti-tumor and body weight effects of compound 60 in the ER+ WHIM20 PDX model bearing a homozygous Y537S mutation. Compound 60 inhibited xenograft growth in a dose dependent manner with 10 mg/kg QD, 30 mg/kg QD and 100 mg/kg QD treatments significantly inhibiting growth on day 22 (TGI of 26%, 36%, and 48% and p<0.05, p<0.01 and p<0.0001, respectively). This dose of compound 60 was tolerated in accordance with internal animal care and use committee guidelines.

Compound 60 was given orally once daily for the duration of the study. Data represent the mean±SEM (Tumor Volume) or mean±SEM (Body Weight) (N=8 for all groups). *p<0.05, **p<0.01 and ***p<0.0001 respectively versus vehicle control on Day 22 (Two-Way ANOVA followed by the Dunnett multiple comparison test).

It will now be apparent that new, improved, and nonobvious compositions have been described in this specification with sufficient particularity as to be understood by one of ordinary skill in the art. Moreover, it will be apparent to those skilled in the art that modifications, variations, substitutions, and equivalents exist for features of the compositions which do not materially depart from the spirit and scope of the embodiments disclosed herein. Accordingly, it is expressly intended that all such modifications, variations, substitutions, and equivalents which fall within the spirit and scope of the invention as defined by the appended claims shall be embraced by the appended claims.

SEQUENCE LISTING

<160> NUMBER OF SEQ ID NOS: 8

<210> SEQ ID NO 1
<211> LENGTH: 39
<212> TYPE: DNA
<213> ORGANISM: artificial sequence
<220> FEATURE:
<223> OTHER INFORMATION: mutagenesis primer

<400> SEQUENCE: 1

aagaacgtgg tgcccctctc tgacctgctg ctggagatg 39

<210> SEQ ID NO 2
<211> LENGTH: 39
<212> TYPE: DNA
<213> ORGANISM: artificial sequence
<220> FEATURE:
<223> OTHER INFORMATION: mutagenesis primer

<400> SEQUENCE: 2

catctccagc agcaggtcag agaggggcac cacgttctt 39

<210> SEQ ID NO 3
<211> LENGTH: 39
<212> TYPE: DNA
<213> ORGANISM: artificial sequence
<220> FEATURE:
<223> OTHER INFORMATION: mutagenesis primer

<400> SEQUENCE: 3

aagaacgtgg tgcccctcaa tgacctgctg ctggagatg 39

<210> SEQ ID NO 4
<211> LENGTH: 39
<212> TYPE: DNA
<213> ORGANISM: artificial sequence
<220> FEATURE:
<223> OTHER INFORMATION: mutagenesis primer

<400> SEQUENCE: 4

catctccagc agcaggtcat tgaggggcac cacgttctt 39

<210> SEQ ID NO 5
<211> LENGTH: 39
<212> TYPE: DNA
<213> ORGANISM: artificial sequence
<220> FEATURE:
<223> OTHER INFORMATION: mutagenesis primer

-continued

<400> SEQUENCE: 5

aagaacgtgg tgcccctctg tgacctgctg ctggagatg 39

<210> SEQ ID NO 6
<211> LENGTH: 39
<212> TYPE: DNA
<213> ORGANISM: artificial sequence
<220> FEATURE:
<223> OTHER INFORMATION: mutagenesis primer

<400> SEQUENCE: 6

catctccagc agcaggtcac agaggggcac cacgttctt 39

<210> SEQ ID NO 7
<211> LENGTH: 39
<212> TYPE: DNA
<213> ORGANISM: artificial sequence
<220> FEATURE:
<223> OTHER INFORMATION: mutagenesis primer

<400> SEQUENCE: 7

aacgtggtgc ccctctatgg cctgctgctg gagatgctg 39

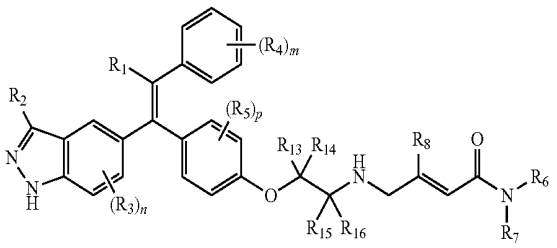
<210> SEQ ID NO 8
<211> LENGTH: 39
<212> TYPE: DNA
<213> ORGANISM: artificial sequence
<220> FEATURE:
<223> OTHER INFORMATION: mutagenesis primer

<400> SEQUENCE: 8

cagcatctcc agcagcaggc catagagggg caccacgtt 39

What is claimed is:

1. A compound given by formula II:



II

wherein:

R_1 is selected from the group consisting of methyl, ethyl, cyclobutyl, cyclopropyl, propyl, isopropyl, —CH_2CF_3, —CH_2CH_2F, and —CH_2CH_2Cl;

R_2 is selected from the group consisting of H and F;

n is 0-1;

R_3 is F when n=1;

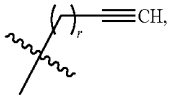
m is 0-2;

R_4 are the same or different and are independently selected from the group consisting of F, CF_3, Cl, isopropyl, —OCH_3, —$OCHF_2$, —OCF_3, ethyl and methyl;

p is 0-1;

R_5 is F when p=1;

R_6 and R_7 are the same or different and are independently selected from the group consisting of methyl, ethyl, propyl, —CH_2CH_2OH and



wherein r is 1 or 2; or, wherein R_6 and R_7 form a 4-6 membered heterocyclic ring with the N to which they are attached, wherein said heterocyclic ring optionally includes an oxygen atom, and wherein said heterocyclic ring is optionally substituted with F, or —CH_2F;

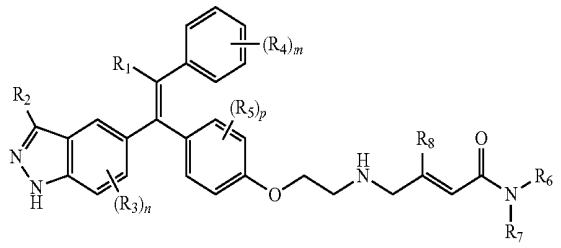
R_8 is selected from the group consisting of H and —CH_3;

and R_{13}, R_{14}, R_{15}, and R_{16} are independently selected from the group consisting of —H or —CH_3;

or a pharmaceutically acceptable salt thereof.

2. The compound or pharmaceutically acceptable salt of claim **1**, given by formula I:

I



wherein:

R_1 is selected from the group consisting of methyl, ethyl, cyclobutyl, cyclopropyl and —CH_2CH_2Cl;

R_2 is selected from the group consisting of H and F;

n is 0-1;

R_3 is F when n=1;

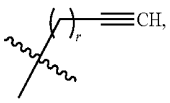
m is 0-2;

R_4 are the same or different and are independently selected from the group consisting of F, CF_3, Cl, isopropyl, —OCH_3, —$OCHF_2$, —OCF_3, ethyl and methyl;

p is 0-1;

R_5 is F when p=1;

R_6 and R_7 are the same or different and are independently selected from the group consisting of methyl, ethyl, propyl, —CH_2CH_2OH and



wherein r is 1 or 2;

or, wherein R_6 and R_7 form a 4-6 membered heterocyclic ring with the N to which they are attached, wherein said heterocyclic ring optionally includes an oxygen atom, and wherein said heterocyclic ring is optionally substituted with F, or —CH_2F;

R_8 is selected from the group consisting of H and CH_3;

or a pharmaceutically acceptable salt thereof.

3. The compound or pharmaceutically acceptable salt according to claim **2**, wherein R_1 is ethyl.

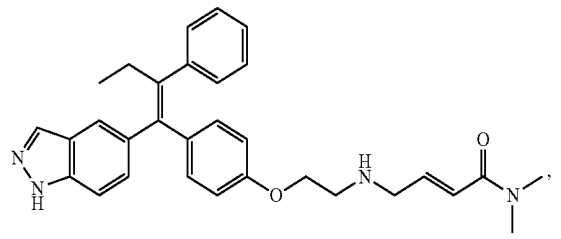
4. The compound or pharmaceutically acceptable salt according to claim **2**, wherein R_6 and R_7 are both methyl.

5. The compound or pharmaceutically acceptable salt according to claim **2**, wherein R_2 and R_8 are H.

6. The compound or pharmaceutically acceptable salt according to claim **2**, wherein R_2 is F.

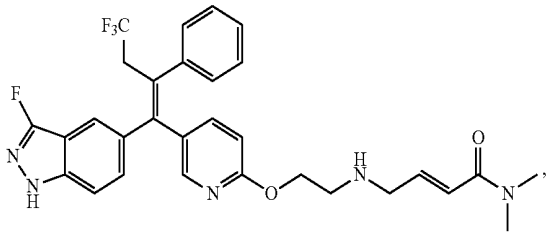
7. The compound or pharmaceutically acceptable salt according to claim **2**, wherein m, n, and p are 0.

8. The compound of claim **2**, having the following formula:



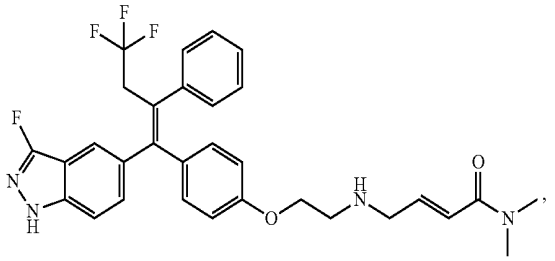
or a pharmaceutically acceptable salt thereof.

9. A compound having the following formula:



or a pharmaceutically acceptable salt thereof.

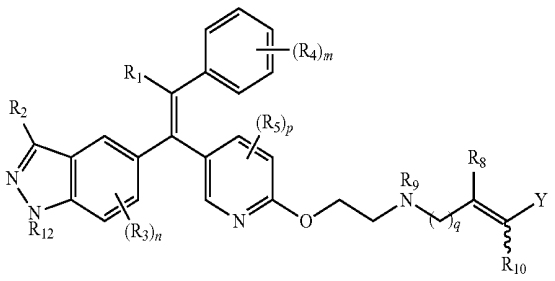
10. The compound of claim **1** having the following formula:



or a pharmaceutically acceptable salt thereof.

11. A compound given by formula III:

III



wherein:

R_1 is selected from the group consisting of C_1-C_6 alkyl, C_3-C_6 cycloalkyl, —CH_2CF_3, and a 4-6 membered heterocyclic ring;

R_2 is selected from the group consisting of H, halogen, hydroxy, C_1-C_3 alkyl, C_3-C_4 cycloalkyl and C_4 heterocyclic ring;

when n is not 0, R_3 are the same or different, and are independently selected from the group consisting of H, halogen, C_1-C_6 alkyl and C_1-C_3 alkoxy optionally substituted with at least one halogen;

n is 0-3;

when m is not zero, R_4 are the same or different and are independently selected from the group consisting of H, halogen, C_1-C_6 alkyl, and OR_{11}, wherein R_{11} is selected from the group consisting of C_3-C_6 cycloalkyl, C_1-C_6 alkyl, aryl, heteroaryl and a 4-6 membered heterocyclic ring;

m is 0-5;

when p is not 0, R_5 are the same or different and are independently selected from the group consisting of

H, halogen, C_1-C_4 alkyl, C_1-C_4 alkoxy, C_3-C_4 cycloalkyl, C_3-C_6 cycloalkoxy and C_4 heterocycle;

p is 0-3;

q is 1-2;

R_8 and R_{10} are the same or different and are independently selected from the group consisting of halogen, H and C_1-C_3 alkyl;

R_9 is selected from the group consisting of H, C_1-C_6 alkyl and C_3-C_6 cycloalkyl;

Y is selected from the group consisting of —$S(O)_2R_6$, —$S(O)_2NR_6R_7$, —$C(O)NR_6R_7$, —$C(O)R_6$, —$C(O)OR_6$, —CN; or wherein Y and R_{10} both represent —CF_3;

R_6 and R_7 are the same or different and are independently selected from the group consisting of H, C_1-C_6 alkyl, C_3-C_6 cycloalkyl, aryl, heteroaryl and a 4-6 membered heterocyclic ring wherein said alkyl is saturated or unsaturated or wherein R_6 and R_7 form a 4-6 membered heterocyclic ring with the N to which they are attached, optionally also containing an O atom;

R_{12} is selected from the group consisting of H, C_3-C_4 cycloalkyl and C_1-C_6 alkyl; and

wherein any carbon containing moiety of R_1-R_{12} may be optionally substituted with one or more halogen atoms, fluoromethane, difluoromethane or trifluoromethane, or —OH;

or pharmaceutically acceptable salts thereof.

12. The compound or pharmaceutically acceptable salt according to claim **11**, wherein R_1 is selected from the group consisting of C_1-C_6 alkyl, C_3-C_6 cycloalkyl, and a 4-6 membered heterocyclic ring.

13. The compound or pharmaceutically acceptable salt according to claim **11**, wherein:

R_2 is selected from the group consisting of H, halogen, methyl and ethyl;

R_3 are the same or different, and are independently selected from the group consisting of H, halogen, methyl and ethyl;

R_4 are the same or different and are independently selected from the group consisting of H, halogen, C_1-C_6 alkyl and C_1-C_6 alkoxy;

R_5 are the same or different and are independently selected from the group consisting of H, halogen, methyl and ethyl;

R_8 and R_{10} are the same or different and are independently selected from the group consisting of H and methyl;

R_9 is selected from the group consisting of H, methyl and ethyl; and

R_6 and R_7 are the same or different and are independently selected from the group consisting of H and C_1-C_6 alkyl or wherein R_6 and R_7 form a 4-6 atom heterocyclic ring with the N to which they are attached, optionally also containing an O atom.

14. The compound or pharmeutically acceptable salt of claim **11**, wherein Y is —$C(O)NR_6R_7$.

15. The compound or pharmaceutically acceptable salt of claim **11**, wherein R_6 and R_7 are methyl.

16. The compound or pharmaceutically acceptable salt of claim **14**, wherein R_2, R_8, R_9, and R_{10} are each H.

17. The compound or pharmaceutically acceptable salt of claim **14**, wherein R_1 is ethyl.

18. The compound or pharmaceutically acceptable salt of claim **14**, wherein R_1 is cyclobutyl.

19. The compound or pharmaceutically acceptable salt of claim **14**, wherein R_2 is F.

20. The compound or pharmaceutically acceptable salt of claim **14**, wherein m, n, and p are 0.

21. A method of treating breast cancer comprising administering to a subject a compound or pharmaceutically acceptable salt of claim **11**.

22. The method of claim **21**, wherein said breast cancer is an ER-positive breast cancer.

23. The method of claim **22**, where said subject expresses a mutant ER-α protein.

24. A method of treating breast cancer comprising administering to a subject a compound or pharmaceutically acceptable salt of claim **9**.

25. The method of claim **24**, wherein said breast cancer is an ER-positive breast cancer.

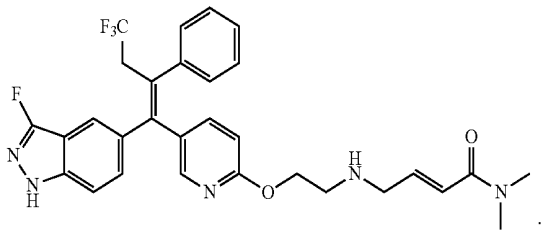
26. The method of claim **25**, where said subject expresses a mutant ER-α protein.

27. A pharmaceutical composition comprising the compound of claim **8** or a pharmaceutically acceptable salt thereof, and further comprising a pharmaceutically acceptable excipient.

28. A pharmaceutical composition comprising the compound of claim **9** or a pharmaceutically acceptable salt thereof, and further comprising a pharmaceutically acceptable excipient.

29. A pharmaceutical composition comprising the compound of claim **10** or a pharmaceutically acceptable salt thereof, and further comprising a pharmaceutically acceptable excipient.

30. The compound of claim **9**, having the following formula:



31. A pharmaceutical composition comprising the compound of claim **30**, and further comprising a pharmaceutically acceptable excipient.

32. A pharmaceutical composition comprising the compound of claim **11** or a pharmaceutically acceptable salt thereof, and further comprising a pharmaceutically acceptable excipient.

* * * * *

SEARCH HISTORY

Application Number	**PCT/US 16/34764**
Search Conducted By	JFK
Search Approved By	SV

IPC/CPC Classifications Searched	IPC(8): A61K 31/00 (2016.01) CPC: C07D 463/00; C07D 505/00; C07D 487/04
Date Conducted	1 August 2016 (01.08.2016)

Documentation Searched	USPC: 514/210.04,210.05
Search Terms Used	PatBase; Keyword limited: Tetrasubstituted alkene; aminosulfonyl/N,N-dimethylaminosulfonyl/N,N-dimethylaminosulfonyl/alkene; tamoxifen; ER-positive breast cancer
Date Conducted	1 August 2016 (01.08.2016)

Electronic Database Searched	PatBase
Files Searched	Full-text: AU BE BR CA CH CN DE DK EP ES FI FR GB IN JP KR SE TH TW US WO Bibliographic: (Europe) AT BA BE BG CH CS CY CZ DD DK EE ES FI GE GR HR HU IE IS IT LT LU LV MC MD MT NL NO PL PT RO RS SE SI SK SM TR UA YU (Asia) EA GC HK ID IL IN KZ MN MY PH RU SG SU TH TJ TW UZ VN (North America) CA CR CU DO GT HN MX NI PA SV TT (South America) AR BR CL CO EC PE UY (Australasia) AU NZ (Africa) AP DZ EG KE MA MW OA ZA ZM ZW
Date Conducted	1 August 2016 (01.08.2016)

Search Logic:

Search 1: IC=(A61K31/00) (Results 38380)
Search 2: CPC=(C07D463/00 or C07D505/00 or C07D487/04) (Results 11848)
Search 3: UC=(514/210.0 or 514/210.05) (Results 91)
Search 4: 1 or 2 or 3 (Results 49583)
Search 5: 4 and FT=(aminosulfonyl and alkene) (Results 159)
Search 6: 4 and FT=(N, N-dimethylaminosulfonyl) (Results 76)
Search 7: 4 and FT=(N, N-dimethylaminosulfonyl and alkene) (Results 2)
Search 8: 4 and FT=(tamoxifen and aminosulfonyl and alkene) (Results 33)

Search 9: 4 and FT=(tamoxifen and N,N-dimethylaminosulfonyl) (Results 17)
Search 10: 9 and FT=(alkene) (Results 2)
Search 11: 4 and FT=(ER-positive) (Results 55)
Search 12: 4 and FT=(ER-receptor) (Results 0)
Search 13: 4 and FT=(ER receptor) (Results 33)
Search 14: 11 or 13 (Results 85)
Search 15: 5 or 6 or 7 or 8 or 9 or 10 (Results 234)
Search 16: 14 and 15 (Results 5)
Search 17: FT=(aminosulfonyl and alkene) (Results 890)
Search 18: FT=(N, N-dimethylaminosulfonyl) (Results 563)
Search 19: FT=(N, N-dimethylaminosulfonyl and alkene) (Results 46)
Search 20: FT=(tamoxifen and aminosulfonyl and alkene) (Results 144)
Search 21: FT=(tamoxifen and N,N-dimethylaminosulfonyl) (Results 43)
Search 22: 21 and FT=(alkene) (Results 4)
Search 23: FT=(ER-positive) (Results 796)
Search 24: FT=(ER-receptor) (Results 12)
Search 25: FT=(ER receptor) (Results 226)
Search 26: 23 or 24 or 25 (Results 981)
Search 27: 17 or 18 or 19 or 20 or 21 or 22 (Results 1435)
Search 28: 26 and 27 (Results 9)

Electronic Database Searched	Google
Files Searched	Web (Articles and Patents)
Date Conducted	1 August 2016 (01.08.2016)

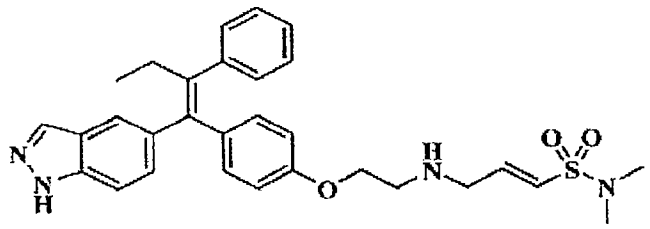
Search Logic:

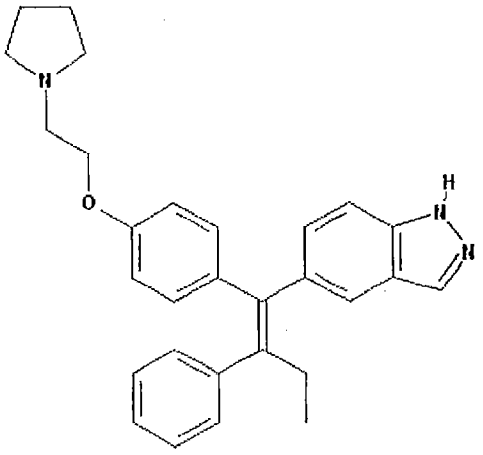
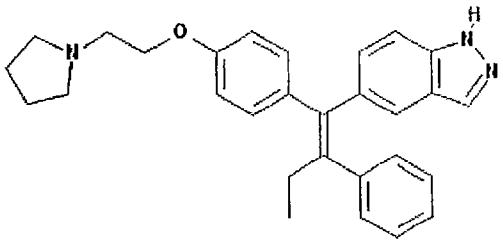
Tetrasubstituted alkene - 57,300 results
aminosulfonyl alkene - 35,100 results
N,N-dimethylaminosulfonyl - 40,200 results
N,N-dimethylaminosulfonyl alkene - 23,900 results
tamoxifen aminosulfonyl alkene - 23,100 results
tamoxifen N,N-dimethylaminosulfonyl - 42,000 results
tamoxifen N,N-dimethylaminosulfonyl alkene - 5,950 results
ER-positive breast cancer aminosulfonyl alkene - 2,060 results
ER-positive breast cancer N,N-dimethylaminosulfonyl - 6,370 results
ER-positive breast cancer N,N-dimethylaminosulfonyl alkene - 272 results
ER-positive breast cancer tamoxifen aminosulfonyl alkene - 758 results
ER-positive breast cancer tamoxifen N,N-dimethylaminosulfonyl - 1,840 results
ER-positive breast cancer tamoxifen N,N-dimethylaminosulfonyl alkene - 174 results

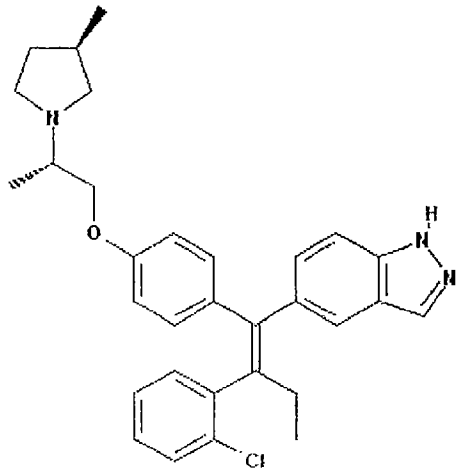
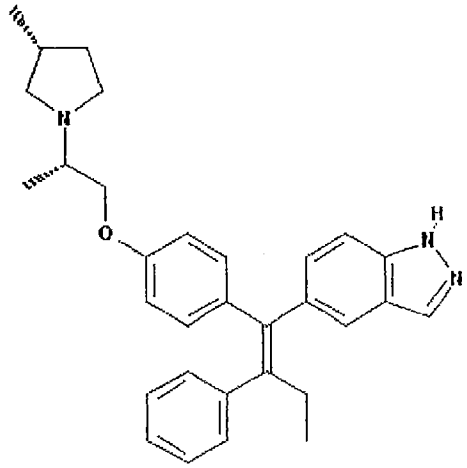
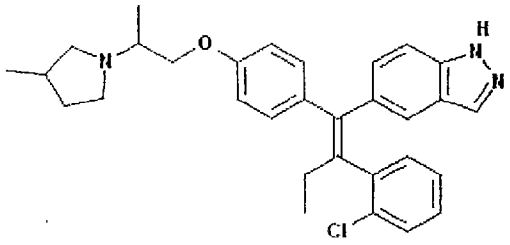
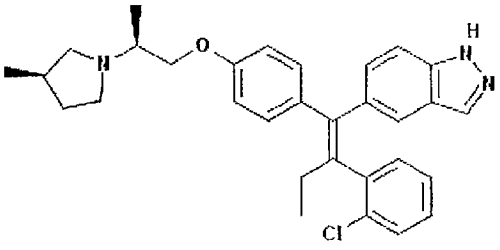
Electronic Database Searched	PubChem Compound
Files Searched	Data Source Categories: Biological Properties, Chemical Vendors, Journal Publishers, NIH Molecular Libraries 68,406,957 records
Date Conducted	1 August 2016 (01.08.2016)

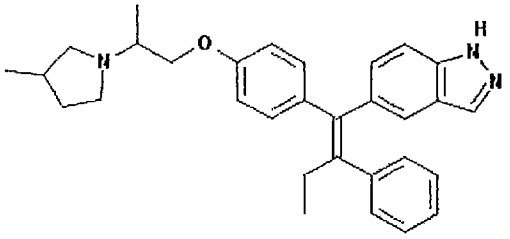
Search Logic:

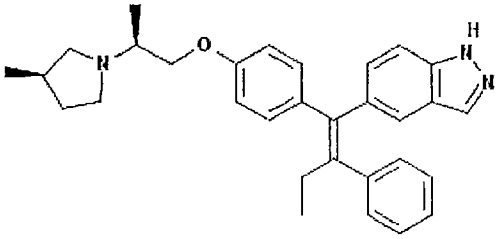
CID = chemical ID; SID = substance ID

Application
Claim 1 - FORMULA

Prior Art / PubChem Compounds

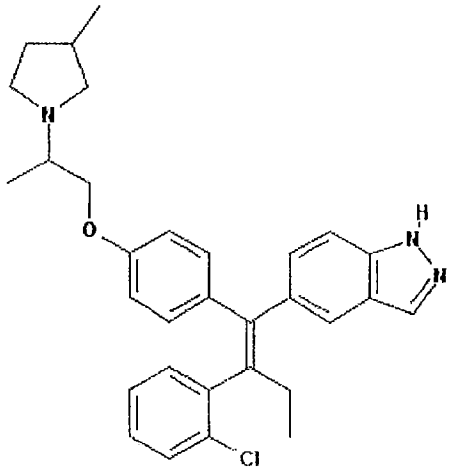
CID=69281185	CID=89780731
	

CID=66802140	CID=66806699
	
CID=87158403	CID=87158404
	
CID=89780569	CID=89780570





CID=90169830



NIH U.S. National Library of Medicine National Center for Biotechnology Information

PubChem OPEN CHEMISTRY DATABASE

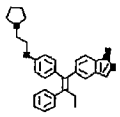
Search Compounds

Compound Summary for CID 69281185

SCHEMBL5019915

Cite this Record

Patents



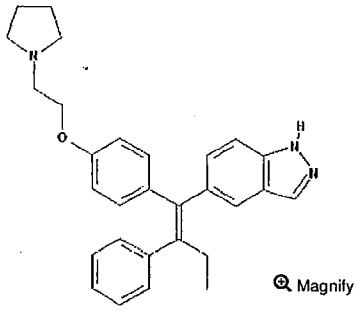
PubChem CID:	69281185
Molecular Formula:	$C_{29}H_{31}N_3O$
Molecular Weight:	437.57594 g/mol
InChI Key:	MMLFMEZBDVFWTR-ORIPQNMZSA-N
Modify Date:	2016-07-30
Create Date:	2012-12-01

Contents

1 2D Structure
2 3D Conformer
3 Names and Identifiers
4 Chemical and Physical Properties
5 Related Records
6 Patents
7 Classification
8 Information Sources

1 2D Structure

Search Download Get Image

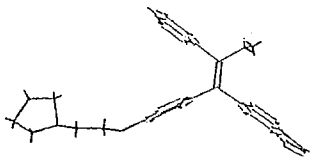


Magnify

from PubChem

2 3D Conformer

Search Download Get Image



Magnify

Show Hydrogens Show Atoms Animate

from PubChem

3 Names and Identifiers

3.1 Computed Descriptors

3.1.1 IUPAC Name

5-[(E)-2-phenyl-1-[4-(2-pyrrolidin-1-ylethoxy)phenyl]but-1-enyl]-1H-indazole

from PubChem

3.1.2 InChI

InChI=1S/C29H31N3O/c1-2-27(22-8-4-3-5-9-22)29(24-12-15-28-25(20-24)21-30-31-28)23-10-13-26(14-11-23)33-19-18-32-16-6-7-17-32/h3-5,8-15,20-21H,2,6-7,16-19H2,1H3,(H,30,31)/b29-27+

from PubChem

3.1.3 InChI Key

MMLFMEZBDVFWTR-ORIPQNMZSA-N

from PubChem

3.1.4 Canonical SMILES

CCC(=C(C1=CC=C(C=C1)OCCN2CCCC2)C3=CC4=C(C=C3)NN=C4)C5=CC=CC=C5

from PubChem

3.1.5 Isomeric SMILES

CC/C(=C(/C1=CC=C(C=C1)OCCN2CCCC2)\C3=CC4=C(C=C3)NN=C4)/C5=CC=CC=C5

from PubChem

3.2 Molecular Formula

$C_{29}H_{31}N_3O$

from PubChem

3.3 Synonyms

3.3.1 Depositor-Supplied Synonyms

SCHEMBL5019915

from PubChem

4 Chemical and Physical Properties

4.1 Computed Properties

Molecular Weight	437.57594 g/mol
XLogP3	7.3
Hydrogen Bond Donor Count	1
Hydrogen Bond Acceptor Count	3
Rotatable Bond Count	8
Exact Mass	437.246713 g/mol
Monoisotopic Mass	437.246713 g/mol
Topological Polar Surface Area	41.2 A^2
Heavy Atom Count	33
Formal Charge	0
Complexity	629
Isotope Atom Count	0
Defined Atom Stereocenter Count	0
Undefined Atom Stereocenter Count	0
Defined Bond Stereocenter Count	1
Undefined Bond Stereocenter Count	0
Covalently-Bonded Unit Count	1

from PubChem

5 Related Records

5.1 Related Compounds with Annotation

▸ *from PubChem*

5.2 Related Compounds

Same Connectivity	2 records
Same Parent, Connectivity	2 records
Similar Compounds	34 records
Similar Conformers	14 records

▸ *from PubChem*

5.3 Substances

5.3.1 Related Substances

Same	1 record

▸ *from PubChem*

5.3.2 Substances by Category

Download

▸ Curation Efforts (1)

▸ Research and Development (1)

▸ *from PubChem*

6 Patents

6.1 Depositor-Supplied Patent Identifiers

Download

1 to 1 of 1

Patent ID	Date	Patent Title
US2013231333	2013-09-05	ESTROGEN RECEPTOR MODULATORS AND USES THEREOF

from PubChem

7 Classification

7.1 Ontologies

7.1.1 WIPO IPC

Refine/Analyze Download

1 to 10 of 12 1 2

List View Tree View

C07D209/08 - with only hydrogen atoms or radicals containing only hydrogen and carbon atom...

C07D215/227 - only one oxygen atom which is attached in position 2

C07D249/18 - Benzotriazoles

C07D265/18 - with hetero atoms directly attached in position 2

C07D277/68 - with hetero atoms or with carbon atoms having three bonds to hetero atoms wit...

C07D279/16 - condensed with one six-membered ring

C07D401/10 - linked by a carbon chain containing aromatic rings

C07D409/10 - linked by a carbon chain containing aromatic rings

C07D471/04 - Ortho-condensed systems

C07D495/04 - Ortho-condensed systems

from WIPO

8 Information Sources

1. **PubChem**
   Data deposited in or computed by PubChem
   https://pubchem.ncbi.nlm.nih.gov https://pubchem.ncbi.nlm.nih.gov

2. **WIPO /source/WIPO**
   International Patent Classification 2014
   http://www.wipo.int/classifications/ipc/ http://www.wipo.int/classifications/ipc/

NIH U.S. National Library of Medicine National Center for Biotechnology Information

PubChem OPEN CHEMISTRY DATABASE

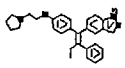
Search Compounds

Compound Summary for CID 89780731

SCHEMBL15226737

Cite this Record

Patents



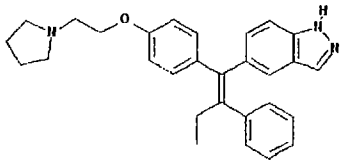
PubChem CID:	89780731
Molecular Formula:	$C_{29}H_{31}N_3O$
Molecular Weight:	437.57594 g/mol
InChI Key:	MMLFMEZBDVFWTR-OHYPFYFLSA-N
Modify Date:	2016-07-30
Create Date:	2015-02-13

Contents

1 2D Structure
2 3D Conformer
3 Names and Identifiers
4 Chemical and Physical Properties
5 Related Records
6 Patents
7 Classification
8 Information Sources

1 2D Structure

Search Download Get Image

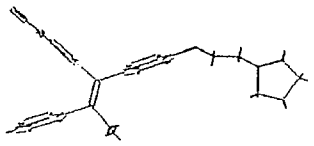


Magnify

from PubChem

2 3D Conformer

Search Download Get Image



Magnify

Show Hydrogens Show Atoms Animate

from PubChem

3 Names and Identifiers

3.1 Computed Descriptors

3.1.1 IUPAC Name

5-[(Z)-2-phenyl-1-[4-(2-pyrrolidin-1-ylethoxy)phenyl]but-1-enyl]-1H-indazole

from PubChem

3.1.2 InChI

InChI=1S/C29H31N3O/c1-2-27(22-8-4-3-5-9-22)29(24-12-15-28-25(20-24)21-30-31-28)23-10-13-26(14-11-23)33-19-18-32-16-6-7-17-32/h3-5,8-15,20-21H,2,6-7,16-19H2,1H3,(H,30,31)/b29-27-

from PubChem

3.1.3 InChI Key

MMLFMEZBDVFWTR-OHYPFYFLSA-N

from PubChem

3.1.4 Canonical SMILES

CCC(=C(C1=CC=C(C=C1)OCCN2CCCC2)C3=CC4=C(C=C3)NN=C4)C5=CC=CC=C5

from PubChem

3.1.5 Isomeric SMILES

CC/C(=C(\C1=CC=C(C=C1)OCCN2CCCC2)/C3=CC4=C(C=C3)NN=C4)/C5=CC=CC=C5

from PubChem

3.2 Molecular Formula

$C_{29}H_{31}N_3O$

from PubChem

3.3 Synonyms

3.3.1 Depositor-Supplied Synonyms

SCHEMBL15226737

from PubChem

4 Chemical and Physical Properties

4.1 Computed Properties

Molecular Weight	437.57594 g/mol
XLogP3	7.3
Hydrogen Bond Donor Count	1
Hydrogen Bond Acceptor Count	3
Rotatable Bond Count	8
Exact Mass	437.246713 g/mol
Monoisotopic Mass	437.246713 g/mol
Topological Polar Surface Area	41.2 A^2
Heavy Atom Count	33
Formal Charge	0
Complexity	629
Isotope Atom Count	0
Defined Atom Stereocenter Count	0
Undefined Atom Stereocenter Count	0
Defined Bond Stereocenter Count	1
Undefined Bond Stereocenter Count	0
Covalently-Bonded Unit Count	1

from PubChem

5 Related Records

5.1 Related Compounds with Annotation

LOADING... PLEASE WAIT...

▸ *from PubChem*

5.2 Related Compounds

Same Connectivity	2 records
Same Parent, Connectivity	2 records
Similar Compounds	34 records
Similar Conformers	16 records

▸ *from PubChem*

5.3 Substances

5.3.1 Related Substances

Same	1 record

▸ *from PubChem*

5.3.2 Substances by Category

Download

▸ Curation Efforts (1)

▸ Research and Development (1)

▸ *from PubChem*

6 Patents

6.1 Depositor-Supplied Patent Identifiers

Download

1 to 1 of 1

Patent ID	Date	Patent Title
US2013231333	2013-09-05	ESTROGEN RECEPTOR MODULATORS AND USES THEREOF

from PubChem

7 Classification

7.1 Ontologies

7.1.1 WIPO IPC

Refine/Analyze Download

1 to 10 of 12 1 2

List View Tree View

C07D209/08 - with only hydrogen atoms or radicals containing only hydrogen and carbon atom...

C07D215/227 - only one oxygen atom which is attached in position 2

C07D249/18 - Benzotriazoles

C07D265/18 - with hetero atoms directly attached in position 2

C07D277/68 - with hetero atoms or with carbon atoms having three bonds to hetero atoms wit...

C07D279/16 - condensed with one six-membered ring

C07D401/10 - linked by a carbon chain containing aromatic rings

C07D409/10 - linked by a carbon chain containing aromatic rings

C07D471/04 - Ortho-condensed systems

C07D495/04 - Ortho-condensed systems

from WIPO

8 Information Sources

1. **PubChem**
   Data deposited in or computed by PubChem
   https://pubchem.ncbi.nlm.nih.gov https://pubchem.ncbi.nlm.nih.gov

2. **WIPO /source/WIPO**
   International Patent Classification 2014
   http://www.wipo.int/classifications/ipc/ http://www.wipo.int/classifications/ipc/

PCT Recordation of Search History

Case/PCT Application Number: PCT/US16/34774

CLIN Number/Technical Field of PCT Application: 0007 Biotechnology

Date(s) During Which the Search was Conducted: 26 July 2016

Date of Completion of Recordation of Search History Form: 26 July 2016

Research Analyst Initials: KAC

Search Approval Official (SAO) Initials: DGF

Field of Search/Classification Information:

IPC(8) Classification(s): C07C 215/46; A61K 31/133 (2016.01)

CPC Classification(s): C07C 317/28, 323/12

Database(s) Searched (Patent and Non-Patent Literature (NPL), Including Sub-Databases and Files Searched) and Search Terms Used:

PatSeer (US, EP, WO, JP, DE, GB, CN, FR, KR, ES, AU, IN, CA, INPADOC Data); ProQuest; Scifinder; Google/Google Scholar; breast, cancer, ER, positive, mutant, alpha, endoxifen

Database Search String Recordation, Including Dates of Searches):

Patent Database Search Strategy/Results:

Patseer:

ID	Search String	Records	Created Date
L29	CPC:(C07C323/12)	4455	26-Jul-16
L28	TACD:((endoxifen OR tamoxifen) AND (analog* OR derivativ*) AND (proliferativ* OR cancer*)) AND CPC:(C07C323/12)	99	26-Jul-16
L27	CPC:(C07C317/28)	4035	26-Jul-16
L26	TACD:((endoxifen OR tamoxifen) AND (analog* OR derivativ*) AND (proliferativ* OR cancer*)) AND CPC:(C07C317/28)	141	26-Jul-16
L25	TAC:((endoxifen OR tamoxifen) AND (analog* OR derivativ*) AND (proliferativ* OR cancer*)) AND CPC:(C07C317*)	10	26-Jul-16
L24	TAC:((endoxifen OR tamoxifen) AND (analog* OR derivativ*) AND (proliferativ* OR cancer*)) AND CPC:(C07C*)	216	26-Jul-16
L23	IC:(A61K31/133)	5067	26-Jul-16
L22	TAC:((endoxifen OR tamoxifen) AND (analog* OR derivativ*) AND (proliferativ* OR cancer*)) AND IC:(A61K31/133)	13	26-Jul-16
L21	TA:((endoxifen OR tamoxifen) AND (analog* OR derivativ*) AND (proliferativ* OR cancer*)) AND IC:(A61K31*)	69	26-Jul-16
L20	TAC:((endoxifen OR tamoxifen) AND (analog* OR derivativ*) AND (proliferativ* OR cancer*)) AND IC:(A61K31*)	3418	26-Jul-16
L19	TAC:((endoxifen OR tamoxifen) AND (analog* OR derivativ*) AND (proliferativ* OR cancer*)) AND IC:(A61K*)	4440	26-Jul-16
L18	IC:(C07C21/54)	1	26-Jul-16
L17	TAC:((endoxifen OR tamoxifen) AND (analog* OR derivativ*) AND (proliferativ* OR cancer*)) AND IC:(C07C21/54)	0	26-Jul-16
L16	TAC:((endoxifen OR tamoxifen) AND (analog* OR derivativ*) AND (proliferativ* OR cancer*) AND breast*) AND IC:(C07C21/54)	0	26-Jul-16
L15	TAC:((endoxifen OR tamoxifen) AND (analog* OR derivativ*) AND (proliferativ* OR cancer*) AND breast*) AND IC:(C07C21*)	30	26-Jul-16
L14	TACD:((endoxifen OR tamoxifen) AND (analog* OR derivativ*) AND (proliferativ* OR cancer*) AND breast*) AND IC:(C07C21*)	772	26-Jul-16
L13	IC:(C07C215/46)	1138	26-Jul-16
L12	TACD:((endoxifen OR tamoxifen) AND (analog* OR derivativ*) AND (proliferativ* OR cancer*) AND breast*) AND IC:(C07C215/46)	14	26-Jul-16
L11	TAC:((endoxifen OR tamoxifen) AND (analog* OR derivativ*) AND (proliferativ* OR cancer*) AND breast*) AND IC:(C07C215/46)	0	26-Jul-16
L10	TAC:((endoxifen OR tamoxifen) AND (analog* OR derivativ*) AND (proliferativ* OR cancer*) AND breast*) AND IC:(C07C215*)	2	26-Jul-16
L9	TAC:((endoxifen OR tamoxifen) AND (analog* OR derivativ*) AND (proliferativ* OR cancer*) AND breast*) AND IC:(C07C*)	129	26-Jul-16
L8	TAC:((endoxifen OR tamoxifen) AND (analog* OR derivativ*) AND (proliferativ* OR cancer*) AND breast*) AND IC:(C07*)	1729	26-Jul-16
L7	TAC:((endoxifen OR tamoxifen) AND (analog* OR derivativ*) AND (proliferativ* OR cancer*) AND breast* AND positive*)	436	26-Jul-16
L6	TAC:((endoxifen OR tamoxifen) AND (analog* OR derivativ*) AND (proliferativ* OR cancer*) AND breast*)	3079	26-Jul-16
L5	TAC:((endoxifen OR tamoxifen) AND (analog* OR derivativ*) AND (proliferativ* OR cancer*))	5181	26-Jul-16

L4	TA:((endoxifen OR tamoxifen) AND (analog* OR derivativ*) AND (proliferativ* OR cancer*))	116	26-Jul-16
L3	TAC:((endoxifen OR tamoxifen) AND (analog* OR derivativ*))	6920	26-Jul-16
L2	TA:((endoxifen OR tamoxifen) AND (analog* OR derivativ*))	354	26-Jul-16
L1	TAC: ((endoxifen OR tamoxifen) AND (analog* OR derivativ*)) AND ASN:(eisai)	21	26-Jul-16

Non-Patent Literature (NPL) Search Strategy/Results:

Google Scholar: 26 July 2016

endoxifen derivative breast cancer	698
endoxifen derivative breast cancer ER-positive	294
endoxifen derivative breast cancer ER-positive mutant alpha	203

PubMed: 26 July 2016

(endoxifen OR tamoxifen) AND (derivative* OR analog*)	4563
(endoxifen OR tamoxifen) AND (derivative* OR analog*) AND cancer	3022
(endoxifen OR tamoxifen) AND (derivative* OR analog*) AND cancer AND breast	2317
(endoxifen OR tamoxifen) AND (derivative* OR analog*) AND cancer AND breast AND (perfluoroalkyl OR perfluoroethyl)	1

EBSCO: 26 July 2016

endoxifen derivative breast cancer	741
endoxifen derivative breast cancer ER-positive	248
endoxifen derivative breast cancer ER-positive mutant alpha	141

PCT Application No.: PCT/US2016/034782
Date of Search: 25 July 2016

Search History:

Limited Classification Search

The Patent Analyst performed a limited classification search within the following US, IPC, CPC, ECLA, or F-Term classification areas:

U.S. Class/Subclass(es): 514/338; 514/359; 514/406

IPC (8) Class/Subclass(es): A61K 31/4439; C07D 317/02; C07D 317/06; C07D 487/04 (2016.01)

CPC Class/Subclass(es): A61K 31/416; A61K 31/3349; C07D 231/56; C07D 317/06; 487/04 (2016.05)

See Global Search Results.

Global Patent Literature Text Search

The Patent Analyst performed the following global text search, which was not limited by classification but may or may not have been limited by other criteria:

Minesoft PatBase: https//www.patbase.com

Search 1:	PN=(WO2013142266 or US20130231333) (Results 2)
Search 2:	(indazol* and vinyl and phenyl) (Results 18675)
Search 3:	TAC=(indazol* and vinyl and phenyl) (Results 511)
Search 4:	3 and ethox* (Results 445)
Search 5:	TAC=((indazol 5 yl) and vinyl and phenoxy) (Results 39)
Search 6:	5 and (breast w3 cancer) (Results 24)
Search 7:	PA=(EISAI) (Results 3063)
Search 8:	6 and 7 (Results 0)
Search 9:	IC=("C07D487/04" OR "A61K31/4439") (Results 34046)
Search 10:	IC=(C07D317/06 or C07D317/02) (Results 141)
Search 11:	CPC=("C07D317/06") (Results 18)
Search 12:	CPC=("C07D487/04") (Results 11665)
Search 13:	CPC=("A61K31/4439") (Results 3512)
Search 14:	CPC=("C07D231/56") (Results 1364)
Search 15:	CPC=("A61K31/416") (Results 501)
Search 16:	UC=("514/406") (Results 3417)
Search 17:	UC=("514/338" OR "514/359") (Results 3994)
Search 18:	((indazol 5 yl) and vinyl and phenoxy) and (breast w3 cancer) (Results 0)
Search 19:	(indazol 5 yl) and vinyl and phenoxy and (breast w3 cancer) (Results 0)

Search 20:	((indazol 5 yl) and vinyl and phenoxy) (Results 0)
Search 21:	3 and (9 or 10 or 11 or 12 or 13 or 14 or 15 or 16 or 17) (Results 215)
Search 22:	21 and (breast w3 cancer) (Results 78)

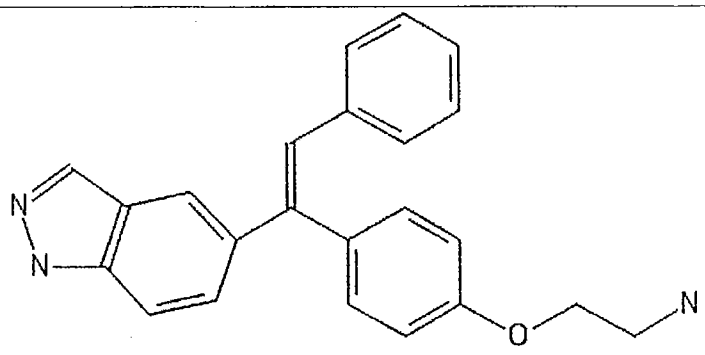
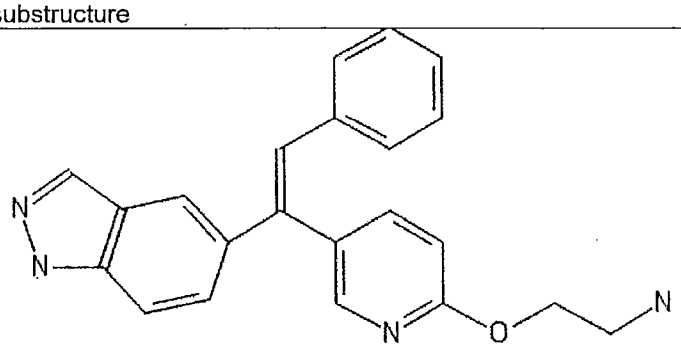
Google Patents: https://patents.google.com

#	Search query	Results
1	"indazol-5-yl" vinyl	55
2	"indazol-5-yl" vinyl phenoxy	22
3	"indazol-5-yl" vinyl phenoxy phenyl	22
4	"indazol-5-yl" vinyl phenoxy pyridine	10

Computer Accessed Text Databases Searched

The Patent Analyst searched the following computer accessed text databases:

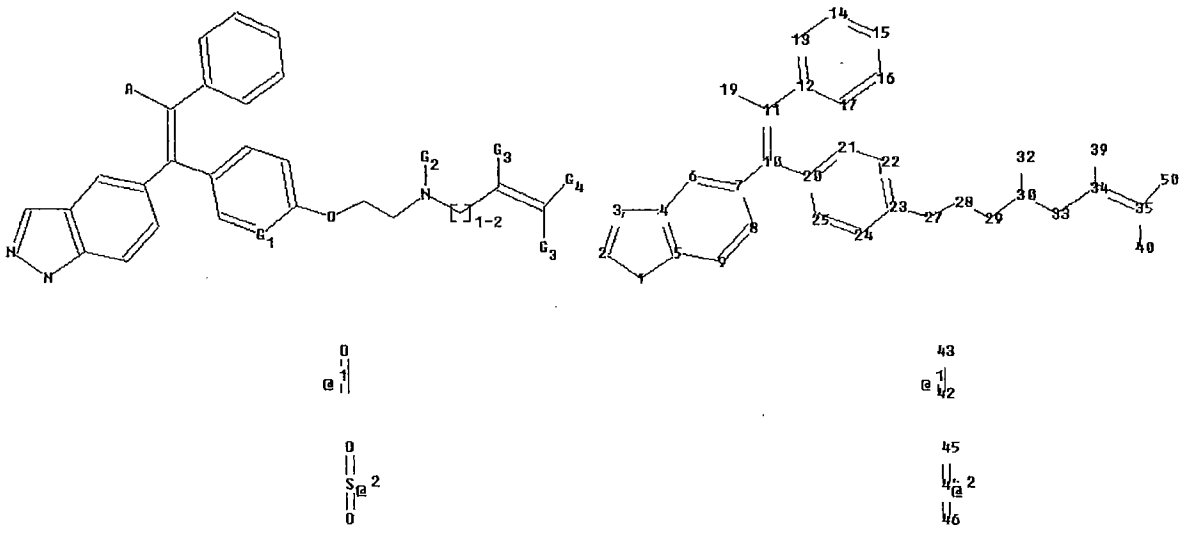
PubChem.gov (NCBI): https://pubchem.ncbi.nlm.nih.gov/

#	Search query	Results
1	 , substructure	9
2	 , substructure	0

STN: http://www.cas.org/products/stn

=>

Uploading C:\Users\al02\Documents\STN Express 8.6\Queries\16-34782.str



chain nodes :
10 11 19 27 28 29 30 32 33 34 35 39 40 42 43 44 45 46
50
ring nodes :
1 2 3 4 5 6 7 8 9 12 13 14 15 16 17 20 21 22 23 24
25
chain bonds :
7-10 10-11 10-20 11-12 11-19 23-27 27-28 28-29 29-30 30-32
30-33 33-34
34-35 34-39 35-40 35-50 42-43 44-45 44-46
ring bonds :
1-2 1-5 2-3 3-4 4-5 4-6 5-9 6-7 7-8 8-9 12-13 12-17 13-14
14-15 15-16
16-17 20-21 20-25 21-22 22-23 23-24 24-25
exact/norm bonds :
1-2 1-5 2-3 3-4 7-10 10-11 10-20 11-12 11-19 20-21 20-25 21-
22 22-23
23-24 23-27 24-25 27-28 28-29 29-30 30-32 30-33 33-34 34-35
34-39 35-40 35-50 42-43
44-45 44-46
normalized bonds :
4-5 4-6 5-9 6-7 7-8 8-9 12-13 12-17 13-14 14-15 15-16 16-17
isolated ring systems :
containing 1 : 12 : 20 :

G1:C,N

G2:C,H

G3:H,CH3,X,CF3

G4:CF3,CN,[@1],[@2]

Match level :
1:Atom 2:Atom 3:Atom 4:Atom 5:Atom 6:Atom 7:Atom 8:Atom 9:Atom

```
10:CLASS
11:CLASS  12:Atom  13:Atom  14:Atom  15:Atom  16:Atom  17:Atom
19:CLASS  20:Atom  21:Atom  22:Atom
23:Atom  24:Atom  25:Atom  27:CLASS  28:CLASS  29:CLASS  30:CLASS
32:CLASS  33:CLASS  34:CLASS
35:CLASS  39:CLASS  40:CLASS  42:CLASS  43:CLASS  44:CLASS  45:CLASS
46:CLASS  50:CLASS



L1      STRUCTURE UPLOADED

=> s l1
SAMPLE SEARCH INITIATED 10:53:33 FILE 'REGISTRY'
SAMPLE SCREEN SEARCH COMPLETED -        0 TO ITERATE

100.0% PROCESSED         0 ITERATIONS                                    0
ANSWERS
SEARCH TIME: 00.00.01

FULL FILE PROJECTIONS:  ONLINE  **COMPLETE**
                        BATCH   **COMPLETE**
PROJECTED ITERATIONS:            0 TO        0
PROJECTED ANSWERS:               0 TO        0

L2            0 SEA SSS SAM L1

=> s l1 full
FULL SEARCH INITIATED 10:53:37 FILE 'REGISTRY'
FULL SCREEN SEARCH COMPLETED -        3 TO ITERATE

100.0% PROCESSED         3 ITERATIONS                                    0
ANSWERS
SEARCH TIME: 00.00.01

L3            0 SEA SSS FUL L1


STN INTERNATIONAL LOGOFF AT 10:53:44 ON 22 JUL 2016
```

Google Scholar: https://scholar.google.com/

#	Search query	Results
1	"indazol-5-yl" vinyl	31
2	"indazol-5-yl" vinyl phenoxy	2
3	"indazol-5-yl" vinyl phenoxy phenyl	2
4	"indazol-5-yl" vinyl phenoxy pyridine	2

Date search was completed: 25 July 2016

ANL/BT

Identification by MALDI-TOF Mass Spectrometry of 17α-Bromoacetamidopropylestradiol Covalent Attachment Sites on Estrogen Receptor α†

Hélène Mattras,‡ Sigrid Aliau,‡ Eric Richard,‡ Jean-Claude Bonnafous,‡ Patrick Jouin,§ and Jean-Louis Borgna*,‡

INSERM U 439, 70 rue de Navacelles, and UPR 9023 CNRS, 141 rue de la Cardonille, 34090 Montpellier, France

Received August 2, 2002; Revised Manuscript Received October 7, 2002

ABSTRACT: Mass spectrometry was used to identify the sites of covalent attachment of [^{14}C]-17α-bromoacetamidopropylestradiol ([^{14}C]17BAPE$_2$, an estradiol agonist) to the ligand-binding domain (LBD) of mouse estrogen receptor α (ERα). A glutathione *S*-transferase (GST)−LBD chimera protein was overexpressed in *Escherichia coli*, using a vector encoding GST fused with a C-terminal portion of mouse ERα (Ser^{313}−Ile^{599}), via a sequence enclosing a thrombin cleavage site (located 14 amino acids ahead of Ser313). [^{14}C]17BAPE$_2$ covalent labeling experiments were carried out on the GST−LBD chimera immobilized on glutathione−Sepharose. After thrombin cleavage of the chimeric LBD, two major [^{14}C]-17BAPE$_2$-labeled species of 34 (∼75%) and 30 kDa (∼25%) were detected by SDS−PAGE and autoradiography. Their identity was assessed by matrix-assisted laser desorption ionization time-of-flight mass spectrometry (MALDI-TOF MS): two main signals were consistent with the mass of the full-length (Ser^{313}−Ile^{599}) and truncated LBD (Ser^{313}−Ala^{573}), both comprising the extra 14 N-terminal amino acids and covalently bound [^{14}C]17BAPE$_2$ (via HBr elimination). A purified ^{14}C-labeled LBD preparation was trypsinized to identify the covalent attachment sites of 17BAPE$_2$. HPLC of tryptic fragments only revealed two discrete and practically equivalent radioactive fractions. MALDI-TOF MS analysis of these two fractions showed only two signals which exactly matched the molecular masses of the [^{14}C]17BAPE$_2$-alkylated Cys^{534}Lys^{535} and Cys^{421}−Arg^{438} peptides, respectively. Hydrolysis of the second ^{14}C-labeled fraction by *Staphylococcus aureus* V8 Glu-C endoproteinase generated signals typical of alkylated the Cys^{421}−Glu^{423} tripeptide. We concluded that Cys421 and Cys534 were equivalent alternative covalent attachment sites of 17BAPE$_2$ on the LBD. These biochemical data were interpreted using the crystallographic structures of estradiol−LBD and raloxifene− or 4-hydroxytamoxifen−LBD complexes. The covalent attachment to Cys421, Cys534, or both could be interpreted according to the starting structure. Various hypotheses based on the biochemical results and molecular modeling simulations are discussed, with the likely involvement of dynamic interconversion between multiple conformational states of the LBD−17BAPE$_2$ complex.

In mammals, two estrogen receptors (ERα[1] and ERβ) (*1*−*4*) mediate the effects of estrogens and antiestrogens in estrogen target cells. These ERs belong to the nuclear receptor superfamily (*5*, *6*), the members of which display a modular structure, usually involving six domains (A−F). Domains C and E, which constitute the DNA-binding domain and the ligand-binding domain (LBD), respectively, are the most conserved domains in nuclear receptors; e.g., human ERα and ERβ are 96 and 59% identical in amino acid sequence in their DNA-binding domains and LBDs, respectively. Since the mid-1990s, a number of X-ray analyses of crystallized nuclear receptor LBDs, either unliganded or bound to agonist or antagonist ligands, have considerably improved our knowledge in this field (*7*). Several of these studies were performed with ERα (*8*−*12*) or ERβ (*13*, *14*) LBDs. Crystal structures of ERα LBD−ligand complexes show the characteristic, predominantly α-helical fold observed with other crystallized nuclear receptor LBDs (*15*). According to the authors, the ERα LBD which includes 12 α-helices [the ERα helix numbering of Brzozowski et al. (*8*) will be used] and two β-strands is folded into a three-layered antiparallel α-helical sandwich. Agonists [estradiol (E_2) and diethylstilbestrol (DES)] and antagonists [4-hy-

† This work was supported by the "Institut National de la Santé et de la Recherche Médicale" and the "Association pour la Recherche sur le Cancer".

* To whom correspondence should be addressed. Telephone: 33 4 67 04 37 14. Fax: 33 4 67 04 37 15. E-mail: Borgna@u439.montp.inserm.fr.

‡ INSERM U 439.

§ UPR 9023 CNRS.

[1] Abbreviations: ER, estrogen receptor; LBD, ligand-binding domain; LBP, ligand-binding pocket; GST, glutathione *S*-transferase; E_2, estradiol; DES, diethylstilbestrol; OHT, 4-hydroxytamoxifen; Ral, raloxifene; 17BAPE$_2$, 17α-bromoacetamidopropylestradiol; SDS, sodium dodecyl sulfate; TFA, trifluoroacetic acid; CHCA, α-cyano-4-hydroxycinnamic acid; SA, 3,5-dimethoxy-4-hydroxycinnamic acid (sinapinic acid); PBS, phosphate-buffered saline; T_{20}, 20 mM Tris-HCl buffer; V8 proteinase (or V8), *Staphylococcus aureus* V8 Glu-C endoproteinase; PAGE, polyacrylamide gel electrophoresis; HPLC, high-pressure liquid chromatography; MALDI-TOF, matrix-assisted laser desorption ionization time-of-flight; MS, mass spectrometry. Θ symbolizes an undefined atom or group of atoms displaying a monoisotopic mass very close to 16.

10.1021/bi0205092 CCC: $22.00 © 2002 American Chemical Society
Published on Web 12/04/2002

droxytamoxifen (OHT) and raloxifene (Ral)] bind at the same site within the LBD core; the ligand-binding pocket (LBP) is predominantly formed by hydrophobic residues located in six portions of the LBD sequence. Many structural features are common to estrogen and antiestrogen complexes, but a major established difference between structures of crystallized ERα LBD−estrogen and LBD−antiestrogen complexes was found to be related to the orientation of helix 12, which harbors the AF-2 activation domain (*16*, *17*) that is involved in coactivator recruitment (*18*). The orientation of helix 12 in an ER−ligand complex was therefore thought to be responsible for the agonist or antagonist activity of the ligand (*8*). However, this dual positioning of helix 12, according to the type of ligand bound to the LBD, did not seem to be a common phenomenon since helix 12 was found to have an "antiestrogen type" orientation in agonist-bound ERβ LBD (*13*) or mutated ERα LBD (*11*) crystals. These results underscored the high degree of positional variability of this helix in crystallized LBD forms.

The crystallization approach cannot account for the possible occurrence of equilibria between multiple conformational states for these complexes in aqueous medium. Moreover, the stacking of LBD monomers in the crystalline network may change the conformation or even the type of peripheral amino acid residues occurring in solute complexes. It is important to determine the potential conformational states of these complexes according to hormone or antihormone binding. Some of them, even if they are a minority, could especially be involved in coactivator or corepressor recruitment and could thus account for ligand-induced modulation of ER transcriptional activity. Therefore, noncrystallization approaches, i.e., using fluorescent, cross-linking, or specific amino acid reagents or affinity labeling agents to probe the structure of solute ER−ligand complexes, could enhance the overall understanding of the molecular action of estrogens and antiestrogens, and help in the rational design of new selective ER modulators (*19*).

In previous studies, we characterized lamb and human ERα affinity labeling by three closely related estrogenic ligands, derived from E_2 by introducing an 17α-bromoacetamidoalkyl substituent (the alkyl group being methyl, ethyl, or propyl). First using an SH-specific reagent, we showed that cysteinyl residues of lamb ERα were involved in covalent attachment of these electrophilic ligands (*20*). Then the inability of electrophiles to alkylate the Cys417Ala/Cys530Ala double-mutant human ERα[2] strongly suggested that Cys417 and Cys530 constituted the covalent attachment sites of these electrophiles in human ERα (*21*). However, this indirect evidence did not allow us to determine the relative involvement of the two cysteines in electrophile covalent attachment processes.

In the study presented here, using mass spectrometry (MS) analysis, we attempted to directly identify the covalent attachment sites within the mouse ERα LBD of 17α-bromoacetamidopropylE_2 (17BAPE$_2$, Figure 1), one of the previously studied estrogenic ER affinity labels, which

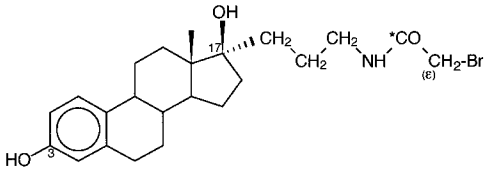


FIGURE 1: Structure of [^{14}C]17BAPE$_2$. The ER affinity labeling agent is derived from E_2 by 17α-substitution. It possesses an electrophilic carbon (terminal bromine-bearing carbon, ε-carbon) and, to facilitate the characterization of the affinity-labeled mouse ERα LBD and fragments, a 88% ^{14}C-enriched carbon (denoted with an asterisk).

displays high affinity for mammal ERαs (K_a estimated to be in the range of 10^8-10^9 M^{-1}, unpublished results). We first report the production in *Escherichia coli* and purification of a chimera protein made of glutathione *S*-transferase (GST) and a C-terminal portion of mouse ERα (Ser^{313}−Ile^{599} sequence, corresponding to the LBD and the adjacent C-terminal region F, and designated LBD). We then describe the affinity labeling of LBD with a ^{14}C-labeled form of the affinity probe, and the characterization of [^{14}C]17BAPE$_2$-labeled LBD. We next report, by means of matrix-assisted laser desorption ionization time-of-flight (MALDI-TOF) MS analysis, the identification of covalently modified LBD tryptic peptides, and labeled residues within these peptides. Finally, using available crystalline models of the ERα LBD bound to estrogen or antiestrogen, we try to interpret by molecular modeling the biochemical results obtained.

EXPERIMENTAL PROCEDURES

Materials. 1-Isopropylthio-β-D-galactopyranoside, protease inhibitor cocktail for bacterial cell extracts [containing 4-(2-aminoethyl)benzenesulfonyl fluoride, pepstatin A, *trans*-epoxy succinyl-L-leucylamido(4-guanidino)butane, bestatin, and EDTA], and *Staphylococcus aureus* V8 Glu-C endoproteinase (V8) were from Sigma-Aldrich. Glutathione−Sepharose 4B and thrombin were purchased from Amersham Biosciences. Trypsin (sequencing grade) was from Roche, and the synthetic CysValGluGlyMetValGlu heptapeptide was purchased from Neosystem. Solvents and reagents used for HPLC and MALDI-TOF MS analyses were HPLC grade (for HPLC, Milli-Q grade water was passed through a C18 preparative column and then sterilized). Matrices for MS, α-cyano-4-hydroxycinnamic acid (CHCA) and 3,5-dimethoxy-4-hydroxycinnamic acid [sinapinic acid (SA)], were purchased from Sigma-Aldrich. [6,7-^{3}H]Estradiol ([^{3}H]-E_2, specific activity of 1.6 PBq/mol, radiochemical purity of >98%) was purchased from New England Nuclear, and bromo[1-^{14}C]acetic acid (specific activity of 2.0 TBq/mol, 88% ^{14}C enrichment, radiochemical purity of >98%) from Amersham Biosciences. [^{3}H]E_2 and synthesized [NHCO-^{14}C]-17α-bromoacetamidopropylE_2 ([^{14}C]17BAPE$_2$) were solubilized in absolute ethanol. Solutions were stored at −20 °C in the dark. The purity of solubilized compounds was checked before use by thin-layer chromatography.

GST−LBD Expression Vector. A pGEX-2TK vector encoding glutathione *S*-transferase (GST) fused with the mouse ERα LBD (Ser^{313}−Ile^{599}), via a sequence enclosing a thrombin cleavage site located 14 amino acids ahead of Ser313 (*22*), was provided by V. Cavaillès (INSERM U 540).

Protein Assay and Radioactivity Determinations. Protein concentrations were measured colorimetrically by the method

[2] As mouse ERα possesses four additional residues as compared to human ERα, the residue numbers are different for the two ERs. The mouse numbering is used in the Results and related Figures 2 and 8; the human numbering is used in Experimental Procedures and the Discussion which deal with crystal models of the human ERα LBD.

of Bradford (*23*) using a dye reagent concentrate (Bio-Rad Laboratories) with bovine serum albumin as a standard. The radioactivity of the various samples (10−200 μL) was counted in 4 mL of Emulsifier Safe (Packard) using an LS 1801 Beckman scintillation counter.

SDS−PAGE Analyses and Autoradiography. Electrophoreses were performed using a Mini Protean II Bio-Rad unit with 1 mm gel slabs containing 12% (w/v) acrylamide in the separation gel and 5% acrylamide in the stacking gel, in 0.1% (w/v) SDS, 25 mM Tris-HCl buffer (pH 8.5). Gels were stained with GelCode Blue Stain Reagent (Pierce). Prestained protein molecular weight markers, a broad range from 6.5 to 175 kDa (BioLabs), were used as a standard. ^{14}C-labeled species were analyzed on dried gels using a Fujix BAS 1000 apparatus.

Synthesis and Characterization of [^{14}C]17BAPE$_2$. The procedure described for the preparation of unlabeled 17BAPE$_2$ (*20*) was used to obtain [NHCO-^{14}C]17BAPE$_2$. Briefly, 17α-aminopropylE$_2$, with the phenolic function protected in the form of *tert*-butyldimethylsilyl ether, was condensed with bromo[1-^{14}C]acetic acid in the presence of 1-ethyl-3-[3-(dimethylamino)propyl] carbodiimide hydrochloride. The silylated protection group was then removed by exposure of the compound to tetrabutylammonium fluoride. The [^{14}C]-17BAPE$_2$ that was obtained was purified on silica gel. The compound purity, assessed by thin-layer chromatography, was >95%.

Expression and Extraction of the GST−LBD Chimera. A 10 mL culture of *E. coli* BL21 cells transformed with the pGEX-2TK plasmid encoding the GST−LBD chimera was grown overnight at 37 °C in LB^A (LB medium with 0.1 mg/mL ampicillin). The cell suspension (OD_{550} = 1.2−1.5) was incubated in 450 mL of LB^A at 37 °C until the OD_{600} had reached 0.6. GST−LBD expression was then induced with 1 mM 1-isopropylthio-β-D-galactopyranoside for 2 h at 37 °C. Cells were then pelleted by centrifugation for 30 min at 3500*g* (4 °C). Bacterial pellets were resuspended in a minimal volume of fresh LB, and centrifuged once more. The final pellet was suspended in extraction buffer [20 mM Tris-HCl (T_{20}) (pH 8) containing 100 mM NaCl, 1 mM EDTA, 10 mM dithiothreitol, and protease inhibitor cocktail] at a ratio of 2 mL of buffer to 1 mL of pellet, and then aliquoted (1.5 mL fractions). Aliquots were centrifuged for 15 min at 3500*g* (4 °C); supernatants were discarded and pellets (0.5 mL) snap-frozen and then stored at −70 °C.

For fusion protein extraction, thawed aliquots were slowly resuspended in ice-cooled extraction buffer [1/1 (v/v)]. Nonidet P-40 (final concentration of 0.1%) was added, and then the cell suspension was incubated for 30 min at 0 °C. The cells were ruptured by sonication at 0 °C, using a Bioblock-Scientific Vibra-cell 72405 instrument (six pulses for 6 s, amplitude of 60), and sonication was repeated 15 min later. Cell breakage was controlled by microscopy (Turk reagent), and the sonicate was centrifuged for 10 min at 20000*g* (4 °C).

Binding Assay. Extracts from induced *E. coli* cells were diluted 200-fold with T_{20} (pH 7.5). The protein concentration of diluted extracts was adjusted to 2 mg/mL with bovine serum albumin. Aliquots were incubated for 15 h at 0 °C with 10 nM [^{3}H]E$_2$ in the absence (to measure the level of total binding) and presence (to measure the level of nonspecific binding) of 1 μM unlabeled E$_2$. Aliquots were treated with an equal volume of a charcoal suspension [1% charcoal, 0.1% dextran T_{70} in T_{20} (pH 7.5)] for 15 min at 0 °C; charcoal was pelleted by centrifugation, and concentrations of bound [^{3}H]E$_2$ in supernatants were determined by radioactivity counting.

Purification and Affinity Labeling of the LBD. Bacterial lysate (1.5 mL) was added to 100 μL of glutathione−Sepharose 4B [equilibrated with T_{20} (pH 8.0)] in an ice-cooled Bio-Spin chromatography column (Bio-Rad Laboratories). The mixture was rotated for 15 h at 4 °C, and then the column was drained and carefully washed with phosphate-buffered saline (PBS), equilibrated to pH 8.5, to remove nonspecifically bound proteins. An ~4-fold excess of [^{14}C]-17BAPE$_2$ (final concentration of 10 μM), relative to the glutathione−Sepharose-bound GST−LBD chimera, was added to the matrix suspended in 1 mL of ice-cooled PBS (pH 8.5) containing 10% dimethylformamide. The mixture was rotated gently for 2 h at 4 °C, washed five times with PBS, and then resuspended in 1 mL of ice-cooled PBS (pH 7.3). Thrombin (1 NIH for a 1 mL mixture) was added to the gel suspension; the mixture was rotated for 15 h at 4 °C and then incubated for 30 min at 4 °C with glutathione (30 mM, pH readjusted to 7.3). The gel was drained and washed twice with 50 μL of PBS (pH 7.3), and the three eluates were pooled. Aliquots of the various samples were analyzed for ^{14}C content, [^{3}H]E$_2$ binding capacity, and protein content (SDS−PAGE).

CysValGluGlyMetValGlu Alkylation with [^{14}C]17BAPE$_2$. Sixty-five microliters of an ethanol solution of [^{14}C]17BAPE$_2$ (1 mM) was added to 195 μL of a solution of the synthetic CysValGluGlyMetValGlu heptapeptide (0.67 mM) in 0.1 M $NaHCO_3$. The mixture was incubated at 20 °C, and equal amounts of heptapeptide were added at 1 and 2 h. After incubation for 3 h, the mixture was submitted to HPLC.

HPLCs. HPLC purifications of [^{14}C]17BAPE$_2$-labeled or unlabeled forms of the GST−LBD chimera and the LBD were performed on a Vydac C4 reversed-phase column (3.2 mm × 250 mm, 5 μm particles, 300 Å pore size) at a flow rate of 500 μL/min, using a Waters gradient system (two 510 pumps, a gradient controller, and a 486 UV detector) equipped with a Shimadzu C-R6A integrator and an Isco Retriever II collector. For compound elution, linear gradients were generated from 10 to 95% CH_3CN over the course of 60−120 min; binary components for these gradients included solvent A [90/10 H_2O/CH_3CN mixture containing 0.05% trifluoroacetic acid (TFA)] and solvent B (5/95 H_2O/CH_3CN mixture containing 0.05% TFA). UV absorption (220 nm) was recorded; 4 min fractions were collected. LBD tryptic fragments were analyzed and purified under the same conditions with a Vydac C4 narrow-bore column (2.1 mm × 250 mm) at a flow rate of 200 μL/min. HPLC purifications of crude and [^{14}C]17BAPE$_2$-labeled heptapeptide and its V8 proteolytic fragments were performed with an Alltima C18 column (4.6 mm × 250 mm, 5 μm particles) at a flow rate of 1 mL/min. Linear gradients from 10 to 95% CH_3CN were generated with solvent A and B over the course of 30−60 min.

Trypsin and Endoproteinase V8 Proteolyses. The radioactive fractions obtained by HPLC purification of the affinity-labeled LBD (or tryptic fragments) or labeled heptapeptide were partially dried to evaporate CH_3CN, and then their pH was adjusted to the appropriate value and the proteolytic

enzyme added. For trypsin proteolysis of the LBD [T_{20} (pH 7.5), enzyme-to-substrate ratio of 1/40], the incubation was carried out for 2 h at 37 °C; for V8 endoproteinase proteolysis of LBD tryptic fragments or labeled heptapeptide [100 mM phosphate buffer (pH 7.8), enzyme-to-substrate ratio of 1/33], the incubation was performed for 15 h at 25 °C.

ZipTip Purification of Affinity-Labeled V8 Proteolytic LBD Fragments. A ZipTip$_{\mu-C18}$ microcolumn (Millipore) was equilibrated with a 50/50 H_2O/CH_3CN mixture. After being washed (three times) with 0.1% TFA, the column was loaded with the V8-proteolyzed sample. The ZipTip was washed (three times) with 0.1% TFA, and then bound peptides were eluted with 4 μL of a 20/80 H_2O/CH_3CN mixture containing 0.02% TFA. Samples were air-dried and then solubilized in 3 μL of 0.1% TFA.

Mass Spectrometry. MALDI mass spectra were obtained on a Bruker BiflexIII time-of-flight mass spectrometer (Bruker-Franzen, Bremen, Germany) equipped with a SCOUT source and Xmass software for data collection and analysis. The matrices were prepared either from a saturated solution of CHCA (analyses of peptides and LBD digests) or from a 4.5 μM solution of SA (LBD analyses) in a 1/1 (v/v) 0.1% TFA/CH_3CN mixture. A 1 μL aliquot of matrix solution was mixed with 1 μL of sample, and 0.4 μL of the mixture was spotted on the probe and allowed to dry at ambient temperature. Desorption and ionization were achieved with an N_2 laser (337 nm, 3 ns pulse width, 3 Hz repetition rate), followed by subsequent gridless delayed extraction. The instrument was used in the positive reflectron mode for synthetic peptides or digests, or linear mode for proteins, with an acceleration voltage of 19 kV. Mass spectra were acquired as a sum of ion signals generated by irradiation of the target with 50−200 laser pulses. Quadratic external calibration was achieved using a mixture of standard peptides containing angiotensin I [$[M + H]^+$, *m/z* (monoisotopic) 1296.69], bombesin ($[M + H]^+$, *m/z* 1619.82), ACTH 1−17 ($[M + H]^+$, *m/z* 2093.09), ACTH 18−36 ($[M + H]^+$, *m/z* 2465.20), and somatostatin 28 ($[M + H]^+$, *m/z* 3147.47). The Swiss-Prot protein data bank was consulted to characterize signals found in the spectra of the mouse ERα LBD and its proteolytic fragments.

Molecular Modeling Studies. Energy minimizations of ERα LBD models were performed using InsightII/Discover software from MSI, and CFF91 as the force field. The starting X-ray crystallographic structures of the human ERα LBD bound to E_2 (PDB entry 2ERE, monomer A), OHT (PDB entry 3ERT, monomer A), or Ral (PDB entry 1ERR, monomer A) (*8*, *10*) were lacking several poorly resolved amino acid residues, and some loop sequences were not specified for LBD−E_2 (residues 330−337 and 461−465) and LBD−Ral (residues 460−469 and 529−534) complexes. Lacking amino acid side chains were introduced in the complexes. All water molecules from crystallographic structures were deleted, with the exception of the one involved in hydrogen bonding of the phenolic OH (E_2 and OHT) or benzothiophene OH (Ral). 17BAPE$_2$ was docked into LBD structures derived from crystallized estrogen− and antiestrogen−LBD complexes to account for the covalent attachment of 17BAPE$_2$ to Cys421 and Cys534 (the mouse homologues of human Cys417 and Cys530, respectively), while firmly bound to the LBD.

(1) Docking of 17BAPE$_2$ into the LBD Structure Derived from Human LBD−E_2 Crystals. 17BAPE$_2$ was superimposed over LBD-bound E_2 by aligning the two A rings. This resulted in almost merged steroid nuclei, with very close locations of the two 17β-OH functions. The flexibility of the 17BAPE$_2$ 17α-substituent was then used to bring the electrophilic carbon (ε-carbon) into the proximity of the S atom of Cys417. Then steric clashes between 17BAPE$_2$ and the LBD were manually suppressed by appropriate rotations of some amino acid side chains and single chemical bonds of the 17α-substituent.

(2) Docking of 17BAPE$_2$ into an LBD Structure Derived from Human LBD−OHT Crystals. This was performed by superimposing the 17BAPE$_2$ A ring over the phenol ring of LBD-bound OHT. The His524 side chain was rotated so that the distance between δ-N of its imidazole ring and steroidal 17β-O would be suitable for N−OH hydrogen bonding (distance of ~3 Å). The flexibility of the helix 11−helix 12 loop was then used to position Cys530 close to the 17BAPE$_2$ ε-carbon; i.e., the helix 11−helix 12 loop was ruptured at the junction of amino acids 530 and 531; by appropriate rotations of single N−C and C−C bonds, the two open sequences were twisted to bring Cys530 closer to helix-3, and then the two sequences were reconnected. The 17α-substituent and (newly conformed) helix 11−helix 12 loop flexibilities were used to bring the ε-carbon and the S atom of Cys530 closer (distance of ~3.5 Å); steric clashes between 17BAPE$_2$ and LBD were suppressed, as described with the LBD−E_2 complex. OHT was then deleted, and a first minimization was carried out with fixed LBD α-carbons, except those of the helix 9−helix 10 and helix 11−helix 12 loops, and constrained interactions of (i) 17BAPE$_2$ 3-O with Glu353 and Arg394 side chains and with the bound water molecule, (ii) 17BAPE$_2$ 17β-O with the His524 imidazole ring, and (iii) the 17BAPE$_2$ ε-carbon with the S atom of Cys530. A second round of minimization was performed as indicated above, except that the LBD−ligand interaction constraints were suppressed.

(3) Docking of 17BAPE$_2$ into an LBD Structure Derived from Human LBD−Ral Crystals. Lacking sequences in the LBD−Ral complex, i.e., amino acids 460−469 (helix 9−helix 10 loop) and 529−534 (helix 11−helix 12 loop), were imported from the crystallized LBD−OHT complex (with a modified helix 11−helix 12 loop conformation, as described in the above paragraph). The modified complex was then minimized with fixed LBD α-carbons, except those of added loops, and constrained interactions of (i) the benzothiophene-linked O of Ral with Glu353 and Arg394 side chains and with the bound water molecule, (ii) the second phenolic O of Ral with the His524 imidazole ring, and (iii) the pyrimidyl N of Ral with the Asp351 side chain. 17BAPE$_2$ was then superimposed over Ral to obtain optimal overlap of the two ligands, i.e., (i) matching of 17BAPE$_2$ 3-O with the benzothiophene-linked O, with very close locations of the two phenol rings, and (ii) the tight proximity of 17BAPE$_2$ 17β-O and the second phenolic O of Ral. The His524 side chain was rotated to allow hydrogen bonding between δ-N of its imidazole ring and 17BAPE$_2$ 17β-OH. Flexibilities of the 17α-substituent and the helix 11−helix 12 loop were used to closely position the ε-carbon with the S atom of Cys530 or of Cys417 (distance of ~3.5 Å). Steric clashes in the two alternative models of the LBD−17BAPE$_2$

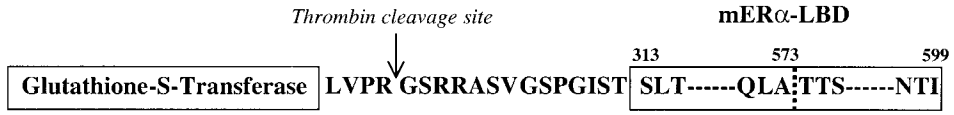


FIGURE 2: Structure of the GST−LBD chimera protein. The chimera encoded by the pGEX-2TK expression vector is schematically represented. Its LBD moiety constituted by the C-terminal half of mouse ERα (Ser^{313}−Ile^{599}) is linked to the GST moiety by an amino acid sequence enclosing a thrombin cleavage site. The major GST−LBD forms expressed in *E. coli* extracts were the full-length form and a C-terminally truncated form ending at Ala573 (cf. the text).

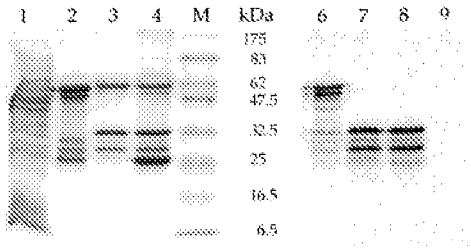


FIGURE 3: SDS−PAGE analysis of the mERα LBD. The cell extract (1.5 mL) from *E. coli*, induced to express the GST−LBD chimera, was rotated for 15 h at 4 °C with glutathione−Sepharose (100 μL). The whole gel was transferred into a column and washed with T_{20} (pH 8.0, 10 mL). Adsorbed species were incubated with or without 10 μM [^{14}C]17BAPE$_2$ (in the absence and presence of 50 μM E_2) for 2 h at 4 °C. Following gel washes, bound species were treated with glutathione, thrombin, or thrombin and glutathione, successively. Aliquots of bacterial extract (lane 1) and proteins released by the action of glutathione (lanes 2 and 6), thrombin (lanes 3 and 7), or thrombin and glutathione successive actions (lanes 4, 8, and 9) were subjected to SDS−PAGE. Proteins from unlabeled samples were revealed with blue stain (lanes 1−4), whereas proteins from samples incubated with [^{14}C]17BAPE$_2$ were visualized by autoradiography (lanes 6−8, samples incubated in the absence of E_2; lane 9, sample incubated in the presence of E_2). Standard molecular mass markers revealed by blue stain are in lane M.

complex were suppressed, as previously described, and then Ral was deleted. Two rounds of minimization, one with and one without constraints, were carried out as described for the minimization with the LBD structure derived from LBD−OHT crystals.

RESULTS

Expression, Purification, and Affinity Labeling of the Mouse ERα LBD. Our goal of identifying the covalent attachment sites of 17BAPE$_2$ (Figure 1) in the ERα LBD by MS analysis required access to large amounts (nanomole range, ~10^{-4} g) of the purified LBD. Expression in *E. coli* of a GST−mouse LBD chimera protein (enclosing a thrombin cleavage site located 14 amino acids ahead of LBD, cf. Figure 2), using a previously described recombinant vector (*21*), allowed us to fulfill these conditions, since (i) binding experiments performed with [^{3}H]E_2 revealed the presence of micromolar concentrations of specific E_2-binding species in soluble bacterial extracts and (ii) incubation with a glutathione−Sepharose absorbent selectively removed these E_2-binding species from extracts (not shown). SDS−PAGE analysis (Figure 3) of crude extracts (lane 1) and of proteins released by glutathione from glutathione−Sepharose (lane 2) showed that four main species (apparent molecular masses of 57, 53, 51, and 28 kDa) were selectively enriched in the glutathione eluate. To differentiate GST−LBD species from other proteins, glutathione−Sepharose-bound proteins were submitted to thrombin action alone or followed by that of glutathione, and then the released proteins were analyzed (lanes 3 and 4, respectively). In both cases, the 57 kDa species was still present, with two new major species (apparent molecular masses of 34 and 30 kDa), whereas the 53 and 51 kDa species were no longer detected. The main difference between the patterns in lanes 3 and 4 was the presence of a prominent band at 28 kDa in the thrombin + glutathione eluate which was absent in the thrombin eluate.

To affinity label the mouse LBD, the glutathione−Sepharose gel loaded with cell extracts was incubated with 10 μM [^{14}C]17BAPE$_2$, a concentration ~4-fold higher than that of E_2 specific-binding sites in adsorbed extracts. Then bound species were released as described above. Following SDS−PAGE, labeled species were revealed by autoradiography. Only two main signals were obtained from the glutathione eluate (lane 6), which precisely corresponded to the 53 and 51 kDa bands in lane 2. The thrombin and thrombin + glutathione eluates exhibited identical autoradiography patterns (lanes 7 and 8, respectively) with two major signals, which accurately corresponded to the 34 and 30 kDa bands in lanes 3 and 4. All of these ^{14}C signals were due to E_2 specific-binding species, since no signal was observed (lane 9) when the labeling step was carried out in the presence of a 5-fold excess of E_2 (relative to the [^{14}C]-17BAPE$_2$ concentration). It is noteworthy that (i) in lanes 6−8 the intensity ratio of signals for the heavy and light species was ~3 and (ii) no ^{14}C signal was observed at levels corresponding to the 57 and 28 kDa bands. The [^{14}C]-17BAPE$_2$ concentration that was used appeared to be quasi-optimal for species labeling, since in another experiment only slight increases (<50%) in signal intensities were obtained when the affinity probe concentration was increased from 6 to 24 μM (not shown).

All of the above results suggested that (i) the 53 and 51 kDa species were two different forms (present at a 3/1 ratio in the glutathione eluate) of the GST−LBD chimera, (ii) the 34 and 30 kDa species were the two corresponding LBD forms, and the 28 kDa species was the GST moiety, all released from the 53 and 51 kDa species by thrombin, (iii) only the LBD moieties of GST−LBD chimeras were specifically alkylated by [^{14}C]17BAPE$_2$, and (iv) the unidentified 57 kDa species may be related to the bacterial chaperonin dnaK involved in protein degradation (*24*) and which seemed to interact with the LBD.

Note that, besides the two major described forms for both GST−LBD and LBD species, two minor forms accounting for less than 10% of labeled species were present in the eluates (Figure 3, lanes 6−8); very weak LBD-like forms were present in the glutathione eluate (lane 6), which could have resulted from partial hydrolysis of GST−LBD forms by a bacterial protease. In some experiments, we observed that the thrombin-induced release of the 30 and 34 kDa species from glutathione−Sepharose was markedly improved when glutathione was subsequently added to the

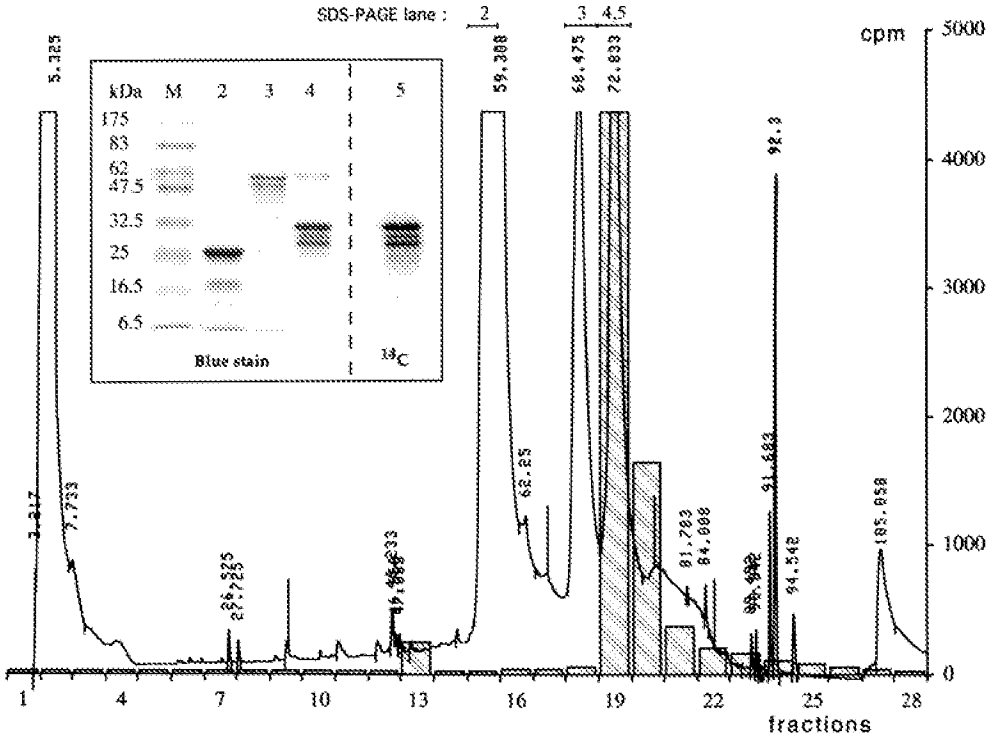


FIGURE 4: HPLC of the [^{14}C]17BAPE$_2$-labeled LBD. *E. coli* cell extracts were incubated with glutathione−Sepharose, and then following gel washes, bound species were exposed to [^{14}C]17BAPE$_2$ in situ. The species released by the action of thrombin and then glutathione were submitted to reverse-phase HPLC. Column elution was performed with a linear CH_3CN gradient. The curve represents the recorded 220 nm absorption according to the elution time, whereas hatched bars indicate the ^{14}C content of the various fractions (counts per minute per milliliter). The contents of major HPLC fractions (15, 18, and 19), analyzed by SDS−PAGE, are shown in the inset: blue staining (lanes 1−4) and autoradiography (lane 5) reveal the unlabeled and labeled species in fractions 15 (lane 2), 18 (lane 3), and 19 (lanes 4 and 5). Standard molecular mass markers are in lane M.

medium. This positive effect could be interpreted in two ways: (i) GST−LBD molecules released by glutathione displayed better accessibility to thrombin, or (ii) glutathione reduced S−S bonds formed between LBD SH groups and those of glutathione−Sepharose or those of glutathione−Sepharose-bound proteins. Regardless of the explanation, in practice we routinely used the successive actions of thrombin and glutathione for the full release of bound species from the absorbent.

Species released from glutathione−Sepharose, following in situ exposure of bound material to [^{14}C]17BAPE$_2$, were submitted to HPLC (Figure 4). Three main components were obtained: the first two (fractions 15, 16, and 18) only included unlabeled species, whereas the third contained practically all of the ^{14}C-labeled species (fractions 19 and 20). SDS−PAGE analysis of these fractions (Figure 4) showed that the first and second components (lanes 2 and 3) mainly contained putative GST (28 kDa) and dnaK (57 kDa) species, respectively, and the third one (lanes 4 and 5) included the ^{14}C-labeled 34 and 30 kDa species together with the two minor companion forms. These results indicated that HPLC was efficient for purifying the LBD forms. To more accurately characterize the two main ^{14}C-labeled LBD forms, whole radioactive fractions were submitted to MALDI-TOF MS analysis (Figure 5). In close accordance with the results of SDS−PAGE blue staining and autoradiography analyses, MS analysis showed only two signals centered at *m/z* 34 089 and 31 297 with relative intensities of 70 and 30%, respectively. The *m/z* 34 000 component was quite likely due to the $[M + H]^+$ form of the full-length LBD with its 14 extra N-terminal amino acids (Figure 2) and, via dehydrobromination, covalently bound [^{14}C]17BAPE$_2$ (average mass increment of 371.50 Da). The *m/z* 31 000 component appeared to correspond to the same species truncated at Ala573. These assumptions were based on acute agreements between (i) the calculated average mass for such species ([M + H], 34198.79 and 31403.78 Da, respectively) and the two experimental *m/z* values (deviation of 0.3%) and (ii) the

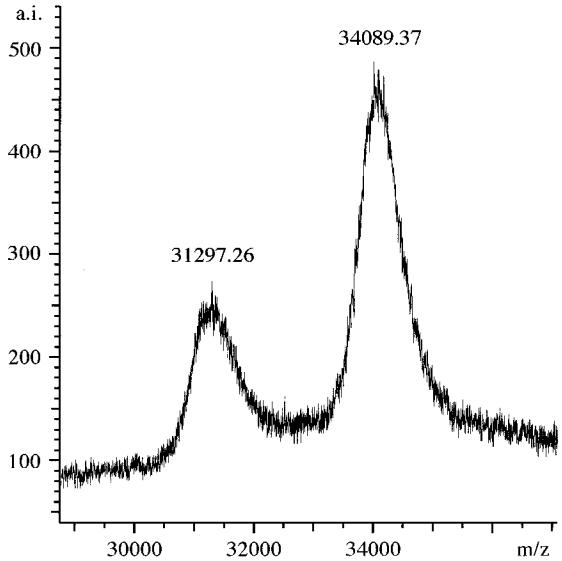


FIGURE 5: MALDI-TOF MS analysis of the [^{14}C]17BAPE$_2$-labeled LBD. The labeled LBD released from glutathione−Sepharose was purified by HPLC, as shown in Figure 4. The main radioactive fractions (19 and 20) were pooled, concentrated, and then analyzed by MS (SA matrix and positive linear mode).

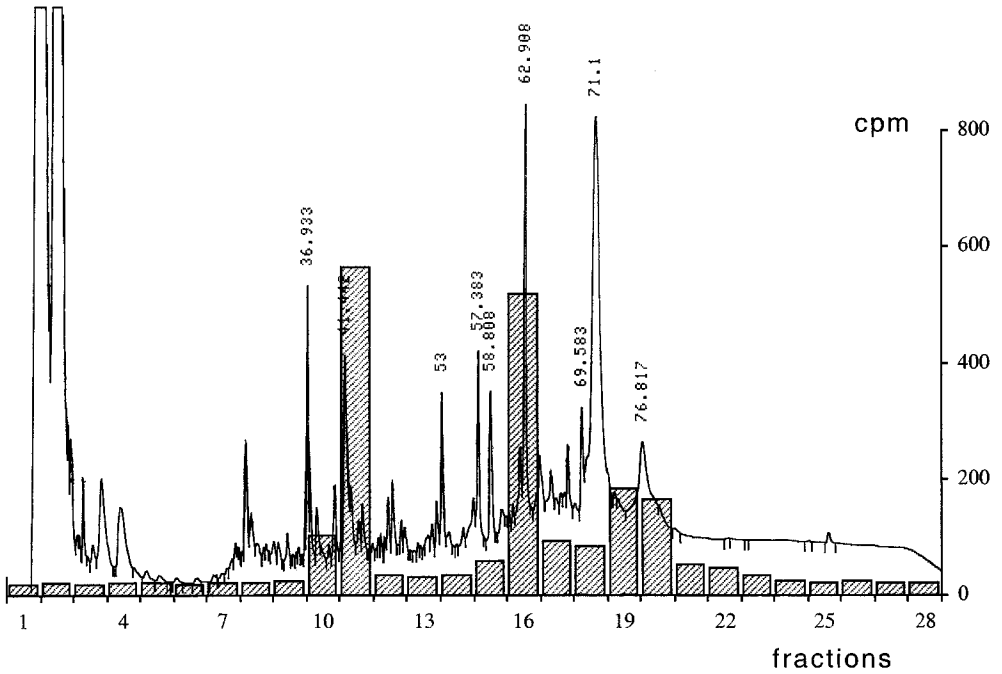


FIGURE 6: HPLC of [^{14}C]17BAPE$_2$-labeled LBD tryptic fragments. The labeled LBD was purified, as shown in Figure 4. The main radioactive fractions (19 and 20) were concentrated, treated with trypsin, and then submitted to reverse-phase HPLC. Column elution was performed with a linear CH_3CN gradient. The curve represents the recorded 220 nm absorption according to the elution time, whereas cross-hatched bars indicate the ^{14}C content of the various fractions (counts per minute per milliliter).

average mass increment ($\Delta M = 2795.01$ Da), corresponding to the postulated lacking Thr^{574}—Ile^{599} (LBD C-terminal) sequence (Figure 2) in the second species and the difference between the two experimental values ($\Delta m/z$ 2792.1, deviation of 0.1%). These interpretations were subsequently confirmed when tryptic fragments of the labeled LBD were analyzed by MALDI-TOF MS: two signals at *m/z* 4279.10 and 1483.55 were observed, which accurately corresponded to [M + H]$^+$ ions of full-length Met^{560}—Ile^{599} and truncated Met^{560}—Ala^{573} tryptic peptides. With regard to the truncated form, a similar form of the human ERα LBD, ending at Ala569, the human homologue of Ala573 of mouse ERα, was previously identified in *E. coli* expressing the human ERα LBD (*25*); this truncated form accounted for 23% of the different LBD forms.

Identification of Covalent Attachment Sites of [^{14}C]-17BAPE$_2$ on the Mouse ERα LBD. To identify 17BAPE$_2$-alkylated sites on the LBD, the HPLC-purified labeled LBD preparation was treated with trypsin, and then submitted to HPLC (Figure 6). Numerous species revealed by 220 nm absorption were present in the HPLC fractions, whereas only two nearly equivalent radioactive species were found (fractions 11 and 16, respectively), together with the nonproteolyzed LBD (fractions 19 and 20). MALDI-TOF MS analysis of the various fractions (example shown in Figure 7) allowed the identification of 23 signals corresponding to pseudomolecular [M + H]$^+$ ions of different LBD tryptic peptides (Figure 8), encompassing 97% of the LBD sequence.

Analyses of the two radioactive fractions gave few signals with, in each case, only one signal compatible with the combined masses of an LBD tryptic fragment and a dehydrobrominated form of [^{14}C]17BAPE$_2$ (monoisotopic mass increment of 371.23 Da). The fine structure of each of the two signals (Figure 9) was constituted by two series of well-resolved peaks, due to the occurrence of ^{12}C, ^{13}C, and ^{14}C isotopes in the alkylated species. In the major series, the peaks at *m/z* 621.47 and 2371.90 matched the [M + H]$^+$ form of alkylated LBD tryptic peptides (Figure 8) Cys^{534}Lys^{535} (calcd value of 621.36 Da, deviation of 0.02%) and Cys^{421}—Arg^{438} (calcd value of 2371.18 Da, deviation of 0.01%), comprising only ^{12}C isotopes and the ^{14}C isotope of 17BAPE$_2$; the peaks at $\Delta m/z$ +1, +2, +3 ... corresponded to alkylated forms involving one, two, three ... ^{13}C atoms, respectively. The minor series of peaks located at $\Delta m/z$ −2 from the major series simply reflected the presence of 12% [NH-^{12}CO] in [NH-^{14}CO]17BAPE$_2$ (cf. the legend of Figure 9). No signal was found that corresponded to the mass of any LBD tryptic peptide increased by one of the following values: 60.01 Da (addition of dehydrobrominated $BrCH_2$-$^{14}CO_2H$, due to hydrolysis of the amide bond in 17BAPE$_2$, following LBD alkylation), 357.22 Da (elimination of CH_3-Br following LBD alkylation by [^{14}C]17BAPE$_2$ at the S atom of methionine), or 45.99 Da (LBD alkylation at the S atom of methionine, followed by hydrolysis of the amide bond in 17BAPE$_2$). Then the results of HPLC and MALDI-TOF MS analyses strongly indicated that two alternative and quantitatively equivalent sites for covalent attachment of 17BAPE$_2$ were located on the Cys^{534}Lys^{535} and Cys^{421}—Arg^{438} LBD segments, respectively.

In the alkylated Cys^{534}Lys^{535} dipeptide, the covalent attachment site of 17BAPE$_2$ could be unambiguously assigned to the S atom of the Cys residue since, under the affinity labeling conditions used (pH 8.5), half of the Cys SH groups should be under their strongly nucleophilic, S^- form, whereas the Lys ϵ-NH_2 groups should be essentially under their unreactive NH_3^+ form.

In the Cys^{421}—Arg^{438} peptide, apart from the Cys residue, other amino acid residues possess a nucleophilic group, especially OH groups of the two Ser residues and the Thr residue. S atoms of the two Met residues are likely not

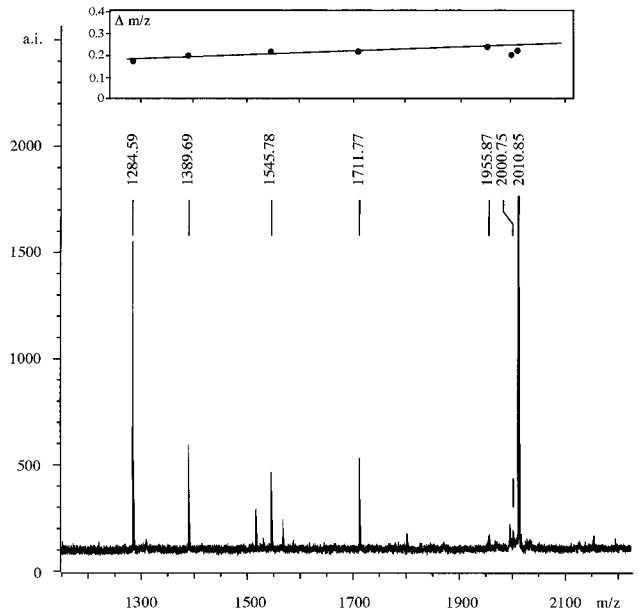


FIGURE 7: MALDI-TOF MS analysis of some unlabeled LBD tryptic fragments. Fractions 14−17 obtained in the HPLC separation of [^{14}C]17BAPE$_2$-labeled LBD tryptic fragments (as shown in Figure 6) were pooled and concentrated for MS analysis (CHCA matrix and positive reflectron mode). The various signals obtained in the range of *m/z* 1200−2200 are shown. *m/z* values which accurately match the monoisotopic mass of the $[M + H]^+$ form of LBD tryptic peptides (as obtained from the SwissProt data bank) are specified: *m/z* 1284.59 (Leu^{406}−Arg^{416}, calcd value of 1284.767 Da), 1389.69 (Leu^{508}−Arg^{519}, calcd value of 1389.894 Da), 1545.78 (Arg^{507}−Arg^{519}, calcd value of 1545.995 Da), 1711.77 (Leu^{406}−Lys^{420}, calcd value of 1711.985 Da), 1955.87 (Ser^{453}−Lys^{471}, calcd value of 1956.105 Da), 2000.75 (Cys^{421}−Arg^{438}, calcd value of 2000.949 Da), and 2010.85 (Asn^{536}−Arg^{552}, calcd value of 2011.068 Da). In the inset, the deviation between the measured *m/z* value and the calculated *m/z* value for the postulated $[M + H]^+$ form of the LBD tryptic peptide is plotted vs the measured value. The good linear correlation that was obtained fully validates the signal attribution.

involved in the covalent attachment of 17BAPE$_2$, as such an event would shift the peptide signal by a $\Delta m/z$ increment of 357.22 (or 45.99) and not of 371.23 (see above). To determine which nucleophilic atom in the Cys^{421}−Arg^{438} peptide was the covalent attachment site of 17BAPE$_2$ and since three potential V8 proteinase cleavage sites were present on the peptide (Figure 8), V8-induced fragmentation of the ^{14}C-labeled peptide, followed by ZipTip purification of fragments, and then MALDI-TOF MS analysis were performed. Four signals corresponding to the $[M + H]^+$ form of peptide fragments [resulting from peptide cleavage at the second (Glu427) and third (Asp430) V8 proteinase sites] devoid of the affinity label were obtained (not shown). Only a single very faint signal was observed at *m/z* 721.30, which could correspond to the $[M + H]^+$ form of the Cys^{421}−Glu^{423} tripeptide with covalently bound dehydrobrominated [^{14}C]-17BAPE$_2$ (calcd value of *m/z* 721.37); several important signals, which at this point were not yet attributed to definite species, were present (Figure 10).

To obtain conclusive evidence, the synthetic CysValGlu-GlyMetValGlu heptapeptide, constituting the 7-mer N-terminal portion of the Cys^{421}−Arg^{438} peptide, was submitted to alkylation by [^{14}C]17BAPE$_2$. Under conditions more drastic (concerning temperature and compound concentrations) than those used for LBD alkylation (cf. Experimental Procedures), the heptapeptide reacted with [^{14}C]17BAPE$_2$ to give only one labeled species revealed by HPLC (not shown). Treatment of the latter with V8 proteinase gave rise to only one labeled fragment, which was purified by HPLC (not shown). The heptapeptide, the alkylated heptapeptide, and its labeled V8 fragment were analyzed by MS. The compared analysis of the patterns (Figure 11 and Table 1) obtained for the three species revealed their homology; it allowed the identification of the $[M + H]^+$ signals, despite the faint intensity of some of them, as well as additional forms which we could almost exhaustively identify (cf. Appendix). In the heptapeptide (Figure 11A) and labeled heptapeptide (Figure 11B) spectra, two major signals accurately matching the masses of $[M + Na]^+$ and $[M + K]^+$ or $[M + Na + O]^+$ ions were higher (heptapeptide) or even much higher (labeled heptapeptide) than those corresponding to $[M + H]^+$ ions, whereas two minor signals matched the masses of $[M + 2Na - H]^+$ and $[M + Na + K - H]^+$ or $[M + 2Na + O - H]^+$ ions. The existence of such Na- and/or K-containing ions, not observed in the MS analysis of LBD tryptic fragments, probably reflected the high affinity of the heptapeptide and labeled heptapeptide with the ubiquitous Na or K contaminants. For the labeled heptapeptide V8 fragment, the *m/z* values of prominent signals (Figure 11C) homologous to the above-mentioned signals indicated that the peptide moiety of this fragment was constituted by the CysValGlu tripeptide. Other homologous signals were present in the labeled heptapeptide and labeled tripeptide spectra. In each case, one signal (particularly strong for the labeled tripeptide) exactly matched the mass of $[M + H - OH_2]^+$ ions. However, two signals matched the masses of ions differing from $[M + H]^+$ and $[M + Na]^+$ species by a $\Delta m/z$ increment of very close to −16, and these ions could be derived from the above species by elimination of an undefined atom or group of atoms (designated Θ). All signals obtained with the [^{14}C]-17BAPE$_2$-labeled heptapeptide and labeled tripeptide, but not those obtained with the unlabeled heptapeptide, were preceded at $\Delta m/z$ −2.00 by weaker satellite signals, which were clearly the mark of 17BAPE$_2$-labeled species.

The results obtained in the analysis of the labeled synthetic heptapeptide and its labeled V8 fragment clearly indicated that the nonattributed signals in the MS analysis of V8 fragments of the labeled Cys^{421}−Arg^{438} peptide (Figure 10) were in fact due to $[M + Na]^+$, $[M + Na - \Theta]^+$, $[M + H - \Theta]^+$, and $[M + H - H_2O]^+$ ions of the labeled Cys^{421}−Glu^{423} tripeptide and labeled Cys^{421}-Glu^{427} heptapeptide (Table 2). Since S^- in Cys residues is a much stronger nucleophile than CO_2^- in Glu residues, as reflected by the absence of a reaction of the C-terminal Glu residue when the heptapeptide was submitted to 17BAPE$_2$ action, we concluded that the S atom of the Cys^{421} residue was the covalent attachment site of 17BAPE$_2$ on the Cys^{421}−Glu^{423} tripeptide, and hence on the Cys^{421}−Arg^{438} LBD tryptic peptide. S atoms of Cys421 and Cys534 constituted the two alternative and equivalent attachment sites of 17BAPE$_2$ on the mouse ERα LBD.

DISCUSSION

This study was devoted to the identification of covalent attachment sites of 17BAPE$_2$, an electrophilic, high-affinity ligand which exhibits estrogenic properties on mouse ERα. After we started with *E. coli* cell extracts containing a GST−

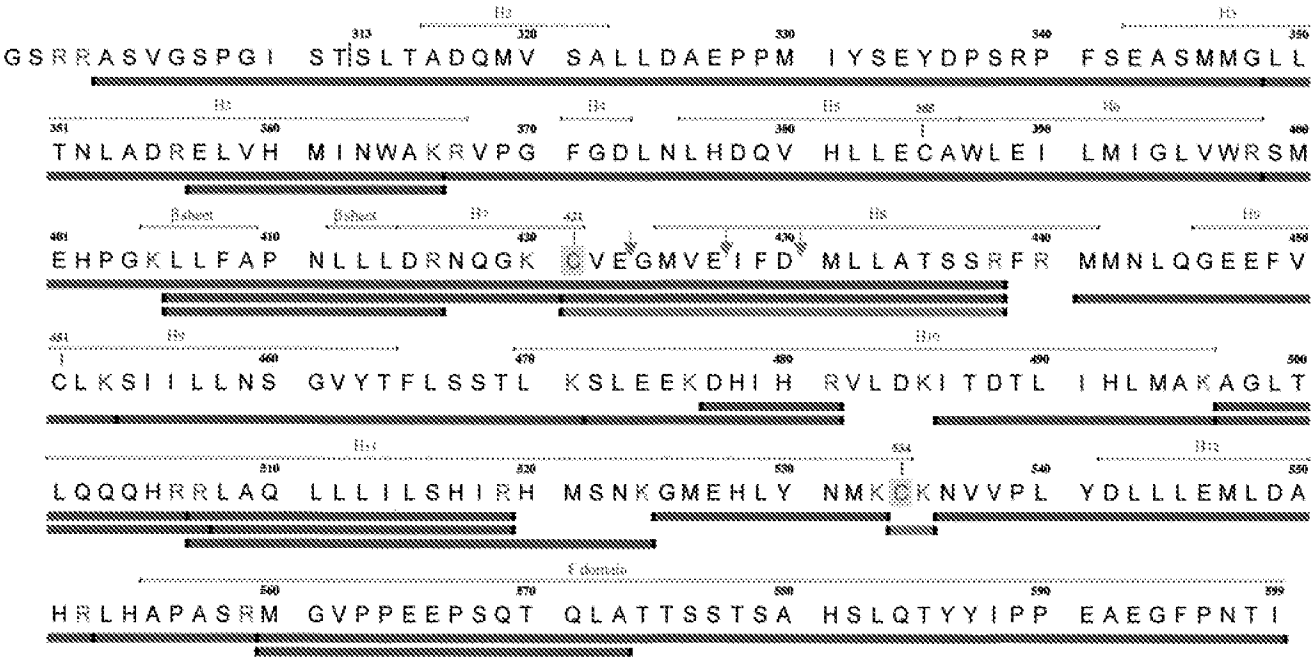


FIGURE 8: Map of LBD tryptic peptides identified by MS analysis. The sequence of the C-terminal moiety of the GST−LBD chimera (starting at the thrombin cleavage site) includes the full mouse ERα LBD encompassing the Ser^{313}−Ile^{599} sequence with the extra N-terminal 14 amino acids following the thrombin cleavage site. As inferred from the structure of the crystallized human ERα LBD−E_2 complex, lacking C-terminal domain F (the Ser^{309}−Pro^{552} human sequence, corresponding to the Ser^{313}−Pro^{556} mouse sequence), the 11 potential α-helices (H_2−H_{12}) and β-sheet which could occur in the mouse ERα LBD are represented (mauve segments above the sequence). Potential trypsin cleavage sites are immediately right of the red letters R and K. Following trypsin hydrolysis of the purified [^{14}C]17BAPE$_2$-labeled LBD, the various peptides identified from signals corresponding to their $[M + H]^+$ forms in MS analyses are materialized under the sequence: unmodified tryptic peptides (red segments) and [^{14}C]17BAPE$_2$-alkylated (via HBr elimination) tryptic peptides (green segments). The three potential V8 proteinase cleavage sites on the Cys^{421}−Arg^{438} tryptic peptide (green) are shown with arrows. The two cysteine residues, which are the covalent attachment sites of [^{14}C]17BAPE$_2$ on the LBD (cf. the text), are shown in green.

Table 1: MS Characteristics of the CysValGluGlyMetValGlu Heptapeptide, the [^{14}C]17BAPE$_2$-Labeled Heptapeptide, and Its Labeled V8 Proteolytic Fragment[a]

ion		CVEGMVE	(CVEGMVE)-APE$_2$	(CVE)-APE$_2$
$[M + H]^+$	*m/z*			
	theoretical	766.31	1137.55	721.37
	experimental	766.30 (51)	1137.94 (10)	721.76 (16)
		experimental Δ*m/z*		
alternative $[M + "X"]^+$	theoretical Δ*m/z*	CVEGMVE	(CVEGMVE)-APE$_2$	(CVE)-APE$_2$
$[M + H - H_2O]^+$	−18.01	nd[c]	−17.97 (13)	−17.97 (100)
$[M + H - Θ]^+$	−16.00[b]	−16.00 (0.5)	−15.99 (16)	−15.79[d] (50)
$[M + Na - Θ]^+$	5.98[b]	nd[c]	nd[c]	6.14[d] (0.5)
$[M + Na]^+$	21.98	21.94 (100)	22.05 (59)	22.06 (58)
$[M + K]^+$/$[M + Na + O]^+$	37.96/37.98	37.91 (30)	38.02 (100)	38.01 (38)
$[M + 2Na - H]^+$	43.96	43.91 (10)	44.04 (1)	44.03 (10)
$[M + K + O]^+$/$[M + Na + 2O]^+$	53.95/53.97	nd[c]	54.00 (14)	nd[c]
$[M + Na + K - H]^+$/$[M + 2Na + O - H]^+$	59.94/59.96	59.89 (10)	60.00 (14)	60.00 (15)

[a] Theoretical and experimental *m/z* values, corresponding to the $[M + H]^+$ ion, of the synthetic CVEGMVE heptapeptide, its [^{14}C]17BAPE$_2$-labeled form, (CVEGMVE)-APE$_2$, and the labeled tripeptide (CVE)-APE$_2$, postulated to be the labeled V8 proteolytic fragment of the latter, are given in the upper part of the table. Alternative ions ($[M + "X"]^+$), as inferred for the main signals found in the MS spectra of the three above-mentioned species (cf Figure 12), are listed in the left column; in the second and third ion species, Θ symbolizes an undefined atom or group of atoms (e.g., O, NH_2, or CH_4) displaying a monoisotopic mass very close to 16. For each of these ion types, the theoretical Δ*m/z* increment (difference in *m/z* values for $[M + "X"]^+$ and $[M + H]^+$ ions, equal to the difference in monoisotopic masses of "X" and H) is given. The corresponding experimental Δ*m/z* values in the MS analyses are given for the three peptide species. Values in brackets indicate, for each particular ion, the relative intensity of the corresponding signal in the spectrum of the analyzed species (expressed as a percentage of the most intense signal in the spectrum). [b] Calculated value assuming a monoisotopic mass of 16.00 for Θ. [c] Not detected (due to the absence of the corresponding signal in the spectrum). [d] Slightly inaccurate value (due to the presence of an interfering signal in the spectrum).

LBD chimera, an affinity chromatography step with in situ affinity labeling of the GST−LBD chimera followed by HPLC separation of eluted species led to the highly purified [^{14}C]17BAPE$_2$-alkylated LBD. The use of a ^{14}C-labeled form of 17BAPE$_2$ considerably facilitated the characterization and then purification of the expressed GST−LBD forms and derived LBD forms. Proteolyses of the alkylated LBD followed by HPLC separation and MALDI-TOF MS analysis of LBD fragments clearly identified Cys421 and Cys534 (the mouse homologues of human ERα Cys417 and Cys530, respectively) as alternative and equivalent covalent attachment sites of the electrophile.

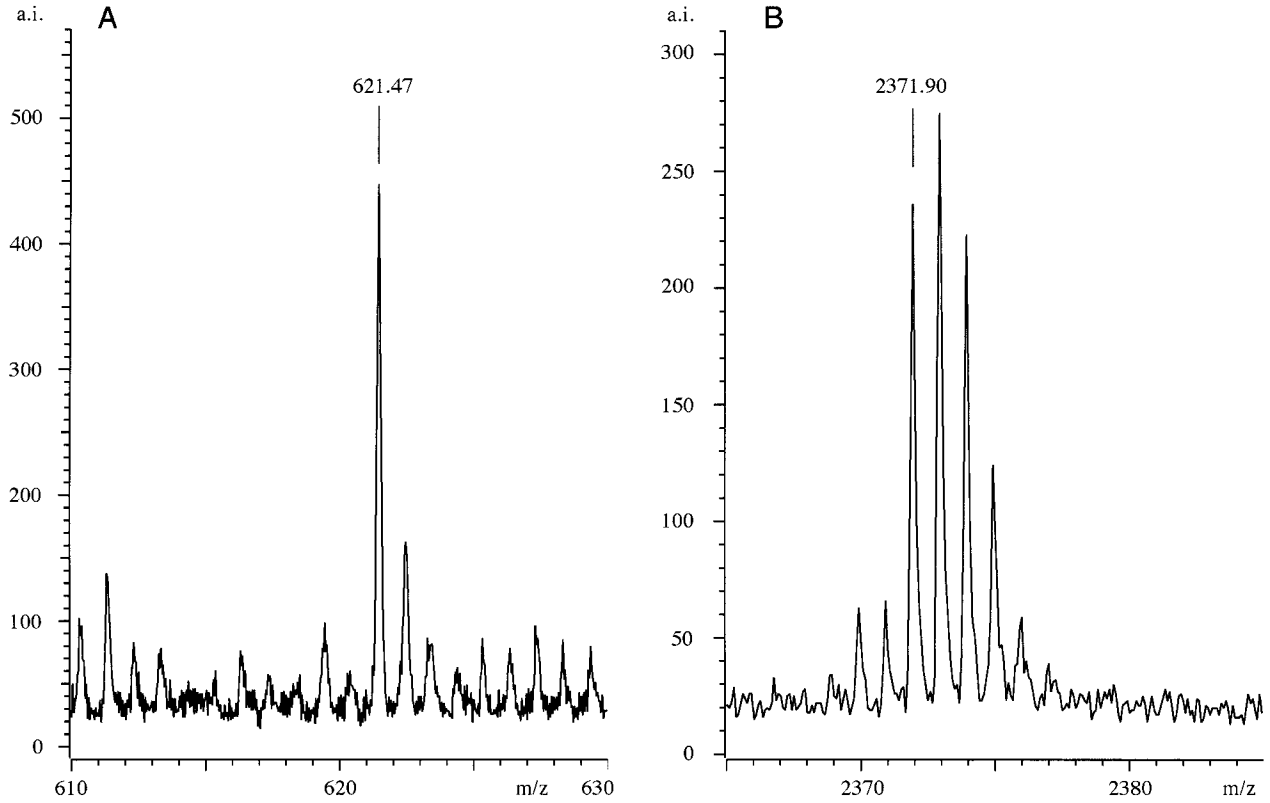


FIGURE 9: MALDI-TOF MS analysis of ^{14}C-labeled species obtained from trypsin hydrolysis of the [^{14}C]17BAPE$_2$-alkylated LBD. The two radioactive fractions (11 and 16 in Figure 6) obtained in the HPLC separation of labeled LBD tryptic fragments were analyzed by MS (CHCA matrix and positive reflectron mode). For each fraction, the obtained signal compatible with a [^{14}C]17BAPE$_2$-alkylated form of a LBD tryptic peptide is shown: (A) analysis of fraction 11 and (B) analysis of fraction 16. Signals at *m/z* 621.47 and 2371.90 accurately match the monoisotopic masses of pseudomolecular $[M + H]^+$ ions of Cys^{534}Lys^{535} and Cys^{421}—Arg^{438} tryptic peptides, respectively, alkylated by the ^{14}C form of 17BAPE$_2$ ([M + H] calcd values of 621.36 and 2372.18 Da for dehydrobrominated adducts, respectively). The companion signals observed just ahead of these two signals (at $\Delta m/z$ −2.00) correspond to tryptic peptides alkylated by nonradioactive 17BAPE$_2$ molecules; their intensities, relative to those of the main signals, closely reflect the proportion of [NHCO-^{12}C]17BAPE$_2$ and [NHCO-^{14}C]-17BAPE$_2$ (1/7.33) in the affinity probe that was used. Note that fine structures of the two major signals, characterized by the relative intensities of $[M + H]^+$, $[M + H + 1]^+$, $[M + H + 2]^+$ ... peaks (due to the occurrence of 1.1% ^{13}C in ^{12}C), reflect the total carbon numbers in alkylated Cys^{534}Lys^{535} (31 unlabeled carbons and one ^{14}C) and alkylated Cys^{421}—Arg^{438} (107 unlabeled carbons and one ^{14}C) LBD tryptic peptides.

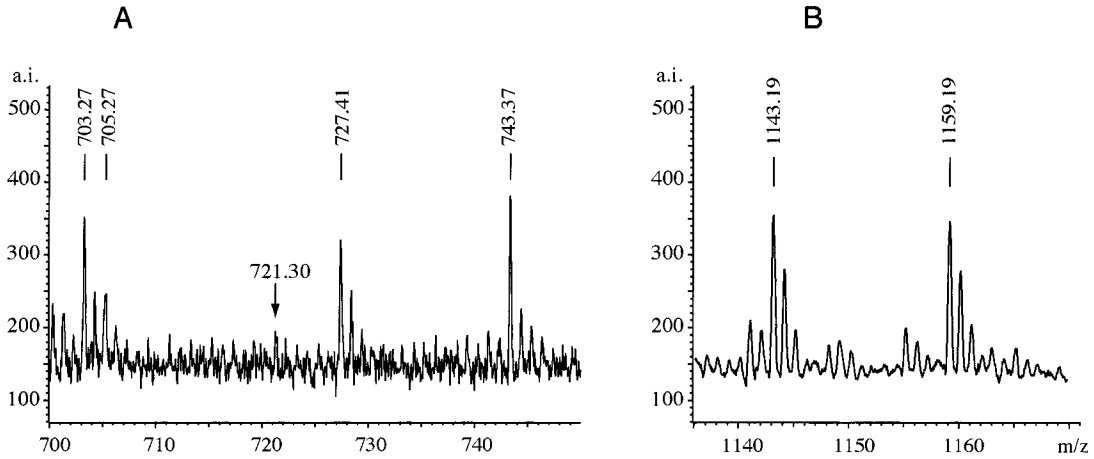


FIGURE 10: MALDI-TOF MS analysis of V8 proteolytic fragments of the [^{14}C]17BAPE$_2$-labeled Cys^{421}—Arg^{438} peptide. The alkylated Cys^{421}—Arg^{438} LBD tryptic peptide (HPLC fraction 16 in Figure 6) was submitted to V8 proteinase hydrolysis, desalted with ZipTip, and then analyzed by MS (CHCA matrix and positive reflectron mode). Signals shown in panels A and B (obtained in two different experiments) characterize $[M + H - H_2O]^+$, $[M + H - \Theta]^+$, $[M + Na - \Theta]^+$, or $[M + Na]^+$ ions of [^{14}C]17BAPE$_2$-labeled Cys^{421}—Glu^{423} (A) and Cys^{421}—Glu^{427} (B) fragments of the alkylated Cys^{421}—Glu^{438} peptide (cf. the text, and the legend of Table 2); only a very faint signal (*m/z* 721.30, shown with an arrow) was obtained for the $[M + H]^+$ ion of the alkylated Cys^{421}—Glu^{423} peptide.

These results validate and supplement those obtained in a previous study (*21*) in which covalent attachment sites of several electrophilic E_2 17α-derivatives, including 17BAPE$_2$, were ascribed to Cys417 and Cys530 of human ERα according to indirect evidence. They were based on the inability of these electrophiles to irreversibly inhibit E_2 binding to the Cys417Ala/Cys530Ala double-mutant ER, whereas the two Cys417Ala and Cys530Ala single mutants,

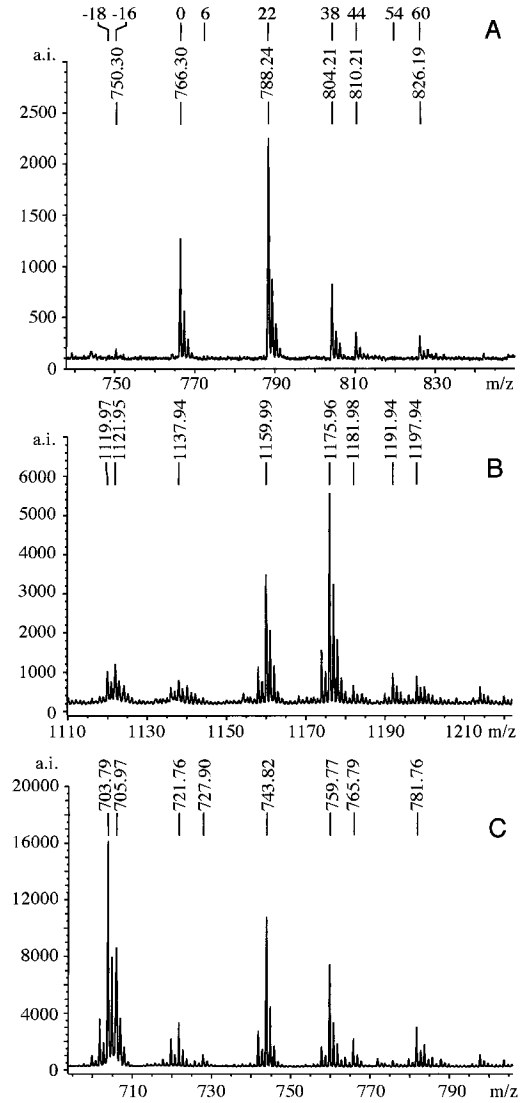


FIGURE 11: MS analysis of the unlabeled CysValGluGlyMetValGlu heptapeptide, the [^{14}C]17BAPE$_2$-labeled heptapeptide, and its labeled V8 proteolytic fragment. The synthetic heptapeptide was labeled with [^{14}C]17BAPE$_2$ in 0.1 M $NaHCO_3$ at 20 °C. Submitting the reaction mixture to HPLC led to only one ^{14}C-containing, 220 nm-absorbing species. An aliquot of the corresponding HPLC fraction was submitted to V8 proteinase hydrolysis. HPLC fractionation of the hydrolysate gave a single fraction showing both UV absorption and a high radioactivity level. The synthetic heptapeptide (A) and the HPLC fractions containing the [^{14}C]-17BAPE$_2$-labeled heptapeptide (B) or its labeled V8 fragment (C) were analyzed by MALDI-TOF MS (CHCA matrix and positive reflectron mode). The obtained spectra are represented so that the *m/z* experimental values of signals corresponding to the monoisotopic $[M + H]^+$ ion of the synthetic heptapeptide (measured *m/z* 766.30, calcd *m/z* 766.31), the [^{14}C]17BAPE$_2$-alkylated heptapeptide (measured *m/z* 1137.94, calcd *m/z* 1137.55), and the [^{14}C]17BAPE$_2$-alkylated CysValGlu tripeptide, postulated to be the labeled V8 fragment of the latter (measured *m/z* 721.76, calcd *m/z* 721.37) are aligned. The values displayed at the top of the figure indicate (for A−C spectra) the various Δ*m/z* increments (starting from the *m/z* values corresponding to the $[M + H]^+$ forms) characterizing ions as opposed to the $[M + H]^+$ ions, i.e., −18 for $[M + H - H_2O]^+$, −16 for $[M + H - \Theta]^+$, 6 for $[M + Na - \Theta]^+$, 22 for $[M + Na]^+$, 38 for $[M + K]^+$ or $[M + Na + O]^+$, 44 for $[M + 2Na - H]^+$, and 60 for $[M + Na + K - H]^+$ or $[M + 2Na + O - H]^+$. Note that, except for the heptapeptide signals, all of the other above-mentioned signals are accompanied by weaker satellite signals at Δ*m/z* −2.00, due to heptapeptide and tripeptide species alkylated by nonradiolabeled 17BAPE$_2$ molecules present in [^{14}C]17BAPE$_2$ (cf. the legend of Figure 9).

Table 2: MS Characteristics of [^{14}C]17BAPE$_2$-Labeled Cys^{421}−Arg^{438} V8 Proteolytic Fragments[a]

	m/z (Cys^{421}−Glu^{423})-APE$_2$		*m/z* (Cys^{421}−Glu^{427})-APE$_2$	
ion	exptl	calcd	exptl	calcd
$[M + H - H_2O]^+$	703.27	703.36	nd[c]	1119.54
$[M - H - \Theta]^+$	705.27	705.37[b]	nd[c]	1121.55
$[M + Na - \Theta]^+$	727.41	727.35[b]	1143.19	1143.53[b]
$[M + Na]^+$	743.37	743.35	1159.19	1159.53

[a] Experimental *m/z* values of signals obtained in the MS analysis of alkylated Cys^{421}−Arg^{438} V8 proteolytic fragments (as shown in Figure 10), which accurately matched the calculated values for various ions corresponding to the alkylated Cys^{421}−Glu^{423} tripeptide, (Cys^{421}−Glu^{423})-APE$_2$, and the alkylated Cys^{421}−Glu^{427} heptapeptide, (Cys^{421}−Glu^{427})-APE$_2$, are given. In the second and third ion species, Θ symbolizes an undefined atom or group of atoms displaying a monoisotopic mass very close to 16. [b] Calculated value assuming a monoisotopic mass of 16.00 for Θ. [c] Not detected (due to the absence of the corresponding signal in the spectrum).

like wild-type ER, were susceptible to irreversible E_2 binding inhibition. However, this did not allow us to clarify the following situations. (i) Both Cys417 and Cys530 might be alternative covalent attachment sites of these electrophiles (note that in this case the approach that is used cannot determine the relative involvements of Cys417 and Cys530 in the alkylation processes). (ii) Only one of the two cysteines might be the covalent attachment site while the other becomes an attachment site when the target cysteine is substituted for alanine [a similar case was observed with tamoxifen aziridine, a triphenylethylene antiestrogen, which alkylated the wild-type ER only at Cys530, but quite likely alkylated the Cys530Ala mutant at Cys381 (*26*)]. (iii) Neither of the two cysteines is a covalent attachment site: the inability of electrophiles to alkylate the Cys417Ala/Cys530Ala double mutant would thus result from ER conformational changes, induced by the two mutations, which move off (or hinder) the ER covalent attachment site from the electrophilic center of the bound steroid. Although unlikely, this possibility cannot be totally excluded since a triple cysteine to serine substitution, especially involving both Cys417 and Cys530, induced pronounced structural changes in a crystallized form of the ERα LBD−E_2 complex (*12*).

To date, only Cys417 and Cys530 have been identified as covalent attachment sites of electrophilic ligands on human ERα. Cys530 is the covalent attachment site common to (i) both steroidal [E_2 17α-derivatives (ref *21* and this study)] and nonsteroidal [ketononestrol aziridine (*27*), a diphenylethane derivative] estrogens and (ii) both steroidal [E_2 11β-derivatives (*28*)] and nonsteroidal [the aforementioned tamoxifen aziridine (*27*)] antiestrogens. Conversely, as confirmed in this study, Cys417 is the covalent attachment site of only the estrogenic E_2 17α-derivatives. Note that non-cysteinyl residues (but not yet identified) appeared to be involved in the covalent attachment of other antiestrogenic E_2 11β-derivatives to lamb ERα (*29*). The unique dual covalent attachment sites of E_2 17α-derivatives on ERαs may result from the particular location of their electrophilic groups relative to the steroid nucleus (17α-orientation) or from their type of activity (they are estrogen agonists, whereas the above-mentioned E_2 11β-derivatives are potent antagonists). To investigate this point, it would be interesting to determine the covalent attachment sites of new E_2-derived electrophiles,

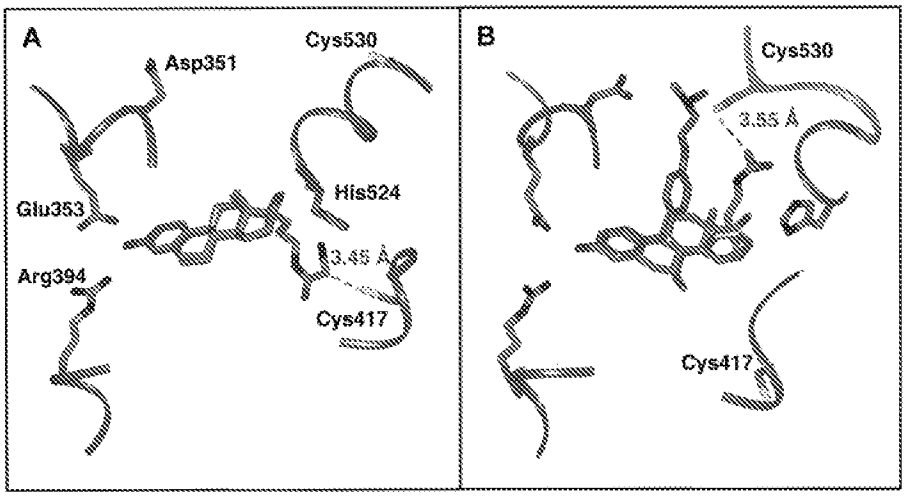


FIGURE 12: Docking of 17BAPE$_2$ into human ERα LBD structures derived from crystallized LBD−E$_2$ and LBD−OHT complexes. (A) 17BAPE$_2$ was manually docked into the fixed LBP structure, deduced from X-ray analysis of the crystallized human LBD−E$_2$ complex, as described in Experimental Procedures. The relative positions of E$_2$ (blue) and that of superimposed 17BAPE$_2$ (green) are shown in the LBP materialized by portions (in blue) of helix 3 (Asp351 and Glu353), helix 6 (Arg394), helix 7 and the helix 7−helix 8 loop (Cys417), and helix 11 (His524 and Cys530). The main characteristics of docked 17BAPE$_2$ are as follows: ϵ-carbon−Cys417 S distance (*d*) of 3.45 Å, 3-OH−Glu353 *d* of 2.31 Å, 3-OH−Arg394 *d* of 3.00 Å, and 17β-OH−His524 *d* of 2.62 Å. (B) 17BAPE$_2$ was docked through a two-step minimization process, into the LBD structure determined for the crystallized human LBD−OHT complex, as described in Experimental Procedures. The relative positions of OHT (blue) and docked 17BAPE$_2$ (green) are shown in the LBP materialized by portions of helix 3, helix 6, helix 7, the helix 7−helix 8 loop, helix 11 (His524), and the helix 11−helix 12 loop (Cys530). LBD original elements are in blue, whereas the helix 11−helix 12 loop, the conformation of which was modified, is in blue-green. The main characteristics of docked 17BAPE$_2$ are as follows: ϵ-carbon−Cys530 S *d* of 3.55 Å, 3-OH−Glu353 *d* of 2.74 Å, 3-OH−Arg394 *d* of 3.01 Å, and 17β-OH−His524 *d* of 3.25 Å.

e.g., estrogens possessing a relatively short 11β-substituent with a terminal bromoacetamido group and 11β-aryl antiestrogens bearing a 17α-bromoacetamidoalkyl group.

Mouse and human ERα LBDs differ by only eight amino acid residues (of more than 250 residues). Hence, with the aim of accounting for the alternative covalent attachments of 17BAPE$_2$ to human ERα Cys417 and Cys530 (i.e., to obtain close locations between S atoms of the two cysteines and the ϵ-carbon of bound compound), 17BAPE$_2$ was docked into available crystallographic structures of the human ERα LBD. In the LBP region, many structural features are common to the four crystallized LBD−estrogen and LBD−antiestrogen complexes (*8*, *10*); especially Glu353, in helix 3, and Arg394, in helix 6, make direct hydrogen bonds with the E$_2$ phenolic OH (or corresponding phenolic OH in DES, OHT, or Ral), and His524, in helix 11, is involved in hydrogen bonding of E$_2$ 17β-OH (or the second phenolic OH of DES or Ral). However, discrete variations were reported between crystallized estrogen and antiestrogen complexes, with some of them specifically affecting the structure of Cys417- and Cys530-bearing segments and then the location of these two amino acids relative to invariant structural elements. LBD structures derived from the crystallized domain bound to E$_2$, OHT, and Ral were therefore used for a manual exploration (followed by minimization) of potential proximities between the 17BAPE$_2$ ϵ-carbon and S atoms of Cys417 and Cys530. This was carried out assuming that (i) LBD helices and β−sheet would not vary and (ii) 17BAPE$_2$ 3-OH and 17β-OH, as observed with their counterparts in crystallized estrogen− and antiestrogen−LBD complexes, would interact with the above-mentioned key amino acids.

Since 17BAPE$_2$ includes the whole E$_2$ structure and displays estrogenic properties (*20*), the LBD structure derived from LBD−E$_2$ crystals (*8*) was first used for the ligand docking. From the steroid moiety of 17BAPE$_2$, positioned like E$_2$ in the LBD−E$_2$ crystals, the flexibility of the 17α-arm (which confers four degrees of freedom to the ϵ-carbon from steroidal C17) allowed us to bring the ϵ-carbon into the proximity of the S atom of Cys417 (distance of ~3.45 Å), with opposite locations of S and Br atoms, and without any steric clashes between 17BAPE$_2$ and LBP amino acids (Figure 12A). However, we could not obtain a distance of less than 6 Å between the ϵ-carbon and the S atom of Cys530. Since the sum of S and C van der Waals radii is ~3.36 Å, the distance of 3.45 Å between the ϵ-carbon and the S atom of Cys417 appeared to be very favorable for nucleophilic attack of the latter, whereas the distance of ~6 Å seems to be unsuitable for attack of the S atom of Cys530.

Due to structural changes (involving helix 7, the helix 7−helix 8 loop, and the helix 11−helix 12 loop) between crystallized LBD−E$_2$ and LBD−OHT complexes (*10*), different results were obtained when 17BAPE$_2$ was docked into the LBD structure inferred from LBD−OHT crystals. (i) The differential orientation of helix 7 moves off Cys417 (still located at the C-terminal end of that helix) from the LBP core and therefore from the ϵ-carbon which, despite the mobility of the 17α-substituent, cannot approach the S atom of Cys417 within <5 Å. (ii) Conversely, the shortening of helix 11 conferred mobility to Cys530 (shift in the helix 11−helix 12 loop); then combining the Cys530 and 17α-substituent mobilities allowed us to bring the S atom of Cys530 and the ϵ-carbon to the very convenient distance of ~3.55 Å in the minimized complex, while maintaining the interactions of 3-OH and 17β-OH with Glu353, Arg394, and His524, respectively (Figure 12B).

Finally, the potential proximities of the electrophilic center with respect to Cys417 and Cys530 in the LBD−17BAPE$_2$ complex were examined using the structure determined for the crystallized LBD−Ral complex (*8*). In the helix 7−helix

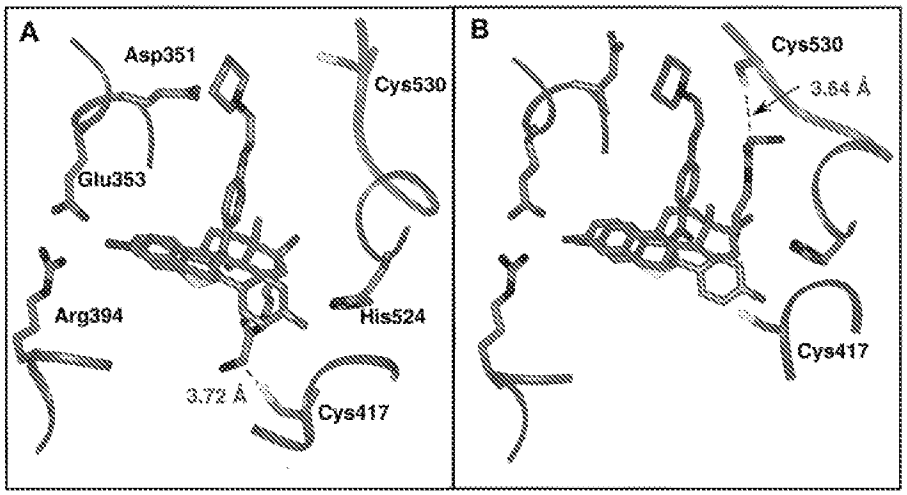


FIGURE 13: Docking of 17BAPE$_2$ into the human ERα LBD structure derived from the crystallized LBD−Ral complex. 17BAPE$_2$ was docked through a two-step minimization process, into the LBD structure determined for the crystallized human LBD−Ral complex (with the helix 11−helix 12 loop imported from the modified LBD−OHT crystallized complex), as described in Experimental Procedures. The docking was performed with the 17α-substituent oriented toward the C-terminal end of either helix 7 (A) or the helix 11−helix 12 loop (B). The relative positioning of Ral (blue) and 17BAPE$_2$ (green) is shown in the LBP materialized by portions of helix 3 (Asp351 and Glu353), helix 6 (Arg394), helix 7 and the helix 7−helix 8 loop (Cys417), helix 11 (His524), and the helix 11−helix 12 loop (Cys530). LBD original elements are in blue, whereas the helix 11−helix 12 loop, the conformation of which was modified, is in blue-green. The main characteristics of docked 17BAPE$_2$ are as follows: (A) ϵ-carbon−Cys417 S distance (*d*) of 3.72 Å, 3-OH−Glu353 *d* of 2.56 Å, 3-OH−Arg394 *d* of 2.88 Å, and 17β-OH−His524 *d* of 4.48 Å and (B) ϵ-carbon−Cys530 S *d* of 3.64 Å, 3-OH−Glu353 *d* of 2.38 Å, 3-OH−Arg394 *d* of 3.07 Å, and 17β-OH−His524 *d* of 3.19 Å.

8 region, the structure of this complex was closer to that of the LBD−E$_2$ complex than that of the LBD−OHT complex. Therefore, using the 17α-substituent flexibility, it was possible to bring the ϵ-carbon close to the S atom of Cys417 (distance of ~3.72 Å, Figure 13A). In the minimized complex, interactions of 3-OH with Glu353 and Arg394 were maintained, whereas the 17β-OH−His524 interaction was lost. In the reported LBD−Ral structure, the helix 11−helix 12 loop (including Cys530) was lacking. Since Ral and OHT belong to the same class of estrogen antagonists, the lacking loop was imported from the LBD−OHT complex. Then, by means of both 17α-substituent and helix 11−helix 12 loop flexibilities, it was possible to bring the ϵ-carbon close to the S atom of Cys530 (distance of ~3.64 Å, Figure 13B). In this case, all 3-OH and 17β-OH interactions (with Glu353, Arg394, and His524) were maintained.

Without any extensive molecular dynamics simulation analyses, the results of 17BAPE$_2$ docking into manually modified and minimized structures derived from the various crystallized complexes accounted well for the LBD specific labeling at Cys417 and Cys530: the proximities of the S atoms of the two cysteines and the ϵ-carbon of 17BAPE$_2$ could be obtained without disruption of canonical ligand−ER interactions. The same two cysteines were alkylated when the human ERα LBD, interacting with E$_2$ covalently linked to Sepharose via a 17α-propylthiopropyl arm (*30*), was exposed to the cysteine reagent iodoacetic acid (*31*−*33*); however, the required iodoacetic acid concentration was 500−2000-fold higher than the 17BAPE$_2$ concentration we used, and the reaction time was also ~10-fold higher. These considerable discrepancies reflect the two types of LBD alkylation processes, i.e., nonspecific with free iodoacetic acid and specific with the E$_2$-linked bromoacetamido group of 17BAPE$_2$.

The fact that only a model deduced from the crystallized LBD bound to Ral [a primarily antiestrogenic compound (*34*)] can account for the simultaneous labeling of Cys417 and Cys530 seems to conflict with the agonist behavior of 17BAPE$_2$. Even though if it is difficult to predict how conformational changes are upset by 17BAPE$_2$ as compared to E$_2$, we favor the hypothesis of alternative labeling of the two cysteines due to equilibria between multiple conformational states of ER−ligand complexes. These interpretations are in agreement with previous crystallographic studies involving a cysteine/serine mutant ERα (*11*) and the partial agonism of some ER ligands (*35*). The fact that the crystal data we used were obtained from the human ER LBD carboxymethylated at its cysteine residues, including Cys417 and Cys530, is an additional handicap for predicting the molecular basis of these conformational changes.

In conclusion, the results obtained suggest that methods other than the crystallization approach could help in gaining further insight into the dynamics of nuclear receptor−ligand interactions: the experimental results and modeling studies point to a view of ER−ligand complexes much more conformationally dynamic than that indicated by the crystal structure of these complexes. A study using specific amino acid reagents is under way to determine, by means of MS analysis, the pattern of modified amino acids in the human ERα LBD according to the type of bound ligand. This ER "footprinting" approach should allow us to establish solvent-exposed surfaces in the various LBD−ligand complexes, information that could be potentially useful for interpreting the agonist and antagonist activities of ER ligands. This work also illustrates that MS is a powerful tool for identifying covalent modifications on nuclear receptors, resulting from either physiological processes (e.g., phosphorylation, glycosylation, acetylation, etc.) or artifactual processes (e.g., affinity labeling to determine nuclear receptor−ligand proximities and specific amino acid derivation to probe conformations of nuclear receptor−ligand complexes).

ACKNOWLEDGMENT

We are grateful to Dr. Vincent Cavaillès for his donation of the plasmid encoding the GST−LBD chimera, and we thank Emmanuelle Demay for MS data acquisition.

APPENDIX

Interpretation of the Signal Diversity in MS Analyses of the Heptapeptide and Derivatives. The occurrence of nonconventional ions in the MS analyses of the synthetic CysValGluGlyMetValGlu heptapeptide, [^{14}C]17BAPE$_2$-labeled heptapeptide, and labeled CysValGlu tripeptide (or labeled Cys^{421}−Arg^{438} V8 proteolytic fragments) deserve commentary.

For these species, most signals attributed to Na- or/and K-containing pseudomolecular ions were stronger than those of classical $[M + H]^+$ ions. This suggests that, due to their particular amino acid sequences (involving hydrophobic residues, one C-terminal Glu residue, and, for heptapeptide species, an additional Glu residue), the heptapeptide and tripeptide species display high affinities for Na^+ and K^+ and therefore form stable complexes with these ubiquitous cation contaminants. Detection of such alkali−metal adducts has previously been reported in MS analyses of various peptidyl or non-peptidyl structures.

Apart from the unpredictable saline forms for all three analyzed species, the occurrence of chemical modifications [mainly oxidation, but also, in the case of labeled species, elimination of H_2O or of an unascribed group ("Θ") displaying a monoisotopic mass very close to 16] contributed to the increase in the ion diversity and therefore the signal number in spectra. First, signals attributed to singly and doubly oxidized forms were likely due to monooxidation at thioether S atoms (commonly observed for methionine-containing peptides) of species enclosing either one thioether function (unlabeled heptapeptide and cysteinyl S-alkylated tripeptide) or two thioether functions (labeled heptapeptide). For the various species, the closeness of the oxygen monoisotopic mass (15.995 Da) and the difference in the K and Na monoisotopic masses (15.974 Da) cannot allow discrimination between the signal of a K form and that of a corresponding monooxidized Na form. Second, the presence in MS spectra of labeled species (mainly labeled tripeptide) of signals at $\Delta m/z$ −18 or −16, which were absent in the spectra of the unlabeled heptapeptide, suggested a role for the steroidal moiety in generating forms derived from $[M + H]^+$ ions by elimination of H_2O or the Θ group, respectively (e.g., the labile tertiary steroidal 17β-OH could be involved in H_2O elimination).

Note that (i) signals at $\Delta m/z$ −18 and −16 were also observed in MS analyses of the labeled Cys^{534}Lys^{535} LBD tryptic fragment, which displays some characteristics very similar to those of labeled tripeptide, i.e., short peptide moiety with S-alkylated cysteine in its N-terminus, (ii) the similarity of the apparent monoisotopic mass of the Θ group with that of O and with the difference in K and Na monoisotopic masses increases the uncertainty concerning the number and the relative involvement of differing forms in a given signal, and (iii) from one experiment to another slight variations in the relative intensities of signals were observed, which probably reflected either differing Na^+/K^+ ratios in samples or differing extents of species oxidation or dehydration.

REFERENCES

1. Green, S., Walter, P., Kumar, V., Krust, A., Bornet, J. M., Argos, P., and Chambon, P. (1986) Human oestrogen receptor cDNA: sequence, expression and homology to v-*erb-A*, *Nature 320*, 134−139.
2. Greene, G. L., Gilna, P., Waterfield, M., Baker, A., Hort, Y., and Shine, J. (1986) Sequence and expression of human estrogen receptor complementary DNA, *Science 231*, 1150−1154.
3. Mosselman, S., Polman, J., and Dijkema, R. (1996) ERβ: identification and characterization of a novel human estrogen receptor, *FEBS Lett. 392*, 49−53.
4. Kuiper, G. G. J. M., Enmark, E., Pelto-Huikko, M., Nilsson, S., and Gustafsson, J. Å. (1996) Cloning of a novel estrogen receptor expressed in rat prostate and ovary, *Proc. Natl. Acad. Sci. U.S.A. 93*, 5925−5930.
5. Tsai, M. J., and O'Malley, B. W. (1994) Molecular mechanisms of action of steroid/thyroid receptor superfamily members, *Annu. Rev. Biochem. 63*, 451−486.
6. Mangelsdorf, D. J., Thummel, C., Beato, M., Herrlich, P., Schultz, G., Umesono, K., Blumberg, B., Kastner, P., Mark, M., Chambon, P., and Evans, R. M. (1995) The nuclear receptor superfamily: the second decade, *Cell 83*, 835−839.
7. Egea, P. F., Klaholz, B. P., and Moras, D. (2000) Ligand-protein interactions in nuclear receptors of hormones, *FEBS Lett. 476*, 62−67.
8. Brzozowski, A. M., Pike, A. C. W., Dauter, Z., Hubbard, R. E., Bonn, T., Engström, O., Öhman, L., Greene, G. L., Gustafsson, J. Å., and Carlquist, M. (1997) Molecular basis of agonism and antagonism in the oestrogen receptor, *Nature 389*, 753−758.
9. Tanenbaum, D. M., Wang, Y., Williams, S. P., and Sigler, P. B. (1998) Crystallographic comparison of the estrogen and progesterone receptor's ligand binding domains, *Proc. Natl. Acad. Sci. U.S.A. 95*, 5998−6003.
10. Shiau, A. K., Barstad, D., Loria, P. M., Cheng, L., Kushner, P. J., Agard, D. A., and Greene, G. L. (1998) The structural basis of estrogen receptor/coactivator recognition and the antagonism of this interaction by tamoxifen, *Cell 95*, 927−937.
11. Gangloff, M., Ruff, M., Eiler, S., Duclaud, S., Wurtz, J., and Moras, D. (2001) Crystal structure of a mutant hERα ligand-binding domain reveals key structural features for the mechanism of partial agonism, *J. Biol. Chem. 276*, 15059−15065.
12. Eiler, S., Gangloff, M., Duclaud, S., Moras, D., and Ruff, M. (2001) Overexpression, purification and crystal structure of native ERα LBD, *Protein Expression Purif. 22*, 165−173.
13. Pike, A. C. W., Brzozowski, A. M., Hubbard, R. E., Bonn, T., Thorsell, A. G., Engström, O., Ljunggren, J., Gustafsson, J. Å., and Carlquist, M. (1999) Structure of the ligand-binding domain of oestrogen receptor beta in the presence of partial agonist and a full antagonist, *EMBO J. 18*, 4608−4618.
14. Pike, A. C. W., Brzozowski, A. M., Walton, J., Hubbard, R. E., Thorsell, A. G., Li, Y. L., Gustafsson, J. Å., and Carlquist, M. (2001) Structural insights into the mode of action of a pure antiestrogen, *Structure 9*, 145−193.
15. Wurtz, J. M., Bourguet, W., Renaud, J. P., Vivat, V., Chambon, P., Moras, D., and Gronemeyer, H. (1996) A canonical structure for the ligand-binding domain of nuclear receptors, *Nat. Struct. Biol. 3*, 87−94.
16. Lees, J. A., Fawell, S. E., and Parker, M. G. (1989) Identification of two transactivation domains in the mouse estrogen receptor, *Nucleic Acids Res. 17*, 5477−5488.
17. Tora, L., White, J., Brou, C., Tasset, D., Webster, N., Scheer, E., and Chambon, P. (1989) The human estrogen receptor has two independent nonacidic transcriptional activation functions, *Cell 59*, 477−487.
18. Feng, W., Ribiero, R. C., Wagner, R. L., Nguyen, H., Apriletti, J. W., Fletterick, R. J., Baxter, J. D., Kushner, P. J., and West, B. L. (1998) Hormone-dependent coactivator binding to a hydrophobic cleft on nuclear receptors, *Science 280*, 1747−1749.
19. Grese, T. A., and Dodge, J. A. (1998) Selective estrogen receptor modulators (SERMs), *Curr. Pharmacol. Des. 4*, 71−92.
20. El Garrouj, D., Aliau, S., Aumelas, A., and Borgna, J. L. (1995) Steroidal affinity labels of the estrogen receptor. 2. 17α-(haloacetamidoalkyl)estradiols, *J. Med. Chem. 38*, 2339−2348.
21. Aliau, S., El Garrouj, D., Yasri, A., Katzenellenbogen, B. S., and Borgna, J. L. (1997) 17α-(Haloacetamidoalkyl)estradiols alkylate the human estrogen receptor at cysteine residues 417 and 530, *Biochemistry 36*, 5861−5867.

22. Cavaillès, V., Dauvois, S., Danielan, P. S., and Parker, M. G. (1994) Interactions of proteins with transcriptionally active estrogen receptors, *Proc. Natl. Acad. Sci. U.S.A. 91*, 10009−10013.
23. Bradford, M. M. (1976) A rapid and sensitive method for the quantitation of microgram quantities of protein utilizing the principle of protein dye binding, *Anal. Biochem. 72*, 248−254.
24. Sherman, M. Y., and Goldberg, A. L. (1992) Involvement of the chaperonin dnaK in the rapid degradation of a mutant protein in *Escherichia coli*, *EMBO J. 11*, 71−77.
25. Seielstad, D. A., Carlson, K. E., Katzenellenbogen, J. A., Kushner, P. J., and Greene, G. L. (1995) Molecular characterization by mass spectrometry of the human estrogen receptor ligand-binding domain expressed in *Escherichia coli*, *Mol. Endocrinol. 9*, 647−658.
26. Reese, J. C., and Katzenellenbogen, B. S. (1991) Mutagenesis of cysteines in the hormone binding domain of the human estrogen receptor, *J. Biol. Chem. 266*, 10880−10887.
27. Harlow, K. W., Smith, D. N., Katzenellenbogen, J. A., Greene, G. L., and Katzenellenbogen, B. S. (1989) Identification of cysteine-530 as the covalent attachment site of an affinity labeling estrogen (ketononestrol aziridine) and antiestrogen (tamoxifen aziridine) in the human estrogen receptor, *J. Biol. Chem. 264*, 17476−17485.
28. Aliau, S., Mattras, H., Richard, E., and Borgna, J. L. (1999) Cysteine 530 of the human estrogen receptor α is the main covalent attachment site of 11β-(aziridinylalkoxyphenyl)estradiols, *Biochemistry 38*, 14752−14762.
29. Aliau, S., Delettre, G., Mattras, H., El Garrouj, D., Nique, F., Teutsch, G., and Borgna, J. L. (2000) Steroidal affinity labels of the estrogen receptor α. 4. Electrophilic 11β-aryl derivatives of estradiol, *J. Med. Chem. 43*, 613−628.
30. Greene, G. L., Nolan, C., Engler, J. P., and Jensen, E. V. (1980) Monoclonal antibodies to human estrogen receptor, *Proc. Natl. Acad. Sci. U.S.A. 77*, 5115−5119.
31. Hegy, G. B., Shackleton, C. H. L., Carlquist, M., Bonn, T., Engström, O., Sjöholm, P., and Witkowska, H. E. (1996) Carboxymethylation of the human estrogen receptor ligand-binding domain-estradiol complex: HPLC/ESMS peptide mapping shows that cysteine 447 does not react with iodoacetic acid, *Steroids 61*, 367−373.
32. Witkowska, H. E., Carlquist, M., Engström, O., Carlsson, B., Bonn, T., Gustafsson, J. Å., and Shackleton, C. H. L. (1997) Characterization of bacterially expressed rat estrogen receptor β ligand binding domain by mass spectrometry: Structural comparison with estrogen receptor α, *Steroids 62*, 621−631.
33. Goldstein, S. W., Bordner, J., Hoth, L. R., and Geoghegan, K. F. (2001) Chemical and biological issues related to X-ray crystallography of the ligand-binding domain of estrogen receptor α, *Bioconjugate Chem. 12*, 406−413.
34. Grese, T. A., et al. (1997) Structure−activity relationships of selective estrogen receptor modulators: modifications to the 2-arylbenzothiophene core of raloxifene, *J. Med. Chem. 40*, 146−167.
35. Bourguet, W., Germain, P., and Gronemeyer, H. (2000) Nuclear receptor ligand-binding domains: three-dimensional structures, molecular interactions and pharmacological implications, *Trends Pharm. Sci. 21*, 381−388.

BI0205092

THE JOURNAL OF BIOLOGICAL CHEMISTRY
© 1991 by The American Society for Biochemistry and Molecular Biology, Inc.

Vol. 266, No. 17, Issue of June 15, pp. 10880-10887, 1991
Printed in U.S.A.

Mutagenesis of Cysteines in the Hormone Binding Domain of the Human Estrogen Receptor

ALTERATIONS IN BINDING AND TRANSCRIPTIONAL ACTIVATION BY COVALENTLY AND REVERSIBLY ATTACHING LIGANDS*

(Received for publication, December 17, 1990)

Joseph C. Reese and Benita S. Katzenellenbogen‡

From the Department of Physiology and Biophysics, University of Illinois, Urbana, Illinois 61801

We have carried out experiments to determine the role of the cysteines in the hormone-binding domain (HBD) of the human estrogen receptor (ER) in receptor function. In each mutant receptor, 1 of the 4 cysteines in the HBD (cysteines 381, 417, 447, and 530) was changed by *in vitro* mutagenesis of the ER cDNA (containing Gly^{400}) from cysteine to alanine; Cys^{530} was also mutated to a serine. The mutant and wild-type receptor cDNAs were expressed in Chinese hamster ovary cells using an expression vector containing the Rous sarcoma virus promoter. The mutant and wild-type receptors were assayed for hormone binding and for their ability to activate estrogen-responsive reporter plasmids. All ER mutants bound estradiol (E_2) with affinity similar to wild-type ER, displaying a K_d between 0.3 and 0.8 nM (wild-type ER K_d = 0.45 ± 0.10 nM). All were capable of covalent labeling by the affinity ligands ketononestrol aziridine, an estrogen agonist, and tamoxifen aziridine, an antagonist. Since in previous work we identified Cys^{530} as the site of covalent attachment of these ligands (Harlow, K. W., Smith, D. N., Katzenellenbogen, J. A., Greene, G. L., and Katzenellenbogen, B. S. (1989) *J. Biol. Chem.* 264, 17476–17485) it appears that an alternate residue(s) can be labeled in the absence of a cysteine at position 530; studies with methyl methanethiosulfonate, a cysteine-specific reagent, suggest that this residue is probably another cysteine in the HBD. The C381A, C417A, C530A and C530S ERs showed E_2-stimulated transcriptional activation profiles similar to wild-type ER whereas the dose response for E_2 for the C447A mutant was shifted to the right, requiring 50 × higher E_2 concentrations to achieve half-maximal response. Tamoxifen aziridine inhibited E_2-stimulated transcription, and ketononestrol aziridine stimulated transcription by wild-type, C530A, and C530S ER, but the effectiveness of these covalently attaching ligands was altered in the C530A and C530S mutants. Thus, these two mutant receptors are altered in their transactivation response to agonist and antagonist affinity labeling ligands but are unaltered in their response to reversibly binding estrogens and antiestrogens. In addition, we show that a mutant ER (C447A) can have an affinity for E_2 similar to that of wild-type ER but differs in its ability to activate transcription in response to E_2, indicating a decoupling of the hormone binding and transcriptional activation functions in this receptor.

The estrogen receptor (ER)[1] is a nuclear regulatory protein that mediates the actions of estrogens in target cells. The binding of ligand is presumed to cause a conformational change in the receptor protein which increases the receptor's affinity for DNA/chromatin elements resulting in a hormone-receptor complex that promotes transcription activation (or repression). The receptor-ligand complex binds as a dimer to a well defined 13-base pair palindromic sequence referred to as an estrogen-responsive element (ERE). The outcome of this interaction is dependent on the nature of the receptor-ligand complex. Although receptors can be occupied by either estrogen agonists or antagonists, receptors bound to antiestrogens fail to activate gene transcription or do so only poorly (1–4). ER-antiestrogen and ER-estrogen complexes also display physicochemical differences that would suggest a dissimilar conformation (1, 3), and gel mobility shift and cotransfection studies show that receptor-antiestrogen complexes fail to recruit transcription factors necessary to elicit the proper response (5, 6).

The cloning of the human estrogen receptor cDNA (7) as well as the development of affinity labels (8–10) and antibodies against ER (10, 11), have allowed the mapping of the hormone binding domain (HBD) of the ER to the carboxyl terminus. Although the boundaries of the hormone binding domain have been identified through deletion analysis (12, 13), the deletions that have been made have been large; therefore, a more detailed and refined analysis is necessary to identify amino acids important in the binding of ligands as well as those implicated in modulating agonist and antagonist activity. In a previous study from this laboratory (14) we identified a cysteine (Cys^{530}) in the HBD of ER as the site of covalent attachment to both an estrogenic (ketononestrol aziridine) and an antiestrogenic (tamoxifen aziridine) affinity-labeling ligand. Others have determined that dexamethasone mesylate, a covalently attaching glucocorticoid, labels a cysteine in the hormone binding region of the glucocorticoid receptor (15). The role of cysteines in the hormone binding regions of steroid receptors seems not to be limited to a site of covalent attachment for affinity labels because studies on glucocorticoid receptor (16–18) reveal that agents that specif-

* The costs of publication of this article were defrayed in part by the payment of page charges. This article must therefore be hereby marked "*advertisement*" in accordance with 18 U.S.C. Section 1734 solely to indicate this fact.

‡ To whom correspondence should be sent: Dept. of Physiology and Biophysics, University of Illinois at Urbana-Champaign, 407 South Goodwin Ave., Urbana, IL 61801.

[1] The abbreviations used are: ER, estrogen receptor; ERE, estrogen-responsive element; HBD, hormone binding domain; E_2, 17β-estradiol; KNA, ketononestrol aziridine; TAZ, tamoxifen aziridine; CHO, Chinese hamster ovary; CAT, chloramphenicol acetyltransferase; vit, vitellogenin; SDS, sodium dodecyl sulfate; MMTS, methyl methanethiosulfonate; WT, wild type.

ically block cysteinyl residues or influence redox transformations of cysteine residues alter receptor function.

Using the results of our previous affinity labeling studies (10, 14) to key the sites for our mutagenesis investigations, we have in this study used recombinant DNA techniques to address the importance of the 4 cysteinyl residues (cysteines 381, 417, 447, and 530) in the ER HBD. Our approach has been to make single amino acid changes that should have local rather than global effects on receptor structure. Thus, we have changed these cysteine residues to alanine residues (and in one case also to serine), and we have examined the effects of these changes on several aspects of receptor function, namely, ligand binding, and specificity with several reversibly binding and covalently attaching ligands, and the transcriptional activation by these ligands. The results of this study document, for the first time, mutations in the HBD of a steroid receptor which affect differentially the activity of affinity labeling *versus* reversibly binding ligands, and mutations that result in a decoupling of the hormone binding and transactivation functions of the receptor.

EXPERIMENTAL PROCEDURES

Chemicals and Materials—Radioinert 17β-estradiol (E_2) was obtained from Calbiochem. The antiestrogen ICI164,384 was kindly provided by Dr. Alan Wakeling and ICI Pharmaceuticals (Macclesfield, Great Britain). The affinity ligands ketononestrol aziridine (KNA), [^{3}H]KNA (67 Ci/mmol), and radioinert tamoxifen aziridine (TAZ) were synthesized as described in Refs. 8 and 9 and were kindly provided by Dr. John Katzenellenbogen, University of Illinois at Urbana-Champaign. [^{3}H]TAZ (21 Ci/mmol) was supplied by Amersham Corp. [2,4,5,6-^{3}H]Estradiol (105 Ci/mmol) and [*dichloroacetyl*-1,2-^{14}C]chloramphenicol (50–60 Ci/mmol) were from Du Pont-New England Nuclear. All sera and antibiotics were from GIBCO. DNA restriction and modification enzymes were purchased from Bethesda Research Laboratories or U. S. Biochemical Corp.

Cell Culture Conditions and Transfections—Chinese hamster ovary (CHO) cells, an estrogen receptor-deficient cell line, were passaged in phenol red-free Dulbecco's modified Eagle's medium/F-12 tissue culture medium (Sigma) supplemented with 10% charcoal-dextran-treated fetal calf serum, penicillin (100 units/ml), and streptomycin (100 μg/ml). Cells transfected for use in receptor binding studies were plated in 100-mm dishes in Dulbecco's modified Eagle's medium/F-12 with 10% charcoal-dextran-treated fetal calf serum at a density of 4×10^5 cells/plate, and for the gene transfer experiments, 2.2×10^5 cells were plated in 60-mm dishes in Dulbecco's modified Eagle's medium/F-12 with 5% charcoal-treated calf serum in a humidified 5% CO_2 atmosphere. At 36–40 h later, the medium was changed, and the cells were transfected 5–6 h later.

Cells were transfected by the calcium phosphate coprecipitation technique (19). The 100-mm plates used in the binding studies were transfected with 20 μg of ER expression plasmid (pRER) plus 10 μg of pTZ19R carrier DNA in 1.5 ml of precipitate, and the 60-mm plates used in the gene transfer studies were transfected with 5 ng of pRER + 0.8 μg of CAT reporter plasmid + 0.4 μg of pCH110 (an internal control plasmid) + 6.8 μg of carrier DNA in 0.4 ml of precipitate. The precipitate remained in contact with the cells for 12–16 h. After calcium phosphate exposure, the cells were glycerol shocked for 2.5 min with 20% glycerol in Hanks' balanced salt solution to facilitate DNA uptake by the cells. Cells were then fed with media, and hormones were added to the media from 1,000 × stocks in ethanol; these cells were harvested 48 h later.

DNA Constructs—All cloning was performed by standard procedures (20). The human ER cDNA clone λOR8 (provided by Dr. G. Greene of the University of Chicago) was digested with Tth 111-I at its restriction site 35 base pairs 5′ to the start codon and with *Sac*I 2 base pairs 3′ of the stop codon to obtain the open reading frame fragment. This 1,770-base pair piece was then blunted using T4 DNA polymerase, and *Sal*I linkers were ligated to the blunted fragment. This fragment was then inserted into the *Sal*I site of pTZ19R (21). This cDNA clone contained a mutation where a previous cloning error caused a replacement of a glycine for a valine residue at position 400 in the amino acid sequence (22). Therefore, the cDNA was reverted by us to the wild-type sequence by *in vitro* mutagenesis as described below. The eucaryotic expression vector pRSV was constructed from the vector pMAMneo (Clonetech) by digestion with *Bam*HI to release the neomycin resistance unit, isolation of the vector fragment, and ligation to generate pMAM. The pMAM vector was then digested with *Hin*dIII and *Nhe*I, blunt ended with mung bean nuclease, the vector fragment isolated from the murine mammary tumor virus sequences, and ligated. The resulting expression vector is under the control of the Rous sarcoma virus long terminal repeat promoter. Wild-type and mutant receptors were placed into the *Sal*I site of pRSV.

For the transcriptional activation studies the estrogen-responsive plasmid pATC-2 or ERE-vit-CAT was used (both provided by Dr. D. Shapiro of the University of Illinois). pATC-2 contains $(ERE)_2$-TATA-CAT with two consensus estrogen-responsive elements 38 base pairs from a TATA region, and the ERE-vit(vitellogenin)-CAT, a more complex promoter containing three endogenous EREs plus a consensus ERE inserted within the promoter (23). The plasmid pCH110 (Pharmacia LKB Biotechnology Inc.), used as an internal control for transfection efficiencies during gene transfer experiments, expresses the β-galactosidase gene constitutively from the SV40 early promoter.

In Vitro Mutagenesis—Oligonucleotide site-directed mutagenesis of the ER cDNA was performed according to the method of Kunkel (24) with modifications (21). The ER cDNA was cloned into pTZ19R, a phagemid vector that will produce a single-stranded DNA copy of itself with infection of the host bacterial strain by a helper phage (M13K07, kindly provided by Dr. B. Kemper, University of Illinois). The host strain used was CJ236.

The synthetic oligonucleotide was phosphorylated with T4 DNA kinase (Bethesda Research Laboratories), and 10 ng was annealed to 1 μg of single-stranded DNA in 30 μl of hybridization buffer (10 mM Tris-HCl, pH 7.5, 5 mM $MgCl_2$) by placing the tube in a 500-ml beaker of water at 70 °C and allowing it to cool slowly to <30 °C. The tube was placed on ice, and a polymerase reaction containing 20 mM Tris-HCl, pH 7.5, 10 mM $MgCl_2$, 5 mM dithiothreitol, 500 μM dNTPs, 1 mM ATP, 2.5 units of DNA polymerase (Klenow fragment), 1 unit of T4 DNA ligase (Bethesda Research Laboratories), and 2–4 μg of gene 32 protein (U. S. Biochemical Corp.) was brought to 100 μl. The reaction was carried out overnight at 16 °C. NM522 cells were transformed (20) with 10 μl of the reaction. Transformants were screened by sequencing using the dideoxy Sequenase kit (U. S. Biochemical Corp.).

Oligonucleotides used in mutagenesis were G400 (to revert the mutant cDNA to the wild-type $Val^{400} \rightarrow$ Gly) pGCACCCAGGGAAGCTACT; A381 (changes Cys^{381} to Ala) pACCTTCTCGAGGCTGCCTGG; A417 (changes Cys^{417} to Ala) pCCCTCTACAGCTTTTCCCTG; A447 (changes Cys^{447} to Ala) pGAGTTTGTGGCCCTCAAATC; A530 (changes Cys^{530} to Ala) pAGCATGAAGGCCAAGAACGT; S530 (changes Cys^{530} to Ser) pAGCATGAAGTCTAAGAACGT; ER SEQ (used as a primer for sequencing) pGTTCACATGATCAACTGG.

CAT Assays—48 h after the addition of hormones the plates were washed with cold phosphate-buffered saline, and 1 ml of TNE (40 mM Tris-HCl, pH 7.5, 140 mM NaCl, 1.5 mM EDTA) was added per plate. After a 5-min incubation at room temperature, cells were collected by scraping with a rubber policeman and transferred to microcentrifuge tubes. Cells were spun at 100 × *g* for 5 min, the supernatant aspirated, and the pellet resuspended in 300–400 μl of cold 250 mM Tris-HCl, pH 7.5. Cells were lysed by three cycles of freeze-thaw. 30–50 μl was used in a β-galactosidase assay as described by Herbomel *et al.* (25). Extracts containing 15–20 units of β-galactosidase activity were used for the CAT assay (26). Extracts were incubated with 0.1 μCi of [^{14}C]chloramphenicol in a total volume of 145 μl. The reaction was started by the addition of 5 μl of 10 mM acetyl-CoA (U. S. Biochemical Corp.) and placed at 37 °C for 90 min. The reaction was stopped by extracting with 1 ml of cold ethyl acetate. The supernatant (900 μl) was recovered and dried down. The residue was resuspended in 15 μl of ethyl acetate and spotted on TLC plates (Polygram Sil G, Sybron-Brinkmann). The reaction products were separated in a solvent of 95:5 (v/v) chloroform:methanol. After autoradiography, radioactive spots were excised for quantification by scintillation counting. CAT activity was expressed as percent conversion of chloramphenicol to its acetylated forms. The basal (control) level was determined as CAT activity in cells transfected with the reporter plasmid in the absence of ER plasmid.

Receptor Binding and Covalent Attachment Assays in Vitro—Plates transfected with 20 μg of pRER were harvested in HE (Hanks' balanced salt solution + 1.2 mM EDTA) by scraping with a rubber policeman. Cells were placed on ice, collected by centrifugation at 100 × *g*, and washed in ice-cold phosphate-buffered saline or TEG

(10 mM Tris-HCl, pH 7.4, 1 mM EDTA, 10% glycerol). Cells were resuspended in a volume of 200 μl/100-mm plate in homogenization buffer (50 mM Tris-HCl, pH 7.4, 1.5 mM EDTA, 10 mM sodium molybdate, 1 mM β-mercaptoethanol, 50 mM NaCl, 10% glycerol, 10 μg/ml leupeptin, 5 μg/ml aprotinin, and 0.1 mM phenylmethylsulfonyl fluoride. Cells were homogenized by 25–30 strokes in a glass Dounce homogenizer (B pestle). The homogenate was then centrifuged at 180,000 × *g* at 4 °C to yield cytosol. The protein concentration was determined by the BCA reagent kit (Pierce Chemical Co.).

For hormone binding assays performed on cytosol, samples were incubated with [^{3}H]estradiol in the absence of (total binding) and the presence of 200-fold excess radioinert estradiol (nonspecific binding) for 2 h at 22 °C. Incubation was terminated by placing the tubes on ice for 5 min and then adding an equal volume of dextran-coated charcoal (0.5% Norit A charcoal, 0.05% dextran T-70 in TEG). Samples were treated for 10 min on ice with periodic mixing, centrifuged at 12,000 × *g* for 5 min, followed by removal of an aliquot of the supernatant for scintillation counting. Affinity of the receptor for estradiol was determined by the method of Scatchard (27).

The covalent attachment assay was performed as described (9). Samples were incubated with radiolabeled TAZ either on ice for 2 h or at 22 °C for 30 min, and those with KNA were at 22 °C for 2 h. Reversible binding was determined by dextran-coated charcoal assay and covalent binding by an ethanol filter disc assay (9).

Labeling of Transfected Cells with Affinity Ligands—Dulbecco's modified Eagle's medium/F-12 containing 0.5% charcoal-dextran-treated fetal calf serum (4 ml) with and without 200-fold excess radioinert E_2 was added to transfected CHO cells on plates (100 mm) and incubated at 37 °C for 15 min. Media were then removed and replaced with media containing 20 nM [^{3}H]TAZ or 40 nM [^{3}H]KNA with or without 200-fold excess radioinert E_2. Plates were incubated at 37 °C for 30 min, ligand-containing media removed, and 10 ml of fresh media added followed by a 10-min incubation at 37 °C. The plates were washed with Hanks' balanced salt solution, harvested in HE, washed in TEG, and the cells homogenized with 500 μl/plate of homogenization buffer (25 strokes with a B pestle). The crude homogenate was spun at 800 × *g* for 10 min; the supernatant was removed, and the pellet was resuspended in 100 μl of nuclear extraction buffer (50 mM Tris-HCl, pH 8.5, 1.5 mM EDTA, 1 mM β-mercaptoethanol, 10 mM sodium molybdate, 10% glycerol, 0.6 M NaCl, 10 μg/ml leupeptin, 0.1 mM phenylmethylsulfonyl fluoride, 5 μg/ml aprotinin). The suspension was extracted for 30 min on ice with resuspension every 10 min and then centrifuged at 180,000 × *g*. Nuclear extract was used in the binding and covalent attachment assays described above. Nuclear extracts containing covalently labeled receptors were also subjected to SDS-polyacrylamide gel electrophoresis as described previously (8, 10).

Immunoprecipitation—Cytosolic extracts were labeled with [^{3}H]TAZ or [^{3}H]KNA as described above. ER was immunoprecipitated as described (28) using the two anti-ER-specific monoclonal antibodies H222 and D547 (10, 11). The immune complex was precipitated using *Staphylococcus* A cells (Zymed), and the ER was then removed by boiling in SDS-polyacrylamide gel electrophoresis loading solution.

Immunoblots—Proteins were fractionated on polyacrylamide gels under reducing conditions. Slab gels containing 9% polyacrylamide and 0.1% SDS were used as described (10). Proteins were transferred from SDS gels to nitrocellulose by electrophoresis and subjected to Western blot analysis using anti-ER monoclonal antibodies as described (29).

RESULTS

Expression of a Functional ER in CHO Cells—To demonstrate the expression of a functional ER in CHO cells, cytosolic extracts were prepared from cells transfected with the ER expression vector pRER, and ER binding was measured by the dextran-coated charcoal assay. The levels of ER expressed by these cells ranged between 150 and 300 fmol/mg of protein, approximately half the level of ER found in the estrogen receptor-rich cell line MCF-7 (30). The wild-type receptor bound E_2 with high affinity, displaying a K_d of 0.5 nM (Fig. 1), and this receptor evokes an estrogen-dependent increase in transcription of estrogen-responsive reporter genes (see below). Western blot analysis of cytosols from cells transfected with either mutant or wild-type cDNAs, using the ER-specific monoclonal antibody H222 (11), revealed a receptor doublet comigrating with the MCF-7 ER with an apparent molecular weight of 66,000 (data not shown). It has been proposed that the slower migrating species of the doublet may be a phosphorylated form of the receptor (29, 31).

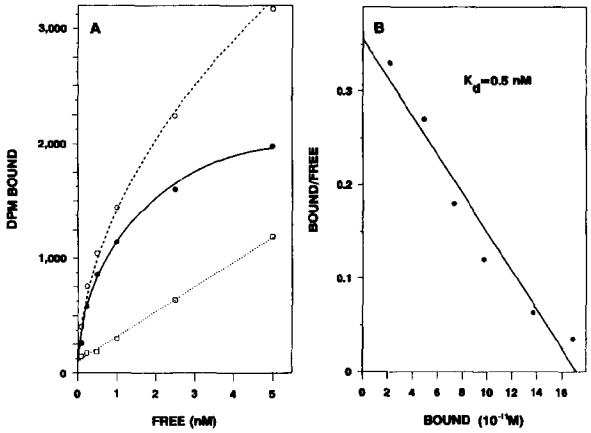


FIG. 1. **Saturation analysis of the binding of estradiol by the wild-type receptor expressed in CHO cells.** *A*, cytosols from cells transfected with pRER were incubated at 22 °C for 2 h with increasing concentrations of [^{3}H]E_2 with (□) or without (○) 200-fold excess radioinert E_2. Free steroid was removed by dextran-coated charcoal treatment. Specific binding (●) was calculated by subtracting nonspecific binding from total binding. *B*, binding was subjected to Scatchard analysis (27). The wild-type receptor bound estradiol with high affinity, displaying a K_d of 0.5 nM.

TABLE I

Estrogen receptors: wild-type and mutants

The equilibrium dissociation constants (K_d) are expressed as means ± S.E. from the number of separate determinations indicated in parentheses. + designates that the mutants were at least 90% as effective as the wild-type at covalent labeling by the ligands TAZ and KNA. [^{3}H]TAZ labeling (20 nM ± 4,000 nM E_2) was for 30 min at 22°C; [^{3}H]KNA labeling (40 nM ± 8,000 nM E_2) was for 2 h at 22 °C. Transactivation data represent the mean ± S.E. from four to six separate experiments.

Receptor	Binding	Covalent Attachment		Transactivation
		TAZ	KNA	
	K_d (E_2) nM			$1/2_{max}$[E_2], M
Wild-type	0.45 ± 0.10 (4)	+	+	$5.8 \pm 0.9 \times 10^{-12}$ (1 ×)
C381A	0.80 ± 0.20 (3)[a]	+	+	$1.3 \pm 0.5 \times 10^{-11}$ (2 ×)
C417A	0.82 ± 0.09 (3)[a]	+	+	$7.6 \pm 0.1 \times 10^{-12}$ (1 ×)
C447A	0.84 ± 0.05 (9)[a]	+	+	$2.8 \pm 0.1 \times 10^{-10}$ (50 ×)
C530A	0.54 ± 0.10 (3)	+	+	$6.8 \pm 0.9 \times 10^{-12}$ (1 ×)
C530S	0.30 ± 0.06 (3)	+	+	$8.3 \pm 0.1 \times 10^{-12}$ (1 ×)

[a] $p < 0.05$ *versus* wild-type ER by Student's *t* test.

Estradiol Binding Studies with Mutated Receptors—The affinity of the various receptor mutants for estradiol was measured by saturation binding (Scatchard) analysis (27). The affinities of the mutant receptors for E_2 were similar to that of the wild-type receptor (Table I), differing from wild type by less than 2-fold, with only three of the mutants showing K_d values statistically different from wild-type.

The stability of the estradiol-receptor complexes of wild-type and mutant receptors was examined, as was the dissociation rate of estradiol from the receptors at 22 °C. The expressed wild-type and mutant receptors were found to be equally stable over 3 h at 22 °C, showing no loss of specific binding (Fig. 2). The wild-type and mutant estradiol-receptor dissociation rates were also similar (Fig. 2), with a $t_{1/2}$ of approximately 5–6 h at 22 °C, a value similar to that of native ER (32).

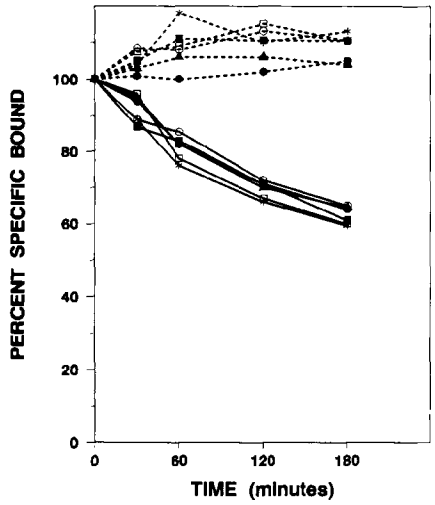


FIG. 2. **Estradiol-receptor complex dissociation and stability studies.** The stability and dissociation studies were performed as described (32). Cytosolic extracts were incubated with 10 nM [^{3}H] estradiol ± 200-fold excess radioinert E_2 for 2 h at 22 °C. The extracts were stripped of free hormone by dextran-coated charcoal treatment, and aliquots were made 10^{-6} M in estradiol (dissociation studies) or 10 nM in [^{3}H]estradiol ± 200-fold E_2 (stability studies) and incubated for the times indicated at 22 °C. Incubations were terminated by placing the tubes on ice for 5 min followed by dextran-coated charcoal treatment. The stabilities (*dashed lines*) and dissociation rates (*solid lines*) of ER mutants C381A (■), C417A (▲), C447A (○), C530A (*), and C530S (□) were compared with WT (●) and were found to be similar.

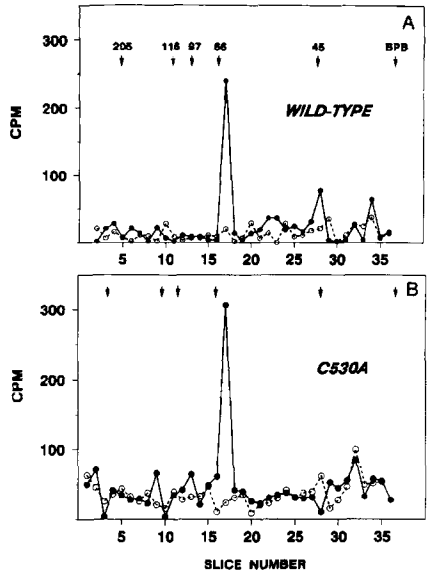


FIG. 3. **SDS-polyacrylamide gel electrophoresis of TAZ-labeled receptors.** Equal amounts of wild-type (*A*) and C530A (*B*) ER were labeled in cytosolic extracts with 20 nM [^{3}H]TAZ with (○) and without (●) a 200-fold excess of radioinert E_2. After a 40-min incubation at 22 °C, the samples were immunoprecipitated as described under "Experimental Procedures" and loaded onto an 8% SDS-polyacrylamide electrophoresis gel. The gels were sliced, processed as described (8, 10), and subjected to liquid scintillation counting to determine radioactivity in each slice. The positions of the molecular weight markers that were run separately are indicated by the *arrows*.

Covalent Attachment of Affinity Labeling Ligands—We examined the ability of the affinity labeling ligands TAZ and KNA to label covalently the wild-type and mutant receptors. We did this both by exposing intact CHO cells expressing the receptors to [^{3}H]TAZ or [^{3}H]KNA in cell culture and by incubating cytosolic extracts from transfected cells expressing ER with these radiolabeled affinity ligands.

Cytosol preparations of wild-type and mutant ERs expressed in CHO cells were covalently labeled by TAZ and KNA. The labeling of wild-type and all receptor mutants by both affinity labels was efficient, with the mutants being labeled to at least 90% the extent of the wild-type ER (Table I). The labeling of the C530A mutant is unexpected because we have previously identified Cys^{530} as the site of covalent attachment of both KNA and TAZ in MCF-7 cell ER (14). We also labeled the transfected ER-expressing CHO cells with affinity ligands and then performed the covalent attachment assay on the receptors in nuclear extracts. The mutant receptors were covalently labeled under these conditions as well, verifying the results of the labeling performed in the cytosolic extracts and eliminating the possibility that the receptor may have been denatured or altered during isolation, thereby allowing attachment at another site.

To verify that the molecular moiety being labeled is the estrogen receptor, cytosols from cells transfected with wild-type, C530A, or C530S ER were labeled with [^{3}H]KNA or [^{3}H]TAZ; cytosols were then immunoprecipitated with anti-ER antibodies, and the material was subjected to SDS-polyacrylamide gel electrophoresis. One major peak was observed for the wild-type or mutant receptor labeled with TAZ which migrated just slightly ahead of the 66,000 molecular weight marker (Fig. 3). This peak was displaced by a 200-fold excess of radioinert estradiol, and it migrates at the same position as native ER from MCF-7 cells (9, 10, 14).

Since the C530A mutant lacks cysteine at position 530, the site of TAZ and KNA labeling in wild-type ER, it appears that an alternative residue is being labeled in this mutant. To establish whether another cysteine residue is involved, the cysteine-specific modifying agent methyl methanethiosulfonate (MMTS) was used. Both estradiol binding and TAZ covalent attachment assays were performed with cytosolic extracts containing either wild-type (WT)-ER or C530A-ER in the presence or absence of MMTS. Although reversible estradiol binding was not reduced significantly by the addition of MMTS, covalent attachment of the affinity ligand was greatly reduced (Fig. 4), providing evidence that the residue (or residues) being labeled is most likely another cysteine.

Cytosolic extracts containing WT-ER or C530A-ER were also labeled with varying concentrations of KNA to see if there were any differences in labeling efficiency that might be observable at low KNA concentrations. We found no differences in KNA labeling curves between WT-ER and C530A-ER, with 20, 50, and 90% of receptors covalently labeled at 10, 25, and 40 nM [^{3}H]KNA, respectively (data not shown), suggesting that the alternate site(s) of labeling in C530A ER is quite similar in reactivity to the C530 residue in WT-ER.

Transcriptional Activation Properties of Mutant Receptors—The transactivating abilities of the mutant and wild-type receptors were studied by measuring CAT activity in CHO cells cotransfected with pRER, the ER expression plasmid, and the estrogen-responsive reporter gene $(ERE)_2$-TATA-CAT. The data in Fig. 5 indicate that the wild-type receptor was sensitive to low levels of E_2. The dose-response curve for wild-type ER shows that maximal response was achieved at 10^{-10} M E_2, and half-maximal response occurred at 6×10^{-12} M E_2 (Fig. 5 and Table I). Cells transfected with wild-type ER and the reporter plasmid, but not treated with E_2, showed a measurable but low level of transcription (Fig. 5) which could

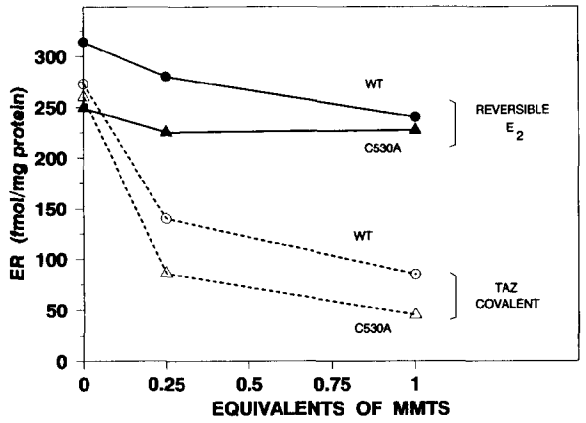


FIG. 4. **Effects of the cysteine-specific blocker MMTS on reversible [^{3}H]E_2 binding and [^{3}H]TAZ covalent labeling.** ER content in cytosols was determined by [^{3}H]E_2 binding from cells transfected with the expression vector for wild-type or C530A ER or by the [^{3}H]TAZ covalent filter assay after the incubation of cytosols with tritiated ligand ± 200-fold excess of E_2 in the presence of increasing concentrations of MMTS. Total —SH group content of the cytosols was determined using the reagent 5,5′-dithiobis(2-nitrobenzoic acid).

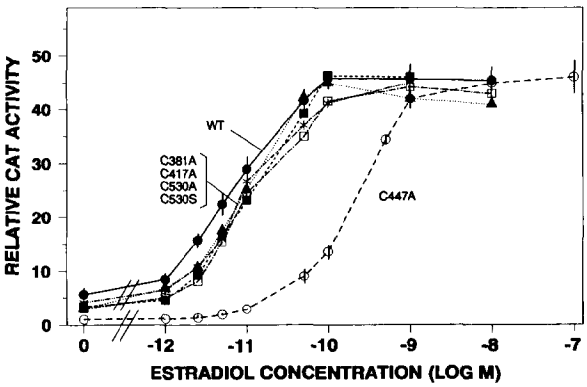


FIG. 5. **Transactivation profiles of mutant and wild-type receptors in response to estradiol.** CHO cells were cotransfected with 5 ng of pRER containing wild-type or mutant ER cDNA and with 0.8 μg of the estrogen-responsive reporter plasmid pATC-2, which contains two perfect EREs and a TATA box linked to the bacterial chloramphenicol acetyltransferase gene. Transfection efficiencies were corrected for by β-galactosidase activity as described under "Experimental Procedures." After transfection the cells were incubated with increasing concentrations of E_2 for 48 h and then harvested. Transactivation was measured as an increase in CAT enzyme activity in the extracts from the cells. Relative CAT activity is the activity in cells transfected with pATC-2 and pRER compared with cells transfected with pATC-2 in the absence of pRER which is set at a value of 1. Points are the mean values from at least four independent transfections. *Error bars* represent S.E. values of the points and are shown for the WT (●) and C447A (○) curves. *Error bars* were omitted from the other curves because of the closeness of these curves, but the S.E. values of the points for the mutants C381A (■), C417A (▲), C530A (*), and C530S (□) were similar to the wild-type and the C447A mutant ERs.

be suppressed by antiestrogens (not shown). This suggests that low levels of estrogen are still present even in charcoal-stripped serum.

The ER mutants C381A, C417A, C530A, and C530S (Fig. 5) showed dose responses that were less than 2-fold different from wild type, achieving maximal response at 10^{-10} M E_2, as observed for wild-type ER, and showing half-maximal responses at concentrations of 7×10^{-12}–1×10^{-11} M E_2. In contrast, the C447A mutant displayed a significant dose-response shift. In this mutant, there was a 50-fold increase in the half-maximal E_2 concentration needed for transcription activation as monitored by CAT activity (Fig. 5); the half-maximal response required 3×10^{-10} M E_2. Since the affinity of this mutant receptor for estradiol binding is only slightly different from wild-type ER (Table I), the data suggest that the C447A mutant receptor is altered in a receptor function other than ligand binding. Similar E_2 dose-response shifts as displayed by the C447A mutant with the $(ERE)_2$-TATA-CAT reporter were also observed when another reporter plasmid (ERE-vit-CAT) was used (33) with the C447A ER, suggesting that this is not a promoter-specific phenomenon.

The ligand structural specificity of these mutant receptors was examined by studying the ability of various estrogenic compounds to stimulate CAT activity. All receptors could stimulate CAT activity in response to estrone, estriol, diethylstilbestrol, and hexestrol, to a level comparable to that achieved with estradiol (data not shown). With the C447A mutant, dose-response studies with hexestrol revealed a 50 × dose-response shift similar to that seen using estradiol (data not shown), indicating that the structurally dissimilar estrogenic compound hexestrol was also a much less effective estrogen agonist in this mutant.

Effect of Antiestrogens on Transcriptional Activation Stimulated by Estrogen—The estradiol-induced transcription by wild-type and mutant receptors could be reversed by antiestrogens. Cells transfected with wild-type or mutant receptors were treated with the lowest maximally stimulatory concentration of E_2 (10^{-10} M for all ERs except C447A, for which 10^{-8} M E_2 was used) and increasing concentrations of the antiestrogens LY 117018, *trans*-hydroxy-tamoxifen, or ICI164,384. The three antiestrogens suppressed estradiol-stimulated CAT activity of all receptor mutants. For each antiestrogen, a similar molar excess of that antiestrogen (relative to E_2) was needed to achieve equal suppression of E_2-stimulated CAT activity (Fig. 6). This indicates that compared to E_2, the antiestrogens were equally less effective as estradiol antagonists in the C447A mutant and, thus, this mutant ER shows a similar (*ca.* 50 ×) dose-response shift for antiestrogen suppression of transcription. It is of note that of the three antiestrogens, ICI164,384 appeared to be the least potent E_2 antagonist despite a good affinity for ER in cell-free extracts (34). This likely reflects the greater difficulty of ICI164,384 in penetrating into intact cells (35).

Effectiveness of TAZ and KNA in Transcriptional Regulation in the C530A and C530S ER Mutants—It appears that the C530A and C530S mutants are covalently labeled by TAZ and KNA at a residue other than C530, probably another cysteine. We postulated that covalent attachment at another site might result in differences in TAZ-inhibited transcription or KNA-activated transcription. Indeed, we have observed that TAZ inhibition of transcription was different between WT and C530A and C530S receptors (Fig. 7). E_2-stimulated transcription was inhibited by TAZ for all three receptors, but TAZ was less effective in inhibiting E_2-stimulated transcription by the C530A and C530S ER compared with wild-type ER. Approximately 10-fold higher TAZ concentrations were required to achieve the same level of suppression as achieved in the wild-type receptor (Fig. 7).

The agonist affinity label KNA was able to stimulate CAT activity by wild-type ER, although only weakly relative to the level stimulated by estradiol (*i.e.* 10–15% of E_2 stimulation). Interestingly, KNA displayed a higher level of activity in the C530A and C530S mutants (Fig. 8), stimulating CAT activity to levels 3–4-fold higher than the wild-type receptor (approximately 50% of E_2-stimulated response). The enhanced effec-

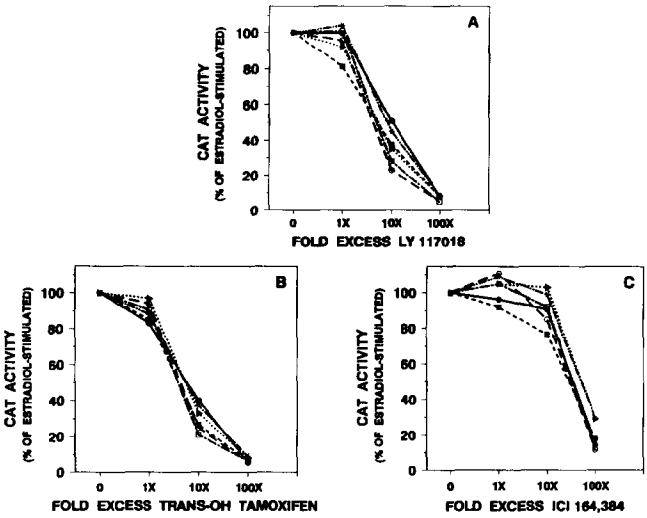


FIG. 6. **The ability of the antiestrogens LY 117018 (*panel A*), *trans*-hydroxytamoxifen (*panel B*), and ICI164,384 (*panel C*) to suppress E_2-stimulated transcription.** CHO cells were cotransfected with pATC-2 and the expression vector for the wild-type, C530A, C530S, C318A, C417A, and C447A ER. The cells were treated for 48 h with the lowest maximally stimulatory concentration of E_2 (10^{-10} M for all receptors except C447A, for which 10^{-8} M E_2 was used) ± the indicated fold excesses of the antiestrogen. CAT activity was then measured. 100% activity is defined as the CAT activity of the cells treated with E_2 alone. It should be noted that C447A is assayed with 10^{-8} M E_2 (the lowest maximally stimulatory concentration of E_2) and that antiestrogen ratios for the C447A receptor are relative to the agonist ligand at 10^{-8} M. The symbols used to designate the wild-type and mutant receptors are the same as in Fig. 5.

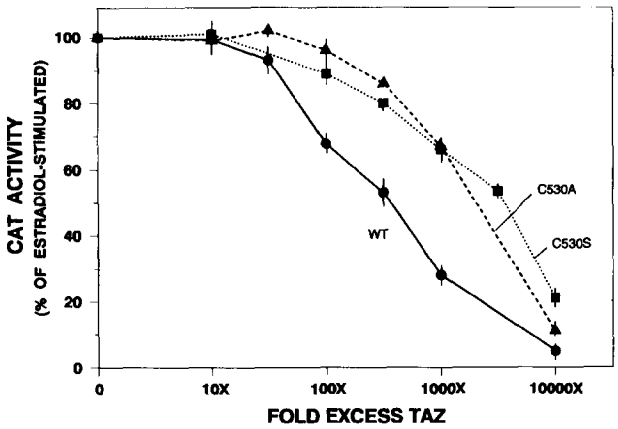


FIG. 7. **The effectiveness of TAZ in suppressing E_2-stimulated transcription.** CHO cells were cotransfected with pATC-2 and the expression vector for the wild-type, C530A, or C530S ER. The cells were treated for 48 h with 10^{-10} M estradiol ± the indicated fold excesses of TAZ. CAT activity in these cells was measured. 100% activity is defined as the CAT activity of the cells treated with E_2 alone. *Points* represent the mean of at least three independent transfections, and *error bars* represent the S.E. of these values.

tiveness of KNA in the C530A and C530S *versus* wild-type ER was also seen when using a different estrogen-responsive reporter plasmid, ERE-vit-CAT, which contains a different promoter (data not shown).

DISCUSSION

The cloning of the ER from various species and the determination of its domain structure have allowed insight into the functioning of this steroid receptor as a ligand-activated

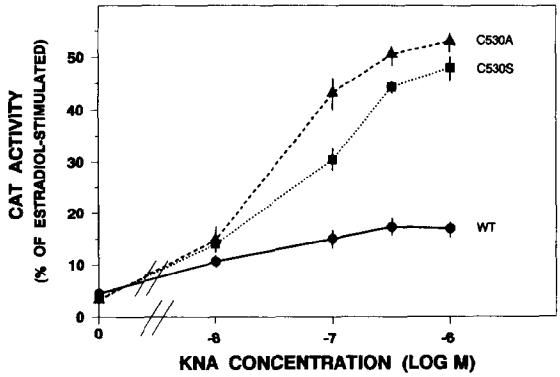


FIG. 8. **The ability of KNA to stimulate CAT activity.** Cells were cotransfected with pATC-2 and the expression vector for wild-type, C530A, or C530S ER and were treated with increasing concentrations of KNA for 48 h. Data are expressed as percent of CAT activity relative to cells treated with 10^{-10} M estradiol, which is considered 100%.

transcriptional regulator (for review see Ref. 2). The DNA binding domain of this and other steroid receptors has been studied extensively through deletion and amino acid replacement analysis (2). The hormone binding domain of these receptors has been more difficult to study because of its complexity and large size. The HBD of the human ER is the largest of the receptor's six proposed domains (12), spanning 251 amino acids. The HBD contains the ligand binding (12), dimerization (5, 36), nuclear localization (12), and hormone-dependent transactivating functions of the receptor (37, 38). Studies to date have introduced large deletions into this region of the ER, and a more detailed analysis is necessary to determine the amino acids critical for various receptor functions. Our study has provided a more refined analysis of this region. We have focused in particular on the role of cysteines in the HBD in the functioning of the ER since our previous studies identified Cys^{530} as the site of covalent attachment of two affinity labeling ligands (14) and because studies on other steroid receptors have implicated cysteines in the HBD as important in ligand binding and receptor activation (15–18).

The data presented here point to two major findings. The first is that receptors (such as C447A) displaying binding affinities for E_2 quite similar to wild-type ER can show marked alteration in the ability of E_2 to induce transcription activation by these receptors, suggesting a "decoupling" of the receptor binding and transactivation functions. The second finding is that although Cys^{530} is covalently labeled by TAZ and KNA in native ER (14), an alternate residue is labeled in the Cys^{530} mutants, most likely a different cysteine in the HBD. Changing the cysteine to an alanine or serine at position 530 alters the transcriptional effectiveness of the affinity labeling ligands TAZ and KNA, reducing the potency of the antiestrogen TAZ and increasing the activity of the estrogenic KNA. Interestingly, however, the effectiveness of reversibly binding estrogenic and antiestrogenic ligands is not affected in these C530A and C530S mutant ERs.

Effects of Mutation of Cysteine 530 on ER Function: Efficacy of Covalently Attaching Versus Reversibly Binding Ligands—Mutation of cysteine 530 to an alanine or serine residue resulted in receptors that showed differences in the efficacy and bioactivity of covalently attaching *versus* reversibly binding ligands. Studies on the covalent attachment site of steroid receptors through the use of covalently attaching affinity ligands have mapped the covalent attachment site to the carboxyl terminus of the protein. In the case of the glucocorticoid receptor affinity ligand dexamethasone mesylate, the

site of covalent attachment has been identified as Cys^{656} of the rat glucocorticoid receptor (Cys^{644} in human) (15). Other reports suggest that sulfhydryl groups are closely associated with hormone binding. Miller and Simons (16) found that blocking sulhydryl groups with the cysteine-specific reagent MMTS caused a reduction in binding of dexamethasone mesylate to glucocorticoid receptor. They postulated that two sulfhydryl groups may play a role in binding and receptor structure. Cys^{530} has been identified as the site of covalent attachment of the ER-specific affinity labels KNA and TAZ (14). This is the fourth, and most carboxyl-terminal, of the cysteines in the HBD of ER. Similar studies conducted on the rat uterine and MCF-7 ER have shown that incubating receptor preparations with low levels of MMTS blocked covalent attachment by TAZ without affecting E_2 binding (14).

Since the binding of estradiol and the affinity labels TAZ and KNA is mutually competitive, it is likely that Cys^{530} is positioned close to or is within the region of receptor that interacts with ligands, the hormone binding pocket. Thus, one might expect that mutational changes at or near this amino acid would affect hormone binding, provided that these changes were substantial enough. Thus, in a study of the mouse ER, Fawell *et al.* (13) demonstrated that estradiol binding was abolished when amino acids 507–538 were deleted. (These are analogous to amino acids 511–534 in human ER.) By contrast, the same group recently replaced Cys^{534} (equivalent to Cys^{530} in the human) with an alanine residue; this single substitution had no effect on estradiol binding (36). We have found that simple substitution of Cys^{530} with alanine or serine has minimal effect on hormone binding.

We did not expect that the C530A mutant would be covalently labeled by the affinity ligands TAZ and KNA, since the nucleophilic cysteine is replaced by a nonnucleophilic alanine residue. However, C530A ER is labeled with TAZ and KNA, as well as is wild-type ER. We presume that TAZ and KNA are labeling C530A ER at an alternate site(s), most likely another cysteine, because the cysteine-specific blocker MMTS, which abolishes covalent attachment but not reversible binding in wild-type ER, does the same with the C530A mutant. We also presume that this alternate site of labeling is in or near the binding pocket of the HBD because labeling with TAZ and KNA is blocked competitively by E_2.

The C530S mutant was prepared to investigate to what degree reaction of TAZ and KNA with the residue at 530 resulted from the inherent nucleophilicity of the residue *versus* its spatial location. If the reactivity factor is the more significant, then the reaction with S530 should not take place whereas if location (that is, the spatial positioning of the reactive aziridine function in TAZ relative to residue 530) were of major importance, then some reaction with the isostructural serine (serine is the oxygen analog of cysteine) might still occur, albeit at a slower rate. The fact that MMTS suppresses TAZ labeling in both C530A and C530S receptors and that these mutants showed nearly identical changes in the potencies of TAZ and KNA in transcriptional repression or stimulation, respectively, suggests that attachment at an alternate cysteine also occurs in the C530S mutant. This suggests that the reactivity of the site is the major determinant.

The mutational changes at 530 (C530A and C530S) have an interesting complementary effect on the potency of *covalently* reacting ligands (TAZ and KNA) *versus reversibly* binding ligands (*trans*-hydroxytamoxifen, E_2, and hexestrol) in terms of the transactivation response measured by alteration of CAT activity. The potency of the covalently reacting antagonist TAZ is reduced; it is 10-fold less potent in suppressing E_2-stimulated CAT activity in the C530A and C530S mutants than in wild-type ER. The reversibly binding antiestrogens (LY117018, ICI164,384, or *trans*-hydroxytamoxifen), however, are equally effective at suppressing CAT activity by both the WT and the Cys^{530} mutants, indicating that this effect is specific for the affinity labeling antagonist TAZ but not other reversibly binding antiestrogens.

With the covalently reacting agonist KNA the effect appears to be in the activity level observed in the Cys^{530} mutants. Although KNA is equally effective as an agonist in wild-type and some receptor mutants, with C530A and C530S ER, KNA stimulated CAT activity to levels 3–4-fold higher than the other receptor types (Fig. 8). The structurally related reversible agonist hexestrol, the compound from which KNA was derived, on the other hand, was equally effective among these three receptors (data not shown). Thus, mutational changes at Cys^{530} which would obviate covalent attachment of the covalently reacting ligands TAZ and KNA at this site (and direct their reaction to a cysteine elsewhere, see above), have a major effect on the potency of the antagonist (decreases 10-fold) and the activity of the agonist (increases 3–4-fold) whereas these mutational changes have no effect on the reversibly binding analogs of these affinity labels. Thus, the potency and activity of these affinity labels in wild-type ER are influenced by their covalent attachment to Cys^{530}.

Effect of Mutation of Cys^{381}, Cys^{417}, and Cys^{447} on ER Functioning: Transactivation Activity—Since the HBD of the receptor contains a hormone-activated transcription activation function (37, 38), it is possible that mutations in this region might have a differential effect, allowing maintenance of hormone binding but producing a reduction in efficiency of transactivation. Although C381A and C417A appear relatively normal, both in terms of ligand binding and transactivation, the C447A receptor appears to be a differential mutant in which E_2 binds with only very slightly (about 2 ×) reduced affinity whereas transactivation activity is greatly reduced (about 50 ×). The shift in the dose response for CAT activity for the C447A mutant was also seen in the effectiveness of the structurally dissimilar ligands LY 117018, ICI164,384, *trans*-hydroxytamoxifen, and hexestrol (Fig. 6 and data not shown). Since the marked reduction in the transactivating effectiveness of these ligands does not reflect altered receptor-ligand binding, this points to possible alterations in the receptor's effectiveness at stages beyond ligand binding, *i.e.* DNA (estrogen response element) binding or interaction with elements of the transcriptional machinery. Studies examining the ability of ER to sequester transcription factors have revealed that the HBD of the receptor is necessary for its ability to compete for these factors (6). In future studies our efforts will be directed toward determining the changes in the C447A mutant functioning which underlie its reduced hormone-dependent transcriptional activation activity. Of interest, two mutations in the mouse ER HBD have been created which impair the receptor's ability to dimerize (36), but the transactivating abilities of these mutants are unknown.

Quantitative Aspects of and Decoupling between Ligand Binding and Hormone-stimulated Transcriptional Activation—It is of note that different concentrations of E_2 are required for half-maximal hormone binding ($K_d \sim 5 \times 10^{-10}$ M) and half-maximal stimulation of transactivation by cotransfection studies using the hormone-responsive reporter plasmids, either $(ERE)_2$-TATA-CAT or ERE-vit-CAT (half-maximal = $\sim 5 \times 10^{-12}$ M). This plus the observation that we need only low levels of receptor for full CAT activity (see "Experimental Procedures") suggest that certain factors that mediate transactivation may be present in very limiting

amounts such that only a small fraction of receptor occupied by ligand may be needed to tie up these limiting factors. In the C447A mutant, in which approximately 50 × more E_2 is needed for maximal transactivation response, it is possible that the interaction between the ligand-occupied mutant receptor and this limiting transcription factor(s) is similarly reduced by a factor of about 50. Such a reduction in affinity of the receptor for transcription factor(s) would require 50 × more of this receptor to be occupied to achieve maximal response. Several studies have shown that ligand binding alters the conformation of receptor such that receptor is able to interact effectively with transactivating or mediating factors (2, 6), and C447A may represent a mutant that has a less favorable conformation for interaction with transcription factors.

To our knowledge, this is the first report of a point mutation in the HBD of a steroid receptor which causes an alteration in transactivation, while such a receptor retains normal, relatively unaltered affinity for ligand. In both the chick progesterone receptor (39) and the v-erbA protein (40), point mutations in the "hinge" region between the DNA and hormone binding receptor domains have been identified which render these receptors unable to activate transcription efficiently while retaining their ability to bind ligand. Characterizing the C447A ER mutant further in terms of its DNA and chromatin interaction should provide a better understanding of how the receptor transduces a hormonal signal into a transcriptional regulator.

Acknowledgements—We are very grateful to Dr. Geoffrey L. Greene for providing the hER cDNA and Abbott Laboratories for providing the ER monoclonal antibodies; Dr. Byron Kemper for the vector pTZ19R, the phage M13K07, and the bacterial strain CJ236; and Dr. David Shapiro for allowing us the use of the vectors ERE-vit-CAT and $(ERE)_2$-TATA-CAT.

REFERENCES

1. Katzenellenbogen, B. S., Miller, M. A., Mullick, A., and Sheen, Y. Y. (1985) *Breast Cancer Res. Treat.* **5,** 231–243
2. Beato, M. (1989) *Cell* **56,** 6335–6344
3. Katzenellenbogen, B. S., Miller, M. A., Eckert, R. L., and Sudo, K. (1983) *J. Steroid Biochem.* **19,** 59–68
4. Thompson, E. W., Katz, D., Shima, T. B., Wakeling, A. E., Lippman, M. E., and Dickson, R. B. (1989) *Cancer Res.* **49,** 6929–6934
5. Kumar, V., and Chambon, P. (1988) *Cell* **55,** 145–156
6. Meyer, M. E., Gronemeyer, H., Turcotte, B., Bocquel, M. T., Tasset, D., and Chambon, P. (1989) *Cell* **57,** 433–442
7. Greene, G. L., Gilna, P., Waterfield, M., Baker, A., Hort, Y., and Shine, J. (1986) *Science* **231,** 11150–11154
8. Elliston, J. F., Zablocki, J. A., Katzenellenbogen, B. S., and Katzenellenbogen, J. A. (1987) *Endocrinology* **121,** 667–676
9. Katzenellenbogen, J. A., Carlson, K. E., Heiman, D. F., Robertson, D. W., Wei, L. L., and Katzenellenbogen, B. S. (1983) *J. Biol. Chem.* **258,** 3487–3495
10. Katzenellenbogen, B. S., Elliston, J. F., Monsma, F. J., Jr., Springer, P. A., Ziegler, Y. S., and Greene, G. L. (1987) *Biochemistry* **26,** 2364–2373
11. Greene, G. L., Sobel, N. B., King, W. J., and Jensen, E. V. (1984) *J. Steroid Biochem.* **20,** 51–56
12. Kumar, V., Green, S., Staub, A., and Chambon, P. (1986) *EMBO J.* **5,** 2231–2236
13. Fawell, S. E., Lees, J. A., and Parker, M. G. (1989) *Molec. Endocrinol.* **3,** 1002–1005
14. Harlow, K. W., Smith, D. N., Katzenellenbogen, J. A., Greene, G. L., and Katzenellenbogen, B. S. (1989) *J. Biol. Chem.* **264,** 17476–17485
15. Simons, S. S., Jr., Pumprey, J. G., Rudikoff, S., and Eisen, H. J. (1987) *J. Biol. Chem.* **262,** 9676–9680
16. Miller, N. R., and Simons, S. S., Jr. (1988) *J. Biol. Chem.* **263,** 15217–15225
17. Meshinchi, S., Matić, G., Hutchison, K. A., and Pratt, W. B. (1990) *J. Biol. Chem.* **265,** 11643–11649
18. Silva, C. M., and Cidlowski, J. A. (1989) *J. Biol. Chem.* **264,** 6638–6647
19. Chen, C., and Okayama, H. (1987) *Mol. Cell. Biol.* **7,** 2745–2752
20. Maniatis, T., Fritsch, E. F., and Sambrook, J. (1982) *Molecular Cloning: A Laboratory Manual,* Cold Spring Harbor Laboratory, Cold Spring Harbor, NY
21. Mead, D. A., Szczesna-Skorupa, E., and Kemper, B. (1986) *Protein Eng.* **1,** 67–74
22. Tora, L., Mullick, A., Metzger, D., Ponglikitmongkol, M., Park, I., and Chambon, P. (1989) *EMBO J.* **8,** 1981–1986
23. Chang, T.-C., and Shapiro, D. J. (1990) *J. Biol. Chem.* **265,** 8176–8182
24. Kunkel, T. A. (1985) *Proc. Natl. Acad. Sci. U. S. A.* **82,** 488–492
25. Herbomel, P., Bourachot, B., and Yaniv, M. (1984) *Cell* **39,** 653–662
26. Gorman, C. M., Moffat, L. F., and Howard, B. H. (1982) *Mol. Cell. Biol.* **2,** 1044–1051
27. Scatchard, G. (1949) *Ann. N. Y. Acad. Sci.* **51,** 660–672
28. Gilmour, D. S., and Lis, J. T. (1985) *Mol. Cell. Biol.* **5,** 2009–2018
29. Wrenn, C. K., and Katzenellenbogen, B. S. (1990) *Mol. Endocrinol.* **4,** 1647–1654
30. Miller, M. A., Lippman, M. E., and Katzenellenbogen, B. S. (1984) *Cancer Res.* **44,** 5038–5045
31. Golding, T. S., and Korach, K. S. (1988) *Proc. Natl. Acad. Sci. U. S. A.* **85,** 69–73
32. Katzenellenbogen, B. S., Pavlik, E. J., Robertson, D. W., and Katzenellenbogen, J. A. (1981) *J. Biol. Chem.* **256,** 2908–2915
33. Reese, J. C., and Katzenellenbogen, B. S. (1990) *Endocrinology* **126,** (suppl.) 96 (Abstr. 287)
34. Wakeling, A. E., and Bowler, J. (1987) *J. Endocrinol.* **112,** R7–R10
35. Poulin, R., Merand, Y., Poirier, D., Levesque, C., Dufour, J. M., and Labrie, F. (1989) *Breast Cancer Res. Treat.* **14,** 65–76
36. Fawell, S. E., Lees, J. A., White, R., and Parker, M. (1990) *Cell* **60,** 953–962
37. Webster, N. J. G., Green, S., and Jin, J. R. (1988) *Cell* **54,** 199–207
38. Tora, L., White, J., Brou, C., Tasset, D., Webster, N., Scheer, E., and Chambon, P. (1989) *Cell* **59,** 477–487
39. Dobson, A. D. W., Conneely, O. M., Beattie, W., Maxwell, B. L., Mak, P., Tsai, M-J., Schrader, W. T., and O'Malley, B. W. (1989) *J. Biol. Chem.* **264,** 4207–4212
40. Monuz, A., Zenke, M., Gehring, U., Sap, J., Berg, H., and Vennstrom, B. (1988) *EMBO J.* **7,** 151–159

Endometrial Cancer in Tamoxifen-Treated Breast Cancer Patients: Findings From the National Surgical Adjuvant Breast and Bowel Project (NSABP) B-14*

*Bernard Fisher, Joseph P. Costantino, Carol K. Redmond, Edwin R. Fisher, D. Lawrence Wickerham, Walter M. Cronin, Other NSABP Contributors***

Background: Tamoxifen is advantageous in treating all stages of breast cancer. However, studies have suggested that incidence and severity of endometrial cancer increase in women treated with tamoxifen. *Purpose:* We compared rates of endometrial and other cancers in tamoxifen- and non–tamoxifen-treated patients and described the pathologic characteristics of the endometrial cancers. *Methods:* Data were analyzed on 2843 patients with node-negative, estrogen receptor-positive, invasive breast cancer randomly assigned to placebo or tamoxifen (20 mg/d) and on 1220 tamoxifen-treated patients registered in NSABP B-14 subsequent to randomization. Average time on study is 8 years for randomly assigned patients and 5 years for registered patients. *Results:* The incidence rates of liver, gastrointestinal, urinary tract, and nonuterine genital tumors were not increased by tamoxifen treatment. Twenty-five endometrial cancers were originally reported, one of which was reclassified after subsequent review. Two cases occurred in the placebo group in patients whose medical status subsequent to random assignment had required tamoxifen treatment. Twenty-three occurred in the tamoxifen groups. Twenty-one of the 24 originally reported endometrial cancers were FIGO stage 1; 18 of 23 gradable cases were of good to moderate histologic grade. Four tamoxifen-treated women died of uterine cancer. The average annual hazard rate of endometrial cancer as a first event within the first 5 years of follow-up in the randomized, tamoxifen-treated group was 1.2/1000 patient-years; the cumulative hazard rate was 6.3/1000. Findings for the registered, tamoxifen-treated group were similar. Including all originally reported endometrial cancers, the annual hazard rate through all follow-up was 0.2/1000 in the placebo group and 1.6/1000 in the randomized, tamoxifen-treated group; the relative risk of endometrial cancer for the latter versus the former group was 7.5. Again for the latter group, using population-based rates of endometrial cancer from SEER data and information from another NSABP (B-06) trial, relative risks were 2.2 and 2.3, respectively. The 5-year cumulative hazard rate for disease-free survival in the randomized tamoxifen group was 38% less than that in the placebo group. Some data in this paper were provided by an investigator who submitted fraudulent data to the NSABP [*see* the "News" section]; therefore, the reader must read the entire text including Table 10 and the Editor's notes. In brief, data on 182 of the 2843 randomly assigned patients and 37 of the 1220 registered patients were provided by the investigator in question. After review, 24 of the 182 records showed falsification, all involving characteristics of patients prior to random assignment. Of the 37 registered-patient records, 8 showed falsification. *Conclusions:* Risk of endometrial cancer increases following tamoxifen therapy for invasive breast cancer; however, net benefit greatly outweighs risk. Endometrial cancers occurring after tamoxifen therapy do not appear to be of a different type with a worse prognosis than are such tumors in non–tamoxifen-treated patients. *Implications:* Tamoxifen treatment for breast cancer should continue. In addition, the relative risk of endometrial cancer observed in B-14 tamoxifen-treated patients is consistent with the twofold relative risk used in the initial risk–benefit computation for the NSABP breast cancer prevention trial.
[J Natl Cancer Inst 86:527-537, 1994]

*Editor's note: The investigators indicate that "irrespective of the data provided by St. Lucs [Hôpital Saint-Luc, Montreal, Quebec, Canada, an NSABP B-14 participating institution whose data are in dispute], the conclusions remain the same in this paper. The actual numbers of patients and endometrial cancers reported by St. Lucs are as follows: 0 endometrial cancers among 88 patients in the placebo group, 1 endometrial cancer among 94 patients in the randomized, tamoxifen-treated group, and 1 endometrial cancer among 37 patients in the registered, tamoxifen-treated group." At the time this manuscript went to press, both women were alive, with no indication of relapse of endometrial cancer. (Four patients from Hôpital Saint-Luc, none of whom developed endometrial cancer, were excluded from analyses in this paper. They were among the ineligible patients always excluded from B-14 analyses.)

**Affiliations of authors:* B. Fisher, D. L. Wickerham (Department of Surgery), J. P. Costantino, C. K. Redmond, W. M. Cronin (Department of Biostatistics), University of Pittsburgh, Pa.

E. R. Fisher, Shadyside Hospital, Pittsburgh.

Other NSABP Contributors, *see* "Notes."

Correspondence to: Bernard Fisher, M.D., Department of Surgery, University of Pittsburgh Medical Center, Pittsburgh, PA 15261.

Reprint requests to: The National Surgical Adjuvant Breast and Bowel Project (NSABP) Headquarters, Rm. 914, Scaife Hall, 3550 Terrace St., Pittsburgh, PA 15261.

See "Notes" section following "References."

Downloaded from http://jnci.oxfordjournals.org/ at Reprints Desk on July 6, 2016

Tamoxifen, a nonsteroidal antiestrogen, has been used in the treatment of breast cancer since the early 1970s (*1*). Subsequent to its proven efficacy for advanced disease, the drug was employed as adjuvant treatment for the management of primary operable breast cancer; it is now the most widely used hormonal therapy for that disease. More than 3 million breast cancer patients have received tamoxifen (*2*) for greater than 5.8 million patient-years. Although the drug has demonstrated a benefit in the treatment of all stages of breast cancer, various adverse effects from tamoxifen therapy have been reported (*3*).

There has been speculation as to whether or not there is an increase in second primary cancers exclusive of those in the ipsilateral or contralateral breast as a result of tamoxifen administration. Such events could have particular clinical significance should they appear with frequency in low-risk patients with stage I disease or in clinical trials evaluating the worth of tamoxifen as a breast cancer preventive agent in women at increased risk for the disease. Because the presence of second primary cancers in either of these circumstances could significantly reduce the net benefit from tamoxifen therapy, knowledge about the frequency of second primary tumors is important.

In 1989 the National Surgical Adjuvant Breast and Bowel Project (NSABP) reported initial findings from a randomized clinical trial (B-14) involving 2843 patients with primary operable estrogen receptor (ER)-positive breast cancers and negative axillary lymph nodes, who were randomly assigned to receive either placebo or tamoxifen (20 mg/d) (*4,5*). Results from that study indicated a benefit from tamoxifen and a reduction in the incidence of breast cancer recurrence, cancer in the opposite breast, and mortality. Because B-14 included a placebo group, the trial provided an opportunity to obtain information likely to be more indicative of the frequency of second primary cancers and of other adverse effects attributed to tamoxifen than could have been obtained from retrospective reports or from clinical trials in which patients and physicians were aware of whether or not tamoxifen was administered. Information relative to the association between tamoxifen and endometrial cancer has been derived mainly from approximately 100 cases described in a series of about 25 reports (*6,7*) that appear in the literature subsequent to the 1985 publication by Killackey et al. (*8*), who observed endometrial cancer in three patients on tamoxifen. The heterogeneity of the information in most of these reports precludes attaching much significance to the findings other than to acknowledge that endometrial tumors have occurred in tamoxifen-treated breast cancer patients. Although findings from these noncontrolled studies suggest a possible association, they fail to provide definitive support for such a relationship because of the few cases in any one report and because of the differences in dosage, duration of therapy, follow-up time, stage of breast cancer, and other variables. This series of reports also includes findings from four randomized studies in which 30 postmenopausal patients treated with adjuvant tamoxifen for primary breast cancer developed endometrial tumors (*9-13*). Although in two of the trials (*9,10,13*) the cumulative frequency of endometrial cancer was found to be greater for tamoxifen-treated patients than for non–tamoxifen-treated controls, in two other studies (*11,14*) no increase in endometrial tumors was noted. Because many of the same shortcomings inherent in the noncontrolled studies are also evident in these four trials, additional information is needed to address the issues related to the association between tamoxifen and endometrial cancer. One issue that requires prompt resolution relates to the thesis that tamoxifen-treated patients are at greater risk for high-grade endometrial cancers with a poorer prognosis than are those who do not receive the drug (*15*).

This article presents information about rates of occurrence of endometrial, liver, gastrointestinal, urinary tract, and nonuterine genital cancers following tamoxifen therapy, discusses findings obtained when those rates were compared with the frequency of such tumors in non–tamoxifen-treated patients, and describes the pathologic characteristics of the endometrial cancers that occurred. It also considers the significance of the findings for the use of tamoxifen in both the treatment of breast cancer patients and in the NSABP Breast Cancer Prevention Trial (BCPT), which is currently being conducted to evaluate the worth of tamoxifen as a preventive agent.

Methods

Between January 1982 and January 1988, 2843 patients at NSABP-participating institutions in Canada and the United States were entered into a randomized clinical trial (protocol B-14) to evaluate the worth of postoperative tamoxifen therapy in women with ER-positive (ER ≥10 fmol/mg cytosol protein), invasive breast cancer and histologically negative axillary lymph nodes. After patients had undergone either lumpectomy followed by breast irradiation or total mastectomy and had given informed consent, they were stratified according to age, tumor size at clinical examination, type of surgery, and tumor ER level. They were then randomly assigned to receive either tamoxifen therapy (Nolvadex; Zeneca Pharmaceuticals, Wilmington, Del.) or placebo for 5 years. Neither patients nor their physicians were aware of the treatment assignment. Women who had completed the initially assigned tamoxifen therapy for 5 years were offered the option to be reassigned randomly to either tamoxifen or placebo for 5 more years. Women who had received 5 years of placebo discontinued that agent, and their follow-up was continued in accordance with protocol requirements. Details of stratification, randomization, tumor ER and progesterone receptor analyses, surgical procedures, and statistical analyses have been presented in reports of the overall findings of the studies (*4,5*). Immediately after completion of patient accrual in the randomized part of the trial, and until October 1988, an additional 1220 women with eligibility criteria identical to those in the randomized study were *registered.* All were to receive tamoxifen for 5 years, then were to be randomly assigned to receive an additional 5 years of tamoxifen or placebo. This method increased the patient population for randomization to compare the worth of 5 years with that of 10 years of tamoxifen therapy. The additional tamoxifen-treated patients also contributed information about the relationship between the drug and the occurrence of endometrial cancer.

The 4063 patients used in these analyses were those eligible with follow-up. In the randomized study, there were 1424 patients in the control group and 1419 in the tamoxifen-treated group. Patients were evenly distributed according to age in the two groups. A total of 437 patients (31%) in the placebo group and 440 (31%) in the tamoxifen-treated group were 49 years of age or less; 987 of the patients who received placebo and 979 tamoxifen-treated patients (69% in both groups) were 50 years of age or older. Distribution according to age was similar in the registered patients (31% in the younger group and 69% in the older group). Complete information is available regarding the number of women with hysterectomies at the time they entered the trial, and there is no imbalance in the number in each of the treatment groups. A history of prior hormone replacement therapy was obtained at the time of protocol entry. Specific information regarding the drug(s), dose, duration, recentness of use, and method of delivery is not available for all patients. Follow-up information from patients entered on this trial was to be obtained every 3 months for the first 3 years and every 6 months thereafter. The average time on study was 8 years for the randomly assigned patients and 5 years for the registered patients. The average time at risk for en-

Downloaded from http://jnci.oxfordjournals.org/ at Reprints Desk on July 6, 2016

dometrial cancer was 6.8 years in the randomly assigned patients and 4.6 years in the registered patients.

Slides prepared from paraffin-embedded tissue blocks from 24 of the 25 patients reported by institutional pathologists to have developed endometrial cancer were submitted to the NSABP Pathology Center for review by the headquarters' pathologist (E. R. Fisher). Specimens were masked so that the reviewer was unaware of the patients' treatment. All nuclear grading was carried out by the headquarters' pathologist. In only one patient was there disagreement with findings obtained by the institutional pathologist relative to the diagnosis of an endometrial cancer. That patient, a 68-year-old woman who had received prior hormone replacement therapy, was reported to have developed endometrial cancer after 4 months of tamoxifen therapy. The cancer had been diagnosed by the hospital pathologist from curettings. Headquarters' review demonstrated an endometrial polyp and cervical adenosis, not endometrial cancer. Although no cancer was found in the review, that patient has been included in the analyses related to the incidence of endometrial cancer.

Endometrial cancers were graded and staged using the International Federation of Gynecology and Obstetrics (FIGO) system (*16,17*). In that system, tumors limited to the endometrium are classified as IA; those that have invaded less than one half of the myometrium, IB; and those invading greater than one half of the myometrium, IC. If tumors display endocervical glandular involvement only or cervical stromal invasion, they are classified as IIA and IIB, respectively. Tumors involving the serosa and/or adnexa and those that demonstrate positive peritoneal cytology are classified as IIIA; those with vaginal metastases, IIIB; and those with metastases to pelvic and/or para-aortic lymph nodes, IIIC. Stage IVA consists of tumors that have invaded the bladder and/or bowel mucosa; those with distant metastases, including intra-abdominal or inguinal lymph nodes, are classified as IVB. Histologic grade was dependent on the degree of solid foci of cancer exclusive of squamous cell type and is classified in this report as "1" (good), "2" (moderate), and "3" (poor). Nuclear grade was assessed as has been described by us for breast cancer (*18*) and is designated in this article as "good" or "poor."

The annual risk of endometrial cancer for patients in each of the treatment groups was estimated by the average annual hazard rate, either through the entire period of follow-up or through 5 years of follow-up. Rates were determined for those endometrial cancers that occurred as a first event after initiation of breast cancer therapy and for those that occurred as any event, i.e., as a first event or subsequent to a breast cancer recurrence or to a second primary cancer. The relative risk for endometrial cancer and its 95% confidence intervals were estimated using a proportional hazards model (*19*). Cumulative hazard rates of endometrial cancer were assessed for both the randomized and registered patient groups through 5 years of follow-up (*20*); all cases of endometrial cancer occurred within these periods. Average annual hazard rates and cumulative rates were also calculated individually for breast cancer recurrence, for cancers in the opposite breast, for deaths without evidence of breast cancer, or for second primary cancers occurring at organ sites other than the breast (*21*).

Results

Second Primary Cancers Other Than Cancer in the Opposite Breast

When the sites and incidence rates for second primary cancers occurring as first events subsequent to removal of a breast cancer were determined, there was no evidence to indicate that there was an increased frequency of such tumors at any site except in the uterus. Of particular relevance was the failure to observe any liver cancers or an increase in the incidence of gastrointestinal, urinary tract, or nonuterine genital tumors. Specifically, cancer of the endometrium is the only second primary cancer site that displays a statistically significant increase in tamoxifen-treated patients (Table 1). There are no significant differences between the treatment arms in second cancers of the colon, rectum, ovary, liver, or other site. The remaining data in this section relate to detailed findings for cancer of the endometrium.

Table 1. Incidence and average annual hazard rates of second cancers as a first event in the randomized groups

Site or type of second cancers	Placebo (n = 1424) No. of events	Placebo (n = 1424) Average annual rate/1000	Tamoxifen (n = 1419) No. of events	Tamoxifen (n = 1419) Average annual rate/1000	*P*
Colon and rectum	13	1.6	15	1.7	.88
Colon	10	1.2	11	1.2	.98
Rectum	3	0.4	4	0.4	.79
Endometrium	0	0	15	1.7	<.001
Esophagus	1	0.1	0	0	.30
Kidney	3	0.4	0	0	.07
Leukemia/myeloproliferative disease	2	0.2	3	0.3	.72
Lung	3	0.4	9	1.0	.11
Lymph nodes	0	0	2	0.2	.18
Ovary	3	0.4	2	0.2	.59
Pancreas	2	0.2	0	0	.14
Peritoneum	0	0	2	0.2	.18
Salivary gland	1	0.1	2	0.2	.61
Skin	3	0.4	2	0.2	.59
Stomach	0	0	3	0.3	.10
Thyroid	3	0.4	2	0.2	.59
Urinary bladder	0	0	3	0.3	.10
Other sites	8	1.0	3	0.3	.10
All second primary cancers, excluding cancer in the opposite breast	42	5.1	63	7.0	.10

Placebo Patients

Two of the 1424 patients randomly assigned to the placebo group developed endometrial cancer (Table 2). Both women were in their sixties, and both were receiving tamoxifen at the time their tumors occurred. One woman (patient 1), who had received hormone replacement therapy before developing breast cancer, had a tumor recurrence in the chest wall 28 months after removal of her primary breast cancer. She was then treated for the recurrence with tamoxifen; after 28 months of treatment, she developed a stage IA G1 endometrial cancer. The second placebo patient (patient 2) developed colon cancer 9 months after breast cancer surgery. The physician treating her colon cancer also elected to give her tamoxifen for the breast cancer. After 45 months of tamoxifen therapy, she developed a stage IC G2 endometrial cancer. Both women are alive and tumor free, for 13 and 31 months, respectively, after the diagnosis of endometrial cancer.

Randomly Assigned, Tamoxifen-Treated Patients

Of the 1419 patients randomly assigned to the tamoxifen treatment group, 15 developed endometrial cancer (Table 3). Only one patient (patient 12) was less than 50 years old, and five were in their fifties at treatment randomization. One woman in the group (patient 1), who was 66 years of age, was randomly assigned to receive tamoxifen; however, on the day after randomization, she chose not to accept therapy. Although she consented to be followed in the study, she never received the drug. She developed endometrial cancer 78 months after treatment randomization. Of the 15 patients randomly assigned to receive

Downloaded from http://jnci.oxfordjournals.org/ at Reprints Desk on July 6, 2016

Table 2. Endometrial cancers in breast cancer patients randomly assigned to receive placebo (n = 1424)*

Patient No.	Time, mo: On TAM	Time, mo: Off TAM to diagnosis of EC	Time, mo: Follow-up after diagnosis of EC	Age, y†	Prior hormone replacement therapy	Pathology of EC: Histologic type	Pathology of EC: Histologic grade	Pathology of EC: Nuclear grade	Pathology of EC: FIGO stage‡	Patient status	Cause of death or comment
1	28	0	13	66	Yes	Endometrioid in polyp	Good	Good	IA G1	Alive	NED; TAM given for breast cancer recurrence
2	45	0	31	63	No	Endometrioid, mucinous, and clear cell	Moderate	Poor	IC G2	Alive	NED; TAM given after colon cancer

*TAM = tamoxifen; EC = endometrial cancer; NED = no evidence of disease.

†At entry into the study.

‡"G" classification relates to degree of differentiation of the adenocarcinoma. G1 signifies 5% or less of a nonsquamous or nonmorular solid growth pattern, G2 signifies 6% to 50% of a nonsquamous or nonmorular solid growth pattern, and G3 signifies more than 50% of a nonsquamous or nonmorular solid growth pattern.

Table 3. Endometrial cancers in breast cancer patients randomly assigned to receive tamoxifen (n = 1419)*

Patient No.	Time, mo: On TAM	Time, mo: Off TAM to diagnosis of EC	Time, mo: Follow-up after diagnosis of EC	Age, y†	Prior hormone replacement therapy	Pathology of EC: Histologic type	Pathology of EC: Histologic grade	Pathology of EC: Nuclear grade	Pathology of EC: FIGO stage‡	Patient status	Cause of death or comment
1	0	§	15	66	Yes	Endometrioid	Good	Good	IB G1	Dead	EC, no TAM received
2	5	0	61	68	Yes	Endometrioid (NC)	U	U	IA	Dead	CV disease
3	8	0	125	59	No	Adenosquamous	Poor	UII	IB G3	Alive	BC mets. to ribs and sternum
4	17	0	82	52	No	Endometrioid	Good	Good	IA G1	Alive	NED
5	22	73	11	58	No	Papillary	Poor	Poor	IB G3	Dead	Most likely EC
6	31	0	30	66	No	Mucinous	Good	Good	IB G1	Alive	NED
7	40	0	34	53	No	Endometrioid	Moderate	Good	IA G2	Alive	NED
8	41	0	24	67	No	Endometrioid	Good	Good	IA G1	Alive	NED
9	42	23	5	54	Yes	Carcinosarcoma	Poor	Poor	IIB G3	Dead	EC
10	53	0	51	67	Yes	Endometrioid	Good	Good	IB G1	Alive	NED
11	58	0	18	67	Yes	Endometrioid	Good	Good	IB G1	Alive	NED
12	64	7	0	35	No	Endometrioid (adenomatous and cystic hyperplasia)	Good	Good	IA G1	Alive	NED
13	65	0	0	68	Yes	Papillary	Good	Poor	IVB G1	Dead	EC, pulmonary embolus after hysterectomy
14	66	34	0	62	No	Carcinosarcoma¶	Poor	Poor	IA G3	Alive	NED
15	76	19	2	65	No	Papillary serous	Good	Good	IIIC G1	Alive	NED

*TAM = tamoxifen; EC = endometrial cancer; NC = not cancer on central pathology review; U = unknown; CV = cardiovascular disease; BC mets. = breast cancer metastasis; NED = no evidence of disease.

†At entry into the study.

‡*See* ‡ footnote in Table 2 for explanation of "G" classification.

§78 months after randomization to treatment group.

‖Slide not available for central pathology review. Findings for histologic grade and FIGO stage are those reported by the institution's pathologist.

¶Graded on epithelial component.

tamoxifen, six had received prior hormone replacement therapy (Table 3). In five patients, tamoxifen therapy had been discontinued before their endometrial tumor occurred. The interval between the discontinuation of tamoxifen and the occurrence of an endometrial cancer in those patients varied from 7 to 73 months.

Ten of the 15 patients in the randomized, tamoxifen-treated group who developed endometrial cancer are currently alive. A review of the five deaths in that group revealed that one occurred in the 66-year-old woman (patient 1) who never received tamoxifen. A stage IB G1 endometrial cancer was detected 78 months after the diagnosis of her breast tumor. Biopsies demonstrated peritoneal carcinomatosis of possibly ovarian or pancreatic origin. Because endometrial cancer could not be excluded, her death is considered to have been due to that disease; she died 15 months after the diagnosis of endometrial cancer. The second death occurred in a 68-year-old woman (patient 2), who had received tamoxifen for 5 months, at which time a stage IA endometrial cancer was diagnosed from curettings by the institutional pathologist. After review by the NSABP headquarters' pathologist, the lesion was considered not to be an endometrial cancer. The patient's death was related to cardiovascular disease. The third of the five deaths occurred in a 58-year-old woman (patient 5), who had received tamoxifen for

Downloaded from http://jnci.oxfordjournals.org/ at Reprints Desk on July 6, 2016

22 months and who developed an endometrial cancer 6 years after she discontinued the drug. Her death occurred from extensive metastatic abdominal carcinomatosis, 11 months after the diagnosis. The fourth death occurred in a woman aged 54 (patient 9), who was diagnosed as having carcinosarcoma of the uterus 23 months after she discontinued tamoxifen, which she had taken for 42 months. Her death was the result of that tumor. The fifth death occurred in a 68-year-old woman (patient 13), who had received tamoxifen for 65 months and who died from a pulmonary embolus after hysterectomy. Autopsy demonstrated metastases from an endometrial cancer.

Registered, Tamoxifen-Treated Patients

Of the 1220 registered, tamoxifen-treated patients, eight developed uterine cancer (Table 4). Seven of the eight tumors were endometrioid, and one (in patient 8) was a stromal sarcoma. In seven women, the cancer occurred as a first event and, in the eighth, subsequent to skin cancer. As with the randomly assigned patients, all but one were more than 50 years of age; three were in their fifties and four were older than age 60. One cancer occurred in a woman, aged 44 at treatment randomization; this woman was reported to have ceased menstruating for at least 6 months before diagnosis of the cancer. One woman (patient 4) had received hormone replacement therapy, and three had been on tamoxifen for less than a year (2, 2, and 9 months) when their endometrial cancer occurred.

Seven of the eight patients are currently alive. One (patient 3), aged 63, who received tamoxifen therapy for 9 months, died 28 months after diagnosis of endometrial cancer. During that interval, she was considered to have sepsis as a result of acute diverticulitis. At her death, however, an autopsy revealed metastatic carcinoma consistent with endometrial cancer. Another patient (patient 2), aged 65, is alive, through 44 months of follow-up, with a retroperitoneal mass; a biopsy specimen was taken, and the mass was found to be endometrial cancer.

Summary of Patient and Tumor Characteristics

Only two patients (8%) were less than 50 years of age at the time of diagnosis of their endometrial tumors; in contrast, of the 23 women who were 50 years of age or older at the time of diagnosis, 19 (76%) were 60 years of age or older (Table 5). The mean age ± SE of women at diagnosis of endometrial cancer (64.5 ± 1.7 years) was 4 years greater than their mean age at the time of entry into the B-14 study (60.6 ± 1.6 years).

While the mean time ± SE on tamoxifen therapy was 34.8 ± 4.6 months, six patients received the drug for less than 12 months (0-9 months), and three received it for between 1 year and 2 years. Thus, 36% received tamoxifen for less than 2 years. Hormone replacement therapy was received by 32% of the women at some time prior to diagnosis of their breast cancer. When six patients who had discontinued tamoxifen therapy for from 7 to 73 months before diagnosis of an endometrial cancer were included, the mean time from the beginning of tamoxifen therapy to the diagnosis of endometrial cancer was 41.6 ± 5.9 months. The mean time on study for patients with endometrial cancer was 77.0 ± 4.8 months.

Review by the NSABP headquarters' pathologist of the pathology material from 24 of the endometrial cancers and information regarding the one tumor not reviewed from the tamoxifen-treated group revealed a variety of histologic tumor types (Table 6). Tumors that occurred most frequently were either endometrioid alone (n = 13; 52%) or endometrioid combined with another cell type (n = 4; 16%). The tumor in the patient who did not take tamoxifen was an endometrioid cancer. A summary of the FIGO stage, histologic grade, and nuclear grade of the endometrial cancers revealed that 21 (88%) of the 24 women with endometrial cancers had stage I cancer and that one each had stage II, III, or IV cancer. One tumor was a sarcoma. Of the 23 endometrial cancers with known histologic grade, 18 (78%) were classified as grades 1 and 2 (good and moderate, respectively). Of the 22 endometrial cancers with known nuclear grade, 15 (68%) were classified as good.

Incidence of Endometrial Cancer

The average annual hazard rate (per 1000 women) of endometrial cancer occurring as *any event* (first event or subsequent to another type of first event such as a breast cancer relapse or a second primary cancer) was determined through the entire period of follow-up for both the randomized, placebo and tamoxifen-treated groups. The average annual hazard rate was

Downloaded from http://jnci.oxfordjournals.org/ at Reprints Desk on July 6, 2016

Table 4. Endometrial cancers in breast cancer patients registered to receive tamoxifen (n = 1220)*

	Time, mo					Pathology of EC					
Patient No.	On TAM	Off TAM to diagnosis of EC	Follow-up after diagnosis of EC	Age, y†	Prior hormone replacement therapy	Histologic type	Histologic grade	Nuclear grade	FIGO stage‡	Patient status	Cause of death or comment
1	2	0	56	59	No	Endometrioid	Moderate	Good	IB G2	Alive	NED
2	2	13	44	65	No	Endometrioid	Good	Good	IB G1	Alive	EC mets.
3	9	0	28	63	No	Endometrioid	Moderate	Good	IB G2	Dead	EC
4	22	0	28	68	Yes	Endometrioid and in part, clear-cell	Good	Good	IB G1	Alive	NED
5	27	0	23	67	No	Endometrioid and papillary	Good	Poor	IB G1	Alive	NED
6	43	0	12	58	No	Endometrioid and papillary	Good	Good	IB G1	Alive	NED
7	46	0	9	56	No	Endometrioid	Poor	Poor	IB G3	Alive	NED
8	59	0	1	44	No	Stromal sarcoma, uterus and cervix	NA	NA	NA	Alive	NED

*TAM = tamoxifen; EC = endometrial cancer; NED = no evidence of disease; EC mets. = endometrial metastasis; NA = not applicable.
†At entry into the study.
‡*See* ‡ footnote in Table 2 for explanation of "G" classification.

Table 5. Characteristics of patients with endometrial cancers (n = 25)

Characteristic	No. of patients	%
Age at study entry, y		
<50	2	8
50-59	8	32
60-69	15	60
≥70	0	0
Mean ± SE	60.6 ± 1.6	
Age at diagnosis,* y		
<50	2	8
50-59	4	16
60-69	11	44
≥70	8	32
Mean ± SE	64.5 ± 1.7	
Time on tamoxifen, mo		
0-12	6	24
13-24	3	12
25-36	3	12
37-60	9	36
>60	4	16
Mean ± SE	34.8 ± 4.6	
Time from start of tamoxifen to diagnosis,* mo		
0-12	5	20
13-36	6	24
37-60	8	32
>60	6	24
Mean ± SE	41.6 ± 5.9	
Time on study, mo		
<60	7	28
60-79	9	36
80-99	4	16
≥100	5	20
Mean ± SE	77.0 ± 4.8	

*Of endometrial cancer.

Table 6. Characteristics of endometrial cancers (n = 25)

Characteristic	No. of patients	%
Histologic type		
Endometrioid	13*	52
Endometrioid, mixed	4	16
Papillary	3	12
Carcinosarcoma	2	8
Mucinous	1	4
Adenosquamous	1	4
Stromal sarcoma	1	4
Histologic grade		
Good	14	56
Moderate	4	16
Poor	5	20
Sarcoma	1	4
Unknown	1*	4
Nuclear grade		
Good	15	60
Poor	7	28
Unknown	2*	8
Sarcoma	1	4
FIGO stage		
IA	7*	28
IB	13	52
IC	1	4
IIB	1	4
IIIC	1	4
IVB	1	4
Sarcoma	1	4

*One case not cancer upon central pathology review is included in the percent distribution of this table. Note that in the text, this case has not been included in the calculation of the percentage of stage I cancers.

0.2/1000 for the placebo group and 1.6/1000 for the randomized, tamoxifen-treated group (Table 7). When compared to that in the placebo group, the relative risk of an endometrial cancer occurring in the randomized, tamoxifen-treated group was 7.5 (95% confidence interval = 1.7-32.7, determined by proportional hazards modeling). When examined according to patient age, the rate for those in the randomized, tamoxifen-treated group who were 50 years of age or older was about seven times greater than the rate for those 49 years of age or younger. In the registered patients receiving tamoxifen, the average annual hazard rate was similar (1.4/1000) to that in the randomized, tamoxifen-treated group.

When patients with endometrial cancer occurring *only as a first event* were evaluated, the average annual hazard rate of endometrial cancer in both the randomized and registered, tamoxifen-treated groups (1.7/1000 and 1.3/1000, respectively) was similar to that observed when endometrial cancer occurred as any event. Because no endometrial cancers occurred as first events in the placebo group, the hazard rate was zero; consequently, the specific relative risk was undefined.

In order to put into perspective the frequency with which various events occurred in the placebo and tamoxifen-treated groups, average annual hazard rates and cumulative hazard rates by type of first event were determined during the first 5 years after surgery (Table 8; Fig. 1). When all categories of events were combined, the net benefit from tamoxifen (38%) was evident. Examination of the rates of specific events indicated a substantial reduction in both breast cancer relapse (46%) and occurrence of cancer in the opposite breast (42%) following tamoxifen administration. By contrast, there was little change in either the cumulative rates of second primary cancers occurring in other organs or non-breast cancer deaths. There was, however, an increase in both the average annual rates and the cumulative rates of endometrial cancer: from 0 in the placebo group to 1.2/1000 and 6.3/1000, respectively, in the randomized, tamoxifen-treated group. Cumulative hazard rates at 5 years demonstrated that the rate of cancer in the opposite breast, though reduced from 40.5/1000 in the placebo group to 23.5/1000 in the tamoxifen-treated group, was greater than the rate of endometrial cancer. The cumulative rate of endometrial cancer in the registered, tamoxifen-treated group was similar to that in the randomized, tamoxifen-treated group (Fig. 1).

Discussion

Despite increased interest in and speculation about the association between tamoxifen administration and the occurrence of endometrial cancer, there are insufficient data from controlled studies to clearly define the nature and extent of that relationship. Most of the information regarding the incidence of endometrial cancer has come from a Swedish randomized trial in which patients received 40 mg of tamoxifen per day for either 2 or 5 years (*9,10*). In a 1989 report of that study (*9*), 13 endometrial cancers occurred in tamoxifen-treated patients, whereas

Downloaded from http://jnci.oxfordjournals.org/ at Reprints Desk on July 6, 2016

Table 7. Average annual hazard rate of endometrial cancer as any event or as a first event through the entire follow-up period

		Randomized						
		Placebo		Tamoxifen		Registered: tamoxifen		
Endometrial cancer	Age, y	No. of events	Average annual rate/1000	No. of events	Average annual rate/1000	No. of events	Average annual rate/1000	Relative risk (95% CI)*
As any event	All	2	0.2	15	1.6	8	1.4	7.5 (1.7-32.7)
	≤49	0	0	1	0.3	1	0.6	—
	≥50	2	0.3	14	2.1	7	1.8	7.1 (1.6-31.1)
As first event	All	0	0	15	1.7	7	1.3	—
	≤49	0	0	1	0.4	1	0.6	—
	≥50	0	0	14	2.3	6	1.6	—

*Comparing tamoxifen with placebo. CI = confidence interval.

Table 8. Average annual hazard and cumulative hazard rates by type of first event within the first 5 years after surgery according to treatment group

	Placebo: randomized (n = 1424)			Tamoxifen: randomized (n = 1419)			Tamoxifen: registered (n = 1220)		
Type of event	No. of events	Average annual rate/1000	Five-year cumulative rate/1000	No. of events	Average annual rate/1000	Five-year cumulative rate/1000	No. of events	Average annual rate/1000	Five-year cumulative rate/1000
All events	382	63.3	315.6	249	38.9	194.8	181	34.1	178.5
Breast cancer relapse*	274	45.4	227.8	156	24.4	123.5	117	22.0	114.5
Cancer in opposite breast	49	8.1	40.5	30	4.7	23.5	15	2.8	12.9
Other second primary cancer†	31	5.1	26.3	29	4.5	21.9	28	5.3	26.9
Dead, no evidence of disease	28	4.6	22.9	26	4.1	20.5	14	2.6	14.2
Endometrial cancer	0	0	0	8	1.2	6.3	7	1.3	6.2

*Excludes cancer in the opposite breast.
†Excludes cancer in opposite breast and endometrial cancer.

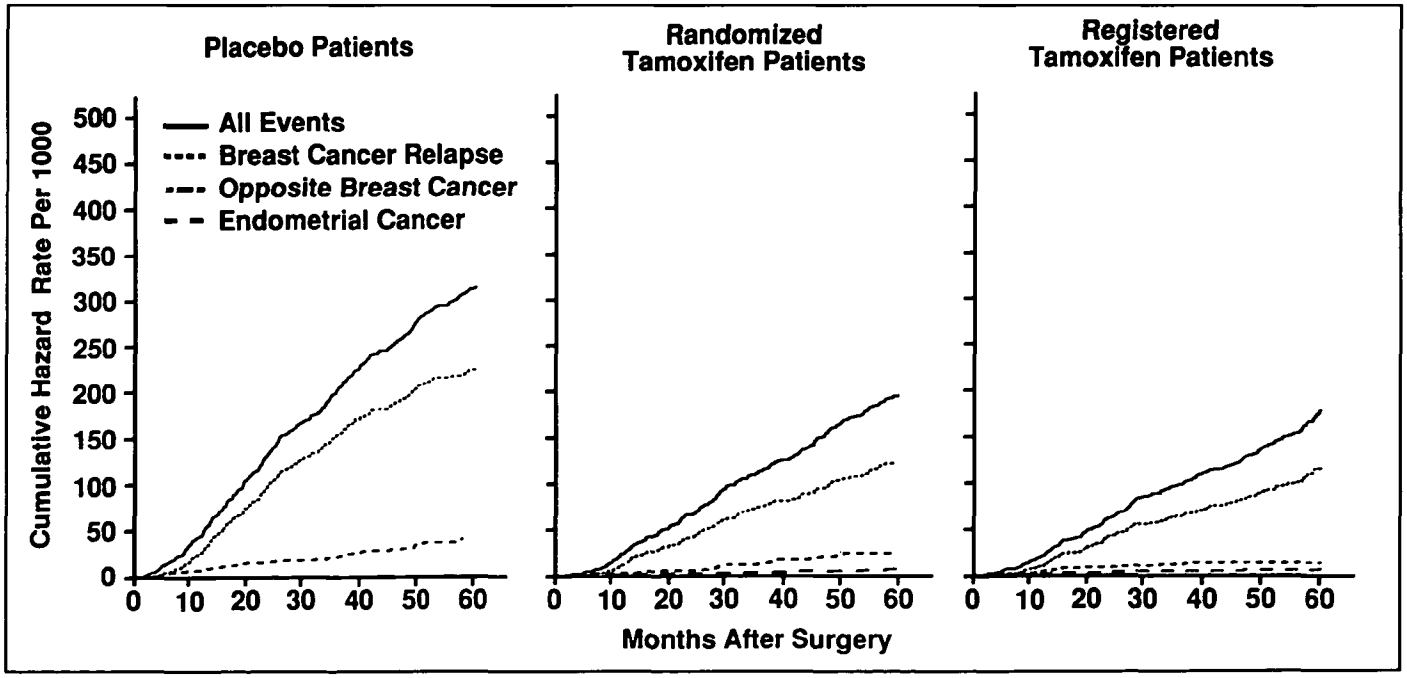


Fig. 1. Cumulative hazard rates through 5 years by type of first event in randomized placebo and tamoxifen-treated groups and in registered tamoxifen-treated group.

Downloaded from http://jnci.oxfordjournals.org/ at Reprints Desk on July 6, 2016

only two tumors occurred in the control group. At 7 years, the cumulative frequency of uterine tumors was approximately 0.4% in the control group, 0.9% in those who received tamoxifen for 2 years, and 5.5% in those treated with tamoxifen for 5 years ($P<.01$). In a recent update (*10*), four additional cancers were identified in the group receiving tamoxifen (a total of 17 tumors), and one more tumor occurred in the control group (a total of three). In a randomized Danish trial (*13*) in which tamoxifen (30 mg/d) was given for 48 weeks, two endometrial cancers occurred in patients who received radiation therapy alone, while there were seven cancers in those treated with radiation therapy plus tamoxifen. The standardized incidence ratio for endometrial cancer was 1.9 (95% confidence interval = 0.8-3.9) for tamoxifen-treated patients; the cumulative incidence in the two groups after 10 years was 0.3% and 1.0%, respectively ($P = .11$).

Findings from two other trials failed to note an increase in the incidence of endometrial cancer following tamoxifen administration. In a Scottish trial (*11,12*), tamoxifen (20 mg/d) was administered for 5 years or until relapse. After 4-10 years of follow-up, there were two endometrial cancers in the untreated control group and three sarcomas in the tamoxifen-treated group (*11*). In a subsequent update (*12*), only two endometrial cancers were recorded, one in each arm of the trial. A report (*14*) from a Manchester, England, adjuvant trial, in which patients received tamoxifen (20 mg/d) for 1 year, noted that the incidence of endometrial cancer in postmenopausal patients after 13 years of follow-up was the same in the tamoxifen-treated and control groups: one of 282 patients in the former and one of 306 in the latter. The limited and divergent findings from these four trials emphasize the need for more information to define the frequency with which endometrial cancers occur in tamoxifen-treated patients and in those who do not receive the drug.

The findings in this study indicate that, in patients randomly assigned to receive tamoxifen, endometrial tumors occurred as a first event within 5 years of surgery at an average annual hazard rate of 1.2/1000 and that the cumulative hazard rate through 5 years was 6.3/1000. The similarity of these rates in the registered, tamoxifen-treated patients (1.3/1000 and 6.2/1000, respectively) supports these findings. Less clear is the frequency with which endometrial cancers occur in non–tamoxifen-treated patients. In this study, no endometrial cancers were observed as a first event in women receiving placebo. The two endometrial cancers in patients who received placebo were detected following tamoxifen administration: one in the woman who received tamoxifen for treatment of a breast cancer recurrence and the other in the woman diagnosed as having a second primary (colon) cancer. Including these cases, the average annual hazard rate of an endometrial cancer occurring as any event in the placebo group was 0.2/1000 patients, which, when compared with the rate of 1.6/1000 in the randomized, tamoxifen-treated group, resulted in a relative risk of 7.5 (95% confidence interval = 1.7-32.7).

While these findings indicate that the average annual and cumulative hazard rates of occurrence of endometrial cancer are greater in the tamoxifen-treated patients than in those receiving placebo, certain factors must be considered before deciding upon the magnitude of the difference in risk between the two randomized groups in the trial. One such consideration relates to possible biases that may have caused a differential between treatment groups in the likelihood of identifying endometrial cancer. Because of gynecologic symptoms associated with tamoxifen therapy, women who received that drug were more likely to have been seen by gynecologists than were women who received placebo. A more frequent "search" may have resulted in the discovery of more uterine cancers in the tamoxifen-treated group than in the placebo group. This and other biases such as lead-time bias might affect obtaining an accurate estimate of the absolute or relative risk of endometrial cancers. The B-14 trial was not designed to assess the risk of endometrial cancer and, therefore, did not incorporate methods to quantify the extent to which these biases were involved.

There is indirect information indicating that the rate of endometrial cancer as a second primary tumor is unusually low in the placebo group of B-14. The 1984-1988 Surveillance, Epidemiology, and End Results (SEER[1]) data (*22*) predicted that 6.9 endometrial cancers would occur in the group of patients who received placebo in our study. With the use of their data to determine the base line for relative risk of endometrial cancer in the randomized, tamoxifen-treated group, that risk is about 2.2. Findings from NSABP B-06 further support the likelihood that the hazard rate of endometrial cancer in our placebo group is low. That trial, which compared the worth of modified radical mastectomy and lumpectomy with and without breast irradiation, accrued 2163 patients between 1976 and 1984. The 1159 patients with negative lymph nodes in that study did not receive systemic therapy; consequently, they provide a population comparable to the placebo group of the B-14 trial and, thus, can be used to estimate the rate of endometrial cancer in a non–tamoxifen-treated group. After an average follow-up time of 98.8 months in the B-06 trial, there have been seven endometrial cancers in that group of patients. The average annual hazard rate was 0.7/1000. When the rate of endometrial cancer in the tamoxifen-treated group in this study (1.7/1000) is compared with the rate in the B-06 trial, the relative risk of 2.3 is commensurate with that obtained using SEER data as the base for the comparison.

Of paramount importance is the need for quantitative information regarding the risk and the benefit of a therapeutic intervention—in this case, the extent of the risk of an endometrial cancer occurring as a result of tamoxifen therapy versus the magnitude of the benefit of tamoxifen in reducing both breast cancer relapse and occurrence of cancer in the opposite breast. In this study, cumulative hazard rates by type of first event occurring within the first 5 years after surgery provide the least biased measurements for estimating the risk and benefit resulting from tamoxifen therapy. The cumulative rate/1000 of breast cancer recurrence was reduced from 227.8 in the placebo group to 123.5 in the randomized, tamoxifen-treated group; the cumulative rate of cancer in the opposite breast was reduced from 40.5 to 23.5, respectively, in the two groups. Thus, there was a benefit in that there were 121.3 fewer breast-related events per 1000 women. On the other hand, the cumulative rate of endometrial cancer was increased: There were 6.3 events per 1000 women. Comparing the tamoxifen with the placebo group and taking into account endometrial cancers, there was a 38%

Downloaded from http://jnci.oxfordjournals.org/ at Reprints Desk on July 6, 2016

reduction in the 5-year cumulative hazard rate in the tamoxifen-treated group, instead of, at most, a 45% reduction if no endometrial cancers had occurred in the tamoxifen-treated group.

The findings reported herein indicating an increase in the rate of endometrial cancers following tamoxifen therapy have two important implications for physicians who treat breast cancer patients with tamoxifen as well as for the patients who receive the drug. First, the benefit from tamoxifen is substantially greater than the incidence of endometrial cancer currently being reported; consequently, tamoxifen should continue to be used in the treatment of breast cancer. Second, because of the increase in the incidence of endometrial cancer following administration of tamoxifen, it is imperative that a program similar to the one currently being used in the NSABP BCPT be implemented to ensure that tamoxifen-treated breast cancer patients receive appropriate surveillance for detection and treatment of endometrial cancers. A gynecologic evaluation that includes medical history and physical examination should be available to all patients. When deemed appropriate, pelvic and/or endovaginal sonography and endometrial sampling should be carried out. Thirty-six percent of the patients in this study developed endometrial cancers after fewer than 2 years of tamoxifen therapy; six of the tumors occurred after 0-9 months of such treatment. These findings suggest that endometrial changes could have been present when tamoxifen therapy was begun. Thus, use of endovaginal ultrasound and/or endometrial sampling before tamoxifen administration deserves further consideration. Most important, gynecologic examinations should be carried out promptly when symptoms are reported. The observation that endometrial cancers occurred in only two patients younger than 50 years of age is in keeping with SEER data indicating that the age-specific rates of endometrial cancer are much lower for women under 50 years of age (*22*). Especially relevant is the fact that 76% of endometrial cancers occurred in women 60 years of age or older—16% in those between 50 and 59 years of age. Because the average annual hazard rate for endometrial cancer as a first event was 0.4/1000 in women 49 years of age or younger versus 2.3/1000 in those 50 years of age or older, particular effort should be directed toward detection and the use of interventions to prevent such tumors in postmenopausal, tamoxifen-treated patients. We recommend that all women who receive tamoxifen therapy have, at a minimum, yearly gynecologic examinations.

The findings in this article have important implications not only for women who receive tamoxifen to treat their breast cancer but also for women in the NSABP BCPT. The risk–benefit analysis used in the design of that trial assumed that there would be an increase in the risk of endometrial cancer that would be twice that expected on the basis of SEER data. Currently, the absolute rate of endometrial cancer observed in the B-14 tamoxifen-treated patients is only slightly greater than that used for the original BCPT risk–benefit analysis. A recent reanalysis using the absolute rate of endometrial cancer observed among B-14 tamoxifen-treated patients and the actual projected risk of breast cancer from the first 8300 women randomly assigned to the BCPT indicates that the risk–benefit analysis for the BCPT continues to favor a benefit. Thus, because the excess risk of endometrial cancer remains close to our original prediction and because the prediction of a benefit is still present, there is justification for continuing the BCPT as planned. Moreover, because a possible risk of endometrial cancer was considered initially, the BCPT has, from its inception, incorporated several safety aspects to diminish that risk. These safety aspects include the routine questioning of participants regarding gynecologic symptoms at each 6-month follow-up visit and a prescribed follow-up procedure to determine the etiology of any problems that may be identified. In addition, all findings from the trial are regularly evaluated by an external safety-monitoring committee. These aspects of the BCPT methodology are similar to those used in women who receive hormone replacement therapy and are designed to ensure that participants in the trial are not subjected to any undue risk for this disease. As previously noted, these aspects of the BCPT are germane to tamoxifen-treated breast cancer patients.

It has been suggested that endometrial cancer occurring after tamoxifen therapy may be more "aggressive" and, perhaps, less easily manageable than are such tumors that occur in non–tamoxifen-treated patients or in those who have received hormone replacement therapy. Little information has been presented to justify that claim (*23*). Recently, however, that concept has received greater attention as a result of a report by Magriples et al. (*15*), who conducted a retrospective study using archival reports from 53 patients in the Yale Tumor Registry (1980-1990). The histologic features of uterine cancers in 15 patients who had received tamoxifen at 40 mg/d for from 3 months to 10 years (mean time on study, 4.2 years) were compared with findings obtained from 38 other patients with breast cancer who did not receive tamoxifen. Seven of the 38 non–tamoxifen-treated patients had been exposed to unopposed estrogen; in five patients, that information was unknown. However, no mention was made of how many of the 15 tamoxifen-treated patients also received estrogen. The investigators found that 67% of tamoxifen-treated patients had high-grade tumors, as compared with 24% in the untreated group. Their classification of low-grade and high-grade tumors does not completely relate to histologic grade but also relates to histologic tumor type. In their classification, low-grade tumors include all grade 1 and 2 endometrioid carcinomas; high-grade tumors include grade 3 endometrioid carcinomas in addition to all papillary-serous, clear-cell, and mixed müllerian tumors, regardless of grade. We refer to tumors in the NSABP series as being of good histologic grade, i.e., good and moderate combined, or of poor histologic grade regardless of histologic tumor type. In the Yale series, some of the tumor types considered to be of high grade are of good or moderate histologic grade in the NSABP series. In the Yale series, five patients on tamoxifen died of endometrial cancer, as compared to one in the untreated group. From their limited information, these investigators concluded that "women receiving tamoxifen as treatment for breast cancer who subsequently develop uterine cancer are at risk for high-grade endometrial cancers that have a poor prognosis" and perhaps have a biologic basis different from that associated with non–tamoxifen-treated tumors.

A comparison between our findings and those in the Yale study indicated that the distribution of patients according to FIGO stage and histologic grade in our tamoxifen-treated patients was similar to that in the *non–tamoxifen*-treated patients

Downloaded from http://jnci.oxfordjournals.org/ at Reprints Desk on July 6, 2016

in the Yale series (Table 9). Moreover, there were fewer tumors with high FIGO stage in tamoxifen-treated patients in our trial than in similar patients in the Yale series. A similar comparison was made between our findings and SEER data (1983-1987) (*22*) from 12 717 patients with endometrial cancers. SEER data indicated that 74% of tumors were localized at the time of diagnosis, that 79% were of histologic grades 1 and 2 (good), and that the 5-year relative survival was 83%. The B-14 findings in tamoxifen-treated patients are comparable to these data: 88% of the endometrial cancers (a greater proportion than in the SEER data) were FIGO stage I (localized), 78% were of good histologic grades (1 and 2), and, although not all patients have been followed for 5 years, there is no indication that relative survival will be poorer.

Two reports recently presented information similar to our findings regarding the lack of evidence to indicate that endometrial cancers resulting from tamoxifen therapy are likely to be more aggressive tumors. Barakat et al. (*24*) found no difference in the stage, grade, or histologic subtype of endometrial cancers occurring in 23 women who received tamoxifen and 51 who did not receive the drug. In another study by van Leeuwen et al. (*25*), the stage distributions and morphology of the endometrial cancers in tamoxifen-treated and non–tamoxifen-treated women showed no striking differences.

After evaluating our data, SEER data, and the Swedish trial findings presented in Table 9, we are unable to agree that endometrial cancers occurring in tamoxifen-treated patients are necessarily different types of tumor with a worse prognosis than are those tumors that occur in non–tamoxifen-treated patients, if for no other reason than that the data are too limited to make such a judgment. Additional well-planned studies are required to further evaluate the Magriples thesis before that concept can be supported.

Since the mid-1970s, when several independent studies (*17,26-30*) provided evidence to suggest an association between the use of exogenous estrogen therapy and the development of endometrial cancer, a plethora of reports has appeared affirming that relationship. Numerous reviews (*31-34*) describe the current status of the issues regarding the use of unopposed estrogens, estrogens and progestins, duration of therapy, estrogen dose, type of estrogen preparation, recentness of use, and other aspects of the estrogen–endometrial cancer issue. Although great effort has been expended to quantify the risks and benefits of hormone replacement therapy as used in postmenopausal women, no completely unified position has been achieved in that regard. Moreover, the extent to which estrogen use is associated with a more advanced stage of such tumors remains unclear (*32*). Because tamoxifen displays an agonist effect that mimics estrogen and because a large proportion of postmenopausal women take hormone replacement therapy for a variety of reasons, there is clinical relevance for comparing the risk of endometrial cancer in women who take either of the two hormonal agents. However, it is difficult to make a meaningful comparison on the basis of information currently available.

Table 9. Comparison of distributions of uterine cancer by selected characteristics within NSABP and other studies

	NSABP: tamoxifen (n = 25)*		Yale Tumor Registry†				Swedish trial‡			
			Tamoxifen (n = 15)*		No tamoxifen (n = 38)*		Tamoxifen (n = 17)*		No tamoxifen (n =3)*	
	No. of events	%	No. of events	%	No. of events	%	No. of events	%	No. of events	%
Histologic type										
Endometrial										
Endometrioid (pure or mixed type)	17	71	9	60	31	89	16	94		
Other	7	29	6	40	4	11	1	6		
Total No. evaluated	24		15		35		17			
FIGO stage										
Endometrial										
I	21	88	7	78	23	88	14	82	3	100
I (A and B)	20	83	5	56	18	69	—	—	—	—
II-IV	3	13	2	22	3	12	3	18	0	0
Total No. staged	24		9		26		17		3	
Histologic grade										
Endometrial										
Low (good)	18	78	5	33	26	74	8§	53	3	100
High (poor)	5	22	10	67	9	26	7‖	47	0	0
Total No. graded	23		15		35		15		3	
Sarcoma	1	—	0	—	3	—	0	—	0	—
Deaths¶	4	16	5	33	1	3	3	18	0	0

*n = number of cases.
†Adapted from Magriples et al. (*15*), Tables 2 and 3.
‡Adapted from Fornander et al. (*10*), Table 2.
§World Health Organization grade I.
‖World Health Organization grade II.
¶Due to endometrial cancer in tamoxifen-treated patients.

Downloaded from http://jnci.oxfordjournals.org/ at Reprints Desk on July 6, 2016

Note added in proof: Institution 97 (Hôpital Saint-Luc) was involved in the submission of fraudulent data to the NSABP. The average annual hazard rates of endometrial cancer as a first event have been recalculated by the investigators with and without the data from Hôpital Saint-Luc (*see* Table 10 *below*); the rates remain essentially the same. Also note the following breakdown of data: Data on 182 of the 2843 randomly assigned patients and 37 of the 1220 registered patients were provided by the Hôpital Saint-Luc. After review, 24 of the 182 records showed falsification, all involving characteristics of patients prior to random assignment. Of the 37 registered-patient records, 8 showed falsification.

Table 10. Average annual hazard of endometrial cancer as a first event (rate/1000)

	Placebo	Tamoxifen	Registered
With Institution 97	0	1.7	1.3
Without Institution 97	0	1.7	1.2

References

(*1*) Mouridsen H, Palshof T, Patterson J, et al: Tamoxifen in advanced breast cancer. Cancer Treat Rev 5:131-141, 1978

(*2*) Powles TJ: The case for clinical trials of tamoxifen for prevention of breast cancer. Lancet 340:1145-1147, 1992

(*3*) Nayfield SG, Karp JE, Ford LG, et al: Potential role of tamoxifen in prevention of breast cancer. J Natl Cancer Inst 83:1450-1459, 1991

(*4*) Fisher B, Costantino J, Redmond C, et al: A randomized clinical trial evaluating tamoxifen in the treatment of patients with node-negative breast cancer who have estrogen-receptor-positive tumors. N Engl J Med 320:479-484, 1989

(*5*) Fisher B, Redmond C, Wickerham L, et al: Systemic therapy in patients with node-negative breast cancer. A commentary based on two National Surgical Adjuvant Breast and Bowel Project (NSABP) clinical trials. Ann Intern Med 111:703-712, 1989

(*6*) Seoud MA, Johnson J, Weed JC Jr: Gynecologic tumors in tamoxifen-treated women with breast cancer. Obstet Gynecol 82:165-169, 1993

(*7*) Segna RA, Dottino PR, Deligdisch L, et al: Tamoxifen and endometrial cancer. Mt Sinai J Med 59:416-418, 1992

(*8*) Killackey MA, Hakes TB, Pierce VK: Endometrial adenocarcinoma in breast cancer patients receiving antiestrogens. Cancer Treat Rep 69:237-238, 1985

(*9*) Fornander T, Rutqvist LE, Cedermark B, et al: Adjuvant tamoxifen in early breast cancer: occurrence of new primary cancers. Lancet 1:117-120, 1989

(*10*) Fornander T, Hellström A-C, Moberger B: Descriptive clinicopathologic study of 17 patients with endometrial cancer during or after adjuvant tamoxifen in early breast cancer. J Natl Cancer Inst 85:1850-1855, 1993

(*11*) Stewart HJ, Knight GM: Tamoxifen and the uterus and endometrium [letter]. Lancet 1:375-376, 1989

(*12*) Stewart HJ: The Scottish trial of adjuvant tamoxifen in node-negative breast cancer. Scottish Cancer Trials Breast Group. Monogr Natl Cancer Inst 11:117-120, 1992

(*13*) Andersson M, Storm HH, Mouridsen HT: Carcinogenic effects of adjuvant tamoxifen treatment and radiotherapy for early breast cancer. Acta Oncol 31:259-263, 1992

(*14*) Ribeiro G, Swindell R: The Christie Hospital adjuvant tamoxifen trial. Monogr Natl Cancer Inst 11:121-125, 1992

(*15*) Magriples U, Naftolin F, Schwartz PE, et al: High-grade endometrial carcinoma in tamoxifen-treated breast cancer patients. J Clin Oncol 11:485-490, 1993

(*16*) Creasman WT: New gynecologic cancer staging. Obstet Gynecol 75:287-288, 1990

(*17*) Gusberg SB, Runowicz CD: Gynecologic cancers. *In* American Cancer Society Textbook of Clinical Oncology (Holleb AI, Fink DJ, Murphy GP, eds). Atlanta: American Cancer Society, 1991, pp 481-497

(*18*) Fisher ER: Identification of risk factors by conventional pathologic and some ancillary techniques in women with breast cancer. *In* High Risk Breast Cancer (Ragaz J, Ariel IM, eds). New York: Springer-Verlag, 1989, pp 233-250

(*19*) Cox DR. Regression models and life-tables. J R Stat Soc [B] 34:187-220, 1972

(*20*) Kalbfleisch JD, Prentice RL: The Statistical Analysis of Failure-Time Data. New York: Wiley, 1980

(*21*) Kay R, Schumacher M: Unbiased assessment of treatment effects on disease recurrence and survival in clinical trials. Stat Med 2:41-58, 1983

(*22*) National Cancer Institute: SEER Cancer Statistics Review 1973-1990. Document #93-2789. Bethesda, Md: NCI, 1993

(*23*) McDonald TW, Annegers JF, O'Fallon WM, et al: Exogenous estrogen and endometrial carcinoma: case-control and incidence study. Am J Obstet Gynecol 127:572-580, 1977

(*24*) Barakat RR, Wong G, Curtin JP, et al: Tamoxifen (T) use in breast cancer patients who subsequently develop corpus cancer is not associated with a higher incidence of adverse histologic features. Memorial Sloan-Kettering Cancer Center, New York, NY. Presented at the 25th annual meeting of the Society of Gynecologic Oncologists, February 6, 1994. In press

(*25*) van Leeuwen FE, Benraadt J, Coebergh JWW, et al: Risk of endometrial cancer after tamoxifen treatment of breast cancer. Lancet 343:448-452, 1994

(*26*) Smith DC, Prentice R, Thompson DJ, et al: Association of exogenous estrogen and endometrial carcinoma. N Engl J Med 293:1164-1167, 1975

(*27*) Ziel HK, Finkle WD: Increased risk of endometrial carcinoma among users of conjugated estrogens. N Engl J Med 293:1167-1170, 1975

(*28*) Mack TM, Pike MC, Henderson BE, et al: Estrogens and endometrial cancer in a retirement community. N Engl J Med 294:1262-1267, 1976

(*29*) Malfetano JH: Tamoxifen-associated endometrial carcinoma in postmenopausal breast cancer patients. Gynecol Oncol 39:82-84, 1990

(*30*) Jick SS, Walker AM, Jick H: Estrogens, progesterone, and endometrial cancer. Epidemiology 4:20-24, 1993

(*31*) Gray LA Sr, Christopherson WM, Hoover RN: Estrogens and endometrial carcinoma. Obstet Gynecol 49:385-389, 1977

(*32*) Grady D, Rubin SM, Petitti DB, et al: Hormone therapy to prevent disease and prolong life in postmenopausal women. Ann Intern Med 117:1016-1037, 1992

(*33*) Herrinton LJ, Weiss NS: Postmenopausal unopposed estrogens. Characteristics of use in relation to the risk of endometrial carcinoma. Ann Epidemiol 3:308-318, 1993

(*34*) Brinton LA, Hoover RN: Estrogen replacement therapy and endometrial cancer risk: unresolved issues. The Endometrial Cancer Collaborative Group. Obstet Gynecol 81:265-271, 1993

Notes

[1]Editor's note: SEER is a set of geographically defined, population-based central tumor registries in the United States, operated by local nonprofit organizations under contract to the National Cancer Institute (NCI). Each registry annually submits its cases to the NCI on a computer tape. These computer tapes are then edited by the NCI and made available for analysis.

The following were major NSABP contributors to this study: David Bowman, Manitoba Cancer Foundation, Winnipeg, Canada; Jean Couture, St. Sacrement Hospital, Quebec City, Canada; Nikolay V. Dimitrov, Michigan State University, East Lansing; James Evans, Geisinger Medical Center, Danville, Pa.; William Farrar, Ohio State University, Columbus; Maureen Kavanah, Boston University, Mass.; H. Lavina Lickley, Women's College Hospital, Toronto, Ontario, Canada; Richard Margolese, Jewish General Hospital, Montreal, Quebec, Canada; A. H. G. Paterson, Cross Cancer Institute, Edmonton, Alberta, Canada; Andre Robidoux, Hotel-Dieu, Montreal; Henry Shibata, Royal Victoria Hospital, Montreal; Jose Terz, City of Hope Medical Center, Duarte, Calif.

Supported by Public Health Service grants NCIU10CA12027, NCIU10CA37377, and NCIU10CA39086 from the National Cancer Institute, National Institutes of Health, Department of Health and Human Services; and by a grant (ACS-R-13) from the American Cancer Society.

We acknowledge the assistance of Tanya Spewock in the preparation of this manuscript.

Manuscript received January 18, 1994; revised March 8, 1994; accepted March 14, 1994.

Downloaded from http://jnci.oxfordjournals.org/ at Reprints Desk on July 6, 2016

For nearly 50 years, the Defense Technical Information Center (DTIC) has been collecting, storing and distributing DoD-sponsored scientific, technical, and engineering information within the Defense community. We provide our users with technical support services and information on topics from aeronautics to medical research to pharmacology. For defense-related information, come to us...

THE DEFENSE TECHNICAL INFORMATION CENTER

DTIC's products and services include:

- Department of Defense Gateway Information System
- Defense Research, Development, Test & Evaluation Online System
- Technical Report Database on CD-ROM
- Technical Reports in Hard Copy or Microfiche
- Nonprint Products
- Customized Bibliographies
- Summaries of Current Research Efforts
- Current Awareness Products
- Information Analysis Centers

PLUS MUCH MORE!

Here's what our customers have to say about our products and services...

"As a result of doing a DTIC search, we eliminated unnecessary. . .work and saved $70,000."

—U.S. Army White Sands Missile Range

"I am able to locate information at DTIC that is available nowhere else."

—Sikorsky Aircraft

"With DTIC databases there is an ease and convenience in ordering documents, they offer good technical and other support personnel who seem to really care about your questions and problems."

—Naval Research Laboratory, Stennis Space Center

"I am a researcher by profession and if I don't want to re-invent the wheel--I use DTIC."

—LTC Robert Clemence, USA, Joint Chiefs of Staff

The Defense Technical Information Center's products and services are available to Government agencies, Government contractors and potential contractors. To find out if your organization may already be registered with DTIC, contact your organization's library or information center. For more information on registering with DTIC or for additional information on DTIC's products and services, please call DTIC's toll free number at 1-800-225-DTIC (3842) or write to:

Defense Technical Information Center
Building 5
Cameron Station
Alexandria, VA 22304-6145

Downloaded from http://jmci.oxfordjournals.org/ at Reprints Desk on July 6, 2016

Cell Reports
Article

Endocrine-Therapy-Resistant *ESR1* Variants Revealed by Genomic Characterization of Breast-Cancer-Derived Xenografts

Shunqiang Li,[1,2,13] Dong Shen,[3,13] Jieya Shao,[1] Robert Crowder,[1] Wenbin Liu,[4] Aleix Prat,[5,6] Xiaping He,[6] Shuying Liu,[4] Jeremy Hoog,[1] Charles Lu,[3] Li Ding,[2,3,8] Obi L. Griffith,[3] Christopher Miller,[3] Dave Larson,[3] Robert S. Fulton,[3] Michelle Harrison,[3] Tom Mooney,[3] Joshua F. McMichael,[3] Jingqin Luo,[2,7] Yu Tao,[7] Rodrigo Goncalves,[1] Christopher Schlosberg,[8] Jeffrey F. Hiken,[8] Laila Saied,[9] Cesar Sanchez,[10] Therese Giuntoli,[1] Caroline Bumb,[1] Crystal Cooper,[1] Robert T. Kitchens,[1] Austin Lin,[1] Chanpheng Phommaly,[1] Sherri R. Davies,[1] Jin Zhang,[3] Megha Shyam Kavuri,[1] Donna McEachern,[11] Yi Yu Dong,[1] Cynthia Ma,[1,2] Timothy Pluard,[1,2] Michael Naughton,[1,2] Ron Bose,[1,2] Rama Suresh,[1] Reida McDowell,[1] Loren Michel,[1,2] Rebecca Aft,[12] William Gillanders,[12] Katherine DeSchryver,[1] Richard K. Wilson,[2,3] Shaomeng Wang,[11] Gordon B. Mills,[4] Ana Gonzalez-Angulo,[4] John R. Edwards,[8] Christopher Maher,[1,2,3] Charles M. Perou,[6] Elaine R. Mardis,[2,3] and Matthew J. Ellis[1,2,*]

[1]Section of Breast Oncology, Division of Oncology, Department of Internal Medicine, Washington University in St. Louis, St. Louis, MO 63110, USA
[2]Siteman Cancer Center Breast Cancer Program, Washington University in St. Louis, St. Louis, MO 63110, USA
[3]The Genome Institute, Washington University in St. Louis, St. Louis, MO 63110, USA
[4]Department of Systems Biology, University of Texas MD Anderson Cancer Center, Houston, TX 77030, USA
[5]Translational Genomics Unit, Vall d'Hebron Institute of Oncology (VHIO), Passeig de la Vall d'Hebron 119-129, Barcelona 08035, Spain
[6]Departments of Genetics, and Pathology and Laboratory Medicine, Lineberger Comprehensive Cancer Center, University of North Carolina, Chapel Hill, NC 27599, USA
[7]Division of Biostatistics, Department of Medicine, Washington University in St. Louis, St. Louis, MO 63110, USA
[8]Center for Pharmacogenomics, Washington University in St. Louis, St. Louis, MO 63110, USA
[9]Residency Program, Department of Internal Medicine, Washington University in St. Louis, St. Louis, MO 63110, USA
[10]Department of Hematology-Oncology, Pontificia Universidad Catolica de Chile, Santiago 8330032, Chile
[11]Departments of Internal Medicine, Pharmacology, and Medicinal Chemistry, University of Michigan Comprehensive Cancer Center, University of Michigan, Ann Arbor, MI 48109, USA
[12]Department of Surgery, Washington University in St. Louis, St. Louis, MO 63110, USA
[13]These authors contributed equally to this work
*Correspondence: mellis@dom.wustl.edu
http://dx.doi.org/10.1016/j.celrep.2013.08.022
This is an open-access article distributed under the terms of the Creative Commons Attribution License, which permits unrestricted use, distribution, and reproduction in any medium, provided the original author and source are credited.

SUMMARY

To characterize patient-derived xenografts (PDXs) for functional studies, we made whole-genome comparisons with originating breast cancers representative of the major intrinsic subtypes. Structural and copy number aberrations were found to be retained with high fidelity. However, at the single-nucleotide level, variable numbers of PDX-specific somatic events were documented, although they were only rarely functionally significant. Variant allele frequencies were often preserved in the PDXs, demonstrating that clonal representation can be transplantable. Estrogen-receptor-positive PDXs were associated with *ESR1* ligand-binding-domain mutations, gene amplification, or an *ESR1/YAP1* translocation. These events produced different endocrine-therapy-response phenotypes in human, cell line, and PDX endocrine-response studies. Hence, deeply sequenced PDX models are an important resource for the search for genome-forward treatment options and capture endocrine-drug-resistance etiologies that are not observed in standard cell lines. The originating tumor genome provides a benchmark for assessing genetic drift and clonal representation after transplantation.

INTRODUCTION

Many stage 3 breast cancers and effectively all stage 4 breast cancers are fatal, with annual worldwide deaths from the disease approaching one-half million (Youlden et al., 2012). Large-scale partial and whole-genome sequencing (WGS) was recently conducted on early-stage, treatment-naive breast cancer samples (Ellis and Perou, 2013). By contrast, the genomic landscape of advanced and treatment-resistant breast cancer is poorly documented. We therefore developed a panel of patient-derived xenografts (PDXs) from patients with poor-prognosis, treatment-resistant disease for genomic and functional studies, because early-passage PDX models reproduce gene expression patterns observed in the originating human tumors

and recapitulate the chemotherapy response (DeRose et al., 2011; Fleming et al., 2010; Kabos et al., 2012; Marangoni et al., 2007; Zhang et al., 2013). However, it has remained unclear to what extent PDX models accurately represent the genomic characteristics of the originating tumor at a whole-genome level. The value of the PDX approach in the setting of estrogen-receptor-positive (ER+) breast cancer has also been questioned because very few breast cancer PDXs expressing ER have been reported.

WGS using massively parallel techniques is the gold standard for comparing an originating tumor with a counterpart PDX because partial-genome sequencing, which focuses on the coding sequence alone (i.e., exome sequencing), does not fully document all mutations, particularly structural variations (SVs) or other mutational events that occur in noncoding space (Ley et al., 2008). Promisingly, WGS of a single example of a breast cancer primary, a brain metastasis, and a PDX basal-like breast cancer "trio" demonstrated that the PDX model efficiently captures almost all of the genome-wide somatic mutations observed in the originating tumor, and displayed enrichment for mutations that were present in the metastatic sample even though they were derived from the primary tumor (Ding et al., 2010). Heterogeneity in mutation frequencies also has not been comparatively evaluated for PDX models and originating tumors, so a customized capture approach (Welch et al., 2012) was used to generate high depth at somatic variant positions genome wide, coupled with statistical analyses for this comparison. RNA sequencing (RNA-seq) was conducted to determine the expression level of individual mutations and to confirm gene fusion events (Iyer et al., 2011). Reverse phase protein array (RPPA) was employed to determine whether protein and phosphoprotein expression patterns were stable upon serial transplantation (Tabchy et al., 2011). We also successfully developed multiple ER+ PDXs from patients with endocrine-therapy-resistant disease, and our genomic and functional analyses revealed mechanistic insights into resistance that have not been achieved with conventional cell line approaches.

RESULTS

Derivation and RNA/Protein Expression Patterns in Xenografts from Advanced Stage Breast Cancer

Samples were obtained from 152 patients (Figure 1A), which yielded 22 serially transplantable PDXs from 20 patients, for an engraftment rate of 13.1%. These PDXs are referred to as "Washington University Human in Mouse" (WHIM) lines and were mostly obtained from patients with advanced disease or larger primary tumors that rapidly developed lethal metastasis (Table S2A). Concordant *ER* and *HER2* status was demonstrated at the mRNA level (Table 1), and PDX expression of ER and HER2 protein was confirmed by western blot (Figure S1). Mouse and human centromere-specific fluorescent in situ hybridization (FISH) assays were conducted to demonstrate that stromal elements were murine in origin, the malignant cells were human, and there was no evidence for interspecies cellular fusion events (Figures S2A–S2C). Agilent 44K Array-based mRNA expression data were generated from the originating tumors and from matched early- and late-passage PDX counterparts. We subjected the matched pairs to unsupervised hierarchical clustering after removing genes that were highly differentially expressed between progenitor and PDX models (FDR = 0) to ensure that this comparison was "tumor centric" and not confounded by differences in the hybridization properties of mRNA arising from human versus mouse stroma (Table S2B). In almost all cases, the originating tumor and WHIM lines derived from the same individual clustered adjacently (Figure 1B). Each sample was also classified into one of five intrinsic gene-expression subtypes; lumenal A (dark blue), lumenal B (light blue), HER2-enriched (pink), basal-like (red), and Claudin-low (yellow) using PAM50 (Parker et al., 2009) and the "Nine-Cell Line Claudin-low subtype predictor" (Prat et al., 2010; Table 1; Figure 1B). The PDX lines derived from ER+ clinical samples were all subtyped lumenal by PAM50 in both the human and mouse samples, with the exception of WHIM11, which was classified as HER2-E. Of note, the human lumenal originating tumors expressed high levels of cytokeratin 14 (*CK14*), *CK5*, and *CK17* mRNA, but there was no evidence for expression of these CKs by the counterpart lumenal PDX. To investigate this discordance, we conducted immunohistochemistry for CK5 on the human lumenal tumor progenitor samples (derived from cutaneous metastases). This revealed normal-appearing CK5-positive epithelial cells arranged in ducts "trapped" among CK5-negative malignant lumenal epithelial cells, thereby "contaminating" the progenitor tumor samples with basal epithelial keratins (Figure S2D). To investigate the lumenal classification further, PDX mRNA was also profiled on a 244K customized UNC Agilent chip (Cancer Genome Atlas Network, 2012a) and the PDX data clustered with clinical breast cancer samples profiled on the same platform. In this analysis, all ER+ PDXs segregated with lumenal B tumors (Figure S3). The WHIM12 line was derived from a metaplastic carcinoma and showed a near-perfect correlation with the claudin-low signature (Figure S4). To address the stability of PDXs at the level of protein and phosphoprotein expression, multiple samples taken from the same passage and upon serial passage were assayed by RPPAs (Tabchy et al., 2011). Data from 110 antibodies for 68 samples harvested from 20 WHIM lines were clustered with the data from 386 primary breast cancers studied by The Cancer Genome Atlas (TCGA) research network (Cancer Genome Atlas Network, 2012a; Table S2C). In every case, the samples from each WHIM line clustered adjacently, including the two double isolates (WHIM2 and WHIM5, and WHIM20 and WHIM23; Figure S5). This suggests that the intra-PDX proteomic heterogeneity was considerably lower than the intertumoral heterogeneity in a large RPPA data set and was relatively stable over time and passage. The PDX samples were dispersed across the breast TCGA data, indicating that they are representative of the heterogeneous biology of breast cancer. An analysis was conducted to determine the relative rank of protein and phosphoprotein levels for each WHIM tumor with respect to the ranges in the TCGA data set (Table S2C). Here, the WHIM lines did not contain any extreme data outliers with respect to the phosphoprotein levels documented in the TCGA data. Phosphorylation of the phosphatidylinositol-3-kinase/AKT pathway proteins represented the highest-ranked pathway activation event (Table 1).

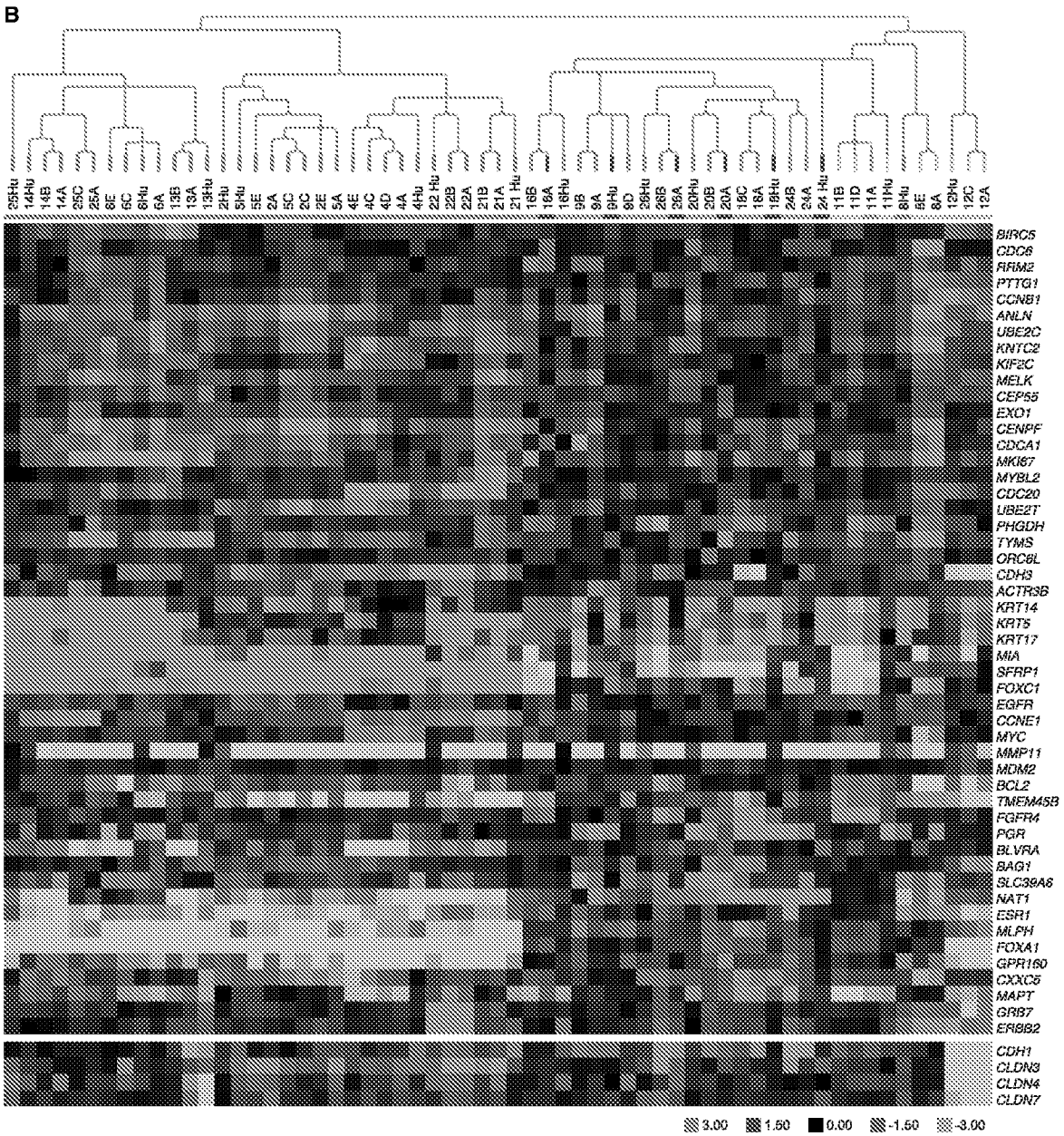
A

152 individuals entered protocol
60 primary tumor samples from patients with early stage disease
132 specimens from patients with advanced disease

ER- HER2- * 65 individuals		HER2+ * 33 individuals		ER+ HER- 54 individuals	
11 successfully grafted	17%	2 successfully grafted	6%	7 successfully grafted	13%
HIM technique		**HIM technique**		**HIM technique**	
7 out of 43 attempts in total	16%	1 out of 25 attempts in total	4%	1 out of 38 attempts in total	3%
1 out of 12 primaries	8%	0 out of 9 primaries	0%	0 out of 10 primaries	0%
6 out of 31 primaries	19%	1 out of 16 primaries	6%	1 out of 28 primaries	4%
Direct Implantation		**Direct Implantation**		**Direct Implantation**	
6 out of 29 attempts in total	21%	1 out of 15 attempts in total	7%	5 out of 44 attempts in total	11%
2 out of 15 primaries	13%	0 out of 7 primaries	0%	0 out of 7 primaries	0%
4 out of 14 primaries	28%	1 out of 8 primaries	12%	5 out of 37 primaries	14%

13 xenografts with adequate sample for whole genome sequencing of normal, human progenitor tumor and xenograft

B



(legend on next page)

Genomic Fidelity of PDX Models

Using paired-end massively parallel sequencing, we sequenced 17 originating tumor, xenograft, and germ-line trio DNA samples to ≥30-fold average whole-genome coverage. For 13 trios, we subsequently validated each candidate mutation using solution-based hybridization capture followed by deep sequencing of the originating tumor, the paired WHIM line, and the normal DNA (for the somatic variants observed in WHIM4, WHIM24, WHIM25, and WHIM26, further validation was not conducted; see Table S2D for the coding region single-nucleotide variation [SNV] observed in these examples). In the 13 cases subjected to validation, a total of 59,189 genome-wide SNVs were confirmed (Table S2E). Of these, 1,056 (1.8%) were nonsilent protein coding mutations or in RNA genes (Table S2F). Across all WHIM lines, there were 241 (range 0–77) out of a total of 58,814 validated genome-wide SNVs that were unique to the originating tumor (0.4%). In contrast, a much higher number of sites (5,450, range 29–1,564, 9.3%) were PDX specific (Table S2G). Seventy-one mutations were detected in "significantly mutated genes" (SMGs) as defined by TCGA data (Cancer Genome Atlas Research Network, 2012b), lumenal tumors (Ellis et al., 2012), or triple-negative tumors (Shah et al., 2012; Table S2H). Each PDX harbored mutation(s) in at least one SMG (WHIM6) and up to 12 SMGs (WHIM14). A small number of potentially significant mutations were observed in the PDX but not in the originating tumor (*WNK2* in WHIM8, *PIK3R4* and *KRAS* in WHIM9, *MAP4K2* in WHIM16, and *CBLB* in WHIM18). Thirty-four PDX-specific missense mutations were identified as potentially deleterious or functionally significant by a mutation impact assessment algorithm (Xi et al., 2004), and all examples contained at least one predicted deleterious PDX-specific SNV, except for WHIM 2 (Table S2I). The PDX data analysis pipeline removed sequence reads contributed by the murine genome, thereby "computationally purifying" the human tumor DNA (Ding et al., 2010). Biallelic deletions (e.g., in *PTEN*) were therefore revealed with clarity in the WHIM analysis (Figure S6) and amplified regions were often enhanced (Figures 2A, B, and S7–S9). Of the 5,336 copy-number variation (CNV) phenotypes that were detected in the 13 cases analyzed, 5,036 (94.4%) had the same call (amplified or deleted) in both the originating tumor and the counterpart PDX line (Table S2L). Remarkably, all SVs (translocations, large deletions, and inversions) were preserved upon transplantation, including regions characteristic of chromothripsis (Stephens et al., 2011; Figures 2A, 2B, and S7).

Genomic Stability of PDX across Early and Late Passages

Subsequent to our earlier report on comparative WGS of a primary tumor, brain metastasis, and primary-derived PDX trio (Ding et al., 2010), a PDX model also was derived from the patient's brain metastasis (WHIM5), enabling a deep genomic analysis of two xenografts from the same patient. The vast majority of the validated somatic SNVs and indels were shared by the four genomes (n = 1,598) as well as seven translocations, 11 deletions, and four inversions. The breast primary tumor and brain metastasis contained no single sample-unique SNV or SV (i.e., all of the SNVs were noted in at least one other sample; Figure 3A). However, in every comparison, more SNVs were observed in the tumor sample taken at a later time point when compared with a sample taken at an earlier time point (whether a PDX sample pair or a human sample pair). For example, in a comparison of the two human specimens, 13 SNVs were unique to the primary tumor, but 231 SNVs were unique to the metastasis. Additionally, both WHIM lines harbored additional sample-unique noncoding SNVs that become detectable after xenografting (39 in the case of WHIM2 and 43 in the case of WHIM5; Figure 3B). Since therapeutic experiments require extensive expansion of PDX models, we also conducted a "late-exome" study to characterize genomic drift in the WHIM2 genome, performing exome sequencing on two separate passage eight tumor grafts (Figure 3C). This experiment detected 38 additional variants in both specimens, although none of the SNVs were clearly damaging mutations in cancer-associated genes (Table S2K).

The Genome-Wide Variant Allele Frequency Is a Transplantable Phenotype

To compare mutant allele representation in the originating tumor isolates versus their corresponding PDX models, we obtained deep coverage through our capture-based validation approach and then calculated the proportion of sequencing reads that contained a mutant allele. This value was expressed as a percentage (variant allele frequency [VAF]) and analyzed by scatterplot (Figures 2C and 2D; see Figures S7–S9 for the remaining examples). The genome-wide correlation coefficients across the 13 tumor/PDX pairs varied from 0.32 (WHIM8) to 0.86 (WHIM5; Table S2L and Figures S7–S9). In the majority of cases, there was statistical evidence for VAF stability genome wide, with nine out of the 13 comparisons showing correlation coefficients above 0.65. For example, WHIM18 (R = 0.85) displayed coding region (yellow) and noncoding region (blue) VAF stability, including all six SMG mutations (Figure 2C). Eight other pairs exhibited correlation coefficients above 0.65 (Table S1L), suggesting that VAF stability was the rule, not the exception. Clearly, differences in tumor purity biased the correlation, as the originating tumors were variably contaminated with DNA from normal stromal elements, whereas the PDX had been computationally purified. However, WHIM8 stood out from the other cases by exhibiting a low correlation coefficient (0.26) and a relatively large

Figure 1. Generation of a Biologically Diverse Panel of PDX Models from Patients with Advanced Breast Cancer

(A) Diagram indicating the genesis of the PDX models from patients with primary and advanced breast cancer, using two different implantation techniques (human in mouse [Kuperwasser et al., 2004] and simple orthotopic).

(B) Unsupervised hierarchical clustering of samples using all genes of the microarrays except the stromal-related genes. The colors of the array tree and the squares below the tree denote the subtype call of each sample. Red, basal-like; pink, HER2-enriched; dark blue, lumenal A; light blue, lumenal B; yellow, Claudin-low. Below the array tree and the subtype identification row, the heatmap of the 50 PAM50 genes as well as selected tight-junction-related genes (E-cadherin [CDH1], claudin 3 [CLDN3], CLDN4, and CLDN7) are shown. The stromal-related genes were identified after a two-class paired SAM was performed with an FDR of 0% between 18 paired progenitor human tumors and xenografts. The complete list of up- and down-regulated genes can be found in Table S2B.

See also Figures S3 and S4.

Table 1. Summary of the WHIM Line Biomarker Status

WHIM Number	Intrinsic Subtype human	P1/Late WHIM passage	HER2 RNA[a] human/P1	ER RNA[a] human/P1	P53 Mutation human/P1	PIK3CA Mutation human/P1	ESR1 Mutation Translocation amplification	Highest Ranked phospho-protein by RPPA
2[c]	basal	basal	1.3	3.1	S166S ins	WT	WT	p90RSK_pT359
Primary		basal	1.0	1.0	S166S ins	WT	WT	rank = 25.5
3	N/A	Her2-E	N/A	N/A	N/A	N/A	WT	Src_pY527
Primary		Her2-E	1.8	3.8	WT	WT	WT	rank = 4.0
4	basal	basal	−5.9	−5.7	R175H	WT	WT	p27_pT198
Skin met		basal	2.2	2.2	R175H	WT	WT	rank = 28.7
5[c]	basal	basal	3.1	1.1	S166S ins	WT	WT	p90RSK_pT359
Brain met		basal	1.8	−1.7	S166S ins	WT	WT	rank = 62.3
6	basal	basal	−1.5	3.1	WT	WT	WT	PRAS40_pT246
Primary		basal	1.2	3.6	WT	WT	WT	rank = 59.2
8	basal	HER2-E	8.6	3.6	Y234H	WT	WT	Shc_pY317
Skin met		HER2-E	16.8	4.9	Y234H	WT	WT	rank = 24.7
9	LumA	LumB	1.2	72.2	WT	H1047R	WT	Akt_pS474
Skin met		LumB	2.1	365.2	WT	H1047R	WT	rank = 25.0
10	N/A	basal	N/A	N/A	N/A	N/A	WT	N/A
Skin met		basal	1.6	−2.1	Y220C	WT	WT	
11	HER2-E	LumB	−1.6	31.8	D184X ins	WT	WT	p70S6K_pT389
Primary		HER2-E	1.2	112.1	D184X ins	WT	WT	rank = 13.3
12	CLDN low	CLDN low	−5.0	2.4	R248Q	WT	WT	Akt_pT308
Primary		CLDN low	−5.0	−1.2	R248Q	WT	WT	rank = 10
13	basal	basal	−4.8	−2.1	C238Y	WT	WT	Src_pY527
Skin met		basal	−1.5	1.0	C238Y	WT	WT	rank = 14.3
14	basal	basal	1.0	5.3	I195T	WT	WT	N/A
Skin met		basal	1.3	1.2	I195T	WT	WT	
16	LumB	LumA	−2.9	40.1	R248W	H1047R	AMP	4E-BP1_pT37
Skin met		LumB	−1.2	171.5	R248W	H1047R	AMP	rank = 13.7
17	N/A	basal	N/A	N/A	N/A	N/A	WT	PKC-delta_pS664
Primary		basal	−22.8	4.1	WT	WT	WT	rank = 2.5
18	LumA	LumB	−3.9	65.5	WT	E545K	ESR1 YAP1	ER-alpha_pS118
Skin met		LumB	3.1	19.9	WT	E545K	ESR1 YAP1	rank = 16.5
20	LumB	LumA	3.1	135.2	C182X	E542K	Y537S	PDK1_pS241
Skin met[c]		LumB	5.9	71.6	C182X	E542K	Y537S	rank = 57.8
21	basal	basal	−7.5	6.4	P151H	WT	WT	Chk1_pS345
Primary		basal	−6.8	−1.9	P151H	WT	WT	rank = 16.7

(*Continued on next page*)

Table 1. Continued

22	basal	basal	2.5	1.2	C275F	WT	WT	EGFR_pY1068	
Skin met		basal	7.7	2.6	C275F	WT	WT	rank = 24.4	
23	N/A	LumA	N/A	N/A	N/A	N/A	N/A	Rb_pS807_S811	
Node met[a]		LumB	−1.3	75.8	C182X	E542K	Y537S	rank = 27.7	
24	LumA	LumB	−2.1	18.9	WT	H1047K	WT	ER-alpha_pS118	
Skin met		LumB	−1.3	719.1	WT	H1047K	E380Q	rank = 7.0	
25	basal	basal	−3.9	−1.1	R273H	WT	WT	MAPK_pT202_Y204	
Skin met		basal	1.8	−1.3	R273H	WT	WT	rank = 20.3	
26	LumB	LumA	1.9	59.6	WT	WT	WT	mTOR_pS2448	
Nodal met		LumB	3.5	52.3	WT	WT	WT	rank = 2.7	

The characteristics of 22 WHIM lines discussed in the text are summarized, including the site of the originating tumor; the PAM50 subtype of the originating tumor ("human") and passage 1 (P1) and a later passage (late); *HER2* and *ESR1* mRNA levels normalized to WHIM2 P1, *PIK3CA*, *TP53*, and *ESR1* mutation status and phosphoprotein ranking based on WHIM RPPA data within the context of 386 TCGA breast tumors (Table S2C; Figure S3).

See also Figures S5 and S12. WT, wild-type.

[a]WHIM2 and WHIM5 from the same patient.

[b]WHIM20 and WHIM23 from the same patient.

[c]Reference WHIM2 early passage.

number of xenograft-specific mutations in the homozygous range of 80% or higher (Figure 2D). This pattern suggests the emergence of a clone that was below the detection limit in the originating tumor sample but had become a significant contributor to the PDX mutational repertoire.

Most PDX-Specific Mutations Are Not Expressed

The RNA-seq approach (Cancer Genome Atlas Research Network, 2012b) detected mRNA expression from 462 (44%) of the 1,056 validated, nonsilent SNVs identified by DNA sequencing of 13 PDX tumors (Table S2M). Expression was detected for only 39 of the 69 SMG mutations. Of the PDX-unique SMG mutations, only *WNK2* in WHIM8, *PIK3R4* and *KRAS* in WHIM9, and *MAP4K2* in WHIM16 were detectable in the RNA-seq data. However, all *TP53* mutations were expressed at high levels (75%–100% of reads; Table S2H). The RNA-seq data were also used to examine the expression of PDX-specific missense mutations predicted to be functionally significant by Polyphen (Xi et al., 2004). Of the 34 mutations in this class, only 11 were expressed according to the RNA-seq reads (Table S2I): *Hist1H1E* in WHIM6, *ABCC1* in WHIM8, *WDR81* in WHIM13, *MAP4K2* in WHIM16, *ZNF687* in WHIM21, and *KRAS*, *SLC23A*, *LRRC58*, *MAPK9*, *KIF21B*, and *PIK3R4* in WHIM9. Since *MAP3K1* mutations have not been previously reported in available cell lines, RNA-seq analysis was used to confirm that a splice site mutation in WHIM20 indeed generated a splice donor, leading to an out-of-frame *MAP3K1* transcript (Figure S10).

The Estradiol Response of ER+ PDX Mirrors the Clinical Phenotype of the Originating Tumor

The estradiol dependence of each ER+ PDX was studied by transplantation into oophorectomized mice with or without estradiol supplementation. Four lumenal PDX exhibited estradiol-independent growth (Figures 4A, 4B, 4D, and 4E) consistent with the fact these xenografted samples were accrued after the development of aromatase inhibitor resistance (Table S2A). WHIM24 was the only example that exhibited estradiol-dependent growth (Figure 4F); the patient who contributed this sample had a protracted clinical course and experienced a durable clinical response to tamoxifen after xenograft sample accrual. The growth of WHIM16 was delayed by estradiol (Figure 4C). Furthermore, established WHIM16 tumors exhibited marked regression in response to estradiol exposure (Figure 4G), modeling the paradoxical estradiol treatment of advanced breast cancer, which produced a modest response in the patient who contributed this sample (Ellis et al., 2009). The patient who donated WHIM18 had a particularly striking history of fulvestrant resistance (progression within 1 month of therapy; Table S2A), and WHIM18 proved to be just as fulvestrant unresponsive in the PDX setting (Figure 4H).

ESR1 Translocation, Point Mutation, or Gene Amplification in ER+ PDX Models

The RNA-seq data analysis identified five interchromosomal in-frame gene fusion events (Figure S11), including a balanced translocation between 6q and 11q in WHIM18 that created a transcript encoding the 5′ four exons of *ESR1* (amino acids

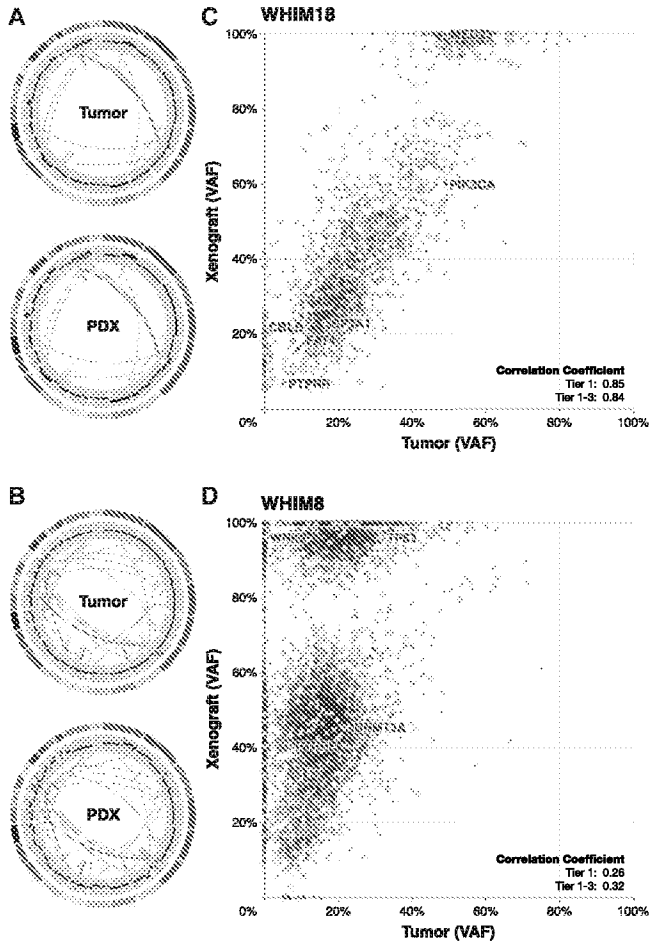


Figure 2. Pairwise Genome-Wide VAF, CNV, and SV Analyses

(A and B) The circos plots for (A) WHIM18 and (B) WHIM8 show the closely matched SVs and CNVs in the tumor of origin and the paired WHIM line. To compare differences in mutant allele frequency between the originating tumor and the PDX counterpart, the read counts for each mutant and wild-type allele were expressed as a percentage of all reads at that position and analyzed by scatterplot and simple correlation coefficient.

(C) WHIM18 has a high correlation coefficient (0.84) in both the coding region (yellow) and noncoding region (blue). The VAF stability was maintained across all six SMG mutations.

(D) WHIM8 represented the opposite extreme with a low correlation coefficient (0.32) and a relatively large number of xenograft-specific mutations in the homozygous range of 80% or higher. Related to this figure are analyses for the other whole-genome sequenced originating tumor/PDX pairs that are displayed in Figures S7A–S9.

See also Figure S6.

1–365), fused to the C terminus of *YAP1* (amino acids 230–504; Figure 5A). Western blots on WHIM18 extracts confirmed the presence of an appropriately sized ESR1/YAP1 fusion protein that was detected by an N-terminal ESR1 antibody and a YAP1 antibody, but not by a C-terminal ESR1 antibody (Figure 5E). Gene amplification across the *ESR1* promoter and coding region was observed in WHIM16 (Figure 5B) and was associated with high levels of ESR1 protein (Figure 5D). To quantify and confirm the degree of amplification in WHIM16, we conducted quantitative PCR (qPCR) of the promoter region and two regions of the coding sequence of ESR1 (Figure 5C). In this experiment, MCF7 cell DNA was used as a nonamplified ESR1 control, and, unexpectedly, MCF7 cells that had been subjected to long-term estrogen deprivation (LTED) (Sanchez et al., 2011), but not parental MCF7 cells, showed marked *ESR1* gene amplification (Figure 5C) with associated increased expression levels of ESR1 protein (Figure 5E). These data suggest that *ESR1* amplification is an adaptation to estrogen deprivation in this well-studied model. WHIM20 expressed an *ESR1-Y537S* point mutation that was present in the majority of reads (96%) in the RNA-seq data (Table S2M). WHIM24 harbored an *ESR1-E380Q* mutation (Table S2D), which was not detected in the originating tumor but was present in 42 of 42 reads in the PDX (Figure S12). Low estradiol xenografting (i.e., no E2 supplementation) may therefore favor the growth of tumors with somatic variants in ESR1, since four out of seven ER+ PDXs analyzed by sequencing contained a mutation or a gene rearrangement. Interestingly, in a recent study by Piccart et al. (2013), *ESR1* sequencing of advanced breast cancer samples from a clinical trial revealed both *ESR1-Y537S* and *ESR1-E380Q*. Piccart et al.'s report, in combination with our observations, clearly delineates a hot spot of ligand-binding-domain *ESR1* mutations in advanced breast cancer (Figure 5D) that complement the initial example (*Y537N*) reported in the 1990s (Zhang et al., 1997).

ESR1/YAP1 and ESR1-Y537S Induce Estradiol-Independent Growth

ESR1-Y537S and ESR1-Y537N are known to induce estradiol-independent transcriptional activity (Weis et al., 1996; Zhang et al., 1997). To compare the properties of *ESR1* point mutations affecting the Y537 residue with the ESR1/YAP1 fusion gene product, MCF7 and T47D lines were engineered to overexpress wild-type ESR1, ESR1YAP1, ESR1-Y537S, and ESR1-Y537N proteins (YFP provided the control). Under low-estrogen conditions, all three mutant ESR1 constructs increased proliferation in T47D and MCF7 cells compared with the YFP control, and the three mutant ESR1 constructs were all more active than wild-type ESR1 (Figure 6A). In T47D cells, the proliferation of cells harboring ESR1-Y537N or ESR1-Y537S was largely estradiol independent, although some estradiol responsiveness was retained for ESR-Y537N in MCF7 cells. ESR1/YAP1 was as active as the two point mutants in inducing estradiol-independent growth, but E2 was able to further stimulate growth in ESR1/YAP1-expressing cells in T47D cells. This indicates that ESR1/YAP1 does not obviously function to inhibit the function of endogenous ESR1 (i.e., it was not dominant negative). Fulvestrant significantly inhibited the growth of cells expressing ESR1-Y537S, ESR1-Y537N, and wild-type ESR1, and induced downregulation of wild-type and mutant ER protein expression (Figure S13). However, growth suppression was incomplete for the two point mutants, suggesting partial resistance to fulvestrant. Cells expressing the ESR1/YAP1 fusion were clearly insensitive to fulvestrant and the fusion protein was not downregulated, since the ligand-binding domain of ESR1 is absent from this chimeric protein (Figure S13). Similar overall findings regarding growth induction under low-estrogen conditions by ESR1 mutants and the ESR1/YAP1 fusion were made in MCF7 cells (Figure 6B). Of note, however, cells expressing

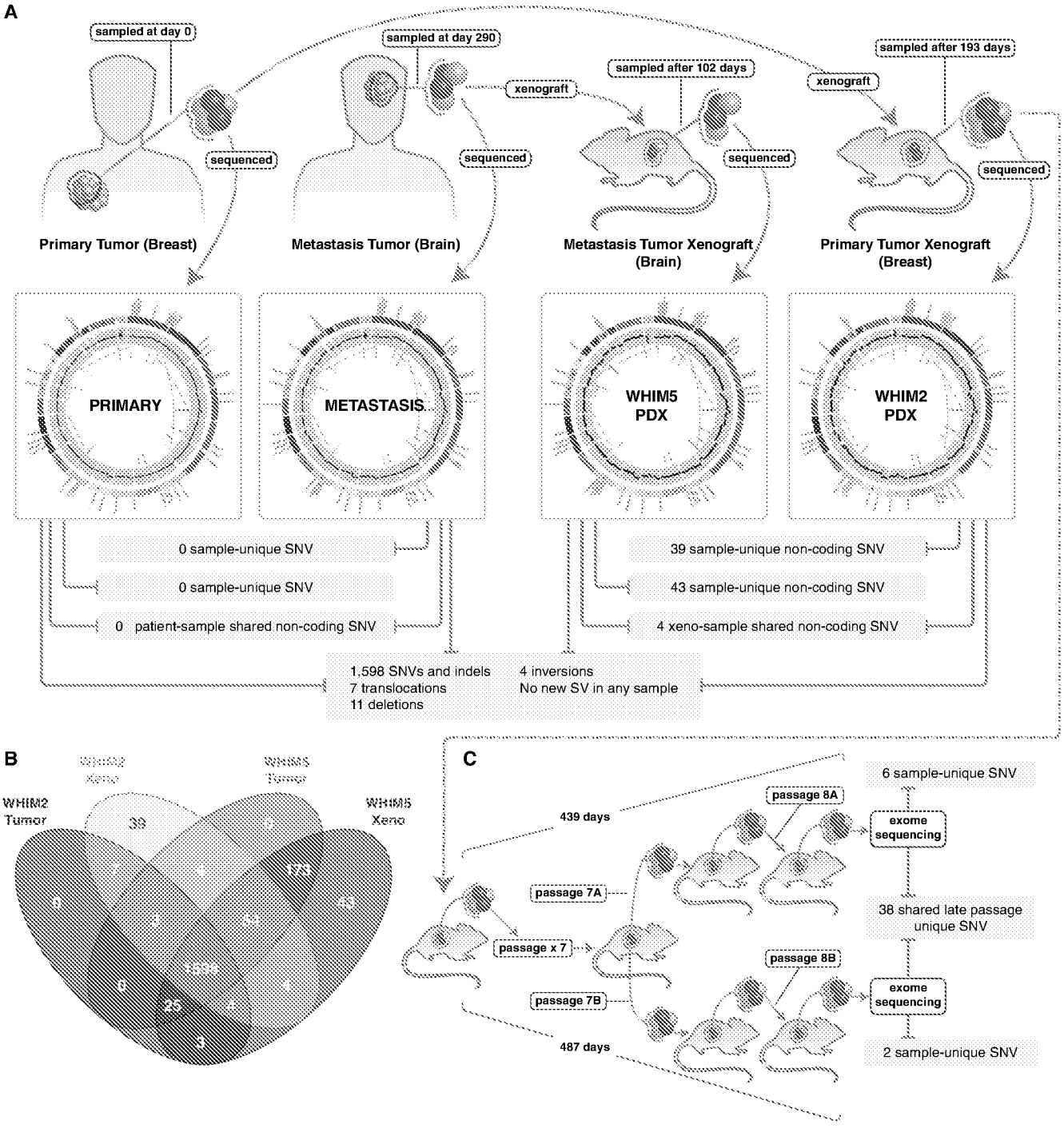


Figure 3. Whole-Genome Comparisons of Breast Primary Tumor and Brain Metastasis with their Counterpart PDX Model Xenografts from the Same Patient

(A) The majority of the validated somatic SNVs were shared by the breast primary tumor, brain metastasis, and xenografts (1,598). In addition, seven translocations, 11 large deletions, and four inversions were present in all samples, without any SV detected or lost upon engraftment.

(B) The breast primary tumor and brain metastasis contained no sample-unique SNVs, i.e., all of the SNVs were noted in at least one other sample. However in every comparison, more SNVs were observed in the later time sample than in the earlier sample. In a comparison of the two human specimens, 13 were unique to the primary tumor and 231 were unique to the metastasis. Additionally, both WHIM lines harbored additional sample-unique noncoding SNVs (39 in the case of WHIM2 and 43 in the case of WHIM5).

(C) Exome sequencing of two separate DNA samples isolated from WHIM2 passage 8, after expansion for therapeutic studies. Mutations in coding space have accumulated, but a study of the 38 mutations observed in both samples suggests that most are passengers rather than biological drivers.

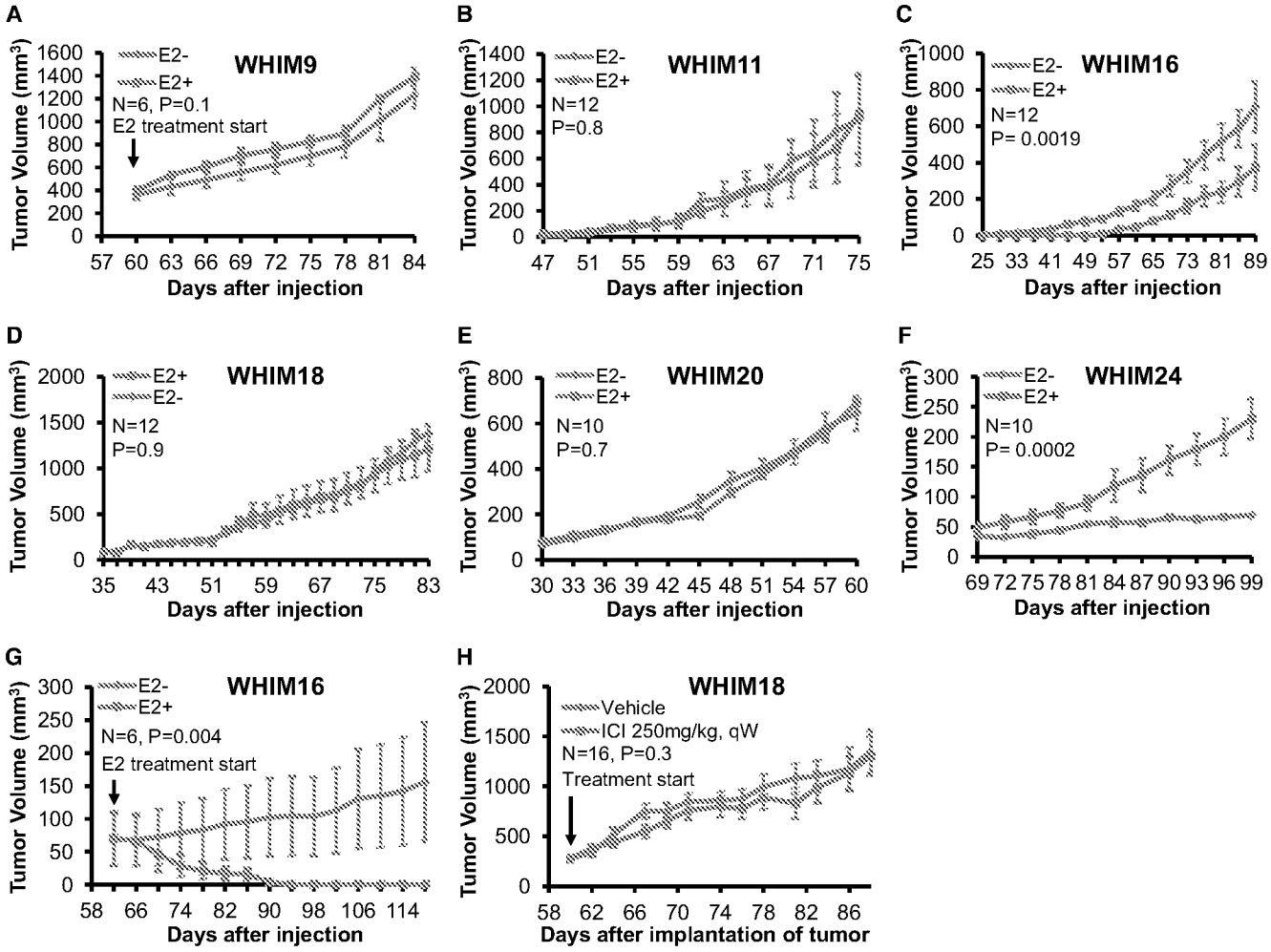


Figure 4. Estradiol Dependency and Tumor Doubling Times for the ER+ WHIM Lines

(A and G) WHIM9 cells (A) or WHIM16 cells (G) were allowed to establish tumor nodules in ovariectomized nonobese diabetic (NOD)/severe combined immunodeficiency (SCID) mice and then treated with or without 17β-estradiol pellets.

(B–F) Tumor cells were subcutaneously injected into ovariectomized NOD/SCID mice and then immediately treated with 17β-estradiol pellets or observed.

(H) Fragments of WHIM18 tumor tissue were subcutaneously engrafted into female CB.17 SCID mice. Tumor-bearing mice were treated in the presence or absence of fulvestrant when tumor size reached 300 mm^3. All data were analyzed in SAS using the PROC MIXED function.

ESR1-Y537S grew poorly relative to cells expressing other ESR1 mutant constructs and exhibited signs of cell death (data not shown). Gain-of-function ESR1 point mutants may therefore require a cellular background that is tolerant of the extreme properties of these constitutively active ESR1 mutants. In accord with this hypothesis, ectopic expression levels for the Y537S mutant were lower than wild-type ER in both T47D and MCF7 (Figures 6C and 6D), and were extremely low in WHIM20, which naturally expresses the ESR1-Y537S mutant (Figure 6E). Lysates from cells grown in charcoal-stripped serum (CSS) media were analyzed for progesterone receptor (PR) and trefoil factor 1 (TFF1) expression by western blot. In both cell lines, the ESR1 point mutations strongly induced PR expression in a hormone-independent fashion relative to wild-type ESR1 and YFP control lines, whereas ESR1/YAP1 had a more modest effect. For TFF1, the two ESR1 point mutants induced expression in MCF7 cells in low-estradiol conditions, but caused less induction in the T47D cells. ESR1/YAP1 strongly induced TFF1 expression relative to wild-type in both cell lines. In the WHIM tumors that expressed these mutations naturally, high PR expression was associated with the lines expressing the mutations or gene rearrangements (WHIM16, WHIM18, WHIM20, and WHIM24). In contrast, WHIM lines with a wild-type ESR1 locus (WHIM9 and WHIM11) but estradiol-independent growth showed very low levels of PR expression (Figure S14).

DISCUSSION

In this study, we assessed the degree to which breast cancer PDX models are genomic replicas of human tumors based on genome-wide analysis, including translocations, insertions, deletions, point mutations, and amplification events. The stability

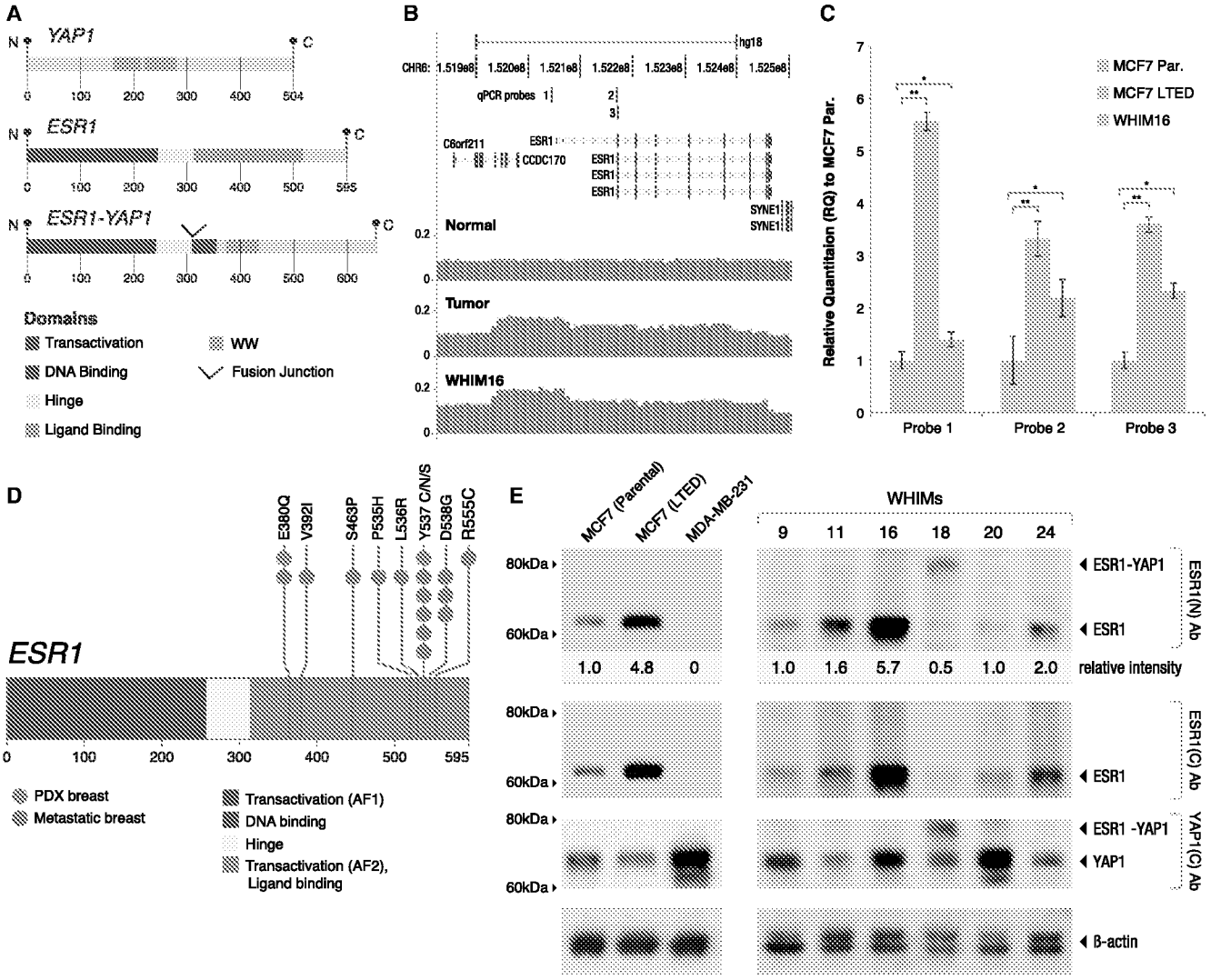


Figure 5. ESR1 Gene Rearrangements and Point Mutations in Lumenal PDX Models

(A) WHIM18 and the originating tumor harbored a balanced translocation between 6q and 11q in WHIM18 that created a fusion-transcript-defected mRNA-seq that encodes the 5′ four exons of *ESR1* (amino acids 1–365, including the DNA-binding domain but not the steroid-binding domain) fused to the C terminus of *YAP1* (amino acids 230–504), thereby excluding the TEAD domain and the first WW motif of *YAP1*, but retaining the second WW motif, the SH3 domain, the YES phosphorylation site, and the transactivation domain.

(B) WHIM16 and the originating tumor harbor amplification of the *ESR1* gene that extends from the promoter region throughout the coding sequence that was mapped using read counts obtained during WGS.

(C) qPCR on genomic DNA using three separate probes was used to confirm gene amplification in WHIM16 cells. The negative control was MCF7 cells. In a screen for *ESR1*-gene-amplified cell lines, MCF7 cells that were adapted after LTED were found to have developed *ESR1* gene amplification. qPCR results were normalized relative to parental MCF7 (Par.). The positions of probes 1, 2, and 3 are displayed in (B). Error bars are ±1 SD of the mean relative quantification (RQ); *$p < 0.05$, ** is $p < 0.01$.

(D) WHIM20 cells harbored and expressed a mutation in *ESR1-Y537S*, and WHIM24 harbors *ESR1-E380Q* (indicated in blue). The finding of *ESR1-V537S* and *ESR1-E380Q* in these PDX lines complements a recent report on *ESR1* sequencing of advanced disease samples in which multiple mutations in the AF2/ligand-binding domain (in pink) were observed (Piccart et al., 2013; mutation positions from this report are indicated in red).

(E) Tumor lysates from six ESR1+ WHIM lines (WHIM9, WHIM11, WHIM16, WHIM18, WHIM20, and WHIM24) were analyzed by western blot using antibodies targeting the N terminus or C terminus of ESR1 or the C terminus of *YAP1*. In parallel, lysates from three breast cancer cell lines (parental MCF7, LTED MCF7, and MDA-MB-231) were analyzed as controls. All blots were replicated four times. ESR1 intensity detected by the N-terminal ER antibody was quantified and normalized against the actin level. For WHIM lines, the normalized ESR1 levels were averaged from four replicate blots and expressed as relative intensities using WHIM9 as the internal reference (arbitrarily set at one). For cell lines, ESR1 levels were similarly normalized against actin and expressed as relative values using parental MCF7 as the internal reference. Lysates from cell lines and WHIM tumors were analyzed in the same blot, but the images displayed reflect different exposure times.

See also Figure S1B.

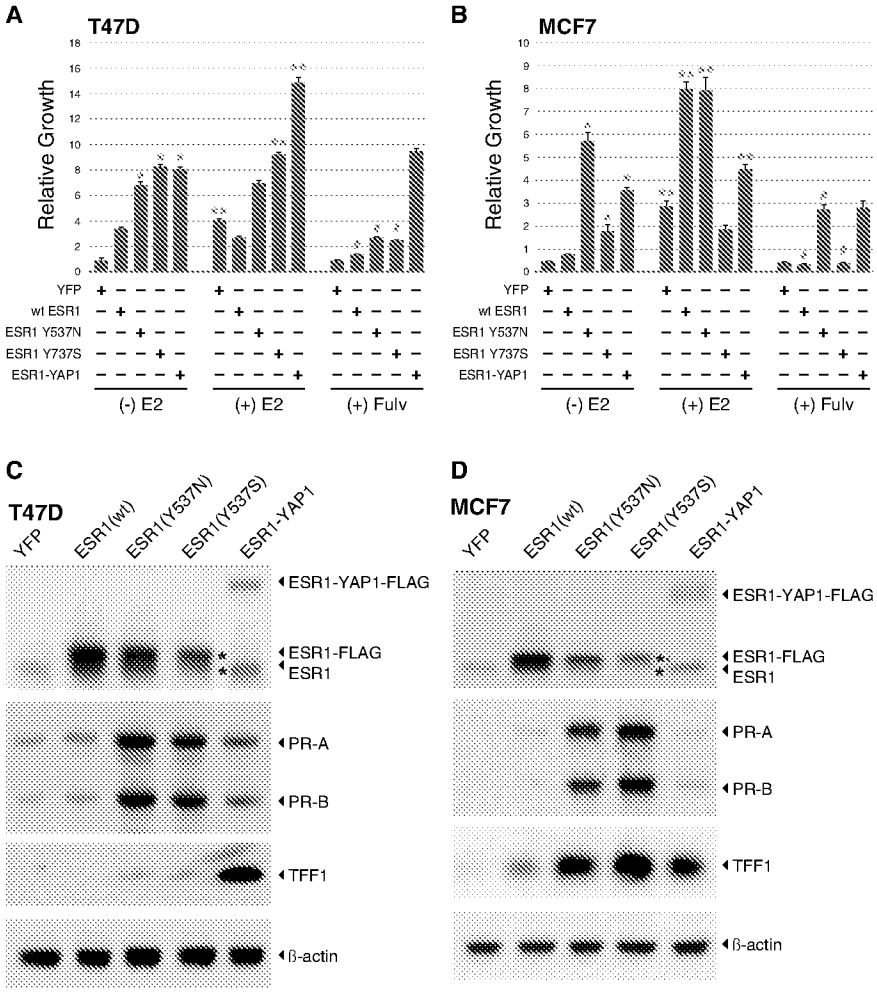


Figure 6. Point Mutations and a Translocation in ESR1 Induce Estradiol-Independent Growth

(A and B) T47D(A) and MCF7 (B) cells stably transduced with lentiviral vectors expressing the YFP control gene (YFP), wild-type ESR1 (WT ESR1), ESR1 point mutants (ESR1-Y537N and ESR1-Y537S), and the ESR1-YAP1 fusion gene (ESR1-YAP1) were grown in CSS medium for at least 2 weeks. Cells were then plated in CSS medium containing no supplemental estrogen (−E2), 10 nM estradiol (+E2), or medium without estrogen +500 nM fulvestrant (+ Fulv), and growth was measured after 10 days by Alamar blue assay. Mean results, with standard SEM as error bars, are shown for four experiments (T47D) and three experiments (MCF7), with each experiment conducted in quadruplicate. Cell growth in each line was normalized to baseline values obtained the day after the cells were plated, prior to the beginning of treatment. Expression of the ESR1 point mutants and ESR1-YAP1 fusion significantly promoted the growth of estrogen-deprived cells compared with WT ESR1 or YFP control (*$p < 0.05$ indicates significant growth stimulation versus YFP or WT ER). The effect of estradiol was then assessed for each lentivirus construct (**$p < 0.05$ indicates a significant stimulatory effect for each construct with and without estradiol). In T47D cells, estradiol stimulated the growth of YFP, ESR1-Y537S (minimally), and ESR1-YAP1, but not WT-ESR1 or ESR1-Y537N. In contrast, in MCF7 cells, estradiol promoted the growth of WT-ESR1, ESR1-Y537N, and to a much lesser extent ESR1-YAP1, but not ESR1-Y537S. Treatment with fulvestrant significantly inhibited estrogen-independent growth of cells expressing WT ER and ER point mutants (#$p < 0.05$), but not the ER-YAP1 fusion.

(C and D) T47D (C) and MCF7(D) cells were cultured for 8 days in CSS medium, followed by western blot for the expression of endogenous and exogenous ESR1 using an N-terminal antibody and two direct ESR1 downstream targets (progesterone receptor [PR-A and PR-B] and TFF1) with an actin loading control. Due to the substantially lower basal TFF1 expression in T47D cells compared with MCF7 cells, the T47D TFF1 blot was intentionally exposed for a longer time for visualization.

See also Figures S13 and S14.

of SVs was striking, suggesting that these genomic features may stabilize early in pathogenesis, perhaps during telomere crisis (Chin et al., 2004). Regarding SNVs, almost all mutations detected in the originating tumor were present in the PDX, but a variable number of SNVs were PDX unique (Table S2I). However, RNA-seq data indicated that most PDX-unique SNVs have expression levels below the detection limit and therefore may be passengers. PDX-unique mutations could arise in the mouse after xenografting or may represent a rare subclone that existed below the detection limit in the originating tumor but increased into the detectable range during growth in the mouse. Deep analysis of a "quartet" of a primary and metastasis pair with their counterpart PDX lines WHIM2 and WHIM5 suggests that xenograft-specific mutations indeed arise over time. When we compared samples taken at a later time point with those obtained an earlier time point, whether in the human setting (primary tumor and brain metastasis) or xenograft setting, we found that the later samples contained multiple SNVs (Figure 3). These mutations may increase "tumor fitness" in the transplanted environment or may just be passengers in a constantly mutating tumor (most were in noncoding regions). PDX-specific SNVs may simply arise from serial population reductions during repeated xenografting events, which can select a passenger mutation at random due to cell attrition during transplantation ("population bottlenecking"; Gisselsson et al., 2010). This might explain the accumulation of seemingly nonfunctional mutations observed with late-passage exome sequencing (Table S2K). However, selection by increasing tumor fitness is a more likely explanation for cases in which the PDX-specific mutations were detectable at the mRNA level and were functionally linked to cancer biology, such as *WNK2* in WHIM8 (Jun et al., 2009; Moniz et al., 2007), *PIK3R4* (Huang et al., 2011; Shull et al., 2012) and *KRAS* (Santos et al., 1984) in WHIM9, *MAP4K2* in WHIM16 (Lau et al., 2012), and *ESR1-E380Q* in WHIM24. Thus, we are not arguing that PDXs are perfect genomic replicas of the originating tumors; rather, we suggest that tracking the

PDX genome, benchmarked against the originating tumor, is a way to assess the ongoing genomic integrity of the model during experimentation. This is something that has never been considered for conventional cell-line approaches, where the progenitor tumor genome is rarely available and analysis of ongoing genetic drift is not a routine aspect of experimental design.

An important issue that was not addressed by previous investigations is the effect of the xenografting process on the VAF, since each mutation can either be present in the founder clone (and therefore present in all cells) or arise later in a subclone and therefore occur with a lower frequency because it is present in only a subpopulation of cells. VAF analysis, perhaps surprisingly, showed that the VAF for many mutations was preserved in the PDX, even in the case of rare mutations. This implies that clonal representation can be transplantable, i.e., different clones maintain their relative prevalence in equilibrium. Since clonal prevalence is maintained despite growth in an immunocompromised host, immunoediting (differential immune responses against particular mutant proteins) is an unlikely explanation for relative clone abundance in this setting (DuPage et al., 2012; Matsushita et al., 2012). Our findings are compatible with other recent studies on the clonal diversity of epithelial cancers, which showed that minor clones are carried at low frequencies for many passages until a section event (e.g., therapeutic intervention or the process of adaption to growth in a new organ) increases the minor mutation prevalence (Ding et al., 2012; Kreso et al., 2013).

Genomic analysis of each ER+ PDX raised tumor-unique hypotheses to explain endocrine-therapy resistance, underscoring the etiological heterogeneity of this common clinical problem. The WHIM11 line was isolated from a patient with a fulminant clinical course and little evidence for sensitivity to endocrine therapy (Table S2A). Despite the patient's ER+ HER2− status, WHIM11 was classified as HER2-E by PAM50. This biomarker pattern predicts poor responsiveness to aromatase inhibition (Ellis et al., 2011). WHIM11 was a *TP53* mutant and harbored a biallelic deletion in *PTEN* (Figure S6). RPPA data confirmed high levels of pS70S5K and 4EBP1 protein phosphorylation, indicating phosphoinositol-3-kinase pathway activation (Figure S3), which has been implicated in endocrine-therapy resistance (Sanchez et al., 2011). WHIM9 harbored monoallelic expression of an R515I mutation in *SMAD4* (Table S2M). *SMAD4* mutations were recently associated with genome instability in head and neck cancer (Bornstein et al., 2009), which could explain why this particular lumenal PDX had a high rate of PDX-specific mutations, although which mutation caused endocrine resistance in this line remains unclear.

WHIM16 exhibited paradoxical regression with estradiol, which is an effective but nonintuitive late-line endocrine therapy for some advanced ER+ breast cancers (Ellis et al., 2009). The *ESR1* amplification and high-level ESR1 protein expression in WHIM16 therefore raise the hypothesis that *ESR1* amplification may be a predictive marker for responsiveness to estradiol therapy in advanced disease. This suggestion is consistent with the finding (Figures 5B and 5C) that MCF7 cells develop *ESR1* gene amplification after LTED in vitro, conditions under which estradiol is well known to induce apoptosis (Lewis et al., 2005; Song et al., 2001). In T47D cells, overexpression of wild-type ESR1 gene/protein increased growth in low-estradiol conditions, supporting the notion that by driving ESR1 overexpression, *ESR1* gene amplification promotes adaptive resistance to estrogen deprivation (Figure 6B). This hypothesis is also compatible with clinical observations indicating that *ESR1* amplification is associated with poor clinical outcome (Ejlertsen et al., 2012; Lin et al., 2013; Nielsen et al., 2011).

The *ESR1-Y537S* hormone-binding-domain mutation is clearly a potent cause of aromatase-inhibitor resistance. Expression of ESR1-Y537S produced greater growth than wild-type ESR1 under estrogen-deprived conditions and very strong induction of PR in the absence of estradiol in both cell lines tested (Figures 6C and 6D). Since *ESR1-Y537S* (or other mutations in this region of *ESR1*) was not observed in >500 exome sequencing experiments by the TCGA, it seems likely that mutations in the hormone-binding domain largely occur as an adaptation to endocrine treatment. Consistent with this conclusion, an *ESR1* mutation hotspot in the ligand-binding-domain/AF2 region was observed in metastatic samples from a clinical trial for patients with nonsteroidal aromatase-inhibitor-resistant advanced breast cancer (Piccart et al., 2013). Our in vitro data indicate that ESR1-Y537S was responsive to fulvestrant, as protein expression was downregulated. However, suppression of growth was incomplete, indicating partial resistance (Figures 6 and S13). The patient whose tumor harbored *ESR1-Y537S* (WHIM20) experienced only 4 months of clinical benefit from fulvestrant, which is compatible with the hypothesis that *ESR1-Y537S*-positive tumors may be less responsive to this commonly used second-line endocrine intervention for advanced breast cancer. WHIM24, a PDX that was estradiol dependent (Figure 4) and associated with a tamoxifen clinical response (but resistance to aromatase inhibition) harbored an *ESR1-E380Q* mutation. This mutation has already been documented to be associated with estradiol hypersensitivity, increased DNA binding, and estradiol-independent activity (Pakdel et al., 1993). However, *ESR1-E380Q* was not detected in the relatively low-coverage WGS analysis of the originating tumor, so the link with the clinical phenotypes observed is uncertain (Figure S11).

The identification of the *ESR1/YAP1* fusion gene in WHIM18 completes the mechanistic spectrum of gain-of-function mutations in ESR1 associated with endocrine-resistant breast cancers. YAP1 plays a central role in organ size and tumorigenesis through the Hippo pathway (Lin et al., 2013); however, the domains that are responsible for most of these biological properties are in the N terminus of *YAP1* and therefore absent from the fusion gene. Analysis of TCGA breast cancer RNA-seq data revealed two other in-frame fusion genes that preserve at least the first four exons of ESR1 (preserving DNA binding). In one case, a fusion was detected with *AKAP12*, a putative tumor-suppressor gene (Gelman, 2012), and in the second case it was detected with *POLH*, a DNA polymerase associated with xeroderma pigmentosum (Ortega-Recalde et al., 2013; Figure S15). These findings indicate that the *ESR1/YAP1* translocation documented in WHIM18 is not a private event, but is a member of a class of translocations that preserve the DNA-binding and AF1 domains of *ESR1* with variable in-frame C-terminal partners that replace the ligand-binding and AF2 domains. Although these in-frame *ESR1* translocations are likely rare, the

denominator for breast cancer is so large that even low percentages of particular somatic events can represent clinically significant patient populations if the effect on the disease course is dramatic (i.e., in this instance, intrinsic and universal endocrine-therapy resistance).

In conclusion, PDX models validated through comparative whole-genome analysis against the originating tumor are a useful starting point for studies of the molecular pharmacology of advanced breast cancer. No actively growing cancer has a static genome, and genetic drift though cell attrition is inherent in the xenografting process. Furthermore, selection of mutations that increase tumor fitness in the murine environment is to be expected. However, unlike conventional cell lines, PDX-specific mutations can be monitored with reference to the genome of the originating human tumor, establishing a tumor "pedigree" that can be checked before and after each functional or pharmacological experiment. This continuous genomic annotation approach is illustrated by the late-passage exome sequencing conducted in WHIM2 (Figure 3).

The identification of endocrine-resistance-associated ESR1 gene rearrangements and point mutations has deep implications for the management of metastatic breast cancer. The choice of endocrine therapy in an advanced-disease setting could be based on the presence and class of *ESR1* gene mutations and rearrangements if more were known about the correlations with outcomes. The detection of these mutations in the xenograft setting establishes the principle that the PDX approach captures genomic events that have been understudied in the past because they are not present in conventional ER+ cell lines even when experimentally selected for endocrine drug resistance in vitro. The availability of authentic PDX-based models of endocrine-therapy-resistant lumenal breast cancer will facilitate the testing of therapeutic interventions and perhaps particularly those designed to more effectively target mutant forms of ESR1.

EXPERIMENTAL PROCEDURES

Generation and Analysis of PDX Breast Cancer Models

All human tissues for these experiments were processed in compliance with NIH regulations and institutional guidelines, and approved by the institutional review board at Washington University. All animal procedures were reviewed and approved by the institutional animal care and use committee at Washington University in St. Louis. Detailed methods are provided in Extended Experimental Procedures. PDX models are available through the application to the Human and Mouse-Linked Evaluation of Tumors core at http://digitalcommons.wustl.edu/hamlet/.

WGS and Capture Validation

Seventeen patients with blood, tumor, and xenograft were selected for WGS. Detailed histories for these patients and xenografts are provided in Table S2A. Libraries were prepared using unamplified genomic DNA from blood (normal), tumor, and xenograft samples. Paired-end sequencing was performed on the Illumina platform as previously described (Ellis et al., 2012; Walter et al., 2012). Variant calling and validation of all mutations using liquid-phase hybridization capture were performed as previously described (Welch et al., 2012). All DNA have been deposited with dbGAP under accession number phs000611 (http://www.ncbi.nlm.nih.gov/projects/gap/cgi-bin/study.cgi?study_id=phs000611.v1.p1).

mRNA-Seq

mRNA-seq was performed as previously described (Cancer Genome Atlas Research Network, 2012b). Reads were mapped using the MapSplice algorithm (Wang et al., 2010). Expressed gene fusions were nominated using ChimeraScan v0.4.3 (Iyer et al., 2011) with default parameters. Gene fusion nominations were required to have at least two independent spanning junction reads. Sequences will be made available upon application to CGHub. TCGA mRNA-seq data can be accessed through the TCGA program (http://cancergenome.nih.gov). All PDX mRNA-seq data have also been deposited with dbGAP under accession number phs000611 (http://www.ncbi.nlm.nih.gov/projects/gap/cgi-bin/study.cgi?study_id=phs000611.v1.p1).

DNA Microarray-Based Gene-Expression Analysis

Agilent's 4x44K Whole Human Gene expression microarray processing, data quality control and processing, and research use only PAM50 subtype classification were previously described (Ellis et al., 2011). The stromal-related genes were identified after a two-class paired significance analysis of microarrays (SAM) with an FDR of 0% between 18 paired progenitor human tumors and xenografts (Table S2B). The GEO accession number for the chip-based gene expression data reported in this paper is GSM41685. PDX tumors were also analyzed by 244K UNC customized Agilent chips for clustering with data with unmatched primary tumors (GEO accession number GSE46604).

Quantification of ESR1 Amplification

A real-time PCR system (Life Technologies) was run for *ESR1* amplifications using control genes *FAM38B* and *ASXL2* as described previously (Reis-Filho et al., 2008).

RPPA, In Vitro Growth Assays, Lentivirus Gene Transduction, and Western Blots

Standard methods were used for RPPA (Tabchy et al., 2011); see Extended Experimental Procedures for other standard protein-analysis approaches.

Statistical Methods

Hierarchical clustering was applied with a distance metric of one minus the Pearson correlation coefficient and using the average linkage method. Clustering results were visualized as dendrograms in heatmaps. Pearson and Spearman rank-based correlation coefficients were separately calculated to demonstrate VAF stability between a PDX and its patient origin.

ACCESSION NUMBERS

The dbGAP accession number for the DNA and PDX mRNA sequences reported in this paper is phs000611. The GEO accession number for the gene-expression data used in Figure 1B is GSM41685. PDX tumors were also analyzed by 244K UNC customized Agilent chips for clustering with data from primary tumors (GEO accession number GSE46604; Figure S3).

SUPPLEMENTAL INFORMATION

Supplemental Information includes Extended Experimental Procedures, 15 figures, and two tables and can be found with this article online at http://dx.doi.org/10.1016/j.celrep.2013.08.022.

ACKNOWLEDGMENTS

This work was funded by grants to M.J.E. by Susan G. Komen for the Cure (BCTR0707808, KG090422, and PG12220321). The DNA sequencing and analysis were performed by the Genome Institute at Washington University School of Medicine and supported by grants to R.K.W. from the National Human Genome Research Institute (NHGRI U54 HG003079). The Tissue Procurement Core was supported by NCI 3P50 CA68438. The HAMLET Core was supported by CTSA grant UL1 RR024992. M.J.E. is also supported as a Susan G. Komen Scholar and by the Breast Cancer Research Fund, the Barnes Jewish Hospital Foundation, the Theresa Harpole Foundation for Metastatic

Breast Cancer, and a gift from the Mary Speak family. The RPPA analysis was supported by NCI grants PO1CA099031, U54CA112970, KG081694, and P30 CA16672 to G.M. The RNA-seq was supported by grants from the TCGA Project (U24-CA143848), the NCI Breast SPORE Program (P50-CA58223-09A1), and the Breast Cancer Research Foundation to C.M.P. M.J.E. and C.M.P. own shares and have leadership positions in Bioclassifier and University Genomics, which has licensing income from patents related to the ProSigna breast cancer intrinsic subtype test.

Received: May 6, 2013
Revised: July 16, 2013
Accepted: August 9, 2013
Published: September 19, 2013

WEB RESOURCES

The URLs for data presented herein are as follows:

The Cancer Genome Atlas, http://cancergenome.nih.gov
Digital Commons, http://digitalcommons.wustl.edu/hamlet/
Index of OOMPA, http://bioinformatics.mdanderson.org/OOMPA
NCBI, http://www.ncbi.nlm.nih.gov/projects/gap/cgi-bin/study.cgi?study_id=phs000611.v1.p1
UNC Microarray Database, https://genome.unc.edu/

REFERENCES

Bornstein, S., White, R., Malkoski, S., Oka, M., Han, G., Cleaver, T., Reh, D., Andersen, P., Gross, N., Olson, S., et al. (2009). Smad4 loss in mice causes spontaneous head and neck cancer with increased genomic instability and inflammation. J. Clin. Invest. *119*, 3408–3419.

Cancer Genome Atlas Network. (2012a). Comprehensive molecular portraits of human breast tumours. Nature *490*, 61–70.

Cancer Genome Atlas Research Network. (2012b). Comprehensive genomic characterization of squamous cell lung cancers. Nature *489*, 519–525.

Chin, K., de Solorzano, C.O., Knowles, D., Jones, A., Chou, W., Rodriguez, E.G., Kuo, W.L., Ljung, B.M., Chew, K., Myambo, K., et al. (2004). In situ analyses of genome instability in breast cancer. Nat. Genet. *36*, 984–988.

DeRose, Y.S., Wang, G., Lin, Y.C., Bernard, P.S., Buys, S.S., Ebbert, M.T., Factor, R., Matsen, C., Milash, B.A., Nelson, E., et al. (2011). Tumor grafts derived from women with breast cancer authentically reflect tumor pathology, growth, metastasis and disease outcomes. Nat. Med. *17*, 1514–1520.

Ding, L., Ellis, M.J., Li, S., Larson, D.E., Chen, K., Wallis, J.W., Harris, C.C., McLellan, M.D., Fulton, R.S., Fulton, L.L., et al. (2010). Genome remodelling in a basal-like breast cancer metastasis and xenograft. Nature *464*, 999–1005.

Ding, L., Ley, T.J., Larson, D.E., Miller, C.A., Koboldt, D.C., Welch, J.S., Ritchey, J.K., Young, M.A., Lamprecht, T., McLellan, M.D., et al. (2012). Clonal evolution in relapsed acute myeloid leukaemia revealed by whole-genome sequencing. Nature *481*, 506–510.

DuPage, M., Mazumdar, C., Schmidt, L.M., Cheung, A.F., and Jacks, T. (2012). Expression of tumour-specific antigens underlies cancer immunoediting. Nature *482*, 405–409.

Ejlertsen, B., Aldridge, J., Nielsen, K.V., Regan, M.M., Henriksen, K.L., Lykkesfeldt, A.E., Müller, S., Gelber, R.D., Price, K.N., Rasmussen, B.B., et al.; Danish Breast Cancer Cooperative Group; BIG 1-98 Collaborative Group; International Breast Cancer Study Group. (2012). Prognostic and predictive role of ESR1 status for postmenopausal patients with endocrine-responsive early breast cancer in the Danish cohort of the BIG 1-98 trial. Ann. Oncol. *23*, 1138–1144.

Ellis, M.J., and Perou, C.M. (2013). The genomic landscape of breast cancer as a therapeutic roadmap. Cancer Discov *3*, 27–34.

Ellis, M.J., Gao, F., Dehdashti, F., Jeffe, D.B., Marcom, P.K., Carey, L.A., Dickler, M.N., Silverman, P., Fleming, G.F., Kommareddy, A., et al. (2009). Lower-dose vs high-dose oral estradiol therapy of hormone receptor-positive, aromatase inhibitor-resistant advanced breast cancer: a phase 2 randomized study. JAMA *302*, 774–780.

Ellis, M.J., Suman, V.J., Hoog, J., Lin, L., Snider, J., Prat, A., Parker, J.S., Luo, J., DeSchryver, K., Allred, D.C., et al. (2011). Randomized phase II neoadjuvant comparison between letrozole, anastrozole, and exemestane for postmenopausal women with estrogen receptor-rich stage 2 to 3 breast cancer: clinical and biomarker outcomes and predictive value of the baseline PAM50-based intrinsic subtype—ACOSOG Z1031. J. Clin. Oncol. *29*, 2342–2349.

Ellis, M.J., Ding, L., Shen, D., Luo, J., Suman, V.J., Wallis, J.W., Van Tine, B.A., Hoog, J., Goiffon, R.J., Goldstein, T.C., et al. (2012). Whole-genome analysis informs breast cancer response to aromatase inhibition. Nature *486*, 353–360.

Fleming, J.M., Miller, T.C., Meyer, M.J., Ginsburg, E., and Vonderhaar, B.K. (2010). Local regulation of human breast xenograft models. J. Cell. Physiol. *224*, 795–806.

Gelman, I.H. (2012). Suppression of tumor and metastasis progression through the scaffolding functions of SSeCKS/Gravin/AKAP12. Cancer Metastasis Rev. *31*, 493–500.

Gisselsson, D., Lindgren, D., Mengelbier, L.H., Øra, I., and Yeger, H. (2010). Genetic bottlenecks and the hazardous game of population reduction in cell line based research. Exp. Cell Res. *316*, 3379–3386.

Huang, J., Zhang, L., Greshock, J., Colligon, T.A., Wang, Y., Ward, R., Katsaros, D., Lassus, H., Butzow, R., Godwin, A.K., et al. (2011). Frequent genetic abnormalities of the PI3K/AKT pathway in primary ovarian cancer predict patient outcome. Genes Chromosomes Cancer *50*, 606–618.

Iyer, M.K., Chinnaiyan, A.M., and Maher, C.A. (2011). ChimeraScan: a tool for identifying chimeric transcription in sequencing data. Bioinformatics *27*, 2903–2904.

Jun, P., Hong, C., Lal, A., Wong, J.M., McDermott, M.W., Bollen, A.W., Plass, C., Held, W.A., Smiraglia, D.J., and Costello, J.F. (2009). Epigenetic silencing of the kinase tumor suppressor WNK2 is tumor-type and tumor-grade specific. Neuro-oncol. *11*, 414–422.

Kabos, P., Finlay-Schultz, J., Li, C., Kline, E., Finlayson, C., Wisell, J., Manuel, C.A., Edgerton, S.M., Harrell, J.C., Elias, A., and Sartorius, C.A. (2012). Patient-derived luminal breast cancer xenografts retain hormone receptor heterogeneity and help define unique estrogen-dependent gene signatures. Breast Cancer Res. Treat. *135*, 415–432.

Kreso, A., O'Brien, C.A., van Galen, P., Gan, O.I., Notta, F., Brown, A.M., Ng, K., Ma, J., Wienholds, E., Dunant, C., et al. (2013). Variable clonal repopulation dynamics influence chemotherapy response in colorectal cancer. Science *339*, 543–548.

Kuperwasser, C., Chavarria, T., Wu, M., Magrane, G., Gray, J.W., Carey, L., Richardson, A., and Weinberg, R.A. (2004). Reconstruction of functionally normal and malignant human breast tissues in mice. Proc. Natl. Acad. Sci. USA *101*, 4966–4971.

Lau, K.S., Zhang, T., Kendall, K.R., Lauffenburger, D., Gray, N.S., and Haigis, K.M. (2012). BAY61-3606 affects the viability of colon cancer cells in a genotype-directed manner. PLoS ONE *7*, e41343.

Lewis, J.S., Meeke, K., Osipo, C., Ross, E.A., Kidawi, N., Li, T., Bell, E., Chandel, N.S., and Jordan, V.C. (2005). Intrinsic mechanism of estradiol-induced apoptosis in breast cancer cells resistant to estrogen deprivation. J. Natl. Cancer Inst. *97*, 1746–1759.

Ley, T.J., Mardis, E.R., Ding, L., Fulton, B., McLellan, M.D., Chen, K., Dooling, D., Dunford-Shore, B.H., McGrath, S., Hickenbotham, M., et al. (2008). DNA sequencing of a cytogenetically normal acute myeloid leukaemia genome. Nature *456*, 66–72.

Lin, J.I., Poon, C.L., and Harvey, K.F. (2013). The Hippo size control pathway—ever expanding. Sci. Signal. *6*, pe4.

Marangoni, E., Vincent-Salomon, A., Auger, N., Degeorges, A., Assayag, F., de Cremoux, P., de Plater, L., Guyader, C., De Pinieux, G., Judde, J.G., et al. (2007). A new model of patient tumor-derived breast cancer xenografts for preclinical assays. Clin. Cancer Res. *13*, 3989–3998.

Matsushita, H., Vesely, M.D., Koboldt, D.C., Rickert, C.G., Uppaluri, R., Magrini, V.J., Arthur, C.D., White, J.M., Chen, Y.S., Shea, L.K., et al. (2012).

Cancer exome analysis reveals a T-cell-dependent mechanism of cancer immunoediting. Nature *482*, 400–404.

Moniz, S., Veríssimo, F., Matos, P., Brazão, R., Silva, E., Kotelevets, L., Chastre, E., Gespach, C., and Jordan, P. (2007). Protein kinase WNK2 inhibits cell proliferation by negatively modulating the activation of MEK1/ERK1/2. Oncogene *26*, 6071–6081.

Nielsen, K.V., Ejlertsen, B., Müller, S., Møller, S., Rasmussen, B.B., Balslev, E., Lænkholm, A.V., Christiansen, P., and Mouridsen, H.T. (2011). Amplification of ESR1 may predict resistance to adjuvant tamoxifen in postmenopausal patients with hormone receptor positive breast cancer. Breast Cancer Res. Treat. *127*, 345–355.

Ortega-Recalde, O., Vergara, J.I., Fonseca, D.J., Ríos, X., Mosquera, H., Bermúdez, O.M., Medina, C.L., Vargas, C.I., Pallares, A.E., Restrepo, C.M., and Laissue, P. (2013). Whole-exome sequencing enables rapid determination of xeroderma pigmentosum molecular etiology. PLoS ONE *8*, e64692.

Pakdel, F., Reese, J.C., and Katzenellenbogen, B.S. (1993). Identification of charged residues in an N-terminal portion of the hormone-binding domain of the human estrogen receptor important in transcriptional activity of the receptor. Mol. Endocrinol. *7*, 1408–1417.

Parker, J.S., Mullins, M., Cheang, M.C., Leung, S., Voduc, D., Vickery, T., Davies, S., Fauron, C., He, X., Hu, Z., et al. (2009). Supervised risk predictor of breast cancer based on intrinsic subtypes. J. Clin. Oncol. *27*, 1160–1167.

Piccart, M., Rugo, H., Chen, D., Campone, M., Burris, A.H., Taran, T., Sahmoud, T., Deleu, I., Hortobagyi, G.N., and Baselga, J. (2013). Assessment of genetic alterations in postmenopausal women with hormone receptor-positive, HER2-negative advanced breast cancer from the BOLERO-2 trial by next-generation sequencing. Ann. Oncol. *24*, iii25–iii26.

Prat, A., Parker, J.S., Karginova, O., Fan, C., Livasy, C., Herschkowitz, J.I., He, X., and Perou, C.M. (2010). Phenotypic and molecular characterization of the claudin-low intrinsic subtype of breast cancer. Breast Cancer Res. *12*, R68.

Reis-Filho, J.S., Drury, S., Lambros, M.B., Marchio, C., Johnson, N., Natrajan, R., Salter, J., Levey, P., Fletcher, O., Peto, J., et al. (2008). ESR1 gene amplification in breast cancer: a common phenomenon? Nat. Genet. *40*, 809–810, author reply 810–812.

Sanchez, C.G., Ma, C.X., Crowder, R.J., Guintoli, T., Phommaly, C., Gao, F., Lin, L., and Ellis, M.J. (2011). Preclinical modeling of combined phosphatidylinositol-3-kinase inhibition with endocrine therapy for estrogen receptor-positive breast cancer. Breast Cancer Res. *13*, R21.

Santos, E., Martin-Zanca, D., Reddy, E.P., Pierotti, M.A., Della Porta, G., and Barbacid, M. (1984). Malignant activation of a K-ras oncogene in lung carcinoma but not in normal tissue of the same patient. Science *223*, 661–664.

Shah, S.P., Roth, A., Goya, R., Oloumi, A., Ha, G., Zhao, Y., Turashvili, G., Ding, J., Tse, K., Haffari, G., et al. (2012). The clonal and mutational evolution spectrum of primary triple-negative breast cancers. Nature *486*, 395–399.

Shull, A.Y., Latham-Schwark, A., Ramasamy, P., Leskoske, K., Oroian, D., Birtwistle, M.R., and Buckhaults, P.J. (2012). Novel somatic mutations to PI3K pathway genes in metastatic melanoma. PLoS ONE *7*, e43369.

Song, R.X., Mor, G., Naftolin, F., McPherson, R.A., Song, J., Zhang, Z., Yue, W., Wang, J., and Santen, R.J. (2001). Effect of long-term estrogen deprivation on apoptotic responses of breast cancer cells to 17beta-estradiol. J. Natl. Cancer Inst. *93*, 1714–1723.

Stephens, P.J., Greenman, C.D., Fu, B., Yang, F., Bignell, G.R., Mudie, L.J., Pleasance, E.D., Lau, K.W., Beare, D., Stebbings, L.A., et al. (2011). Massive genomic rearrangement acquired in a single catastrophic event during cancer development. Cell *144*, 27–40.

Tabchy, A., Hennessy, B.T., Gonzalez-Angulo, A.M., Bernstam, F.M., Lu, Y., and Mills, G.B. (2011). Quantitative proteomic analysis in breast cancer. Drugs Today (Barc) *47*, 169–182.

Walter, M.J., Shen, D., Ding, L., Shao, J., Koboldt, D.C., Chen, K., Larson, D.E., McLellan, M.D., Dooling, D., Abbott, R., et al. (2012). Clonal architecture of secondary acute myeloid leukemia. N. Engl. J. Med. *366*, 1090–1098.

Wang, K., Singh, D., Zeng, Z., Coleman, S.J., Huang, Y., Savich, G.L., He, X., Mieczkowski, P., Grimm, S.A., Perou, C.M., et al. (2010). MapSplice: accurate mapping of RNA-seq reads for splice junction discovery. Nucleic Acids Res. *38*, e178.

Weis, K.E., Ekena, K., Thomas, J.A., Lazennec, G., and Katzenellenbogen, B.S. (1996). Constitutively active human estrogen receptors containing amino acid substitutions for tyrosine 537 in the receptor protein. Mol. Endocrinol. *10*, 1388–1398.

Welch, J.S., Ley, T.J., Link, D.C., Miller, C.A., Larson, D.E., Koboldt, D.C., Wartman, L.D., Lamprecht, T.L., Liu, F., Xia, J., et al. (2012). The origin and evolution of mutations in acute myeloid leukemia. Cell *150*, 264–278.

Xi, T., Jones, I.M., and Mohrenweiser, H.W. (2004). Many amino acid substitution variants identified in DNA repair genes during human population screenings are predicted to impact protein function. Genomics *83*, 970–979.

Youlden, D.R., Cramb, S.M., Dunn, N.A., Muller, J.M., Pyke, C.M., and Baade, P.D. (2012). The descriptive epidemiology of female breast cancer: an international comparison of screening, incidence, survival and mortality. Cancer Epidemiol *36*, 237–248.

Zhang, Q.X., Borg, A., Wolf, D.M., Oesterreich, S., and Fuqua, S.A. (1997). An estrogen receptor mutant with strong hormone-independent activity from a metastatic breast cancer. Cancer Res. *57*, 1244–1249.

Zhang, X., Claerhout, S., Prat, A., Dobrolecki, L.E., Petrovic, I., Lai, Q., Landis, M.D., Wiechmann, L., Schiff, R., Giuliano, M., et al. (2013). A renewable tissue resource of phenotypically stable, biologically and ethnically diverse, patient-derived human breast cancer xenograft models. Cancer Res. *73*, 4885–4897.

Human Cancer Biology
See related article by Segal and Dowsett, p. 1724

Clinical Cancer Research

Emergence of Constitutively Active Estrogen Receptor-α Mutations in Pretreated Advanced Estrogen Receptor–Positive Breast Cancer

Rinath Jeselsohn[1,2,3], Roman Yelensky[6], Gilles Buchwalter[1,2,3], Garrett Frampton[6], Funda Meric-Bernstam[7], Ana Maria Gonzalez-Angulo[8], Jaime Ferrer-Lozano[9], Jose A. Perez-Fidalgo[10], Massimo Cristofanilli[11], Henry Gómez[12], Carlos L. Arteaga[13], Jennifer Giltnane[13], Justin M. Balko[13], Maureen T. Cronin[6], Mirna Jarosz[6], James Sun[6], Matthew Hawryluk[6], Doron Lipson[6], Geoff Otto[6], Jeffrey S. Ross[6], Addie Dvir[14], Lior Soussan-Gutman[14], Ido Wolf[15], Tamar Rubinek[15], Lauren Gilmore[4], Stuart Schnitt[4], Steven E. Come[5], Lajos Pusztai[16], Philip Stephens[6], Myles Brown[1,2], and Vincent A. Miller[6]

Abstract

Purpose: We undertook this study to determine the prevalence of estrogen receptor (ER) α (*ESR1*) mutations throughout the natural history of hormone-dependent breast cancer and to delineate the functional roles of the most commonly detected alterations.

Experimental Design: We studied a total of 249 tumor specimens from 208 patients. The specimens include 134 ER-positive ($ER^+/HER2^-$) and, as controls, 115 ER-negative (ER^-) tumors. The ER^+ samples consist of 58 primary breast cancers and 76 metastatic samples. All tumors were sequenced to high unique coverage using next-generation sequencing targeting the coding sequence of the estrogen receptor and an additional 182 cancer-related genes.

Results: Recurring somatic mutations in codons 537 and 538 within the ligand-binding domain of ER were detected in ER^+ metastatic disease. Overall, the frequency of these mutations was 12% [9/76; 95% confidence interval (CI), 6%–21%] in metastatic tumors and in a subgroup of patients who received an average of 7 lines of treatment the frequency was 20% (5/25; 95% CI, 7%–41%). These mutations were not detected in primary or treatment-naïve ER^+ cancer or in any stage of ER^- disease. Functional studies in cell line models demonstrate that these mutations render estrogen receptor constitutive activity and confer partial resistance to currently available endocrine treatments.

Conclusions: In this study, we show evidence for the temporal selection of functional *ESR1* mutations as potential drivers of endocrine resistance during the progression of ER^+ breast cancer. *Clin Cancer Res; 20(7); 1757–67. ©2014 AACR.*

Introduction

Estrogen receptor α (ERα) is a nuclear transcription factor that drives proliferation and growth of luminal-type breast cancers and is the target of endocrine therapies in this disease. Although such antiestrogen treatments are highly effective, a major clinical limitation is the development of acquired resistance to these therapies. Despite the fact that approximately 50% of patients with ER^+ breast cancer benefit from adjuvant endocrine treatment, a significant fraction of them recur with metastatic disease (1–3). Furthermore, all patients with ER^+ metastatic breast cancer who respond to endocrine treatment will eventually

Authors' Affiliations: [1]Center for Functional Cancer Epigenetics, [2]Department of Medical Oncology, Dana-Farber Cancer Institute; [3]Department of Medicine, Brigham and Women's Hospital; Departments of [4]Pathology and [5]Breast Medical Oncology Program, Beth Israel Deaconess Medical Center, Harvard Medical School, Boston; [6]Foundation Medicine, Cambridge, Massachusetts; [7]Departments of Investigational Cancer Therapeutics, Surgical Oncology, and [8]Systems Biology and Breast Medical Oncology, The University of MD Anderson Cancer Center, Houston, Texas; [9]Fundacion de Investigacion INCLIVA-Institute for Health Research; [10]Departments of Hematology-Oncology, Hospital Clinico Universitario de Valencia, Valencia, Spain; [11]Jefferson Breast Care Center, Kimmel Cancer Center, Thomas Jefferson University, Philadelphia, Pennsylvania; [12]Instituto Nacional de Enfermedades Neoplásicas (INEN), Lima, Perú; [13]Breast Cancer Program, Vanderbilt-Ingram Cancer Center, Vanderbilt University Medical Center, Nashville, Tennessee; [14]Teva Pharmaceuticals, Petach Tikva; [15]Oncology Division, Tel Aviv Sourasky Medical Center, Tel Aviv, Israel; and [16]Section of Breast Medical Oncology, Yale School of Medicine, New Haven, Connecticut

Note: Supplementary data for this article are available at Clinical Cancer Research Online (http://clincancerres.aacrjournals.org/).

R. Jeselsohn, R. Yelensky, G. Buchwalter, and G. Frampton contributed equally to this work.

Corresponding Author: Myles Brown, Dana-Farber Cancer Institute, 450 Brookline Ave, D730, Boston, MA 02215. Phone: 611-631-3948; Fax: 611-581-8501; E-mail: myles_brown@dfci.harvard.edu

doi: 10.1158/1078-0432.CCR-13-2332

©2014 American Association for Cancer Research.

Translational Relevance

This study demonstrates an overall 12% frequency of somatic *ESR1* mutations in metastatic ER$^+$ breast cancer and absence of detectable mutations in the primary tumors. In preclinical models, we show that these mutations render constitutive activity and relative resistance to endocrine therapy. Taken together, these results suggest clonal evolution as the mechanism of resistance. Thus, we propose that these mutations are biomarkers and drivers of endocrine resistance in ER$^+$ metastatic breast cancer. As such, these mutations can assist in clinical decision making as disease progresses, underscoring the value of serial biopsies and profiling of metastatic recurrences. In addition, further studies are warranted to investigate therapeutic strategies to circumvent the resistance conferred by these mutations.

progress with antiestrogen-resistant, hormone-independent disease.

In most cases of acquired endocrine resistance, ER continues to be expressed. Proposed mechanisms of resistance include activation of growth factor receptor, cell survival and cell-cycle signaling pathways, as well as stress-induced pathways (4, 5). In addition, aberrant expression of ER coactivators and corepressors has been implicated in endocrine resistance (6, 7). ER mutations have also been explored as a potential mechanism of drug resistance and initially it was postulated that loss-of-function mutations could contribute to resistance. However, several preclinical studies analyzed the effects of point mutations in ER and found a number of mutations that can actually enhance ER function similar to androgen receptor mutations in castrate-resistant prostate cancer (1–10). One such functional mutation in *ESR1* leads to the substitution of tyrosine by serine or alanine at position 537 in the ligand-binding domain (LBD) and results in ligand-independent ER transcriptional activity that does not respond to endocrine manipulation (11–13). Despite these preclinical findings, the frequency of ER mutations in primary breast cancers was found to be extremely rare. In one early study of 118 ER$^+$ and 70 ER$^-$ primary breast cancers, only two ESR1 mutations of unknown significance were found and both were in ER$^-$ breast cancers (14). More recently, several studies describing next-generation sequencing (NGS) in hundreds of primary breast cancer samples detected multiple significant somatic alterations, but none were detected in *ESR1* (11–17). Two small studies conducted in the 1990s detected mutations in the ER LBD with a frequency of 1% to 10% in metastatic breast cancer samples, suggesting that the frequency of ER mutations in metastatic disease may be higher (18, 19). However, these studies were small and had not been validated with more sensitive sequencing technology and/or integrated with clinical correlations. Therefore, in this study, we sought to comprehensively study the frequency and functional significance of ER mutations in both primary and metastatic breast cancer using targeted NGS.

Materials and Methods

Breast cancer human tissue specimens and clinical data

Paraffin-embedded blocks from formalin-fixed ER$^+$/HER2$^-$ primary and in-breast local recurrence/metastatic breast cancer specimens were obtained from the Pathology Departments of three institutions (MD Anderson Cancer Center, Houston, TX; Beth Israel Deaconess Medical Center, Boston, MA; and Hospital Clínico Universitario in Valencia, Spain), including samples from the NCT00780676 trial (a phase II trial for patients with advanced metastatic breast cancer treated with dasatinib or selumetinib based on the expression profile of their metastatic tumor). ER$^+$/HER2$^+$ tumors were excluded as they are known to be resistant to endocrine therapy.

All samples were stained for ER, progesterone receptor (PR), and HER2 and reviewed by a pathologist at each institution but were not centrally reviewed. ER positivity was defined as more than 1% of cells with strong staining. Anti-ERα antibodies were from Thermo Scientific and Ventana (clone SP1). HER2 was defined as positive either by immunohistochemistry of 3+ or FISH HER2/CEP17 ratio of greater than 2.2. The anti-HER2 antibody was purchased from Dako or Ventana. Clinical data were also collected. For comparison, additional ER$^-$ (either ER−/HER2− or ER−/HER2+) primary breast cancer samples were obtained (MD Anderson Cancer Center and Instituto Nacional de Enfermedades Neoplásicas), as well as a small number of specimens from ER− metastatic disease (MD Anderson Cancer Center). Brief descriptions of all studied cohorts can be found in Table 1, and more detailed information about the ER+ metastatic cohort is in Supplementary Table S1. All tissue collections were done with the approval of the corresponding institutional review boards.

Sequencing and primary sequence data analysis

Tumor tissue sections of 40 μm were macrodissected using hematoxylin and eosinophil staining to identify areas of at least 80% cellularity. Genomic DNA was extracted using the Maxwell 16 FFPE Plus LEV DNA Purification Kit (Promega) and quantified using a PicoGreen fluorescence assay (Invitrogen); ≥50 ng and up to 200 ng of extracted DNA was sheared to approximately 101–400 bp by sonication, followed by end repair, dA addition and ligation of indexed, Illumina sequencing adaptors. Sequencing libraries were hybridization captured using RNA-based baits (Agilent), targeting a total of 3,320 exons of 182 cancer-related genes (most commonly altered in cancer, from http://www.sanger.ac.uk/genetics/CGP/cosmic/) plus 37 introns from 14 genes often rearranged in cancer (Supplementary Table S1). Paired-end sequencing (49 × 49 cycles) was performed using the HiSeq2000 (Illumina). Sequence data from gDNA were mapped to the reference human genome (hg19) using the BWA aligner (20). PCR duplicate read removal and sequence metric collection was performed using Picard (http://picard.sourceforge.net) and SAMtools

Table 1. Patient cohorts

	Patient cohort	No. of specimens	Average number of treatments[a] before biopsy
LM^+	Metastases from patients with advanced ER^+ disease that were heavily pretreated before biopsy (participants in "Personalized Treatment Selection for Metastatic Breast Cancer" trial NCT00780676)	25	7
EM^+	Metastases from patients with early metastatic ER^+ disease	51	1–2
P^+	Primary ER^+ tumors	58	NA
M^-	Metastases from patients with ER^- disease	11	NA
P^-	Primary ER^- primary breast cancer disease	104	NA

Abbreviations: EM^+, early metastatic ER^+ disease; LM^+, late metastatic ER^+ breast cancer; M^-, ER^- metastatic disease; P^+, ER^+ primary breast cancer; and P^-, ER^- primary breast cancer.

[a]Including endocrine treatments and chemotherapy regimens.

(21). Local alignment optimization was performed using GATK (22).

Genomic alteration detection

Base substitution detection was performed using a Bayesian methodology, which allows detection of novel somatic mutations at low mutation annotation format and increased sensitivity for mutations at hotspot sites (23) through the incorporation of tissue-specific prior expectation: P (Mutation present| Read data "R") = P(Frequency of mutation "F" > $0|R) \propto 1 - P(R|F = 0)\,P(F = 0)$, where $P(R|F)$ is evaluated with a multinomial distribution of the observed allele counts using empirically observed error rates and $P(F = 0)$ is the prior expectation of mutation in the tumor type. To detect indels, *de novo* local assembly in each targeted exon was performed using the de-Bruijn approach (24). Candidate calls are filtered using a series of quality metrics, including strand bias, read location bias, and a custom database of sequencing artifacts derived from normal controls. Germline alterations are identified and filtered using dbSNP (version 135, www.ncbi.nlm.nih.gov/projects/SNP/) and subsequently annotated for known and likely somatic mutations using the COSMIC database (version 62, http://cancer.sanger.ac.uk/cancergenome/projects/cosmic/). Detection of copy number alterations was performed by obtaining a log-ratio profile of the sample by normalizing the sequence coverage obtained at all exons against a process-matched normal control. The profile is segmented and interpreted using allele frequencies of approximately 1,800 additional genome-wide SNPs to estimate tumor purity and copy number based on established methods (21–27) by fitting parameters of the equation $\text{copy}\,lr_{\text{seg}} \sim N\left(\log_2 \frac{p*C_{\text{seg}}+(1-p)*2}{p*\text{tumor ploidy}+(1-p)*2}\right)$, where lr_{seg} and C_{seg} are numbers at each segment and sample purity, respectively. Focal amplifications are called at segments with ≥ 6 copies (1–8 in high aneuploidy samples) and homozygous deletions at 0 copies, in samples with purity >20%.

Cell and tissue culture

293T and MCF7 cells (purchased from the American Type Culture Collection and early passage used) were maintained in Dulbecco's Modified Eagle Medium supplemented with 10% FBS and penicillin/streptomycin. Hormone depletion was carried out for 48 hours using phenol red–free DMEM (Cellgro) + 10% charcoal dextran-treated FBS (Omega Scientific) and was followed by estradiol (E_2, 10 nmol/L) stimulation. Transient transfections were accomplished using Lipofectamine 2000 (Life Technologies) as per the manufacturer's protocol.

Luciferase assays

Luciferase reporter assay system (Promega) was used to monitor luciferase activity in 293T cells as per the manufacturer's recommendations, using a single tube luminometer (BD Monolight 2010). Briefly, 1×10^5 293T cells were plated in 6-well plate in hormone-depleted medium. Transient transfections were accomplished using Lipofectamine 2000 (Life Technologies) with the following vectors: pcDNA-wt/mut ER (0.1 μg/well), ERE-TK-Luc (2 copies of Estrogen Response Element upstream Luciferase reporter, minimal TK promoter, 1 μg/well), pCMV-βGal (internal control normalization vector, 0.1 μg/well), pcDNA3.1 (empty vector, 0.8 μg/well). Forty-eight hours after transfection, cells were treated with E_2 or vehicle. For the dose response studies, doses ranged between 100 and 1,500 nmol/L for the 4-hydroxytamoxifen (Sigma-Aldrich, catalog # H7904) and between 50 and 2,500 nmol/L for fulvestrant (AstraZeneca). All transfection studies were performed in triplicates and luciferase results are reported as relative light units (RLU) and normalized with β-galactosidase activity using the Mammalian β-gal assay kit (Thermo Scientific).

Site-directed mutagenesis

The GeneArt Site-Directed mutagenesis system (Life Technologies) was used to generate Y537N, Y537C, and D538G mutations within ER LBD. Wild-type ER expression vector (pcDNA-ER) was used as a template with the following mutagenesis primers: Y537N: Forward, 5′-AACGTGGTGCCCCTCAATGACCTGCTGCTGGAGA T-3′ Reverse, 5′-ATCTCCAGCAGCAGGTCATTGAGGGGCAC-CACGTT-3′

Y537C: Forward, 5′-AACGTGGTGCCCCTCTGTGACCT-GCTGCTGGAGAT-3′

Reverse, 5′-ATCTCCAGCAGCAGGTCACAGAGGGGCA-CCACGTT-3′

D538G: Forward, 5′-AACGTGGTGCCCCTCTATGGCCT-GCTGCTGGAGAT-3′

Reverse, 5′-ATCTCCAGCAGCAGGCCATAGAGGGGCA-CCACGTT-3′.

Western blot and real-time PCR

The following antibodies were used for ER (sc-543, Santa Cruz Biotechnology) and β-Actin (A5441, Sigma) protein detection. For mRNA level measurement, total RNA was prepared using TRIzol reagent (Life Technologies), and cDNA were synthesized using a high-capacity cDNA reverse transcription kit (Applied Biosystems). The following primers were used for *GREB1*, *pS2/TFF1*, *PR*, *CA12*, β-*Actin* mRNAs detection, using ABI 7300 Real-time PCR system in combination with Power SYBR Green PCR Master Mix (Life Technologies):

GREB1 mRNA: Forward, 5′-CTG CCC CAG AAT GGT TTT TA-3′

Reverse, 5′-GGA CTG CAG AGT CCA GAA GC-3′ *pS2/TFF1* mRNA: Forward, 5′-CCGAGCTCTGGGACTAATCA-3′ Reverse, 5′-TTG TGG TTT TCC TGG TGT CA-3′; β-*Actin* mRNA: Forward, 5′-CAC ACG CAG CTC ATT GTA GA-3, Reverse, 5′-GGC ATG GGT CAG AAG GAT T-3′; *PR* mRNA:

Forward: 5′-AGC CAG AGC CCA CAA TAC AG-3′, Reverse: 5′-GAC CTT ACA GCT CCC ACA GG-3′; *CA12* mRNA:

Forward: 5′-GTG GTG TCC ATT TGG CTT TT-3′, Reverse: 5′-GTG TCG CAA GTG TCC AGA GA-3′.

Results

Sequencing studies

To examine the prevalence and clinical implications of ER mutations in human breast cancer, we assembled a dataset of 249 specimens, obtained from 208 patients, representing both $ER^+/HER2^-$ and ER^- disease (Table 1). The cohorts selected enabled the analysis of the different stages of breast cancer, ranging from diagnostic biopsies of early breast cancers to samples from metastatic recurrences used for biomarker assessment before enrollment in clinical trials. DNA sequencing was performed for 3,230 exons of 182 cancer-related genes plus 37 introns of 14 genes commonly fused on indexed hybridization-captured libraries to an average unique coverage of >500×.

Across the 249 specimens, a total of 16 *ESR1* point mutations (substitutions or indels) and 2 instances of locus focal amplification were observed. Although matched normal specimens were unavailable for definitive somatic status determination in our study, a computational assessment of variant allele frequencies supported the germline hypothesis for 4 of 16 observed events (see methods, Supplementary Table S1). Of the remaining 12 somatic variants (Table 2), 9 (75%) occurred at the known recurrent mutation sites in the ER LBD, codons 537/538, while the rest were elsewhere in the LBD (Fig. 1A).

Focusing on the recurrent codon 537/538 LBD mutations, we observed a striking enrichment of these variants in ER^+ metastatic disease (Fig. 1B): Of the 76 ER^+ metastatic specimens profiled, the recurring ER LBD mutations were found in 9 (12%) cases. The specific mutations include: Y537N (33%), D538G (33%), Y537S (22%), and Y537C (11%). The prevalence was even higher with a frequency of 20% (5/25 patients) in heavily pretreated patients who received an average of seven lines of treatment, including at least two endocrine treatments for metastatic disease. The mutations were not found in any of the 58 ER^+ primary treatment-naïve tumors or the 115 ER^- tumors.

Our study included 37 matched primary and metastatic pairs. In two of these pairs, EM8 and EM11 the point mutations Y537C and D538G were detected in the metastatic samples but not in the matching untreated primary tumors. For one patient with a mutation (sample EM43), we were able to sequence tissue from an earlier metastatic specimen. Both biopsies were from the same metastatic site but were attained at two time points from a patient who did not receive adjuvant hormonal treatment. The first metastatic lesion, without a detectable *ESR1* mutation, was obtained before the initiation of tamoxifen and the second one, found to have a Y537C mutation, was obtained at the time of disease progression after 8 years of treatment. Finally, in 3 specimens, codon 537/538 mutations exhibited allele frequencies consistent with subclonal cell populations. Collectively, these findings suggest a clonal selection of an endocrine-resistant phenotype.

We then broadened our analysis to the genomic context of ER alterations by examining the full spectrum of genomic alterations in primary and metastatic ER^+ disease. The list of the 182 genes that were sequenced can be found in Supplementary Table S3. All 25 advanced metastatic, as well as 46 early metastatic and primary, specimens were considered in this analysis. A similar analysis of the other 63 ER^+ specimens has been presented previously (28). ER alterations were not mutually exclusive with any other commonly altered gene in ER^+ breast cancer (*P53*, *PIK3CA*, *CCND1*, *MYC*, *FGFR1*, *MCL1*), although HER2 copy gains could not be assessed in our dataset as clinical $ER^+/HER2^+$ cases were excluded. Nonetheless, we believe more samples will be needed to verify this observation (Supplementary Fig. S1). Of the most frequently altered genes (altered in >5 samples), all but *ESR1* alterations displayed similar frequencies across primary and metastatic specimens, suggesting a role for aberrant ER in the development of recurrent disease (Fig. 2).

Functional studies

To delineate the functional roles of the mutations in codons 537/538 found in metastatic breast cancer patient samples, we performed site-directed mutagenesis to prepare three ER expression constructs containing 2 different amino acid substitutions at position 537 (Y537C and Y537N) and one amino acid substitution at position D538 (D538G). All ER mutations were confirmed by sequencing. The constitutive activity of the Y537N and Y537S mutations has been

Table 2. Detailed description of the detected somatic ESR1 variants

Cohort/ sample ID	Primary/ metastasis	ER status	HER2 status	Biopsy site	Transcript change	Protein change	Known somatic variant (literature)	Predicted variant zygosity in tumor	Endocrine treatment before biopsy
LM3	Metastasis	+	–	Liver	1033_1034 insGCT	344insC	No	Clonal homozygous	Anastrozole Tamoxifen Exemestane Fulvestrant
EM29	Metastasis	+[a]	–[a]	Bone	1138G>C	E380Q	No	Unknown[b]	Anastrazole
P371	Primary	–	+		1507C>T	R503W	No	Subclonal	None
LM17	Metastasis	+	–	Lymph node	1609T>A	Y537N	Yes	Subclonal	Tamoxifen Exemestane Fulvestrant Letrozole Megestrol
EM43	Metastasis	+	–	Lymph node	1609T>A	Y537N	Yes	Clonal heterozygous	Tamoxifen
LM12	Metastasis	+	–	Bone	1610A>C	Y537C	Yes	Clonal heterozygous	Tamoxifen Goserelin Anastrozole
EM11	Metastasis	+	–	Lung	1610A>C	Y537C	Yes	Subclonal	Anastrazole
LM4	Metastasis	+	–	Liver	1610A>C	Y537S	Yes	Clonal heterozygous	Tamoxifen Goserelin Letrozole Exemestane Fulvestrant
EM51	Metastasis	+	–	Liver	1610A>C	Y537S	Yes	Subclonal	Tamoxifen
LM19	Metastasis	+	–	Liver	1613A>G	D538G	Yes	Clonal homozygous	Tamoxifen Anastrozole Fulvestrant
LM2	Metastasis	+	–	Bone	1613A>G	D538G	Yes	Clonal heterozygous	Anastrozole Exemestane Fulvestrant
EM8	Metastasis	+	–	Skin	1613A>G	D538G	Yes	Unknown	Anastrazole

[a]Inferred (assessed on another specimen from patient).

[b]Tumor purity or coverage too low for assessment.

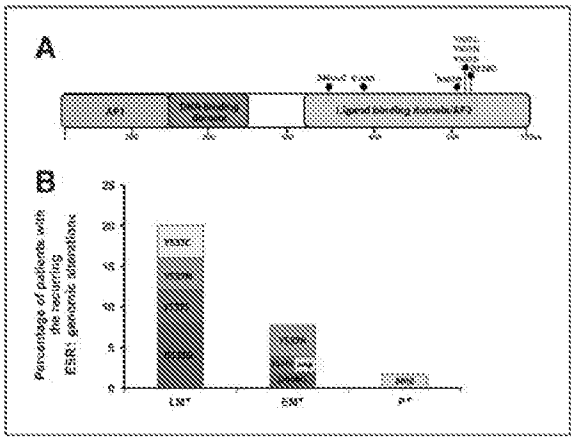


Figure 1. Location of the ER mutations and frequencies per cohort. A, diagram of ER with detected predicted somatic point mutations designated with a circle at the representative protein position. *, a mutation found in a primary ER$^+$ breast cancer. B, frequency of the 538/537 substitution mutations and ER amplifications per cohort in ER$^+$ tumors showing an increase in frequency with the progression and increase in number of treatment lines for ER$^+$ breast cancer. Each bar represents the percentage of patients with a mutation and the different colors within the bars represent the frequency of the indicated alteration. In the EM$^+$ cohort one patient had both an ER amplification and a Y537S mutation. AF1, activation function 1; AF2, activation function 2; EM$^+$, early metastatic ER$^+$ disease; LM$^+$, late metastatic ER$^+$ breast cancer.

established previously (11, 19). To assess the transcriptional activity of the Y537C, Y537N, and D538G mutants we transiently transfected ER$^-$ 293T cells with wild-type (WT) ER or the mutant ER constructs and an estrogen-responsive promoter-reporter construct, ERE-TK-Luc (Fig. 3). Cells were treated with either control vehicle or estradiol (E_2) and luciferase activity was measured. As expected, the WT-ER construct exhibited activity only with E_2 stimulation. In contrast, all three ER mutants possessed constitutive activity in the absence of E_2 stimulation, whereas the addition of E_2 did not increase the reporter activity significantly. In addition, both the ligand and nonligand–dependent activity in the mutants was higher than the ligand-stimulated activity of the WT-ER. We next treated the cells with increasing doses of 4-hydroxytamoxifen or fulvestrant with or without E_2. Cells expressing the WT-ER responded to 4-hydroxytamoxifen and fulvestrant with a significant and dose-dependent reduction in luciferase activity. The ER mutants also responded to 4-hydroxytamoxifen and fulvestrant in a dose-dependent manner; however, the mutant ER displayed a significantly reduced response to all doses of antiestrogens except for the highest dose of 4-hydroxytamoxifen. Mutant ER exhibited decreased response to 4-hydroxytamoxifen and fulvestrant and higher doses of these antiestrogens were required to achieve the level of inhibition seen in the WT receptor. To confirm the decreased response of the mutant ER to fulvestrant, we examined ER degradation after 24 hours with increasing doses of fulvestrant. As we expected, mutant ER degradation compared with WT-ER was less pronounced at all doses of fulvestrant tested (Fig. 3C). In addition, since it has been shown that endocrine-resistant breast cancer can respond to estrogen treatment (29, 30), we tested the response of the Y537N and D538G mutants to a wide range of E_2 levels but did not detect a significant change in the luciferase activity (Supplementary Fig. S2). These results suggest that the ER mutants would be relatively resistant to established clinical doses of tamoxifen and fulvestrant as well as estrogen treatment and higher doses of SERMS or newer selective estrogen receptor degraders (SERDS) with improved pharmacokinetics may be required to inhibit mutant ER activity.

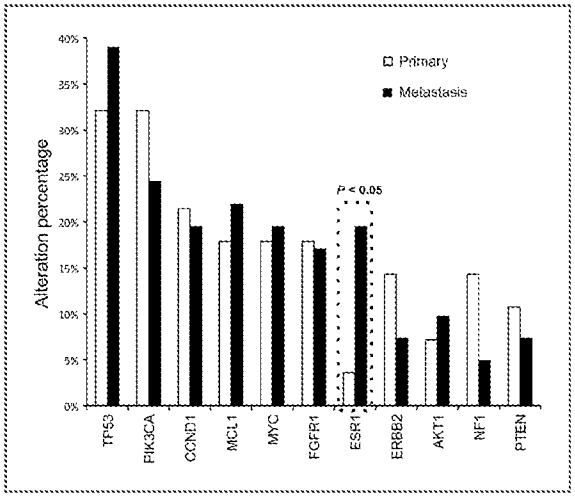


Figure 2. Genetic alteration in primary versus metastatic breast cancer. The frequencies of the common genomic alterations found in our cohorts comparing primary tumors versus metastatic samples shows a significant increase in the ESR1 alterations in metastatic samples. *P* value calculated using the Fisher exact test.

To study the transcriptional activity of the ER mutant in ER$^+$ breast cancer cells, we transfected a WT-ER construct and the Y537N construct in MCF7 cells. WT and mutant ER signaling was measured by determining the expression levels of ER regulated transcripts with or without E_2. As shown in Fig. 4A, PR, GREB1, CA12, and PS2 transcript levels were comparable between the WT and ER-mutant in full media, whereas in E_2-deprived conditions these ER-regulated genes are induced by the Y537N mutant but not the WT-ER. In addition, when we examined cell proliferation in estrogen-deprived conditions, which mimic aromatase inhibitor treatment, as well as treatment with 4-hydroxytamoxifen or fulvestrant, we found a significant growth advantage for the Y537N mutant (Fig. 4B). These results demonstrate that cells expressing the Y537N mutant exhibit constitutive transcriptional activity of ER target genes and an abrogated growth inhibitory response to E_2 deprivation, tamoxifen, or fulvestrant treatment.

Discussion

The advances in sequencing technologies over the past few years have led to a new paradigm in the understanding of the mutational landscape of breast cancer and tumor

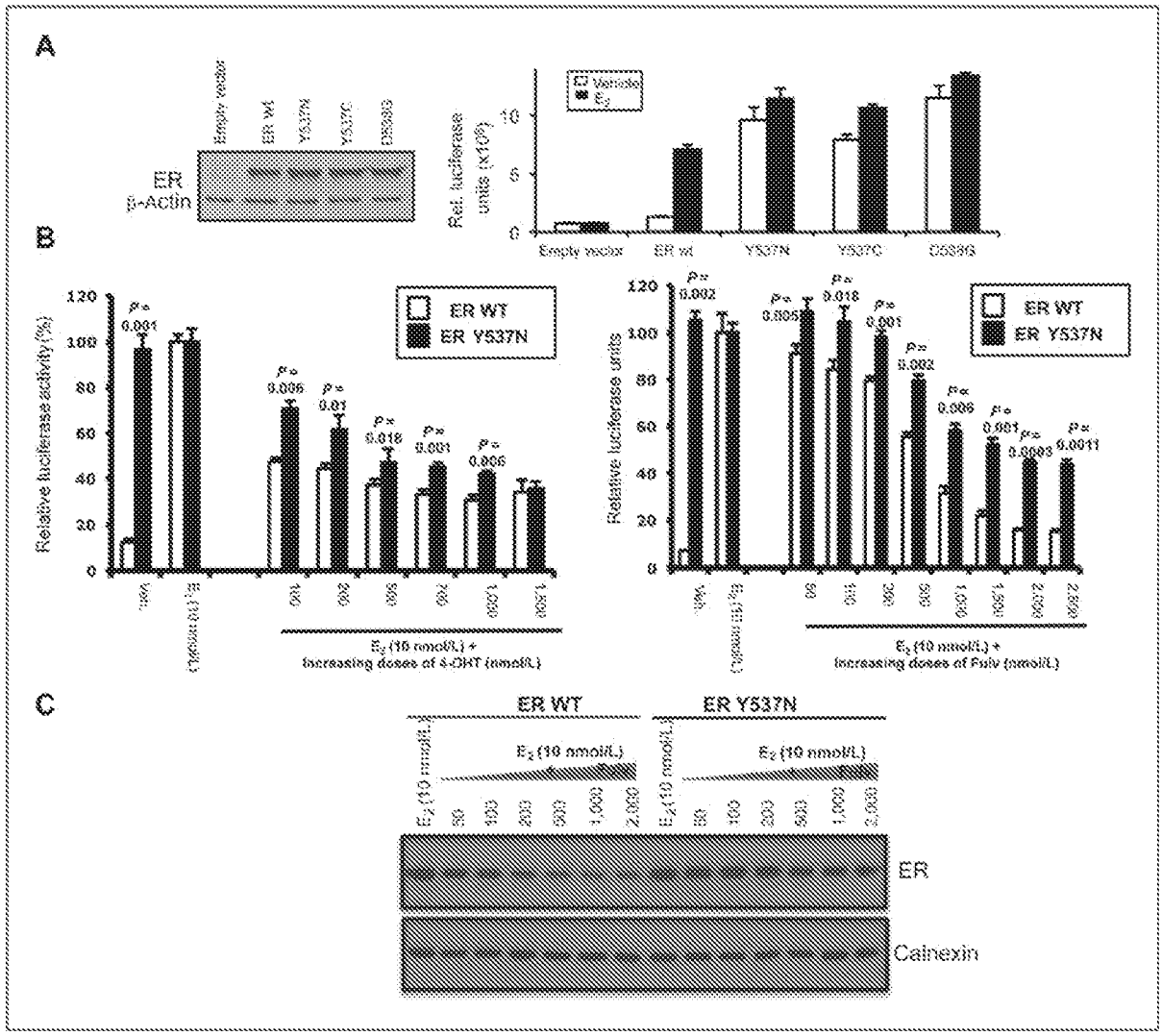


Figure 3. Analysis of the transcriptional activity of the recurring mutant ER and dose response to tamoxifen and fulvestrant. A, transient transfection of 293T cells with WT or mutant ER expression vectors in addition to ERE-TK-Luc reporter vector. ER expression levels were determined to be equivalent by Western blot analysis. β-Actin expression level is shown as an internal loading control (left). Luciferase activity comparison of transfected 293T cells then treated for 24 hours with 10 nmol/L estrogen (E_2) or vehicle (ethanol) for 24 hours. Experiments were done in triplicates and repeated three times. Data represent mean ± SD and are normalized by β-galactosidase internal control activity (left). B, luciferase activity comparison of 293 T cells transfected with WT or mutant ER expression vectors in addition to ERE-TK-Luc reporter vector, then treated with vehicle (ethanol) or indicated dose of E_2 and increasing doses of 4-hydroxytamoxifen (4-OHT) or fulvestrant (Fulv) for 24 hours. Response to 4-OHT and fulvestrant is normalized to the response to E_2 stimulation. Data represent mean ± SD and are normalized by β-galactosidase internal control activity. An unpaired two-tailed *t* test was used to examine the statistical differences between the WT and Y537N mutant, and *P* values are shown. C, R levels determined by immunoblotting 24 hours after treatment with increasing doses of fulvestrant.

heterogeneity. In this study, we performed targeted NGS, which enables high levels of sequencing coverage to detect low frequency mutations within limited cellular populations, in order to study ER mutations in breast cancer. In this study, which is an international effort, we assembled a large sample set of breast cancers comprised primarily of ER^+/$HER2^-$ metastatic samples and associated treatment histories as well as ER^+ primary tumors and control ER^- tumors. The majority of the ER^+ metastatic samples were obtained from patients who received at least one form of endocrine treatment, to focus on endocrine-resistant tumors.

In this report, we detected in 11 of the 76 (14%) metastatic tumors *ESR1* mutations in the LBD. Nine of these mutations are substitution mutations affecting Y537 and D538. In addition, we identified two mutations, 344insC and E380Q, that were not described in the literature previously and further studies are needed to test their

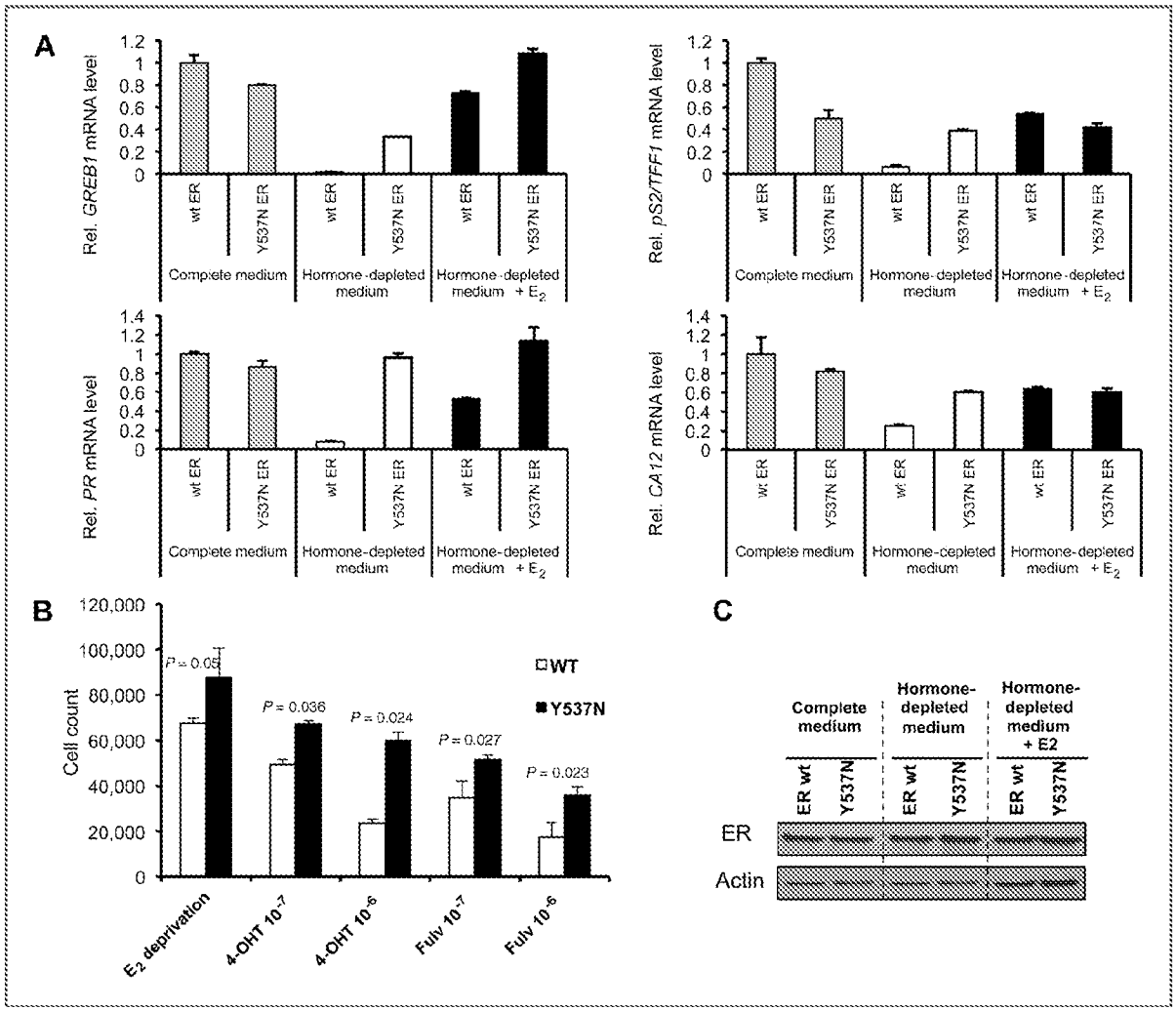


Figure 4. Transcriptional activity and growth of mutant ER in a breast cancer cell line. A, transient transfection of MCF7 cells with empty vector (EV), wt, or mutant Y537N ER expression vectors, then grown in complete medium (gray bars), hormone-depleted medium (white bars), or hormone-depleted medium with 10 nmol/L E_2 (black bars). Relative mRNA levels of ER target genes *GREB1 and PR* (left) and *pS2/TFF1* and *CA12* (right) were determined by real-time PCR. Bars, fold change ± SD of two independent experiments. B, MCF7 cells were transfected with WT or Y537N ER. Cells were grown in E_2-deprived conditions alone, with 4-OHT or fulvestrant and monitored for 5 days. Histograms depict cell count at day 5. Unpaired two-tailed *t* test was used to examine the statistical difference and *P* value is shown. C, Western blot analysis of ER levels in MCF7 cells after transfection of either WT-ER or Y537N mutant ER showing similar expression levels.

functional significance. In line with our data, other groups have recently identified the Y537 and D538 mutations and additional other mutations (31–34). The mutations detected in these studies are clustered in the LBD in a substantial number of metastatic ER^+ cancers Among these three studies, the largest cohorts consisted of 36 and 44 metastatic tumors with a mutation frequency of 25% and 11%, respectively, supporting the significance of these mutations in advanced disease. We did not detect LBD *ESR1* mutations in 58 primary ER^+ tumors and is consistent with the findings of The Cancer Genome Atlas of more than 450 cases (35). In contrast, LBD mutations were detected in 3% of the primary tumors from the BOLERO 2 study, where patients with ER^+ metastatic breast cancer that had progressed in the metastatic setting were randomized to exemestane ± the TORC1 inhibitor everolimus (32, 36). This discrepancy may be due to the fact that the primary tumors in the BOLERO 2 represent a selective group of patients who all developed resistance to endocrine treatment, among them approximately 20% developed resistance early after adjuvant hormonal adjuvant treatment. Thus, the frequency of the recurrent *ESR1* LBD mutations in primary disease remains an open and important question, as the existence of these mutations in early disease has important implications for the selection of adjuvant treatment for thousands of patients annually.

The recurring LBD mutations in positions Y537 and D538 are at the start of helix 12, a highly conserved α-helix that undergoes conformational changes during ER activation. Therefore, it is not surprising that mutations in these positions would have functional implications. Similar to previous studies that focused on the Y537N, Y537S, and D538A mutations (11, 19, 37), our functional studies indicate that the Y537N, Y537C, and D538G mutations lead to ligand-independent activity that is relatively resistant to tamoxifen, fulvestrant, and estrogen deprivation. Prior studies led by Katzenellenbogen and colleagues have shed light on the mechanisms of these findings by demonstrating that the ER mutants that confer constitutive activity adopt a conformation that resembles the WT ligand-bound ER and the Y537S mutant has a decreased affinity to E_2 with increased binding to coactivators (12, 38). The mutant ER affinity to tamoxifen and fulvestrant has not been tested; however, we hypothesize that it is also reduced and together with increased coactivator binding leads to the relative resistance to these drugs. Our studies show that higher doses of tamoxifen or fulvestrant are able to partially decrease the mutant transcriptional activity, suggesting the possibility that higher doses of these agents could be a strategy to circumvent this relative resistance. This might explain in part the results of the CONFIRM trial in which a higher dose of fulvestrant improved progression-free survival (39). Further experiments to understand the detailed mechanism of the endocrine resistance of these mutants and test this hypothesis are under way.

Previous studies in xenograft models of MCF7 cells demonstrated the emergence of a D351Y LBD mutation in a tamoxifen-resistant and stimulated tumor (40, 41). In this study, we analyzed tumor specimens obtained at different stages of ER^+ breast cancer, including primary treatment-naïve primary disease, local recurrent and/or metastatic disease with an average of two lines of treatment for metastatic disease, and metastatic disease biopsied after an average of seven treatments. The frequencies of the recurring ER-LBD mutations in these three cohorts were 0%, 8%, and 20%, respectively, demonstrating a correlation between the increase in the frequency of these mutations and tumor progression. In addition, in a case from which serial biopsies were available, we were able to detect the emergence of the LBD mutation as the patient developed resistance to tamoxifen treatment. Taken together, these findings suggest a temporal evolution of ER mutations with emergence of an endocrine-resistant phenotype.

In our study, we detected ESR1 amplifications in a primary and metastatic tumor. Multiple studies have investigated the frequency of *ESR1* amplifications in ER^+ primary breast cancer though the data have been controversial. Two large studies found *ESR1* amplifications in approximately 20% of cancers, which correlated with an increased response to tamoxifen, whereas in other studies, amplifications were detected in just 1% to 3% of tumors (41–45). Our study is consistent with the latter studies as we observed an *ESR1* amplification rate of 1.7% (1/58) in primary ER^+ tumors. Similarly, the frequency of amplifications in metastatic samples was also very low (1.3%, 1/76). This is the first study to report the frequency of *ESR1* amplifications in metastatic breast cancer.

In summary, our study demonstrates an overall 14% frequency of somatic *ESR1* mutations in a large cohort of metastatic ER^+ breast cancers though the retrospective nature of our study limits our ability to precisely determine the frequency. The absence of detectable mutations in the primary tumors suggests clonal evolution as the mechanism of resistance. Thus, we propose that these mutations are a genomic mechanism of endocrine resistance. As such, the detection of these mutations can assist in clinical decision making as disease progresses, underscoring the value of serial biopsies and profiling of metastatic recurrences. In addition, since the frequencies of these mutations are substantial when sensitive testing methods are used in patients with ER^+ breast cancer, studies to identify alternative dosing schedules of currently approved antiestrogens and novel therapeutics that can overcome this resistance are warranted.

Disclosure of Potential Conflicts of Interest

R. Yelensky, M.T. Cronin, M. Jarosz, M. Hawryluk, and D. Lipson have ownership interest (including patents) in Foundation Medicine. G. Frampton and P. Stephens are employees of and have ownership interest (including patents) in Foundation Medicine. M. Cristofanilli is a consultant/advisory board member for Cynvenio. J. Sun is an employee of Foundation Medicine. J.S. Ross is an employee of, has a commercial research grant from, and has ownership interest (including patents) in Foundation Medicine Inc. A. Dvir is an employee of Teva pharmaceuticals. L. Pusztai has received a commercial research grant from Foundation Medicine. M. Brown has received a commercial research grant from and is a consultant/advisory board member for Novartis Pharmaceuticals. No potential conflicts of interest were disclosed by the other authors.

Authors' Contributions

Conception and design: R. Jeselsohn, R. Yelensky, G. Buchwalter, A.M. Gonzalez-Angulo, M.T. Cronin, J.S. Ross, L. Soussan-Gutman, P. Stephens, M. Brown, V.A. Miller

Development of methodology: R. Jeselsohn, R. Yelensky, G. Buchwalter, G. Frampton, J. Ferrer-Lozano, M.T. Cronin, M. Jarosz, G. Otto, J.S. Ross, V.A. Miller

Acquisition of data (provided animals, acquired and managed patients, provided facilities, etc.): R. Jeselsohn, G. Buchwalter, F. Meric-Bernstam, A.M. Gonzalez-Angulo, J. Ferrer-Lozano, A. Perez-Fidalgo, M. Cristofanilli, H. Gómez, C.L. Arteaga, J.M. Balko, M. Hawryluk, J.S. Ross, A. Dvir, L. Gilmore, S. Schnitt, L. Pusztai, V.A. Miller

Analysis and interpretation of data (e.g., statistical analysis, biostatistics, computational analysis): R. Jeselsohn, R. Yelensky, G. Buchwalter, G.M. Frampton, F. Meric-Bernstam, A.M. Gonzalez-Angulo, M.T. Cronin, J. Sun, M. Hawryluk, D. Lipson, J.S. Ross, S.E. Come, L. Pusztai, P. Stephens, V.A. Miller

Writing, review, and/or revision of the manuscript: R. Jeselsohn, R. Yelensky, G. Buchwalter, G. Frampton, F. Meric-Bernstam, A.M. Gonzalez-Angulo, J. Ferrer-Lozano, M. Cristofanilli, H. Gómez, C.L. Arteaga, J. Giltnane, J.M. Balko, M. Hawryluk, J.S. Ross, L. Soussan-Gutman, I. Wolf, T. Rubinek, S.J. Schnitt, S.E. Come, L. Pusztai, P. Stephens, M. Brown, V.A. Miller

Administrative, technical, or material support (i.e., reporting or organizing data, constructing databases): R. Jeselsohn, G. Buchwalter, J. Ferrer-Lozano, J.A. Perez-Fidalgo, H. Gómez, C.L. Arteaga, J.M. Balko, J.S. Ross, L. Gilmore, L. Pusztai

Study supervision: R. Jeselsohn, M. Brown, V.A. Miller

Grant Support

This study was supported in part by grants from Susan G. Komen for the Cure (to M. Brown), the NCI (P01 CA080111; to M. Brown), and NIDDK (R01 DK074967; to M. Brown).

The costs of publication of this article were defrayed in part by the payment of page charges. This article must therefore be hereby marked *advertisement* in accordance with 18 U.S.C. Section 1734 solely to indicate this fact.

Received August 25, 2013; revised December 9, 2013; accepted December 13, 2013; published OnlineFirst January 7, 2014.

References

1. Bonneterre J, Thurlimann B, Robertson JF, Krzakowski M, Mauriac L, Koralewski P, et al. Anastrozole versus tamoxifen as first-line therapy for advanced breast cancer in 668 postmenopausal women: results of the Tamoxifen or Arimidex Randomized Group Efficacy and Tolerability study. J Clin Oncol 2000;18:3741–57.
2. Nabholtz JM, Buzdar A, Pollak M, Harwin W, Burton G, Mangalik A, et al. Anastrozole is superior to tamoxifen as first-line therapy for advanced breast cancer in postmenopausal women: results of a North American multicenter randomized trial. J Clin Oncol 2000;18:3751–67.
3. Baum M, Budzar AU, Cuzick J, Forbes J, Houghton JH, Klijn JG, et al. Anastrozole alone or in combination with tamoxifen versus tamoxifen alone for adjuvant treatment of postmenopausal women with early breast cancer: first results of the ATAC randomised trial. Lancet 2002;359:2131–9.
4. Osborne CK, Schiff R. Mechanisms of endocrine resistance in breast cancer. Annu Rev Med 2011;62:231–47.
5. Garcia-Becerra R, Santos N, Diaz L, Camacho J. Mechanisms of resistance to endocrine therapy in breast cancer: focus on signaling pathways, miRNAs and genetically based resistance. Int J Mol Sci 2012;14:101–45.
6. Osborne CK, Bardou V, Hopp TA, Chamness GC, Hilsenbeck SG, Fuqua SA, et al. Role of the estrogen receptor coactivator AIB1 (SRC-3) and HER-2/neu in tamoxifen resistance in breast cancer. J Natl Cancer Inst 2003;95:353–61.
7. Lavinsky RM, Jepsen K, Heinzel T, Torchia J, Mullen TM, Schiff R, et al. Diverse signaling pathways modulate nuclear receptor recruitment of N-CoR and SMRT complexes. Proc Natl Acad Sci U S A 1998;95:2921–5.
8. Veldscholte J, Ris-Stalpers C, Kuiper GG, Jenster G, Berrevoets C, Claassen E, et al. A mutation in the ligand binding domain of the androgen receptor of human LNCaP cells affects steroid binding characteristics and response to anti-androgens. Biochem Biophys Res Commun 1990;173:531–40.
9. Zhao XY, Malloy PJ, Krishnan AV, Swami S, Navone NM, Peehl DM, et al. Glucocorticoids can promote androgen-independent growth of prostate cancer cells through a mutated androgen receptor. Nat Med 2000;6:703–6.
10. Herynk MH, Fuqua SA. Estrogen receptor mutations in human disease. Endoc Rev 2004;25:861–98.
11. Weis KE, Ekena K, Thomas JA, Lazennec G, Katzenellenbogen BS. Constitutively active human estrogen receptors containing amino acid substitutions for tyrosine 537 in the receptor protein. Mol Endocrinol 1996;10:1381–98.
12. Carlson KE, Choi I, Gee A, Katzenellenbogen BS, Katzenellenbogen JA. Altered ligand binding properties and enhanced stability of a constitutively active estrogen receptor: evidence that an open pocket conformation is required for ligand interaction. Biochemistry 1997;36:14891–905.
13. White R, Sjoberg M, Kalkhoven E, Parker MG. Ligand-independent activation of the oestrogen receptor by mutation of a conserved tyrosine. EMBO J 1997;16:1421–35.
14. Roodi N, Bailey LR, Kao WY, Verrier CS, Yee CJ, Dupont WD, et al. Estrogen receptor gene analysis in estrogen receptor-positive and receptor-negative primary breast cancer. J Natl Cancer Inst 1995;87:441–51.
15. Ellis MJ, Ding L, Shen D, Luo J, Suman VJ, Wallis JW, et al. Whole-genome analysis informs breast cancer response to aromatase inhibition. Nature 2012;486:351–60.
16. Stephens PJ, Tarpey PS, Davies H, Van Loo P, Greenman C, Wedge DC, et al. The landscape of cancer genes and mutational processes in breast cancer. Nature 2012;486:401–4.
17. Banerji S, Cibulskis K, Rangel-Escareno C, Brown KK, Carter SL, Frederick AM, et al. Sequence analysis of mutations and translocations across breast cancer subtypes. Nature 2012;486:401–9.
18. Karnik PS, Kulkarni S, Liu XP, Budd GT, Bukowski RM. Estrogen receptor mutations in tamoxifen-resistant breast cancer. Cancer Res 1994;54:341–53.
19. Zhang QX, Borg A, Wolf DM, Oesterreich S, Fuqua SA. An estrogen receptor mutant with strong hormone-independent activity from a metastatic breast cancer. Cancer Res 1997;57:1241–9.
20. Li H, Durbin R. Fast and accurate short read alignment with Burrows-Wheeler transform. Bioinformatics 2009;25:1751–60.
21. Li H, Handsaker B, Wysoker A, Fennell T, Ruan J, Homer N, et al. The sequence alignment/map format and SAMtools. Bioinformatics 2009;25:2071–9.
22. DePristo MA, Banks E, Poplin R, Garimella KV, Maguire JR, Hartl C, et al. A framework for variation discovery and genotyping using next-generation DNA sequencing data. Nat Genet 2011;43:491–8.
23. Forbes SA, Bindal N, Bamford S, Cole C, Kok CY, Beare D, et al. COSMIC: mining complete cancer genomes in the catalogue of somatic mutations in cancer. Nucleic Acids Res 2011;39:D941–50.
24. Compeau PE, Pevzner PA, Tesler G. How to apply de Bruijn graphs to genome assembly. Nat Biotechnol 2011;29:981–91.
25. Carter SL, Cibulskis K, Helman E, McKenna A, Shen H, Zack T, et al. Absolute quantification of somatic DNA alterations in human cancer. Nat Biotechnol 2012;30:411–21.
26. VanLoo P, Nordgard SH, Lingjaerde OC, Russnes HG, Rye IH, Sun W, et al. Allele-specific copy number analysis of tumors. Proc Natl Acad Sci U S A 2010;107:16911–5.
27. Yau C, Mouradov D, Jorissen RN, Colella S, Mirza G, Steers G, et al. A statistical approach for detecting genomic aberrations in heterogeneous tumor samples from single nucleotide polymorphism genotyping data. Genome Biol 2010;11:R92.
28. Meric-Bernstam F, Frampton G, Ferrer-Lozano J, Yelensky R, Palmer GA, Cronin MT, et al. Cancer gene profile of metastatic breast cancer. J Clin Oncology 2012;30 (suppl; abstract 1015).
29. Swaby RF, Jordan VC. Low-dose estrogen therapy to reverse acquired antihormonal resistance in the treatment of breast cancer. Clin Breast Cancer 2008;8:121–33.
30. Ellis MJ, Gao F, Dehdashti F, Jeffe DB, Marcom PK, Carey LA, et al. Lower-dose vs high-dose oral estradiol therapy of hormone receptor-positive, aromatase inhibitor-resistant advanced breast cancer: a phase 2 randomized study. JAMA 2009;302:771–80.
31. Li S, Shen D, Shao J, Crowder R, Liu W, Prat A, et al. Endocrine-therapy-resistant ESR1 variants revealed by genomic characterization of breast-cancer-derived xenografts. Cell Rep 2013;4:1111–30.
32. Toy W, Shen Y, Won H, Green B, Sakr RA, Will M, et al. ESR1 ligand-binding domain mutations in hormone-resistant breast cancer. Nat Genet 2013;45:1439–45.
33. Robinson DR, Wu YM, Vats P, Su F, Lonigro RJ, Cao X, et al. Activating ESR1 mutations in hormone-resistant metastatic breast cancer. Nat Genet 2013;45:1446–51.
34. Merenbakh-Lamin K, Ben-Baruch N, Yeheskel A, Dvir A, Soussan-Gutman L, Jeselsohn R, et al. D538G mutation in estrogen receptor-alpha: a novel mechanism for acquired endocrine resistance in breast cancer. Cancer Res 2013;73:6856–64.
35. The Cancer Genome Atlas Network. Comprehensive molecular portraits of human breast tumours. Nature 2012;490:61–70.
36. Baselga J, Campone M, Piccart M, Burris HAIII, Rugo HS, Sahmoud T, et al. Everolimus in postmenopausal hormone-receptor-positive advanced breast cancer. N Engl J Med 2012;366:521–9.
37. Pearce ST, Liu H, Jordan VC. Modulation of estrogen receptor alpha function and stability by tamoxifen and a critical amino acid (Asp-538) in helix 12. J Biol Chem 2003;278:7631–8.
38. Lazennec G, Ediger TR, Petz LN, Nardulli AM, Katzenellenbogen BS. Mechanistic aspects of estrogen receptor activation probed with constitutively active estrogen receptors: correlations with DNA and

coregulator interactions and receptor conformational changes. Mol Endoc 1997;11:1371–86.
39. Di Leo A, Jerusalem G, Petruzelka L, Torres R, Bondarenko IN, Khasanov R, et al. Results of the CONFIRM phase III trial comparing fulvestrant 250 mg with fulvestrant 500 mg in postmenopausal women with estrogen receptor-positive advanced breast cancer. J Clin Oncol 2010;28:4591–600.
40. Wolf DM, Jordan VC. The estrogen receptor from a tamoxifen stimulated MCF-7 tumor variant contains a point mutation in the ligand binding domain. Breast Cancer Res Treat 1994;31:121–38.
41. Wolf DM, Jordan VC. Characterization of tamoxifen stimulated MCF-7 tumor variants grown in athymic mice. Breast Cancer Res Treat 1994;31:111–27.
42. Holst F, Stahl PR, Ruiz C, Hellwinkel O, Jehan Z, Wendland M, et al. Estrogen receptor alpha (ESR1) gene amplification is frequent in breast cancer. Nat Genet 2007;39:655–60.
43. Tomita S, Zhang Z, Nakano M, Ibusuki M, Kawazoe T, Yamamoto Y, et al. Estrogen receptor alpha gene ESR1 amplification may predict endocrine therapy responsiveness in breast cancer patients. Cancer Sci 2009;100:1011–7.
44. Adelaide J, Finetti P, Charafe-Jauffret E, Wicinski J, Jacquemier J, Sotiriou C, et al. Absence of ESR1 amplification in a series of breast cancers. Int J Cancer 2008;123:2971–2.
45. Brown LA, Hoog J, Chin SF, Tao Y, Zayed AA, Chin K, et al. ESR1 gene amplification in breast cancer: a common phenomenon? Nat Genet 2008;40:801–7.

Priority Report

Cancer Research

D538G Mutation in Estrogen Receptor-α: A Novel Mechanism for Acquired Endocrine Resistance in Breast Cancer

Keren Merenbakh-Lamin[1,2], Noa Ben-Baruch[5], Adva Yeheskel[3], Addie Dvir[6], Lior Soussan-Gutman[6], Rinath Jeselsohn[8], Roman Yelensky[9], Myles Brown[8], Vincent A. Miller[9], David Sarid[1], Shulamith Rizel[7], Baruch Klein[4], Tami Rubinek[1], and Ido Wolf[1,2]

Abstract

Resistance to endocrine therapy occurs in virtually all patients with estrogen receptor α (ERα)-positive metastatic breast cancer, and is attributed to various mechanisms including loss of ERα expression, altered activity of coregulators, and cross-talk between the ERα and growth factor signaling pathways. To our knowledge, acquired mutations of the ERα have not been described as mediating endocrine resistance. Samples of 13 patients with metastatic breast cancer were analyzed for mutations in cancer-related genes. In five patients who developed resistance to hormonal therapy, a mutation of A to G at position 1,613 of ERα, resulting in a substitution of aspartic acid at position 538 to glycine (D538G), was identified in liver metastases. Importantly, the mutation was not detected in the primary tumors obtained prior to endocrine treatment. Structural modeling indicated that D538G substitution leads to a conformational change in the ligand-binding domain, which mimics the conformation of activated ligand-bound receptor and alters binding of tamoxifen. Indeed, experiments in breast cancer cells indicated constitutive, ligand-independent transcriptional activity of the D538G receptor, and overexpression of it enhanced proliferation and conferred resistance to tamoxifen. These data indicate a novel mechanism of acquired endocrine resistance in breast cancer. Further studies are needed to assess the frequency of D538G-ERα among patients with breast cancer and explore ways to inhibit its activity and restore endocrine sensitivity. *Cancer Res; 73(23); 6856–64. ©2013 AACR.*

Introduction

The human estrogen receptor-α (ERα) belongs to the superfamily of nuclear hormone receptors that function as ligand-activated transcription factors (1). Upon binding of estrogen, the ER dimerizes and binds to coactivators. The complex is then recruited to the estrogen-responsive elements (ERE) on the promoters of ER target genes. Approximately 75% of all breast cancers express ERα, and targeting ERα signaling, either by reducing levels of the ligand or inhibiting the receptor, is a key treatment strategy in these tumors. However, some patients with metastatic breast cancer (MBC) do not respond to any form of endocrine treatment (*de novo* resistance), and virtually all patients who initially respond eventually develop endocrine resistance (acquired resistance). Mechanisms associated with the development of acquired resistance include reduced expression of ERα, altered activity of coregulators, and increased activity of growth factor signaling pathways (2). Although mutation of key proteins is a common event in tumorigenesis, mutation of ERα is a rare event, occurring in only 1% of primary tumors (3). To our knowledge, acquired mutations of ERα have not been linked to the development of endocrine resistance yet.

We report here on a novel mutation of ERα, in which an A to G substitution at position 1,613 resulted in substitution of aspartic acid at position 538 to glycine (D538G). The mutation was identified in liver metastases obtained from patients who developed endocrine resistance, but not in samples of primary tumors obtained prior to commencing endocrine treatment. Structural modeling indicates that D538G substitution creates a conformational change that disrupts the interaction between the receptor and either estrogen or tamoxifen, but mimics the conformation of the activated receptor. Studies in cell lines confirmed ligand-independent, constitutive activity of the mutated receptor. Taken together, these data indicate the mutation D538G as a novel mechanism conferring acquired endocrine resistance.

Materials and Methods

Patients and genetic analyses

Samples of patients with metastatic breast cancer were submitted, at the discretion of their physicians, for

Authors' Affiliations: [1]Department of Oncology, Tel Aviv Sourasky Medical Center; [2]Sackler Faculty of Medicine; [3]The Bioinformatics Unit, Goerge S. Wise Faculty of Life Sciences, Tel Aviv University; [4]Assuta Medical Center, Tel Aviv; [5]Kaplan Medical Center, Rehovot; [6]Oncotest-Teva Pharmaceutical Industries; [7]Institute of Oncology, Davidoff Center, Rabin Medical Center, Petach Tikva, Israel; [8]Department of Medical Oncology, Dana-Farber Cancer Institute and Department of Medicine, Brigham and Women's Hospital, Harvard Medical School, Boston; and [9]Foundation Medicine, Cambridge, Massachusetts

K. Merenbakh-Lamin and N. Ben-Baruch contributed equally to this work.

Corresponding Author: Ido Wolf, Department of Oncology, Tel Aviv Sourasky Medical Center, 6 Weizmann st., 64239, Tel Aviv, Israel. Phone: 972-52-736-0558; Fax: 972-3-697-3030. E-mail: wolf-i@inter.net.il

doi: 10.1158/0008-5472.CAN-13-1197

©2013 American Association for Cancer Research.

commercially available genetic analysis aiming at identifying novel targets for treatment (Foundation One, Foundation Medicine, Cambridge, MA). The test has been described previously (4), and comprises deep sequencing of cancer-related genes on DNA extracted from paraffin-embedded tissue samples. Clinical data was obtained from the treating physicians.

Chemicals and antibodies

17β-estradiol (E2) and 4-hydroxytamoxifen (4-HT) were obtained from Sigma. Fulvestrant (ICI 182,780) was obtained from Tocris Bioscience. The antibodies used include anti-ERα (F-10) and anti-p-ERα (Tyr 537), both from Santa Cruz Biotechnology, and anti-SRC-1(MA1-840) from Thermo Fisher Scientific.

Constructs

The ERα expression vector (HEGO) was a generous gift of P. Chambon (University of Strasbourg, France). The ERE-luciferase reporter construct, kindly provided by D. Harris, (UCLA, Los Angeles, CA), consists of 2 repeats of the upstream region of the vitellogenin ERE promoter.

Generation of pcDNA3 ER-WT and 538G-ERα constructs: full-length ERα was subcloned into EcoRI site of pcDNA3 (Invitrogen) using the primers: 5′-primer: TTGGAATTCATGACCATGACCCTCCACAC, 3′-primer: AAACTCGAGTCAGACTGTGGCAGGGAAA. Generation of 538G-ER: site-directed mutagenesis was performed using the QuikChange Site-Directed Mutagenesis Kit according to the manufacturer's instructions (Stratagene). The ER expression vector was used as a template for PCR. Primers used were as follows: 5′-primer: GTGCCCCTCTATGGCCTGCTGCTGGAG, 3′-primer: CTCCAGCAGCAGGCCATAGAGGGGCAC. All subcloned constructs were sequenced.

Cells and transfections

Cell lines were obtained from the American Type Culture Collection. MCF-7 were grown in Dulbecco's Modified Eagle's Medium (DMEM) containing 10% fetal calf serum (FCS); MDA-MB-231 were grown in RPMI medium containing 10% FCS. All transfections used Jet Pei (Polyplus Transfection). For all E2, 4-HT, and fulvestrant studies, cells were cultured in phenol-free media using 10% charcoal-treated serum for 2 days before treatment.

Western blot analysis

Cells were harvested, lysed, and the total protein was extracted with radioimmunoprecipitation assay (RIPA) buffer (50 mmol/L Tris–HCl pH 7.4, 150 mmol/L NaCl, 1% NP-40, 0.25% Na-deoxycholate, 1 mmol/L EDTA, 1 mmol/L NaF), together with a protease and phosphatase inhibitor cocktails (Sigma). Lysates were resolved on 10% SDS-PAGE and immunoblotted with the indicated antibodies.

Coimmunoprecipitation studies

Studies were conducted essentially as described previously (5). Cells were harvested in immunoprecipitation (IP) buffer (50 mmol/L Tris–HCl pH 7.5, 1% NP-40, 150 mmol/L NaCl, 5 mmol/L EDTA). Total protein was extracted, and 1 mg protein lysate was incubated with 5 μL of anti SRC-1 antibody overnight at 4°C. Then, protein A/G beads (Pierce) were added and, after a 2-hour incubation, the beads were washed once with IP-buffer and 3 times with PBS. The immunoprecipitated materials were separated by SDS-PAGE and detected by Western blot analysis.

Luciferase assays

Cells were plated in 24-well plates and transfected with the reporter vector and the various constructs. Luciferase assay was conducted using the Luciferase Assay System kit (Promega, CA) according to the manufacturer's instructions. Luciferase units were normalized to protein concentration.

Real-time quantitative PCR

Two days after transfection with the various constructs, total RNA was prepared using the RNA isolation kit (Sigma). Total RNA (1 μg) was reverse transcribed using RevertAid (Fermentas). The cDNA was then used for real-time quantitative PCR using StepOne Plus (Applied Biosystems). The TGF-α–specific primers used were: 5′CCCGCTGAGTGCAGACC and 3′ACGTACCCAGAATGGCAGAC. The progesterone receptor (PR)-specific primers used were: 5′CGCGCTCTACCCTGCACTC and 3′TGAATCCGGCCTCAGGTAGTT. The GREB1a-specific primers used were: 5′-ACGTGTGGTGACTGGAGTAGC and 3′CCACGCAAGGTAGAAGGTGA. Equal loading was determined using β-actin–specific primers.

Proliferation and migration assays

Proliferation was assessed using the MTT assay as previously described (5). For the assay, MCF-7 cells were transfected with either a control vector, WT-ERα, or 538G-ERα, plated in 96-well plates (3,000 cells/well), cultured in phenol-free media with 10% charcoal-treated serum for 2 days, and then treated for 48 hours as indicated.

Migration was assessed using the wound healing ("scratch") assay as described previously (6). For the assay, MCF-7 cells were transfected with the indicated constructs and grown to confluency in a six-well plate in phenol-free media with 10% charcoal-treated serum. The cell monolayer was then scraped in a straight line with a 200-μL tip and photographed at 48 hours.

Structure modeling

Mutant D538G ERα was modeled twice: (i) according to PDB 2OCF (7) for the estrogen-bound conformation, and (ii) PDB 3ERT (8) for the tamoxifen-bound conformation. Both models were created using Jacakl as implemented in the Fold and Function Assignment System (FFAS) server (9), and then refined using the Relax protocol of Rosetta version 3.4 (10). On thousand models were generated for each initial model structure and then clustered using the Rosetta cluster protocol. A representative of the largest cluster was selected for further analysis. The wild-type (WT) structure of the estrogen-bound conformation was also modeled based on PDB 2OCF.

Molecular docking

Molecular docking of estrogen and tamoxifen were performed for both conformations using Dock version 6.5

(http://dock.compbio.ucsf.edu/DOCK_6/) and SwissDock (11). The results of both tools were similar. In addition, estrogen and tamoxifen were docked on the WT structures for method validation. Docking of both ligands was performed with and without the SRC-1 peptide taken from PDB.

Results

Identification of D538G mutation in ERα in breast cancer samples

From December 2011 to April 2013, tumor samples of 13 Israeli patients with ERα-positive metastatic infiltrating ductal carcinoma (IDC), who have failed multiple lines of treatment, were submitted for genetic analysis aiming at identifying novel treatment options. Surprisingly, a novel mutation (A1613G) leading to the substitution D538G in ERα was identified in liver metastases obtained from 5 patients (38%). Importantly, the mutation was not detected in the primary tumor of these patients, obtained at diagnosis prior to commencing endocrine treatment. All 5 patients received at least two lines of endocrine treatment for a prolonged duration (from 67 to 97 months of treatment) for the adjuvant and metastatic setting, prior to the development of endocrine resistance (Table 1). The frequency of the mutated allele was 16% to 41% and correlated with the percentage of tumor cells in the samples.

All biopsies containing the mutation were obtained from liver metastases. On the other hand, only one of the eight samples with WT-ERα was obtained from the liver, and the other seven were obtained from bone or soft tissues ($P = 0.005$ for the comparison between the groups). In one patient who carried the mutation, pulmonary metastasis was analyzed simultaneously and did not harbor the mutation. This observation may suggest either emergence of this specific mutation in the liver or predilection of cells harboring the mutation to the liver tissue.

Structural modeling of D538G-ERα

Asp-538 is positioned within a critical area of the ligand-binding domain (LBD), termed helix 12, and *in vitro* substitution of it to alanine or asparagine reduced the activity of the receptor (12). Aspartic acid contains a fairly large negative side-chain whereas glycine contains only a hydrogen substituent as its side-chain. Thus, the D538G substitution is expected to affect the tertiary structure of ERα. Analysis of the crystal structure of the LBD in the WT-ERα indicates the important role of helix 12 in mediating the interaction between the receptor and various coactivators, including the steroid receptor coactivator (SRC)-1 and -2 (1). Upon binding of estrogen, helix 12 is positioned over the ligand-binding pocket, thus forming a surface for the recruitment of coactivators (Fig. 1A). However, upon binding of tamoxifen, helix 12 is displaced into a position that prevents binding of coactivators (Fig. 1B and 1C). The model structure of D538G-ERα (Fig. 1D) suggests that the conformation of helix 12 in the mutated protein is similar to that observed in the WT-ERα upon estrogen binding (Fig. 1D). Thus, the model predicts ligand-independent constitutive activity of D538G-ERα.

We next compared the effects of D538G substitution to that of Y537S substitution, which also induces constitutive activity of the receptor (13). The model demonstrates a change in side-chain rotamers. The hydrogen bonds Y537-N348 and D351-L540 exist in the WT structure, but the Y537-N348 bond cannot exist in the Y537S mutant (Fig. 1E). Similarly, the D538G substitution prevents the Y537-N348 hydrogen bond but allows the D351-L540 bond to exist (Fig. 1F). These changes in the network of hydrogen bonds may cause higher flexibility in helix 12, thus enabling binding of coactivators even in the absence of a ligand.

We next modeled the docking of estrogen and tamoxifen. The model structure of estrogen- or tamoxifen-bound WT-ERα (based on 2OCF and 3ERT) yielded a similar pose to the one observed in the X-ray structure (1ERE, 2OCF, and 3ERT). The

Table 1. Clinical and pathologic characteristics of 5 patients with infiltrating ductal carcinoma carriers of the D538G-ER mutation

Stage at diagnosis	Hormone receptors at primary tumor	ER mutation status at diagnosis	Adjuvant hormonal treatments (months)	Hormonal treatments for metastatic disease (months)	Hormone receptors at metastasis	Tumor content (%)	ER minor allele frequency (mutant/WT, %)
Local	NA	WT	NA	Aromazin (24) Fulvestrant (13)	NA	70	35
Local	ER 0 PR +1	WT	Tamoxifen (60)	Anastrazole (3)	ER +2 PR +3	50	22
Local	ER +1 PR +3	WT	Tamoxifen (60)	Anastrazole (14) Fulvestrant (9)	ER +1	30	16
Local	ER +3 PR +3,	WT	Tamoxifen (20) Anastrazole (32)	Exemestane (15) Fulvestrant (28)	ER +3, PR +3,	80	31
Metastatic	ER +3, PR +3,	WT	NA	Tamoxifen + goserelin (14) Anastrazola + goserelin (14) Fulvestrant (8)	NA	80	41

Abbreviations: ER, estrogen receptor; IDC, infiltrating ductal carcinoma; NA, not available; PR, progesterone receptor; WT, wild-type.

model of D538G-ERα suggests a conformational change in the position of helix 12 that enables binding of coactivators in the absence of estrogen and interferes with binding of estrogen and tamoxifen (Fig. 1G and H). Thus, the D538G receptor is predicted to be resistant to tamoxifen. The molecular docking used here is based on the assumption that the WT protein is rigid. Substitution of Asp by Gly at position 538 allows the protein to be more flexible and may help to understand the low affinity of D538G-ERα to tamoxifen.

Ligand-independent transcriptional activity of D538G-ERα

In order to study the activity of the mutated receptor, an ERα harboring the D538G substitution (538G-ERα) was generated and its transcriptional activity was studied compared to WT-ERα using the ERE-luciferase reporter (14). MCF-7 cells were cotransfected with the ERE-luciferase reporter and either pcDNA3, WT-ERα or 538G-ERα. Cells were grown in estrogen-depleted medium and treated with either vehicle control or E2. In the absence of E2, WT-ERα increased ERE activity by 10-fold compared with pcDNA3-transfected cells, whereas 538G-ERα increased ERE activity by 45-fold (Fig. 2A, black bars, $P = 0.002$). Treatment with E2 significantly increased ERE activity only in pcDNA3- and WT-ERα–transfected cells but activity remained lower compared with 538G-ERα–transfected cells (Fig 2A, gray bars). In addition, similar results were noted in the ERα-negative MDA-MB-231 cells. Overexpression of 538G-ERα increased ERE activity by 11-fold compared with pcDNA3-transfected cells (Fig. 2B, $P = 0.0002$) or WT-ERα–transfected cells ($P = 0.0004$), and treatment with E2 increased activity in WT-ERα–transfected cells but not in 538G-ERα–transfected cells. In order to further validate the transcriptional activity of 538G-ERα, we also examined its ability to induce transcription of the ERα-regulated genes *PR*, *GREB1*, and *TGF-α* (12). Expression of 538G-ERα in MCF-7 cells increased mRNA levels of PR by 15.7-fold and of GREB1 by 28-fold compared with pcDNA3-transfected cells (Fig. 2C and D), and by 3- and 4-fold, respectively, compared with WT-ERα–transfected cells ($P < 0.01$ for all comparisons). Similarly, overexpression of 538G-ERα in MDA-MB-231 cells significantly increased TGF-α mRNA levels (Fig. 2E, $P = 0.01$). Due to the activation of the endogenous ERα, treatment with E2 increased the transcriptional activity in MCF-7 cells transfected with 538G-ERα (Fig. 2C and 2D), but not in MDA-MB-231 cells (Fig. 2E).

Taken together, these data clearly indicate ligand-independent, constitutive activity of D538G-ERα in breast cancer cells.

D538G-ERα interacts with SRC-1 constitutively in a ligand-independent manner but does not affect phosphorylation of Tyr 537

Our model predicts that the conformational alteration induced by the substitution of Asp538 to glycine will confer the receptor active conformation allowing ligand-independent interaction with coactivators. In order to test this hypothesis, we examined the interaction between overexpressed WT-ERα or 538G-ER and endogenous SRC-1 in MDA-MB-231 cells (Fig. 3A). Although WT-ERα interacted with SRC-1 only upon treatment with E2, 538G-ERα interacted with SRC-1 in a ligand-independent manner.

Phosphorylation of Tyr-537 may inhibit activity of ERα, and substitution of it by Asn (Y537N) is associated with increased activity of the receptor (13, 15). We examined the effect of 538G on phosphorylation of Tyr-537, using a phospho–Tyr-537-directed antibody. No change in phosphorylation pattern was noted, suggesting that increased activity of D538G is not mediated by altered phosphorylation of Tyr 537 (Fig. 3B).

D538G-ERα enhances proliferation and migration of breast cancer cells

We next tested the ability of 538G-ERα to enhance the proliferation of MCF-7 cells. Cells were transfected with control vector, WT-ERα, or 538G-ERα, grown in estrogen-depleted medium, and treated with either vehicle or E2 for 48 hours. Viability was studied by the MTT assay. The 538G-ERα enhanced proliferation compared with either pcDNA3 or WT-ERα by 33% in untreated cells and by 28% in E2-treated cells (Fig. 4A, $P < 0.01$ for both comparisons).

In order to study the ability of the mutation to affect migration, we conducted a wound healing ("scratch") assay. MCF-7 cells were transfected with control vector, WT-ERα, or 538G-ERα, grown in estrogen-depleted medium, and the cell monolayer was scraped in a straight line and then treated with either vehicle or E2 for 48 hours. 538G-ERα enhanced migration compared with either pcDNA3 or WT-ERα in both untreated and treated cells (Fig. 4B).

D538G-ERα is resistant to tamoxifen and fulvestrant

We tested the ability of the active metabolite of tamoxifen, 4-HT, and of the selective ER downregulator (SERD) fulvestrant to inhibit the transcriptional activity of 538G-ERα. To this aim, we employed the ER-negative MDA-MB-231 cells, which do not show intrinsic transcriptional activity (Fig. 2B). Cells were transfected with either WT-ERα or 538G-ERα, grown in estrogen-depleted medium and treated with 4-HT (Fig. 5A) or fulvestrant (Fig. 5B) as indicated. The mutated receptor demonstrated relative resistance to both 4-HT and fulvestrant.

Discussion

We show here, for the first time, that acquired resistance to hormonal treatment in metastatic breast cancer may be mediated through an activating mutation of ERα. Despite the central role of ERα in the development of breast cancer, mutation of ERα is a rare event (3). Two activating mutations of the ERα have been described previously, Y537N and K303R, and both occur in less than 1% of primary tumors (15–17). To our knowledge, the D538G mutation in ERα has not been described as yet. Furthermore, no other acquired mutations of the ERα are currently known. There are two possible explanations for this. First, prior studies focused mainly on the presence of mutations in the primary tumor at diagnosis and, thus, were not able to detect acquired

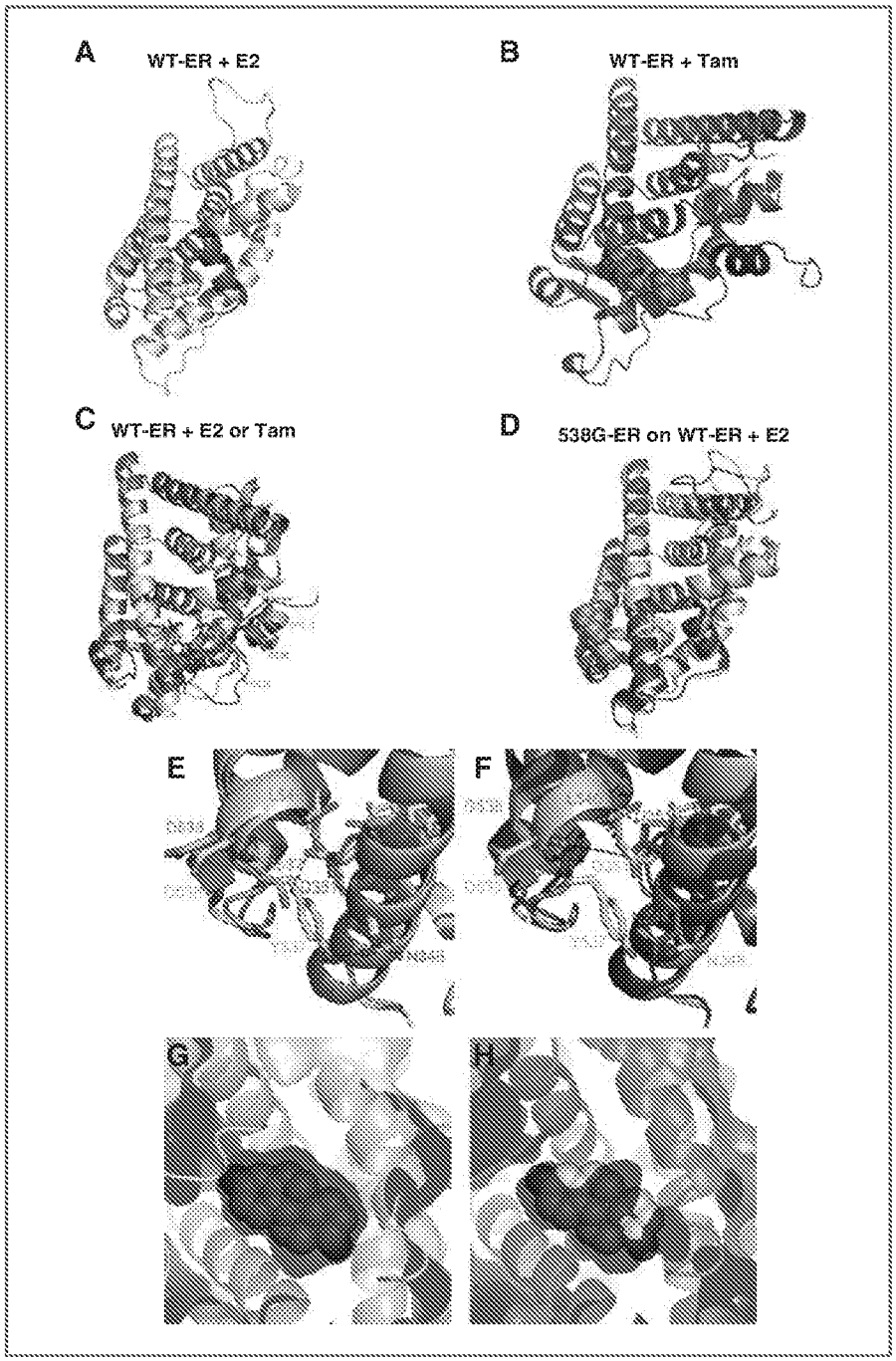


Figure 3. D538G mutation enables ligand-independent binding of coactivators. A, WT-ERα in the estrogen-bound conformation (PDB 1ERE) is shown by beige ribbons. Helix 12 (H12) colored in brown. E2 of the X-ray structure is shown by yellow VdW spheres, and the docking result is shown by green VdW spheres. B, WT-ERα in the tamoxifen-bound conformation (PDB 3ERT) is shown by blue ribbons. H12 colored in dark blue. Tamoxifen of the X-ray structure is shown by red VdW spheres and the docking result is shown by pink VdW spheres. C, WT-ERα in the estrogen-bound conformation (PDB 1ERE) is shown by beige ribbons. WT-ERα in the tamoxifen-bound conformation (PDB 3ERT) is shown by blue ribbons. The wild-type X-ray structure of Src-1 (PDB 3UUD) is shown by orange ribbons. Estrogen is shown by yellow sticks, and tamoxifen is shown by red sticks. The location of D538 is shown in both conformations by sticks. The direction of H12 in both conformations is shown by a black arrow. SRC-1 cannot bind the tamoxifen-bound receptor because H12 is located in the SRC-1 binding site. D, WT-ERα in the estrogen-bound conformation (PDB 1ERE) is shown by beige ribbons. E2 of the X-ray structure is shown by yellow VdW spheres. The D538G-ERα model structure is shown by dark red ribbons, and the docking result of E2 is shown by green VdW spheres. (*Continued on the following page.*)

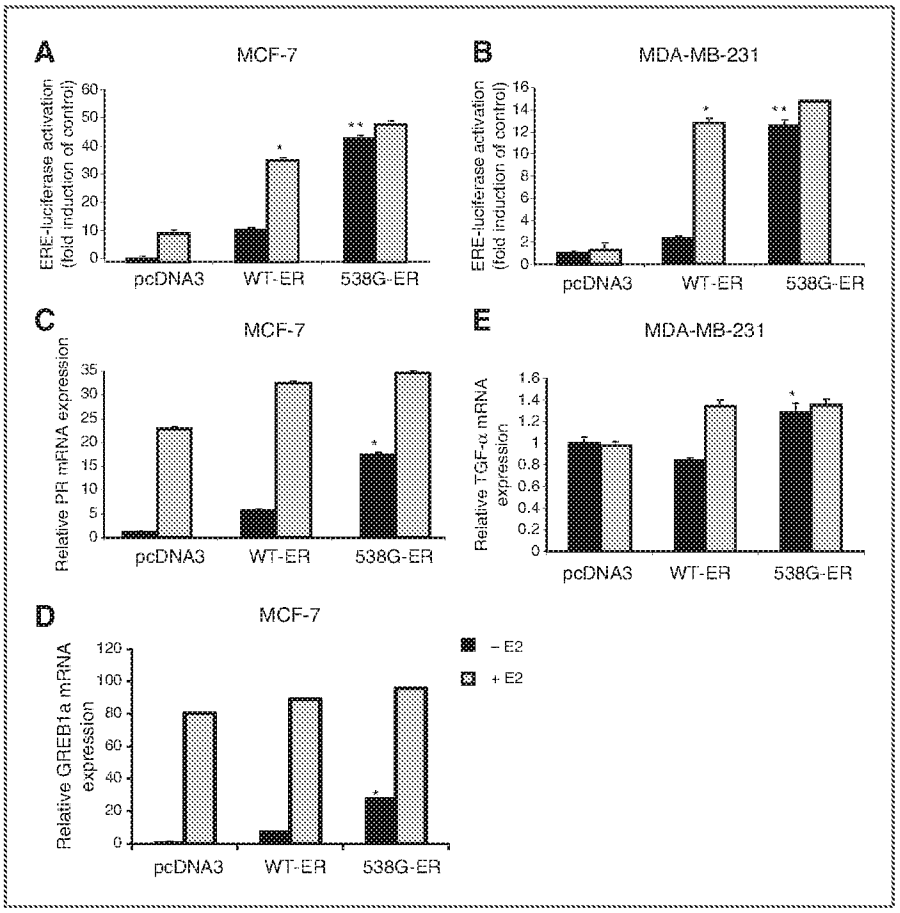


Figure 2. 538G-ERα possess constitutive, ligand-independent transcriptional activity. A, MCF-7 cells were transiently transfected with WT-ERα, 538G-ERα, or control vector, together with the ERE-luciferase reporter. Cells were treated with E2 (10 nmol/L) as indicated, for 24 hours. The luciferase activities were analyzed and normalized to total protein concentration, and are shown relative to the control vector. *, $P < 0.01$, WT-ERα versus control; **, $P < 0.005$ 538G-ERα versus control and WT-ERα. B, MDA-MB-231 cells were transiently transfected and treated as in A, and luciferase activity was analyzed. *, $P < 0.005$ WT-ERα versus control; **, $P < 0.005$ 538G-ERα versus control and WT-ERα. C and D, MCF-7 cells were transiently transfected with WT-ERα, 538G-ERα constructs, or a control vector. Cells were then treated with E2 or control vehicle for 24 hours. PR (C) and GREB1a (D) mRNA levels were determined 48 hours after transfection by quantitative RT-PCR. *, $P < 0.01$, 538G-ERα versus WT-ERα. E, MDA-MB-231 cells were transiently transfected and treated as in C, and TGF-α mRNA levels were determined 48 hours after transfection by quantitative RT-PCR. *, $P < 0.01$, 538G-ERα versus WT-ERα. All figures show representative results of at least three independent experiments, each performed in quadruplicates (ERE-luciferase) or triplicates (RT-PCR). Each bar represents the mean ± SD.

mutations in the metastases. Second, it is possible that sequencing methods used previously were less sensitive than current methods. We noted the presence of this mutation in 5 out of 13 (38%) patients with ERα-positive metastatic breast cancer. However, these are highly selected, heavily pretreated patients and may not represent the general population of patients with breast cancer. The actual prevalence of the D538G mutation needs to be determined in large cohorts of patients. If indeed the mutation is identified in a significant proportion of patients, direct testing of it may be an easy and cheap method to predict response to hormonal treatment.

(*Continued.*) The conformation of H12 in the mutated protein is predicted to allow binding of SRC-1 in the absence of E2. D538G mutation alters hydrogen bonds in helix 12. WT-ERα X-ray structure is shown by beige ribbons and 537S-ERα X-ray structure (E) or 538G-ER (F) in the estrogen-bound conformation are shown by gray ribbons. Estrogen is shown by yellow sticks. Specific residues are shown by sticks, with their nitrogen atoms colored in blue and oxygen atoms in red. S537 (E) and G538 (F) are colored in green. The hydrogen bonds network is shown by dashed black lines. The hydrogen bonds Y537-N348 and D351-L540 exist in the WT, but both mutants are predicted to lack the Y537-N348 hydrogen bond. In 537S-ER, Ser-537 may bind D351. In D538G, Tyr-537 is too far from Asp-351 (7.3 Å) but, similarly to the WT-ERα, Asp-351 may bind Leu-540. The D538G mutation alters docking of E2 and tamoxifen. G, the wild-type X-ray structure of estrogen receptor in the estrogen bound conformation (PDB 1ERE) is shown by beige ribbons and molecular surface. The estrogen atoms are shown by VdW spheres, carbons in yellow, and oxygen in red. H, the mutant model structure is in gray. The estrogen atoms are shown by VdW spheres, carbons in yellow, and oxygen in red. The binding site of the mutant is not fitted for estrogen.

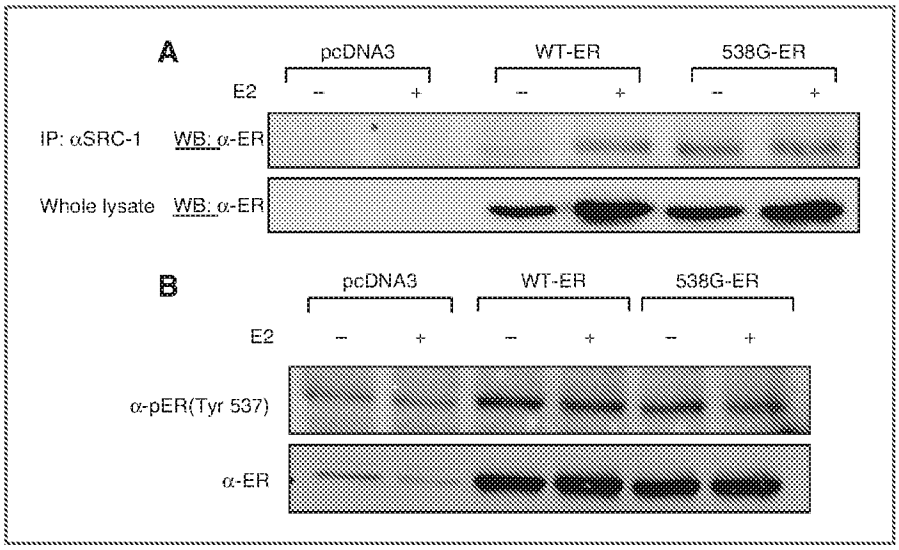


Figure 3. Ligand-independent interaction between 538G-ERα and SRC1. A, MDA-MB-231 cells were transfected with WT-ERα, 538G-ERα, or control vector. Cells were then treated with vehicle or E2 (10 nmol/L) for 45 minutes; then cells were lysed and SRC1 was immunoprecipitated. Immunocomplexes were resolved on SDS-PAGE gel and immunoblotted with anti-ER antibodies. B, MCF-7 cells were transfected with WT-ERα, 538G-ERα, or control vector. Cells were then treated with vehicle or E2 (10 nmol/L) for 24 hours. Forty-eight hours after transfection, cells were lysed and immunoblotted with antibodies as indicated.

Helix 12 in the LBD plays a major regulatory role in the activity of the ER and is involved in the interaction of the ER with E2, coregulators and inhibitors (1). Our structure model suggested a conformational change in helix 12 following the D538G substitution and predicted the mutated receptor to be constitutively active ligand-independent and bound to coactivators. The experimental data strongly support this model. Although no mutations in helix 12 have been identified in clinical samples as yet, ample laboratory data indicate the role of specific amino acids within this region. Most amino acid substitutions either do not change or decrease transcriptional activity (reviewed in ref. 3). Specifically, D538A substitution is associated with decreased activation and increased degradation of the receptor (12), and several substitutions of Tyr-537

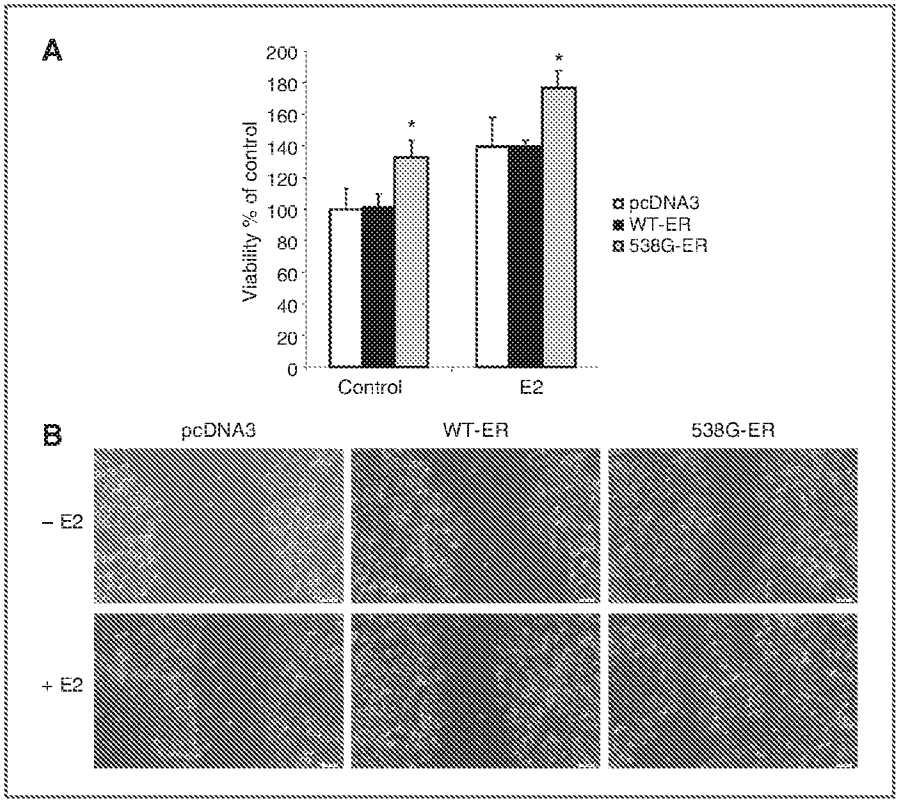


Figure 4. 538G-ERα enhances viability and migration of breast cancer cells. A, MCF-7 cells were seeded in 60-mm dishes and were transiently transfected with WT-ERα, 538G-ERα, or empty vector, and 24 hours later were seeded in 96-well plates. Cells then were treated with E2 (10 nmol/L) or control vehicle. Viability was assessed after 48 hours using MTT assay. *, $P < 0.0001$, 538G-ERα versus control and WT-ERα. B, MCF-7 cells were transfected as in A and grown to confluency in phenol-free media with 10% charcoal-treated serum. The monolayer was scraped, treated with E2 or control vehicle for 48 hours, and photographed.

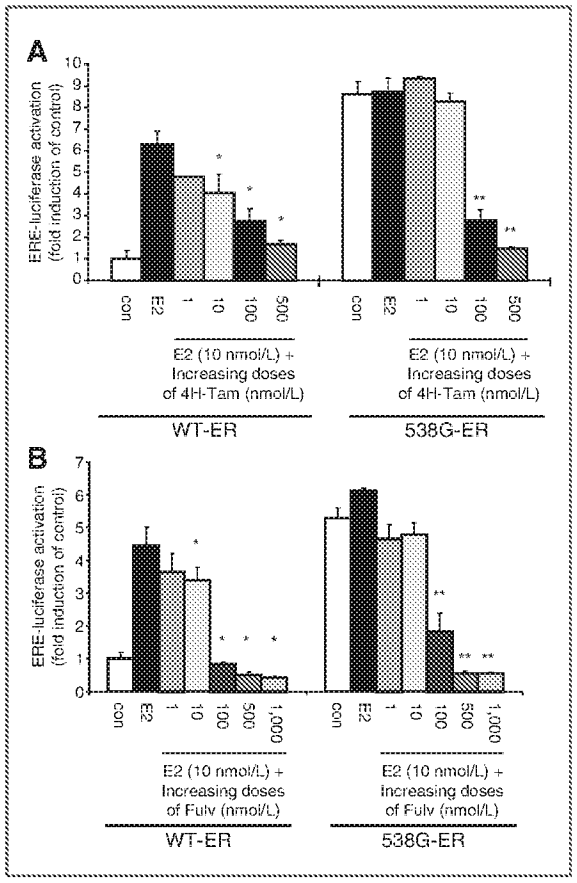


Figure 5. 538G-ERα confers resistance to 4HT and fulvestrant. A, MDA-MB-231 cells were transfected with either WT-ERα or 538G-ERα, together with the ERE-luciferase reporter. Cells were then treated with a vehicle control or with E2 (10 nmol/L) together with increasing doses of 4HT, as indicated, for 24 hours. Luciferase activities were analyzed and normalized to total protein concentration, and are shown relative to the control WT-ERα. *, $P < 0.01$ for WT-ERα treated with E2 alone compared to treatment with 4HT at 10 nmol/L and higher concentrations. **, $P < 0.05$ for 538G-ERα treated with E2 alone compared with treatment with 4HT at 100 nmol/L and higher concentrations. B, MDA-MB-231 cells were transfected as in A, and treated with elevated fulvestrant concentrations. *, $P < 0.03$ for WT-ERα treated with E2 alone compared with treatment with fulvestrant at 10 nmol/L and higher concentrations. **, $P < 0.05$, 538G-ERα treated with E2 alone compared with treatment with fulvestrant at 100 nmol/L and higher concentrations. The figure shows representative results of two independent experiments, each performed in quadruplicates. Each bar represents the mean ± SD.

alter the affinity of the ER to E2 (13). However, there are several examples for increased activation and resistance to inhibitors. For example, certain mutations of Leu-536 increased ligand-independent constitutive activity (13), and substitution of Glu-542 to alanine increased E2-dependent activity (12). Thus, the increased activity of D538G-ERα observed by us is in line with current knowledge regarding helix 12 structure and function.

D538G-ERα seems to enhance viability and migration of MCF-7 cells, even compared with E2 stimulation. It remains to be elucidated whether this phenomenon translates into more aggressive clinical course upon acquisition of the mutation. The mechanisms governing this increased activity are not known. One possibility is altered degradation. Upon E2 binding and transcriptional activity, the half-life of the ER is shortened from 5 days to 3 hours, and this may serve as a negative regulatory mode of the estrogen pathway (18). It is possible that, as D538G-ERα does not bind to the ligand, its degradation is altered and its half-life, and therefore activity, is increased.

Although no acquired mutations of ER-α were noted in the clinic, a series of articles from the laboratory of Craig Jordan reported and characterized an acquired mutation occurring *in vivo*. The mutation, D351Y, was discovered in MCF-7 cells grown as tumors in athymic mice chronically treated with tamoxifen (19). This is an important laboratory proof to our clinical observation. Although D351 does not reside within helix 12, upon binding of E2, D351 lies next to D538 and plays a major role in the regulation of E2-dependent and -independent activation and is also involved in mediating the agonist effects of tamoxifen (20, 21).

The presence of the mutation may represent the genetic heterogeneity of the primary tumor followed by Darwinian selection of resistance clones. This mechanism was noted in a relatively fast-growing basal-like breast cancer (22). Alternatively, *de novo* mutations may appear during disease progression. This was noted in a lobular breast tumor, where 32 mutations appeared during a period of 9 years (23). Regardless of the mechanism, our observation clearly indicates that genomic analyses aimed at predicting response to treatment and identifying novel potential therapeutic targets should be conducted on the most recent metastatic lesions available. Preferably, both the metastases and the primary tumor should be evaluated.

The mutation was noted only in liver metastases. In one patient, the mutation was noted in a liver metastasis and not in a pulmonary metastasis, and, in the 8 patients without the mutation, all but one sample were obtained from extrahepatic sites. This is a very preliminary observation and needs to be validated in a much larger cohort. However, it may indicate a special predilection of cancer cells with active estrogen signaling to the liver. Tropism of breast cancer cells to specific organs, especially to the lung, bone, and brain, is a well-described phenomenon (24). In accordance with our observation, a recent study noted an association between the expression of hormones receptors and liver metastases (25).

All our patients developed resistance to several forms of endocrine treatments (Table 1). Ligand-independent activity explains clinical resistance to treatment with aromatase inhibitors, which inhibit estrogen production. Resistance to tamoxifen and fulvestrant is predicted to result from a conformational change in helix 12 interfering with their binding to the receptor (Fig. 1). Studies in cell lines indicated that both tamoxifen and fulvestrant can inhibit the mutated receptor, although at high, supraphamacologic concentrations. Thus, the concentration of tamoxifen that inhibited the mutated receptor is 1,400-fold higher than that observed in breast cancer tissue following administration of standard dose of 20 mg tamoxifen (0.07 nmol/L) and predicts complete clinical resistance to tamoxifen (26). Similarly, the effective fulvestrant concentration was higher than the plasma concentration of

fulvestrant (27, 28). The observation that a high concentration of tamoxifen and fulvestrant can inhibit D538G-ERα is still encouraging and indicates that other compounds may be able to bind the receptor, prevent its activation, and restore endocrine sensitivity.

In conclusion, we identified a novel acquired mutation of ERα in metastases obtained from patients with metastatic breast cancer who developed resistance to endocrine treatment. The mutation induces a conformational change, which mimics the conformation of activated ligand-bound receptor and confers ligand-independent activity as well as resistance to endocrine treatment. This discovery may lead to the development of novel endocrine treatments for patients who develop resistance to currently available endocrine treatments.

Disclosure of Potential Conflicts of Interest

A. Dvir and L. Soussan-Gutman are employees of Oncotest-Teva Pharmaceutical Industries, the Israeli distributer of Foundation One. R. Yelensky has ownership interest (including patents) in association with Foundation Medicine. M. Brown is a consultant for and has received commercial research funding from Novartis Pharmaceuticals. No potential conflicts of interest were disclosed by the other authors.

Authors' Contributions

Conception and design: N. Ben-Baruch, V.A. Miller, I. Wolf
Development of methodology: R. Yelensky, T. Rubinek, I. Wolf
Acquisition of data (provided animals, acquired and managed patients, provided facilities, etc.): K. Merenbakh Lamin, A. Dvir, L. Soussan-Gutman, R. Jeselsohn, D. Sarid, S. Rizel, B. Klein, I. Wolf
Analysis and interpretation of data (e.g., statistical analysis, biostatistics, computational analysis): K. Merenbakh Lamin, A. Yeheskel, R. Yelensky, M. Brown, V.A. Miller, T. Rubinek, I. Wolf
Writing, review, and/or revision of the manuscript: N. Ben-Baruch, A. Dvir, L. Soussan-Gutman, R. Jeselsohn, M. Brown, V.A. Miller, D. Sarid, I. Wolf
Administrative, technical, or material support (i.e., reporting or organizing data, constructing databases): A. Dvir, L. Soussan-Gutman, D. Sarid
Study supervision: I. Wolf
Other (bioinformatics): A. Yeheskel
Other (medical oncologic patient care): S. Rizel

Grant Support

This work was financially supported by the Israel Cancer Association; The Margaret Stultz foundation, the Sackler Faculty of Medicine, Tel Aviv University, Tel Aviv, Israel; the Israel Science Foundation (grant no. 1112/09); and TASMC excellence fund.

The costs of publication of this article were defrayed in part by the payment of page charges. This article must therefore be hereby marked *advertisement* in accordance with 18 U.S.C. Section 1734 solely to indicate this fact.

Received April 23, 2013; revised September 10, 2013; accepted September 20, 2013; published OnlineFirst November 11, 2013.

References

1. Ascenzi P, Bocedi A, Marino M. Structure-function relationship of estrogen receptor alpha and beta: impact on human health. Mol Aspects Med 2006;27:299–402.
2. Osborne CK, Schiff R. Mechanisms of endocrine resistance in breast cancer. Annu Rev Med 2011;62:233–47.
3. Herynk MH, Fuqua SA. Estrogen receptor mutations in human disease. Endocr Rev 2004;25:869–98.
4. Giulino-Roth L, Wang K, MacDonald TY, et al. Targeted genomic sequencing of pediatric Burkitt lymphoma identifies recurrent alterations in antiapoptotic and chromatin-remodeling genes. Blood 2012;120:5181–4.
5. Wolf I, Levanon-Cohen S, Bose S, et al. Klotho: a tumor suppressor and a modulator of the IGF-1 and FGF pathways in human breast cancer. Oncogene 2008;27:7094–105.
6. Liang C, Park A, Guan J. In vitro scratch assay: a convenient and inexpensive method for analysis of cell migration in vitro. Nat Protoc 2007;2:329–33.
7. Koide A, Abbatiello S, Rothgery L, Koide S. Probing protein conformational changes in living cells by using designer binding proteins: application to the estrogen receptor. Proc Natl Acad Sci U S A 2002;99:1253–8.
8. Shiau AK, Barstad D, Loria PM, et al. The structural basis of estrogen receptor/coactivator recognition and the antagonism of this interaction by tamoxifen. Cell 1998;95:927–37.
9. Jaroszewski L, Li Z, Cai XH, Weber C, Godzik A. FFAS server: novel features and applications. Nucleic Acids Res 2011;39:W38–44.
10. Misura KM, Baker D. Progress and challenges in high-resolution refinement of protein structure models. Proteins 2005;59:15–29.
11. Grosdidier A, Zoete V, Michielin O. SwissDock, a protein-small molecule docking web service based on EADock DSS. Nucleic Acids Res 39:W270–7.
12. Pearce ST, Liu H, Jordan VC. Modulation of estrogen receptor alpha function and stability by tamoxifen and a critical amino acid (Asp-538) in helix 12. J Bio Chem 2003;278:7630–8.
13. Zhong L, Skafar DF. Mutations of tyrosine 537 in the human estrogen receptor-alpha selectively alter the receptor's affinity for estradiol and the kinetics of the interaction. Biochemistry 2002;41:4209–17.
14. Fan S, Wang J, Yuan R, et al. BRCA1 inhibition of estrogen receptor signaling in transfected cells. Science 1999;284:1354–6.
15. Barone I, Brusco L, Fuqua SA. Estrogen receptor mutations and changes in downstream gene expression and signaling. Clin Cancer Res 2010;16:2702–8.
16. Fuqua SA, Wiltschke C, Zhang QX, et al. A hypersensitive estrogen receptor-alpha mutation in premalignant breast lesions. Cancer Res 2000;60:4026–9.
17. Zhang QX, Borg A, Wolf DM, Oesterreich S, Fuqua SA. An estrogen receptor mutant with strong hormone-independent activity from a metastatic breast cancer. Cancer Res 1997;57:1244–9.
18. Reid G, Denger S, Kos M, Gannon F. Human estrogen receptor-alpha: regulation by synthesis, modification and degradation. Cell Mol Life Sci 2002;59:821–31.
19. Wolf D, Jordan VC. The estrogen receptor from a tamoxifen stimulated MCF-7 tumor variant contains a point mutation in the ligand binding domain. Breast Cancer Res Treat 1994;31:129–38.
20. Liu H, Lee ES, Deb Los Reyes A, Zapf JW, Jordan VC. Silencing and reactivation of the selective estrogen receptor modulator-estrogen receptor alpha complex. Cancer Res 2001;61:3632–9.
21. MacGregor Schafer J, Liu H, Bentrem DJ, Zapf JW, Jordan VC. Allosteric silencing of activating function 1 in the 4-hydroxytamoxifen estrogen receptor complex is induced by substituting glycine for aspartate at amino acid 351. Cancer Res 2000;60:5097–105.
22. Ding L, Ellis MJ, Li S, et al. Genome remodelling in a basal-like breast cancer metastasis and xenograft. Nature 2010;464:999–1005.
23. Shah SP, Morin RD, Khattra J, et al. Mutational evolution in a lobular breast tumour profiled at single nucleotide resolution. Nature 2009;461:809–13.
24. Lorusso G, Ruegg C. New insights into the mechanisms of organ-specific breast cancer metastasis. Semin Cancer Biol 2012;22:226–33.
25. Koo JS, Jung W, Jeong J. Metastatic breast cancer shows different immunohistochemical phenotype according to metastatic site. Tumori 2010;96:424–32.
26. Kisanga ER, Gjerde J, Guerrieri-Gonzaga A, et al. Tamoxifen and metabolite concentrations in serum and breast cancer tissue during three dose regimens in a randomized preoperative trial. Clin Cancer Res 2004;10:2336–43.
27. Addo S, Yates RA, Laight A. A phase I trial to assess the pharmacology of the new oestrogen receptor antagonist fulvestrant on the endometrium in healthy postmenopausal volunteers. Br J Cancer 2002;87:1354–9.
28. Estevez L, Alvarez I, Tusquets I, et al. Finding the right dose of fulvestrant in breast cancer. Cancer Treat Rev 2013;39:136–41.

Role of the Estrogen Receptor Coactivator AIB1 (SRC-3) and HER-2/neu in Tamoxifen Resistance in Breast Cancer

C. Kent Osborne, Valerie Bardou, Torsten A. Hopp, Gary C. Chamness, Susan G. Hilsenbeck, Suzanne A. W. Fuqua, Jiemin Wong, D. Craig Allred, Gary M. Clark, Rachel Schiff

Background: **AIB1 (SRC-3) is an estrogen receptor (ER) coactivator that, when overexpressed in cultured cells, can reduce the antagonist activity of tamoxifen-bound ERs. Signaling through the HER-2 receptor pathway activates AIB1 by phosphorylation. To determine whether high AIB1 expression alone or together with HER-2 reduces the effectiveness of tamoxifen in breast cancer patients, we quantified expression of AIB1 and HER-2 in tumors from breast cancer patients with long-term clinical follow-up who received either no adjuvant therapy or adjuvant tamoxifen therapy after breast cancer surgery.** ***Methods:*** **AIB1 and HER-2 protein levels in tumors from 316 breast cancer patients were determined using western blot analysis. Molecular variables (e.g., expression of AIB1, ER, progesterone receptor, p53, Bcl-2), tumor characteristics, and patient outcome were assessed using Spearman rank correlation. Disease-free survival (DFS) curves were derived from Kaplan–Meier estimates, and the curves were compared by log-rank tests. The effect of AIB1 on DFS adjusted for other prognostic factors was assessed by multivariable analysis using the Cox proportional hazards model. All statistical tests were two-sided.** ***Results:*** **High AIB1 expression in patients not receiving adjuvant tamoxifen therapy was associated with better prognosis and longer DFS ($P = .018$, log-rank test). In contrast, for patients who did receive tamoxifen therapy, high AIB1 expression was associated with worse DFS ($P = .049$, log-rank test), which is indicative of tamoxifen resistance. The test for interaction between AIB1 expression and tamoxifen therapy was statistically significant ($P = .004$). When expression of AIB1 and HER-2 were considered together, patients whose tumors expressed high levels of both AIB1 and HER-2 had worse outcomes with tamoxifen therapy than all other patients combined ($P = .002$, log-rank test).** ***Conclusions:*** **The antitumor activity of tamoxifen in patients with breast cancer may be determined, in part, by tumor levels of AIB1 and HER-2. Thus, AIB1 may be an important diagnostic and therapeutic target. [J Natl Cancer Inst 2003;95:353–61]**

The estrogen receptor (ER) mediates the effects of estrogen on the development and progression of breast cancer, and it serves as an important diagnostic and therapeutic target for prevention and treatment. The ER regulates the expression of genes that contribute to tumor progression by both classical (e.g., binding to specific response elements in a gene promoter) and nonclassical (e.g., activating growth factor pathways in the membrane) mechanisms. The selective estrogen receptor modulator (SERM) drug tamoxifen, which binds to the ER and partially inhibits its activity, is effective in the treatment and prevention of breast cancer.

ER-mediated gene transcription is regulated not only by the binding of estrogens or SERMs to the ER but also by other post-translational events, such as receptor phosphorylation, which can be induced both by the binding of estrogen and SERMs and by mitogen-activated protein kinase (MAPK) pathways *(1–6)*. ER function is also modulated by interactions with coactivators and corepressors *(7)*. These coregulatory proteins may also alter ER activity when the receptor is bound by SERMs such as tamoxifen, a drug that has mixed estrogen agonist/antagonist properties. Increased coactivator levels can enhance the agonist activity of tamoxifen-bound ER, whereas increased corepressor levels can enhance antagonist activity, at least in cultured cells, in which the levels of these proteins can be raised or lowered dramatically *(8–12)*.

AIB1, also called SRC-3, RAC3, ACTR, and p/CIP, is an ER coactivator that is thought to be important in breast cancer *(13–16)*. AIB1 is overexpressed in breast cancer cells compared with normal duct epithelial cells and is amplified in a small proportion of breast tumors *(13,17–19)*. AIB1 is highly expressed in cultured MCF-7 human breast cancer cells, and its activity is essential for the growth of these cells both *in vitro* and *in vivo* *(20)*. AIB1, like the ER itself, is phosphorylated and thereby functionally activated by MAPKs; therefore, high levels of activated AIB1 could reduce the antagonist effects of tamoxifen, especially in tumors that also overexpress the HER-2 receptor, a member of the epidermal growth factor (EGF) receptor family that activates MAPKs *(21)*.

Laboratory studies suggest that ER-positive breast cancers that overexpress HER-2 may be less responsive to tamoxifen than breast cancers with low HER-2 expression *(22)*. The mechanisms for this resistance are not yet clear; however, li-

Affiliation of authors: C. K. Osborne, S. A. W. Fuqua (Departments of Medicine and Molecular and Cellular Biology and the Breast Center), V. Bardou, T. A. Hopp, G. C. Chamness, S. G. Hilsenbeck, R. Schiff, G. M. Clark (Department of Medicine and the Breast Center), J. Wong (Department of Molecular and Cellular Biology), D. C. Allred (Department of Pathology and the Breast Center), Baylor College of Medicine, Houston, TX.

Correspondence to: C. Kent Osborne, M.D., Baylor College of Medicine, One Baylor Plaza, BCM 600, Houston, TX 77030 (e-mail: kosborne@breastcenter.tmc.edu).

See "Notes" following "References."

Journal of the National Cancer Institute, Vol. 95, No. 5, © Oxford University Press 2003, all rights reserved.

Downloaded from http://jnci.oxfordjournals.org/ at Eisai-Andover on July 6, 2016

gand-independent activation of the ER by MAPKs, which themselves are phosphorylated and thereby activated by HER-2 signaling in such tumors, may contribute to it *(4–6)*. High HER-2 expression has also been shown to be associated with tamoxifen resistance in some clinical studies *(23,24)*, but this association is not strong and other studies have failed to confirm it *(23,24)*.

The cumulative data on the role of coregulators in ER function suggest that they are important contributors to estrogen-mediated tumor growth and, potentially, to breast tumor sensitivity or resistance to endocrine therapy such as tamoxifen. Tumors with a relatively high abundance of coactivators such as AIB1, especially those with enhanced HER-2 signaling which can activate AIB1, should be less responsive to tamoxifen therapy because of increased estrogen agonist activity of tamoxifen-bound ER *(12,25)*. To explore these hypotheses, we determined AIB1 protein levels in extracts from frozen tumors from 316 patients with long-term clinical follow-up, some of whom had received no adjuvant systemic therapy after breast cancer surgery and others of whom had received adjuvant tamoxifen therapy. Correlations among expression levels of AIB1 and other molecular variables, including ER, progesterone receptor (PR), HER-2, p53, and Bcl-2, and tumor characteristics, including S-phase fraction and patient outcome, were analyzed. Given the biologic relationship between HER-2 and AIB1 activation, the predictive significance of the combination of AIB1 and HER-2 expression levels was also assessed in both groups of patients.

Patients and Methods

Patients

Frozen tumor specimens from 316 breast cancer patients, all of whom had positive axillary lymph nodes at the time of initial surgery, were selected for study. Such patients have higher recurrence rates after primary treatment (i.e., initial surgery) than lymph node-negative patients, resulting in more events for better statistical power. One hundred nineteen of these patients received no adjuvant chemotherapy or tamoxifen therapy after initial surgery and 187 patients received adjuvant tamoxifen therapy. The other 10 patients received both adjuvant chemotherapy and tamoxifen therapy. The median follow-up for patients still living is 95 months. These studies were approved by the Baylor College of Medicine Institutional Review Board.

Tumor Specimens

Proteins (30 mg) from tumor tissue from each patient were extracted in 300 μL of 5% sodium dodecyl sulfate (SDS) at 90 °C for 5 minutes. Protein concentration was determined using the bicinchoninic acid (BCA) method (Pierce, Rockford, IL), according to the manufacturer's instructions, with typical yields of 2–5 μg/μL. Protein samples were stored at –70 °C until use.

Cell Line Standard

MCF-7 human breast cancer cell extracts were used as a standard on each gel to correct for gel-to-gel variations in band intensity. Cells were grown in 100-mm tissue culture dishes and then harvested. Proteins were then extracted in a single-step process in the culture dish. Briefly, cells were washed twice with cold phosphate-buffered saline (PBS), and proteins were extracted with 5% SDS in distilled water at 90 °C for 5 minutes. The mixture was centrifuged at 13 000*g* for 5 minutes, and the protein remaining in the supernatant (approximate yield = 1 μg/μL) was determined using the BCA method. Standard samples were stored at –70 °C until use.

Western Blot Assay for AIB1

AIB1 expression levels were measured by an investigator blinded to all clinical information. Briefly, 20 μg of extracted protein in sample buffer (0.05 *M* Tris [pH 6.8] containing 2% SDS, 2.5% β-mercaptoethanol, 10% glycerol, and 0.1% bromophenol blue as tracking dye) was placed in boiling water for 2 minutes, cooled to room temperature, and centrifuged at 13 000*g* for 1 minute. Protein extracted from MCF-7 cells was used as a reference standard (5 μg of protein/lane) and was included on each gel as a normalization control. Proteins were subjected to electrophoresis on 8% Tricine-Glycine polyacrylamide gels (Invitrogen, Carlsbad, CA) and transferred onto nitrocellulose membranes at 4 °C overnight at 20 mA.

Blots were then rinsed for 5 minutes with Tris-buffered saline (TBS) (100 m*M* Tris [pH 7.5] and 0.9% NaCl) containing 0.1% Tween-20 (TBST). After blocking with 5% nonfat dry milk in TBST, the blots were incubated overnight at 4 °C in primary antibody (1 : 1000 rabbit anti-RAC3 antiserum). This polyclonal antibody was raised in rabbits against a maltodextrin binding protein (MBP) fusion protein containing amino acid residues 582–842 of human RAC3 (i.e., AIB1). This antibody is specific for AIB1 and does not cross-react with other members of the SRC family *(26)*. The blots were washed three times in TBST and then incubated for 1 hour at room temperature in 5% nonfat dry milk in TBST and horseradish peroxidase-labeled anti-rabbit Ig (1 : 5000) as secondary antibody (Amersham Pharmacia Biotech, Piscataway, NJ). The blots were then washed five times in TBST, after which the labeled protein was visualized on a FluorChem digital imaging system (Alpha Innotech Corp., San Leandro, CA) using an enhanced chemiluminescence detection system. Band intensities were measured densitometrically using AlphaEase FC software (Alpha Innotech Corp.). AIB1 levels in tumor samples were normalized to AIB1 levels in the MCF-7 standard control from the same immunoblot. AIB1 levels were measured once in each breast tumor extract. For most analyses, AIB1 levels were considered as a continuous variable, and no attempt was made to identify an optimal cutpoint. For some analyses, levels were arbitrarily divided into quartiles.

Other Tumor Markers

The amount of ER and PR in the tumor tissue was measured by ligand binding assays as previously described *(27)*. Briefly, cytosols were extracted from tumor tissues that had been pulverized in liquid nitrogen. ^{125}I-labeled estradiol and tritiated-ORG 2058 (Amersham Pharmacia Biotech) allowed for simultaneous determination of levels of both ER and PR in the standard multipoint dextran-coated charcoal assay. Tumors with an ER content of at least 3 fmol/mg protein (the limit of detection in this assay) and with a PR content of at least 10 fmol/mg protein were considered to be positive for ER and PR, respectively. These levels were based on prior studies calibrated to clinical outcome *(27)*.

S-phase fraction was calculated by DNA flow cytometry and classified as low, intermediate, or high, as previously described *(28)*. Briefly, DNA flow cytometry was performed on tumor extracts, and the histograms were analyzed by Modfit (Verity Software House, Topsham, ME) using single-cut debris strip-

Downloaded from http://jnci.oxfordjournals.org/ at Eisai-Andover on July 6, 2016

ping *(28)*. Cut points were determined by calibrating S-phase fraction with clinical outcome in a group of more than 28 800 patients with breast cancer (low, <6%; intermediate, 6%–10%; high, >10%).

Immunohistochemistry was used to semiquantitatively measure p53 and Bcl-2 protein expression *(29)*. Briefly, 5-μm sections of each paraffin-embedded specimen were stained with hematoxylin and eosin to verify adequate numbers of invasive tumor cells. Additional 5-μm sections underwent antigen retrieval in boiling citrate buffer (pH 6) in a pressure cooker for 5 minutes. For Bcl-2 immunostaining, sections were incubated for 1 hour in monoclonal antibody 124 (DAKO, Carpinteria, CA). For p53 immunostaining, sections were incubated overnight in a humidity chamber with monoclonal antibody 1801 (Novocastra Laboratories, Ltd., Newcastle upon Tyne, U.K.). A secondary biotinylated anti-mouse antibody was applied to the slides for 30 minutes at room temperature, followed by incubation with streptavidin horseradish peroxidase for 30 minutes at room temperature. The slides were then rinsed in PBS and exposed to diaminobenzidine tetrahydrochloride for 10 minutes at room temperature. Slides were then counterstained with methyl green and scored by a pathologist. A cut point of more than or equal to 10% positively stained cells was used for both Bcl-2 and p53, based on prior calibrations with clinical outcome *(29)*.

HER-2 expression was determined by western blot analysis as described previously *(30)*. Briefly, proteins were extracted in 5% SDS and subjected to electrophoresis on 7.5% polyacrylamide gels. An SDS extract of the T47D human breast cancer cell line was used as a reference standard. Resolved proteins were electroblotted onto a nitrocellulose membrane at 20 mA for 16 hours at 4 °C. Blots were incubated with anti-HER-2 protein antiserum overnight at 4 °C, followed by incubation with ^{125}I-labeled donkey anti-rabbit whole antibody for 30 minutes at room temperature. The level of HER-2 protein in individual tumors was determined by densitometric scanning of the 190-kd band and expressed in terms of HER-2 units based on the T47D laboratory standard. The cut points for low (i.e., grade 0 or 1) and high (i.e., grades 2–4) HER-2 expression accurately predicted disease-free survival (DFS) in a prior study and thus were used as the cut points in this study *(29,30)*.

Statistical Analysis

Clinical and prognostic characteristics of study patients are grouped as shown in Table 1 and are summarized by frequency distributions. Differences in frequency distributions between patients who did and did not receive adjuvant tamoxifen therapy were assessed by Fisher's exact test. Associations between clinical and molecular factors, which were all treated as continuous variables, were assessed by the Spearman rank correlation.

DFS was calculated from the date of diagnosis. First recurrence (local or distant) was scored as an event, and patients without recurrence were censored at the time of last follow-up or death from any cause. For graphical presentation, follow-up was truncated at 120 months. Overall survival (OS) was calculated from the date of diagnosis, with death from any cause being scored as an event. Patients who were alive at the last follow-up were censored at the last follow-up date. Survival curves were derived from Kaplan–Meier estimates *(31)*, and the curves were compared by log-rank tests *(32)*.

Separate analyses were performed for those patients who did and did not receive adjuvant tamoxifen therapy. The association of the level of AIB1 expression with patient outcome, adjusted for other prognostic factors, was assessed in multivariable analysis by Cox proportional hazards models *(33)*. The assumption of proportional hazards was verified separately in each treatment group by using the method of Grambsch and Therneau *(34)*. Explanatory variables conformed to the assumption of proportionality, except for ER (dichotomized ER-positive versus -negative) in patients who did not receive adjuvant tamoxifen therapy ($P = .005$). The nonproportionality resulted from a loss of prognostic effect for ER after the first 3 years of follow-up. Multivariable analyses that did or did not include an additional time-dependent variable to account for this change in the effect of ER after 3 years yielded virtually identical results for other explanatory variables, and therefore only the simpler, time-independent analyses are presented *(34)*. All statistical tests were two-sided at the 5% level of statistical significance and were performed using SAS (version 8.0) or SPLUS (version 6.1) (SAS Institute, Cary, NC). A Wald test was used to assess the statistical significance of individual prognostic factors. Survival rates and hazard ratios are presented with their 95% confidence intervals (CIs).

Results

Characteristics of Patients and Tumor Specimens

Patient and tumor characteristics for the entire study population and for each treatment group are shown in Table 1. The majority of patients (85%) were at least 50 years old and, by definition, all patients had positive axillary lymph nodes, with 55% having 1–3 positive lymph nodes. Most of the tumors were of small or intermediate size (82%) and had intermediate or high S-phase fractions (77%). Eighty-nine percent of the patients had ER-positive tumors (reflecting the patient selection criteria), 62% of patients had PR-positive tumors, and 31% of patients had HER-2 grade 2–4 tumors. The characteristics of the treatment (i.e., tamoxifen therapy or no adjuvant therapy) groups were similar, with the exception of a slightly older age, a greater proportion of ER and/or PR positivity, and a lower proportion of p53 positivity in the patients who received tamoxifen therapy.

AIB1 Expression and Correlations With Molecular Markers and Clinical Variables

Expression of AIB1 in different tumors varied widely (Fig. 1). Normalized band intensity, using the MCF-7 reference standard, ranged from 0.26 to 5.7 densitometry units, a difference of more than 20-fold. The mean band intensity across all tumors was 1.3 (95% CI = 1.22 to 1.39), and the median was 1.15.

When we examined the correlations between various molecular markers and clinical variables in the tumor specimens, ER protein expression was positively correlated with age, PR expression, and Bcl-2 expression and inversely correlated with p53 expression, S-phase fraction, and tumor size (data not shown). AIB1 protein expression (as a continuous variable), by contrast, showed a weak inverse correlation with PR expression (correlation coefficient [r] = –0.11; $P = .05$) and no correlation with ER expression ($r = -0.07$; $P = .20$) (Table 2). Statistically significant but weak positive correlations were observed between AIB1 expression and S-phase fraction ($r = 0.21$; $P = .003$) and HER-2 expression ($r = 0.22$; $P<.001$). The positive correlations between AIB1 expression and factors typically associated with a more aggressive phenotype

Downloaded from http://jnci.oxfordjournals.org/ at Eisai-Andover on July 6, 2016

Table 1. Patient and tumor characteristics*

Variable	All patients, No. (%)	Untreated patients, No. (%)	Tamoxifen-treated patients, No. (%)	*P* value†
Age, y				
⩾50	269 (85)	95 (80)	168 (90)	
<50	47 (15)	24 (20)	19 (10)	.018
Lymph nodes				
1–3	172 (55)	64 (54)	104 (56)	
>3	143 (45)	54 (46)	83 (44)	.81
Missing	1	1	0	
Tumor size, cm				
Small (<2)	78 (25)	23 (20)	51 (27)	
Intermediate (2–5)	180 (57)	69 (58)	107 (57)	
Large (>5)	57 (18)	26 (22)	29 (16)	.17
Missing	1	1	0	
S-phase fraction, %				
Low (<6)	72 (23)	20 (17)	49 (27)	
Intermediate (6–10)	101 (33)	41 (35)	59 (32)	
High (>10)	137 (44)	57 (48)	75 (41)	.13
Missing	6	1	4	
ER				
Positive (⩾3 fmol/mg)	281 (89)	96 (81)	177 (95)	
Negative (<3 fmol/mg)	35 (11)	23 (19)	10 (5)	<.001
PR				
Positive (⩾10 fmol/mg)	187 (62)	58 (53)	122 (66)	
Negative (<10 fmol/mg)	116 (38)	52 (47)	62 (34)	.026
Missing	13	9	3	
p53 IHC score				
0–4	256 (82)	88 (76)	160 (86)	
5–8	55 (18)	28 (24)	26 (14)	.030
Missing	5	3	1	
HER-2 grade				
0–1	218 (69)	84 (71)	127 (68)	
2–4	97 (31)	35 (29)	60 (32)	.70
Missing	1	0	0	
Bcl-2 IHC score				
0–4	125 (41)	50 (44)	72 (40)	
5–8	177 (59)	63 (56)	108 (60)	.54
Missing	14	6	7	
AIB1 expression, units				
1st quartile	84 ⩽ .78	30 ⩽ 0.79‡	48 ⩽ 0.76‡	
2nd quartile	85 > .78–1.15	30 > 0.79–1.17	46 > 0.76–1.11	
3rd quartile	79 > 1.15–1.61	30 > 1.17–1.67	47 > 1.11–1.55	
4th quartile	68 > 1.61	29 > 1.67	46 > 1.55	

*Ten patients treated with adjuvant chemotherapy plus tamoxifen were included in the "All patients" category and were used for initial correlations, but they are not included in the "Untreated" or "Tamoxifen-treated" categories. The number of patients with missing data is shown, but they are not included in the calculation of percentages or in Fisher's exact test. ER = estrogen receptor; PR = progesterone receptor; IHC = immunohistochemistry.

†*P* values were derived from Fisher's exact test.

‡Corrected densitometry units from western blots were normalized to the MCF-7 reference standards.

(i.e., HER-2 and S-phase fraction) suggested that AIB1 expression might correlate with relatively poor prognosis.

AIB1 Expression and Prognosis

To examine the relationship between AIB1 expression and prognosis, we analyzed tumors from the 119 patients who did not receive adjuvant therapy. The exclusion of patients who received adjuvant therapy allowed us to discriminate between

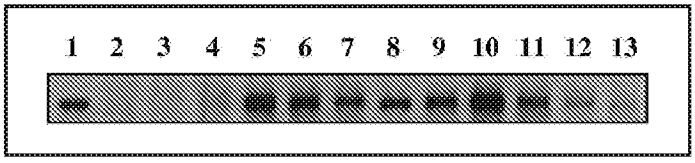


Fig. 1. Example of a western blot showing AIB1 expression from extracts of 12 representative tumors. **Lane 1** is the standard (5 μg of MCF-7 extract protein) that was used to normalize AIB1 levels between blots. Protein (20 mg) was added to each lane.

Table 2. Spearman rank correlations of AIB1 expression with molecular markers and clinical variables*

Variable	N	AIB1 correlation coefficient†	*P* value‡
ER	316	−0.07	.20
PR	303	−0.11	.05
p53	311	0.09	.10
HER-2	315	0.22	<.001
Age	316	0.008	.88
Tumor size	315	0.09	.09
S-phase fraction	310	0.21	.003
Bcl-2	302	−0.08	.15
Lymph nodes	315	0.07	.22

*ER = estrogen receptor; PR = progesterone receptor; N = number of patients for whom data were available.

†All variables are continuous.

‡*P* values were derived from a two-sided one-sample *t* test.

Downloaded from http://jnci.oxfordjournals.org/ at Eisai-Andover on July 6, 2016

the prognostic (natural progression) and predictive (response to drug) effects of AIB1 expression. Although high AIB1 expression was correlated weakly with higher S-phase fraction and HER-2, both indicators of poor prognosis, high levels of AIB1 expression were associated, instead, with better prognosis (log-rank test, $P = .018$); 5-year DFS was 77% (95% CI = 59% to 95%) for patients in the top quartile of AIB1 expression compared with 47% (95% CI = 35% to 59%) for patients in the lower three quartiles combined (Fig. 2, A). When AIB1 expression was considered as a continuous variable, high AIB1 expression was not statistically significantly associated with better prognosis ($P = .07$). AIB1 expression was also not statistically significantly associated with OS, an endpoint that can be confounded by multiple treatments given after recurrence.

Several of the other prognostic factors investigated in this patient subset that had statistically significant associations with better DFS included ER positivity ($P = .008$) and PR positivity ($P = .017$). Poorer DFS was predicted by high HER-2 expression ($P = .024$), high S-phase fraction ($P = .013$), more than three positive lymph nodes ($P<.001$), and large tumor size (>5 cm) ($P = .004$). When AIB1 expression and these six prognostic factors were included in a Cox multivariable analysis of DFS (in which the values for AIB1, ER, PR, and HER-2 expression and the number of lymph nodes were dichotomized; the values for tumor size were trichotomized; and the values for S-phase fraction were treated as continuous variables [Table 3]), only the number of lymph nodes, ER status, AIB1 expression, and HER-2 expression remained statistically significant—that is, more than three positive lymph nodes, negative ER status, low AIB1 expression, and high HER-2 expression (grade 2–4) were all associated with an increased risk of recurrence. In a similar analysis, in which AIB1 expression was treated as a continuous variable, the number of positive lymph nodes ($P<.001$), HER-2 expression ($P = .038$), ER negativity ($P = .006$), and low AIB1 expression ($P = .043$) all remained statistically significant risk factors for recurrence. AIB1 protein expression (continuous or dichotomized) was still not associated with OS, even though the number of positive lymph nodes, ER expression level, and HER-2 expression were statistically significantly associated with OS (data not shown). Thus, among patients who did not receive adjuvant tamoxifen therapy, high AIB1 expression was associated with a more indolent tumor and more favorable patient outcome than was low AIB1 expression.

AIB1 and Effect of Adjuvant Tamoxifen Therapy

To examine the effect of AIB1 expression on the benefit of adjuvant tamoxifen therapy, we analyzed tumors from the 187 patients who had received adjuvant tamoxifen therapy. AIB1 expression levels in these patients were similar to those observed in the patients who had not received adjuvant tamoxifen therapy (Table 1). AIB1 expression was not a favorable factor for DFS in the tamoxifen-treated patients compared with DFS in untreated patients. Patients in the top quartile of AIB1 expression had worse DFS than patients in the lower three quartiles combined, although the difference did not reach statistical significance. When the 10 known ER-negative patients were omitted from the analysis and AIB1 expression was considered as a continuous variable, high AIB1 expression was statistically significantly associated with poorer DFS (hazard ratio [HR] = 1.43, 95% CI = 1.03 to 1.97; $P = .031$) (data not shown). High AIB1 expression, when treated as a continuous variable, remained a statistically significant adverse factor in a multivariable analysis (HR = 1.45, 95% CI = 1.06 to 1.97; $P = .028$), along with more than three positive lymph nodes (HR = 2.73, 95% CI = 1.64 to 4.54; $P<.001$) (Table 3), whereas ER and PR status, HER-2 expression, and S-phase fraction were not statistically significant predictors of outcome. As was the case in patients who did not receive adjuvant therapy, AIB1 expression was not a predictor of OS in patients who had received adjuvant tamoxifen.

Thus, although high AIB1 expression was associated with better DFS for patients who had not received adjuvant therapy, high levels of AIB1 were associated with poorer DFS in patients who had received tamoxifen. A test for interaction between AIB1 expression and treatment (tamoxifen-treated patients) or not (untreated patients) was highly statistically significant ($P = .004$), thus confirming that the association of AIB1 expression with DFS is different in the tamoxifen-treated patients (data not shown). These data suggest that tumors expressing high levels of AIB1 protein may be tamoxifen resistant.

Interaction of AIB1 and HER-2

Because one of the consequences of HER-2 signaling is the activation of AIB1 and because some studies *(23,24)* have suggested that high HER-2 expression may be associated with tamoxifen resistance, we examined whether high HER-2 expression might, via activation of AIB1, further modulate the response of ER to tamoxifen and thus cause a higher level of resistance. An analysis of the interaction of HER-2 and AIB1 in patients who did not receive adjuvant therapy (Table 4) showed that when HER-2 expression was low, high AIB1 expression (top quartile) predicted better DFS than lower AIB1 expression (lower three quartiles combined) (log-rank test, $P = .013$); 5-year DFS was 88% (95% CI = 73% to 100%) and 53% (95% CI = 39% to 67%), respectively. Fig. 2, B, shows that the patients with high AIB1 expression and low HER-2 expression, although relatively few in number (n = 19), had statistically significantly better DFS than patients with low AIB1 expression and low HER-2 expression, high AIB1 expression and high HER-2 expression, or low AIB1 expression and high HER-2 expression as a group (log-rank test, $P = .005$). Thus, high HER-2 expression was an adverse prognostic factor for DFS in the untreated patients, and the level of AIB1 expression did not appear to have an additional effect on patient outcome.

Among patients receiving adjuvant tamoxifen therapy who had low HER-2 expression (Table 4), high AIB1 expression was not statistically significantly associated ($P = .20$) with an unfavorable outcome, perhaps because that group of patients lacked the high HER-2 expression needed to functionally activate AIB1. Among patients receiving adjuvant tamoxifen therapy who had high HER-2 expression, however, high AIB1 expression was an adverse predictive factor ($P = .003$). Kaplan–Meier estimates of DFS comparing patients in the high AIB1/high HER-2 group with all other patients combined are shown in Fig. 2, C. DFS in the group of patients with high AIB1 expression and high HER-2 expression was much worse (5-year DFS = 42%, 95% CI = 22% to 63%) than the other three groups of patients combined (5-year DFS = 70%, 95% CI = 62% to 77%) (log-rank test, $P = .002$). Interestingly, the group of patients with high HER-2 expression but low AIB1 expression had favorable DFS, despite having high HER-2 expression (5-year DFS = 77%, 95% CI = 63% to 92%). Thus, in the presence of

Downloaded from http://jnci.oxfordjournals.org/ at Eisai-Andover on July 6, 2016

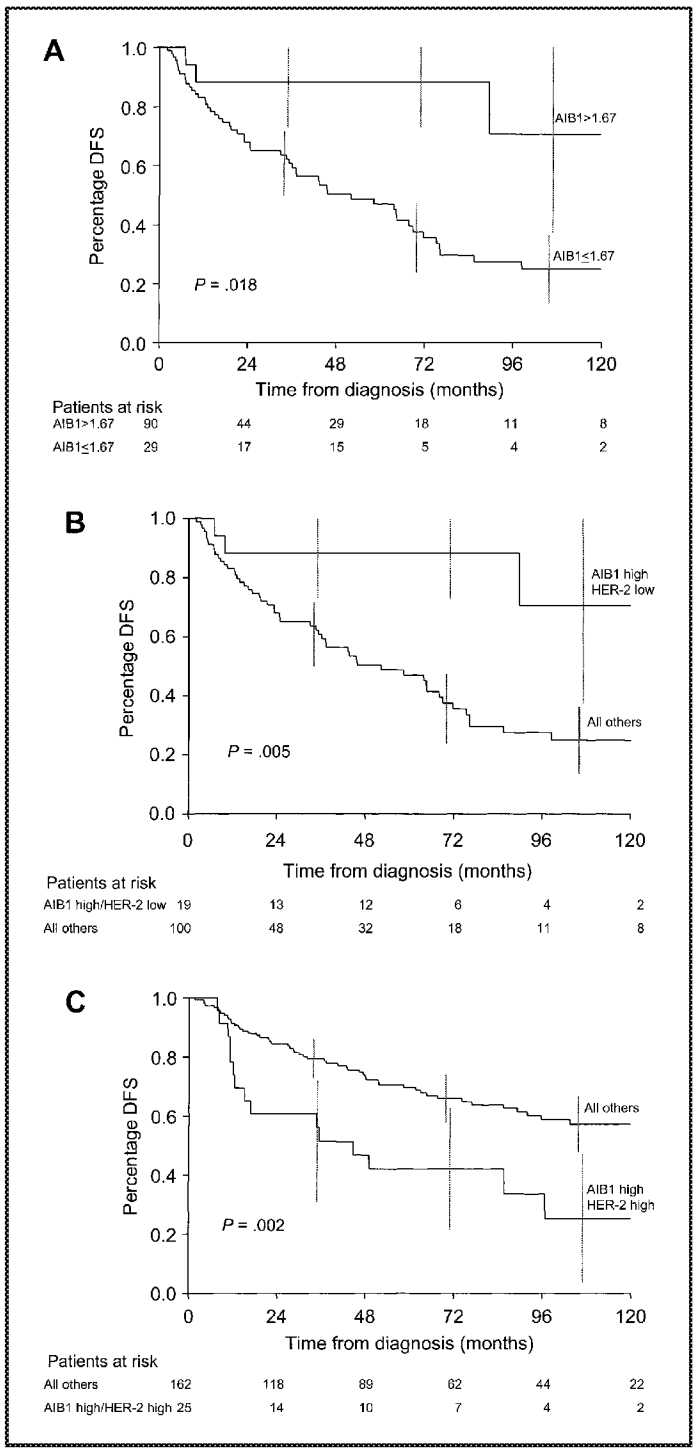


Fig. 2. Kaplan–Meier estimates of disease-free survival (DFS). **A)** DFS according to AIB1 expression for patients who did not receive adjuvant therapy (n = 119). Patients with high AIB1 expression (top quartile: AIB1>1.67 densitometric units) were compared with patients with lower AIB1 expression (≤1.67 densitometric units). **B)** DFS curves for patients who did not receive adjuvant therapy (n = 119). Patients with high AIB1 expression (top quartile) and low HER-2 expression were compared with patients with high expression of both AIB1 and HER-2, low expression of both AIB1 and HER-2, or low AIB1 expression and high HER-2 expression. **C)** DFS for patients who received adjuvant tamoxifen therapy (n = 187). Patients with high AIB1 expression (top quartile) and high HER-2 expression (grades 2–4) were compared with patients with high expression of both AIB1 and HER-2, low expression of both AIB1 and HER-2, or low AIB1 expression and high HER-2 expression. All *P* values refer to two-sided log-rank tests. Numbers below each graph indicate the number of patients remaining at risk in each group. Vertical lines are the 95% confidence intervals at selected time points.

tamoxifen, high HER-2 expression may be an indicator of poor outcome and, therefore, perhaps of tamoxifen resistance, only if high levels of AIB1 are available to mediate the adverse effect.

Discussion

To our knowledge, this is the first article comparing protein expression levels of the ER coactivator AIB1 with tumor and clinical variables in patients with primary breast cancer. Because the tumor specimens were not derived from patients randomly assigned to either a no-adjuvant-treatment group or to an adjuvant tamoxifen group and because many of the analyses are exploratory, the results presented here are not definitive with regard to their clinical implications. Nevertheless, our results confirm and extend hypotheses derived from preclinical studies that suggest that high AIB1 expression levels might reduce the antagonist activity of tamoxifen, and they provide a direct demonstration that ER coactivators can be important in the pathophysiology of disease in humans.

We found that, in patients known to have ER-positive primary breast cancer who were treated by surgery followed by adjuvant tamoxifen therapy, high levels of the ER coactivator AIB1 are associated with poor DFS in both univariate and multivariable analyses. These data support the hypothesis that the estrogen agonist activity of SERMs such as tamoxifen can be enhanced by high levels of ER coactivators, as has been observed in laboratory studies *(12,25)*, rendering the drug less antiestrogenic in patients with high AIB1 levels. In multivariable analyses of these primarily ER-positive patients, AIB1 expression was an even more important predictor of tamoxifen responsiveness than expression of PR or HER-2, molecular markers previously shown to predict tamoxifen benefit or resistance *(23,24)*. These results are even more striking when viewed in the context that, among patients who did not receive adjuvant therapy, higher AIB1 expression was associated with a less aggressive clinical course and better patient outcome than lower AIB1 expression. Thus, the test for interaction between AIB1 and tamoxifen treatment (or no treatment) was highly statistically significant.

Ample biologic evidence suggests a mechanism whereby ER coactivators like AIB1 might modulate the estrogen agonist or antagonist properties of tamoxifen or other SERMs to reduce their antitumor activity in patients *(9,12,25)*. Moreover, our data suggest that AIB1 may contribute to the reduced benefit from tamoxifen that has been reported in some, although not all, studies of patients with ER-positive tumors that also express high levels of HER-2 *(23,24)*. Signaling through the HER-2 receptor activates MAPK, which in turn phosphorylates not only the ER but also AIB1 *(21)*. Increased agonist activity of tamoxifen-bound ER induced by AIB1 might thereby reduce the clinical benefit of adjuvant tamoxifen therapy. Our observations of a positive correlation between AIB1 and HER-2 protein levels, which has also been observed at the RNA level *(19)*, and of worse outcome for tamoxifen-treated patients whose tumors express high levels of both AIB1 and HER-2 are, therefore, clinically important. Our data suggest that only those tumors with high levels of HER-2 expression that also express high levels of AIB1, a downstream target of this kinase signaling pathway, are relatively resistant to tamoxifen treatment. The inconsistent results in prior studies *(23,24)*, in which only HER-2 was measured in tamoxifen-treated patients, could be due in part to the failure of these studies to include consideration

Downloaded from http://jnci.oxfordjournals.org/ at Eisai-Andover on July 6, 2016

Table 3. Cox multivariable analyses of disease-free survival in patients who received no adjuvant therapy and patients who received adjuvant tamoxifen therapy*

Variable	No adjuvant therapy (N = 108; 47 recurrences)†		Adjuvant tamoxifen therapy (N = 180; 64 recurrences)†	
	HR (95% CI)	*P* value‡	HR (95% CI)	*P* value‡
More than three positive lymph nodes	4.04 (2.16 to 7.58)	<.001	2.73 (1.64 to 4.54)	<.001
ER negative	2.84 (1.36 to 5.93)	.006	—	NS
AIB1 (top quartile)	0.32 (0.13 to 0.75)	.009	1.45 (1.06 to 1.97)§	.028
HER-2 (grade 2–4)	1.90 (1.02 to 3.51)	.039	—	NS

*Multivariable analysis was performed using stepwise Cox proportional hazards regression with forward selection (*see* "Patients and Methods" section). Candidate exploratory variables included lymph nodes, tumor size, estrogen receptor (ER), progesterone receptor, HER-2, and AIB1. HR = hazard ratio; CI = confidence interval; NS = variable not statistically significant in model; — = variable was not included in the statistical model.

†Patients with missing data could not be included in the analysis.

‡*P* values were derived from a two-sided Wald test.

§AIB1 was treated as a continuous variable in adjuvant tamoxifen therapy patients.

Table 4. Five-year disease-free survival (DFS) by AIB1 and HER-2 status in patients stratified by treatment group*

Variable	No adjuvant therapy (N = 119)			Adjuvant tamoxifen therapy (N = 187)		
	No. of patients	5-year DFS (95% CI)	*P* value†	No. of patients	5-year DFS (95% CI)	*P* value†
High HER-2 (grade 2–4)						
High AIB1 (top quartile)	10	36% (0% to 88%)	.40	25	42% (22% to 63%)	.003
Low AIB1 (lower three quartiles)	25	33% (13% to 54%)		35	77% (63% to 92%)	
Low HER-2 (grade 0–1)						
High AIB1 (top quartile)	19	88% (73% to 100%)	.013	21	83% (64% to 100%)	.20
Low AIB1 (lower three quartiles)	65	53% (39% to 67%)		106	64% (54% to 74%)	

*CI = confidence interval.

†*P* value was derived from two-sided log-rank test.

of AIB1, which may also be necessary to elicit the agonist activity of tamoxifen, and in part to the lack of assay standardization for the measurement of HER-2. It is also clinically important to emphasize that, in our study, patients with tumors that had high HER-2 expression alone, without high levels of AIB1, responded to adjuvant tamoxifen treatment just as well as patients with tumors that had low HER-2 expression.

More study is required to determine the levels of HER-2 expression relative to AIB1 expression that are necessary for the tamoxifen-resistant tumor phenotype. The highly amplified levels of HER-2 found in some breast cancers, which are necessary for tumor response to HER-2-targeted therapies, may not be necessary to induce an increased estrogen agonist function of tamoxifen-bound ER. Furthermore, given the relatively high level of EGFR expression in normal breast ductal epithelium, AIB1 levels in normal and premalignant breast epithelium may have implications for the effectiveness of tamoxifen in cancer prevention. A recent report *(34)* suggests that AIB1 is an important modifier gene contributing to the high incidence of breast cancer in patients carrying BRCA1 mutations *(35)*. AIB1 is, therefore, a potential diagnostic as well as therapeutic target for breast cancer prevention and treatment.

The association we observed between high levels of AIB1 and more favorable DFS in patients not receiving adjuvant therapy is more difficult to explain. Breast cancers arising in women taking estrogen replacement therapy (ERT) are known to be less aggressive and to be associated with more favorable patient outcome than breast cancers arising in women who did not take ERT *(36–38)*. It is possible that enhanced signaling through the ER in women taking exogenous estrogen promotes and maintains a more differentiated and less biologically aggressive tumor. High AIB1 levels, by further augmenting ER agonist activity, might then promote a tumor that is not only less aggressive but also less responsive to tamoxifen therapy. The correlations between high AIB1 expression and both high S-phase fraction and high HER-2 expression observed in this study may seem inconsistent with less aggressive tumor behavior, but these correlations were weak, albeit highly statistically significant. Thus, further study of AIB1 in untreated patients is necessary, not only to confirm these observations, but also to clarify the mechanism(s) by which high AIB1 expression is associated with better DFS in patients who did not receive adjuvant therapy.

Only a few studies *(13,17–19,39)* have investigated the expression of ER coactivators in clinical breast cancer samples, and only one *(39)* measured protein rather than mRNA. That study showed that AIB1 protein is expressed at higher levels in breast tumors than in normal breast tissue *(39)*. The AIB1 gene is amplified in a small proportion of ER-positive breast cancers, and it is overexpressed at the RNA level in 30%–60% of breast cancers compared with normal breast epithelium *(13,17–19)*. One study *(18)* found a correlation between ER status and AIB1 expression. Another study *(19)* reported that AIB1 RNA expression was higher in tumors of high histologic grade, in tumors that were ER- and PR-negative, and in tumors with p53 mutations or high HER-2 expression. In contrast, we found no correlation between high AIB1 expression and ER expression, although we did find a positive correlation with HER-2 expression.

To our knowledge, no prior studies have correlated AIB1 protein expression with clinical outcome. One small study of 21

Downloaded from http://jnci.oxfordjournals.org/ at Eisai-Andover on July 6, 2016

primary breast tumors *(40)* measured mRNA levels of SRC-1, an ER coactivator related to AIB1. SRC-1 expression was reduced in tumor tissues compared with normal ductal epithelium, and high levels of SRC-1 in the primary tumor correlated with response to tamoxifen when it was given later, at the time of distant metastases *(39)*. In endometrial cells, high levels of SRC-1 were associated with increasing tamoxifen agonist activity, suggesting a mechanism for the proliferative effects of tamoxifen in that tissue *(41)*. Clearly, further research is needed to evaluate AIB1, SRC-1, and other ER coregulators in clinical breast cancer samples.

In summary, our results suggest that high expression of AIB1 and possibly other ER coactivators can reduce the estrogen antagonist activity of tamoxifen-bound ER in breast cancer patients, so that the level of AIB1 expression in the tumor may be an important predictive marker for tamoxifen resistance in clinical breast cancer. Our data also suggest that high levels of AIB1 must be present for the tamoxifen resistance associated with high HER-2 expression to be clinically manifest. Ideally, the prognostic significance of AIB1 expression should be confirmed in patients who are randomly assigned to no systemic adjuvant therapy, and the predictive significance of AIB1 expression should be evaluated by testing the interaction between AIB1 expression and treatment in a randomized setting *(42)*. It will also be important to determine whether levels of AIB1 and HER-2 correlate with response to endocrine therapies that work by mechanisms different from that of tamoxifen. ER coactivator levels and ligand-independent activation of ER (induced by the HER-2 pathway) may be less important for therapies such as aromatase inhibitors, which are designed to reduce the estrogen concentration (the natural ligand for ER), than for treatment with SERMs, which are receptor ligands that have mixed agonist and antagonist properties on the ER. Results from a recent clinical trial showing a much higher response for aromatase inhibitors compared with tamoxifen in ER-positive tumors that express high levels of HER-2 support this possibility *(43)*. Although ER and PR status are clinically useful tumor markers, many patients with ER-positive tumors still fail to benefit from hormone therapies. Therefore, other biomarkers are needed to identify these patients. This study suggests that AIB1 is one such potential marker that deserves additional investigation as both a diagnostic and a therapeutic target.

References

(1) Ali S, Metzger D, Bornert JM, Chambon P. Modulation of transcriptional activation by ligand-dependent phosphorylation of the human oestrogen receptor A/B region. EMBO J 1993;12:1153–60.

(2) Arnold SF, Obourn JD, Jaffe H, Notides AC. Serine 167 is the major estradiol-induced phosphorylation site on the human estrogen receptor. Mol Endocrinol 1994;8:1208–14.

(3) Le Goff P, Montano MM, Schodin DJ, Katzenellenbogen BS. Phosphorylation of the human estrogen receptor. Identification of hormone-regulated sites and examination of their influence on transcriptional activity. J Biol Chem 1994;269:4458–66.

(4) Kato S, Endoh H, Masuhiro Y, Kitamoto T, Uchiyama S, Sasaki H, et al. Activation of the estrogen receptor through phosphorylation by mitogen-activated protein kinase. Science 1995;270:1491–4.

(5) Bunone G, Briand PA, Miksicek RJ, Picard D. Activation of the unliganded estrogen receptor by EGF involves the MAP kinase pathway and direct phosphorylation. EMBO J 1996;15:2174–83.

(6) Pietras RJ, Arboleda J, Reese DM, Wongvipat N, Pegram MD, Ramos L, et al. HER-2 tyrosine kinase pathway targets estrogen receptor and promotes hormone-independent growth in human breast cancer cells. Oncogene 1995;10:2435–46.

(7) McKenna NJ, Lanz RB, O'Malley BW. Nuclear receptor coregulators: cellular and molecular biology. Endocr Rev 1999;20:321–44.

(8) Jackson TA, Richer JK, Bain DL, Takimoto GS, Tung L, Horwitz KB. The partial agonist activity of antagonist-occupied steroid receptors is controlled by a novel hinge domain-binding coactivator L7/SPA and the corepressors N-CoR or SMRT. Mol Endocrinol 1997;11:693–705.

(9) McInerney EM, Tsai MJ, O'Malley BW, Katzenellenbogen BS. Analysis of estrogen receptor transcriptional enhancement by a nuclear hormone receptor coactivator. Proc Natl Acad Sci U S A 1996;93:10069–73.

(10) Lavinsky RM, Jepsen K, Heinzel T, Torchia J, Mullen TM, Schiff R, et al. Diverse signaling pathways modulate nuclear receptor recruitment of N-CoR and SMRT complexes. Proc Natl Acad Sci U S A 1998;95:2920–5.

(11) Shiau AK, Barstad D, Loria PM, Cheng L, Kushner PJ, Agard DA, et al. The structural basis of estrogen receptor/coactivator recognition and the antagonism of this interaction by tamoxifen. Cell 1998;95:927–37.

(12) Smith CL, Nawaz Z, O'Malley BW. Coactivator and corepressor regulation of the agonist/antagonist activity of the mixed antiestrogen, 4-hydroxytamoxifen. Mol Endocrinol 1997;11:657–66.

(13) Anzick SL, Kononen J, Walker RL, Azorsa DO, Tanner MM, Guan XY, et al. AIB1, a steroid receptor coactivator amplified in breast and ovarian cancer. Science 1997;277:965–8.

(14) Torchia J, Rose DW, Inostroza J, Kamei Y, Westin S, Glass CK, et al. The transcriptional co-activator p/CIP binds CBP and mediates nuclear-receptor function. Nature 1997;387:677–84.

(15) Li H, Gomes PJ, Chen JD. RAC3, a steroid/nuclear receptor-associated coactivator that is related to SRC-1 and TIF2. Proc Natl Acad Sci U S A 1997;94:8479–84.

(16) Chen H, Lin RJ, Schiltz RL, Chakravarti D, Nash A, Nagy L, et al. Nuclear receptor coactivator ACTR is a novel histone acetyltransferase and forms a multimeric activation complex with P/CAF and CBP/p300. Cell 1997;90:569–80.

(17) Murphy LC, Simon SL, Parkes A, Leygue E, Dotzlaw H, Snell L, et al. Altered expression of estrogen receptor coregulators during human breast tumorigenesis. Cancer Res 2000;60:6266–71.

(18) Bautista S, Valles H, Walker RL, Anzick S, Zeillinger R, Meltzer P, et al. In breast cancer, amplification of the steroid receptor coactivator gene AIB1 is correlated with estrogen and progesterone receptor positivity. Clin Cancer Res 1998;4:2925–9.

(19) Bouras T, Southey MC, Venter DJ. Overexpression of the steroid receptor coactivator AIB1 in breast cancer correlates with the absence of estrogen and progesterone receptors and positivity for p53 and HER2/neu. Cancer Res 2001;61:903–7.

(20) List HJ, Lauritsen KJ, Reiter R, Powers C, Wellstein A, Riegel AT. Ribozyme targeting demonstrates that the nuclear receptor coactivator AIB1 is a rate-limiting factor for estrogen-dependent growth of human MCF-7 breast cancer cells. J Biol Chem 2001;276:23763–8.

(21) Font de Mora J, Brown M. AIB1 is a conduit for kinase-mediated growth factor signaling to the estrogen receptor. Mol Cell Biol 2000;20:5041–7.

(22) Benz CC, Scott GK, Sarup JC, Johnson RM, Tripathy D, Coronado E, et al. Estrogen-dependent, tamoxifen-resistant tumorigenic growth of MCF-7 cells transfected with HER2/neu. Breast Cancer Res Treat 1993;24:85–95.

(23) Mass R. The role of HER-2 expression in predicting response to therapy in breast cancer. Semin Oncol 2000;27:46–52; discussion 92–100.

(24) Ciocca DR, Elledge R. Molecular markers for predicting response to tamoxifen in breast cancer patients. Endocrine 2000;13:1–10.

(25) Takimoto GS, Graham JD, Jackson TA, Tung L, Powell RL, Horwitz LD, et al. Tamoxifen resistant breast cancer: coregulators determine the direction of transcription by antagonist-occupied steroid receptors. J Steroid Biochem Mol Biol 1999;69:45–50.

(26) Wu RC, Qin J, Hashimoto Y, Wong J, Xu J, Tsai SY, et al. Regulation of SRC-3 (pCIP/ACTR/AIB-1/RAC-3/TRAM-1) coactivator activity by I kappa B kinase. Mol Cell Biol 2002;22:3549–61.

(27) Harvey JM, Clark GM, Osborne CK, Allred DC. Estrogen receptor status by immunohistochemistry is superior to the ligand-binding assay for predicting response to adjuvant endocrine therapy in breast cancer. J Clin Oncol 1999;17:1474–81.

(28) Wenger CR, Clark GM. S-phase fraction and breast cancer—a decade of experience. Breast Cancer Res Treat 1998;51:255–65.

Downloaded from http://jnci.oxfordjournals.org/ at Eisai-Andover on July 6, 2016

(29) Elledge RM, Green S, Howes L, Clark GM, Berardo M, Allred DC, et al. bcl-2, p53, and response to tamoxifen in estrogen receptor-positive metastatic breast cancer: a Southwest Oncology Group study. J Clin Oncol 1997;15:1916–22.
(30) Tandon AK, Clark GM, Chamness GC, Ullrich A, McGuire WL. HER-2/neu oncogene protein and prognosis in breast cancer. J Clin Oncol 1989; 7:1120–8.
(31) Kaplan E, Meier P. Non-parametric estimation for incomplete observation. J Am Stat Assoc 1958;53:457–71.
(32) Peto R, Peto J. Asymptotically efficient rank invariant test procedures (with discussion). J R Stat Soc A 1972;135:185–207.
(33) Cox D. Regression models and life table (with discussion). J R Stat Soc B 1972;34:187–202.
(34) Grambsch P, Therneau T. Proportional hazards tests and diagnostics based on weighted residuals. Biometrika 1994;81:515–26.
(35) Rebbeck TR, Wang Y, Kantoff PW, Krithivas K, Neuhausen SL, Godwin AK, et al. Modification of BRCA1- and BRCA2-associated breast cancer risk by AIB1 genotype and reproductive history. Cancer Res 2001;61: 5420–4.
(36) Bergkvist L, Adami HO, Persson I, Bergstrom R, Krusemo UB. Prognosis after breast cancer diagnosis in women exposed to estrogen and estrogen-progestogen replacement therapy. Am J Epidemiol 1989;130:221–8.
(37) Jernstrom H, Frenander J, Ferno M, Olsson H. Hormone replacement therapy before breast cancer diagnosis significantly reduces the overall death rate compared with never-use among 984 breast cancer patients. Br J Cancer 1999;80:1453–8.
(38) Gapstur SM, Morrow M, Sellers TA. Hormone replacement therapy and risk of breast cancer with a favorable histology: results of the Iowa Women's Health Study. JAMA 1999;281:2091–7.
(39) List HJ, Reiter R, Singh B, Wellstein A, Riegel AT. Expression of the nuclear coactivator AIB1 in normal and malignant breast tissue. Breast Cancer Res Treat 2001;68:21–8.
(40) Berns EM, van Staveren IL, Klijn JG, Foekens JA. Predictive value of SRC-1 for tamoxifen response of recurrent breast cancer. Breast Cancer Res Treat 1998;48:87–92.
(41) Shang Y, Brown M. Molecular determinants for the tissue specificity of SERMs. Science 2002;295:2465–8.
(42) Clark GM. Interpreting and integrating risk factors for patients with primary breast cancer. J Natl Cancer Inst Monogr 2001;30:17–21.
(43) Ellis MJ, Coop A, Singh B, Mauriac L, Llombert-Cussac A, Janicke F, et al. Letrozole is more effective neoadjuvant endocrine therapy than tamoxifen for ErbB-1- and/or ErbB-2-positive, estrogen receptor-positive primary breast cancer: evidence from a phase III randomized trial. J Clin Oncol 2001;19:3808–16.

NOTES

Supported in part by Public Health Service grants P01CA30195 and P50CA50183 (Breast Cancer Specialized Projects of Oncology Research Excellence [SPORE] grant) from the National Cancer Institute, National Institutes of Health, Department of Health and Human Services.

Manuscript received March 18, 2002; revised December 11, 2002; accepted December 26, 2002.

Downloaded from http://jnci.oxfordjournals.org/ at Eisai-Andover on July 6, 2016

Annu. Rev. Med. 2011.62:233-247. Downloaded from www.annualreviews.org
Access provided by EISAI Research Institute on 07/06/16. For personal use only.

Mechanisms of Endocrine Resistance in Breast Cancer

C. Kent Osborne and Rachel Schiff

Dan L. Duncan Cancer Center, Lester & Sue Smith Breast Center, Departments of Medicine and Molecular and Cellular Biology, Baylor College of Medicine, Houston, Texas 77030; email: kosborne@bcm.edu, rschiff@bcm.edu

Annu. Rev. Med. 2011. 62:233–47

First published online as a Review in Advance on September 27, 2010

The *Annual Review of Medicine* is online at med.annualreviews.org

This article's doi: 10.1146/annurev-med-070909-182917

Copyright © 2011 by Annual Reviews. All rights reserved

0066-4219/11/0218-0233$20.00

Keywords

estrogen receptor, endocrine therapy, growth factor receptor signaling, crosstalk, combination therapy

Abstract

The estrogen receptor (ER) pathway plays a pivotal role in breast cancer development and progression. Endocrine therapy to block the ER pathway is highly effective, but its usefulness is limited by common intrinsic and acquired resistance. Multiple mechanisms responsible for endocrine resistance have been proposed and include deregulation of various components of the ER pathway itself, alterations in cell cycle and cell survival signaling molecules, and the activation of escape pathways that can provide tumors with alternative proliferative and survival stimuli. Among these, increased expression or signaling of growth factor receptor pathways, especially the EGFR/HER2 pathway, has been associated with both experimental and clinical endocrine therapy resistance. New treatment combinations targeting both ER and growth factor receptor signaling to block the crosstalk between these pathways and eliminate escape routes have been proven highly effective in preclinical models. Results of recent clinical studies, while partly supporting this approach, also highlight the need to better identify a priori the patients whose tumors are most likely to benefit from these specific cotargeting strategies.

ER: estrogen receptor

HER2: human epidermal growth factor receptor 2

PR: progesterone receptor

INTRODUCTION

The name endocrine therapy is given to those breast cancer treatments that target the estrogen receptor (ER) by blocking receptor binding with an antagonist or by depriving the tumor of estrogen. The ER, which has nuclear (genomic) and nonnuclear (nongenomic) functions, is the major driver in the majority of breast cancers. It is expressed in 75% of breast cancers overall, with its detection being slightly more frequent in tumors from postmenopausal women and less in younger women (1). ER expression is related to patient age and correlates with lower tumor grade, lower tumor proliferation, less aneuploidy, less frequent amplification of the c-erbB2 (HER2) oncogene and concomitant loss of the p53 tumor suppressor gene, positive expression of progesterone receptor (PR), metastases (preferentially to soft tissue and bone), and slower rates of disease recurrence (1–3). It is not related to initial nodal metastases, and thus it does not correlate with long-term disease recurrence and death after primary therapy (3).

These clinical factors, along with ER expression itself, are used to make treatment decisions in patients, especially those with metastatic disease. In some cases, multigene tests are performed on the primary breast tumor to assist in adjuvant therapy decision making and to distinguish which patients might benefit most from a combination of endocrine therapy plus chemotherapy, rather than endocrine therapy alone. The 21-gene and 70-gene profiles can classify ER-positive tumors according to their aggressiveness, risk of recurrence, and likelihood of benefiting from adjuvant endocrine or chemotherapy (4, 5). The stratification of ER-positive tumors on this basis indicates that some tumors are more resistant to endocrine therapy than others, despite expressing ER. In general, patients are more likely to benefit from endocrine therapy and less (if at all) likely to benefit from chemotherapy if their tumors have high levels of ER and PR, are negative for HER2 amplification, are slowly proliferating, are lower grade histologically, and have low-risk 21-gene or 70-gene profile scores. In contrast, patients with ER-positive tumors that are more aggressive, morphologically and genetically, are less likely to benefit from endocrine therapy, although there are exceptions. Additional recent molecular profiling studies have stratified ER-positive tumors into luminal A and luminal B subtypes. The more aggressive and endocrine-resistant tumors largely overlap with the luminal B subtype, whereas the more indolent and endocrine-responsive tumors generally correspond to the luminal A subtypes. Currently, however, no tests exist that can predict resistance to endocrine therapy with certainty, although tumors with absent ER and PR rarely respond. Most patients with ER-positive primary tumors are, therefore, treated with endocrine adjuvant therapy, whereas cases of ER-positive metastatic disease are treated with endocrine therapy initially and serially until the tumor demonstrates independence from estrogen.

Endocrine therapy is the most effective treatment for ER-positive metastatic breast cancer, but its effectiveness is limited by high rates of de novo resistance and resistance acquired during treatment. Only ~30% of patients with metastatic disease have objective regression of tumor with initial endocrine treatment, and another 20% have prolonged stable disease. Thus, ER is not the only survival pathway driving most of these tumors, and escape pathways when ER is targeted are already functioning or begin to function during treatment.

Understanding the pathways responsible for resistance in the metastatic setting may provide important clues to the mechanisms of resistance to adjuvant endocrine therapy given before or after primary surgery to eradicate distant micrometastases. Treatment in this setting is much more effective; the risk of recurrence is reduced by as much as 60% with estrogen deprivation therapies using aromatase inhibitors in postmenopausal women (6, 7). Unfortunately, biopsying patients with metastatic disease in the lung, bone, or liver is difficult and can be associated with high morbidity rates. However, such tissue is crucial for the molecular profiling of

Annu. Rev. Med. 2011.62:233-247. Downloaded from www.annualreviews.org
Access provided by EISAI Research Institute on 07/06/16. For personal use only.

resistant tumors in order to understand escape pathways. Despite these challenges, progress is being made in understanding potential mechanisms of resistance. The advances come largely from preclinical models of endocrine resistance as well as a greater understanding of the molecular mechanisms by which estrogen works to stimulate the growth of the tumor.

MECHANISM OF ESTROGEN ACTION

All biological networks have similar characteristics. In order to provide important functions in normal cells under a variety of conditions and stress factors, as well as to keep the cell alive, these networks must be complex with multiple levels of regulation, fine tuning capabilities, redundancy, and evolvability. Collectively these features allow the cell to adapt to cellular stress, toxins, and potentially hostile environments. Cancer cells exploit these normal functions, which are often altered genetically during oncogenesis, to provide them with a survival advantage and the ability to escape the effects of treatment. The ER signaling pathway is an example of a complex biological pathway that controls a variety of functions, such as cell proliferation, apoptosis, invasion, and angiogenesis, and is exploited by breast cancer cells to serve as a major survival pathway driven by the female hormone estrogen (**Figure 1**).

The classic function of ER is its nuclear function, also referred to as genomic activity, to alter the expression of genes important for normal cellular function and tumor growth and survival. ER modulates the expression of hundreds of genes, some by upregulation and others by downregulation (8). Upon binding to estrogen, ER dimerizes with another receptor monomer and attracts a complex of coactivators and corepressors to specific sites on DNA (3, 9). ER can also bind to other transcription factors such as AP-1 (activator protein-1) and SP-1 (specificity protein-1) at their specific sites on DNA, thereby functioning as a coregulator (3, 10). Coregulators serve as a fine-tuning mechanism by increasing or reducing the transcriptional activity of the receptor (11). Several coregulators have been implicated in cancer, most notably AIB1 (SRC-3), which is gene-amplified in a small percentage—but overexpressed in two thirds—of all breast cancers. Overexpression of this gene has been implicated in tamoxifen resistance (12).

The ER signaling pathway is also regulated by membrane receptor tyrosine kinases, including epidermal growth factor receptor (EGFR), HER2, and insulin-like growth factor receptor (IGF1-R) (13). These membrane kinases activate signaling pathways that eventually result in phosphorylation of ER as well as its coactivators and corepressors at multiple sites to influence their specific functions (13–16). This activation of ER by growth factor receptor signaling is sometimes referred to as ligand-independent receptor activation. Crosstalk between the growth factor receptor and ER pathways has been established through several other mechanisms as well. Estrogen can increase the expression of ligands such as transforming growth factor-α (TGFα) and IGF1 (10, 17–19), which can then activate the growth factor receptor pathway (13, 18, 20). On the other hand, estrogen signaling downregulates the expression of EGFR and HER2 while increasing the expression of IGF1-R (21–23). Activation of the PI3K/AKT and the p42/44 mitogen-activated protein kinase (MAPK) pathways by these receptors, in turn, downregulates the expression of ER and PR (24–29). Thus, while these receptor tyrosine kinases can activate the transcriptional function of ER, they can also reduce estrogen dependence by downregulating the expression of ER, perhaps contributing to the relative resistance to endocrine therapies in tumors amplified for HER2 (25, 30).

Studies also suggest that ER may work by nontranscriptional mechanisms. Low levels of ER have been found outside the nucleus in the membrane, cytoplasm, or even mitochondria, although the exact location for this receptor remains controversial (31). Some of the nongenomic action of estrogen appears to be too rapid for a transcriptional effect to activate growth factor receptor signaling, including

AIB1: amplified in breast cancer–1

SRC: steroid receptor coactivator

EGFR: epidermal growth factor receptor

IGF1-R: insulin-like growth factor receptor

PI3K: phosphoinositide 3-kinase

MAPK: mitogen-activated protein kinase

Annu. Rev. Med. 2011.62:233-247. Downloaded from www.annualreviews.org
Access provided by EISAI Research Institute on 07/06/16. For personal use only.

Annu. Rev. Med. 2011.62:233-247. Downloaded from www.annualreviews.org
Access provided by EISAI Research Institute on 07/06/16. For personal use only.

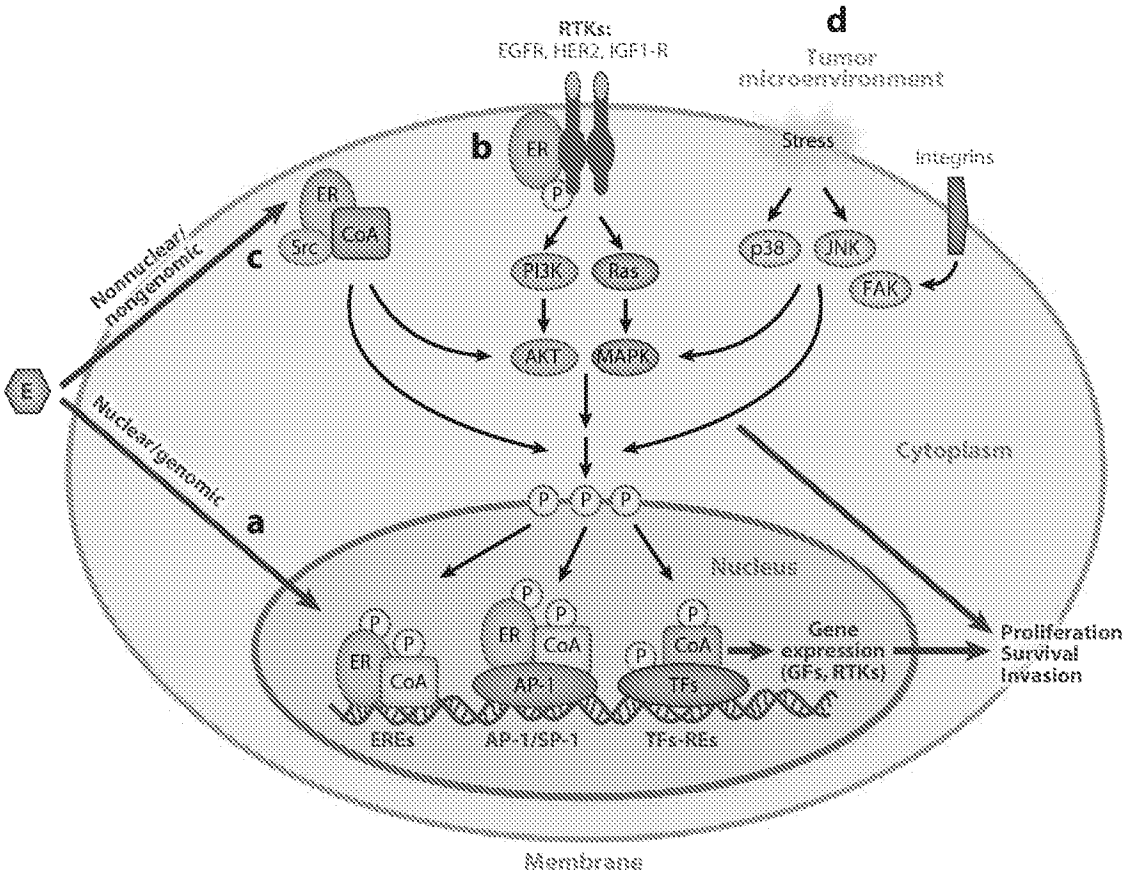


Figure 1

Mechanisms of estrogen receptor (ER) action in breast cancer. Estrogen (E)-bound ER, acting as a transcription factor in the nucleus (nuclear/genomic activity), binds to DNA sequences in promoter regions of target genes either directly [at estrogen response elements (EREs)] or indirectly via protein-protein interaction with other transcription factors at their cognate DNA-responsive sites (e.g., members of the AP-1 or the SP-1 transcription complexes at AP-1 or SP-1 sites). Upon estrogen binding, ER generally recruits coactivator complexes (CoA) to induce or modulate gene transcription, including genes encoding growth factors (GFs) and receptor tyrosine kinases (RTKs) (*a*). A small subset of the cellular pool of ER localized outside the nucleus and/or at the cell membrane associates in response to estrogen with GF RTKs (e.g., EGFR, HER2, and IGF1-R) (*b*) and with additional signaling and coactivator molecules (e.g., the Src kinase) (*c*). This interaction, similar to GF activation of these pathways, activates multiple downstream kinase pathways (e.g., SRC, PI3K/AKT, and Ras/p42/44 MAPK), which in turn phosphorylate various transcription factors (TFs) and coregulators, including components of the ER pathway that enhance gene expression on EREs and other response elements (REs). The nonnuclear/nongenomic activity, which can also be activated by tamoxifen, is enhanced in the presence of overexpression and hyperactivation of RTKs and can contribute to endocrine therapy resistance. Overall, the nuclear/genomic and nonnuclear/nongenomic ER activities work in concert to provide breast tumor cells with proliferation, survival, and invasion stimuli. Signaling from the microenvironment activates stress-related pathways and members of the integrin family. These pathways then trigger downstream kinase pathways [e.g., FAK (focal adhesion kinase), JNK (c-Jun N-terminal kinase), and p38 MAPK] that can further modulate components of the transcriptional machinery, including ER (*d*). Alterations in each of these transcriptional and signaling elements can mediate resistance to endocrine therapy either by modulating ER activity or by acting as escape pathways to provide alternative proliferation and survival stimuli.

the PI3K/AKT and the Ras/p42,44 MAPK pathways (13). Thus, ER—through this nongenomic activity—can alter the expression of genes normally regulated by growth factors (13, 31, 32). Finally, the stress kinase pathway via p38 and JNK (c-Jun N-terminal kinase) can also modulate ER function by phosphorylation of ER and its coregulators (33, 34). The microenvironment and its associated integrin signaling may exert a similar activity (35). Thus, ER activity and signaling are modulated by a variety of pathways that could also contribute to resistance to ER-targeted therapies, especially when the pathways display aberrant activity in a cancer cell.

MECHANISM OF ACTION OF ENDOCRINE THERAPIES

Various endocrine therapies work by different mechanisms to antagonize the growth-promoting activity of estrogen. Selective estrogen receptor modulators (SERMs) such as tamoxifen bind ER and antagonize the effects of estrogen on specific target genes (8, 36). Tamoxifen also has some estrogen-agonist effects on certain genes and tissues, and augmentation of this property may play a role in resistance (8, 37). Estrogen deprivation is another mechanism utilized to antagonize ER (38). In premenopausal women, tamoxifen or pharmacological or surgical ovarian ablation is standard, and in postmenopausal women, aromatase inhibitors are prescribed to block the conversion of weak androgens of adrenal origin to estrogen in peripheral tissues as well as breast cancer tissue itself. Fulvestrant is an ER downregulator and a more potent antiestrogen that reduces ER levels in cells (39). Older endocrine therapies such as high-dose or physiological-dose estrogens and androgens work by less well-known mechanisms, although it has been proposed that high-dose estrogen can induce apoptosis by activation of the Fas ligand (40). Tamoxifen, but not estrogen deprivation or fulvestrant, activates the nongenomic ER, another property that could contribute to endocrine resistance in some cases.

CLINICAL CLUES TO ENDOCRINE THERAPY RESISTANCE

Several clinical observations provide clues to potential mechanisms for resistance to endocrine therapy (**Table 1**). ER loss over time in the tumor occurs in ~20% of patients treated with endocrine therapy (41–43). Such tumors would no longer be driven by estrogen, but the escape pathways that take over with loss of estrogen dependence have not been well defined. Upregulation of HER2 by either acquisition of gene amplification or overexpression has been shown to occur in some tumors (42, 44, 45). HER2 may subsequently assume the driving role in tumor progression by serving as an alternative survival pathway or by reducing the level of ER, thus rendering the tumor less responsive to estrogen (25, 46). Preclinical and clinical data suggest the possibility that tumors can alternate between ER and HER2 as the dominant pathway, with targeted therapy against one pathway causing reactivation of the other (23, 25, 42, 44, 45, 47–51). PR, on the other hand, is lost more frequently than ER with intervening endocrine therapy, and with this loss the tumor becomes more aggressive and patients have a worse survival outcome than patients who maintain PR expression after resistance to one endocrine therapy (52, 53). In this case, PR loss might be associated with increased growth factor signaling and upregulation of the PI3K pathway, which downregulates PR and ER expression (27, 29, 54).

Table 1 Clinical clues to mechanisms of resistance to endocrine therapy

Decrease or loss of ER
Upregulation of HER2 in some patients after endocrine therapy
Loss of PR after progression on endocrine therapy
Response to sequential endocrine therapies
Shorter response duration and less frequent responses with sequential endocrine therapies
Withdrawal response after high-dose estrogen therapy
Eventual loss of dependence on estrogen with resistance to all endocrine therapies
Lower clinical benefit to endocrine therapy in high-grade, highly proliferating, high 21-gene profile score ER-positive tumors

Abbreviations: ER, estrogen receptor; HER2, human epidermal growth factor receptor 2; PR, progesterone receptor.

Annu. Rev. Med. 2011.62:233-247. Downloaded from www.annualreviews.org
Access provided by EISAI Research Institute on 07/06/16. For personal use only.

Annu. Rev. Med. 2011.62:233-247. Downloaded from www.annualreviews.org
Access provided by EISAI Research Institute on 07/06/16. For personal use only.

Response to one form of endocrine therapy after progression on another is a historically recognized observation that is the key to management of patients with metastatic disease. Tumors in such patients are still estrogen dependent but have become resistant to the ER-targeted therapy being given. Responses to an aromatase inhibitor or fulvestrant after progression on tamoxifen are good examples of this phenomenon (55, 56). Subsequent responses to serial endocrine therapy tend to be shorter, coincident with a decline in ER level, suggesting a gradual shift from dependence on ER to an alternative escape pathway. High-dose estrogen therapy was the first additive endocrine therapy for breast cancer, later replaced by tamoxifen and aromatase inhibitors owing to their more favorable toxicity profile. It is important to note that patients responding and then progressing on high-dose estrogen therapy frequently respond simply to estrogen withdrawal. Occasionally the disease can be controlled for many years by initiating and then sequencing high-dose estrogen with estrogen withdrawal over time. In one such patient treated by Dr. Osborne, metastatic bone disease was controlled for more than eight years by alternating high-dose estrogen with estrogen withdrawal three separate times. Eventually all tumors completely lose estrogen dependence, even when ER is still expressed, by mechanisms that are poorly understood and are likely to be multiple as the tumor progresses to a more aggressive phenotype.

These observations suggest several types of endocrine therapy resistance (**Table 2**). Resistance can occur de novo (existing before any treatment is given) or be acquired (developing during a given therapy after an initial period of response). Some tumors lose estrogen dependence with loss of ER expression, although preclinical data suggest that ER can sometimes be reexpressed during subsequent treatment (25, 49, 51). Other tumors lose estrogen dependence while still expressing ER, indicating that an escape pathway has developed to replace ER. Still other tumors continue to express ER but have not lost estrogen dependence and will respond to an alternative form of endocrine therapy. These tumors have developed resistance to the specific ER-targeted therapy. The fact that subsequent remissions tend to be shorter and the fact that ER levels decline over time suggest that other survival pathways are beginning to exert their effects or that an endocrine-resistant clone is slowly emerging over time. Whether tumor cells with stem cell–like qualities play a role in the development of endocrine resistance remains to be clarified.

Table 2 Types of endocrine therapy resistance

De novo
Acquired during treatment
Loss of estrogen dependence due to loss of estrogen receptor
Loss of estrogen dependence despite presence of estrogen receptor
Resistance to a specific therapy; tumor still estrogen dependent

SIGNALING MOLECULES AND PATHWAYS IMPLICATED IN RESISTANCE TO ENDOCRINE THERAPY

Multiple pathways and molecules have been implicated in the diverse mechanisms responsible for endocrine resistance. These pathways and their gene networks, recently reviewed elsewhere (57), have mostly been investigated in the preclinical setting with a focus on tamoxifen. However, several alternative pathways have been shown or suggested to play a more general role in resistance to various other forms of endocrine therapy. Deregulation of these pathways most often arises from genetic or epigenetic changes in the tumor cells themselves. These changes influence uptake and metabolism of the endocrine agents and cellular responses to their inhibitory effects.

Tumor Microenvironment and Host-Associated Mechanisms of Resistance

The importance of the tumor microenvironment as a modulator of these processes and contributor to endocrine sensitivity has been

recognized in recent years. Evidence to support this notion has emerged from studies involving gene expression profiling and biomarkers associated with endocrine therapy responses (58, 59), and from more sophisticated in vitro and in vivo experimental model systems (35). Components of the microenvironment implicated in endocrine resistance include stromal cells (e.g., fibroblasts, endothelial, and immune system cells), structural elements of the extracellular matrix (ECM), and soluble factors (e.g., growth factors and cytokines), as well as additional microenvironmental conditions such as hypoxia and acidity (60). The role of tumor cell pathways engaged in mediating these microenvironmental and extracellular matrix stimuli, especially the integrin family and other adhesion molecules (e.g., CAS^{p130}), has also recently been documented (61, 62), suggesting novel signaling axes (e.g., integrin/FAK/SRC kinase) that may be targeted to circumvent endocrine resistance. In addition, as a result of recent pharmacogenomic and high-throughput studies, the list of additional host genome–associated factors governing endocrine sensitivity is growing.

Tumor-Associated Mechanisms of Resistance

As suggested above, however, most pathways potentially involved in endocrine resistance stem from the tumor cells themselves. These pathways fall broadly into three conceptual categories with overlapping components and mechanisms.

ER and ER coregulators. The first category consists of the ER itself, its coregulators, and additional factors that deregulate ER activity and modulate the receptor functions in response to endocrine therapy. As mentioned, loss of ER expression (i.e., the ERα isoform) in refractory endocrine tumors, though uncommon, results in an endocrine-insensitive phenotype (41, 42). Importantly, however, therapies inhibiting growth factor receptor pathways known to downregulate ER can restore ER expression and endocrine sensitivity in both preclinical and clinical settings (25, 49, 51). The expression of ER splicing variants, specifically the newly identified short variant ERα36 (63) and estrogen-related receptors, has also been implicated in reducing endocrine response. In addition, evidence indicates that negative (corepressors) and positive (coactivators) ER coregulators, which directly influence the balance of agonistic versus antagonistic activities of SERMs such as tamoxifen and the ligand-independent activity of the ER, are critical in determining endocrine sensitivity and resistance (16 and references therein). Overexpression of the ER coactivator AIB1 (also known as SRC3 or NCoA3) is associated with clinical and experimental tamoxifen resistance (12, 14), and downregulation of the corepressor NCoR was documented in tamoxifen-refractory experimental tumors (64). ER and its coregulators are also intimately regulated by posttranslational modifications. Growth factor receptors [e.g., EGFR/HER2, IGF1-R, and FGFR (fibroblast growth factor receptor)] and additional cellular and stress-related kinases [e.g., AKT, p42/44, JNK, and p38 MAPKs, PKA (protein kinase A), PAK1 (p21-activated kinase), IKK (IκB kinase), SRC, and CDK7 (cyclin-dependent kinase)] regulate multiple posttranslational modifications (16, 57, 65 and references therein). Phosphorylation, methylation, ubiquitination, and additional posttranslational modifications of ER and its coregulators have all been shown to influence ER activity and sensitivity to various endocrine therapies (57). ER can also reside outside the nucleus, engaging with cytoplasmic and membrane signaling complexes, and can activate and regulate various growth factor receptors and other cellular signaling pathways as a result (13, 14, 31, 32). Intriguingly, hyperactivation of these signaling pathways increases nonnuclear ER localization and its nongenomic activity, thus creating a positive feedback loop of crossactivation between the ER and growth factor receptor pathways. Importantly, this nonnuclear ER activity can be activated by both estrogen and tamoxifen, thus contributing to resistance (13, 14, 32). Other

Annu. Rev. Med. 2011.62:233-247. Downloaded from www.annualreviews.org
Access provided by EISAI Research Institute on 07/06/16. For personal use only.

endocrine therapies, however, such as the more potent ER degrader fulvestrant or strategies of estrogen deprivation, fail to trigger this nongenomic ER activity. Last, increased levels of transcription factors, such as NFkB and AP-1, that tether ER to specific gene promoters, have also been associated with endocrine resistance (66–68).

Cell cycle signaling molecules. The second category of endocrine resistance–related pathways includes molecules involved in the cellular and biological responses to endocrine therapy such as inhibition of cell proliferation and induction of apoptosis. Most of the evidence for the role of these pathways stems from preclinical studies. Both upregulation of positive regulators of the cell cycle, especially those controlling G1 phase progression, and downregulation of negative regulators of the cell cycle have been documented to interrupt and block the antiproliferative effects of endocrine therapy, leading to resistance (57, 69). For example, overexpression of the positive regulators MYC and cyclins E1 and D1 results in endocrine resistance, either by activating cyclin-dependent kinases critical for G1 phase or by relieving the inhibitory effects of the negative cell cycle regulators p21 and p27 (69, 70). Likewise, reduced expression, stability, or activity of p21 and p27 (71, 72), as well as inactivation of the RB (retinoblastoma) tumor suppressor, are also associated with poor response to endocrine therapy, especially tamoxifen. Of note, multiple growth factor receptors and their downstream signaling pathways, by modulating specific transcription factors or microRNAs, or by protein phosphorylation, downregulate expression or activity of these negative cell cycle regulators. Overexpression of HER2 and hyperactivation of AKT and SRC kinase are prominent examples of such pathways. Consistent with the cytotoxic effect of endocrine therapy, upregulation of cell survival signaling and antiapoptotic molecules, such as BCL-X_L, and decreases in expression of proapoptotic molecules, such as BIK (BCL2-interacting killer) and caspase 9, can also lead to endocrine resistance (73). As before, activation of growth factor receptor signaling via the PI3K/AKT pathway is an important modulator of these apoptotic/survival molecules, but additional molecules such as NFκB (nuclear factor κB) have also been implicated (66). Finally, whether autophagy, recently shown to mediate cell survival, plays a more general role in endocrine resistance is yet to be determined (74).

Growth factor receptor pathways. The third category of pathways involved in endocrine resistance comprises those that can provide alternative proliferation and survival stimuli to the tumors in the presence of effective inhibition of the ER pathway. Importantly, these pathways—such as growth factor and other cellular kinase pathways—can also circumvent the inhibitory effects of endocrine therapy via bidirectional crosstalk and modulation of the ER. However, many of these pathways can, either initially or eventually during the course of treatment, emerge to act as ER-independent drivers of tumor growth and survival, thus conferring resistance to all types of endocrine therapy. Pathways such as the HER tyrosine kinase receptor family and receptors for insulin/IGF1, fibroblast growth factor (FGF), and vascular endothelial growth factor (VEGF), as well as cellular Src, AKT, and stress-related kinases, have been implicated (75–78). These pathways can be activated by amplification and/or overexpression of the receptors or their cognate ligands. Pathway activation can also be achieved by deregulation of downstream signaling moieties, such as activating mutations in the PI3K catalytic subunit or loss of expression of the PTEN tumor suppressor of this pathway (79). The androgen receptor and potentially additional nuclear receptors have also been implicated as alternative growth stimulators that can bypass ER inhibition and lead to resistance (80). Importantly, although these pathways and mechanisms are varied and span a wide range of signaling cascades and gene networks, EGFR and HER2 have been recognized as important contributors to endocrine resistance. As a result, many clinical strategies have focused on cotargeting

Annu. Rev. Med. 2011.62:233-247. Downloaded from www.annualreviews.org
Access provided by EISAI Research Institute on 07/06/16. For personal use only.

this pathway together with ER to circumvent endocrine resistance and improve patient outcome.

CLINICAL TRIALS DESIGNED TO OVERCOME ENDOCRINE RESISTANCE

Many clinical trials have begun to test the idea that growth factor receptor signaling contributes to de novo or acquired endocrine resistance (75, 81, 82). Some of these trials were short-term neoadjuvant trials, some phase II, some randomized phase II, and some phase III in patients with metastatic disease. Some focused on HER2-positive patients whereas others included all ER-positive patients, regardless of HER2 status.

The TAnDEM trial randomized patients with HER2-positive tumors to anastrozole alone or anastrozole plus trastuzumab (83). The results clearly showed an advantage for the combination, although both arms did poorly, exemplifying the difficulty of controlling ER-positive HER2-positive disease. Despite targeting both major pathways, remissions are few and brief owing to the rapid development of more dominant survival pathways in metastatic disease.

Because preclinical studies suggest a major role for the EGFR (HER1) in acquired endocrine resistance, many trials incorporated gefitinib into the endocrine therapy regimen with tamoxifen or an aromatase inhibitor (23). Some of these studies have not yet been published but have been presented at meetings and published as abstracts. Two randomized phase II trials of somewhat similar design randomized patients with ER-positive metastatic breast cancer to either tamoxifen +/− gefitinib or anastrozole +/− gefitinib (84, 85). One of these trials was terminated early because of slow patient accrual, but it showed a numerical advantage in clinical benefit rate and progression-free survival with the addition of gefitinib to anastrozole (85). The other larger trial with 290 patients also showed a numerical advantage in favor of gefitinib added to tamoxifen (84). Both trials reported that the advantage was confined to previously untreated patients and suggested that an advantage was seen even in patients whose tumors were initially negative for HER2 overexpression (84, 85). These studies concluded that the strategy of combining an EGFR inhibitor with an endocrine agent was of sufficient interest to warrant further study and that studies designed to select the appropriate patients for combined treatment were paramount. A much smaller trial in more heavily treated patients failed to confirm these data and showed a high rate of patient withdrawal from the study (30%) owing to side effects of gefitinib (86). Finally, another trial comparing anastrozole plus gefitinib with fulvestrant plus gefitinib showed that the regimens were tolerable and suggested a slight advantage for the anastrozole combination (87).

The largest trial by far (1,286 patients) compared letrozole with and without lapatinib in patients with ER-positive metastatic breast cancer (88). The addition of lapatinib conferred a significant advantage in progression-free survival and response rate in the HER2-positive subset. In the HER2-negative subset, there was no overall significant benefit from lapatinib, but a preplanned Cox regression analysis showed a 23% reduction in the risk of progression with the addition of lapatinib. The benefit was seen in those who had discontinued tamoxifen therapy within six months of entering the study. A more recent analysis showed that patients with tumors exhibiting lower ER levels received the most benefit (89). This result, which will require confirmation from other trials, is consistent with data suggesting that growth factor signaling downregulates ER expression (3, 25, 29). Perhaps those tumors with lower ER expression are also those that rely on the HER pathway when ER is blocked by endocrine therapy. These tumors would be expected to respond well to a HER inhibitor.

Two randomized neoadjuvant studies have compared anastrozole and gefitinib (90, 91). One small study in patients selected for higher expression of EGFR evaluated gefitinib alone versus gefitinib plus anastrozole (91). Both

Annu. Rev. Med. 2011.62:233-247. Downloaded from www.annualreviews.org
Access provided by EISAI Research Institute on 07/06/16. For personal use only.

treatment regimens reduced phosphorylation of EGFR, Ki67 index, and tumor size, suggesting that gefitinib is effective in tumors selected by EGFR expression. The other study compared anastrozole alone to anastrozole plus gefitinib in patients selected only by ER status (90). If EGFR expression is important for the response to gefitinib, and if expression rises over time in patients treated with endocrine therapy, then the neoadjuvant setting, where EGFR levels would be low, may not be optimal to investigate this new strategy. Like the preclinical studies that led to testing this strategy in patients (23), gefitinib would be expected to delay the onset of acquired resistance but exert a minimal impact on initial response. In fact, this neoadjuvant trial showed no benefit from gefitinib, and even showed a trend for a reduced antitumor effect on Ki67 and tumor response with the combination (90).

Other trials in metastatic disease evaluated inhibitors of signaling molecules downstream from HER receptors. Two trials of mTOR inhibitors have been reported in combination with endocrine therapy (92, 93). A randomized phase II study compared letrozole alone to letrozole plus temsirolimus in hormone receptor–positive metastatic breast cancer and suggested a benefit. The trial was expanded to a phase III trial that was terminated early owing to lack of efficacy of the combination (92). The phase III portion of the study used a lower dose than the phase II portion because of toxicity with the higher dose. A randomized phase II trial of letrozole with or without everolimus, using an optimal dose of the inhibitor in the neoadjuvant setting, showed a statistically significant increase in response with the combination (93).

CONCLUSIONS

ER-targeted therapy has improved the quality of life and survival of millions of women with breast cancer around the world in the past three decades, but resistance to therapy continues to be a major problem. The ER signaling pathway is a complex network with many levels of control including extensive crosstalk with growth factor signaling pathways, thus offering several possible mechanisms of resistance. Clinical trials in patients suggest that HER2-overexpressing, ER-positive breast cancers should be treated with a combination of ER-targeted and HER-targeted therapies. Early results from clinical trials also suggest that subsets of patients with ER-positive, HER2-negative breast cancers may benefit from a combination of a growth factor pathway inhibitor with ER-targeted therapy such as tamoxifen or an aromatase inhibitor. Further studies are needed to confirm and expand these observations and to identify a priori those patients most likely to benefit from this approach. Finally, ongoing and planned additional studies combining ER-targeted and growth factor pathway–targeted therapy will determine whether this strategy is of value.

It is likely that there are many causes of resistance to endocrine therapy once a tumor becomes independent of estrogen. One factor limiting our understanding of these varied mechanisms is the lack of tumor tissue for detailed studies before treatment and after resistance has developed. This type of study will be crucial if we are to learn which escape pathways become activated in endocrine resistance and which targeted therapies can prevent or overcome this type of tumor progression.

DISCLOSURE STATEMENT

Dr. Schiff receives research grant support from AstraZeneca and GlaxoSmithKline.

ACKNOWLEDGMENTS

This work was supported in part by National Cancer Institute (NCI) grants P30CA125123 and P50CA058183, and by funding from the Stand Up to Cancer–Breast Cancer Dream Team.

Annu. Rev. Med. 2011.62:233-247. Downloaded from www.annualreviews.org
Access provided by EISAI Research Institute on 07/06/16. For personal use only.

LITERATURE CITED

1. Clark GM, Osborne CK, McGuire WL. 1984. Correlations between estrogen receptor, progesterone receptor, and patient characteristics in human breast cancer. *J. Clin. Oncol.* 2:1102–9
2. Wenger CR, Beardslee S, Owens MA, et al. 1993. DNA ploidy, S-phase, and steroid receptors in more than 127,000 breast cancer patients. *Breast Cancer Res. Treat.* 28:9–20
3. Schiff R, Osborne CK, Fuqua SA. 2009. Clinical aspects of estrogen and progesterone receptors. In *Diseases of the Breast*, ed. JR Harris, ME Lippman, M Morrow, CK Osborne, pp. 408–30. Philadelphia: Wolters Kluwer/Lippincott Williams & Wilkins. 4th ed.
4. Paik S, Shak S, Tang G, et al. 2004. A multigene assay to predict recurrence of tamoxifen-treated, node-negative breast cancer. *N. Engl. J. Med.* 351:2817–26
5. van de Vijver MJ, He YD, van't Veer LJ, et al. 2002. A gene-expression signature as a predictor of survival in breast cancer. *N. Engl. J. Med.* 347:1999–2009
6. Baum M, Budzar AU, Cuzick J, et al. 2002. Anastrozole alone or in combination with tamoxifen versus tamoxifen alone for adjuvant treatment of postmenopausal women with early breast cancer: first results of the ATAC randomised trial. *Lancet* 359:2131–39
7. Coates AS, Keshaviah A, Thurlimann B, et al. 2007. Five years of letrozole compared with tamoxifen as initial adjuvant therapy for postmenopausal women with endocrine-responsive early breast cancer: update of study BIG 1–98. *J. Clin. Oncol.* 25:486–92
8. Frasor J, Stossi F, Danes JM, et al. 2004. Selective estrogen receptor modulators: discrimination of agonistic versus antagonistic activities by gene expression profiling in breast cancer cells. *Cancer Res.* 64:1522–33
9. Klinge CM. 2001. Estrogen receptor interaction with estrogen response elements. *Nucleic Acids Res.* 29:2905–19
10. Kushner PJ, Agard DA, Greene GL, et al. 2000. Estrogen receptor pathways to AP-1. *J. Steroid Biochem. Mol. Biol.* 74:311–17
11. Smith CL, O'Malley BW. 2004. Coregulator function: a key to understanding tissue specificity of selective receptor modulators. *Endocr. Rev.* 25:45–71
12. Osborne CK, Bardou V, Hopp TA, et al. 2003. Role of the estrogen receptor coactivator AIB1 (SRC-3) and HER-2/neu in tamoxifen resistance in breast cancer. *J. Natl. Cancer Inst.* 95:353–61
13. Schiff R, Massarweh SA, Shou J, et al. 2004. Cross-talk between estrogen receptor and growth factor pathways as a molecular target for overcoming endocrine resistance. *Clin. Cancer Res.* 10:331S–36S
14. Shou J, Massarweh S, Osborne CK, et al. 2004. Mechanisms of tamoxifen resistance: increased estrogen receptor-HER2/neu cross-talk in ER/HER2-positive breast cancer. *J. Natl. Cancer Inst.* 96:926–35
15. Wu RC, Smith CL, O'Malley BW. 2005. Transcriptional regulation by steroid receptor coactivator phosphorylation. *Endocr. Rev.* 26:393–99
16. Schiff R, Massarweh S, Shou J, et al. 2003. Breast cancer endocrine resistance: how growth factor signaling and estrogen receptor coregulators modulate response. *Clin. Cancer Res.* 9:447S–54S
17. Vyhlidal C, Samudio I, Kladde MP, et al. 2000. Transcriptional activation of transforming growth factor alpha by estradiol: requirement for both a GC-rich site and an estrogen response element half-site. *J. Mol. Endocrinol.* 24:329–38
18. Lee AV, Cui X, Oesterreich S. 2001. Cross-talk among estrogen receptor, epidermal growth factor, and insulin-like growth factor signaling in breast cancer. *Clin. Cancer Res.* 7:4429S–35S, discussion (4411S–12S)
19. Umayahara Y, Kawamori R, Watada H, et al. 1994. Estrogen regulation of the insulin-like growth factor I gene transcription involves an AP-1 enhancer. *J. Biol. Chem.* 269:16433–42
20. Nicholson RI, Hutcheson IR, Hiscox SE, et al. 2005. Growth factor signaling and resistance to selective oestrogen receptor modulators and pure antioestrogens: the use of antigrowth factor therapies to treat or delay endocrine resistance in breast cancer. *Endocr. Relat. Cancer* 12(Suppl. 1):S29–S36
21. Yarden RI, Wilson MA, Chrysogelos SA. 2001. Estrogen suppression of EGFR expression in breast cancer cells: a possible mechanism to modulate growth. *J. Cell Biochem. Suppl.* 36:232–46
22. Newman SP, Bates NP, Vernimmen D, et al. 2000. Cofactor competition between the ligand-bound oestrogen receptor and an intron 1 enhancer leads to oestrogen repression of ERBB2 expression in breast cancer. *Oncogene* 19:490–97

Annu. Rev. Med. 2011.62:233-247. Downloaded from www.annualreviews.org
Access provided by EISAI Research Institute on 07/06/16. For personal use only.

23. Massarweh S, Osborne CK, Creighton CJ, et al. 2008. Tamoxifen resistance in breast tumors is driven by growth factor receptor signaling with repression of classic estrogen receptor genomic function. *Cancer Res.* 68:826–33
24. Bayliss J, Hilger A, Vishnu P, et al. 2007. Reversal of the estrogen receptor negative phenotype in breast cancer and restoration of antiestrogen response. *Clin. Cancer Res.* 13:7029–36
25. Lopez-Tarruella S, Schiff R. 2007. The dynamics of estrogen receptor status in breast cancer: reshaping the paradigm. *Clin. Cancer Res.* 13:6921–25
26. Cui X, Zhang P, Deng W, et al. 2003. Insulin-like growth factor-I inhibits progesterone receptor expression in breast cancer cells via the phosphatidylinositol 3-kinase/Akt/mammalian target of rapamycin pathway: progesterone receptor as a potential indicator of growth factor activity in breast cancer. *Mol. Endocrinol.* 17:575–88
27. Cui X, Schiff R, Arpino G, et al. 2005. Biology of progesterone receptor loss in breast cancer and its implications for endocrine therapy. *J. Clin. Oncol.* 23:7721–35
28. Guo S, Sonenshein GE. 2004. Forkhead box transcription factor FOXO3a regulates estrogen receptor alpha expression and is repressed by the Her-2/neu/phosphatidylinositol 3-kinase/Akt signaling pathway. *Mol. Cell Biol.* 24:8681–90
29. Creighton CJ, Fu X, Hennessy BT, et al. 2010. Proteomic and transcriptomic profiling reveals a link between the PI3K pathway and lower estrogen-receptor (ER) levels and activity in ER+ breast cancer. *Breast Cancer Res.* 12(3):R40
30. Brinkman JA, El-Ashry D. 2009. ER re-expression and resensitization to endocrine therapies in ER-negative breast cancers. *J. Mammary Gland Biol. Neoplasia* 14:67–78
31. Levin ER, Pietras RJ. 2008. Estrogen receptors outside the nucleus in breast cancer. *Breast Cancer Res. Treat.* 108:351–61
32. Santen RJ, Fan P, Zhang Z, et al. 2009. Estrogen signals via an extranuclear pathway involving IGF-1R and EGFR in tamoxifen-sensitive and -resistant breast cancer cells. *Steroids* 74:586–94
33. Wu RC, Qin J, Yi P, et al. 2004. Selective phosphorylations of the SRC-3/AIB1 coactivator integrate genomic reponses to multiple cellular signaling pathways. *Mol. Cell* 15:937–49
34. Lee H, Bai W. 2002. Regulation of estrogen receptor nuclear export by ligand-induced and p38-mediated receptor phosphorylation. *Mol. Cell Biol.* 22:5835–45
35. Pontiggia O, Rodriguez V, Fabris V, et al. 2009. Establishment of an in vitro estrogen-dependent mouse mammary tumor model: a new tool to understand estrogen responsiveness and development of tamoxifen resistance in the context of stromal-epithelial interactions. *Breast Cancer Res. Treat.* 116:247–55
36. Jordan VC. 2006. The science of selective estrogen receptor modulators: concept to clinical practice. *Clin. Cancer Res.* 12:5010–13
37. Jordan VC, O'Malley BW. 2007. Selective estrogen-receptor modulators and antihormonal resistance in breast cancer. *J. Clin. Oncol.* 25:5815–24
38. Jordan VC, Brodie AM. 2007. Development and evolution of therapies targeted to the estrogen receptor for the treatment and prevention of breast cancer. *Steroids* 72:7–25
39. Dowsett M, Nicholson RI, Pietras RJ. 2005. Biological characteristics of the pure antiestrogen fulvestrant: overcoming endocrine resistance. *Breast Cancer Res. Treat.* 93(Suppl. 1):S11–18
40. Lewis-Wambi JS, Jordan VC. 2009. Estrogen regulation of apoptosis: How can one hormone stimulate and inhibit? *Breast Cancer Res.* 11:206–17
41. Encarnacion CA, Ciocca DR, McGuire WL, et al. 1993. Measurement of steroid hormone receptors in breast cancer patients on tamoxifen. *Breast Cancer Res. Treat.* 26:237–46
42. Gutierrez MC, Detre S, Johnston S, et al. 2005. Molecular changes in tamoxifen-resistant breast cancer: relationship between estrogen receptor, HER-2, and p38 mitogen-activated protein kinase. *J. Clin. Oncol.* 23:2469–76
43. Hull DF 3rd, Clark GM, Osborne CK, et al. 1983. Multiple estrogen receptor assays in human breast cancer. *Cancer Res.* 43:413–16
44. Lipton A, Leitzel K, Ali SM, et al. 2005. Serum HER-2/neu conversion to positive at the time of disease progression in patients with breast carcinoma on hormone therapy. *Cancer* 104:257–63
45. Meng S, Tripathy D, Shete S, et al. 2004. HER-2 gene amplification can be acquired as breast cancer progresses. *Proc. Natl. Acad. Sci. USA* 101:9393–98

Annu. Rev. Med. 2011.62:233-247. Downloaded from www.annualreviews.org
Access provided by EISAI Research Institute on 07/06/16. For personal use only.

46. Arpino G, Green SJ, Allred DC, et al. 2004. HER-2 amplification, HER-1 expression, and tamoxifen response in estrogen receptor-positive metastatic breast cancer: a Southwest Oncology Group study. *Clin. Cancer Res.* 10:5670–76
47. Massarweh S, Osborne CK, Jiang S, et al. 2006. Mechanisms of tumor regression and resistance to estrogen deprivation and fulvestrant in a model of estrogen receptor-positive, HER-2/neu-positive breast cancer. *Cancer Res.* 66:8266–73
48. Creighton CJ, Massarweh S, Huang S, et al. 2008. Development of resistance to targeted therapies transforms the clinically associated molecular profile subtype of breast tumor xenografts. *Cancer Res.* 68:7493–501
49. Munzone E, Curigliano G, Rocca A, et al. 2006. Reverting estrogen-receptor-negative phenotype in HER-2-overexpressing advanced breast cancer patients exposed to trastuzumab plus chemotherapy. *Breast Cancer Res.* 8:R4
50. Reid G, Denger S, Kos M, Gannon F. 2002. Human estrogen receptor-alpha: regulation by synthesis, modification and degradation. *Cell Mol. Life Sci.* 59:821–31
51. Xia W, Bacus S, Hegde P, et al. 2006. A model of acquired autoresistance to a potent ErbB2 tyrosine kinase inhibitor and a therapeutic strategy to prevent its onset in breast cancer. *Proc. Natl. Acad. Sci. USA* 103:7795–800
52. Brankovic-Magic M, Jankovic R, Neskovic-Konstantinovic Z, et al. 2002. Progesterone receptor status of breast cancer metastases. *J. Cancer Res. Clin. Oncol.* 128:55–60
53. Gross GE, Clark GM, Chamness GC, et al. 1984. Multiple progesterone receptor assays in human breast cancer. *Cancer Res.* 44:836–40
54. Arpino G, Weiss H, Lee AV, et al. 2005. Estrogen receptor-positive, progesterone receptor-negative breast cancer: association with growth factor receptor expression and tamoxifen resistance. *J. Natl. Cancer Inst.* 97:1254–61
55. Dodwell D, Wardley A, Johnston S. 2006. Postmenopausal advanced breast cancer: options for therapy after tamoxifen and aromatase inhibitors. *Breast* 15:584–94
56. Robertson JF, Osborne CK, Howell A, et al. 2003. Fulvestrant versus anastrozole for the treatment of advanced breast carcinoma in postmenopausal women: a prospective combined analysis of two multicenter trials. *Cancer* 98:229–38
57. Musgrove EA, Sutherland RL. 2009. Biological determinants of endocrine resistance in breast cancer. *Nat. Rev. Cancer* 9:631–43
58. Helleman J, Jansen MP, Ruigrok-Ritstier K, et al. 2008. Association of an extracellular matrix gene cluster with breast cancer prognosis and endocrine therapy response. *Clin. Cancer Res.* 14:5555–64
59. Jansen MP, Foekens JA, van Staveren IL, et al. 2005. Molecular classification of tamoxifen-resistant breast carcinomas by gene expression profiling. *J. Clin. Oncol.* 23:732–40
60. Generali D, Berruti A, Brizzi MP, et al. 2006. Hypoxia-inducible factor-1α expression predicts a poor response to primary chemoendocrine therapy and disease-free survival in primary human breast cancer. *Clin. Cancer Res.* 12:4562–68
61. Folgiero V, Avetrani P, Bon G, et al. 2008. Induction of ErbB-3 expression by α6β4 integrin contributes to tamoxifen resistance in ERβ1-negative breast carcinomas. *PLoS One* 3:e1592
62. Brinkman A, de Jong D, Tuinman S, et al. 2010. The substrate domain of BCAR1 is essential for antiestrogen-resistant proliferation of human breast cancer cells. *Breast Cancer Res. Treat.* 120:401–8
63. Shi L, Dong B, Li Z, et al. 2009. Expression of ER-α36, a novel variant of estrogen receptor α, and resistance to tamoxifen treatment in breast cancer. *J. Clin. Oncol.* 27:3423–29
64. Lavinsky RM, Jepsen K, Heinzel T, et al. 1998. Diverse signaling pathways modulate nuclear receptor recruitment of N-CoR and SMRT complexes. *Proc. Natl. Acad. Sci. USA* 95:2920–25
65. Ali S, Coombes RC. 2002. Endocrine-responsive breast cancer and strategies for combating resistance. *Nat. Rev. Cancer* 2:101–12
66. Zhou Y, Yau C, Gray JW, et al. 2007. Enhanced NFκB and AP-1 transcriptional activity associated with antiestrogen resistant breast cancer. *BMC Cancer* 7:59
67. Johnston SR, Lu B, Scott GK, et al. 1999. Increased activator protein-1 DNA binding and c-Jun NH2-terminal kinase activity in human breast tumors with acquired tamoxifen resistance. *Clin. Cancer Res.* 5:251–56

Annu. Rev. Med. 2011.62:233-247. Downloaded from www.annualreviews.org
Access provided by EISAI Research Institute on 07/06/16. For personal use only.

68. Schiff R, Reddy P, Ahotupa M, et al. 2000. Oxidative stress and AP-1 activity in tamoxifen-resistant breast tumors in vivo. *J. Natl. Cancer Inst.* 92:1926–34
69. Span PN, Tjan-Heijnen VC, Manders P, et al. 2003. Cyclin-E is a strong predictor of endocrine therapy failure in human breast cancer. *Oncogene* 22:4898–904
70. Butt AJ, McNeil CM, Musgrove EA, et al. 2005. Downstream targets of growth factor and oestrogen signaling and endocrine resistance: the potential roles of c-Myc, cyclin D1 and cyclin E. *Endocr. Relat. Cancer* 12(Suppl. 1):S47–59
71. Chu IM, Hengst L, Slingerland JM. 2008. The Cdk inhibitor p27 in human cancer: prognostic potential and relevance to anticancer therapy. *Nat. Rev. Cancer* 8:253–67
72. Perez-Tenorio G, Berglund F, Esguerra Merca A, et al. 2006. Cytoplasmic p21WAF1/CIP1 correlates with Akt activation and poor response to tamoxifen in breast cancer. *Int. J. Oncol.* 28:1031–42
73. Riggins RB, Bouton AH, Liu MC, et al. 2005. Antiestrogens, aromatase inhibitors, and apoptosis in breast cancer. *Vitam. Horm.* 71:201–37
74. Schoenlein PV, Periyasamy-Thandavan S, Samaddar JS, et al. 2009. Autophagy facilitates the progression of ERalpha-positive breast cancer cells to antiestrogen resistance. *Autophagy* 5:400–3
75. Arpino G, Wiechmann L, Osborne CK, et al. 2008. Crosstalk between the estrogen receptor and the HER tyrosine kinase receptor family: molecular mechanism and clinical implications for endocrine therapy resistance. *Endocr. Rev.* 29:217–33
76. Chakraborty AK, Welsh A, Digiovanna MP. 2010. Co-targeting the insulin-like growth factor I receptor enhances growth-inhibitory and proapoptotic effects of antiestrogens in human breast cancer cell lines. *Breast Cancer Res. Treat.* 120:327–35
77. Kern FG, McLeskey SW, Zhang L, et al. 1994. Transfected MCF-7 cells as a model for breast-cancer progression. *Breast Cancer Res. Treat.* 31:153–65
78. Morgan L, Gee J, Pumford S, et al. 2009. Elevated Src kinase activity attenuates tamoxifen response in vitro and is associated with poor prognosis clinically. *Cancer Biol. Ther.* 8:1550–58
79. Shoman N, Klassen S, McFadden A, et al. 2005. Reduced PTEN expression predicts relapse in patients with breast carcinoma treated by tamoxifen. *Mod. Pathol.* 18:250–59
80. De Amicis F, Thirugnansampanthan J, Cui Y, et al. 2009. Androgen receptor overexpression induces tamoxifen resistance in human breast cancer cells. *Breast Cancer Res. Treat.* 121:1–11
81. Johnston SR. 2010. New strategies in estrogen receptor-positive breast cancer. *Clin. Cancer Res.* 16:1979–87
82. Johnston SR. 2006. Clinical efforts to combine endocrine agents with targeted therapies against epidermal growth factor receptor/human epidermal growth factor receptor 2 and mammalian target of rapamycin in breast cancer. *Clin. Cancer Res.* 12:1061S–68S
83. Kaufman B, Mackey JR, Clemens MR, et al. 2009. Trastuzumab plus anastrozole versus anastrozole alone for the treatment of postmenopausal women with human epidermal growth factor receptor 2-positive, hormone receptor-positive metastatic breast cancer: results from the randomized phase III TAnDEM study. *J. Clin. Oncol.* 27:5529–37
84. Osborne K, Neven P, Dirix L, et al. 2007. Randomized phase II study of gefitinib (IRESSA) or placebo in combination with tamoxifen in patients with hormone receptor positive metastatic breast cancer. *Breast Cancer Res. Treat.* 106(S1):S107 (Abstr. 2067)
85. Cristofanilli M, Valero V, Mangalik A, et al. 2010. Phase II, randomized trial to compare anastrozole combined with gefitinib or placebo in postmenopausal women with hormone receptor-positive metastatic breast cancer. *Clin. Cancer Res.* 16:1904–14
86. Mauriac L, Cameron D, Dirix L, et al. 2009. *Results of randomized phase II trial combining Iressa® (gefitinib) and arimidex in women with advanced breast cancer (ABC). EORTC protocol 10021.* Presented at San Antonio Breast Cancer Symp., 31st, San Antonio, TX. *Cancer Res.* 69(2S) (Abstr. 6133)
87. Carlson RW, O'Neill A, Vidaurre T, et al. 2009. *Randomized phase II trial of gefitinib plus anastrozole or fulvestrant in postmenopausal, metastatic breast cancer.* Presented at Annu. Meet. Am. Soc. Clin. Oncol., 45th, Orlando, FL. *J. Clin. Oncol.* 27:15s (Abstr. 1013)
88. Johnston S, Pippen J Jr, Pivot X, et al. 2009. Lapatinib combined with letrozole versus letrozole and placebo as first-line therapy for postmenopausal hormone receptor-positive metastatic breast cancer. *J. Clin. Oncol.* 27:5538–46

Annu. Rev. Med. 2011.62:233-247. Downloaded from www.annualreviews.org
Access provided by EISAI Research Institute on 07/06/16. For personal use only.

89. Finn RS, Press M, Dering J, et al. 2009. *Progression-free survival (PFS) of patients with HER2-negative, estrogen-receptor (ER)-low metastatic breast cancer (MBC) with the addition of lapatinib to letrozole: biomarker results of EGF30008*. Presented at Annu. Meet. Am. Soc. Clin. Oncol., 45th, Orlando, FL. *J. Clin. Oncol.* 27:15s (Abstr. 1018)
90. Smith IE, Walsh G, Skene A, et al. 2007. A phase II placebo-controlled trial of neoadjuvant anastrozole alone or with gefitinib in early breast cancer. *J. Clin. Oncol.* 25:3816–22
91. Polychronis A, Sinnett HD, Hadjiminas D, et al. 2005. Preoperative gefitinib versus gefitinib and anastrozole in postmenopausal patients with oestrogen-receptor positive and epidermal-growth-factor-receptor-positive primary breast cancer: a double-blind placebo-controlled phase II randomised trial. *Lancet Oncol.* 6:383–91
92. Chow L, Sun Y, Jassem J, et al. 2006. Phase 3 study of temsirolimus with letrozole or letrozole alone in postmenopausal women with locally advanced or metastatic breast cancer. *Breast Cancer Res. Treat.* 100(Suppl. 1):S28 (Abstr. 6091)
93. Baselga J, Semiglazov V, van Dam P, et al. 2009. Phase II randomized study of neoadjuvant everolimus plus letrozole compared with placebo plus letrozole in patients with estrogen receptor-positive breast cancer. *J. Clin. Oncol.* 27:2630–37

Annu. Rev. Med. 2011.62:233-247. Downloaded from www.annualreviews.org
Access provided by EISAI Research Institute on 07/06/16. For personal use only.

Annual Review of Medicine

Volume 62, 2011

Contents

Role of Postmarketing Surveillance in Contemporary Medicine
Janet Woodcock, Rachel E. Behrman, and Gerald J. Dal Pan 1

Genome-Wide Association Studies: Results from the First Few Years and Potential Implications for Clinical Medicine
Joel N. Hirschhorn and Zofia K.Z. Gajdos 11

Imaging of Atherosclerosis
D.R.J. Owen, A.C. Lindsay, R.P. Choudhury, and Z.A. Fayad 25

Novel Oral Factor Xa and Thrombin Inhibitors in the Management of Thromboembolism
Bengt I. Eriksson, Daniel J. Quinlan, and John W. Eikelboom 41

The Fabry Cardiomyopathy: Models for the Cardiologist
Frank Weidemann, Markus Niemann, David G. Warnock, Georg Ertl, and Christoph Wanner 59

Kawasaki Disease: Novel Insights into Etiology and Genetic Susceptibility
Anne H. Rowley 69

State of the Art in Therapeutic Hypothermia
Joshua W. Lampe and Lance B. Becker 79

Therapeutic Potential of Lung Epithelial Progenitor Cells Derived from Embryonic and Induced Pluripotent Stem Cells
Rick A. Wetsel, Dachun Wang, and Daniel G. Calame 95

Therapeutics Development for Cystic Fibrosis: A Successful Model for a Multisystem Genetic Disease
Melissa A. Ashlock and Eric R. Olson 107

Early Events in Sexual Transmission of HIV and SIV and Opportunities for Interventions
Ashley T. Haase 127

HIV Infection, Inflammation, Immunosenescence, and Aging
Steven G. Deeks 141

Annu. Rev. Med. 2011.62:233-247. Downloaded from www.annualreviews.org
Access provided by EISAI Research Institute on 07/06/16. For personal use only.

The Increasing Burden of HIV-Associated Malignancies in Resource-Limited Regions
Corey Casper 157

Biliary Atresia: Will Blocking Inflammation Tame the Disease?
Kazuhiko Bessho and Jorge A. Bezerra 171

Advances in Palliative Medicine and End-of-Life Care
Janet L. Abrahm 187

Clostridium difficile and Methicillin-Resistant *Staphylococcus aureus*: Emerging Concepts in Vaccine Development
David C. Kaslow and John W. Shiver 201

Antiestrogens and Their Therapeutic Applications in Breast Cancer and Other Diseases
Simak Ali, Laki Buluwela, and R. Charles Coombes 217

Mechanisms of Endocrine Resistance in Breast Cancer
C. Kent Osborne and Rachel Schiff 233

Multiple Myeloma
Jacob Laubach, Paul Richardson, and Kenneth Anderson 249

Muscle Wasting in Cancer Cachexia: Clinical Implications, Diagnosis, and Emerging Treatment Strategies
Shontelle Dodson, Vickie E. Baracos, Aminah Jatoi, William J. Evans, David Cella, James T. Dalton, and Mitchell S. Steiner 265

Pharmacogenetics of Endocrine Therapy for Breast Cancer
Michaela J. Higgins and Vered Stearns 281

Therapeutic Approaches for Women Predisposed to Breast Cancer
Katherine L. Nathanson and Susan M. Domchek 295

New Approaches to the Treatment of Osteoporosis
Barbara C. Silva and John P. Bilezikian 307

Regulation of Bone Mass by Serotonin: Molecular Biology and Therapeutic Implications
Gerard Karsenty and Vijay K. Yadav 323

Alpha-1-Antitrypsin Deficiency: Importance of Proteasomal and Autophagic Degradative Pathways in Disposal of Liver Disease–Associated Protein Aggregates
David H. Perlmutter 333

Hepcidin and Disorders of Iron Metabolism
Tomas Ganz and Elizabeta Nemeth 347

Annu. Rev. Med. 2011.62:233-247. Downloaded from www.annualreviews.org
Access provided by EISAI Research Institute on 07/06/16. For personal use only.

Interactions Between Gut Microbiota and Host Metabolism Predisposing to Obesity and Diabetes
Giovanni Musso, Roberto Gambino, and Maurizio Cassader 361

The Brain-Gut Axis in Abdominal Pain Syndromes
Emeran A. Mayer and Kirsten Tillisch 381

Cognitive Therapy: Current Status and Future Directions
Aaron T. Beck and David J.A. Dozois 397

Toward Fulfilling the Promise of Molecular Medicine in Fragile X Syndrome
Dilja D. Krueger and Mark F. Bear 411

Stress- and Allostasis-Induced Brain Plasticity
Bruce S. McEwen and Peter J. Gianaros 431

Update on Sleep and Its Disorders
Allan I. Pack and Grace W. Pien 447

A Brain-Based Endophenotype for Major Depressive Disorder
Bradley S. Peterson and Myrna M. Weissman 461

Indexes

Cumulative Index of Contributing Authors, Volumes 58–62 475

Cumulative Index of Chapter Titles, Volumes 58–62 479

Errata

An online log of corrections to *Annual Review of Medicine* articles may be found at http://med.annualreviews.org/errata.shtml

Annu. Rev. Med. 2011.62:233-247. Downloaded from www.annualreviews.org
Access provided by EISAI Research Institute on 07/06/16. For personal use only.

CCR Translations
See related article by Jeselsohn et al., p. 1757

Clinical Cancer Research

Estrogen Receptor Mutations in Breast Cancer—New Focus on an Old Target

Corinne V. Segal[1,2] and Mitch Dowsett[1,2]

Recent studies have provided strong evidence for the emergence of substantial numbers of constitutively active *ESR1* mutations in estrogen receptor–positive metastatic breast cancer that are undetected in primary disease. Some of these mutants remain partially sensitive to current anti-estrogen therapies but effective therapeutics targeted at them may require new approaches. *Clin Cancer Res; 20(7); 1724–6. ©2014 AACR.*

In this issue of *Clinical Cancer Research*, Jeselsohn and colleagues (1) report an overall 12% frequency of mutations in the coding sequence of *ESR1* in metastatic estrogen receptor–positive (ER^+) breast cancers but the lack of their detection in primary disease.

About 80% of primary breast cancers express estrogen receptor α (ERα), the product of the *ESR1* gene, and are described as ER^+. Estrogen is the primary stimulant of the development and continued growth of ER^+ tumors: withdrawal of estrogen from primary ER^+ breast tumors decreases proliferation in >90%, although this reduction may be modest in some (2). The mainstay of treatment of ER^+ breast cancer is endocrine therapy, in the form of drugs that antagonize the ER (e.g., tamoxifen), therapies that result in estrogen deprivation (e.g., aromatase inhibitors), or fulvestrant, a drug that destabilizes and antagonizes the receptor. Most patients receive endocrine therapy for 5 years starting shortly after surgery (adjuvant therapy).

Endocrine therapy for breast cancer has resulted in markedly reduced recurrence and mortality rates; however, a significant proportion of patients relapse with metastatic disease. If the recurrence has not arisen within a few months of starting adjuvant therapy, these patients will be treated with an alternative endocrine treatment (first-line metastatic treatment). Resultant shrinkage or stasis of metastatic lesions is achieved in many patients and those showing a response have a good chance of responding to subsequent lines of endocrine treatments: patients whose cancer has progressed on tamoxifen often respond to fulvestrant or an aromatase inhibitor and *vice versa* (3). The lack of cross-resistance suggests that the mechanisms by which this occurs may vary depending upon the prior treatment. Eventually, pan-endocrine resistance develops.

Many mechanisms have been elucidated in model systems of resistance to tamoxifen, and more recently to estrogen deprivation and fulvestrant. These include altered expression of growth factor receptors, such as HER2, or aberrant expression of ER coregulators leading to either ER-independent growth or ER-dependent/ligand-independent growth (4). However, there has been limited confirmation of these findings in the clinic. Although some patients with acquired resistance to tamoxifen show loss of ER in metastases, an obvious route to loss of sensitivity, the majority continue to express ER and there is less evidence for ER loss with resistance to aromatase inhibitors (4, 5). Thus, resistance mechanisms remain incompletely explained and there is little biomarker-related guidance of therapy for metastatic disease.

Despite the central role of estrogens in the development of breast cancer, ERα mutations in primary disease have thus far proved rare (Fig. 1). For example, no *ESR1* mutations were identified in a study of 390 ER^+ primary tumors (6). In metastatic disease, the presence of an *ESR1* mutation unique to the metastases was first noted 20 years ago (7), but until very recently, surprisingly few further data accumulated. However, three groups have recently reported substantial numbers of *ESR1* mutations in metastatic breast cancer (8–10). The current work of Jeselsohn and colleagues (1) is consistent with and extends these reports. They sequenced the coding region of *ESR1*, and 182 additional cancer-related genes, in 58 treatment-naïve primary and 76 metastatic ER^+ $HER2^-$ breast tumors and set out to describe better the functional relevance of the observed *ESR1* mutations. None of the primaries contained detectable *ESR1* mutations but 11 (14.5%) of the metastatic samples contained previously reported mutations (8, 9), clustered in the ligand-binding domain (LBD), predominantly at amino acids 537 or 538, as well as a novel 344insC mutation. Notably, a direct correlation was apparent between the number of endocrine treatments and mutation frequency, which was 5/25 (25%) in tumors from patients receiving an average of seven lines of treatment. All of the other 182 cancer-related genes

Authors' Affiliations: [1]Breakthrough Breast Cancer Research Centre at The Institute of Cancer Research and [2]Academic Department of Biochemistry, The Royal Marsden Hospital, London, United Kingdom

Corresponding Author: Mitch Dowsett, Academic Department of Biochemistry, Royal Marsden Hospital, London SW3 6JJ, United Kingdom. Phone: 020-7808-2885; Fax: 020-7376-3918; E-mail: Mitch.dowsett@icr.ac.uk

doi: 10.1158/1078-0432.CCR-14-0067

©2014 American Association for Cancer Research.

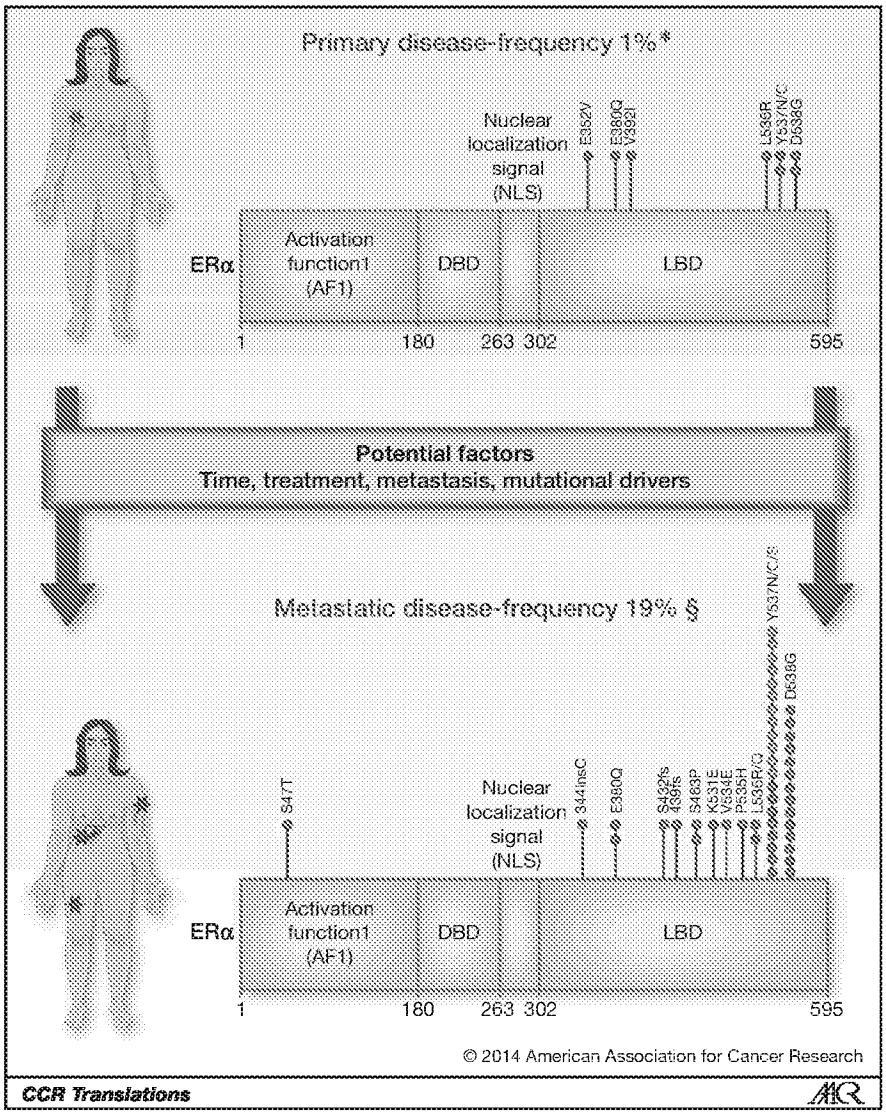


Figure 1. Schematic of *ESR1* mutations identified in primary and metastatic advanced ER$^+$ breast cancer and factors that may influence their development. The majority of the mutations affect the ligand-binding domain in helix 12 (H12). Collated from refs. (1, 6–12). *, total number of patients with mutations in primary disease (7/674). 0/58, ref. (1); 0/390, ref. (6); 1/35, ref. (7); 6/183, ref. (8); 0/3, ref. (9); 0/5, ref. (10). §, total number of patients with mutations in metastatic disease (43/222). 11/76, ref. (1); 2/5, ref. (7); 14/80, ref (8); 6/11, ref. (9); 5/13, ref. (10); 2/7, ref. (11); 3/30 (NB ER$^+$ status unconfirmed), ref (12).

sequenced exhibited similar mutation frequencies between the primary and metastasis.

In the largest of the other recent reports, Toy and colleagues (8) found nine LBD mutations in 36 cases enrolled in a metastatic collection program. In the two cases in which they could also test the primary tumor, the mutation was absent. They also found that 5 of 44 cases from the BOLERO-2 clinical trial of letrozole ± everolimus harbored *ESR1* mutations with the frequency enriched in cases with a long duration of endocrine therapy (8). Similarly, Robinson and colleagues (9) and Merenbakh-Lamin and colleagues (10) reported that 6 of 11 and 5 of 13 cases, respectively, of breast cancer metastases contained LBD-localized *ESR1* mutations. In each of these reports, mutations at 537 and 538 were the most frequent, but others at 534 or 536 were also noted. Given the consistent finding of mutations in the LBD of ERα, elucidation of their functional significance and susceptibility to therapeutic targeting is of paramount importance.

Functional studies by Jeselsohn and colleagues (1) and others (8–12) provide evidence that many of the mutants are strong promoters of ER signaling and, importantly, are constitutively active in the absence of estradiol and therefore likely to elicit resistance to estrogen deprivation strategies. They stimulate increased expression of ER-regulated genes, and increase proliferation and migration *in vitro* compared with wild-type *ESR1*. The *ESR1* mutants have also generally been found to confer reduced sensitivity to anti-estrogens compared with wild-type *ESR1*. Although signaling is reduced by 4-hydroxytamoxifen and fulvestrant, much higher doses are required to reach a similar level of inhibition observed in the wild type (1, 8–12). These *in vitro* findings are supported by molecular modeling that indicate

that the mutants favor the agonist conformation and mediate their effects through influence of coactivator or corepressor binding (8). It is also notable that in ER-Y537N–mutant cells, fulvestrant induces much more modest ER degradation compared with wild type (1) and therefore reduced ability to inhibit ligand-independent activity of ER. This relative resistance to degradation seems less apparent with ER-Y537S (11).

Interestingly, while it has been difficult to sustain patient-derived xenografts (PDX) from ER^+ breast cancer tissues, aberrations in the *ESR1* gene were found in 4 of 5 luminal breast cancer metastases. This included one case with ER-Y537S that was found in a further PDX in which the ER status was not available. A fusion gene (*ESR1/YAP1*) was also discovered in an ER^+ PDX that, like the point mutations, induced estradiol-independent growth. It is plausible that the drive provided by certain constitutively active *ESR1* alterations is a major advantage in promoting survival and growth in the low-estrogen environment of the PDX system. These PDXs are likely to be particularly valuable in elucidation of the best therapeutic approaches for tumors with specific *ESR1* alterations.

In summary, there is now substantial evidence for the emergence of functionally aberrant *ESR1* mutations, particularly in the LBD, in metastatic ER^+ breast cancer, which are undetectable in primary tumors. Correlative evidence is consistent with this emergence being due to selective pressure of multiple endocrine therapies. The genomic instability associated with advanced disease may contribute to the prevalence of the mutations, for example through self-perpetuating defects in DNA-repair mechanisms. *ESR1* mutations might also promote the success of the metastatic process and be apparently enriched as a result, although this hypothesis requires their presence below the detection limits of the high-depth sequencing conducted to date. To confirm the role of the mutations as resistance mechanisms and their potential as targets for new therapies requires careful prospective study of metastatic disease aligned with comprehensive genomic and functional analyses.

Disclosure of Potential Conflicts of Interest

No potential conflicts of interest were disclosed.

Authors' Contributions

Conception and design: C.V. Segal, M. Dowsett
Analysis and interpretation of data (e.g., statistical analysis, biostatistics, computational analysis): C.V. Segal, M. Dowsett
Writing, review, and/or revision of the manuscript: C.V. Segal, M. Dowsett

Acknowledgments

The authors thank the Mary-Jean Mitchell Green Foundation and Breakthrough Breast Cancer for funding. They also thank NHS for providing funding to the NIHR Royal Marsden Hospital, and the Institute of Cancer Research Biomedical Research Centre.

Received January 31, 2014; accepted February 7, 2014; published OnlineFirst February 28, 2014.

References

1. Jeselsohn R Yelensky R, Buchwalter G, Frampton G, Meric-Bernstam F, Gonzalez-Angulo AM. Emergence of constitutively active estrogen receptor-a mutations in pretreated advanced estrogen receptor–positive breast cancer Clin Cancer Res 2014;20:1757–67.
2. Dowsett M, Smith IE, Ebbs SR, Dixon JM, Skene A, Griffith C, et al. Short-term changes in Ki-67 during neoadjuvant treatment of primary breast cancer with anastrozole or tamoxifen alone or combined correlate with recurrence-free survival. Clin Cancer Res 2005;11:951s–8s.
3. Ingle JN, Suman VJ, Rowland KM, Mirchandani D, Bernath AM, Camoriano JK, et al. Fulvestrant in women with advanced breast cancer after progression on prior aromatase inhibitor therapy: North Central Cancer Treatment Group Trial N0032. J Clin Oncol 2006;24:1052–6.
4. Ring A, Dowsett M. Mechanisms of tamoxifen resistance. Endocr Relat Cancer 2004;11:643–58.
5. Arnedos M, Drury S, Afentakis M, A'Hern R, Hills M, Salter J, et al. Biomarker changes associated with the development of resistance to aromatase inhibitors (AIs) in oestrogen receptor-positive breast cancer. Ann Oncol 2014;25:605–10.
6. Cancer Genome Atlas Network. Comprehensive molecular portraits of human breast tumours. Nature 2012;490:61–70.
7. Karnik PS, Kulkarni S, Liu XP, Budd GT, Bukowski RM. Estrogen receptor mutations in tamoxifen-resistant breast cancer. Cancer Res 1994;54:349–53.
8. Toy W, Shen Y, Won H, Green B, Sakr RA, Will M, et al. ESR1 ligand-binding domain mutations in hormone-resistant breast cancer. Nat Genet 2013;45:1439–45.
9. Robinson DR, Wu YM, Vats P, Su F, Lonigro RJ, Cao X, et al. Activating ESR1 mutations in hormone-resistant metastatic breast cancer. Nat Genet 2013;45:1446–51.
10. Merenbakh-Lamin K, Ben-Baruch N, Yeheskel A, Dvir A, Soussan-Gutman L, Jeselsohn R, et al. D538G mutation in estrogen receptor-alpha: a novel mechanism for acquired endocrine resistance in breast cancer. Cancer Res 2013;73:6856–64.
11. Li S, Shen D, Shao J, Crowder R, Liu W, Prat A, et al. Endocrine-therapy-resistant ESR1 variants revealed by genomic characterization of breast-cancer-derived xenografts. Cell Rep 2013;4:1116–30.
12. Zhang QX, Borg A, Wolf DM, Oesterreich S, Fuqua SA. An estrogen receptor mutant with strong hormone-independent activity from a metastatic breast cancer. Cancer Res 1997;57:1244–9.

Mechanisms of Tamoxifen Resistance: Increased Estrogen Receptor-HER2/neu Cross-Talk in ER/HER2–Positive Breast Cancer

Jiang Shou, Suleiman Massarweh, C. Kent Osborne, Alan E. Wakeling, Simale Ali, Heidi Weiss, Rachel Schiff

Background: **Patients receiving adjuvant tamoxifen whose tumors express high levels of both HER2/neu (HER2) and the estrogen receptor (ER) coactivator AIB1 often develop tamoxifen resistance. We used a breast cancer model system with high expression of AIB1 and HER2 to investigate the possible mechanisms underlying this resistance.** ***Methods:*** **MCF-7 breast cancer cells, which express high levels of AIB1, and a tamoxifen-resistant derivative cell line engineered to overexpress HER2 (MCF-7/HER2-18) were treated with estrogen, tamoxifen, epidermal growth factor (EGF), or heregulin in the absence or presence of the EGF receptor (EGFR) tyrosine kinase inhibitor gefitinib. We analyzed phosphorylation of signaling intermediates by immunoblotting, ER transcriptional activity with reporter gene constructs and immunoblot analysis of endogenous gene products, promoter assembly by chromatin immunoprecipitation (ChIP) assay, and tumor cell growth *in vitro* by anchorage-independent colony formation and *in vivo* using xenografts in nude mice.** ***Results:*** **MCF-7/HER2-18 tumors were completely growth inhibited by estrogen deprivation but were growth stimulated by tamoxifen. Molecular cross-talk between the ER and HER2 pathways was increased in the MCF-7/HER-2 cells compared with MCF-7 cells, with cross-phosphorylation and activation of both the ER and the EGFR/HER2 receptors, the signaling molecules AKT and ERK 1,2 mitogen-activated protein kinase (MAPK), and AIB1 itself with both estrogen and tamoxifen treatment. Tamoxifen recruited coactivator complexes (ER, AIB1, CBP, p300) to the ER-regulated pS2 gene promoter in MCF-7/HER2-18 cells and corepressor complexes (NCoR, histone deacetylase 3) in MCF-7 cells. Gefitinib pretreatment blocked receptor cross-talk, reestablished corepressor complexes with tamoxifen-bound ER on target gene promoters, eliminated tamoxifen's agonist effects, and restored its antitumor activity both *in vitro* and *in vivo* in MCF-7/HER2-18 cells.** ***Conclusions:*** **Tamoxifen behaves as an estrogen agonist in breast cancer cells that express high levels of AIB1 and HER2, resulting in *de novo* resistance. Gefitinib's ability to eliminate this cross-talk and to restore tamoxifen's antitumor effects should be tested in the clinic. [J Natl Cancer Inst 2004; 96:926–35]**

The binding of estrogen to the estrogen receptor (ER) induces receptor phosphorylation, alters its conformation, triggers receptor dimerization, and facilitates binding of the receptor complex to the promoter region of target genes to activate transcription *(1)*. These transcriptional effects of the ER are modulated by interactions with coregulatory proteins that function as either coactivators or corepressors *(2)*. The conformation of estrogen-bound ER favors the recruitment of coactivators that augment transcriptional activity. By contrast, the ER conformation induced by binding of the selective estrogen receptor modulator (SERM) tamoxifen favors the recruitment of corepressors that inhibit transcriptional activity. Tamoxifen has different partial agonist–antagonist activities in different tissues, however, and the differences may be related in part to the milieu of ER coactivators and corepressors in these tissues *(3)*. For example, increased levels of coactivators such as AIB1 (SRC3) or SRC1 enhance the estrogen agonist properties of tamoxifen *in vitro (4)*.

ER can generate multiple growth-promoting signals both inside and outside the nucleus. Estrogen-induced expression of genes encoding growth factors, their receptors, and other signaling molecules can provide cell proliferation and survival stimuli *(5,6)*. ER can also complex with other transcription factors, such as Fos and Jun proteins on AP1 response elements, to alter the transcription of genes not normally thought to be classical estrogen targets, such as cyclin D1, insulin-like growth factor 1, and collagenase *(7)*. Finally, new evidence also indicates that ER located in or near the cell membrane can activate growth factor receptor tyrosine kinases, such as epidermal growth factor receptor (EGFR) and HER2/neu (HER2), providing another mechanism for the growth-promoting effects of estrogen *(8)*.

The receptor cross-talk between the ER and growth factor receptors travels in both directions. For example, ERK1,2 mitogen-activated protein kinase (MAPK) that has been activated by signaling from the EGFR or HER2 phosphorylates both ER and the ER coactivator AIB1 *(9)*. The resulting ER phosphorylation in the N-terminal region, which can also be induced by estrogen binding, increases transcription arising from the AF-1 domain of the ER; the resulting phosphorylation of AIB1, which is not directly induced by estrogen, augments its coactivator activity *(9,10)*.

These data raise the possibility that high tumor levels of ER coactivators, such as AIB1, could cause tamoxifen resistance and that HER2 cross-talk with ER could enhance the estrogen agonist activity of tamoxifen-bound ER. Tamoxifen's agonist properties might require both high AIB1 levels and growth

Affiliations of authors: The Breast Center (JS, SM, CKO, HW, RS) and the Departments of Medicine (JS, SM, CKO, HW, RS) and Molecular and Cellular Biology (CKO), Baylor College of Medicine, Houston, TX; Cancer and Infection Bioscience, AstraZeneca, Macclesfield, Cheshire, UK (AEW); Department of Cancer Medicine, Imperial College of Science, Technology & Medicine, London, UK (SA).

Correspondence to: Rachel Schiff, PhD, Breast Center, Baylor College of Medicine, One Baylor Plaza, MS 600, Houston, TX 77030 (e-mail: rschiff@breastcenter.tmc.edu).

See "Notes" following "References."

DOI: 10.1093/jnci/djh166

Journal of the National Cancer Institute, Vol. 96, No. 12, © Oxford University Press 2004, all rights reserved.

Downloaded from http://jnci.oxfordjournals.org/ at Eisai-Andover on July 6, 2016

factor receptor cross-talk, which phosphorylates and further activates both AIB1 and ER. In support of this hypothesis, we recently reported that tamoxifen-treated breast cancer patients whose ER-positive tumors express high levels of AIB1 and HER2 experience substantially more recurrences than those with ER-positive tumors that have lower expression of one or both proteins *(11)*. Furthermore, there was a strong correlation between overexpression of AIB1 and overexpression of HER2 in these tumors, suggesting that high levels of the two proteins provide a strong selective growth advantage for tumor cells with this genotype.

The goal of the present study was to identify the mechanism for the tamoxifen resistance displayed by ER-positive tumors that express high levels of both AIB1 and HER2. We studied as an experimental model MCF-7 breast cancer cells, which express high levels of AIB1, and a derivative line, MCF-7/HER2-18, which expresses high levels of both AIB1 and HER2. We compared the estrogen agonist activity of tamoxifen-bound ER on *in vivo* tumor growth induced by estrogen and tamoxifen in the two cell lines, and we examined cross-talk between the HER2 and ER signaling pathways. We also investigated the components of the coregulatory complexes recruited by tamoxifen-bound ER to the promoter of a target gene. Finally, we examined the effect of a growth factor receptor tyrosine kinase inhibitor, gefitinib (ZD1839 or Iressa), on tamoxifen's effects in both cell lines.

Materials and Methods

Reagents, Hormones, and Antibodies

EGF and heregulin were from Invitrogen (Carlsbad, CA) and R&D Systems (Minneapolis, MN), respectively. 17β-Estradiol (E2), 4-hydroxy-tamoxifen (for all *in vitro* studies) and tamoxifen citrate (for *in vivo* studies), and all other reagents were from Sigma (St. Louis, MO) unless otherwise indicated. Gefitinib was provided by AstraZeneca (Macclesfield, UK). Antibodies used for immunoblotting were to phospho-Ser118-ER and AIB1 *(11,12)*; ERα and HSP27 (NeoMarkers, Fremont, CA); progesterone receptor (PR) (DAKO, Carpinteria, CA); cathepsin D (BD Biosciences, San Diego, CA); Bcl-2 (Oncogene, Cambridge, MA); total and different phospho-forms of EGFR (Tyr^{845},Tyr^{992},Tyr^{1045}, or Tyr^{1068}), HER2 (Tyr^{887},Tyr^{1112}, or Tyr^{1248}), Akt (Ser^{437}), and ERK1,2 MAPK (Thr^{202}/Tyr^{204}) (Cell Signaling Technology, Beverly, MA); IRS-1 (Upstate Biotechnology, Lake Placid, NY); cyclin D1 (Santa Cruz, Santa Cruz, CA); and β-actin (Chemicon, Temecula, CA). Antibodies used for chromatin immunoprecipitation (ChIP) assays were to AIB1 and NCoR (Affinity Bioreagents, Golden, CO), ERα and histone deacetylase 3 (HDAC3) (Santa Cruz), p300 and acetylated histone 3 (Upstate Biotechnology), and CREB binding protein (CBP) (NeoMarkers).

Xenograft Studies

MCF-7/HER2-18 xenografts were established in ovariectomized 5- to 6-week-old BALB/c athymic nude mice (Harlan Sprague Dawley, Madison, WI) supplemented with 0.25-mg 21-day–release estrogen pellets (Innovative Research, Sarasota, FL) by inoculating the mice subcutaneously with 5×10^6 cells, as described previously *(17)*. When tumors reached 150–200 mm^3 (i.e., in 2–4 weeks), the animals were randomly allocated (n = 12 per group) to continued estrogen (E2), estrogen withdrawal alone (–E2; by removal of the estrogen pellets), or to estrogen withdrawal plus tamoxifen citrate (Tam; 500 μg/animal given subcutaneously in peanut oil, 5 days/week) *(17)*, with either gefitinib (100 mg/kg of body weight, 5 days/week) or vehicle (1% Tween 80) administered via gavage. Tumor growth was assessed and tumor volumes were measured as described previously *(17)*. Tumors were harvested either after 3 weeks of treatment (n = 4 per group) or when they reached 1000 mm^3 (n = 8 per group). Mice were anesthetized with isoflurane before tumor removal. Each tumor analyzed was from a different mouse; tumor tissues were removed from each individual mouse and kept at –190 °C for later analyses. Animal care was in accordance with institutional guidelines.

Cells and Treatment

MCF-7 breast cancer cells, the derivative MCF-7/neo and MCF/HER2-18 cell lines (stably transfected with the control vector alone and a HER2 overexpression vector, respectively), and BT-474 breast cancer cells were maintained as described previously *(13,14)*. Before treatment, tumor cells, in 10-cm dishes, were starved in phenol red–free (PRF), serum-free improved modified Eagle medium (IMEM) for 24 hours. For phosphorylation studies, cells were pretreated for 3 hours with gefitinib (1 μ*M*) or vehicle (dimethyl sulfoxide [DMSO [0.001%]) followed by short-term treatment with vehicle (ethanol), estrogen (1 n*M*, 20 minutes), tamoxifen (100 n*M*, 20 minutes), EGF (100 ng/mL, 10 minutes), or heregulin (10 ng/mL, 20 minutes) in the presence or absence of gefitinib (1 μ*M*). For long-term induction studies, the cells were pretreated for 3 hours with gefitinib (1 μ*M*) or vehicle (DMSO) and were then treated for 48 hours with vehicle (ethanol), estrogen, tamoxifen, EGF, or heregulin at the same concentrations as used in the short-term treatments. Endogenous gene expression was analyzed in cells treated in the same way but for 12 hours. All of the experiments involving parental cells were carried out with both MCF-7 and MCF-7/neo cells. Because similar results were obtained with both cell lines (data not shown), only results for MCF-7 cells are reported.

Cell and Tumor Extracts and Immunoblots

After treatment, cells were rinsed twice with ice-cold phosphate-buffered saline (PBS) and were then lysed immediately with 0.5 mL of lysis buffer/10-cm plate. The lysis buffer (Cell Signaling Technology) was supplemented with 10% glycerol, 1 m*M* phenylmethylsulfonyl fluoride (PMSF), 1× protease inhibitor cocktail (Roche Molecular Biochemicals, Indianapolis, IN), 1 μ*M* okadaic acid, and 10 μg of Microcystin per milliliter. Cell lysates were collected, sonicated (five times for 5 seconds on ice), and microcentrifuged at 15 300*g* for 10 minutes at 4 °C. Cell supernatants were aliquoted and stored at –70 °C. Frozen tumor samples from the different treatment groups (n ≥ 4/group) were pulverized by a tissue pulverizer (Biospec Products, Bartlesville, OK) that was precooled with liquid nitrogen. Tumor powders were manually homogenized in the same supplemented lysis buffer (50 mg/0.5 mL) and extracted as above. Protein concentration was measured with the Bio-Rad Protein Assay kit (Bio-Rad Laboratories, Hercules, CA) according to the manufacturer's directions. Aliquots (20–25 μg) of protein from each sample were separated under denaturing conditions by

Downloaded from http://jnci.oxfordjournals.org/ at Eisai-Andover on July 6, 2016

electrophoresis in 8%–10% polyacrylamide gels containing sodium dodecyl sulfate (SDS–PAGE) and transferred to nitrocellulose membranes by electroblotting (Schleicher & Schuell, Keene, NH). The blots were first stained with Ponceau S to confirm uniform transfer of all samples and were then incubated with specific antibodies according to the manufacturers' directions. Briefly, blots were blocked with blocking buffer (5% [wt/vol] nonfat dry milk in Tris-buffered saline [TBS; 100 m*M* Tris, pH 7.5, and 0.9% NaCl] containing 0.1% Tween 20 (TBS–T)] for 1 hour and then incubated with primary antibodies at dilutions per the manufacturers' directions. For all phospho antibodies, the incubations were done in 5% bovine serum albumin in TBS–T overnight at 4 °C; for other antibodies, the incubations were done in blocking buffer for 2 hours at room temperature. The blots were washed three times in TBS–T and then incubated for 1 hour at room temperature in 5% nonfat dry milk in TBS–T with horseradish peroxidase–labeled anti–rabbit or anti–mouse immunoglobulin G (IgG) (1:2000 and 1:4000 dilutions, respectively) secondary antibodies (Amersham Pharmacia Biotech, Piscataway, NJ). The blots were then washed in TBS–T, and the labeled proteins were detected with an enhanced chemiluminescence detection system (Amersham Pharmacia) and exposure of the membranes to X-ray film (Kodak, Rochester, NY). To detect the mobility shift in AIB1 due to phosphorylation, 10 μg of cell or tumor extracts was first preincubated in the presence or absence of protein λ-phosphatase (λ-PPase) (New England BioLabs, Beverly, MA) as previously described *(9)* and then electrophoresed on SDS–6% polyacrylamide gels. All experiments were repeated three times, and representative blots are presented.

Cell Cycle Analysis

Proliferating MCF-7 and MCF-7/HER2-18 cells were serum starved for 24 hours, were pretreated for 3 hours with gefitinib (1 μ*M*) or vehicle (DMSO), and were then treated, in the presence or absence of gefitinib, for 16 hours with vehicle (ethanol), E2, tamoxifen, or heregulin, as mentioned above. Cells were then subjected to flow cytometric analysis as described previously *(14)*, using a Beckman Coulter EPICS XL-MCS (Fullerton, CA).

Transient Transfection and Luciferase ER Reporter Assays

A total of 1.5×10^6 cells/10-cm dish were serum starved for 24 hours and transfected for 12 hours with 7.5 μg of a 2× estrogen response element (ERE)–luciferase construct *(15)* using LipofectAmine (Invitrogen) in PRF Opti-MEM reduced-serum medium (Invitrogen) containing 1% charcoal-stripped fetal calf serum (CS-FCS) (HyClone, Logan, UT) according to the manufacturer's directions. Cells were then pooled (two dishes per cell line) and split into 12-well plates in PRF IMEM supplemented with 0.5% CS-FCS. After 12 hours, the cells were treated for an additional 16 hours with estrogen or tamoxifen, with or without heregulin and with or without gefitinib, at the concentrations given above. Activity of the luciferase reporter gene was determined by using the Luciferase Assay System (Promega, Madison, WI).

ChIP Assays

ChIP assays were carried out with the ChIP assay kit (Upstate Biotechnology) as previously described *(16)*, with minor modifications. All reagents and buffers were from the kit unless otherwise indicated. Cells were grown on 15-cm plates to 90% confluence in steroid-starved medium (PRF IMEM containing 10% CS-FCS [HyClone]) for 7 days and then were serum starved for 24 hours. Cells were pretreated for 3 hours with gefitinib (1 μ*M*) or vehicle (DMSO) and then treated for 45 minutes with vehicle (ethanol), 100 n*M* estradiol, or 1 μ*M* tamoxifen with or without gefitinib, and immediately cross-linked with 1% formaldehyde (final concentration) added directly to the cell medium for 10 minutes at 37 °C. Cells were washed with cold PBS containing 1× protease inhibitor cocktail and 1 m*M* PMSF, scraped, microcentrifuged for 4 minutes at 4 °C, 420*g*, and lysed by incubation with 1 mL of 1× SDS lysis buffer for 10 minutes on ice. Lysates were sonicated three times for 10 seconds each at 50% duty cycle using an Out Control intensity of 3 (Sonifier 450; Branson, Danbury, CT) followed by microcentrifugation at 4 °C, 18 000*g* for 10 minutes. Protein concentration was measured with the Bio-Rad Protein Assay kit (Bio-Rad Laboratories, Hercules, CA). Two hundred micrograms of supernatant protein was diluted 10-fold with ChIP dilution buffer and immunocleared with 80 μL of salmon sperm DNA–Protein A/G agarose in the presence of preimmune serum (Santa Cruz). Collected agarose beads were saved as control IgG. Immunoprecipitation was performed overnight at 4 °C with specific antibodies (2 μg/1 mL of precleared supernatant). Immunocomplexes were extracted by adding 80 μL of salmon sperm DNA–Protein A/G agarose for 1 hour at 4 °C followed by gentle centrifugation (110*g*, 1 minute, 4 °C). Precipitates were washed sequentially with 1 mL of low-salt wash buffer, high-salt wash buffer, and LiCl wash buffer and were washed twice with 1 mL of TE buffer (10 m*M* Tris–HCl and 1m*M* EDTA, pH 8.0) and extracted twice sequentially by 15 minutes of incubation at room temperature with 250 μL of freshly made elution buffer (1% SDS, 0.1 *M* $NaHCO_3$). The two sequential eluates (×2) were pooled in a total volume of 500 μL, and after the addition of 20 μL of 5 *M* NaCl, were heated at 65 °C for 4 hours to reverse the formaldehyde cross-linking. DNA fragments were then purified with a Qiagen Gel Extraction kit (Qiagen, Valencia, CA) in a final volume of 30 μL.

Five microliters from the 30-μL DNA extraction was amplified by polymerase chain reaction (PCR) with the following pairs of primers for the promoter region of the PS2 gene: 5′-GGC CATCTCTCACTATGAATCACTTCTGCA-3′ (forward) and 5′-GGCAGGCTCTGTTTGCTTAAAGAGCGTTAGATA-3′ (reverse). The PCR amplification was carried out with Sigma reagents in a final reaction volume of 20 μL containing 1× PCR buffer, all four deoxynucleoside triphosphates (each at 0.2 m*M*), 1 U of *Taq* DNA polymerase, and 1.25 p*M* primers. The reactions were performed in an MJ Research PTC-200 Peltier thermal cycler (MJ Research, Reno, NV), with the following program: initial 2 minutes of denaturing at 94 °C followed by 28 cycles of denaturing for 30 seconds at 94 °C, annealing for 30 seconds at 63 °C, and elongating for 1 minute at 72 °C; the final extension took place at 72 °C for 10 minutes. Equal volumes of each PCR sample were subjected to electrophoresis in a 2% agarose gel, which was then stained with ethidium bromide and photographed under UV illumination.

Downloaded from http://jnci.oxfordjournals.org/ at Eisai-Andover on July 6, 2016

Anchorage-Independent Growth Assays

Cells were steroid starved for 7 days in PRF IMEM containing 10% CS-FCS (HyClone) and then treated for 3 hours with gefitinib at the indicated concentrations or vehicle. Colony-forming assays in soft agarose were performed as described previously *(14)*. In brief, tumor cells in top soft agar in steroid starvation medium–containing vehicle, 10 n*M* E2, or 100 n*M* tamoxifen with gefitinib at the original treatment concentration were plated on solidified agar in steroid starvation medium. After 3 weeks, tumor cell colonies measuring at least 50 μm were counted from six replicates per treatment under a dissecting microscope.

Statistical Analysis

Values are expressed as means with 95% confidence intervals (CIs). Tumor growth curves were constructed from the mean tumor volume at each time point of measurement, with error bars representing 95% CI of the mean. The two-sample *t* test was used for two-group comparisons of relative luciferase activity and percentage of cells in S phase. Major analyses, unless otherwise specified, were for gefitinib effects (i.e., comparison of with versus without gefitinib for each specific hormonal treatment and cell group). For the anchorage-independent colony growth assays, effects of increasing concentrations of gefitinib were tested with analysis of variance. After statistically significant differences across various concentrations were established, contrasts were generated in the analysis of variance model to perform pairwise comparisons between control and each concentration of gefitinib in each treatment and cell group. In addition, to assess the magnitude of gefitinib inhibition in the tamoxifen-treated groups versus that of the estrogen-treated groups, we used linear regression models to compare the decrease in number of colonies from that of vehicle-treated cells to that of cells treated with each concentration of gefitinib between these two groups.

Results

HER2 Overexpression and Tamoxifen-Stimulated Growth

We previously showed that growth of wild-type MCF-7 xenografts, which express moderate levels of the ER, low levels of EGFR and HER2, and high levels of AIB1, is stimulated by estrogen and inhibited by estrogen deprivation, either alone or in the presence of tamoxifen *(17)*. Stable MCF-7 transfectants overexpressing HER2 (MCF-7/HER2-18 cells) are tamoxifen resistant and rapidly form xenografts in mice treated with tamoxifen or estrogen *(13)*. To analyze the endocrine sensitivity of HER2-overexpressing breast tumors in more detail, we established MCF-7/HER2-18 xenografts in ovariectomized athymic nude mice in the presence of estrogen. Mice were then randomized to continued treatment with estrogen supplementation, estrogen withdrawal, or estrogen withdrawal plus the antiestrogen tamoxifen, and tumor growth was monitored over time (Fig. 1, A). Growth of MCF-7/HER2-18 tumors was stimulated by estrogen and completely inhibited by estrogen withdrawal nearly 60 days after removal of the estrogen pellet, indicating absolute estrogen dependence. Growth of these tumors was also stimulated when tamoxifen was added to estrogen withdrawal. This result is in contrast to the findings we previously reported for

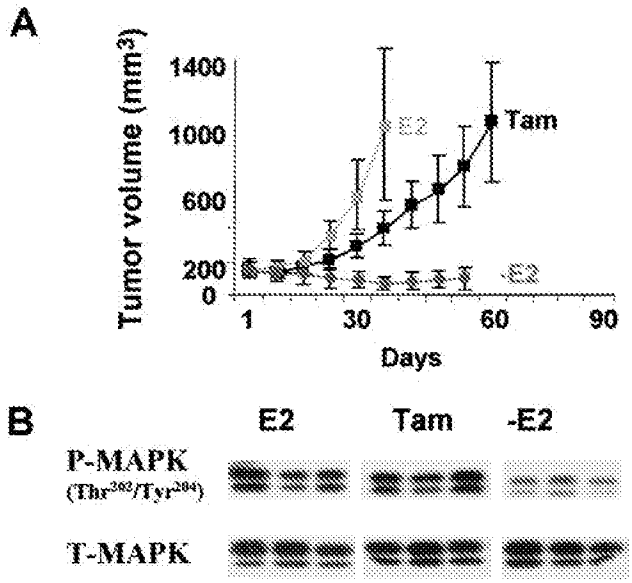


Fig. 1. Effect of estrogen and tamoxifen on HER2-overexpressing tumors. **A)** MCF-7 cells stably transfected with HER2 (MCF-7/HER2-18 clone) were established as xenografts in ovariectomized athymic nude mice in the presence of estrogen. Mice were assigned randomly (day 1), in groups of 12, to continued estrogen supplementation (E2), estrogen withdrawal (–E2), or estrogen withdrawal plus the antiestrogen tamoxifen (Tam), and tumor growth was monitored over time. Four mice from each group were harvested after 3 weeks of treatment. Tumor growth of the remaining eight mice in each group appears as the mean of tumor volumes in each treatment group; bars show 95% confidence intervals. **B)** Levels of phospho Thr^{202}/Tyr^{204}–ERK1,2 mitogen-activated protein kinase (MAPK) (P-MAPK) and total ERK1,2 MAPK (T-MAPK, doublets represent the 42- and 44-kd forms) in three individual tumor extracts from the different treatment groups (after 3 weeks of treatment) assessed by immunoblot analysis. Blots were repeated three times.

parental MCF-7 tumors, whose growth is inhibited by the combination of tamoxifen plus estrogen withdrawal *(17)*. These data indicate that tamoxifen, like estrogen, functions like an estrogen agonist to enhance tumor growth when HER2 is overexpressed.

To investigate the effects of estrogen and tamoxifen on growth factor receptor downstream signaling, we analyzed the levels of phosphorylated ERK 1,2 MAPK in tumor extracts (Fig. 1, B). The level of this activated kinase was increased by tamoxifen as well as by estrogen compared with estrogen withdrawal alone (Fig. 1, B).

Cross-Talk Between Growth Factor Receptor and ER Pathways

To further investigate the mechanism by which the estrogen agonist properties of tamoxifen are increased in MCF-7 cells when HER2 is overexpressed, we examined the short-term effects of estrogen, EGF, heregulin, and tamoxifen on phosphorylation of ER, EGFR, HER2, ERK1,2 MAPK, and AKT in the presence or absence of the receptor tyrosine kinase inhibitor gefitinib, which has been shown to inhibit signaling from both the EGFR and HER2 *(18)*. Treatment of parental MCF-7 cells with either estrogen or tamoxifen led to phosphorylation of the ER via a process that is independent of EGFR or HER2 signaling because it was not inhibited by gefitinib (Fig. 2, A). Treatment with heregulin, and to a much lesser extent, EGF, also caused ER phosphorylation via a process that was inhibited by gefitinib. We did not detect phosphorylation of EGFR or HER2 with EGF

Downloaded from http://jnci.oxfordjournals.org/ at Eisai-Andover on July 6, 2016

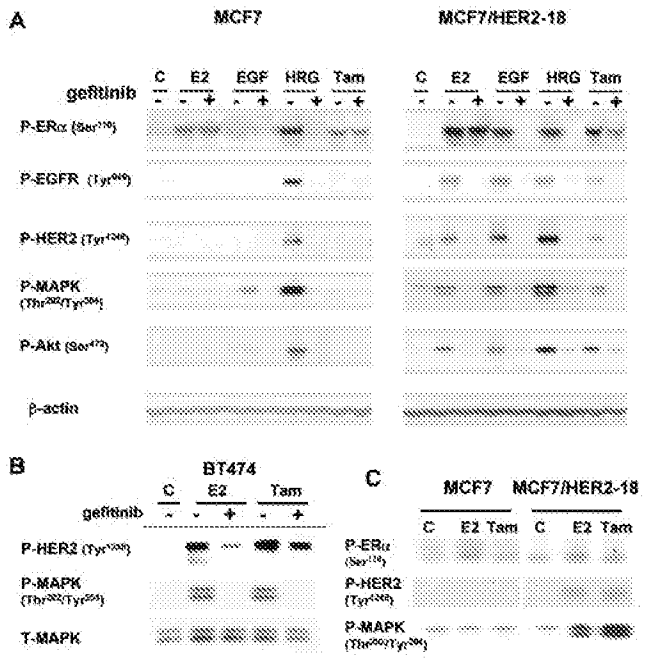


Fig. 2. Effect of HER2 overexpression and gefitinib on cross-phosphorylation between ER and EGFR/HER2 signaling components in MCF-7 and MCF-7/HER2-18 cells. **A)** MCF-7 and MCF-7/HER2-18 cells in serum-free medium, after 3 hours of preincubation with vehicle (dimethyl sulfoxide) or with the tyrosine kinase inhibitor gefitinib, were subjected to a 10–20 minute treatment with vehicle (ethanol [C]), estrogen (E2), EGF, heregulin (HRG), or 4-OH tamoxifen (Tam) in the continuous presence or absence of gefitinib. Levels of phosphorylated (P) ERα, EGF receptor (EGFR), HER2, ERK1,2 mitogen-activated protein kinase (MAPK), and AKT, at the indicated residues, were measured in cellular extracts by immunoblot analysis. Blots are representative of three experiments. β-Actin was used as a control for equal loading and transfer. **B)** BT474 cells, which naturally express high levels of AIB1 and HER2, were treated and analyzed as in panel A. Blots are representative of three experiments. β-Actin was used as a control for equal loading and transfer (not shown). **C)** Parental MCF-7 and MCF-7/HER2-18 cells were induced for long-term (48 hours) as in panel A and phosphorylation levels of ER, HER2, and ERK1,2 MAPK in cellular extracts were measured as in panel A. Blots are representative of three experiments. β-Actin was used as a control for equal loading and transfer (not shown).

treatment in MCF-7 cells under these conditions, although EGF treatment induced slightly higher levels of phosphorylated MAPK and phosphorylated AKT (Fig. 2, A), indicating that EGFR is functional in these cells. Heregulin treatment, on the other hand, led to strong phosphorylation of ER, EGFR, HER2, AKT, and ERK1,2 MAPK, and phosphorylation of all of these targets was inhibited by gefitinib. We did not detect phosphorylation of EGFR, HER2, ERK1,2 MAPK, or AKT in MCF-7 cells treated with estrogen or tamoxifen.

In contrast with parental MCF-7 cells, MCF-7/HER2-18 cells showed substantial bidirectional cross-talk between ER, on the one hand, and EGFR and HER2, on the other (Fig. 2, A). Treatment of MCF-7/HER2-18 cells with estrogen, EGF, heregulin, and tamoxifen all led to ER phosphorylation on Ser-118, as was the case in MCF-7 cells. Gefitinib inhibited the effect of EGF and heregulin on MCF-7/HER2-18 cells, and it partially inhibited the ER phosphorylation induced by tamoxifen but not that induced by estrogen, again as in MCF-7 cells. However, in the MCF-7/HER2-18 cells, both estrogen and tamoxifen induced phosphorylation of EGFR, HER2, AKT, and ERK1,2 MAPK, similar to the phosphorylation induced by EGF and heregulin. Similar results were obtained in both cell lines by using other antibodies specific for detecting phosphorylation of Tyr-992, -1045, or -1068 on EGFR, and Tyr-887 or -1112 on HER2 (data not shown). Phosphorylation of all of these growth factor signaling molecules was abolished by gefitinib. Effects of estrogen and tamoxifen on phosphorylation of downstream effectors of EGFR and HER2 similar to those in MCF-7/HER2-18 cells were observed in another cell line, BT474, which expresses ER and is naturally gene amplified for HER2 and AIB1 *(19,20)* (Fig. 2, B).

All of these experiments in both cell lines involved a maximum of a 20-minute treatment with estrogen, EGF, heregulin, and tamoxifen. The effects of estrogen and tamoxifen treatments on phosphorylated levels of HER2 and MAPK were observed as early as 3 minutes (BT474 cells, data not shown) and were still evident after 48 hours (Fig. 2, C), indicating that they were not transient. Thus, in these HER2-overexpressing cells, estrogen and tamoxifen activate growth factor signaling, while at the same time growth factor signaling activates ER. The receptor tyrosine kinase inhibitor gefitinib eliminated the cross-talk in both directions.

Phosphorylation of AIB1 and Effects of Gefitinib

Because ERK 1,2 MAPK, a downstream target of HER2, phosphorylates the ER coactivator AIB1 *(9)*, we reasoned that tamoxifen-stimulated growth in the presence of high levels of HER2 may be mediated, in part, by the functional activation of AIB1 by HER2 signaling, which would in turn enhance tamoxifen's estrogen agonist activity. In parental MCF-7 cells, treatment with heregulin but not estrogen or tamoxifen led to AIB1 phosphorylation (Fig. 3), and this AIB1 phosphorylation was completely prevented by gefitinib. In contrast, in MCF-7/HER2-18 cells, phosphorylation of AIB1 was observed not only in cells treated with heregulin but also in cells treated with estrogen and tamoxifen. Gefitinib blocked these effects, suggesting that the AIB1 phosphorylation by estrogen and tamoxifen in MCF-7/HER2-18 cells was due to ER-mediated activation of the EGFR and/or HER2 pathway.

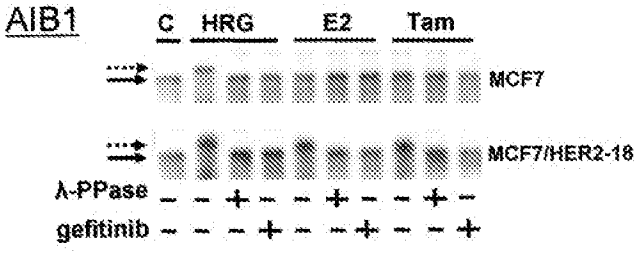


Fig. 3. Effects of HER2 overexpression and gefitinib on AIB1 phosphorylation by estrogen and tamoxifen in MCF-7 and MCF-7/HER2-18 cells. MCF-7 and MCF-7/HER2-18 cells were treated for 20 minutes with vehicle (C), heregulin (HRG), estrogen (E2), or 4-OH tamoxifen (Tam) in the presence or absence of the tyrosine kinase inhibitor gefitinib as in Fig 1, A. AIB1 expression was examined by immunoblot analysis of cell extracts, some of which had been preincubated with protein λ-phosphatase (λ-PPase) prior to electrophoresis. More slowly migrating AIB1 bands (marked by **dashed arrows**) represent the phosphorylated form of the protein, because this change in mobility was reversed by pretreatment of the extracts with λ-PPase to restore the dephosphorylated form (solid arrows). Blots are representative of three experiments.

Downloaded from http://jnci.oxfordjournals.org/ at Eisai-Andover on July 6, 2016

Tamoxifen Agonist Effects and ER-Dependent Gene Transcription in MCF-7/HER2-18 Cells

To determine if the activation of growth factor signaling, ER phosphorylation, and AIB1 phosphorylation by tamoxifen has functional significance, we examined tamoxifen's effects on ER-dependent gene transcription. Mean luciferase activity observed with estrogen induction in each cell line was not set to 1.0. In parental MCF-7 cells, gefitinib had no effect on ER-dependent transcription of an ERE–luciferase reporter gene induced by estrogen (Fig. 4, A). The addition of heregulin, however, increased luciferase activity by more than twofold (to levels of 2.2, 95% CI = 2.05 to 2.35), and the effect was growth factor receptor dependent, as reflected by gefitinib inhibition. Relative luciferase activity was reduced by more than fourfold (to levels of 0.49, 95% CI = 0.4 to 0.58) when gefitinib was combined with heregulin ($P<.001$). As expected, tamoxifen had no agonist activity in MCF-7 cells; i.e., ERE-luciferase transcription was not induced by tamoxifen (relative activity = 0.18, 95% CI = 0.17 to 0.19), although the combination of heregulin and tamoxifen did increase luciferase activity by a small amount. By contrast, in the MCF-7/HER2-18 cells, tamoxifen-induced–luciferase activity was similar to that induced by estrogen (relative activity = 0.82, 95% CI = 0.63 to 1.01) and gefitinib treatment resulted in statistically significant inhibition of both estrogen and tamoxifen-induced activity (Fig. 4, A; 55%, P = .003 and 40%, P = .008 for gefitinib inhibition effect on estrogen and tamoxifen treatments, respectively). Heregulin treatment further enhanced luciferase activity in response to estrogen (by more than fourfold, relative activity = 4.37, 95% CI = 4.13 to 4.61) and tamoxifen (by more than 2.5-fold, relative activity = 2.24, 95% CI = 2.06 to 2.42), an effect that was statistically significantly inhibited by more than 50% by gefitinib ($P<.001$).

To confirm the agonist properties of tamoxifen on gene expression in a more physiologically relevant context, we examined a panel of endogenous estrogen-responsive gene products (Fig. 4, B). In MCF-7 cells, estrogen treatment resulted in variable increases in the expression of all the proteins examined. Most of these effects were partially inhibited by gefitinib, with the notable exception of the progesterone receptor (both A and B isoforms), which showed no reduction with the addition of gefitinib. As expected, tamoxifen demonstrated no agonist activity on any of these genes in MCF-7 cells. Heregulin by itself induced the expression of all of the genes, again except for the progesterone receptor A and B isoforms, and these effects were abolished by gefitinib. Whether the induction by heregulin is mediated through its activation of ER or by some other mechanism remains to be determined.

In the MCF-7/HER2-18 cells, estrogen had similar effects on the expression of endogenous estrogen-responsive genes, and gefitinib reduced these effects (Fig. 4, B), indicating a contribution from the growth factor signaling pathway, as was evident in the luciferase assays (Fig. 4, A). However, in contrast to its behavior in MCF-7 cells, tamoxifen also behaved as an estrogen agonist on all of the genes examined. This agonist activity was completely dependent on growth factor receptor activity—that is, it was abolished by gefitinib. Heregulin also had dramatic effects on several of these genes. Thus, in the setting of HER2 overexpression, tamoxifen behaves as an estrogen agonist on a variety of estrogen-dependent genes, and in distinct contrast to the agonist effects of estrogen, those of tamoxifen are com-

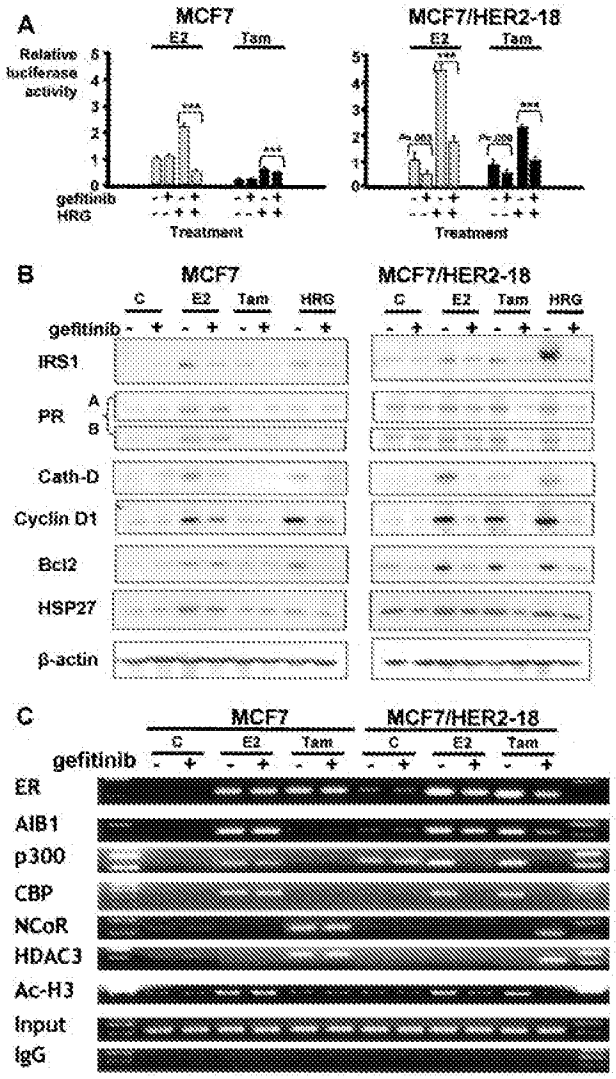


Fig. 4. Effect of HER2 overexpression and gefitinib on tamoxifen agonist activity in MCF-7 and MCF-7/HER2-18 cells. **A)** Serum-starved MCF-7 and MCF-7/HER2-18 cells were transiently transfected with a vector containing a luciferase reporter gene under the control of two estrogen response elements *(15)*. Transfected cells were replated and 12 hours later were treated for 16 hours with estrogen (E2, **gray bars**) or 4-OH tamoxifen (Tam, **solid bars**) in the absence or presence of heregulin (HRG) and/or gefitinib. Mean luciferase activity observed with E2 induction in each cell line was set to 1.0. Each column represents the mean luciferase activity relative to estrogen induction of six replicate dishes. Bars indicate 95% confidence intervals. *P* values indicate statistical significance of inhibition in the presence of gefitinib in each treatment group (two-sample *t* test); *** = $P<.001$. **B)** Cells in serum-free medium were treated for 12 hours with control vehicle (C), E2, Tam, or heregulin (HRG), in the absence or presence of gefitinib. Expression of endogenous estrogen-responsive genes was assessed in immunoblot assays of whole-cell extracts by using antibodies against the following proteins: IRS-1, insulin receptor substrate 1; PR, progesterone receptor (which recognizes the A and B isoforms); Cath-D, cathepsin D; HSP27, heat shock protein 27, cyclin D1, and Bcl2. Blots are representative of three experiments. **C)** Steroid-starved, serum-starved cells were treated with vehicle (C), E2, or Tam in the presence or absence of gefitinib for 45 minutes. Occupancy of the estrogen-responsive pS2 promoter by ERα; the coactivators AIB1, p300, and CBP; the corepressors NCoR and histone deacetylase H3 (HDAC3); and acetylated histone 3 (Ac-H3) was examined by chromatin immunoprecipitation (ChIP) assay. Relevant pS2 promoter sequences were PCR amplified from complexes immunoprecipitated with each antibody. Input lane shows DNA that was PCR amplified from extracts before immunoprecipitation. In the control immunoglobulin G (IgG), PCR was done in eluates from beads collected after preclearing of these extracts by using preimmune (normal) serum. Gels are representative of three experiments.

Downloaded from http://jnci.oxfordjournals.org/ at Eisai-Andover on July 6, 2016

pletely dependent on cross-talk with the EGFR and/or HER2 pathway.

Having shown that tamoxifen has estrogen agonist activity on estrogen target genes in MCF-7/HER2-18 cells, we next examined the assembly of ER transcription complex components on the well-characterized estrogen-responsive pS2 promoter by using ChIP assays (Fig. 4, C). We reasoned that, under conditions of enhanced EGFR and HER2 signaling and activation of ER and AIB1, tamoxifen-bound ER may recruit coactivators instead of corepressors as previously reported *(21)*. In MCF-7 cells, estrogen treatment induced occupancy of the pS2 promoter by ER and coactivator complexes, including AIB1 and the histone acetylases P300 and CBP, leading to acetylated histones. Tamoxifen, by contrast, induced occupancy by ER, the corepressor NCoR, and histone deacetylase (HDAC3). In MCF-7/HER2-18 cells, both estrogen and tamoxifen induced occupancy by ER, AIB1, P300, and CBP, resulting in the formation of acetylated histones. NCoR and HDAC3 replaced the coactivator complex when gefitinib was added to tamoxifen-treated cells to block growth factor signaling. The presence of coactivator complexes on the promoter when the receptor is bound by tamoxifen may explain its agonist properties on target gene expression in the MCF-7/HER2-18 cells.

Gefitinib Effects on Tamoxifen Stimulation of Tumor Growth

Because gefitinib blocked EGFR and HER2 cross-talk with ER, dissociated coactivator complexes from tamoxifen-bound ER on the promoters of target genes, and restored tamoxifen's antagonist effects on gene expression, we investigated its effects on tamoxifen stimulation of tumor growth. As expected, treatment of MCF-7 cells with estrogen increased anchorage-independent colony formation, and treatment with tamoxifen reduced it (Fig. 5, A). Tamoxifen's antagonist properties on colony formation were further enhanced by gefitinib, because the number of colonies grown in the presence of tamoxifen was further reduced by gefitinib by more than 40% ($P<0.001$, F test) at 1 μM and by more than 50% ($P<0.001$, F test) at 10 μM. Gefitinib only slightly reduced the effects of estrogen on colony formation, and only at the highest concentration (10 μM). Thus, even in cells with low levels of EGFR and HER2—i.e., MCF-7 cells—tamoxifen's antagonist activity can be strengthened further by inhibiting growth factor signaling with the tyrosine kinase inhibitor.

In MCF-7/HER2-18 cells, by contrast, both tamoxifen and estrogen stimulated colony formation, although colony growth even in control conditions was higher than that of MCF-7 cells (Fig. 5, A). The agonist activity of tamoxifen was entirely dependent on growth factor signaling because it was partially inhibited by even a low concentration of gefitinib (0.1 μM) and eliminated at the higher concentrations ($\geq$1μM) that restored tamoxifen's antagonist activity ($P<.001$). Estrogen-induced colony formation was also partially inhibited by gefitinib in these MCF7/HER2-18 cells (50% at 10 μM, $P<0.001$, F test). Yet, in these cells, the magnitude of the decrease in number of colonies caused by gefitinib at all concentrations was statistically significantly larger in the tamoxifen-treated group than in the estrogen-treated group ($P<.001$, F test from a linear regression model), suggesting that the tamoxifen agonist activity is more dependent on the growth factor signaling than that of estrogen.

We also examined the S-phase fraction as another way to assess cell proliferation. Both the basal S-phase fraction in

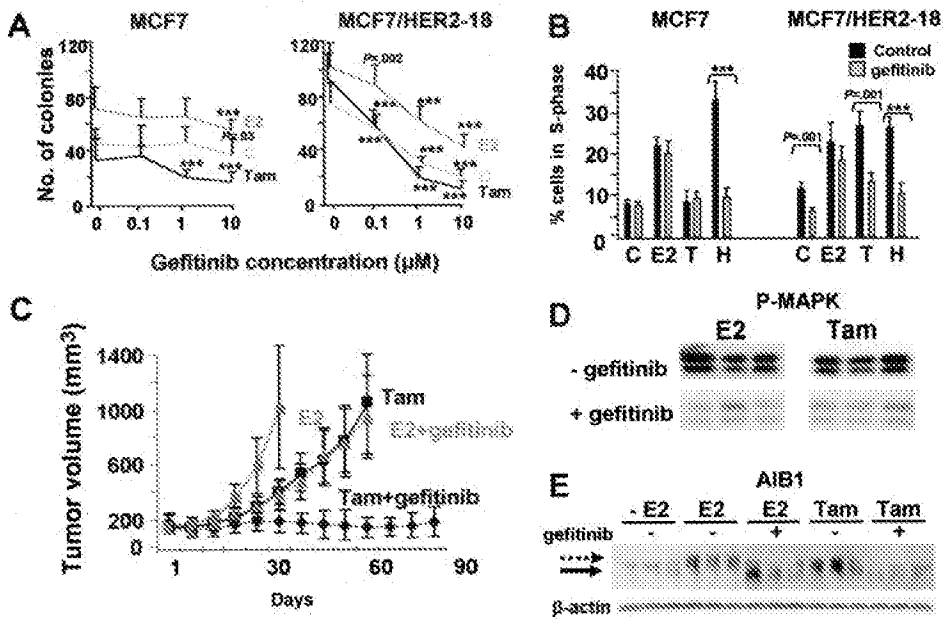


Fig. 5. Effect of gefitinib on tamoxifen antitumor activity *in vitro* and *in vivo*. **A)** Anchorage-independent growth of steroid-starved MCF-7 or MCF-7/HER2-18 cells was assessed by soft agarose colony-forming assays in the presence of vehicle (C), estrogen (E2), or 4-OH tamoxifen (Tam) in combination with gefitinib at the indicated concentrations. Graphs represent the mean colony number of six dishes. Bars indicate 95% confidence intervals (CIs). P values, based on the F test from contrasts generated in an analysis of variance model, indicate statistical significance of inhibition between control and each concentration of gefitinib within each treatment group; *** = $P<.001$. Only statistically significant P values are shown. **B)** Serum-starved MCF-7 and HER2-18 cells were treated with vehicle (C), estrogen (E2), 4-OH tamoxifen (T), or heregulin (H) for 16 hours and analyzed by DNA flow cytometry. Each column represents the mean of the percentage of cells in S phase of triplicate plates; bars indicate 95% CI; P values indicate statistical significance of the reduction in S-phase fraction in the presence of gefitinib compared with its absence in each treatment group (a two-sample t test); *** = $P<.001$. Only statistically significant P values are shown. **C)** Athymic nude mice bearing MCF-7/HER2-18 tumors were treated with estrogen (E2) or tamoxifen (Tam), either alone or in combination with gefitinib, and tumor growth was monitored. Graph shows the mean tumor volume in each group (n = 8); bars show 95% CI. **D)** Immunoblot analysis of phospho-Thr^{202}/Tyr^{204}–ERK1,2 mitogen-activated protein kinase (MAPK) (P-MAPK) in three individual tumor extracts from the different treatment groups in panel C (after 3 weeks of treatment). Total ERK 1,2 MAPK levels were unchanged (not shown). Blots were repeated three times. **E)** Immunoblot analysis of AIB1 in tumor extracts from the different tumor treatment groups (including E2 withdrawal [–E2]). More slowly migrating AIB1 bands (**dashed arrow**) represent the phosphorylated form of the protein, and the unphosphorylated form is marked by a **solid arrow.** Blots are representative of three experiments.

Downloaded from http://jnci.oxfordjournals.org/ at Eisai-Andover on July 6, 2016

untreated MCF-7/HER2-18 cells and the S-phase fraction in MCF-7/HER2-18 cells treated with tamoxifen were higher than those in MCF-7 cells (by 1.4- and 3.1-fold; $P = .005$ and $<.001$ for control untreated and tamoxifen-treated cells, respectively). However, the pronounced induction in S-phase fraction by tamoxifen compared with that of control in the MCF-7/HER2-18 cells (more than twofold) suggests that tamoxifen behaves as a strong estrogen agonist on cell proliferation in these HER2-overexpressing cells (Fig. 5, B). Heregulin also substantially increased the S-phase fraction above that of control treatment in these cells (more than twofold). Gefitinib inhibited the stimulatory effect of both tamoxifen ($P = 0.001$) and heregulin ($P<0.001$) in the MCF-7/HER2-18 cells by more than 50% but only modestly inhibited the effects of estrogen, again demonstrating the complete growth factor receptor dependence of tamoxifen's agonist activity, in contrast with that of estrogen, which is only minimally dependent on this pathway.

Similar effects of tamoxifen and gefitinib on tumor growth were observed *in vivo* (Fig. 5, C). In contrast with parental MCF-7 tumors, the estrogen-mediated growth of which was unaffected by gefitinib (data not shown), gefitinib modestly slowed estrogen-induced growth of MCF-7/HER2-18 tumors and totally blocked their tamoxifen-stimulated growth. Despite its limited effects on estrogen-induced growth of MCF-7/HER2-18 tumors, gefitinib also strikingly reduced the levels of phosphorylated ERK1,2 MAPK in tumors from mice treated with either estrogen or tamoxifen (Fig. 1, B and 5, D). These data again indicate that estrogen-induced tumor growth is only partially dependent on EGFR- and HER2-mediated activation of ERK1,2 MAPK, whereas that induced by tamoxifen is totally dependent on this pathway. Estrogen and tamoxifen treatment of mice with MCF-7/HER2-18 xenografts also led to increases in levels of both total and phosphorylated AIB1, effects that were inhibited by gefitinib, consistent with gefitinib inhibition of tamoxifen's agonist activity (Fig. 5, E).

Discussion

We have previously reported that ER-positive human breast cancers that overexpress AIB1, especially those that also overexpress HER2, are resistant to adjuvant therapy with tamoxifen *(11)*. Given the interaction between HER2 and the ER coactivator AIB1, which are often overexpressed together in ER-positive tumors, we hypothesized that the antagonist effects of tamoxifen-bound ER in such overexpressing tumors might be reduced, and the agonist properties increased, as a mechanism for tamoxifen resistance *(11)*. Here, we have demonstrated a plausible mechanism for this resistance in an experimental model system using ER-positive breast cancer cells that also overexpress both AIB1 and HER2. Although we did not address the exclusive role of coactivators and especially AIB1, the current data, together with the clinical data *(11)*, strongly suggest that both HER2 and AIB1 are needed for the resistant phenotype. The agonist activity of tamoxifen on gene expression and cell proliferation was strongly increased in MCF-7/HER2-18 cells, which express high levels of both HER2 and AIB1, resulting in tumor growth stimulation by the drug. These effects are in stark contrast to tamoxifen's antagonist effects in parental MCF-7 cells, which have high AIB1 but low HER2 expression *(17)*.

Our results provide an explanation for tamoxifen's estrogen-like activity in MCF-7/HER2-18 cells (Fig. 6). Enhanced signaling from the EGFR and HER2 tyrosine kinases activates ERK1,2 MAPK, which then phosphorylates and functionally activates both ER and AIB1, as has also been found in prior reports *(9,22–24)*. Activation of AKT by these same tyrosine kinase receptors may have a similar effect *(25)*. In addition, both estrogen and tamoxifen rapidly activate EGFR, HER2, AKT, and ERK1,2 MAPK in these cells, thereby establishing bidirectional cross-talk and a vicious cycle of cell survival and proliferative stimuli even when the ER is bound by tamoxifen. This cross-talk is less evident, and tamoxifen acts an antagonist, in cells with low growth factor receptor levels *(13,17)* or in cells with high growth factor levels in the presence of gefitinib.

In agreement with previous reports *(12)*, we found that tamoxifen, like estrogen, induces phosphorylation of the ER on Ser-118, even in the parental cells in which it behaves as an antagonist. This interesting observation indicates that Ser-118 phosphorylation of the ER alone does not increase the agonist effects of tamoxifen sufficiently to cause resistance to the drug. Our data do suggest, however, that phosphorylation of the ER coactivator AIB1 by HER2 signaling is important for the development of resistance. In the HER2-overexpressing MCF-7/HER2-18 cells, both estrogen and tamoxifen recruited ER and AIB1 coactivator complexes to the promoter of an estrogen target gene, whereas in the parental MCF-7 cells, tamoxifen-bound ER recruited corepressor complexes with NCoR and HDAC3. In MCF-7/HER2-18 cells, gefitinib restored the recruitment of corepressor complexes with tamoxifen-bound ER

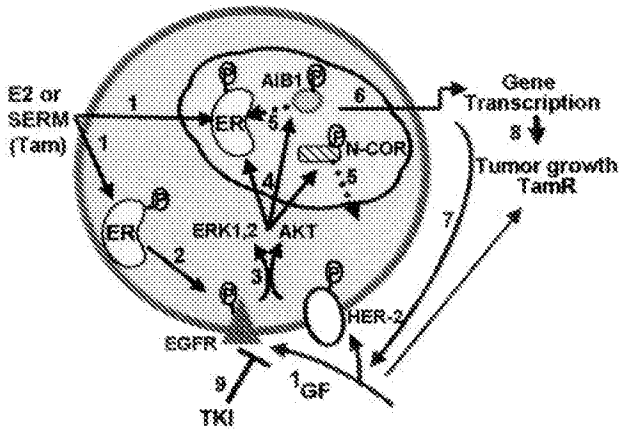


Fig. 6. Tamoxifen resistance model: Increased bidirectional ER/HER2 cross-talk converts tamoxifen into an agonist. In HER2-overexpressing tumors, peptide growth factors (1), as well as estrogen and tamoxifen via nongenomic activities (1 and 2), activate EGFR and HER2 signaling pathways (3). Activated downstream kinases, including ERK 1,2 mitogen-activated protein kinase (MAPK) and AKT, then phosphorylate both the ER and its accessory proteins (4). Corepressor complexes with NCoR are inactivated and dismissed from Tam-bound ER-promoter complexes, allowing instead the recruitment of the phosphorylated/activated coactivator complexes with AIB1 (5). This results in an increase in the agonist versus the antagonist activity of tamoxifen on gene transcription (6), which can lead to even further activation of the growth factor signaling pathways (7), thereby establishing bidirectional cross-talk and a vicious cycle of cell survival and proliferative stimulation even when ER is bound by tamoxifen. The net effect is tamoxifen resistance and tumor growth (8). This cross-talk is less evident, and tamoxifen remains an antagonist, in tumor cells with low growth factor receptor levels. In tumor cells with high levels of EGFR and/or HER2, this cross-talk can be blocked by gefitinib and presumably by other growth factor pathway inhibitors (9).

Downloaded from http://jnci.oxfordjournals.org/ at Eisai-Andover on July 6, 2016

on the promoter. Blocking ERK1,2 MAPK also blocks phosphorylation of NCoR and restores its nuclear localization *(26)*, thereby increasing its availability to bind and repress ER *(27,28)*. The presence on the promoter of coactivator complexes explains why tamoxifen behaves as an estrogen agonist on a panel of endogenous target genes and on *in vitro* and *in vivo* proliferation of MCF-7/HER2-18 cells. Thus, in these HER2-overexpressing cells, the classical action of ER on transcription is enhanced by its nongenomic effects to activate the growth factor receptor tyrosine kinases EGFR and HER2 in response to binding of estrogen or tamoxifen. The relative contribution of classical effects of ER on gene transcription versus the rapid nonclassical (nongenomic) ER activities on the growth factor receptors in the membrane to this and other forms of tamoxifen resistance requires further investigation.

It is not clear from our data how AIB1 interacts with tamoxifen-bound ER. Coactivators like AIB1 are thought to bind ER in the hydrophobic groove in its AF-2 domain *(29)*. When estrogen, but not tamoxifen, is bound to ER, helix 12 in the AF2 domain opens to allow access by coactivators to their binding site *(29)*. Whether the conformation of ER is somehow altered in the presence of growth factor signaling to allow the interaction of AIB1 with this region, or whether phosphorylated AIB1 binds there or to another site on the receptor, remains to be clarified. Coactivators can bind to other sites on the ER, including the AF-1 domain, causing enhanced transactivation arising from this domain *(27,30,31)*, and it is possible that AIB1 binds to one of these other sites in response to activation of the ER and AIB1 by growth factor signaling.

Although ligand-independent activation of the ER by ERK1,2 MAPK has been implicated as a mechanism for resistance to therapies designed to reduce endogenous estrogen levels, such as ovarian ablation or aromatase inhibitors *(32)*, we detected only very low levels of ER and no coactivator complexes on the pS2 promoter in the absence of estrogen or tamoxifen in MCF-7/HER2-18 cells. Furthermore, in MCF-7/HER2-18 tumors from mice treated by estrogen withdrawal alone, phosphorylated ERK1,2 MAPK levels fell markedly compared with those in mice treated with estrogen or tamoxifen, and we could no longer detect phosphorylated AIB1. Finally, estrogen withdrawal was a strikingly effective inhibitor of MCF-7/HER2-18 tumor growth. Together, these observations suggest that ligand-independent activation of ER in the absence of estrogen or tamoxifen may be insufficient to trigger tumor growth and, consequently, that ovariectomy in premenopausal women and aromatase inhibition in postmenopausal women may still be worthwhile endocrine therapies for women with ER-positive tumors that overexpress EGFR, HER2, and/or AIB1. A recent clinical trial reporting a high rate of regression of primary tumors overexpressing EGFR/HER2 in patients treated with an aromatase inhibitor but not with tamoxifen supports this idea *(33)*.

In summary, our data suggest that tamoxifen-stimulated growth of MCF-7/HER2-18 tumors is highly dependent on bidirectional cross-talk between ER and HER2. Treatment with the receptor tyrosine kinase inhibitor gefitinib blocked the cross-talk, prevented activation of ER and AIB1, reduced the recruitment of coactivator complexes, and enhanced recruitment of corepressor complexes to tamoxifen-bound ER on gene promoters. Tamoxifen's estrogen antagonist effects on gene expression and tumor growth were then restored. Gefitinib also blocked the rapid nongenomic effects of ER by which tamoxifen can activate EGFR and HER2. Other studies have reported that receptor-blocking antibodies and an inhibitor of ERK1,2 MAPK can also inhibit growth of HER2-overexpressing breast tumor cells when given together with tamoxifen *(14,34)*. *In vitro (35)* and *in vivo* studies of acquired tamoxifen resistance in parental MCF-7 cells also implicate enhanced EGFR and HER2 signaling cross-talk with ER as a mechanism for resistance *(36)*. Gefitinib only minimally slowed MCF-7/HER2-18 tumor growth in estrogen-treated mice but totally blocked tamoxifen-stimulated growth. This finding indicates that estrogen enhances tumor growth largely by growth factor receptor–independent mechanisms, whereas the growth-stimulatory effects of tamoxifen are totally growth factor receptor dependent. Our data imply that monotherapy with growth factor pathway inhibitors like gefitinib may have little or only modest benefits on ER-positive, HER2-overexpressing breast cancer, but the results do provide a strong rationale for combining tamoxifen with gefitinib or other EGFR/HER2 pathway inhibitors to overcome *de novo* resistance in such tumors. Clinical trials of this new strategy are under way.

References

(1) Schiff R, Saw F. The importance of the estrogen receptor in breast cancer. In Pasqualini JR, editor. Breast cancer: prognosis, treatment, and prevention. New York (NY): Marcel Dekker; 2002. p. 149–86.

(2) McKenna NJ, Lanz RB, O'Malley BW. Nuclear receptor coregulators: cellular and molecular biology. Endocr Rev 1999;20:321–44.

(3) Graham JD, Bain DL, Richer JK, Jackson TA, Tung L, Horwitz KB. Thoughts on tamoxifen resistant breast cancer. Are coregulators the answer or just a red herring? J Steroid Biochem Mol Biol 2000;74:255–9.

(4) Smith CL, Nawaz Z, O'Malley BW. Coactivator and corepressor regulation of the agonist/antagonist activity of the mixed antiestrogen, 4-hydroxytamoxifen. Mol Endocrinol 1997;11:657–66.

(5) Nicholson RI, McClelland RA, Robertson JF, Gee JM. Involvement of steroid hormone and growth factor cross-talk in endocrine response in breast cancer. Endocr Relat Cancer 1999;6:373–87.

(6) Lee AV, Cui X, Oesterreich S. Cross-talk among estrogen receptor, epidermal growth factor, and insulin-like growth factor signaling in breast cancer. Clin Cancer Res 2001;7:4429s–35s; discussion 11s–12s.

(7) Kushner PJ, Agard DA, Greene GL, Scanlan TS, Shiau AK, Uht RM, et al. Estrogen receptor pathways to AP-1. J Steroid Biochem Mol Biol 2000; 74:311–7.

(8) Razandi M, Pedram A, Park ST, Levin ER. Proximal events in signaling by plasma membrane estrogen receptors. J Biol Chem 2003;278:2701–12.

(9) Font de Mora J, Brown M. AIB1 is a conduit for kinase-mediated growth factor signaling to the estrogen receptor. Mol Cell Biol 2000;20:5041–7.

(10) Ali S, Coombes RC. Endocrine-responsive breast cancer and strategies for combating resistance. Nat Rev Cancer 2002;2:101–12.

(11) Osborne CK, Bardou V, Hopp TA, Chamness GC, Hilsenbeck SG, Fuqua SWA, et al. Role of the estrogen receptor coactivator AIB1 (SRC-3) and HER-2/neu in tamoxifen resistance in breast cancer. J Natl Cancer Inst 2003;95:353–61.

(12) Chen D, Washbrook E, Sarwar N, Bates GJ, Pace PE, Thirunuvakkarasu V, et al. Phosphorylation of human estrogen receptor alpha at serine 118 by two distinct signal transduction pathways revealed by phosphorylation-specific antisera. Oncogene 2002;21:4921–31.

(13) Benz CC, Scott GK, Sarup JC, Johnson RM, Tripathy D, Coronado E, et al. Estrogen-dependent, tamoxifen-resistant tumorigenic growth of MCF-7 cells transfected with HER2/neu. Breast Cancer Res Treat 1993;24:85–95.

(14) Kurokawa H, Lenferink AE, Simpson JF, Pisacane PI, Sliwkowski MX, Forbes JT, et al. Inhibition of HER2/neu (erbB-2) and mitogen-activated protein kinases enhances tamoxifen action against HER2-overexpressing, tamoxifen-resistant breast cancer cells. Cancer Res 2000;60:5887–94.

(15) Oesterreich S, Zhang Q, Hopp T, Fuqua SA, Michaelis M, Zhao HH, et al. Tamoxifen-bound estrogen receptor (ER) strongly interacts with the nuclear matrix protein HET/SAF-B, a novel inhibitor of ER-mediated transactivation. Mol Endocrinol 2000;14:369–81.

Downloaded from http://jnci.oxfordjournals.org/ at Eisai-Andover on July 6, 2016

(16) Shang Y, Hu X, DiRenzo J, Lazar MA, Brown M. Cofactor dynamics and sufficiency in estrogen receptor-regulated transcription. Cell 2000;103: 843–52.
(17) Osborne CK, Coronado-Heinsohn EB, Hilsenbeck SG, McCue BL, Wakeling AE, McClelland RA, et al. Comparison of the effects of a pure steroidal antiestrogen with those of tamoxifen in a model of human breast cancer. J Natl Cancer Inst 1995;87:746–50.
(18) Moasser MM, Basso A, Averbuch SD, Rosen N. The tyrosine kinase inhibitor ZD1839 ("Iressa") inhibits HER2-driven signaling and suppresses the growth of HER2-overexpressing tumor cells. Cancer Res 2001;61: 7184–8.
(19) Lin YZ, Li SW, Clinton GM. Insulin and epidermal growth factor stimulate phosphorylation of p185HER-2 in the breast carcinoma cell line, BT474. Mol Cell Endocrinol 1990;69:111–9.
(20) Anzick SL, Kononen J, Walker RL, Azorsa DO, Tanner MM, Guan XY, et al. AIB1, a steroid receptor coactivator amplified in breast and ovarian cancer. Science 1997;277:965–8.
(21) Shang Y, Brown M. Molecular determinants for the tissue specificity of SERMs. Science 2002;295:2465–8.
(22) Kato S, Endoh H, Masuhiro Y, Kitamoto T, Uchiyama S, Sasaki H, et al. Activation of the estrogen receptor through phosphorylation by mitogen-activated protein kinase. Science 1995;270:1491–4.
(23) Joel PB, Smith J, Sturgill TW, Fisher TL, Blenis J, Lannigan DA. pp90rsk1 regulates estrogen receptor-mediated transcription through phosphorylation of Ser-167. Mol Cell Biol 1998;18:1978–84.
(24) Bunone G, Briand PA, Miksicek RJ, Picard D. Activation of the unliganded estrogen receptor by EGF involves the MAP kinase pathway and direct phosphorylation. EMBO J 1996;15:2174–83.
(25) Campbell RA, Bhat-Nakshatri P, Patel NM, Constantinidou D, Ali S, Nakshatri H. Phosphatidylinositol 3-kinase/AKT-mediated activation of estrogen receptor alpha: a new model for anti-estrogen resistance. J Biol Chem 2001;276:9817–24.
(26) Hong SH, Privalsky ML. The SMRT corepressor is regulated by a MEK-1 kinase pathway: inhibition of corepressor function is associated with SMRT phosphorylation and nuclear export. Mol Cell Biol 2000; 20:6612–25.
(27) Lavinsky RM, Jepsen K, Heinzel T, Torchia J, Mullen TM, Schiff R, et al. Diverse signaling pathways modulate nuclear receptor recruitment of N-CoR and SMRT complexes. Proc Natl Acad Sci U S A 1998;95:2920–5.
(28) Baek SH, Ohgi KA, Rose DW, Koo EH, Glass CK, Rosenfeld MG. Exchange of N-CoR corepressor and Tip60 coactivator complexes links gene expression by NF-kappaB and beta-amyloid precursor protein. Cell 2002;110:55–67.
(29) Shiau AK, Barstad D, Loria PM, Cheng L, Kushner PJ, Agard DA, et al. The structural basis of estrogen receptor/coactivator recognition and the antagonism of this interaction by tamoxifen. Cell 1998;95:927–37.
(30) Webb P, Nguyen P, Shinsako J, Anderson C, Feng W, Nguyen MP, et al. Estrogen receptor activation function 1 works by binding p160 coactivator proteins. Mol Endocrinol 1998;12:1605–18.
(31) Ma H, Hong H, Huang SM, Irvine RA, Webb P, Kushner PJ, et al. Multiple signal input and output domains of the 160-kilodalton nuclear receptor coactivator proteins. Mol Cell Biol 1999;19:6164–73.
(32) Yue W, Wang JP, Conaway M, Masamura S, Li Y, Santen RJ. Activation of the MAPK pathway enhances sensitivity of MCF-7 breast cancer cells to the mitogenic effect of estradiol. Endocrinology 2002;143:3221–9.
(33) Ellis MJ, Coop A, Singh B, Mauriac L, Llombert-Cussac A, Janicke F, et al. Letrozole is more effective neoadjuvant endocrine therapy than tamoxifen for ErbB-1- and/or ErbB-2-positive, estrogen receptor-positive primary breast cancer: evidence from a phase III randomized trial. J Clin Oncol 2001;19:3808–16.
(34) Witters LM, Kumar R, Chinchilli VM, Lipton A. Enhanced anti-proliferative activity of the combination of tamoxifen plus HER-2-neu antibody. Breast Cancer Res Treat 1997;42:1–5.
(35) Nicholson RI, Hutcheson IR, Harper ME, Knowlden JM, Barrow D, McClelland RA, et al. Modulation of epidermal growth factor receptor in endocrine-resistant, oestrogen receptor-positive breast cancer. Endocr Relat Cancer 2001;8:175–82.
(36) Massarweh S, Shou J, DiPietro M, Mohsin SK, Hilsenbeck SG, Wakeling AE, et al. Targeting the epidermal growth factor receptor pathway improves the anti-tumor effect of tamoxifen and delays acquired resistance in a xenograft model of breast cancer. San Antonio Breast Cancer Symposium. Breast Cancer Res Treat 2002;76:S33.

NOTES

J. Shou and S. Massarweh contributed equally to this work.

Supported by NCI grant P50 CA058183 (Breast Cancer SPORE Grant) and in part by a grant from AstraZeneca.

C. Kent Osborne conducts research with grants from AstraZeneca (manufacturer of gefitinib). A. Wakeling is a full-time employee of AstraZeneca. R. Schiff has a research grant from AstraZeneca. AstraZeneca supplied the gefitinib used in this study.

Manuscript received August 11, 2003; revised April 19, 2004; accepted April 27, 2004.

Downloaded from http://jnci.oxfordjournals.org/ at Eisai-Andover on July 6, 2016

nature genetics

ESR1 ligand-binding domain mutations in hormone-resistant breast cancer

Weiyi Toy[1], Yang Shen[2], Helen Won[1], Bradley Green[3], Rita A Sakr[4], Marie Will[5], Zhiqiang Li[1], Kinisha Gala[1], Sean Fanning[3], Tari A King[4], Clifford Hudis[5,6], David Chen[7], Tetiana Taran[7], Gabriel Hortobagyi[8], Geoffrey Greene[3], Michael Berger[1,9], José Baselga[1,5] & Sarat Chandarlapaty[1,5,6]

© 2013 Nature America, Inc. All rights reserved.

Seventy percent of breast cancers express estrogen receptor (ER), and most of these are sensitive to ER inhibition. However, many such tumors for unknown reasons become refractory to inhibition of estrogen action in the metastatic setting. We conducted a comprehensive genetic analysis of two independent cohorts of metastatic ER-positive breast tumors and identified mutations in *ESR1* affecting the ligand-binding domain (LBD) in 14 of 80 cases. These included highly recurrent mutations encoding p.Tyr537Ser, p.Tyr537Asn and p.Asp538Gly alterations. Molecular dynamics simulations suggest that the structures of the Tyr537Ser and Asp538Gly mutants involve hydrogen bonding of the mutant amino acids with Asp351, thus favoring the agonist conformation of the receptor. Consistent with this model, mutant receptors drive ER-dependent transcription and proliferation in the absence of hormone and reduce the efficacy of ER antagonists. These data implicate LBD-mutant forms of ER in mediating clinical resistance to hormonal therapy and suggest that more potent ER antagonists may be of substantial therapeutic benefit.

ER is a member of the nuclear receptor family and regulates the transformed phenotype of the majority of breast cancers. Pharmacological inhibitors of estrogen-driven signaling are effective in many of these cases[1]. Therapeutics in this class include drugs that suppress estrogen production (aromatase inhibitors and gonadotropin-releasing hormone agonists) and direct inhibitors of ER (selective ER modulators (SERMs) or selective ER degraders (SERDs))[2]. Although most patients with ER-positive breast cancer derive a benefit from these drugs, resistance often emerges after prolonged exposure[1,3–5]. The mechanisms underlying this phenomenon are unclear, and a better understanding of acquired resistance to hormone antagonists is essential for the development of more durable and effective therapeutics.

RESULTS

ESR1 mutations in metastatic breast cancer

To identify possible genetic mechanisms underlying acquired resistance to hormonal therapy, we sought to characterize tumors from individuals with metastatic ER-positive breast cancer treated for at least 3 months with hormonal therapy and whose tumors had grown or spread to new sites while on therapy. As part of a metastatic breast tumor procurement protocol (National Clinical Trials Registry 00897702), we identified 38 of 71 samples that met these criteria and had sufficient tumor DNA for analysis. We used a targeted approach to genomic characterization, surveying for mutations and copy number alterations in 230 genes commonly mutated in cancer through massively parallel sequencing (MSKCC sequencing panel)[6]. Two cases were excluded from the analysis because they did not pass quality control testing for being from a single source. In the MSKCC cohort, we had normal DNA from white blood cells for comparison in 22 cases. Analysis of these 22 matched samples identified an average of 4.3 mutations per tumor with a mean coverage depth of ~500× (normal sample, 441×; metastatic sample, 696×) (**Supplementary Table 1**). Six genes were mutated in more than 10% of the matched cases. We compared the prevalence of mutations in these genes in our set of relapsed tumors with their prevalence in The Cancer Genome Atlas (TCGA) invasive primary (untreated) breast cancer and luminal A and luminal B primary breast cancer cases and found that the prevalence of mutations in *TP53*, *PIK3CA* and *GATA3* was comparable in all sets (**Fig. 1a**)[7]. By contrast, *ESR1*, *RPTOR* and *ERBB3* mutations were detected at much higher rates in our samples than in those reported by TGCA. The fact that these mutations are enriched among tumors from patients who had relapsed while on hormonal therapy suggests that they may have a role in the development of acquired resistance. Gene copy number was also analyzed in these samples, and the genes that were frequently amplified are shown in **Figure 1b**. Amplification of *ERBB2* (refs. 8–10), *CCND1* (ref. 11) or *FGFR1* (ref. 12) was common and has previously been associated with hormone resistance, but these amplifications were not commonly observed to be acquired in those cases where we had information on the primary tumor.

[1]Human Oncology and Pathogenesis Program, Memorial Sloan-Kettering Cancer Center (MSKCC), New York, New York, USA. [2]Toyota Technological Institute at Chicago, Chicago, Illinois, USA. [3]Ben May Department of Cancer Research, University of Chicago, Chicago, Illinois, USA. [4]Breast Service, Department of Surgery, MSKCC, New York, New York, USA. [5]Weill Cornell Medical College, New York, New York, USA. [6]Breast Cancer Medicine Service, Solid Tumor Division, Department of Medicine, MSKCC, New York, New York, USA. [7]Novartis Pharmaceuticals Corporation, East Hanover, New Jersey, USA. [8]Department of Breast Medical Oncology, MD Anderson Cancer Center, Houston, Texas, USA. [9]Department of Pathology, MSKCC, New York, New York, USA. Correspondence should be addressed to S.C. (chandars@mskcc.org).

Received 28 June; accepted 10 October; published online 3 November 2013; doi:10.1038/ng.2822

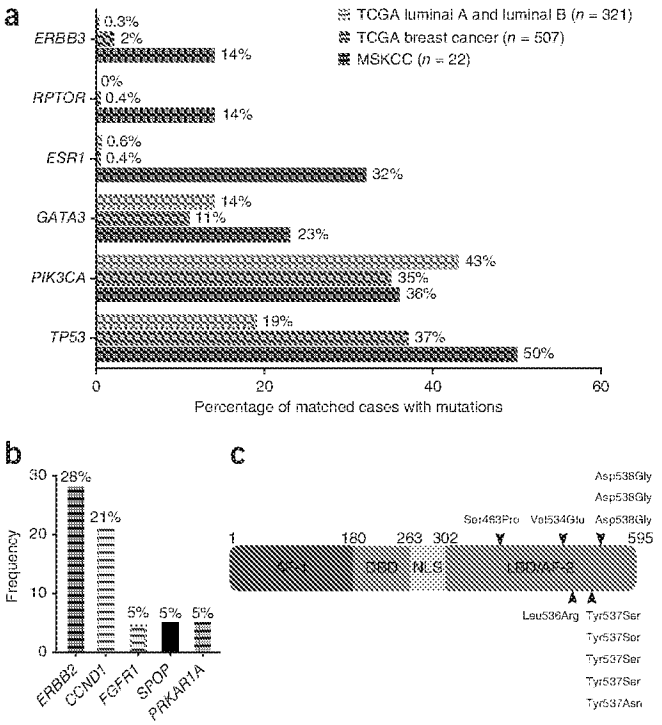


Figure 1 *ESR1* mutations in ER-positive metastatic breast cancers. (**a**) Percentage of matched cases with gene mutations detected in our patient samples (MSKCC) were compared to those of TCGA invasive breast cancer and luminal A and luminal B cases. Only genes found to be mutated in three or more cases are shown. (**b**) Top amplified genes detected in patient samples. Genes were considered amplified when the ratio of their copy number in tumor and normal samples was greater than two. (**c**) Diagram of ERα domains with the locations of the identified alterations indicated. AF-1, activation function-1; DBD, DNA-binding domain; NLS, nuclear localization signal; LBD, ligand-binding domain; AF-2, activation function-2.

The mutations in *ESR1* clustered in a small region that encodes its LBD and were obvious candidates for mediating hormone resistance. In addition to the 7 tumors with these mutations out of the 22 that had matched normal DNA, 2 more tumors with mutations affecting the LBD were detected in the 14 samples without matched normal DNA (in a total of 9/36 cases). The clinical histories of these patients showed that they were treated with multiple lines of hormonal therapy for an average of 4.9 years (range of 1–10 years) (**Table 1**). Of note, all nine patients with *ESR1* mutations were treated at some point with aromatase inhibitors, drugs that reduce the levels of circulating estrogens. We were able to obtain pretreatment, primary tumor samples from two of the nine patients with *ESR1* mutations, and the mutation was not present in these samples in either case, although these primary tumors did harbor several other alterations that were identified in the paired metastatic sample. Of all the cases with *ESR1* mutation, two cases harbored concurrent *PIK3CA* mutations, two cases had concurrent *GATA3* mutations, and one case had both concurrent *PIK3CA* and *GATA3* mutations. No other mutations were concurrent with *ESR1* mutation. In a separate analysis of 26 ER-negative tumors, no *ESR1* LBD mutation was detected (S.C., unpublished data). All *ESR1* mutations affected the LBD of the receptor, and the majority specifically altered amino acid 537 or 538 in helix 12 (H12; **Fig. 1c**).

The finding of LBD alterations in our small cohort of metastatic samples but not in several large whole-genome analyses of untreated, primary tumors was notable, and we sought to validate this observation in another cohort of tumors. We analyzed tumors collected from patients who enrolled in the BOLERO-2 clinical trial (NCT00863655), which studied patients with ER-positive metastatic breast cancer whose tumors had progressed during treatment with an aromatase inhibitor[13]. Most of these tumors were collected before any exposure to hormonal therapy (primary tumors); however, a subset was collected after some exposure to hormonal therapy (metastatic tumors). Among the metastatic tumors analyzed (Foundation Medicine sequencing panel; >600× average coverage), *ESR1* mutations were observed in 11% of the cases (5/44), with only 3% (6/183) of the primary tumors mutated in this gene (**Supplementary Fig. 1**). Once again, mutation affecting Tyr537 or Asp538 of the LBD was frequently observed and occurred in patients with prolonged hormonal treatment (average of 4 years) (**Table 2** and **Supplementary Table 2**). Although there were not sufficient mutant tumors to formally analyze the usefulness of these mutations in predicting response to therapy in the BOLERO-2 clinical trial, there did not seem to be obvious differences in how patients with mutant and wild-type *ESR1* fared on the aromatase inhibitor plus placebo arm of the study. This result is not surprising, as all patients had already had tumor progression during treatment with an aromatase inhibitor. Given the strong correlation of LBD alterations in these two tumor sets with hormone-resistant disease, we set out to characterize the functional consequences of the more frequent mutations (encoding p.Asp538Gly, p.Tyr537Ser and p.Ser463Pro alterations) for ER activity and sensitivity to hormonal therapy.

ERα LBD alterations promote receptor activation

Alteration of Tyr537 to serine was previously demonstrated to promote the ERα agonist conformation and activation of its transcriptional functions[14,15]. To determine the activity of the newly identified mutants, we used site-directed mutagenesis to introduce specific mutations into *ESR1* constructs encoding HA-tagged protein. Constructs were cotransfected into breast cancer cells along with reporter plasmids carrying estrogen-responsive element (ERE)-luciferase and *Renilla* luciferase (pRL-TK). In ER-negative SK-BR-3 cells, the levels of luciferase activity in the absence of 17β-estradiol (E2) were highest in cells expressing the Tyr537Ser mutant (60 times wild-type levels), followed by cells expressing the Ser463Pro/Asp538Gly double mutant (30 times wild-type levels) and cells expressing the Asp538Gly mutant (15 times wild-type levels) (**Fig. 2a**). The addition

Table 1 Relationship of *ESR1* mutations to previous hormonal therapy

Case	*ESR1*-encoded alteration	Primary tumor	Mutation frequency	Duration of hormonal therapies (years)	Types of hormonal therapies given
1	p.Tyr537Ser	WT	0.528	2.5	AI, SERM
2	p.Asp538Gly	WT	0.285	6.5	AI, SERM
3	p.Ser463Pro/p.Asp538Gly	N/A	0.122/0.280	7.5	AI, SERM
4	p.Tyr537Ser/p.Asp538Gly	N/A	0.082/0.103	3.3	AI, SERD, SERM
5	p.Leu536Arg	N/A	0.114	10.0	AI, SERM
6	p.Val534Glu	N/A	0.056	5.5	AI, SERD
7	p.Tyr537Asn	N/A	0.839	5.5	AI, SERM
8	p.Tyr537Ser	N/A	0.253	1.5	AI, SERD
9	p.Tyr537Ser	N/A	0.265	2.0	AI, SERM, SERD

WT, wild type; N/A, not available; AI, aromatase inhibitor; SERM, selective ER modulator; SERD, selective ER degrader.

© 2013 Nature America, Inc. All rights reserved.

Table 2 ***ESR1*** **mutations in metastatic samples from the BOLERO-2 clinical trial**

Case	*ESR1*-encoded alteration	Mutation frequency	Duration of aromatase inhibitor therapy (years)	Affected ER domain
1	p.Ser463Pro/p.Tyr537Asn	0.18/0.10	2.0	LBD/AF-2
2	p.Pro535His	0.22	5.0	LBD/AF-2
3	p.Tyr537Cys	0.75	3.0	LBD/AF-2
4	p.Tyr537Ser	0.09	5.0	LBD/AF-2
5	p.Asp538Gly	0.13	6.0	LBD/AF-2

of 10 nM E2 potently induced the activities of the wild-type receptor (5 times basal wild-type levels) and the Ser463Pro mutant (3 times basal Ser463Pro levels), whereas it only weakly increased the already high levels driven by the Tyr537Ser (1.4 times basal Tyr537Ser levels), Asp538Gly (1.5 times basal Asp538Gly levels) and Ser463Pro/Asp538Gly (1.6 times basal Ser463Pro/Asp538Gly levels) mutants. In ER-driven MCF7 cells, these assays again showed that the mutants with alterations at residues 537 and 538 had very high basal activity with modest further induction by E2 (**Fig. 2a**). Expression of the Ser463Pro mutant induced modest activity in the absence of hormone and required E2 addition to achieve activity levels near those seen with alterations at residue 537 or 538 without hormone. We examined the activity of the mutants in four other cell lines (consisting of models of breast and endometrial cancer) and found in all cases that the Tyr537Ser and Asp538Gly mutants potently induced activity in the absence of hormone to near or above the levels achieved by E2 activation of wild-type receptor, whereas the Ser463Pro mutant was weakly activating (**Supplementary Fig. 2a–f**). These results suggest that the alterations at residues 537 and 538 can effectively promote ER transactivation function in the absence of hormone, although mutants still bind and are responsive to ER agonists.

Given the elevated activity of the mutants on an ERE reporter, we next asked whether they could activate known ER-dependent transcripts. HA-ERα constructs were transfected into MCF7 cells in hormone-depleted medium, and mRNA levels of ER target genes (*GREB1*, *MYC*, *PGR*, *TFF1*, *XBP1* and *CTSD*) were measured. To control for potential differences in expression of the ERα constructs, mRNA levels of ER target genes were normalized to total *ESR1* mRNA levels (similar data were obtained when normalized to *ACTB*; **Supplementary Fig. 3**). Compared to cells expressing wild-type ERα, cells expressing the Tyr537Ser, Ser463Pro;Asp538Gly and Asp538Gly mutants had significantly higher levels of *GREB1*, *MYC*, *PGR* and *TFF1* mRNA (**Fig. 2b**). To further assess whether the mutants promote transcriptional function in the absence of hormone, we performed gene expression analysis of MCF7 cells transfected with the various ERα mutant constructs in hormone-depleted medium. In comparison to wild-type ERα, the mutants differentially regulated a total of 203 genes, of which 92 were shared among the mutants. Hierarchical clustering of these genes showed that the Tyr537Ser, Asp538Gly and Ser463Pro/Asp538Gly mutants grouped together and induced a shared gene expression pattern distinct from that of the wild-type protein (**Fig. 2c**). This finding is in agreement with the quantitative PCR and ERE-luciferase results, and these data, taken together, demonstrate that, in the absence of E2, the Tyr537Ser and Asp538Gly mutants activate ER transcriptional function much more potently than wild-type ERα.

Ser118 is one of the major phosphorylation sites of ERα (ref. 16). Phosphorylation of Ser118, located within the AF-1 domain, has been shown to modulate the ligand-independent activity of ER[17]. All mutants displayed elevated levels of Ser118 phosphorylation compared to wild-type ERα, with the Tyr537Ser and Ser463Pro/Asp538Gly mutants showing the highest levels (**Fig. 2d**). The degree to which the mutant receptors were phosphorylated corresponded with the degree to which they activated expression of luciferase in the reporter assays and induction of ER target gene expression, further suggesting that the mutants possess greater estrogen-independent activity.

Coregulators recruited by ER can either promote (coactivators) or suppress (corepressors) the transcription of ER target genes. The binding of these coregulators specifies the response of target genes to a particular receptor-ligand complex. Among these coregulators, AIB1 has a critical role as a coactivator in ER target gene expression[18,19]. We sought to determine the effect of LBD alterations on the interaction of ER and AIB1 by coimmunoprecipitation. In comparison to wild-type ERα, the Asp538Gly mutant coimmunoprecipitated a substantially greater amount of AIB1 (**Fig. 2e**). These data further suggest that the Asp538Gly mutant promotes ER function through a direct effects on ER conformation.

In the absence of ligand, ER associates with the heat shock protein 90 (HSP90) complex, which promotes its conformational stability[20]. As the ERα mutants are able to promote transcription in an estrogen-independent manner, we speculated that they might be less dependent on chaperone function for their stability. To test this hypothesis, we transfected MCF7 cells with constructs encoding HA-tagged wild-type or mutant ERα and treated cells with an ATP competitive inhibitor of HSP90, SNX2112 (ref. 21), for 3 h. We assessed ERα protein levels by immunoblotting. The level of both the Tyr537Ser and Asp538Gly mutants were unaffected by HSP90 inhibition, whereas the levels of wild-type protein substantially decreased in a dose-dependent fashion (**Fig. 2f**). In further support of our hypothesis, SNX2112 treatment in hormone-deprived medium resulted in more rapid and profound depletion of wild-type than mutant ERα (**Supplementary Fig. 4**). These data further suggest that there are differences in the conformations and activities of wild-type and mutant ERα receptors.

The higher activities of the Tyr537Ser and Asp538Gly mutant receptors suggested that they might promote hormone-independent tumor cell growth. To test this idea, we generated stable MCF7 cell lines in which expression of HA-tagged wild-type ERα and Tyr537Ser and Asp538Gly mutants was under the control of the tetracycline promoter (**Supplementary Fig. 5**). These MCF7 sublines were used to establish tumors in nude mice in the presence of E2 pellets that were surgically implanted in mice 3 d before injection with cells. Pellets were removed when the tumors reached a size of ~250 mm^3 to mimic estrogen deprivation therapy. To induce the expression of the HA-tagged wild-type ERα and mutant proteins in tumor cells, mice received water containing 0.2 or 0.5 mg/ml doxycycline and 1% sucrose 1 week after the removal of the E2 pellets. The growth rates of all tumors were significantly reduced during the week when estrogen and doxycycline were absent (**Fig. 2g**), indicating that the tumors are dependent on ER signaling. However, inducing expression of the Tyr537Ser or Asp538Gly mutant dramatically increased tumor growth (**Fig. 2g**). These data further confirm the sufficiency of the Tyr537Ser and Asp538Gly mutants in facilitating hormone-independent ER function.

Residual activity of ERα mutants after drug inhibition

Mutations affecting residues 537 and 538 appeared to strongly promote various ER activities in the absence of ligand. One of the primary modes of treatment of ER-positive breast cancer is estrogen deprivation. Our data suggest that Asp538Gly and Tyr537Ser mutant forms of ERα can adopt an agonist confirmation irrespective of

© 2013 Nature America, Inc. All rights reserved.

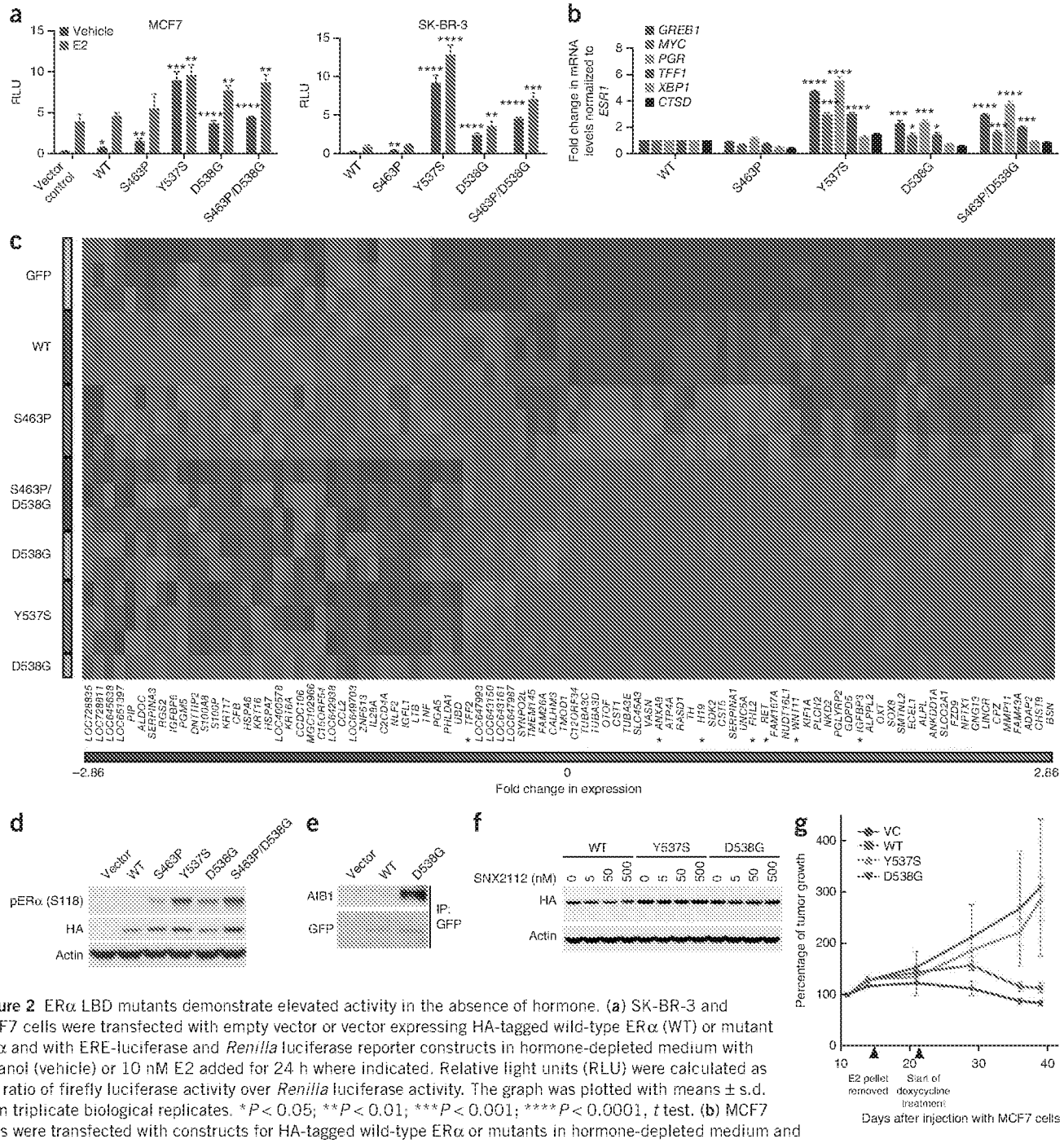


Figure 2 ERα LBD mutants demonstrate elevated activity in the absence of hormone. (**a**) SK-BR-3 and MCF7 cells were transfected with empty vector or vector expressing HA-tagged wild-type ERα (WT) or mutant ERα and with ERE-luciferase and *Renilla* luciferase reporter constructs in hormone-depleted medium with ethanol (vehicle) or 10 nM E2 added for 24 h where indicated. Relative light units (RLU) were calculated as the ratio of firefly luciferase activity over *Renilla* luciferase activity. The graph was plotted with means ± s.d. from triplicate biological replicates. $^{*}P < 0.05$; $^{**}P < 0.01$; $^{***}P < 0.001$; $^{****}P < 0.0001$, *t* test. (**b**) MCF7 cells were transfected with constructs for HA-tagged wild-type ERα or mutants in hormone-depleted medium and collected 48 h after transfection. ERα target gene mRNA levels were measured by quantitative RT-PCR using gene-specific primers. Bars represent the means ± s.d. from triplicate technical replicates normalized to *ESR1* expression. $^{*}P < 0.05$; $^{***}P < 0.001$; $^{****}P < 0.0001$, *t* test. Data shown are representative of two biological replicates. (**c**) Gene expression microarray analysis was performed using RNA derived from MCF7 cells transfected with empty vector or with vector expressing GFP fused to wild-type ERα or mutants in hormone-depleted medium for 48 h. A total of 92 genes were commonly up- or downregulated by the ERα mutants, and these genes were hierarchically clustered to generate a heat map. Selected genes previously well established as estrogen-responsive genes are marked with asterisks. (**d**) Lysates of MCF7 cells transfected with empty vector or with vector expressing HA-tagged wild-type ERα or mutants in hormone-depleted medium for 48 h were immunoblotted with antibodies to phosphorylated Ser118 of ERα (pERα), HA and actin. The immunoblots shown are representative of experiments repeated at least three times. (**e**) Lysates generated from MCF7 cells transfected with empty vector or with vector expressing GFP fused with wild-type ERα or the Asp538Gly mutant were immunoprecipitated with GFP-Trap beads (IP) and immunoblotted with antibodies to AIB1 and GFP. The immunoblots shown are representative of experiments repeated three times. (**f**) MCF7 cells transfected with vector expressing HA-tagged wild-type ERα or mutants were treated with SNX2112 at various doses for 3 h before collection. Lysates were then immunoblotted with antibodies to HA and actin. The immunoblots shown are representative of experiments repeated three times. (**g**) Mice bearing tumors derived from MCF7 cells with inducible vector control (VC) or vector encoding HA-tagged wild-type ERα or the Tyr537Ser or Asp538Gly mutants had their E2 pellets removed when the tumors reached an approximate volume of 250 mm^3 and received water containing 0.2 or 0.5 mg/ml doxycycline 1 week later for the induction of wild-type and mutant ERα expression. Results are presented as percentage tumor growth by normalizing to the first mean tumor volume measured for each group ± s.e.m. ($n = 10$ mice/group).

© 2013 Nature America, Inc. All rights reserved.

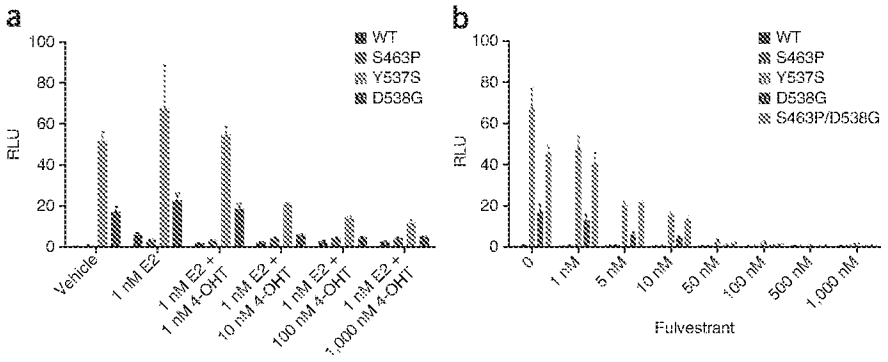


Figure 3 ER antagonists partially inhibit mutant ERα transcriptional activity. SK-BR-3 cells were transfected with vectors expressing HA-tagged wild-type or mutant ERα and with ERE-luciferase and *Renilla* luciferase reporter constructs in hormone-depleted medium. (**a**,**b**) Cells were then treated with either ethanol (vehicle) or 1 nM E2 alone or in combination with 4-OHT (**a**) or fulvestrant (**b**) at the indicated doses for 24 h before measurement of luciferase activity. Relative light units (RLU) were calculated as the ratio of firefly luciferase activity over *Renilla* luciferase activity. The graph was plotted with the means ± s.d. from triplicate biological replicates. $^{*}P < 0.05$; $^{**}P < 0.01$; $^{***}P < 0.001$; $^{****}P < 0.0001$.

hormone availability. However, drugs directly targeting ER, such as tamoxifen or fulvestrant, might still be effective against the mutant forms of ERα. To test whether LBD mutants resist ER-targeted therapies, we examined the effect of 4-hydroxytamoxifen (4-OHT) or fulvestrant over a range of doses in transfected SK-BR-3 cells. Given the mixed agonist/antagonist effects of 4-OHT, a low dose of E2 (1 nM) was used to focus on the antagonist property in these experiments[22]. Consistent with previous reports, 4-OHT potently inhibited the transcriptional activity of the Tyr537Ser mutant in ERE-driven luciferase expression[23]. The drug also potently antagonized the Asp538Gly mutant, with ~70% inhibition of the activities of the Asp538Gly and Tyr537Ser mutants using 10 nM 4-OHT (**Fig. 3a**). However, the amount of residual activity in these cells is also notable. To reduce ER activity to levels close to those observed with the vector-transfected cells, substantially higher doses of drug were required. We examined this phenomenon across a panel of cell lines and found similar results: 4-OHT potently antagonized the Tyr537Ser and Asp538Gly mutants, but, at lower doses (for example, 1–10 nM), there was higher residual activity than with wild-type ERα or empty vector (**Supplementary Figs. 2** and **6**). Bazedoxifene, which is a third-generation SERM, exhibited similar effects as 4-OHT (data not shown). The pure anti-estrogen fulvestrant also resulted in a similar phenomenon as 4-OHT (**Fig. 3b**), with low doses (1–5 nM) decreasing the activity of mutants with alteration at residue 537 or 538, whereas substantially higher doses (50–100 nM) were needed to bring activity levels closer to those of wild-type ERα. As the doses at which potent ER inhibition is achieved in the mutant-expressing models may exceed the steady-state, intratumoral levels achieved in patients, these data raise the possibility that more potent or selective ER antagonists will be required to effectively inhibit ERα mutants with alteration at residue 537 or 538.

Molecular dynamics simulation of Asp538Gly

The crystal structures of agonist-bound wild-type ERα and Tyr537Ser mutant ERα were previously determined[14,24]. To directly examine the possible effects of the p.Asp538Gly alteration on ERα conformation, we performed molecular dynamics simulations on structures for wild-type ERα and the Tyr537Ser and Asp538Gly mutants, each in the absence of ligand and with a coactivator (TIF2) bound. The stability of each ERα variant in an agonist conformation was then assessed by the root-mean-square deviation (r.m.s.d.) between the starting agonist conformation and the final conformation after 10-ns molecular dynamics simulations.

Of the three coactivator-bound ERα variants, wild-type ERα showed the largest difference from the starting agonist conformation (**Fig. 4a**), with the cofactor-recruiting H12 helix (starting at residue 538) drifting away from the rest of the ERα structure (including helix 3, H3) by 2.1 Å in r.m.s.d. The Tyr537Ser mutant clearly contrasted with wild-type ERα, as its H12 helix stayed close to the starting agonist conformation (**Fig. 4b**),

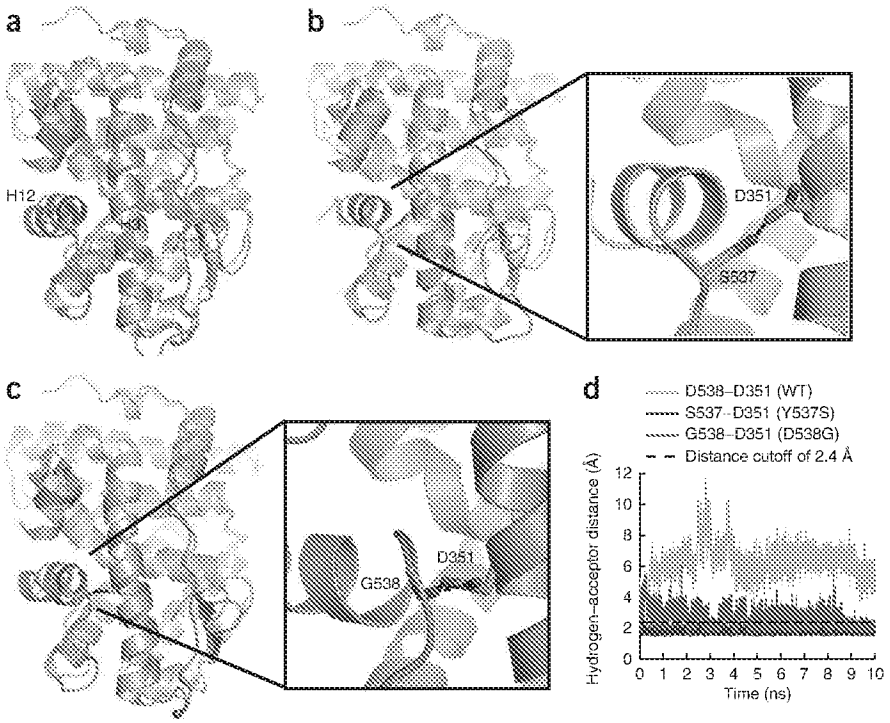


Figure 4 Molecular dynamics–modeled structures of wild-type and mutant forms of ERα. (**a**–**c**) Wild-type (cyan) (**a**), Tyr537Ser (green) (**b**) and Asp538Gly (red) (**c**) at 10 ns, overlaid with a co-crystallized structure (Protein Data Bank (PDB) accession 1GWQ) of wild-type ERα in an agonist conformation (gray) bound to TIF2 (wheat). (**d**) Hydrogen-to-acceptor distances between Asp538, Ser537 or Gly538 and Asp351 in wild-type, Tyr537Ser and Asp538Gly ERα, respectively, over the course of 10-ns molecular dynamics simulations.

© 2013 Nature America, Inc. All rights reserved.

with an H12 r.m.s.d. value of 1.2 Å. A hydrogen bond between the side chains of Ser537 and Asp351 was observed in the 10-ns molecular dynamics structure of the Tyr537Ser mutant (**Fig. 4b**, inset). This hydrogen bond was found to be stable throughout the molecular dynamics simulation and existed for 99.8% of the last 1 ns (**Fig. 4d**). In other studies, the p.Tyr537Ser alteration was introduced to facilitate structural determination of ER-agonist complexes, and the hydrogen bond with Asp351 was observed in corresponding X-ray crystal structures[14].

In the case of the Asp538Gly mutant, the starting residue 538 of the H12 helix shifted toward the H3 helix by 3.5 Å (**Fig. 4c**). Remarkably, hydrogen bonds were formed between the backbone of Gly538 (with a nitrogen atom acting as a donor) and the side chain of Asp351 (with two oxygen atoms acting as acceptors). For simplicity, a single distance between the hydrogen and its closer acceptor at Asp351 was measured for each snapshot of the simulations. Judging by a standard 2.4-Å cutoff in hydrogen-to-acceptor distance, Gly538–Asp351 hydrogen bond(s) were stable during the simulation and existed for 94.3% of the last 1 ns (**Fig. 4d**). In contrast, no hydrogen bond was found between Gly538 and Asp351 in wild-type ERα, either in the crystal structure or during the simulation. Even though the rest of the H12 helix drifted away from the H3 helix by 2.8 Å, we speculate that the hydrogen bonds can keep H12 from moving substantially further away from its agonist conformation. Judging from the slightly longer hydrogen-to-acceptor distances and lower existence percentage in the last 1 ns of simulations, the Gly538–Asp351 hydrogen bond(s) in the Asp538Gly mutant appeared weaker than those between Tyr537Ser and Asp351. The Gly538–Asp351 hydrogen bond(s) were very likely enabled by the substituent glycine, which is the smallest and most flexible of all natural amino acids and can adopt backbone conformations inaccessible to other amino acids. Indeed, this hypothesis was supported by the unique ϕ angle (the dihedral around an N–C_α bond) at residue 538 modeled for the Asp538Gly mutant (~125° compared to around ~49° for wild-type ERα and the Tyr537Ser mutant; crystallized or simulated by molecular dynamics). This hypothesis was further supported by a functional experiment in which mutating residue 538 to an alanine (uncharged and small like glycine) had no effect on ER transactivation function (**Supplementary Fig. 7**).

Taken together, the conformational choices of wild-type ERα and the Tyr537Ser and Asp538Gly mutants correlated with their basal activity levels and provide a mechanistic explanation for the newly discovered activating alteration p.Asp538Gly.

DISCUSSION

In this report, we identify for the first time, to our knowledge, recurrent mutations of *ESR1* affecting its LBD in approximately 20% of metastatic ER-positive breast cancers. The mutations occur in a population of patients with hormone-refractory disease. Our biochemical and structural data demonstrate that these mutations promote the agonist conformation of ERα in the absence of ligand and likely represent one of the major causes of acquired resistance to estrogen depletion therapies such as aromatase inhibitors. The mutants appear to retain some sensitivity to drugs directly targeting the receptor, suggesting potential pharmacological strategies for patients with these mutant receptors.

A natural LBD mutation of *ESR1* was first described in a patient with metastatic breast cancer in 1997 (ref. 15). Subsequent studies interrogating the exomes and genomes of primary breast cancers have failed to identify similar lesions, causing many to question whether the initial finding was merely an outlier[7]. In our study of metastatic breast cancer samples, we identified 9 of 36 tumors with mutations affecting the LBD of ERα. Independently, analysis of ER-positive metastatic breast cancers from the BOLERO-2 trial also identified 5 of 44 patients with *ESR1* mutations affecting its LBD. In many regards, these two studies were highly comparable, with alterations in the same amino acids, lack of alterations in other domains of the protein and mutations found in patients with prolonged exposure to hormonal therapy. There are two obvious differences between these two metastatic tumor cohorts and the primary tumors in which few or no *ESR1* mutations were found. First, analyzing metastatic tumors rather than primary tumors enforced a selection bias for more aggressive and lethal tumors. Second, in our population, patients with *ESR1* mutations were exposed to an average of 5 years of hormonal therapy. Our selection of this population was imposed to facilitate understanding of a specific and understudied clinical entity, patients with acquired resistance to hormonal therapy.

In our analysis of frequently mutated oncogenes and tumor suppressors, *ESR1* mutations stood out as a common and plausible event that could contribute to resistance. We found that the mutations affecting both Tyr537 and Asp538 strongly promoted ER signaling in the absence of ligand. This effect was observed biochemically as increased phosphorylation of Ser118, increased association with AIB1 and diminished sensitivity to HSP90 inhibitors. Functionally, the mutations promoted the expression of classical ER target genes *in vitro* in the absence of hormone. Moreover, expression of the Tyr537Ser or Asp538Gly mutant was sufficient to render a hormone-sensitive tumor model, MCF-7 cells, resistant to estrogen deprivation *in vivo*. Interestingly, the Ser463Pro mutant was also observed in three patients and in all cases co-occurred with alteration at Tyr537 or Asp538. Expression of the Ser463Pro mutant was associated with a rather modest induction in ER activity in the absence of hormone, as evaluated by ER target gene expression, with expression not increased to levels close to those seen with the Tyr537Ser or Asp538Gly mutant. Expression of this mutant together with Asp538Gly did induce activity above the levels seen with Asp538Gly alone. Given the location of this residue near the dimerization interface of ERα, it will be of interest to study whether the mutation alters ER dimer formation and what complementary roles it might have with the Tyr537Ser and Asp538Gly mutants in mediating hormone resistance.

Computer modeling of the structural effects of the p.Tyr537Ser and p.Asp538Gly alterations helped to decipher the molecular mechanisms responsible for the hormone-independent activities of the mutants. Molecular dynamics stimulations of the Tyr537Ser and Asp538Gly mutants bound to TIF2 (a coactivator) showed that both mutants favor formation of the agonist conformation of ERα (**Fig. 4**). Provocatively, hydrogen bonds were detected between Gly538 or Ser537 and Asp351 (on H3), which existed for 94.3% and 99.8% of the last 1 ns of stimulation, respectively. Formation of the latter bond is validated in the crystal structure of the Tyr537Ser mutant and is associated with the constitutive activity of the mutant[14]. The newly discovered hydrogen bond involving Gly538 is likely caused by altered backbone conformations inaccessible to all natural amino acids except glycine, a hypothesis supported by the fact that the Asp538Ala mutant was non-activating. Furthermore, these stimulations agree with the activity levels of the mutants, suggesting that these hydrogen bonds stabilize the agonist conformation, especially for the coactivator-recruiting H12 helix and its surroundings, and may contribute to the elevated activity of the mutants. The simulations do not, however, show obvious effects of the alterations on the ligand-binding pocket that might hinder ER antagonists from binding. Indeed, *in vitro* ligand binding assays confirmed the ability of mutant LBDs to bind E2

© 2013 Nature America, Inc. All rights reserved.

(data not shown). Rather, the effects on helix H12 are likely to influence coactivator and/or corepressor binding.

Although the mutant ERα isoforms were not effectively inhibited by hormone withdrawal, they could be partially inhibited by direct antagonists of the receptor, such as tamoxifen and fulvestrant. These findings validate previously reported data on the effect of tamoxifen on the activity of the Tyr537Ser mutant[23]. However, the ability of these drugs to inhibit the mutants is somewhat impaired. When we examined the effect of different doses of these compounds on mutant-expressing cells, at the lower doses, residual activity was observed, and this activity may be sufficient to confer drug resistance. Moreover, expression of the mutants was observed to raise the dose of tamoxifen needed to inhibit MCF7 cell growth *in vitro* (data not shown). By way of anecdote, one of nine patients in the MSKCC set did receive treatment with direct ER antagonists (tamoxifen followed by fulvestrant) after detection of this mutation and had no tumor response to either.

The fact that higher doses of fulvestrant and tamoxifen were able to fully antagonize mutant ERα signaling *in vitro* is nonetheless notable. These data and structural modeling results suggest that more potent or specific antagonists of the mutant forms may be effective at blocking ER signaling and may benefit patients where hormonal therapies can have a very high therapeutic index. As next-generation SERMs and SERDs are currently in development, analysis of their effects on the activity and stability of ERα mutants is now a pressing need given the apparent prevalence of these lesions in individuals with metastatic disease. Going further, the fact that these lesions are clearly more prevalent in metastatic disease suggests a possible causal role in this process. Given the widespread use of hormone antagonists as adjuvants to prevent metastatic recurrence, it will be important to determine whether the identified mutations can be implicated in such recurrences and, then, whether newer SERMs or SERDs that more potently block mutant function can be curative when given as adjuvants.

METHODS

Methods and any associated references are available in the online version of the paper.

Accession codes. Accession codes. Gene expression array data for MCF7 cells transfected with constructs expressing wild-type or mutant ERα fused with GFP have been deposited in the Gene Expression Omnibus (GEO) under accession GSE51448.

Note: Any Supplementary Information and Source Data files are available in the online version of the paper.

ACKNOWLEDGMENTS

We would like to thank N. Rosen and C. Sawyers for their insights and critical reading of the manuscript, P. Chi and S. Lowe (MSKCC) for plasmids and J.S. Reis-Filho (MSKCC) for cell lines. S.C. is funded by the Damon Runyon Cancer Research Foundation and a Louis V. Gerstner Jr. Young Investigator Award. M.B. and H.W. are funded by the Starr Cancer Consortium and the Geoffrey Beene Cancer Research Center, respectively. Individual support for this study was also provided by Julie Laub (to C.H.). Molecular dynamics simulations were performed using computational resources awarded to Y.S. by the Argonne Leadership Computing Facility at the Argonne National Laboratory, which is supported by the Office of Science of the US Department of Energy under contract DE-AC02-06CH11357. Y.S. is partially funded by the Toyota Technological Institute at Chicago.

AUTHOR CONTRIBUTIONS

S.C., W.T., Y.S., G.G., J.B., G.H. and M.B. conceived and designed the experiments. W.T., Y.S., H.W., B.G., S.F., R.A.S., M.W., Z.L., K.G. and S.C. conducted the experiments. W.T., S.C., Y.S., G.G., M.B., H.W., D.C., T.T., J.B., G.H., T.A.K. and C.H. analyzed the data. W.T., S.C., Y.S. and H.W. wrote the manuscript.

COMPETING FINANCIAL INTERESTS

The authors declare no competing financial interests.

Reprints and permissions information is available online at http://www.nature.com/reprints/index.html.

1. Early Breast Cancer Trialists' Collaborative Group (EBCTCG). Effects of chemotherapy and hormonal therapy for early breast cancer on recurrence and 15-year survival: an overview of the randomised trials. *Lancet* **365**, 1687–1717 (2005).
2. Ariazi, E.A., Ariazi, J.L., Cordera, F. & Jordan, V.C. Estrogen receptors as therapeutic targets in breast cancer. *Curr. Top. Med. Chem.* **6**, 181–202 (2006).
3. Strasser-Weippl, K. & Goss, P.E. Advances in adjuvant hormonal therapy for postmenopausal women. *J. Clin. Oncol.* **23**, 1751–1759 (2005).
4. Forbes, J.F. *et al.* Effect of anastrozole and tamoxifen as adjuvant treatment for early-stage breast cancer: 100-month analysis of the ATAC trial. *Lancet Oncol.* **9**, 45–53 (2008).
5. Peng, J., Sengupta, S. & Jordan, V.C. Potential of selective estrogen receptor modulators as treatments and preventives of breast cancer. *Anticancer. Agents Med. Chem.* **9**, 481–499 (2009).
6. Wagle, N. *et al.* High-throughput detection of actionable genomic alterations in clinical tumor samples by targeted, massively parallel sequencing. *Cancer Discov.* **2**, 82–93 (2012).
7. Cancer Genome Atlas Network. Comprehensive molecular portraits of human breast tumours. *Nature* **490**, 61–70 (2012).
8. Gutierrez, M.C. *et al.* Molecular changes in tamoxifen-resistant breast cancer: relationship between estrogen receptor, HER-2, and p38 mitogen-activated protein kinase. *J. Clin. Oncol.* **23**, 2469–2476 (2005).
9. Lipton, A. *et al.* Serum HER-2/neu conversion to positive at the time of disease progression in patients with breast carcinoma on hormone therapy. *Cancer* **104**, 257–263 (2005).
10. Meng, S. *et al. HER-2* gene amplification can be acquired as breast cancer progresses. *Proc. Natl. Acad. Sci. USA* **101**, 9393–9398 (2004).
11. Jirström, K. *et al.* Adverse effect of adjuvant tamoxifen in premenopausal breast cancer with cyclin D1 gene amplification. *Cancer Res.* **65**, 8009–8016 (2005).
12. Turner, N. *et al. FGFR1* amplification drives endocrine therapy resistance and is a therapeutic target in breast cancer. *Cancer Res.* **70**, 2085–2094 (2010).
13. Baselga, J. *et al.* Everolimus in postmenopausal hormone-receptor-positive advanced breast cancer. *N. Engl. J. Med.* **366**, 520–529 (2012).
14. Nettles, K.W. *et al.* NFκB selectivity of estrogen receptor ligands revealed by comparative crystallographic analyses. *Nat. Chem. Biol.* **4**, 241–247 (2008).
15. Zhang, Q.X., Borg, A., Wolf, D.M., Oesterreich, S. & Fuqua, S.A. An estrogen receptor mutant with strong hormone-independent activity from a metastatic breast cancer. *Cancer Res.* **57**, 1244–1249 (1997).
16. Kato, S. *et al.* Activation of the estrogen receptor through phosphorylation by mitogen-activated protein kinase. *Science* **270**, 1491–1494 (1995).
17. Le Goff, P., Montano, M.M., Schodin, D.J. & Katzenellenbogen, B.S. Phosphorylation of the human estrogen receptor. Identification of hormone-regulated sites and examination of their influence on transcriptional activity. *J. Biol. Chem.* **269**, 4458–4466 (1994).
18. Anzick, S.L. *et al.* AIB1, a steroid receptor coactivator amplified in breast and ovarian cancer. *Science* **277**, 965–968 (1997).
19. Azorsa, D.O., Cunliffe, H.E. & Meltzer, P.S. Association of steroid receptor coactivator AIB1 with estrogen receptor-α in breast cancer cells. *Breast Cancer Res. Treat.* **70**, 89–101 (2001).
20. Fan, M., Park, A. & Nephew, K.P. CHIP (carboxyl terminus of Hsc70-interacting protein) promotes basal and geldanamycin-induced degradation of estrogen receptor-α. *Mol. Endocrinol.* **19**, 2901–2914 (2005).
21. Chandarlapaty, S. *et al.* SNX2112, a synthetic heat shock protein 90 inhibitor, has potent antitumor activity against HER kinase–dependent cancers. *Clin. Cancer Res.* **14**, 240–248 (2008).
22. Shang, Y. & Brown, M. Molecular determinants for the tissue specificity of SERMs. *Science* **295**, 2465–2468 (2002).
23. Weis, K.E., Ekena, K., Thomas, J.A., Lazennec, G. & Katzenellenbogen, B.S. Constitutively active human estrogen receptors containing amino acid substitutions for tyrosine 537 in the receptor protein. *Mol. Endocrinol.* **10**, 1388–1398 (1996).
24. Brzozowski, A.M. *et al.* Molecular basis of agonism and antagonism in the oestrogen receptor. *Nature* **389**, 753–758 (1997).

© 2013 Nature America, Inc. All rights reserved.

ONLINE METHODS

Reagents. We obtained 4-hydroxytamoxifen (4-OHT) and 17β-estradiol (E2) from Sigma-Aldrich. Fulvestrant (ICI 182780) was purchased from Selleck Chemicals, and bazedoxifene acetate (BZA) was purchased from Toronto Research Chemical. SNX2112 was obtained from Pfizer. All drugs were dissolved in ethanol except for BZA and SNX2112, which were reconstituted in DMSO. Antibodies to ER-α phosphorylated at Ser118 (11072), hemagglutinin (HA) tag (2367, 6E2), AIB1 (611105, 34/AIB-1) and β-actin (5441, AC-15) were purchased from Signalway Antibody, Cell Signaling Technology, BD Transduction Laboratories and Sigma, respectively. GFP-trap_A kit was obtained from Chromotek. pcDNA 3.1 (+), pCL-Ampho and pVSVG vectors were kind gifts from P. Chi, and pSIN-TREtight-IRES-Cherry vector was a kind gift from S. Lowe. pRL-TK *Renilla* Luciferase plasmid was obtained from Promega, 3×-ERE-TATA-Luciferase reporter and pEGFP-C1-ERα were obtained from Addgene (Addgene plasmids11354 and 28230, deposited by D. McDonnell and M. Mancini, respectively).

Cell culture. All cell lines were maintained at 37 °C and 5% CO_2 in a humidified atmosphere. SK-BR-3 MCF7, ZR-75-1, MDA-MB-361 and MDA-MB-231 cell lines were obtained from the American Type Culture Collection, and MCF Tet-On cells were obtained from Clontech. The Ishikawa cell line was obtained from the laboratory of J.S. Reis-Filho. SK-BR-3, MCF7 and MDA-MB-361 cells were grown in DMEM-F12, ZR-75-1 and MDA-MB-231 cells were grown in RPMI, and Ishikawa cells were grown in DMEM, supplemented with 5% heat-inactivated FBS, 100 μg/ml penicillin, 100 mg/ml streptomycin and 4 mM glutamine. MCF Tet-On cells were grown in similar medium except that FBS was replaced with 10% Tet System Approved FBS from Clontech. All cell lines tested negative for mycoplasma.

Transfections. Cells were either transfected with Lipofectamine 2000 (Invitrogen) or X-tremeGENE (Roche) according to the manufacturers' protocols. For experiments involving estrogen induction, cells were transfected in phenol red–free DMEM-F12 containing 10% charcoal-stripped FBS (hormone-depleted medium) (Invitrogen), and E2 was added 24 h after transfection.

Cloning and mutagenesis. A sequence encoding an HA tag was inserted onto the 5′ end of *ESR1* by PCR amplifying it from pEGFP-C1-ERα using the primers listed in **Supplementary Table 3**. This fragment encoding HA-ERα was cloned into pcDNA3.1 (+) using ApaI and BamHI restriction sites and into pSIN-TREtight-IRES-Cherry using BamHI and ApaI restriction sites. Point mutations were introduced into pEGFP-C1-ERα, pcDNA-HA-ERα and pSIN-TREtight-HA-ERα using the QuikChange II XL Site-Directed Mutagenesis kit (Stratagene) as described in the manufacturer's instructions.

Clinical samples (MSKCC set). Patients with breast cancer and either recurrence of disease after receiving adjuvant therapy or World Health Organization (WHO)-defined progression of metastatic disease on therapy were prospectively enrolled on an institutional review board (IRB)-approved tissue collection protocol from February 2007 through January 2013. Informed consent was obtained from all participants. All patients underwent biopsy of at least one site to document progressive disease. Mutational analysis of the metastatic biopsy was performed on fresh-frozen specimens. Formalin-fixed, paraffin-embedded blocks of each primary tumor before treatment were obtained, where possible, for comparison. The presence of tumor, in both frozen samples and formalin-fixed, paraffin-embedded tissue sections, was confirmed by the study pathologist. Extraction of genomic DNA was performed using a QuickGene DNA tissue kit (Fujifilm). A minimum of 5 mg of fresh-frozen tumor was suspended in 360 μl of tissue lysis buffer (MDT) to which 40 μl of proteinase K was added, and samples were incubated for 48 h at 55 °C. Lysis buffer LDT (360 μl) was then added, and samples were incubated at 70 °C for 30 min. Samples were washed with 100% ethanol and wash buffer. DNA was eluted in 50 μl of EDTA buffer. Quantification of DNA by Nanodrop Fluorospectrometer showed an average yield of 20 μg (average yield with PicoGreen was 250 ng). A prespecified effect size was not estimated in our discovery efforts using next-generation sequencing to characterize hormone-refractory breast cancers.

IMPACT next-generation sequencing and analysis. Extracted genomic DNA from the MSKCC clinical samples underwent next-generation sequencing using an Illumina HiSeq 2000 instrument, and analysis was performed using our custom IMPACT assay (Integrated Mutation Profiling of Actionable Cancer Targets). The IMPACT assay uses specially designed target-specific probes to capture all the protein-coding exons of 230 genes of interest for hybrid selection (Agilent SureSelect or Nimblegen SeqCap) as previously described[25]. The list of genes included commonly implicated oncogenes, tumor suppressor genes and components of pathways deemed actionable by current targeted therapies (see **Supplementary Table 4** for the complete list of targets). In addition to targeting exons from the 230 cancer-related genes, we also designed probes to target >1,000 common SNPs across the genome. For each sample, we examined all sites that were homozygous, and we calculated the average minor allele frequency across these sites. Tumors for which the average minor allele frequency at homozygous sites was >2% were removed, as this frequency suggests the presence of contaminating DNA from another individual. By closely monitoring this value and removing samples harboring evidence of contamination, we increased our confidence that variants with low allele frequencies were bona fide mutations and not false-positive artifacts.

Two protocols were followed during the course of the study. For eight samples (four tumor-normal pairs), barcoded sequence libraries (Illumina TruSeq) were prepared using 500 ng of input tumor or matched normal DNA according to the manufacturer's instructions. Libraries were pooled at equimolar concentrations (100 ng per tumor library and 50 ng per normal sample library) for a single exon capture reaction (Agilent SureSelect) as previously described[26]. For the remaining samples, barcoded sequence libraries were prepared with 250 ng of input DNA using a hybrid protocol based on the NEBNext DNA Library-Prep kit (New England Biolabs). The manufacturer's instructions were followed with two substitutions: instead of the specified reagents, we used NEXTflex barcoded adapters (Bio Scientific) and HiFi DNA polymerase (Kapa Biosystems). Libraries were pooled at 100 ng per tumor library and 50 ng per normal sample library for a single exon capture reaction (Nimblegen SeqCap). To prevent off-target hybridization in all capture reactions, we spiked libraries with a pool of blocker oligonucleotides complementary to the full sequences of all barcoded adaptors (to a final total concentration of 10 μM). Hybridized DNA was sequenced on an Illumina HiSeq 2000 instrument to generate paired-end 75-bp reads.

Data were demultiplexed using CASAVA, and reads were aligned to the reference human genome (hg19) using the Burrows-Wheeler Alignment tool[27]. Local realignment and quality score recalibration were performed using the Genome Analysis Toolkit (GATK) according to GATK best practices[28]. We achieved mean exon sequence coverage of 512× (628× for all tumor samples and 418× for all normal samples). Deep sequencing ensured sensitivity in detecting mutations in multiclonal and stroma-admixed samples and enabled accurate determination of mutation allele frequencies.

Sequence data were analyzed to identify three classes of somatic alterations: single-nucleotide variants, small insertions-deletions (indels) and copy number alterations. Single-nucleotide variants were called using muTect[29] and retained if variant allele frequency in the tumor was >5 times that in the matched normal sample. Indels were called using the SomaticIndelDetector tool in GATK. All candidate mutations and indels were reviewed manually using the Integrative Genomics Viewer[30]. Mean sequence coverage was calculated using the DepthOfCoverage tool in GATK and was used to compute copy number as described previously[6].

Clinical samples (BOLERO-2 sample set). The study design for BOLERO-2 has been described previously[13]. Archival tissue samples with sufficient tumor content (10 slides per patient) were identified and analyzed by next-generation sequencing.

Foundation Medicine next-generation sequencing and analysis (BOLERO-2 set). Next-generation sequencing and analysis by Foundation Medicine was performed as described previously[31]. DNA sequencing was performed on 3,230 exons from 182 cancer-related genes on indexed, adaptor-ligated, hybridization-captured (Agilent SureSelect custom kit) libraries using DNA isolated from 272 formalin-fixed, paraffin-embedded tumors along with matched normal DNA from white blood cells. A total of 227 samples (183 primary and 44 metastatic) with coverage of >250× and average coverage of 602 ± 202× were included in the final analysis.

Retroviral infection and generation of stable cell lines. We plated 293CT packaging cells at 2.5 × 10^7 cells/ tissue culture dish (10 cm in diameter) and

© 2013 Nature America, Inc. All rights reserved.

doi:10.1038/ng.2822

transfected them with 2.25 μg of the pSIN-TREtight retroviral vector (empty or encoding HA-tagged wild-type or mutant ERα), 2.25 μg of pCL-Ampho and 0.5 μg of pVSVG with X-tremeGENE (Roche) according to the manufacturer's protocol. Conditioned medium containing recombinant retroviruses was collected and filtered through non-pyrogenic filters with a pore size of 0.45 μm (Millipore). Samples of these supernatants were applied immediately to MCF Tet-On cells, which had been plated 18 h before infection at a density of 4×10^6 cells/tissue culture dish (10 cm in diameter). Polybrene (Sigma) was added to a final concentration of 8 μg/ml, and supernatants were incubated with cells for 12 h. After infection, cells were placed in fresh growth medium and cultured as usual. Selection with 500 μg/ml hygromycin was initiated 72 h after infection. After 14 d of selection, the hygromycin concentration was lowered to 100 μg/ml, and cells were cultured as usual.

Mouse studies. We obtained 6- to 8-week-old *nu/nu* athymic BALB/c female mice from Harlan Laboratories and maintained them in pressurized, ventilated caging. All studies were performed in compliance with institutional guidelines under an institutional animal care and use committee (IACUC)-approved protocol (MSKCC 12-10-016). Xenograft tumors of MCF7 cells inducibly expressing HA-ERα were established in nude mice by subcutaneously implanting 0.72 mg of sustained-release 17β-estradiol pellets with a 10-g trocar into one flank and injecting 1×10^7 cells suspended 1:1 in reconstituted basement membrane (Matrigel, Collaborative Research) into the opposite flank 3 d later. We removed 17β-estradiol pellets from the mice when tumors reached a size of ~250 mm^3, and mice then received water containing 0.2 or 0.5 mg/ml doxycycline (0.2 mg/ml for mice with xenografts expressing wild-type ERα and 0.5 mg/ml for mice with xenografts expressing vector control or Tyr537Ser or Asp538Gly mutant ERα) and 0.1% sucrose for induction of ER expression 7 d after pellet removal. Tumor dimensions were measured with vernier calipers, and tumor volume was calculated ($\pi/6 \times$ larger diameter $\times$ (smaller diameter)^2). In this study, no blinding of investigators or randomization of mice was performed. On the basis of our previous work measuring the variability in size and growth of MCF7 xenografts, we estimated that ten mice per group would allow us to detect differences in tumor size of >200 mm^3.

Coimmunoprecipitation. Coimmunoprecipitation was performed with the GFP-Trap_A kit according to the manufacturer's protocol. In brief, cell pellets were resuspended in coimmunoprecipitation lysis buffer (10 mM Tris-HCl, pH 7.5, 150 mM NaCl, 0.5 mM EDTA, 0.5% NP-40 and 1× protease and phosphatase inhibitors (Pierce)). Cells were lysed by pipetting the pellet up and down every 10 min for a total of 30 min while on ice. Lysates were cleared by spinning them at 20,000*g* for 10 min. For coimmunoprecipitation, 1 mg of lysate was used for each sample with 100 μl of equilibrated GFP-Trap_A beads, and samples were incubated on a rotator overnight at 4 °C. Beads were then washed twice with ice-cold wash buffer, resuspended in 2× LDS sample buffer (Invitrogen) and boiled for 10 min at 70 °C before loading onto SDS-PAGE gels.

Immunoblotting. Cells were washed once with cold PBS and scraped off the plate with a rubber policeman. The cell suspension was briefly centrifuged to pellet cells, PBS was removed, and the cell pellet was stored at −80 °C until lysis. For cell lysis, pellets were resuspended in a non-denaturing lysis buffer (Cell Signaling Technology) supplemented with protease and phosphatase inhibitors (Pierce) and were sonicated briefly for 30 s. Lysates were cleared by centrifugation at 14,000*g* for 10 min, and protein concentration was determined using the BCA kit (Pierce), which measures the reduction of Cu^{2+} to Cu^{1+} by protein in an alkaline medium. For each sample, 30 μg of protein lysate was loaded onto 4–12% SDS-PAGE minigels (Invitrogen) for electrophoresis and immunoblotting.

Luciferase assays. Cells were plated at a density of 0.1×10^6 cells per well of a 24-well plate 1 d before transfection. Cells were transfected with 100 ng (per well) of vector encoding HA-tagged wild-type or mutant ERα, 250 ng (per well) of 3×-ERE-TATA-Luciferase reporter and 50 ng (per well) of pRL-TK *Renilla* Luciferase plasmid using Lipofectamine 2000. Cells were treated with either E2, 4-OHT or ICI 1 d after transfection for 24 h, and luciferase activities were determined using the Dual-Luciferase Reporter Assay System (Promega) according to the manufacturer's instructions. Luciferase bioluminescence measurements were performed with the Veritas Microplate Luminometer (Promega). All experiments were conducted in triplicate, and firefly luciferase activity was normalized by *Renilla* luciferase activity for each sample.

Quantitative RT-PCR. RNA was extracted from cells 48 h after transfection using the RNeasy Mini kit (Qiagen) according to the manufacturer's protocol. cDNA was synthesized with 2 μg of RNA from each sample using the SuperScript First-Strand Synthesis System for RT-PCR (Invitrogen) according to the manufacturer's protocol. Synthesized cDNA was diluted with one volume of DEPC-treated water, and 2 μl of the mixture was added to TaqMan PCR Master Mix (Applied Biosystems) along with primers. Relative quantification for each mRNA was performed using the comparative C_T method with a ViiA 7 Real-Time PCR system (Applied Biosystems)[32]. Samples were run in triplicate, and mRNA levels were normalized to those of *ESR1* for each reaction.

Microarrays. RNA was extracted from MCF7 cells transfected with vector expressing wild-type or mutant ERα fused with GFP using TRIzol reagent and was analyzed with the HumanHT-12 v4 Expression BeadChip (Illumina). Statistical analysis of differences between groups was performed using standard ANOVA tests. Data were analyzed using the Partek Genomics Suite.

Molecular dynamics simulations. Crystal structures for TIF2-bound wild-type and Tyr537Ser ERα were obtained from PDB[6] (accessions 1GWQ and 3Q95, respectively), and corresponding agonist ligands were removed. A few terminal residues of ERα or TIF2 were also removed so that the two structures shared the same segment. The structure of TIF2-bound Asp538Gly ERα was first constructed by removing the side chain atoms at residue 538. For all three structures, missing atoms were placed with geometries parameterized by CHARMM22 (ref. 33) and were then minimized, with the rest harmonically constrained, using the molecular modeling program CHARMM[34]. Minimization was performed with a distance-dependent dielectric constant to approximate solvation effects. No distance cutoff for non-bonded interactions was used.

The resulting structures were used as starting points for explicit-solvent molecular dynamics simulation. Each was first placed in a water box whose boundaries were at least 15 Å away from the nearest ERα or TIF2 atoms. Sodium and chloride ions were also added to reach a physiological concentration (0.145 M) and total charge neutrality. The two steps above were performed with the program VMD[35]. Each system of TIF2-bound ERα (wild type, Tyr537Ser or Asp538Gly), water molecules and ions was minimized for 5,000 steps and then run for a 10-ns molecular dynamics stimulation using the program NAMD[36]. Constant temperature (300 K) and pressure (1 atm, with the Nosé-Hoover Langevin piston method) were used for the molecular dynamics simulations. Force-field parameters were adopted from CHARMM22. Electrostatic interactions were treated with a particle mesh Ewald (PME) method (1-Å grid spacing and 14-Å distance cutoff). Dynamics were run with a 2-fs time step, and the list of non-bonded interactions was updated every ten steps.

Statistics. All reported values represent the average of triplicate experiments. Statistical analysis of differences between samples was performed using standard two-tailed Student's *t* tests, and $P < 0.05$ was defined as significant. Analysis was conducted using Prism v6.0c (GraphPad Software).

25. Won, H.H., Scott, S.N., Brannon, A.R., Shah, R.H. & Berger, M.F. Detecting somatic genetic alterations in tumor specimens by exon capture and massively parallel sequencing. *J. Vis. Exp.* **80**, e50710 (2013).
26. Li, H. *et al.* The Sequence Alignment/Map format and SAMtools. *Bioinformatics* **25**, 2078–2079 (2009).
27. Li, H. & Durbin, R. Fast and accurate short read alignment with Burrows-Wheeler transform. *Bioinformatics* **25**, 1754–1760 (2009).
28. DePristo, M.A. *et al.* A framework for variation discovery and genotyping using next-generation DNA sequencing data. *Nat. Genet.* **43**, 491–498 (2011).
29. Cibulskis, K. *et al.* Sensitive detection of somatic point mutations in impure and heterogeneous cancer samples. *Nat. Biotechnol.* **31**, 213–219 (2013).
30. Robinson, J.T. *et al.* Integrative genomics viewer. *Nat. Biotechnol.* **29**, 24–26 (2011).
31. Lipson, D. *et al.* Identification of new *ALK* and *RET* gene fusions from colorectal and lung cancer biopsies. *Nat. Med.* **18**, 382–384 (2012).
32. Chandarlapaty, S. *et al.* AKT inhibition relieves feedback suppression of receptor tyrosine kinase expression and activity. *Cancer Cell* **19**, 58–71 (2011).
33. MacKerell, A.D. *et al.* All-atom empirical potential for molecular modeling and dynamics studies of proteins. *J. Phys. Chem. B* **102**, 3586–3616 (1998).
34. Brooks, B.R. *et al.* CHARMM: the biomolecular simulation program. *J. Comput. Chem.* **30**, 1545–1614 (2009).
35. Humphrey, W., Dalke, A. & Schulten, K. VMD: visual molecular dynamics. *J. Mol. Graph.* **14**, 33–38 (1996).
36. Phillips, J.C. *et al.* Scalable molecular dynamics with NAMD. *J. Comput. Chem.* **26**, 1781–1802 (2005).

© 2013 Nature America, Inc. All rights reserved.

Escherichia coli causing primary pyelonephritis. *Lancet* 1981; ii: 1366–69.
24 Korhonen TK, Valtonen MV, Parkkinen J, et al. Serotype, hemolysin production, and receptor recognition of Escherichia coli stains associated with neonatal sepsis and meningitis. *Infect Immun* 1985; **48:** 486–91.
25 Old DC. Inhibition of the interaction between fimbrial hemagglutinins and erythrocytes by D-mannose and other carbohydrates. *J Gen Microbiol* 1972; **71:** 149–57.
26 Green CP, Thomas VL. Hemagglutination of human type O erythrocytes, hemolysin production and serogrouping of Escherichia coli isolates from patients with acute pyelonephritis cystitis, and asymptomatic bacteriuria. *Infect Immun* 1981; **31:** 309–15.
27 Okada Y, Tsuji T. Immunohistochemical application of monoclonal antibodies to reveal the structure and localization of carbohydrate antigens: N-acetyl-lactosamine related carbohydrates antigens in human biliary epithelial cells. *J Immunol Method* 1988; **112:** 243–49.
28 Sung JY, Costerton JW, Shaffer EA. Defense system in the biliary tract against bacterial infection. *Dig Dis Sci* 1992; **37:** 689–96.
29 Hamadeh RM, Mandrell RE, Griffiss JM. Immunophysical characterization of human isolates of *Serratia marcescens*. *J Clin Microbiol* 1990; **28:** 20–26.

Risk of endometrial cancer after tamoxifen treatment of breast cancer

Flora E van Leeuwen, Jantien Benraadt, Jan Willem W Coebergh, Lambertus A L M Kiemeney, Charles H F Gimbrère, Renée Otter, Leo J Schouten, Ronald A M Damhuis, Marijke Bontenbal, Fred W Diepenhorst, Alexandra W van den Belt-Dusebout, Harm van Tinteren

Summary

Since large trials have been set up to assess whether tamoxifen decreases the risk of breast cancer in healthy women, it has become important to investigate the drug's potential adverse effects, including occurrence of endometrial cancer. We undertook a case-control study in the Netherlands to assess the effect of tamoxifen on the risk of endometrial cancer after breast cancer.

Through the population-based Netherlands Cancer Registry and two older, hospital-based, registries, we identified 98 patients who had endometrial cancer diagnosed at least 3 months after a diagnosis of primary breast cancer. Detailed information about treatment was obtained for all these patients, and for 285 controls, who were matched to the cases for age, year of breast cancer diagnosis, and survival time with intact uterus. Tamoxifen had been used by 24% of patients with subsequent endometrial cancer and 20% of controls (relative risk 1·3 [95% CI 0·7–2·4]). Women who had used tamoxifen for more than 2 years had a 2 3 (0 9–5 9) times greater risk of endometrial cancer than never users. There was a significant trend of increasing risk of endometrial cancer with duration of tamoxifen use ($p=0\ 049$), and also with cumulative dose ($p=0·046$). The duration-response trends were similar with daily doses of 40 mg or 30 mg and less.

These findings support the hypothesis that tamoxifen use increases the risk of endometrial cancer. This oestrogenic effect on the endometrium was not related to the dose intensity. Physicians should be aware of the higher risk of endometrial cancer in tamoxifen users.

Lancet 1994; **343:** 448–52

Department of Epidemiology, Netherlands Cancer Institute, Amsterdam (F E van Leeuwen MSPH, A W van den Belt-Dusebout); **Comprehensive Cancer Centers—Amsterdam** (F E van Leeuwen, J Benraadt MD, F W Diepenhorst, H van Tinteren MSc), **South Netherlands** (J W W Coebergh MD), **East Netherlands** (L A L M Kiemeney PhD), **Middle Netherlands** (C H F Gimbrère MD), **Northern Netherlands** (R Otter MD), **Limburg** (L J Schouten MD), **Rotterdam** (R A M Damhuis MD), **and Stedendriehoek Twente** (J Benraadt); **and Dr Daniel den Hoed Cancer Center, Rotterdam** (M Bontenbal MD), **Netherlands**

Correspondence to: Ms Flora E van Leeuwen, Department of Epidemiology, Netherlands Cancer Institute, Plesmanlaan 121, 1066 CX, Amsterdam, Netherlands

Introduction

Since its introduction in the early 1970s, tamoxifen has been widely and effectively used to treat advanced breast cancer. Adjuvant tamoxifen therapy in early-stage breast cancer became common in the 1980s, and has been convincingly shown to improve disease-free survival as well as overall survival for women older than 50 years.[1] Several large trials have suggested, furthermore, that tamoxifen reduces the risk of cancer in the contralateral breast.[1–4] Based on these findings, chemoprevention trials have been set up in the USA and Europe to find out whether tamoxifen decreases the risk of breast cancer developing in healthy women judged to be at high risk of the disease.[5,6]

Our knowledge of the long-term effects of tamoxifen is still limited. Tamoxifen's mixed oestrogen-agonist and oestrogen-antagonist properties have led to concern that the drug may increase the risk of endometrial cancer. The Stockholm trial[4] found that women receiving 40 mg tamoxifen daily for at least 2 years had a more than six-fold excess risk of endometrial cancer in comparison with untreated controls. No significant increase in risk has been reported in other major adjuvant trials,[7] although a non-significant excess of endometrial cancer after tamoxifen treatment was noted in an evaluation of Danish trials and in an unpublished Southwest Oncology Group Trial.[8–10] The 10-year cumulative risk of endometrial cancer in postmenopausal women is estimated to be 0·3% or less. Thus, a follow-up study with sufficient power to settle the question of whether there is an excess risk of endometrial cancer after tamoxifen treatment would require long-term follow-up of many thousands of breast cancer patients. We therefore used a case-control design to investigate, in a nationwide study, whether tamoxifen, at different doses and for different durations, increases the risk of endometrial cancer.

Patients and methods

Since 1989, the Netherlands has had a population-based, nationwide cancer registry served by nine regional cancer registries.[11] Most registries have been operating since 1986, the Eindhoven Cancer Registry since 1975,[12] and the Middle Netherlands Breast Cancer Registry since 1973.[13] Patients with endometrial cancer after breast cancer were identified from eight of the nine regional cancer registries; other cases (most with endometrial cancer diagnosed before 1986) were identified from the hospital tumour registries of two major cancer treatment

centres (the Netherlands Cancer Institute [NKI], Amsterdam, and the Dr Daniel den Hoed Cancer Center [DDHK], Rotterdam).

Women were eligible for the study if they had a histologically or cytologically confirmed diagnosis of infiltrating endometrial carcinoma at least 3 months after a diagnosis of primary breast cancer; if the breast cancer developed after Jan 1, 1976 (Jan 1, 1972 in NKI and DDHK; before these dates tamoxifen was not commonly used); and if they had no other second malignant disorder after breast cancer, except for carcinoma in situ of the uterine cervix, basal-cell carcinoma of skin, or contralateral breast cancer. We required that the diagnosis of breast cancer had been made in a hospital that, at the time, was taking part in any type of registration of all breast cancer cases diagnosed in that hospital. This eligibility criterion was necessary because the method of selecting controls was based on calendar year of breast cancer diagnosis. 98 patients with endometrial cancer after breast cancer met these eligibility criteria.

Controls were women with breast cancer in whom endometrial cancer had not been diagnosed. For each case patient, 3 controls were sought. They were individually matched to the patient for date of birth (within 3 years), date of diagnosis of breast cancer (within 2 years), and pathology laboratory where the breast cancer diagnosis was made. In addition, each control had to have survived, with an intact uterus, for at least as long as the time between the diagnoses of breast cancer and endometrial cancer in the corresponding case. Furthermore, we required that the control had not had a second primary cancer (other than carcinoma in situ of the cervix, basal-cell carcinoma of skin, or contralateral breast cancer) before the date the case patient developed endometrial cancer. When more than 3 controls per case met the above criteria, we selected those with the closest year of diagnosis of breast cancer, and then closest date of birth, to the case. For endometrial cancer patients whose breast cancer diagnoses were recorded in the cancer registries, controls were drawn through the registries. For those whose breast cancer registration records were not present in the registries (since they were not operating at the time), controls were selected through the Dutch Network and National Database for Pathology. This database contains records of all cytological and histological diagnoses made in the Netherlands, with computerised data submission by the individual pathology laboratories. The database was set up in 1977, and complete national coverage was achieved in 1989. Control selection through this database was allowed only if the breast cancer diagnosis of the case patient was also recorded in the pathology database. 3 controls were found for 91 case patients, 2 controls for 5 cases, and 1 control for 2 cases.

For each case and her matched controls, full medical records were obtained for detailed data abstraction. Information was collected on stage of breast cancer, menopausal status at diagnosis of breast cancer, occurrence of contralateral disease, vital status, date of latest follow-up examination or date of death, and cause of death. We recorded for each period of tamoxifen treatment the starting date, the stopping date, and the dosage. The use of radiotherapy, chemotherapy, and hormonal treatment other than tamoxifen for breast cancer was also recorded. For each control, we checked extensively whether she had undergone hysterectomy (in which case she was excluded from the study). If necessary, information was obtained from the patient's general practitioner. Complete information on all treatments, including periods of tamoxifen use and dosage, was eventually available for all women. For cases, we also sought information from the medical record on the endometrial cancer diagnosis (stage of endometrial cancer, full pathology report, treatment for endometrial cancer). All pathology reports of endometrial cancer were reviewed centrally by one of us (JB). If reports were incomplete or diagnosis uncertain, the slides were reviewed by the local pathologist.

The relative risk of endometrial cancer associated with tamoxifen use was estimated by comparison of the case patient's treatment history with that of her matched controls, by conditional logistic regression methods.[14] Relative risk estimates, two-sided p values, and 95% CI were calculated with the microcomputer programme EGRET (SERC, Seattle, Washington, USA); comparisons between exposure categories were based on likelihood-ratio tests. For analysis, only the treatment of case patients during the time between the diagnoses of breast cancer and of endometrial cancer was included. For controls, treatment was studied for an equivalent time, starting with the date that breast cancer was diagnosed. Total duration of tamoxifen use and total dose were examined specifically as relevant factors in determining risk. The cumulative dose of tamoxifen was grouped into quartiles to calculate relative risks for each category in relation to the reference group of patients not treated with tamoxifen. Tests for trend in relative risk of endometrial cancer by duration (or cumulative dose) of tamoxifen were calculated by fitting the actual months (or mg) of use as a continuous variable in the logistic regression analyses. To assess the effect of dose intensity, duration-response slopes were estimated simultaneously for women who had received daily doses of 40 mg and 30 mg or less. Multivariate analyses were done to account for potentially confounding effects of radiotherapy (yes/no), chemotherapy (yes/no), hormonal treatment other than tamoxifen, and breast cancer stage. For this purpose, hormonal treatment other than tamoxifen was classified according to the expected effect on the endometrium (oestrogen stimulation, yes/no; progestagenic protection yes/no).

	No (%)	
	Cases (n = 98)	Controls (n = 285)
Age at diagnosis (yr)*		
≤55	13 (13)	36 (13)
56–65	36 (37)	103 (36)
66–75	31 (32)	97 (34)
>75	18 (18)	49 (17)
Year of diagnosis*		
1972–1979	26 (27)	69 (24)
1980–1983	21 (21)	69 (24)
1984–1986	22 (23)	67 (24)
1987–1990	29 (30)	80 (28)
Time between diagnoses (mo)†		
≤18	21 (21)	
19–36	31 (32)	
37–72	26 (27)	
>72	20 (20)	
Stage of breast cancer		
Localised	51 (52)	152 (53)
Regional	36 (37)	122 (43)
Distant	9 (9)	10 (4)
Unknown	2 (2)	1
Menopausal status at diagnosis*‡		
Premenopausal	6 (6)	28 (10)
Postmenopausal	90 (92)	254 (89)
Perimenopausal	2 (2)	1
Unknown	0	2
Treatment§		
Radiotherapy	65 (66)	212 (74)
Chemotherapy	7 (7)	22 (8)
Tamoxifen treatment	23 (24)	58 (20)
Other hormonal therapy	6 (6)	16 (6)

*Breast cancer †Breast and endometrial cancers. ‡Premenopausal = last menstruation <3 mo previously; postmenopausal = last menstruation >1 yr previously. §Treatment within matched intervals; percentages add to more than 100 because of overlapping categories.

Table 1: **Characteristics of case patients with endometrial cancer after breast cancer and matched controls**

Results

Most of the women were over 55 years old and postmenopausal when breast cancer was diagnosed (table 1). Date of birth was matched within 1 year for 78% of controls and within 2 years for 94%. Most (74%) of the endometrial cancers occurred in patients whose breast cancer had been diagnosed in the 1980s. 89% of controls matched cases within 1 year for diagnosis of breast cancer. The median time between the diagnoses of breast cancer and endometrial cancer was 34 (5–201) months. More cases than controls were diagnosed with advanced breast cancer (9 *vs* 4%, p = 0·03, Fisher's exact test). Controls were slightly more likely than case patients to have received

	Cases	Controls	Matched RR (95% CI)
Duration (mo)			
Never	75	227	1·0
≤12	6	28	0·6 (0·2–1·7)
13–24	7	14	1·9 (0·6–5·8)
25–60	7	12	2·2 (0·8–6·5)
>60	3	4	3·0 (0·6–15·8)
Cumulative dose (mg)			
0	75	227	1·0
1·8670	3	17	0·7 (0·2–2·3)
8671–14 680	5	16	0·8 (0·2–2·6)
14 681–31 720	8	12	2·5 (0·9–7·1)
>31 720	7	13	2·1 (0·7–6·0)

Table 2: **Relative risk (RR) of endometrial cancer according to total duration of tamoxifen use and cumulative dose**

radiotherapy for breast cancer. However, there were no significant differences between endometrial cancer patients and controls in the types of treatments used for breast cancer.

24% of the case patients and 20% of controls had used tamoxifen at some time, and the relative risk of endometrial cancer for women who had ever been treated with tamoxifen compared with those who had not was 1·3 (95% CI 0·7–2·4). The median duration of tamoxifen use was higher for case patients than for controls (19 *vs* 13 months, p = 0·07). The risk of endometrial cancer increased with duration (table 2). Women who had used tamoxifen for more than 2 years had a 2·3 (0·9–5·9) times greater risk of endometrial cancer than never users and the risk rose to 3·0 (0·6–15·8) for those treated for more than 5 years. None of the risk estimates for categories of duration reached significance, but the inclusion of duration of tamoxifen use as a linear continuous variable in the logistic regression model produced a significant trend (p = 0·049). The cumulative dose of tamoxifen was also associated with the risk of endometrial cancer (table 2, p for trend = 0·046). The effect of tamoxifen was best fitted by including a binary term (ever/never use) and the log-transformed duration of tamoxifen use as a continuous variable in the model (p = 0·026). Similar duration and dose-response patterns were found when analyses were restricted to the 89 women (and their matched controls) in whom endometrial cancer was diagnosed more than 1 year after the initial breast cancer diagnosis. Adjustment for the variables chemotherapy, radiotherapy, hormonal treatment other than tamoxifen, and stage of breast cancer did not substantially alter the risk estimates in table 2.

Of the 81 tamoxifen users in our study, most (59%) had received daily doses of 40 mg, 17% received 30 mg, and 23% received 20 mg or less. We attempted to separate the effects of dose intensity, duration of tamoxifen use, and cumulative dose. The average dose of tamoxifen taken daily did not affect the risk of endometrial cancer in a model accounting for total duration of use (p = 0·54). The inclusion of dose intensity in the model hardly affected the duration-response trend (0·05). To explore further the effect of dose intensity, duration-response slopes were fitted simultaneously for women who had received 40 mg daily and those who received 30 mg or less. The relative risk per year of tamoxifen use (with a multiplicative model, based on actual months of use) was 1·22 for a daily dose of 30 mg or less and 1·24 for 40 mg (tests for linear trend p = 0·18 and p = 0·10, respectively). The two doses did not differ in duration-response trends (p = 0·73).

Within the case group, we studied whether the endometrial cancers in women who had used tamoxifen had different characteristics from those diagnosed in women who had never been treated with the drug (table 3). The stage distributions[15] and morphology of the endometrial cancers in these two groups showed no striking differences. During median follow-up of 15 months after the diagnosis of endometrial cancer, none of the tamoxifen-treated women died of this cancer. Median follow-up in never users was 29 months. 2-year actuarial survival after the diagnosis of endometrial cancer was similar for women who had received breast cancer treatment with tamoxifen and for those who had never received the drug (68% and 71%, respectively).

	No (%)	
	Never users (n = 75)	Ever users (n = 23)
Stage*		
I	62 (83)	17 (74)
II	7 (9)	3 (13)
III	1 (1)	0
IV	1 (1)	0
Unknown	4 (5)	3 (13)
Morphology		
Adenocarcinoma	54 (72)	15 (65)
Papillary adenocarcinoma	13 (17)	4 (17)
Clear cell adenocarcinoma	2 (3)	1 (4)
Adenosquamous carcinoma	3 (4)	1 (4)
Adenoacanthoma	3 (4)	2 (9)
Treatment		
Surgery alone	29 (39)	11 (48)
Surgery + RT	34 (45)	6 (26)
Surgery + HT	6 (8)	4 (17)
HT ± RT	2 (3)	1 (4)
None	4 (5)	1 (4)
Deaths		
Total	25 (33)	9 (39)
Breast cancer	13	4
Endometrial cancer	4	0
All other causes	5	4
Unknown	3	1

RT = radiotherapy; HT = hormonal therapy. *FIGO.[16]

Table 3: **Characteristics of patients with endometrial cancer according to use of tamoxifen**

Discussion

Our results support the hypothesis that use of tamoxifen increases the risk of endometrial cancer. We found a significant trend in risk of endometrial cancer with total duration of tamoxifen treatment, whatever the dose intensity.

In interpreting our results we considered several potential sources of bias. Increased medical surveillance in tamoxifen users, as well as the presence of gynaecological symptoms due to tamoxifen treatment (eg, vaginal bleeding) might lead to earlier diagnosis of endometrial cancer in such women than in untreated patients, which might result in a spurious association between tamoxifen and endometrial cancer. We found no evidence for such bias. First, the stage distribution of the endometrial cancers did not differ between ever and never users. Furthermore, women who had used tamoxifen for a year or less did not have an increased risk of endometrial cancer, and in the (small) subgroup of endometrial cancers diagnosed within 1 year from the breast cancer diagnosis we found no association with tamoxifen use.

Since the Netherlands did not have a nationwide cancer registry in the 1970s and early 1980s, some patients with endometrial cancer after breast cancer were not eligible for our study, solely because there was no sampling frame for control breast cancer patients diagnosed in the same

calendar period. Although this feature reduces the study's power, we do not believe that it introduces bias to our results. For each endometrial cancer case included in the study, all the corresponding matched controls were drawn from a source that also included the breast cancer diagnosis of the case patient. Given this design, selection bias could arise only in the unlikely event that an association between tamoxifen and risk of endometrial cancer depended on the presence of a regional cancer registry at the time of the breast cancer diagnosis.

By matching controls with case patients, we incorporated adjustment for important confounders such as age and calendar year at breast cancer diagnosis. The additional matching, according to the pathology laboratory where the breast cancer diagnosis was made, was introduced for practical reasons, and enabled us to include case patients with a long time between the diagnoses of endometrial and breast cancer. However, matching for pathology laboratory may have resulted in greater similarity in treatment between case patients and controls than would otherwise have been observed. This notion is not just theoretical, since the introduction date of tamoxifen, the indications for its use, and the dose and duration of administration have varied between regions in the Netherlands. Overmatching may thus have led us to underestimate risk of endometrial cancer associated with tamoxifen use. On the other hand, we may have adjusted for determinants of regional differences in incidence of endometrial cancer. Since the possibility of overmatching cannot be excluded, our risks must be viewed as minimum estimates of the true effect of tamoxifen.

Evidence for an association between the use of tamoxifen and risk of endometrial cancer has, to date, come from only two other studies. In the Stockholm trial[4] the relative risk was 6·4 ($p<0·01$) for women who received 40 mg/day tamoxifen for at least 2 years compared with untreated women. In the Danish studies[8,9] there was a non-significant three-fold excess in women who received 30 mg daily for 48 weeks compared with untreated women. These estimates were based on 15 and 20 cases of endometrial cancer, respectively. Our risk estimates, based on much larger numbers of cases, are somewhat lower than these previous estimates (relative risk 2·3 for 2 years' use, 3·0 for >5 years' use), possibly because of overmatching in the study design. In several other large trials of adjuvant tamoxifen therapy, no increased risk of endometrial cancer has been observed.[3,7,16] However, no full statistical evaluation of second cancer incidence in these trials has been published, and incomplete registration of second cancers, or lack of sufficient follow-up time, may have led to negative findings in some trials.

The observation of increased risk of endometrial cancer after tamoxifen treatment is biologically plausible and may be explained as a partial oestrogen-agonistic effect of tamoxifen on the endometrium.[17,18] Endometrial lesions, such as hyperplasia, are more common in breast cancer patients who have received a cumulative dose of tamoxifen of 15 g or more than in those receiving smaller doses.[19] Interestingly, in our study the risk of endometrial cancer was also increased only after cumulative doses above 15 g. It has been suggested that the oestrogenic effect of tamoxifen, especially the proliferative effect on the endometrium, depends upon the dose intensity of the drug. Our results do not support this suggestion. We must emphasise, however, that few women in our study received 30 mg daily or less, and neither of the duration-response trends for the two subcategories of tamoxifen dose intensity reached statistical significance. Numbers did not permit a separate risk calculation for women who took 20 mg per day, which is the dose used in the continuing chemoprevention trials. The Danish study[8,9] also reported increased risk (though not significantly) of endometrial cancer at a dose of 30 mg. Oestrogenic effects of a daily dose of 20 mg tamoxifen on the postmenopausal vagina have also been reported.[20,21] With regard to a similar association, that between postmenopausal oestrogen replacement therapy and risk of endometrial cancer, elevated risks have also been reported for the lowest dose levels.[22]

It has been postulated that any increase of endometrial cancer risk due to the oestrogenic effects of tamoxifen would yield a high proportion of highly differentiated, prognostically favourable tumours, as has been observed with endometrial carcinomas associated with oestrogen replacement therapy.[23-25] We found no substantial differences in histological features of the endometrial cancers diagnosed in tamoxifen-treated patients and in non-treated women. The only suggestion of a difference was in the proportion of well-differentiated tumours (52% in tamoxifen users and 32% in women not treated with tamoxifen). Since the histological slides of endometrial cancers were not reviewed centrally, this finding must be interpreted cautiously. In Magriples and colleagues' study[26] of the clinical and histological features of endometrial cancers in breast cancer patients who had or had not received tamoxifen, there was a significant excess of poorly differentiated tumours in the tamoxifen-treated group'[26] However, the number of tamoxifen users in that study, as well as in ours, was small (15 and 23, respectively), and in both studies the age distribution of the tamoxifen-treated group differed from that in the untreated patients. A much larger patient population would be needed to refute or confirm an association between tamoxifen use and specific histological characteristics of endometrial cancer.

Increased risk of endometrial cancer after tamoxifen use will cause some morbidity in breast cancer patients treated with the drug. However, the proven clinical benefit of tamoxifen in controlling breast cancer[1] clearly outweighs the modest increase of endometrial cancer risk. Endometrial cancer has a more favourable prognosis than breast cancer, so no patient should be denied tamoxifen treatment of her breast tumour because of anticipated adverse effects on the endometrium.

The issue of whether tamoxifen should be used to prevent cancer in healthy women, who do not have a medical need for treatment, is different, however. Even if, at the population level, the postulated reduction in the incidence of breast cancer were to outweigh the apparently increased risk of endometrial cancer, it is debatable whether the use of a medical intervention can be justified when it prevents breast cancer in some women at the cost of inducing endometrial cancer in others. This issue will continue to provoke discussion in the medical community,[27-29] until more is known about tamoxifen's long-term benefits and adverse effects. Further studies are needed to quantify the risk for women taking 30 mg or 20 mg per day, to assess the effect of very long durations of use (5 years or more), and to determine the risk for ex-users.

Meanwhile, we believe that, on the basis of our results, physicians should be alert to the higher risk of endometrial cancer in all women using tamoxifen, both breast cancer patients and healthy participants in prevention trials. Regular gynaecological examinations may be worth while for long-term users.

We thank Dr I J A M G Casparie-van Velsen (Dutch Network and National Database for Pathology), Prof H J A Collette (Department of Epidemiology, University of Utrecht), and the hospital cancer registries of the Netherlands Cancer Institute and the Dr Daniel den Hoed Cancer Center for making control selection possible; the treating specialists for providing access to patients' medical charts; and the abstracting teams from the regional cancer registries for data collection. This study was supported partly by a grant (NKI 88–11) from the Dutch Cancer Society.

References

1 Early Breast Cancer Trialists' Collaborative Group. Systemic treatment of early breast cancer by hormonal, cytotoxic, or immune therapy: 133 randomised trials involving 31 000 recurrences and 24 000 deaths among 75 000 women. *Lancet* 1992; **339:** 1–15, 71–85.
2 CRC Adjuvant Breast Trial Working Party. Cyclophosphamide and tamoxifen as adjuvant therapies in the management of breast cancer. *Br J Cancer* 1988; **57:** 604–07.
3 Fisher B, Constantino J, Redmond C, et al. A randomized trial evaluating tamoxifen in the treatment of patients with node-negative breast cancer who have estrogen-receptor-positive tumors. *N Engl J Med* 1989; **320:** 489–84.
4 Fornander T, Rutqvist LE, Cedermark B, et al. Adjuvant tamoxifen in early breast cancers: occurrence of new primary cancers. *Lancet* 1989; i: 117–20.
5 Powles TJ, Tillyer CR, Jones AL, et al. Prevention of breast cancer with tamoxifen: an update on the Royal Marsden pilot programme. *Eur J Cancer* 1990; **26:** 680–84.
6 Fisher B, Redmond C. New perspective on cancer of the contralateral breast: a marker for assessing tamoxifen as a preventive agent. *J Natl Cancer Inst* 1991; **83:** 1278–80.
7 Nayfield SG, Karp JE, Ford LG, Dorr FA, Kramer BS. Potential role of tamoxifen in prevention of breast cancer. *J Natl Cancer Inst* 1991; **83:** 1450–59.
8 Andersson M, Storm HH, Mouridsen HT. Incidence of new primary cancers after adjuvant tamoxifen therapy and radiotherapy for early breast cancer. *J Natl Cancer Inst* 1991; **83:** 1013–17.
9 Andersson M, Storm HH, Mouridsen HT. Carcinogenic effects of adjuvant tamoxifen treatment and radiotherapy for early breast cancer. *Acta Oncol* 1992; **31:** 259–63.
10 Sunderland MC, Osborne CK. Tamoxifen in premenopausal patients with metastatic breast cancer: a review. *J Clin Oncol* 1991; **9:** 1283–97.
11 LOK/Coordinating Council of Comprehensive Cancer Centers, ed. Incidence of cancer in the Netherlands 1989: First report of the Netherlands Cancer Registry. Utrecht: LOK, 1992.
12 Muir C, Waterhouse J, Mack T, et al, eds. Cancer incidence in five continents, vol V, no 88. Lyon: IARC Scientific Publications, 1987.
13 Collette HJA, Day NE, Rombach JJ, De Waard F. Evaluation of screening for breast cancer in a non-randomised study (the DOM project) by means of a case-control study. *Lancet* 1984; i: 1224–26.
14 Breslow NE, Day NE. Statistical methods in cancer research: the analysis of case-control studies, vol 1, no 32. Lyon: IARC Scientific Publications, 1980.
15 Creasman WT. New gynecologic cancer staging. *Obstet Gynecol* 1990; **75:** 287–88.
16 Stewart HJ, Knight GM. Tamoxifen and the uterus and endometrium. *Lancet* 1989; **1:** 375–76.
17 Gottardis MM, Robinson SP, Satyaswaroop PS, Jordan VC. Contrasting actions of tamoxifen on endometrial and breast cancer tumor growth in the athymic mouse. *Cancer Res* 1988; **48:** 812–15.
18 Boccardo F, Guarnieri D, Rubagotti A, et al. Endocrine effects of tamoxifen in postmenopausal breast cancer patients. *Tumori* 1984; **70:** 61–68.
19 De Muylder X, Neven P, De Somer M, Van Belle Y, Vanderick G, De Muylder E. Endometrial lesions in patients undergoing tamoxifen therapy. *Int J Gynaecol Obstet* 1991; **36:** 127–30.
20 Ferrazzi E, Cartei G, Mattarazzo R, Fiorentino M. Oestrogen-like effect of tamoxifen on vaginal epithelium. *BMJ* 1977; i: 1351–52.
21 Boccardo F, Bruzzi P, Rugagotti A, et al. Estrogen-like action of tamoxifen on vaginal epithelium in breast cancer patients. *Oncology* 1981; **38:** 281–85.
22 Grady D, Rubin SM, Petitti DB, et al. Hormone therapy to prevent disease and prolong life in postmenopausal women. *Ann Intern Med* 1992; **117:** 1016–37.
23 Elwood JM, Boyes DA. Clinical and pathological features and survival of endometrial cancer patients in relation to prior use of estrogens. *Gynecol Oncol* 1980; **10:** 173–87.
24 Buring JE, Bain CJ, Ehrmann RL. Conjugated estrogen use and risk of cancer registries. *Am J Epidemiol* 1986; **124:** 434–41.
25 Collins J, Donner A, Allen LN, Adams O. Oestrogen use and survival in endometrial cancer. *Lancet* 1980; i: 961–14.
26 Magriples U, Naftolin F, Schwartz PE, Carcangiu ML. High-grade endometrial carcinoma in tamoxifen-treated breast cancer patients. *J Clin Oncol* 1993; **11:** 485–90.
27 Fugh-Berman A, Epstein S. Tamoxifen: disease prevention or disease substitution? *Lancet* 1992; **340:** 1143–45.
28 Powles TJ. The case for clinical trials of tamoxifen for prevention of breast cancer. *Lancet* 1992; **340:** 1145–47.
29 Neven P. Tamoxifen and endometrial lesions. *Lancet* 1993; **342:** 452.

Short reports

α_1-antitrypsin deficiency in intracranial aneurysms and cervical artery dissection

Wouter I Schievink, Udaya B S Prakash, David G Piepgras, Bahram Mokri

The pathogenesis of ruptured intracranial aneurysms and cervical artery dissections is poorly understood but may be similar in these two disorders. We report four patients with α_1-antitrypsin deficiency who developed a ruptured intracranial aneurysm or spontaneous dissection of the cervical internal carotid artery. Three patients were heterozygous for the deficient allele (PiMZ or PiGZ) and one was homozygous (PiZZ). A deficiency of α_1-antitrypsin or one of the other protease inhibitors could result in degradation of the arterial wall through an imbalance between proteolytic enzymes and their inhibitors, thereby predisposing the arterial wall to dissection or aneurysm formation.

Lancet 1994; **343:** 452–53

The pathogenesis of ruptured intracranial aneurysms and spontaneous cervical artery dissections is not well understood but an underlying arteriopathy is usually suspected. Except for some patients with fibromuscular dysplasia or certain heritable connective tissue disorders, investigations into the nature of this arteriopathy have been unsuccessful.[1] Deficiencies of α_1-antitrypsin or other inhibitors of proteolytic enzymes may have a role in the development of abdominal arterial aneurysms.[2,3] Such deficiency could undermine the integrity of the vascular extracellular matrix, predisposing the arterial wall to dissection or aneurysm formation. We report a group of patients with α_1-antitrypsin deficiency who developed aneurysmal subarachnoid haemorrhage or spontaneous cervical artery dissection.

All patients with α-antitrypsin deficiency, who were evaluated at the Mayo Clinic between 1976 and 1992, were identified through a computerised and coded diagnostic index. This group consisted of 168 women and 194 men (mean age 48·1 years). All had symptoms of α_1-antitrypsin deficiency, which had been diagnosed with similar methods throughout the study period. During this time, about 140 patients with spontaneous carotid dissection and 1250 patients with aneurysmal subarachnoid haemorrhage were seen at our institution.

CANCER THERAPY

Ex vivo culture of circulating breast tumor cells for individualized testing of drug susceptibility

Min Yu,[1,2]* Aditya Bardia,[1,3] Nicola Aceto,[1] Francesca Bersani,[1] Marissa W. Madden,[1] Maria C. Donaldson,[1] Rushil Desai,[1] Huili Zhu,[1] Valentine Comaills,[1] Zongli Zheng,[1,4,5] Ben S. Wittner,[1] Petar Stojanov,[6] Elena Brachtel,[4] Dennis Sgroi,[1,4] Ravi Kapur,[7] Toshihiro Shioda,[1,3] David T. Ting,[1,3] Sridhar Ramaswamy,[1,3] Gad Getz,[1,6,8] A. John Iafrate,[1,4] Cyril Benes,[1,3] Mehmet Toner,[7,8] Shyamala Maheswaran,[1,3]† Daniel A. Haber[1,2,3]†

Circulating tumor cells (CTCs) are present at low concentrations in the peripheral blood of patients with solid tumors. It has been proposed that the isolation, ex vivo culture, and characterization of CTCs may provide an opportunity to noninvasively monitor the changing patterns of drug susceptibility in individual patients as their tumors acquire new mutations. In a proof-of-concept study, we established CTC cultures from six patients with estrogen receptor–positive breast cancer. Three of five CTC lines tested were tumorigenic in mice. Genome sequencing of the CTC lines revealed preexisting mutations in the *PIK3CA* gene and newly acquired mutations in the estrogen receptor gene (*ESR1*), *PIK3CA* gene, and fibroblast growth factor receptor gene (*FGFR2*), among others. Drug sensitivity testing of CTC lines with multiple mutations revealed potential new therapeutic targets. With optimization of CTC culture conditions, this strategy may help identify the best therapies for individual cancer patients over the course of their disease.

Circulating tumor cells (CTCs) are present in the blood of many patients with solid tumors. Most of these cells, which are thought to be involved in metastasis, die in the circulation, presumably due to the loss of matrix-derived survival signals or circulatory shear stress. Nonetheless, if CTCs can be isolated from cancer patients as viable cells that can be genotyped and functionally characterized over the course of therapy, they have the potential to identify treatments that most effectively target the evolving mutational profile of the primary tumor (*1*). The isolation of viable CTCs is technically challenging: Most methods yield low numbers of partially purified CTCs that are fixed before isolation, damaged during the cell purification process, or irreversibly immobilized on an adherent matrix [see review (*2*)]. We recently reported a microfluidic technology, the CTC-iChip, which efficiently depletes normal blood cells, leaving behind unmanipulated CTCs (*3*). The cytological appearance, staining properties, and intact RNA evident within a subset of CTCs isolated by means of this tumor antigen-agnostic CTC isolation platform suggested that the cells may be viable.

To investigate whether the CTCs were in fact viable, we applied the CTC-iChip to blood samples from patients with metastatic estrogen receptor (ER)–positive breast cancer. After testing a range of culture conditions (*4*–*7*) (see supplementary methods), we found that CTCs proliferated best as tumor spheres when cultured in serum-free media supplemented with epidermal growth factor (EGF) and basic fibroblast growth factor (FGF) (*8*) under hypoxic conditions (4% O_2) (Fig. 1A). Nonadherent culture conditions were critical, because CTCs senesced after a few cell divisions in adherent monolayer culture (fig. S1). We established long-term oligoclonal CTC

[1]Massachusetts General Hospital Cancer Center, Harvard Medical School, Charlestown, MA 02129, USA. [2]Howard Hughes Medical Institute, Chevy Chase, MD 20815, USA. [3]Department of Medicine, Harvard Medical School, Charlestown, MA 02129, USA. [4]Department of Pathology, Harvard Medical School, Charlestown, MA 02129, USA. [5]Department of Medical Epidemiology and Biostatistics, Karolinska Institutet, Stockholm, Sweden. [6]Broad Institute of Harvard and MIT, Cambridge, MA 02142, USA. [7]Center for Bioengineering in Medicine, Harvard Medical School, Charlestown, MA 02129, USA. [8]Department of Surgery, Harvard Medical School, Charlestown, MA 02129, USA. *Present address: Department of Stem Cell Biology and Regenerative Medicine, University of Southern California, Los Angeles, CA 90033, USA. †Corresponding author. E-mail: maheswaran@helix.mgh.harvard.edu (S.M.); haber@helix.mgh.harvard.edu (D.A.H.)

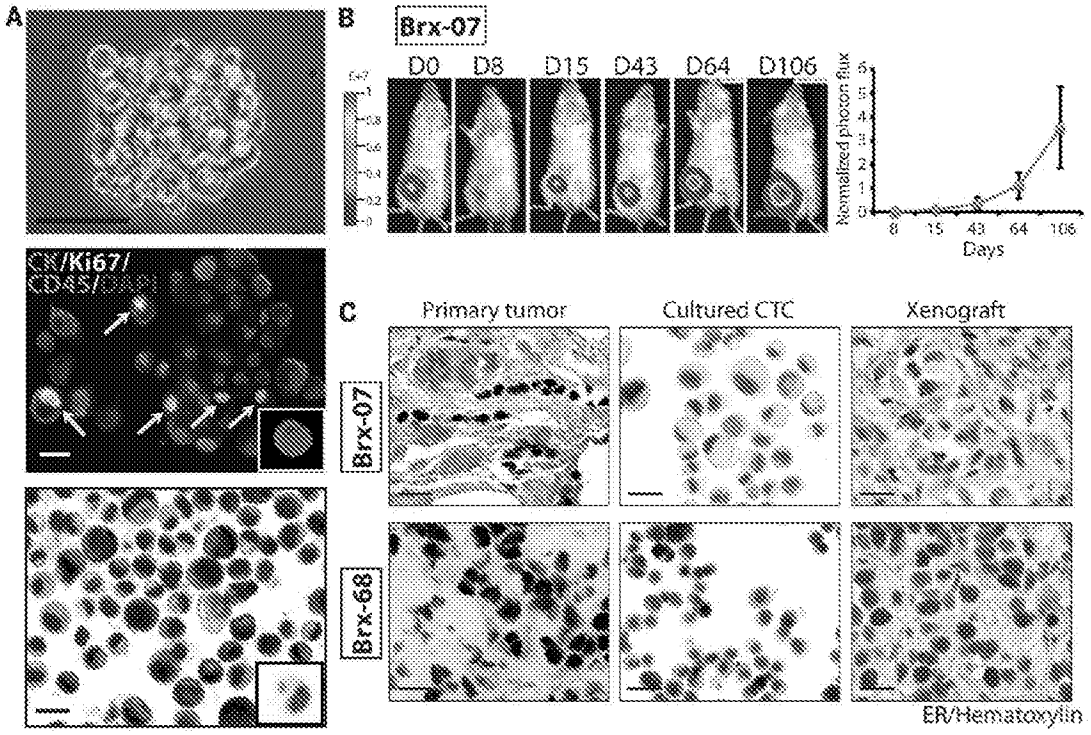


Fig. 1. Ex vivo expansion of breast cancer CTCs. (A) Representative images of nonadherent CTC culture (BRx-07). Top: Phase contrast. Scale bar, 100 μm. Middle: immunofluorescent staining for cytokeratin (CK, red), Ki67 (yellow), CD45 (green), nuclei [4′,6-diamidino-2-phenylindole (DAPI), blue]. Scale bar, 20 μm. Bottom: Light microscopic imaging with Papanicolaou staining. Comparable images for uncultured primary CTCs are shown in the insets. Scale bar, 20 μm. **(B)** (Left) Bioluminescent images showing growth of NSG mouse xenografts, after implantation of 20,000 cultured CTCs (BRx-07) into the mammary fat pad. (Right) Quantification of bioluminescent signals for BRx-07–derived mouse xenografts (mean ± SD, $n = 6$). **(C)** Histology of matched primary breast tumors, cultured CTCs, and CTC-derived mouse xenografts for two CTC lines. All panels show cellular staining with hematoxylin (blue) and immunohistochemical staining for ER expression (brown). Scale bar, 20 μm.

Downloaded from http://science.sciencemag.org/ on July 6, 2016

cultures (sustained in vitro for >6 months) from CTCs isolated from six patients with metastatic luminal subtype breast cancers (table S1). One or more CTC cell lines were successfully generated from 6 of 36 patients who were either off therapy or progressing on treatment. We were unable to generate CTC cell lines from nine patients who were responding to treatment at the time of attempted CTC culture. For three patients, four additional CTC cell lines were established from blood samples drawn at multiple different time points during therapy (table S1). In these cases, CTCs were successfully cultured only when patients were progressing on treatment (fig. S1).

Cultured CTCs shared cytological features with the matched primary CTCs captured on the CTC-iChip (Fig. 1A), and consistent with standard CTC definitions, they stained positive for epithelial cytokeratin (>95% of cells) and negative for the leukocyte marker CD45 (Fig. 1A) (fig. S2). The proliferative index of CTC cultures was ~30%, as defined by Ki67 staining (mean 28.1%, range 24 to 32%), and the initial doubling time of CTC cultures varied from 3 days to 3 weeks (table S1). All six primary tumors were positive for ER expression. Five CTC lines retained ER positivity in culture (>10% of cells), whereas one line (BRx-07) lost ER expression in vitro (Fig. 1C and fig. S2).

We undertook RNA sequencing analysis of each cell line and compared the results with those of 29 uncultured single CTCs from a total of 10 patients, as well as a panel of 13 commonly used established breast cancer cell lines, all using low-template single-cell resolution analysis (fig. S3). CTC cultures clustered with each other, and separately from established breast cancer cell lines or uncultured single CTCs. As expected, both CTC cultures and established breast cancer cell lines had increased proliferative signature, compared with primary uncultured single CTCs (fig. S3). We did not observe increased expression in CTC cultures of defined signaling pathways, including stem cell–related signatures, compared with established breast cancer cell lines.

To test the tumorigenicity of CTC lines, we used lentiviral transduction to label them with both green fluorescent protein (GFP) and luciferase and inoculated 20,000 cells into the mammary fat pad of immunosuppressed non-obese diabetic *scid* gamma (NSG) female mice implanted with subcutaneous estrogen pellets. Of five CTC lines tested, three (BRx-07, BRx-68, and BRx-61) generated tumors within 3 months at this low inoculum (Fig. 1B and figs. S4 and S5). CTC-derived tumors shared histological and immunohistochemical features with the matched primary patient tumor, including BRx-07, which regained ER expression (Fig. 1C).

All six patients with metastatic breast cancer had received sequential courses of hormonal and other therapies before CTC collection (fig. S6). As part of standard clinical care at Massachusetts General Hospital, a mutational panel [SNaPShot (*9*)] covering ~140 mutations in 25 genes had been performed on primary tumor specimens (BRx-68 and BRx-42) or on pretreatment biopsies of metastatic lesions (BRx-33, BRx-07, BRx-50 and BRx-61). Point mutations in *PIK3CA* (H1047R and G1049R), hot-spot mutations in breast cancer, were identified in two cases (BRx-68 and BRx-42), whereas no mutations were found in the four other cases (table S1). The availability of CTC cultures made it possible to undertake more comprehensive mutational analysis from a more abundant and purified tumor cell population. CTC lines were screened for mutations in a panel of 1000 annotated cancer genes, with a hybrid-capture–based next-generation sequencing (NGS) platform. The *PIK3CA* mutations identified by SNaPShot testing of primary tumors were confirmed by NGS in both CTC cultures (BRx-68 and BRx-42), and multiple additional mutations in other cancer-related genes were identified (Table 1). For all mutations identified in the 1000 cancer gene panel, candidate driver mutations were defined by their absence from matched germline DNA and by their annotation in pan-cancer (*10*) and COSMIC (Catalogue of somatic mutations in cancer) databases (Table 1), whereas additional mutations in known cancer genes were of uncertain relevance (table S2). To ensure that the candidate driver mutations were not acquired during the in vitro establishment of CTC cell lines, we tested for selected mutations in four additional CTC lines, which had been independently isolated at different time points from each of three patients (BRx-68, BRx-42, and BRx-61). The acquired

Table 1. Mutations detected in cultured CTC lines.

Case	Gene	DNA	Protein	Allele frequency†	In pretreatment tumor‡	In multiple CTC lines	Known mutation§
BRx33‖	ESR1	A1613G	D538G	0.24	–	–	Br,# En
	NUMA1	C5501T	S1834L	0.39	–	–	Br
BRx07‖	TP53	G853A	E285K	0.99	No	–	Bl, Br, Co, HN, Lu
	PIK3CA	A3140T	H1047L	1	No	–	Br, Co, GBM, HN, K_i, Lu, Me, Mel, Ov, En
	FGFR2	T1647A	N549K	0.46	No	–	Br, En
	CDH1	C790T	Q264*	1	Yes	–	Br
	APC	G7225A	G2409R	0.47	Yes	–	Mel
	DGKQ	G2530A	D844N	0.55	–	–	Lu
	MAML2	A2569G	M857V	0.52	–	–	Lu
BRx68	TP53	C1009T	R337C	0.99	No	Yes	Br, Co, HN, Hem, Ov
	ESR1	A1610C	Y537S	0.47	No	Yes	Br#, En
	PIK3CA	A3140G	H1047R	0.7	Yes	Yes	Br, Co, GBM, HN, K_i, Lu, Me, Mel, Ov, En
	MSN	G1153A	E385K	0.25	–	–	En
BRx50‖	ESR1	T1607C	L536P	0.06††	–	–	Br#
	IKZF1	G1444T	G482C	0.09	–	–	Hem
	BRCA2¶	T6262del	L2039fs	–	–	–	Br (germ line)
BRx42	PIK3CA	G3145C	G1049R	0.60	Yes	Yes	Br, En, K_i
	PIK3CA	C1097G	P366R	0.54	–	–	Br
	KRAS	G35T	G12V	0.99	No	Yes	Br, Co, Hem, Es, GBM, Lu, Ov, En
	IGF1R	G3613A	A1205T	0.06	–	–	Hem
BRx61	TP53	G610T	E204*	0.98	No	Yes	Bl, Br, K_i, Lu, Ov

†Mutant allele frequency within oligoclonal cultured CTC populations was calculated as the ratio of mutant sequence reads to total reads for each gene. ‡Where sufficient material was available for analysis, matched archival pretreatment tumor specimens were subjected to Sanger sequencing to confirm selected mutations identified in CTC cultures. Insufficient tumor material is marked (–). §List of tumor types reported to harbor the same mutation in pan-cancer (*10*) or COSMIC databases. Abbreviations: breast (Br), endometrial (En), central nervous system (CNS), bladder (Bl), colorectal (Co), pancreas (Pa), stomach (St), head and neck (HN), lung (Lu), thyroid (Th), glioblastoma (GBM), kidney (Ki), prostate (Pr), medulloblastoma (Me), melanoma (Mel), ovarian (Ov), cervix (Ce), esophageal (Es), hematopoietic and lymphoid tissue (Hem), sarcoma (Sar), cholangiocarcinoma (Ch). ‖Cases for which DNA from matched normal tissue was not available. ¶Germline BRCA2 mutation was detected as part of genetic counseling for familial breast cancer. #Mutations reported in recent publications (*12*–*15*). ††ESR1 T1607C mutant allele frequency increased to 0.49 after prolonged in vitro culture under low-estrogen conditions (>6 months). *Chain termination codon. fs: frameshift mutation. Abbreviations for amino acid residues: A, Ala; C, Cys; D, Asp; E, Glu; F, Phe; G, Gly; H, His; I, Ile; K, Lys; L, Leu; M, Met; N, Asn; P, Pro; Q, Gln; R, Arg; S, Ser; T, Thr; V, Val; W, Trp; and Y, Tyr.

Downloaded from http://science.sciencemag.org/ on July 6, 2016

mutations in *ESR1* (BRx-68), *TP53* (BRx-68, BRx-61), and *KRAS* (BRx-42) were universally present in all independent CTC cell lines (Table 1), confirming that they are tumor-derived mutations. In addition, the *ESR1* mutation (Y537S) present in multiple BRx-68 CTC lines was also detectable by direct RNA sequencing of uncultured CTCs isolated from this patient (fig. S7).

Activating mutations in the estrogen receptor (*ESR1*) were first identified in 1997 and are rare in primary breast cancer (*11*). While this manuscript was in preparation, multiple research groups reported *ESR1* mutations in 18 to 54% of patients treated with aromatase inhibitors (AIs), drugs that suppress estrogen synthesis and thus may favor the emergence of these ligand-independent ER mutants (*12*–*15*). We also detected *ESR1* mutations in three of six CTC lines (BRx-33, BRx-68, and BRx-50). Each of these patients had received extensive treatment with AIs, and reanalysis of the primary tumor or the pre-AI treatment biopsy of a metastatic lesion showed no evidence of *ESR1* mutations (Table 1). Other mutations identified included newly arising mutations in *PIK3CA*, *TP53*, *KRAS*, and fibroblast growth factor receptor–2 (*FGFR2*) (Table 1). Consistent with its lobular histological subtype, an E-cadherin (*CDH1*) mutation was detected in one CTC line (BRx-07). Although most mutant allele frequencies indicated heterozygous or homozygous truncal mutations shared by all CTCs, rare mutated alleles consistent with emerging tumor subpopulations were also evident. An *ESR1* mutation initially present at 6% allele frequency in BRx-50 increased to 49% allele frequency upon prolonged culture in low-estrogen–containing medium (Table 1), suggesting a proliferative advantage under these conditions. Notably, *TP53* mutations, which are thought to be rare in primary luminal breast cancers (*16*), emerged during tumor progression in three of six cases.

The availability of comprehensive tumor cell genotyping brings with it the challenge of identifying the subset of mutations whose therapeutic targeting is likely to be beneficial to an individual patient. To begin to explore this opportunity, we tested CTC lines for sensitivity to panels of single drug and drug combinations, including standard clinical regimens, as well as experimental agents targeting specific mutations. Conditions were optimized for highly reproducible testing of viability in small numbers of cells (200 cells per well) cultured as aggregates in solution. For each drug, we tested five concentrations (table S3), centered around median inhibitory concentration (IC_{50}) levels established in large-scale cancer cell line screens (*17*), with relative sensitivity or resistance defined by comparison among the CTC cell lines (Fig. 2 and figs. S8 to S10). Although CTC drug sensitivity testing was blinded to clinical history, and patient treatment selections were not informed by CTC testing, some CTC drug sensitivity measurements were concordant with clinical histories, including sensitivity to paclitaxel (BRx-07)

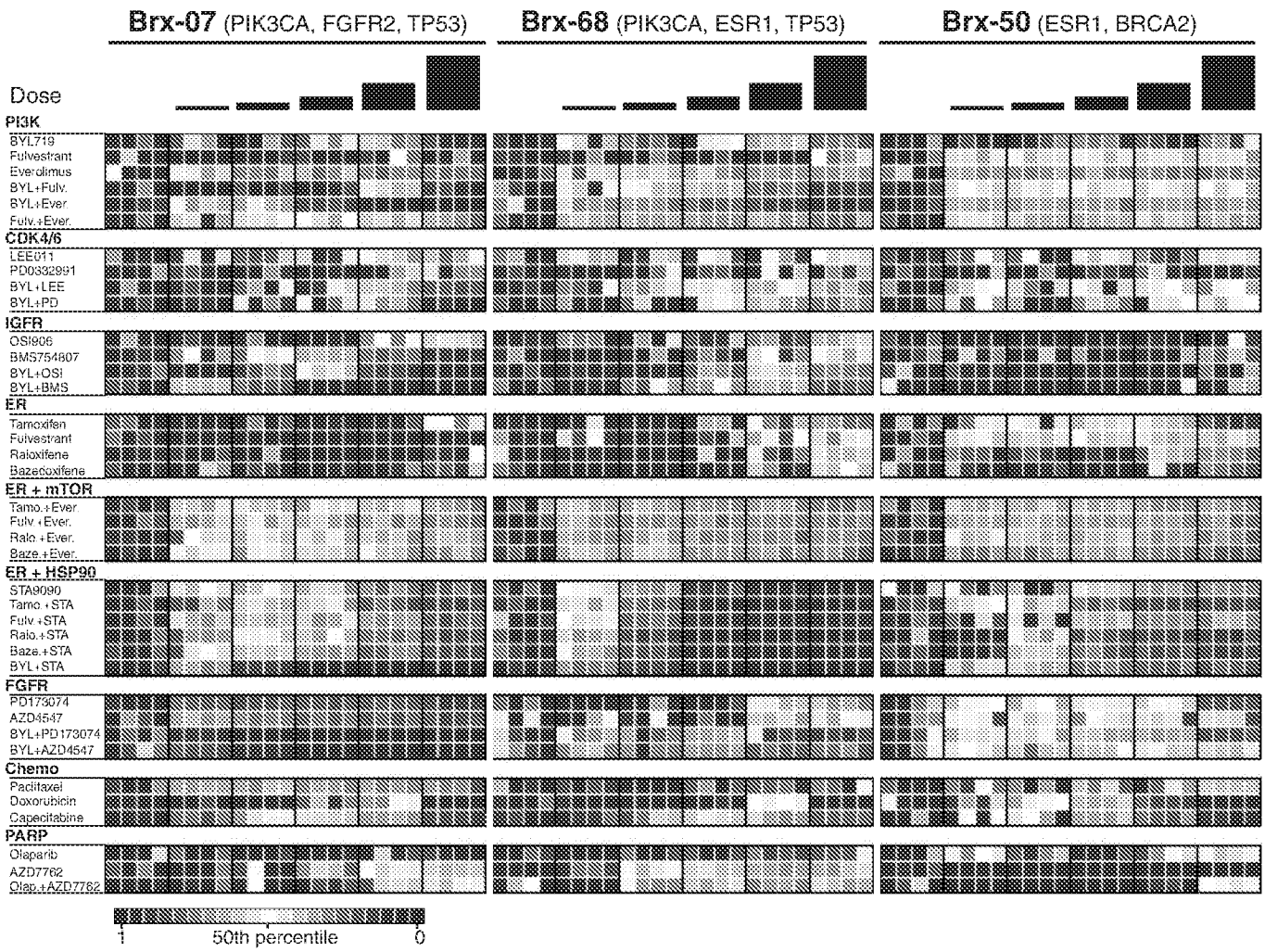


Fig. 2. Drug sensitivity of cultured CTCs. Heatmaps representing cell viability after treatment of BRx-07, BRx-68, and BRx-50 CTC lines with selected anticancer drugs, either alone or in combination. The presumed driving mutation for each CTC line is noted, and drugs are grouped according to therapeutic class and targeted pathway. For each drug, the range of concentrations tested is centered around the IC_{50} derived from large-scale breast cancer cell line screens (*17*), and each concentration represents a twofold increase from the previous dose, with each concentration tested in quadruplicate. Drug concentrations are listed in table S3. Signal from viable cells remaining after drug treatment is normalized to corresponding vehicle [dimethyl sulfoxide (DMSO)]–treated controls, with ratios plotted ranging from red (more viable) to blue (less viable). Drug abbreviations: BYL, BYL719; Fulv, fulvestrant; Ever, everolimus; LEE, LEE011; PD, PD0332991; OSI, OSI906; BMS, BMS754807; Tamo, tamoxifen; Ralo, raloxifene; Baze, bazedoxifene; STA, STA9090; Olap, Olaparib.

Downloaded from http://science.sciencemag.org/ on July 6, 2016

and capecitabine (BRx-68 and BRx-50), and resistance to fulvestrant (BRx-07 and BRx-68), doxorubicin (BRx-07), and olaparib (BRx-50) (fig. S11).

We selected two mutated drug targets identified in CTCs but not in the primary tumor for more detailed analysis; namely, *ESR1* and *PIK3CA* mutations (additional drug responses in cultured CTCs are shown in fig. S12). To facilitate interpretation of the effect of drug combinations, responses to selected drugs are represented in a 2 × 2 matrix highlighting cooperative drug effects versus independent cytotoxicity (Fig. 3; see quantitation in fig. S13). The three de novo acquired *ESR1* mutations affected distinct but adjacent residues within the ER ligand-binding domain and were present at different allele frequencies within the oligoclonal CTC cell lines. The most commonly reported *ESR1* mutation, Y537S (*12–14*), was observed in BRx-68 (47% allele frequency, consistent with a heterozygous mutation in all cells), with two other mutations, D538G and L536P, in BRx-33 and BRx-50 (24 and 6% allele frequencies, respectively). Each mutation arose within the context of distinct additional mutations (Table 1 and table S2). Of note, all *ESR1* mutation-positive CTC lines maintained ER expression in culture.

The optimal therapy for breast cancer patients whose ER$^+$ tumor has acquired an *ESR1* mutation is unknown; consistent with previous models (*12–14*, *18*), we found that the selective estrogen receptor modulators (SERMs) tamoxifen and raloxifene, and the selective ER degrader (SERD) fulvestrant, were ineffective in BRx-68 cells, either alone or in the clinically approved combination with inhibitors of the phosphatidylinositol 3-kinase–mammalian target of rapamycin (PI3K-mTOR) pathway (everolimus) (*19*) (Fig. 2). However, the HSP90 inhibitor STA9090 demonstrated cytotoxicity alone and in combination with both raloxifene and fulvestrant (Fig. 3A). ER is a client protein for HSP90, and mutated receptors are highly dependent on this chaperone for their stability (*20*). Indeed, treatment with a low dose of STA9090 (32 nM) suppressed ER levels in BRx-68 cells but had no effect in MCF7 breast cancer cells with wild-type ER, or in BRx-50 cells, where the low allele frequency of mutant *ESR1* is not associated with sensitivity to HSP90 inhibitors (Fig. 3B and figs. S12 to S14). Clinical studies of HSP90 inhibitors, along with novel ER inhibitors, will be required to define the optimal treatment for breast cancer patients whose tumor has acquired an *ESR1* mutation.

The BRx-07 cell line is noteworthy because it harbors activating mutations in both *PIK3CA* and *FGFR2*, both of which were acquired de novo during the course of therapy. Based on their respective allele frequencies, *PIK3CA* was homozygously mutated in all cells, whereas the *FGFR2* mutation was heterozygous (Table 1). Cultured CTCs were highly sensitive to the PIK3CA inhibitor BYL719 (*21*) and the FGFR2 inhibitor AZD4547 (*22*), and moderately responsive to the FGFR1 inhibitor PD173074 (*23*) (Fig. 2). Combined inhibition of both PIK3CA and FGFR2 showed cooperative effects (Fig. 3C and fig. S13), suggesting that both of these mutations may function as acquired oncogenic drivers in this tumor. Because combinations of PIK3CA and FGFR inhibitors have not been tested in clinical settings, we further quantified responses in a panel of established

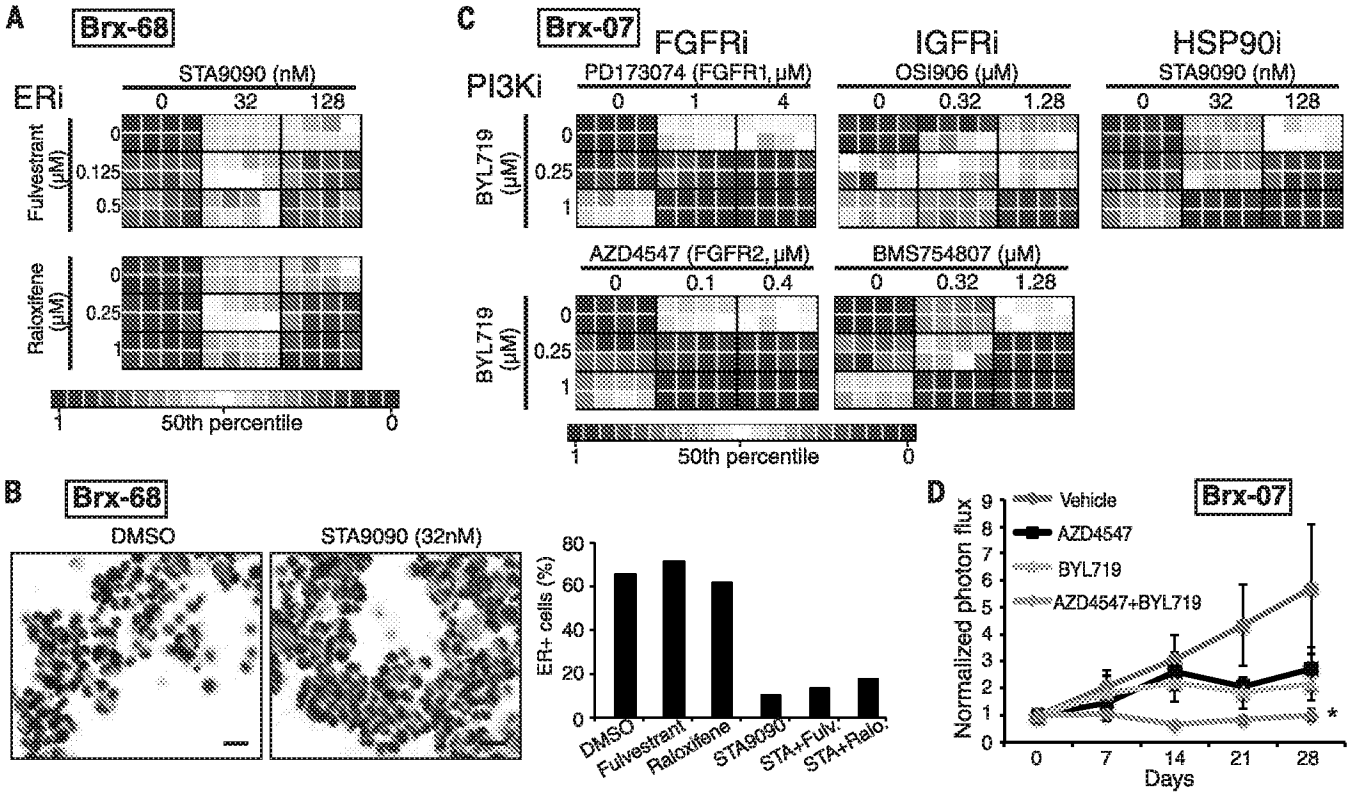


Fig. 3. Combinatorial drug targeting of mutant *ESR1* and *PIK3CA* in CTC lines. (**A**) Heatmaps representing cell viability in the BRx-68 CTC line, carrying an *ESR1* mutation (allele frequency 47%), treated with HSP90 inhibitor (STA9090) together with the selective estrogen receptor modulator (SERM) tamoxifen or degrader (SERD) fulvestrant. For these drug-combination studies, the concentrations of each drug was varied independently, and results are shown in eight replicates. Cooperative drug interactions are represented by a diagonal gradient, showing increasing cell killing as both drug concentrations increase independently. (**B**) Down-regulation of ER protein expression measured by immunohistochemical staining (brown) of BRx-68 CTC cultures treated for 24 hours with an HSP90 inhibitor (STA9090) versus vehicle (DMSO). Nuclei are stained with hematoxylin. Scale bar, 20 μm. Bar graph shows quantification of percent ER-positive cells. More than 200 cells were quantified in each condition. (**C**) Heatmaps representing cell viability in the BRx-07 line harboring mutations in *PIK3CA* (99% allele frequency) and *FGFR2* (46% allele frequency). Drugs targeting the products of these mutated oncogenic drivers were tested, along with compounds inhibiting nonmutated targets (IGFR and HSP90). Drug combinations shown are PI3Ki + FGFRi; PIK3Ki + IGFRi; PIK3Ki + HSP90i. (**D**) Response of BRx-07 CTC-derived mouse xenografts to the PI3K inhibitor BYL719 (n = 4), the FGFR2 inhibitor AZD4547 (n = 3), the combination of the two inhibitors (BYL719+AZD4547) (n = 4), or diluent control (n = 4). Mean ± SD. In vivo drug administration was initiated after mammary fat pad inoculation with genotyped CTC cultures and establishment of an expanding tumor xenograft, and tumor-derived bioluminescent measurements were normalized to pretreatment levels.

Downloaded from http://science.sciencemag.org/ on July 6, 2016

breast cancer cell lines. Of seven *PIK3CA*-mutant breast cancer lines, six were responsive to BYL719 (fig. S15). In addition to their characteristic *PIK3CA* mutation, two lines harbored mutations of unknown importance in *FGFR4* (Y367C; MDA-MB-453 cells) and in *FGFR2* (K570E; EFM-19 cells). The former showed cooperative cytotoxicity by BYL719 and AZD4547, whereas the latter was insensitive to FGFR inhibition (fig. S15). One of five *PIK3CA*-mutant breast cancer lines without an *FGFR* gene mutation showed modest sensitivity to AZD4547 (CAL51), whereas the other four were resistant. Thus, the combination of genotyping and functional testing for drug susceptibility is essential to defining therapeutically relevant driver mutations in both breast cancer cell lines and CTC cultures.

In vitro screening of additional drugs for cooperation with PIK3CA-targeted agents identified inhibitors of the insulin-like growth factor receptor 1 (*IGF1R*, inhibitors OSI906 and BMS754807) and HSP90 (inhibitor STA9090, Ganetespib) (Fig. 3C). Although neither of these is mutated in BRx-07 cells, IGF1R has been implicated in modulating signaling loops that mitigate sensitivity to PI3K inhibitors (*24*), and HSP90 is involved in stabilization of mutant kinases (*20*). To extend drug sensitivity studies to mouse xenografts, we generated BRx-07–derived mammary tumors and treated these with BYL719, AZD4547, the two agents in combination, or diluent control. In vivo tumor suppression was observed after treatment with either drug individually, whereas the combination completely abrogated tumor growth (Fig. 3D).

In this proof-of-concept study, we have shown that the culture of tumor cells circulating in the blood of patients with breast cancer provides an opportunity to study patterns of drug susceptibility, linked to the genetic context that is unique to an individual tumor. In patients with hormone-responsive breast cancer, most of whom have bone metastases that are not readily biopsied, the ability to noninvasively and repeatedly analyze live tumor cells shed into the blood from multiple metastatic lesions may enable monitoring of emerging subclones with altered mutational and drug sensitivity profiles. The successful culture of CTCs stems partly from the application of a microfluidic device capable of effectively depleting leukocytes from a blood specimen while preserving viable tumor cells for ex vivo expansion (*3*). The proliferation of cultured CTCs as nonadherent spheres differs from that of characteristic epithelial cancer cell cultures and may reflect intrinsic properties of tumor cells that remain viable in the bloodstream after loss of attachment to basement membrane. A recent report documented direct inoculation of the mouse femur with blood-derived cancer cells from a patient who had very high numbers of CTCs, but in vitro culture was not successful (*25*). Our results differ from the adherent in vitro CTC cultures described by Zhang *et al.* (*26*), but these lines appear to share the identical *TP53*, *BRAF*, and *KRAS* genotype of the highly tumorigenic MDA-MB-231 cell line.

Optimization of CTC culture conditions will be needed before this strategy can be incorporated into clinical practice. In addition, further characterization of the nonadherent CTC-derived cell lines described here will be required to define how they differ from cells cultured from primary tumor biopsies or directly implanted into mouse models (*4*, *14*). In the future, strategies such as that described here may be an essential component of "precision medicine" in oncology, where treatment decisions are based on evolving tumor mutational profiles and drug sensitivity patterns in individual patients.

REFERENCES AND NOTES

1. D. A. Haber, N. S. Gray, J. Baselga, *Cell* **145**, 19–24 (2011).
2. M. Yu, S. Stott, M. Toner, S. Maheswaran, D. A. Haber, *J. Cell Biol.* **192**, 373–382 (2011).
3. E. Ozkumur *et al.*, *Sci. Transl. Med.* **5**, 179ra47 (2013).
4. X. Liu *et al.*, *Am. J. Pathol.* **180**, 599–607 (2012).
5. T. Sato, H. Clevers, *Methods Mol. Biol.* **945**, 319–328 (2013).
6. T. A. Ince *et al.*, *Cancer Cell* **12**, 160–170 (2007).
7. J. Debnath, S. K. Muthuswamy, J. S. Brugge, *Methods* **30**, 256–268 (2003).
8. G. Dontu *et al.*, *Genes Dev.* **17**, 1253–1270 (2003).
9. D. Dias-Santagata *et al.*, *EMBO Mol. Med.* **2**, 146–158 (2010).
10. M. S. Lawrence *et al.*, *Nature* **505**, 495–501 (2014).
11. Q. X. Zhang, A. Borg, D. M. Wolf, S. Oesterreich, S. A. Fuqua, *Cancer Res.* **57**, 1244–1249 (1997).
12. D. R. Robinson *et al.*, *Nat. Genet.* **45**, 1446–1451 (2013).
13. W. Toy *et al.*, *Nat. Genet.* **45**, 1439–1445 (2013).
14. S. Li *et al.*, *Cell Reports* **4**, 1116–1130 (2013).
15. K. Merenbakh-Lamin *et al.*, *Cancer Res.* **73**, 6856–6864 (2013).
16. The Cancer Genome Atlas Network, *Nature* **490**, 61 (2012).
17. M. J. Garnett *et al.*, *Nature* **483**, 570–575 (2012).
18. K. E. Weis, K. Ekena, J. A. Thomas, G. Lazennec, B. S. Katzenellenbogen, *Mol. Endocrinol.* **10**, 1388–1398 (1996).
19. J. Baselga *et al.*, *N. Engl. J. Med.* **366**, 520–529 (2012).
20. Y. Wang, J. B. Trepel, L. M. Neckers, G. Giaccone, *Curr. Opin. Investig. Drugs* **11**, 1466–1476 (2010).
21. P. Furet *et al.*, *Bioorg. Med. Chem. Lett.* **23**, 3741–3748 (2013).
22. P. R. Gavine *et al.*, *Cancer Res.* **72**, 2045–2056 (2012).
23. M. Mohammadi *et al.*, *EMBO J.* **17**, 5896–5904 (1998).
24. M. Pollak, *Nat. Rev. Cancer* **12**, 159–169 (2012).
25. I. Baccelli *et al.*, *Nat. Biotechnol.* **31**, 539–544 (2013).
26. L. Zhang *et al.*, *Sci. Transl. Med.* **5**, 180ra48 (2013).

ACKNOWLEDGMENTS

We are grateful to all the patients who participated in this study. We thank Dr. Lecia Sequist for coordinating the clinical studies, A. McGovern, C. Hart, and the Massachusetts General Hospital (MGH) clinical research coordinators P. Spuhler, A. Shah, J. Ciciliano, and V. Pai for bioengineering technical support; R. Milano, K. Lynch, H. Robinson, and M. Liebers for technical support; L. Collins (Beth Israel Deaconess Medical Center) for providing pathological specimens; and L. Libby for mouse studies. N. Aceto is a fellow of the Human Frontiers Science Program, the Swiss National Science Foundation, and the Swiss Foundation for Grants in Biology and Medicine. This work was supported by grants from the Breast Cancer Research Foundation (D.A.H), Stand Up to Cancer (D.A.H., M.T., S.M.), the Wellcome Trust (D.A.H., C.B.), National Foundation for Cancer Research (D.A.H.), NIH CA129933 (D.A.H.), NIBIB EB008047 (M.T., D.A.H.), Susan G. Komen for the Cure KG09042 (S.M.), National Cancer Institute–MGH Proton Federal Share Program (S.M.), the MGH-Johnson and Johnson Center for Excellence in CTCs (M.T., S.M.), and the Howard Hughes Medical Institute (M.Y., D.A.H.). A.J.I. holds equity in, and is a paid consultant for, Enzymatics, Inc. M.T., D.A.H., and the Massachusetts General Hospital have filed for patent protection for the CTC-iChip technology. RNA-Seq reads have been deposited into Gene Expression Omnibus: uncultured CTCs (accession no. GSE51827); the six cultured CTC lines (accession no. GSE55807).

SUPPLEMENTARY MATERIALS

www.sciencemag.org/content/345/6193/216/suppl/DC1
Materials and Methods
Figs. S1 to S15
Tables S1 to S3
References (*27*–*30*)

13 January 2014; accepted 10 June 2014
10.1126/science.1253533

BACTERIAL CELL WALL

MurJ is the flippase of lipid-linked precursors for peptidoglycan biogenesis

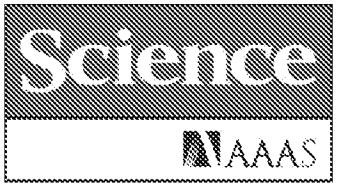
Lok-To Sham,[1] Emily K. Butler,[2] Matthew D. Lebar,[3] Daniel Kahne,[3,*] Thomas G. Bernhardt,[1,*] Natividad Ruiz[2,*]

Peptidoglycan (PG) is a polysaccharide matrix that protects bacteria from osmotic lysis. Inhibition of its biogenesis is a proven strategy for killing bacteria with antibiotics. The assembly of PG requires disaccharide-pentapeptide building blocks attached to a polyisoprene lipid carrier called lipid II. Although the stages of lipid II synthesis are known, the identity of the essential flippase that translocates it across the cytoplasmic membrane for PG polymerization is unclear. We developed an assay for lipid II flippase activity and used a chemical genetic strategy to rapidly and specifically block flippase function. We combined these approaches to demonstrate that MurJ is the lipid II flippase in *Escherichia coli*.

Bacteria use polyisoprenoid-linked oligosaccharides to assemble the essential peptidoglycan (PG) matrix that surrounds their cytoplasmic membrane and fortifies their cell envelope against high internal osmotic pressure (*1*). The building block of PG is a disaccharide-pentapeptide that is synthesized at the cytoplasmic leaflet of the inner membrane (IM) as a precursor known as lipid II (Fig. 1A) (*1*, *2*). This precursor must be flipped across the membrane for cell wall synthesis. The identity of the lipid II flippase has been controversial, with the debate centered on two candidates: MurJ-like and FtsW/RodA-like proteins

[1]Department of Microbiology and Immunobiology, Harvard Medical School, Boston, MA 02115, USA. [2]Department of Microbiology, Ohio State University, Columbus, OH 43210, USA. [3]Department of Chemistry and Chemical Biology, Harvard University, Cambridge, MA 02138, USA. [4]Department of Biological Chemistry and Molecular Pharmacology, Harvard Medical School, Boston, MA 02115, USA.
*Corresponding author. E-mail: thomas_bernhardt@hms.harvard.edu (T.G.B.); ruiz.82@osu.edu (N.R.)

Downloaded from http://science.sciencemag.org/ on July 6, 2016



Ex vivo culture of circulating breast tumor cells for individualized testing of drug susceptibility

Min Yu, Aditya Bardia, Nicola Aceto, Francesca Bersani, Marissa W. Madden, Maria C. Donaldson, Rushil Desai, Huili Zhu, Valentine Comaills, Zongli Zheng, Ben S. Wittner, Petar Stojanov, Elena Brachtel, Dennis Sgroi, Ravi Kapur, Toshihiro Shioda, David T. Ting, Sridhar Ramaswamy, Gad Getz, A. John Iafrate, Cyril Benes, Mehmet Toner, Shyamala Maheswaran and Daniel A. Haber

(July 10, 2014)
Science **345** (6193), 216-220. [doi: 10.1126/science.1253533]

Editor's Summary

Staying one step ahead of tumors

Cancer treatments require continual adjustment. A drug that works initially will lose its potency as the tumor acquires new mutations that allow it to bypass the drug's lethal effects. To stay ahead of the tumor, oncologists need a noninvasive way to collect tumor cells from patients over the course of their treatment. Analyzing the mutations in these samples may help them choose the right drugs as the tumors change. In a small study of breast cancer patients, Yu *et al.* show that rare tumor cells circulating in the blood can be captured in viable form and used for this purpose.

Science, this issue p. 216

This copy is for your personal, non-commercial use only.

Article Tools Visit the online version of this article to access the personalization and article tools:
http://science.sciencemag.org/content/345/6193/216

Permissions Obtain information about reproducing this article:
http://www.sciencemag.org/about/permissions.dtl

Science (print ISSN 0036-8075; online ISSN 1095-9203) is published weekly, except the last week in December, by the American Association for the Advancement of Science, 1200 New York Avenue NW, Washington, DC 20005. Copyright 2016 by the American Association for the Advancement of Science; all rights reserved. The title *Science* is a registered trademark of AAAS.

Downloaded from http://science.sciencemag.org/ on July 6, 2016

nature genetics

Activating *ESR1* mutations in hormone-resistant metastatic breast cancer

Dan R Robinson[1,2,12], Yi-Mi Wu[1,2,12], Pankaj Vats[1,2], Fengyun Su[1,2], Robert J Lonigro[1,3], Xuhong Cao[1,4], Shanker Kalyana-Sundaram[1,2], Rui Wang[1,2], Yu Ning[1,2], Lynda Hodges[1], Amy Gursky[1,2], Javed Siddiqui[1,2], Scott A Tomlins[1,2], Sameek Roychowdhury[5], Kenneth J Pienta[6], Scott Y Kim[7], J Scott Roberts[8], James M Rae[3,9], Catherine H Van Poznak[9], Daniel F Hayes[9], Rashmi Chugh[9], Lakshmi P Kunju[1,2], Moshe Talpaz[9], Anne F Schott[9] & Arul M Chinnaiyan[1–4,10,11]

© 2013 Nature America, Inc. All rights reserved.

Breast cancer is the most prevalent cancer in women, and over two-thirds of cases express estrogen receptor-α (ER-α, encoded by *ESR1*). Through a prospective clinical sequencing program for advanced cancers, we enrolled 11 patients with ER-positive metastatic breast cancer. Whole-exome and transcriptome analysis showed that six cases harbored mutations of *ESR1* affecting its ligand-binding domain (LBD), all of whom had been treated with anti-estrogens and estrogen deprivation therapies. A survey of The Cancer Genome Atlas (TCGA) identified four endometrial cancers with similar mutations of *ESR1*. The five new LBD-localized *ESR1* mutations identified here (encoding p.Leu536Gln, p.Tyr537Ser, p.Tyr537Cys, p.Tyr537Asn and p.Asp538Gly) were shown to result in constitutive activity and continued responsiveness to anti-estrogen therapies *in vitro*. Taken together, these studies suggest that activating mutations in *ESR1* are a key mechanism in acquired endocrine resistance in breast cancer therapy.

Advances in high-throughput sequencing technologies are beginning to establish a molecular taxonomy for a spectrum of human diseases and has facilitated a move toward 'precision medicine' (refs. 1,2). With regard to oncology, defining the mutational landscape of a patient's tumor will lead to more precise treatment and management of individuals with cancer. Comprehensive clinical sequencing programs for cancer patients have been initiated at a variety of medical centers, including our own[3,4]. In addition to the potential for identifying 'actionable' therapeutic targets in cancer patients, these clinical sequencing efforts may also shed light on acquired resistance mechanisms developed against targeted therapies[5–7].

ER is the primary therapeutic target in breast cancer and is expressed in 70% of cases[8]. Drugs directly antagonizing ER, such as tamoxifen and fulvestrant, are a mainstay of breast cancer treatment; however, approximately 30% of ER-positive breast cancers exhibit *de novo* resistance, whereas 40% acquire resistance to these therapies[9]. In addition to anti-estrogen therapies, patients with ER-positive breast cancer are also treated with aromatase inhibitors such as letrozole and exemestane[10]. Aromatase inhibitors block the peripheral conversion of androgens into estrogen and, in post-menopausal women, lead to over a 98% decrease in circulating levels of estrogen. As with anti-estrogens, treatment with aromatase inhibitors results in the development of resistance, but this is presumably due to different mechanisms, as patients with breast cancer who develop resistance to aromatase inhibitors often still respond to anti-estrogen therapies[11]. The molecular mechanisms of endocrine resistance in ER-positive breast cancer continues to be an active area of research[12].

Our institutional review board (IRB)-approved clinical sequencing program, called MI-ONCOSEQ (the Michigan Oncology Sequencing Program), enrolls patients with advanced cancer across all histologies[3]. Since April 2011, we have enrolled over 200 patients in this program, which involves obtaining a current tumor biopsy with matched normal samples (blood and/or buccal swab). Samples are then subjected to integrative sequencing, which includes whole-exome sequencing of the tumor and matched normal sample, transcriptome sequencing and, as needed, low-pass whole-genome sequencing[3]. This combination of DNA and RNA sequencing technologies allows one to be relatively comprehensive with regard to the mutational landscape of coding genes, including analysis of point mutations, indels, amplifications, deletions, gene fusions or translocations, and outlier gene expression profiles. These results are generated within a 5- to 7-week time frame and are presented at an institutional 'precision medicine tumor board' to deliberate upon potentially actionable findings.

[1]Michigan Center for Translational Pathology, University of Michigan Medical School, Ann Arbor, Michigan, USA. [2]Department of Pathology, University of Michigan Medical School, Ann Arbor, Michigan, USA. [3]Comprehensive Cancer Center, University of Michigan Medical School, Ann Arbor, Michigan, USA. [4]Howard Hughes Medical Institute, University of Michigan Medical School, Ann Arbor, Michigan, USA. [5]Department of Internal Medicine, Ohio State University, Columbus, Ohio, USA. [6]Brady Urological Institute, Johns Hopkins University School of Medicine, Baltimore, Maryland, USA. [7]Center for Bioethics and Social Science in Medicine, University of Michigan, Ann Arbor, Michigan, USA. [8]Department of Health Behavior & Health Education, University of Michigan, Ann Arbor, Michigan, USA. [9]Department of Internal Medicine, University of Michigan Medical School, Ann Arbor, Michigan, USA. [10]Department of Urology, University of Michigan Medical School, Ann Arbor, Michigan, USA. [11]Center for Computational Medicine and Biology, University of Michigan, Ann Arbor, Michigan, USA. [12]These authors contributed equally to this work. Correspondence should be addressed to A.M.C. (arul@umich.edu).

Received 22 July; accepted 10 October; published online 3 November 2013; doi:10.1038/ng.2823

Table 1 Clinical sequencing of 11 metastatic ER-positive breast cancer cases

Case	Age (years)	ER/PR/ERBB2	Treatment[a]	Number of SNVs/fusions	Genetic aberration[b]
MO_1031	41	+/+/–	Tamoxifen, letrozole, fulvestrant	266/18	*ESR1* (p.Leu536Gln), gene copy gains of *FGFR1*, *FGFR2*, *CCND1* and *GNRHR*
MO_1051	31	+/–/–	Oophorectomy, letrozole, fulvestrant	248/5	*ESR1* (p.Tyr537Ser), *PIK3CA* (p.His1047Arg), *TP53* (p.Gly199Glu), *FGFR2-AFF3* fusion
MO_1069	62	+/+/–	Tamoxifen, letrozole, fulvestrant	74/9	*ESR1* (p.Asp538Gly), *ARID2* (p.Glu245*), gene copy losses of *TP53*, *BRCA1*, *RB1*, *ARID1A* and *SMARCA4*
MO_1129	44	+/+/–	Tamoxifen, oophorectomy, anastrozole, fulvestrant, exemestane	32/3	*ESR1* (p.Tyr537Ser), *PIK3CA* (p.Glu542Lys), gene copy gains of *CCND1* and *PAK1*
MO_1030	78	+/+/–	Tamoxifen (short), anastrozole, fulvestrant	26/2	*PIK3CA* (p.Glu545Ala), *TP53* copy loss
MO_1068	65	+/–/–	Tamoxifen, anastrozole	83/10	*PIK3CA* (p.His1047Arg), *TP53* (p.Glu51*), *MSH2* copy loss
MO_1090	52	+/+/–	Tamoxifen, anastrozole	28/11	No significant drivers identified
MO_1107	46	+/+/–	Tamoxifen, oophorectomy, anastrozole, fulvestrant, exemestane	63/12	*BRCA1* (c.5385_5386insC), frameshift deletions in *TP53*, *SMARCA4* and *NF1*
MO_1167	60	+/–/–	Tamoxifen, letrozole	47/3	*ESR1* (p.Asp538Gly)
MO_1185	58	+/+/–	Tamoxifen, letrozole, fulvestrant, exemestane	88/1	*ESR1* (p.Tyr537Ser), *CDH1* (p.Gln641*), *NOTCH2* (frameshift deletion), *TP53* copy loss
TP_2004[c]	52	+/–/–	Tamoxifen (short)	29/22	*MDM2* gene amplification, gene copy losses of *CDKN2A* and *CDKN2B*

PR, progesterone receptor; SNVs, single-nucleotide variants.
[a]Only anti-estrogen–related treatments are listed. Patients also received chemotherapies, radiation or mastectomy in the interim between diagnosis and MI-ONCOSEQ sequencing. [b]Amino acid substitutions caused by nonsynonymous somatic mutations are given in parentheses. [c]TP_2004 is male.

© 2013 Nature America, Inc. All rights reserved.

As part of the MI-ONCOSEQ program, we enrolled and sequenced 11 patients with metastatic ER-positive breast cancer (**Table 1** and **Supplementary Table 1**). A diverse array of aberrations were identified in individual patients, some of which are potentially actionable, including mutations in *PIK3CA* ($n = 4$), *BRCA1* aberrations ($n = 2$), *FGFR2* aberrations ($n = 2$)[13], *NOTCH2* frameshift deletion ($n = 1$), cyclin and associated cyclin-dependent kinase aberrations ($n = 3$) and *MDM2* amplification and overexpression ($n = 1$). Aberrations were also frequently found in the tumor suppressor *TP53* ($n = 6$), the DNA mismatch repair gene *MSH2* ($n = 1$) and in epigenetic regulators ($n = 2$), including *ARID2*, *ARID1A* and *SMARCA4*, among others. The complete spectra of somatic mutations with associated alterations in expression levels and copy number in the index patients are given in **Supplementary Figure 1** and **Supplementary Tables 2** and **3**. Two of the index patients, MO_1031 and MO_1051, exhibited a high level of mutations consistent with 'signature B' identified in a whole-genome study of mutational processes in breast cancer[14]. There were 39 gene fusions identified in the 6 index patients, with 11 encoding in-frame fusion proteins (**Supplementary Fig. 2** and **Supplementary Tables 4** and **5**), including an activating *FGFR2-AFF3* fusion[13].

The most notable observation in the mutational landscapes of these treated patients with ER-positive breast cancer was the finding of nonsynonymous mutations in *ESR1* affecting the LBD ($n = 6$). The six index patients MO_1031, MO_1051, MO_1069, MO_1129, MO_1167 and MO_1185 had mutations encoding p.Leu536Gln, p.Tyr537Ser, p.Asp538Gly, p.Tyr537Ser, p.Asp538Gly and p.Tyr537Ser alterations in the LBD, respectively. The respective mutation in each case was detected by whole-exome sequencing of the tumor relative to the matched normal sample and was corroborated by whole-transcriptome sequencing, as *ESR1* was expressed at moderate to high levels (**Supplementary Table 2**). The clinical histories of the index patients are depicted in timelines in **Figure 1**. For three of the patients (MO_1051, MO_1069 and MO_1129), we had access to primary diagnostic material and showed that the *ESR1* mutations were not present at an earlier stage, indicating that they were acquired after endocrine therapy (**Fig. 1** and **Supplementary Table 2**). Interestingly, all of the index patients were treated with anti-estrogens (tamoxifen and/or fulvestrant) and aromatase inhibitors (letrozole, anastrozole and/or exemestane). Two of the patients also had an oophorectomy. Comparison of the mutations present in each primary versus post-treatment pair showed a substantial number of shared mutations in both samples of the pair, including activating mutations in *PIK3CA* in two of the cases. Thus, it is clear that the index cases presented with recurrent disease of the original primary tumor surviving in an estrogen-deprived state and having acquired *ESR1* mutations. Of note, neither *ESR1* amplifications nor gene fusions were observed in these cases.

The five new LBD alterations of ESR1 identified in this study are depicted in **Figure 2**. Each occurred in the vicinity of the synthetic alterations of ESR1 that are inverted in response to tamoxifen and involve p.Met543Ala and p.Leu544Ala alterations (Inv-mut-AA2)[15] and served as a positive control for our subsequent *in vitro* studies. We next investigated the occurrence of *ESR1* mutations in a range of breast cancer types. Here we took advantage of data from the TCGA Project, which has generated whole-exome sequences for 27 tumor types across at least 4,000 individual samples. As expected, LBD-disrupting mutations of *ESR1* were not detected in the 390 ER-positive breast cancers sequenced by TCGA, as these were primary resection samples before hormonal treatment[16], nor did we detect *ESR1* mutations in a cohort of 80 triple-negative breast carcinoma transcriptomes (D.R.R., Y.-M.W., X.C., S.K.-S., A.M.C. *et al.*, unpublished data).

As the LBD-disrupting mutations of *ESR1* we identified were somatic and were acquired after treatment, we next assessed whether the encoded proteins were dependent on estrogen for activation. We cloned into expression vectors each of the five *ESR1* mutants identified in this study (encoding p.Leu536Gln, p.Tyr537Ser, p.Asp538Gly, p.Tyr537Cys and p.Tyr573Asn alterations) and subsequently cotransfected these constructs into HEK293T cells with an estrogen response element (ERE)-luciferase reporter system. We then exposed steroid hormone–deprived cells to β-estradiol for 24 h and assessed ERE reporter levels. Surprisingly, unlike wild-type ESR1, which had little ERE reporter activity in the absence of ligand, all five of the ESR1 mutants had strong constitutive activation of the ERE reporter that was not markedly enhanced with β-estradiol (**Fig. 3**). This finding suggested that each of the mutations developed in the context of evolution during

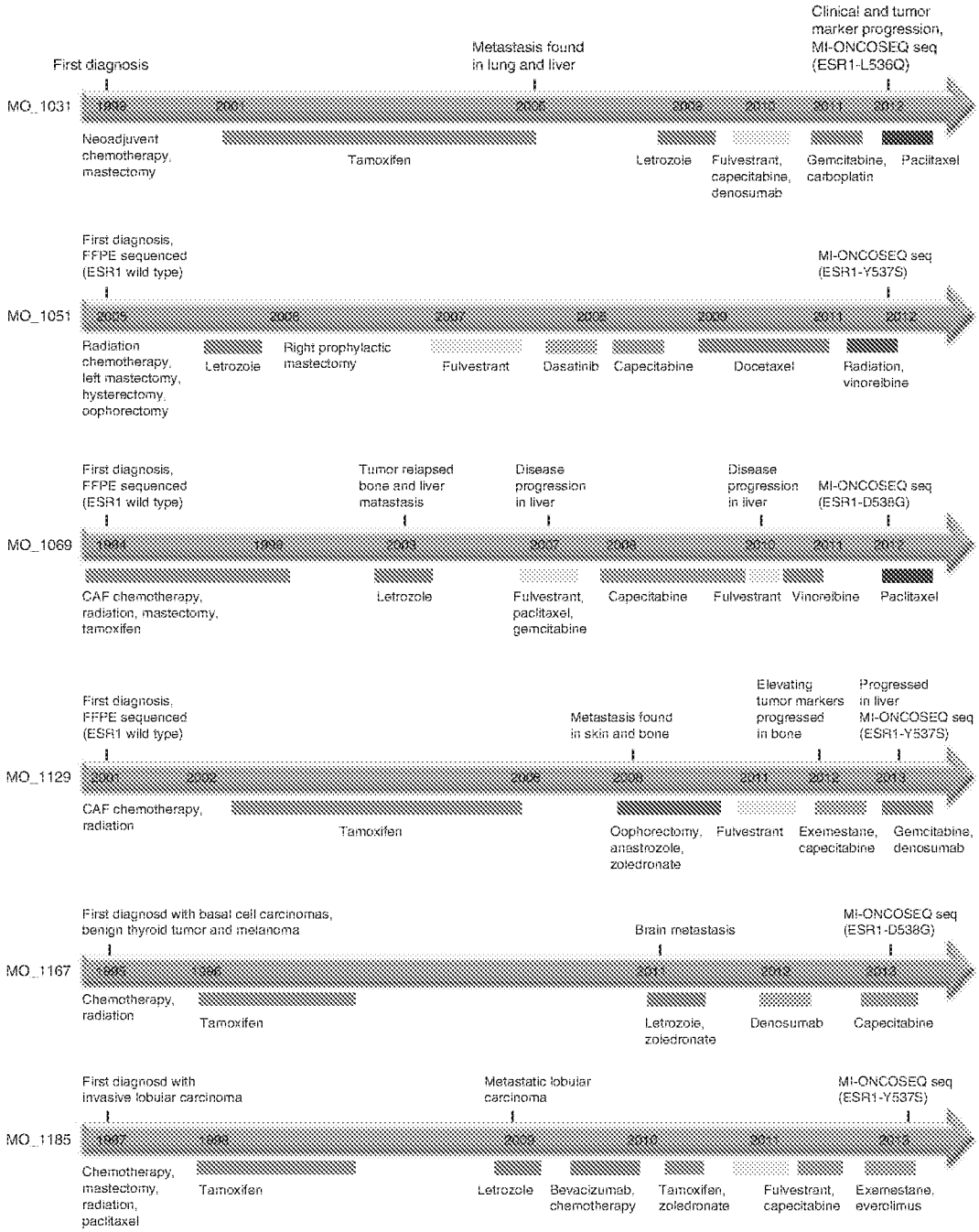


Figure 1 Clinical timelines for the six index ER-positive metastatic breast cancer patients harboring *ESR1* mutations. Shown are patients' histories of clinical treatment from first diagnosis until enrollment in the MI-ONCOSEQ study. Each bar represents the timeframe of treatment. FFPE, formalin fixed, paraffin embedded; CAF, cyclophosphamide, doxorubicin, fluorouracil chemotherapy.

an estrogen-deprived state. Consistent with this idea, a whole-genome sequencing study of 46 patients with ER-positive breast cancer enrolled in 2 aromatase inhibitor trials did not identify any of these *ESR1* mutations in the pretreatment samples analyzed[17].

Next, we assessed whether anti-estrogen therapies affected the functional activity of the LBD mutants. As effects on inhibition can be influenced by the levels of ectopic ER expression, we performed a dose response study with expression plasmid and selected a dose of 50 ng for the following experiments[18] (**Supplementary Fig. 3**). As expected, wild-type ESR1 was inhibited in a dose-dependent fashion by the anti-estrogens 4-hydroxytamoxifen, fulvestrant and endoxifen (**Fig. 4** and **Supplementary Figs. 4–6**). In addition, the mutant corresponding to the synthetic *ESR1* mutation (Inv-mut-AA2) was activated in a dose-dependent fashion by these anti-estrogens (**Fig. 4**), which has been reported previously[15]. Interestingly, ESR1 with each of the five LBD alterations identified in this study was inhibited by tamoxifen and fulvestrant in a dose-dependent fashion and did not exhibit the inverted response to anti-estrogens that the synthetic Inv-mut-AA2 mutant did. One could speculate that the corresponding mutations did not arise under selective pressure of anti-estrogen treatment but rather in the context of an estrogen deprivation setting, such as treatment with aromatase inhibitors and/or oophorectomy. The IC_{50} (half-maximal

© 2013 Nature America, Inc. All rights reserved.

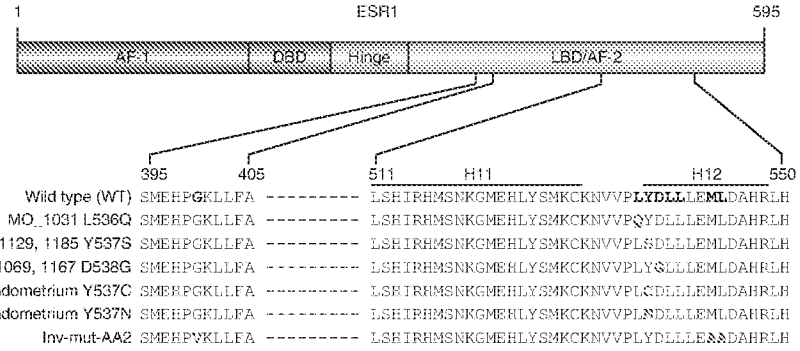


Figure 2 Schematic of ESR1 alterations identified in this study. The structural domains of ESR1 are illustrated on top, including the transcription activation function-1 domain (AF-1), the DNA-binding domain (DBD), the hinge domain and the ligand-binding domain (LBD/AF-2). Altered residues identified in mutants are marked in red, and reference residues are shown in bold in the wild-type sequence. Endometrium p.Tyr537Cys and p.Tyr537Asn are two alterations discovered in endometrial cancer samples from the TCGA study. Inv-mut-AA2 represents a ligand activity inversion mutant of ESR1 that confers inverted responses to anti-estrogen and estrogen. H11, helix 11; H12, helix 12.

inhibitory concentration) values for both 4-hydroxytamoxifen and fulvestrant were two- to fourfold higher for all mutants compared to wild-type ESR1. Fulvestrant exhibited greater maximal inhibition than 4-hydroxytamoxifen for all the mutants tested (**Supplementary Figs. 4** and **5**).

The ESR1 alterations identified in this study cluster near the beginning of helix 12 (**Fig. 2**). Structural studies have demonstrated a key role for the position of helix 12 in the response of the ER to agonists and antagonists[19], and Tyr537 has been postulated to form a capping motif contributing to the activity of the receptor[20]. Specifically, the p.Tyr537Ser mutant has been reported to have higher affinity for estrogen than wild-type ESR1 and interacts with the SRC1 coactivator in the absence of ligand[21,22]. Several studies using experimental mutagenesis have implicated the same three residues identified here as critical determinants of the transcriptional activity of the receptor[21,23,24].

As estrogen therapy has been shown to have a positive effect in treating aromatase inhibitor–resistant advanced breast cancers, we tested the effect of low- to high-dose estrogen on the activity of the mutants in the transient luciferase reporter assays (**Supplementary Fig. 7**)[25,26]. The results did not suggest that the effectiveness of this therapy is mediated through direct control of the transcriptional activity of these mutants, if encoded by the responding patients.

Although the primary intent of our broad-based clinical sequencing program is to identify actionable and/or driver mutations in advanced cancers, this study demonstrates how such prospective, real-time sequencing efforts can also shed light on resistance mechanisms that develop against targeted therapies. A number of resistance mechanisms have been suggested to function in the evasion of endocrine treatment, including activation of the mTOR and phosphoinositide 3-kinase (PI3K) pathways, among others[9,27]. Although the total number of ER-positive breast cancers we have sequenced is modest, we have done so in a comprehensive fashion in terms of delineating mutational landscapes and incorporating both DNA and RNA sequencing. This analysis identified *de novo* driver mutations and/or potentially acquired mutations in breast cancer such as mutations resulting in PI3K activation, *PAK1* amplification and *FGFR* fusion and amplification, which have been described previously[13,28,29]. Among potential new mechanisms described, we identified profound focal amplification of *MDM2* (which encodes a negative regulator of p53 that is targetable) and copy gains of *GNRHR* (encoding gonadotropin-releasing hormone receptor), which may be related to past endocrine therapy.

As the LBD-disrupting mutations of *ESR1* identified in this study result in constitutive activity, the encoded mutant proteins can function in the absence of ligand and maintain ER signaling. In 1997, an *ESR1* mutation affecting the LBD, encoding a p.Tyr537Asn alteration, was detected in a single individual with stage IV metastatic breast cancer who had been treated with diethylstibesterol, but, since then, this mutation has been considered to be very rare[30]. With the advent of widespread aromatase inhibitor therapy, we suggest that alteration of the ESR1 LBD is likely a common mechanism of resistance that develops in low-estrogen states. Interestingly, LBD-disrupting mutations of *ESR1* were detected somatically in 4 of 373 cases of endometrial cancer[31]. We speculate that the four TCGA endometrial tumors that harbor LBD-affecting mutations likely came from patients with concurrent breast cancer, as tamoxifen treatment is known to be associated with higher incidence of this tumor type and such patients also often receive estrogen deprivation treatment[32].

Our study suggests that it is unlikely that these LBD alterations develop in the context of anti-estrogen treatment, as the mutated *ESR1* variants continue to be responsive to direct ER antagonists such as tamoxifen and fulvestrant. This finding is consistent with clinical reports showing that patients that develop resistance to aromatase inhibitors still respond to anti-estrogen treatment[11]. Although this prospective clinical sequencing study was not designed to characterize a specific cancer type or treatment resistance mechanism,

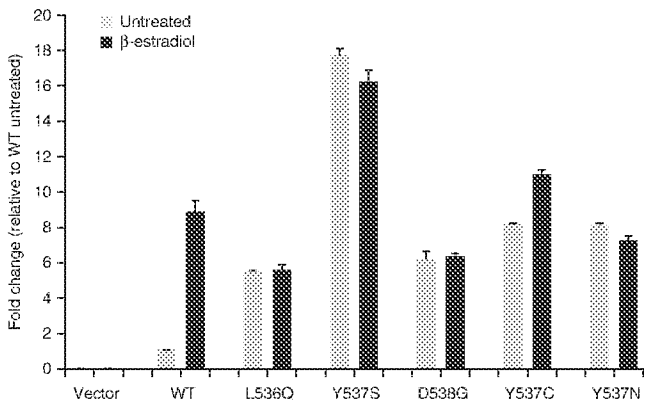


Figure 3 *ESR1* with acquired mutations encodes constitutively active protein. HEK293T cells were cotransfected with an ERE–firefly luciferase reporter plasmid, a plasmid constitutively expressing *Renilla* luciferase as an internal control and various *ESR1* constructs (as illustrated in **Fig. 2**). Steroid hormone–deprived cells were either untreated or stimulated with 5 nM β-estradiol for 24 h. Firefly luciferase activities were normalized using corresponding *Renilla* luciferase activities for each condition. Fold change in ESR1-driven transcriptional activity was calculated using untreated wild type as a control for each condition. Data shown are the means from triplicate experiments. Amino acid changes in respective ESR1 mutants are indicated. WT, wild-type ESR1. Error bars, s.d.

© 2013 Nature America, Inc. All rights reserved.

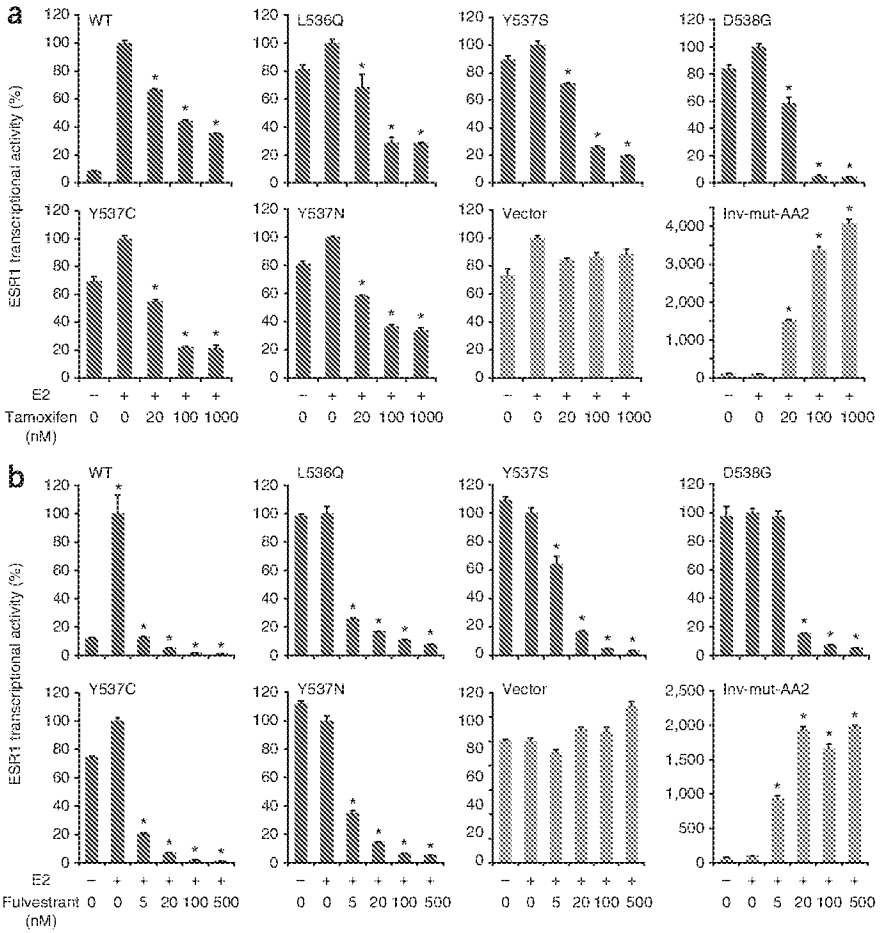


Figure 4 Acquired *ESR1* mutations result in maintained sensitivity to anti-estrogen therapies. HEK293T cells were cotransfected with an ERE–firefly luciferase reporter plasmid, a plasmid constitutively expressing *Renilla* luciferase and various *ESR1* constructs as indicated. (**a**,**b**) Steroid hormone–deprived cells were either untreated or treated with increasing doses of the anti-estrogen drugs tamoxifen (**a**) and fulvestrant (**b**) in the presence of 5 nM β-estradiol (E2) for 24 h. Percentage change in ESR1-driven transcriptional activity was calculated using E2-treated cells as the control for each tested construct. Data shown are the means from triplicate experiments. Error bars, s.d. $^*P < 0.001$. Red, wild type; blue, clinically identified mutants; orange, synthetic ligand-inversion mutant; green, vector control.

future studies comprising larger cohorts of breast cancer patients with disease that recurs after varied endocrine treatments will more precisely delineate the incidence of this acquired resistance mechanism. The focused nature of these mutations and their role in aromatase inhibitor resistance suggest the possibility of monitoring patients undergoing treatment using circulating tumor DNA methods[33,34]. In this manner, treatment could be shifted to head off evolving tumor resistance.

URLs. BLAT, http://genome.ucsc.edu/cgi-bin/hgBlat; ORF Finder, http://www.ncbi.nlm.nih.gov/gorf/gorf.html.

METHODS

Methods and any associated references are available in the online version of the paper.

Accession codes. Sequence data have been deposited in the database of Genotypes and Phenotypes (dbGaP), which is hosted by the National Center for Biotechnology Information (NCBI), under accessions phs000602.v1.p1 and phs000673.v1.p1.

Note: Any Supplementary Information and Source Data files are available in the online version of the paper.

ACKNOWLEDGMENTS

The authors thank D. Miller, T. Barrette and D. Gibbs for hardware and database management, K. Giles for assistance with manuscript preparation, physicians M. Wicha, L. Pierce, D. Smith, K. Levin and F. Feng for referring patients, and C. Betts and J. Athanikar for assistance with tumor boards. We also thank the larger MI-ONCOSEQ team, including clinical research coordinator E. Williams, pathologist R. Mehra, genetic counselors J. Everett, S. Gustafson and V. Raymond, and radiologists E. Higgins, E. Caoili and R. Dunnick. This project is supported in part by the Prostate Cancer Foundation with funding for our sequencing infrastructure, the National Cancer Institute Early Detection Research Network (U01 CA111275), National Human Genome Research Institute Clinical Sequencing Exploratory Research (CSER) Consortium (1UM1HG006508), US Department of Defense contract W81XWH-12-1-0080 and a Department of Defense Era of Hope Scholar Award. A.M.C. is also supported by the Alfred A. Taubman Institute, the American Cancer Society, the Howard Hughes Medical Institute and a Doris Duke Charitable Foundation Clinical Scientist Award.

AUTHOR CONTRIBUTIONS

D.R.R., Y.-M.W. and A.M.C. conceived the experiments. D.R.R., Y.-M.W., X.C., R.W., F.S. and Y.N. performed exome and transcriptome sequencing. P.V., R.J.L., S.K.-S. and D.R.R. carried out bioinformatics analysis of high-throughput sequencing data for somatic mutation, copy number and tumor content determination and performed gene expression and gene fusion analysis. D.R.R., Y.-M.W. and F.S. generated *ESR1* constructs and carried out *in vitro* experiments. L.H. coordinated patients for clinical research. J.S. and A.G. collected and processed clinical tissue samples for next-generation sequencing. L.P.K. and S.A.T. provided pathology review. J.M.R. provided experimental analysis. C.H.V.P., D.F.H., R.C. and A.F.S. enrolled patients and provided clinical data and consultation at tumor boards. D.R.R., X.C., Y.-M.W., P.V., R.J.L., S.K.-S., S.Y.K., J.S.R., S.R., M.T., K.J.P. and A.M.C. developed the integrated clinical sequencing protocol. D.R.R., Y.-M.W. and A.M.C. prepared the manuscript, which was reviewed by all authors.

COMPETING FINANCIAL INTERESTS

The authors declare no competing financial interests.

Reprints and permissions information is available online at http://www.nature.com/reprints/index.html.

1. Chin, L., Andersen, J.N. & Futreal, P.A. Cancer genomics: from discovery science to personalized medicine. *Nat. Med.* **17**, 297–303 (2011).
2. Meyerson, M., Gabriel, S. & Getz, G. Advances in understanding cancer genomes through second-generation sequencing. *Nat. Rev. Genet.* **11**, 685–696 (2010).
3. Roychowdhury, S. *et al.* Personalized oncology through integrative high-throughput sequencing: a pilot study. *Sci. Transl. Med.* **3**, 111ra121 (2011).
4. Welch, J.S. *et al.* Use of whole-genome sequencing to diagnose a cryptic fusion oncogene. *J. Am. Med. Assoc.* **305**, 1577–1584 (2011).
5. Gorre, M.E. *et al.* Clinical resistance to STI-571 cancer therapy caused by *BCR-ABL* gene mutation or amplification. *Science* **293**, 876–880 (2001).
6. Korpal, M. *et al.* An F876L mutation in androgen receptor confers genetic and phenotypic resistance to MDV3100 (enzalutamide). *Cancer Discov.* **3**, 1030–1043 (2013).
7. Joseph, J.D. *et al.* A clinically relevant androgen receptor mutation confers resistance to 2nd generation anti-androgens enzalutamide and ARN-509. *Cancer Discov.* **3**, 1020–1029 (2013).
8. Ariazi, E.A., Ariazi, J.L., Cordera, F. & Jordan, V.C. Estrogen receptors as therapeutic targets in breast cancer. *Curr. Top. Med. Chem.* **6**, 181–202 (2006).
9. Riggins, R.B., Schrecengost, R.S., Guerrero, M.S. & Bouton, A.H. Pathways to tamoxifen resistance. *Cancer Lett.* **256**, 1–24 (2007).

© 2013 Nature America, Inc. All rights reserved.

10. Lønning, P.E. & Eikesdal, H.P. Aromatase inhibition 2013: clinical state of the art and questions that remain to be solved. *Endocr. Relat. Cancer* **20**, R183–R201 (2013).
11. Ingle, J.N. *et al.* Fulvestrant in women with advanced breast cancer after progression on prior aromatase inhibitor therapy: North Central Cancer Treatment Group Trial N0032. *J. Clin. Oncol.* **24**, 1052–1056 (2006).
12. Osborne, C.K. & Schiff, R. Mechanisms of endocrine resistance in breast cancer. *Annu. Rev. Med.* **62**, 233–247 (2011).
13. Wu, Y.M. *et al.* Identification of targetable *FGFR* gene fusions in diverse cancers. *Cancer Discov.* **3**, 636–647 (2013).
14. Nik-Zainal, S. *et al.* Mutational processes molding the genomes of 21 breast cancers. *Cell* **149**, 979–993 (2012).
15. Feil, R., Wagner, J., Metzger, D. & Chambon, P. Regulation of Cre recombinase activity by mutated estrogen receptor ligand-binding domains. *Biochem. Biophys. Res. Commun.* **237**, 752–757 (1997).
16. TCGA. Comprehensive molecular portraits of human breast tumours. *Nature* **490**, 61–70 (2012).
17. Ellis, M.J. *et al.* Whole-genome analysis informs breast cancer response to aromatase inhibition. *Nature* **486**, 353–360 (2012).
18. Huang, H.J., Norris, J.D. & McDonnell, D.P. Identification of a negative regulatory surface within estrogen receptor α provides evidence in support of a role for corepressors in regulating cellular responses to agonists and antagonists. *Mol. Endocrinol.* **16**, 1778–1792 (2002).
19. Shiau, A.K. *et al.* The structural basis of estrogen receptor/coactivator recognition and the antagonism of this interaction by tamoxifen. *Cell* **95**, 927–937 (1998).
20. Skafar, D.F. Formation of a powerful capping motif corresponding to start of "helix 12" in agonist-bound estrogen receptor-α contributes to increased constitutive activity of the protein. *Cell Biochem. Biophys.* **33**, 53–62 (2000).
21. Carlson, K.E., Choi, I., Gee, A., Katzenellenbogen, B.S. & Katzenellenbogen, J.A. Altered ligand binding properties and enhanced stability of a constitutively active estrogen receptor: evidence that an open pocket conformation is required for ligand interaction. *Biochemistry* **36**, 14897–14905 (1997).
22. Weis, K.E., Ekena, K., Thomas, J.A., Lazennec, G. & Katzenellenbogen, B.S. Constitutively active human estrogen receptors containing amino acid substitutions for tyrosine 537 in the receptor protein. *Mol. Endocrinol.* **10**, 1388–1398 (1996).
23. Pearce, S.T., Liu, H. & Jordan, V.C. Modulation of estrogen receptor α function and stability by tamoxifen and a critical amino acid (Asp-538) in helix 12. *J. Biol. Chem.* **278**, 7630–7638 (2003).
24. Zhao, C. *et al.* Mutation of Leu-536 in human estrogen receptor-α alters the coupling between ligand binding, transcription activation, and receptor conformation. *J. Biol. Chem.* **278**, 27278–27286 (2003).
25. Ellis, M.J. *et al.* Lower-dose vs high-dose oral estradiol therapy of hormone receptor–positive, aromatase inhibitor–resistant advanced breast cancer: a phase 2 randomized study. *J. Am. Med. Assoc.* **302**, 774–780 (2009).
26. Swaby, R.F. & Jordan, V.C. Low-dose estrogen therapy to reverse acquired antihormonal resistance in the treatment of breast cancer. *Clin. Breast Cancer* **8**, 124–133 (2008).
27. Sokolosky, M.L. *et al.* Involvement of Akt-1 and mTOR in sensitivity of breast cancer to targeted therapy. *Oncotarget* **2**, 538–550 (2011).
28. Kan, Z. *et al.* Diverse somatic mutation patterns and pathway alterations in human cancers. *Nature* **466**, 869–873 (2010).
29. Shrestha, Y. *et al. PAK1* is a breast cancer oncogene that coordinately activates MAPK and MET signaling. *Oncogene* **31**, 3397–3408 (2012).
30. Barone, I., Brusco, L. & Fuqua, S.A. Estrogen receptor mutations and changes in downstream gene expression and signaling. *Clin. Cancer Res.* **16**, 2702–2708 (2010).
31. Kandoth, C. *et al.* Integrated genomic characterization of endometrial carcinoma. *Nature* **497**, 67–73 (2013).
32. Fisher, B. *et al.* Endometrial cancer in tamoxifen-treated breast cancer patients: findings from the National Surgical Adjuvant Breast and Bowel Project (NSABP) B-14. *J. Natl. Cancer Inst.* **86**, 527–537 (1994).
33. Dawson, S.J. *et al.* Analysis of circulating tumor DNA to monitor metastatic breast cancer. *N. Engl. J. Med.* **368**, 1199–1209 (2013).
34. Diehl, F. *et al.* Circulating mutant DNA to assess tumor dynamics. *Nat. Med.* **14**, 985–990 (2008).

© 2013 Nature America, Inc. All rights reserved.

ONLINE METHODS

Clinical study and specimen collection. Sequencing of clinical samples was performed under IRB-approved studies at the University of Michigan. Patients were enrolled and consented for integrative tumor sequencing in MI-ONCOSEQ (Michigan Oncology Sequencing Protocol, HUM00046018). Medically qualified patients 18 years or older with advanced or refractory cancer were eligible for the study. Informed consent detailed the risks of integrative sequencing and includes up-front genetic counseling. Informed consent was obtained from all subjects included in this study. Biopsies were arranged for safely accessible tumor sites. Needle biopsies were snap frozen in OCT (Optimal Cutting Temperature) compound, and a longitudinal section was cut. Frozen sections stained with hematoxylin and eosin were reviewed by pathologists to identify cores with the highest tumor content. Remaining portions of each needle biopsy core were retained for nucleic acid extraction.

Extraction of DNA and RNA. Genomic DNA from frozen needle biopsies and blood was isolated using the Qiagen DNeasy Blood and Tissue kit, according to the manufacturer's instructions. Total RNA was extracted from frozen needle biopsies using the Qiazol reagent with disruption using a 5-mm bead on a Tissuelyser II (Qiagen) and was purified using a miRNeasy kit (Qiagen) with DNase I digestion, according to the manufacturer's instructions. RNA integrity was verified on an Agilent 2100 Bioanalyzer using RNA Nano reagents (Agilent Technologies).

Preparation of next-generation sequencing libraries. Transcriptome libraries were prepared using 1–2 μg of total RNA. Polyadenylated RNA was isolated using Sera-Mag oligo(dT) beads (ThermoScientific) and fragmented with the Ambion Fragmentation Reagents kit. cDNA synthesis, end repair, A-base addition and ligation of the Illumina indexed adaptors were performed according to Illumina's TruSeq RNA protocol. Libraries were selected for DNA fragments of 250–300 bp in size on a 3% Nusieve 3:1 agarose gel (Lonza), recovered using QIAEX II gel-extraction reagents (Qiagen) and PCR amplified using Phusion DNA polymerase (New England BioLabs). Amplified libraries were purified using AMPure XP beads (Beckman Coulter). Library quality was measured on an Agilent 2100 Bioanalyzer by product size and concentration. Paired-end libraries were sequenced with the Illumina HiSeq 2000 platform (2 × 100-nucleotide read length). Reads that passed the chastity filter of Illumina BaseCall software were used for subsequent analysis.

Exome libraries of matched pairs of tumor and normal genomic DNA were generated using the Illumina TruSeq DNA Sample Prep kit, following the manufacturer's instructions. In brief, 1–3 μg of each genomic DNA sample was sheared using a Covaris S2 to a peak target size of 250 bp. Fragmented DNA was concentrated using AMPure XP beads, and end repair, A-base addition and ligation of Illumina indexed adaptors were performed. Adaptor-ligated libraries were electrophoresed on 3% Nusieve agarose gels, and fragments of 300–350 bp were recovered using QIAEX II gel-extraction reagents. Recovered DNA was amplified using Illumina index primers for eight cycles and purified using AMPure XP beads, and DNA concentration was determined using a Nanodrop spectrophotometer. Libraries (1 μg) were hybridized to the Agilent SureSelect Human All Exon v4 chip at 65 °C for 60 h, following the manufacturer's protocol (Agilent Technologies). Targeted exon fragments were captured on Dynal M-280 streptavidin beads (Invitrogen) and enriched by amplification with the Illumina index primers for nine additional PCR cycles. PCR products were purified with AMPure XP beads and analyzed for quality and quantity using an Agilent 2100 Bioanalyzer and DNA 1000 reagents.

We used the publicly available software FastQC to assess sequencing quality. For each lane, we examined per-base quality scores across the length of the reads. Lanes were deemed passing if the per-base quality score box plot indicated that >85% of the reads had >Q20 for bases 1–100. In addition to raw sequence quality, we also assessed alignment quality using the Picard package. This allows monitoring of duplication rates and chimeric reads that may result from ligation artifacts, crucial statistics for interpreting the results of copy number and structural variant analysis.

Gene fusion detection. Paired-end transcriptome sequencing reads were aligned to the human reference genome (GRCh37/hg19) using an RNA sequencing (RNA-seq) spliced read mapper Tophat2 (ref. 35) (Tophat 2.0.4) with the '–fusion-search' option turned on to detect potential gene fusion transcripts. In the initial process, Tophat2 internally deploys an ultrafast short-read alignment tool, Bowtie (Version 0.12.8), to map the transcriptome data. Potential false-positive fusion candidates were filtered out using the 'Tophat-Post-Fusion' module. Further, fusion candidates were manually examined for annotation and ligation artifacts. Junction reads supporting the fusion candidates were realigned using the BLAT alignment tool to confirm fusion breakpoints. Full-length sequence of each fusion gene was constructed on the basis of supporting junction reads and evaluated for potential ORFs using an ORF Finder. For gene fusions with robust ORFs, the amino acid sequences of the fused proteins were explored using the Simple Modular Architecture Research Tool (SMART) to examine the gain or loss of known functional domains in the fusion proteins.

Gene expression. BAM 'accepted_hits.bam' files, which were generated by the Tophat mapping module, were used to quantify the expression data through Cufflinks[36] (Version 2.0.2), an isoform assembly and RNA-seq quantification package. The structural features of 56,369 transcripts from the Ensembl resource (Ensembl 66) were used as an annotation reference to quantify the expression of individual transcripts and isoforms. The 'Max Bundle Length' parameter was set to '10000000', and 'multi-read-correct' was flagged on to perform an initial estimation procedure to more accurately weight reads mapping to multiple locations in the genome.

Mutation analysis. Whole-exome sequencing was performed on an Illumina HiSeq 2000 or HiSeq 2500 instrument in paired-end mode, and primary base call files were converted into FASTQ sequence files using the bcl2fastq converter tool bcl2fastq-1.8.4 in the CASAVA 1.8 pipeline. FASTQ sequence files were then processed through an in-house pipeline constructed for whole-exome sequence analyses of paired cancer and normal genomes. Sequencing reads were aligned to reference genome build hg19 (GRCh37) using Novoalign multithreaded (Version 2.08.02, Novocraft) and converted into BAM files using SAMtools (Version 0.1.18)[37]. Sorting and indexing of BAM files used Novosort threaded (Version 1.00.01), and duplicate reads were removed using Picard (Version 1.74). Mutation analysis was performed using VarScan2 algorithms (Version 2.3.2)[38] with the pileup files created by SAMtools mpileup for tumor and matched normal samples, simultaneously performing pairwise comparisons of base call and normalized sequence depth at each position. For SNV detection, filtering parameters including coverage, variant read support, variant frequency, *P* value, base quality, the presence of homopolymers and strandedness were applied. For indel analysis, Pindel (Version 0.2.4) was used on tumor and matched normal samples, and indels common to both samples were classified as germline, whereas indels present in tumor but not in normal samples were classified as somatic. Finally, a list of candidate indels as well as of somatic and/or germline mutations was generated by excluding synonymous SNVs. ANNOVAR[39] was used to functionally annotate the detected genetic variants, and positions are based on Ensembl 66 transcript sequences.

Tumor content for each tumor exome library was estimated from the sequence data by fitting a binomial mixture model with two components to the set of most likely SNV candidates from two-copy genomic regions. The set of candidates used for estimation consisted of coding variants that (i) were supported by at least 3 variant fragments in the tumor sample, (ii) were not supported by variant fragments in the matched benign sample, with at least 16 fragments of coverage, (iii) were not present in dbSNP, (iv) were within a targeted exon or within 100 bp of a targeted exon, (v) were not in homopolymer runs of 4 or more bases and (vi) exhibited no evidence of amplification or deletion. To filter out regions of possible amplification or deletion, we used exon coverage ratios to infer copy number changes, as described below. Resulting SNV candidates were not used for the estimation of tumor content if the segmented log ratio exceeded 0.2 in absolute value. Candidates on the Y chromosome were also eliminated because they were unlikely to exist in two-copy genomic regions. Using this set of candidates, we fit a binomial mixture model with two components using the R package flexmix, version 2.3-8. One component consisted of SNV candidates with very low variant fractions, presumably resulting from recurrent sequencing errors and other artifacts. The other component, consisting of the set of likely true SNVs, was informative of tumor content in the tumor sample. Specifically,

© 2013 Nature America, Inc. All rights reserved.

doi:10.1038/ng.2823

under the assumption that most or all of the observed SNV candidates in this component are heterozygous SNVs, we expect the estimated binomial proportion of this component to represent one-half of the proportion of tumor cells in the sample. Thus, the estimated binomial proportion obtained from the mixture model was doubled to obtain an estimate of tumor content.

Copy number aberrations were quantified and reported for each gene as the segmented, normalized, $\log_2$-transformed exon coverage ratio between each tumor sample and its matched normal sample[30]. To account for observed associations between coverage ratios and variation in GC content across the genome, lowess normalization was used to correct per-exon coverage ratios before segmentation analysis. Specifically, mean GC percentage was computed for each targeted region, and a lowess curve was fit to the scatterplot of $\log_2$ coverage ratios versus mean GC content across the targeted exome using the lowess function in R (version 2.13.1) with smoothing parameter $f = 0.05$.

Partially redundant sequencing of areas of the genome affords the ability for cross-validation of findings. We cross-validated exome-based point mutation calls by manually examining the genomic and transcriptomic reads covering the mutation using the UCSC Genome Browser. Likewise, gene fusion calls from the transcriptome data can be further supported by structural variant detection in the genomic sequence data, as well as by copy number information derived from genome and exome sequencing.

Chemicals and reagents. β-estradiol, (Z)-4-hydroxytamoxifen, (E/Z)-endoxifen hydrochloride hydrate and fulvestrant were purchased from Sigma-Aldrich.

Plasmids and cloning. cDNA for wild-type *ESR1* was PCR amplified from a breast cell line MCF7 (ATCC) with the introduction of a sequence encoding an N-terminal Flag tag. cDNAs encoding the relevant mutations of *ESR1* were generated by site-directed mutagenesis (QuikChange, Agilent Technologies), and full-length constructs were fully sequenced. All *ESR1* variants were placed in the lentiviral vector pCDH (System Biosciences) for eukaryotic expression.

ERE-luciferase reporter assays. For cell transfection experiments, HEK293T cells (ATCC) were plated at a density of $1–2 \times 10^5$ cells per well (24-well plates) in phenol red–free DMEM containing 10% FBS and antibiotics. Once cells attached, the medium was replaced with DMEM containing 10% charcoal/dextran-treated FBS (HyClone), and cells were cultured overnight. The next day, cells were transiently cotransfected with *ESR1* expression plasmid (50 ng/well) and luciferase reporter constructs (25 ng/well; SABiosciences) using FuGene 6 reagent (Promega). The ER-responsive luciferase plasmid encoding the firefly luciferase reporter gene is driven by a minimal CMV promoter and tandem repeats of the estrogen transcriptional response element (ERE). A second plasmid constitutively expressing *Renilla* luciferase served as an internal control for normalizing transfection efficiencies (Cignal ERE Reporter, SABiosciences). After transfection for 18 h, cells were serum starved for a few hours before treatment with β-estradiol or anti-estrogen drugs. Cells were harvested 18 h after treatment, and luciferase activity was measured using the Dual-Luciferase Reporter Assay System (Promega). IC_{50} values were computed using the GraphPad Prism application to fit a four-parameter dose response curve.

35. Kim, D. & Salzberg, S.L. TopHat-Fusion: an algorithm for discovery of novel fusion transcripts. *Genome Biol.* **12**, R72 (2011).
36. Trapnell, C. *et al.* Differential gene and transcript expression analysis of RNA-seq experiments with TopHat and Cufflinks. *Nat. Protoc.* **7**, 562–578 (2012).
37. Li, H. *et al.* The Sequence Alignment/Map format and SAMtools. *Bioinformatics* **25**, 2078–2079 (2009).
38. Koboldt, D.C. *et al.* VarScan 2: somatic mutation and copy number alteration discovery in cancer by exome sequencing. *Genome Res.* **22**, 568–576 (2012).
39. Wang, K., Li, M. & Hakonarson, H. ANNOVAR: functional annotation of genetic variants from high-throughput sequencing data. *Nucleic Acids Res.* **38**, e164 (2010).
40. Lonigro, R.J. *et al.* Detection of somatic copy number alterations in cancer using targeted exome capture sequencing. *Neoplasia* **13**, 1019–1025 (2011).

© 2013 Nature America, Inc. All rights reserved.

Journal of Medicinal Chemistry

Article

pubs.acs.org/jmc

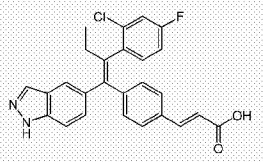
Identification of GDC-0810 (ARN-810), an Orally Bioavailable Selective Estrogen Receptor Degrader (SERD) that Demonstrates Robust Activity in Tamoxifen-Resistant Breast Cancer Xenografts

Andiliy Lai,[†] Mehmet Kahraman,[†] Steven Govek,[†] Johnny Nagasawa,[†] Celine Bonnefous,[†] Jackie Julien,[†] Karensa Douglas,[†] John Sensintaffar,[‡] Nhin Lu,[‡] Kyoung-jin Lee,[§] Anna Aparicio,[§] Josh Kaufman,[§] Jing Qian,[‡] Gang Shao,[‡] Rene Prudente,[‡] Michael J. Moon,[‡] James D. Joseph,[‡] Beatrice Darimont,[‡] Daniel Brigham,[‡] Kate Grillot,[‡] Richard Heyman,[‡] Peter J. Rix,[§] Jeffrey H. Hager,[‡] and Nicholas D. Smith*[,†]

[†]Department of Chemistry, [‡]Department of Biology, [§]Department of Drug Safety and Disposition, Seragon Pharmaceuticals, 12780 El Camino Real, Suite 302, San Diego, California 92130, United States

Supporting Information

ABSTRACT: Approximately 80% of breast cancers are estrogen receptor alpha (ER-α) positive, and although women typically initially respond well to antihormonal therapies such as tamoxifen and aromatase inhibitors, resistance often emerges. Although a variety of resistance mechanism may be at play in this state, there is evidence that in many cases the ER still plays a central role, including mutations in the ER leading to constitutively active receptor. Fulvestrant is a steroid-based, selective estrogen receptor degrader (SERD) that both antagonizes and degrades ER-α and is active in patients who have progressed on antihormonal agents. However, fulvestrant suffers from poor pharmaceutical properties and must be administered by intramuscular injections that limit the total amount of drug that can be administered and hence lead to the potential for incomplete receptor blockade. We describe the identification and characterization of a series of small-molecule, orally bioavailable SERDs which are potent antagonists and degraders of ER-α and in which the ER-α degrading properties were prospectively optimized. The lead compound **11l** (GDC-0810 or ARN-810) demonstrates robust activity in models of tamoxifen-sensitive and tamoxifen-resistant breast cancer, and is currently in clinical trials in women with locally advanced or metastatic estrogen receptor-positive breast cancer.



11l (GDC-0810 or ARN-810)
ER-α degradation IC_{50} = 0.7 nM
ER-α degradation Efficacy = 91%

INTRODUCTION

The estrogen receptors ER-α and ER-β are members of the nuclear hormone receptor superfamily and are ligand-regulated transcription factors that mediate the activity of estrogens in a number of important physiological processes, including reproduction, cardiovascular maintenance, and bone density/remodeling.[1] ER-α has been an important target in the pharmaceutical industry for many years, with ER antagonists such as tamoxifen (**1**) and aromatase inhibitors (that block the production of estrogen) such as anastrozole being a mainstay in the treatment of ER-positive breast cancer.[2] Tamoxifen (**1**) and its active metabolite 4-hydroxytamoxifen (**2**) (Figure 1) are selective estrogen receptor modulators (SERMs), in that they can behave as agonists or antagonists depending on the tissue context.[1] Unfortunately, despite many women with breast cancer initially responding well to tamoxifen, resistance often emerges. Although a variety of resistance mechanism may be at play in this state,[3] there is evidence that in many cases ER still plays a central role and that tumor cells still utilize pro-growth signaling pathways downstream of ER.[4] Recently, there has been increasing clinical evidence following treatment with aromatase inhibitors, of the involvement of mutations in the ligand-binding domain of ER-α rendering it transcriptionally active in the absence of ligand, leading to resistance to antihormonal therapy.[5] On the basis of this observation, it might be expected that a next-generation ER-α ligand that both antagonizes and degrades (i.e., removes) the ER-α would be of benefit to patients that have progressed on antihormonal therapy such as tamoxifen or aromatase inhibitors.

Fulvestrant (**3**) is a steroid-based estrogen receptor antagonist originally selected for development due its lack of agonism across all tissue types tested; however, it was retrospectively found to also be a selective estrogen receptor degrader (SERD) as well as antagonist.[6] Fulvestrant is approved for the treatment of ER-positive, metastatic breast cancer in postmenopausal women whose disease has progressed following treatment with endocrine therapy (i.e., tamoxifen or an aromatase inhibitor). However, fulvestrant is limited by poor pharmaceutical properties and is being administered by intramuscular injections (500 mg total dose in 2 × 5 mL injections) that limits the total amount of drug that may be administered and hence circulating levels. Even at the recently approved higher dose of 500 mg, FES-PET imaging data

Received: January 12, 2015
Published: April 16, 2015

ACS Publications © 2015 American Chemical Society

DOI: 10.1021/acs.jmedchem.5b00054
J. Med. Chem. 2015, 58, 4888−4904

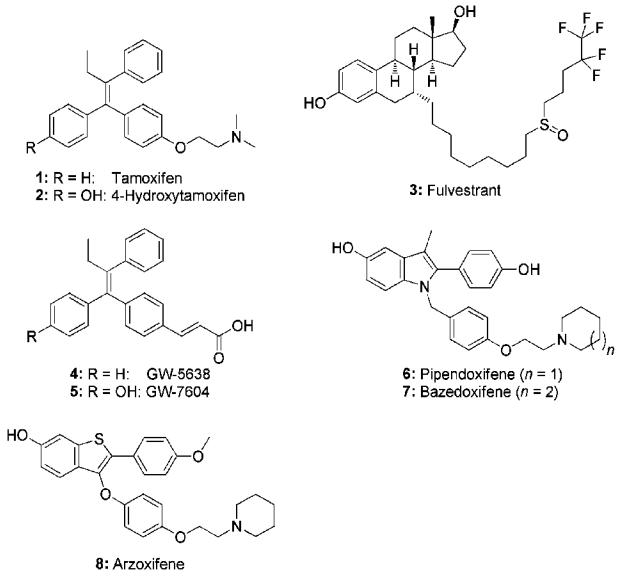


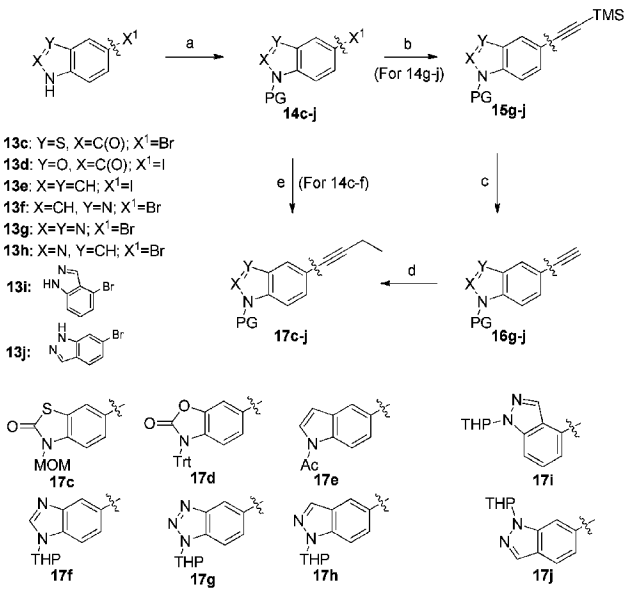
Figure 1. Estrogen receptor ligands.

supports the notion that the limitations of fulvestrant intramuscular dosing leads to incomplete estrogen receptor engagement in the clinic.[7] GW-5638 (**4**) is a nonsteroidal ER antagonist originally selected for development for its lack of undesired uterotrophic activity in tamoxifen treated animals and patients but, like fulvestrant, was also retrospectively determined to be a SERD.[8] Like tamoxifen, GW-5638 may be considered a prodrug as it is metabolized to produce the active metabolite GW-7604 (**5**) in vivo. Importantly, tamoxifen-resistant breast cancer cell lines were not cross-resistant to GW-5638 treatment, and the compound was ultimately progressed to a phase 1 clinical trial, although development was discontinued for unknown reasons. Thus, the activity of fulvestrant in relapsed patients in the clinic, and GW-5638 in models of tamoxifen-resistance, support the notion that ER still plays a critical role in tamoxifen-resistant breast cancer. We therefore set out to identify nonsteroidal SERDs where the ER-α degradation efficacy of the compounds was optimized prospectively and were orally bioavailable, allowing rapid achievement of robust, therapeutic levels of exposure.

CHEMISTRY

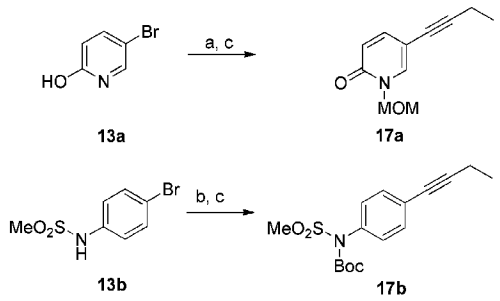
The compounds presented in this manuscript were prepared as outlined in Schemes 1−6. The synthetic strategy involved preparation of an appropriately substituted alkyne which was converted in the key synthetic step to the desired tetra-substituted alkene with regio- and stereocontrol. Heteroaryl alkynes **17c−j** were synthesized from commercial heteroaryl halides **13c−j** as shown in Scheme 1. Heteroaryl halides **13c−j**, containing a free NH, gave low yields in the Sonogashira coupling, and so a variety of protecting groups were employed. Benzothiazolone **13c**, benzoxazolone **13d**, and indole **13e** were protected with MOM, trityl, and acetyl, respectively, to give **14c**, **14d**, and **14e**. Meanwhile, benzimidazole **13f**, benzotriazole **13g**, and indazoles **13h−j** were protected with THP using 3,4-dihydro-2*H*-pyran and catalytic pyridinium *p*-toluenesulfonate to afford **14h−j** in 56−89% yield.[9] In the case of benzimidazole **14f** and benzotriazole **14g**, a 1:1 mixture of THP regioisomers was obtained. This mixture was used without separation in the Sonagashira reaction and then

Scheme 1. [a]



[a]Reagents and conditions: (a) For **13c**: MOM, MOM-Cl, K_2CO_3, DMF, 96%. **13d**: Tr-Cl, TEA, DCM, 83%. **13e**: Ac_2O, TEA, DMAP, DCE, 97%. **13f−j**: DHP, PPTS, DCM, 56−89%. (b) Cat. $Pd(Ph_3P)_2Cl_2$, CuI, trimethylsilylacetylene, THF−TEA (5:1), 80 °C, 97−100%. (c) K_2CO_3, MeOH, rt, 49−98%. (d) *n*-BuLi, Et-I, THF/TMEDA (9:1), −78 °C to 40 °C, 52−58%. (e) Cat. Pd(OAc)2, dppf, CuI, Cs_2CO_3, but-1-yn-1-yltrimethylsilane, DMA 80 °C, 47−93%.

Scheme 2. [a]



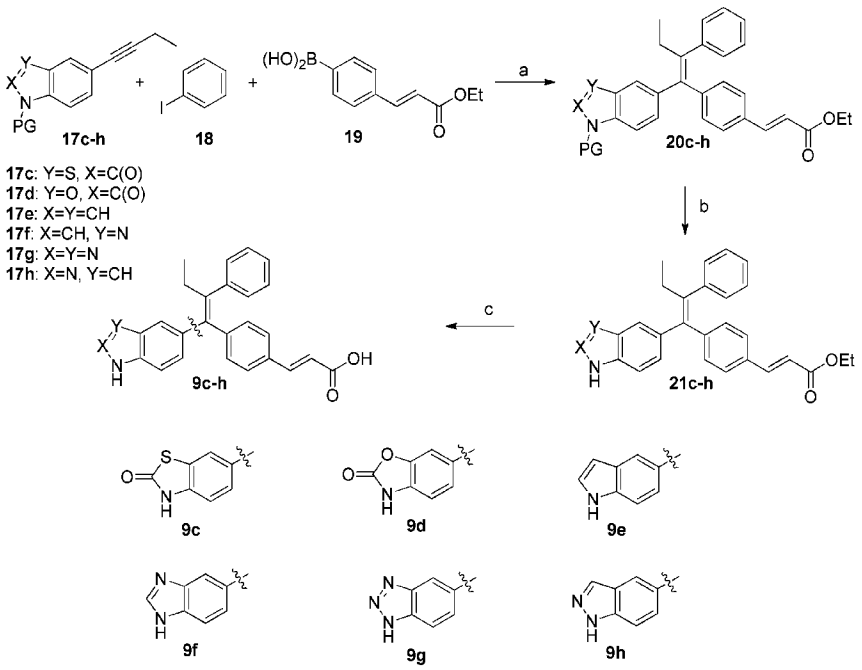
[a]Reagents and conditions; (a) MOM-Cl, K_2CO_3, DMF 40%; (b) Boc_2O, DMAP, DCM, 83%; (c) $Pd(OAc)_2$, dppf, CuI, Cs_2CO_3, but-1-yn-1-yltrimethylsilane 72−77%.

subsequently separated. Having suitably protected heteroaryl halides in hand, compounds **14c−j** were converted to alkynes **17c−j** via one of two routes. Initially, for **17g−j**, a three-step procedure was utilized. Coupling of **14g−j** and trimethylsilylacetylene under Sonogashira cross-coupling conditions[10] afforded alkynes **15g−j**, which were then desilylated using potassium carbonate. Then, a base-mediated alkylation of terminal alkynes **16g−j** with ethyl iodide gave the desired internal alkynes **17g−j**. Later, a more efficient one-pot procedure was used: halides **14c−f** were coupled with but-1-yn-1-yltrimethylsilane in the presence of palladium(II) acetate catalyst, 1,1′-bis(diphenylphosphino)ferrocene, copper iodide, and cesium carbonate to afford the desired internal alkynes **17c−f** directly in 47−93% yields.

In a similar way, alkynes **17a** and **17b** were synthesized from heteroaryl bromide **13a** or aryl bromide **13b** as shown in

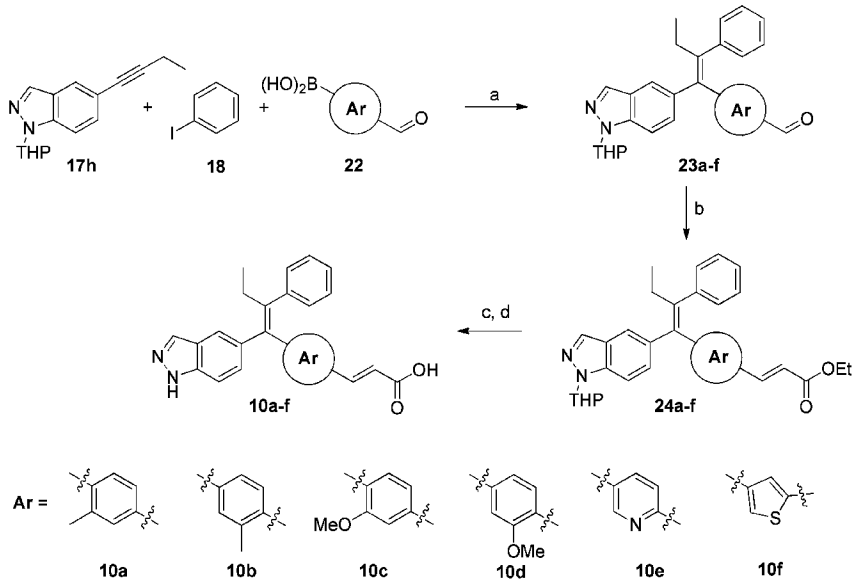
DOI: 10.1021/acs.jmedchem.5b00054
J. Med. Chem. 2015, 58, 4888−4904

Scheme 3. [a]



[a]Reagents and conditions: (a) cat. $Pd(PhCN)_2Cl_2$, K_2CO_3, DMF/H_2O, 13–82%; (b) HCl, EtOH, 90–100%; (c) LiOH, THF–EtOH, 45–60%.

Scheme 4. [a]



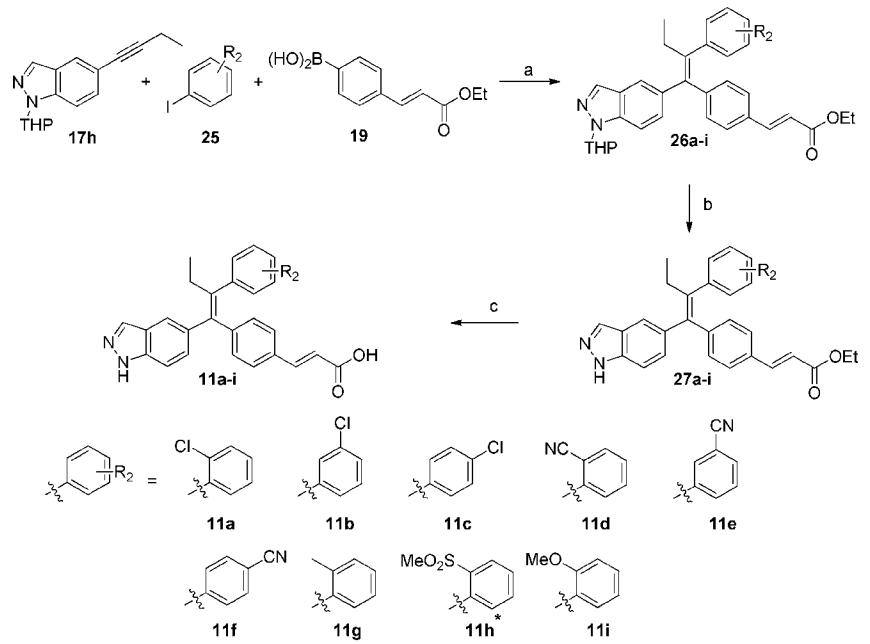
[a]Reagents and conditions: (a) cat. $Pd(PhCN)_2Cl_2$, K_2CO_3, DMF/H_2O, 30–68%; (b) triethylphosphonoacetate, LiCl, DBU, MeCN, 75–100%; (c) HCl, EtOH, 90–100%; (d) LiOH, THF–Et_2O, 54–60%.

Scheme 2. Thus, bromopyridine **13a** was protected as the *N*-MOM intermediate in 40% yield, while sulfonamide **13b** was protected as the carbamate in 83% yield. Using Sonagashira cross-coupling conditions, both intermediates were converted to the alkynes **17a** and **17b** in 72–77% yield.

To efficiently carry out structure–activity relationship (SAR) studies, we utilized a regioselective, stereospecific, three-component coupling followed by deprotection and saponification to prepare final compounds **9c–h** (Scheme 3).[11] To this end, heteroaryl alkynes **17c–h**, iodobenzene, and boronic acid **19** were coupled in 13–82% yield using catalytic $Pd(PhCN)_2Cl_2$ and K_2CO_3 in DMF–water. The tetra-substituted olefins **20c–h** were formed with good regioselectivity (typically >10:1), and any undesired regioisomer and biaryl (derived from Suzuki coupling of **18** and **19**) side-products were removed by silica gel chromatography. The fully constructed tetra-substituted alkenes **20c–h** were then deprotected under acidic condition to give acrylic esters **21c–h** in high yield. Finally, the acrylic ester was hydrolyzed using lithium hydroxide to afford the acrylic acids **9c–h**. In an analogous way, alkynes **17a–b** and

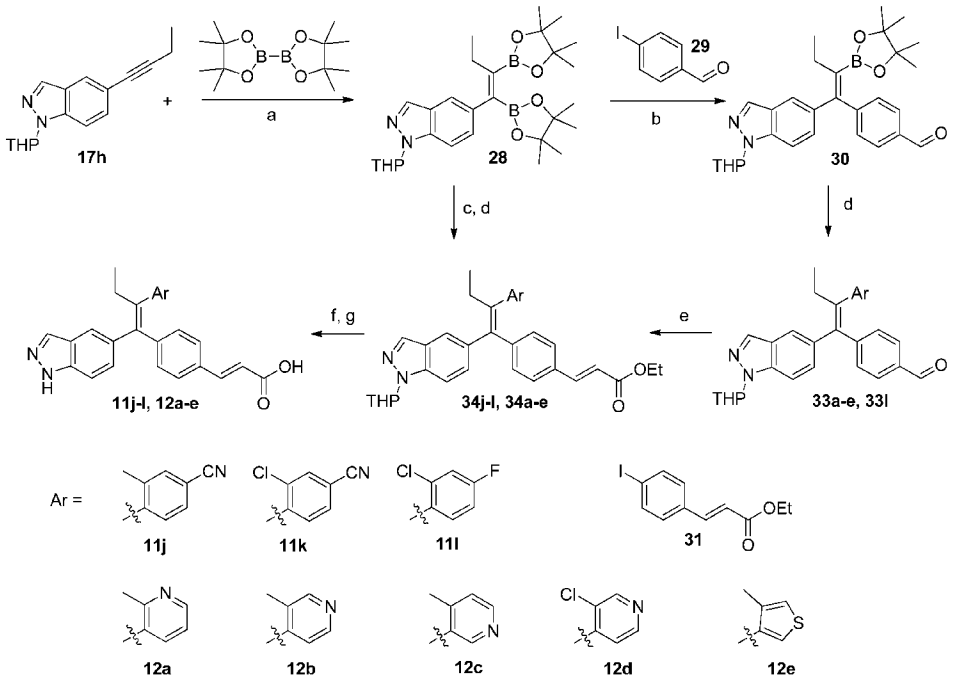
DOI: 10.1021/acs.jmedchem.5b00054
J. Med. Chem. 2015, 58, 4888–4904

Scheme 5. [a]



[a]Reagents and conditions: (a) cat. $Pd(PhCN)_2Cl_2$, K_2CO_3, DMF/H_2O, 8–62%; (b) HCl, EtOH, 95–100%; (c) LiOH, THF–EtOH, 11–77%. *2-iodothioanisole (**25**) was used in step (a) followed by oxone oxidation to give **26h**.

Scheme 6. [a]



[a]Reagents and conditions: (a) cat. $Pt(PPh_3)_4$, bis(pinacolato)diboron, 2-MeTHF, 80 °C; (b) **29**, cat. $PdCl_2(PPh_3)_2$, Cs_2CO_3, 2-MeTHF, 0 °C–rt; (c) **31**, cat. $PdCl_2(PPh_3)_2$, Cs_2CO_3, 2-MeTHF, 0 °C–rt; (d) Ar-X (**32**), cat. $PdCl_2(PPh_3)_2$, KOH (or K_2CO_3 in 1:1 2-MeTHF/DMSO), 2-MeTHF, reflux 21–99% (3 steps); (e) triethyl-phosphonoacetate, LiCl, DBU, MeCN, rt, 56–96%; (f) HCl, EtOH; (g) LiOH, THF–EtOH, 26–93% (2 steps).

17i–j were converted to the respective final compounds **9a–b,i–j**.

To investigate substitution on the phenyl-linker region, compounds **10a–f** were prepared (Scheme 4) by employing the same three-component coupling described in Scheme 3. Boronic acids **22** were used as coupling partners and afforded aryl aldehydes **23a–f** with good regioselectivity and moderate yields (30–68%). Aldehydes **23a–f** were then converted to (*E*)-acrylic esters **24a–f** via a Horner–Wadsworth–Emmons (HWE) reaction with triethylphosphonoacetate. Finally,

DOI: 10.1021/acs.jmedchem.5b00054
J. Med. Chem. 2015, 58, 4888–4904

compounds **10a–f** were obtained after removal of the THP protecting group and hydrolysis of the acrylic ester under standard conditions.

Compounds investigating substitution of the pendant phenyl ring were initially prepared (Scheme 5) using the three-component coupling described above. However, for systems with an ortho-subtituent (i.e.**11a**) and/or an electron withdrawing substituent (i.e., **11e**), these coupling conditions gave poor yields (<30%), or in some cases did not work due to the competing Suzuki cross-coupling of aryl iodide **25** and boronic acid **19**. Despite its inefficiency, this chemistry was used to produce intermediates **26a–i** in 8–62% yield. Removal of the THP group and hydrolysis of the ester gave the desired compounds **11a–i** in good yields.

Alternate chemistry was used for the efficient synthesis of tetra-substituted alkenes containing ortho-substituted and/or electron-deficient aryls and heteroaryls as outlined in Scheme 6. Alkyne **17h** was converted to bis(pinacolato)diboryl-alkene intermediate **28** in high yield,[12] and this intermediate was sufficiently stable to be stored for future synthesis. More typically, it was used immediately in a sequential bis-arylation to prepare the desired tetra-substituted alkene with high regio- and stereocontrol and in good yields.[13] Thus, in a one-pot reaction from **17h**, intermediate **28** (not isolated) was reacted with 4-iodo benzaldehyde **29** to give the intermediate aldehyde **30**, which was coupled with aryl halide **32** in the presence of catalytic $PdCl_2(PPh_3)_2$ and aqueous KOH to give intermediates **33a–e** and **33l** in 21–99% yield overall. These were then homologated using a HWE reaction to give **34a–e** and **34l**. It was observed that lower temperatures (0–25 °C) resulted in higher regiocontrol in the key arylation reaction and that intermediate **30** could also be isolated and stored for future use. Alternatively, intermediate **28** was coupled with ethyl 3-(4-iodophenyl)acrylate **31** in the presence of $PdCl_2(PPh_3)_2$ and Cs_2CO_3, followed by coupling with **32** in the presence of $PdCl_2(PPh_3)_2$ and aqueous potassium carbonate, to provide tetra-substituted alkenes **34j–k**. Lastly, the protecting groups of compounds **34a–e** and **34j–l** were removed under standard conditions to afford the targeted acrylic acid analogues **11j–l** and **12a–e**.

RESULTS AND DISCUSSION

In addition to more typical assays used in nuclear hormone receptor drug discovery programs such as binding and transcriptional assays, we also developed a cell-based immunofluorescence assay (in-cell western assay, "ICW") which monitored total ER-α protein levels in an MCF-7 breast cancer cell line. This assay was central to the program and was used to drive SAR to maximize ER-α degradation (SERD efficacy) of our ligands. Figure 2 shows an example of the assay with benchmark compounds, including fulvestrant, which was used as an internal control in each run of the assay, and we report degradation efficacy of compounds as a percent of this fulvestrant control. It should be noted that a small percentage of the ER-α still remains after fulvestrant treatment. This may reflect an inaccessible ER-α population resistant to degradation such as a nuclear insoluble fraction that is revealed upon cell permeabilization and antibody interrogation.[14]

Table 1 shows the profiles of the SERMs arzoxifene (discontinued following a phase 3 in patients with metastatic breast cancer)[15] and pipendoxifene (phase 2, discontinued for unknown reasons)[16] and the SERDs fulvestrant and GW-5638/7604 in the key ER-α degradation assay. A number of points are worth highlighting, first that arzoxifene, although potent in the ER-α degradation assay, has relatively poor degradation efficacy at 71% of the fulvestrant control. Second, GW-7604, the active metabolite of GW-5638, is much more potent than the parent in this ER-α degradation assay. At 91% of the fulvestrant control, GW-7604 is also an efficacious degrader of ER-α.

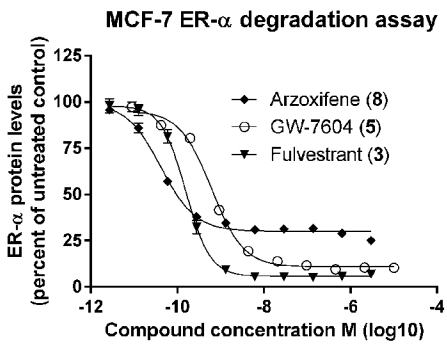


Figure 2. MCF-7 ER-α degradation assay. ER-α in-cell western in MCF-7 breast cancer cells in phenol-red free RPMI medium containing 5% charcoal dextran treated FBS; readings taken after 4 h incubation using a SP-1 anti-ER rabbit monoclonal antibody.

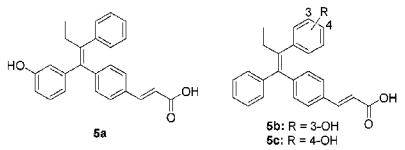
Table 1. MCF-7 ER-α Degradation Profile of ER Modulators

	MCF-7 ER-α degradation[a]		
compd	EC_{50} (μM)	maximum efficacy (%)	efficacy % of control[b]
fulvestrant (**3**)	0.0004	94	100
GW-5638 (**4**)	0.39	82	90
GW-7604 (**5**)	0.0017	86	91
pipendoxifene (**6**)	0.0001	83	87
arzoxifene (**8**)	0.0002	67	71

[a]ER-α in-cell western in MCF-7 breast cancer cells in phenol-red free RPMI medium containing 5% charcoal dextran treated FBS; readings taken after 4 h incubation using a SP-1 anti-ER rabbit monoclonal antibody. [b]Efficacy recorded as percent of efficacy of fulvestrant control.

For a prodrug strategy to be maximally effective, the active species should be efficiently produced in humans. When we examined the cross-species microsome profile of GW-5638, we found that, in all species, the active metabolite GW-7604 was indeed produced, but the ratio varied between species (Table 2). For example, in rat liver microsomes, 82% of GW-7604 was produced after a 4 h incubation, while in human liver

Table 2. Cross-Species in Vitro Liver Microsome Profile of GW-5638



	compd detected (%)[a]				
species	GW-5638 (**4**)	GW-7604 (**5**)	**5a**	**5b**	**5c**
mouse	50	21	0	0	30
rat	16	82	0	0	1
dog	92	5	0	0	3
human	63	16	0	0	21

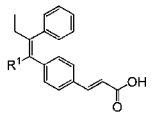
[a]Following 4 h incubation in liver microsomes.

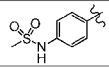
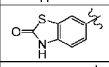
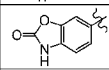
DOI: 10.1021/acs.jmedchem.5b00054
J. Med. Chem. 2015, 58, 4888–4904

microsomes, only 16% of GW-7604 was produced. In addition, we found that another oxidative metabolite **5c** was produced in human liver microsomes (21% after 4 h) and that it was 100-fold less potent an ER-α degrader than GW-7604 (ERα degradation EC_{50} = 0.113 μM). Further, the exposure of GW-7604 in mice following dosing of the parent GW-5638 was found to be relatively low (dosing of 100 mg/kg of GW-5638, gave: AUC (GW-5638) = 137 μg·h/mL, AUC (GW-7604) = 13 μg·h/mL). Thus, metabolism of GW-5638 to the desired active species GW-7604 is inefficient across species in vitro and in mouse PK studies.

We investigated a variety of scaffolds toward our goal of identifying fully efficacious ER-α degraders that had good exposure following oral dosing, and this paper will describe our investigation of the GW-5638 triphenylalkene scaffold. We initially explored the SAR in the region of the phenyl ring that is the site of metabolism of GW-5638 to the active 4-hydroxyphenyl metabolite, GW-7604 (Table 3).

Table 3. SAR of the Phenol Region of the Triphenylalkene Scaffold



Compound	R^1	ER-α Degradation[a]		MCF-7 Viability[b]
		EC_{50} (μM)	Efficacy[c]	IC_{50} (μM)
4 (GW-5638)		0.39	90%	0.985
5 (GW-7604)		0.0017	91%	0.005
9a		6.28	ND[d]	ND
9b		1.05	ND[d]	2.31
9c		0.101	92%	0.158
9d		0.023	90%	0.056
9e		0.003	93%	0.009
9f		0.957	ND[d]	1.18
9g		0.014	92%	0.053
9h		0.003	90%	0.006
9i		0.006	92%	0.021
9j		0.357	ND[d]	0.57

[a]ER-α in-cell western in MCF-7 breast cancer cells in phenol-red free RPMI medium containing 5% charcoal dextran treated FBS; readings taken after 4 h incubation using a SP-1 anti-ER rabbit monoclonal antibody. [b]MCF-7 viability assay in RPMI medium containing 10% FBS; 5 day incubation. [c]Efficacy recorded as percent of efficacy of fulvestrant control. [d]Not determined due to incomplete floor of dose response curve because of relative low potency of compound.

Single-ring systems such as pyridyl **9a** and sulfonamide **9b** both lost a considerable amount of activity (>1 μM in the ER-α degradation assay) compared to **GW-7604** (EC_{50} = 0.0017 μM), potentially due to the high polarity of these moieties and/or the pyridone nature of **9a**. However, when we examined bicyclic heterocycles such as the benzothiazolone **9c** and benzoxazolone **9d**, where a weakly acidic N−H exists in the cyclic structure (pK_a 8.7),[17] improved activity was observed. Exploration of [6,5] systems improved the potency further; thus, indole **9e** (EC_{50} = 0.003 μM), benzotriazole **9g** (EC_{50} = 0.014 μM), and indazole **9h** (EC_{50} = 0.003 μM) were high potency compounds, with the indole and indazole effectively equipotent to **GW-7604**. In contrast to these systems, basic benzimidazole **9f** was considerably less active (EC_{50} = 0.957 μM). In addition to good potency, indazole **9h** was also an efficacious ER-α degrader (90% of the fulvestrant control) and importantly delivered good exposure in mice following oral dosing (100 mpk po: AUC = 240 μg·h/mL versus **GW-7604** AUC = 13 μg·h/mL, from 100 mpk po dosing of **GW-5638**).

The importance of the directionality of the indazole N−H was highlighted when different isomers of **9h** were prepared. Thus, the 4-indazole **9i** (EC_{50} = 0.006 μM) maintained potency compared to **9h**, while the 6-indazole isomer **9j** lost >100× potency (EC_{50} = 0.357 μM), presumably as it is unable to form the key hydrogen bond in the ligand binding domain of the estrogen receptor that **9h** is able to. Of note, all potent compounds were efficacious ER-α degraders, achieving ≥90% of the efficacy of the fulvestrant control. This was found to be the case in general for the triphenylalkene scaffold derivatives that contained the acrylic acid side chain. The potency in an MCF-7 breast cancer cell viability assay generally tracked with the ER-α degradation EC_{50}, with **9h** and **9e** both having an IC_{50} < 0.010 μM in this viability assay. With the identification of indazole **9h** as a potent, efficacious SERD, we proceeded to examine the SAR of the phenyl linker region of the scaffold (Table 4).

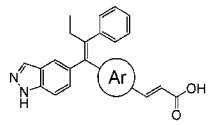
Although introduction of a methyl or methoxy substituent at either the "internal" (**10a**, **10c**) or "external" (**10b**, **10d**) positions relative to the core was tolerated, it did not lead to an increase in potency. Replacement of the phenyl ring with a heterocycle such as pyridine **10e** and thiophene **10f** led to a substantial drop-off in potency, indicating that these heterocyclic rings are not well tolerated in this region. It is interesting that **10d** is one of the few potent acrylic acid examples where a reduction of degradation efficacy was observed in the ER-α in-cell western assay. This suggests the importance of this region for maximal ER-α degradation efficacy and may reflect the ability of the methoxy substituent to modulate the pK_a of the key acrylic acid moiety.

In general, nuclear hormone receptor ligands such as estradiol are lipophilic in nature,[18] and so introduction of polar groups while maintaining potency can be difficult. Throughout the program we explored typical lipophilic groups as well as trying to incorporate heteroatoms in the series, and Tables 5 and 6 show some of the SAR that was carried out on the pendent phenyl ring of indazole **9h** toward this goal.

Table 5 shows that substitution at the ortho position (**11a**, **11d**) is preferred over the meta- or para-position (**11c**, **11e**, **11f**) for both a more polar substituent (−CN) or a lipophilic substituent (−Cl). Of note, *ortho*-chloro **11a** gives a 3−5-fold increase in potency over the unsubstituted phenyl **9h**, while *ortho*-nitrile **11d** is equipotent to **9h**. Additional substituents were examined at the ortho-position, with a strongly polar

DOI: 10.1021/acs.jmedchem.5b00054
J. Med. Chem. 2015, 58, 4888−4904

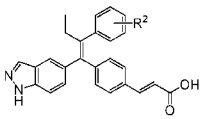
Table 4. SAR in the Phenyl Linker Region of the Triphenylalkene Scaffold



Compound	Ar	ER-α Degradation[a]		MCF-7 Viability[b]
		EC_{50} (μM)	Efficacy[c]	IC_{50} (μM)
9h		0.003	90%	0.006
10a		0.015	92%	0.036
10b		0.006	90%	0.014
10c		0.004	90%	0.012
10d		0.011	85%	0.031
10e		0.11	85%	0.21
10f		1.13	ND[d]	2.9

[a]ER-α in-cell western in MCF-7 breast cancer cells in phenol-red free RPMI medium containing 5% charcoal dextran treated FBS; readings taken after 4 h incubation using a SP-1 anti-ER rabbit monoclonal antibody. [b]MCF-7 viability assay RPMI medium containing 10% FBS; 5 day incubation. [c]Efficacy recorded as percent of efficacy of fulvestrant control. [d]Not determined due to incomplete floor of dose response curve because of relative low potency of compound.

Table 5. SAR of the Pendent Phenyl Ring

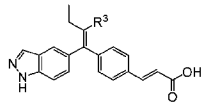


compd	R^2	ER-α degradation[a]		MCF-7 viability[b]
		EC_{50} (μM)	efficacy (%)[c]	IC_{50} (μM)
9h	H	0.003	90	0.006
11a	o-Cl	0.0007	92	0.002
11b	m-Cl	0.002	91	0.012
11c	p-Cl	0.010	93	0.015
11d	o-CN	0.003	93	0.012
11e	m-CN	0.028	87	0.100
11f	p-CN	0.036	93	0.047
11g	o-Me	0.0008	92	0.004
11h	o-SO_2Me	0.049	91	0.070
11i	o-OMe	0.004	93	0.025
11j	o-Me, p-CN	0.001	89	0.005
11k	o-Cl, p-CN	0.0009	92	0.004
11l	o-Cl, p-F	0.0007	91	0.002

[a]ER-α in-cell western in MCF-7 breast cancer cells in phenol-red free RPMI medium containing 5% charcoal dextran treated FBS; readings taken after 4 h incubation using a SP-1 anti-ER rabbit monoclonal antibody. [b]MCF-7 viability assay in RPMI medium containing 10% FBS; 5 day incubation. [c]Efficacy recorded as percent of efficacy of fulvestrant control.

ortho-sulfone substituent leading to a drop-off in activity, i.e., compare **11h** (ER-α degradation EC_{50} = 0.049 μM) to *ortho*-methyl **11g** (ER-α degradation EC_{50} = 0.0008 μM). We found

Table 6. Select Pendant Heterocycles Are Tolerated



Compound	R^3	ER-α Degradation[a]		MCF-7 Viability[b]
		EC_{50} (μM)	Efficacy[c]	IC_{50} (μM)
11g		0.0008	92%	0.004
12a		0.16	ND[d]	0.20
12b		0.008	89%	0.016
12c		0.11	91%	0.15
12d		0.002	90%	0.004
12e		0.0005	90%	0.002

[a]ER-α in-cell western in MCF-7 breast cancer cells in phenol-red free RPMI medium containing 5% charcoal dextran treated FBS; readings taken after 4 h incubation using a SP-1 anti-ER rabbit monoclonal antibody. [b]MCF-7 viability assay in RPMI medium containing 10% FBS; 5 day incubation. [c]Efficacy recorded as percent of efficacy of fulvestrant control. [d]Not determined due to incomplete floor of dose response curve because of relative low potency of compound.

that adding an *ortho*-methyl or *ortho*-chloro substituent to otherwise less active derivatives (such as the *para*-cyano derivative **11f**; ER-α degradation EC_{50} = 0.036 μM), resulting in disubstituted systems such as **11j** and **11k**, gave a substantial 30-fold increase in potency (**11j** and **11k**: ER-α degradation $EC_{50} \leq 0.001$ μM). The *ortho*-chloro, *para*-fluoro derivative **11l** was also a high potency compound. We also found that heterocycles could be incorporated in this region (Table 6), the 4-pyridyl **12b** (ER-α degradation EC_{50} = 0.008 μM) being the preferred substitution pattern compared to **12a** and **12c** (ER-α degradation EC_{50} > 0.10 μM). Chloro-pyridyl **12d** and thiophene **12e** were also potent heterocyclic compounds in this region. As with SAR on the indazole region, potency in the ER-α degradation assay generally tracked with the MCF-7 breast cancer cell viability IC_{50}, with compounds such as **11a**, **11k**, **11l**, and **12d** all having an IC_{50} < 0.005 μM.

As illustrated in Tables 3−6, a number of potent and efficacious ER-α degraders were identified. To quickly determine those that had good exposure and activity following oral dosing, we heavily utilized a 4-day immature rat uterine wet weight assay, which allowed rapid determination of compound antagonist activity in an ER responsive tissue (immature rat uterus) while competing against the native ER ligand estradiol (i.e., antagonist mode).[19] Drug plasma levels were also obtained from this assay. Table 7 shows the reduction in immature rat uterine weight for select compounds when compared to estradiol-only treated animals (the table also includes exposure in mice from separate PK studies).

In general, compounds that effectively antagonized estradiol-induced uterine weight gain (>75% compared to vehicle) when dosed at 1 mg/kg orally had good potency in the ER-α degradation assay (EC_{50} <0.001 μM) and also had measurable drug levels at the end of the study (C_{24} > 3 nM following a 1 mg/kg po dose). In this way, the uterine assay identified promising compounds such as **11a**, **11l**, and **12e** while de-emphasizing otherwise potent in vitro compounds such as

DOI: 10.1021/acs.jmedchem.5b00054
J. Med. Chem. 2015, 58, 4888−4904

Table 7. Immature Rat Uterine Wet Weight Assay (Antagonist Mode) and Mouse Pharmacokinetics

		rat uterine wet weight[a]		mouse PK
compd	ER-α degradation EC_{50} (μM)	percent inhibition[b]	drug levels (nM)[c]	po AUC (μg·h/mL)
9d	0.023	28	0.2	3.0
9e	0.003	47	ND	9.4
9g	0.014	15	ND	2.3
9h	0.003	69	3.8	5.8
9i	0.006	35	0.1	2.8
11a	0.0007	82	3.7	15
11b	0.002	81	11	11
11d	0.003	27	ND	0.2
11g	0.0008	72	1.7	7.2
11j	0.001	48	14[d]	4.3
11k	0.0009	60	10[d]	2.9
11l	0.0007	81	5.2	8.8
12b	0.008	7	7.6	0.081
12d	0.002	66	0.5	0.11
12e	0.0005	105[e]	10	3.8

[a]Compounds administered orally (1 mg/kg po) followed by an oral dose of 0.1 mg/kg ethynyl estradiol each day for 3 days. On the fourth day, 24 h post dose, the animals were euthanized and the uterus was removed and weighed. Plasma was taken at the time point indicated. [b]100[(Vehicle$_{EE}$ − Compd)/(Vehicle$_{EE}$ − Vehicle)], where "Vehicle$_{EE}$" is the uterine wet weight of the of the vehicle animals dosed with ethynyl estradiol (0.1 mg/kg); "Compd" is the uterine wet weight of the of the compound treated animals dosed with ethynyl estradiol (0.1 mg/kg); "Vehicle" is the uterine wet weight of the of the vehicle animals. [c]Measured at 24 h after last dose unless otherwise indicated. [d]Measured at 6 h after last dose. [e]In same assay, **11l** = 112%.

indole **9e** or indazole **9i**. Although **12e** demonstrated robust activity in the UWW model, it had lower exposure in mouse PK (mouse po AUC @ 10 mg/kg =3.8 μg·h/mL) than **11a** and **11l** (mouse po AUC @ 10 mg/kg =15 μg·h/mL and 8.8 μg·h/mL respectively). In addition, the presence of a thiophene in **12e** was of concern due to the potential for reactive metabolite formation in vivo, and so we did not pursue **12e** further.[20] Compounds **11a** and **11l** had a similar in vitro and uterine assay profile and were subsequently profiled in additional assays including a tamoxifen-resistant MCF-7 xenograft model. Ultimately, **11l** was selected for development and Table 8 shows a comparison to clinical benchmarks. **11l** is a potent ER-α binder (IC_{50} = 6.1 nM), a full transcriptional antagonist with no agonism (3× ERE, IC_{50} = 2 nM), and displays good potency

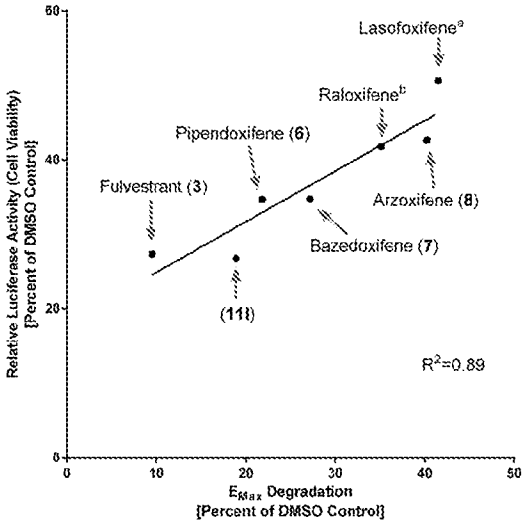


Figure 3. Optimization of efficacy in the ER-α degradation assay correlates with increased efficacy in the MCF-7 breast cancer cell line viability assay. (a) SERM for osteoporosis.[21] (b)SERM for osteoporosis.[22]

and efficacy in ER-α degradation (EC_{50} = 0.7 nM) and MCF-7 breast cancer cell viability (IC_{50} = 2.5 nM) assays.

Of particular note are the optimized levels of ER-α degradation for **11l** (91%) compared to arzoxifene (**8**) (71%) and pipendoxifene (**6**) (87%) and that these efficacy levels translate into increased efficacy in the MCF-7 viability assay (**11l**, 99% efficacy, 4; arzoxifene (**8**), 73% efficacy; pipendoxifene (**6**), 89% efficacy). Indeed, we observed a correlation between ER-α degradation efficacy and MCF7-viability efficacy which extended across chemical scaffolds and is captured graphically in Figure 3. Although not definitively causative, this correlation indicates that optimization of ER-α degradation efficacy leads to compounds with improved efficacy in a breast cancer cell viability assay. As will be presented below, this increase in in vitro efficacy also led to improved efficacy in a xenograft model of tamoxifen resistance.

The robust degradation of **11l** in the in cell western assay was confirmed in a Western blot assay as shown in Figure 4. Similar to fulvestrant, **11l** displays robust degradation of ER-α in this assay format. Of note is that, although an agonist, estradiol also leads to degradation of ER-α while 4-hydroxytamoxifen (**2**), as is known the literature, leads to stabilization of ER-α (an increase in protein levels).

Table 8. 11l Shows a Favorable in Vitro Profile Compared to Benchmark Compounds

	binding (nM)[a]		transcriptional antagonism[b]	ER-α degradation[c]		MCF-7 viability[d]	
compd	ER-α IC_{50}	ER-β IC_{50}	IC_{50} (nM)	EC_{50} (nM)	efficacy (%)[e]	IC_{50} (nM)	efficacy (%)[e]
11l	6.1	8.8	2.0	0.7	91	2.5	99
Fulvestrant (**3**)	24	21	0.6	0.4	100	0.6	100
GW-7604 (**5**)	6.0	3.0	18	1.8	91	5.0	98
pipendoxifene (**6**)	ND	ND	0.6	0.1	87	0.4	89
arzoxifene (**8**)	42	240	0.3	0.2	71	0.4	73

[a]Competitive radiometric binding in TEGM; 2.5 nM ER-α or 1.5 nM ER-β, 1.5 nM ^{3}H-E2. [b]3× ERE-TK-Luc reporter vector, phenol-red free RPMI containing 10% charcoal dextran treated FBS plus 17β-estradiol (0.1 nM), 24 h. [c]ER-α in-cell western in MCF-7 breast cancer cells in phenol-red free RPMI medium containing 5% charcoal dextran treated FBS; readings taken after 4 h incubation using a SP-1 anti-ER rabbit monoclonal antibody. [d]MCF-7 viability assay in RPMI medium containing 10% FBS; 5 day incubation. [e]Efficacy recorded as percent of efficacy of fulvestrant control.

DOI: 10.1021/acs.jmedchem.5b00054
J. Med. Chem. 2015, 58, 4888−4904

Table 9. Cross-Species Pharmacokinetic of 11l[a]

species	CL (mL/min/kg)	V_{ss} (L/kg)	$t_{1/2}$ (iv) (h)	C_{max} (oral) (μg/mL)	AUC (oral) (μg·h/mL)	oral %F
mouse	11	1.2	4.2	4.4	8.8	61
rat	14	1.9	3.9	1.8	5.8	49
dog	1.6	0.2	11	20	69	61
cyno	7.0	0.5	13	6.1	10	42

[a]Dosed intravenously at 3 mg/kg and per orally at 10 mg/kg in PEG400/PVP/TW80/0.5% CMC in water, 9:0.5:0.5:90.

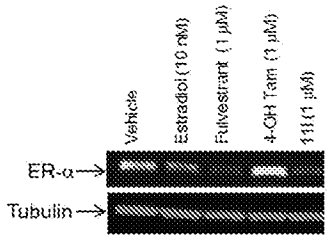


Figure 4. Western blot analysis confirms **11l** is a robust degrader of ER-α. MCF-7 cells in RPMI supplemented with 10% charcoal dextran treated FBS; compound treatment for 20 h, cell lysates separated electrophoretically using NuPAGE 4–12% Bis Tris Gels; SP-1 anti-ERα antibody and imaged using a LI-COR Odyssey infrared imaging system.

The pharmacokinetic profile of **11l** (Table 9) shows it is a low clearance molecule across species, with good bioavailability (40–60%). As would be expected for a lipophilic carboxylic acid, the compound is highly bound to plasma proteins (>99.5% across species) and has a low to moderate volume of distribution (V_{ss} = 0.2–2.0 L/kg across species).

Metabolism profiling of **11l** conducted in microsomes, with phase 1 and phase 2 cofactors added, showed the acyl glucuronide to be the major metabolite across species. The stability of this acyl glucuronide in physiological medium (pH 7.4 phosphate buffer at 37 °C) was examined to understand its potential for reactivity (Figure 5).[23]

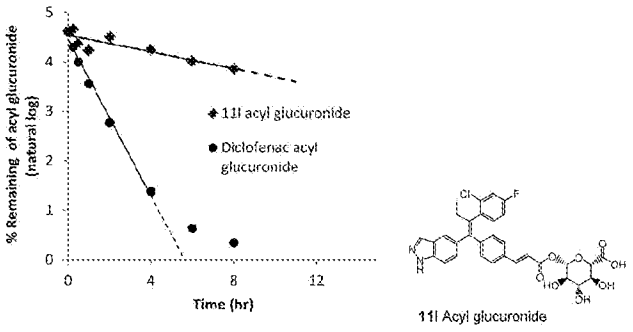


Figure 5. Percent remaining of **11l** acyl glucuronide in pH 7.4 phosphate buffer at 37 °C.

Compared to the diclofenac *O*-glucuronide positive control ($t_{1/2}$ = 0.9 h), the stability of the **11l** *O*-glucuronide was good at $t_{1/2}$ = 8.1 h, leading to the conclusion that the potential risk for idiosyncratic toxicity of **11l** was low. Cytochrome P450 inhibition profiling of **11l** indicated it had little to no inhibition against CYP1A2, CYP2D6, or CYP3A4 (IC_{50} > 20 μM), modest inhibitory effect on CYP2C9 and CYP2C19 (IC_{50} = 2.2 and 3.3 μM respectively), and potent inhibition of CYP2C8 (IC_{50} of <0.1 μM). Inhibition of CYP2C8 was not considered a major liability, as few therapeutics are metabolized exclusively by CYP2C8, suggesting the potential for drug–drug interactions is low.[24]

Selectivity of **11l** over other nuclear hormone receptors was found to be good. In transcriptional reporter assays for the mineralocorticoid (MR), progesterone-A (PR-A), progesterone-B (PR-B), and glucocorticoid (GR) receptors, **11l** had minimal activity (IC_{50} > 1 μM). While in binding assays, **11l** displayed little activity toward the androgen receptor (AR; IC_{50} > 4 μM) and GR (IC_{50} = 0.99 μM). In a CEREP panel of radioligand binding assays for 54 diverse targets (protein-free conditions), **11l** at 10 μM displayed >50% binding to seven targets. However, the only appreciable activity seen in cell-based functional assays for these seven targets was for the GABA-gated chloride channel (IC_{50} = 1.1 μM) and the dopamine transporter (IC_{50} = 3.4 μM). In light of the high plasma protein binding of **11l**, these low micromolar activities were not considered an issue, as selectivity for the estrogen receptor is >500-fold (MCF-7 viability = 2 nM; ER-α degradation = 0.7 nM). **11l** produced no significant inhibition of hERG current at doses up to 30 μM in a patch clamp assay and was Ames negative in the TA-98 and TA-100 tester strains.

Compound **11l** was extensively characterized in xenograft models of breast cancer. In these models, supplemental estradiol (E2) is used to drive xenograft tumor growth in vivo (in the form of an implanted slow-release pellet), and these high E2 ligand concentrations (300–400 pg/mL) require higher concentrations of **11l** in order to out-compete the native ligand (E2) and so mediate an inhibitory effect. This is of relevance, as plasma E2 levels in the target patient population of postmenopausal women (~5 pg/mL)[25] are substantially lower than those of the various preclinical models. Thus, preclinical models run in the context of high E2 plasma concentrations likely significantly overestimate **11l** dose and plasma levels necessary to drive efficacy in a postmenopausal setting.

Figure 6 shows the robust activity of **11l** in a tamoxifen-sensitive MCF-7 xenograft model, with 3 mg/kg/day dosed orally showing substantial tumor-growth inhibition, while at the highest dose of 100 mg/kg/day, all animals showed tumor regression of more than 50%. No weight loss was observed. Fulvestrant was run as a positive control in this assay at a dose of 200 mg/kg subcutaneously 3× per week and caused only tumor stasis. The mediocre activity of fulvestrant in this and other xenograft models is not due to an insufficient exposure, as this regimen produces sustained fulvestrant levels that are 30-fold greater than those obtained in the clinic (fulvestrant xenograft C_{max}~ 0.75 and C_{min} ~0.45 ng/mL versus clinical C_{max} = 0.028 and C_{min} ~0.012 ng/mL).[26]

Continued dosing of **11l** to the 100 mg/kg/day cohort in this model beyond the initial 28 days produced a durable response with a median time to progression for **11l** of >1 year. In contrast, emergence of resistance with tamoxifen occurred at about 70 days, clearly showing the differential profile of **11l**.

The initial target patient population for the SERD program is women who have progressed on endocrine therapy such as

DOI: 10.1021/acs.jmedchem.5b00054
J. Med. Chem. 2015, 58, 4888–4904

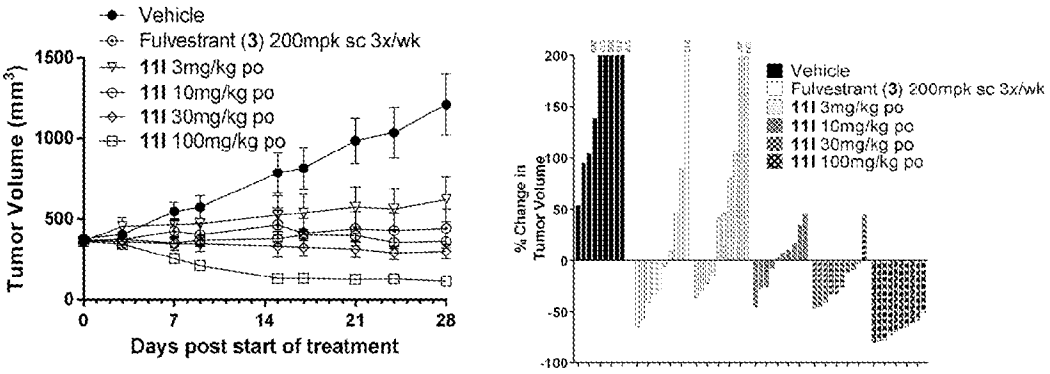
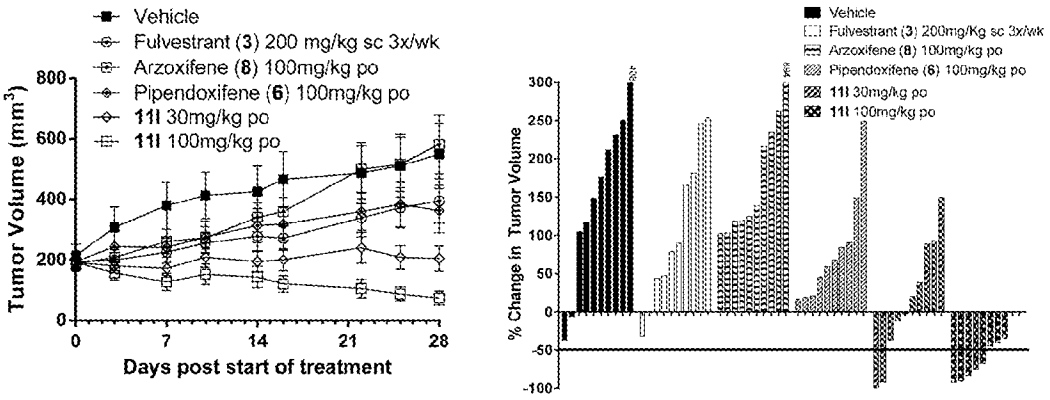


Figure 6. **11l** shows robust dose-responsive activity in a tamoxifen-sensitive MCF-7 xenograft model. MCF-7 tamoxifen-sensitive xenograft in nu/nu mice using subcutaneous 0.72 mg estradiol pellets. MCF-7 cells subcutaneously injected 2–3 days post pellet implantation. n = 9–10 animals per group. Tumor volume (length × width^2/2) was monitored weekly. Animals were treated with vehicle or compound daily. Left panel shows tumor growth time course; right panel shows individual tumor volume on day 28.



	Tamoxifen-resistant xenograft study		
Compound	**Dose (mg/kg)**	**Tumor Volume (Fold over start)**	**AUC_{day28} (μg.hr/mL)**
Vehicle	-	2.6	-
Fulvestrant	200 SC 3xwk	2.1	11
Pipendoxifene	100 po	1.8	7
Arzoxifene	100 po	3.3	50
11l	30 po	1.1	21
11l	100 po	0.34	45

Figure 7. **11l** shows robust activity in an MCF-7 tamoxifen-resistant xenograft model and is superior to benchmark compounds. MCF-7 tamoxifen-resistant xenograft in nu/nu mice using subcutaneous 0.72 mg estradiol pellets. n = 8–10 animals per group. Tumor volume (length × width^2/2) was monitored weekly. Animals were treated with vehicle or compound daily. Left panel shows tumor growth time course; right panel shows individual tumor volume on day 28.

tamoxifen. To mimic this preclinically, we developed models of endocrine resistance by continuous dosing of tamoxifen to mice in an MCF-7 xenograft until tumor regrowth occurred. These individual tumors that were resistant were then propagated in the presence of tamoxifen and used as the source material for tamoxifen-resistant xenograft studies. Figure 7 illustrates the activity of **11l** in this tamoxifen-resistant setting compared to fulvestrant (**3**), pipendoxifene (**6**), and arzoxifene (**8**). Compound **11l** showed robust activity, with a dose of 30 mg/kg giving tumor stasis (tumor volume fold over start = 1.1), and all tumors regressing at 100 mg/kg (tumor volume fold over start = 0.34). Fulvestrant and pipendoxifene showed only tumor-growth inhibition (tumor volume fold over start = 2.1 and 1.8, respectively), while arzoxifene had no inhibitory activity compared to vehicle (tumor volume fold over start = 3.3).[27] The poor performance of arzoxifene in the tamoxifen-resistant setting is noteworthy considering that it is more potent than **11l** in the ER-α degradation and viability assays (Table 8) and has equivalent exposure to **11l** on day 28 of the xenograft study (arzoxifene AUC_{day28} = 50 μg·h/mL; **11l** AUC_{day28} = 45 μg·h/mL). Of note is that arzoxifene has poor *efficacy* in the ER-α degradation assay compared to **11l** (ER-α degradation efficacy: **11l** (91%) versus arzoxifene (71%)).

The improved profile of **11l** over GW-5638 was clearly demonstrated in this MCF-7 tamoxifen-resistant xenograft setting where at a dose of 100 mg/kg po, GW-5638 only resulted in tumor growth inhibition (tumor volume fold over start = 2.6, separate experiment, data not shown) compared to tumor regression for **11l** at this dose (tumor volume fold over start = 0.34).

DOI: 10.1021/acs.jmedchem.5b00054
J. Med. Chem. 2015, 58, 4888–4904

CONCLUSION

Through our SAR studies on a triphenylalkene scaffold, we identified a series of indazole ER-α modulators that exhibited a dual mode of action being both potent transcriptional antagonists and degraders of the estrogen receptor (SERDs). Importantly, the series of compounds in general and the clinical candidate **11l** in particular are high efficacy degraders of the ER-α, reducing the levels of ER-α to a similar extent as fulvestrant. **11l** exhibited good bioavailability across species and displayed robust activity in tamoxifen-sensitive and tamoxifen-resistant xenograft models of breast cancer. Activity was superior to fulvestrant and other benchmark compounds in these studies. Compound **11l** (GDC-0810 or ARN-810) is currently in clinical trials in women with locally advanced or metastatic estrogen receptor-positive breast cancer.

EXPERIMENTAL SECTION

Experimental Procedures (Chemistry). All air and moisture sensitive reactions were carried out under an inert atmosphere of nitrogen. All reactive liquid reagents were transferred by syringe or cannula and were added into the flask through a rubber septum. All other solvents and reagents were obtained from commercial sources and used as received unless otherwise stated. Both ^{1}H and ^{13}C spectra were obtained on a Bruker 400 spectrometer at 400 and 100 MHz, respectively. Chemical shifts are reported in parts per million (δ) from an internal standard of residual DMSO (2.50 or 39.5 ppm), methanol (3.31 or 49.0 ppm), or chloroform (7.26 or 77.2 ppm). Proton chemical shift data are reported as follows: chemical shift, multiplicity (s = singlet, d = doublet, t = triplet, q = quartet, m = multiplet, b = broad), integration, coupling constant (J) reported in hertz. Analytical thin-layer chromatography (TLC) was performed on commercial silica plates (Merck 60-F 254, 0.25 mm thickness); compounds were visualized by UV light (254 nm). All yields reported are not optimized. Normal phase purifications were performed on silica gel columns using a Biotage (SP1 or SP4), an ISCO Combiflash Companion XL, or ISCO Combiflash Torrent using prepacked silica gel columns. Reversed phase semipreparative HPLC purifications were carried out using a Shimadzu Discovery VP system with a SPD-20A prominence UV/vis detector (190−700 nm range). The columns used were a Waters SunFire C18 (19 mm × 150 mm) or a YMC-Pack Pro ODS-A (20 mm × 150 mm) or a Phenomenex, Luna 5 μ C18 semipreparative (250 mm × 10 mm) column with a acetonitrile−water solvent mixture in the presence of 0.1% TFA. The purity of target compounds was determined by ^{1}H NMR, analytical HPLC/MS, and high resolution mass spectroscopy and shown to be >95% pure prior to biological testing. Low-resolution mass spectra (LRMS) were recorded on a WatersMicromass ZQ using electrospray positive ionization. High-resolution mass spectra (HRMS) were obtained on an Agilent ESI-TOF mass spectrometer using electrospray positive or negative ionization.

*5-Bromo-1-(tetrahydro-2H-pyran-2-yl)-1H-indazole (**14h**).* A 250 mL round-bottom flask equipped with a magnetic stir bar, a rubber septum, and a N_2 inlet was charged with 5-bromo-1*H*-indazole (10 g, 50.7 mmol) and anhydrous dichloromethane (101 mL). To this solution, 3,4-dihydro-2*H*-pyran (23 mL, 253.8 mmol) was added in one portion at room temperature followed by addition of PPTS (1.28 g, 5 mmol). The resulting mixture was stirred at room temperature for 48 h. Upon completion by TLC (or LCMS), the reaction mixture was quenched with water and extracted with dichloromethane (3 × 100 mL). The combined organic extracts were washed with water (100 mL), washed with brine (50 mL), dried over sodium sulfate, filtered, concentrated, and purified by silica gel chromatography (0−10% ethyl acetate in hexanes) to give 5-bromo-1-(tetrahydro-2*H*-pyran-2-yl)-1*H*-indazole as a pale-yellow oil (89% yield). ^{1}H NMR (400 MHz, DMSO-d_6): δ 8.10 (s, 1H), 8.00 (d, 1H, J = 1.85 Hz), 7.72 (d, 1H, J = 8.90 Hz), 7.53 (dd, 1H, J = 1.85 Hz, J = 8.90 Hz), 5.83 (dd, 1H, J = 2.60 Hz, J = 9.80 Hz), 3.89−3.83 (m, 1H), 3.75−3.69 (m, 1H), 2.43−2.31(m, 1H), 2.04−1.92 (m, 2H), 1.80−1.64 (m, 1H), 1.60−150 (m, 2H). ^{13}C NMR (100 MHz, DMSO-d_6): δ 137.9, 132.8, 128.9, 125.7, 123.2, 113.4, 112.4, 84.1, 66.5, 28.8, 24.7, 22.0.

Method B: General Procedure for Sonagashira Coupling of Protected Aryl or Heteroaryl Halides with But-1-yn-1-yltrimethylsilane. A mixture of the appropriate aryl or heteroaryl halide (1.0 equiv), Cs_2CO_3 (1.3−3.0 equiv), CuI (0.05−0.2 equiv), $Pd(OAc)_2$ (0.05−0.2 equiv), dppf (0.05−0.2 equiv), and *N*,*N*-dimethylacetamide (DMA, 1−2 mL/mmol) was degassed with three vacuum/nitrogen cycles. But-1-yn-1-yltrimethylsilane (1.3−2.0 equiv) was added, and the reaction was heated at 80 °C under N_2 for 2−24 h (until complete by TLC or LCMS). The reaction was allowed to cool to room temperature, diluted with ethyl acetate and water, and then filtered through Celite. The aqueous layer was separated and extracted with ethyl acetate. The organics were combined, dried, filtered, concentrated, and then purified by silica gel column chromatography to give the corresponding butynyl-aryl or butynyl-heteroaryl.

*5-(But-1-yn-1-yl)-1-(tetrahydro-2H-pyran-2-yl)-1H-indazole (**17h**). Step 1: 1-(Tetrahydro-2H-pyran-2-yl)-5-((trimethylsilyl)-ethynyl)-1H-indazole (**15h**).* To a 250 mL pressure tube, 5-bromo-1-(tetrahydro-2*H*-pyran-2-yl)-1*H*-indazole (11.9 g, 42.3 mmol), $Pd(Ph_3P)_2Cl_2$ (1.48 g, 0.05 mmol), CuI (0.8 g, 4.2 mmol), and THF/triethylamine (5:1, 85 mL) were added. This mixture was degassed with three vacuum/N_2 cycles, and then trimethylsilylacetylene (9 mL, 63.5 mmol) was added. The pressure tube was sealed and heated at 80 °C for 2 days. Upon completion by LCMS, the reaction mixture was cooled down to room temperature and filtered through Celite with ethyl acetate (200 mL). The filtrate was concentrated to give the crude product that was used directly in the next step.

*Step 2: 5-Ethynyl-1-(tetrahydro-2H-pyran-2-yl)-1H-indazole (**16h**).* A 250 mL round-bottom flask equipped with a magnetic stir bar, a rubber septum, and a N_2 inlet was charged with a solution of 1-(tetrahydro-2*H*-pyran-2-yl)-5-((trimethylsilyl)ethynyl)-1*H*-indazole (12.6 g, 42.2 mmol) in MeOH. To this solution, solid K_2CO_3 (0.58 g, 4.2 mmol) was added in one portion. The resulting mixture was stirred at room temperature for 4 h. Upon completion by TLC, the reaction mixture was filtered, concentrated, and purified by silica gel chromatography (0−10% ethyl acetate in hexanes) to give 5-ethynyl-1-(tetrahydro-2*H*-pyran-2-yl)-1*H*-indazole (4.7 g) as a pale-yellow solid. ^{1}H NMR (400 MHz, DMSO-d_6): δ 8.13 (s, 1H), 7.96 (s, 1H), 7.75 (d, 1H, J = 8.75 Hz), 7.47 (dd, 1H, J = 1.45 Hz, 8.75 Hz), 5.86 (dd, 1H, J = 2.60 Hz, J = 9.80 Hz), 4.10 (s, 1H), 3.90−3.86 (m, 1H), 3.78−3.68 (m, 1H), 2.43−2.32 (m, 1H), 2.06−1.93 (m, 2H), 1.81−1.66 (m, 1H), 1.60−1.50 (m, 2H).

*Step 3: 5-(But-1-yn-1-yl)-1-(tetrahydro-2H-pyran-2-yl)-1H-indazole (**17h**).* A 250 mL round-bottom flask equipped with a magnetic stir bar, a rubber septum, and a N_2 inlet was charged with 5-ethynyl-1-(tetrahydro-2*H*-pyran-2-yl)-1*H*-indazole (4.2 g, 18.6 mmol) and anhydrous THF/TMEDA (9:1, 93 mL). This solution was cooled to −78 °C in an IPA/dry ice bath, and *n*-BuLi (17.4 mL solution in hexanes, 27.84 mmol) was added dropwise over 15 min. The resulting mixture was stirred for 30 min at −78 °C, and then iodoethane (2.23 mL, 27.84 mmol) was added dropwise over 5 min. The mixture was gradually warmed to room temperature, stirred for 1 h, and then heated at 40 °C overnight. Upon completion by LCMS, the reaction mixture was cooled to room temperature, quenched with water (100 mL), and extracted with ethyl acetate (2 × 100 mL). The combined organics were washed with water (100 mL), washed with brine (50 mL), dried over sodium sulfate, filtered, concentrated, and purified by silica gel chromatography (0−10% ethyl acetate in hexanes) to give 5-(but-1-yn-1-yl)-1-(tetrahydro-2*H*-pyran-2-yl)-1*H*-indazole (1.42 g) as a pale-yellow solid. ^{1}H NMR (400 MHz, DMSO-d_6): δ 8.08 (s, 1H), 7.82 (s, 1H), 7.68 (d, 1H, J = 8.75 Hz), 7.39 (dd, 1H, J = 1.60 Hz, 8.75 Hz), 5.82 (dd, 1H, J = 2.60 Hz, J = 9.90 Hz), 3.90−3.84 (m, 1H), 3.77−3.69 (m, 1H), 2.43 (q, 2H, J = 7.50 Hz), 2.40−2.33 (m, 1H), 2.04−1.92 (m, 2H), 1.78−1.67 (m, 1H), 1.60−1.53 (m, 2H), 1.18 (t, 3H, J = 7.50 Hz). LCMS: 255 $(M + H)^+$.

*Method B: Alternate Preparation of 5-(But-1-yn-1-yl)-1-(tetrahydro-2H-pyran-2-yl)-1H-indazole (**17h**).* A mixture of 5-bromo-1-(tetrahydro-2*H*-pyran-2-yl)-1*H*-indazole (39.6 g, 0.142 mol), Cs_2CO_3

DOI: 10.1021/acs.jmedchem.5b00054
J. Med. Chem. 2015, 58, 4888−4904

(60.0 g, 184 mmol), CuI (1.35 g, 7.08 mmol), $Pd(OAc)_2$ (1.59 g, 7.08 mmol), dppf (3.93 g, 7.08 mmol), and *N*,*N*-dimethylacetamide (DMA, 160 mL) was degassed with three vacuum/nitrogen cycles. But-1-yn-1-yltrimethylsilane (23.2 g, 184 mmol) was added, and the resulting mixture was heated at 80 °C for 5 h under N_2. Upon completion by LCMS, the reaction mixture was diluted with EtOAc (300 mL) and H_2O (300 mL) and then filtered. The organic layer of the filtrate was separated, and the aqueous layer was extracted with EtOAc (3 × 150 mL). The combined organic layers were washed with brine (2 × 100 mL), dried over anhydrous Na_2SO_4, filtered, and concentrated. The residue was purified on silica gel column (300–400 mesh, 20 cm in diameter and 15 cm in height) using EtOAc/petroleum ether (1 L of petroleum ether, then 1 L of EtOAc/petroleum ether = 1/50, and then EtOAc/petroleum ether = 1/30 until the byproduct was washed out, then EtOAc/petroleum ether = 1/10 to collect the product), affording a yellow oil (33 g) which solidified over time in the refrigerator. The resulting solid was further washed with petroleum ether (200 mL, then 3 × 50 mL), affording the title compound as an off-white solid (26 g, 73%). ^{1}H NMR (400 MHz, DMSO-d_6): δ 8.08 (s, 1H), 7.82 (s, 1H), 7.68 (d, 1H, J = 8.75 Hz), 7.39 (dd, 1H, J = 1.60 Hz, 8.75 Hz), 5.82 (dd, 1H, J = 2.60 Hz, J = 9.90 Hz), 3.90–3.84 (m, 1H), 3.77–3.69 (m, 1H), 2.43 (q, 2H, J = 7.50 Hz), 2.40–2.33 (m, 1H), 2.04–1.92 (m, 2H), 1.78–1.67 (m, 1H), 1.60–1.53 (m, 2H), 1.18 (t, 3H, J = 7.50 Hz). ^{13}C NMR (100 MHz, DMDO-d_6): δ 138.2, 133.5, 129.4, 124.0, 123.9, 115.9, 110.7, 90.2, 84.1, 80.1, 66.5, 28.8, 24.7, 22.1, 13.8, 12.3. LCMS: 255 $(M + H)^+$.

Method C: General Procedure for Multicomponent Cross-Coupling of the Butynyl-aryls or Butynyl-heteroaryls. A mixture of the appropriate butynyl-aryl or butynyl-heteroaryl (1.0 equiv), aryl-iodide (3.0 equiv), aryl-boronic acid (3.0 equiv), K_2CO_3 (3.0 equiv), and *N*,*N*-dimethylformamide (DMF)/water (2:1, 50 mL/mmol) was degassed with three vacuum/N_2 cycles and then heated at 45 °C. After 10 min (or when homogeneous), a solution of $Pd(PhCN)_2Cl_2$ (0.01 equiv) in DMF was added (note 1). The reaction was stirred at 45 °C for 4–24 h (until complete by TLC or LCMS; note 2), allowed to cool to room temperature, quenched with water, and then extracted with ethyl acetate. The extracts were washed with water, washed with brine, dried, filtered, concentrated, and purified by silica gel chromatography to give the desired tetra-substituted alkene.

Note 1: In some instances, all chemicals were simply mixed at room temperature, degassed, and then heated. In other instances, the boronic acid was added last as a DMF/water solution. *Note 2*: When incomplete conversion of butynyl-heteroaryl was observed (especially with ortho-substituted aryl-iodides), additional aryl-iodide, aryl-boronic acid, and K_2CO_3 (1–3 equiv each) were added and heating was continued for 8–24 h.

Method D: General Procedure for an Alternate Multicomponent Cross-Coupling of the Butynyl-heteraryls. Step 1: Preparation of Bis(pinacolato)diboryl-alkene. A solution of the appropriate butynyl-heteroaryl (1.0 equiv), bis(pinacolato)diboron (1.01 equiv), $Pt(PPh_3)_4$ (0.01 equiv), and 2-methyltetrahydrofuran (2 mL/mmol) was degassed with three vacuum/N_2 cycles and then heated at reflux under N_2 for 1–8 h (until complete by TLC or LCMS). The reaction was allowed to cool to room temperature and then either (1) taken directly into step 2, or (2) concentrated to give a crude residue (usually a foam), or (3) concentrated and purified by silica gel chromatography to afford the pure bis(pinacolato)diboryl-alkene.

Step 2: Cross-Coupling of the Bis(pinacolato)diboryl-alkene. A mixture of bis(pinacolato)diboryl-alkene (1.0 equiv), an appropriate 4-iodoaryl-aldehyde or (*E*)-ethyl 3-(4-iodophenyl)acrylate (1.0 equiv), $PdCl_2(PPh_3)_2$ (0.1 equiv), Cs_2CO_3 (2 equiv), 2-methyltetrahydrofuran (4 mL/mmol, note 1), and water (0–3% v/v; note 2) was stirred vigorously at 20–40 °C (note 3) under N_2 for 1–24 h (until complete by TLC or LCMS). The reaction was then either (1) taken directly into step 3 or (2) processed to isolate the 1-aryl-2-(pinacolato)boryl-alkene (The reaction was diluted with ethyl ether (or ethyl acetate) and washed with water (1–3 times). The aqueous phases were back extracted with ethyl ether (or ethyl acetate). The extracts were combined, dried, filtered, concentrated, and then purified by silica gel chromatography.).

Note 1: When the bis(pinacolato)diboryl-alkene was brought into this step as a solution from step 1, solvent (2 mL/mmol) was added to make the final volume of solvent approximately 4 mL/mmol. *Note 2*: Most commonly, anhydrous Cs_2CO_3 and anhydrous solvent were used, so 1–2% water (v/v with respect to solvent) was added to the reaction. When the Cs_2CO_3 and/or solvent were not anhydrous, no water was added. *Note 3*: Most commonly, reactions were run at room temperature. resulting in higher regiocontrol.

Step 3: Cross-Coupling of the 1-Aryl-2-(pinacolato)boryl-alkene. A mixture of 1-aryl-2-(pinacolato)boryl-alkene (1.0 equiv), an appropriate aryl-halide or heteroaryl-halide (1.5 equiv), $PdCl_2(PPh_3)_2$ (0.1 equiv), 2-methyltetrahydrofuran (4 mL/mmol; note 1), and KOH (3–6M, 5–6 equiv; note 2) was degassed with three vacuum/N_2 cycles and then heated at reflux under N_2 for 1–24 h (until complete by TLC or LCMS). The reaction was allowed to cool to room temperature, diluted with ethyl ether (or ethyl acetate), and washed with water (1–3 times). The aqueous phases were back extracted with ethyl ether (or ethyl acetate). The extracts were combined, dried, filtered, concentrated, and then purified by silica gel chromatography to give the desired tetra-substituted alkene.

Note 1: When the 1-aryl-2-(pinacolato)boryl-alkene was brought into this step directly from step 2, no additional solvent or $PdCl_2(PPh_3)_2$ was added. Only the aryl-halide (or heteroaryl-halide) and KOH were added. *Note 2*: Most commonly, 6 equiv of KOH were used, and the aqueous solution of KOH was 4 M or 6 M. For some compounds, especially those with base-sensitive functionality (e.g., a nitrile or ester), K_2CO_3 (6 equiv, 4 M aqueous) was used in place of KOH and DMSO was used as either the sole solvent or a cosolvent.

Method E: Horner–Wadsworth–Emmons Coupling of the Aryl-aldehydes. 1,8-Diazabicyclo[5.4.0]undec-7-ene (DBU, 1.1 equiv) was added dropwise to a mixture of the appropriate aryl-aldehyde (1.0 equiv), triethylphosphonoacetate (1.1–1.3 equiv), lithium chloride (2.0 equiv), and anhydrous acetonitrile (2 mL/mmol) at room temperature. The resulting mixture was stirred for 1–4 h (until complete by TLC or LCMS) and then concentrated. Dichloromethane (or ethyl acetate or ether) was added, and the mixture was washed with water, washed with brine, dried, filtered, concentrated, and purified by silica gel column chromatography to give the desired acrylic ester.

Method F: Removal of Protecting Groups. I. Deprotection of a THP Group. A solution of HCl (note 1) was added to a solution of the protected-heteroaryl (1.0 equiv) in ethanol (2–5 mL/mmol; note 2) at room temperature. The mixture was heated at 70 °C (note 3) for 2–8 h (until complete by TLC or LCMS), allowed to cool to room temperature, and concentrated to give a crude product that was either carried on directly to the next step or purified by silica gel chromatography.

Note 1: Most commonly, 2 M HCl in diethyl ether or 1.25 M HCl in ethanol were used. Most commonly, 10% v/v HCl solution was used. *Note 2:* Most commonly, the concentration was 5 mL/mmol. *Note 3*: In some instances, the reaction was heated at 80 °C or reflux.

ii. Deprotection of a MOM Group. A variety of conditions have been utilized to remove the MOM protecting group, including (1) the same as above for removing THP, (2) ethereal HCl in refluxing THF, and (3) aqueous HCl in refluxing ethanol

iii. Deprotection of a Trt or a Boc Group. Most commonly, Trt and Boc groups were removed under the conditions described for THP group.

iv. Deprotection of an Acetyl Group. The *N*-acetyl group was removed during the hydrolysis of the acrylic ester with LiOH as described in method G.

Method G: Hydrolysis of the Acrylic Ester to the Acrylic Acid. An aqueous solution of LiOH (2–20 equiv; note 1) was added to a solution of the appropriate ester (1.0 equiv) in ethanol/tetrahydrofuran (1:1, 10 mL/mmol; note 2) at room temperature, and the mixture was stirred for 4–24 h (until complete by TLC or LCMS). A solution of HCl (1 M aqueous) was added until the pH was 3 (note 3). The mixture was diluted with water and extracted with ethyl acetate. The organic layer was washed with water, washed with brine, dried, filtered,

DOI: 10.1021/acs.jmedchem.5b00054
J. Med. Chem. 2015, 58, 4888–4904

concentrated, and purified by silica gel chromatography or preparative-HPLC to give the desired acrylic acid.

Note 1: Most commonly, a 2 M solution of aqueous LiOH was used, or the LiOH was dissolved in minimum amount of water. *Note 2*: In some instances, a single solvent (ethanol, dioxane, or tetrahydrofuran) was used. *Note 3*: Alternate workup procedures have been employed including: (i) the use of satd NH_4Cl in place of aqueous HCl and (ii) removal of the organic solvent by rotary evaporation prior to acid quench.

*(E)-3-(4-((E)-1-(1H-Indol-5-yl)-2-phenylbut-1-en-1-yl)phenyl)-acrylic Acid (**9e**).* The title compound was prepared using 1-(5-(but-1-yn-1-yl)-1*H*-indol-1-yl)ethanone, (*E*)-(4-(3-ethoxy-3-oxoprop-1-en-1-yl)phenyl)boronic acid, and iodobenzene following methods C and G. ^{1}H NMR (300 MHz, DMSO-d_6): δ OH resonance not observed, 12.30 (br, 1H), 11.13 (s, 1H), 7.43−7.31 (m, 5H), 7.24−7.12 (m, 5H), 6.93−6.88 (m, 1H), 6.87 (d, 2H, J = 8.5 Hz), 6.44−6.40 (m, 1H), 6.36 (d, 1H, J = 16.0 Hz), 2.46 (q, 2H, J = 7.3 Hz), 0.88 (t, 3H, J = 7.3 Hz). HRMS-ESI$^+$: m/z [M + H]$^+$ calcd for $C_{27}H_{23}NO_2$, 394.1807; found, 394.1809.

*(E)-3-(4-((E)-1-(1H-Benzo[d][1,2,3]triazol-5-yl)-2-phenylbut-1-en-1-yl)phenyl)acrylic Acid (**9g**).* The title compound was prepared using 5-(but-1-yn-1-yl)-1-(tetrahydro-2*H*-pyran-2-yl)-1*H*-benzo[*d*][1,2,3]-triazole, (*E*)-(4-(3-ethoxy-3-oxoprop-1-en-1-yl)phenyl)boronic acid, and iodobenzene following methods C, F, and G. ^{1}H NMR (300 MHz, DMSO-d_6): δ 15.65 (br, 1H), 12.29 (br, 1H), 7.92 (d, 1H, J = 8.40 Hz), 7.78 (s, 1H), 7.41 (d, 1H, J = 16.0 Hz), 7.35 (d, 2H, J = 8.40 Hz), 7.24−7.13 (m, 6H), 6.91 (d, 2H, J = 8.40 Hz), 6.37 (d, 1H, J = 16.0 Hz), 2.39 (q, 2H, J = 7.50 Hz), 0.89 (t, 3H, J = 7.50 Hz)). ^{13}C NMR (100, MHz, DMSO-d_6): δ 167.5, 144.5, 143.3 (2C), 143.2, 143.2, 141.1, 137.3, 131.8, 130.7, 129.3, 128.0, 127.5, 126.6, 118.8, 28.6, 13.2. HRMS-ESI$^+$: m/z [M + H]$^+$ calcd for $C_{25}H_{21}N_3O_2$, 396.1712; found, 396.1704.

*(E)-3-(4-((E)-1-(1H-Indazol-5-yl)-2-phenylbut-1-en-1-yl)phenyl)-acrylic Acid (**9h**). Step 1: (E)-Ethyl 3-(4-((E)-2-Phenyl-1-(1-(tetrahydro-2H-pyran-2-yl)-1H-indazol-5-yl)but-1-en-1-yl)phenyl)acrylate (**20h**).* A solution of 5-(but-1-yn-1-yl)-1-(tetrahydro-2*H*-pyran-2-yl)-1*H*-indazole (2.5 g, 9.83 mmol), iodobenzene (6 g, 29.5 mmol), (*E*)-(4-(3-ethoxy-3-oxoprop-1-en-1-yl)phenyl)boronic acid (6.49 g, 29.5 mmol), K_2CO_3 (4.08 g, 29.5 mmol), and *N*,*N*-dimethylformamide/water (2:1, 492 mL) was degassed with 3 vacuum/N_2 cycles and then heated at 45 °C until it was a homogeneous solution. A solution of $Pd(PhCN)_2Cl_2$ (38 mg, 0.098 mmol) in *N*,*N*-dimethylformamide (0.5 mL) was added. The resulting mixture was stirred at 45 °C overnight. Upon completion, the reaction mixture was cooled to room temperature, quenched with water (500 mL), and extracted with ethyl acetate (3 × 500 mL). The combined organics were washed with water, washed with brine, dried over sodium sulfate, filtered, and concentrated to give the crude product. This crude material was purified on a silica gel column eluted with 0−50% ethyl acetate in hexanes, affording the title compound as off-white foam (3.71 g). LCMS: 423 [(M − THP + H) + H]$^+$.

*Step 2: (E)-Ethyl 3-(4-((E)-1-(1H-Indazol-5-yl)-2-phenylbut-1-en-1-yl)phenyl)acrylate (**21h**).* To a solution of (*E*)-ethyl 3-(4-((*E*)-2-phenyl-1-(1-(tetrahydro-2*H*-pyran-2-yl)-1*H*-indazol-5-yl)but-1-en-1-yl)phenyl)acrylate (3.5 g, 6.9 mmol) in ethyl alcohol (69 mL), HCl (6 mL, 2 M in diethyl ether) was added at room temperature. The resulting mixture was then heated at 70 °C for 2 h. Upon completion, the mixture was cooled to room temperature and concentrated to give the crude product. This crude material was purified on a silica gel column eluted with 0−100% ethyl acetate in hexanes, affording an off-white solid (2.5 g, 86% yield). ^{1}H NMR (300 MHz, DMSO-d_6): δ 13.10 (s, 1H), 8.08 (s, 1H), 7.69 (s, 1H), 7.53 (d, 1H, J = 8.70 Hz), 7.48 (d, 1H, J = 16.0 Hz), 7.39 (d, 2H, J = 8.40 Hz), 7.27−7.11 (m, 6 H), 6.89 (d, 2H, J = 8.40 Hz), 6.45 (d, 1H, J = 16.0 Hz), 4.14 (q, 2H, J = 7.30 Hz), 2.43 (q, 2H, J = 7.50 Hz), 1.22 (t, 3H, J = 7.30 Hz), 0.87 (t, 3H, J = 7.50 Hz). LCMS: 423 (M + H)$^+$.

*Step 3: (E)-3-(4-((E)-1-(1H-Indazol-5-yl)-2-phenylbut-1-en-1-yl)-phenyl)acrylic Acid (**9h**).* To a solution of (*E*)-ethyl 3-(4-((*E*)-1-(1*H*-indazol-5-yl)-2-phenylbut-1-en-1-yl)phenyl)acrylate (2.5 g, 5.9 mmol) in THF−EtOH (1:1, 59 mL), an aqueous solution of LiOH (2.8 g, 118 mmol; dissolved in a minimum amount of water) was added at room temperature. The resulting mixture was stirred at room temperature overnight. The reaction was monitored by LCMS. Upon completion, 1 N aqueous HCl was added until pH was 3. Then, the mixture was diluted with water and extracted with ethyl acetate (3 × 200 mL). The combined organic layers were washed with water, washed with brine, dried over sodium sulfate, filtered, and concentrated to give the crude product. This crude material was purified on a silica gel column eluted with 0−20% methanol in dichloromethane, affording the title compound as a pale-yellow solid (1.9 g). ^{1}H NMR (400 MHz, DMSO-d_6): δ OH resonance not observed, 12.7 (br, 1H), 8.08 (d, 1H, J = 0.9 Hz), 7.65 (br, 1H), 7.54 (d, 1H, J = 8.50 Hz), 7.44 (d, 1H, J = 16. 0 Hz), 7.33 (d, 2H, J = 8.50 Hz), 7.20−7.08 (m, 6 H), 6.88 (d, 2H, J = 8.40 Hz), 6.37 (d, 1H, J = 16.0 Hz), 2.41 (q, 2H, J = 7.50 Hz), 0.86 (t, 3H, J = 7.50 Hz). ^{13}C NMR (100, MHz, DMSO-d_6): δ 166.4, 144.1, 142.4, 141.4, 140.4, 137.8, 137.0, 133.5, 132.4, 130.4, 129.7, 128.2, 126.8, 126.6, 126.3, 125.3, 121.8, 119.2, 117.4, 108.9, 27.5, 12.2. HRMS-ESI$^+$: m/z [M + H]$^+$ calcd for $C_{26}H_{22}N_2O_2$, 395.1760; found, 395.1759.

*(E)-3-(4-((E)-1-(1H-Indazol-4-yl)-2-phenylbut-1-en-1-yl)phenyl)-acrylic Acid (**9i**).* The title compound was prepared using 4-(but-1-yn-1-yl)-1-(tetrahydro-2*H*-pyran-2-yl)-1*H*-indazole, (*E*)-(4-(3-ethoxy-3-oxoprop-1-en-1-yl)phenyl)boronic acid, and iodobenzene following methods C, F, and G. ^{1}H NMR (400 MHz, DMSO-d_6): δ 13.14 (br s, 1H), 12.31 (br s, 1H), 7.78 (d, 1H, J = 1.0 Hz), 7.49 (d, 1H, J = 8.5 Hz), 7.42−7.37 (m, 2H), 7.33 (d, 2H, J = 8.3 Hz), 7.26−7.22 (m, 4H), 7.20−7.14 (m, 1H), 7.08 (dd, 1H, J = 0.67 Hz, J = 6.9 Hz), 6.95 (d, 2H, J = 8.3 Hz), 6.34 (d, 1H, J = 16.0 Hz), 2.32 (q, 2H), 0.79 (t, 3H). ^{13}C NMR (100 MHz, DMSO-d_6): δ 167.5, 144.2, 143.6, 143.4, 141.0, 140.2, 135.5, 135.0, 132.7, 131.8, 130.2, 129.4, 128.0, 127.5, 126.6, 126.0, 122.4, 120.2, 118.6, 109.1, 28.8, 13.1. HRMS-ESI$^+$: m/z [M + H]$^+$ calcd for $C_{26}H_{22}N_2O_2$, 395.1760; found, 395.1760.

*(E)-3-(4-((E)-1-(1H-Indazol-6-yl)-2-phenylbut-1-en-1-yl)phenyl)-acrylic Acid (**9j**).* The title compound was prepared using 6-(but-1-yn-1-yl)-1-(tetrahydro-2*H*-pyran-2-yl)-1*H*-indazole, (*E*)-(4-(3-ethoxy-3-oxoprop-1-en-1-yl)phenyl)boronic acid, and iodobenzene following methods C, F, and G. ^{1}H NMR (400 MHz, DMSO-d_6): δ 112.94 (br, 1H), 12.40 (br, 1H), 8.07 (d, 1H, J = 0.9 Hz), 7.75−7.73 (m, 1H), 7.43−7.34 (m, 3H), 7.23−7.12 (m, 5H), 6.94−6.88 (m, 3H), 6.37 (d, 1H, J = 16.0 Hz), 2.43 (q, 2H, J = 7.50 Hz), 0.88 (t, 3H, J = 7.50 Hz). ^{13}C NMR (100 MHz, DMSO-d_6): δ 167.5, 144.7, 143.3, 142.7, 141.3, 140.3, 140.0, 138.0, 133.3, 131.7, 130.7, 129.3, 128.0, 127.4, 126.5, 122.1, 121.6, 120.4, 118.7, 109.9, 28.6, 13.3. HRMS-ESI$^+$: m/z [M + H]$^+$ calcd for $C_{26}H_{22}N_2O_2$, 395.1760; found, 395.1752.

*(E)-3-(4-((E)-2-(2-Chlorophenyl)-1-(1H-indazol-5-yl)but-1-en-1-yl)phenyl)acrylic Acid (**11a**).* The title compound was prepared using 5-(but-1-yn-1-yl)-1-(tetrahydro-2*H*-pyran-2-yl)-1*H*-indazole, (*E*)-(4-(3-ethoxy-3-oxoprop-1-en-1-yl)phenyl)boronic acid, and 1-chloro-2-iodobenzene following methods C, F, and G. ^{1}H NMR (400 MHz, DMSO-d_6): δ 8.32 (br, 2H), 8.12 (s, 1H), 7.74 (s, 1H), 7.61 (d, 1H, J = 16.0 Hz), 7.53 (d, 1H, J = 7.50 Hz), 7.33−7.27 (m, 2H), 7.22−7.20 (m, 2H), 7.17−7.11 (m, 3H), 7.01 (d, 2H, J = 8.50 Hz), 6.32 (d, 1H, J = 16.0 Hz), 2.48 (q, 2H, J = 7.50 Hz), 0.98 (t, 3H, J = 7.50 Hz). ^{13}C NMR (100 MHz, DMSO-d_6): δ 171.3, 146.2, 145.2, 140.9, 140.4, 139.8, 138.9, 135.1, 134.3, 133.3., 131.9, 131.7, 130.2, 129.5, 129.3, 128.0, 127.4, 126.3, 123.2, 121.2, 117.0, 109.9, 28.3, 12.9. HRMS-ESI$^+$: m/z [M + H]$^+$ calcd for $C_{26}H_{21}ClN_2O_2$, 429.1370; found, 429.1370.

*(E)-3-(4-((E)-2-(2-Cyanophenyl)-1-(1H-indazol-5-yl)but-1-en-1-yl)phenyl)acrylic Acid (**11d**).* The title compound was prepared using 5-(but-1-yn-1-yl)-1-(tetrahydro-2*H*-pyran-2-yl)-1*H*-indazole, (*E*)-(4-(3-ethoxy-3-oxoprop-1-en-1-yl)phenyl)boronic acid, and 2-iodobenzonitrile following methods C, F, and G. ^{1}H NMR (300 MHz, DMSO-d_6): δ OH resonance not observed, 13.17 (s, 1H), 8.13 (br, 1H), 7.68−7.63 (m, 4H), 7.59 (d, 1H, J = 8.50 Hz), 7.43−7.36 (m, 4H), 7.19 (dd, 1H, J = 1.5 Hz, J = 8.50 Hz), 6.92 (d, 2H, J = 8.50 Hz), 6.38 (d, 1H, J = 16.0 Hz), 2.47 (q, 2H, J = 7.50 Hz), 0.93 (t, 3H, J = 7.50 Hz). HRMS-ESI$^+$: m/z [M + H]$^+$ calcd for $C_{27}H_{21}N_3O_2$, 420.1712; found, 420.1712.

*(E)-3-(4-((E)-1-(1H-Indazol-5-yl)-2-(o-tolyl)but-1-en-1-yl)phenyl)-acrylic Acid (**11g**).* The title compound was prepared using 5-(but-1-

DOI: 10.1021/acs.jmedchem.5b00054
J. Med. Chem. 2015, 58, 4888−4904

yn-1-yl)-1-(tetrahydro-2*H*-pyran-2-yl)-1*H*-indazole, (*E*)-(4-(3-ethoxy-3-oxoprop-1-en-1-yl)phenyl)boronic acid, and 1-iodo-2-methylbenzene following methods C, F, and G. ^{1}H NMR (400 MHz, DMSO-d_6): δ 13.17 (s, 1H), 12.39 (br s, 1H), 8.09 (dd, 1H, J = 1.0 Hz), 7.68 (s, 1H), 7.54 (d, 1H, J = 8.5 Hz), 7.38 (d, 1H, J = 15.9 Hz), 7.31 (d, 2H, J = 8.3 Hz), 7.23 (m, 1H), 7.18 (dd, 1H, J = 1.5 Hz, J = 8.6 Hz), 7.14 (dt, 1H, J = 1.5 Hz, J = 7.3 Hz), 7.08 (dt, 1H, J = 1.5 Hz, J = 7.5 Hz), 7.05–7.03 (m, 1H), 6.87 (d, 2H, J = 8.3 Hz), 6.34 (d, 1H, J = 16.0 Hz), 2.38–2.29 (m, 2H), 2.12 (s, 3H), 0.87 (t, 3H, J = 7.50 Hz). ^{13}C NMR (100 MHz, DMSO-d_6): δ 167.5, 144.8, 143.4, 141.0, 140.6, 138.9, 138.5, 135.0, 134.3, 133.6, 131.7, 129.9, 129.5, 127.8, 127.2, 126.6, 125.3, 122.9, 120.4, 118.6, 110.1, 29.3, 19.4, 12.4. HRMS-ESI$^+$: m/z [M + H]$^+$ calcd for $C_{27}H_{24}N_2O_2$, 409.1916; found, 409.1916.

*(E)-3-(4-((E)-1-(1H-Indazol-5-yl)-2-(2-(methylsulfonyl)phenyl)but-1-en-1-yl)phenyl)acrylic Acid (**11h**). Step 1: (E)-Ethyl 3-(4-((E)-2-(2-(Methylthio)phenyl)-1-(1-(tetrahydro-2H-pyran-2-yl)-1H-indazol-5-yl)but-1-en-1-yl)phenyl)acrylate.* The title compound was prepared using 5-(but-1-yn-1-yl)-1-(tetrahydro-2*H*-pyran-2-yl)-1*H*-indazole, (*E*)-(4-(3-ethoxy-3-oxoprop-1-en-1-yl)phenyl)boronic acid, and 2-iodothioanisole following method C. ^{1}H NMR (300 MHz, DMSO-d_6): δ 8.14 (s, 1H), 7.75 (d, 1H, J = 8.50 Hz), 7.72–7.65 (m, 1H), 7.44 (d, 1H, J = 16.0 Hz), 7.35 (d, 2H, J = 8.50 Hz), 7.29–7.24 (m, 1H), 7.22–7.11 (m, 3H), 7.09–7.03 (m, 1H), 7.01 (d, 2H, J = 8.30 Hz), 6.44 (d, 1H, J = 16.0 Hz), 5.85 (dd, 1H, J = 2.50 Hz, J = 10.0 Hz), 4.13 (q, 2H, J = 7.20 Hz), 3.94–3.83 (m, 1H), 3.80–3.68 (m, 1H), 2.47–2.27 (m, 6H), 2.09–1.93 (m, 2H), 1.83–1.69 (m, 1H), 1.67–1.52 (m, 2H), 1.20 (t, 3H, J = 7.20 Hz), 0.88 (t, 3H, J = 7.60 Hz).

*Step 2: (E)-Ethyl 3-(4-((E)-2-(2-(Methylsulfonyl)phenyl)-1-(1-(tetrahydro-2H-pyran-2-yl)-1H-indazol-5-yl)but-1-en-1-yl)phenyl)acrylate (**26h**).* Oxone (potassium peroxymonosulfate; 521 mg, 0.85 mmol) was added to a slurry of (*E*)-ethyl 3-(4-((*E*)-2-(2-(methylthio)-phenyl)-1-(1-(tetrahydro-2*H*-pyran-2-yl)-1*H*-indazol-5-yl)but-1-en-1-yl)phenyl)acrylate (156 mg, 0.28 mmol) in MeOH:H_2O (1:1, 6 mL) at room temperature, and the reaction was stirred overnight. Dichloromethane and water were added, and the layers were separated. The aqueous layer was washed with dichloromethane (×2). The organic layers were combined, washed with water, washed with brine, dried over Na_2SO_4, filtered, and concentrated. The crude material was purified on a silica gel column eluted with 0–50% ethyl acetate in hexane affording the title compound. ^{1}H NMR (300 MHz, DMSO-d_6): δ 8.15 (s, 1H), 7.91 (d, 1H, J = 8.0 Hz), 7.77–7.71 (m, 2H), 7.49–7.46 (m, 3H), 7.41–7.31 (m, 4H), 7.01 (d, 2H, J = 8.20 Hz), 6.45 (d, 1H, J = 16.0 Hz), 5.87 (dd, 1H, J = 2.50 Hz, J = 10.0 Hz), 4.12 (q, 2H, J = 7.20 Hz), 3.92–3.85 (m, 1H), 3.82–3.69 (m, 1H), 2.93 (s, 3H), 2.46–2.27 (m, 2H), 2.09–1.97 (m, 3H), 1.85–1.67 (m, 1H), 1.63–1.51 (m, 2H), 1.18 (t, 3H, J = 7.20 Hz), 0.83 (t, 3H, J = 7.60 Hz). LCMS: 501 [(M − THP + H) + H]$^+$.

*Step 3: (E)-3-(4-((E)-1-(1H-Indazol-5-yl)-2-(2-(methylsulfonyl)-phenyl)but-1-en-1-yl)phenyl)acrylic Acid (**11h**).* The title compound was prepared from (*E*)-ethyl 3-(4-((*E*)-2-(2-(methylsulfonyl)phenyl)-1-(1-(tetrahydro-2*H*-pyran-2-yl)-1*H*-indazol-5-yl)but-1-en-1-yl)-phenyl)acrylate following methods F and G. ^{1}H NMR (300 MHz, DMSO-d_6): δ 13.14 (br s, 1H), 12.29 (br s, 1H), 8.11 (d, 1H, J = 0.9 Hz), 7.92 (dd, 1H, J = 0.9 Hz, 8.5 Hz), 7.71 (s, 1H), 7.66–7.54 (m, 2H), 7.51–7.44 (m, 2H), 7.40–7.33 (m, 3H), 7.26 (dd, 1H, J = 1.50 Hz, J = 8.45 Hz), 7.01 (d, 2H, J = 8.45 Hz), 6.34 (d, 1H, J = 16. 0 Hz), 2.94 (s, 3H), 2.42–2.30 (m, 2H), 0.83 (t, 3H, J = 7.60 Hz). HRMS-ESI$^+$: m/z [M + H]$^+$ calcd for $C_{27}H_{24}N_2O_4S$, 473.1535; found, 473.1535.

*(E)-3-(4-((E)-1-(1H-Indazol-5-yl)-2-(2-methoxyphenyl)but-1-en-1-yl)phenyl)acrylic Acid (**11i**).* The title compound was prepared using 5-(but-1-yn-1-yl)-1-(tetrahydro-2*H*-pyran-2-yl)-1*H*-indazole, (*E*)-(4-(3-ethoxy-3-oxoprop-1-en-1-yl)phenyl)boronic acid, and 1-iodo-2-methoxybenzene following methods C, F, and G. ^{1}H NMR (400 MHz, DMSO-d_6): δ 13.06 (s, 1H), 12.32 (br, 1H), 8.08 (d, 1H, J = 0.9 Hz), 7.65 (s, 1H), 7.53 (d, 1H, J = 8.50 Hz), 7.39 (d, 1H, J = 16.0 Hz), 7.32 (d, 2H, J = 8.50 Hz), 7.18–7.12 (m, 2H), 6.96–6.89 (m, 4H), 6.75 (dt, 1H, J = 0.9 Hz, J = 7.40 Hz), 6.34 (d, 1H, J = 16. 0 Hz), 3.76 (s, 3H), 2.42–2.29 (m, 2H), 0.87 (t, 3H, J = 7.50 Hz). ^{13}C NMR (100 MHz, DMSO-d_6): δ 167.5, 156.8, 145.4, 143.5, 139.9, 138.8, 138.6, 134.0, 133.6, 131.6, 131.0, 130.3, 129.7, 128.0, 127.9, 127.3, 122.8, 120.4, 120.0, 118.4, 110.9, 109.9, 55.3, 27.3, 13.1. HRMS-ESI$^+$: m/z [M + H]$^+$ calcd for $C_{27}H_{24}N_2O_3$, 425.1865; found, 425.1862.

*(E)-Ethyl 3-(4-((Z)-1-(1-(Tetrahydro-2H-pyran-2-yl)-1H-indazol-5-yl)-2-(4,4,5,5-tetramethyl-1,3,2-dioxaborolan-2-yl)but-1-en-1-yl)-phenyl)acrylate. Step 1: (Z)-5-(1,2-Bis(4,4,5,5-tetramethyl-1,3,2-dioxaborolan-2-yl)but-1-en-1-yl)-1-(tetrahydro-2H-pyran-2-yl)-1H-indazole (**28**).* The title compound was prepared from of 5-(but-1-yn-1-yl)-1-(tetrahydro-2*H*-pyran-2-yl)-1*H*-indazole, bis(pinacolato)-diboron, and $Pt(PPh_3)_4$ following method D, step 1. ^{1}H NMR (400 MHz, DMSO-d_6): δ 8.06 (br, 1H), 7.66 (d, 1H, J = 8.70 Hz), 7.33 (br, 1H), 7.05 (dd, 1H, J = 1.60 Hz, J = 8.70 Hz), 5.81 (dd, 1H, J = 2.50 Hz, J = 9.80 Hz), 3.89 (d, 1H, J = 11.0 Hz), 3.76–3.70 (m, 1H), 2.46–2.36 (m, 1H), 2.0–1.94 (m, 4H), 1.77–1.68 (m, 1H), 1.61–1.54 (m, 2H), 1.27 (s, 12H), 1.16 (s, 12H), 0.87 (t, 3H, J = 7.60 Hz).

Step 2: (E)-Ethyl 3-(4-((Z)-1-(1-(Tetrahydro-2H-pyran-2-yl)-1H-indazol-5-yl)-2-(4,4,5,5-tetramethyl-1,3,2-dioxaborolan-2-yl)but-1-en-1-yl)phenyl)acrylate. The title compound was prepared from (*Z*)-5-(1,2-bis(4,4,5,5-tetramethyl-1,3,2-dioxaborolan-2-yl)but-1-en-1-yl)-1-(tetrahydro-2*H*-pyran-2-yl)-1*H*-indazole and (*E*)-ethyl 3-(4-iodophenyl)acrylate following method D, step 2. ^{1}H NMR (400 MHz, DMSO-d_6): δ 8.09 (s, 1H), 7.70 (d, 1H, J = 8.80 Hz), 7.58–7.63 (m, 3H), 7.49 (s, 1H), 7.11 (d, 2H, J = 8.40 Hz), 6.58 (d, 1H, J = 16.0 Hz), 5.84 (dd, 1H, J = 2.60, J = 9.90 Hz), 4.18 (q, 2H, J = 7.20 Hz), 3.86–3.91 (m, 1H), 3.70–3.77 (m, 1H), 2.36–2.48 (m, 1H), 2.08–2.15 (m, 2H), 1.95–2.08 (m, 2H), 1.70–1.81 (m, 1H), 1.56–1.62 (m, 2H), 1.25 (t, 3H, J = 7.20 Hz), 1.12 (s, 12H), 1.01 (t, 3H, J = 7.50 Hz). LCMS: 473 [(M − THP + H) + H]$^+$.

*(E)-3-(4-((E)-2-(2-Chloro-4-fluorophenyl)-1-(1H-indazol-5-yl)but-1-en-1-yl)phenyl)acrylic Acid (**11l**). Steps 1: (E)-4-(2-(2-Chloro-4-fluorophenyl)-1-(1-(tetrahydro-2H-pyran-2-yl)-1H-indazol-5-yl)but-1-en-1-yl)benzaldehyde (**33l**).* A round-bottom flask equipped with a magnetic stir bar, a reflux condenser, an internal thermometer, and a N_2 inlet was charged with 5-(but-1-yn-1-yl)-1-(tetrahydro-2*H*-pyran-2-yl)-1*H*-indazole (50.0 g, 197 mmol), bis(pinacolato)diboron (50.4 g, 199 mmol), and anhydrous 2-methyltetrahydrofuran (393 mL) followed by $Pt(PPh_3)_4$ (1.83 g, 1.5 mmol). This mixture was degassed with three vacuum/N_2 cycles, heated at 83 °C (internal temperature; oil bath at 95 °C) for 5 h under N_2, and then allowed to cool to room temperature. 2-Methyltetrahydrofuran (393 mL), cesium carbonate (128.1 g, 393 mmol), and water (11.8 mL, 1.5% v/v) were added, and the reaction was cooled to 4 °C. 4-Iodobenzaldehyde (45.6 g, 197 mmol) and $PdCl_2(PPh_3)_2$ (6.90 g, 9.8 mmol) were added, and the reaction was degassed with three vacuum/N_2 cycles. The mixture was allowed to warm to room temperature and stirred overnight. Aqueous KOH solution (4M, 275 mL, 1100 mmol) and 2-chloro-4-fluoroiodobenzene (70.6 g, 275 mmol) were added. The reaction was degassed with three vacuum/N_2 cycles, heated at 75 °C (internal temperature; oil bath at 90 °C) for 7 h under N_2, and then allowed to cool to room temperature. The layers were separated, and the organic layer was washed with brine (800 mL), dried over sodium sulfate, filtered, and concentrated. The crude product was purified by silica gel chromatography (0–20% ethyl acetate in hexanes) to give the title compound (82.6 g, 7:1 mixture of regioisomers) as a pale-yellow foam. Data for major isomer (*E*)-4-(2-(2-chloro-4-fluorophenyl)-1-(1-(tetrahydro-2*H*-pyran-2-yl)-1*H*-indazol-5-yl)but-1-en-1-yl)-benzaldehyde: ^{1}H NMR (300 MHz, DMSO-d_6) δ 9.82 (s, 1H), 8.15 (s, 1H), 7.78–7.71 (m, 2H), 7.61 (d, 2H, J = 8.40 Hz), 7.43–7.27 (m, 3H), 7.15 (m, 3H), 5.86 (dd, 1H, J = 2.40 Hz, J = 9.90 Hz), 3.93–3.85 (m, 1H), 3.79–3.68 (m, 1H), 2.44–2.36 (m, 3H), 2.10–1.96 (m, 2H), 1.81–1.67 (m, 1H), 1.63–1.53 (m, 2H), 0.92 (t, 3H, J = 7.20 Hz); LCMS: 405 [(M − THP + H) + H]$^+$.

*Step 2: (E)-Ethyl 3-(4-((E)-2-(2-Chloro-4-fluorophenyl)-1-(1-(tetrahydro-2H-pyran-2-yl)-1H-indazol-5-yl)but-1-en-1-yl)phenyl)acrylate (**34l**).* A round-bottom flask equipped with a magnetic stir bar, an addition funnel, and a N_2 inlet was charged with (*E*)-4-(2-(2-chloro-4-fluorophenyl)-1-(1-(tetrahydro-2*H*-pyran-2-yl)-1*H*-indazol-5-yl)but-1-en-1-yl)benzaldehyde (82.6 g, 169 mmol), triethylphosphonoacetate (40.6 mL, 203 mmol), lithium chloride (14.5 g, 338 mmol), and anhydrous acetonitrile (338 mL). The reaction was cooled to 0 °C and then degassed with three vacuum/N_2 cycles. A solution of DBU (27.8

DOI: 10.1021/acs.jmedchem.5b00054
J. Med. Chem. 2015, 58, 4888–4904

mL, 186 mmol) in acetonitrile (60 mL) was added dropwise over 35 min, and then the ice water bath was removed. The reaction was stirred at room temperature for 1 h, concentrated, and then partitioned between dichloromethane (250 mL) and H_2O (250 mL). The layers were separated, and the organic layer was washed with brine (400 mL), dried over sodium sulfate, filtered, and concentrated. The crude product was purified on a silica gel column (300 g column, 20% ethyl acetate in hexanes) to give the title compound (89.6 g) as a pale-yellow foam. ^{1}H NMR (300 MHz, DMSO-d_6): δ 8.14 (s, 1H), 7.75 (d, 1H, J = 8.70 Hz), 7.70–7.69 (m, 1H), 7.47 (d, 1H, J = 16.0 Hz), 7.42 (d, 2H, J = 8.40 Hz), 7.37–7.33 (m, 2H), 7.29 (m, 1H), 7.14 (dt, 1H, J = 2.60 Hz, J = 8.50 Hz), 6.95 (d, 2H, J = 8.40 Hz), 6.48 (d, 1H, J = 16.0 Hz), 5.86 (dd, 1H, J = 2.42 Hz, J = 9.80 Hz), 4.14 (q, 2H, J = 7.20 Hz), 3.90–3.86 (m, 1H), 3.78–3.70 (m, 1H), 2.45–2.34 (m, 1H), 2.37 (q, 2H, J = 7.50 Hz), 2.06–1.95 (m, 2H), 1.78–1.67 (m, 1H), 1.62–1.53 (m, 2H), 1.19 (t, 3H, J = 7.20 Hz), 0.90 (t, 3H, J = 7.50 Hz). LCMS: 475 [(M − THP + H) + H]$^+$.

Step 3: (E)-Ethyl 3-(4-((E)-2-(2-Chloro-4-fluorophenyl)-1-(1H-indazol-5-yl)but-1-en-1-yl)phenyl)acrylate Hydrochloride. A round-bottom flask equipped with a magnetic stir bar was charged with (*E*)-ethyl 3-(4-((*E*)-2-(2-chloro-4-fluorophenyl)-1-(1-(tetrahydro-2*H*-pyran-2-yl)-1*H*-indazol-5-yl)but-1-en-1-yl)phenyl)acrylate (255.9 g, 457.8 mmol) and a solution of HCl (732 mL, 1.25 M in ethyl alcohol). The reaction was heated at 80 °C for 2.5 h, allowed to cool to room temperature, and then concentrated to an orange gel. *tert*-Butyl methyl ether (2.3 L) was added. After stirring for 5 min, solids began to precipitate. The mixture was stirred at room temperature for 2 h and then filtered. The solids were washed with MTBE (700 mL) and dried to give the title compound (193 g) as an off-white solid. ^{1}H NMR (400 MHz, DMSO-d_6): δ NH resonance not observed, 8.11 (d, 1H, J = 0.9 Hz), 7.69 (br, 1H), 7.56 (d, 1H, J = 8.60 Hz), 7.46 (d, 1H, J = 16.0 Hz), 7.41 (d, 2H, J = 8.40 Hz), 7.35–7.33 (m, 2H), 7.19 (dd, 1H, J = 1.60 Hz, J = 8.40 Hz), 7.12 (dt, 1H, J = 2.60 Hz, J = 8.60 Hz), 6.96 (d, 2H, J = 8.40 Hz), 6.48 (d, 1H, J = 16.0 Hz), 4.14 (q, 2H, J = 7.20 Hz), 2.38 (q, 2H, J = 7.60 Hz), 1.19 (t, 3H, J = 7.20 Hz), 0.90 (t, 3H, J = 7.50 Hz). LCMS: 475 (M + H)$^+$.

Step 4: (E)-3-(4-((E)-2-(2-Chloro-4-fluorophenyl)-1-(1H-indazol-5-yl)but-1-en-1-yl)phenyl)acrylic Acid (11l). A round-bottom flask equipped with a magnetic stir bar was charged with (*E*)-ethyl 3-(4-((*E*)-2-(2-chloro-4-fluorophenyl)-1-(1*H*-indazol-5-yl)but-1-en-1-yl)-phenyl)acrylate hydrochloride (198.5 g, 388 mmol) and ethyl alcohol (517 mL). A solution of LiOH (27.9 g, 1164 mmol) in water (388 mL) was added, and the mixture was stirred at room temperature overnight. The ethyl alcohol was removed by rotary evaporation, and the remaining solution was cooled to 0 °C and acidified with 2 M aqueous HCl to pH 3. Dichloromethane (500 mL) was added, the mixture was stirred, and then the layers were separated. The organic layer was washed with water, washed with brine, dried over sodium sulfate, filtered, and concentrated. The crude product was purified on a silica column (800 g column, 5% MeOH in DCM) to give the title compound. The product was then dissolved in DCM (400 mL), and acetonitrile (500 mL) was added. Approximately 200 mL of DCM was removed by rotary evaporation (solids began to precipitate). Acetonitrile (550 mL) was added followed by water (25 mL). The mixture was stirred at room temperature for 2 h. The solvent was decanted, and then acetonitrile:DCM (10:1; 550 mL) was added. The mixture stirred at room temperature for 1.5 h, the solvent was again decanted, and then acetonitrile:DCM (10:1; 550 mL) was added. The mixture was again stirred at room temperature for 1.5 h and then filtered. The solids were resuspended in acetonitrile:DCM (10:1; 550 mL), stirred at room temperature for 1.5 h, filtered, and washed to give the title compound (123.9 g) as an off-white powder. ^{1}H NMR (400 MHz, DMSO-d_6): δ 13.11 (br s, 1H), 12.32 (br, 1H), 8.10 (d, 1H, J = 1.0 Hz), 7.68 (s, 1H), 7.55 (d, 1H, J = 8.6 Hz), 7.42–7.33 (m, 5H), 7.18 (dd, 1H, J = 1.5 Hz, J = 8.6 Hz), 7.13 (dt, 1H, J = 2.8 Hz, J = 8.4 Hz), 6.95 (d, 2H, J = 8.4 Hz), 6.37 (d, 1H, J = 16.0 Hz), 2.37 (q, 2H, J = 7.50 Hz), 0.90 (t, 3H, J = 7.50 Hz). ^{13}C NMR (100 MHz, DMSO-d_6): δ 167.5, 160.7 (1C, J = 245 Hz), 144.4, 143.3, 140.7, 139.0, 138.2, 136.4 (1C, J = 3 Hz), 133.6, 133.5, 133.2 (1C, J = 9 Hz), 133.1 (1C, J = 11 Hz), 132.1, 129.6, 127.5, 127.4, 122.8, 120.3, 118.9, 116.13 (1C, J = 25 Hz), 114.0 (1C, J = 21 Hz), 110.18, 27.9, 12.5. HRMS-ESI$^+$: [M + H]$^+$ calcd for $C_{26}H_{20}ClFN_2O_2$, 447.1276; found, 447.1276.

Experimental Protocols (Biology). *Breast Cancer Cell ER-α In Cell Western Assay (ER-α Degradation Assay).* MCF-7 cells were trypsinized and washed twice in phenol red free RPMI containing 5% charcoal dextran stripped FBS with 20 mM HEPES and NEAA and adjusted to a concentration of 200000 cells per mL with the same medium. Next, 16 μL of the cell suspension (3200 cells) was added to each well of a poly-D-lysine coated 384-well plate, and the cells were incubated at 37 °C over 4 days to allow the cells to adhere and grow. On day 4, a 10-point, serial 1:5 dilution of each compound was added to the cells in 16 μL at a final concentration ranging from 10^{-5} M to 5.12×10^{-12} M or 10–6 M to 5.12×10^{-13} M for fulvestrant. At 4 h post compound addition, the cells were fixed by adding 16 μL of 30% formalin to the 32 μL of cells and compound (10% formalin final concentration) for 20 min. Cells were then washed twice with PBS Tween 0.1% and then permeabilized in PBS 0.1% Triton (50 μL/well) for additional 15 min. The PBS 0.1% triton was decanted, and the cells were washed: LI-COR blocking buffer (50 μL/well) was added, the plate was spun at 3000 rpm, and then the blocking buffer was decanted. Additional LI-COR blocking buffer (50 μL/well) was added, and the cells were incubated overnight at 4 °C. The blocking buffer was decanted, and the cells were incubated overnight at 4 °C with SP1 (Thermo Scientific) anti-ER rabbit monoclonal antibody diluted 1:1000 in LI-COR blocking buffer/0.1% Tween-20. Wells, which were treated with blocking buffer with Tween but no antibody, were used as a background control. Wells were washed twice with PBS Tween 0.1% to remove free SP1 antibodies, and the cells were incubated at room temp for 60–90 min in LI-COR goat antirabbit IRDyeTM 800CW (1:1000) and DRAQ5 DNA dye (1:10000 of 5 mM stock solution) diluted in LI-COR blocking buffer containing 0.1% Tween-20 and 0.01% SDS. Cells were then washed with 0.1%Tween-20/PBS three times. Plates were scanned on a LI-COR Odyssey infrared imaging system. Integrated intensities in the 800 and 700 nm channels were measured to determine levels of ER-α and DNA respectively. Percent ER levels were determined as follows: (integrated intensity 800 nm sample/integrated intensity 700 nm sample)/(integrated intensity 800 nm untreated cells/integrated intensity 700 nm untreated cells) × 100 = %ER-α levels.

Breast Cancer Cell Viability Assay (MCF-7 Viability Assay). MCF-7 cells were adjusted to a concentration of 40000 cells per mL in RPMI containing 10% FBS and 20 mM HEPES. Then 16 μL of the cell suspension (640 cells) was added to each well of a 384-well plate, and the cells were incubated overnight to allow the cells to adhere. The following day a 10-point, serial 1:5 dilution of each compound was added to the cells in 16 μL at a final concentration ranging from 10 to 0.000005 μM. After 5 days' compound exposure, 16 μL of CellTiter-GLo (Promega) was added to the cells, and the relative luminescence units (RLUs) of each well were determined. CellTiter-Glo added to 32 μL of medium without cells was used to obtain a background value. The percent viability of each sample was determined as follows: (RLU sample − RLU background/RLU untreated cells − RLU background) × 100 = %viability.

Immature Uterine Wet Weight-Antagonist Mode. Female immature CD-IGS rats (21 days old upon arrival) were dosed daily for 3 days. Vehicle or test compound was administered orally by gavage followed 15 min later by an oral dose of 0.1 mg/kg ethynyl estradiol. On the fourth day 24 h after dose, plasma was collected for pharmacokinetic analysis. Immediately following plasma collection, the animals were euthanized and the uterus was removed and weighed.

In Vivo Xenograft Breast Cancer Model (MCF-7; Tamoxifen-Sensitive). Time release pellets containing 0.72 mg 17-β estradiol were subcutaneously implanted into nu/nu mice. MCF-7 cells were grown in RPMI containing 10% FBS at 5% CO_2, 37 °C. Trypsinized cells were pelleted and resuspended in 50% RPMI (serum free) and 50% Matrigel at 1×10^7 cells/mL. MCF-7 cells were subcutaneously injected (100 μL/animal) on the right flank 2–3 days post pellet implantation. Tumor volume (length × width^2/2) was monitored biweekly. When tumors reached an average volume of ~200 mm^3 animals were randomized and treatment was started. Animals were

DOI: 10.1021/acs.jmedchem.5b00054
J. Med. Chem. 2015, 58, 4888–4904

treated with vehicle or compound daily for 4 weeks. Tumor volume and body weight were monitored biweekly throughout the study.

In Vivo Xenograft Breast Cancer Model (Tamoxifen-Resistant Model). Female nu/nu mice (with supplemental 17-β estradiol pellets; 0.72 mg; 60 day slow release) bearing MCF-7 tumors (mean tumor volume 200 mm^3) were treated with Tamoxifen (citrate) by oral gavage. Tumor volume (length × $width^2/2$) and body weight were monitored twice weekly. Following a significant antitumor response in which tumor volume remained static, evident tumor growth was first observed at approximately 100 days of treatment. At 120 days of treatment, tamoxifen dose was increased. Rapidly growing tumors were deemed tamoxifen resistant and selected for in vivo passage into new host animals. Tumor fragments (~100 mm^3/animal) from the tamoxifen resistant tumors were subcutaneously implanted into the right flank of female nu/nu mice (with 17-β estradiol pellets (0.72 mg; 60 day slow release)). Passaged tumors were maintained under constant Tamoxifen selection, and tumor volume (length × $width^2/2$) was monitored weekly. When tumor volume reached ~150–250 mm^3, animals were randomized into treatment groups (mean tumor volume 200 mm^3) and tamoxifen treatment was terminated. Animals were treated with vehicle or compound daily for 4 weeks. Tumor volume and body weight were monitored twice weekly for the duration of the study.

■ ASSOCIATED CONTENT

Supporting Information

Experimental procedures for all compounds and intermediates. The Supporting Information is available free of charge on the ACS Publications website at DOI: 10.1021/acs.jmedchem.5b00054.

■ AUTHOR INFORMATION

Corresponding Author

*Phone: 858-369-7604. E-mail: nicholas.d.smith10@gmail.com.

Notes

The authors declare no competing financial interest.

■ ABBREVIATIONS USED

AUC, area under the curve; Cl, clearance; C_{24}, concentration at 24 h; compd, compound; C_{max}, maximum concentration; C_{min}, minimum concentration; CYP, cytochrome; DBU, diazabicycloundecene; DHP, 3,4-dihydro-2*H*-pyran; dppf, 1,1′-bis(diphenylphosphino)ferrocene; DMAP, 4-dimethylaminopyridine; E2, estradiol; EE, ethynyl estradiol; ER, estrogen receptor; ERE, estrogen response element; FES-PET, 18F-fluoroestradiol positron emission tomography; MOM-Cl, chloro(methoxy)methane; %*F*, percent oral bioavailability; iv, intravenous; PG, protecting group; po, per oral; PPTS, pyridinium *p*-toluenesulfonate; SAR, structure–activity relationship; SERD, selective estrogen receptor degrader; SERM, selective estrogen receptor modulator; $t_{1/2}$, half-life; TEA, triethylamine; THP, tetrahydropyran; Tr, triphenylmethane; UWW, uterine wet weight; V_{ss}, volume of distribution at steady state

■ REFERENCES

(1) Nilsson, S.; Gustafsson, J. A. Estrogen receptors: therapies targeted to receptor subtypes. *Clin. Pharmacol. Ther.* **2011**, *89* (1), 44–55.

(2) Ariazi, E. A.; Ariazi, J. L.; Cordera, F.; Jordan, V. C. Estrogen receptors as therapeutic targets in breast cancer. *Curr. Top. Med. Chem.* **2006**, *6* (3), 181–202.

(3) Riggins, R. B.; Schrecengost, R. S.; Guerrero, M. S.; Bouton, A. H. Pathways to tamoxifen resistance. *Cancer Lett.* **2007**, *256* (1), 1–24.

(4) Musgrove, E. A.; Sutherland, R. L. Biological determinants of endocrine resistance in breast cancer. *Nature Rev. Cancer* **2009**, *9* (9), 631–643.

(5) (a) Li, S.; Shen, D.; Shao, J.; Crowder, R.; Liu, W.; Prat, A.; He, X.; Liu, S.; Hoog, J.; Lu, C.; Ding, L.; Griffith, O. L.; Miller, C.; Larson, D.; Fulton, R. S.; Harrison, M.; Mooney, T.; McMichael, J. F.; Luo, J.; Tao, Y.; Goncalves, R.; Schlosberg, C.; Hiken, J. F.; Saied, L.; Sanchez, C.; Giuntoli, T.; Bumb, C.; Cooper, C.; Kitchens, R. T.; Lin, A.; Phommaly, C.; Davies, S. R.; Zhang, J.; Kavuri, M. S.; McEachern, D.; Dong, Y. Y.; Ma, C.; Pluard, T.; Naughton, M.; Bose, R.; Suresh, R.; McDowell, R.; Michel, L.; Aft, R.; Gillanders, W.; DeSchryver, K.; Wilson, R. K.; Wang, S.; Mills, G. B.; Gonzalez-Angulo, A.; Edwards, J. R.; Maher, C.; Perou, C. M.; Mardis, E. R.; Ellis, M. J., Endocrine-Therapy-Resistant ESR1 Variants Revealed by Genomic Characterization of Breast-Cancer-Derived Xenografts. *Cell Rep.* *4* (6), 1116–1130;. (b) Robinson, D. R.; Wu, Y.-M.; Vats, P.; Su, F.; Lonigro, R. J.; Cao, X.; Kalyana-Sundaram, S.; Wang, R.; Ning, Y.; Hodges, L.; Gursky, A.; Siddiqui, J.; Tomlins, S. A.; Roychowdhury, S.; Pienta, K. J.; Kim, S. Y.; Roberts, J. S.; Rae, J. M.; Van Poznak, C. H.; Hayes, D. F.; Chugh, R.; Kunju, L. P.; Talpaz, M.; Schott, A. F.; Chinnaiyan, A. M. Activating ESR1 mutations in hormone-resistant metastatic breast cancer. *Nature Genet.* **2013**, *45* (12), 1446–1451. (c) Toy, W.; Shen, Y.; Won, H.; Green, B.; Sakr, R. A.; Will, M.; Li, Z.; Gala, K.; Fanning, S.; King, T. A.; Hudis, C.; Chen, D.; Taran, T.; Hortobagyi, G.; Greene, G.; Berger, M.; Baselga, J.; Chandarlapaty, S. ESR1 ligand-binding domain mutations in hormone-resistant breast cancer. *Nature Genet.* **2013**, *45* (12), 1439–1445.

(6) (a) Johnston, S. J.; Cheung, K. L. Fulvestrant—a novel endocrine therapy for breast cancer. *Curr. Med. Chem.* **2010**, *17* (10), 902–914. (b) Pike, A. C.; Brzozowski, A. M.; Walton, J.; Hubbard, R. E.; Thorsell, A. G.; Li, Y. L.; Gustafsson, J. A.; Carlquist, M. Structural insights into the mode of action of a pure antiestrogen. *Structure* **2001**, *9* (2), 145–153. (c) Gradishar, W. J.; Sahmoud, T. Current and future perspectives on fulvestrant. *Clin. Breast Cancer* **2005**, *6* (Suppl 1), S23–S29.

(7) Van Kruchten, M.; de Vries, E. G.; Glaudemans, A. W.; van Lanschot, M. C.; van Faassen, M.; Kema, I. P.; Brown, M.; Schroder, C. P.; de Vries, E. F.; Hospers, G. A. Measuring residual estrogen receptor availability during fulvestrant therapy in patients with metastatic breast cancer. *Cancer Discovery* **2015**, *5* (1), 72–81.

(8) (a) Willson, T. M.; Henke, B. R.; Momtahen, T. M.; Charifson, P. S.; Batchelor, K. W.; Lubahn, D. B.; Moore, L. B.; Oliver, B. B.; Sauls, H. R.; Triantafillou, J. A.; Wolfe, S. G.; Baer, P. G. 3-[4-(1,2-Diphenylbut-1-enyl)phenyl]acrylic acid: a non-steroidal estrogen with functional selectivity for bone over uterus in rats. *J. Med. Chem.* **1994**, *37* (11), 1550–1552. (b) Wu, Y. L.; Yang, X.; Ren, Z.; McDonnell, D. P.; Norris, J. D.; Willson, T. M.; Greene, G. L. Structural basis for an unexpected mode of SERM-mediated ER antagonism. *Mol. Cell* **2005**, *18* (4), 413–424.

(9) Slade, D. J.; Pelz, N. F.; Bodnar, W.; Lampe, J. W.; Watson, P. S. Indazoles: regioselective protection and subsequent amine coupling reactions. *J. Org. Chem.* **2009**, *74* (16), 6331–6334.

(10) Negishi, E.; Anastasia, L. Palladium-catalyzed alkynylation. *Chem. Rev.* **2003**, *103* (5), 1979–2017.

(11) Zhou, C.; Larock, R. C. Regio- and stereoselective route to tetrasubstituted olefins by the palladium-catalyzed three-component coupling of aryl iodides, internal alkynes, and arylboronic acids. *J. Org. Chem.* **2005**, *70* (10), 3765–3777.

(12) Tatsuo, I.; Nobuo, M.; Miki, M.; Fumiyuki, O. Platinum(0)-Catalyzed Diboration of Alkynes with Tetrakis(alkoxo)diborons: An Efficient and Convenient Approach to cis-Bis(boryl)alkenes. *Organometallics* **1996**, *15*, 713–720.

(13) Brown, S. D.; Armstrong, R. W. Parallel Synthesis of Tamoxifen and Derivatives on Solid Support via Resin Capture. *J. Org. Chem.* **1997**, *62* (21), 7076–7077.

(14) (a) Marsaud, V.; Gougelet, A.; Maillard, S.; Renoir, J. M. Various phosphorylation pathways, depending on agonist and antagonist binding to endogenous estrogen receptor alpha (ERalpha), differentially affect ERalpha extractability, proteasome-mediated stability, and transcriptional activity in human breast cancer cells. *Mol. Endocrinol.* **2003**, *17* (10), 2013–2027. (b) Wittmann, B. M.; Sherk, A.; McDonnell, D. P. Definition of functionally important mechanistic

DOI: 10.1021/acs.jmedchem.5b00054
J. Med. Chem. 2015, 58, 4888–4904

differences among selective estrogen receptor down-regulators. *Cancer Res.* **2007**, *67* (19), 9549−9560.

(15) (a) Detre, S.; Riddler, S.; Salter, J.; A'Hern, R.; Dowsett, M.; Johnston, S. R. Comparison of the selective estrogen receptor modulator arzoxifene (LY353381) with tamoxifen on tumor growth and biomarker expression in an MCF-7 human breast cancer xenograft model. *Cancer Res.* **2003**, *63* (19), 6516−6522. (b) Deshmane, V.; Krishnamurthy, S.; Melemed, A. S.; Peterson, P.; Buzdar, A. U. Phase III double-blind trial of arzoxifene compared with tamoxifen for locally advanced or metastatic breast cancer. *J. Clin. Oncol.* **2007**, *25* (31), 4967−4973.

(16) Greenberger, L. M.; Annable, T.; Collins, K. I.; Komm, B. S.; Lyttle, C. R.; Miller, C. P.; Satyaswaroop, P. G.; Zhang, Y.; Frost, P. A new antiestrogen, 2-(4-hydroxy-phenyl)-3-methyl-1-[4-(2-piperidin-1-yl-ethoxy)-benzyl]-1*H*-indol-5-ol hydrochloride (ERA-923), inhibits the growth of tamoxifen-sensitive and -resistant tumors and is devoid of uterotropic effects in mice and rats. *Clin. Cancer Res.* **2001**, *7* (10), 3166−3177.

(17) Poupaert, J.; Carato, P.; Colacino, E.; Yous, S. 2(3*H*)-Benzoxazolone and bioisosters as "privileged scaffold" in the design of pharmacological probes. *Curr. Med. Chem.* **2005**, *12* (7), 877−885.

(18) Leeson, P. D.; Springthorpe, B. The influence of drug-like concepts on decision-making in medicinal chemistry. *Nature Rev. Drug Discovery* **2007**, *6* (11), 881−890.

(19) Ashby, J.; Odum, J.; Foster, J. R. Activity of raloxifene in immature and ovariectomized rat uterotrophic assays. *Regulatory Toxicol. Pharmacol.* **1997**, *25* (3), 226−231.

(20) Stepan, A. F.; Walker, D. P.; Bauman, J.; Price, D. A.; Baillie, T. A.; Kalgutkar, A. S.; Aleo, M. D. Structural alert/reactive metabolite concept as applied in medicinal chemistry to mitigate the risk of idiosyncratic drug toxicity: a perspective based on the critical examination of trends in the top 200 drugs marketed in the United States. *Chem. Res. Toxicol.* **2011**, *24* (9), 1345−1410.

(21) Rosati, R. L.; Da Silva Jardine, P.; Cameron, K. O.; Thompson, D. D.; Ke, H. Z.; Toler, S. M.; Brown, T. A.; Pan, L. C.; Ebbinghaus, C. F.; Reinhold, A. R.; Elliott, N. C.; Newhouse, B. N.; Tjoa, C. M.; Sweetnam, P. M.; Cole, M. J.; Arriola, M. W.; Gauthier, J. W.; Crawford, D. T.; Nickerson, D. F.; Pirie, C. M.; Qi, H.; Simmons, H. A.; Tkalcevic, G. T. Discovery and preclinical pharmacology of a novel, potent, nonsteroidal estrogen receptor agonist/antagonist, CP-336156, a diaryltetrahydronaphthalene. *J. Med. Chem.* **1998**, *41* (16), 2928−2931.

(22) Grese, T. A.; Cho, S.; Finley, D. R.; Godfrey, A. G.; Jones, C. D.; Lugar, C. W., III; Martin, M. J.; Matsumoto, K.; Pennington, L. D.; Winter, M. A.; Adrian, M. D.; Cole, H. W.; Magee, D. E.; Phillips, D. L.; Rowley, E. R.; Short, L. L.; Glasebrook, A. L.; Bryant, H. U. Structure−activity relationships of selective estrogen receptor modulators: modifications to the 2-arylbenzothiophene core of raloxifene. *J. Med. Chem.* **1997**, *40* (2), 146−167.

(23) (a) Benet, L. Z.; Spahn-Langguth, H.; Iwakawa, S.; Volland, C.; Mizuma, T.; Mayer, S.; Mutschler, E.; Lin, E. T. Predictability of the covalent binding of acidic drugs in man. *Life Sci.* **1993**, *53* (8), PL141−146. (b) Baba, A.; Yoshioka, T. Structure−activity relationships for degradation reaction of 1-beta-*o*-acyl glucuronides: kinetic description and prediction of intrinsic electrophilic reactivity under physiological conditions. *Chem. Res. Toxicol.* **2009**, *22* (1), 158−172.

(24) Kim, K. A.; Park, P. W.; Kim, K. R.; Park, J. Y. Effect of multiple doses of montelukast on the pharmacokinetics of rosiglitazone, a CYP2C8 substrate, in humans. *Br. J. Clin. Pharmacol.* **2007**, *63* (3), 339−345.

(25) Lee, J. S.; Ettinger, B.; Stanczyk, F. Z.; Vittinghoff, E.; Hanes, V.; Cauley, J. A.; Chandler, W.; Settlage, J.; Beattie, M. S.; Folkerd, E.; Dowsett, M.; Grady, D.; Cummings, S. R. Comparison of methods to measure low serum estradiol levels in postmenopausal women. *J. Clin. Endocrinol. Metab.* **2006**, *91* (10), 3791−3797.

(26) Fulvestrant Package insert: http://www1.astrazeneca-us.com/pi/faslodex.pdf.

(27) Tamoxifen itself (60 mg/kg po QD, 28 days) was found to have agonist activity in this tamoxifen-resistant xenograft, increasing tumor volume above vehicle: Tumor volume fold over start = 4.4 (versus vehicle tumor volume fold over start of 2.6), n = 2 studies.

DOI: 10.1021/acs.jmedchem.5b00054
J. Med. Chem. 2015, 58, 4888−4904

Design, Synthesis and Biochemical Evaluation of Estrogen Receptor Ligand Conjugates as Tumour Targeting Agents

Niall O. Keely[1], Daniela M. Zisterer[2] and Mary J. Meegan*,[1]

[1]*School of Pharmacy and Pharmaceutical Sciences, Centre for Synthesis and Chemical Biology, Trinity College Dublin, Dublin 2, Ireland*

[2]*School of Biochemistry & Immunology, Trinity College Dublin, Dublin 2, Ireland*

Received July 29, 2011: Revised October 07, 2011: Accepted October 24, 2011

Abstract: The estrogen receptors (ERα and ERβ), are ligand inducible nuclear receptors which play a key role in many cellular functions through specific gene expression regulation. The estrogen receptor is regarded as an attractive therapeutic target for hormone-dependent breast cancers. The antiestrogen drug tamoxifen is useful in the treatment of breast cancer. To develop new ER targeting agents as probes of estrogen receptor action, the synthesis and preliminary biochemical evaluation of five structurally varied estrogen receptor ligand conjugates containing the tamoxifen metabolite endoxifen are now reported. These structurally varied conjugates bind to the estrogen receptor (commonly overexpressed in breast cancer cells) and contain DNA alkylating, aromatase inhibitor and COX2 inhibitor moieties. The ER targeting group endoxifen (*E/Z* 4-hydroxy-N-desmethyltamoxifen) was selected for its ability to bind to the estrogen receptor. Compound **11** exhibited moderate antiproliferative activity IC_{50} = 1.64 μM in MCF-7 breast cancer cells, while compound **9b** demonstrated the most potent ER binding effects with IC_{50} values of 35.6 nM(ERα), 19.5 nM(ERβ).

Keywords: Estrogen receptor, Conjugates, Tamoxifen, Tumour targeting, Antiproliferative activity, Breast cancer.

INTRODUCTION

Nuclear receptors play a key role in many cellular functions through specific gene expression regulation and are targeted by a large number of both endogenous and exogenous ligands [1]. The majority of early stage breast cancers, in both pre- and postmenopausal women, are hormone-dependent [2]. Estradiol, the endogenous hormonal ligand, has a key role in the development and progression of the tumour and the estrogen receptor is regarded as an attractive target for hormone-dependent breast cancers [3-5]. Tamoxifen **1a** is widely used as an estrogen receptor antagonist in the treatment of breast cancer. However, many cancer chemotherapies lack specificity which can lead to toxicity and undesirable side effects and more selective chemotherapeutic approaches have been investigated to target tumours. For example, agents targeting nuclear receptors over-expressed in tumours can be directed to malignant tissue and result in improved chemotherapeutic treatments. In hormone-dependent cancers, such as certain breast cancers, a number of structurally varied estrogen receptor ligand conjugates have previously been investigated, attempting to take advantage of the presence of over-expressed estrogen receptor [6]. Conjugate compounds containing multiple ligands, separated by covalent linking groups, can exert a synergistic and improved selective action on the target disease [7]. Many examples of the coupling of cytotoxic agents to the steroid estradiol and related scaffolds, hexestrol, diethylstilbestrol and tamoxifen have been reported [8-10]. Conjugates of estradiol with geldanamycin [11], the indole alkaloid ellipticine [12], mitomycin C [13], doxorubicin [14, 15] and 5-fluorouracil [16] have been found to show lower ER binding affinities and variable cytotoxicity effects in ER positive breast tumour cells. Doxorubicin–formaldehyde conjugates linked to the antiestrogen 4-hydroxytamoxifen incorporating a base labile N-Mannich linking group have been reported to inhibit the growth of breast cancer cell lines with enhanced activity relative to doxorubicin [17, 18]. 17β-Estradiol platinum (II) complexes have demonstrated antiproliferative enhanced activity (when compared to cisplatinum) in ER positive and ER negative breast cancer cell lines [19, 20].

To develop new ER targeting agents as probes of estrogen receptor action, the synthesis and ER binding effects of novel conjugates containing components with known activity in the prevention of breast cancer proliferation (e.g. chlorambucil and indomethacin), linked to the tamoxifen metabolite endoxifen are now reported. The ER targeting group endoxifen (*E/Z* 4-hydroxy-N-desmethyltamoxifen, **1c**) was selected for its ability to bind to the estrogen receptor. Endoxifen has been shown to be the major metabolite of tamoxifen **1a,** and is present at greater concentrations than 4-hydroxytamoxifen **1b** in human plasma in breast cancer patients treated with tamoxifen [21].

Chlorambucil **2** is a nitrogen mustard alkylating agent used in the treatment of select chronic lymphocytic leukaemia and advanced ovarian and breast carcinomas. Alkylating agents have limited selectivity towards malignant cells over normal tissue and as a result can be quite toxic. By coupling alkylating agents such as chlorambucil, to a carrier agent such as endoxifen which targets tumour cells, the selectivity of the agents would be increased, their toxicity diminished and their efficacy improved. The synthesis of an endoxifen conjugate with indomethacin **3** was of interest as there is considerable evidence showing that prostaglandins

*Address correspondence to this author at the School of Pharmacy and Pharmaceutical Sciences, Centre for Synthesis and Chemical Biology, Trinity College Dublin, Dublin 2, Ireland; Tel: +353-1-8962798; Fax: +353-1-8962793; E-mail: mmeegan@tcd.ie

1875-628X/12 $58.00+.00 © 2012 Bentham Science Publishers

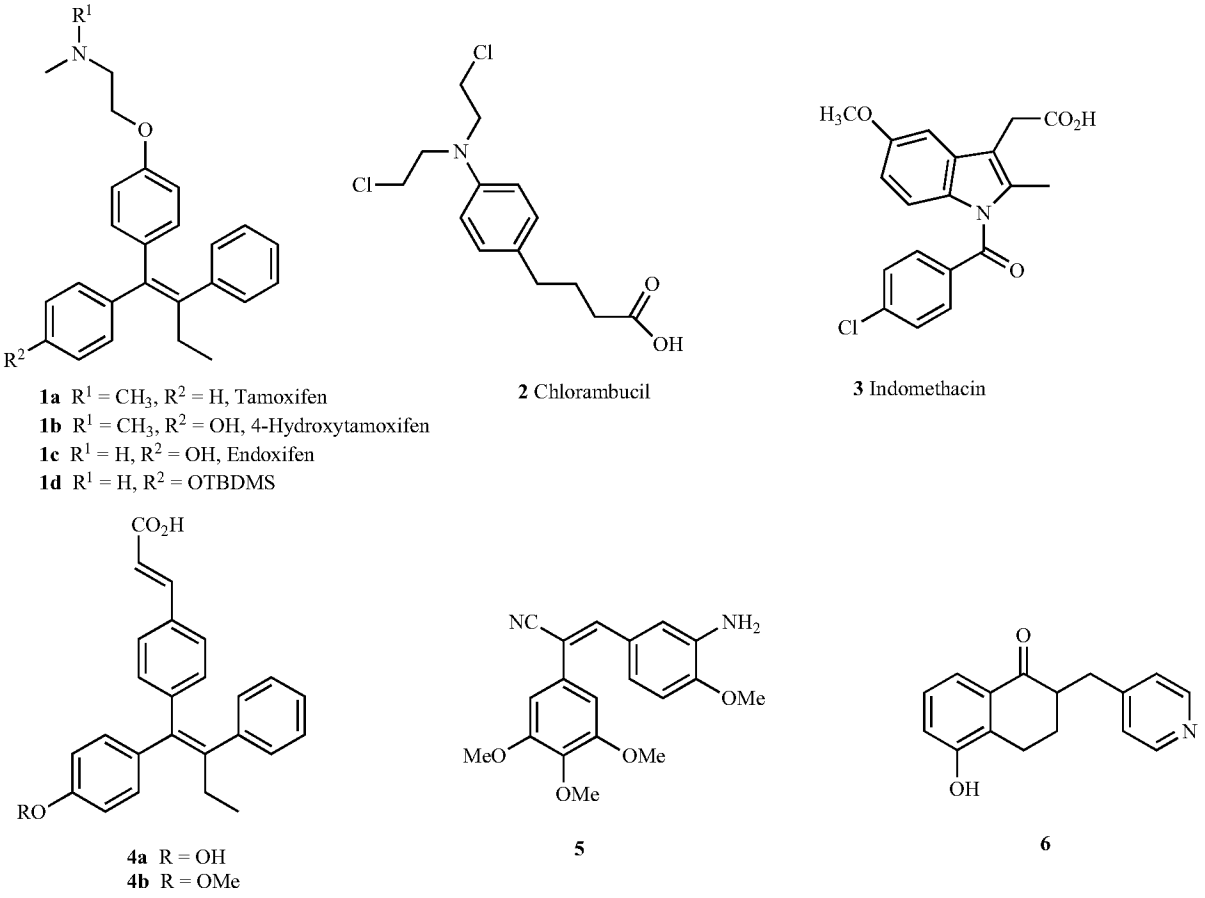


Fig. (1). Structures of estrogen receptor antagonists **1a-d** and compounds **2-6**.

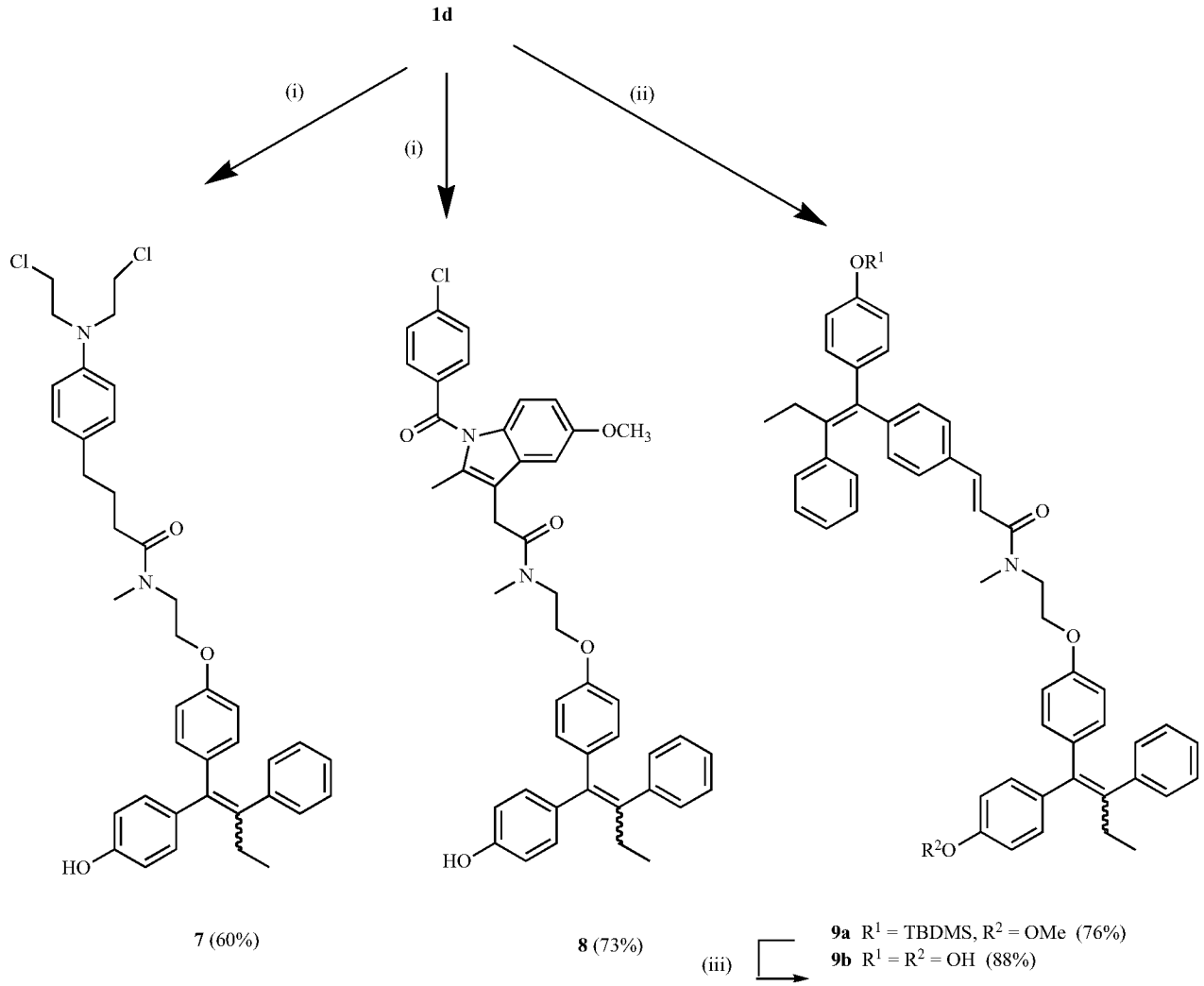
(PGs) play an important role in breast cancer development and growth [22] and there has been interest in a possible role of COX inhibitors such as indomethacin in the prevention of malignancy. Cyclooxygenase-2 (COX-2) is overexpressed in several epithelial tumours, including breast cancer. The COX-2 inhibitor indomethacin **3** has been shown to induce apoptosis and reduce the proliferation rate of HT-29 colon cancer [23], and MCF-7 cancer cell lines [24] and also exerts a synergistic effect when combined with other chemotherapeutic drugs such as doxorubicin and vincristine [25]. We wished to determine if the indomethacin fragment of the conjugate, covalently bound *via* an amide linkage to endoxifen, would act as a bulky side chain to displace the helix-12 in the ER binding site resulting in increased (or pure) antagonist activity.

A dual ER-ligand conjugate was also synthesised comprising of the fragments endoxifen **1c** and GW7604, **4a**, a selective estrogen receptor downregulator [26], in which the dimethylaminoethoxy group of tamoxifen is replaced by an acrylate side chain. A secondary binding site exists on the ER, also known as the antiestrogen binding site (AEBS) that demonstrates high affinity binding of triarylethylene antiestrogens (i.e. specifically tamoxifen and its hydroxy derivatives) which is not in competition with the binding of estrogens [27, 28]. By synthesising a bivalent ER-ligand conjugate we wish to probe the possibility of binding in both the ER and AEBS sites concurrently. The binding properties of bivalent ER targeting ligands based on the nonsteroidal estrogen hexestrol have been reported by Bergmann [29]. We wished to investigate any antagonistic effect that the presence of one ER-ligand covalently linked to a second ER-ligand would have on antiproliferative activity through the displacement of Helix-12 in the ER binding site.

The acrylonitrile combretastatin analogue **5** was chosen for conjugation with endoxifen **1c** as an example of a potent antitubulin drug with cytotoxic effects in against murine Colon 26 adenocarcinoma [30]. A conjugate incorporating the tetralone aromatase inhibitor **6** [31] was also examined. Inhibitors of aromatase enzyme reduce the production of estrogen thus decreasing the stimulation of breast tumours, hence developing multitargeting agents may result in more selective drug delivery to the tumour target site.

CHEMISTRY

Endoxifen **1c** was synthesised [17], and used as the protected *tert*-butyldimethylsilyl ether **1d** in the subsequent coupling reactions. The chlorambucil conjugate **7** was obtained by the reaction of chlorambucil **2** with the silyl-protected endoxifen ligand **1d** *via* a DCC/DMAP coupling reaction, immediately followed by the TBAF deprotection step (Scheme **1**) to afford a 1:1 *E/Z* isomeric mixture of the desired product **7** (60 % yield). Previous work has demonstrated that *p*-hydroxy substituted triarylbutenes may isomerise under cell culture conditions, having little impact on ER binding activity [32, 33]. In the ^{13}C-NMR spectrum,

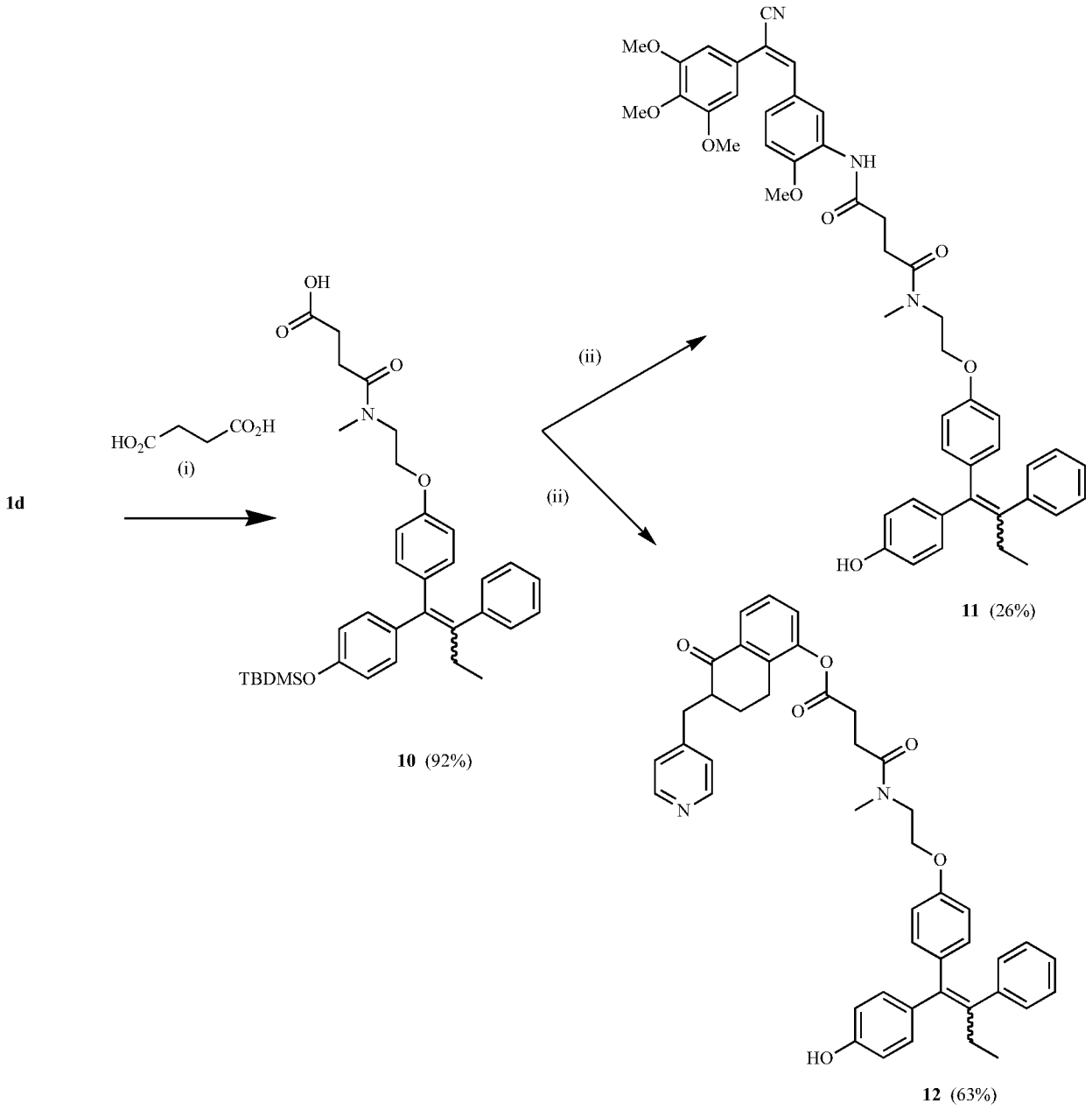


Scheme 1. Synthesis of conjugates **7, 8, 9a** and **9b**.

Reagents and conditions: (i) (a) DCC, DMAP, **2** or **3**, CH_2Cl_2, rt, 24h (b) TBAF, THF, rt, 24h (c) CH_2Cl_2, 10 % HCl, rt, 5min; (ii) DCC, DMAP, **4b**, CH_2Cl_2, rt, 24h (iii) (a) BBr_3, CH_2Cl_2, -78°, 45min, then rt, 3h (b) TBAF, THF, rt, 24h (c) 10 % HCl, CH_2Cl_2, rt, 5min.

the amide carbon is observed at 173.2 ppm while in the IR spectrum, the amide signal is observed at 1723.9 cm^{-1} and the broad hydroxyl signal at 3401.5 cm^{-1}. The conjugate **8** was synthesised by reaction of indomethacin **3** with the silyl-protected endoxifen ligand **1d** *via* a DCC/DMAP coupling reaction, immediately followed by the TBAF deprotection step (Scheme **1**) to afford a 1:1 *E/Z* isomeric mixture of the desired product **8** in 73 % yield. The main diagnostic signal of the coupled conjugate is observed in the ^{13}C-NMR spectra, where three amide carbons (due to the *E*- and *Z*-isomers of conjugate and also the indomethacin moiety) are observed at 171.82 ppm, 171.88 ppm, 172.22 ppm. In the IR spectrum, the amide signal is observed at 1724.5 $cm^{-1}$and the broad hydroxyl signal at 3327.2 cm^{-1}. The GW7604 analogue **4b** [34] was coupled with **1d** using a DCC/DMAP reaction (Scheme **1**) to afford the protected-conjugate product **9a** (76 %). Following demethylation with boron tribromide and subsequent silyl deprotection steps, the product **9b** was afforded in a 1:1 *E/Z* isomeric mixture (88 % yield).

For the synthesis of the endoxifen conjugates with **5** and **6**, the protected endoxifen was first reacted with succinic acid to afford the endoxifen-succinimide **10**, (Scheme **2**). The *cis*-acrylonitrile **6** was prepared following the literature method [30], and was reacted with endoxifen analogue **10** *via* a DCC/HOBt coupling, immediately followed by the TBAF deprotection step (Scheme **2**) to afford a 1:1 *E/Z* isomeric mixture of the product **11** (26 % yield). The two amide carbons of the linker fragment are observed at 171.48 and 173.27 ppm in the ^{13}C-NMR spectrum of the coupled conjugate **11** with the nitrile, amide and hydroxyl signals observed at 2208.6, 1734.8 and 3401.5 cm^{-1} in the IR spectrum. The conjugate **12** was obtained by reaction of the aromatase inhibitor **5** and the protected endoxifen ligand **10** *via* a DCC/HOBt coupling reaction, followed by the TBAF deprotection step to afford a 1:1 *E/Z* isomeric mixture of the desired product **12** in 63 % yield, (Scheme **2**). The coupled conjugate is observed in the ^{13}C-NMR spectrum, where the ester and amide carbons are identified at 171.45 and 172.00 ppm and the carbonyl group of the aromatase inhibitor fragment at 198.52 ppm. In the IR spectrum, the ester signal



Scheme 2. Synthesis of conjugates **11** and **12**.

Reagents and conditions:(i) CH_2Cl_2, rt, 16h (ii) (a) DCC, HOBt, **5** or **6**, CH_2Cl_2, rt, 24h (b) TBAF, THF, rt, 24h (c) 10 % HCl, CH_2Cl_2, rt, 5min.

is observed at ν1738.0 cm^{-1}, the amide signal at ν1631.2 cm^{-1} and the broad hydroxyl signal at ν3435.0 cm^{-1}.

BIOLOGICAL RESULTS AND DISCUSSION

The conjugates in this series contain an ER-ligand component (i.e. endoxifen) linked *via* amide and/or ester linkages, with or without a succinic acid linker group, to another compound with bioactivity towards cancers and tumours. The subset of bioactive compounds include an aromatase inhibitor, an alkylating agent (chlorambucil), a tubulin targeting agent, an ER antagonist and the NSAID indomethacin (shown to have synergistic effects when used in combination with the DNA intercalating drugs doxorubicin). Therefore, some structural comparison may highlight possible mechanistic features regarding the functionality of the conjugates.

The antiproliferative and cytotoxicity data for the conjugates evaluated in the ER positive MCF-7 breast cancer cells are shown in Table **1**. The data obtained for this series of conjugates ranged from low micromolar antiproliferative IC_{50} values to IC_{50} values greater than 50 μM. All the conjugates displayed low cytotoxicity levels at 10 μM in the lactate dehydrogenase assay [35]. The endoxifen-acrylonitrile conjugate **11** displays the most potent antiproliferative activity of the series, with IC_{50} = 1.64 μM,

Table 1. Antiproliferative and ER Binding Affinities for Conjugates 7, 8, 9b, 11 and 12

Compound	MCF-7 IC_{50} (μM) [a]	Cytotoxicity 10 μM [c]	ER α IC_{50} (nM) [d]	ER β IC_{50} (nM) [d]	Selectivity α/ β ratio	RBA [f] (ERα)	RBA [f] (ERβ)
7	30.3	0	490	415	0.85	1	1
8	11.6	0	78.9	200	2.5	7	3
9b	>50	0	35.6	19.5	0.55	16	29
11	1.64	1.7	524	269	0.51	1	2
12	12.6	0	51.4	51.6	1.00	11	11
Tamoxifen	4.12[b]	13.4	70 [e]	170 [e]	2.42	8.14	2.97

[a]IC_{50} values are half maximal inhibitory concentrations required to block the growth stimulation of MCF-7 cells. Values represent the mean ± S.E.M (error values x 10^{-6}) for three experiments performed in triplicate.

[b]The IC_{50} value obtained for Tamoxifen using the MTT assay is 4.12± 0.038 μM, with cytotoxicity value 13.4 % (10 μM) is in good agreement with the reported IC_{50} value for tamoxifen on human MCF-7 cells, (reference 36).

[c]Lactate Dehydrogenase assay: Following treatment of the cells, the amount of LDH was determined using LDH assay kit from Promega. Data is presented as % cell lysis at compound concentration of 10 μM (reference 35).

[d]Values are an average of at least nine replicate experiments, for ERα with typical standard errors below 15%, and six replicate experiments for ERβ, with typical standard errors below 15%.

[e]The ER binding values obtained are in agreement with the reported ER IC_{50} binding data for tamoxifen (ERα 60.9 nM ERβ188 nM, Panvera/Invitrogen).

[f]The RBA (Relative Binding Affinity value, %) is calculated as the ratio of the binding IC_{50} value for the reference ligand (estradiol) divided by the binding IC_{50} value for the selected ligand, multiplied by 100.

comparable to activity of the acid **6** (IC_{50} = 0.83 μM) in this cell line, with low cytotoxicity in the LDH assay. The endoxifen conjugates of chlorambucil **7**, indomethacin **8** and the aromatase inhibitor **12** displayed moderate antiproliferative activity when compared to tamoxifen [36]. The IC_{50} values for these conjugates were in the range of 11.6 - 30.3 μM and displayed virtually no cytotoxicity at 10 μM in the lactate dehydrogenase assay [35]. The aromatase inhibitor conjugate **12** contains an ester linkage between the tetralone and the succinate linker fragment which may be enzymatically hydrolysed *in vivo,* thus possibly exerting a dual-effect through aromatase inhibition and ER-antagonism. The dual ER-ligand conjugate **9b** containing the amide linking groups, did not display significant antiproliferative activity, with an IC_{50} value greater than 50 μM, resulting in negligible cytotoxicity. The presence of the amide linkage may restrict the conformation of this conjugates unfavourably. This suggests that presence of the bulky ligand side chain in this case has a detrimental effect on the antiproliferative activity of either the endoxifen or GW7604 ER-ligand fragment at the ER site. As the conjugate **9b** contains an amide linkage in the scaffold, it is possible that **9b** may not be easily hydrolysed *in vivo* and could act as a possible pure ER antagonist due to the large bulky side chain group.

The conjugates were investigated for their ERα and ERβ binding abilities in a fluorescence polarization based-competitor assay. The ER-binding data for these selected conjugates is reported in Table **1**. In order to function as ER-targeting agents, the conjugates should display some binding affinity towards the receptor target. All the conjugates display binding affinities for the ERα and ERβ with IC_{50} values below 1 μM, confirming their ability to act as ER-targeting agents. The acrylonitrile conjugate **11** and chlorambucil conjugate **7** showed the least affinity for either ER isoform yet still demonstrated sub-micromolar competitive binding IC_{50} values towards ERα (96 and 490 nM respectively) and ERβ (415 and 61 nM respectively). The indomethacin conjugate **8** and aromatase inhibitor conjugate **12**, which did not demonstrate potent antiproliferative activity, display impressive binding affinities towards ERα and ERβ with competitive binding IC_{50} values in the range 50 – 200 nM. The acrylonitrile conjugate **11** displayed the lowest ER binding of the series with IC_{50} of 524 nM(ERα) and 269 nM(ERβ). The bivalent ER-ligand conjugate **9b** which also did not display significant antiproliferative activity, demonstrated potent competitive binding with IC_{50} values of 35.6 nM (ERα) and 19.5 nM (ERβ). This may suggest that these conjugates bind in orientations or sites which as a result do not displace helix-12 in the ER, hence, do not display a significant antagonistic activity *in vitro*. The phenolic hydroxy group present on the endoxifen fragment can interact favourably with residues Glu353, Arg394 and His524 in the ER binding site through hydrogen bonding which can explain the high binding affinity for all conjugates which make them useful probes for the estrogen receptor action.

The relative binding affinity (RBA) of the estrogen receptor ligands is reported. Estradiol is the reference ligand, with 100 % binding value. Using the IC_{50} binding values obtained for estradiol for ERα (5.7 nM) and ERβ (5.6 nM), the relative binding affinities of the selected conjugates were calculated (Table **1**). As the estrogen receptor has between 1000 and 10000 molecules per cell and calculations on the basis of the number of receptors per cell and the possible drug concentration show that the relative binding affinity (RBA) value should be at least 1% of that of estradiol for effective activity [12]. All of the conjugates investigated in the ER competitor binding assays had RBA values greater than or equal to 1%. The bivalent ER conjugate **9b** demonstrates impressive RBA values of 16 for ERα and 29 for ERβ.

CONCLUSION

We have synthesised a new series of estrogen receptor ligand conjugates, which contain components with known activity in the prevention of breast cancer proliferation

covalently linked to the tamoxifen metabolite endoxifen. Preliminary *in vitro* evaluation of the antiproliferative and cytotoxic activities of the compounds in MCF-7 breast cancer cells, together with determination of the ER binding indicated that some of these estrogen receptor ligand conjugate molecules may be useful as probes of estrogen receptor action and may also result in a more selective and targeted delivery of non-specific agents such as chlorambucil to breast tumour cells. The bivalent ER conjugate **9b** demonstrates potent ER binding with IC_{50} values of 35.6 nM(ERα), 19.5 nM(ERβ) and RBA values of 16 (ERα) and 29 (ERβ) and provides a template scaffold for the development of further ER ligands.

EXPERIMENTAL SECTION

General

Uncorrected melting points were measured on a Stuart SMP11 apparatus. Infra-red spectra were recorded on a Perkin Elmer Paragon 100 Spectrometer. Band positions are given as cm^{-1}. Solid and resin samples were analysed by KBr disc, while oils were analysed as neat films on NaCl plates. ^1H and ^{13}C Nuclear magnetic resonance (NMR) spectra were recorded at 20°C on a Bruker DPX 400 spectrometer (400.13 MHz, ^1H; 100.61 MHz, ^{13}C) in $CDCl_3$, with internal standard trimethylsilane (TMS), or CD_3OD. ^1H-NMR spectra were assigned relative to the TMS peak at 0.00. ^{13}C NMR spectra were assigned relative to the centre peak of the $CDCl_3$ triplet at 77.00 ppm. Coupling constants are reported in Hertz (Hz). High resolution molecular ion determinations (HRMS) were acquired on a Micro mass spectrometer (E.I. Mode) at the Department of Chemistry, Trinity College Dublin and a Micro mass spectrometer (E.I. Mode) at the Centre for Synthesis and Chemical Biology, University College Dublin. Thin layer chromatography (TLC) was carried out using Merck F-254 silica plates. Flash chromatography was carried out on Merck Kieselgel $60F_{254}$ silica. Solvents were dried according to the standard protocols.

[2-(4-{(E/Z)-1-[4-(tert-Butyldimethylsilanyloxy)phenyl]-2-phenylbut-1-enyl}phenoxy)ethyl] methylamine (1d)

(4-{(*E/Z*)-1-[4-(2-Bromoethoxy)phenyl]-2-phenylbut-1-enyl}phenoxy)-*tert*-butyldimethylsilane (0.54 g, 1.00 mmol) was reacted with methylamine in anhydrous tetrahydrofuran (20 mL) in a sealed tube at 60 °C under pressure while stirring for 48 – 72 h, [17]. After this time the reaction container was allowed sufficient time to cool, and then sodium carbonate/sodium hydrogen carbonate pH 10 buffer solution (50 mL) was added. The mixture was then extracted with CH_2Cl_2 (3 x 50 mL). The organic phases were combined, dried over sodium sulfate and the solvent evaporated *in vacuo* to afford a crude product which was then purified *via* flash chromatography over silica gel (CH_2Cl_2:MeOH, 4:1) to afford the product as a brown oil (0.38 g, 78 %, *Z/E* = 1:1.3). ^1H-NMR (400 MHz, $CDCl_3$): δ 0.13 (s, 0.57 x 6H, $Si(CH_3)_2$), 0.26 (s, 0.43 x 6H, $Si(CH_3)_2$), 0.95 – 1.03 (m, 12H, $(CH_3)_3$, CH_3), 2.45 – 2.53 (m, 5H, NCH_3, CH_2), 2.89 (s, 0.43 x 2H, CH_2), 2.99 (s, 0.57 x 2H, CH_2), 3.36 (s, 1H, NH), 3.95 (t, 0.43 x 2H, *J* = 5.0 Hz, CH_2), 4.11 (t, 0.57 x 2H, *J* = 5.0 Hz, CH_2), 6.50 – 7.20 (m, 13H, ArH). ^{13}C-NMR (100 MHz, $CDCl_3$): (*Z/E* mixture) δ -4.91, -4.80, 13.21, 13.24, 17.75, 25.24, 25.26, 28.47, 28.60, 35.39, 35.26, 49.47, 50.03, 50.12, 65.73, 65.99, 112.80, 113.54, 118.54, 119.12, 125.44, 125.48, 127.33, 127.41, 129.25, 130.12, 130.20, 131.43, 131.57, 135.68, 136.02, 136.06, 136.35, 137.44, 137.53, 140.59, 140.65, 142.11, 142.19, 153.06, 153.84, 156.10, 156.94. IR: ν_{max} (KBr) cm^{-1}: 3340.9, 2956.9, 2930.0, 2857.0, 1605.5. HRMS (EI): Found 488.2980 (M^++H), $C_{31}H_{42}NO_2Si$ requires 488.2985.

4-{4-[Bis-(2-chloroethyl)amino]phenyl}-N-(2-{4-[(E/Z)-1-(4-hydroxyphenyl)-2-phenylbut-1-enyl]phenoxy}ethyl)-N-methylbutyramide (7)

Chlorambucil **7** (0.06 g, 0.21 mmol), DCC (0.04 g, 0.21 mmol) and DMAP (0.03, 0.21 mmol) were stirred for 10 mins in anhydrous CH_2Cl_2 (4 mL). A solution of the amine **1d** (0.10 g, 0.21 mmol) in dry CH_2Cl_2 (4 mL) was added to the reaction mixture and then allowed stir for 24 h under nitrogen at room temperature. Reaction was monitored *via* TLC (CH_2Cl_2:MeOH, 4:1) until no more starting materials were visible. The reaction mixture was diluted to 15 mL with anhydrous CH_2Cl_2 and filtered to remove DCU. The filtrate was evaporated to dryness under reduced pressure. The residue was dissolved in 3 mL anhydrous THF and stirred under a nitrogen atmosphere. A solution of 0.1 M TBAF (0.21 mL, 0.21 mmol) was added to the mixture and allowed stir for 24 h. The mixture was evaporated to dryness under reduced pressure. The residue was dissolved in CH_2Cl_2 and washed with 10 % HCl solution. The resulting organic phase was dried over sodium sulfate and evaporated to dryness under vacuum. The residue was purified *via* flash chromatography (CH_2Cl_2:MeOH, 20:1) to yield an isomeric mixture of the product **7** as a brown oil (81.0 mg, 60 %, *E/Z* = 1:1). ^1H-NMR (400 MHz, $CDCl_3$): δ 0.91- 0.96 (m, 3H, CH_3), 1.29 - 2.63 (m, 8H, $4xCH_2$), 2.97 - 3.15 (m, 3H, NCH_3), 3.60 - 4.16 (m, 12H, $3xCH_2N$, CH_2O, $2xCH_2Cl$), 6.45 – 7.18 (m, 17H, ArH), OH not observed. ^{13}C-NMR (100 MHz, $CDCl_3$), (*Z/E* mixture): δ 13.30, 24.45, 25.12, 25.22, 16.15, 26.49, 28.48, 29.26, 29.26, 29.88, 32.27, 32.76, 33.42, 33.66, 37.25, 40.13, 44.94, 47.61, 48.73, 53.12, 111.68, 112.69, 113.37, 113.99, 114.51, 114.65, 118.16, 128.65, 129.24, 130.21, 130.34, 131.59, 133.71, 136.64, 133.71, 136.64, 143.81, 154.11, 154.67, 156.85, 173.23. IR: ν_{max} (KBr) cm^{-1}: 3401.5, 2929.6, 2850.2, 1723.9, 1609.5. HRMS (EI): Found 659.2803 (M^++H), $C_{39}H_{45}$ $Cl_2N_2O_3$ requires 659.2807.

2-[1-(4-Chlorobenzoyl)-5-methoxy-2-methyl-1H-indol-3-yl]-N-(2-{4-[(E/Z)-1-(4-hydroxyphenyl)-2-phenylbut-1-enyl]phenoxy}ethyl)-N-methylacetamide (8)

Indomethacin **3** (0.33 g, 0.91 mmol), DCC (0.19 g, 0.91 mmol) and DMAP (0.11, 0.91 mmol) were stirred for 10 mins in anhydryous CH_2Cl_2 (7 mL). A solution of the amine **1d** (0.45 g, 0.91 mmol) in dry CH_2Cl_2 (8 mL) was added to the reaction mixture and then allowed stir for 24 h under nitrogen at room temperature. Reaction was monitored *via* TLC (CH_2Cl_2:MeOH, 4:1) until no more starting materials were visible. The reaction mixture was diluted to 15 mL with anhydrous CH_2Cl_2 and filtered to remove DCU. The filtrate was evaporated to dryness under reduced pressure. The residue was dissolved in 3 mL anhydrous THF and stirred under a nitrogen atmosphere. A solution of 0.1 M TBAF (0.91 mL, 0.91 mmol) was added to the mixture and allowed

stir for 24 h. The mixture was evaporated to dryness under reduced pressure. The residue was dissolved in CH_2Cl_2 and washed with 10 % HCl solution. The resulting organic phase was dried over sodium sulfate and evaporated to dryness under vacuum. The residue was purified *via* flash chromatography (CH_2Cl_2:MeOH, 20:1) to yield an isomeric mixture of the product **8** as a brown oil (472 mg, 73 %, *E/Z* = 1:1). ^{1}H-NMR (400 MHz, $CDCl_3$): δ 0.93 - 0.97 (m, 3H, endoxifen CH_3), 2.21 – 2.29 (m, 3H, indomethacin CH_3), 2.48 - 2.53 (m, 2H, CH_2), 2.97 - 3.18 (m, 3H, NCH_3), 3.69 - 4.16 (m, 9H, OCH_3, CH_2N, CH_2O, $COCH_2$), 6.44 – 7.19 (m, 20H, ArH), OH not observed. ^{13}C-NMR (100 MHz, $CDCl_3$), (*E/Z* mixture): δ 11.42, 11.46, 13.14, 13.25, 28.63, 29.28, 30.53, 30.58, 33.89, 36.07, 37.54, 48.12, 48.82, 55.36, 55.43, 64.50, 64.92, 65.96, 66.21, 99.73, 99.82, 99.89, 103.67, 103.73, 104.20, 110.28, 110.33, 112.77, 113.49, 113.94, 114.62, 125.43, 127.40, 128.37, 129.33, 129.73, 129.80, 130.15, 130.26, 131.51, 131.59, 132.54, 132.69, 132.76, 134.68, 135.08, 136.23, 137.40, 137.51, 140.27, 140.45, 142.29. 142.32, 153.49, 153.51, 153.86, 154.75, 155.61, 155.93, 156.74, 171.82, 171.88, 172.22. IR: ν_{max} (KBr) cm^{-1}: 3327.2, 2929.2, 2851.9, 1724.5, 1626.2. HRMS (EI): Found 735.2620(M^++Na), $C_{44}H_{41}ClN_2O_5Na$ requires 735.2601.

(E)-N-[2-(4-{(E/Z)-1-[4-(tert-Butyldimethylsilanyloxy)-phenyl]-2-phenylbut-1-enyl}-phenoxy)ethyl]-3-{4-[(E/Z)-1-(4-methoxyphenyl)-2-phenylbut-1-enyl]phenyl}-N-methylacrylamide (9a)

The acid **4b** [34] (0.13 g, 0.34 mmol, 1 eq.), DCC (0.07 g, 0.34 mmol, 1 eq.), DMAP (0.04 g, 0.34 mmol, 1 eq.) was stirred in 5 mL of anhydrous CH_2Cl_2 for 10 mins. **1d** (0.166 g, 0.34 mmol, 1 eq.) was added to the reaction mixture and allowed stir at room temperature for 24 h under nitrogen atmosphere. After which time the reaction was diluted with 20 mL CH_2Cl_2 and filtered to remove insoluble solids. The solvent was removed *in vacuo* and the residue was purified *via* flash chromatography (CH_2Cl_2:MeOH, 20:1) to afford the product **9a** as a resin (220 mg, yield = 76 %, *E/Z* = 1:1). ^{1}H-NMR (400 MHz, $CDCl_3$): δ 0.12 – 0.25 (m, 6H, $Si(CH_3)_2$), 0.94 – 1.02 (m, 15H, CH_3 ,$SiC(CH_3)_3$), 2.49 – 2.53 (m, 4H, CH_2), 3.04 – 4.33 (m, 10H, NCH_3, NCH_2, OCH_2, OCH_3), 6.49 – 7.77 (m, 28H, ArH, CH=CH). ^{13}C-NMR (100 MHz, $CDCl_3$), (*E/Z* mixture): δ -4.91, -4.80, 13.19, 17.76, 25.25, 28.61, 33.54, 36.06, 48.56, 54.57, 112.39, 112.69, 113.14, 113.47, 116.41, 118.52, 119.10, 125.42, 125.73, 125.86, 126.55, 127.30, 127.48, 129.20, 129.26, 129.54, 130.80, 131.39, 131.51, 134.64, 136.23, 142.12, 145.03, 156.44, 157.16, 162.10. IR: ν_{max} (KBr) cm^{-1}: 3430.0, 3326.2, 2928.7, 2850.8, 1625.3, 1575.8. HRMS (EI): Found 876.4424, $C_{57}H_{63}NO_4SiNa$ requires 876.4424.

(E)-N-(2-{4-[(E/Z)-1-(4-Hydroxyphenyl)-2-phenylbut-1-enyl]phenoxy}ethyl)-3-{4-[(E/Z)-1-(4-hydroxyphenyl)-2-phenylbut-1-enyl]phenyl}-N-methylacrylamide (9b)

A solution of **9a** (0.18 g, 0.21 mmol, 1 eq.) was stirred in anhydrous CH_2Cl_2 (5 mL). The mixture was cooled to -78 °C and 1.0 M boron tribromide solution (0.84 mL, 0.84 mmol, 4 eq.) was added slowly to the reaction mixture. The reaction was allowed stir at -78 °C for 45 minutes then allow return to room temperature while stirred for three hours. The reaction was quenched through the addition of 3 mL of methanol. The mixture was evaporated to dryness *in vacuo* and the residue was dissolved in 5 mL of anhydrous THF. To the solution, 1.0M TBAF in THF (0.50 mL, 0.50 mmol, 2.5eq.) was added. The reaction was allowed stir overnight. The reaction was diluted with 20 mL of THF and washed with 10 % HCl solution. The organic layer was separated, dried over sodium sulfate and evaporated to dryness *in vacuo*. The residue was purified *via* flash chromatography (CH_2Cl_2:MeOH, 20:1) to afford the product **9b** as a resin (135 mg, yield = 88 %, *E/Z* = 1:1). ^{1}H-NMR (400 MHz, $CDCl_3$): δ 0.91 – 0.96 (m, 6H, CH_3), 2.44 - 2.55 (m, 4H, CH_2), 2.91 – 3.22 (m, 3H, NCH_3), 3.65 – 4.41 (6H, NCH_2, OCH_2, 2xOH), 6.51 – 7.35 (m, 28H, ArH, CH=CH). ^{13}C-NMR (100 MHz, $CDCl_3$), (*E/Z* mixture): δ 13.60, 13.68, 24.90, 25.57, 28.93, 29.03, 30.99, 33.88, 49.26, 65.92, 68.11, 113.98, 114.33, 114.94, 115.06, 115.31, 116.56, 125.82, 126.99, 127.28, 127.81, 127.90, 128.04, 129.52, 129.67, 129.76, 130.02, 130.70, 130.85, 131.31, 132.06, 132.10, 135.54, 135.89, 138.06, 140.63, 142.79, 153.99, 154.95, 157.13. IR: ν_{max} (KBr) cm^{-1}: 3326.6, 2928.9, 2850.8, 1626.2, 1575.2. HRMS (MALDI-TOF): Found 726.3588; $C_{50}H_{48}NO_4$ requires 726.3583(M^++H).

N-[2-(4-{(E/Z)-1-[4-(tert-Butyldimethylsilanyloxy)phenyl]-2-phenylbut-1-enyl}phenoxy)ethyl]-N-methylsuccinamic acid (10)

The amine **1d** (0.20 g, 0.41 mmol, *E/Z* = 1:1) and succinic anhydride (0.04 g, 0.41 mmol) were dissolved in 5ml of dry CH_2Cl_2. The reaction was allowed stir at room temperature for 16 h. Reaction was monitored *via* TLC (CH_2Cl_2:MeOH = 4:1). Reaction mixture was worked up *via* the addition of CH_2Cl_2 (10 mL), washed with 1M NaOH solution (10 mL). The aqueous phase was extracted with CH_2Cl_2 (10 mL x3). The combined organic layers were acidified with dilute HCl dropwise, washed with water (10 mL) and brine (10 mL), dried over sodium sulfate and then evaporated to dryness *in vacuo* to afford an isomeric mixture (*E:Z* = 1:1) of the product (222 mg, 92%) as a light brown oil. ^{1}H-NMR (400 MHz, $CDCl_3$): δ 0.12 – 0.25 (m, 6H, $Si(CH_3)_2$), 0.94 – 1.02 (m, 12H, $SiC(CH_3)_3$, CH_3), 2.48 – 2.52 (m, 2H, CH_2), 2.65 - 2.87 (m, 4H, succinic CH_2), 3.00 - 3.22 (m, 3H, NCH_3), 3.70 – 4.17 (m, 4H, CH_2N, CH_2O), 6.49 – 7.20 (m, 13H, ArH), COOH not observed. ^{13}C-NMR (100 MHz, $CDCl_3$), (*E/Z* mixture): δ -4.92, -4.80, 13.18, 13.22, 17.75, 25.22, 25.24, 28.46, 28.60, 37.04, 37.10, 47.91, 65.78, 66.12, 112.65, 113.42, 118.53, 119.10, 125.46, 127.31, 127.39, 127.43, 129.26, 130.09, 130.22, 130.30, 131.38, 131.57, 131.65, 135.73, 136.20, 136.27, 137.37, 137.44, 140.65, 142.08, 153.06, 156.68, 172.69, 176.78; IR: ν_{max} (KBr) cm^{-1}: 3435.7, 2927.5, 1696.5, 1624.0, 1603.6. HRMS (EI): Found 610.2972 $(M+Na)^+$, $C_{35}H_{45}NO_5SiNa$ requires 610.2965.

N-{5-[2-Cyano-2-(3,4,5-trimethoxyphenyl)vinyl]-2-methoxyphenyl}-N'-(2-{4-[(E/Z)-1-(4-hydroxyphenyl)-2-phenylbut-1-enyl]phenoxy}ethyl)-N'-methylsuccinamide (11)

The protected endoxifen succinic acid linker compound **10** (0.10 g, 0.17 mmol, *E:Z* = 1:1), dicyclohexylcarbodiimide (0.04 g, 0.17 mmol) and 1-hydroxybenzotriazole hydrate (0.02 g, 0.17 mmol) were dissolved in dry CH_2Cl_2 (5 mL) under a N_2 environment. The mixture was allowed to stir for 20 minutes before adding a solution of the *cis*-acrylonitrile **6** (0.06 g, 0.17 mmol) in dry CH_2Cl_2 (3 mL). The reaction was

allowed stir at room temperature for 24 h until no starting material was visible by TLC (CH_2Cl_2:MeOH, 4:1). The reaction mixture was filtered to remove the dicyclohexylurea byproduct. The mixture was evaporated to dryness *in vacuo*. The residue was dissolved in 3 mL anhydrous THF and stirred under a nitrogen atmosphere. A quantity of 0.1 M TBAF (0.20 mL, 0.02 mmol) was added to the mixture and allowed stir for 24 h. The mixture was evaporated to dryness under reduced pressure. The residue was dissolved in CH_2Cl_2 and washed with 10 % HCl solution. The resulting organic phase was dried over sodium sulfate and evaporated to dryness under vacuum. The residue was purified *via* flash chromatography on silica gel (CH_2Cl_2:MeOH, 20:1) to yield an isomeric mixture (*E:Z* = 1:1) of the product **12** (35 mg, 26 %). ^{1}H-NMR (400 MHz, $CDCl_3$): δ 0.87 – 0.95 (m, 3H, CH_3), 2.44 – 3.23 (m, 9H, NCH_3, CH_2, 2xsuccinic-CH_2), 3.65 – 4.28 (m, 16H, NCH_2, 4xOCH_3, OCH_2), 6.33 – 7.80 (m, 20H, ArH, C=CH, NH), OH not observed. ^{13}C-NMR (100 MHz, $CDCl_3$), (*E/Z* mixture): δ 13.18, 14.24, 17.93, 27.87, 27.92, 28.55, 28.80, 29.25, 31.14, 36.20, 36.96, 47.62, 51.43, 55.70, 58.03, 66.26, 105.43, 106.13, 112.79, 113.40, 114.06, 114.57, 114.73, 115.03, 127.12, 127.37, 128.13, 128.52, 128.66, 129.25, 129.54, 130.21, 130.57, 130.64, 131.24, 131.56, 131.83, 132.14, 134.85, 162.32, 171.48, 173.27. IR: ν_{max} (KBr) cm^{-1}: 3467.8, 2208.6, 1734.8, 1636.3, 1508.9. HRMS (MALDI-TOF):. Found 808.3398; $C_{47}H_{49}N_2O_8K$ requires 808.3126.

N-(2-{4-[(E/Z)-1-(4-Hydroxyphenyl)-2-phenylbut-1-enyl] phenoxy}ethyl)-N-methyl-succinamic acid 5-oxo-6-pyridin-4-ylmethyl-5,6,7,8-tetrahydronaphthalen-1-yl ester (12)

The acid **10** (1 equivalent, 0.25 mmol), DCC (1 equivalent, 0.25 mmol, 0.05 g) and HOBt (1 equivalent, 0.25 mmol, 0.03 g) were suspended in 3 mL of anhydrous CH_2Cl_2 and stirred for 10 minutes under a nitrogen atmosphere. The phenol **5** was then dissolved in 3 mL of anhydrous DCM and slowly added to the mixture *via* syringe. Reaction was allowed stir for 24 h. Reaction was monitored *via* TLC (CH_2Cl_2:MeOH, 4:1) until no more starting materials were visible. The reaction mixture was diluted to 15 mL with anhydrous CH_2Cl_2 and filtered to remove DCU. The filtrate was evaporated to dryness under reduced pressure. The residue was dissolved in 3 mL anhydrous THF and stirred under a nitrogen atmosphere. A solution of 0.1 M TBAF (2 equivalents) was added to the mixture and allowed stir for 24 h. The mixture was evaporated to dryness under reduced pressure. The residue was dissolved in CH_2Cl_2 and washed with 10 % HCl solution. The resulting organic phase was dried over sodium sulfate and evaporated to dryness under vacuum. The residue was purified *via* flash chromatography (CH_2Cl_2:MeOH, 20:1) to yield an isomeric mixture of the product as a brown oil (112 mg, 63%, *E/Z* = 1:1). ^{1}H-NMR (400 MHz, $CDCl_3$): δ 0.99 (t, J = 7.5Hz, 3H, CH_3), 1.27 - 1.43 (m, 2H, CH_2), 1.74 (m, 2H, CH_2), 2.50 (m, 2H, CH_2), 2.64 – 2.87 (m, 4H, CH_2), 3.17 – 3.03 (m, 5H, CH_2, NCH_3), 3.45 (dd, 1H, *J* = 4 Hz, 13.5 Hz, CH), 3.66 (m, 1H, CH_2N), 3.77 (m, 1H, CH_2N), 3.97 (m, 1H, CH_2O), 4.12 (m, 1H, CH_2O), 6.51 (m, 1H, ArH), 6.70 (m, 1H, ArH), 6.77 (d, 1H, ArH, *J* = 8 Hz), 6.85 (m, 2H, ArH), 7.12 (m, 7H, ArH), 7.17 (s, br, 2H, ArH), 7.36 (s, 2H, ArH), 7.62 (d, 1H, ArH, *J* = 8 Hz), 7.71 (d, 1H, ArH, *J* = 5.0 Hz), 8.63 (d, 2H, pyridine-H, *J* = 5.2 Hz), OH not observed. ^{13}C-NMR (100 MHz, $CDCl_3$), (*E/Z* mixture): δ 13.09, 19.53, 21.24, 21.89, 24.26, 24.89, 25.03, 26.17, 26.96, 28.57, 28.86, 29.25, 32.45, 34.81, 47.66, 47.84, 52.38, 112.64, 113.36, 113.43, 113.96, 114.66, 118.40, 119.20, 119.30, 119.55, 125.42, 125.54, 126.91, 127.37, 129.25, 130.04, 130.20, 130.40, 131.59, 132.01, 133.02, 133.71, 139.04, 148.43, 149.02, 153.49, 153.80, 171.45, 172.00, 198.52. IR: ν_{max} (KBr) cm^{-1}: 3435.0, 2930.7, 1738.0, 1631.2, 1605.9. HRMS (MALDI-TOF): Found 709.3290; $C_{44}H_{45}N_2O_6$ requires 709.3278(M^++H).

Biochemistry

Estrogen Receptor (ER) Competitor Assay

ERα and ERβ fluorescence polarization based-competitor assay kits were obtained from Invitrogen. The recombinant ER and the fluorescent estrogen ligand were removed from the -80°C freezer and thawed on ice for one-hour prior to use. The assay was performed using a protocol described by the manufacturer. The fluorescent estrogen (2 nM) was added to the ER (30 nM for ERα and 20 nM for ERβ), screening buffer (100 nM potassium phosphate (pH 7.4), 100 μg/ml BGG, 0.02 M NaN_3) was added to make up a final volume that was dependent on the number of tubes used. Test compound, 1 μL, in varying concentrations, was added to 49 μL screening buffer in 96-well black plates, 50 μL of the fluorescent estrogen/ER complex was added to make up the total volume to 100 μL. A vehicle control contained 1 % DMSO (v/v). A negative control contained 50 μL of screening buffer and 50 μL of fluorescent estrogen/ER complex. This control was used to determine the polarization value when no competitor was present (theoretical maximum polarization). 1 μL of 1 mM estradiol (final concentration 10 μM) was used as complete displacement (minimum polarization value). The tubes were incubated in the dark at room temperature for 2 hours and were mixed by shaking on a plate shaker. The polarization instrument contained 485 nM excitation and 530 nM emission interference filters.

Cell Proliferation Assays

All assays were performed in triplicate for the determination of mean values reported. Compounds were assayed as the free bases isolated from reaction. The human breast tumour cell line MCF-7 was cultured in Eagles Minimum Essential (MEM) medium in a 95% O_2/5% CO_2 atmosphere supplemented with 10% foetal bovine serum, 2 mM L-glutamine and 100 μg/mL penicillin/streptomycin The medium was further supplemented with 1% non-essential amino acids. Cells were trypsinised and seeded at a density of 2.5 x 10^4 cells/mL into a 96-well plate and incubated for 24 h. After this time they were treated with 2 μl volumes of test compound which had been pre-prepared as stock solutions in ethanol to furnish the final concentration range of study, 1nM-100 μM, and re-incubated for a further 72 h. Control wells contained the equivalent volume of the vehicle ethanol (1% v/v). The culture medium was then removed and the cells washed with 100 μL phosphate buffer saline (PBS) and 50 μL of 1 mg/mL MTT solution was added. Cells were incubated for 2 h in darkness at 37°C. At this point solubilisation was begun through the addition of 200 μL DMSO and the cells maintained at room temperature in darkness for 20 min to ensure thorough

colour diffusion before reading the absorbance at 595 nm. The absorbance value of control cells (vehicle treated) was set to 100 % cell viability and from this graphs of absorbance versus cell density per well were prepared to assess cell viability and from these, graphs of percentage cell viability versus concentration of subject compound were drawn.

Lactate Dehydrogenase (LDH) Assay

Cytotoxicity was determined using the Cyto-Tox 96 non-radioactive cytotoxicity assay by Promega [37]. The assay quantitatively measures lactate dehydrogenase (LDH) a stable cytosolic enzyme that is released upon cell lysis. Released LDH in culture supernatant is measured in a 30 minute coupled enzymatic assay, which results in the conversion of a tetrazolium salt (INT) into a red formazan product. MCF-7 and MDA-MB-231 cells were seeded in 96-well plates, incubated for 24 hours and then treated with compounds as above. After 72 hours 20 µl of lysis solution (10X) was added to the 'blank' wells, they were then left for 1 hour to ensure 100 % death, 50 µL was removed from each well and transferred into a new 96-well plate for use in the LDH assay. 50 µL of substrate mix from the LDH assay kit was added and the plate was placed in the dark at room temperature for 30 minutes. After this period, 50 µL of stop solution was added to each well before reading the absorbance at a wavelength of 490 nm using a Dynatech MR5000 plate reader. Percentage death was calculated at 10 µM.

CONFLICT OF INTEREST

Declared none.

ACKNOWLEDGEMENTS

This study was supported by the Irish Research Council for Science, Engineering and Technology (IRCSET). Nuclear magnetic spectroscopy was carried out by Dr. Manuel Ruethers and Dr. John O'Brien at the Department of Chemistry, Trinity College Dublin. High-resolution mass spectroscopy was carried out by Dr. Martin Feeney at the Department of Chemistry, Trinity College Dublin.

REFERENCES

[1] Gronemeyer, H.; Gustafsson, J. A.; Laudet, V. Principles for modulation of the nuclear receptor superfamily. *Nat. Rev. Drug Discov.*, **2004**, *3*, 950-964.

[2] Pasqualini, J. R.; Chetrite, G. S. Recent insight on the control of enzymes involved in estrogen formation and transformation in human breast cancer. *J. Steroid Biochem. Mol. Biol.*, **2005**, *93*, 221-236.

[3] Ascenzi, P.; Bocedi, A.; Marino, M. Structure-function relationship of estrogen receptor alpha and beta: impact on human health. *Mol. Aspects Med.*, **2006**, *27*, 299-402.

[4] Brzozowski, A. M.; Pike, A. C.; Dauter, Z.; Hubbard, R. E.; Bonn, T.; Engstrom, O.; Ohman, L.; Greene, G. L.; Gustafsson, J. A.; Carlquist, M.; Molecular basis of agonism and antagonism in the oestrogen receptor. *Nature*, **1997**, *389*, 753-758.

[5] Pike, A. C. W. Lessons learnt from structural studies of the oestrogen receptor. *Best Pract. Res. Cl. En.*, **2006**, *20*, 1-14.

[6] Keely, N. O.; Meegan, M. J. Targeting tumors using estrogen receptor ligand conjugates. *Curr. Cancer Drug Targets*, **2009**, *9*, 370-380.

[7] Morphy, R.; Rankovic, Z. Designed multiple ligands. An emerging drug discovery paradigm. *J. Med. Chem.*, **2005**, *48*, 6523-6543.

[8] Krohn, K.; Kulikowski, K.; Leclercq, G. Diethylstilbestrol-linked cytotoxic agents: synthesis and binding affinity for estrogen receptors. *J. Med. Chem.*, **1989**, *32*, 1532-1538.

[9] Kohle, H.; Krohn, K.; Leclercq, G. Hexestrol-linked cytotoxic agents: synthesis and binding affinity for estrogen receptors. *J. Med Chem.*, **1989**, *32*, 1538-1547.

[10] Sharma, U.; Marquis, J. C; Dinaut, A. N; Hillier, S. M.; Fedeles, B.; Rye, P. T.; Essigmann, J. M.; Croy, R. G. Design, synthesis, and evaluation of estradiol-linked genotoxicants as anti-cancer agents. *Bioorg. Med. Chem. Lett.*, **2004**, *14*, 3829-3833.

[11] Kuduk, S. D.; Zheng, F. F.; Sepp-Lorenzino, L.; Rosen, N.; Danishefsky, S. J. Synthesis and evaluation of geldanamycin-estradiol hybrids. *Bioorg. Med. Chem. Lett.*, **1999**, *9*, 1233-1238.

[12] Devraj, R.; Barrett, J. F.; Fernandez, J. A.; Katzenellenbogen, J. A.; Cushman, M. Design, synthesis, and biological evaluation of ellipticine-estradiol conjugates. *J. Med. Chem.*, **1996**, *39*, 3367-3374.

[13] Ishiki, N.; Onishi, H.; Machida, Y. Evaluation of antitumor and toxic side effects of mitomycin C-estradiol conjugates. *Int. J. Pharm.*, **2004**, *279*, 81-93.

[14] Kasiotis, K. M.; Magiatis, P.; Pratsinis, H.; Skaltsounis, A.; Abadji, V.; Charalambous, A.; Moutsatsou, P.; Haroutounian, S. A. Synthesis and biological evaluation of novel daunorubicin-estrogen conjugates. *Steroids*, **2001**, *66*, 785-791.

[15] Fenick, D. J.; Taatjes, D. J.; Koch, T. H. Doxoform and Daunoform: anthracycline-formaldehyde conjugates toxic to resistant tumor cells. *J. Med. Chem.*, **1997**, *40*, 2452-2461.

[16] Ali, H.; Ahmed, N.; Tessier, G.; van Lier, J. E. Synthesis and biological activities of nucleoside-estradiol conjugates. *Bioorg. Med. Chem. Lett.*, **2006**, *16*, 317-319.

[17] Burke, P. J.; Koch, T. H. Design, synthesis, and biological evaluation of doxorubicin-formaldehyde conjugates targeted to breast cancer cells. *J. Med. Chem.*, **2004**, *47*, 1193-1206.

[18] Burke, P. J.; Kalet, B. T; Koch, T. H. Antiestrogen binding site and estrogen receptor mediate uptake and distribution of 4-hydroxytamoxifen-targeted doxorubicin-formaldehyde conjugate in breast cancer cells. *J. Med. Chem.*, **2004**, *47*, 6509-6518.

[19] Descoteaux, C.; Provencher-Mandeville, J.; Mathieu, I.; Perron, V.; Mandal, S. K.; Asselin, E.; Berube, G. Synthesis of 17beta-estradiol platinum(II) complexes: biological evaluation on breast cancer cell line. *Bioorg. Med. Chem. Lett.*, **2003**, *13*, 3927-3931.

[20] Perron, V.; Rabouin, D.; Asselin, E.; Parent, S.; Gaudreault, R. C.; Berube, G. Synthesis of 17beta-estradiol-linked platinum(II) complexes and their cytocidal activity on estrogen-dependent and -independent breast tumor cells. *Bioorg. Chem.*, **2005**, *33*, 1-15.

[21] Lim, Y. C.; Desta, Z.; Flockhart, D. A.; Skaar, T. C. Endoxifen (4-hydroxy-N-desmethyl-tamoxifen) has anti-estrogenic effects in breast cancer cells with potency similar to 4-hydroxy-tamoxifen. *Cancer Chemother. Pharmacol.*, **2005**, *55*, 471-478.

[22] Mazhar, D.; Ang, R.; Waxman, J. COX inhibitors and breast cancer. *Br. J. Cancer*, **2006**, *94*, 346-350.

[23] Kapitanovic, S.; Cacev, T.; Antica, M.; Kralj, M.; Cavric, G.; Pavelic, K.; Spaventi, R. Effect of indomethacin on E-cadherin and beta-catenin expression in HT-29 colon cancer cells. *Exp. Mol. Pathol.*, **2006**, *80*, 91-96.

[24] Planchon, P.; Veber, N.; Magnien, V.; Prevost, G.; Starzec, A. B.; Israel, L. Evidence for separate mechanisms of antiproliferative action of indomethacin and prostaglandin on MCF-7 breast cancer cells. *Life Sci.*, **1995**, *57*, 1233-1240.

[25] Duffy, C. P.; Elliott, C. J.; O'Connor, R. A.; Heenan, M. M.; Coyle, S.; Cleary, I. M.; Kavanagh, K.; Verhaegen, S.; O'Loughlin, C. M.; NicAmhlaoibh, R.; Clynes, M. Enhancement of chemotherapeutic drug toxicity to human tumour cells *in vitro* by a subset of non-steroidal anti-inflammatory drugs (NSAIDs). *Eur. J. Cancer*, **1998**, *34*, 1250-1259.

[26] Willson, T. M.; Henke, B. R.; Momtahen, T. M.; Charifson, P. S.; Batchelor, K. W.; Lubahn, D. B.; Moore, L. B.; Oliver, B. B.; Sauls, H. R.; Triantafillou, J. A.; Wolfe, S. G.; Baer, P. G. 3-[4-(1,2-Diphenylbut-1-enyl)phenyl]acrylic acid: a non-steroidal estrogen with functional selectivity for bone over uterus in rats. *J. Med. Chem.*, **1994**, *37*, 1550-1552.

[27] Faye, J. C.; Jozan, S.; Redeuilh, G.; Baulieu, E. E.; Bayard, F. Physicochemical and genetic evidence for specific antiestrogen binding sites. *Proc. Natl. Acad. Sci. U. S. A.*, **1983**, *80*, 3158-3162.

[28] Wang, Y.; Chirgadze, N. Y.; Briggs, S. L.; Khan, S.; Jensen, E. V.; Burris, T. P. A second binding site for hydroxytamoxifen within the coactivator-binding groove of estrogen receptor beta. *Proc. Natl. Acad. Sci. U. S. A.,* **2006**, *103*, 9908-9911.

[29] Bergmann, K. E.; Wooge, C. H.; Carlson, K. E.; Katzenellenbogen, B. S.; Katzenellenbogen, J. A. Bivalent ligands as probes of estrogen receptor action. *J. Steroid Biochem. Mol. Biol.*, **1994**, *49,* 139-152.

[30] Ohsumi, K.; Nakagawa, R.; Fukuda, Y.; Hatanaka, T.; Morinaga, Y.; Nihei, Y.; Ohishi, K.; Suga, Y.; Akiyama, Y.; Tsuji, T. Novel combretastatin analogues effective against murine solid tumors: design and structure-activity relationships. *J. Med. Chem.*, **1998**, *41*, 3022-3032.

[31] Bayer, H.; Batzl, C.; Hartmann, R. W.; Mannschreck, A. New aromatase inhibitors. Synthesis and biological activity of pyridyl-substituted tetralone derivatives. *J. Med. Chem.,* **1991**, *34*, 2685-2691.

[32] Katzenellenbogen, J. A.; Carlson, K. E.; Katzenellenbogen, B. S. Facile geometric isomerization of phenolic non-steroidal estrogens and antiestrogens: limitations to the interpretation of experiments characterizing the activity of individual isomers. *J. Steroid Biochem.*, **1985**, *22*, 589-596.

[33] Maximov, P. Y.; Myers, C. B.; Curpan, R. F.; Lewis-Wambi, J. S.; Jordan, V. C. Structure-function relationships of estrogenic triphenylethylenes related to endoxifen and 4-hydroxytamoxifen. *J. Med. Chem.*, **2010**, *53*, 3273-3283.

[34] Eaddy, J. F.; Heyer, D.; Katamreddy, S. R.; Martin, M. T.; McClure, M. S.; Randhawa, A. S.; Samano, V.; Ray, J. A. Preparation of acyloxydiphenylbutenylcinnamates as estrogen receptor modulator prodrugs. PCT Int. Appl. **2005**, WO 2005033056, A2 20050414 2005.

[35] Bidlack, J. M.; Lockshin, R. A. Evolution of LDH isozymes during programmed cell death. *Comp. Biochem. Physiol. B,* **1976**, *55*, 161-166.

[36] Reddel, R. R.; Murphy, L. C.; Hall, R. E.; Sutherland, R. L. Differential sensitivity of human breast cancer cell lines to the growth-inhibitory effects of tamoxifen. *Cancer Res.,* **1985**, *45*, 1525-1531.

[37] Allen, M. J.; Rushton, N. Use of the CytoTox 96™ Assay in Routine Biocompatibility Testing *in vitro*. *Promega Notes,* **1994**, *45,* 7-10.

The Molecular Pharmacology of SERMs

Donald P. McDonnell

Estrogen-containing medicines have been used successfully for the past 50 years for the treatment of conditions associated with menopause. Although initially considered a reproductive hormone, millions of years of clinical exposure to estrogen(s) have indicated that its influence extends to a variety of target tissues not generally considered to be involved in reproduction. Specifically, estrogen has positive actions in the skeleton, the cardiovascular system and possibly the central nervous system, activities that combine to have a positive impact on mortality and morbidity. However, despite the medical benefits afforded by estrogen replacement therapy, the number of women who initiate or remain on therapy for longer than one year is relatively small. This is due in part to the fear that estrogens increase the risk for breast cancer. Consequently, it was realized several years ago that novel estrogen receptor modulators were needed, which would retain the beneficial effects of estrogens in most target organs but be inactive in the breast. Although the perfect tissue-selective estrogen remains to be identified, progress in this direction has been made. In the past year, for example, we have seen selective estrogen receptor modulators (SERMs) enter into the clinic for the prevention of osteoporosis. Compounds of this class, which function as estrogens in the skeletal system but oppose estrogen action in the breast, are the first step in developing the perfect hormone replacement therapy. This review summarizes the complex pharmacology of the SERMs and illustrates how they differ mechanistically from estradiol, the physiological ligand of the estrogen receptor.

Estrogen is a key regulator of the cellular processes involved in the development and maintenance of reproductive function[1]. However, as early as the 1940s, when estrogen-containing medicines were first approved for the treatment of the vasomotor symptoms associated with menopause, it was clear that this hormone had activities in target organs that were not involved in reproduction. This has been confirmed by over 50 years of clinical exposure to estrogen replacement therapy (ERT), where the influence of this class of hormones has been shown to extend to several functionally unrelated target organs. For example, estrogens can inhibit bone resorption and, as a result, they can be used for the treatment and prevention of osteoporosis[2,3]. In addition, many different types of studies have indicated that estrogens have beneficial activities in the cardiovascular system and might decrease the incidence of coronary heart disease by as much as 50% (Refs 4,5). ERT may also have beneficial activities in the central nervous system, as several studies have linked it to improvements in cognitive function and in delaying the onset of Alzheimer's disease[6,7]. Although the positive effects of estrogens on the cardiovascular and central nervous systems remain to be confirmed in randomized, blinded, placebo-controlled clinical trials, it is likely that when studies of this nature are completed, they will reinforce the importance of estrogen as a regulator of cellular processes unrelated to reproduction. It is clear that we are far from understanding the full spectrum of estrogen's actions in the body. However, there is overwhelming evidence that ERT has a positive effect on mortality and morbidity in postmenopausal women[8,9]. It has been predicted that by the year 2000 over 30% of a woman's lifespan will be spent under conditions of estrogen deprivation and, consequently, that the number of patients seeking ERT will increase[9]. Thus, within the next decade, ERT might emerge as one of the most important medical interventions in terms of both health benefits and economics.

D.P. McDonnell is at the Department of Pharmacology and Cancer Biology, Duke University Medical Center, Durham, NC 27710, USA.

• Selective Estrogen Receptor Modulators: an Unmet Medical Need

Given the overall health benefits of estrogens, it is surprising, that relatively few postmenopausal women actually consider ERT and, of those who initiate therapy, a significant number discontinue treatment within one year. Although a complex issue, it is clear that one of the overriding factors that influences compliance with therapy is the potential link between ERT and breast cancer. Indeed, several large studies have shown that the incidence of breast cancer is raised in patients taking ERT (Ref. 10). Although it is difficult to achieve a consensus on the magnitude of this increased risk, most studies put the relative risk somewhere between 1.1 and 1.3 (Ref. 10). This issue is further complicated by studies indicating that women who are diagnosed with breast cancer while taking ERT have a better survival rate than non-users[11]. Clinically, the distinction between incidence and mortality is an important one; however, among healthy women considering their options for hormone replacement therapy, the distinction is blurred. Therefore, although the need for ERT will increase, the concerns about breast cancer will have to be addressed to

 1043-2760/99/$ – see front matter © 1999 Elsevier Science Ltd. All rights reserved. PII: S1043-2760(99)00177-0

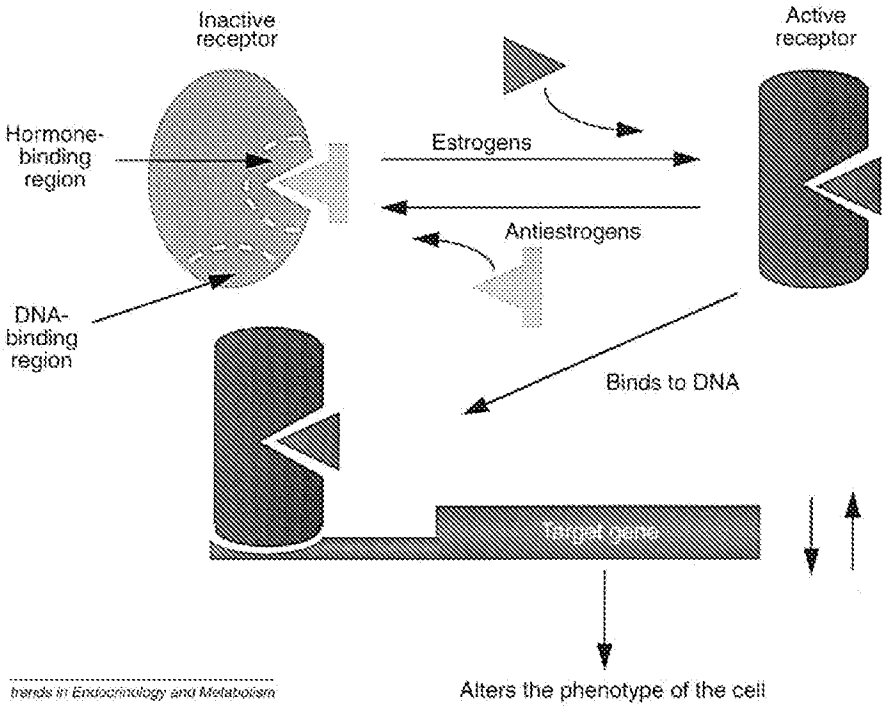


Figure 1. Early models of estrogen receptor (ER) action do not explain the complex pharmacology of known ER ligands. The classic models of estrogen action suggested that, in the absence of ligand, the ER existed in the nuclei of target cells in an inactive form. Upon binding an agonist, the ER underwent an activating transformation event, which facilitated the interaction of the receptor with specific DNA response elements within target gene promoters. Within the confines of this model it was hard to explain the molecular pharmacology of tamoxifen and other ligands whose agonist/antagonist activity differs from cell to cell.

maximize the number of women who initiate and remain on therapy. Wider acceptance of ERT will be facilitated by studies that provide a clearer understanding of the estrogen–breast cancer link and the application of this knowledge to the improvement of current therapies. Notwithstanding these efforts, there is clearly an unmet medical need for novel therapies that retain the beneficial effects of ERT but which are not associated with an increased risk of breast cancer. It is this need that has provided the impetus to the pharmaceutical industry to search for new estrogens that might modulate estrogen receptors (ERs) in a tissue-selective manner. This endeavor, although still in its infancy, has already seen the emergence of several new selective ER modulators (SERMs), and the first approval of a SERM for the prevention of osteoporosis[12]. This is the first fundamentally different hormone replacement therapy drug in over 50 years and heralds a new era in the treatment and management of conditions associated with menopause.

• Tamoxifen is a SERM

Since the 1970s, there has been interest in developing new classes of ER modulators that exhibit their biological activity in a tissue-selective manner. However, within the confines of the traditional models of ER action, where the only function of estrogen was to switch the inactive receptor to a transcriptionally active form, it was difficult to understand how tissue-selective ER modulators could be developed (Fig. 1)[13]. These models held that, when corrected for affinity, all ER agonists were qualitatively similar. Antagonists, on the other hand, were thought to function solely in a competitive manner, binding to the inactive receptor and blocking agonist access. Consequently, it was assumed that all antagonists were functionally identical. This implied that selectivity at the receptor level would be difficult to achieve and that reliance would have to be placed on empirical differences in the pharmacokinetic properties of a ligand to achieve the desired pharmaceutical profile. Fortunately, data from clinical studies designed to evaluate the activity of tamoxifen in bone indicated that the simple models of ER action were oversimplified and that mechanism-based approaches could be used to develop novel antiestrogens[14].

The antiestrogen tamoxifen is used in the clinic for the treatment of metastatic breast cancer and as adjuvant chemotherapy[15]. The rationale for its use is based on the fact that estrogen is a mitogen in ER-containing breast cancer cells and this activity can be inhibited by an ER antagonist[16–18]. However, because estrogen is also required for the preservation of skeletal integrity in postmenopausal women, it was believed that the administration of tamoxifen in breast cancer patients would lead to deterioration in bone quality. A fundamental change in the way we think about the pharmacology of estrogens and antiestrogens was prompted by the results of a 24-month, placebo-controlled study in breast cancer patients, which indicated that tamoxifen could mimic the actions of estrogen in the lumbar spine, leading to an increase in bone mineral density[14]. This study was not the first to indicate that tamoxifen could function as a tissue-selective estrogen agonist/antagonist. However, most of the previous studies had been performed in rodents and the importance of these findings to humans was unclear[19,20]. Cumulatively, the human and rodent studies suggested that it would be possible to develop tissue-selective estrogens. Furthermore, these findings necessitated a re-evaluation of the classic models of estrogen action and a re-examination of the pharmacology of ER. Interestingly, tamoxifen was the first compound identified with noticeable SERM activity and, were it not for its unfavorable uterotrophic activity, it would probably be a viable pharmaceutical for the treatment and prevention of osteoporosis[21–23].

The finding that tamoxifen is a SERM that functions as an agonist in

bone and in the cardiovascular system, while manifesting antagonist activity in the breast, was an important milestone in our understanding of ER pharmacology[14,24]. First, it suggested that the pharmacology of ER antagonists was more complex than predicted from the early models of ER action. Second, it provided a potential explanation for the observation that some breast tumors that initially recognize tamoxifen as an antagonist switch and respond to this drug as if it were an agonist[25]. Specifically, if there were cells in the breast that recognize tamoxifen as an agonist (which there are in bone), then it was possible that the selective pressure of tamoxifen administration could lead to the selection of a subpopulation of cells that are capable of recognizing this drug as an ER agonist. This model proposes that some breast tumor cells can 'learn' to see tamoxifen as an agonist. There is a substantial amount of data to support this hypothesis. In athymic nude mice, for example, it has been shown that the growth of estrogen-dependent MCF-7 cell xenografts can be inhibited by tamoxifen. Over time however, these tumors escape tamoxifen inhibition and actually become tamoxifen dependent[25]. This observation, implying that tamoxifen can function as a growth stimulator in some circumstances, is supported by the finding that some patients whose disease progresses while on tamoxifen therapy actually demonstrate a withdrawal response when administration of the drug is discontinued[26]. In addition, it has been suggested recently by data emerging from the NSABBP-B14 trial that patients who receive adjuvant tamoxifen therapy for breast cancer for five years have a better rate of survival than those who remain on therapy for ten years[27]. These observations suggest that there might be a link between tamoxifen resistance and the ability of this compound to manifest agonist activity in some cell contexts.

The demonstration that the agonist and antagonist activities of tamoxifen could differ in different cell contexts predicted that additional SERMs with unique tissue selectivity could be developed. This prediction was realized recently when the SERM raloxifene was approved for the prevention of osteoporosis. Raloxifene was developed originally as a treatment for tamoxifen-refractory breast cancer[28]. Although it was not successful in this role, it was found to have similar properties to tamoxifen in bone; however, it lacks significant uterotrophic activity[29–32]. Neither tamoxifen nor raloxifene were designed specifically as SERMs, yet the insights gleaned from studies of their mechanism of action have facilitated the development of additional SERMs, which we hope will exhibit improved therapeutic profiles. Within the next few years, the SERMs idoxifene, droloxifene, CP336-156, GW5638 and LY353381 will make their way through the clinical trials process, and clinicians will be faced with the task of comparing these drugs at a mechanistic and functional level (Fig. 2)[33–36].

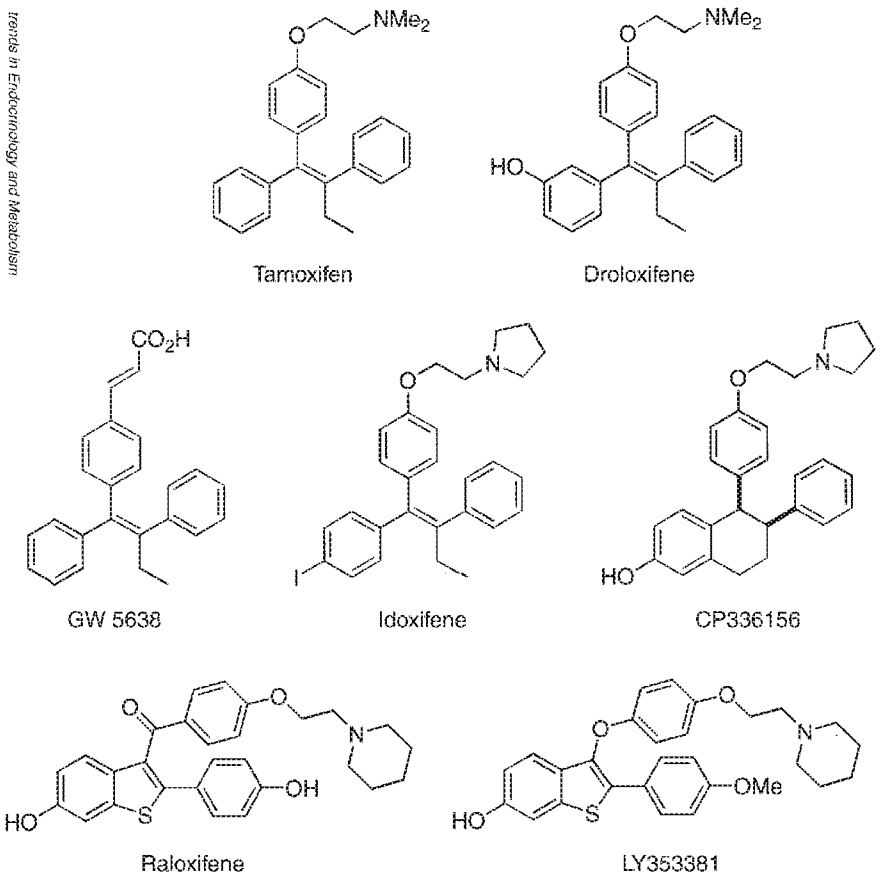


Figure 2. Comparison of the structures of commonly studied estrogen receptor agonists and antagonists.

• Tissue-selective ER Modulators: a Concept Borrowed from Nature

The identification of synthetic ER ligands, like tamoxifen and raloxifene, which exhibit their activity in a selective manner, has raised the issue of whether these drugs are mimicking a physiological process or whether their activity reflects a pharmacological phenomenon. With respect to the ER, this question remains to be answered; however, in the case of other nuclear hormone receptors, there is a large amount of evidence to suggest that a single receptor might respond to more than one different physiologically occurring ligand[37,38]. The classic example is the androgen receptor (AR), which has at least two naturally occurring ligands: testosterone and dihydrotestosterone. Although both of these hormones bind to AR, testosterone functions primarily as a regulator of processes involved

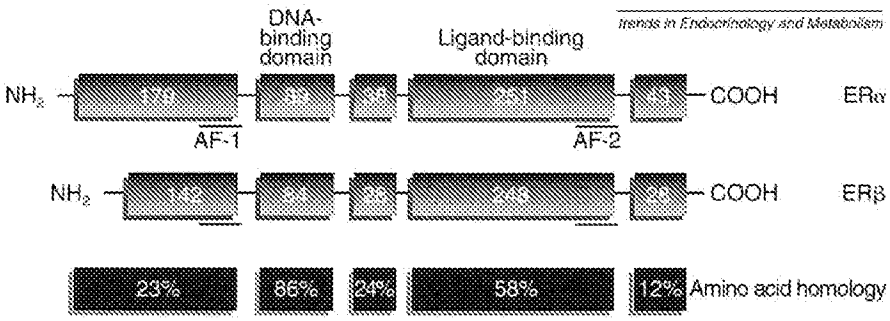


Figure 3. Estrogens and antiestrogens manifest their biological activity through two distinct receptors: estrogen receptor α (ERα) and ERβ. Numbers in boxes indicate number of amino acids or percentage homology between domains (as indicated).

in defining primary sexual function, whereas dihydrotestosterone is involved in determining secondary sexual characteristics[39]. The molecular basis for this differential activity has yet to be determined; however, it provides a conceptual framework upon which to base a hypothesis that there are a series of steroidal estrogens that interact with the ER and regulate different processes within target cells.

There is strong evidence supporting this hypothesis. For example, in some early animal studies that compared estrone with estradiol it was noted that, when corrected for affinity, these compounds had distinct actions in the uterus. Moreover, estrone was found to be an impeded estrogen that could oppose some of the biological responses to estradiol in the uterus[40]. More compelling, however, are the clinical studies with the estrogen Δ8,9 dehydroestrone sulfate (Δ8,9)[41]. This estrogen is one of the active ingredients in the conjugated estrogen preparation Premarin®. In a clinical study that compared estrone sulfate with Δ8,9 in postmenopausal women, it was found that both compounds effectively treated moderate to severe hot flushes and had favorable effects on markers of bone modeling[41]. However, in these same patients, estrone sulfate alone could exert an estrogenic activity in the cardiovascular system. The ability of Δ8,9 to manifest tissue-selective estrogenic activity was also seen in rodent studies, where it was shown that with respect to progesterone receptor regulation, a marker of estrogen action in the brain, Δ8,9 was an effective estrogen (A. Negro-Vilar, pers. commun.). On other endpoints, however, such as the induction of prolactin or stimulation of uterine hypertrophy, this estrogen was not effective. These data suggest that naturally occurring estrogens can act as *bona fide* SERMs, lending support to the hypothesis that nature has developed systems to enable a single receptor to manifest different biological responses upon binding different estrogens.

• Receptor Subtypes as Determinants of ER Pharmacology

There has been, and continues to be, a high level of interest in defining the molecular basis underlying tissue selectivity of the known ER ligands, particularly because of the potential pharmaceutical implications. Until recently, it was thought that all the biological actions of estrogens and antiestrogens were manifested through a single ER, which was biochemically identical in all cells[1]. However, the discovery in 1996 of a second ER significantly increased the biological complexity of estrogen[42]. Unexpectedly, Kuiper and co-workers identified a novel receptor cDNA in the prostate of male rats, which encoded a protein that bound 17 β-estradiol with an affinity equivalent to that of the previously identified 'breast/uterus' estrogen receptors[42]. The human homolog of this novel ER, now called ERβ, has been cloned[43]. With respect to ER pharmacology, the identification of this novel estrogen receptor is probably one of the most important discoveries in the past 20 years (Fig. 3).

The emergence of a second ER immediately suggested that the differential affinity of ligands for each of these receptors, coupled with tissue-specific differences in their synthesis, could explain some aspects of SERM selectivity. Indeed, the results of a preliminary analysis of the *in vitro* pharmacology of ERα and ERβ support this idea[44]. Specifically, it has been noted that, whereas 17 β-estradiol has equivalent affinities for both receptors, there are significant differences with respect to estrone and estriol binding. However, SERM action is likely to involve more than receptor selectivity, because it has been noted that most of the existing SERMs do not distinguish between ERα and ERβ (Ref. 44). In addition, it has been shown that the biological activity of some SERMs can differ among tissues or cells that synthesize the same ER subtype[30,45]. For example, using ERα-responsive transcription systems reconstituted in a variety of cells, we have shown that tamoxifen can function in some backgrounds as an antagonist, whereas in others it can manifest partial agonist activity[45,46]. Furthermore, in those cells where tamoxifen manifests partial agonist activity, raloxifene, GW5638, droloxifene and idoxifene function as pure ERα antagonists[35,45–48]. This suggests that there are differences in the mechanism of action of different SERMs. When this analysis was extended to ERβ, it was found that all of the SERMs examined function as pure antagonists (J. Hall and D.P. McDonnell, unpublished).

As yet, no simple explanation has emerged to explain how SERMs can manifest cell-selective agonist activity. It is possible that the cellular backgrounds in which the *in vitro* experiments were performed do not reflect the target cells *in vivo*, and that factors within these cells are important for SERM agonist activity. However, it is clear that differential activation of ERα or ERβ is not sufficient to explain the tissue-selective actions of the currently available SERMs.

• Definition of the Mechanism of Action of Tamoxifen

It is well established that the primary activity of ER is to function as a ligand-dependent transcription factor[49]. However, there is still considerable debate about how this activity is accomplished and how it is influenced by estrogens and antiestrogens. The prevailing model, to which we subscribe, is that the ER regulates target gene promoters by binding directly to specific estrogen-response elements (EREs) located within the regulatory regions of target genes and that the impact of the receptor on transcription is determined both by the cellular and promoter environment and the nature of the bound ligand[45,46,50]. In support of this model, we have shown that tamoxifen functions as a partial ER agonist in cultured hepatocellular carcinoma (HepG2) cells, and that in this system a direct interaction of the receptor with an ERE is required for this activity on all the promoters tested so far[45,46,50]. This model predicts that events occurring downstream of ER–DNA binding are the primary determinants of the estrogenic or antiestrogenic activity of ligands. This conclusion is complicated slightly by the observation that the sequence of the DNA-response element also influences the pharmacology of ER ligands[51]. Therefore, it is likely that the cellular factors that determine the agonist/antagonist activity of a given ligand recognize a complex of ligand, ER and DNA-response element[49]. This finding suggests that, as the pharmaceutical exploitation of ER continues, we may see the emergence of gene-specific or -selective compounds.

The observation that ligands such as tamoxifen could function as cell-selective agonists, or SERMs, was at variance with the uncomplicated pharmacology implied by the classic models of ER action. Specifically, these models suggest that, in the absence of hormone, ER resides in target cell nuclei in an inactive conformation and that the role of agonists, such as estradiol, was to serve merely as a switch, converting the ER into an active conformation, and that antagonists functioned by blocking agonist access. However, work from our group and others has indicated that the ligand plays a much more complex role in regulating ER function[45,46]. Specifically, it has been found that different compounds induce different alterations within the ER structure[45]. This was shown initially by studies using differential sensitivity to proteases to assess ligand-induced alterations within the ER (Refs 45,52). Unexpectedly, these studies revealed that antagonists such as tamoxifen do not function solely by blocking activation of the ER, but that they induce a conformational change within the receptor, which distinguishes it from both apo (receptor without ligand) and ligand-bound receptor.

The crystal structure of ERα in the presence of the agonist estradiol, or with the SERM raloxifene, has now been resolved, confirming the central role of the ligand in modulating ER conformation[53,54]. The crystal structure also provided insights into the mechanism by which different SERMs could interact with the ligand-binding pocket of the ER, and how this could lead to alterations in overall ER structure. Several important conclusions can be drawn from this work. First, the ER is not a rigid molecule existing in either an active or inactive state, but rather its conformation is determined by the nature of the bound ligand. Although it remains to be proven whether these conformational states exist *in vivo*, the data obtained *in vitro* provide a molecular explanation for the differential biological activity of different ER ligands. In addition, it suggests that the ability of tamoxifen to function as an antiestrogen in some settings is not the result solely of its ability to function passively as a competitive antagonist, freezing the ER in an apo-unactivated conformation. Rather, it indicates that tamoxifen functions as an active antagonist, inducing a unique structural alteration within the ER, and permitting it to interfere with the ER–estradiol complex at multiple steps in the signal transduction pathway. Another important finding that has emerged is that different SERMs have different effects on ER structure[55]. Thus, at least with respect to their molecular mechanism of action, SERMs can be classified according to their effect on ER structure. The mechanism by which these conformational changes are distinguished by target cells is currently under investigation.

• Receptor Conformation Affects the Way the ER is Presented to the Transcription Apparatus

Considerable progress has been made recently in defining how the cell distinguishes between different ER ligand structures. Many of these insights have come from reverse genetic studies, where the effects of specific ER mutations on ligand responsiveness could be assessed in transfected mammalian cells. This approach permitted the definition of the domains within the ER required for DNA and ligand binding and also led to the discovery of two 'activation' domains within the receptor, which facilitated the interaction of the ER with the transcription apparatus[46,47,56–58]. These activation domains – activation domain 1 (AF-1) contained within the N-terminus, and AF-2 contained within the ligand-binding domains – were shown to be required for maximal ER transcriptional activity in most cell contexts[46,59]. However, in some contexts, ER–AF-1 or ER–AF-2 activity alone was sufficient for transcriptional activity[46]. The finding that these activation domains were not functionally equivalent and that their activity was influenced by cell and promoter context suggested that compounds which differentially affected ER structure could influence the presentation of these domains to the transcription apparatus (Fig. 4). It was thought that because tamoxifen could function as a cell-selective ER mixed agonist, and because the activation domains of ER were manifest in a cell-selective manner, the two might be linked[46]. It has been found that, in all contexts where AF-2 is required for ER transcriptional activity, tamoxifen functions as a pure antagonist[45]. Conversely, in contexts where AF-2 is not required, and AF-1 is sufficient for ER transcriptional activity, tamoxifen functions as a partial agonist[45,46]. Thus, tamoxifen, in addition to functioning as

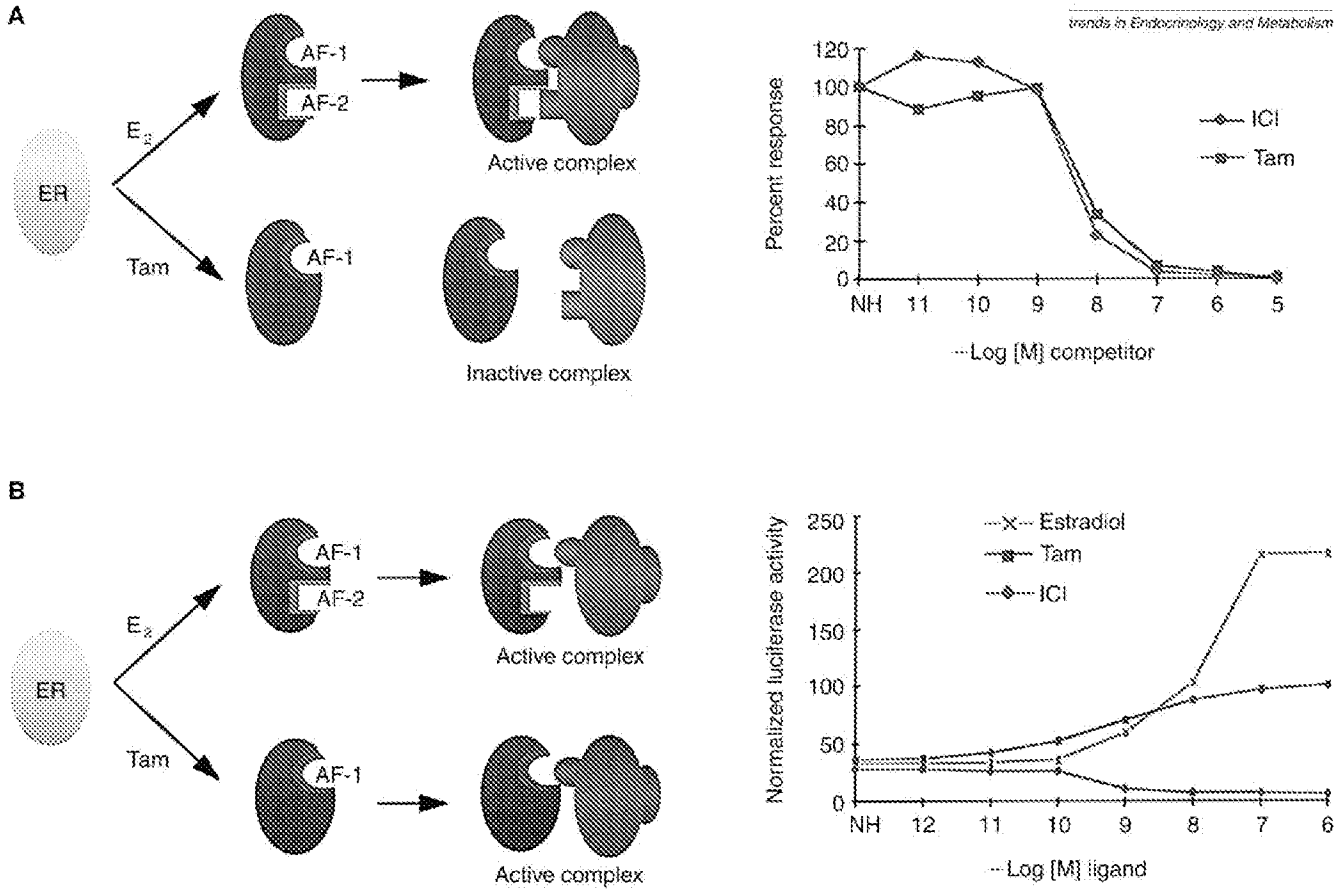


Figure 4. Genetic dissection of the structure of the estrogen receptor (ER) reveals a mechanism to explain the tissue-selective agonist activity of tamoxifen. The ER contains two distinct activation functions (AF-1 and AF-2), whose activities are manifest in a cell-selective manner. (**A**) In some cell contexts, the interaction of both ER–AFs with a cellular target is required for transcriptional activity. In these contexts, estradiol (E_2), but not tamoxifen, functions as an agonist. This can be demonstrated pharmacologically by assaying the ability of the ER to regulate the expression of an estrogen-responsive reporter in HeLa cells, a context where both AF-1 and AF-2 are required. In the experiment shown, ER-dependent transcriptional activity was assessed in the presence of estradiol alone (100% response) or in the presence of 4-OH-tamoxifen (Tam) or the pure antagonist ICI182,780 (ICI). This, together with a large number of similar published experiments, has allowed us to conclude that tamoxifen is an AF-2 antagonist. (**B**) In other cell contexts, ER–AF-1 alone is required for ER transcriptional activity. In HepG2 cells, for example, where AF-2 is not required, estrogen functions as an agonist of ER-mediated transcription. Under the same conditions, however, the pure antiestrogen ICI182,780 displays inverse agonist activity, whereas tamoxifen manifests partial agonist activity. This observation has led to the conclusion that tamoxifen is an AF-1 agonist.

an AF-2 antagonist, is also an AF-1 agonist. Therefore, it appeared that the ability of tamoxifen to manifest AF-1 activity in a cell-specific manner explained its SERM activity. Specifically, it was proposed that, in tissues such as breast, where tamoxifen exhibited pure antagonist activity, AF-2 was required for transcriptional activity. On the other hand, in the uterus, bone and the cardiovascular system, where tamoxifen exhibits estrogenic activity, it was concluded that AF-1 activity was sufficient. This model was supported by the observation that ICI182,780, which does not exhibit AF-1 agonist activity, is not bone-protective[45,60]. However, ICI182,780 is a complex antiestrogen that, in addition to inhibiting AF-1 and AF-2 activity, induces turnover of the receptor[61,62]. It is difficult therefore to relate its biological actions to a specific molecular characteristic.

Cumulatively, these data indicated that AF-1 activity correlated with the partial agonist activity of tamoxifen in bone, the cardiovascular system and the uterus. However, there was no direct evidence that AF-1 activity was required for agonist activities in these organs. An ER ligand, devoid of AF-1 agonist activity, which did not induce ER degradation, was required to test the relationship between AF-1 activity and the tissue-selective actions of SERMs, such as tamoxifen. In 1995, Willson *et al.* published the structures of a series of ER ligands that were chemically related to tamoxifen but that exhibited unique biological activities[63]. In particular, one compound they identified, GW5638, was shown to prevent bone loss in ovariectomized rats but did not display uterotrophic activity[35]. This finding was at odds with the hypothesis that the bone and uterotrophic activities of compounds were linked, and implied that these

compounds function by different mechanisms in bone and uterus. Indeed, we showed that GW5638 could inhibit ER–AF-1 and ER–AF-2 in all contexts examined and could also inhibit the partial agonist activity of tamoxifen[35]. Thus, ER–AF-1 activity, at least as measured in our assays, was not required for bone protection; however, it does seem to be required for uterotrophic activity.

The identification of GW5638, a bone protective ER ligand that lacked AF-1 activity, prompted us to extend our studies to other bone-protective ER modulators. These studies confirmed that AF-1 activity correlated with uterotrophic activity. In addition, however, we found that the SERM raloxifene, which demonstrates estrogenic activity in the skeleton, is not an AF-1 agonist, but functions as a pure antagonist in most circumstances[35]. These data complicate our understanding of the pharmacology of ER antagonists, as they suggest that the mechanisms by which SERMs exhibit their agonist activity in bone and the uterus are not the same. Thus, whereas we believed previously that ER partial agonists were a single mechanistic class, it is now clear that there are at least two different classes.

- **The Role of Coactivators and Corepressors in Determining ER Pharmacology**

The existence of steroid receptor coactivator proteins was postulated several years ago when it was observed that overproduction of the progesterone receptor could inhibit the transcriptional activity of the ER without affecting the basal transcriptional activity of the promoter and without affecting the activity of other unrelated transcription factors[57,64]. This process, called 'squelching', led many groups to consider that the steroid receptors interacted with transcription coactivator proteins, which were present in limiting amounts in target cells. In 1995, Onate *et al.* reported the identification and characterization of the first steroid receptor coactivator protein, SRC-1 (Ref. 65). A large number of potential coactivator proteins have been found since, although not all have been as well validated as SRC-1 (Ref. 66). A comprehensive discussion of their activities is beyond the scope of this review. In short, however, these coactivator proteins bind to agonist-activated ERs and nucleate a large complex of proteins that link the ER to the transcription apparatus. In addition, many of these coactivator proteins possess intrinsic acetylase activity. Consequently, their recruitment to target gene promoters leads to the acetylation of histones and a subsequent decondensation of chromatin in the vicinity of the DNA-bound receptor complex[67]. The biological importance of these proteins was revealed when it was shown that overproduction of coactivators, such as SRC-1, enhanced the transcriptional activity of the ER (Refs 48,65). In addition, the recent demonstration that knockout of the gene encoding SRC-1 in mice leads to a mild form of steroid resistance confirms the role of SRC-1 in steroid hormone signaling[68]. Of equal importance, however, was the observation that overexpression of the gene encoding SRC-1 enhanced the partial agonist activity of tamoxifen in target cells[48]. Therefore, it is possible that the differential activity of tamoxifen in different cells is a reflection of the level of expression of the gene encoding SRC-1 (or another co-factor), and that epigenetic changes which affect the activity or expression level of these cofactors are at the root of ER pharmacology.

The discovery of SRC-1 and other coactivators that positively affect ER transcriptional activity was predicted on the basis of the results of *in vitro* squelching experiments. However, as is the norm in biology, each positive-acting factor or process is opposed by some system that operates in the opposite manner. Thus, it was not surprising that transcriptional corepressors that acted on nuclear receptors were identified[69,70]. To date, there are two nuclear corepressor proteins that have been shown to interact with the ER. These proteins, nuclear receptor corepressor (NCoR) and 'silencing mediator of retinoid and thyroid hormone' (SMRT), were initially identified as proteins that bound to DNA-bound thyroid hormone or retinoid X receptors and enabled these proteins to repress basal transcription in the absence of hormone[69,70]. With respect to the ER, these corepressor proteins are functionally the opposite of coactivators. They bind to the ER either in the absence of hormone or in the presence of antagonists[48]. Like coactivators, the corepressors nucleate a large protein complex; however, the corepressor complex is responsible for deacetylating histones, facilitating chromatin condensation and subsequent inhibition of target gene transcription. The potential importance of the corepressors in ER pharmacology was suggested by the recent studies of Lavinsky *et al.*, who showed that passage of tumors in mice from a state of tamoxifen sensitivity to an insensitive state was accompanied by a decrease in the production of the corepressor NCoR (Ref. 71). A similar process, if it occurs in humans, could explain how cells become resistant to the antiestrogenic actions of tamoxifen.

The identification of steroid receptor coactivators and corepressors and the demonstration that their ability to interact with the ER is influenced by the structure of the receptor–ligand complex has provided a potential mechanism to explain how the same estrogen can have different activities in different cells, and has also provided a potential explanation for the tissue-selective actions of SERMs. Specifically, it has been observed that full agonists appear to facilitate high-affinity interactions of the ER with coactivators, such as SRC-1, glucocorticoid receptor interacting protein 1 (GRIP-1), transcription intermediary factor 2 (TIF-2) or 'amplified in breast cancer 1' (AIB1); whereas pure antagonists promote the interaction of the receptor with the corepressors NCoR and SMRT. Thus, the response of a cell to these classes of ligands will probably depend on the relative levels of different coactivators/corepressors and on the properties of the specific factor with which the ER interacts. A further level of complexity is apparent when the SERMs are considered because these drive the ER into a conformational state different from that induced by pure agonists and

antagonists. Because different SERMs induce different conformational changes within the ER, it is likely that the resulting receptor–ligand complexes do not interact with all coactivators or corepressors in an equivalent manner. Thus, SERM agonist activity will be restricted to cells in which the particular ER–SERM complex can find an appropriate coactivator protein. Therefore, it is likely that it will be possible to develop highly selective SERMs by screening for compounds that modulate a specific ER–coactivator interaction.

- **Alternative Pathways by which the ER can Regulate Target Gene Transcription**

The observation that tamoxifen can manifest partial agonist activity through a functional ERE within some promoters does not exclude the possibility that additional mechanisms might also operate. Indeed, it has been shown recently that the ER can associate with target gene promoters in an indirect manner through protein–protein contacts with transcription factors that are pre-bound to target gene promoters. In one situation, Webb *et al.* showed that ligand-activated ER could interact with and positively regulate the collagenase gene promoter by associating with the activating protein 1 (AP-1) transcription factor complex within target cells[72,73]. In this particular pathway, both ER agonists and SERMs, such as tamoxifen, functioned as transcriptional activators. Interestingly, several groups have shown a correlation between the activity of the AP-1 complex in this system and the ability of tamoxifen to manifest partial agonist activity[72,73]. The ER–AP-1 pathway is particularly active in cell lines derived from the endometrium, where tamoxifen is an agonist, whereas it is less active in cultured breast cancer cells, where tamoxifen has antagonist activity. This suggests that the ability to activate the ER–AP-1 pathway might correlate with the ability of a cell to support tamoxifen partial agonist activity[72,73]. These initial studies were performed in systems where the gene encoding ERα was expressed; however, it has now been shown that ERβ can also participate in this regulatory pathway, although it displays a unique pharmacology[74]. Specifically, when this AP-1-dependent transcription system was reconstituted in cells where the gene encoding ERβ was expressed, it was seen that both tamoxifen and raloxifene functioned as agonists and that their activity was inhibited by estradiol and other ERα agonists. These findings introduce a new complexity into ER action; however, the physiological significance of these novel pathways has yet to be determined.

The ER–AP-1 interaction is the most studied of the indirect transcriptional regulatory pathways involved in ER pharmacology. However, there are other systems where these types of interactions have been shown to be important. For example, it has been shown in rodents that the retinoic acid receptor β (RARβ) promoter is upregulated both by estrogens and antiestrogens[75]. What makes this system so remarkable is that the pure antiestrogen ICI182,780 functions as an agonist on this promoter[75]. Genetic dissection of the RARβ promoter revealed that, in this system, ER exerts its regulatory activities in an indirect manner through a pre-bound transcription factor. The identity of this factor remains to be determined[75]. In a different system, Montano *et al.* showed that antagonist-activated ER stimulated quinone reductase gene transcription through a previously defined electrophile-response element[76]. It has been shown that the ER does not bind directly with this element, leading to the hypothesis that it interacts with a factor that is already occupying this site. The finding that the ER can contact the transcription apparatus in an indirect manner through several distinct types of protein–protein interactions was not anticipated. However, it indicates that there are at least two distinct mechanisms by which the ER can function as a transcriptional activator in target cells.

The ability of the ER to interact with DNA, either directly or indirectly, appears to explain the activity of estrogens and antiestrogens in most systems. There is some evidence, however, that these pharmaceutical agents might have additional activities. As discussed above, it has yet to be determined how SERMs, such as tamoxifen, raloxifene and GW5638, can function as agonists in bone and the cardiovascular system[14,24,29,35]. It appears that any compound that activates the ER, and that has the ability to deliver the ER to DNA, can act as an estrogen in bone and the cardiovascular system, implying that the ER functions similarly in both systems. Several recent studies have provided evidence to support this hypothesis. In bone for example, it has been shown that estrogens and antiestrogens effectively suppress production of interleukin 6 (IL-6), a cytokine required for osteoclastogenesis and osteoblastogenesis[77–79]. In addition, estrogen can inhibit the production of macrophage chemoattractant protein (MCP-1) and consequently may block macrophage infiltration and subsequent atherosclerotic plaque formation in the arterial endothelium. It now appears that the mechanism by which the ER regulates the genes encoding IL-6 and MCP-1 is the same. Upon activation by ligand, the ER physically interacts with the p65 subunit of nuclear factor κB (NF-κB), thus blocking its ability to bind to target sequences located within the regulatory regions of the MCP-1 or IL-6 genes[80]. Thus, the ER is functioning as a transcriptional inhibitor in a way that does not require the receptor to bind DNA. This regulatory paradigm might extend beyond NF-κB, as it has been shown that the ER can inhibit the transcriptional activity of CCAAT/enhancer binding protein β (C/EBPβ) and GATA-1 in a similar way[80,81]. Together, these findings strongly support the physiological relevance of the novel inhibitory activity of ER.

It is clear from the discussion above that the pharmacology of estrogens, SERMs and antiestrogens is complex and that no one model is sufficient to explain the activity of these compounds in all tissues. The fact that the ER can act as a transcriptional activator by binding to target gene promoters or as a transcriptional repressor by mechanisms that do not involve DNA binding suggests that nature has engineered flexibility into ER biology to permit a

single protein to have different functions in different cells.

• An Updated Model of Estrogen Action

The classic models of ER action suggested that the role of agonists was that of a switch, converting the receptor from an inactive to an active state, and that antagonists functioned solely by blocking agonist–receptor interactions. However, the identification of compounds such as tamoxifen, raloxifene and GW5638, which function as cell-selective agonists/antagonists, indicates that ER pharmacology is more complex. Accordingly, the classic models of ER action need to be replaced by new models that reflect the changes in our understanding of ER action (Fig. 5).

In the absence of hormone, the ER resides within the nucleus of target cells in an inactive form associated with a large inhibitory protein complex. Upon binding hormone, the ER undergoes a conformational change, displacing the heat shock protein complex and permitting the receptor to participate in any of a number of pathways within the cells. Each of the three major pathways will be considered separately:

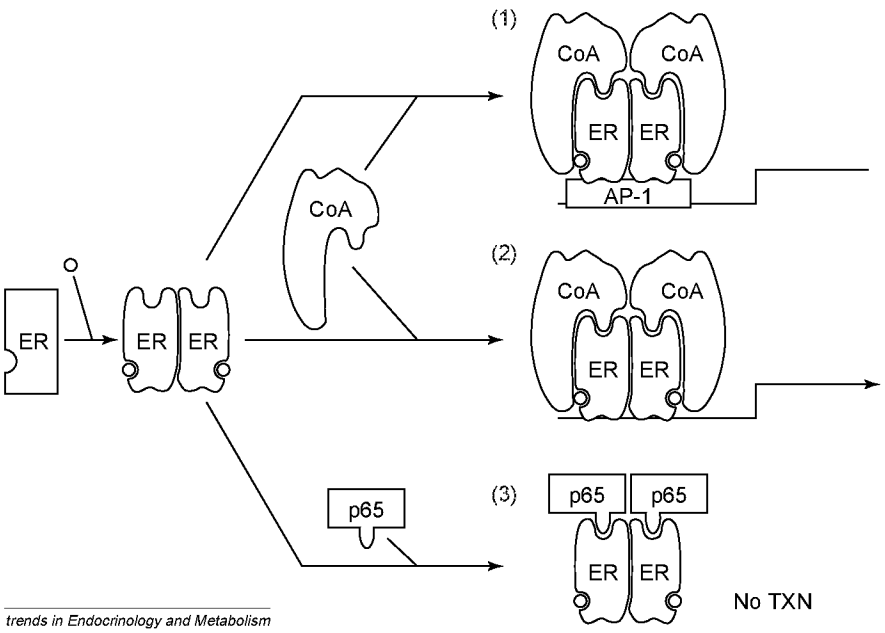


Figure 5. An updated model of ER action. The current models of ER action have evolved considerably from those proposed in the 1970s. After activation and dimerization, the ER can participate in the regulation of target gene transcription in either of three ways: (1) the ligand-activated ER can associate with target gene promoters by binding to transcription factors, such as AP-1, which are sitting on the DNA. The resulting complex can then recruit transcriptional coactivators such as SRC-1. (2) The ER can form a ternary complex with a coactivator protein after its direct interaction with specific regulatory sequences within target gene promoters. (3) The ER can also function as a transcriptional repressor by inhibiting the ability of transcription factors like the p65 subunit of NF-κB from interacting with its cognate targets. Abbreviations: AP-1, activating protein 1; CoA, coactivator; ER, estrogen receptor; NF-κB, nuclear factor κB; SRC-1, steroid receptor coactivator protein 1; TXN, transcription.

Pathways Involving Direct Interaction of the ER with DNA

In this case, the activated receptor can interact as a dimer with specific DNA response elements within target genes. This activity is accomplished by all of the known ER ligands. However, it is now apparent that the conformation of the receptor is influenced by the nature of the bound ligand and that the shape of the ER is a crucial determinant of whether or not it can activate transcription. In the presence of a full agonist, the conformation adopted by the ER facilitates a displacement of the corepressor proteins and a recruitment of coactivator proteins. This permits the assembly of a histone-acetylating complex on the DNA, with a concomitant increase in target gene transcription. In this model, pure antagonists drive the ER into a conformation that favors corepressor interaction, whereas SERMs, such as tamoxifen, function as partial agonists because they can drive the ER into a structure that partially displaces the corepressors and frees part of the ER for interactions with coactivators, such as SRC-1. Based on this model, it is predicted that the efficacy of pure antagonists and pure agonists would not be as sensitive to the cell context as that of SERMs, such as tamoxifen, which permit the ER to interact with both coactivators and corepressors to some degree. It is likely therefore that the agonist/antagonist activities of tamoxifen and other SERMs will be influenced greatly by the levels of specific coactivators within the cell. Superimposed on this already complex model is the fact that there are several different coactivators and corepressors whose level varies from cell to cell. These will probably be shown to possess different affinities for the different liganded states of the ER and thus their relative and absolute levels will influence ER pharmacology. Finally, ER signal transduction, complex as it is, does not exist in a vacuum. It is clear that signaling events initiated at the cell membrane, such as those generating increased levels of cAMP, also impinge on this ER signaling pathway[82,83]. These signaling pathways might function by affecting receptor phosphorylation or they might operate by modifying the interaction of the ER with nuclear receptor coactivators and corepressors.

Pathways in which the ER Interacts in an Indirect Manner with Target Gene Promoters

The ligand-activated receptor associates with target gene promoters by interacting with transcription factors that are on the DNA. In this pathway, the conformation of the receptor affects both its ability to interact with its tethering partner on DNA and the ability of the tethered ER to recruit transcriptional coactivator proteins.

Pathways in which the ER Functions as a Transcriptional Repressor

This is one of the least well-defined pathways in which the ER operates. In this situation, the ligand-activated ER, in the presence of all but pure antagonists, can bind to and inhibit the activity of transcription factors such as NF-κB or GATA-1 (Refs 80,81). The role of coactivator or corepressor proteins in this system has not yet been determined.

• Final Comments

In summary, the complex pharmacology of the known ER ligands is being unraveled slowly. Importantly, a firm relationship between antagonist efficacy and receptor conformation has been established and some of the components that enable the cell to distinguish between these conformations have been identified. This evolving complexity is likely to identify novel drug targets within the ER signal transduction pathway and lead to the discovery and development of new SERMs with improved therapeutic profiles.

• Acknowledgements

I would like to thank my colleagues for helpful suggestions and comments on the content and presentation of this article. Some of the research was supported by a research grant to DPM (NIH DK 48807).

References

1 Clark, J.H. and Markaverich, B.M. (1988) **Actions of ovarian steroid hormones.** In *The Physiology of Reproduction* (Knobil, E. and Neill, J., eds), pp 675–724, Raven Press

2 Felson, D.T. *et al.* (1993) **The effect of postmenopausal estrogen therapy on bone density in elderly women.** *New Engl. J. Med.* 329, 1141–1146

3 Turner, R.T., Riggs, B.L. and Spelsberg, T.C. (1994) **Skeletal effects of estrogen.** *Endocr. Rev.* 15, 275–300

4 Iafrati, M.D. *et al.* (1997) **Estrogen inhibits the vascular injury response in estrogen receptor α-deficient mice.** *Nat. Med.* 3, 545–548

5 Zumoff, B. (1993) **Hormone replacement and cardiovascular risk factors.** *New Engl. J. Med.* 329, 1041–1043

6 Grady, D., Rubin, S.M. and Petitti, D.B. (1992) **Hormone therapy to prevent disease and prolong life in postmenopausal women.** *Ann. Int. Med.* 117, 1016–1037

7 Tang, M-X. *et al.* (1996) **Effect on oestrogen during menopause on risk and age at onset of Alzheimer's disease.** *Lancet* 348, 429–432

8 Henderson, B.E., Paganini-Hill, A. and Ross, R.K. (1991) **Decreased mortality in users of estrogen replacement therapy.** *Arch. Intern. Med.* 151, 75–78

9 Soules, M.R. and Bremmer, W.J. (1982) **The menopause and climacteric: endocrinological basis and associated symptomatology.** *J. Am. Geriatr. Soc.* 30, 547–561

10 Dupont, W.D. and Page, D.L. (1991) **Menopausal estrogen replacement therapy and breast cancer.** *Arch. Int. Med.* 151, 67–72

11 Willis, D.B., Calle, E.E., Miracle-McMahill, H.L. and Heath, C.W. (1996) **Estrogen replacement therapy and risk of fatal breast cancer in a prospective cohort of postmenopausal women in the United States.** *Cancer Causes Control* 7, 449–457

12 Delmas, P.D. *et al.* (1997) **Effects of raloxifene on bone mineral density, serum cholesterol concentrations, and uterine endometrium in postmenopausal women.** *New Engl. J. Med.* 337, 1641–1647

13 O'Malley, B.W. and Schrader, W.T. (1976) **The receptors of steroid hormones.** *Sci. Am.* 234, 32–43

14 Love, R.R. *et al.* (1992) **Effects of tamoxifen on bone mineral density in postmenopausal women with breast cancer.** *New Engl. J. Med.* 326, 852–856

15 Jordan, V.C. (1992) **The strategic use of antiestrogen to control the development and growth of breast cancer.** *Cancer* 70, 977–982

16 Jordan, V.C., Collins, M.M., Rowsby, L. and Prestwich, G. (1977) **A monohydroxylated metabolite of tamoxifen with potent antioestrogen activity.** *J. Endocrinol.* 75, 305–316

17 Osborne, C.K., Hobbs, K. and Clark, G.M. (1985) **Effect of estrogens and antiestrogens on growth of human breast cancer cells in athymic nude mice.** *Cancer Res.* 45, 584–590

18 Gottardis, M.M., Jiang, S-Y., Jeng, M-H. and Jordan, V.C. (1989) **Inhibition of tamoxifen-stimulated growth of an MCF-7 tumor variant in athymic mice by novel steroidal antiestrogens.** *Cancer Res.* 49, 4090–4093

19 Jordan, V.C., Phelps, E. and Lindgren, J.U. (1987) **Effects of anti-estrogens in castrated and intact female rats.** *Breast Cancer Res. Treat.* 10, 31–35

20 Jordan, V.C., ed. (1996) *Tamoxifen: a Guide for Clinicians and Patients*, Huntington

21 Ismail, S.M. (1994) **Effects of tamoxifen on uterus.** *Lancet* 344, 622–624

22 Ugwumadu, A.H.N., Bower, D. and Ho, P.K-H. (1993) **Tamoxifen induced adenomyosis and adenomyomatous endometrial polyp.** *Br. J. Obstet. Gynaecol.* 100, 386–392

23 Kilackey, M.A., Hakes, T.B. and Pierce, V.K. (1985) **Endometrial adenocarcinoma in breast cancer patients receiving antiestrogens.** *Cancer Treat. Rep.* 69, 237–238

24 Love, R.R. *et al.* (1991) **Effects of tamoxifen on cardiovascular risk factors in postmenopausal women.** *Ann. Int. Med.* 115, 860–864

25 Gottardis, M.M. and Jordan, V.C. (1988) **Development of tamoxifen-stimulated growth of MCF-7 tumors in athymic mice after long-term antiestrogen administration.** *Cancer Res.* 48, 5183–5187

26 Stein, W., Hortobagyi, G.N. and Blumenschein, G.R. (1983) **Response of metastatic breast cancer to tamoxifen withdrawal: report of a case.** *J. Surg. Oncol.* 22, 45–46

27 Fisher, B. *et al.* (1996) **Five versus more than five years of tamoxifen therapy for breast cancer patients with negative lymph nodes and estrogen receptor-positive tumors.** *J. Natl. Cancer Inst.* 88, 1529–1542

28 Howell, A., Downey, S. and Anderson, E. (1996) **New endocrine therapies for breast cancer.** *Eur. J. Cancer* 32A, 576–588

29 Black, L.J. *et al.* (1994) **Raloxifene (LY139481 HCl) prevents bone loss and reduces serum cholesterol without causing uterine hypertrophy in ovariectomized rats.** *J. Clin. Invest.* 93, 63–69

30 Sato, M., Rippy, M.K. and Bryant, H.U. (1996) **Raloxifene, tamoxifen, nafoxidine, or estrogen effects on reproductive and nonreproductive tissues in ovariectomized rats.** *FASEB J.* 10, 905–912

31 Turner, C.H., Sato, M. and Bryant, H.U. (1994) **Raloxifene preserves bone strength and bone mass in ovariectomized rats.** *Endocrinology* 135, 2001–2005

32 Draper, M.W., Flowers, D.E., Huster, W.J. and Neild, J.A. (1993) **Effects of raloxifene (LY 139481 HCl) on biochemical markers of bone and lipid metabolism in healthy post-menopausal women.** In *Proceedings 1993. Fourth International Symposium on Osteoporosis and Consensus Development Conference* (Christiansen, C. and Riis, B., eds), pp 119–121, Handelstrykkeriet

33 Johnston, S.R. *et al.* (1997) **The novel anti-oestrogen idoxifene inhibits the growth of human MCF-7 breast cancer xenografts and reduces the frequency of acquired anti-oestrogen resistance.** *Br. J. Cancer* 75, 804–809

34 Rosati, R.L. *et al.* (1998) **Discovery and preclinical pharmacology of a novel, potent, nonsteroidal estrogen receptor agonist/antagonist.** *J. Med. Chem.* 41, 2928–2931

35 Willson, T.M. *et al.* (1997) **Dissection of the molecular mechanism of action of GW5638, a novel estrogen receptor ligand, provides insights into the role of ER in bone.** *Endocrinology* 138, 3901–3911

36 Rauschning, W. and Pritchard, K.I. (1994) **Droloxifene, a new antiestrogen: its role in metastatic breast cancer.** *Breast Cancer Res. Treat.* 31, 83–94

37 Heyman, R.A. *et al.* (1992) **9-*cis* retinoic acid is a high affinity ligand for the retinoid X receptor.** *Cell* 68, 397–406

38 Deslypere, J-P., Young, M., Wilson, J.D. and McPhaul, M.J. (1992) **Testosterone and 5α-dihydrotestosterone interact differently with the androgen receptor to enhance transcription of the MMTV-CAT reporter gene.** *Mol. Cell. Endocrinol.* 88, 15–22

39 Grumbach, M.M. and Conte, F.A. (1992) **Disorders of sex differentiation.** In *Williams Textbook of Endocrinology* (8th

edn) (Wilson, J.D. and Foster, D.W., eds), pp 853–951, W.B. Saunders
40 Ruh, T.S., Katzenellenbogen, B.S., Katzenellenbogen, J.A. and Gorski, J. (1973) **Estrone interaction with the rat uterus: *in vitro* response and nuclear uptake.** *Endocrinology* 92, 125–134
41 Baracat, E. *et al.* (1999) **Estrogen activity and novel tissue selectivity of Δ8,9 dehydroestrone sulfate in postmenopausal women.** *J. Clin. Endocrinol. Metab.* 84, 2020–2027
42 Kuiper, G.G.J.M., Enmark, E., Pelto-Huikko, M., Nilsson, S. and Gustafsson, J-A. (1996) **Cloning of a novel estrogen receptor expressed in rat prostate and ovary.** *Proc. Natl. Acad. Sci. U. S. A.* 93, 5925–5930
43 Mosselman, S., Polman, J. and Dijkema, R. (1996) **ERβ: identification and characterization of a novel human estrogen receptor.** *FEBS Lett.* 392, 49–53
44 Kuiper, G.G.J.M. *et al.* (1997) **Comparison of the ligand binding specificity and transcript tissue distribution of estrogen receptors α and β.** *Endocrinology* 138, 863–870
45 McDonnell, D.P., Clemm, D.L., Hermann, T., Goldman, M.E. and Pike, J.W. (1995) **Analysis of estrogen receptor function *in vitro* reveals three distinct classes of antiestrogens.** *Mol. Endocrinol.* 9, 659–668
46 Tzukerman, M.T. *et al.* (1994) **Human estrogen receptor transactivational capacity is determined by both cellular and promoter context and mediated by two functionally distinct intramolecular regions.** *Mol. Endocrinol.* 8, 21–30
47 Berry, M., Metzger, D. and Chambon, P. (1990) **Role of the two activating domains of the oestrogen receptor in the cell-type and promoter-context dependent agonistic activity of the anti-oestrogen 4-hydroxytamoxifen.** *EMBO J.* 9, 2811–2818
48 Smith, C.L., Nawaz, Z. and O'Malley, B.W. (1997) **Coactivator and corepressor regulation of the agonist/antagonist activity of the mixed antiestrogen, 4-hydroxytamoxifen.** *Mol. Endocrinol.* 11, 657–666
49 Katzenellenbogen, J.A., O'Malley, B.W. and Katzenellenbogen, B.S. (1996) **Tripartite steroid hormone receptor pharmacology: interaction with multiple effector sites as a basis for the cell- and promoter-specific action of these hormones.** *Mol. Endocrinol.* 10, 119–131
50 Norris, J.D., Fan, D. and McDonnell, D.P. (1996) **Identification of the sequences within the human complement 3 promoter required for estrogen responsiveness provides insight into the mechanism of tamoxifen mixed agonist activity.** *Mol. Endocrinol.* 10, 1605–1616
51 Dana, S.L., Hoener, P.A., Wheeler, D.L., Lawrence, C.L. and McDonnell, D.P. (1994) **Novel estrogen response elements identified by genetic selection in yeast are differentially responsive to estrogens and antiestrogens in mammalian cells.** *Mol. Endocrinol.* 8, 1193–1207
52 Beekman, J.M., Allan, G.F., Tsai, S.Y., Tsai, M-J. and O'Malley, B.W. (1993) **Transcriptional activation by the estrogen receptor requires a conformational change in the ligand binding domain.** *Mol. Endocrinol.* 7, 1266–1274
53 Brzozowski, A.M. *et al.* (1997) **Molecular basis of agonism and antagonism in the oestrogen receptor.** *Nature* 389, 753–758
54 Tanenbaum, D.M., Wang, Y., Williams, S.P. and Sigler, P.B. (1998) **Crystallographic comparison of the estrogen and progesterone receptor's ligand binding domains.** *Proc. Natl. Acad. Sci. U. S. A.* 95, 5998–6003
55 Paige, L.A. *et al.* (1999) **Estrogen receptor (ER) modulators each induce distinct conformational changes in ERα and ERβ.** *Proc. Natl. Acad. Sci. U. S. A.* 96, 3999–4004
56 Kumar, V. *et al.* (1987) **Functional domains of the human estrogen receptor.** *Cell* 51, 941–951
57 Tasset, D., Tora, L., Fromental, C., Scheer, E. and Chambon, P. (1990) **Distinct classes of transcriptional activating domains function by different mechanisms.** *Cell* 62, 1177–1187
58 Danielian, P.S., White, R., Lees, J.A. and Parker, M.G. (1992) **Identification of a conserved region required for hormone dependent transcriptional activation by steroid hormone receptors.** *EMBO J.* 11, 1025–1033
59 Metzger, D., Losson, R., Bornert, J-M., Lemoine, Y. and Chambon, P. (1992) **Promoter specificity of the two transcriptional activation functions of the human oestrogen receptor in yeast.** *Nucleic Acids Res.* 20, 2813–2817
60 Gallagher, A., Chambers, T.J. and Tobias, J.H. (1993) **The estrogen antagonist ICI 182,780 reduces cancellous bone volume in female rats.** *Endocrinology* 133, 2787–2791
61 Dauvois, S., Danielian, P.S., White, R. and Parker, M.G. (1992) **Antiestrogen ICI 164,384 reduces cellular estrogen receptor content by increasing its turnover.** *Proc. Natl. Acad. Sci. U. S. A.* 89, 4037–4041
62 Dauvois, S., White, R. and Parker, M.G. (1993) **The antiestrogen ICI 182,780 disrupts estrogen receptor nucleocytoplasmic shuttling.** *J. Cell Sci.* 106, 1377–1388
63 Willson, T.M. *et al.* (1994) **3-[4-(1,2-diphenylbut-1-enyl)phenyl]acrylic acid: a non-steroidal estrogen with functional selectivity for bone over uterus in rats.** *J. Med. Chem.* 37, 1550–1552
64 Conneely, O.M. *et al.* (1988) **Structure–function relationships of the chicken progesterone receptor.** *Biochem. Soc. Trans.* 16, 683–687
65 Onate, S.A., Tsai, S., Tsai, M-J. and O'Malley, B.W. (1995) **Sequence and characterization of a coactivator for the steroid hormone receptor superfamily.** *Science* 270, 1354–1357
66 Horwitz, K.B. *et al.* (1996) **Nuclear receptor coactivators and corepressors.** *Mol. Endocrinol.* 10, 1167–1177
67 Spencer, T.E. *et al.* (1997) **Steroid receptor coactivator-1 is a histone acetyltransferase.** *Nature* 389, 194–198
68 Xu, J. *et al.* (1998) **Partial hormone resistance in mice with disruption of the steroid receptor coactivator-1 (SRC-1) gene.** *Science* 279, 1922–1925
69 Chen, J.D. and Evans, R.M. (1995) **A transcriptional co-repressor that interacts with nuclear hormone receptors.** *Nature* 377, 454–457
70 Hörlein, A.J. *et al.* (1995) **Ligand-independent repression by the thyroid hormone receptor mediated by a nuclear receptor co-repressor.** *Nature* 377, 397–403
71 Lavinsky, R.M. *et al.* (1998) **Diverse signaling pathways modulate nuclear receptor recruitment of N-CoR and SMRT complexes.** *Proc. Natl. Acad. Sci. U. S. A.* 95, 2920–2925
72 Webb, P., Lopez, G.N., Uht, R.M. and Kushner, P.J. (1995) **Tamoxifen activation of the estrogen receptor/AP-1 pathway: potential origin for the cell-specific estrogen-like effects of antiestrogens.** *Mol. Endocrinol.* 9, 443–456
73 Savouret, J-F. *et al.* (1994) **Interplay between estrogens, progestins, retinoic acid and AP-1 on a single regulatory site in the progesterone receptor gene.** *J. Biol. Chem.* 269, 28955–28962
74 Paech, K. *et al.* (1997) **Differential ligand activation of estrogen receptors ERα and ERβ at AP1 sites.** *Science* 277, 1508–1510
75 Elgort, M.G., Zou, A., Marschke, K.B. and Allegretto, E.A. (1996) **Estrogen and estrogen receptor antagonists stimulate transcription from the human retinoic acid receptor-β-1 promoter via a novel sequence.** *Mol. Endocrinol.* 10, 477–487
76 Montano, M.M. and Katzenellenbogen, B.S. (1997) **The quinone reductase gene: a unique estrogen receptor-regulated gene that is activated by antiestrogens.** *Proc. Natl. Acad. Sci. U. S. A.* 94, 2581–2586
77 Girasole, G. *et al.* (1992) **17β-estradiol inhibits interleukin-6 production by bone marrow-derived stromal cells and osteoblasts *in vitro*: a potential mechanism for the antiosteoporotic effect of estrogens.** *J. Clin. Invest.* 89, 883–891
78 Jilka, R.L. *et al.* (1992) **Increased osteoclast development after estrogen loss: mediation by interleukin-6.** *Science* 257, 88–91
79 Ray, A., Prefontaine, K.E. and Ray, P. (1994) **Down-modulation of interleukin-6 gene expression by 17β-estradiol in the absence of high affinity DNA binding by the estrogen receptor.** *J. Biol. Chem.* 269, 12940–12946
80 Stein, B. and Yang, M.X. (1995) **Repression of the interleukin-6 promoter by estrogen receptor is mediated by NF-κB and C/EBPβ.** *Mol. Cell. Biol.* 15, 4971–4979
81 Blobel, G.A., Sieff, C.A. and Orkin, S.H. (1995) **Ligand-dependent repression of the erythroid transcription factor GATA-1 by the estrogen receptor.** *Mol. Cell. Biol.* 15, 3147–3153
82 Smith, C.L., Conneely, O.M. and O'Malley, B.W. (1993) **Modulation of the ligand-independent activation of the human estrogen receptor by hormone and antihormone.** *Proc. Natl. Acad. Sci. U. S. A.* 90, 6120–6124
83 Ignar-Trowbridge, D.M., Pimentel, M., Parker, M.G., McLachlan, J.A. and Korach, K.S. (1996) **Peptide growth factor cross-talk with the estrogen receptor requires the A/B domain and occurs independently of protein kinase C or estradiol.** *Endocrinology* 137, 1735–1744

A second binding site for hydroxytamoxifen within the coactivator-binding groove of estrogen receptor β

Yong Wang*, Nickolay Y. Chirgadze*, Stephen L. Briggs*, Sohaib Khan†, Elwood V. Jensen†‡, and Thomas P. Burris*‡§

*Lilly Research Laboratories, Indianapolis, IN 46285; †Department of Cell Biology, University of Cincinnati College of Medicine, Cincinnati, OH 45267-0521; and §Department of Pharmacology and Toxicology, Indiana University School of Medicine, Indianapolis, IN 46202

Contributed by Elwood V. Jensen, December 9, 2005

Evidence is presented that the estrogen antagonist 4-hydroxytamoxifen (HT) can occupy not only the core binding pocket within the ligand-binding domain of estrogen receptor (ER) β but also a second site on its surface. The crystal structure of the ligand-binding domain (LBD) associated with HT was determined to 2.2 Å and revealed two molecules of HT bound to the protein. One was located in the consensus ligand-binding pocket, whereas the other bound to a site that overlaps with the hydrophobic groove of the coactivator recognition surface. Relative to the ERα-tamoxifen structure, helix 12 has been displaced from the coactivator recognition surface and occupies a unique position. Although it has been demonstrated that association of the antagonist with the core ligand-binding pocket is sufficient to induce an antagonist ligand-binding domain conformation, this structure suggests that small molecules may directly antagonize receptor–coactivator interactions. These results provide a direct demonstration of two binding sites for HT in ERβ, as has been previously suggested for ERα by using biochemical methods, and represent a crystal structure of a small nonpeptide molecule occupying the coactivator recognition site.

antiestrogen | crystallography | nuclear receptor

The estrogen receptor (ER) is a member of the nuclear hormone receptor (NHR) superfamily of ligand-activated transcription factors. Members of this class of proteins display a conserved structural organization consisting of an amino terminal transactivation domain (AF-1), a highly conserved DNA-binding domain, and ligand-binding domain in the carboxyl terminus, which also contains a ligand-activated transactivation function, AF-2 (1). The role that ligands play in modulation of receptor activity has been well characterized by using both biochemical and structural methods and indicates that ligands induce a significant conformational change within the receptor ligand-binding domain (LBD). The structures of several liganded NHRs have been solved, indicating that the ligand binds within the core of the globular LBD. In fact, a "mouse trap" model has been proposed (2) in which an agonist accesses the core of the LBD via a pore and, once bound, is "trapped" by a conformational shift of a structural component of the LBD itself, helix (H)12. This carboxyl-terminal α-helix folds against the surface of the LBD and partially obscures the pore. The conformational shift of H12 also completes the formation of a favorable surface on the LBD that is recognized by transcriptional coactivators that mediate the agonist-dependent transactivation properties of the nuclear receptors. The coactivator recognition surface of the receptor is created by helices 3, 4, 5, and 12 of the LBD and is composed of a hydrophobic groove that is capped on either side by two charged residues (charge clamp), a lysine from H3, and a glutamate from H12 (3, 4). The coactivator motif that is recognized by this groove within the LBD is a conserved amphipathic α-helical structure with the consensus sequence, LXXLL (L = leucine and X = any amino acid), also known as an NR box (5–9). The recognition of the LXXLL motif by the LBD is mediated by the hydrophobic side chains of the leucine residues displayed on one face of the helix interacting with the hydrophobic surface of the LBD and hydrogen bonding between the charge clamp residues and the backbone of the LXXLL peptide motif (3, 4). Thus, this ligand-regulated protein–protein interaction is critical for the mediation of transcriptional activation by nuclear receptors.

ER antagonists and selective ER modulators (SERMs) have been shown (4, 10) to induce distinct conformations relative to the agonists, estradiol-17β (E_2) and diethylstilbestrol, within the LBD of the receptor (4, 10). SERMs, such as raloxifene and 4-hydroxytamoxifen (HT), which display mixed agonist/antagonist pharmacology, occupy the identical site as the agonists within the core of the LBD but prevent productive positioning of H12 by hindrance due to basic side-chain extensions of these ligands. With either of these selective ER modulators bound, H12 actually occupies the coactivator-binding groove of the receptor, preventing NR box recognition and, thus, functionally antagonizing receptor–coactivator interaction (4, 10). When bound to ERα, the pure antagonist, ICI 164,384, results in a unique structure in which H12 cannot be resolved in the crystal structure, but a portion of the ICI molecule itself protrudes from the LBD occupying the coactivator binding site, thus preventing both the correct positioning of H12 and binding of the NR box (11). Recently, a third mode of antagonism was reported in which the antagonist still occupies the ligand-binding site within the core of the LBD but allosterically prevents productive H12 positioning (12).

Immunoassay performed on tumor specimens from breast cancer patients in the presence of hydroxytamoxifen demonstrated increased antiestrogen binding as a consequence of the exposure of an additional epitope in the receptor, specifically for the marker antibody, H222 (13). In these and later (14) studies, sedimentation patterns demonstrated that the total binding for HT was nearly twice that of E_2 and, despite the high affinity of HT for the receptor, the total binding capacity was not saturated until the HT concentration was well above that required to saturate E_2 binding. This finding indicated that binding of HT to the secondary site was of considerably lower affinity than to the primary site. Moreover, two other groups (15–17), reported a biphasic proliferation response to HT in breast cancer cell lines in that this agent acts as an agonist at low concentrations and an antagonist at higher levels, consistent with the two-binding-site model. In this model, we proposed that the primary, high-affinity

Conflict of interest statement: No conflicts declared.

Abbreviations: ER, estrogen receptor; E_2, estradiol-17β; H*n*, helix *n*; HT, 4-hydroxytamoxifen; LBD, ligand-binding domain; NHR, nuclear hormone receptor.

Data deposition: The atomic coordinates have been deposited in the Protein Data Bank, www.pdb.org (PDB ID code 2FSZ).

‡To whom correspondence may be addressed. E-mail: elwood.jensen@uc.edu or burris@lilly.com.

© 2006 by The National Academy of Sciences of the USA

site was responsible for agonist activity of the antiestrogen, whereas the secondary, low-affinity site was responsible for antagonist activity (17). Interestingly, a second ligand-binding site within the vitamin D receptor has recently been proposed based on computational modeling (18).

In the present study, we used x-ray crystallography to identify a second binding site for HT within the LBD of ERβ. Similar to the HT-ERα evidence, in addition to the primary site recognized by estradiol, HT associates with a secondary site located in the coactivator-binding groove. The predominant interactions between the second HT and the LBD are van der Waals contacts, consistent with the second binding site having much less affinity than the primary one. H12, which has been demonstrated to associate with the coactivator-binding groove in the HT-ERα structure, occupies a unique position, folded against the LBD surface. This structure provides insight into a previously uncharacterized mechanism of antagonism of a nuclear receptor in which a small nonpeptide molecule binds within the coactivator recognition.

Results and Discussion

The structure of the ERβ/HT complex exhibited the classical three-layered α-helical sandwich conformation, similar to other ERβ structures published in refs. 12 and 20 with other ligands (Fig. 1*a*). In this structure, two molecules of HT per ERβ molecule were observed in the electron density. One of the HT molecules is located in the cognate ligand-binding site with a conformation indistinguishable from that in the ERα/HT structure (Fig. 1*b*). The second HT, clearly indicated by the electron density map (Fig. 2*a*), is located at a site that overlaps with the coactivator binding site (Fig. 1*a*). H12 in the C-terminal tail is displaced based on the location of the second HT molecule and, thus, is not in the typical antagonist-bound conformation but interacts with a neighboring molecule within the crystal. This type of positioning of H12 is not unusual because different conformations of H12 in ERs or other nuclear receptors have been observed in refs. 11 and 21–23. The binding of the second HT appears mostly due to hydrophobic and van der Waals interactions between HT and ERβ with the 4-OH group and the amine group exposed to solvent. This interaction is mediated partly by the coactivator-binding site known to contain hydrophobic patches that, along with two charged residues Lys 314 and Glu 493 (charge clamp), are responsible for recognition of the LXXLL motif of the coactivator. Several key interactions that are used for high-affinity interaction with the LXXLL motif, such as the charge-clamp residues, are not exploited by the second HT. This region is also the site where H12 in the antagonist-bound conformation binds as seen in structures in refs. 4 and 10. The comparison between the bound second HT and a bound coactivator LXXLL peptide or H12 is shown in Fig. 2*b*.

Compared with bound peptides, the unsubstituted phenyl group of HT is buried deeper into a hydrophobic cavity and is likely the main contributor to binding (Fig. 2*c*). Residues surrounding the binding site display nearly identical conformations compared to those of previously reported structures of ER. As in binding coactivators, several residues in H3, such as Leu 306, Met 309, and Ile 310, form important interactions with the second HT. Trp 335 also is in close contact with the unsubstituted phenyl ring and the ethyl group. The side chain of Glu 332 has van der Waals contact with the phenolic ring, but there is no evidence of polar interaction between the two. The Leu 331 and Val 328 residues in H4 contribute to the interaction, with the side chain bearing the phenyl ring of HT. In addition to these interactions, the second HT also has some interaction with the H12 of a neighboring molecule in the crystal. Side chains of Leu 490 and Met 497 are the main contributors, whereas the backbones of Leu 447 and Arg 448 are within van der Waals contact distance. Compared to the binding site formed by H3, H4, and H5, the contribution from H12 is secondary. This type of binding is reminiscent of the corepressor binding to PPARα,

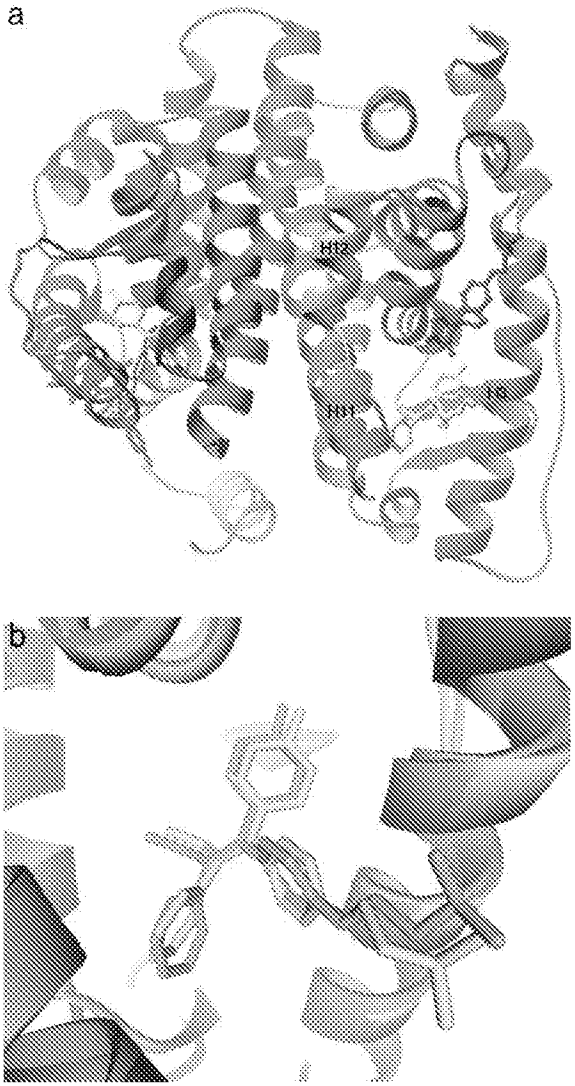


Fig. 1. Crystal structure of estrogen receptor β associated with 4-hydroxytamoxifen. (*a*) The overall structure of ERβ with two HT molecules bound. The HT bound to the cognate binding site is in yellow, whereas the second HT is colored by element. H12 is in gold. This figure was constructed with RIBBONS (19). (*b*) Comparison between HTs bound to ERα and ERβ. View is of the HT in the cognate-binding site in ERβ superimposed to the bound HT in ERα. The superposition was based on the alignment of the protein structure. The ERα/HT structure as reported in ref. 4 is in yellow, and the ERβ/HT structure is in cyan.

where the H12 is displaced from the coactivator binding groove but is still within van der Waals contact with the bound corepressor peptide (25).

The observation of a second binding site for HT in ERβ is particularly remarkable given previous suggestions of its existence by using biochemical methods and its localization within an essential protein–protein recognition surface of the LBD. This finding is welcome given that previous proposals of an antagonist-specific binding site in ER had not been widely accepted. Martin *et al.* (13) noted that the addition of HT to ER derived from breast cancer cytosol or MCF-7 cells resulted in exposure of an additional epitope recognized by a particular monoclonal antibody. Interestingly, this effect was still noted even when the receptor was saturated with excess E_2, suggesting for the first time that HT may also bind to a distinct site, not recognized by E_2, resulting in an additional conformational change. Analysis of binding capacity of the receptor with either

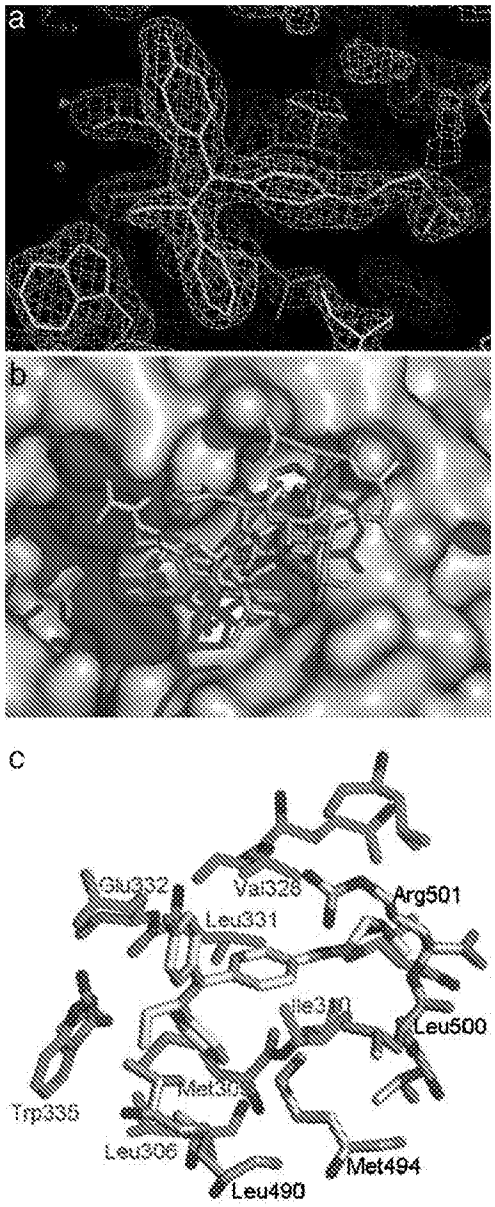


Fig. 2. Analysis of a second binding site for hydroxytamoxifen in estrogen receptor β (*a*) Electron-density map of the second bound HT. The $2F_c - F_o$ Sigma A weighted electron-density map contoured at 1.5 σ shows the second bound HT in the ERβ/HT structure. The protein portion is drawn in yellow, whereas the HT molecule is colored by element. This figure was constructed with QUANTA. (*b*) Comparison between the second HT and coactivator binding. View of the second HT on the surface of ERβ bound with the first HT shows the overlap with a coactivator (GRIP) peptide from an ERα structure (4). The second HT is colored by element, whereas the GRIP peptide is in purple. (*c*) ERβ residues interacting with the second HT. Residues within 4 Å of the second HT are shown. Atoms are colored by element. Carbon atoms from the main ERβ are in green, and the residue labels are in blue, whereas carbon atoms from the H12 of a neighboring ERβ in the crystal are in gray, and the residue labels are in black.

radiolabeled E_2 or HT indicated that the total binding capacity of HT was nearly twice that of E_2 (14). In addition, the second HT binding site appeared to be of considerably less affinity. Our results are consistent with these studies, suggesting a second HT binding site, but we are currently unable to conclude that they are identical. These previous studies used crude extracts that were likely dominated by ERα, whereas our structure demonstrates the second site in crystalline ERβ. Analysis of the residues responsible for interaction with the second HT indicates that they are absolutely conserved between the two ER subtypes, suggesting that ERα may also have the capacity to interact with a second HT. However, this second HT binding site was not observed in the previous structure of HT/ERα published in ref. 4, and our attempts to crystallize ERα with HT under the similar conditions have been unsuccessful. The second HT is not fully buried like the HT bound in the cognate binding site and has higher temperature factors in the x-ray crystallographic refinement relative to the first HT. Thus, we expect that the second binding site would be of low affinity. It is possible that the crystallization conditions that we used were conducive to preserving the weak binding of the second HT, whereas the conditions used in the HT/ERα structure were not.

The pharmacological significance of this second binding site for HT is unclear given that binding of HT within the primary site is sufficient to cause a conformational change that results in placement of H12 into the coactivator-binding groove, yielding antagonist activity. Nevertheless, binding of a small drug-like molecule within the coactivator-binding groove is itself an interesting observation given recent efforts examining the potential for using this protein–protein interaction surface as an alternative site for NHR drug design. Until recently, one fundamental concern was that the coactivator recognition surface of the NHR LBD may not display sufficient diversity between various receptors to allow design of selective drugs. However, we and others (24, 25) have demonstrated that short peptidomimetics based on the LXXLL motif can be designed displaying high-affinity binding to NHRs while retaining significant receptor selectivity. Evolution of this approach to drug design will require transition from the peptidomimetics to more drug-like molecules. Recently, Rodriguez *et al.* (26) took the first step toward this transition by using structure-based design to develop nonpeptide small-molecule coactivator-binding inhibitors (CBIs) against ERα. Even though the best CBIs identified were relatively low affinity ($K_i \approx 30$ μM), the fact that they were rationally designed based on the mode of LXXLL recognition of the receptor and our discovery of the ability of HT to bind to a coactivator recognition surface provides validation of this approach to design a new class of NHR antagonists. In the search for more effective estrogen antagonists, the affinity for the secondary site should be an important factor.

Materials and Methods

ERβ Expression and Purification. For crystallographic studies, the human ERβ LBD (residues 204–448) was overexpressed as an N-terminally His-6-tagged protein in BL21(DE3) cells by using expression vector pET19 (Novagen) and purified by PanVera (Madison, WI).

Crystallization and Data Collection. The protein was concentrated to 5–8 mg/ml in solution containing 20 mM Tris·HCl (pH 8.0), 100 mM NaCl, 1 mM benzamidine, 12 μM leupetin, 10 μM E-64, 1 mM PMSF, and 3% DMSO. The HT concentration was 10 times the molar concentration of the protein. Crystallization was carried out by the hanging drop vapor diffusion method at room temperature by using a reservoir solution of 100 mM sodium citrate (pH 5.6)/1–2 M NaCl/4% wt/vol ethyleneimine polymer. Crystals belong to space group I4 with unit cell parameters $a = b = 105.04$ Å, $c = 102.39$ Å. There are two molecules of the complex per asymmetric unit.

Several diffraction data sets were collected on Industrial Macromolecular Crystallography Association (IMCA) beam lines. The data (resolution of 2.2 Å; $R_{merge} = 5.7\%$ and completeness of 95.7%) used for the final refinement were collected by using a MarCCD detector on IMCA beam line

ID-17 at the Advanced Photon Source, Argonne National Laboratories. The crystal was cooled at 100K by using 15–20% glycerol plus the mother liquor as cryoprotectant. The diffraction data were processed by using HKL2000 (27).

Structure Determination and Refinement. The crystal structure was determined by the method of molecular replacement with AMORE (28) by using the ERβLBD/raloxifene structure as a search model (20). The program suite QUANTA 98 (Molecular Simulations, San Diego) was used for model building between rounds of refinement. Structure refinement was carried out by CNX2000 (29) by using rigid-body, positional, and individual B factor refinements with bulk solvent correction (R_{work} = 0.273, R_{free} = 0.30). Ninety-four percent of residues were found in the most favorable region, and 6% of residues were found in additionally allowed region of a Ramachandran plot.

This work was partially supported by National Institutes of Health Grant CA72039 (to S.K.)

1. Burris, T. P. (2001) in *Nuclear Receptors and Genetic Disease*, eds. Burris, T. P. & McCabe, E. R. B. (Academic, San Diego), pp. 1–57.
2. Moras, D. & Gronemeyer, H. (1998) *Curr. Opin. Cell Biol.* **10**, 384–391.
3. Nolte, R. T., Wisely, G. B., Westin, S., Cobb, J. E., Lambert, M. H., Kurokawa, R., Rosenfeld, M. G., Willson, T. M., Glass, C. K. & Milburn, M. V. (1998) *Nature* **395**, 137–143.
4. Shiau, A. K., Barstad, D., Loria, P. M., Cheng, L., Kushner, P. J., Agard, D. A. & Greene, G. L. (1998) *Cell* **95**, 927–937.
5. Ding, X. F., Anderson, C. M., Ma, H., Hong, H., Uht, R. M., Kushner, P. J. & Stallcup, M. R. (1998) *Mol. Endocrinol.* **12**, 302–313.
6. Heery, D. M., Kalkhoven, E., Hoare, S. & Parker, M. G. (1997) *Nature* **387**, 733–736.
7. Le Douarin, B., Nielsen, A. L., Garnier, J. M., Ichinose, H., Jeanmougin, F., Losson, R. & Chambon, P. (1996) *EMBO J.* **15**, 6701–6715.
8. Torchia, J., Rose, D. W., Inostroza, J., Kamei, Y., Westin, S., Glass, C. K. & Rosenfeld, M. G. (1997) *Nature* **387**, 677–684.
9. Savkur, R.S. & Burris, T.P. (2004) *J. Peptide Res.* **63**, 207–212.
10. Brzozowski, A. M., Pike, A. C., Dauter, Z., Hubbard, R. E., Bonn, T., Engstrom, O., Ohman, L., Greene, G. L., Gustafsson, J-Å. & Carlquist, M. (1997) *Nature* **389**, 753–758.
11. Pike, A. C., Brzozowski, A. M., Walton, J., Hubbard, R. E., Thorsell, A. G., Li, Y.L., Gustafsson, J-Å. & Carlquist, M. (2001) *Structure (London)* **9**, 145–153.
12. Shiau, A. K., Barstad, D., Radek, J. T., Meyers, M. J., Nettles, K. W., Katzenellenbogen, B. S., Katzenellenbogen, J. A., Agard, D. A. & Greene, G. L. (2002) *Nat. Struct. Biol.* **9**, 359–364.
13. Martin, P. M., Berthois, Y. & Jensen, E. V. (1988) *Proc. Natl. Acad. Sci. USA* **85**, 2533–2537.
14. Hedden, A., Müller, V. & Jensen, E. V. (1995) *Ann. N.Y. Acad. Sci.* **761**, 109–120.
15. Katzenellenbogen, B. S., Kendra, K.L., Norman, M.J. & Berthois, Y. (1987) *Cancer Res.* **47**, 4355–4360.
16. Poulin, R., Merand, Y., Poirer, D., Levesque, C., Dufour, J. M. & Labrie, F. (1989) *Breast Cancer Res. Treat.* **14**, 65–76.
17. Jensen, E. V. & Khan, S. A. (2004) *Mech. Ageing Dev.* **125**, 672–682.
18. Mizwicki, M. T., Keidel, D., Bula, C. M., Bishop, J. E., Zanello, L. P., Wurtz, J.-M., Moras, D. & Norman, A. W. (2004) *Proc. Natl. Acad. Sci. USA* **101**, 12876–12881.
19. Carson, M. (1997) *Macromol. Crystallogr. Pt. B* **277**, 493–505.
20. Pike, A. C., Brzozowski, A. M., Hubbard, R. E., Bonn, T., Thorsell, A. G., Engstrom, O., Ljunggren, J., Gustafsson, J-Å. & Carlquist, M. (1999) *EMBO J.* **18**, 4608–4618.
21. Tanenbaum, D. M., Wang, Y., Williams, S. P. & Sigler, P. B. (1998) *Proc. Natl. Acad. Sci. USA* **95**, 5998–6003.
22. Gangloff, M., Ruff, M., Eiler, S., Duclaud, S., Wurtz, J. M. & Moras, D. (2001) *J. Biol. Chem.* **276**, 15059–15065.
23. Xu, H. E., Stanley, T. B., Montana, V. G., Lambert, M. H., Shearer, B. G., Cobb, J. E., McKee, D. D., Galardi, C. M., Plunket, K. D., Nolte, R. T., *et al.* (2002) *Nature* **415**, 813–817.
24. Leduc, A.-M., Trent, J. O., Wittliff, J. L., Bramlett, K. S., Briggs, S. L., Chirgadze, N. Y., Wang, Y., Burris, T. P. & Spatola, A. F. (2003) *Proc. Natl. Acad. Sci. USA* **100**, 11273–11278.
25. Geistlinger, T. R. & Guy, R. K. (2003) *J. Am. Chem. Soc.* **125**, 6852–6853.
26. Rodriguez, A. L., Tamrazi, A., Collins, M. L. & Katzenellenbogen, J. A. (2004) *J. Med. Chem.* **47**, 600–611.
27. Otwinowski, Z. & Minor, W. (1997) *Macromol Crystallogr. Pt. A* **276**, 307–326.
28. Navaza, J. (1994) *Acta Crystallogr. A* **50**, 157–163.
29. Brunger, A. T., Adams, P. D., Clore, G. M., DeLano, W. L., Gros, P., Grosse-Kunstleve, R. W., Jiang, J. S., Kuszewski, J., Nilges, M., Pannu, N. S., *et al.* (1998) *Acta Crystallogr. D* **54**, 905–921.

Global analysis of ligand sensitivity of estrogen inducible and suppressible genes in MCF7/BUS breast cancer cells by DNA microarray

Kathryn R. Coser*†, Jessica Chesnes*†, Jingyung Hur*, Sandip Ray‡, Kurt J. Isselbacher*, and Toshi Shioda*§

*Department of Tumor Biology and DNA Microarray Core Facility, Massachusetts General Hospital Cancer Center, Charlestown, MA 02129; and ‡X-Mine Inc., Brisbane, CA 94005

Contributed by Kurt J. Isselbacher, September 12, 2003

To obtain comprehensive information on 17β-estradiol (E2) sensitivity of genes that are inducible or suppressible by this hormone, we designed a method that determines ligand sensitivities of large numbers of genes by using DNA microarray and a set of simple Perl computer scripts implementing the standard metric statistics. We used it to characterize effects of low (0–100 pM) concentrations of E2 on the transcriptome profile of MCF7/BUS human breast cancer cells, whose E2 dose-dependent growth curve saturated with 100 pM E2. Evaluation of changes in mRNA expression for all genes covered by the DNA microarray indicated that, at a very low concentration (10 pM), E2 suppressed ≈3–5 times larger numbers of genes than it induced, whereas at higher concentrations (30–100 pM) it induced ≈1.5–2 times more genes than it suppressed. Using clearly defined statistical criteria, E2-inducible genes were categorized into several classes based on their E2 sensitivities. This approach of hormone sensitivity analysis revealed that expression of two previously reported E2-inducible autocrine growth factors, transforming growth factor α and stromal cell-derived factor 1, was not affected by 100 pM and lower concentrations of E2 but strongly enhanced by 10 nM E2, which was far higher than the concentration that saturated the E2 dose-dependent growth curve of MCF7/BUS cells. These observations suggested that biological actions of E2 are derived from expression of multiple genes whose E2 sensitivities differ significantly and, hence, depend on the E2 concentration, especially when it is lower than the saturating level, emphasizing the importance of characterizing the ligand dose-dependent aspects of E2 actions.

Estrogens bind to estrogen receptors (ERs), which belong to the steroid receptor family of transcription factors, and the liganded ERs activate or suppress transcription of genes by recruiting coactivator or corepressor proteins. ERs bind directly to genomic DNA sequences that are known as estrogen response elements, or they interact with genomic DNA indirectly through other DNA-binding proteins such as AP-1 or Sp1. ERs also interact with key components of other signal transduction pathways such as the Src tyrosine kinase or phosphatidyl inositol 3-kinase, affecting gene expression indirectly through these pathways (1). Moreover, changes in gene expression that occur as primary responses to estrogens may exert secondary influences on expression of other genes. Thus, the majority of the biological actions of estrogens are derived from, or at least associated with, induction or suppression of certain sets of genes, even when such actions are considered indirect or nongenomic.

To characterize estrogen effects on gene expression, several laboratories have used DNA microarrays and determined the transcriptome profiles of estrogen-dependent human breast cancer cells cultured in the presence or absence of 17β-estradiol (E2) (2–4). In these experiments, cells were subjected to hormone starvation for up to 5 days and then stimulated with 1–10 nM E2, which are high concentrations that usually saturate the E2 dose-dependent growth curves of ER-positive breast cancer cell cultures (5, 6). Therefore, the changes in transcriptome profiles reported in these previous studies, each of which handled only a single, high E2 concentration, were likely reflecting the maximum or near-maximum E2 effects. However, information on E2 dose-dependent effects at a lower, unsaturated range of concentrations would be critically important to understand estrogen actions *in vivo*, where cells are unlikely to be exposed to saturating concentrations of estrogens continuously.

The E2 sensitivity of a gene may be characterized by three aspects of the E2 dose-dependent profiles of the mRNA expression, namely, (*i*) the minimum E2 concentration required to induce or suppress expression of mRNA transcripts significantly, (*ii*) the E2 concentration that saturates E2 effects on mRNA expression, and (*iii*) the shape of the E2 dose–response curve for mRNA expression (i.e., linear, convex, or concave). The E2 sensitivity thus characterized may be determined by multiple factors: affinity of E2 to each of the two isoforms of ERs (i.e., ERα and ERβ), affinity of the liganded ERs to estrogen response element (EREs) (7, 8), location of the EREs in the transcriptional control sequences of genomic DNA (8), and availability of transcriptional coactivators and cosuppressors that are recruited to the transcriptional protein complexes formed around the liganded ERs (9). When the E2 sensitivity differs among genes, effects of a subsaturating concentration of E2, which would involve only a part of the whole repertoire of the E2-regulatable genes, may be different from the effect of a saturating concentration of estrogen not only quantitatively but also qualitatively. To examine such possibilities, it is necessary to develop a method that characterizes the quantitative aspects of E2 sensitivity of a large number of genes with a reasonable precision and a statistical basis.

In the present study, we applied the Affymetrix high-density oligonucleotide DNA microarray to determine the ligand sensitivity of E2-inducible and E2-suppressible genes in ER-positive MCF7/BUS human breast cancer cells. Using the Perl programming language, we developed a set of simple computer scripts that processed the DNA microarray data and characterized E2 sensitivity of each gene, implementing a standard test of metric statistics.

Materials and Methods

Cell Culture. MCF7/BUS cells (5, 10) were provided by A. M. Soto and C. Sonnenschein (Tufts University, Boston) and maintained in DMEM (4.5 mg/liter glucose) supplemented with 5% FCS that contained bioactive estrogens equivalent to ≈60 pM E2 (HyClone, defined grade) in xenoestrogen-free plastic ware (Corning). Their E2 dose-dependent growth curves were drawn following the E-SCREEN protocol (5, 10). To determine E2 effects on the transcriptome, cells were washed three times with phenol

Abbreviations: E2, 17β-estradiol; ER, estrogen receptor; RRM2, ribonucleotide reductase M2, TGF-α, transforming growth factor α; SDF-1, stromal cell-derived factor 1.

†K.R.C. and J.C. contributed equally to this study.

§To whom correspondence should be addressed. E-mail: tshioda@partners.org.

© 2003 by The National Academy of Sciences of the USA

www.pnas.org/cgi/doi/10.1073/pnas.2235866100

red-free DMEM and cultured for 48 h in the presence of varying concentrations of E2; in these experiments, medium was supplemented with 5% charcoal/dextran-stripped FCS (HyClone) that did not contain significant amounts of steroid hormones. Throughout the experiments, all plastic ware was carefully selected to avoid xenoestrogen contamination.

DNA Microarray Experiment and RT-PCR. Total RNA samples were isolated from cell cultures by using a RNeasy mini-kit (Qiagen, Chatsworth, CA), and their amounts, purity, and integrity were evaluated by UV spectrophotometry and a RNA-nano Bioanalyzer (Agilent, Palo Alto, CA). Solid-phase archives of all RNA samples described in this study will be provided to investigators on request. Probe synthesis and hybridization of human U-133A GeneChip DNA microarrays (Affymetrix, Santa Clara, CA) were performed following the manufacturer's instructions. Gene expression data (CHP file of Affymetrix MICROARRAY SUITE 5.0 software) were normalized to a global target intensity of 500; by our hands, the background noise intensity was <50. RT-PCR primers and conditions for semiquantitative detection of E2-responsive genes are available on request.

Microarray Data Analysis. A master data set spreadsheet for E2 dose-dependent gene expression was generated from the CHP files by MICROARRAY SUITE 5.0 and converted into a tab-delimited text file. Each row of this text file represented a single gene and consisted of gene name, Affymetrix ID number, and normalized signal intensities of five repeated sets of E2 dose–response experiments. Each set of the E2 dose–response experiments consisted of data for 0, 10, 30, 60, and 100 pM E2. About 22,000 rows in this file represented all genes covered by the human U-133A chip.

When $e(i,j)$ is a normalized signal intensity of a gene in experiment number i at E2 concentration of j [i = 1, 2, 3, 4, 5; j = 0, 10, 30, 60, 100 (pM)], distribution of E defined in the following equation approximates to the normal distribution (11, 12). This approximation, although not mathematically rigorous, is usually satisfactory for practical purposes (11, 12):

$$E(i, j1, j2) = \log_2\{e(i, j1)/e(i, j2)\}.$$

Because E is 0 when $e(j1) = e(j2)$, and because E is > 0 when $e(j1)$ is $> e(j2)$, a single-tail Student's t test for a null hypothesis,

$$H_0: \bar{E} = 0 \ [\bar{E} \text{ is mean of } E(i, j1, j2) \text{ with fixed } j1 \text{ and } j2],$$

determines whether $e(j1)$ is significantly greater than $e(j2)$ or not.

Using the programming language Perl (13), simple computer scripts were developed to calculate $E(i, j1, j2)$ for all combinations of $(i, j1, j2)$ and to perform the above t test. Separate scripts were produced for each cutoff P value (P = 0.05, 0.01, 0.001) and each fold-increase cutoff number f. Thus, a script $S(p,f)$ read a row from the master data set text file and copied it to another text file named $(p,f,j1,j2)$ if $e(j1)$ was significantly greater than $e(j2)$ (P value $< p$) *and* $e(j1)$ was more than f-fold greater than $e(j2)$. Therefore, genes whose $e(j1)$ was smaller than $e(j2)$ were copied to file $(p,f,j2,j1)$. The script then read the next row and repeated the process until it reached to the end of the master data set file, and text files $(p,f,j1,j2)$ were generated for all possible combinations of the four parameters. Gene expression data for the hormone starvation experiments were processed similarly.

Computer-Aided Knowledge Extraction. Medline citations that relate E2-responsive genes to estrogen, cancer, E2F1, or cell cycle were extracted from public and commercial literature databases by the OPUS knowledge extraction engine (X-Mine), which discovers meaningful relationships between gene names and the key words even when these do not appear in the title or abstract of a single publication. Extracted literature was verified manually to confirm the suggested relationships.

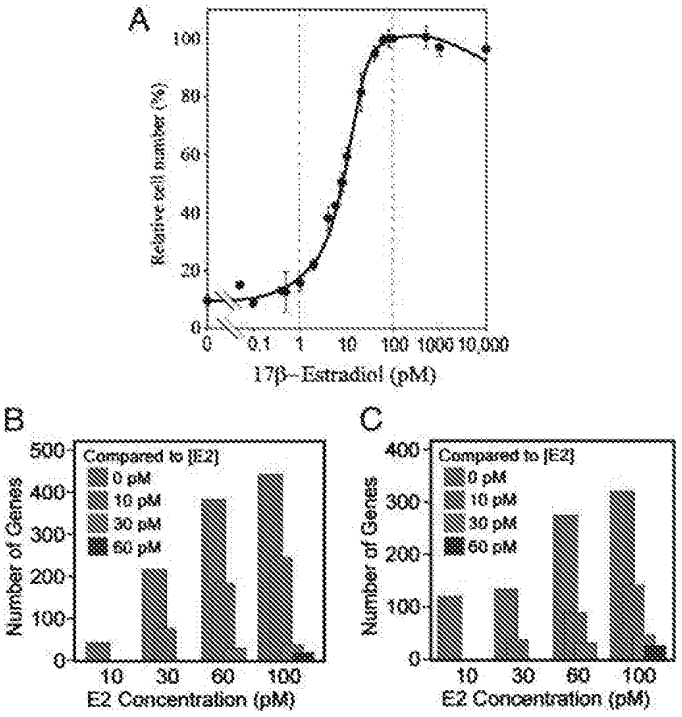


Fig. 1. Global effects of E2 on MCF7/BUS cell growth and transcriptome. (*A*) E2 dose-dependent growth profile of MCF7/BUS cells. Cells were cultured in the presence of indicated concentrations of E2 for 120 h, and cell numbers were determined. Each point represents mean ± SEM of five independent experiments. (*B* and *C*) Global profiles of sensitivities of E2-induced (*B*) and E2-suppressed (*C*) genes. BUS cells were exposed to varying concentrations of E2 for 48 h, and their transcriptome profiles were determined by DNA microarray. Columns indicate numbers of genes whose strength of mRNA expression was stronger (*B*) or weaker (*C*) [>2-fold difference and $P < 0.01$ (n = 5)] in the presence of E2 concentrations shown in the x axis than in the presence of the color-coded E2 concentrations.

Results

Determination of Numbers of Genes Induced or Suppressed by Varying Low Concentrations of E2. The BUS subline of MCF7 human breast cancer cells has been used widely for quantitative detection of low concentrations of natural and xenobiotic estrogens (5, 10). Consistent with previous studies (5, 10), BUS cells showed a highly reproducible E2 dose-dependent growth curve that showed a significant response with as low as 2 pM E2 and saturated with 80–100 pM E2 (Fig. 1*A*). The growth-stimulating effect of 100 pM E2 was completely blocked by pure antiestrogen ICI182,780 (100 nM; data not shown), indicating that E2 binding to ERs is necessary for the BUS cell growth. Western blotting detected ERα protein, but not ERβ, in BUS cells and in an MCF7 cell stock obtained from the American Type Culture Collection (data not shown). In the present study, BUS cells were not subjected to hormone starvation before E2 treatment because, in a carefully controlled xenoestrogen-free cell culture environment, the viability of BUS cells was severely impaired after complete hormone starvation beyond 48 h.

To obtain comprehensive information on effects of subsaturating concentrations of E2 on gene expression, BUS cells were exposed to 0, 10, 30, 60, and 100 pM E2 for 48 h, and their transcriptome profiles were determined by DNA microarray.

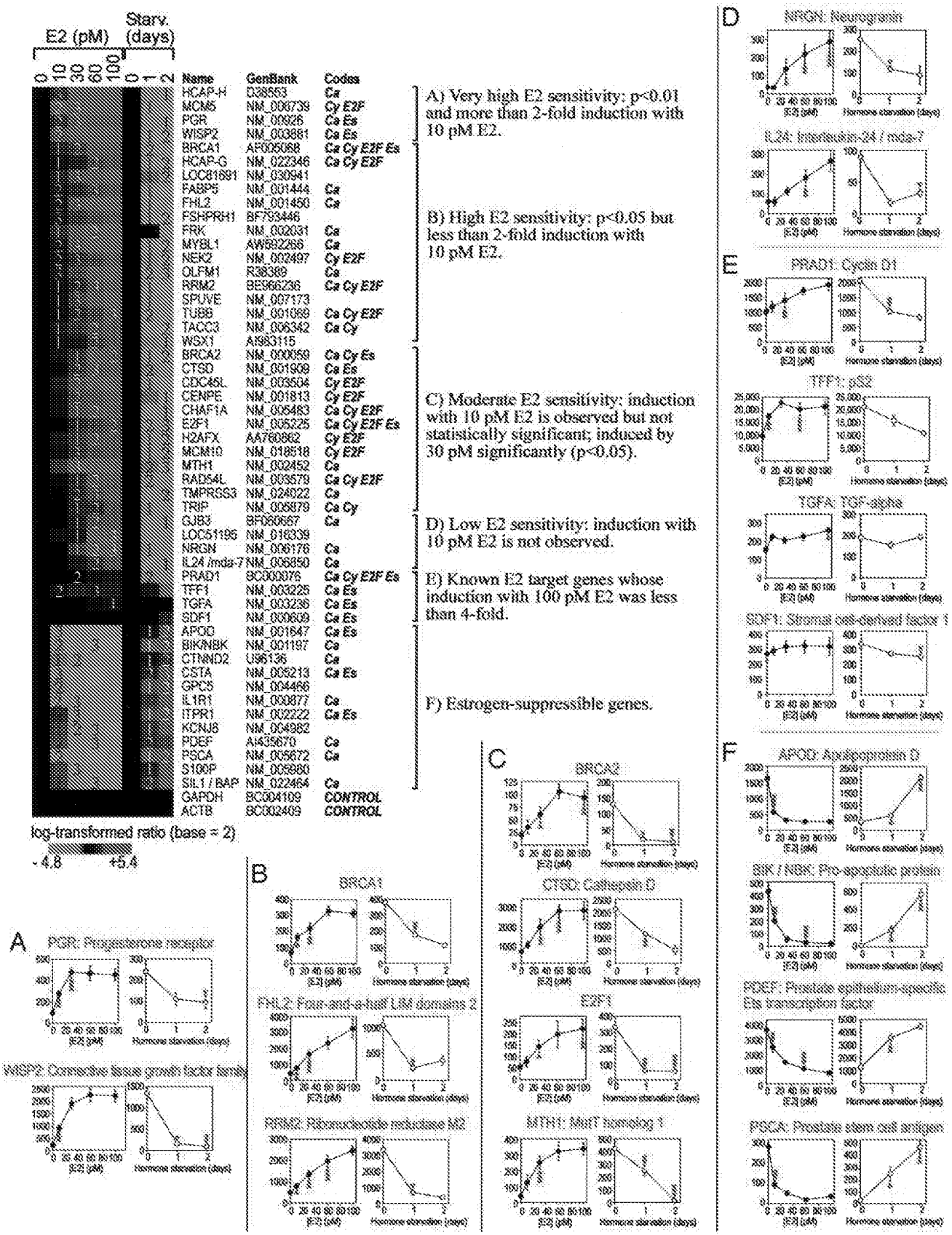


Fig. 2. E2 sensitivity analysis. Color diagram shows induction (red) and suppression (green) of genes with E2 treatment and hormone starvation. Numbers in the diagram indicate statistical significance of induction or suppression determined by Student's *t* test; namely, 1, 2, and 3 indicate $P < 0.05$, $P < 0.01$, and $P < 0.001$, respectively. Each column represents one experimental condition, and each row represents a single gene, whose name and GenBank accession number are shown. The codes indicate known relationships of each gene with estrogen, cancer, cell cycle, and E2F family transcription factors retrieved from databases

Data from five independent repeats of this experiment were compiled in a text file format, and the mean ± SEM of the signal intensity, which reflected the amount of the mRNA transcript, was calculated for each gene and each E2 concentration. The mean signal intensities were then compared between two E2 concentrations (denoted as $j1$ and $j2$), and genes whose strength of expression was significantly stronger when E2 concentration was $j1$ compared with $j2$ (cutoff P value $\leq p$) with at least f-fold changes were copied from this text file to another text file labeled with the four parameters as ($p, f, j1, j2$) ($P = 0.05$, 0.01, or 0.001; $f = 1$, 2, or 4; $j1, j2 = 0$, 10, 30, 60, or 100 pM). Thus, a text file ($p, f, j1, j2$) lists E2-inducible genes when $j1 > j2$; on the contrary, it lists E2-suppressible genes when $j1 < j2$. A set of simple Perl scripts developed in our laboratory generated these gene lists for all possible combinations of the four parameters. Effects of hormone starvation on gene expression were analyzed similarly by using a DNA microarray data set from three independent repeats of hormone starvation experiments, and another class of gene lists ($p, f, d1, d2$), where $d1$ and $d2$ represented starvation periods (0, 1, or 2 days), were generated. Importantly, a gene list ($p, f, j1, j2$) is not identical to a list generated merely by subtracting one gene list ($p, f, j2$, 0 pM) from another gene list ($p, f, j1$, 0 pM). A gene list generated by subtraction between any two other gene lists will not be associated with meaningful parameters p or f.

To understand the global aspects of E2 effects on the transcriptome, we determined numbers of genes induced or suppressed significantly in the presence of one concentration of E2 ($j1$ pM) compared with another ($j2$ pM; $j1 > j2$). Fig. 1 *B* and *C* shows examples of such analyses ($P = 0.01, f = 2; j1$ is indicated by the x axis, and $j2$ is indicated by the color-coded inset). When $j2 = 0$ pM (red columns), numbers of both E2-inducible genes (Fig. 1*B*) and E2-suppressible genes (Fig. 1*C*) increased sharply along with the increasing $j1$, as expected. However, when $j2 = 10$ pM (purple columns), numbers of E2-inducible and suppressible genes were remarkably smaller than those with $j2 = 0$ pM, although they still showed steady increase along with increasing $j1$. When $j2 = 30$ pM (blue columns) or 60 pM (dark blue columns), numbers of E2-inducible or suppressible genes were trivial. Similar results were obtained with several different cutoff values for parameters p and f. These observations may imply that preexposing cells to very low concentrations of E2 (≤ 10 pM) might exert a significant influence on the efficiency of higher concentrations of E2 (such as 100 pM) to induce or suppress genes.

Fig. 1 *B* and *C* also shows that overall profiles of the numbers of E2-inducible and E2-suppressible genes were comparable, with the former being ≈1.5- to 2-fold greater than the latter. This feature was conserved with different cutoff P values ($P = 0.05$ or 0.001; data not shown), suggesting that E2 is as potent a gene suppressor as it is an inducer. However, the numbers of genes induced or suppressed with 10 pM E2 compared with no E2 were exceptions. When three different cutoff P values ($P = 0.05$, 0.01, and 0.001) were applied, the number of E2-inducible and E2-suppressible genes were 190 vs. 602, 38 vs. 122, and 3 vs. 16, respectively, thus consistently indicating that greater numbers of genes were suppressed than induced with this lowest-end E2 concentration. Although the present analysis does not provide information on the mechanistic aspects of gene induction and suppression by E2, it is tempting to speculate that these observations could imply that recruitment of transcriptional corepressors to liganded ERα might be more efficient than recruitment of coactivators when the E2 concentration is strictly limited.

Characterization of E2 Sensitivity of E2-Inducible and E2-Suppressible Genes. We next characterized the E2 sensitivity of each E2-inducible and E2-suppressible gene by using gene lists ($P = 0.05$, $f = 4, j1$, 0 pM) and ($P = 0.05, f = 4, d1$, 0 day) ($j1 = 0$, 10, 30, 60, 100 pM; $d1 = 0$, 1, 2 days). As shown in Fig. 2, mRNA expression of E2-inducible genes was enhanced with increasing E2 concentrations and, conversely, suppressed during hormone starvation. These genes were categorized into four classes of E2 sensitivity, namely, genes showing (*i*) significant ($P < 0.01$) and >2-fold induction with 10 pM E2 (class A); (*ii*) significant ($P < 0.05$) but <2-fold induction with 10 pM E2 (class B); (*iii*) significant ($P < 0.05$) induction with 30 pM E2 but not with 10 pM E2, although there were slight increases in amounts of mRNA transcripts with 10 pM E2 (class C); and (*iv*) no apparent changes in amounts of mRNA transcripts with 10 pM E2 (class D). Class E included several known E2 target genes that were not identified as E2-inducible genes with the strict criteria used to define other classes. Similarly, the mRNA expression profiles of E2-suppressible genes (class F) showed reduction along with increasing E2 concentration and enhancement during hormone starvation. Thus, Fig. 2 concisely shows the three attributes of E2 sensitivity, namely, the minimum E2 concentration required for significant gene induction or suppression, the E2 concentration that saturates transcriptional effects, and the shape of the E2 dose–response curve of gene expression. Moreover, computer-aided knowledge extraction demonstrated that many E2-regulated genes identified in the present study have been reported as genes related to cancer and/or cell cycle regulation (Fig. 2, codes).

E2 Sensitivity Analysis Revealed Dissociation Between E2 Induction of Autocrine Growth Factors and E2 Dose-Dependent Growth Profile of MCF7/BUS Cells. Transforming growth factor-α (TGF-α) and stromal cell derived factor-1 (SDF-1) have been reported as E2-inducible autocrine growth factors that support E2-dependent growth of MCF7 cells (14, 15). Therefore, the apparent absence of induction of the mRNA transcripts for these genes with up to 100 pM E2 (Fig. 2, class E) seemed contradictory because MCF7/BUS cell growth was enhanced with 2–80 pM E2 (Fig. 1*A*). Semiquantitative RT-PCR analysis, which was performed with limited cycles of amplification that did not reach to saturation, confirmed E2 dose-dependent induction and hormone starvation-dependent reduction of the mRNA transcripts for well-established E2 target genes *CTSD/Cathepsin D* and *WISP2*, whereas expression of the mRNA transcripts for control gene *GAPDH* was not affected by either E2 treatment or hormone starvation (Fig. 3*A*). When analyzed similarly, weak and consistent expression of the TGF-α mRNA transcript was observed with no evidence of influence of E2 treatment or hormone starvation (Fig. 3*A*), and this observation was persistent with several different numbers of PCR amplification cycles (data not shown). On the other hand, mRNA transcript for SDF-1 was not detected at all with varying conditions of RT-PCR (Fig. 3*A*). These results confirmed the DNA microarray data that had indicated that neither low concentrations of E2 (≤ 100 pM) nor hormone starvation exerted any significant influence on expression of the mRNA transcripts for TGF-α and SDF-1 genes.

by a computer-aided knowledge extraction engine and denoted by symbols *Es*, *Ca*, *Cy*, and *E2F*, respectively. (*A–F*) Classes A–F are defined based on the E2 sensitivity of genes, and details of the mRNA expression profiles of representative genes for each class are presented as paired line graphs. The left of each pair (filled symbols) shows the E2 dose–response profile ($n = 5$); right graphs (open symbols) shows profile of hormone starvation ($n = 3$). Each data point represents mean ± SEM. Single, double, and triple arrowheads indicate $P \leq 0.05$, 0.01, and 0.001, respectively. Detailed mRNA expression profiles of all of the genes shown in the color diagram are in Fig. 4, which is published as supporting information on the PNAS web site.

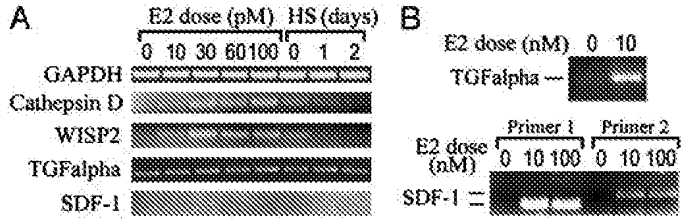


Fig. 3. mRNA expression profiles of E2-inducible genes with high or low E2 sensitivities: Semiquantitative RT-PCR. (*A*) mRNA expression in BUS cells exposed to the indicated concentrations of E2 for 48 h or hormone-starved (HS) for up to 2 days. (*B*) Expression of TGF-α and SDF-1 mRNA transcripts in BUS cells exposed to 10 or 100 nM E2 for 48 h. Primer pair 1 for SDF-1 detection was used for the experiment of *A*.

Because experiments described in previous reports that characterized TGF-α and SDF-1 as E2-inducible autocrine growth factors used 10 nM E2 [a concentration that was >100 times greater than that which saturated the E2 dose-dependent growth curves of MCF7 cells (5) and MCF7/BUS cells (Fig. 1*A*)] we presumed that induction of the mRNA transcripts for these genes might require higher E2 concentrations than we had in the DNA microarray experiments. In fact, TGF-α mRNA transcripts were strongly induced with 10 nM E2 (Fig. 3*B*; the apparent absence of the RT-PCR product for the cells cultured in the absence of E2 was caused by the reduction of the PCR cycle number applied to avoid PCR saturation). The SDF-1 mRNA transcripts were also induced dramatically when cells were exposed to 10 nM E2 and 100 nM E2 (Fig. 3*B*). Specific detection of the SDF-1 mRNA was confirmed by using two different pairs of PCR primers. These results indicated that E2-dependent induction of the TGF-α and SDF-1 mRNA transcripts required an E2 concentration that was far higher than an E2 concentration that saturated the E2 dose-dependent growth curve of MCF7/BUS cells.

Discussion

Information on ligand sensitivity of E2-inducible and E2-suppressible genes may provide important insights into not only the biological actions of E2 itself but also factors that influence E2 effects such as expression of ER coregulator proteins (9, 16), ER interactions with other signaling pathways (1), and the presence of other estrogenic agonists and antagonists such as selective ER modulators or xenobiotic estrogens. To obtain systematic data on E2 sensitivity of large numbers of genes, in the present study we designed a simple method for determining E2 sensitivity of gene expression by using Affymetrix DNA microarray and Perl scripts and applied it to characterize the E2 responses of ERα-positive MCF7/BUS human breast cancer cells. In this study, the E2 exposure time was fixed to 48 h, when expression of the mRNA transcripts for several representative E2 target genes (e.g., progesterone receptor or WISP2; see Fig. 2) reached a maximum level after E2 stimulation (time course data not shown). Characterization of the combined aspects of the ligand sensitivity and the time course of E2 effects on the transcriptome is an important issue and should be addressed in future studies.

The present E2 sensitivity analysis identified a number of known E2 target genes successfully as indicated with code ***Es*** in Fig. 2, supporting the validity of our approach and method. The list of E2-inducible genes also included many genes involved in cell cycle progression and cancer as indicated by codes ***Cy***, ***E2F***, and ***Ca*** in Fig. 2; induction of some of these genes may involve BRCA1 and/or E2F1, which are E2-inducible transcription factors and key regulators of cell cycle and carcinogenesis (see Fig. 2 and refs. 17 and 18). On the other hand, *cyclin D1* and *c-MYC*, two representative E2-inducible genes in human breast cancer cells, were not picked, although cyclin D1 mRNA expression showed a moderate increase with increasing E2 concentration (Fig. 2, class E). This increase is likely caused by the transient nature of induction of their mRNA transcripts, which peaks at ≈8 h after E2 exposure and decreases thereafter (19, 20). We also attempted to identify genes whose E2 dose-dependent curves of mRNA expression showed U-shape or inverted U-shape. However, analyses using several different criteria identified only false positives, whose nonstandard mRNA expression profiles were not confirmed by RT-PCR (data not shown).

A number of additional E2-inducible and E2-suppressible genes have been identified in the present study (Fig. 2), although some of them may not be direct targets of ERs. Elucidation of mechanisms of the E2 responsiveness of their mRNA expression and the biological significance of such regulation awaits further studies. Among these genes, the *FHL2/four-and-a-half LIM domains 2* (Fig. 2, class B) is especially interesting because this gene encodes a transcriptional coactivator for AP-1 (21) and β-catenin (22). The *FHL2* induction with E2 may imply possible interactions between the E2 actions and the mitogen-activated protein kinase signaling pathway (which involves formation of the AP-1 transcription factor) and/or Wnt signaling pathway (which involves stabilization of β-catenin transcriptional coactivator). Another interesting gene was *ribonucleotide reductase M2 (RRM2)*, which encodes the rate-limiting enzyme of deoxyribonucleotide production during DNA synthesis. It has been reported that RRM2 mRNA transcripts are inducible by E2F proteins (23) and BRCA1 (24). Moreover, a recent study identified *RRM2* as a marker gene whose expression was stronger in invasive ductal carcinoma breast cancers than the ductal carcinoma *in situ* (25). These observations suggest a potential importance of RRM2 in growth and malignancy of breast cancer cells, and it would be interesting to determine whether the E2 sensitivity of *RRM2* gene changes during the malignant progression of breast cancers.

Previous studies have reported that TGF-α and SDF-1 are E2-inducible autocrine growth factors for ERα-positive human breast cancer cells. The mRNA transcripts for both TGF-α (14) and SDF-1 (15) were strongly induced in MCF7 cells with 10 nM E2. Suppression of TGF-α production by small interfering RNA (14), and blocking the secreted SDF-1 peptide by a neutralizing antibody (15), resulted in significant inhibition of the E2-dependent growth of this cell line. However, although we were able to reproduce the induction of these mRNA transcripts in MCF7/BUS cells with 10–100 nM E2 (Fig. 3*B*), we also found that lower E2 concentrations that enhanced cell growth in a dose-dependent manner (i.e., 2–80 nM; Fig. 1*A*) did not affect mRNA expression of these factors (Figs. 2*E* and 3*A*). Data shown in Fig. 3*A* rather suggested weak and consistent expression of TGF-α when cells were growing in the presence of subsaturating concentrations of E2. Interestingly, it has been proposed recently that TGF-α may enhance E2 sensitivity of MCF7 cells up to 10–100 times through activating the mitogen-activated protein kinase signaling pathway and, thereby, might facilitate E2-dependent cell growth (6). Moreover, we recently demonstrated that an ER coactivator CITED1 selectively enhanced the E2-dependent induction of the TGF-α mRNA transcript without affecting expression of pS2 mRNA transcript (E2 concentration was 10 nM) (26). Taken together, these observations may imply that induction of TGF-α might be regulated at the level of E2 sensitivity, which is determined by the availability of ER coactivators, and that TGF-α may function as an autocrine modifier of the growth-stimulating effects of E2 rather than as a classical autocrine growth factor. On the other hand, the inability to detect the SDF-1 mRNA in the presence of subsaturating concentrations of E2 (Fig. 3*A*) may suggest that

this factor could function as an autocrine growth factor only when the cancer cells are exposed to saturating concentrations of E2, a situation that may occur in premenopausal women. Further studies are necessary to clarify the biological roles of these factors in relation to the E2 dose-dependent growth of breast cancer cells.

DNA microarray data analysis is a growing field of science, and there are a number of software designed specifically for this application. However, it is not uncommon that specifications of such software do not exactly fit for the experimental design and objectives of a research project. In the present study, we used the Perl programming language to generate simple scripts to implement the algorithm of data processing. Recently, the use of Perl in biological research has been becoming increasingly popular (13), and the present study, together with some studies from other laboratories (27), has demonstrated the usefulness of the Perl scripting technique in DNA microarray data analysis. Although complicated methods of DNA microarray data analysis, such as unsupervised clustering, would require a complete software package, Perl scripting seems convenient and effective for the purpose of quickly implementing simple algorithms that are often sufficient to extract meaningful information from DNA microarray data.

In summary, we have designed a method for characterizing E2 sensitivity of large numbers of genes expressed in cell culture by using DNA microarray and Perl scripting. By applying this method to ERα-positive MCF7/BUS human breast cancer cells, we performed a comprehensive E2 sensitivity analysis and identified a number of E2-responsive genes. The importance of E2 sensitivity analysis was exemplified by the finding that E2 concentration required to induce the mRNA transcripts for TGF-α and SDF-1, two representative E2-inducible autocrine growth factors of MCF7 cells, was actually far greater than the E2 concentration that saturated the E2 dose-dependent MCF7/BUS growth curve.

We thank Ana Soto and Carlos Sonnenschein for providing MCF7/BUS cells and technical advice and Emmett Schmidt, Nick Dyson, Dennis Sgroi, and Myles Brown for helpful discussions and critiques. This work was supported by the Avon Breast Cancer Program and National Institutes of Health Grant R01-CA82230 (to T.S.).

1. Pedram, A., Razandi, M., Aitkenhead, M., Hughes, C. C. & Levin, E. R. (2002) *J. Biol. Chem.* **277**, 50768–50775.
2. Levenson, A. S., Svoboda, K. M., Pease, K. M., Kaiser, S. A., Chen, B., Simons, L. A., Jovanovic, B. D., Dyck, P. A. & Jordan, V. C. (2002) *Cancer Res.* **62**, 4419–4426.
3. Soulez, M. & Parker, M. G. (2001) *J. Mol. Endocrinol.* **27**, 259–274.
4. Inoue, A., Yoshida, N., Omoto, Y., Oguchi, S., Yamori, T., Kiyama, R. & Hayashi, S. (2002) *J. Mol. Endocrinol.* **29**, 175–192.
5. Villalobos, M., Olea, N., Brotons, J. A., Olea-Serrano, M. F., Ruiz de Almodovar, J. M. & Pedraza, V. (1995) *Environ. Health Perspect.* **103**, 844–850.
6. Yue, W., Wang, J. P., Conaway, M., Masamura, S., Li, Y. & Santen, R. J. (2002) *Endocrinology* **143**, 3221–3229.
7. Nardulli, A. M., Romine, L. E., Carpo, C., Greene, G. L. & Rainish, B. (1996) *Mol. Endocrinol.* **10**, 694–704.
8. Klinge, C. M. (2001) *Nucleic Acids Res.* **29**, 2905–2919.
9. Shang, Y. & Brown, M. (2002) *Science* **295**, 2465–2468.
10. Soto, A. M., Sonnenschein, C., Chung, K. L., Fernandez, M. F., Olea, N. & Serrano, F. O. (1995) *Environ. Health Perspect.* **103**, Suppl. 7, 113–122.
11. Jagota, A. (2001) *Microarray Data Analysis and Visualization* (Bioinformatics-By-the-Bay Press, Santa Cruz, CA).
12. Affymetrix (2003) *GeneChip Expression Analysis* (Affymetrix, Santa Clara, CA).
13. Stajich, J. E., Block, D., Boulez, K., Brenner, S. E., Chervitz, S. A., Dagdigian, C., Fuellen, G., Gilbert, J. G., Korf, I., Lapp, H., *et al.* (2002) *Genome Res.* 12, 1611–1618.
14. Kenney, N. J., Saeki, T., Gottardis, M., Kim, N., Garcia-Morales, P., Martin, M. B., Normanno, N., Ciardiello, F., Day, A., Cutler, M. L., *et al.* (1993) *J. Cell Physiol.* **156**, 497–514.
15. Hall, J. M. & Korach, K. S. (2003) *Mol. Endocrinol.* **17**, 792–803.
16. Shang, Y., Hu, X., DiRenzo, J., Lazar, M. A. & Brown, M. (2000) *Cell* **103**, 843–852.
17. Spillman, M. A. & Bowcock, A. M. (1996) *Oncogene* **13**, 1639–1645.
18. Wang, W., Dong, L., Saville, B. & Safe, S. (1999) *Mol. Endocrinol.* **13**, 1373–1387.
19. Prall, O. W., Sarcevic, B., Musgrove, E. A., Watts, C. K. & Sutherland, R. L. (1997) *J. Biol. Chem.* **272**, 10882–10894.
20. Jeng, M. H., Shupnik, M. A., Bender, T. P., Westin, E. H., Bandyopadhyay, D., Kumar, R., Masamura, S. & Santen, R. J. (1998) *Endocrinology* **139**, 4164–4174.
21. Morlon, A. & Sassone-Corsi, P. (2003) *Proc. Natl. Acad. Sci. USA* **100**, 3977–3982.
22. Wei, Y., Renard, C. A., Labalette, C., Wu, Y., Levy, L., Neuveut, C., Prieur, X., Flajolet, M., Prigent, S. & Buendia, M. A. (2003) *J. Biol. Chem.* **278**, 5188–5194.
23. Ishida, S., Huang, E., Zuzan, H., Spang, R., Leone, G., West, M. & Nevins, J. R. (2001) *Mol. Cell. Biol.* **21**, 4684–4699.
24. Welcsh, P. L., Lee, M. K., Gonzalez-Hernandez, R. M., Black, D. J., Mahadevappa, M., Swisher, E. M., Warrington, J. A. & King, M. C. (2002) *Proc. Natl. Acad. Sci. USA* **99**, 7560–7565.
25. Ma, X. J., Salunga, R., Tuggle, J. T., Gaudet, J., Enright, E., McQuary, P., Payette, T., Pistone, M., Stecker, K., Zhang, B. M., *et al.* (2003) *Proc. Natl. Acad. Sci. USA* **100**, 5974–5979.
26. Yahata, T., Shao, W., Endoh, H., Hur, J., Coser, K. R., Sun, H., Ueda, Y., Kato, S., Isselbacher, K. J., Brown, M. & Shioda, T. (2001) *Genes Dev.* **15**, 2598–2612.
27. Dudley, A. M., Aach, J., Steffen, M. A. & Church, G. M. (2002) *Proc. Natl. Acad. Sci. USA* **99**, 7554–7559.

ARTICLE

OPEN

doi:10.1038/nature12113

Integrated genomic characterization of endometrial carcinoma

The Cancer Genome Atlas Research Network*

We performed an integrated genomic, transcriptomic and proteomic characterization of 373 endometrial carcinomas using array- and sequencing-based technologies. Uterine serous tumours and ~25% of high-grade endometrioid tumours had extensive copy number alterations, few DNA methylation changes, low oestrogen receptor/progesterone receptor levels, and frequent *TP53* mutations. Most endometrioid tumours had few copy number alterations or *TP53* mutations, but frequent mutations in *PTEN*, *CTNNB1*, *PIK3CA*, *ARID1A* and *KRAS* and novel mutations in the SWI/SNF chromatin remodelling complex gene *ARID5B*. A subset of endometrioid tumours that we identified had a markedly increased transversion mutation frequency and newly identified hotspot mutations in *POLE*. Our results classified endometrial cancers into four categories: *POLE* ultramutated, microsatellite instability hypermutated, copy-number low, and copy-number high. Uterine serous carcinomas share genomic features with ovarian serous and basal-like breast carcinomas. We demonstrated that the genomic features of endometrial carcinomas permit a reclassification that may affect post-surgical adjuvant treatment for women with aggressive tumours.

Endometrial cancer arises from the lining of the uterus. It is the fourth most common malignancy among women in the United States, with an estimated 49,500 new cases and 8,200 deaths in 2013 (ref. 1). Most patients present with low-grade, early-stage disease. The majority of patients with more aggressive, high-grade tumours who have disease spread beyond the uterus will progress within 1 year (refs 2, 3). Endometrial cancers have been broadly classified into two groups[4]. Type I endometrioid tumours are linked to oestrogen excess, obesity, hormone-receptor positivity, and favourable prognosis compared with type II, primarily serous, tumours that are more common in older, non-obese women and have a worse outcome. Early-stage endometrioid cancers are often treated with adjuvant radiotherapy, whereas serous tumours are treated with chemotherapy, similar to advanced-stage cancers of either histological subtype. Therefore, proper subtype classification is crucial for selecting appropriate adjuvant therapy.

Several previous reports suggest that *PTEN* mutations occur early in the neoplastic process of type I tumours and co-exist frequently with other mutations in the phosphatidylinositol-3-OH kinase (PI(3)K)/AKT pathway[5,6]. Other commonly mutated genes in type I tumours include *FGFR2*, *ARID1A*, *CTNNB1*, *PIK3CA*, *PIK3R1* and *KRAS*[7–9]. Microsatellite instability (MSI) is found in approximately one-third of type I tumours, but is infrequent in type II tumours[10]. *TP53*, *PIK3CA* and *PPP2R1A* mutations are frequent in type II tumours[11,12]. Most of these studies have been limited to DNA sequencing only with samples of heterogeneous histological subtypes and tumour grades. We present a comprehensive, multiplatform analysis of 373 endometrial carcinomas including low-grade endometrioid, high-grade endometrioid, and serous carcinomas. This integrated analysis provides key molecular insights into tumour classification, which may have a direct effect on treatment recommendations for patients, and provides opportunities for genome-guided clinical trials and drug development.

Results

Tumour samples and corresponding germline DNA were collected from 373 patients, including 307 endometrioid and 66 serous (53) or mixed histology (13) cases. Local Institutional Review Boards approved all tissue acquisition. The clinical and pathological characteristics of the samples generally reflect a cross-section of individuals with recurrent endometrial cancer[2,3] (Supplementary Table 1.1). The median follow-up of the cohort was 32 months (range, 1–195 months); 21% of the patients have recurred, and 11% have died. Comprehensive molecular analyses were performed at independent centres using six genomic or proteomic platforms (Supplementary Table 1.2). MSI testing performed on all samples using seven repeat loci (Supplementary Table 1.3) found MSI in 40% of endometrioid tumours and 2% of serous tumours.

Somatic copy number alterations

Somatic copy number alterations (SCNAs) were assessed in 363 endometrial carcinomas. Unsupervised hierarchical clustering grouped the tumours into four clusters (Fig. 1a). The first three copy-number clusters were composed almost exclusively (97%) of endometrioid tumours without significant differences in tumour grades. Cluster 1 tumours were nearly devoid of broad SCNAs, averaging less than 0.5% genome alteration, with no significant recurrent events. Cluster 1 tumours also had significantly increased non-synonymous mutation rates compared to all others (median 7.2×10^{-6} versus 1.7×10^{-6} mutations per megabase (Mb), $P < 0.001$). Copy-number clusters 2 and 3 consisted mainly of endometrioid tumours, distinguished by more frequent 1q amplification in cluster 3 than cluster 2 (100% of cluster 3 tumours versus 33% of cluster 2 tumours) and worse progression-free survival ($P = 0.003$, log-rank versus clusters 1 and 2; Fig. 1b).

Most of the serous (50 out of 53; 94%) and mixed histology (8 out of 13; 62%) tumours clustered with 36 (12%) of the 289 endometrioid tumours, including 24% of grade 3 and 5% of grade 1 or 2, into copy-number cluster 4; a single group characterized by a very high degree of SCNAs (Supplementary Fig. 2.1; focal SCNAs with false discovery rate (FDR) < 0.15, and Supplementary Data 2.1). Cluster 4 tumours were characterized by significantly recurrent previously reported focal amplifications of the oncogenes *MYC* (8q24.12), *ERBB2* (17q12) and *CCNE1* (19q12)[13], and by SCNAs previously unreported in endometrial cancers including those containing *FGFR3* (4p16.3) and *SOX17* (8q11.23). Cluster 4 tumours also had frequent *TP53* mutations (90%),

*Lists of participants and their affiliations appear at the end of the paper.

©2013 Macmillan Publishers Limited. All rights reserved

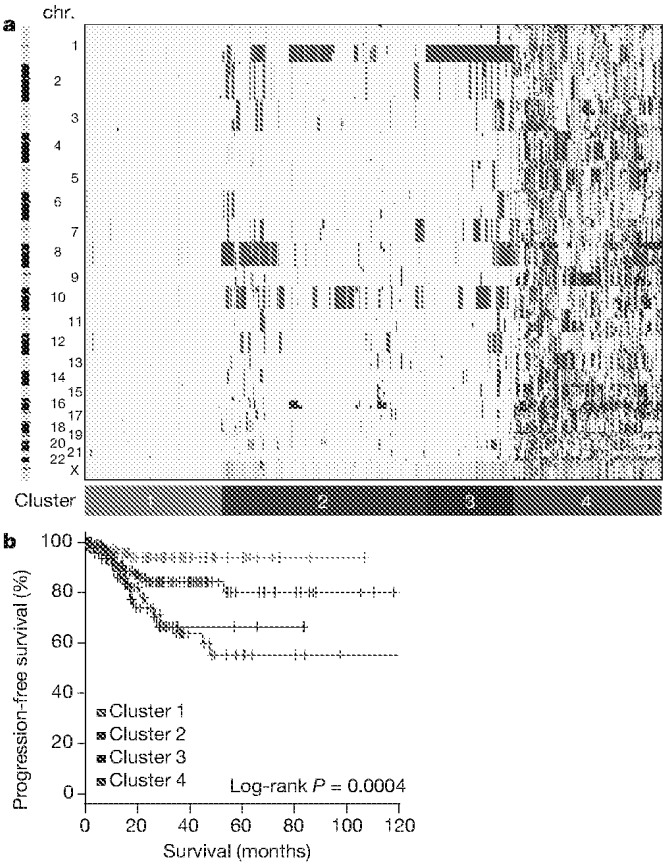


Figure 1 | SCNAs in endometrial carcinomas. a, Tumours were hierarchically clustered into four groups based on SCNAs. The heat map shows SCNAs in each tumour (horizontal axis) plotted by chromosomal location (vertical axis). Chr., chromosome. **b**, Kaplan–Meier curves of progression-free survival for each copy-number cluster.

little MSI (6%), and fewer *PTEN* mutations (11%) than other endometrioid tumours (84%). Overall, these findings suggest that a subset of endometrial tumours contain distinct patterns of SCNAs and mutations that do not correlate with traditional tumour histology or grade.

As expected, tumours in the 'serous-like' cluster (cluster 4) had significantly worse progression-free survival than tumours in the endometrioid cluster groups ($P = 0.003$, log-rank, Fig. 1b). Potential therapeutically relevant SCNAs included the cluster 2 15q26.2 focal amplification, which contained *IGF1R*; and cluster 4 amplifications of *ERBB2*, *FGFR1* and *FGFR3*, and *LRP1B* deletion, which was recently associated with resistance to liposomal doxorubicin in serous ovarian cancer[14].

Exome sequence analysis

We sequenced the exomes of 248 tumour/normal pairs. On the basis of a combination of somatic nucleotide substitutions, MSI and SCNAs, the endometrial tumours were classified into four groups (Fig. 2a, b): (1) an ultramutated group with unusually high mutation rates (232×10^{-6} mutations per Mb) and a unique nucleotide change spectrum; (2) a hypermutated group (18×10^{-6} mutations per Mb) of MSI tumours, most with *MLH1* promoter methylation; (3) a group with lower mutation frequency (2.9×10^{-6} mutations per Mb) and most of the microsatellite stable (MSS) endometrioid cancers; and (4) a group that consists primarily of serous-like cancers with extensive SCNA (copy-number cluster 4) and a low mutation rate (2.3×10^{-6} mutations per Mb). The ultramutated group consisted of 17 (7%) tumours exemplified by an increased C→A transversion frequency, all with mutations in the exonuclease domain of *POLE*, and an improved progression-free survival (Fig. 2a, c). *POLE* is a catalytic subunit of DNA polymerase epsilon involved in nuclear DNA replication and repair. We identified hotspot mutations in *POLE* at Pro286Arg and Val411Leu present in 13 (76%) of the 17 ultramutated samples. Significantly mutated genes (SMGs) identified at low FDRs (Q) in this subset included *PTEN* (94%, $Q = 0$), *PIK3R1* (65%, $Q = 8.3 \times 10^{-7}$), *PIK3CA* (71%, $Q = 9.1 \times 10^{-5}$), *FBXW7* (82%, $Q = 1.4 \times 10^{-4}$), *KRAS* (53%, $Q = 9.2 \times 10^{-4}$) and *POLE* (100%, $Q = 4.2 \times 10^{-3}$). Mutation rates in *POLE* mutant endometrial and previously reported ultramutated colorectal tumours exceeded those found in any other lineage including lung cancer and melanoma[15–17]. Germline susceptibility variants have been reported in *POLE* (Leu424Val) and *POLD1* (Ser478Asn), but were not found in our endometrial normal exome-seq reads[18].

The MSI endometrioid tumours had a mutation frequency approximately tenfold greater than MSS endometrioid tumours, few SCNAs, frameshift deletions in *RPL22*, frequent non-synonymous *KRAS* mutations, and few mutations in *FBXW7*, *CTNNB1*, *PPP2R1A* and *TP53*. The MSS, copy-number low, endometrioid tumours had an unusually high frequency of *CTNNB1* mutations (52%); the only gene with a higher mutation frequency than the MSI samples. The copy-number high group contained all of the remaining serous cases and one-quarter of the grade 3 endometrioid cases. Most of these tumours had *TP53* mutations and a high frequency of *FBXW7* (22%, $Q = 0$) and *PPP2R1A* (22%, $Q = 1.7 \times 10^{-16}$) mutations, previously reported as common in uterine serous but not endometrioid carcinomas. Thus, a subset of high-grade endometrioid tumours had similar SCNAs and mutation spectra as uterine serous carcinomas, suggesting that these patients might benefit from treatment approaches that parallel those for serous tumours.

There were 48 genes with differential mutation frequencies across the four groups (Fig. 2d and Supplementary Data 3.1). *ARID5B*, a member of the same AT-rich interaction domain (ARID) family as *ARID1A*, was more frequently mutated in MSI (23.1%) than in either MSS endometrioid (5.6%) or high SCNA serous tumours (0%), a novel finding for endometrial cancer. Frameshifting *RPL22* indels near a homopolymer at Lys 15 were almost exclusively found in the MSI group (36.9%). The *TP53* mutation frequency (>90%) in serous tumours differentiated them from the endometrioid subtypes (11.4%). However, many (10 out of 20; 50%) endometrioid tumours with a non-silent *TP53* mutation also had non-silent mutations in *PTEN*, compared to only 1 out of 39 (2.6%) serous tumours with non-silent *TP53* mutations. Although *TP53* mutations are not restricted to serous tumours, the co-existing *PTEN* mutations in the endometrioid cases suggest a distinct tumorigenic mechanism.

Comparisons of 66 SMGs between traditional histological subtypes are provided (Supplementary Methods 3), and SMGs across other subcohorts can be found in Supplementary Data 3.2. The spectrum of *PIK3CA* and *PTEN* mutations in endometrial cancer also differed from other solid tumours (Supplementary Methods 3). Integrated analysis may be useful for identifying histologically misclassified cases. For example, a single serous case was identified without a *TP53* mutation or extensive SCNAs and with a *KRAS* mutation and high mutation rate. After re-review of the histological section, the case was deemed consistent with a grade 3 endometrioid tumour, demonstrating how molecular analysis could reclassify tumour histology and potentially affect treatment decisions.

Multiplatform subtype classifications

All of the endometrial tumours were examined for messenger RNA expression ($n = 333$), protein expression ($n = 293$), microRNA expression ($n = 367$), and DNA methylation ($n = 373$) (Supplementary Methods 4–7). Unsupervised k-means clustering of mRNA expression from RNA sequencing identified three robust clusters termed 'mitotic', 'hormonal' and 'immunoreactive' (Supplementary Fig. 4.1) that were significantly correlated with the four integrated clusters; *POLE*, MSI, copy-number low and copy-number high ($P < 0.0001$). Supervised analysis identified signature genes of the *POLE* cluster ($n = 17$) mostly involved in cellular metabolism (Fig. 3a). Among the few signature genes

©2013 Macmillan Publishers Limited. All rights reserved

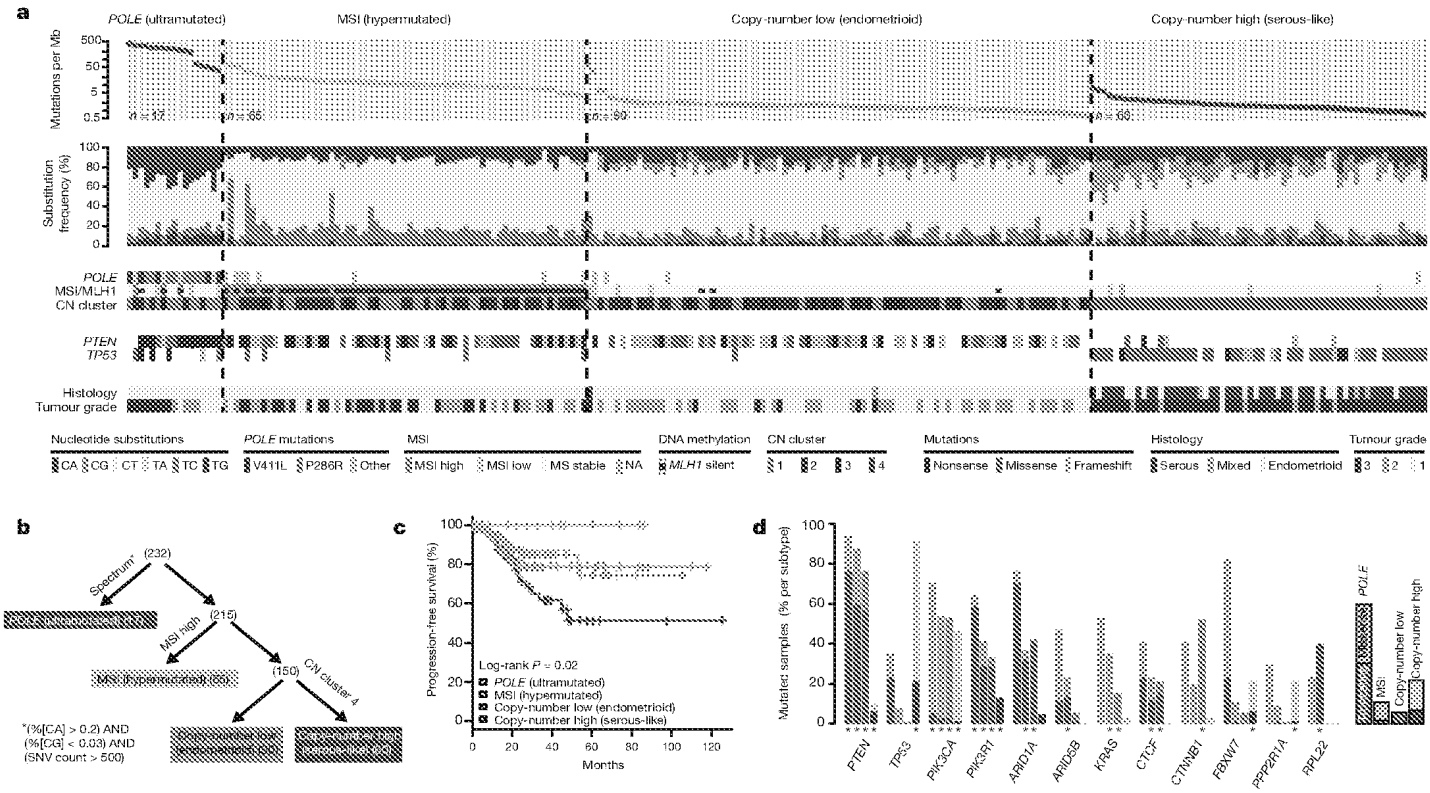


Figure 2 | Mutation spectra across endometrial carcinomas. a, Mutation frequencies (vertical axis, top panel) plotted for each tumour (horizontal axis). Nucleotide substitutions are shown in the middle panel, with a high frequency of C-to-A transversions in the samples with *POLE* exonuclease mutations. CN, copy number. **b**, Tumours were stratified into the four groups by (1) nucleotide substitution frequencies and patterns, (2) MSI status, and (3) copy-number cluster. SNV, single nucleotide variant. **c**, *POLE*-mutant tumours have significantly better progression-free survival, whereas copy-number high tumours have the poorest outcome. **d**, Recurrently mutated genes are different between the four subgroups. Shown are the mutation frequencies of all genes that were significantly mutated in at least one of the four subgroups (MUSiC, asterisk denotes FDR < 0.05).

in the MSI cluster was decreased *MLH1* mRNA expression, probably due to its promoter methylation. Increased progesterone receptor (*PGR*) expression was noted in the copy-number low cluster, suggesting responsiveness to hormonal therapy. The copy-number high cluster, which included most of the serous and serous-like endometrioid tumours, exhibited the greatest transcriptional activity exemplified by increased cell cycle deregulation (for example, *CCNE1*, *PIK3CA*, *MYC* and *CDKN2A*) and *TP53* mutation (Supplementary Figs 4.2 and 4.3). This is consistent with reports that increased CDKN2A can distinguish serous from endometrioid carcinomas[19]. Approximately 85% of cases in the copy-number high cluster shared membership with the 'mitotic' mRNA subtype.

Supervised clustering of the reverse phase protein array (RPPA) expression data was consistent with loss of function for many of the mutated genes (Fig. 3b). *TP53* was frequently mutated in the copy-number high group ($P = 2.5 \times 10^{-27}$) and its protein expression was also increased, suggesting that these mutations are associated with increased expression. By contrast, *PTEN* ($P = 2.8 \times 10^{-19}$) and *ARID1A* ($P = 1.2 \times 10^{-6}$) had high mutation rates in the remaining groups, but their expression was decreased, suggesting inactivating mutations in both genes. The copy-number high group also had decreased levels of phospho-AKT, consistent with downregulation of the AKT pathway. The copy-number low group had raised RAD50 expression, which is associated with DNA repair, explaining some of the differences between the copy-number high and low groups. The *POLE* group had high expression of ASNS and CCNB1, whereas the MSI tumours had both high phospho-AKT and low PTEN expression.

Unsupervised clustering of DNA methylation data generated from Illumina Infinium DNA methylation arrays revealed four unique subtypes (MC1–4) that support the four integrative clusters. A heavily methylated subtype (MC1) reminiscent of the CpG island methylator phenotype (CIMP) described in colon cancers and glioblastomas[20–22] was associated with the MSI subtype and attributable to promoter hypermethylation of *MLH1*. A serous-like cluster (MC3) with minimal DNA methylation changes was composed primarily of serous tumours and some endometrioid tumours (Supplementary Fig. 7.1) and contained most of the copy-number high tumours.

Integrative clustering using the iCluster framework returned two major clusters split primarily on serous and endometrioid histology highlighting *TP53* mutations, lack of *PTEN* mutation and encompassing almost exclusively copy-number high tumours[23] (Supplementary Fig. 8.1). We developed a new clustering algorithm, called SuperCluster, to derive overall subtypes based on sample cluster memberships across all data types (Supplementary Fig. 9.1). SuperCluster identified four clusters that generally confirmed the contributions of individual platforms to the overall integrated clusters. No major batch effects were identified for any platform (Supplementary Methods 10).

Structural aberrations

To identify somatic chromosomal aberrations, we performed low-pass, paired-end, whole-genome sequencing on 106 tumours with matched normals. We found recurrent translocations involving genes in several pathways including WNT, EGFR–RAS–MAPK, PI(3)K, protein kinase A, retinoblastoma and apoptosis. The most frequent translocations (5 out of 106) involved a member of the BCL family (*BCL2*, *BCL7A*, *BCL9* and *BCL2L11*). Four of these were confirmed by identification of the translocation junction point and two were also confirmed by high-throughput RNA sequencing (RNA-Seq). In all cases the translocations result in in-frame fusions and are predicted to result in activation or increased expression of the BCL family members (Supplementary Fig. 3.2). Translocations involving members of the BCL family leading to reduced apoptosis have been

©2013 Macmillan Publishers Limited. All rights reserved

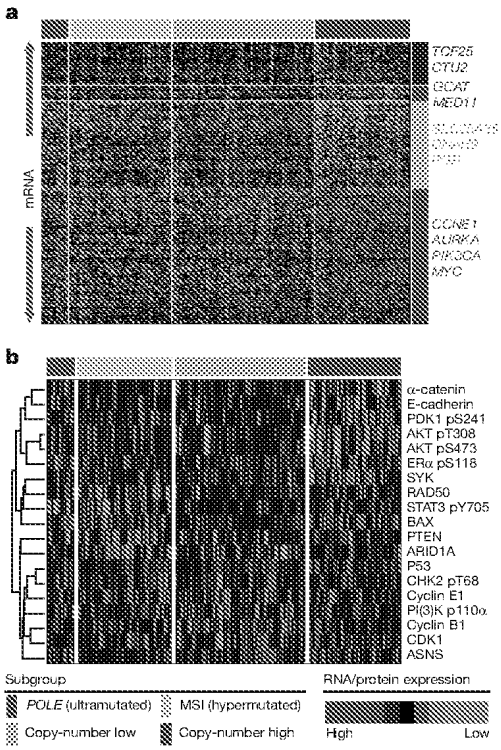


Figure 3 | Gene expression across integrated subtypes in endometrial carcinomas. a, Supervised analysis of ~1,500 genes significantly associated with integrated subtypes. **b**, Heat map of protein expression clusters, supervised by integrated subtypes. Samples are in columns; genes or proteins are in rows.

described in other tumour types[24] and our results suggest that similar mechanisms may be operative here.

Pathway alterations

Multiple platform data were integrated to identify recurrently altered pathways in the four endometrial cancer integrated subgroups. Because of the high background mutation rate and small sample size, we excluded the *POLE* subgroup from this analysis. Considering all recurrently mutated, homozygously deleted, and amplified genes, we used MEMo[25] to identify gene networks with mutually exclusive alteration patterns in each subgroup. The most significant module was found in the copy-number low group and contained *CTNNB1*, *KRAS* and *SOX17* (Fig. 4a). The very strong mutual exclusivity between mutations in these three genes suggests that alternative mechanisms activate WNT signalling in endometrioid endometrial cancer. Activating *KRAS* mutations have been shown to increase the stability of β-catenin via glycogen synthase kinase 3β (GSK-3β), leading to an alternative mechanism of β-catenin activation other than adenomatous polyposis coli degradation[26]. *SOX17*, which mediates proteasomal degradation of β-catenin[27,28], is mutated exclusively in the copy-number low group (8%) at recurrent positions (Ala96Gly and Ser403Ile) not previously described. Other genes with mutually exclusive alteration patterns in this module were *FBXW7*, *FGFR2* and *ERBB2* (ref. 29). *ERBB2* was focally amplified with protein overexpression in 25% of the serous or serous-like tumours, suggesting a potential role for human epidermal growth factor receptor 2 (HER2)-targeted inhibitors. A small clinical trial of trastuzumab found no activity in endometrial carcinoma, but accrued few HER2 fluorescence *in situ* hybridization (FISH)-amplified serous carcinomas[30].

PIK3CA and *PIK3R1* mutations were frequent and showed a strong tendency for mutual exclusivity in all subgroups, but unlike other tumour types, they co-occurred with *PTEN* mutations in the MSI and copy-number low subgroups as previously reported[5,9] (Fig. 4b). The copy-number high subgroup showed mutual exclusivity between alterations of all three genes. Overall, 93% of endometrioid tumours had mutations that suggested potential for targeted therapy with PI(3)K/AKT pathway inhibitors.

Consensus clustering of copy number, mRNA expression and pathway interaction data for 324 samples yielded five PARADIGM clusters with distinct pathway activation patterns[31] (Fig. 4c and Supplementary Methods 11). PARADIGM cluster 1 had the lowest level of MYC pathway activation and highest level of WNT pathway activation, consistent with its composition of copy-number low cases having frequent *CTNNB1* mutations. PARADIGM cluster 3 was composed predominantly of the copy-number high cases, with relatively high MYC/MAX signalling but low oestrogen receptor/FOXA1 signalling and p53 activity. Only *TP53* truncation and not missense mutations were implicated as loss-of-function mutations, suggesting different classes of p53 mutations may have distinct signalling consequences. PARADIGM cluster 5 was enriched for hormone receptor expression.

Comparison to ovarian and breast cancers

The clinical and pathologic features of uterine serous carcinoma and high-grade serous ovarian carcinoma (HGSOC) are quite similar. HGSOC shares many similar molecular features with basal-like breast carcinoma[32]. Focal SCNA patterns were similar between these three tumour subtypes and unsupervised clustering identified relatedness (Fig. 5a and Supplementary Fig. 12.1). Supervised analysis of transcriptome data sets showed high correlation between tumour subtypes (Supplementary Fig. 12.2). The MC3 DNA methylation subtype with minimal DNA methylation changes was also similar to basal-like breast and HGSOCs (Supplementary Fig. 12.3). A high frequency of *TP53* mutations is shared across these tumour subtypes (uterine serous, 91%; HGSOC, 96%; basal-like breast, 84%)[33,34], as is the very low frequency of *PTEN* mutations (uterine serous, 2%; HGSOC, 1%; basal-like breast, 1%). Differences included a higher frequency of *FBXW7*, *PPP2R1A* and *PIK3CA* mutations in uterine serous compared to basal-like breast and HGSOCs (Fig. 5b). We showed that uterine serous carcinomas share many molecular features with both HGSOCs and basal-like breast carcinomas, despite more frequent mutations, suggesting new opportunities for overlapping treatment paradigms.

Discussion

This integrated genomic and proteomic analysis of 373 endometrial cancers provides insights into disease biology and diagnostic classification that could have immediate therapeutic application. Our analysis identified four new groups of tumours based on integrated genomic data, including a novel *POLE* subtype in ~10% of endometrioid tumours. Ultrahigh somatic mutation frequency, MSS, and common, newly identified hotspot mutations in the exonuclease domain of *POLE* characterize this subtype. SCNAs add a layer of resolution, revealing that most endometrioid tumours have few SCNAs, most serous and serous-like tumours exhibit extensive SCNAs, and the extent of SCNA roughly correlates with progression-free survival.

Endometrial cancer has more frequent mutations in the PI(3)K/AKT pathway than any other tumour type studied by The Cancer Genome Atlas (TCGA) so far. Endometrioid endometrial carcinomas share many characteristics with colorectal carcinoma including a high frequency of MSI (40% and 11%, respectively), *POLE* mutations (7% and 3%, respectively) leading to ultrahigh mutation rates, and frequent activation of WNT/CTNNB1 signalling; yet endometrial carcinomas have novel exclusivity of *KRAS* and *CTNNB1* mutations and a distinct mechanism of pathway activation. Uterine serous carcinomas share many similar characteristics with basal-like breast and HGSOCs; three tumour types with high-frequency non-silent *TP53* mutations and extensive SCNA. However, the high frequency of *PIK3CA*, *FBXW7*, *PPP2R1A* and *ARID1A* mutations in uterine serous carcinomas are not found in basal-like breast and HGSOCs. The frequency of mutations in *PIK3CA*, *FBXW7* and *PPP2R1A* was ~30% higher than in a recently

©2013 Macmillan Publishers Limited. All rights reserved

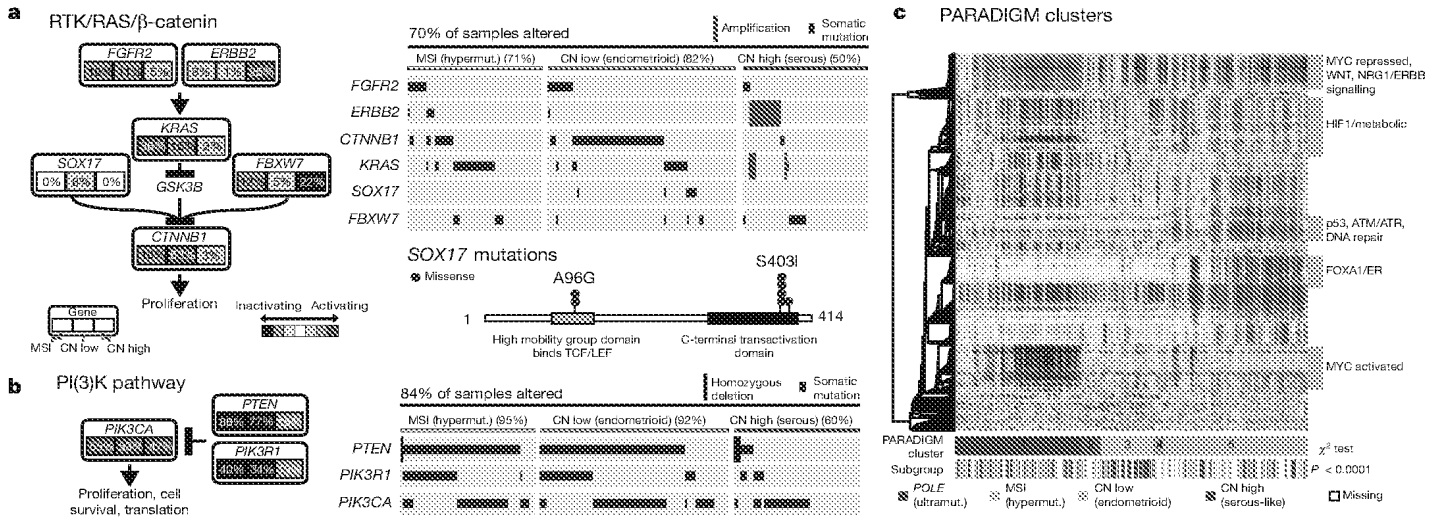


Figure 4 | Pathway alterations in endometrial carcinomas. **a**, The RTK/RAS/β-catenin pathway is altered through several mechanisms that exhibit mutually exclusive patterns. Alteration frequencies are expressed as a percentage of all cases. The right panel shows patterns of occurrence. **b**, The PI(3)K pathway has mutually exclusive *PIK3CA* and *PIK3R1* alterations that frequently co-occur with *PTEN* alterations in the MSI and copy-number low subgroups. **c**, Heat map display of top 1,000 varying pathway features within PARADIGM consensus clusters. Samples were arranged in order of their consensus cluster membership. The genomic subtype for each sample is displayed below the consensus clusters.

reported study of 76 uterine serous carcinomas[11], but similar to another study[12]. Uterine serous carcinomas have *ERBB2* amplification in 27% of tumours and *PIK3CA* mutations in 42%, which provide translational opportunities for targeted therapeutics.

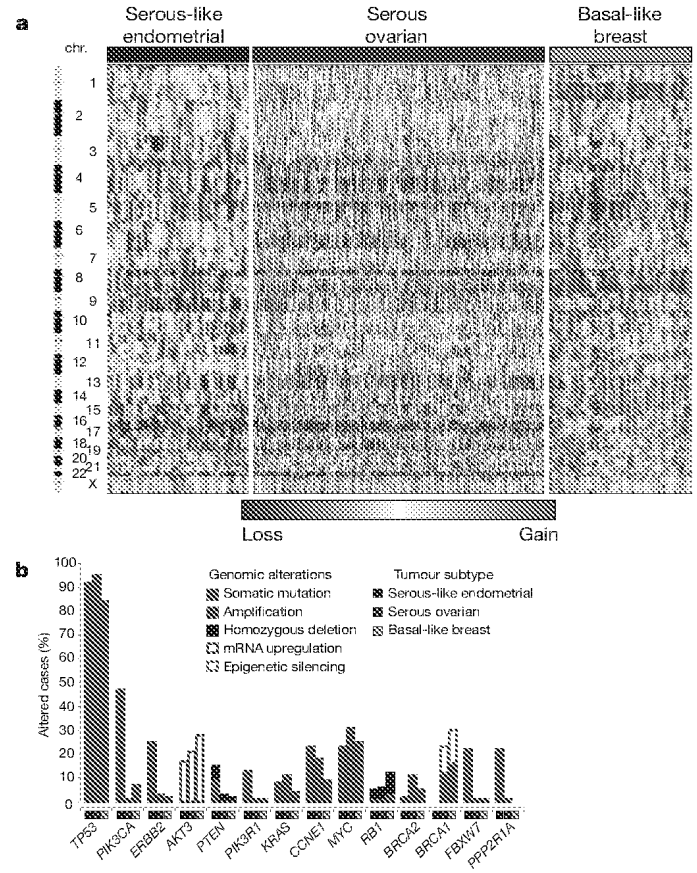


Figure 5 | Genomic relationships between endometrial serous-like, ovarian serous, and basal-like breast carcinomas. **a**, SCNAs for each tumour type. **b**, Frequency of genomic alterations present in at least 10% of one tumour type.

Early stage type I endometrioid tumours are often treated with adjuvant radiotherapy, whereas similarly staged type II serous tumours are treated with chemotherapy. High-grade serous and endometrioid endometrial carcinomas are difficult to subtype correctly, and intra-observer concordance among speciality pathologists is low[7,34–36]. Our molecular characterization data demonstrate that ~25% of tumours classified as high-grade endometrioid by pathologists have a molecular phenotype similar to uterine serous carcinomas, including frequent *TP53* mutations and extensive SCNA. The compelling similarities between this subset of endometrioid tumours and uterine serous carcinomas suggest that genomic-based classification may lead to improved management of these patients. Clinicians should carefully consider treating copy-number-altered endometrioid patients with chemotherapy rather than adjuvant radiotherapy and formally test such hypotheses in prospective clinical trials. Furthermore, the marked molecular differences between endometrioid and serous-like tumours suggest that these tumours warrant separate clinical trials to develop the independent treatment paradigms that have improved outcomes in other tumour types, such as breast cancer.

METHODS SUMMARY

Biospecimens were obtained from 373 patients after Institutional Review Board-approved consents. DNA and RNA were co-isolated using a modified AllPrep kit (Qiagen). We used Affymetrix SNP 6.0 microarrays to detect SCNAs in 363 samples and GISTIC analysis to identify recurrent events[37]. The exomes of 248 tumours were sequenced to a read-depth of at least ×20. We performed low-pass whole-genome sequencing on 107 tumours to a mean depth of ×6. Consensus clustering was used to analyse mRNA, miRNA, RPPA and methylation data with methods previously described[38–40]. Integrated cross-platform analyses were performed using MEMo, iCluster and PARADIGM[25,31].

Received 10 December 2012; accepted 21 March 2013.

1. Siegel, R., Naishadham, D. & Jemal, A. Cancer statistics, 2013. *CA Cancer J. Clin.* **63,** 11–30 (2013).
2. Fleming, G. F. *et al.* Phase III trial of doxorubicin plus cisplatin with or without paclitaxel plus filgrastim in advanced endometrial carcinoma: a Gynecologic Oncology Group Study. *J. Clin. Oncol.* **22,** 2159–2166 (2004).
3. Sutton, G. *et al.* Whole abdominal radiotherapy in the adjuvant treatment of patients with stage III and IV endometrial cancer: a gynecologic oncology group study. *Gynecol. Oncol.* **97,** 755–763 (2005).
4. Lax, S. F. & Kurman, R. J. A dualistic model for endometrial carcinogenesis based on immunohistochemical and molecular genetic analyses. *Verh. Dtsch. Ges. Pathol.* **81,** 228–232 (1997).

©2013 Macmillan Publishers Limited. All rights reserved

5. Cheung, L. W. *et al.* High frequency of *PIK3R1* and *PIK3R2* mutations in endometrial cancer elucidates a novel mechanism for regulation of PTEN protein stability. *Cancer Discov.* **1,** 170–185 (2011).
6. Levine, R. L. *et al. PTEN* mutations and microsatellite instability in complex atypical hyperplasia, a precursor lesion to uterine endometrioid carcinoma. *Cancer Res.* **58,** 3254–3258 (1998).
7. McConechy, M. K. *et al.* Use of mutation profiles to refine the classification of endometrial carcinomas. *J. Pathol.* **228,** 20–30 (2012).
8. Byron, S. A. *et al. FGFR2* point mutations in 466 endometrioid endometrial tumors: relationship with MSI, *KRAS*, *PIK3CA*, *CTNNB1* mutations and clinicopathological features. *PLoS ONE* **7,** e30801 (2012).
9. Urick, M. E. *et al. PIK3R1* (p85α) is somatically mutated at high frequency in primary endometrial cancer. *Cancer Res.* **71,** 4061–4067 (2011).
10. Zighelboim, I. *et al.* Microsatellite instability and epigenetic inactivation of *MLH1* and outcome of patients with endometrial carcinomas of the endometrioid type. *J. Clin. Oncol.* **25,** 2042–2048 (2007).
11. Kuhn, E. *et al.* Identification of molecular pathway aberrations in uterine serous carcinoma by genome-wide analyses. *J. Natl. Cancer Inst.* **104,** 1503–1513 (2012).
12. Le Gallo, M. *et al.* Exome sequencing of serous endometrial tumors identifies recurrent somatic mutations in chromatin-remodeling and ubiquitin ligase complex genes. *Nature Genet.* **44,** 1310–1315 (2012).
13. Salvesen, H. B. *et al.* Integrated genomic profiling of endometrial carcinoma associates aggressive tumors with indicators of PI3 kinase activation. *Proc. Natl Acad. Sci. USA* **106,** 4834–4839 (2009).
14. Cowin, P. A. *et al.* LRP1B deletion in high-grade serous ovarian cancers is associated with acquired chemotherapy resistance to liposomal doxorubicin. *Cancer Res.* **72,** 4060–4073 (2012).
15. The Cancer Genome Atlas Network. Comprehensive molecular characterization of human colon and rectal cancer. *Nature* **487,** 330–337 (2012).
16. Govindan, R. *et al.* Genomic landscape of non-small cell lung cancer in smokers and never-smokers. *Cell* **150,** 1121–1134 (2012).
17. Pleasance, E. D. *et al.* A comprehensive catalogue of somatic mutations from a human cancer genome. *Nature* **463,** 191–196 (2010).
18. Palles, C. *et al.* Germline mutations affecting the proofreading domains of POLE and POLD1 predispose to colorectal adenomas and carcinomas. *Nature Genet.* **45,** 136–144 (2013).
19. Bartosch, C. *et al.* Endometrial carcinomas: a review emphasizing overlapping and distinctive morphological and immunohistochemical features. *Adv. Anat. Pathol.* **18,** 415–437 (2011).
20. Toyota, M. *et al.* CpG island methylator phenotype in colorectal cancer. *Proc. Natl Acad. Sci. USA* **96,** 8681–8686 (1999).
21. Hinoue, T. *et al.* Genome-scale analysis of aberrant DNA methylation in colorectal cancer. *Genome Res.* **22,** 271–282 (2012).
22. Noushmehr, H. *et al.* Identification of a CpG island methylator phenotype that defines a distinct subgroup of glioma. *Cancer Cell* **17,** 510–522 (2010).
23. Shen, R., Olshen, A. B. & Ladanyi, M. Integrative clustering of multiple genomic data types using a joint latent variable model with application to breast and lung cancer subtype analysis. *Bioinformatics* **25,** 2906–2912 (2009).
24. Hockenbery, D., Nunez, G., Milliman, C., Schreiber, R. D. & Korsmeyer, S. J. Bcl-2 is an inner mitochondrial membrane protein that blocks programmed cell death. *Nature* **348,** 334–336 (1990).
25. Ciriello, G., Cerami, E., Sander, C. & Schultz, N. Mutual exclusivity analysis identifies oncogenic network modules. *Genome Res.* **22,** 398–406 (2012).
26. Li, J., Mizukami, Y., Zhang, X., Jo, W. S. & Chung, D. C. Oncogenic K-*ras* stimulates Wnt signaling in colon cancer through inhibition of GSK-3β. *Gastroenterology* **128,** 1907–1918 (2005).
27. Zorn, A. M. *et al.* Regulation of Wnt signaling by Sox proteins: XSox17 α/β and XSox3 physically interact with β-catenin. *Mol. Cell* **4,** 487–498 (1999).
28. Sinner, D. *et al.* Sox17 and Sox4 differentially regulate β-catenin/T-cell factor activity and proliferation of colon carcinoma cells. *Mol. Cell. Biol.* **27,** 7802–7815 (2007).
29. Pollock, P. M. *et al.* Frequent activating FGFR2 mutations in endometrial carcinomas parallel germline mutations associated with craniosynostosis and skeletal dysplasia syndromes. *Oncogene* **26,** 7158–7162 (2007).
30. Fleming, G. F. *et al.* Phase II trial of trastuzumab in women with advanced or recurrent, HER2-positive endometrial carcinoma: a Gynecologic Oncology Group study. *Gynecol. Oncol.* **116,** 15–20 (2010).
31. Vaske, C. J. *et al.* Inference of patient-specific pathway activities from multi-dimensional cancer genomics data using PARADIGM. *Bioinformatics* **26,** i237–i245 (2010).
32. The Cancer Genome Atlas Network. Comprehensive molecular portraits of human breast tumours. *Nature* **490,** 61–70 (2012).
33. The Cancer Genome Atlas Research Network. Integrated genomic analyses of ovarian carcinoma. *Nature* **474,** 609–615 (2011).
34. Clarke, B. A. & Gilks, C. B. Endometrial carcinoma: controversies in histopathological assessment of grade and tumour cell type. *J. Clin. Pathol.* **63,** 410–415 (2010).
35. Yemelyanova, A. *et al.* Utility of p16 expression for distinction of uterine serous carcinomas from endometrial endometrioid and endocervical adenocarcinomas: immunohistochemical analysis of 201 cases. *Am. J. Surg. Pathol.* **33,** 1504–1514 (2009).
36. Gilks, C. B., Oliva, E. & Soslow, R. A. Poor inter-observer reproducibility in the diagnosis of high-grade endometrial carcinoma. *Am. J. Surg. Pathol.* **91,** 248A (2012).
37. Mermel, C. H. *et al.* GISTIC2.0 facilitates sensitive and confident localization of the targets of focal somatic copy-number alteration in human cancers. *Genome Biol.* **12,** R41 (2011).
38. Gaujoux, R. & Seoighe, C. A flexible R package for nonnegative matrix factorization. *BMC Bioinformatics* **11,** 367 (2010).
39. Houseman, E. A. *et al.* Model-based clustering of DNA methylation array data: a recursive-partitioning algorithm for high-dimensional data arising as a mixture of beta distributions. *BMC Bioinformatics* **9,** 365 (2008).
40. Brunet, J. P., Tamayo, P., Golub, T. R. & Mesirov, J. P. Metagenes and molecular pattern discovery using matrix factorization. *Proc. Natl Acad. Sci. USA* **101,** 4164–4169 (2004).

Supplementary Information is available in the online version of the paper.

Acknowledgements We wish to thank all patients and families who contributed to this study. We thank M. Sheth and L. Lund for administrative coordination of TCGA activities, G. Monemvasitis for editing the manuscript, and C. Gunter for critical reading of the manuscript. This work was supported by the following grants from the US National Institutes of Health: 5U24CA143799-04, 5U24CA143835-04, 5U24CA143840-04, 5U24CA143843-04, 5U24CA143845-04, 5U24CA143848-04, 5U24CA143858-04, 5U24CA143866-04, 5U24CA143867-04, 5U24CA143882-04, 5U24CA143883-04, 5U24CA144025-04, U54HG003067-11, U54HG003079-10 and U54HG003273-10.

Author Contributions The TCGA Research Network contributed collectively to this study. Biospecimens were provided by the tissue source sites and processed by the biospecimen core resource. Data generation and analyses were performed by the genome sequencing centres, cancer genome characterization centres and genome data analysis centres. All data were released through the data coordinating centre. The National Cancer Institute and National Human Genome Research Institute project teams coordinated project activities. We also acknowledge the following TCGA investigators who made substantial contributions to the project: N.S. (manuscript coordinator); J. Gao (data coordinator); C.K. and L. Ding (DNA sequence analysis); W.Z. and Y.L. (mRNA sequence analysis); H.S. and P.W.L. (DNA methylation analysis); A.D.C. and I.P. (copy number analysis); S.L. and A. Hadjipanayis (translocations); N.S., N.W. G.C., C.C.B. and C.Y. (pathway analysis); Andy C. and A.G.R. (miRNA sequence analysis); R. Broaddus, P.J.G., G.B.M. and R.A.S. (pathology and clinical expertise); G.B.M., H.L. and R.A. (reverse phase protein arrays); P.J.G. and R.B. (disease experts); G.B.M. and R.K. (manuscript editing); D.A.L. and E.R.M. (project chairs).

Author Information The primary and processed data used to generate the analyses presented here are deposited at the Data Coordinating Center (https://tcga-data.nci.nih.gov/tcga/tcgaDownload.jsp); all of the primary sequence files are deposited in CGHub (https://cghub.ucsc.edu/). Sample lists, data matrices and supporting data can be found at: (https://tcga-data.nci.nih.gov/docs/publications/ucec_2013/). The data can be explored via the cBio Cancer Genomics Portal (http://cbioportal.org). Reprints and permissions information is available at www.nature.com/reprints. The authors declare no competing financial interests. Readers are welcome to comment on the online version of the paper. Correspondence and requests for materials should be addressed to D.A.L. (levine2@mskcc.org).

This work is licensed under a Creative Commons Attribution-NonCommercial-Share Alike 3.0 Unported licence. To view a copy of this licence, visit http://creativecommons.org/licenses/by-nc-sa/3.0

The Cancer Genome Atlas Research Network (Participants are arranged by area of contribution and then by institution.)

Genome sequencing centres: Broad Institute Gad Getz[1], Stacey B. Gabriel[1], Kristian Cibulskis[1], Eric Lander[1], Andrey Sivachenko[1], Carrie Sougnez[1], Mike Lawrence[1]; **Washington University in St Louis** Cyriac Kandoth[2], David Dooling[2], Robert Fulton[2], Lucinda Fulton[2], Joelle Kalicki-Veizer[2], Michael D. McLellan[2], Michelle O'Laughlin[2], Heather Schmidt[2], Richard K. Wilson[2], Kai Ye[2], Li Ding[2], Elaine R. Mardis[2]

Genome characterization centres: British Columbia Cancer Agency Adrian Ally[3], Miruna Balasundaram[3], Inanc Birol[3], Yaron S. N. Butterfield[3], Rebecca Carlsen[3], Candace Carter[3], Andy Chu[3], Eric Chuah[3], Hye-Jung E. Chun[3], Noreen Dhalla[3], Ranabir Guin[3], Carrie Hirst[3], Robert A. Holt[3], Steven J. M. Jones[3], Darlene Lee[3], Haiyan I. Li[3], Marco A. Marra[3], Michael Mayo[3], Richard A. Moore[3], Andrew J. Mungall[3], Patrick Plettner[3], Jacqueline E. Schein[3], Payal Sipahimalani[3], Angela Tam[3], Richard J. Varhol[3], A. Gordon Robertson[3]; **Broad Institute** Andrew D. Cherniack[1], Itai Pashtan[1,4,5], Gordon Saksena[1], Robert C. Onofrio[1], Steven E. Schumacher[1], Barbara Tabak[1], Scott L. Carter[1], Bryan Hernandez[1], Jeff Gentry[1], Helga B. Salvesen[1,6,7], Kristin Ardlie[1], Gad Getz[1], Wendy Winckler[1], Rameen Beroukhim[1,8], Stacey B. Gabriel[1], Matthew Meyerson[1,8]; **Harvard Medical School/Brigham & Women's Hospital/MD Anderson Cancer Center** Angela Hadjipanayis[9], Semin Lee[10], Harshad S. Mahadeshwar[11], Peter Park[10,12], Alexei Protopopov[11], Xiaojia Ren[9], Sahil Seth[11], Xingzhi Song[11], Jiabin Tang[11], Ruibin Xi[10], Lixing Yang[10], Dong Zeng[11], Raju Kucherlapati[9], Lynda Chin[1,11], Jianhua Zhang[11]; **University of North Carolina** J. Todd Auman[13,14], Saianand Balu[15], Tom Bodenheimer[15], Elizabeth Buda[15], D. Neil Hayes[15,16], Alan P. Hoyle[15], Stuart R. Jefferys[15], Corbin D. Jones[17], Shaowu Meng[15], Piotr A. Mieczkowski[18], Lisle E. Mose[15], Joel S. Parker[15], Charles M. Perou[15,18,19], Jeff Roach[20], Yan Shi[15], Janae V. Simons[15], Mathew G. Soloway[15], Donghui Tan[15], Michael D. Topal[15,19], Scot Waring[15], Junyuan Wu[15], Katherine A. Hoadley[15,18]; **University of Southern California & Johns Hopkins** Stephen B. Baylin[21], Moiz S. Bootwalla[22], Phillip H. Lai[22], Timothy J. Triche Jr[22], David J. Van Den Berg[22], Daniel J. Weisenberger[22], Peter W. Laird[22], Hui Shen[22]

Genome data analysis centres: Broad Institute Lynda Chin[1,11], Jianhua Zhang[11], Gad Getz[1], Juok Cho[1], Daniel DiCara[1], Scott Frazer[1], David Heiman[1], Rui Jing[1], Pei Lin[1], Will Mallard[1], Petar Stojanov[1], Doug Voet[1], Hailei Zhang[1], Lihua Zou[1], Michael Noble[1], Mike

©2013 Macmillan Publishers Limited. All rights reserved

Lawrence[1]; **Institute for Systems Biology** Sheila M. Reynolds[23], Ilya Shmulevich[23]; **Memorial Sloan-Kettering Cancer Center** B. Arman Aksoy[24], Yevgeniy Antipin[24], Giovanni Ciriello[24], Gideon Dresdner[24], Jianjiong Gao[24], Benjamin Gross[24], Anders Jacobsen[24], Marc Ladanyi[25], Boris Reva[24], Chris Sander[24], Rileen Sinha[24], S. Onur Sumer[24], Barry S. Taylor[26], Ethan Cerami[24], Nils Weinhold[24], Nikolaus Schultz[24], Ronglai Shen[27]; **University of California, Santa Cruz/Buck Institute** Stephen Benz[28], Ted Goldstein[28], David Haussler[28], Sam Ng[28], Christopher Szeto[28], Joshua Stuart[28], Christopher C. Benz[29], Christina Yau[29]; **The University of Texas MD Anderson Cancer Center** Wei Zhang[30,31], Matti Annala[30,31,32], Bradley M. Broom[33], Tod D. Casasent[33], Zhenlin Ju[33], Han Liang[33], Guoyan Liu[30,31], Yiling Lu[34], Anna K. Unruh[33], Chris Wakefield[33], John N. Weinstein[33], Nianxiang Zhang[33], Yuexin Liu[30,31], Russell Broaddus[31], Rehan Akbani[33], Gordon B. Mills[34]

Biospecimen core resource: Nationwide Children's Hospital Christopher Adams[35], Thomas Barr[35], Aaron D. Black[35], Jay Bowen[35], John Deardurff[35], Jessica Frick[35], Julie M. Gastier-Foster[35,36], Thomas Grossman[35], Hollie A. Harper[35], Melissa Hart-Kothari[35], Carmen Helsel[35], Aaron Hobensack[35], Harkness Kuck[35], Kelley Kneile[35], Kristen M. Leraas[35], Tara M. Lichtenberg[35], Cynthia McAllister[35], Robert E. Pyatt[35], Nilsa C. Ramirez[35,36], Teresa R. Tabler[35], Nathan Vanhoose[35], Peter White[35], Lisa Wise[35], Erik Zmuda[35]

Tissue source sites: Asterand Nandita Barnabas[37], Charlenia Berry-Green[37], Victoria Blanc[37], Lori Boice[38], Michael Button[37], Adam Farkas[37], Alex Green[37], Jean MacKenzie[37], Dana Nicholson[37]; **British Columbia Cancer Agency** Steve E. Kalloger[39,40], C. Blake Gilks[39,40]; **Cedars-Sinai Medical Center** Beth Y. Karlan[41], Jenny Lester[41], Sandra Orsulic[41]; **Christiana Care** Mark Borowsky[42], Mark Cadungog[42], Christine Czerwinski[42], Lori Huelsenbeck-Dill[42], Mary Iacocca[42], Nicholas Petrelli[42], Brenda Rabeno[42], Gary Witkin[42]; **Cureline** Elena Nemirovich-Danchenko[43], Olga Potapova[43], Daniil Rotin[43]; **Duke University** Andrew Berchuck[44]; **Gynecologic Oncology Group** Michael Birrer[45], Phillip DiSaia[46], Laura Monovich[47]; **International Genomics Consortium** Erin Curley[48], Johanna Gardner[48], David Mallery[48], Robert Penny[48]; **Mayo Clinic** Sean C. Dowdy[49], Boris Winterhoff[49], Linda Dao[50], Bobbie Gostout[49], Alexandra Meuter[49], Attila Teoman[49]; **Memorial Sloan-Kettering Cancer Center** Fanny Dao[51], Narciso Olvera[51], Faina Bogomolniy[51], Karuna Garg[52], Robert A. Soslow[52], Douglas A. Levine[51]; **N. N. Blokhin Russian Cancer Research Center** Mikhail Abramov[53]; **Ontario Tumour Bank** John M. S. Bartlett[54], Sugy Kodeeswaran[54], Jeremy Parfitt[55]; **St Petersburg Academic University** Fedor Moiseenko[56]; **University Health Network** Blaise A. Clarke[57]; **University of Hawaii** Marc T. Goodman[58,59], Michael E. Carney[58], Rayna K. Matsuno[58]; **University of North Carolina** Jennifer Fisher[38], Mei Huang[38], W. Kimryn Rathmell[15], Leigh Thorne[38], Linda Van Le[38]; **University of Pittsburgh** Rajiv Dhir[60], Robert Edwards[60], Esther Elishaev[60], Kristin Zorn[60]; **The University of Texas MD Anderson Cancer Center** Russell Broaddus[31]; **Washington University School of Medicine** Paul J. Goodfellow[36,61], David Mutch[61]

Disease analysis working group: Nikolaus Schultz[24], Yuexin Liu[30,31], Rehan Akbani[33], Andrew D. Cherniack[1], Ethan Cerami[24], Nils Weinhold[24], Hui Shen[22], Katherine A. Hoadley[15,18], Ari B. Kahn[62], Daphne W. Bell[63], Pamela M. Pollock[64], Chen Wang[65], David A.Wheeler[66], Eve Shinbrot[66], Beth Y. Karlan[41], Andrew Berchuck[44], Sean C. Dowdy[49], Boris Winterhoff[49], Marc T. Goodman[58,59], A. Gordon Robertson[3], Rameen Beroukhim[1,8], Itai Pashtan[1,4,5], Helga B. Salvesen[1,6,7], Peter W. Laird[22], Michael Noble[1], Joshua Stuart[28], Li Ding[2], Cyriac Kandoth[2], C. Blake Gilks[39,40], Robert A. Soslow[52], Paul J. Goodfellow[36,61], David Mutch[61], Russell Broaddus[31], Wei Zhang[30,31], Gordon B. Mills[34], Raju Kucherlapati[9], Elaine R. Mardis[2], Douglas A. Levine[51]

Data coordination centre: Brenda Ayala[62], Anna L. Chu[62], Mark A. Jensen[62], Prachi Kothiyal[62], Todd D. Pihl[62], Joan Pontius[62], David A. Pot[62], Eric E. Snyder[62], Deepak Srinivasan[62], Ari B. Kahn[62]

Project team: National Cancer Institute Kenna R. Mills Shaw[67], Margi Sheth[67], Tanja Davidsen[67], Greg Eley[68]; Martin L. Ferguson[69], John A. Demchok[67], Liming Yang[67]; **National Human Genome Research Institute** Mark S. Guyer[70], Bradley A. Ozenberger[70], Heidi J. Sofia[70]

Writing committee: Cyriac Kandoth[2], Nikolaus Schultz[24], Andrew D. Cherniack[1], Rehan Akbani[33], Yuexin Liu[30,31], Hui Shen[22], A. Gordon Robertson[3], Itai Pashtan[1,4,5], Ronglai Shen[27], Christopher C. Benz[29], Christina Yau[29], Peter W. Laird[22], Li Ding[2], Wei Zhang[30,31], Gordon B. Mills[34], Raju Kucherlapati[9], Elaine R. Mardis[2] & Douglas A. Levine[51]

[1]The Eli and Edythe L. Broad Institute of Massachusetts Institute of Technology and Harvard University Cambridge, Massachusetts 02142, USA. [2]The Genome Institute, Washington University, St Louis, Missouri 63108, USA. [3]Canada's Michael Smith Genome Sciences Centre, BC Cancer Agency, Vancouver, British Columbia V5Z, Canada. [4]Department of Radiation Oncology, Dana-Farber Cancer Institute and Brigham and Women's Hospital, Boston, Massachusetts 02115, USA. [5]Dana-Farber Cancer Institute, Boston, Massachusetts 02215, USA. [6]Department of Obstetrics and Gynecology, Haukeland University Hospital, 5021 Bergen, Norway. [7]Department of Clinical Medicine, University of Bergen, 5020 Bergen, Norway. [8]Department of Medical Oncology, Dana-Farber Cancer Institute, Boston, Massachusetts 02215, USA. [9]Department of Genetics, Harvard Medical School, Boston, Massachusetts 02115, USA. [10]Center for Biomedical Informatics, Harvard Medical School, Boston, Massachusetts 02115, USA. [11]Institute for Applied Cancer Science, Department of Genomic Medicine, University of Texas MD Anderson Cancer Center, Houston, Texas 77054, USA. [12]Informatics Program, Boston Children's Hospital, Boston, Massachusetts 02115, USA. [13]Eshelman School of Pharmacy, University of North Carolina at Chapel Hill, Chapel Hill, North Carolina 27599, USA. [14]Institute for Pharmacogenetics and Individualized Therapy, University of North Carolina at Chapel Hill, Chapel Hill, North Carolina 27599, USA. [15]Lineberger Comprehensive Cancer Center, University of North Carolina at Chapel Hill, Chapel Hill, North Carolina 27599, USA. [16]Department of Internal Medicine, Division of Medical Oncology, University of North Carolina at Chapel Hill, Chapel Hill, North Carolina 27599, USA. [17]Department of Biology, University of North Carolina at Chapel Hill, North Carolina 27599, USA. [18]Department of Genetics, University of North Carolina at Chapel Hill, Chapel Hill, North Carolina 27599, USA. [19]Department of Pathology and Laboratory Medicine, University of North Carolina at Chapel Hill, Chapel Hill, North Carolina 27599, USA. [20]Research Computing Center, University of North Carolina at Chapel Hill, Chapel Hill, North Carolina 27599, USA. [21]Cancer Biology Division, The Sidney Kimmel Comprehensive Cancer Center at Johns Hopkins University, Baltimore, Maryland 21231, USA. [22]University of Southern California Epigenome Center, University of Southern California, Los Angeles, California 90089, USA. [23]Institute for Systems Biology, Seattle, Washington 98109, USA. [24]Computational Biology Center, Memorial Sloan-Kettering Cancer Center, New York, New York 10065, USA. [25]Human Oncology and Pathogenesis Program, Memorial Sloan-Kettering Cancer Center, New York, New York 10065, USA. [26]Helen Diller Family Comprehensive Cancer Center, University of California, San Francisco, San Francisco, California 94158, USA. [27]Department of Epidemiology and Biostatistics, Memorial Sloan-Kettering Cancer Center, New York, New York 10065, USA. [28]Department of Biomolecular Engineering and Center for Biomolecular Science and Engineering, University of California Santa Cruz, Santa Cruz, California 95064, USA. [29]Buck Institute for Age Research, Novato, California 94945, USA. [30]Cancer Genomics Core Laboratory, University of Texas MD Anderson Cancer Center, Houston, Texas 77054, USA. [31]Department of Pathology, University of Texas MD Anderson Cancer Center, Houston, Texas 77030, USA. [32]Tampere University of Technology Korkeakoulunkatu 10, FI-33720 Tampere, Finland. [33]Department of Bioinformatics and Computational Biology, The University of Texas MD Anderson Cancer Center, Houston, Texas 77030, USA. [34]Department of Systems Biology, The University of Texas MD Anderson Cancer Center, Houston, Texas 77030, USA. [35]The Research Institute at Nationwide Children's Hospital, Columbus, Ohio 43205, USA. [36]The Ohio State University, Columbus, Ohio 43210, USA. [37]Asterand, Detroit, Michigan 48202, USA. [38]University of North Carolina, Chapel Hill, North Carolina 27599, USA. [39]OvCaRe British Columbia, British Columbia Cancer Agency, Vancouver, British Columbia V5Z 4E6, Canada. [40]Department of Pathology & Laboratory Medicine, The University of British Columbia, Vancouver, British Columbia V6T 2B5, Canada. [41]Women's Cancer Program at the Samuel Oschin Comprehensive Cancer Institute, Cedars-Sinai Medical Center, Los Angeles, California 90048, USA. [42]Helen F Graham Cancer Center at Christiana Care, Newark, Delaware 19713, USA. [43]Cureline, Inc., South San Francisco, California 94080, USA. [44]Duke University Medical Center, Duke Cancer Institute, Durham, North Carolina 27710, USA. [45]Harvard Medical School, Massachusetts General Hospital Cancer Center, Boston, Massachusetts 02114, USA. [46]University of California Medical Center, Irvine, Orange California 92868, USA. [47]GOG Tissue Bank, The Research Institute at Nationwide Children's Hospital, Columbus, Ohio 43205, USA. [48]International Genomics Consortium, Phoenix, Arizona 85004, USA. [49]Department of OB Gyn, Division of Gynecologic Oncology, Mayo Clinic, Rochester, Minnesota 55905, USA. [50]Department of Pathology, Mayo Clinic, Rochester, Minnesota 55905, USA. [51]Gynecology Service, Department of Surgery, Memorial Sloan-Kettering Cancer Center, New York, New York 10065, USA. [52]Department of Pathology, Memorial Sloan-Kettering Cancer Center, New York, New York 10065, USA. [53]N. N. Blokhin Russian Cancer Research Center RAMS, Moscow 115478, Russia. [54]Ontario Tumour Bank, Ontario Institute for Cancer Research, Toronto, Ontario M5G 0A3, Canada. [55]Ontario Tumour Bank, London Health Sciences Centre, London, Ontario N6A 5A5, Canada. [56]St Petersburg Academic University, St Petersburg 199034, Russia. [57]Department of Pathology, University Health Network, Toronto, Ontario M5G 2C4, Canada. [58]University of Hawaii, Honolulu, Hawaii 96813, USA. [59]Cedars-Sinai Medical Center, Los Angeles, California 90024, USA. [60]University of Pittsburgh, Pittsburgh, Pennsylvania 15213, USA. [61]Washington University School of Medicine, St Louis, Missouri 63110, USA. [62]SRA International, Fairfax, Virgina 22033, USA. [63]Cancer Genetics Branch, National Human Genome Research Institute, National Institutes of Health, Bethesda, Maryland 20892, USA. [64]Institute of Health and Biomedical Innovation, Queensland University of Technology, Brisbane 4059, Australia. [65]Department of Biomedical Statistics and Informatics, Mayo Clinic, Rochester, Minnesota 55905, USA. [66]Human Genome Sequencing Center, Baylor College of Medicine, Houston, Texas 77030, USA. [67]The Cancer Genome Atlas Program Office, National Cancer Institute, National Institutes of Health, Bethesda, Maryland 20892, USA. [68]Scimentis, LLC, Atlanta, Georgia 30666, USA. [69]MLF Consulting, Arlington, Maryland 02474, USA. [70]National Human Genome Research Institute, National Institutes of Health, Bethesda, Maryland 20892, USA.

©2013 Macmillan Publishers Limited. All rights reserved

ERRATUM
doi:10.1038/nature12325

Erratum: Integrated genomic characterization of endometrial carcinoma

The Cancer Genome Atlas Research Network

Nature **497,** 67–73 (2013); doi:10.1038/nature12113

In the 'Results' section of this Article, the range in the sentence "The median follow-up of the cohort was 32 months (range, 1–19 months); 21% of the patients have recurred, and 11% have died." should have been 1–195 months. This error has been corrected in the HTML and PDF versions of the paper.

©2013 Macmillan Publishers Limited. All rights reserved